ISCBFM
International Society for
Cerebral Blood Flow & Metabolism

Brain
CHICAGO
2009

XXIVth International Symposium on Cerebral Blood Flow, Metabolism and Function
&
IXth International Conference on Quantification of Brain Function with PET

June 29-July 3, Chicago, IL, USA

---

www.kenes.com/brain

www.iscbfm.org

3

Brain Poster Session: Experimental Cerebral Ischemia: In Vitro

LIPID METABOLISM AND CELL CYCLE: ANTI-PROLIFERATIVE EFFECTS OF PC-PLC INHIBITOR D609 IN STROKE

R. Adibhatla[1,2,3,4], J. Hatcher[1], R. Dempsey[1], H. Kalluri[1]

[1]Neurological Surgery, [2]Neuroscience Training Program, [3]Cardiovascular Research Center, University of Wisconsin School of Medicine and Public Health, [4]Research, William S Middleton Veteran Affairs Hospital, Madison, WI, USA

Introduction: The pro-inflammatory response after stroke due to up-regulation of TNF-α and IL-1 can activate phospholipases and stimulate ROS production. Transient middle cerebral artery occlusion (tMCAO) in rat significantly increased (4-fold) PC-PLC activity, up-regulated sphingomyelinases (SMase, neutral- and acidic-) and down-regulated PC synthesis and sphingomyelin (SM) synthases (SMS-1 and 2) in the ipsi cortex, causing significant PC and SM loss (1).

Lipid second messengers 1,2-diacylglycerol (DAG) and ceramide, produced by hydrolysis of PC and SM, respectively, are key regulators of the cell cycle. The PC-PLC product DAG can stimulate cyclin D1 expression through pERK by activation of protein kinase C, either directly or through ASMase/ceramide pathway, and activation of AKT via ASMase/ceramide/PI3 kinase pathway. Up-regulation of cyclin D1 can trigger the cell cycle, inducing proliferation of astrocytes and microglia/macrophages. However, for post-mitotic neurons, cell cycle entry results in their death.

Results: In tMCAO (1 hr by intraluminal suture method in SHR), PC-PLC inhibitor, tricyclodecan-9-yl-xanthogenate (D609) attenuated infarction by 35±5%. D609 blocked proliferation (BrdU uptake) of rat neural progenitor cells by 75±5% and attenuated pERK, pAKT and cyclin D1 expression (Western blotting). D609 did not alter expression of pAKT, pERK and cyclin D1 after stroke. This may be due to heterogeneous populations of neuronal (< 5%) and non-neuronal cells and changes might have been blunted, unlike in the homogeneous rat neural progenitor cells. However, treatment with D609 did increase ceramide levels and expression of endogenous cell cycle inhibitor, $p21^{cip1}$, suggesting cell cycle arrest at G1-phase after stroke. SM synthase transfers the phosphocholine group of PC to ceramide to form SM and DAG. D609 also inhibits SM synthase, which could account for the increase in ceramide following D609 treatment. Ceramide can induce G0/G1 cell cycle arrest by up-regulation of CDK inhibitor $p21^{Cip1}$ (2). Recent studies indicate that $p21^{cip1}$ exerts neuroprotection via mechanisms independent of its nuclear role in cell cycle inhibition (3). In addition to PC hydrolysis and impaired synthesis, oxidation of PC to oxidized-PC (OxPC, detected by EO6-monoclonal antibodies) due to ROS generation was also observed after tMCAO (4). OxPC may serve as a marker of neuroinflammation and apoptosis and also enhance pro-inflammatory signals. D609 also attenuated formation of OxPC-modified proteins after tMCAO, which could be mediated by increased p21 expression or reduction in pro-inflammatory cytokine levels.

Conclusions: We hypothesize that PC-PLC regulates cell cycle through DAG in proliferating non-neuronal cells and mediates cell death in mature post-mitotic neurons. D609 prevented bFGF stimulated astrocyte proliferation in other studies (5). D609 may inhibit proliferation of cytokine-expressing microglia/macrophages and simultaneously prevent mature neurons from entering into cell cycle and dying, thus providing protection after stroke. Funded by NIH, AHA and UW Med School.

References:

1. Adibhatla RM and Hatcher JF (2008) Front. Biosci. **13**, 1250-1270.

2. Ogretmen B and Hannun YA (2004) Nat. Rev. Cancer **4**, 604-616.

3. Langley B et al. (2008) J. Neurosci. **28**, 163-176.

4. Adibhatla RM and Hatcher JF (2008) BMB Reports **41**, 560-567.

5. Riboni L, et al. (2001) J. Biol. Chem. **276**, 12797-12804.

8

Brain Poster Session: Neurovascular Unit in Health & Disease

AGE-RELATED DECREASE ACTIVITY OF NEUROVACULAR COUPLING: A TCD STUDY

M. Zaletel, B. Zvan, J. Pretnar Oblak

Neurology, University Medical Centre Ljubljana, Ljubljana, Slovenia

Background: A noninvasive assessment of neurovascular coupling, during normal ageing, would be of great importance. For this purpose, we simultaneously recorded visual evoked potentials (VEP) and visually evoked cerebral blood flow velocity responses (VEFR).

Methods: The records were made from a group of healthy younger subjects (37.5±9.4 years) as well as healthy older ones (69.5±5.9 years). The stimulus was a black-and-white checkerboard with visual contrasts of 1%, 10% and 100%. The VEFR were measured in the posterior cerebral artery using transcranial Doppler (TCD), and the VEP were recoded from occipital leads.

Results: To test the relationship between the VEFR, the VEP and the visual contrast, a linear regression analysis was performed which showed a significant positive association between the VEP in the VEFR ($r=0.66$, $p< 0.01$) of the younger and older subjects ($r=0.74$, $p< 0.01$). The regression coefficient of the younger subjects was significantly higher ($b=0.54$) than that of the older ones ($b=0.40$) ($p< 0.01$).

Discussion: We found a linear relationship between VEP and VEFR in younger as well as in older subjects. Our major finding was that the regression coefficient was significantly lower in older subjects as compared to younger ones. This finding suggested a diminished function of neurovascular coupling in older subjects. Although the studies have explored the relationship between evoked potentials and vascular responses detected by fMRI and near infrared spectroscopy (NIRS), none of them has studied the effect of ageing on this relationship. An indirect study with TCD using control system analysis has suggested that neurovascular coupling mechanism is unaffected by moderate ageing as estimated by Doppler parameters. In our study as well as in the other TCD studies that have also reported diminished responses in older subjects, however, the age of the subjects was importantly greater.

Conclusions: We concluded that a simultaneous recording of VEFR and VEP at graded visual contrasts indicates diminished neurovascular coupling in older subjects.

Brain Poster Session: Cerebral Vascular Regulation

IS CEREBRAL OXYGENATION NEGATIVELY AFFECTED BY INFUSION OF NORADRENALINE IN HEALTHY SUBJECTS?

P. Brassard, T.S. Larsen, N.H. Secher

Department of Anaesthesia, The Copenhagen Muscle Research Centre, Rigshospitalet, Faculty of Health Sciences, University of Copenhagen, Copenhagen, Denmark

Introduction: One approach of increasing mean arterial pressure (MAP), in order to secure a pressure gradient for vital organs, is provided by the use of vasopressor agents. The consequence of augmenting MAP by elevating vascular resistance or cardiac output (CO) on blood flow and oxygenation of the brain is not clear. More specifically, the influence of noradrenaline (NA), which is an α-agonist causing vasoconstriction, on cerebral hemodynamics is ambiguous. Furthermore, the influence of NA on cerebral oxygenation has not been investigated.

Aim: The aim of this study was to evaluate the impact of the infusion of NA on cerebral oxygenation in healthy subjects.

Methods: Three doses of NA (0.05, 0.1 and 0.15 mg kg^{-1} min^{-1} for 20 min each) were infused in nine healthy subjects (6 males; 26±6 years old, mean±SD). MAP, cerebral oxygenation characterized by frontal lobe oxygenation (S_cO_2) and jugular venous oxygen saturation ($S_{jv}O_2$), middle cerebral artery mean flow velocity (MCA V_{mean}), cardiac output (CO) and arterial pressure for carbon dioxide (P_aCO_2) were evaluated.

Results: MAP increased from 88 (22) [median (range)] to 115 (30) mmHg with increasing doses of NA ($p< 0.05$ for 0.1 and 0.15 mg kg^{-1} min^{-1} of NA) and reflected an increase in total peripheral resistance (20.3 (13.7) to 25.2 (12.1) mmHg 1/L min^{-1}; $p< 0.05$) as CO remained at a baseline value (Table). S_cO_2 and $S_{jv}O_2$ lowered with increasing doses of NA, reaching statistical significance with NA infused at 0.1 mg kg^{-1} min^{-1} and higher (S_cO_2: 78 (19) to 69 (22) %; $p< 0.05$; $S_{jv}O_2$: 67±8 to 64±7 %; $p< 0.01$). MCA V_{mean} was reduced with each doses of NA (56.9±11.2 to 55.0±11.7 cm sec^{-1}; $p< 0.05$). Finally, P_aCO_2 lowered with increasing doses of NA (5.4±0.4 to 5.1±0.4 kPa; $p< 0.001$).

	MAP(mmHg)	S_cO_2(%)	$S_{jv}O_2$(%)	MCA V_{mean}(cm sec^{-1})	CO(L min^{-1})	TPR(mmHg 1/min^{-1})	P_aCO_2(kPa)
Saline	88(22)	78(19)	67±8	56.9±11.2	4.8 (3.3)	20.3 (13.7)	5.4±0.4
0.05	100(26)	72(20)	66±8	54.8±11.9*	4.6 (2.4)	23.0 (13.6)	5.3±0.4
0.1	108(27)*	69(23)*	64±7†	55.0±11.0*	4.8 (2.3)	23.9 (12.3)*	5.1±0.4‡
0.15	115(30)*	69(22)*	64±7†	55.0±11.7*	4.8 (2.3)	25.2	5.1±0.4‡

						(12.1)*	

[Systemic and cerebral parameters changes with NA]
Data are mean±SD or median (range). Infusions of NA are in mg kg^{-1} min^{-1}**;** * p< 0.05, † p< 0.01, and ‡ p< 0.001 vs. saline.

Conclusion: This study suggests that infusion of 0.1 mg kg^{-1} min^{-1} and higher doses of NA negatively affects cerebral oxygenation as it increases MAP by peripheral vasoconstriction.

10

Brain Poster Session: Cerebral Metabolic Regulation

INTER-INDIVIDUAL VARIATIONS OF CBF AND OXYGEN CONSUMPTION IN RELATION TO HEMOGLOBIN CONCENTRATION: A PET STUDY

M. Ibaraki, Y. Shinohara, K. Nakamura, S. Miura, T. Kinoshita

Akita Research institute of Brain and Blood Vessels, Akita, Japan

Introduction: Control mechanism of CBF and its relation to oxygen metabolism are not fully understood. Hemoglobin (Hb) concentration is one of important factors that directly affect oxygen delivery to brain tissue. Variations of Hb concentration, even in normal range, may induce biological response in cerebral circulation to keep oxygen consumption constant. The aim of the study was to investigate the relationship between Hb and CBF and oxygen metabolism measured by ^{15}O-PET in humans.

Methods: Healthy volunteers (n=17) and patients with unilateral major arterial steno-occlusive disease who had no obvious infarct lesion in T2-weighted MR image (n=44) were studied retrospectively. CBF, CBV, $CMRO_2$, and OEF were measured by the sequential administration of $H_2{}^{15}O$, $^{15}O_2$, and $C^{15}O$ (autoradiographic 3-step method) with 3D-dedicated PET scanner, SET-3000GCT/M [1]. Region-of-interests with elliptical shape (16-mm x 48-mm) were defined on cerebral cortical region on a slice at the centrum semiovale level. Values of CBF, CBV, $CMRO_2$, and OEF obtained from both hemispheres of the volunteers and non-affected hemisphere of the patients were pooled and examined by multiple linear regression analysis. Independent variables included Hb concentration (g/dL), age (yr), sex (male or female), and subject type (healthy or stroke). The optimal models were determined by backward selection method based on Akaike information criterion.

Results: Average values (mean ± standard deviation) for Hb concentration, CBF, CBV, $CMRO_2$, and OEF were 12.9 ± 1.6 (g/dL), 40 ± 6 (mL/100 mL/min), 3.2 ± 0.5 (mL/100 mL), 3.1 ± 0.5 (mL/100 mL/min), and 45 ± 6 (%), respectively. CBF and OEF were inversely related to Hb concentration (Fig 1). In contrast, the analyses for CBV and $CMRO_2$ showed no statistically-significant relation to Hb. The optimal model for CBF was described as CBF = 73.3 - (0.191 x Age) - (1.65 x Hb). In the OEF analysis, adding CBF term as an independent variable improved goodness of fit described as OEF (%) = 80.5 - (1.75 x Hb) - (0.317 x CBF). $CMRO_2$ calculated from the optimal models for CBF and OEF (=arterial oxygen content x CBF x OEF) were relatively insensitive to changes in Hb concentration (Fig 1).

Conclusion: In contrast to the inverse relations of CBF and OEF to Hb concentration, $CMRO_2$ tends to keep constant value over the normal range in Hb concentration. The present result may support an existence of CBF control mechanism that keeps oxygen consumption constant against the variation of Hb concentration.

References:

[1] Ibaraki M et al., Quantification of Cerebral Blood Flow and Oxygen Metabolism with 3-Dimensional PET and Oxygen-15: Validation by Comparison to 2-Dimensional PET. J Nucl Med. 2008;49:50-59.

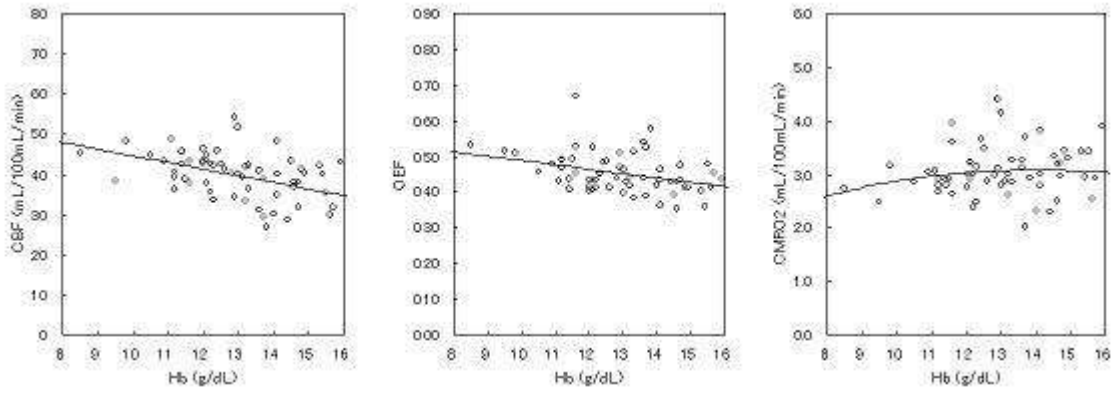

[Figure.1]

Figure 1: Relation between Hb and CBF, OEF, and $CMRO_2$. Solid lines represent predictions by the optimal models for Age = 64 yr (group average).

11

Brain Poster Session: Experimental Cerebral Ischemia: Blood Flow & Metabolism

COLLOID BASED RESUSCITATION FROM ASPHYXIAL CARDIAC ARREST: ASSESSMENT OF CEREBRAL BLOOD FLOW AND FUNCTIONAL OUTCOME

M.D. Manole[1], L.M. Foley[2], H. Bayir[3], T.K. Hitchens[2], C. Ho[2], H. Alexander[3], R.W. Hickey[1], C.D. Marco[3], P.M. Kochanek[3], R.S.B. Clark[3]

[1]Pediatrics, Children's Hospital of Pittsburgh, [2]Carnegie Mellon University, NMR Center for Biomedical Research, [3]Critical Care Medicine, University of Pittsburgh, Pittsburgh, PA, USA

Background: Pediatric cardiac arrest (CA) is caused by asphyxia in most cases and results in dismal neurological outcome. Reactive oxygen species play a role in cerebral blood flow (CBF) disturbances and neurological outcome after CA. We reported that CBF after asphyxial CA in 17 day old rats (PND 17) is characterized by early hyperemia at 5 min followed by resolution of normal CBF in all brain regions except cortex, where early hypoperfusion is seen.

Objectives: Determine the effects of albumin and colloid antioxidant polynitroxyl albumin (PNA) administered at resuscitation from asphyxial CA in PND 17 rats on CBF and neurological outcome.

Design/methods: Asphyxial CA was induced in PND 17 rats for 9 min. The rats were resuscitated with chest compressions, epinephrine and randomized to receive albumin, PNA or normal saline (NS), 20 cc/kg iv (n=10/group). Sham operated rats also received albumin, PNA or NS (n=12). CBF was measured serially at 5, 10, 15, 30, 60, 90, 120 and 150 min after resuscitation in five anatomic regions by arterial spin label MRI in 36 rats. Functional outcome was assessed on d 1-5: motor evaluation by beam balance and inclined plane test, and d 7-14: spatial memory acquisition assessed by Morris Water Maze (MWM). MWM consists of training period with a visible platform (d 7-9), testing with hidden platform (d 10-13) and probe trial (d 14). Data were analyzed using repeated measure ANOVA. Neuronal survival in hippocampus, brain weight, cortical thickness, and cortical surface area 5 weeks post CA were compared using ANOVA.

Results: PNA given at resuscitation prevented the early hyperemia seen at 5 min after NS ($p< 0.05$). In contrast, albumin treated rats had global intense and prolonged hyperemia: 200% increase from baseline in thalamus and sustained to 60 min after resuscitation. In the delayed period after resuscitation, CBF was comparable among treatment groups (figure).

PNA treated rats performed better in the MWM on d 10 vs. NS ($p< 0.05$). In the probe trial, rats treated with PNA or albumin performed better vs. NS treated or shams ($p< 0.05$). There appeared to be a greater benefit in males treated with PNA and albumin vs. females. Histological parameters tested were similar in the treatment groups. Hippocampal neuronal counts were 4000(±1330) in the CA groups vs. 7519(±1100) in shams, without difference among treatment groups.

Conclusion: A combination of colloid and antioxidant therapy produces changes of CBF and improves functional outcome after asphyxial CA in immature rats. Males demonstrate a greater response to PNA vs. females, suggesting that males would benefit more from antioxidants. Given that PNA and albumin cause divergent CBF changes in the early postresuscitation period, the improved functional outcome appears to be independent of early postresuscitation CBF.

Supported by NIH-K08HD058798-01.

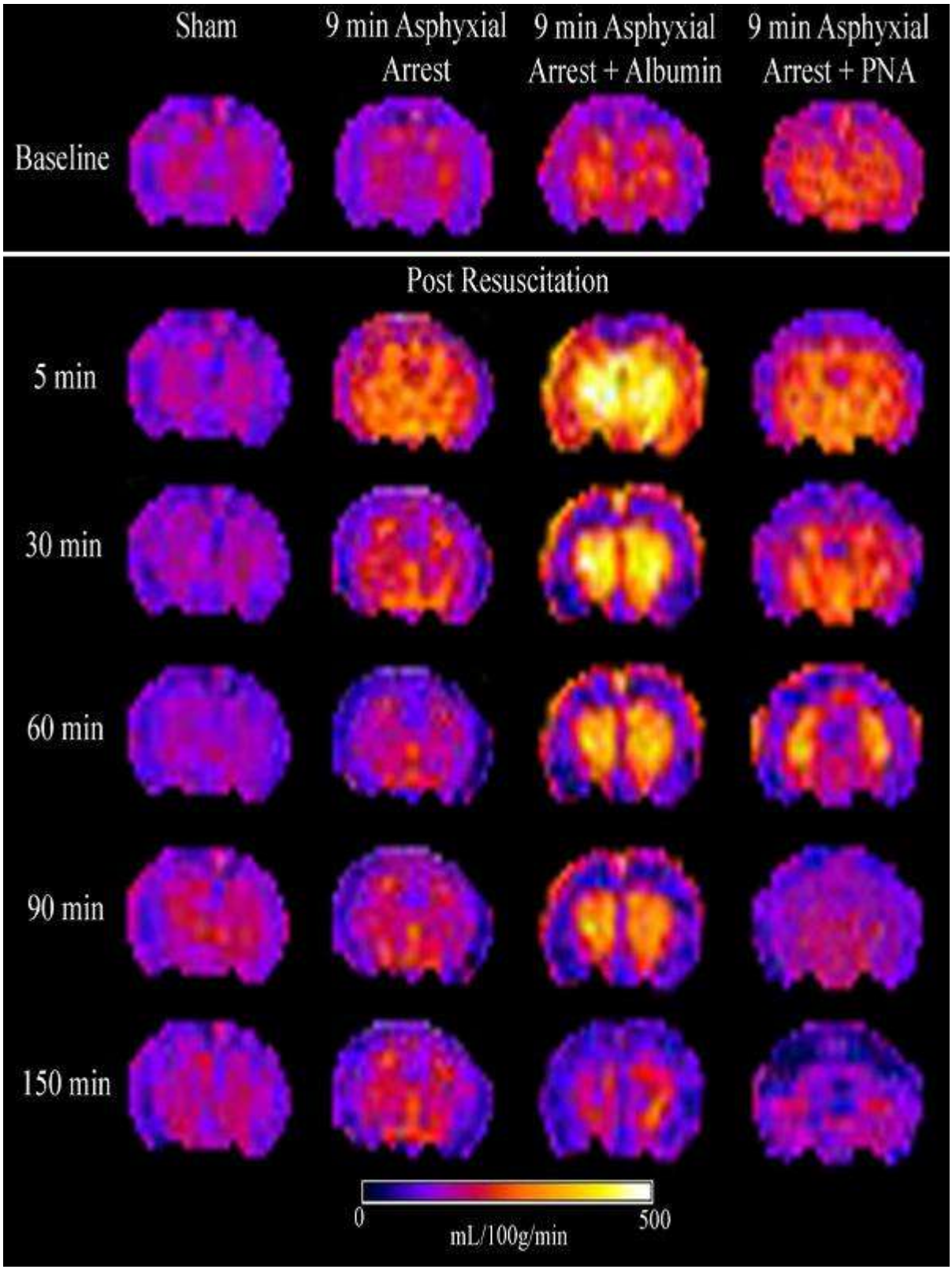

[CBF after CA resuscitated with NS, Albumin or PNA]

ANALYSIS OF THE DOPAMINE D3/D2 SYSTEM WITH [^{11}C]PHNO: SUBCORTICAL PARCELLATION OF ANATOMY AND SIGNAL

A. Tziortzi[1], G. Searle[1], S. Tzimopoulou[1], J. Beaver[1], E. Rabiner[1], R. Gunn[1,2]

[1]Clinical Imaging Centre, GlaxoSmithKline, Imperial College, London, [2]Dept of Engineering Science, University of Oxford, Oxford, UK

Objectives: [^{11}C]PHNO is a D3/D2 agonist radioligand with preferential affinity for D3 receptors. As the [^{11}C]PHNO pinding potential (BP_{ND}) is a mixture of D3 and D2 signal, assessment of the D3 component of [^{11}C]PHNO binding relies on regional differences in D3 and D2 receptor numbers [1]. A robust delineation of regions of interest (ROI) with a relatively homogenous proportion of D3:D2 receptors is therefore important for accurate quantification of the components of [^{11}C]PHNO binding. We report the development of robust criteria to define ROI for the analysis of human [^{11}C]PHNO scans. Both manual and automated definitions of these ROI are evaluated and the reproducibility and accuracy of these methods are assessed.

Methods: The striatum (ST) was subdivided into 6 subregions incorporating information from connectivity/autoradiography studies and the distribution of [^{11}C]PHNO. Putamen (PU) was subdivided into precommissural dorsal/ventral (preDPU, preVPU) and postcommisural (posPU). Caudate (CD) was divided into precommissural/ postcommisural (preCD, posCD), while accumbens and the medial-ventral parts of PU and CD were designated as ventral-striatum (VST). ST and globus-pallidus (GP) ROI were delineated on T1-MR images. Substantia-nigra (SN) was defined on PET integral images using a fixed-size ROI. [^{11}C]PHNO PET and T1-MR images from 12 subjects were analysed. Each subject's PET data was motion corrected and coregistered to their T1-MR image. ROI were defined using three different approaches: I. Manual definition of regions on two occasions (>one month apart), II. Manual definition of regions according to a previously published method developed for raclopride [2] to provide a benchmark for reproducibility, III. Automated definition using a nonlinear deformation of regions defined on the MNI_T1 template according to the criteria in Method I (except SN). Time activity curves (TAC) were derived and SRTM was applied with cerebellum as reference region to determine regional BP_{ND} estimates.

ROI volume overlap (DICE) and BP_{ND} variability (VAR_{BP}), were assessed for; i) intra-operator reproducibility for Methods I and II, ii) inter-method agreement for Methods I and III.

Results: The average inter-subject BP_{ND} values, obtained with Method I, in order of magnitude are, GP=3.0±0.4, VST=2.9±0.3, preVPU=2.7±0.2, preDPU=2.3±0.2, posPU=2.2±0.1 preCD=1.9±0.2 SN=1.6±0.3 and posCD=1.3±0.2.

Intra-operator agreement was high for volume overlap and BP_{ND} for both Methods I and II (DICE; Method I: preCD=91±1%, posCD=85±2%, preDPU=92±2%, preVPU=92±1%, posPU=91±2%, VST=89±2%, GP=85±3% and SN=80±13%, Method II: preCD=89±5%, posCD=82±5% prePU=89±2%, posPU=86±4% and VST=78±3%.

VAR_{BP}; Method I: preCD=0.9±1%, posCD=3.8±2.3%, preDPU=2.7±1.3%, preVPU=1.6±0.71%, posPU=1.7±1.6%, VST=1.4±1%, GP=3.1±2.0% and SN=5±4%, Method II: preCD=1.2±1%, posCD=4±4% prePU=1±1%, posPU=1±1% and VST=2±1%).

The agreement between Methods I and III was generally good. (DICE: preCD=75±4%, posCD=56±16%, preDPU=65±11%, preVPU=74±9%, posPU=58±13%, GP=76±6%, VST=67±10%, VAR_{BP}; preCD=6.4±4%, posCD=7.3±6.2%, preDPU=4.4±2.8%, preVPU=5.9±4.5%,

posPU=3.3±3.4%, VST=5.8±6%, GP=4.9±4.5%). Note that the lower DICE coefficients for the posCD and posPU are not reflected in those for the gross regions (DICE: CD=76±4%, PU=77±8%).

Conclusions: The criteria developed for the analysis of [^{11}C]PHNO scans provide robust and reproducible results for the manual delineation of ROI. The automated ROI, approach the performance of the manual at the level of CD, PU and VST.

References:

1. Rabiner et al. Synapse (In Press).

2. Martinez et al. JCBFM,**23:**285-300, 2003.

15

Brain Poster Session: Spreading Depression

HIPPOCAMPAL SPREADING DEPRESSION IS ASSOCIATED WITH A SEVERE BLOOD FLOW - GLUCOSE USE MISMATCH BUT NOT WITH CA1 NEURON INJURY

G. Mies

Max Planck Institute for Neurological Research, Cologne, Germany

Objectives: Prolonged cortical spreading depression (CSD) has not been associated with neuronal injury (Nedergaard, 1987) because of a close coupling between cerebral blood flow (CBF) and cerebral metabolic rate of glucose (CMRG). The hippocampal formation, however, is known for its selective vulnerability of CA1 neurons even after a brief episode of transient cerebral ischemia. It, therefore, was of interest to examine the hippocampal CBF/CMRG coupling and the histological outcome after repetitive hippocampal spreading depression (HSD).

Methods: Male BD IX rats (n=21) were used for this investigation under pentobarbital anesthesia and mechanical ventilation. HSD was induced by micropipette injections of 4 Mol KCl into the CA1 layer of the hippocampus. Hippocampal EEG activity and DC waves were recorded from a neighbouring glass microelectrode attached to a calomel electrode. In 5 rats, double tracer autoradiography was applied during repetitive HSD using ^{14}C-deoxyglucose (DG) for local CMRG starting at 15 min after HSD onset and ^{131}I-iodoantipyrine (IAP) at 44 min for CBF. In other animals, CBF was examined at 15 min and CMRG after 45 min of continuous HSD. The histological outcome was examined in a separate group following 45 min of several HSD waves after 7 days of survival.

Results: The most striking finding of this investigation was the absence of CA1 neuron loss at one week after 45 min of repetitive HSD despite a pronounced mismatch of the early hippocampal CBF/CMRG coupling. After several evoked HSD-waves at 45 min, CMRG had increased by 66% (41 ± 8 vs. 68 ± 16 µmol/100g/min; $p < 0.05$) whereas CBF declined by 38% (78 ± 14 vs. 56 ± 8 ml/100g/min; $p < 0.05$) (see Figure), accounting for a severe mismatch of the flow / metabolism relationship (0.9 ± 0.3 vs. 1.9 ± 0.3 ml/µmol; $p < 0.05$). CMRG and CBF measured at 15 min or 45 min following HSDs were comparable. At day 7 after 60 min of repeated HSDs, however, no significant difference in the number of hippocampal CA1 neurons was observed.

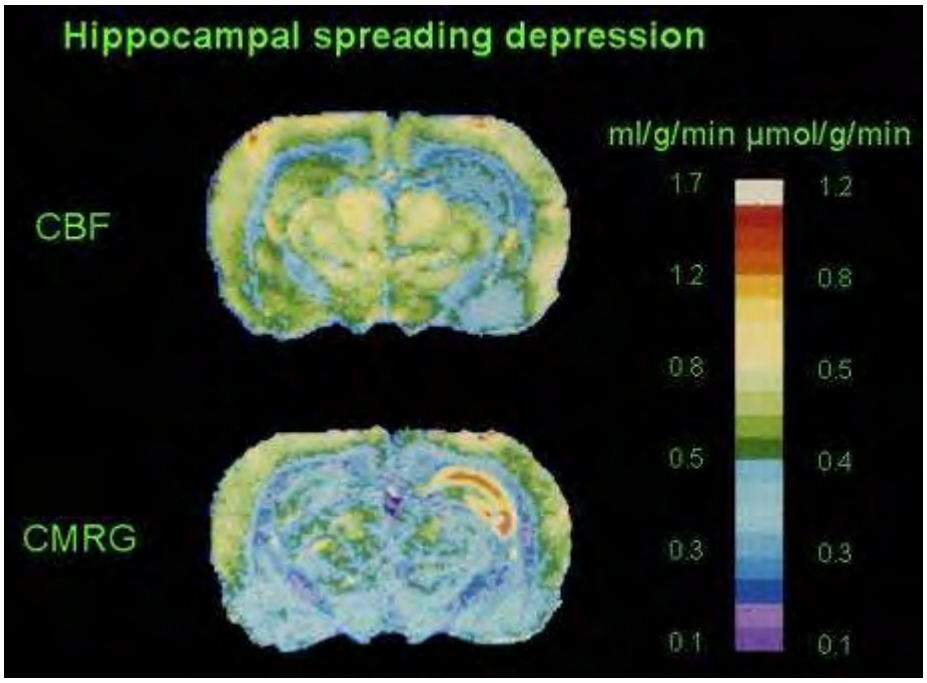

[Mies-BR09-fin.jpg]

Conclusions: In this study, it has been shown for the first time that a severe mismatch in CBF/CMRG alone does not cause neuronal injury, even in most selectively ischemic vulnerable CA1 neurons. These findings suggests that not the transient decrease in CBF and/or the rise in CMRG trigger neuronal injury per se but a critical level of hypoxia and its duration seems to determine neuronal survival. Further studies are in progress to elucidate the observed pathogenetic differences of hippocampal CA1 injury in transient ischemia and HSD.

References: Nedergaard M (1987) Acta Neuropathol 73(3):267-274.

16

BrainPET Poster Session: Molecular Brain Imaging: Clinical Applications

POSITRON EMISSION TOMOGRAPHY IMAGING IN REFRACTORY GILLES DE LA TOURETTE SYNDROME AND FOR STEREOTACTIC BILATERAL CAPSULOTOMY

L. Kangyong[1], S. Liwei[1], G. Yihui[2]

[1]Neurology, 5th Hospital of Fudan University, [2]PET Center of Huashan Hospital, Fudan University, Shanghai, China

Objective: To explore glucose metabolism changes of refractory Gilles de la Tourette syndrome (GTS) in PET scan and observe the effect of stereotactic bilateral capsulotomy for refractory GTS patients.

Methods: We examined the localized orbitofrontal and subcortical metabolic changes in FDG-PET by employing the region of interest (ROI) method in pre-operation and 6 months after operation. 7 cases refractory GTS underwent MRI guided stereotactic bilateral capsulotomy. The post-operation outcome of brain metabolic and clinical scales including tic severity, cognitive performance, and psychiatric status are under investigation by contrast to pre-operation so as to detect and evaluate the effects of capsulotomy for refractory GTS.

Results: There was a remarkable difference between the patients and control team in regional glucose metabolic changes ($P < 0.01$). Moreover stereotactic capsulotomy induces localized orbitofrontal and subcortical metabolic changes and improves clinical symptoms in refractory GTS. No any serous side effects happened except transient urpclepsia and weight loss in our study.

Conclusion: The metabolic abnormalities of FDG are universal and remarkable in PET to refractory GTS, especially in frontal Lobe, orbitofrontal lobe, cingulated cortices, and caudate. FDG-PET changes demonstrated that capsulotomy do decrease remarkably regional hypermetabolism, which might be related to mechanism of surgical treatment of refractory GTS. MRI guided stereotactic capsulotomy is a precise, safe, very effective therapy in some ways for refractory GTS.

17

Brain Poster Session: Stem Cells & Gene Therapy

THE STEM CELL MARKER PROMININ-1/CD133 ON MEMBRANE PARTICLES IN HUMAN CEREBROSPINAL FLUID OFFERS NOVEL APPROACHES FOR STUDYING CNS DISEASE

H. Huttner[1], M. Köhrmann[1], J. Jászai[2], C. Nimsky[3], E. Jüttler[4], S. Schwab[1], M. Wilsch-Bräuninger[5], A.-M. Marzesco[5], D. Corbeil[2]

[1]Neurology, University of Erlangen, Erlangen, [2]Tissue Engineering Laboratories (Biotec), University of Dresden, Dresden, [3]Neurosurgery, University of Erlangen, Erlangen, [4]Neurology, University of Heidelberg, Heidelberg, [5]Max-Planck-Institute of Molecular Cell Biology and Genetics, Dresden, Germany

Objective: Cerebrospinal fluid (CSF) is routinely used for diagnosing and monitoring neurological diseases. The CSF proteins used so far for diagnostic purposes (except for those associated with whole cells) are soluble (1). Here we investigated whether CSF contains membrane particles carrying the somatic stem cell marker prominin-1/CD133.

Methods: CSF samples of 61 healthy adult subjects and 14 patients with different stages of glioblastoma were analyzed. Differential and equilibrium centrifugation as well as detergent solubility analyses were performed followed by quantitative immunoblotting for prominin-1/CD133 using the monoclonal antibody (mAb) 80B258 (2, 3). Caco-2 cells were used as positive control (4) and a standard curve (R^2 = 0.9892) served to determine the amount of membrane particle-associated prominin-1/CD133.

Results: Differential centrifugation of CSF followed by immunoblotting of the resulting fractions revealed the presence of prominin-1 in the 200,000 g (P4) pellet (2). All healthy individuals analyzed showed a narrow range of membrane particle-associated prominin-1/CD133 levels in the CSF (7.4 ± 3.8 ng of bound prominin-1 antibody). The membrane particles were similar in physical properties and microdomain organization to small membrane vesicles previously shown to be released from neural stem cells in the mouse embryo (5). Glioblastoma patients showed elevated levels of membrane particle-associated prominin-1/CD133 (see Figure), which decreased dramatically in the final stage of the disease (2).

Conclusions: Our observations represent the first demonstration that a somatic stem cell marker present in central nervous system (CNS) tissue is released into the CSF. This finding strongly suggests that CSF has a greater potential for diagnosis and monitoring of neurological diseases than previously assumed. To analyze the amount of membrane particle-associated prominin-1/CD133 in CSF reflects a novel approach and may open up new avenues for studying CNS disease (2, 6).

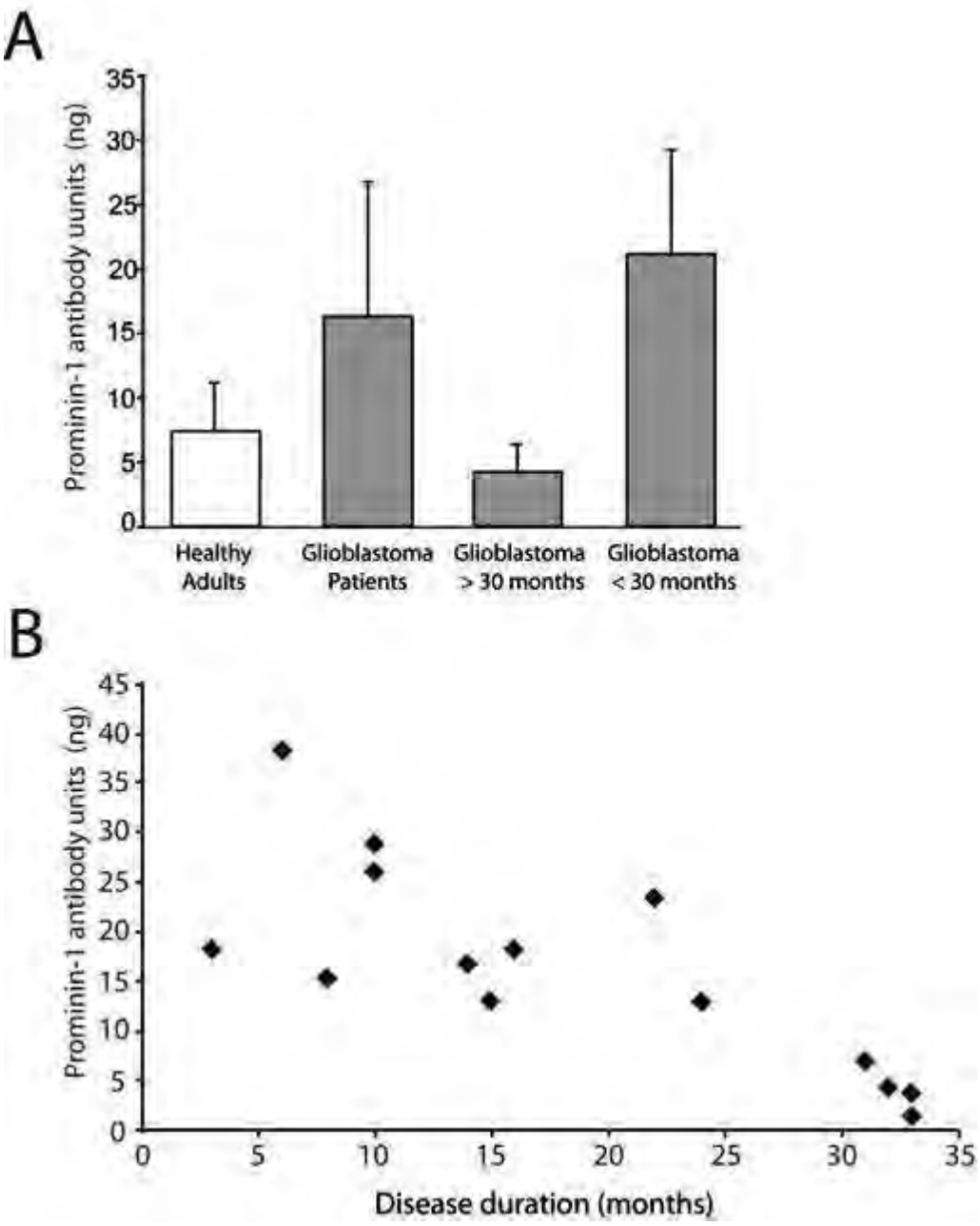

[Figure]

References:

1. Huhmer AF, et al. Protein analysis in human cerebrospinal fluid: Physiological aspects, current progress and future challenges. Dis Markers. 2006;22:3-26.

2. Huttner HB, et al. The stem cell marker prominin-1/CD133 on membrane particles in human cerebrospinal fluid offers novel approaches for studying central nervous system disease. Stem Cells. 2008 Mar;26(3):698-705.

3. Florek M, et al. Prominin-1/CD133, a neural and hematopoietic stem cell marker, is expressed in adult human differentiated cells and certain types of kidney cancer. Cell Tissue Res. 2005;319:15-26.

4. Corbeil D, et al. The human AC133 hematopoietic stem cell antigen is also expressed in epithelial cells and targeted to plasma membrane protrusions. J Biol Chem. 2000;275:5512-5520.

5. Marzesco AM, et al. Release of extracellular membrane particles carrying the stem cell marker prominin-1 (CD133) from neural progenitors and other epithelial cells. J Cell Sci. 2005;118:2849-2858.

6. Bao S, et al. Glioma stem cells promote radioresistance by preferential activation of the DNA damage response. Nature. 2006;444:756-760.

18

Brain Poster Session: Cell Signaling

INDUCTION OF LC3 AND GABARAP IN MOTOR NEURONS AFTER TRANSIENT SPINAL CORD ISCHEMIA IN RABBITS

H. Baba[1], M. Sakurai[2], K. Abe[3], R. Tominaga[1]

[1]Department of Cardiovascular Surgery, Kyushu University Gaduate School of Medicine, Fukuoka, [2]Department of Cardiovascular Surgery, National Hospital Organization Sendai Medical Center, Sendai, [3]Department of Neurology, Okayama University Graduate School of Medicine, Okayama, Japan

Background and aims: Spinal cord injury is considered to be related to a vulnerability of spinal motor neurons to ischemia. However, the mechanisms underlying this vulnerability are not fully understood.

Methods: We used a rabbit spinal cord ischemia model with use of a balloon catheter. The spinal cord was removed at 8 hours, 1, 2, or 7 days after 15 min of transient ischemia, and histological changes were examined with hematoxylin-eosin staining. Western blot analysis for LC3 and GABARAP, temporal profiles of LC3 and GABARAP immunoreactivity, and double-label fluorescence immunocytochemical studies were performed.

Purpose: We previously reported that spinal motor neurons might be lost by programmed cell death, and investigated the role of autophagy at motor neuron as a potential mechanism of neuronal death by immunohistochemical analysis for microtubule-associated protein light chain3 (LC3) and γ-aminobutyric-acid type-A-receptor-associated protein (GABARAP).

Results: In the ischemia group, the majority of motor neurons were preserved until 2 days after reperfusion, but were selectively lost at 7 days. Western blot analysis demonstrated slight immunoreactivity for LC3 and GABARAP in the sham-operated spinal cords. In contrast, in the ischemia group LC3 and GABARAP immunoreactivity became apparent at 8 hours after reperfusion. LC3 was strongly induced up to 2 days, but GABARAP was decreased at 2 days after reperfusion. At 8hours after reperfusion, co-labeling of LC3 and GABARAP was observed in the same motor neurons that eventually died.

Conclusion: This study demonstrated that immunoreactivities for both LC3 and GABARAP were induced in the same motor neurons which eventually die. These results suggest that autophagy was induced in motor neurons by transient spinal cord ischemia in rabbits.

References:

1. W M Moore J, Hollier LH. The influence of severity of spinal cord ischemia in the etiology of delayed-onset paraplegia. Annals of surgery. 1991;213(5):427-432.

2. Sakurai M, Aoki M, Abe K, Sadahiro M, Tabayashi K. Selective motor neuron death and heat shock protein induction after spinal cord ischemia in rabbits. The Journal of Thoracic and Cardiovascular Surgery. 1997;113(1):159-164.

3. Sakurai M, Nagata T, Abe K, Horinouchi T, Itoyama Y, Tabayashi K. Survival and death-promoting events after transient spinal cord ischemia in rabbits: Induction of Akt and caspase3 in motor neurons. Journal of Thoracic and Cardiovascular Surgery. 2003;125(2):370-377.

4. Yamauchi T, Sakurai M, Abe K, Matsumiya G, Sawa Y. Ubiquitin-Mediated Stress Response in the Spinal Cord After Transient Ischemia. Stroke. 2008;39(6):1883-1889.

20

Brain Poster Session: Glial Functions

ROLE OF ASTROGLIAL PENTOSE PHOSPHATE PATHWAY IN ROS PRODUCTION UNDER ACUTELY INCREASING GLUCOSE CONCENTRATIONS

Y. Izawa, S. Takahashi, N. Suzuki

Department of Neurology, Keio University School of Medicine, Tokyo, Japan

Objectives: Brain function is exclusively dependent on the oxidative metabolism of glucose. Reactive oxygen species (ROS) derived from mitochondria in the neural cells play an essential role in brain aging as well as in neurodegenerative disorders. Hyperglycemia is well known to enhance ROS production, resulting in oxidative stress in vascular endothelial cells (Brownlee, Diabetes 54: 1615-25, 2005). Although acute hyperglycemia does not alter the rates of glucose utilization in the brain as measured using the [^{14}C]deoxyglucose method (Orzi et al, J Cereb Blood Flow Metab 8: 346-56, 1988), whether the oxidative metabolism of glucose is affected remains to be elucidated (Blomqvist et al, Acta Physiol Scand 163: 403-15, 1998). Therefore, the effect of acutely increasing glucose concentrations on oxidative stress in different types of neural cells remains unclear.

We reported that chronic (2 weeks) exposure to a high glucose environment (22 mM) suppresses the oxidative metabolism of glucose in astroglia but not in neurons (Abe et al, J Cereb Blood Flow Metab 26: 153-60, 2006). Moreover, even short-term exposure (24 h) to high glucose elicits a similar suppression in astroglia. In the present study, we examined the effect of acutely increasing glucose concentrations on the rates of conversion of D-[^{14}C]glucose ([^{14}C]glc) to $^{14}CO_2$, production of ROS, and GSH formation in cultured rat neurons and astroglia.

Methods: Primary neurons and secondary astroglia were prepared from SD rats, as described previously. The rates of total glucose oxidation (y: pmol glucose/mg protein/60 min) based on the conversion from [U-^{14}C]glc to $^{14}CO_2$ over 60 min were measured at different concentrations of D-glucose (x: 2, 10, 20 mM) containing tracer doses of [U-^{14}C]glc (0.5, 2.5, and 5 mM, respectively).

The activity of the pentose phosphate pathway (PPP) was measured essentially as described by Hothersall et al. (Arch Biochem Biophys 198: 478-492, 1979) based on the determination of the difference in $^{14}CO_2$ production from [1-^{14}C]glucose (decarboxylated by the 6-phosphogluconate dehydrogenase-catalyzed reaction and by the Krebs cycle) and from [6-^{14}C]glucose (decarboxylated only by the Krebs cycle).

The production of ROS, mainly H_2O_2, in cells was assessed using H_2DCFDA and semi-quantitative fluorometric measurements (Ex/Em: 485/530 nm) and that of GSH in astroglia was assessed using monochlorobimane (Chatterjee et al, Glia 27: 152-161, 1999) (Ex/Em: 360/460 nm); the results were expressed as the percent-increase in the fluorescent signal over 60 min.

Results: Increasing glucose concentrations elicited linear increases in glucose oxidation both in neurons ($y_n = 0.26x + 9.81$; $R^2 = 0.996$) and astroglia ($y_a = 0.04x + 0.75$; $R^2 = 0.995$). ROS production in neurons also increased (100, 115, 145%), while ROS production decreased somewhat in astroglia (100, 70, 15%). Neither mixed cultures of neurons & astroglia nor neurons grown on an astroglial cell layer showed an increase in ROS production. Increasing glucose concentrations enhanced PPP activities in astroglia, resulting in elevated CO_2 production, GSH formation, and ROS reduction.

Conclusions: These results indicate that astroglial PPP exerts a protective role against oxidative stress under acutely elevated glucose environments, such as hyperglycemia in diabetic patients.

22

Brain Poster Session: Experimental Cerebral Ischemia: Vascular & Endothelial

EFFECTS OF LONG-TERM ADMINISTRATION OF HMG-COA REDUCTASE INHIBITOR, ATORVASTATIN, ON MICROVESSELS IN THE BRAIN OF STROKE-PRONE SPONTANEOUSLY HYPERTENSIVE RATS

K. Nomura[1], T. Katsumata[1], N. Tanaka[1], M. Ghazizadeh[2], E. Jin[2], M. Fujiwara[2], S. Egawa[2], H. Shimizu[2], Y. Nishiyama[1], T. Otori[1], O. Kawanami[2], Y. Katayama[1]

[1]Department of Neurology, Nippon Medical School, Tokyo, [2]Department of Molecular Pathology, Institute of Development and Aging Sciences, Nippon Medical School, Kawasaki, Japan

Objective: The objective of this study was to determine whether the long-term administration of an HMG-CoA reductase inhibitor, atorvastatin, confers antioxidative effect in microvessels in the brain of stroke-prone spontaneously hypertensive rats (SHRSPs).

Method: Atorvastatin (20 mg/kg) or vehicle was orally administered to 8-week-old SHRSPs for 5 weeks. As normal controls, vehicle was orally administered to 8-week-old WKYs over the same period. The animals were decapitated and the brains were removed. The brains were then quickly frozen, and were sliced into horizontal sections of 6-mm-thickness using a cryostat. The markers for oxidative stresses on lipids (4HNE) and DNA (8OHdG) were immunohistochemically detected. The numbers of positive vessels in the 6 randomized 0.25 mm^2 areas in a horizontal section were counted. The ratio of positive vessels for each maker to all vessels (positive for von Wille brand factor) was calculated.

Results: The positive ratio of oxidative stress markers was significantly higher in the vehicle group than in the normal controls. Then the positive ratio was significantly lower in the atorvastatin group than in the vehicle group. Atorvastatin significantly reduced immunoreactivities for oxidative stress markers in microvessels. Lipids such as total cholesterol (T-cho), HDL-cholesterol (HDL-cho), LDL-cholesterol (LDL-cho), and triglyceride (TG) did not differ among the vehicle, the statin, and normal control groups.

Conclusions: The results suggest that statins may confer the antioxidative properties and have the protective effects in the endothelial cells, even in the brain microvessels.

USE OF [^{11}C]-(+)-A-DIHYDROTETRABENAZINE (DTBZ) TO MONITOR DISEASE PROGRESSION IN A TRANSGENIC MOUSE MODEL OF PARKINSON'S DISEASE

I. Guenther[1], D. Rubins[1], K. Schlingmann[1], X. Meng[1], S.E. Brown[2], S. Sanabria[1], J.J. Cook[1]

[1]Imaging Department, [2]Parkinson's Disease Department, Merck & Co, West Point, PA, USA

Objectives: The aim of this study was to evaluate the use of the vesicular monoamine transporter 2 (VMAT2) ligand (+)-[11C]dihydrotetrabenazine (DTBZ) as a potential biomarker for the in vivo quantification of disease progression in the transgenic "MitoPark" (MP) mouse model of Parkinson Disease (PD). MP mice express a conditional knockout of mitochondrial transcription factor A (Tfam) targeted to dopaminergic neurons. This results in a parkinsonism phenotype, with adult onset of slowly progressing impairment in motor function accompanied by loss of dopaminergic neurons(1).

Methods: A series of PET studies was performed in 8 MP mice and 8 age-matched littermate wild type (WT) controls (age 6 to 23 weeks). Animals were anesthetized with isofluorane (1-2%) and were administered ~0.2 mCi [^{11}C]DTBZ via tail vein. Dynamic PET images were acquired for 30 min in a microPET Focus 220. PET images were reconstructed using a 3-D maximum a-posteriori reconstruction (MAP) algorithm. Reconstructed images were aligned with a standard mouse brain regional template and time-activity curves were obtained in the striatum and cerebellum. From the resulting image data, [^{11}C]DTBZ binding potential (BP) in striatum was calculated using the Logan Plot with cerebellum as reference region.

Results: MitoPark mice show progressive bradykinesia, akinesia, and tremor phenotypes reminiscent of PD, before dying prematurely at 26-33 weeks of age(2). A full characterization of this strain is currently underway by the Merck PD team. Figure 1 summarizes measured BP of all [^{11}C]DTBZ scans (21 scans on WT and 20 scans on PD mice with 1-5 scans per animal). MP mice exhibit a significant reduction in [^{11}C]DTBZ BP compared to WT mice at 13 weeks of age. BP in WT slightly increased with age, while longitudinal imaging of MP mice showed a progressive reduction of BP with increased age. These results demonstrate that the degeneration of the striatal dopaminergic neurons in this transgenic animal model of PD can be followed in vivo by imaging the progressive loss of VMAT2 using the PET tracer [^{11}C]DTBZ. This is consistent with findings previously reported for other animal models of PD such as the 6-OHDA lesioned rat and the MPTP lesioned monkey(3,4) and in PD patients(5).

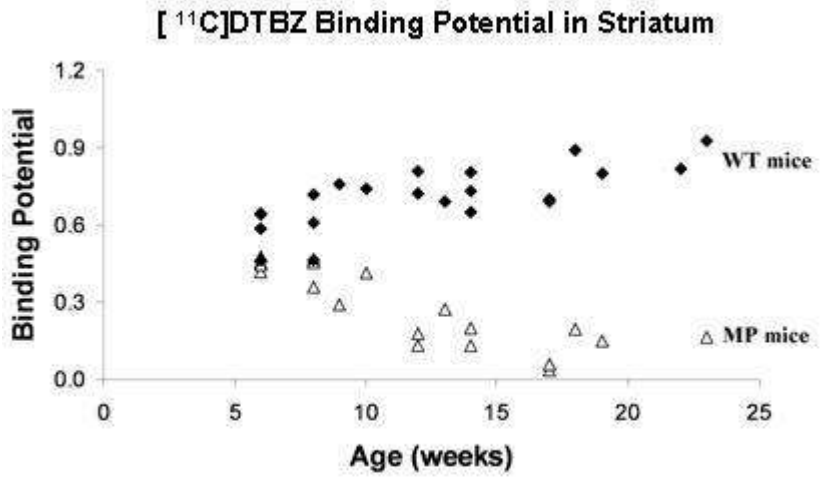

[Figure 1]

Conclusions: In vivo imaging using the PET tracer [^{11}C]DTBZ shows a progressive loss of striatal VMAT2 in the MitoPark mouse model of PD. This parallels the progressive degeneration of the striatal dopaminergic system in this model(1). Thus, VMAT2 imaging in this model may be useful for evaluating potential neuroprotective therapeutics for PD.

References:

(1) Ekstrand et al: PNAS, 104(4), 1325-30(2007).

(2) Renzi et al.: Soc. for Neurosciences, Abstracts 741.2(2008).

(3) Collantes et al: Rev Esp Med Nucl, 27(2), 103-11(2008).

(4) Doudet et al: NeuroImage, 30, 26-35(2006).

(5) Bohnen et al: J Cereb Blood Flow Metab, 26, 1198-1212(2006).

24

BrainPET Poster Session: Radiotracers and Quantification

QUANTIFICATION OF PERIPHERAL BENZODIAZEPINE RECEPTORS IN HUMAN BRAIN WITH ^{18}F-PBR06

Y. Fujimura, S. Zoghbi, F. Simeon, A. Taku, P. Victor, R. Innis, M. Fujita

Molecular Imaging Branch, National Institute of Mental Health, Bethesda, MD, USA

Objectives: The peripheral benzodiazepine receptor (PBR) is upregulated on activated microglia and macrophages and is, thus, a biomarker of inflammation. We previously reported that a ^{11}C-labeled aryloxyanilide ($T_{1/2}$ = 20 min) was able to quantify PBRs in healthy human brain. Since many PET centers would benefit from a longer-lived ^{18}F-labeled radioligand ($T_{1/2}$ = 110 min), the objective of this study was to evaluate the ability of a closely related aryloxyanilide (^{18}F-N-fluoroacetyl-N-(2,5-dimethoxybenzyl)-2-phenoxyaniline; ^{18}F-PBR06) to quantify PBRs in healthy human brain.

Methods: Nine human subjects were injected with about 185 MBq of ^{18}F-PBR06 and scanned over five hours, with rest periods outside the camera. The concentrations of ^{18}F-PBR06, separated from radiometabolites, were measured in arterial plasma.

Results: Modeling of regional brain and plasma data showed that a two-tissue compartment model was superior to a one-tissue compartment model, consistent with measurable amounts of both receptor-specific and nonspecific binding. Concentrations of brain activity measured with PET were consistently greater than the modeled values at late (280 to 300 min) but not at early time points, which may have been caused by the slow accumulation of radiometabolite(s) in brain. To determine an adequate time for more accurate measurement of distribution volume (V_T), which is the summation of receptor binding and nondisplaceable activity, we investigated which scan duration would be associated with maximal or near maximal identifiability. We found that a scan duration of 120 min provided the best identifiability of V_T: approximately two percent. The images showed no significant defluorination.

Conclusion: ^{18}F-PBR06 can quantify PBRs in healthy human brain using 120 min of image acquisition and concurrent measurements of radioligand in plasma. Although brain activity is likely contaminated with radiometabolites, the percentage contamination is thought to be small (< 10%), since values of distribution volume are stable during 60 to 120 min and vary by less than 10%. ^{18}F-FBR is a longer-lived and promising alternative to ^{11}C-labeled radioligands to measure PBRs as a biomarker of inflammation in the body.

Reference:

[1] J Med Chem. 2009; DOI 10.1021/jm8011855.

[2] Synapse. 2007;61:595-605.

Disclosure: This research was supported by the Intramural Program of NIMH (project # Z01-MH-002852-04). Y.F. was supported by the JSPS Research Fellowship in Biomedical and Behavioral Research at NIH.

Figure: Time-activity data and curve fitting for temporal cortex. The two-compartment model provided significantly better fitting than the one-compartment model in all regions for all subjects.

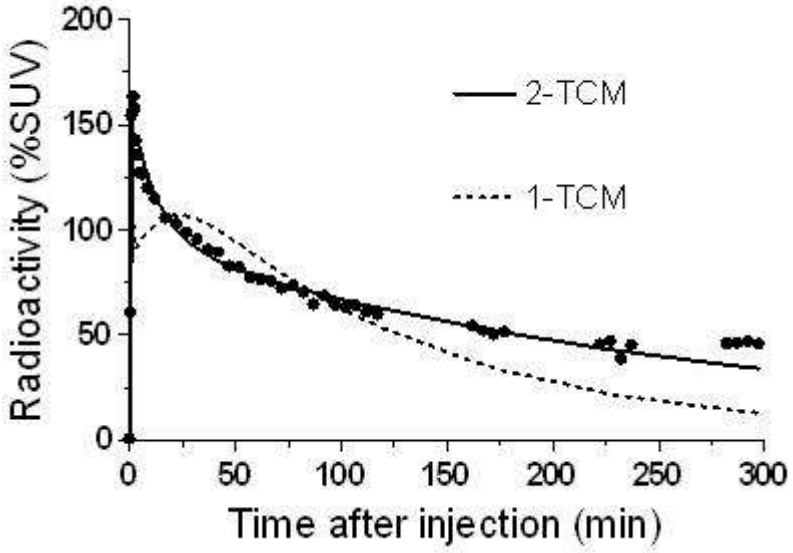

[Time-activity data and curve fitting]

25

Brain Poster Session: Subarachnoid Hemorrhage

THE EFFECT OF ENERGY METABOLISM AND INTRACELLULAR FREE MAGNESIUM OF BRAIN AFTER GOOD GRADE SUBARACHNOID HAEMORRHAGE

G. Wong, D. Yeung, A. Ahuja, A. King, M. Chan, C. Lam, W. Poon

The Chinese University of Hong Kong, Hong Kong, Hong Kong S.A.R.

Objective: Disturbance in energy status happens in many disease entities and had not been previously investigated in patients with subarachnoid hemorrhage. Pilot studies had indicated that hypermagnesemic treatment may improve outcome in patients with aneurysmal subarachnoid hemorrhage but the exact mechanism is not known.

Methods: We designed the current studies to investigate the energy metabolism and intracellular free magnesium using ^{31}P MRS Brain, in good grade aneurysmal subarachnoid hemorrhage patients with and without hypermagnesemic treatment.

Results: A total of 35 eligible patients and 23 healthy volunteers were recruited into the study. A total of 102 MRS studies were performed. Hypermagnesemic treatment after aneurysmal subarachnoid hemorrhage produced a small (15.6%) but significant elevation of intracellular free magnesium during the first week. Aneurysmal subarachnoid hemorrhage produced a depressed cerebral metabolism with higher ATP/Pi and a depressed membrane metabolism with higher PDE/total phosphates, which recovered with time and lasted beyond the initial two weeks.

Interpretation: The finding of elevated brain free intracellular magnesium with intravenous magnesium sulfate infusion is novel. It provides a possible mechanism for intravenous magnesium sulfate infusion to improve outcome in patients with aneurysmal subarachnoid hemorrhage. The finding of depressed cerebral and membrane metabolism provides insight into the metabolic effects of aneurysmal subarachnoid hemorrhage and future pathophysiological studies.

Brain Poster Session: Traumatic Brain Injury

HYPERCAPNEA DOES NOT CONSISTENTLY INCREASE THE OXIDATION OF CYTOCHROME C OXIDASE IN TRAUMATIC BRAIN INJURY

I. Tachtsidis[1], C. Pritchard[2], M.M. Tisdall[2], T.S. Leung[1], C.E. Elwell[1], M. Smith[2]

[1]Medical Physics and Bioengineering, University College London, [2]Department of Neuroanaesthesia and Neurocritical Care, The National Hospital for Neurology and Neurosurgery, London, UK

Background and aim: Using broadband near-infrared spectroscopy (BBS), we have previously demonstrated an increase in aerobic metabolism in the human healthy brain following hypercapnea and hyperoxia[1]. We also observed oxidation in cerebral cellular and mitochondrial redox states, using cerebral microdialysis (MD) and BBS respectively, following hyperoxia in patients with traumatic brain injury (TBI)[2]. In this study we investigate the effect of hypercapnea on regional metabolism in the injured brain using BBS and MD.

Methods: Following ethics approval and assent from nominated representatives, 6 sedated patients with severe TBI were studied 3-5 days after injury. Cerebral blood flow velocity (Vmca) was measured using transcranial Doppler ultrasonography. Changes in cellular and mitochondrial redox state were measured from the changes in brain tissue lactate and pyruvate concentration using MD and the change in oxidized cytochrome c oxidase concentration ([oxCCO]) using BBS. [oxCCO] was measured in a region of interest adjacent to the site of the MD catheter. Intracranial pressure (ICP) was also monitored continuously. During a period of cardiovascular stability, the rate of mechanical ventilation was reduced in a stepwise manner to produce an increase in $PaCO_2$ of approximately 1.5kPa. Changes in the continuously measured variables ([oxCCO], ICP and Vmca) during hypercapnea were compared with baseline values using a Student's paired t-test (significance at $p < 0.05$).

Results: In all patients hypercapnea caused a significant increase in Vmca and ICP. Analysis of the BBS data demonstrated two patterns of [oxCCO] change in response to hypercapnea, Group A showing a significant increase in [oxCCO] and Group B a significant decrease ($p< 0.05$).

	GROUP A (n=4) Baseline	GROUP A (n=4) Hypercapnea	GROUP B (n=2) Baseline	GROUP B (n=2) Hypercapnea
PaCO2 (kPa)	4.6(0.2)	6.1(0.7)	3.9(1.1)	6.0(0.0)
ΔVmca (%)	-	22(11.3)*	-	31(34.3)*
ICP (mmHg)	14.5(4.0)	23.4(7.9)*	7.5(5.5)	14.3(0.9)*
LPR	23(10.1)	23(10.1)	20(5.5)	20(7.3)
Lactate (mM)	4.9(2.7)	4.6(2.6)	3.4(1.6)	2.7(1.0)

Pyruvate (µM)	209(27.3)	193(41.2)	166(32.5)	137(0.7)
Δ[oxCCO] (µM)	-	0.342(0.336)*	-	-0.397(0.412)*

[Summary of results (LPR = lactate;pyruvate ratio).]

*p< 0.05 for within group changes from baseline for continuously measured variables.

Conclusions: In our previous study in TBI, hyperoxia resulted in an increase in [oxCCO] in all patients, consistent with an increase in aerobic metabolism secondary to the induced increase in cerebral oxygen delivery[2]. Hypercapnea can also increase cerebral oxygen delivery via an increase in cerebral blood flow. In this study Vmca increased in all patients during hypercapnea. However despite the likely increase in cerebral oxygen delivery, we did not see an increase in the oxidation status of [oxCCO] in every patient. Interestingly, changes in MD measured metabolic variables were similar in all patients. Further work is required to determine why the continuous optically measured metabolic variable was able to identify two distinct patterns of change in [oxCCO] in response to hypercapnea whereas the non continuous MD variables were not.

References:

[1] Tachtsidis I., et al., Advances in Experimental Medicine and Biology, 645:315-320 (2009).

[2] Tisdall M.M., et al., Journal of Neurosurgery, 109:424-432 (2008).

28

Brain PET Oral 3: Miscellaneous Targets

THE EFFECT OF CAMP DEPENDENT PROTEIN KINASE ACTIVATOR AND INHIBITOR ON [^{11}C]ROLIPRAM BINDING TO PHOSPHODIESTERASE 4 IN CONSCIOUS RATS

T. Itoh[1,2], K. Abe[2,3], O. Inoue[3], J. Hong[1], V.W. Pike[1], R.B. Innis[1], **M. Fujita**[1]

[1]National Institute of Mental Health, Bethesda, MD, USA, [2]Shionogi & Co., Ltd., [3]Osaka University Graduate School of Medicine, Osaka, Japan

Background and aims: Phosphodiesterase-4 (PDE4), a major phosphodiesterase isozyme hydrolyzing the second messenger cAMP, may play a pivotal role in brain diseases and the effects of centrally acting drug. Rolipram is a selective inhibitor of PDE4 and the binding study using [^{11}C]rolipram with PET should allow the function of the cAMP second messenger cascade to be explored. cAMP Dependent protein kinase (PKA) has been reported to phosphorylate PDE4 and affect the enzyme activity. We recently found that both in vivo B_{max} and K_D values of [^{11}C](<i>R</i>)-rolipram were significantly greater in conscious rats than in anesthetized rats. In the present PET study, we examined effects of PKA modulators on the binding of [^{11}C](<i>R</i>)-rolipram and [^{11}C](S)-rolipram (affinity of (S) is 1/20 of that of (R)) using conscious rats.

Methods: For PET scans using conscious rats (n = 26), an acrylic plate was permanently attached to the skull. The animals were trained to acclimate to the scanning holder for at least ten days before the PET experiment. On the day of PET scan, 10 nmol of db-cAMP (cAMP analogue and PKA activator) or 100 nmol of Rp-cAMPS (PKA inhibitor) was injected into the left striatum using 30-gauge needle three times before the scan. At the same time, saline was administered into the right striatum. The animals were given an intravenous bolus injection of [^{11}C](<i>R</i>)-rolipram (61.1±18.3 MBq) or [^{11}C](<i>S</i>)-rolipram (46.3±9.0 MBq) and were imaged for 100 min. The binding activity of [^{11}C](<i>R)- and (<i>S</i>)-rolipram in striatum was measured and expressed as percent standardized uptake value (%SUV), which is normalized to injected activity and body weight. The time-activity curves were drawn and their area under the curves (AUC) were compared between left and right-side striatum for each of [^{11}C](R)- and (S)-rolipram.

Results: When using [^{11}C](R)-rolipram, db-cAMP significantly increased the AUC in left striatum ($p < 0.002$). In contrast, a significant decrease of AUC was found by pretreatment of Rp-cAMPS ($p < 0.002$). On the other hand, these effects of neither of these PKA modulators were not observed in [^{11}C](S)-rolipram PET experiments.

Table. Effects of db-cAMP and Rp-cAMPS on [11C]-rolipram binding in conscious rats

	$AUC_{0\text{-}100\ min}$ (%SUV*min)			
	[^{11}C](<i>R</i>)-rolipram		[^{11}C](S)-rolipram	
	Left striatum	Right striatum[1)]	Left striatum	Right striatum[1)]
db-cAMP	17518 ± 4233	15804 ± 3784	3636 ± 1350	3561 ± 1395

Rp-cAMPS	14508 ± 2346	16311 ± 3002	3633 ± 517	3658 ± 592
[1)]Control saline was administered into the right striatum.				

[Effects of db-cAMP and Rp-cAMPS on [11C]rolipram]

Conclusions: Significant increase and decrease of [^{11}C](<i>R</i>)-rolipram binding were observed by PKA activator and inhibitor, respectively. These effects were not caused by changes in brain regional blood flow, since there were no effects when [^{11}C](<i>S</i>)-rolipram was used. These results support the value of measuring [^{11}C]rolipram binding in brain for assessing responses to physiological or pharmacological challenges to the cAMP second messenger system.

QUANTITATIVE ANALYSIS OF PERIPHERAL BENZODIAZEPINE RECEPTOR IN HUMAN BRAIN USING PET WITH [^{11}C]AC-5216

M. Miyoshi[1,2], H. Ito[1], R. Arakawa[1], H. Takahashi[1], H. Takano[1], M. Okumura[1], T. Otsuka[1], F. Kodaka[1], M. Sekine[1], T. Sasaki[1], S. Fujie[1], C. Seki[1], R. Nakao[3], T. Fukumura[3], K. Suzuki[3], M. Matsumoto[2], T. Suhara[1]

[1]Molecular Neuroimaging Group, Molecular Imaging Center, National Institute of Radiological Sciences, Chiba, [2]Department of Clinical Neuroscience and Therapeutics, Hiroshima University School of Medicine, Hiroshima, [3]Molecular Prrobe Group, Molecular Imaging Center, National Institute of Radiological Sciences, Chiba, Japan

Objectives: Peripheral benzodiazepine receptor (PBR) is upregulated on activated glial cells and is therefore a useful biomarker of inflammation in the injured brain and neurodegenerative disorders, such as Alzheimer's disease [1, 2]. We developed a new PET radioligand, [^{11}C]AC-5216, that allows the imaging and quantification of PBRs in monkey and mouse brains [3]. [^{11}C]AC-5216 can be applied to clinical investigation of PBR expression and therefore also microglia activation in neurological diseases. The aim of this study was to evaluate a quantification method of [^{11}C]AC-5216 binding in human brain using PET measurements performed on healthy human subjects.

Methods: A 90-min dynamic PET scan was performed on each of twelve healthy men (age range 20 - 33 years; mean ± SD, 24.6 ± 4.5) after intravenous injection of [^{11}C]AC-5216. Regions-of-interest were drawn on several brain regions. Binding potential compared to non-displaceable uptake (BP_{ND}) was calculated by nonlinear least-squares fitting (NLS) method with the two-tissue compartment model, and total volume of distribution (V_T) was also estimated by NLS and graphical analysis (GA) method. For these analyses, PMOD ver.2.8 was used.

Results: The distribution of radioactivity was widespread and fairly uniform in gray matter of the cerebral cortices and cerebellum, striatum, and thalamus. After intervenous injection of [^{11}C]AC-5216, radioactivity peaked at about 2-3 min, followed by slow washout. BP_{ND} was highest in the thalamus (4.6 ± 1.0) and lowest in the striatum (3.5 ± 0.7). V_T values calculated by NLS were 6.9 ± 1.8 and 4.9 ± 1.5 mL/mL for the thalamus and striatum, respectively. K_1/k_2 values (K_1: influx rate constant, k_2: efflux rate constant) ranged from 1.3 ± 0.4 to 1.6 ± 0.3 mL/mL. The inter-individual variation of BP_{ND} was larger than V_T, indicating that the inter-individual variation of V_T is mainly caused by the variation of K_1/k_2 rather than BP_{ND}. V_T obtained by NLS or GA showed similar regional distribution to BP_{ND}. However, there was no correlation between BP_{ND} and V_T (V_T by NLS, $r = 0.31$; V_T by GA, $r = 0.19$) because of relatively larger inter-individual variation of K_1/k_2.

Conclusion: The regional distribution of [^{11}C]AC-5216 was in good agreement with previous PET studies of PBRs in human brain, e.g., [^{11}C]PK11195[4] and [^{11}C]DAA1106[5]. BP_{ND} is more appropriate for estimating [^{11}C]AC-5216 binding than V_T due to the inter-individual variation of K_1/k_2. [^{11}C]AC-5216 is a promising PET ligand for quantifying PBR in human brain.

References:

[1] Maeda J, Ji B, Irie T, et al. J Neurosci. 2007; 27: 10957-10968.

[2] Yasuno F, Ota M, Kosaka J, et al. Biol Psychiatry. 2008; 64: 835-841.

[3] Zhang MR, Kumata K, Maeda J, et al. J Med Chem. 2007; 50: 848-855.

[4] Cagnin A, Brooks DJ, Kennedy AM, et al. Lancet. 2001; 358: 461-467.

[5] Ikoma Y, Yasuno F, Ito H, et al. J Cereb Blood Flow Metab. 2007; 27: 173-184.

[^{18}F]NS10743: A POTENTIAL RADIOTRACER FOR IMAGING OF ALPHA-7 NICOTINIC ACETYLCHOLINE RECEPTORS (α7-NACHRS)

P. Brust[1], W. Deuther-Conrad[1], S. Fischer[1], A. Hiller[1], P.-G. Hoffmeister[1], C. Donat[1], R. Bauer[2], E. Østergaard Nielsen[3], D. Brunicardi Timmermann[3], O. Sabri[4], J. Steinbach[1], D. Peters[3]

[1]Radiopharmacy, Institute of Interdisciplinary Isotope Research, Leipzig, [2]Institute of Molecular Cell Biology, Friedrich Schiller University, Jena, Germany, [3]NeuroSearch A/S, Ballerup, Denmark, [4]Nuclear Medicine, University of Leipzig, Leipzig, Germany

Objectives: The α7-nAChR properties are impaired in schizophrenia, brain trauma and neurodegenerative diseases. Furthermore, α7-nAChRs are overexpressed in numerous tumor cells and represent a potential target for therapy. The outstanding diversity of cellular properties mediated by neuronal and non-neuronal α7-nAChRs points to the diagnostic potential of quantitative molecular imaging of α7-nAChRs. We have developed [^{18}F]NS10743 (K_D = 7.7 nM), the first ^{18}F-labeled radioligand for PET imaging of α7-nAChRs, and assessed the radiotracer selectivity in mice and pigs.

Methods: [^{18}F]NS10743 was synthesised by nucleophilic substitution of the nitro precursor with specific activity > 150 GBq/µmol and radiochemical purity > 99%. Its biodistribution was determined in mice at 5 min, 20 min and 60 min p.i. To determine the specificity, separate animals were pre-treated with the α7 agonist SSR180711 (10 mg/kg). Ex vivo autoradiography was performed on mice brain at 60 min after injection of 250 MBq [^{18}F]NS10743. In vitro autoradiography was performed on porcine brain using [^{125}I]α-bungarotoxin as α7 ligand. Furthermore, anesthetized piglets were intravenously injected with 250-500 MBq of [^{18}F]NS10743. Selected animals additionally received 3 mg/kg SSR180711 at 10 min prior to radiotracer application followed by a continuous infusion (2 mg/kg/2h). Acquisition of dynamic PET scans (2 h) started with injection of [^{18}F]NS10743. About 50 plasma samples were obtained, and plasma metabolites were analyzed with HPLC. Regions of interest (brain and eye) were drawn on summed PET images and distribution volumes were estimated.

Results: The brain uptake of [^{18}F]NS10743 in mice was 4.8 ± 0.4 %ID/g at 5 min, 4.0 ± 0.4 %ID/g at 20 min, and 1.6 ± 0.3 %ID/g at 60 min p.i. High initial radioactivity uptake was also observed in adrenal glands (11.3 %ID/g), spleen (7.7 %ID/g), pancreas (6.0 %ID/g), and thymus (4.4 %ID/g). Organ distribution of mice pre-treated with SSR180711 shows a significant reduction of radioactivity uptake at 60 min p.i. in adrenals, brain, thymus, and pancreas, all organs which express α7-nAChRs. Ex vivo autoradiography revealed a pattern of [^{18}F]NS10743 binding in anatomically defined brain structures such as hippocampus and cortex which closely matches regions with high α7-nAChRs expression. Summed PET images obtained in piglets show a distribution pattern similar to in vitro autoradiographs of [^{125}I]α-bungarotoxin with high radiotracer binding in cortex, moderate binding in cerebellum and low binding in white matter. The brain uptake is comparable to that of the α4β2 nAChR-ligand 2-[^{18}F]F-A-85380. Application of SSR180711 resulted in more than two-fold increase of brain uptake. However, the distribution volume was decreased by about 20%, indicating inhibition of specific radiotracer binding. Furthermore, the flow-independent uptake of [^{18}F]NS10743 in eye, which is known to express α7-nAChRs, was reduced by about 30%. Metabolite studies revealed the presence of a single major metabolite in mice and piglets, which is probably the result of an enzymatic oxidation of the nitrogen at position 1 in the diaza-bicyclononane moiety of NS10743.

Conclusions: [^{18}F]NS10743 is a high affinity ligand for α7-nAChRs with good brain uptake, specific receptor binding in vivo and good metabolic stability, which makes it suitable for neuroimaging with PET.

ASIALOERYTHROPOIETIN ATTENUATES NEURONAL CELL DEATH IN HIPPOCAMPAL CA1 REGION AFTER TRANSIENT FOREBRAIN ISCHEMIA IN GERBIL MODEL

T. Yamashita, N. Nonoguchi, N. Ikeda, S. Kawabata, S. Miyatake, T. Kuroiwa

Neurosurgery, Osaka Medical College, Takatsuki, Japan

Objectives: In the central nervous system, recombinant human erythropoietin (rhEPO) attenuates ischemic injury in vitro and in vivo.

However, megadose of rhEPO is required to attain the protective effect, and that is afraid of accumulating thrombus and aggravating brain damage by up-regulating the red blood cell count and hyperactive platelet.

The nonerythropoietic asialoerythropoietin (asialoEPO),which is generated by total enzymatic desialylation of rhEPO, has extremely short plasma half life and has possibility of neuroprotective effect to the brain ischemia.

In this study, we showed that asialoEPO protects neurons against delayed neuronal death in the hippocampal pyramidal cells after transient forebrain ischemia.

Methods: 23 adult gerbils received 3 minutes bilateral common carotid artery occlusion.

The drug (asialoEPO 10U/g, rhEPO 10U/g) or vehicle was injected intraperitoneally three times, 3 hours before, just after, and 24 hour after the insult.

Animals were allowed to survive for 7 days.

Learning ability test and retention test were carried out at day 6 and 7 respectively.

Results: In the training session, the vehicle injected group was received 7.5±2.56 footshocks in the learning trial. rhEPO (5.5 ± 1.93 footshocks) and asialoEPO (4.86 ± 1.07 footshocks) treated group were less than vehicle group statistically.

The latency of the vehicle treated animals to enter the dark compartment (37 ±54.3 sec) was significantly shorter than rhEPO (230 ±72.5 sec) and asialoEPO (264 ±71.9 sec) treated group.

AsialoEPO didn't affect bone marrow and didn't increase hemoglobin level.

The viable cells in CA1 field were counted by Nissl staining, the rhEPO treated group (103.57±78.91 cells/mm) and asialoEPO treated group (144.99±92.26 cells/mm) were significantly suppressed the neuronal cell death than vehicle treated group (19.53±10.72 cells/mm).

TUNEL (terminal deoxynucleotidyltransferase-mediated 2'-deoxyuridine 5'-triphosphate-biotin nick end labeling) staining showed that rhEPO (33.40± 23.0 cells/mm) and asialoEPO (25.61±41.96 cells/mm) injection caused a significant reduction than vehicle treatment (76.67 ± 23.02 cells/mm) in the number of CA1 neurons 7 days after ischemia.

Conclusion: Multiple dosing of asialoEPO protects hippocampal CA1 neurons from ischemic damage by preventing from falling into apoptosis, and it does not affect erythropoiesis in the bone marrow.

References:

1. Xiaoyang Wang, Changlian Zhu, Xinhua Wang, Jens Gammeltoft Gerwien,

Andre Schrattenholz, Mats Sandberg, Marcel Leist and Klas Blomgren. The nonerythropoietic asialoerythropoietin protects against neonatal hypoxia-ischemia as potently as erythropoietin. Journal of Neurochemistry, 2004, 91, 900-910.

2. Serhat Erbayraktar, Giovanni Grasso, Alessandra Sfacteria, Qiao-wen Xie, Thomas Coleman, Mads Kreilgaard, Lars Torup, Thomas Sager, Zubeyde Erbayraktar, Necati Gokmen_, Osman Yilmaz_, Pietro Ghezzi, Pia Villa, Maddalena Fratelli, Simona Casagrande, Marcel Leist, Lone Helboe, Jens Gerwien, Søren Christensen, Marie Aavang Geist, Lars Østergaard Pedersen, Carla Cerami-Hand,Jean-Paul Wuerth, Anthony Cerami, and Michael Brines. Asialoerythropoietin is a nonerythropoietic cytokine with broad neuroprotective activity in vivo. PNAS, 2003, 100, 5741-5746.

3. Michael Brines and Anthony Cerami. Emerging biological roles for erythropoietin in the nervous system. Nature reviews, 2005, 6, 484-494.

35

Brain Poster Session: Experimental Cerebral Ischemia: Vascular & Endothelial

CONCOMITANT TREATMENT WITH MEDROXYPROGESTERONE AND CONJUGATED EQUINE ESTROGENS ATTENUATES ESTROGEN'S PROTECTIVE EFFECT ON POSTISCHEMIC PIAL ARTERY VASODILATION TO ACETYLCHOLINE

C. Miyazaki[1], E. Zeynalov[1], **M. LIttleton-Kearney**[2]

[1]Anesthesia/Critical Care Medicine, [2]Nursing/Anesthesia Critical Care Medicine, Johns Hopkins University, Baltimore, MD, USA

Background and aims: Chronic estrogen replacement partially preserves postischemic pial arteriole vasodilation to endothelium-dependent vasodilators. It is unclear if concomitantly administered equine estrogens (EE) and medroxyprogesterone (MP), hormone replacement therapy commonly prescribed for women, alters estrogen´s effect on postischemic pial arterial vasodilation. We determined if:

1. EE preserves postischemic pial artery dilation to acetylcholine (Ach),
2. concomitant administration of MP and EE alters the effect of EE alone on postichemic Ach-evoked dilation,
3. natural hormone depletion associated with aging depresses postischemic pial artery Ach-evoked dilation and
4. concomitantly administered EE and MP has the same effect on postischemic pial artery dilation in young ovariectomized (OVX)and aged reproducively senescent rats (RS).

Methods: Young OVX (2-3.5 months) or aged RS female rats (20-22 months) were used for these studies. The young groups included; OVX, EE-treated (EE) and EE plus MP (EEMP). The aged groups included; RS, EE-treated (RSEE) and EE plus MP (RSEEMP). The hormones were administered via gavage daily for 1-1.5 months. Drug dosages, based on normal dosages for women (EE-0.625 mg; MP-2.5 mg), were weight-adjusted for rat. Rats were subjected to 15 minutes forebrain ischemia. Pial artery responses to the endothelium-dependent vasodilator Ach (10μM) were examined through closed cranial windows before and 1 hour postischemia.

Purpose: To determine if concomitant EE and MP treatment alters estrogen's beneficial effect on postischemic pial arteriole vasodilatory capacity in response to Ach.

Results: Compared to the young, preischemic pial artery dilation was markedly reduced in the aged groups ($p=0.001$). Postischemic dilation to Ach was profoundly depressed in OVX and in the RS groups ($p=0.001$) compared to preischemia. EE preserved the postischemic pial artery response in the EE and the RSEE groups. EE combined with MP attenuated the effect of EE in the young and the aged rats ($p=0.001$). Because we found that aging alters pial artery vasodilatory capacity we evaluated the magnitude (delta) of the postischemic reduction in Ach-evoked vasodilation between the young and aged groups. The change between the pre and the postischemic response was similar between the

OVX and the RS rats. However, the magnitude of the reduction in postischemic response to Ach was greater in the EEMP (25.3 ± 4.7) compared to the REEMP (14.1 ± 3.0) animals (p=0.001).

Conclusions: Aging alters the ability of pial arterioles to dilate in response to Ach. Postischemic pial artery vasodilatory dysfunction in both young OVX and RS rats is attenuated by chronic EE administration, but not if MP is combined with EE. Concomitantly administered MP and CE may interfere with estrogen´s ability to protect the cerebrovasculature during early reperfusion.

	Preischemia	Postischemia
OVX (n=6)	24.7 ± 5.0	8.1 ± 1.2
EE (n=6)	24.4 ± 2.9	22.2 ± 3.4
EEMP (n=5)	26.6 ± 5.8	1.3 ± 2.0
RS (n=6)	14.4 ± 2.0	0.64 ± 1.2
RSEE (n=6)	14.4 ± 2.4	13.2 ± 1.2
RSEEMP (n=6	13.5 ± 0.8	-0.5 ± 3.1

[Pre and Postischemic Dilation]

Brain PET Oral 2: Novel Radiotracers and Modeling

MODELING OF BRAIN NK1 RECEPTOR BINDING-PLASMA CONCENTRATION RELATIONSHIP WITH A NOVEL NK1 ANTAGONIST

S. Zamuner[1], E.A. Rabiner[2], S.A. Fernandes[3], R.N. Gunn[2,4], R. Gomeni[1], V.J. Cunningham[2]

[1]Clinical Pharmacology Modelling & Simulation, GlaxoSmithKline, Verona, Italy, [2]GlaxoSmithKline Clinical Imaging Centre, Imperial College, London, UK, [3]Discovery Medicine, Neurosciences Centre for Excellence in Drug Discovery, GlaxoSmithKline, Verona, Italy, [4]Dept. of Engineering Science, University of Oxford, Oxford, UK

Objectives: There is growing evidence of the importance of integrating drug receptor-occupancy (RO) data acquired by Positron Emission Tomography (PET) with the plasma pharmacokinetics (PK) of the drug, in order to establish optimal dose selection in subsequent clinical trials. The object of the present work was to develop such a PK-RO model in human subjects for Casopitant, a selective NK1 antagonist currently in development for prevention of chemotherapy-induced and postoperative nausea and vomiting. The relationship between individual plasma concentrations of Casopitant and its binding to receptors was investigated using a population approach applied to RO data from PET occupancy studies carried out with the radioligand and selective NK1 receptor antagonist, [^{11}C]GR205171.

Methods: Eight adult healthy male volunteers entered and completed an [^{11}C]GR205171 brain PET study to estimate the PK-RO relationship following oral doses of Casopitant. All subjects underwent a baseline scan and subsequently received a single dose of 2.5, 5, 20, 50, or 120 mg Casopitant, 24 hrs before a second PET scan. Compartmental models (described elsewhere) were applied to the PET data to obtain regional estimates of binding potential (BP_{ND}). RO in the presence of Casopitant was estimated from changes in BP_{ND} relative to the baseline scans. In order to estimate inter-subject variability on the baseline measurements, a population approach analysis using untransformed data (BP_{ND}) was performed[1]. Moreover, all data were simultaneously fitted and potential differences in model parameters from different regions were considered including a within subject variability term. The population PK/PD analysis was performed using the non-linear mixed effect modelling approach as implemented in the NONMEM (version V) software.

Results: A population approach leading to a PK-RO model of the relationship between the plasma concentration of Casopitant and receptor binding parameters was successfully carried out. All data were fitted simultaneously and potential differences in model parameters from different regions were considered including a within subject variability term. The population estimate Casopitant plasma concentration leading to 50% of the maximal decrease of binding potential is approximately 0.6 ng/mL (median EC50 equal to 0.5 ng/mL in frontal and occipital cortex, 0.7 ng/mL in parietal and lateral temporal cortex, and 1 ng/mL in striatum). Casopitant plasma concentrations above 10 ng/mL produced RO above 90% and plasma concentrations above 20 ng/mL produced RO above 95%. Finally, considering that Casopitant has an accumulation ratio of approximately 2-3 folds at steady state, concentrations above 10 ng/mL at trough and RO above 90% in all brain regions can be achieved by doses of 5-10mg, while RO above 95% can be achieved by doses of 15-30mg.

Conclusions: A suitable integration of plasma and receptor occupancy data was successfully developed using a mixed effect approach. PK-RO model was also used to predict NK1 occupancy levels after Casopitant chronic treatment and for dose selection in subsequent clinical trials.

References: [1] S. Zamuner, R. Gomeni, A. Bye. Nucl. Med. Biol. 29 (2002) 115- 123.

IDENTIFICATION OF HUMAN "NON-BINDERS" AND MEASUREMENT OF SPECIFIC BINDING WITH [^{11}C](R)-PK 11195: IMPLICATIONS FOR PET IMAGING OF BRAIN INFLAMMATION

W.C. Kreisl, Y. Fujimura, N. Kimura, J.S. Hong, C.L. Morse, S.S. Zoghbi, R.L. Gladding, V.W. Pike, M. Fujita, R.B. Innis

Molecular Imaging Branch, National Institute of Mental Health, Bethesda, MD, USA

Objective: Ten percent of subjects scanned with [^{11}C]PBR28 show unusual behavior in that the radioligand is unable to bind to the 18 kDa translocator protein (TSPO, formerly known as the peripheral benzodiazepine receptor) in brain and in peripheral organs [1]. "Non-binders" have not previously been reported using the older radioligand [^{11}C](R)-PK 11195, possibly because of low specific signal. We measured the displaceable (i.e., specific) binding of [^{11}C](R)-PK 11195 in monkey brain to compare to reported values for [^{11}C]PBR28. We also sought to determine if [^{11}C](R)-PK 11195 could distinguish binders from non-binders in human subjects.

Methods: Monkey brain study: Two rhesus monkeys had dedicated brain PET imaging with [^{11}C](R)-PK 11195, both at baseline and after TSPO-blockade using 5 mg/kg of non-radiolabeled PBR28. Total brain activity was measured by calculating total distribution volume (V_T) in each scan using an unconstrained two-tissue compartment model and metabolite-corrected arterial input function. Human whole-body study: Eight healthy human subjects received whole body PET imaging with both [^{11}C](R)-PK 11195 and [^{11}C]PBR28. Four subjects had previously been identified as non-binders with [^{11}C]PBR28. Concentration of radioactivity in organs that express TSPO was measured and corrected for body weight and injected dose. The area under the time-activity curve from 5 to 20 min was used to measure uptake of radioligand in tissue.

Results: Monkey brain study: V_T values for [^{11}C](R)-PK 11195 decreased by 52% after pre-treatment with unlabelled PBR28. Specific binding (V_S), calculated as the difference in V_T at baseline and blocked conditions, was 57-fold lower than that reported for [^{11}C]PBR28 [2]. Human whole-body study: In the [^{11}C]PBR28 scans, non-binders had less uptake than binders in brain, heart, lung, kidney, and spleen ($p < 0.001$). In the [^{11}C](R)-PK 11195 scans, non-binders had less uptake (SUV • min) than binders in the heart [42.6 ± 3.0 (SD) vs. 52.8 ± 2.8, $P < 0.03$] and lung (16.2 ± 2.5 vs. 23.1 ± 2.8, $P < 0.03$). However, [^{11}C](R)-PK 11195 could not distinguish binders and non-binders in the brain, kidney, or spleen. Specific binding of [^{11}C]PBR28, operationally defined as the difference in organ uptake between normal subjects and non-binders, was several-fold higher than that of [^{11}C](R)-PK 11195 in the brain (41-fold), heart (4-fold), lung (4-fold), kidney (15-fold), and spleen (8-fold).

Conclusions: In monkey brain, the specific binding of [^{11}C](R)-PK 11195 was 57-fold lower than that of [^{11}C]PBR28. In humans, [^{11}C]PBR28 clearly distinguishes binders from non-binders in each organ studied. We cannot determine if non-binding is a phenomenon shared by [^{11}C](R)-PK 11195, since this radioligand distinguishes non-binders only in the heart and lung, which may be a result of multiple comparisons or of high amounts of nonspecific binding of this ligand. However, [^{11}C]PBR28 has much greater specific binding in monkey and man than [^{11}C](R)-PK 11195 and [^{11}C]PBR28 is preferred in the 90% of human subjects who display usual receptor kinetics.

References:

[1] NeuroImage. 2008;40:43-52.

[2] NeuroImage. 2008;39:1289-98.

41

Brain Poster Session: Oxidative Mechanisms

PARKINSON'S DISEASE RELATED PROTEINS INDUCTION AFTER TRANSIENT SPINAL CORD ISCHEMIA IN RABBITS

M. Sakurai[1], T. Kawamura[2], H. Nishimura[2], H. Suzuki[2], F. Tezuka[2], K. Abe[3]

[1]Cardiovascular Surgery, [2]National Hospital Organization Sendai Medical Center, Sendai, [3]Neurology, Okayama University, Okayama, Japan

Background and aims: The mechanism of spinal cord injury has been thought to be related to the vulnerability of spinal motor neuron cells against ischemia. However, the mechanisms of such vulnerability are not fully understood.

Methods: We used a rabbit spinal cord ischemia model with use of a balloon catheter. The spinal cord was removed at 8 hours, 1, 2, or 7 days after 15 min of transient ischemia, and histological changes were studied with hematoxylin-eosin staining. Western blot analysis for DJ-1, PINK1 and α-Synuclein, temporal profiles of DJ-1, PINK1 and α-Synuclein immunoreactivity, and double-label fluorescence immunocytochemical studies were performed.

Purpose: Because we previously reported that spinal motor neurons were lost probably by programmed cell death, we investigated a possible mechanism of neuronal death by immunohistochemical analysis for DJ-1, PINK1 and α-Synuclein.

Results: The majority of motor neurons were preserved until 2 days, but were selectively lost at 7 days of reperfusion. Western blot analysis revealed scarce immunoreactivity for DJ-1, PINK1 and α-Synuclein in the sham-operated spinal cords. However, they became apparent at 8 hours after transient ischemia, which returned to the baseline level at 1 day. Double-label fluorescence immunocytochemical study revealed that both DJ-1andPINK1, and DJ-1 and α-Synuclein were positive at 8 hours of reperfusion in the same motor neurons, which eventually die.

Conclusion: This study demonstrated that immunoreactivities for both DJ-1and PINK1, and DJ-1 and α-Synuclein were induced in the same motor neuron, which eventually die. The induction of DJ-1 and PINK1 proteins in motor neurons at the early stage of reperfusion may indicate oxidative stress, and the induction ofα-Synuclein may be implicated in the programmed cell death change after transient spinal cord ischemia**.**

References:

1. Sakurai M, Nagata T, Abe K, Horinouchi T, Itoyama Y, Tabayashi K. Oxidative damage and reduction of redox factor-1 expression after transient spinal cord ischemia in rabbits. J. Vasc. Surg. 2003; 37: 446-452.

2. Sakurai M, Takahashi G, Abe K, Horinouchi T, Itoyama Y, Tabayashi K. Endoplasmic reticulum stress induced in motor neurons by transient spinal cord ischemia in rabbits. J. Thorac. Cardiovasc. Surg. 2005; 130: 640-645.

3. Yamauchi T, Sakurai M, Abe K, Sawa Y. Ubiquitin-mediated stress response in the spinal cord after transient ischemia. Stroke. 2008; 39(6): 1883-1889.

43

Brain Poster Session: Translational Studies

CONTINUOUS ASSESSMENT OF CEREBROVASCULAR RESISTANCE AND CEREBRAL BLOOD FLOW BEFORE AND FOLLOWING TRAUMATIC BRAIN INJURY

M. Daley[1], N. Narayanan[1], C. Leffler[2]

[1]The University of Memphis, [2]The University of Tennessee Health Science Center, Memphis, TN, USA

Background and aims: Published guidelines for the management of adult patients with severe traumatic brain injury prescribe the maintenance of a general threshold of cerebral perfusion pressure (CPP) of 60 mmHg during intensive care monitoring of arterial blood pressure (ABP) and intracranial pressure (ICP) [1]. This threshold value of CPP is near the critical threshold for ischemia, the lower limit of cerebrovascular autoregulation, which is generally thought to be between 50-60 mmHg [2]. These guidelines point out the need for the development of methods that individualize patient CPP management and minimize secondary ischemic complications associated with traumatic brain injury [1].

We have developed a laboratory method to determine model-derived assessments of cerebrovascular resistance (mCVR) and cerebral blood flow (mCBF) from cerebrovascular pressure transmission, the dynamic relationship between ABP and ICP [3]. The aim of this twofold study is to:

1. evaluate relative changes in the model-derived parameters of mCVR and mCBF with corresponding changes in the pial arteriolar vascular parameters of pial arteriolar resistance (PAR) and relative pial arteriolar blood flow (rPABF); and
2. examine the efficacy of the proposed modeling methodology for continuous assessment of the state of cerebrovascular regulation by evaluating relative changes in the model-derived parameters, mCVR and mCBF, in relation to changes of CPP induced by pressor challenge prior to and following fluid percussion brain injury.

Methods: Changes of arterial blood pressure (ABP), intracranial pressure (ICP), pial arteriolar resistance (PAR) and relative blood flow (rPABF) induced by acute pressor challenge (norepinephrine (1uk/kg/min)) were evaluated in both uninjured and fluid percussion brain injured piglets (N=6) equipped with cranial windows. Assessments of model-derived cerebrovascular resistance (mCVR) and cerebral blood flow (mCBF) were obtained by a computational modeling method of cerebrovascular pressure transmission for each challenge.

Results: Consistent with functional autoregulation of the uninjured cerebrovascular circulation, hypertensive challenge resulted in a significant increase of PAR and mCVR; whereas, both rPABF and mCBF remained constant. For all injured piglets, hypertensive challenge resulted in a significant decrease of PAR and mCVR consistent with impaired autoregulation. Hypertensive challenge also significantly increased both rPABF, and mCBF with increased CPP with correlation values of ($r= 0.96$, $p< 0.01$) and ($r=0.97$, $p\leq 0.01$) respectively.

Conclusions: Assessment of model-derived cerebrovascular resistance and cerebral blood flow with changes of CPP may provide a means to continuously monitor the state of cerebrovascular regulation and cerebral perfusion.

References:

1. Bullock MR, Povlishshock JT. Guidelines for the management of severe traumatic brain injury. J. Neurotrauma 2007; 24(1): S59-S64.

2. Howells T, Elf K, Jones P, Ronne-Engstrom E, Piper I, Nilson P, Andrews P, Enbald, P. Pressure reactivity as a guide in the treatment of cerebral perfusion pressure in patients with brain trauma. J. Neurosurg. 2005; 102(2): 311-317.

3. Narayanan, N., Leffler, C.W., and Daley M.L. Influence of hypercapnic vasodilation on cerebrovascular autoregulation and pial arteriolar bed resistance in piglets. J. Appl. Physiology. 2008. [Epub ahead of print]

Brain Poster Session: Translational Studies

VALIDATION OF COMPUTATIONAL MODELING METHOD TO ASSESS CEREBRAL BLOOD FLOW AND REGULATION FROM ARTERIAL BLOOD PRESSURE AND INTRACRANIAL PRESSURE RECORDINGS

N. Narayanan[1], C. Leffler[2], **M. Daley**[1]

[1]The University of Memphis, [2]The University of Tennessee Health Science Center, Memphis, TN, USA

B**ackground and aims:** Guidelines for the management of adult patients with severe traumatic brain injury prescribe the maintenance of cerebral perfusion pressure (CPP) near the lower limit of cerebrovascular regulation during intensive care monitoring of arterial blood pressure (ABP) and intracranial pressure (ICP) [1]. The lower limits of regulation for pediatric patients are age-dependent [2] and generally unknown. To prevent either excessive or insufficient perfusion during management, a method designed to continuously evaluate cerebral blood flow (CBF) and cerebrovascular resistance (CVR) of each patient is needed. The aim of this study is to validate a computational method based on a biomechanical model of the dynamic relationship between ABP and ICP. This method is designed to continuously assess to model derived parameters of cerebral blood flow (mCBF) and cerebrovascular resistance (mCVR). Comparisons between experimental and model derived assessments of CBF and CVR were made to examine the validity of the proposed modeling methodology.

Methods: ABP, ICP, CPP, CBF by H_2 clearance, and pial arteriolar diameter (PAD) were measured in piglets equipped with cranial windows during normocapnia (N=6) and permissive hypercapnia (N=4). Corresponding mCVR and mCBF were calculated. Experimental CVR was computed as CPP/CBF and pial arterial resistance (PAR) was derived from PAD. Grand mean parameter values (±S.D.) were derived for each experimental condition.

Results: A summary of the comparisons between experimentally derived values of CBF, CVR, and PAR and the model-derived values of mCBF and mCVR is given in Table 1. Experimental and model-derived values of CBF and CVR were not significantly different.

Table 1. Comparison of Grand Mean Values (+/-S.D.) of ABP, ICP, CPP, Experimental CBF, CVR, PAR and Model-Derived Assessments of CBF and CVR during Normocapnia and Permissive Hypercapnia.

Condition	N	ABP (±S.D.) mmHg	ICP (±S.D.) mmHg	CPP (±S.D.) mmHg	CBF (±S.D.) ml/100g/min	mCBF (±S.D.) ml/100g/min	CVR (±S.D.) mmHg 100g/ml/min	mCVR (±S.D.) mmHg100g/ml/min	PAR (±S.D.) mmHg100g/ml/min
Normocapn	6	82.6	6.1	75.8	31.3	30.3	2.4	2.5	5075.2

ic **Group**		(±5.7)	(±2.4)	(±2.5)	(±2.2)	(±4.0)	(±0.2)	(±0.1)	(±285.1
Permissive **Hypercapnia** **Group**	4	78.2 (±2.7)	11.5 (±0.9)[1]	66.9 (±3.2)[1]	34.5 (±0.4)	34.7 (±1.8)	1.9 (±0.1)[1]	1.9 (±0.2)[1]	4968.0 (±126.7

[Table 1]

[1] Denotes a significant degree of difference between mean values of normocapnic and permissive hypercapnic groups at $p < 0.01$.

Conclusions: Assessment of model-derived cerebrovascular resistance and cerebral blood flow with changes of CPP may provide a means to continuously monitor the state of cerebrovascular regulation and cerebral perfusion.

References:

1. Bullock MR, Povlishshock JT. Guidelines for the management of severe traumatic brain injury. J Neurotrauma 2007; 24(1): S59-S64.

2. Chambers IR, Jones PA, Lo TYM, Forsyth RJ, Fulton B, Andrews PJD, Mendelow AD, Minns RA: Critical thresholds of intracranial pressure and cerebral perfusion pressure related to age in paediatric head injury. J Neurol Neurosurg Psychiatry 2006, 77: 234-240.

RUTIN PROTECTS AGAINST TRANSIENT FOCAL CEREBRAL ISCHEMIA IN RATS

M. Khan[1], F. Islam[1,2]

[1]Department of Medical Elementology and Toxicology, [2]Jamia Hamdard (Hamdard University), New Delhi, India

Background and purpose: Free radical induced neuronal damage is implicated in cerebral ischemia reperfusion (IR) injury and antioxidants are reported to have neuroprotective activity.The present study was designed to assess the neuroprotective mechanisms of rutin (Vitamin P), a free radical scavenger, through antioxidative, anti-inflammatory and anti-apoptotic pathways.

Methods: The middle cerebral artery of adult male wistar rat was occluded for 2 h and reperfused for 22 h. Rats were pretreated with Rutin (50 mg/kg) for 15 days. Infarct volume and neurological deficit scores were evaluated at several time points after ischemia. 24 hrs after MCAO, the brains were removed for assays of antioxidants, calcium, H_2O_2, DNA fragmentation, PARP, caspase-3, release of mitochondrial cytochrome c and p53.

Results: Neurological deficits were significantly decreased in rats treated with rutin. Rutin pre-treatment improved the antioxidant status, diminished the cytochrome-c expression, decrease DNA fragmentation and brain infarct. Furthermore, rutin markedly suppressed the p53 protein expression and calcium level.

Conclusions: These results indicate that rutin attenuates ischemic neuronal apoptosis by inhibiting cytochrome c release, increasing endogenous antioxidant enzymatic activities and reducing the p53 expression. Thus, rutin shows an excellent neuroprotective effect against ischemia/reperfusion brain injury.

Keywords: Middle Cerebral Artery Occlusion; Brain infract, Rutin, Oxidative stress; Apoptosis. Neuroprotection.

49

Brain Poster Session: Neurologic Disease

WHAT TO DO WITH ALL THAT DATA?!

L. Martens

EMBL-EBI, Hinxton, Cambridge, UK

Novel technologies in different OMICS fields are generating vast amounts of data when applied to samples such as brain tissue biopsies, autopsies, or CSF fluid. Once the analysis is complete, the difficult task of interpreting the output data begins. Here we aim to provide some pointers into possible analyses that can be performed based on a large amount of across-experiments proteomics data from central nervous system tissues, as well as some analyses we have done for human plasma and serum. Taken together, these tools indicate that large amounts of data can be a blessing, and that they can enable powerful analyses that can inform the use of technology in analysing a specific sample, as well as the understanding of the underlying biology.

50

BrainPET Poster Session: Kinetic Modeling

VOXEL-BASED QUANTIFICATION OF L-[1-^{11}C]LEUCINE KINETICS FOR DETERMINATION OF REGIONAL RATES OF CEREBRAL PROTEIN SYNTHESIS

G. Tomasi[1], A. Bertoldo[2], S. Bishu[3], A. Unterman[3], C. Beebe Smith[3], K. Schmidt[3]

[1]Department of Diagnostic Radiology, Yale University, New Haven, CT, USA, [2]Department of Information Engineering, University of Padova, Padova, Italy, [3]Section on Neuroadaptation and Protein Metabolism, National Institute of Mental Health, Bethesda, MD, USA

Objective: The L-[1-^{11}C]leucine PET method (1,2) for measurement of regional rates of cerebral protein synthesis (rCPS) has been employed to date only at the Region-of-Interest (ROI) level (2,3). We adapted and validated a Basis Function Method (BFM) (4) to estimate parameters of the homogeneous tissue kinetic model of L-[1-^{11}C]leucine at the voxel level, and determined rCPS and the fraction (λ) of unlabeled leucine in the tissue precursor pool for protein synthesis derived from arterial plasma.

Methods: At the voxel level BFM performance was assessed both on simulated data, where time-activity curves (TACs) with noise levels typical of voxel data were generated, and on measured data, where BFM estimates were compared to those determined with nonlinear least squares (NLLS). Performance indices were bias% and RMSE% (Root Mean Square Error). BFM parameter estimates, averaged over all voxels in a ROI, were also compared to estimates obtained by fitting the ROI TAC to either a homogeneous or heterogeneous tissue model; both simulated data and data from L-[1-^{11}C]leucine PET studies in six healthy subjects were analyzed.

Results: In simulations of voxel data BFM yielded low-bias estimates of λ and rCPS; when tested on measured data BFM estimates at the voxel level were in good agreement with those determined with NLLS. In simulation of large numbers of voxels comprising a ROI (Figure) fits of the ROI TAC with the homogeneous tissue model gave substantial negative biases for the parameters K_1 and k_2+k_3, and positive biases for rCPS; results on measured data were consistent with the simulations. The heterogeneity model fit of the ROI TAC provided good parameter estimates in simulation, but did not perform well on measured data. rCPS estimated with BFM was slightly negatively biased, but its variability was low.

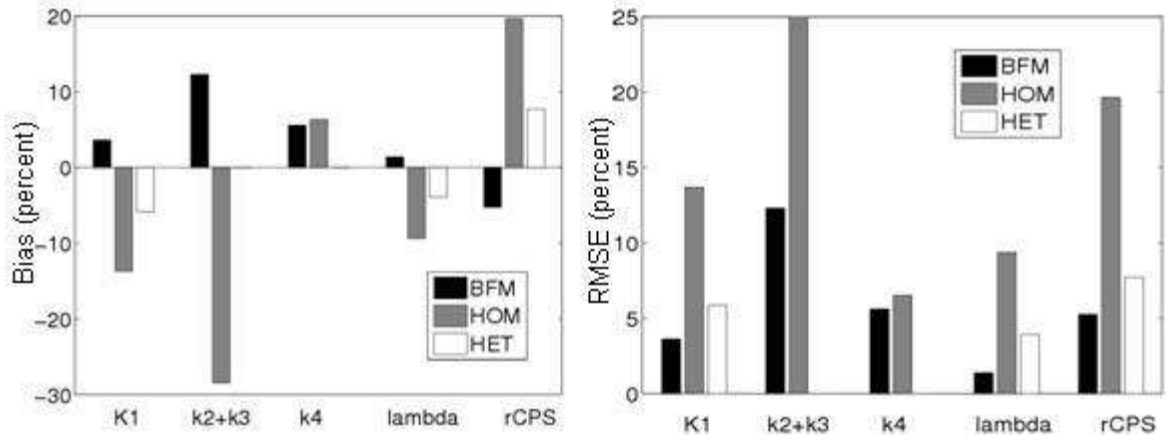

[Figure 1]

Figure: Simulation of all voxels comprising occipital cortex. Parameters were computed in three ways: averaging BFM estimates over all voxels within the ROI (BFM), and fitting the homogeneous tissue model (HOM) and heterogeneous tissue model (HET) to the simulated ROI TAC. The heterogeneity model does not provide estimates of k_2+k_3 and k_4 in the mixed tissue.

Conclusion: BFM is a useful and robust method for analyzing L-[1-^{11}C]leucine PET data at the voxel level. It provides reliable estimates with a computational cost substantially lower than that of NLLS. At the ROI level parameters computed by averaging BFM estimates over all voxels within the ROI were less biased on simulated data, and less variable on both simulated and measured data, than parameter estimates obtained by fitting the ROI TAC to either a homogeneous or heterogeneous tissue model.

References:

(1) Smith et al., JCBFM 2005;25:629-40.

(2) Schmidt et al., JCBFM 2005;25:617-28.

(3) Bishu et al., JCBFM 2008;28:1502-1513.

(4) Gunn et al., Neuroimage 1997;6:279-287.

Supported by: IRP/NIMH/NIH.

Brain Poster Session: Brain Imaging: Neurologic Disease

COMPARISON OF TWO DECONVOLUTION METHODS IN A CBF STUDY OF LUPUS PATIENTS VS HEALTHY CONTROLS WITH PERFUSION MRI

U. Sakoglu[1], C. Gasparovic[1,2], H.J. Bockholt[1], C.R. Qualls[3], J. Sharrar[4], W. Sibbitt[5], C. Roldan[4]

[1]The Mind Research Network, [2]Department of Neurology, [3]Clinical Translational Science Center, GCRC, [4]Department of Internal Medicine, Division of Cardiology, [5]Department of Internal Medicine, Division of Rheumatology, University of New Mexico Health Sciences Center, Albuquerque, NM, USA

Objectives: To compare an established and a recently developed deconvolution method to estimate cerebral blood flow (CBF) of lupus patients and healthy controls from dynamic susceptibility contrast MRI data.

Introduction: Estimating perfusion reliably in brain diseases reveals important information about the diseases´ characteristics. Dynamic susceptibility contrast (DSC) MRI technique based on bolus-pass of contrast agent in the brain vasculature has proved to be a useful technique to estimate important perfusion parameters, such as the cerebral blood flow (CBF). The mathematical model based on DSC MRI technique that links the perfusion parameters and the MR signal involves a convolution relation [1], and requires the deconvolution of the voxel time-concentration curves by an arterial input function (AIF) to estimate CBF. Different deconvolution methods have been used to solve the problem within the last two decades. Among these, the circular singular value decomposition-based (oSVD) deconvolution method has been widely accepted [2]. In this work, we have applied a recently developed Fourier Transform-based minimum mean-squared error (FT-MMSE) deconvolution method [3,4] to estimate CBF in lupus patients and healthy controls and we compared the results of the new method with the established oSVD method.

Methods: Upon approval from institutional ethics review committee, subjects were recruited. In this work, data from 14 patients (ages 26-55) and 6 healthy controls (ages 21-54) were used. 1.5T Siemens Sonata MRI system was used to collect MRI data. 220mmx220mm FOV, 128x128 matrix, 12 axial slices with thickness/gap: 5/5mm, TR/TE: 1600/78ms, 50 time-points were used for the T2*-weighted GE-EPI perfusion MRI scan. 0.1mM/kg Gd-DTPA was administred 10s after the scan start by 5mls/s injector, followed by a saline flush. MATLAB-based program [5] was used to perform deconvolution and to generate CBF maps with both methods based on the same AIF selection [3]. The CBF maps were motion-corrected, coregistered and normalized to MNI EPI template by SPM5 [6], and CBF in tissue with lesions (TWL) and normal tissue (NT) were measured.

Results: The preliminary results revealed the following:

a. CBF is significantly less in patients´ TWL, when compared to their NT,
b. CBF in NT of patients was higher than NT of healthy controls,
c. significance of the results were more prominent with the FT-MMSE method when compared to the oSVD method.

The research is ongoing and the results need to be confirmed with greater subject population.

Conclusions: The preliminary results based on 14 lupus patients and 6 controls revealed significantly less CBF in lupus lesions but more CBF in their normal tissues when compared to controls. Significance of results were more pronounced by the FT-MMSE deconvolution method than by the

oSVD method. The results, especially by FT-MMSE method, support the hypothesis that there is a compensatory flow in lupus patients with lesions.

References:

[1] Ostergaard L, et al. Magn. Res. Med. 1996; 36(5):715-25.

[2] Wu O, et al. Magn. Res. Med. 2003; 50(1):164-74.

[3] Sakoglu U, et al. Magn. Res. Img. 2008; 26(3):313-22.

[4] Sakoglu U, et al. Magn. Res. Img. 2009; in press.

[5] http://www.cfin.au.dk/software/penguin, 5/5/2007.

[6] http://www.fil.ion.ucl.ac.uk/spm, 5/5/2007.

Brain Poster Session: Angiogenesis

BRAIN PROBES FOR MRI OF DE NOVO NEURAL PROGENITOR CELLS IN LIVE BRAINS AFTER GLOBAL CEREBRAL ISCHEMIA

P.K. Liu[1], Z. You[2], C.H. Liu[1]

[1]Massachusetss General Hospital/Harvard Medical School, [2]Pediatrics, MGH/HMS, Charlestown, MA, USA

Cardiac arrest induces global cerebral ischemia (GCI) and hypothermia is the only treatment to reproducibly reduce neurological deficits after cardiac arrest. Gliogenesis, revascularization (angiogenesis), and neurogenesis are three major events thought to contribute to brain repair. The interaction of these three processes after GCI in the brain is not totally understood. Gene expression at the transcription level during brain repair that follows GCI may be related to metabolic response and plasticity, and all involve the presence of neural progenitor cells (NPC); therefore, understanding the changes that occur throughout the repair process will aid translation of gene targeting for therapies that will benefit patients. However, detection of de novo NPC in the brain is not routinely performed clinically because the techniques used to track de novo NPC rely on the use of biopsy or autopsy samples. The biopsy procedure to obtain brain tissue severely limits the utility of these methods because they remove the same cells that we wish to save in vivo, and often clearly precludes longitudinal therapeutic evaluation. To overcome these problems, we developed an alternative method that uses brain probes for magnetic resonance imaging (MRI); this novel method provides a powerful and less invasive means of in vivo detection of gene action in brain cells. Superparamagnetic iron oxide nanoparticles (SPION, a T_2 susceptibility MR contrast agent) are linked to phosphorothioate-modified antisense oligodeoxynucleotides (sODN) to target endogenous gene transcripts of astroglia in live C57black6 mouse brains. Because sODN are charged molecules, they are taken up by the brain cells along with SPION; sODN retention is determined by sequence homology with cellular mRNA targets. By virtue of its coupling with the complementary sODN, SPION retention in living brains can thus imaged by MRI. We induced GCI by transient bilateral carotid occlusion for 60 minutes. We detected abnormal water diffusion by way of hyperintense diffusion-weighted imaging and calculated significant reduction using the apparent diffusion coefficient (rADC) at one day of reperfusion. BBB leakage was detected in the region of rADC at four weeks after GCI. We detected angiogenesis using MR probe targeting cells with high actin gene transcript in the 8th week, and gliosis using MR probe targeting astroglia in the 9th week post GCI. We found gliosis and angiogenesis in close and adjacent regions, but not in the same cells. The MRI data were confirmed by immunohistology in the 10th week. Nestin antigen was found in microvasculature that expressed Actin, but not in GFAP-expressing astroglia. This finding is consistent with the presence of pericytes during angiogenesis in the brain. This method has applications for cell typing based on specific mRNA and exclusion of unbound probe by living cells in vivo, and has potential for translation from bench to bedside application. These brain probes can detect various cell types before enough proteins are translated to enable detection using antibodies. Supported by NINDS (R01NS45845; R21NS057556), NIA (R21DA 024235), NCRR (P41RR14075).

BrainPET Poster Session: Brain Imaging: MRI/fMRI

ASSESSING THE EXISTENCE OF ISCHEMIC PENUMBRA THROUGH AUTOMATICALLY ANALYZING BASELINE DIFFUSION-WEIGHTED IMAGING

Q. Hu[1,2,3], P. Gao[4], L. Ma[4], Z. Chen[1,2], J. Wu[1,2], X. Ma[1,2]

[1]Shenzhen Institute of Advanced Integration Technology, Chinese Academy of Sciences/The Chinese University of Hong Kong, [2]Shenzhen Institute of Advanced Technology, [3]Key Laboratory for Biomedical Informatics and Health Engineering, Chinese Academy of Sciences, Shenzhen, [4]Beijing Tiantan Hospital, Beijing, China

Objectives: Even though the PWI-DWI (perfusion- and diffusion-weighted imaging) mismatch model has been challenged, it remains the major clinical tool and has been proven useful [1]. Serious problems with PWI-DWI mismatch include the delineation of lesions manually (error prone and time consuming), invasiveness and interpretation uncertainty of PWI. A method to determine the existence of salvageable tissues fast and reliably is thus highly desirable and of vital clinical significance, which is our objective.

Methods: An image analysis system is developed to automatically determine the existence of salvageable ischemic tissues. It takes the baseline DWI as input and consists of the following steps:

1. reference ADC_{ref} of normal brain tissues is taken as the most frequent value of apparent diffusion coefficient (ADC);
2. regions with ADC smaller than $0.65*ADC_{ref}$ are approximated as the infarct regions (IRs) while those with ADC in between [$0.65*ADC_{ref}$, $0.85*ADC_{ref}$] as the transition regions (TRs);
3. only those TRs neighboring IRs (area>10mm^2) are kept;
4. the region with the largest area of IR, and the region with the maximum area of the sum of IR and TR, are found;
5. for each region, the areas of the IR and TR are denoted as A_{IR} and A_{TR}, respectively; the radial distance (RD) of the TR is approximated as RD = sqrt ((A_{IR}+A_{TR})/3.14)-sqrt(A_{IR}/3.14) (sqrt for square root); ADC gradient of a point is the ADC difference between the maximum within the 8-neighbors and this point's ADC divided by their distance; the expected ADC change in the TR (δADC) is the product of the average of the ADC gradient of all points within the TR and the radial distance RD divided by ADC_{ref};
6. if both δADCs are not smaller than 0.18 and at least one is larger than 0.21 with the volume of IR not greater than 100 ml, then this patient has salvageable ischemic tissues.

Results: Thirty-nine patients retrospectively retrieved from Tiantan Hospital (Siemens 3.0 T) in the last 5 years within 6 hours of symptom onset without cerebral hemorrhage were tested. The lesions were measured by neurologists to determine the existence of PWI-DWI mismatch (33 with and 6 without mismatch). Taking the PWI-DWI mismatch as gold standard, the image analysis system can yield a sensitivity of 97.0% (32/33) and a specificity of 100% within 1 minute on Pentium 4 PC. Fig. 1 shows an axial slice of ADC and the detected IR (red) and TR (green).

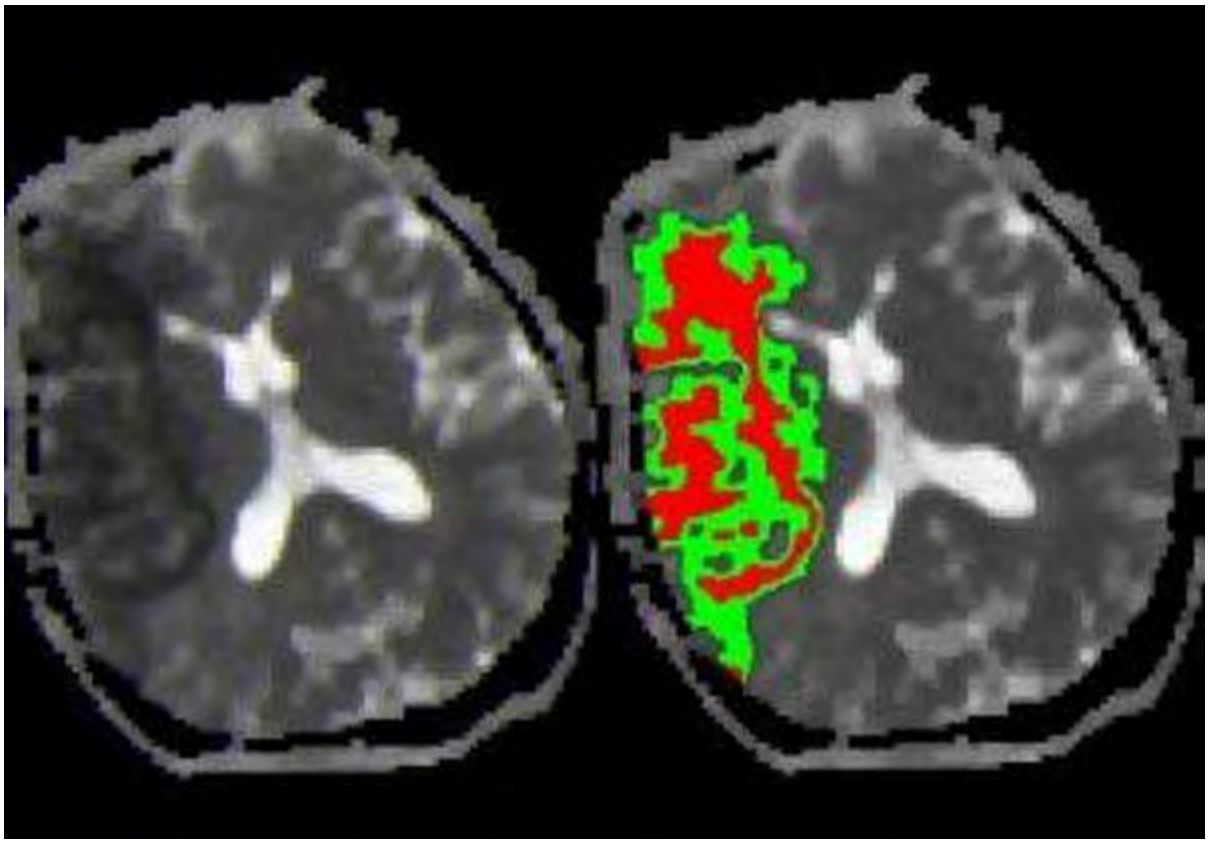

[Fig. 1]

Conclusions: The novelty and main contribution is to judge mismatch based on defining and quantifying spatial distribution instead of the exact volume of ADC within TR. The developed system is now used to test prospective data on both Siemens and GE scanners with encouraging results. It may be used to guide thrombolysis clinically.

References: 1. Thomalla G et al. Outcome and symptomatic bleeding complications of intravenous thrombolysis within 6 hours in MRI-selected stroke patients comparison of a German multicenter study with the pooled data of ATLANTIS, ECASS, and NINDS tPA trials. Stroke 2006; 37: 852-858.

55

BrainPET Poster Session: Brain Imaging: MRI/fMRI

PRE-SYMPTOMATIC DETECTION OF EXPERIMENTAL AUTOIMMUNE ENCEPHALOMYELITIS USING IN VIVO MAGNETIC RESONANCE IMAGING OF VCAM-1

S. Mardiguian[1], S. Serres[2,3], A. Akhtar[4], M. McAteer[4], R. Choudhury[4], D. Anthony[1], N. Sibson[2,3]

[1]Department of Pharmacology, [2]Department of Physiology, Anatomy and Genetics, University of Oxford, [3]Department of Radiation Oncology and Biology, Radiobiology Research Institute, [4]Department of Cardiovascular Medicine, University of Oxford, Oxford, UK

Currently, Multiple Sclerosis (MS) is diagnosed clinically when contrast-enhancing lesions are visible using MRI, yet this identifies late-stage lesions in which BBB breakdown has occurred. The initial recruitment of leukocytes in MS takes place across an intact, but activated, brain endothelium expressing vascular cell adhesion molecules such as VCAM-1, preceding BBB breakdown. Identification and quantification of VCAM-1, therefore, represents an attractive imaging target to accelerate diagnosis and to guide specific therapy in neurological disease. We have previously demonstrated that an anti-VCAM-1 antibody conjugated to 1μm microparticles of iron oxide (MPIO) enables detection of VCAM-1 expression in vivo using MRI, with high specificity and exceptional conspicuity following the unilateral injection of Interleukin-1β into the brain. In this study, using a relapsing- remitting EAE mouse model of MS, we show the expression of VCAM-1 in pre-symptomatic EAE mice, at a time when pathology is otherwise undetectable. In particular, we show the accumulation of anti-VCAM-1-MPIO in EAE lesions of the brain stem and cerebellum in the absence of gadolinium enhancement, indicating that endothelial VCAM-1 expression can be identified in lesions prior to BBB breakdown. We report that the expression of VCAM-1 significantly increases with the progression of disease as well as with increasing disability. Our findings demonstrate that our novel contrast agent reveals pathology previously inaccessible to conventional, clinically-used MRI techniques, raising the possibility of early diagnosis of MS and targeting treatment to patients with elevated VCAM-1 expression.

Reference: McAteer MA, Sibson NR, Von Zur Muhlen C, Schneider JE, Lowe AS, Warrick N, Channon KM, Anthony DC, Choudhury RP. (2007). "In vivo magnetic resonance imaging of acute brain inflammation using microparticles of iron oxide". Nature Medicine 13: 1253-1258.

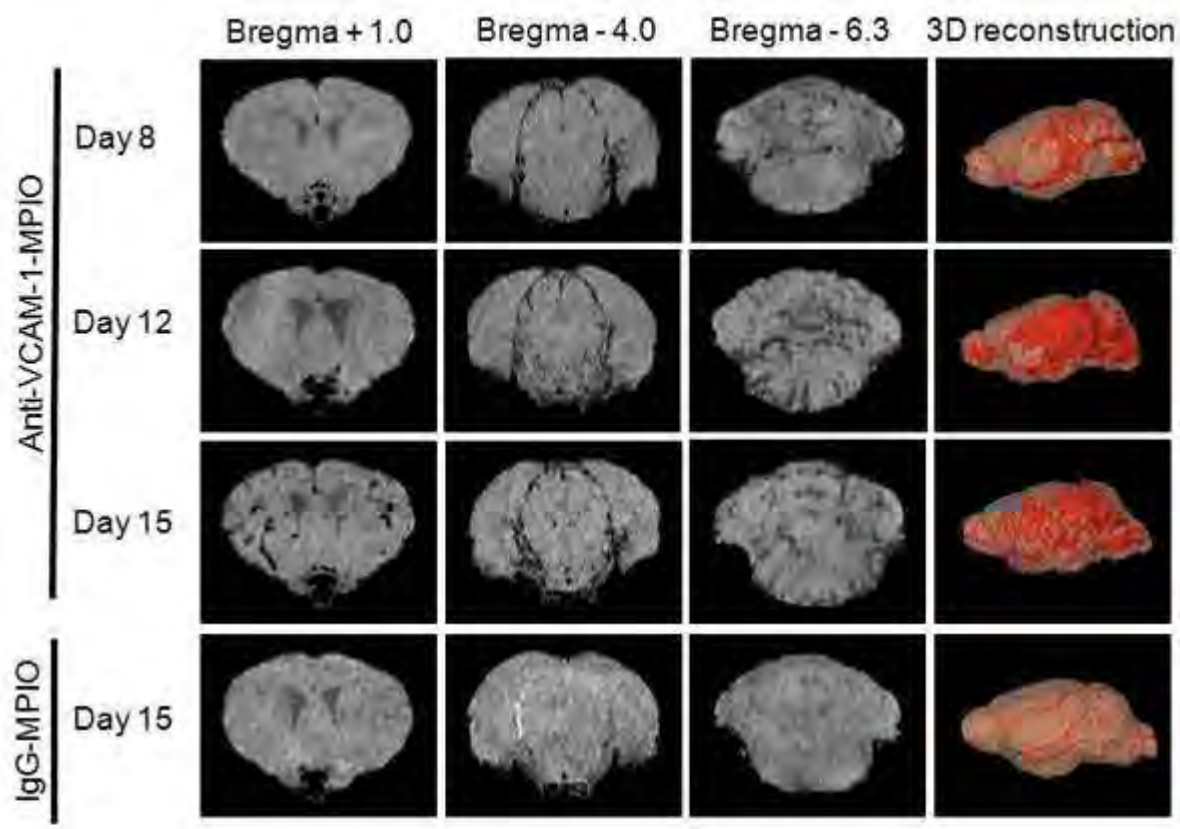

Anti-VCAM-1-MPIO reveals early presence of EAE.
T2*-weighted images of the forebrain (bregma +1.0), midbrain (bregma -4.0), and cerebellum (bregma -6.3) of EAE-SJL mice at days 8 (pre-symptomatic), 12 and 15 (symptomatic) after the injection of anti-VCAM-1-MPIO. VCAM-1 expression is detected in pre-symptomatic EAE mice at day 8 when pathology is otherwise 'invisible'. MPIO binding significantly increases with the progression of disease with evidence of VCAM-1 expression in the forebrain at day 15, when the disease is most severe. No MPIO binding was detected in EAE mice injected with IgG-MPIO demonstrating the specificity of our anti-VCAM-1 contrast agent. The 3D reconstructed images show the expression of VCAM-1 (in red) in the whole brain with binding being highest at day 15.

[Anti-VCAM-1-MPIO reveals early presence of EAE]

Brain PET Oral 3: Miscellaneous Targets

PROPOFOL ANESTHESIA ALTERS TISSUE CLEARANCE OF LEUCINE BUT NOT REGIONAL RATES OF CEREBRAL PROTEIN SYNTHESIS

S. Bishu[1], K. Schmidt[1], A. Unterman[1], A. Zametkin[1], M. Channing[2], Z.-H. Liu[1], M. Qin[1], W. Kammerer[3], P. Herscovitch[2], Z. Quezado[3], C. Beebe Smith[1]

[1]Section on Neuroadaptation and Protein Metabolism, National Institute of Mental Health, [2]PET Department, [3]Department of Anesthesia, National Institute of Health, Bethesda, MD, USA

Objectives: Determine the effect of propofol anesthesia on regional rates of cerebral protein synthesis (rCPS) and leucine kinetics in adult males with the L-[1-^{11}C]leucine PET method (Schmidt et al, JCBFM 2005 25:617-28; Smith et al, JCBFM 2005 25:629-40; Bishu et al.JCBFM 2008 28:1502-13).

Methods: Subjects (20-24y; n=10) were dynamically scanned on the High Resolution Research Tomograph for 90 min following ^{11}C-leucine injection. Region of interest-based analyses were used to estimate kinetic model rate constants. rCPS, λ (fraction of unlabeled leucine in the tissue precursor pool for protein synthesis derived from arterial plasma), and C_E (concentration of unlabeled leucine in tissue precursor pool) were calculated. Sedation was monitored with the bi-spectral index (BIS) monitor® (Gan et al, Anesth1997 87:808-15).

Results: Mean (±SD) plasma leucine concentrations were similar in awake (118±14 nmol/ml) and propofol-anesthetized (109±21) states at baseline as were physiological variables. Clearance curves of arterial plasma ^{11}C-leucine were also similar in both states. Tissue ^{11}C-leucine clearance was slower in the propofol-anesthetized state in 6/8 cortical and 2/6 subcortical regions examined, indicating an increased half-life of unlabeled leucine in tissue. Estimated C_E was 30% higher in most cortical (7/8) and subcortical (4/6) regions. Under propofol anesthesia, λ tended to be slightly higher (NS); rCPS was unchanged (table). In both awake and anesthetized conditions, rCPS varied regionally, whereas λ was more uniform. The mean BIS score was 34, consistent with anesthesia.

Conclusions: Since leucine participates in glutamate trafficking and leucine metabolites are oxidized via the TCA cycle, the longer half-life of unlabeled leucine in tissue is consistent with the effect of anesthetics to decrease neuronal activity and the rate of cerebral energy metabolism. Despite these changes in kinetics, rCPS remained unaffected.

Region	λ		rCPS (nmol g -1 min -1)		Half-life of Precursor Pool (min)	
	Awake	Propofol	Awake	Propofol	Awake	Propofol
Cerebellum	0.75 ± 0.02	0.77 ± 0.02	2.39 ± 0.27	2.39 ± 0.23	3.6 ± 0.4	4.0 ± 0.4
Occipital Cortex	0.73 ± 0.03	0.75 ± 0.02	2.52 ± 0.34	2.38 ± 0.30	4.3 ± 0.4	5.2 ± 0.3*
Frontal Cortex	0.71 ± 0.03	0.73 ± 0.02	2.29 ± 0.26	2.28 ± 0.21	5.4 ± 0.4	6.3 ± 0.5*

Temporal Cortex	0.70 ± 0.03	0.72 ± 0.02	2.07 ± 0.23	2.03 ± 0.22	6.0 ± 0.3	7.0 ± 0.6*
Hippocampus(a)	0.67 ± 0.04	0.68 ± 0.02	1.85 ± 0.24	1.91 ± 0.31	7.5 ± 1.3	8.0 ± 1.0
Thalamus	0.75 ± 0.02	0.77 ± 0.02	1.84 ± 0.18	1.74 ± 0.21	4.4 ± 0.4	4.9 ± 0.4*
Values are means ± SD for 10 subjects, except were indicated; (a): 9 subjects; *: Statistically significant after bonferroni correction, $p<0.05$						

[Table I]

Supported by IRP/NIMH; CC,NIH.

POSTOPERATIVE CORTICAL NEURAL LOSS ASSOCIATED WITH CEREBRAL HYPERPERFUSION AND COGNITIVE IMPAIRMENT AFTER CAROTID ENDARTERECTOMY: ^{123}I-IOMAZENIL SPECT STUDY

K. Chida, K. Ogasawara, Y. Suga, H. Saito, M. Kobayashi, K. Yoshida, Y. Otawara, A. Ogawa

Neurosurgery, School of Medicine, Iwate Medical University, Morioka, Japan

Background and aims: Aithough cerebral hyperperfusion after carotid endarterectomy (CEA) often impairs cognitive function, MRI does not always demonstrate structural brain damage associated with postoperative cognitive impairment. The purpose of the present study was to determine whether postoperative cortical neural loss, which can be detected by ^{123}I-iomazenil (IMZ) single-photon emission CT, is associated with cerebral hyperperfusion after CEA and whether it correlates with postoperative cognitive impairment.

Methods: In 60 patients undergoing CEA for ipsilateral internal carotid artery stenosis (> 70%), cerebral blood flow was measured using N-isopropyl-p-[^{123}I]-iodoamphetamine single-photon emission CT before and immediately after CEA and on the third postoperative day. The distribution of benzodiazepine receptor binding potential in the cerebral cortex was assessed using ^{123}I-iomazenilsingle-photon emission CT before and one month after surgery and was analyzed using three-dimensional stereotactic surface projection. Neuropsychological testing was also performed preoperatively and at the first postoperative month.

Results: Post-CEA hyperperfusion and postoperative cognitive impairment were observed in 9 patients (15%) and 8 patients (13%), respectively. Post-CEA hyperperfusion was significantly associated with postoperative hemispheric reduction of benzodiazepine receptor binding potential (95% CIs, 2.765 to 148.804; $p = 0.0031$). Post-CEA hyperperfusion (95% CIs, 1.183 to 229.447; $p = 0.0370$) and postoperative hemispheric reduction of benzodiazepine receptor binding potential (95% CIs, 1.003 to 77.381; $p = 0.0496$) were also significantly associated with postoperative cognitive impairment.

Conclusions: Cerebral hyperperfusion after CEA results in postoperative cortical neural loss that correlates with postoperative cognitive impairment.

STRUCTURAL MRI-MEASURED T_1 MAP REFLECTS FUNCTIONAL TOPOGRAPHY IN PRIMARY SOMATOSENSORY CORTEX OF A NON-HUMAN PRIMATE

J. Liu, N. Bock, A. Kocharyan, Y. Hirano, A. Silva

CMU, LFMI, NINDS, National Institutes of Health, Bethesda, MD, USA

Objectives: Functional organization in cerebral cortex, for example the somatotopy in primary somatosensory cortex, is well revealed by non-invasive measurements of blood oxygenation (BOLD) using functional MRI [1]. However, a corresponding anatomical organization is rarely shown in structural MRI, where cortical gray matter usually appears homogeneous. We hypothesize that high-resolution T_1 maps acquired by structural MRI can show heterogeneity within gray matter, because T_1 contrast in brain often arises from myelin concentration differences, and a heterogeneous myelin distribution within gray matter (myeloarchitecture) is shown by postmortem histology [2]. We further test the hypothesis that the T_1 heterogeneity within cortical gray matter matches the functional organization mapped by BOLD, thus providing an anatomical substrate that corroborates the functional mapping.

Methods: Three common marmosets were anesthetized by propofol and positioned into a 7 Tesla MRI scanner. For T_1 mapping, inversion-recovery (IR) was added to a conventional multi-slice echo-planar imaging (EPI) sequence (field-of-view: 31.8×21.0 mm, in-plane resolution: 0.3×0.3 mm, thickness: 0.5 mm, TE/TR: 21/11000 ms). Data under 18 IR time values (sampled from 60 to 9859 ms with geometric factor 1.35) were fitted to a three-parameter, single-exponential T1-recovery function [3]. A T_1 map of 20 slices was acquired in 10 minutes. For functional mapping, BOLD response was measured using the same EPI sequence, but with shorter TR (667 ms) and no IR. Stimuli were electrical stimulation of peripheral nerves in either arm or foot, delivered in periodic repeats of epochs (2.5 mA 0.4 ms pulses at 40 Hz, each epoch 8/32 s on/off). The T_1 and BOLD measurements were in good coregistration as they had identical EPI-related geometric distortions.

Results: Within the gray matter of dorsolateral cortex, the primary somatosensory cortex (SI) had significantly low T_1 (~1700 ms) whereas the cingulate cortex (medial to SI) and the secondary somatosensory cortex (lateral to SI) had high T_1 (~1850 ms). Furthermore, a fine structure was identified within SI. A band running lateral to medial had the smallest T_1 (~1650 ms), and this band was interrupted at least two gaps with higher T_1 (~1700 ms). Functional MRI showed two clusters of stimulus-evoked BOLD responses within SI. The relatively medial cluster was driven by stimulation to the foot, and the relatively lateral driven by stimulation to the arm. Both clusters centered at the smallest-T_1 band, and were separated by a gap with higher T_1.

Conclusions: The non-invasively acquired T_1 map is in line with known cortical myeloarchitecture. SI, especially area 3b, has high concentration of myelin, and the major body subareas (foot, hand, etc.) in area 3b are separated by several gaps with low myelin concentration [2]. Correspondingly, we found that a high-T_1 (low-myelin) gap separates the two low-T_1 (high-myelin) regions that are responsive to foot and arm, respectively, in BOLD imaging. Thus the somatotopy (foot vs. arm) may be reflected by structures in T_1 map within SI.

References:

[1] Servos et al., Neuroreport 9(4): 605-9 (1998).

[2] Krubitzer and Kass, J. Neurosci. 10(3): 952-74 (1990).

[3] Deichmann et al., Neuroimage 12(1): 112-27 (2000).

Lassen Award: Lassen Award Symposium

GABA, GLUTAMATE AND ASTROGLIAL MEDIATORS IN THE CORTICAL NEUROVASCULAR COUPLING RESPONSE TO BASAL FOREBRAIN CHOLINERGIC INPUT

C. Lecrux[1], A. Kocharyan[1], P. Fernandes[1], E. Vaucher[2], E. Hamel[1]

[1]Laboratory of Cerebrovascular Research, Montréal Neurological Institute, McGill University, [2]Ecole d'Optométrie, Université de Montréal, Montréal, QC, Canada

Background and aims: Neurovascular coupling or the tight adjustment of cerebral blood flow (CBF) to neurons displaying increased activity is widely used in functional neuroimaging techniques to map changes in neuronal activity. GABA interneurons contribute to the cortical CBF response to basal forebrain (BF) stimulation (Kocharyan et al., JCBFM. 2008;28:221-31). However, little is known about their interactions with other cortical neurons and astrocytes in this response. Hence, we investigated the neuroglial components involved in the CBF response to BF stimulation by blocking GABA and/or glutamatergic receptors, astroglial function or vasoactive mediators.

Methods: Bilateral cortical CBF responses to electrical BF stimulation were measured in urethane-anesthetised rats by Laser-Doppler flowmetry at baseline and after intracisternal (3µl, 10^{-4}M, pH 7.4 buffered solution) injection of vehicles, antagonists of NMDA (MK-801), AMPA (CNQX), metabotropic glutamate (mGluR) (MPEP+LY367385), GABA-A (picrotoxin), epoxyeicosatrienoic acids (EETs) (14,15-EEZE), muscarinic (scopolamine) receptors, blockers of astroglial metabolism (fluorocitrate), or inhibitors of EET-producing P450-epoxygenase (MS-PPOH) or prostaglandin-synthesizing cyclooxygenase-1 and 2 (COX-1 and 2, SC-560 and NS-398, respectively). Body temperature, blood gases and arterial blood pressure were stable throughout the experiments. Changes in CBF, expressed as mean±SEM, were compared by repeated-measures analysis of variance (ANOVA) or by one-way ANOVA for three group comparisons.

Results: The role of glutamate and GABA was evidenced by the significant decrease in the CBF response to BF stimulation after MK-801 (-32.2±5.3%, $p< 0.01$), CNQX (-30.2±5.5%, $p< 0.01$), LY367385+MPEP (-19.6±4.5%, $p< 0.05$) and picrotoxin (-24.5±4.1%, $p< 0.05$). MK-801 and picrotoxin administered together had an additive inhibitory effect on this response (-45.9±6.2%, $p< 0.01$). As previously reported, scopolamine reduced the CBF response (-55.5±4.2%, $p< 0.01$), but no further decrease was found when combined with MK-801 (-54.7±9.5%, $p< 0.01$), suggesting that the glutamate effect is downstream of muscarinic receptor activation. Inhibition of astroglial metabolism reduced (-43.6±5.9%, $p< 0.001$) the CBF response, as did blockade of EET synthesis (MS-PPOH, -44.2±6.2%, $p< 0.01$) or receptors (14,15-EEZE, -52.5±3.6%, $p< 0.01$). The combined administration of MS-PPOH with MK-801 or picrotoxin had no significant additive effect as compared to MS-PPOH alone (-34.5±3.5%, $p< 0.01$ and -35.1±4.3%, $p< 0.001$), suggesting that glutamate and GABA act partly through the astroglial EET cascade. In contrast, COX-1 or COX-2 inhibition had no effect on the evoked CBF response (-9.8±10.2%, ns and +6.9±9.5%, ns).

Conclusion: Our results demonstrate that (i) specific networks of cortical GABA and glutamate neurons are involved in the cortical CBF response induced by BF stimulation, (ii) these cortical neurons act, at least in part, through vasoactive EETs derived from astroglial arachidonic acid metabolism and (iii) COX-2 derivatives are not involved in the perfusion response to BF stimulation, in contrast to the thalamocortical pathway (Niwa et al., J Neurosci. 2000;20:763-70; Fernandes et al., Brain07, Abstract #BO12-3, and this meeting). Together with previous studies, these results suggest that neurovascular coupling in the cerebral cortex is input-specific, and that different vasoactive mediators are involved depending on the neurons recruited locally by a given afferent pathway.

Supported by CIHR (MOP-84209, EH) and Heart & Stroke Foundation of Canada/Canadian Stroke Network fellowship (CL).

61

Brain Poster Session: Inflammation

PIVOTAL ROLE OF CEREBRAL INTERLEUKIN-17-PRODUCING γδT CELLS IN THE LATE PHASE OF ISCHEMIC BRAIN INJURY

T. Shichita[1,2], H. Ooboshi[2], T. Kobayashi[1], Y. Sugiyama[1], H. Sugimori[2], D.J. Cua[3], Y. Iwakura[4], M. Iida[2], A. Yoshimura[1]

[1]Department of Microbiology and Immunology, Keio University, School of Medicine, Tokyo, [2]Department of Medicine and Clinical Science, Graduate School of Medical Sciences, Kyushu University, Fukuoka, Japan, [3]Department of Immunology, DNAX Research Inc, Palo Alto, CA, USA, [4]Center for Experimental Medicine and Department of Cancer Biology, Institute of Medical Science, Tokyo University, Tokyo, Japan

Objectives: Recently, inflammatory cytokines and lymphocyte recruitment / activation have been implicated in the progression of cerebral ischemia-reperfusion (I/R) injury[1,2]. However, the roles of specific lymphocyte subpopulations and their cytokines in stroke remain to be clarified. Because both IL-17 and IL-23 are critical cytokine for the onset of experimental autoimmune encephalomyelitis (EAE) and modify many inflammatory responses in central nervous system, we examined the role of IL-23 and IL-17 in the evolution of brain infarction.

Methods: Transient focal ischemia using a suture occlusion model was applied to the following gene-deficient mice: IL-17$^{-/-}$, IL-23p19$^{-/-}$, IFN-γ$^{-/-}$, IL-6$^{-/-}$, and γδTCR$^{-/-}$. The infiltrating inflammatory cells in the ischemic brain were collected by Percoll density gradient centrifugation. The expression levels of IL-17, IL-23, and other neurotoxic factors in the infiltrating inflammatory cells and ischemic brain tissue were investigated by intracellular FACS or quantitative real time PCR.

Results: Infarct volume of IL-23-deficient mice was significantly smaller than wild-type at 1-7 days after ischemia, while that of IL-17 KO mice was smaller at 4 and 7 days but not at 1 day after ischemia. Disruption of IFN-γ or IL-6 gene did not affect infarct volume. The improvement of neurological deficits in IL-17 and IL-23 KO mice was also observed at day 4 but not at day 1. The expression of IL-23 in the brain increased 1 day after I/R, while IL-17-producing cells were infiltrated into the brain after day 3. IL-17-producing cells were not observed in the brain of IL-23 KO mice with I/R injury, suggesting that IL-17-producing cells induced by IL-23 are important effectors for the progression of ischemic brain damage. The expression of neurotoxic factors including IL-1β, TNFα, MMP-9, and ICAM-1 was extremely reduced in the ischemic brain by IL-17 and IL-23 deficiency. Intracellular cytokine staining indicated that γδT lymphocytes, but not CD4-positive helper T cells, were a major source of IL-17. Depletion of γδT lymphocytes by gene disruption or by anti- γδTCR antibody pre-treatment ameliorated the brain I/R injury to the levels seen in IL-17 deficient mice. Furthermore, a neuroprotective effect was also observed even when the administration of anti-TCRγδ antibody was delayed to 24 hours after the induction of brain ischemia.

Conclusions: Our findings indicate that infiltrated γδT lymphocytes activated by IL-23 mainly produce IL-17 and contribute to the inflammatory responses to ischemic brain injury. We propose that γδT lymphocytes could be a therapeutic target for the later inflammatory events which amplify the initial damage in cerebral ischemia.

References:

1. Ooboshi H, Ibayashi S, Shichita T, et al. Postischemic gene transfer of interleukin-10 protects against both focal and global brain ischemia. Circulation. 111, 913-919 (2006).

2. Yilmaz G, Arumugam TV, Stokes KY, Granger DN. Role of T lymphocytes and interferon-gamma in ischemic stroke. Circulation. 113, 2105-2112 (2006).

A STATISTICAL ANALYSIS OF THE HYPOTHESIS OF THE STANDARD TWO-COMPARTMENT MODEL FOR DYNAMIC PET-FDG DATA IN NORMAL BRAIN

F. O'Sullivan[1,2], N. Fitzgerald[1], J. O'Sullivan[1], M. Muzi[2], D.A. Mankoff[2], A.M. Spence[2], K.A. Krohn[2]

[1]Statistics, University College Cork, Cork, Ireland, [2]Radiology, University of Washington, Seattle, WA, USA

Objectives: While most PET-FDG studies focus on late time retention characteristics in tissue, there is often an opportunity to use the dynamic time-course to obtain a more complete kinetic description of factors influencing FDG metabolism. The usual approach models the tissue residue with the established 2-compartment model(1). But non-parametric approaches to residue modeling are used with dynamic contrast MR and CT data (2,3) and recently we have developed a corresponding non-parametric approach that is applicable to dynamic PET data. The present study uses this technique to more carefully evaluate local cerebral residues from dynamic PET-FDG data.

Methods: The residue description of PET time-course data presents a density deconvolution estimation problem. Our solution uses the method of regularization with cross-validation. The computational implementation uses adaptive cubic B-spline and quadratic programming. Numerical simulation is used for evaluation of sampling variation and is also critically used as a way to assess the 2-compartment residue model hypothesis with FDG.Time-course datasets corresponding to 10 MR-identified brain regions in 12 normal subjects were analysed using the non-parametric and parametric (2-compartment) residue models. The 2-compartment model hypothesis was assessed by the data-fit, with appropriate adjustment for the increased flexibility of the non-parametric procedure.

Results: Strong (p-vlaues< 0.05l) statistical evidence against the compartment model is found in 7 out of 8 gray matter regions considered (cerebellum, putamen, thalamus, and occipital, temporal, frontal and parietal lobes). The only exception is the caudate. The deficit in the 2-compartment model, is its inability to correctly represent the early temporal structure of the tracer residence. The impact of deviations from the compartmental residue on the quantitation of summary characteristics of FDG metabolism including flux, flow, transit time and extraction were also evaluated. In all cases statistically significant deviations were found. The magnitude of deviations in flux are, not-surprisingly, small (4%).

Conclusions: Our study does not refute the basic biochemistry of the 2-compartment model for FDG, this has been well validated by in-vitro test-tube experimentation. Rather the difficulty arises from the realization that a typical PET region of interest need not behave as a well-stirred test-tube sample. Our result is most likely explained in terms of tissue heterogeneity. The brain regions considered here, similar to those in many PET studies, are relatively large. Within these regions it is likely that neither the vascular delivery characteristics nor local biochemistry will be homogeneous. More generally, the non-parametric residue technique has broader application to the quantification of PET imaging data for which compartmental model structures may not be sufficiently validated.

References:

1. Phelps, M.E., Huang, S.C., Hoffman, E.J., Selin, C., Sokoloff, L., Kuhl, D.E., (1979), Tomographic measurement of local cerebral glucose metabolic rate in humans with [F-18]2-Fluoro-2-deoxy-D-glucose: validation of method. Ann. Neurol., 6:371-388.

2. Ostergaard, L., Chesler, D.A., Weisskoff, R.M., Sorensen, A.G., Rosen, B.R., (1999), Modeling cerebral blood flow and flow heterogeneity from Magnetic Resonance residue data. Magn. Reson. Med., 19:690-699.

3. Meier, P., and Zierler, K.L., (1954), On the theory of the indicator-dilution method for measurement of blood flow and volume. J. Appl. Physiol. 6:731--744.

63

Brain Poster Session: Blood-Brain Barrier

A FREE RADICAL SCAVENGER, EDARAVONE, PROTECTS CEREBRAL MICROVASCULAR INTEGRITY AFTER THROMBOLYSIS IN A RAT STROKE MODEL

T. Yamashita[1], T. Kamiya[1], **K. Deguchi**[1], S. Nagotani[1], T. Inaba[2], H. Zhang[1], K. Miyazaki[1], A. Ohtsuka[3], Y. Katayama[2], K. Abe[1]

[1]Department of Neurology, Okayama University, Okayama, [2]Divison of Neurology, Second Department of Internal Medicine, Nippon Medical School, Tokyo, [3]Department of Human Morphology, Okayama University, Okayama, Japan

Background: After stroke, the thrombolytic effect of tissue plasminogen activator (tPA) is beneficial, if it is given within a short time. However, delayed reperfusion with tPA sometimes causes hemorrhagic transformation (HT), strictly limiting its clinical use. An understanding of the mechanism underlying the HT and new therapeutic methods are both needed.

Methods: We used a spontaneously hypertensive rat model of middle cerebral artery occlusion (MCAO). Rats were treated with vehicle alone (n = 6), tPA alone (n = 16), or tPA plus edaravone, a free radical scavenger (n = 11). Edaravone (i.v., 3 mg/kg) was administrated every 1.5 hours during the 4.5 hours of MCAO, followed by tPA treatment (i.v., 10 mg/kg) at reperfusion. At 24 hours after MCAO, the surviving rats were sacrificed.

Results: Administration of tPA alone significantly ($p < 0.05$) worsened the survival rate compared with vehicle. However, treatment with edaravone plus tPA significantly ($p < 0.05$) increased the survival rate, improved motor function, and significantly decreased HT. Immunostaining revealed that edaravone suppressed the tPA-induced lipid peroxidation and matrix metalloproteinase-9 (MMP-9) activation around cerebral microvessels. Moreover, electron microscopic analysis demonstrated that the basement membrane disintegrated and became detached from the astrocyte endfeet in rats treated with tPA alone, whereas treatment with edaravone plus tPA prevented the microvessels from dissociating.

Conclusions: Edaravone can protect the cerebral microvascular integrity, presumably by safeguarding the basement membrane from excess free radicals and MMP-9, leading to a decrease in HT, and an improved survival rate and neurological outcome.

RAPID CEREBRAL HEMODYNAMIC MODULATION DURING SET SHIFTING: EVIDENCE OF TIME-LOCKED ASSOCIATIONS WITH COGNITIVE CONTROL IN FEMALES

D. Schuepbach[1], S. Duschek[2], D. Hell[1]

[1]Psychiatric University Hospital, University of Zürich, Zürich, Switzerland, [2]Department of Psychology, University of Munich, Munich, Germany

Objectives: Set shifting provokes specific alterations of cerebral hemodynamics in large basal cerebral arteries (Schuepbach et al., 2002). However, no clear gender differences have been reported so far. In the following functional transcranial Doppler (fTCD) study, we introduced cerebral hemodynamic modulation, a means that assesses rapid changes of brain perfusion, to gender aspects of set shifting during Wisconsin Card Sorting Test.

Methods: Male and female participants underwent the WCST during measurements of the middle and anterior cerebral arteries. Parameters of task performance and cerebral hemodynamic modulation during set maintenance and set shifting were investigated by means of multi- and univariate analyses of variance. Correlation analyses examined the linkage between task performance and rapid cerebral hemodynamic modulation.

Results: Males showed mostly positive values of cerebral hemodynamic modulation during set shifting whereas in females, maximum modulation was restricted to the behaviorally relevant time point of set shifting. Further, we observed time-locked associations between slowing during set shifting and early rapid cerebral hemodynamic modulation of the left and the right MCA in females ($R=-0.82$, $P=0.0036$ and $R=-0.90$, $P=0.0004$, respectively), but not in males.

Conclusions: This study provides evidence of gender related cerebral hemodynamic modulation during set shifting and of time-locked brain behavior relationship during cognitive control in females, and it emphasizes the importance of temporal dynamics of brain perfusion during cognitive control in both genders. Future fTCD studies are urgently needed to examine neurovascular mechanisms that mediate rapid cerebral hemodynamic modulation and time-locked associations during cognitive control.

Reference: Schuepbach D, Merlo MCG, Goenner F, Staikov I, Mattle HP, Dierks T, Brenner HD (2002) Cerebral hemodynamic response induced by the Tower of Hanoi puzzle and the Wisconsin Card Sorting test. Neuropsychologia 40:39-53.

65

Brain Poster Session: Experimental Cerebral Ischemia: In Vitro

THE HMGB1 RECEPTOR RAGE MEDIATES ISCHEMIC BRAIN DAMAGE

S. Muhammad[1], B. Waleed[1], S. Murikinati[1], S. Stoyanov[2], H. Yang[3], K.J. Tracey[3], M. Bendszus[4], P.P. Nawroth[2], A. Bierhaus[2], G. Rossetti[5], M. Schwaninger[1]

[1]Pharmacological Institute, [2]Department of Internal Medicine, University of Heidelberg, Heidelberg, Germany, [3]Feinstein Institute for Medical Research, Manhasset, NY, USA, [4]Department of Neuroradiology, University of Heidelberg, Heidelberg, Germany, [5]HMGBiotech, Milan, Italy

In ischemic stroke, the necrotic core is surrounded by a zone of inflammation, in which delayed cell death aggravates the initial insult. Here, we provide evidence that the receptor for advanced glycation end products (RAGE) functions as a sensor of necrotic cell death and contributes to inflammation and ischemic brain damage. The RAGE ligand high mobility group box 1 (HMGB1) was elevated in serum of stroke patients and was released from ischemic brain tissue in a mouse model of cerebral ischemia. A neutralizing anti-HMGB1 antibody and HMGB1 box A, an antagonist of HMGB1 at the receptor RAGE, ameliorated ischemic brain damage. Interestingly, genetic RAGE deficiency and the decoy receptor soluble RAGE (sRAGE) reduced the infarct size. In vitro, expression of RAGE in (micro)glial cells mediated the toxic effect of HMGB1. Addition of macrophages to neural cultures further enhanced the toxic effect of HMGB1. To test whether immigrant macrophages in the ischemic brain mediate the RAGE effect, we generated chimeric mice by transplanting RAGE-/- bone marrow to wild-type mice. RAGE deficiency in bone marrow-derived cells significantly reduced the infarct size. Thus, HMGB1-RAGE signaling links necrosis with macrophage activation and may provide a target for anti-inflammatory therapy in stroke.

67

BrainPET Poster Session: Molecular Brain Imaging: Clinical Applications

CHANGES OF BRAIN PHOSPHODIESTERASE 4 IN MAJOR DEPRESSION

M. Fujita[1], S. Zoghbi[1], C. Zarate[2], A. Mallinger[2], J. Hong[1], H. Ozaki[1], V. Pike[1], R. Innis[1], W. Drevets[3]

[1]Molecular Imaging Branch, [2]Mood and Anxiety Disorders Research Unit, [3]Neuroimaging of Mood and Anxiety Disorders, National Institute of Mental Health, Bethesda, MD, USA

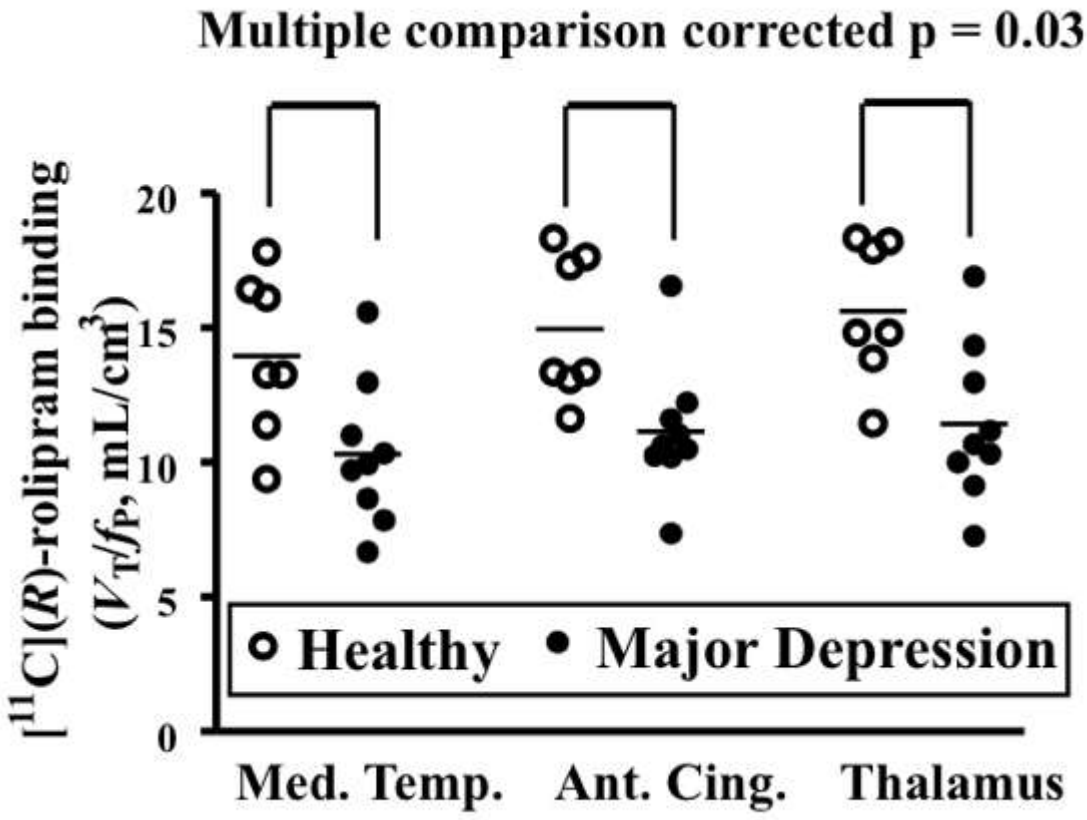

[png]

Objectives: The mechanism of action for some antidepressant treatments may involve upregulation of the 3´-5´-cyclic adenosine monophosphate (cAMP) cascade (1). This hypothesis is based on rodent studies consistently reporting upregulation of the cAMP cascade induced by chronic antidepressant drug administration. A post mortem human study also showed a decrease in cAMP regulatory element protein in unmedicated patients with major depressive disorder (MDD) and its normalization with antidepressants (2). The objectives of the current study were to image brain phosphodiesterase (PDE) 4, which metabolizes the second messenger cAMP, using the selective ligand [C-11](R)-rolipram in MDD patients before and after antidepressant treatment and in healthy controls to compare PDE4 levels between diagnostic groups and before versus after antidepressant treatment. Based on the

human post mortem and rodent studies reviewed above, we hypothesized that unmedicated depressed subjects would show lower PDE4 levels than controls and that antidepressant drug treatment would increase PDE4 levels toward normal in MDD subjects.

Methods: [C-11](R)-rolipram PET scans with metabolite-corrected arterial input function were performed on 9 unmedicated MDD patients (5 females/4 males, age=36±12) and 7 healthy controls (3 females/4 males, age=32±13). So far only 3 patients repeated a scan 4 - 8 weeks after sertraline or escitalopram treatment. Preliminary analyses were performed by comparing V_T/f_P (total distribution volume normalized to plasma free fraction) measured with an unconstrained two-tissue compartment model in large brain regions of frontal, parietal, occipital, lateral and medial temporal, and anterior cingulate cortices, thalamus, caudate, putamen, and cerebellum. Depression symptom severity was rated using the Montgomery-Asberg Depression Rating Scale and Hamilton Anxiety Rating Scale.

Results: The two-compartment model well identified V_T/f_P in all regions with average identifiability of < 2% in both controls and patients. Unmedicated patients showed 21 - 31% lower levels of V_T/f_P than controls in all brain regions (Fig.). After correction for multiple comparisons by applying the False Discovery Rate, the decreases were significant ($p < 0.05$) in all regions except frontal cortex. However, there was no significant correlation between the depression or anxiety scale scores and V_T/f_P in unmedicated patients. The three patients who had PET scans before and after treatment did not show consistent changes in V_T/f_P with two showing average increases of 18 and 27% and one showing an average decrease of 19% across the brain regions.

Conclusions: As we hypothesized, the current PET study showed lower levels of PDE4 in unmedicated MDD patients than healthy subjects, indicating downregulation of the cAMP cascade in depression. Additional patients will be studied before and after antidepressant treatment, and the regional specificity of abnormalities in PDE4 will be investigated via voxel-based analysis.

References:

1. Arch Gen Psychiatry. 1997;54:597.

2. Lancet. 1998;352:1754.

71

Brain Poster Session: Neurogenesis

LIVE IMAGING OF STROKE INDUCED NEUROGENESIS IN THE MOUSE BRAIN

T.D. Farr[1], T. Kallur[1], D. Wiedermann[1], S. Couillard-Després[2], L. Aigner[2], M. Hoehn[1]

[1]In Vivo NMR Laboratory, Max-Planck Institute for Neurological Research, Cologne, [2]Department of Neurology, University of Regensburg, Regensburg, Germany

Background and aims: Neurogenesis is upregulated following stroke, and may contribute to brain repair. Neurogenesis is typically studied invasively. Recently, transgenic mice were generated that express either Discoma sp reef coral red fluorescent protein (DsRed) (Couillard-Després, et al., 2006. Eur J Neurosci. 24: 1535-45), or the bioluminescent enzyme luciferase (LUC) (Couillard-Després, et al., 2008. Mol Imaging. 7: 28-34), under the control of the migrating neuroblast promoter doublecortin (DCX). Therefore, the aims of this project were to employ noninvasive multimodal imaging to observe the timecourse and expression patterns of the neurogenic response following focal ischemia, in vivo.

Methods: Male CD1 DCX-LUC mice (37-44g) (n=4) and C57/BL6 DCX-DsRed mice (29-35g) (n=3) received different durations (30, 20, or 10min) of transient middle cerebral artery occlusion (MCAO); one DsRed mouse received a sham procedure. Optical imaging was performed to detect fluorescence, or bioluminescence (using intraperitoneal administration of 150mg/kg of luciferin), at 23 days prior to and 12 days post MCAO. Anatomical magnetic resonance imaging (MRI) scans (spin echo T_2-weighted, and 3D fast low angle shot (FLASH) images) were acquired 4 days prior to and 7days post-MCAO at 11.7T. Two DsRed mice (including the sham) were sacrificed at 7 days post-MCAO and the other animals at 12 days. Brain tissue was processed for fluorescent immunohistochemistry for the imaging reporters in combination with DCX and GFAP.

Results: Ischemia durations of 30min produced extensive lesions and mortality, as observed from T_2 maps, whereas smaller subcortical insults were produced using 10-20min of occlusion. No fluorescent signal was detected from the C57/BL6 DCX-DsRed animals in vivo, but photons produced from the oxidation of luciferin in the CD1 DCX-LUC mice were observed and counted. Emission was highest in the head in a pattern similar to the pathway of the rostral migratory stream in the brain (Figure 1C-D). Following MCAO the bioluminescent signal increased and appeared to shift laterally towards the injured hemisphere (Figure 1E-F). Improved localization will be possible using co-registration of the optical images to the FLASH 3D MRI data set (Figure 1A-B).

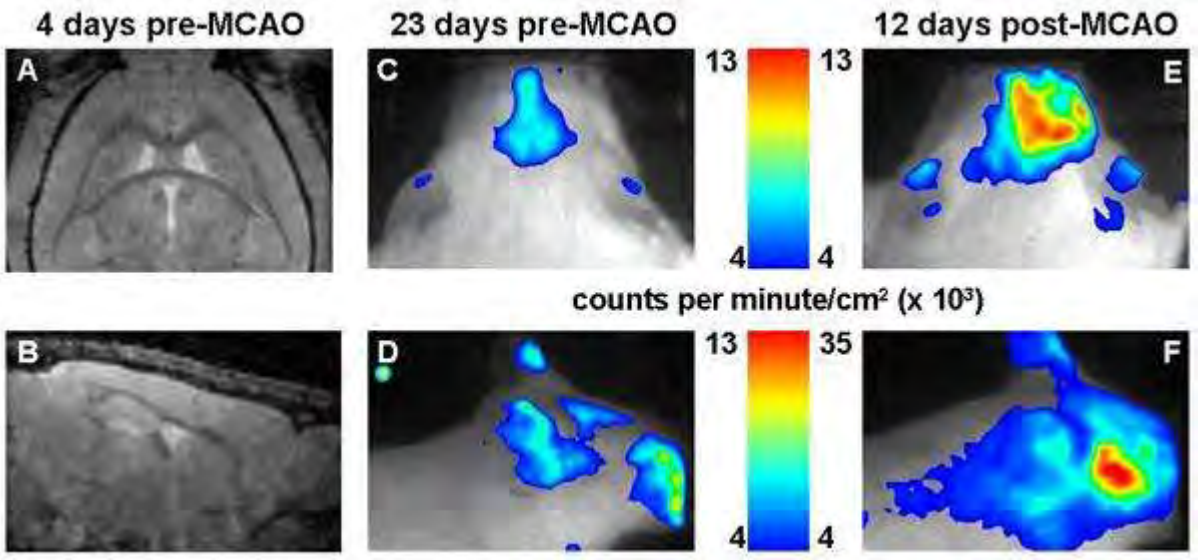

[Figure 1.]

Figure 1 A-B: Horizontal and sagital FLASH images from a CD1 DCX-LUC animal at 4 days prior to MCAO. C-D: Corresponding bioluminescent images (counts/minute/cm^2) from the same animal 23 days prior to and 12 days post MCAO (E-F). Note the increase in bioluminescence after MCAO, and shift towards the ischemic hemisphere.

Conclusions: These preliminary results indicate that monitoring the neurogenic response in vivo following stroke is possible. Ongoing work is being performed to characterize the location, intensity, and timecourse of this response using a multimodal imaging protocol combined with histological validation.

Acknowledgements: This work was supported by the StemStroke EU-FP6 program (LSHB-CT-2006-037526), ENCITE EU-FP7 program (HEALTH-F5-2008-201842), and an Alexander von Humboldt Fellowship to TDF.

SEXUAL STEROIDS OF A BRAIN AND SEXUAL FEATURES OF CONDITIONED-REFLECTED ACTIVITY

V. Sashkov

Institute of Age Physiology, Moscow, Russia

Sexual steroids render potent influence on morphology and functions of brain. It is supposed, that sexual hormones can be involved in a regulation of behavior process, learning and memory both formed in gonads, and synthesized in brain. According to it to understand the role of sexual steroids in a conditioned-reflected activity we need to find out their level in separate structures of brain during the learning process and the decrease process of conditional reflex.

Researches were executed on adult rats´ males and females Vistar´s line. A conditioned reflex was developed on the basis of an electrodermal reinforcement. Testing of conservation of a conditioned reflex was held in 24 h, and during the next 5 days was observed its decrease. During all stages of conditioned-reflected activity the amount of testosteron and estradiol in blood plasma, hypothalamus, hippocampus, amygdale, cingular and frontal corex were found.

The carried out results have shown, that learning to a conditioned reflex of adult rats hasn´t sexual dimorphism, however the decrease of a skill of males occurs rather quickly, and talking about rats it happens females gradually during five days of the tested period. Results of the correlation analysis have shown the selectivity of involving sexual hormones in mechanisms of conditioned-reflected activity rats´ males and females.

Definition of sexual steroids level of during forming of a conditioned reflex has revealed the increasing of the male rats´ testosterone value in all investigated structures of brain at its constant level in blood plasma. During female rats´ training to a conditioned reflex the level of testosterone raises in blood plasma, hypothalamus, hippocampus, amygdale, cingular and frontal corex. When a conditioned reflex decreases, the level of testosterone of both rats´ gender it is reduced in blood plasma and in all investigated structures of brain.

The level of estradiole during the males rats´ training to a conditioned reflex is raised in blood plasma and amygdale. During female training to the conditioned reflex, the level of estradiole remains constant in blood plasma, but it grows in amygdale. In decrease process a conditioned reflex the males rats´ level of estradiole is reduced in blood plasma, hypothalamus and hippocampus. During decrease of conditioned reflex females rats have a reduced concentration of estradiole in blood plasma, hypothalamus and amygdale and raised amount of estradiole in cingular corex and hippocampus.

The revealed rising of testosterone value in hypothalamus, hippocampus, amygdale, cingular and frontal corex according to its constant plasma level that males have during formation of conditioned reflex specifies gives us an opportunity to suppose that this steroid can be formed in brain. The increase of estradiole concentration in amygdale female during training to a conditioned reflex, and also in hippocampus and cingular corex at its decrease also testifies to a cerebral parentage of these quantities of the hormone. It is possible, that except for gonadal sexual hormones penetrating through a blood-brain barrier, androgens at males and estrogens at females, having a cerebral parentage, can provide optimum neurochemistry environment in brain, modulating processes of learning and memory.

SUPPRESSION OF ATHEROSCLEROTIC CHANGES IN CCA OF SHR-SP WITH A HMG-COA REDUCTASE INHIBITOR

S. Nagotani, K. Deguchi, T. Yamashita, V. Lukic-Panin, M. Takamiya, T. Kamiya, K. Abe

Department of Neurology, Okayama University, Okayama, Japan

Objectives: Statin reduces cerebrovascular events independent of its cholesterol lowering effect. We hypothesized statin inhibits early atherosclerotic change in common carotid artery (CCA), and investigated its effect on lectin-like oxidized-LDL receptor-1 (LOX-1) and monocyte chemoattractant protein-1 (MCP-1) expression, both of which are early atherosclerotic markers.

Methods: Stroke-prone spontaneous hypertensive rats (SHR-SP) were divided into 3 groups. Each group was treated with vehicle or simvastatin for 2 or 4 weeks and fed high fatty food and 1% NaCl water for 2 weeks, and CCA was removed. LOX-1 and MCP-1 expression as well as macrophage infiltration were histologically investigated. Lipid deposition was also investigated by Sudan III staining.

Results: Simvastatin groups showed significantly smaller amount of lipid deposition and LOX-1 and MCP-1 expressions, independent of serum lipid levels. Macrophage infiltration was also inhibited.

Conclusions: Simvastatin suppresed atherosclerotic change in CCA of hypertensive rats with high fatty diet. Reduction of cerebrovascular event by statins may be brought by the direct inhibition against atherosclerotic change.

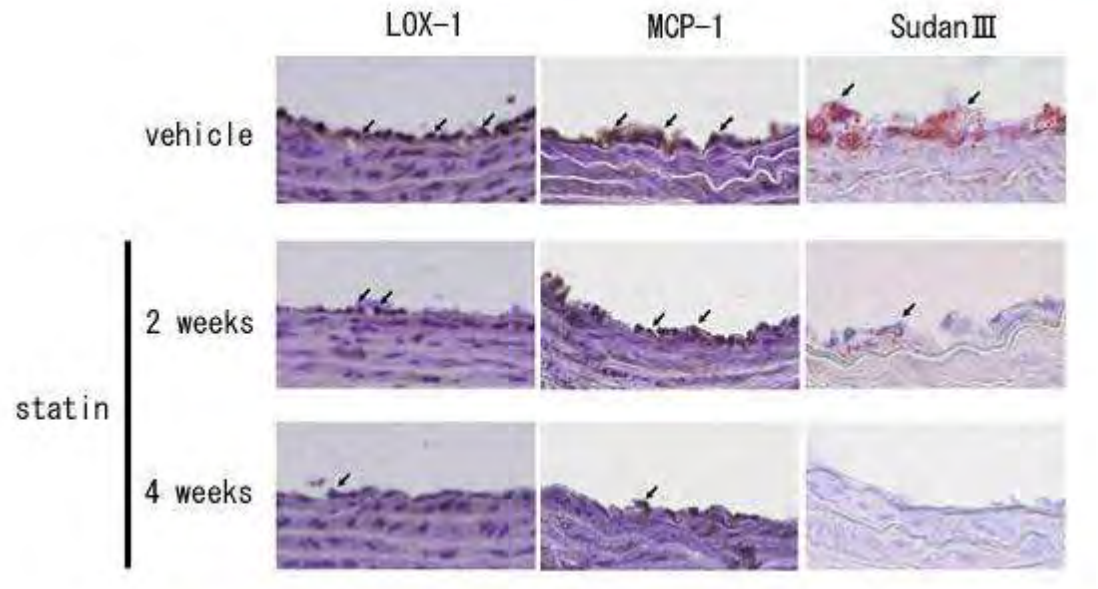

[figure(IHC)]

Figure legend: Representative photomicrographs of immunohistochemistry for LOX-1 and MCP-1 and Sudan III staining. Note strong expression of LOX-1 and MCP-1 and lipid deposition in the

vessel wall of the vehicle group. Simvastatin decreased LOX-1 and MCP-1 expression and lipid deposition in a treatment-period dependent manner.

EFFECTS OF SECOND-GENERATION ANTIPSYCHOTIC DRUG ON DOPAMINE SYNTHESIS IN HUMAN BRAIN MEASURED BY PET WITH L-[C-11]DOPA

H. Ito, H. Takano, H. Takahashi, R. Arakawa, M. Miyoshi, F. Kodaka, M. Okumura, T. Otsuka, T. Suhara

Molecular Neuroimaging Group, Molecular Imaging Center, National Institute of Radiological Sciences, Chiba, Japan

Objectives: Effects of antipsychotic drugs have widely been considered to be mediated by blockade of dopamine D2 receptors. Effects of antipsychotics on presynaptic functions of dopaminergic neurotransmission might also be related to therapeutic effects of antipsychotics. In the present study, changes in dopamine synthesis rate by administration of single dose of second-generation antipsychotics in relation with occupancy of dopamine D2 receptors were measured by positron emission tomography (PET) in healthy human subjects.

Methods: PET studies were performed on 12 healthy men (21-29 years of age) under resting condition (baseline study) and oral administration of single dose of antipsychotic drug, risperidone of 0.5-2.0 mg, (drug challenge study) on separate days. In each study, both PET scans with [C-11]raclopride and L-[C-11]DOPA were performed sequentially to measure dopamine D2 receptor binding and dopamine synthesis rate, respectively. For [C-11]raclopride PET, the binding potential (BP) in the striatum was calculated by the reference tissue model method with use of the cerebellum as a reference region. The occupancy of dopamine D2 receptors by risperidone was calculated from BP values in baseline and drug challenge studies. The uptake rate constant, Ki, for L-[C-11]DOPA in the striatum indicating the dopamine synthesis rate was estimated by the graphical analysis with use of the occipital cortex as a reference region [1]. The percentage change in Ki by risperidone was calculated from Ki values in baseline and drug challenge studies.

Results: The occupancies of dopamine D2 receptors ranged from 39% to 75% in the putamen. The dopamine synthesis rate Ki values were 0.0136 ± 0.0017 (1/min) and 0.0142 ± 0.0010 (1/min) (mean ± SD) in the putamen for the baseline and drug challenge studies, respectively. While occupancy of dopamine D2 receptors corresponding dose of risperidone was observed, no significant change in dopamine synthesis rate by risperidone was observed. No significant correlation between the occupancy of dopamine D2 receptors and the change in dopamine synthesis rate by risperidone was also observed. On the other hand, a significant negative correlation was observed between the baseline dopamine synthesis rate and the change in dopamine synthesis rate by risperidone ($r = -0.87$, $P < 0.001$).

Conclusions: The negative correlation between the baseline dopamine synthesis rate and the change in dopamine synthesis rate by risperidone, and smaller coefficient of variation of dopamine synthesis rate Ki in drug challenge studies than in baseline studies indicate that second-generation antipsychotic, risperidone, can be considered to stabilize the level of dopamine synthesis rate. The concept of phasic and tonic dopamine release with relation to the modulation of dopaminergic neurotransmission has been proposed, and abnormal responsivity in both the phasic and tonic dopamine release in schizophrenia have been considered [2]. Therapeutic effects of risperidone might be related to stabilizing effects on such dopaminergic neurotransmission responsivity.

References:

[1] Patlak CS, Blasberg RG. J Cereb Blood Flow Metab 1985; 5: 584-590.

[2] Grace AA. Neuroscience 1991; 41: 1-24.

INCREASE IN THALAMIC BINDING OF [^{11}C]PE2I IN PATIENTS WITH SCHIZOPHRENIA: A POSITRON EMISSION TOMOGRAPHY STUDY OF DOPAMINE TRANSPORTER

R. Arakawa[1,2], T. Ichimiya[1,2], H. Ito[1], A. Takano[1], M. Okumura[1,2], H. Takahashi[1], H. Takano[1], F. Yasuno[1], M. Kato[3], Y. Okubo[2], T. Suhara[1]

[1]Molecular Neuroimaging Group, Molecular Imaging Center, National Institute of Radiological Sciences, Chiba, [2]Department of Neuropsychiatry, Nippon Medical School, [3]Department of Neuropsychiatry, Keio University School of Medicine, Tokyo, Japan

Objectives: Previous in vivo imaging studies using positron emission tomography (PET) or single photon emission computed tomography (SPECT) reported no difference in dopamine transporter (DAT) bindings between control subjects and patients with schizophrenia[1,2]. However, those studies evaluated DAT binding only in the striatum, as DAT density in extrastriatal regions is very low. The recent development of [^{11}C]PE2I, which has high affinity and selectivity for DAT, allows the evaluation of extrastiatal DAT bindings[3].

Methods: Eight patients (6 men, 2 women; mean age 36.5 ± 9.5 yr, range 25-52 yr) diagnosed with schizophrenia participated in this study. Six of them were antipsychotic naïve and two had been antipsychotic free for at least six months before PET measurement. Psychopathological symptoms were assessed on the same day as the PET scans using the Positive and Negative Syndrome Scale (PANSS). Twelve normal control subjects (10 men, 2 women; mean age 33.2 ± 12.0 yr, range 23-56 yr) also participated. A dynamic PET scan was performed for 90 minutes after intravenous bolus injection of 214.7 ± 13.7 MBq of [^{11}C]PE2I. The specific radioactivity of [^{11}C]PE2I was 344.5 ± 355.3 MBq/nmol. All PET images were transformed into the standard brain size and shape using the statistical parametric mapping (SPM2) system. Regions of interest (ROIs) were drawn on all anatomically standardized PET images with reference to the T1-weighted MR images. ROIs were defined for the cerebellar cortex, caudate head, putamen, substantia nigra and thalamus. Binding potential (BP_{ND}) was calculated by the simplified reference tissue model method. The cerebellum was used as reference region because of its negligible density of DAT. After complete description of this study, written informed consent was obtained from all subjects. The study was approved by the Ethics and Radiation Safety Committee of the National Institute of Radiological Sciences, Chiba, Japan.

Results: The BP_{ND} value in the thalamus was significant higher in patients with schizophrenia (0.36 ± 0.07) than in controls (0.28 ± 0.08) (two-tailed t-test; d.f.=18, t=2.16, P=0.044). There were no significant differences in BP_{ND} between the two groups in the caudate, putamen or substantia nigra. In patients with schizophrenia, there were significant positive correlations between BP_{ND} in the thalamus and total PANSS score (Pearson's correlation coefficient; r=0.75, P=0.032), positive (r=0.78, P=0.023) and negative scores (r=0.82, P=0.014), but no correlation was observed with the general PANSS score. There was no significant correlation between BP_{ND} in other regions and any of PANSS scores.

Conclusions: Although the function of DAT in the thalamus has remained unclear, high DAT bindings may suggest a hyper-dopaminergic state of pre-synaptic dopamine function in patients with schizophrenia.

References:

[1] Laakso A et al. Am J Psychiatry 2000; 157: 269-71.

[2] Schmitt GJ et al. Schizophr Res 2008; 101: 133-41.

[3] Hirvonen J et al. J Cereb Blood Flow Metab 2008; 28: 1059-69.

THE BRAIN REVASCULARIZATION FOR THE PATIENTS WITH BICAROTID ATHEROSCLEROTIC DISEASES

V. Byvaltsev, E. Belykh

State Establishment Scientific Center of Reconstructive and Restorative Surgery of East Siberian Scientific Center Siberian Branch of Russian Academy of Medical Sciences, Irkutsk, Russia

Background and aims: There are 9 million people suffering from brain vascular diseases in the world. The main place belongs to the stroke of more than 6.6 million people. Despite the previous conclusions about the inefficiency of surgical brain revascularization under the conditions of ishemic stroke (1988), the latest research works prove their clinical expediency.

Purpose: The purpose of work was the analysis of treatment results of patients with the chronic cerebral ishemia caused by plural impacts of the main arteries of a brain.

Methods: Are presented by 18 patients with plural stenosis and occlusion effects of carotids which had 20 extra-intracranial microvascular anastamoses (EC-IC bypass). The median age of the patients was 54 years. The estimation of total neurological deficiency of the patients was carried out with the use of the scale of ishemic stroke NIHSS consequences. The complex tool research included: TCDG with defining cerebrovascular reserves, duplex scanning of extra-cranial arteries, CTA, MRA and in some cases a DSA (angiography). Operations were performed under the general anesthesia with the use of an operational microscope. All patients had a two-sided effect of the carotid pool. In 16 cases (88,9 %) there were post-thrombotic occlusion of the internal carotid from one side in the combination with a hemodynamically significant stenosis or a pathological deformation from the opposite side. For these patients an EC-IC bypass on the side of occlusion was performed. In two cases (11,1 %) post-thrombotic occlusions of both carotids was diagnosed which required the creation EC-IC bypass from both sides.

Results: There were the recourse of attributes of a cerebral ishemia according to the scale NIHSS, and also authentic increase of the total brain blood-flow and normalization of autoregulation parameters of cerebral hemodynamics (15 patients - 83,3 %). There were complications of surgical treatment in two cases (11,1 %). One patient had epidural hematoma which required its emergency removal. In another case there was an increase of neurological deficiency during the operation. During the control inspections the thrombosis of microanastomosis (inconsistency) was revealed in one case (catamnesis - 5 years).

Conclusions: The creation of EC-IC bypass of the bicarotid is an effective revasculation operation in cases of its performance on the side of clinical symptomatic prevalence, provide good condition of cerebral reserves and well passable external carotid.

81

Brain Poster Session: Oxidative Mechanisms

THIAMINE DEFICIENCY INCREASES β-SECRETASE ACTIVITY AND ACCUMULATION OF β-AMYLOID PEPTIDES

Q. Zhang, J. Luo, **Z.-J. Ke**

Key Laboratory of Nutrition and Metabolism, Institute for Nutritional Sciences, Shanghai Institutes for Biological Sciences, Chinese Academy of Sciences, Shanghai, China

Thiamine pyrophosphate (TPP) and the activities of thiamine-dependent enzymes are reduced in Alzheimer's disease (AD) patients. In this study, we analyzed the relationship between thiamine deficiency (TD) and amyloid precursor protein (APP) processing in both cellular and animal models of TD. In SH-SY5Y neuroblastoma cells overexpressing APP, TD promoted maturation of b-site APP cleaving enzyme 1(BACE1) and increased b-secretase activity which resulted in elevated levels of β-amyloid (Ab) as well as b-secretase cleaved C-terminal fragment (b-CTF). An inhibitor of b-secretase efficiently reduced TD-induced up-regulation of Ab and b-CTF. Importantly, thiamine supplementation reversed the TD-induced alterations. Furthermore, TD treatment caused a significant accumulation of reactive oxygen species (ROS); antioxidants suppressed ROS production and maturation of BACE1, as well as TD-induced Ab accumulation. On the other hand, exogenous Ab_{1-40} enhanced TD-induced production of ROS. A study on mice indicated that TD also caused Aβ accumulation in the brain, which was reversed by thiamine supplementation. Taken together, our study suggests that TD could enhance Ab generation by promoting b-secretase activity, and the accumulation of Ab subsequently exacerbated TD-induced oxidative stress.

TRANSIENT HEMIPARESIS AFTER TOPICAL APPLICATION OF 0.3 M KCL TO THE SENSORIMOTOR CORTEX IN UNRESTRICTED AWAKE MICE

H. Hattori[1], M. Tomita[1], H. Toriumi[1], Y. Tomita[2], M. Unekawa[1], N. Suzuki[1]

[1]Department of Neurology, [2]Department of Preventive Medicine for Cerebrovascular Disease, Keio University School of Medicine, Tokyo, Japan

Purpose: Cortical spreading depression (CSD) is a fundamental process in brain pathology, but visualization of its occurrence is difficult without employing invasive techniques. Here we report a novel model in which CSD occurrence is noninvasively evaluated from objective clinical symptoms.

Method: We used sixteen male C57BL/6J mice, anesthetized with isoflurane. A pinhole was drilled above the left parieto-temporal cortex, 1 mm lateral from the sagittal suture and 1 mm posterior from the bregma and 10 ml of 0.3 M KCl solution was injected through the hole onto the dura of the left cerebral cortex (n=8). The same amount of saline was injected in control mice (n=6). In 2 additional mice, DC potential was continuously recorded to confirm CSD occurrence with an enamel-covered 150 mm platinum electrode (implanted 300 mm deep into the cerebral cortex through another hole 3 mm anterior to the first hole), which was fixed tightly with dental cement to the skull bone. An Ag-AgCl electrode inserted into the space between the skull and scalp was used as the reference electrode. The wires were securely sutured to the back skin and were long enough to allow free movement. The mouse was released from the head holder and its behavior after recovery from anesthesia was videotaped and analyzed.

Results: Each mouse awoke within a few minutes, and attempted to stand up. In the CSD group the mouse showed a right-twisted posture with hemiparesis of the right extremities: the right fingers took a flexor position and the leg was loosely extended. Most mice struggled to lift their body, but were not able to do so because of the weakness of the right extremities. The mice could use only the left extremities, and so could only move in circles. Hemiparesis was observed in all KCl-treated mice. It was transient, lasting approximately 5 min, and was followed by recovery. In the DC potential recording group, we detected negative repetitive deflections of ca. 20 mV in DC potential. When the mouse awoke, the base-line level of the DC potential slightly shifted up, but negative deflection was seen occasionally, overlapping on the baseline record. The alert mouse became quiet with eyes closed concomitantly with the negative deflections. In one mouse the DC potential was recorded for more than one hour, but the recording was terminated when the mouse pulled out the electrode from its brain with its hands.

Discussion: Such transient symptoms as abnormal posture and hemiparesis, comparable to those in cases of MCA occlusion, have not been reported previously, since the animals in previous CSD studies were anesthetized and were immobilized with the head fixed to a head holder. We are not certain yet that the hemiparesis observed here reflects the DC potential deflection alone. However, since the same amount of K was administered in exactly the same manner as in the previous reports, we consider that the clinical symptoms elicited were attributable to the CSD. [Conclusion] Although the approach used here is quite simple, the model may be useful to investigate CSD.

85

Brain Poster Session: Experimental Cerebral Ischemia: In Vitro

HGTD-P PLAYS A PRO-APOPTOTIC ROLE IN RAT BRAIN WITH HYPOXIA-ISCHEMIA

Y. Qu, **D. Mu**

Department of Pediatrics, Westchina Second University Hospital, Sichuan University, Chengdu, China

Background: HGTD-P is a newly founded pro-apoptotic protein and an effector of hypoxia-ischemia (HI) induced cell death. The function of HGTD-P has been investigated in human prostate cancer cells. However, whether HGTD-P is involved in regulating apoptosis of rat neurons is not clear.

Objective: To elucidate the roles of HGTD-P in cellular apoptosis both in vitro and in vivo following HI.

Methods: Samples from primary cultured neurons and postnatal day 10 rat brains with HI were collected. RT-PCR, Western blots, and immunocytochemistry were used to detect the expression and distribution of HGTD-P. MTT assay, DAPI, TUNEL and flowcytometry were used to detect cell viability and apoptosis.

Results: We found that HGTD-P mRNA and protein expression were upregulated in cultured neurons and rat brains following HI. Antisense oligonuecleotides (AS) targeted to HGTD-P could inhibit the expression of HGTD-P, and thus rescued cell viability and attenuated cell apoptosis. In addition, we found that HGTD-P might play a pro-apoptotic role through the activation of caspase 3 and inducing the translocation of apoptosis inducible factor (AIF) to the nucleus.

Conclusions: Our findings suggested that HGTD-P plays a pro-apoptotic role in the developing rat brain after HI and targeting HGTD-P may be a potential therapy for HI-induced neonatal brain damage.

References:

1. Lee MJ, Kim JY, Suk K, Park JH. Identification of the hypoxia-inducible factor 1 alpha-responsive HGTD-P gene as a mediator in the mitochondrial apoptotic pathway. Mol Cell Biol. 2004; 24: 3918-3927.

2. Cho YE, Ko JH, Kim YJ, Yim JH, Kim SM, Park JH. mHGTD-P mediates hypoxic neuronal cell death via the release of apoptosis-inducing factor. Neurosci Lett. 2007; 416: 144-149.

3. Li L, Qu Y, Li J, Xiong Y, Mao M, Mu D. Relationship between HIF-1alpha expression and neuronal apoptosis in neonatalrats with hypoxia-ischemia brain injury. Brain Res. 2007; 1180: 133-139.

86

Brain Poster Session: Neonatal Ischemia

PTEN/AKT/FOXO3A PATHWAY IN NEURONAL APOPTOSIS IN THE DEVOLOPING RAT BRAIN AFTER HYPOXIA-ISCHEMIA

D. Li, Y. Qu, **D. Mu**

Department of Pediatrics, Westchina Second University Hospital, Sichuan University, Chengdu, China

Background: The pro-apoptotic function of phosphatase PTEN has been linked to its capacity to antagonize the phosphatidylinositol 3-kinase (PI3K) /Akt signaling pathway. However, the roles and the underlying mechanisms of PTEN in neuronal apoptosis after hypoxia-ischemia (HI) are not clear. Previous studies have revealed that Foxhead transcription factor (FOXO3a), a substrate of Akt, is a critical effector of PTEN-mediated tumor suppressor.

Objective: To test whether PTEN/Akt/ FOXO3a pathway is involved in neuronal apoptosis in developing rat brain after HI.

Methods: Postnatal day 10 rats were subjected to HI by ligating common carotid artery followed by hypoxia. Immunohistochemistry and Western blot analysis were used to detect the expression and phosphoralation of PTEN, Akt, as well as FOXO3a and its target gene Bim, a pro-apoptotic member of Bcl-2 family.

Results: We found that dephosphorylation of PTEN, Akt, FOXO3a were accompanied by FOXO3a translocation into the nucleus at 0.5h after HI. Simultaneously, Bim was significantly induced at 0.5h, peaked at 2h, preceding the neuronal apoptosis which occurred after 4 h following HI. Furthermore, we found that pretreatment of rats with bpv, a potential inhibitor for PTEN, significantly increased the phosphorylation of PTEN, Akt, and FOXO3a, which leads to a decrease of FOXO3a translocation into nucleus and a decrease of Bim expression after HI. The downregulation of Bim caused by PTEN inhibition decreased cellular apoptosis in the developing rat brain.

Conclusions: Our findings suggest that PTEN/Akt/FOXO3a pathway is involved in neuronal apoptosis in neonatal rat brain after HI. Agents targeting PTEN may offer a promise to rescue neurons from HI brain damage.

87

Brain Poster Session: Neonatal Ischemia

UNILATERAL CEREBRAL BLOOD FLOW PERTURBATIONS INDUCE CELLULAR RESPONSES IN MIRROR IN P7 RAT BRAIN

C. Charriaut-Marlangue[1], S. Villapol[1], S. Fau[1], P. Bonnin[2], S. Renolleau[1]

[1]NPA - Case 14, UMR-CNRS 7102, [2]Hôpital Lariboisière, Physiologie - Explorations Fonctionnelles, Paris, France

Objectives: Very few experimental studies have addressed the vascular and haemodynamic responses to arterial occlusion in the developing brain in animal models of brain injury and no studies have been published on mechanisms underlying cerebral blood flow (CBF) perturbations in the immature brain. The aim of this study was to explore the relationship between cerebral haemodynamic changes in P7 rat brain and molecular pathways implicated in cell survival and/or demise.

Methods: Wistar 7 day-old rats of both sexes were anaesthetized (Chloral hydrate 350 mg/kg) and subjected to transient (50 min) left common carotid artery (CCAo) using a vascular clip. Rats were subjected to ultrasound measurements using an echocardiograph (Vivid 7, GE Medical Systems ultrasound®, Horten, Norway) equipped with a 12-MHz linear transducer as previously reported (Bonnin et al., 2008). Doppler spectral recordings in the main arteries were evaluated:

1. before surgery,
2. during ischemia and
3. after reperfusion.

Rats were killed at 48 hours post-injury. Caspase-3 (C3) cleavage (p17 protein) was monitored either by immunohistochemistry on cryostat sections or by western blotting. DNA fragmentation was determined using the TUNEL assay and cell death by Fluoro Jade B.

Results: Unilateral transient CCAo (uni-tCCAo) did not induce cell death (no TUNEL and Fluoro Jade B staining) but induced cleavage of C3 in both ipsilateral (IL) and contralateral (CL) cortical layers II-III and VI. Using double immunofluorescence and confocal analysis we determined that cleaved C3 was mainly located in neurons (NeuN-positive) and in immature cells (nestin-positive). Cleaved C3 was expressed by GABAergic neurons (layer III). Blood flow monitoring indicated that during ischemia left ICA (internal carotid artery) was no injected. In contrast, right (CL) ICA and basilar trunk (BT) mean blood flow velocities (mBFVs) significantly increased (by 40%, $p< 0.01$ and 39 %, $p< 0.05$, respectively) to supply the arterial terminal branches of the left ICA through the anterior and posterior communicating arteries. After release of the left uni-tCCAo, left ICA was re-injected and left ACA was anterogradelly injected but these two arteries exhibited reduced mBFVs (by 50 and 45%, $p< 0.05$, respectively). However, mBFV was not significantly modified in the CL middle cerebral artery during ischemia and after reperfusion. A negative significant correlation between the percentage of immediate CCA reflow and the number of cells positive for cleaved C3 was found in both sides. Upstream caspase-2 cleavage and cytochrome c release from mitochondria were detected in both IL and CL cortex tissues at 48 h post-injury.

Conclusions: This study represents the first demonstration that an ipsilateral (IL) hemodynamic stress (50 min left CCA occlusion), not sufficient to induce cell death, produces a bilateral and symmetric cellular response in the MCA territory giving images in mirror in the developing brain. Data suggest that IL energetic deficit only produces upstream apoptotic markers in GABA interneurons (in layer II-

III) and glutamatergic neurons (in layer VI), which can transmute signals to the CL side either by transcallosal fibers and/or directly by their long distance axons.

Bonnin et al. Ultrasound in Med & Biol., 2008, 34:913-922.

BrainPET Poster Session: Molecular Brain Imaging: Clinical Applications

REPETITIVE TRANSCRANIAL MAGNETIC STIMULATION AS A COMPLEMENTARY TREATMENT OF POST-STROKE APHASIA

N. Weiduschat[1,2], A. Thiel[3], A. Hartmann[4], I. Rubi-Fessen[4], J. Kessler[2], P. Merl[4], L. Kracht[1], A. Schuster[1], R. Krais[1], W. Möller-Hartmann[5], T. Rommel[4], W.D. Heiss[1]

[1]Max-Planck-Institute for Neurological Research, [2]Neurology, University of Cologne, Cologne, Germany, [3]Neurology and Neurosurgery, McGill University, Montreal, QC, Canada, [4]RehaNova, [5]Radiology, University of Cologne, Cologne, Germany

Objective: Recovery of post-stroke aphasia seems to be most effective, when ipsilesional regions can be functionally (re-)integrated. In contrast, interhemispheric compensation might represent an inferior strategy. The objective of utilising repetitively administered TMS (rTMS) in neurorehabilition is mainly to decrease the cortical excitability in specific regions that are presumed to hinder optimal recovery. Accordingly, the aim of the present study is to investigate the impact of rTMS over the right-hemispheric Broca-homologous area in aphasic stroke patients concerning the clinical course and its neuronal correlates using a randomized and placebo-controlled design.

Methods: We investigated right-handed patients with aphasia due to first-time stroke. Within 16 weeks post-stroke, the regional cerebral blood flow (rCBF) at rest and during an acoustic verb-generation task was measured using H_2O^{15} positron emission tomography (PET). After randomization, the patients received either rTMS over the right triangular part of the inferior frontal gyrus (BA45) or sham-stimulation, each with subsequent conventional speech therapy. Repetitive TMS was conducted for 20 minutes with a frequency of 1 Hz and an intensity of 90% of the individual motor threshold five times per week for a two-week period. The language performance was tested before and after the two-week rehabilitation period. Additionally, further H_2O^{15}-PET-scans were obtained after the last TMS-session using the same verb-generation paradigm.

Results: Single subject language activation PET studies were analyzed in the first 6 patients (3 in the intervention group, 3 in the control group). Preceding the intervention, activations in the left and the right BA45 were comparable in both groups (fig. 1). After the rehabilitation period, activations in the left BA45 were higher in the treatment group ($p=0.07$; fig. 1). Activation in the right BA45 did not differ between groups. Improvement of language performance scores was higher in the intervention group on every task of the Aachener Aphasie Test.

Conclusions: In accordance with the theory of transcallosal inhibition, rTMS over right BA45 as adjuvant therapy for post-stroke aphasia treatment causes increased activity in left BA45 as compared to sham-stimulation. This imaging finding has its clinical correlate in improved language performance of the treatment group. It has no permanent effect on right BA45 activity although this area was directly stimulated. These preliminary data suggest that TMS-intervention over right BA45 facilitates conventional speech and language therapy with a long-lasting transcallosal effect on left BA45.

Figure 1: Activation intensity of the left and right BA45, as measured in Z-scores, specified for different groups and time points (Group 0: sham stimulation; Group 1: rTMS over right BA45).

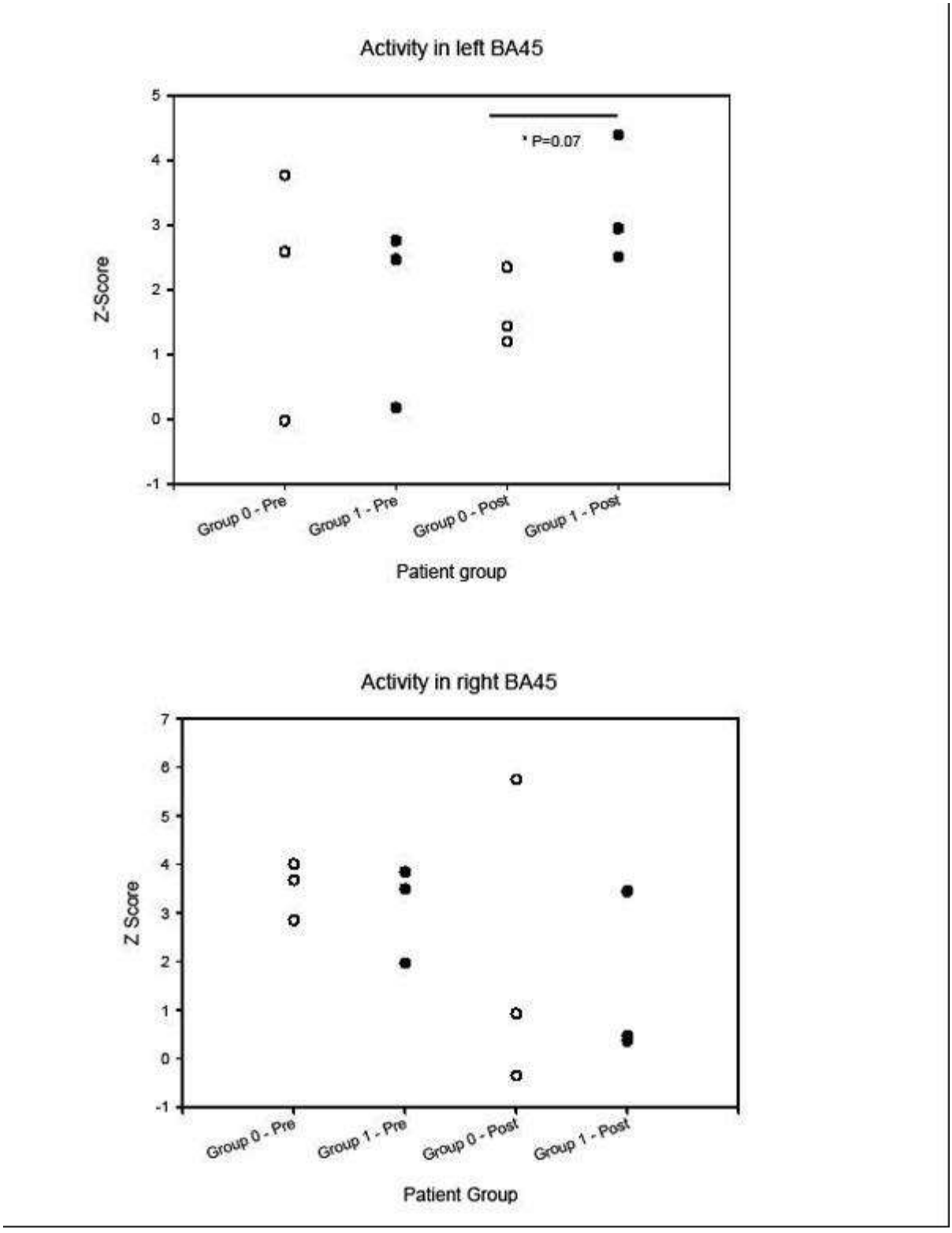
Activity in left BA45
Z-Score
5
4
3
2
1
0
-1
* P=0.07
Group 0 - Pre
Group 1 - Pre
Group 0 - Post
Group 1 - Post
Patient group
Activity in right BA45
Z Score
7
6
5
4
3
2
1
0
-1
Group 0 - Pre
Group 1 - Pre
Group 0 - Post
Group 1 - Post
Patient Group

[Figure 1]

93

Brain Poster Session: Blood-Brain Barrier

CURCUMIN REDUCES MATRIX METALLOPROTEINASE-9 EXPRESSION AND AMELIORATES BLOOD BRAIN BARRIER DYSFUNCTION IN STROKE

N. Tyagi, S. Kundu, S. Givvimani, W. Gillespie, P. Mishra, L. Lominadze, S. Tyagi

Physiology & Biophysics, University of Louisville, Louisville, KY, USA

Purpose: Curcumin, a yellow polyphenolic compound from the plant Curcuma ionga, is a commonly used spice and coloring agent with beneficial effects of anti-tumor, anti-inflammatory, and antioxidant activities. The objective of this study was to determine whether curcumin ameliorates blood-brain barrier (BBB) dysfunction in stroke by reducing matrix metalloproteinase in hyperhomocystemic mice.

Methods: Stroke was induced by a 1-h middle cerebral artery (MCA) occlusion using an intraluminal filament in all groups. Brain infarction was measured and neurological deficits were scored. BBB dysfunction was determined by examining brain edema and Evans Blue extravasation. Expression of collagen IV, the major component of basal lamina essential for maintenance of the endothelial permeability barrier, was quantitatively detected by Western blot and immunocytochemistry. Temporal relationship of expression of MMP-9 and its endogenous inhibitor, the tissue inhibitors of metalloproteinase-1 (TIMP-1), was determined by real-time PCR for mRNA and Western blot for protein during reperfusion.

Results: Brain edema and Evans Blue leakage were both significantly ($P< 0.01$) reduced after stroke in the curcumin treated group as compared to hyperhomocystemic group, in association with reduced brain infarct volume and neurological deficits. Western blot analysis indicated that curcumin enhanced collagen IV expression and reduced the collagen loss after stroke. Immunocytochemistry demonstrated that collagen IV-labeled vessels were significantly ($P< 0.01$) increased in curcumin treated mice. The ex vivo study also revealed a key role of MMP-9 in curcumin treated mice-strengthened collagen IV expression against I/R injury. TIMP-1 protein levels were significantly ($P< 0.01$) increased by curcumin treatment.

Conclusion: These data demonstrate that curcumin effectively reduces brain injury by improving BBB function and enhancing basal lamina integrity in stroke. This study suggests a therapeutic role of dietary curcumin in patients with stroke.

Reference:

1. Cole GM, Teter B, Frautschy SA. Neuroprotective effects of curcumin. Adv Exp Med Biol. 2007;595:197-212.

2. Jiang J, Wang W, Sun YJ, Hu M, Li F, Zhu DY. Neuroprotective effect of curcumin on focal cerebral ischemic rats by preventing blood-brain barrier damage. Eur J Pharmacol. 2007 Apr 30;561(1-3):54-62.

3. Thiyagarajan M, Sharma SS. Neuroprotective effect of curcumin in middle cerebral artery occlusion induced focal cerebral ischemia in rats. Life Sci. 2004 Jan 9;74(8):969-85.

95

Brain Poster Session: Experimental Cerebral Ischemia: Vascular & Endothelial

ESSENTIAL ROLE OF INTERLEUKIN-6 FOR POST-STROKE ANGIOGENESIS

K. Gertz[1], G. Kronenberg[1], T. Baldinger[1], M. Balkaya[1], C. Werner[2], U. Laufs[2], M. Endres[1]

[1]Experimental Neurology, Charité - University Medicine Berlin, Berlin, [2]Department of Internal Medicine, University of Saarland, Homburg, Germany

Background: There is a paucity of studies investigating longer-term endpoints after brain ischemia. The pleiotropic cytokine interleukin (IL)-6 mediates multiple effects which may be both beneficial and detrimental to the injured brain. Here, we pursued the hypothesis that IL-6 is an essential part of the regenerative long-term response of the brain to cerebral ischemia - and in particular plays a role for post-stroke angiogenesis.

Methods: We investigated the influence of IL-6 on long-term outcome in a well-characterized model of mild ischemic stroke. To do so, IL-6 knockout vs. wildtype mice (C57Bl6 background) were subjected to 30 minutes of middle cerebral artery occlusion (MCAo) followed by up to four weeks of reperfusion. Proliferating cells were pulse-labelled with bromodeoxyuridine (BrdU). Functional outcome was assessed by Morris water maze. Following sacrifice we determined ischemic lesion size and performed immunohistological studies. Additionally, we counted vessel density via Evans blue perfusion signal and measured VEGF-levels in serum. Because endothelium-derived nitric oxide (NO) is known to be essential for the growth of new vessels, we also measured protein levels of endothelial nitric oxide synthase (eNOS) in brain, aorta and myocardial tissue. In wildtype mice we evaluated time-dependent regulation of inflammatory cytokines IL-1beta, IL-6, tumor necrosis factor (TNF)-alpha and the IL-6-receptor (IL-6R) as well as gp130.

Results: While there was a significant up-regulation of TNF-alpha and IL-1beta mRNA at early time-points after ischemia, both IL-6R and gp130, and to a lesser extent also IL-6 itself, showed a delayed up-regulation up to four weeks after MCAo/reperfusion. Whereas in wildtype mice, eNOS and VEGF protein levels were significantly elevated at two days after MCAo/reperfusion, this effect was absent in IL-6 deficient animals. At four weeks after MCAo IL-6 knockout mice showed significantly lower BrdU+ cell density in ischemic striatum. Importantly, not only the number of BrdU/Iba-1 double labelled cells was reduced within the ischemic lesion of IL-6 deficient mice, but also the number of newly generated endothelial cells (2.6-fold decrease compared to wildtype mice; $p< 0.05$). In addition, while in wildtype animals the density of perfused microvessels within the ischemic lesion was significantly increased compared to the contralateral side this effect was completely absent in IL-6 knockout mice.Interestingly, this failure in post-stroke angiogenesis in IL-6 knockout mice was associated with significant long-term functional and cognitive impairment assessed with Morris water maze. In the place task, latencies to find the platform were significantly longer in IL-6-deficient mice. In the probe trial, IL-6-deficient animals visited the target zone more frequently in the latter 60 sec of the trial, indicative of a distinct deficit in strategy-switching. In addition, at 4 weeks after MCAo IL-6 knockout mice presented larger lesions compared to wildtype mice while acute lesion size at two days was not significantly different.

Conclusion: We demonstrate that loss of IL-6 results in impaired long-term histological and functional protection four weeks after cerebral ischemia. IL-6 augments inflammation and angiogenesis during the chronic phase after brain ischemia, and this is associated with improved recovery. These effects may in part been mediated by eNOS.

97

Brain Poster Session: Neonatal Ischemia

ABNORMAL RESPONSES OF THALAMOCORTICAL NEURONS AFTER ASPHYXIAL CARDIAC ARREST IN DEVELOPING RATS

M. Shoykhet[1,2], D.J. Simons[3], P.M. Kochanek[1,2], R.S. Clark[1,2]

[1]Critical Care, University of Pittsburgh School of Medicine, [2]Safar Center for Resuscitation Research, University of Pittsburgh, [3]Neurobiology, University of Pittsburgh School of Medicine, Pittsburgh, PA, USA

Background: Children who survive cardiac arrest (CA) often suffer from devastating neurologic consequences. Yet, how CA disrupts behaviorally-relevant neuronal circuits during development remains unknown. The rat somatosensory system is well-suited for defining in vivo neuronal function after CA because it mediates sophisticated sensorimotor behaviors and because its thalamocortical circuitry is well characterized. Neurons in the thalamic ventrobasal (VB) nucleus receive sensory input, process it, and relay it to the cerebral cortex. Neurons in the thalamic reticular (RT) nucleus provide essential inhibitory regulation of VB neurons. RT neurons are thought to be particularly vulnerable to hypoxic-ischemic insult. However, the extent of this vulnerability and its impact on functional organization of developing thalamic circuitry are unknown.

Objective: To characterize responses of VB neurons to tactile stimuli after asphyxial CA in developing rats.

Design/methods: Postnatal day 17 rats underwent either sham insult or asphyxial CA followed by clinically-realistic resuscitation. Two to 3 days post-CA, we utilized extracellular microelectrodes to record responses of single VB neurons to controlled whisker deflections in different directions. Spontaneous and evoked firing rates, as well as firing evoked by movements of different whiskers in multiple directions were compared in sham and CA rats. After recordings, the rats were anesthetized, and the brains were fixed for immunohistochemical analyses.

Results: We recorded responses of 21 and 28 VB neurons in 3 sham and 3 CA rats, respectively. VB neurons in CA animals, like those in sham rats, have a clearly-identifiable response to one or a few neighboring whiskers. However, after CA, VB neurons display abnormally high spontaneous and whisker-evoked firing rates. VB neurons are also somewhat less selective for whisker movement in different directions in CA vs sham rats. In addition, responses occur at longer latency post-CA, suggesting abnormalities in response timing.

Conclusions: Results suggest that thalamic input to the cerebral cortex is abnormal in survivors of asphyxial CA. Our preliminary findings are consistent with injury to inhibitory RT neurons and suggest that the thalamus is a potentially important therapeutic target after asphyxial CA. Further characterization of post-CA thalamic neuropathology and alteration in thalamocortical circuit function are ongoing.

103

Brain Poster Session: Neuroprotection

KETAMINE DECREASED ISCHEMIC NEURONAL DAMAGE BY SHORTENING THE DURATION OF ISCHEMIC DEPOLARIZATION; QUANTITATIVE EVALUATION IN GERBILS

H. Taninishi, Y. Takeda, T. Sasaki, K. Shiraishi, K. Morita

Anesthesiology and Resuscitology, Okayama University Medical School, Okayama-city, Japan

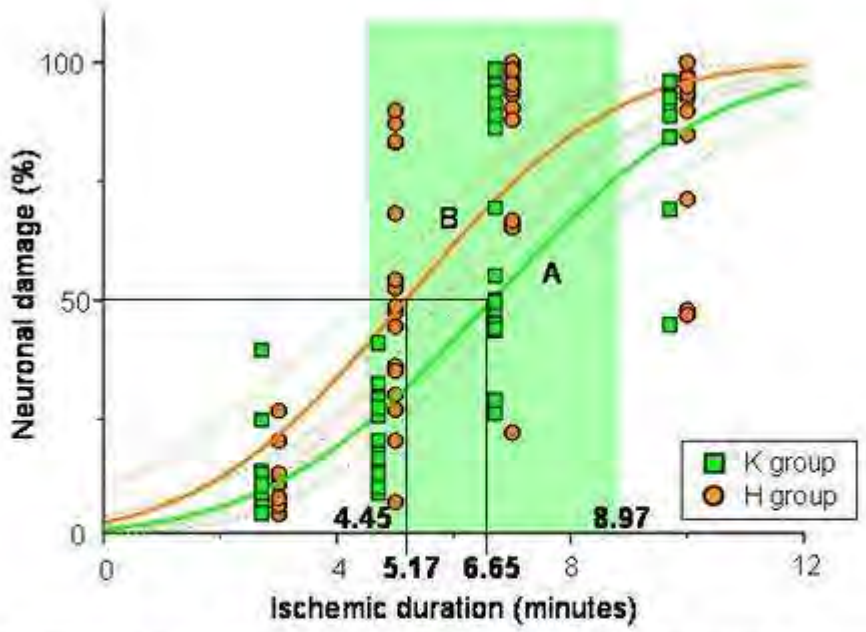

Figure: *Relationship between neuronal damage and ischemic duration. The logistic regression curves show close relationships between damaged neurons and ischemic duration (K group (line A, rectangles), r^2=0.60, p<0.0001, H group (line B, circles), r^2=0.52, p<0.0001). P50-ischemia in the K group and H group were 6.65 and 5.17 minutes respectively. The 95% confidence intervals (dashed lines) were not overlapped from 4.45 to 8.97 minutes of ischemic duration, suggesting that there is a significant difference in the two groups during this ischemic duration.*

[Figure P50 ischemia]

Objectives: The effect of ketamine on ischemic neuronal damage was quantitatively evaluated. For this purpose, ischemia of four different intensities was induced in the same experimental model, and ischemic duration necessary for 50% neuronal damage (P50-ischemia) and duration of ischemic depolarization necessary for 50% neuronal damage (P50-depolarization) were determined.

Materials and methods: In 30% oxygen, sixty male gerbils were randomly assigned to a group receiving 1% halothane (H group; n = 30) and a group receiving 1 mg/kg/min of intravenous ketamine (K group; n = 30) Forebrain ischemia was initiated by occlusion of bilateral common carotid arteries for 3, 5, 7 or 10 minutes (n = 6 in each group for 3 or 10 minutes of ischemia, n = 9 in each group for 5 or 7 minutes of ischemia). Duration of ischemic depolarization was recorded from the bilateral hippocampal CA1 regions. Histological outcome in the bilateral hippocampal CA1 region was evaluated five days after the ischemia. During the experimental period, cerebral and rectal

temperatures were maintained at 37.0 ± 0.5 °C. Relationships of neuronal damage with ischemic duration and duration of ischemic depolarization were shown by probit curves, and P50-ischemia and P50-depolarization were determined. Statistical analysis was performed with multiple comparisons followed by Scheffe's test. A level of $p < 0.05$ was considered to be significant.

Results: Duration of ischemic depolarization in the K group was shorter than that in the H group in each ischemic duration, and the difference in the case of 7 minutes of ischemia was significant (K group vs. H group: 7.50 ± 1.91 minutes vs. 10.01 ± 1.86 minutes). With 5 and 7 minutes of ischemia, the percentages of neuronal damage in the K group (21.2 ± 8.2 % and 63.1 ± 24.7 %, respectively) were significantly lower than those in the H group (50.9 ± 23.8 % and 86.5 ± 19.9 %, respectively). P-50 ischemia in the K group and that in the H group were 6.65 minutes and 5.17 minutes, respectively. P-50 depolarization in the K group and that in the H group were 7.23 minutes and 6.69 minutes, respectively.

Conclusion: Administration of ketamine decreased ischemic neuronal damage. Since duration of ischemic depolarization affects the degree of ischemic neuronal damage[1)], reduction in the duration of ischemic depolarization was a factor that contributed to the decrease in neuronal damage by ketamine rather than factors occurring after the onset of ischemic depolarization.

Reference: 1) Li J, et al. J Neurosurg Anesthesiol 12: 247-54. 2000.

104

Brain Poster Session: Neonatal Ischemia

COLOR-CODED PULSED DOPPLER ULTRASOUND IMAGING PREDICTS ISCHEMIC CEREBRAL LESION IN RAT PUPS

C. Charriaut-Marlangue[1], N. Deroide[2], S. Renolleau[1], P.-L. Leger[1], S. Fau[1], P. Bonnin[2]

[1]NPA - Case 14, UMR-CNRS 7102, [2]Hôpital Lariboisière, Physiologie - Explorations Fonctionnelles, Paris, France

Background and aims: Models of ischemic brain lesion in neonatal rats displayed heterogeneous lesion volumes. Moreover, several rat pups could present an absence of brain lesion, whenever ischemic procedure is well applied. Because of those variations, neuroprotection studies need numerous animals to demonstrate any significant inter-group difference. Color-coded duplex ultrasound give access to measurement of blood flow velocities in cerebral arteries in small animals. We tested whether absence of cerebral lesion could depend on intra cerebral hemodynamic adaptations during and/or after procedure of cerebral ischemia-reperfusion.

Methods: Blood flow velocities of cerebral arteries were measured by ultrasound imaging (Bonnin et al., 2008) in 39 anaesthetized (chloral hydrate 350 mg/kg) Wistar 7 day-old rats:

1. before,
2. during permanent left middle cerebral artery and transient left common carotid artery (50 min) occlusions (Renolleau et al., 1998) and
3. after release of occlusion of the left common carotid artery.

Results: Forty-eight % of rats did not present an ischemic brain lesion. In those rats, ultrasound imaging evidenced:

1. an early rise of the blood flow velocities in large upstream arteries and
2. increased blood flow velocities in Willis's circle arteries giving anastomoses to the left MCA territory.

Conclusions: Ultrasound imaging can predict the absence of ischemic cerebral lesion despite arterial occlusions. Homogeneous groups of rat pups all presenting ischemic brain lesions can be built, making, thus, preclinical neuroprotection studies easier, less time-consuming and more specific and cost-effective by lowering the intra-group variations and the required number of animals.

107

Brain Oral Session: Blood Brain Barrier

MICROGLIA CONTRIBUTE TO SEPSIS INDUCED INJURY TO BBB COMPONENTS VIA THE NF-κ B, JAK-STAT AND MAP KINASE PATHWAYS

R. Kacimi[1], R. Giffard[2], M. Yenari[3]

[1]Neurology Department, University of California San Francisco and Stanford University, San Francisco, [2]Department of Anesthesia, Stanford University, Stanford, [3]Neurology Department, University of California San Francisco, San Francisco, CA, USA

Cerebral inflammation can lead to stress-induced cell death during sepsis and exacerbates injury during ischemia and stroke. Microgliosis or microglia activation and subsequent inflammatory mediator release can promote neurovascular dysfunction in the injured brain. The present study was undertaken to evaluate whether iNOS signaling modulation is a prosurvival strategy in endotoxin-activated microglia. We used 3 cell types (microglia BV2, bEND.3 endothelial cell and primary astrocytes) studied either alone or in co-culture to assess whether BV2 cells potentiates injury to microvascular bEND.3. LPS was highly effective in stimulating NO production in BV2 cells. LPS also induced de novo synthesis of iNOS protein. Furthermore, viability assays showed that LPS induced cell death under these conditions. Moreover, NO and the peroxynitrite donor SIN-1 induced dose dependent NO accumulation and mimiked LPS induced nitrosative stress. While oxidative stress (OGD or H_2O_2) increased bEND.3 permeability and induced cell death, LPS had no effect on eNOS/NO or viability in bEND.3 microvascular endothelial cells alone. Interestingly, in co-culture with BV2 and bEND.3 cells, microglia induced monolayer disruption after LPS exposure. Pretreatment with NOS inhibitors (L-NMMA and aminoguanidine, $p< 0.01$), ROS inhibitors (apocynin and allopurinol, $p< 0.01$), and minocycline ($p< 0.01$) to prevent microglia activation, prevented bEND.3 injury in co-culture. We further assessed the signaling implicated in iNOS/NO activation. Inhibitors of NF-κB and JAK-STAT (PDTC and AG490) respectively, abrogated NO accumulation. While Worthmanin, PD9805, SB203850 (PI3K, ERK, and p38 kinase inhibitors) respectively did not prevent NO accumulation by LPS in BV2 cells. SP600125, a C-jun N-terminal kinase (JNKs/SAPKs) inhibitor, however, partially prevented NO accumulation. Conversely, NF-kB, JAK/STAT, JNKs/SAPKs pathways blockade were shown to be protective against LPS induced cell death (60 to 70% viable cell vs. 20% in LPS treated cell, $p < 0.01$). Our data show that differential signaling pathways mediates endotoxin- dependent activation of inducible nitric oxide synthase involving transcription factor NF- κB and JAK-STAT. Our data confort the importance of microglia iNOS in inflammation induced injury. This possibility is emphasized by the observation that its modulation prevents the underlying oxidative/nitrosative stress induced injury in brain murine microglia BV2 cells. We also show that activated microglia -induced blood barrier disruption and microvascular endothelial cell death in co-culture model. In a similar fashion as NOS inhibitors (that inhibits NOS activity) ROS inhibitors (apocynin, allopurinol), JAK-STAT and NF-κB and JNK signaling pathways appears to be potent negative regulator of iNOS expression and/or NOS activity and show to be useful anti-inflammatory strategy to confer cytoprotection to maintain the integrity of BBB vascular unit. Our observations also shed light on new pathways that may be potential therapeutic targets to modify pro-inflammatory responses leading to increased damage of the BBB and its subsequent neuronal damage during sepsis, cerebral ischemia and stroke.

109

Brain Poster Session: Neuroprotection

IS THERE ANY UNCOUPLING OF NOS DURING CEREBRAL ISCHEMIA AND REPERFUSION? (NO PRODUCTION, HYDROXYL RADICAL METABOLISM IN MICE)

M. Yamazato[1], N. Araki[2], Y. Asano[2], K. Hattori[2], Y. Ito[2], Y. Kato[2], H. Nagoya[2], T. Ohkubo[2], T. Shimazu[2], K. Shimazu[2]

[1]Department of Neurology, Saitama Medical School, Medical Center, Saitama, [2]Department of Neulorogy, Saitama Medical University, Moroyama, Japan

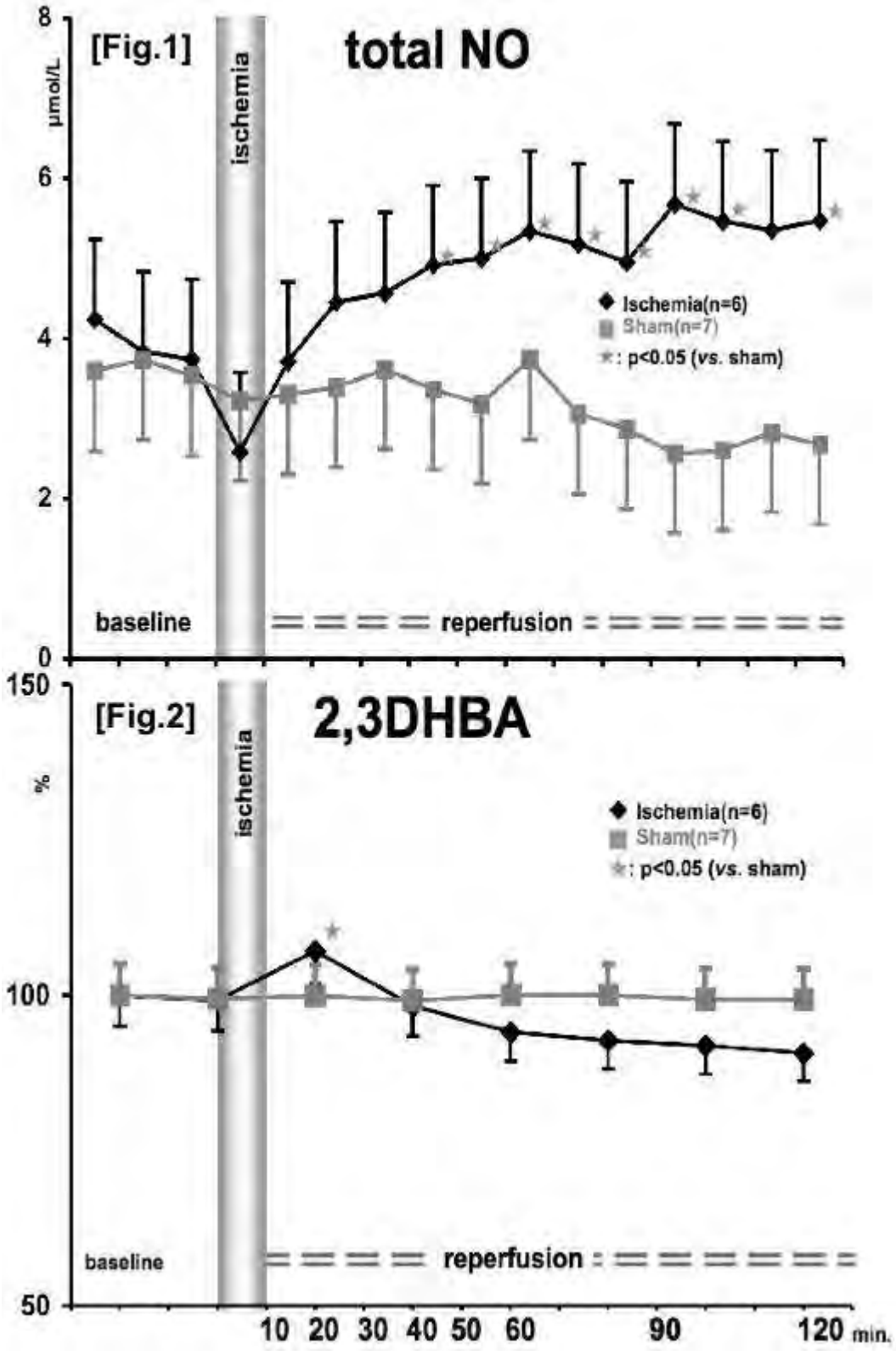

[yamazato`s]

Objectives: The transformation of eNOS from a protective enzyme to uncoupled eNOS, which is a contributor of oxidative stress, has been observed in several in vitro models[1]. The purpose of this study was to measure both hydroxyl radical and nitric oxide simultaneously in brain during cerebral ischemia and reperfusion, in order to analyze the uncoupling of eNOS.

Methods: Thirteen male C57BL/6 mice were used. Both NO production and hydroxyl radical metabolism were continuously monitored by in vivo microdialysis. Microdialysis probes were inserted into the bilateral striatum. The in vivo salicylate trapping method was applied for monitoring hydroxyl radical formation via 2,3 dihydroxybenzoic acid (2,3-DHBA), and 2,5 dihydroxybenzoic acid (2,5-DHBA). A laser Doppler probe was placed on the skull surface. Blood pressure, blood gases and temperature were monitored and maintained within normal ranges throughout the procedure. Forebrain cerebral ischemia was produced in 7 mice (ischemia group) by occlusion of both common carotid arteries for 10 minutes. Six mice were used as sham group. Levels of nitric oxide metabolites, nitrite (NO_2^-) and nitrate (NO_3^-), in the dialysate were determined using the Griess reaction.

Results:

1. Blood Pressure: Ischemia group (73.9 ±13.5, 84.7 ±10.7, 79.9 ±12.4, 79.5 ±12.9 mmHg, mean ±SD) showed significantly higher than that of the sham group (48.1±22.9, 47.2 ±22.3, 46.4 ±27.0, 57.5 ± 9.8) in 10 to 40 minutes after reperfusion ($p< 0.05$).
2. Cerebral blood flow: Ischemia group (16.2 ±11.0, 74.2 ±22.2, 68.2 ±13.0, 66.8 ±10.6%) showed significantly lower than that of sham group (99.9 ±4.3, 98.4 ±11.7, 98.5 ±11.1, 99.8 ±7.7) in ischemia and 30 to 50 minutes after reperfusion.
3. The level of $NO2^-$; There was no significant differences between the two groups.
4. The level of total NO ($NO2^- + NO3^-$) [Fig.1]: Ischemia group (4.9 ±1.0, 5.0 ±1.0, 5.3 ±0.8, 5.2 ±1.2, 5.0 ±1.2, 5.7 ±2.6, 5.5 ±2.7, 5.5 ±2.2μmol/L, mean ±SD) showed significantly higher than that of sham group (3.7 ±0.98, 3.2 ±0.6, 3.7 ±0.9, 3.1 ±0.7, 2.9 ±0.8, 3.0 ±0.5, 3.0 ±0.7, 3.1 ±0.6) in 40-100 and 120minutes after reperfusion ($p< 0.05$).
5. The level of 2,3DHBA [Fig.2]: Ischemia group (107.1±7.4%, mean ±SD)showed significantly higher than that of sham group (99.9±3.2) in 10minutes after reperfusion ($p< 0.05$).
6. The level of 2,5DHBA was no significant differences between the two groups.

Conclusion: Although NO production increased continuously after cerebral ischemia and reperfusion, hydroxyl radical increased temporarily after the start of reperfusion. These data suggests that uncoupling of NOS may play a little role in cerebral ischemia and reperfusion.

References: [1] Forstermann U, et al: Circulation 2006;113:1708-1714.

111

Brain Poster Session: Neurologic Disease

MACHANISMS ASSOCIATED WITH ALZHEIMER'S DISEASE IN ISCHEMIC HIPPOCAMPUS DEGENERATION

M. Ułamek[1], M. Jabłoński[2], R. Pluta[1]

[1]Neurodegenerative Disorders, Mossakowski Medical Research Centre, Polish Academy of Sciences, Warsaw, [2]Orthopedic and Rehabilitation, Skubiszewski Medical University of Lublin, Lublin, Poland

Objectives: For several reasons the favored brain sector for the investigation of ischemic degeneration is the hippocampus. First of all the hippocampus is the region which displays the characteristic neuropathology in ischemic and Alzheimer's brain. Second the hippocampus is implicated in spatial learning and memory. Third the hippocampus especially its sector CA1 is one of the brain areas very sensitive to ischemic and Alzheimer's injury. Finally the relationship of etiology and between ischemic injury dementia and Alzheimer's disease type dementia are recently much debated. Moreover the characterization of the neuronal cells death in ischemic hippocampus is crucial for the development of new effective therapies for both diseases. Additionally brain ischemia is well known for its ability to influence the function of the blood-brain barrier. We assessed blood-brain barrier permeability for horseradish peroxidase and different parts of amyloid precursor protein in animal hippocampus exposed to global brain ischemia.

Methods: Using rats (n=10) blood-brain barrier and amyloid precursor protein changes were studied after 10 min brain ischemia [1] with 6 months survival. As controls sham-operated animals (n=6) were sacrificed in due time. Rats were perfusion fixed for these investigations. Five brains were cut at 60 μm slices in the coronal plane by a vibratome for horseradish peroxidase staining [2]. Next after putting slices on microscope slides they were investigated. Paraffin sections from other 5 brains were selected for amyloid precursor protein staining [3] and structural studies. Control brains went through the same procedures as ischemic.

Results: The blood-brain barrier leakage especially in the medial part of the hippocampus was associated with increased staining of C-terminal of amyloid precursor protein/β-amyloid peptide in perivascular space. At 6 months after ischemia in CA1 area complete pyramidal neurons loss was noted in 93% of brains. At 7% of brains we observed incomplete neuronal loss with degenerating neurons in a trace of the hippocampal CA1 pyramidal cell layer. Additionally acute and chronic neuronal degeneration appeared in CA2, CA3 and CA4 areas and dentate gyrus that were not involved in early pathology. Atrophy of the hippocampus was found after ischemia. Generally atrophic hippocampus is indicative of an active progressing neurodegenerative processes.

Conclusions: These data indicate that late neurotoxic C-terminal of amyloid precursor protein and β-amyloid peptide accumulation around blood-brain barrier vessels in hippocampus postischemia may represent a secondary injuring process that could exacerbate stroke outcome by additional delayed neuronal death with development dementia [4]. Prolongation of survival time results in neuronal changes within hippocampal areas of non-selective vulnerability. These data also suggest that gradual accumulation of above proteins and the amount accumulation correlate very well with extent of pathology in hippocampus and survival time after ischemia [4]. It is looking that amyloid precursor protein products control neurodegeneration in ischemic hippocampus.

References:

1) Pluta R et al.: Acta Neuropathol., 83:1-11,1991.

2) Pluta R et al.: Brain Res., 633:41-52,1994.

3) Pluta R et al.: Brain Res., 649:323-328,1994.

4) Pluta R.: Ischemia-reperfusion pathways in Alzheimer's disease. Nova Science Publishers, New York. 2007.

112

Brain Poster Session: Experimental Cerebral Ischemia: Vascular & Endothelial

NORMOBARIC HYPEROXIA ATTENUATES BLOOD BRAIN BARRIER DISRUPTION BY INHIBITING MATRIX METALLOPROTEINASE-9 IN TRANSIENT FOCAL CEREBRAL ISCHEMIA

W. Liu[1], J. Hendren[1], R. Sood[2], Q. Chen[1], X. Qin[1], K.J. Liu[1,2]

[1]College of Pharmacy, [2]Department of Neurology, University of New Mexico, Albuquerque, NM, USA

Objectives: Using in vivo electron paramagnetic resonance oximetry, we have shown that normobaric hyperoxia (NBO) treatment during ischemia can maintain penumbral tissue oxygenation at the physiological level, which leads to a significant reduction in stroke lesion volumes in ischemic stroke[1, 2]. In this study, we evaluated the effect of NBO on blood brain barrier (BBB) damage and the underlying mechanisms using a rat model of transient focal cerebral ischemia.

Methods: Rats were subjected to NBO (95% O_2) or normoxia (21% O_2) during 90

min filament occlusion of the middle cerebral artery (MCAO), followed by 3 or 22.5 hrs of reperfusion. Infarction volume was evaluated by MRI apparent diffusion coefficient (ADC) analysis and 2,3,5-triphenyltetrazolium chloride (TTC) stain. BBB damage was assessed by measuring Evan's blue extravasation or the permeability coefficient with MRI in ischemic brain. Western blot and immunohistochemistry were used to analyze the protein levels of tight junction protein occludin and NADPH oxidase in the cerebral microvessels. Matrix metalloproteinase-9 (MMP-9) was analyzed by in situ and gel gelatin zymography.

Results: NBO treatment during ischemia significantly reduced infarction volume, Evan's blue extravasation, BBB permeability and brain edema in the ischemic brain after 90-min MCAO with 3 or 22.5 hrs of reperfusion. At the early reperfusion time point (3 hr), we observed that Evan's blue leakage was accompanied by increased gelatinolytic activity and reduced immunostaining for tight junction protein occludin. Moreover, incubation of brain slices or isolated microvessels with purified MMP-9 revealed specific degradation of occludin. At late reperfusion time point (22.5 hr), MMP-9 induction concurrently occurred with the upregulation of NADPH oxidase catalytic subunit $gp91^{phox}$ in the ischemic cerebral microvessels. Gel gelatin zymography identified that MMP-9, but not MMP-2, was the major gelatinotylic enzyme in the cerebral microvessels. Inhibition of NADPH oxidase with apocynin reduced MMP-9 increase, supporting a causal link between NADPH oxidase-derived superoxide and MMP-9 induction in the BBB microvasculature at late reperfusion (22.5 hr). Importantly, NBO treatment significantly inhibited MMP-9 induction in the ischemic cerebral microvessels under both experimental stroke conditions.

Conclusions: Our results indicate that NBO treatment protects BBB integrity in focal cerebral ischemia, and its inhibitory actions on NADPH oxidase and MMP-9-mediated tight junction disruption may represent important mechanisms for this protection.

Key words: Normobaric hyperoxia, cerebral ischemia, matrix metalloproteinases, NADDPH oxidase, occludin.

Reference:

1. Liu S, Liu W, Ding W, Miyake M, Rosenberg GA, Liu KJ. Electron paramagnetic resonance-guided normobaric hyperoxia treatment protects the brain by maintaining penumbral oxygenation in a rat model of transient focal cerebral ischemia. J Cereb Blood Flow Metab. 2006;26:1274-1284.

2. Liu S, Shi H, Liu W, Furuichi T, Timmins GS, Liu KJ. Interstitial po2 in ischemic penumbra and core are differentially affected following transient focal cerebral ischemia in rats. J Cereb Blood Flow Metab. 2004;24:343-349.

113

Brain Poster Session: Experimental Cerebral Ischemia: Blood Flow & Metabolism

OCCLUSION OF SINGLE CORTICAL VENULES RESULTS IN DECREASED BLOOD FLOW IN UPSTREAM CAPILLARIES

J. Nguyen[1], N. Nishimura[1], C. Iadecola[2], C. Schaffer[1]

[1]Biomedical Engineering, Cornell University, Ithaca, [2]Neurology and Neuroscience, Weill Cornell Medical College, New York, NY, USA

Background and aims: Microvascular lesions in the brain play an important role in the development of cognitive decline [1]. While recent animal models of small strokes have investigated the changes in blood flow that result from the occlusion of cortical arterioles and capillaries, the redistribution of blood flow following a venule occlusion remains poorly understood. This is largely due to the lack of an appropriate animal model. To study the consequences of single venule occlusions on cortical blood flow we use nonlinear optical techniques to induce clot formation in targeted venules and to study blood flow changes in upstream capillary beds.

Methods: Through a craniotomy in urethane-anesthetized rats, vascular topology (Fig.1a) and blood flow is measured using two-photon excited fluorescence microscopy of intravenously injected fluorescein-dextran. Blood flow velocity is determined by tracking the motion of unlabeled red blood cells. Occlusions are induced by tightly focusing high intensity, femtosecond laser pulses into a targeted venule. Nonlinear absorption of the laser energy in the focal volume injures the vessel wall, initiating the natural clotting cascade (Fig.1b) [2].

Results: Measurements of blood flow in brain capillaries were taken before and after the occlusion of an ascending venule, i.e. a venule that brings flow from the cortical capillary beds to a vein on the brain surface (Fig.1c). For capillaries one and two branches upstream from the clotted venule, flow decreased to 20% +/- 3% (average +/- SEM; 16 clots across 16 rats; $p < 0.001$, one-way t-test) of baseline value, while for vessels three and four branches upstream, speed decreased to 51% +/- 7% ($p < 0.001$) of baseline. Additionly, we observed reversed blood flow in 55% of the capillaries one or two branches upstream from the occlusion (red arrows, Fig.1c).

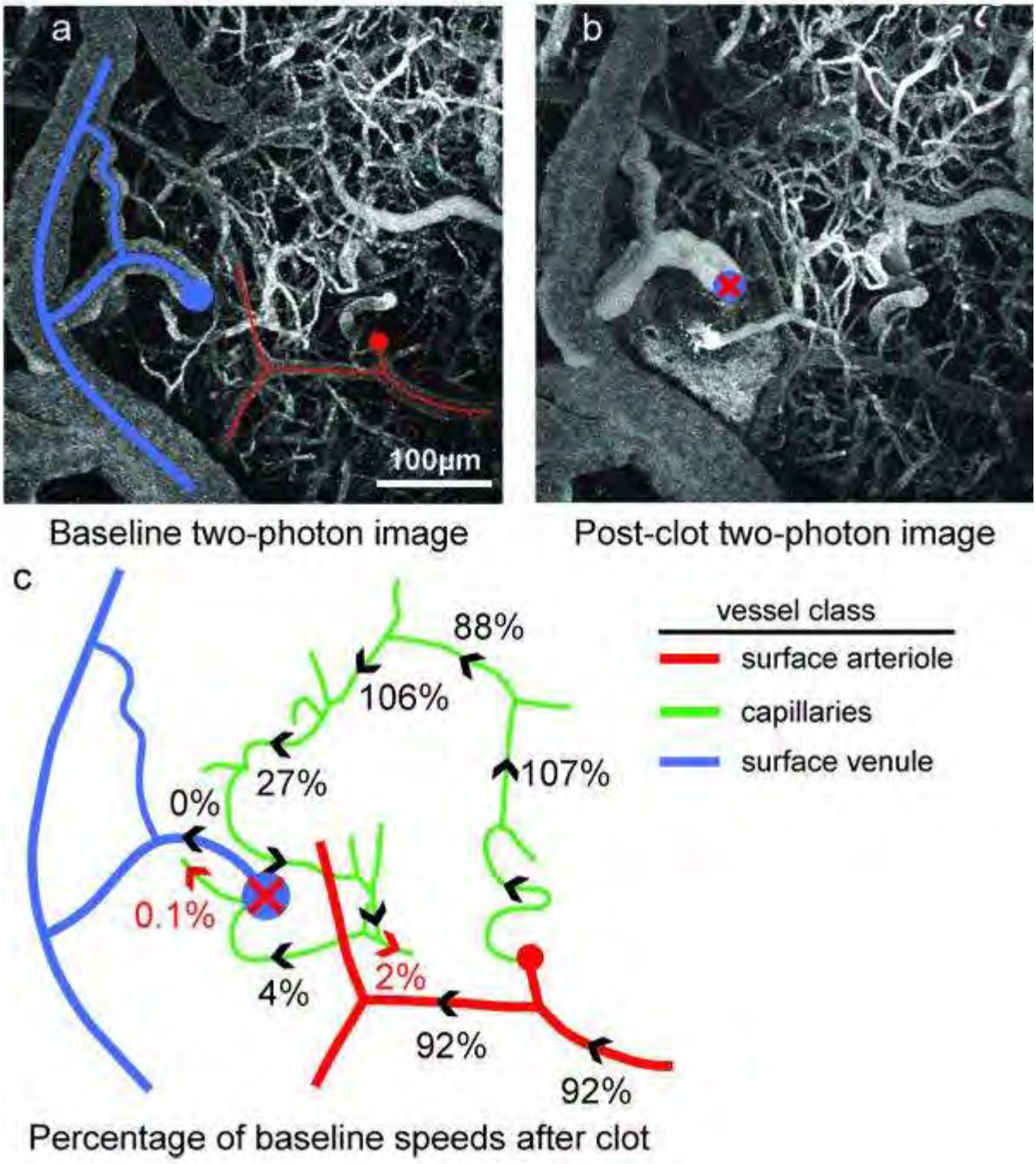

[Case study of an ascending venule occllusion]

Figure 1. Case study of flow changes in capillaries after the occlusion of an ascending venule.

a. Baseline two-photon image of vasculature. Surface venule and arteriole outlined in blue and red, respectively. Red circle indicates a penetrating arteriole and blue circle represents an ascending venule.
b. Post-clot two-photon image. Red "X" indicates location of clot.

c. Mapped vessel network with flow speed after the clot as a percentage of baseline speed in individual vessels. Red arrows indicate vessels that have reversed flow direction after clot.

Conclusions: This reduction in blood flow speed suggests that occlusion of a single venule perturbs microvascular flow in upstream capillaries over a relatively large vascular territory. Such previously unrecognized reduction in flow can deprive nearby neurons of the nutrients required for normal function leading to cell injury and death, and may potentially play a role in the brain lesions responsible for cognitive decline.

References:

[1] Vermeer et. al. NEJM, 348:1215, 2003.

[2] Nishimura et. al. Nat. Meth., 3:99, 2006.

114

Brain Poster Session: Experimental Cerebral Ischemia: In Vitro

PROTEASOME INHIBITION BY LACTACYSTIN IN AN OPTIMAL CONCENTRATION PROTECTS NEURONAL CELLS FROM ISCHEMIA AND REPERFUSION INJURY IN VITRO

R. Liu, T. Urabe, K. Yamashiro, N. Hattori

Neurology, Juntendo University School of Medicine, Tokyo, Japan

Objectives: We have reported the magnitude of an intrinsic neuroprotectant, erythropoirtin (EPO) and its transcription factor hypoxia inducible factor-1 (HIF-1) α. However, reoxygenation significantly degraded HIF-1α activation, reduced subsequent transcription of EPO. In the present study, we design to investigate the neuroprotective effect of proteasome inhibition by Lactacystin against ischemia/reperfusion injury.

Methods: Primary cultures of cerebral cortical cells were obtained from embryos (E 16-17) of Wistar rats. In vitro ischemia/reperfusion was induced by hypoxia (2%) and reoxygenation using primary cerebral cortical culture cells. Cortical cultures were treated with 0.1-60μM lactacystin (Calbiochem, CA), a specific inhibitor of the proteasome, for 24h under normoxic or hypoxia/reoxygenation condition before hypoxia or after onset of reoxygenation. The neuronal survival was assessment by immunofluorescence staining of PI and FDA, and the expression of HIF-1a as well as EPO protein and was detected by Reverse transcription-polymerase chain reaction (RT-PCR) and Western blotting analysis in culture cells under normoxia, 6h hypoxia followed 24h reoxygenation only without lactacystin treatment (H6R24 Lac-), and the same period of hypoxia/reoxygenation with lactacysticn (H6R24 Lac+).

Results: We found that lactacystin is contributed to block the degradation of HIF-1α and EPO during oxygenation by using immuoblot analysis and RT-PCR. We also determined that near-complete blockade of proteasome activity (< 5%) by Lactacystin (≥20μM) during reoxygenation or throughout hypoxia/reoxygenation improved neuronal survival to a range to 61.2% or 47.9% respectively, compared with that of 6h hypoxia followed 24h oxygenation only without Lactacytin treatment (24.3%, P< 0.001~0.0001). Our results indicated that application of Lactacystin in an optimal Aconcentration dose promote an neuronprotective effect against in vitro ischemia/reperfusion injury, and interfering with the progression of apoptosis might partially by preventing degradation of HIF-1α and EPO.

Conclusion: Our initial studies confirmed the observations that proteasome inhibition by lactacystin especially during reoxygenation leads to an up-regulation of HIF-1a and EPO and promote as a neuroprotectant against ischemia/reperfusion injury. Our study suggests that the proteasome inhibition strategies is a potential therapeutic target for acute stroke.

References:

1. Liu R., Suzuki A., Guo Z., Mizuno Y.and Urabe T. (2006) Intrinsic and extrinsic erythropoietin enhances neuroprotection against ischemia and reperfusion injury in vitro. J Neurochem. 96. 1101-1110.

2. Meiners S., Heyken D., Weller A. et al. (2003) Inhibition of proteasome activity induces concerted expression of proteasome genes and de novo formation of. 3. Mammalian proteasomes. J. Biol. Chem. 278, 21 517-21 525.

4. Pasquini L. A., Besio M. M., Adamo A. M. et al. (2000) Lactacystin, a specific inhibitor of the

proteasome, induces apoptosis and activates caspase-3 in cultured cerebellar granule cells. J. Neurosci. Res. 59, 601-611.

5. Rideout H.J. and Stefanis L. (2002) Proteasomal inhibition-induced inclusion formation and death in cortical neurons require transcription and ubiquitination. Mol. Cell. Neurosci. 21, 223-238.

6. Sun J., Lee YE. and Gwag BJ. (2005) Induction and attenuation of neuronal apoptosis by proteasome inhibitors in murine cortical cell cultures. J Neurochem. 95, 684-694.

115

Brain Poster Session: Blood-Brain Barrier

EXPOSURE OF ENGINEERED NANOPARTICLES FROM METALS ALTERS CEREBRAL BLOOD FLOW, BLOOD-BRAIN BARRIER PERMEABILITY, BRAIN EDEMA AND INDUCES NEUROTOXICITY IN RATS

H.S. Sharma[1], A. Sharma[1], D.F. Muresanu[2]

[1]Surgical Sciences, Uppsala University Hospital, Uppsala, Sweden, [2]Neurology, University of Medicine & Pharmacy, Cluj-Napoca, Romania

Influence of nanoparticles on brain function in vivo situations is still not well known. It appears that the magnitude and intensity of exposure to nanoparticles from the environment, food and/or water could affect neuronal functions and eventually may lead to neurotoxicity. This hypothesis was examined in present investigation using systemic administration of engineered nanoparticles from metals, i.e., Al, Ag and Cu (≈50 to 60 nm) on neurotoxicity in rats and mice. Intraperitoneal (50 mg/kg), intravenous (30 mg/kg), intracarotid (2.5 mg/kg) or intracerebroventricular administration (20 μg) of nanoparticles significantly altered the blood-brain barrier (BBB) function to Evans blue and radioiodine in several regions of the brain and spinal cord following 24 h and 48 h after its administration. Marked decreases in local cerebral blood flow (CBF) and pronounced edema formation was seen in several brain and spinal cord areas associated with BBB leakage. Neuronal cell injuries, glial cell activation, heat shock protein (HSP 72 kD) expression and loss of myelinated fibers are quite common in these brain areas. These light microscopical changes were further confirmed using transmission electron microscopy. These pathological changes were most significant in mice compared to rats. Cu and Ag nanoparticles exerted marked effects on neuronal changes when administered in systemic circulation or into the brain ventricular spaces. Intraperitoneal administration was lest effective. Our results clearly demonstrate that that nanoparticles from metals by affecting regional CBF and BBB function are able to induce selective and specific neuronal, glial and myelin changes in the brain and spinal cord. This effect of nanoparticles on neurotoxicity, however, largely depends on the type of metals, route of administration and the species used.

ANAESTHETICS INFLUENCE CLOSED HEAD INJURY INDUCED BLOOD-BRAIN BARRIER DISRUPTION, CEREBRAL BLOOD FLOW, BRAIN EDEMA AND BRAIN PATHOLOGY

H.S. Sharma[1], L. Wiklund[1], R. Patnaik[1,2]

[1]Surgical Sciences, Uppsala University Hospital, Uppsala, Sweden, [2]Biomaterials, School of Bioengineering, Banaras Hindu University, Varanasi, India

Closed head injury (CHI) is a leading cause of death and induces severe neurological disability in surviving victims. In the United States alone the incidence of CHI admitted to hospitals is estimated to be at least 2000 per million populations and more than 400,000 new cases are added each year in which large number of victims demonstrates significant long-term disabilities. The effect of anesthetics on neurological outcomes in head injury patients and the potential benefits of total systemic anesthesia compared with volatile gas anesthesia on various brain functions are still not been well evaluated. This investigation was undertaken to study the development of brain pathology and functional outcome following a well-established model of closed head injury (CHI) in rats under different intravenous or volatile gas anesthesia. Since previous works from our laboratory shows a profound rise of plasma and brain serotonin level following CHI, the effect of different anesthetics on plasma and brain serotonin level in relation to changes in blood-brain barrier (BBB) permeability, brained mea development, alteration in cerebral blood flow (CBF) and brain pathology was also evaluated.

The CHI was produced by an impact of 0.224 N on the right parietal bone under volatile ether anesthesia or systemic ketamine, pentobarbital or equithesin anaesthesia administered intraperitoneally. The CHI was inflicted by dropping a weight of 114.6 g on the skull from a height of 20 cm through a guide tube. This concussive brain injury resulted in profound leakage of Evans blue and radioiodine tracers in both the hemispheres and underlying sub cortical tissues that closely correspond to brain edema formation and volume swelling at 5 h after the CHI. These changes were most pronounced in the contralateral cerebral hemisphere. At this time a marked decrease in the regional CBF was seen in both the hemispheres that was most marked in the contralateral side. The plasma and brain serotonin showed a pronounced increase and exhibited a good correlation with the edema formation. Profound cell damage is seen in many parts of the brain at 5 h that are most marked in left uninjured hemisphere compared to the right injured side. These pathophysiological changes were most marked when the CHI was produced under ether anesthesia compared to systemic anesthesia. Mild but significantly less pathological changes are seen when the injury was made under ketamine aesthesia compared to pentobarbital anesthesia. The equithesin anesthesia showed moderate brain pathology quite comparable to that seen under pentobarbital anesthesia. Interestingly, the plasma and brain serotonin levels were highly correlated with the development of brain edema in animals subjected to CHI under various anesthetics. This suggest that anesthetic stress plays important roles in inducing serotonin levels in the brain and plasma following brain injury that could be detrimental in brain pathology. The functional outcome as seen using rota rod performances or grid walking following CHI were most adversely affected under ether anesthesia followed by pentobarbital, equithesin and ketamine. This indicates that that anesthetics are able to markedly influence the functional and pathological outcome of CHI.

117

Brain Poster Session: Blood-Brain Barrier

CHRONIC EXPOSURE OF NANOPARTICLES EXACERBATE HYPERTHERMIA INDUCED BLOOD-BRAIN BARRIER BREAKDOWN, COGNITIVE DYSFUNCTION AND BRAIN PATHOLOGY. NEUROPROTECION BY NANOWIRED-ANTIOXIDANT COMPOUND H-290/51

D.F. Muresanu[1], A. Sharma[2], H.S. Sharma[2]

[1]Neurology, University of Medicine & Pharmacy, Cluj-Napoca, Romania, [2]Surgical Sciences, Uppsala University Hospital, Uppsala, Sweden

There are reasons to believe that nanoparticles in the ambient air is translocated to the autonomic nervous system via circulation or to the CNS through sensory nerves in the respiratory tract, and induce serious cardiovascular or neurological effects. Thus, the translocated nanoparticles in humans can enter rapidly into the deeper brain structures in short exposure time and induce brain dysfunction. However, the possibility that chronic exposure of nanoparticles may alter stress reaction following hyperthermia and brain pathology is still not known. In this investigation, we examined the effects of chronic exposure of engineered nanoparticles from metals in rats on possible alterations and brain dysfunction in heat stress. For this purpose, engineered nanoparticles from Ag or Cu (≈50-60 nm) were administered (30 mg/kg, i.p.) once daily for 1 week in young male rats. On the 8th day these animals were subjected to 4 h heat stress at 38° C in a BOD incubator and stress reaction, blood-brain barrier (BBB) permeability and brain pathology were examined. Subjection of nanoparticle treated rats to heat stress showed exacerbation stress symptoms i.e., hyperthermia, salivation and prostration and exhibited greater BBB disruption, brain edema formation and brain damage compared to normal animals. This effect of enhanced brain pathology in heat stress was most marked in animals that received Ag nanoparticles compared to Cu treatment. Since nanoparticles of various sizes and different chemical compositions influence mitochondria to stimulate ROS overproduction and interfere with antioxidant defense mechanism, we used the effects of a potent antioxidant compound H-290/51 to induce neuroprotection in heat stress. Treatment with antioxidant compound H-290/51 either 30 min or 60 min after heat stress did not significantly attenuate hyperthermia induce brain pathology in nanoparticle treated rats. Whereas, administration of nanowirded-H-290/51 after 30 min or 60 min heat stress markedly attenuated BBB disruption and brain pathology in these groups. Our results show that chronic nanoparticles treatment exacerbate hypertehrmia induced brain pathology that is significantly attenuated by nanowired but not normal H-290/51 compound, not reported earlier. Taken together, these observations suggest that nano-wired drug delivery of H-290/51 is a promising approach to induce neuroprotection in hypertehrmia induced brain pathology.

119

Brain Poster Session: Neuroprotection

NEUROPROTECTIVE EFFECTS OF CEREBROLYSIN IN ANIMAL MODELS OF CNS INJURIES

H.S. Sharma[1], S. Zimmermann-Meinzingen[2], A. Sharma[1], D.F. Muresanu[3]

[1]Surgical Sciences, Uppsala University Hospital, Uppsala, Sweden, [2]EBEWE Pharma, Unterach, Austria, [3]Neurology, University of Medicine & Pharmacy, Cluj-Napoca, Romania

Previous reports from our laboratory suggest that a suitable combination of neurotrophic factors attenuates CNS pathologies following traumatic or metabolic insults to the brain or spinal cord. Since, Cerebrolysin (Ebewe Pharma, Austria) contains a mixture of neurotrophic peptides, we have undertaken a series of investigations to examine the neuroprotective efficacy of the drug in various animal models of CNS injuries.

We developed a new model of closed head injury (CHI) in which an impact of 0.224 N was applied on the right parietal bone under anesthesia by dropping a weight of 114.6 g on the skull from a height of 20 cm through a guide tube. This concussive CHI resulted in profound edema formation and volume swelling at 5 h after the insult that was most pronounced in the contralateral cerebral hemisphere. The microvascular permeability disturbances to protein tracers were prominent in both the cerebral hemispheres and the underlying cerebral structures. Pretreatment with cerebrolysin (10 µl, 20 µl or 40 µl/min for 10 min) infused into the left lateral cerebral ventricle either 30 min before or 30 min after CHI significantly attenuated brain edema formation, volume swelling and brain pathology. This effect was most pronounced with 20 µl and 40 µl/min cerebrolysin infusions. On the other hand, no reduction in brain edema, BBB permeability or brain pathology was seen when cerebrolysin was administered 60 min post-CHI.

Using a new model of spinal cord injury (SCI) in which an incision to the right dorsal horn at the T10-11 level induces profound disruptions of the blood-spinal coed barrier (BSCB) in rats after 5 h, the effects of topical application of cerebrolysin was evaluated. Topical application of cerebrolysin 5 min after SCI (100, 2000 and 400 µl over 10 min) over the traumatized cord markedly attenuated spinal cord edema formation at 5 h compared to untreated control group. This effect of cerebrolysin was dose related. In these animals cerebrolysin treatment in high doses (200 and 400 µl) significantly improved the motor functions and reduced the BSCB breakdown, edema formation and cell injury at 5h. However, these potential beneficial effects of cerebrolysin were absent when the treatment was initiated 60 min or 90 min after SCI.

To further test the neuroprotective efficacy of cerebrolysin, we used a new model of hyperthermic brain injury (HBI). HBI was produced by subjection of animals to 4 h heat stress at 38° C that resulted in massive blood-brain barrier (BBB) disruption and brain edema formation. Pretreatment with cerebrolysin (5 ml or 10 ml/kg, i.p. 30 min, before heat stress) markedly attenuated the BBB dysfunction and brain pathology. Interestingly, treatment with high dose of cerebrolysin (10 ml/kg) 30 min after heat stress was also neuroprotective. However, administration of the drug 60 or 90 min after the onset of heat stress was ineffective in reducing brain damage.

Taken together these observations suggest that an early intervention with cerebrolysin may have added therapeutic value for the treatment of various cases of CNS injuries.

120

Brain Poster Session: Blood-Brain Barrier

INHIBITION OF MYOSIN LIGHT CHAIN KINASE PREVENTS BLOOD BRAIN BARRIER BREAKDOWN AFTER CLOSED SKULL TRAUMATIC BRAIN INJURY IN THE MOUSE

J. Rossi[1,2], F. Patel[2,3], M. Chrzaszcz[2,3], M. Wainwright[2,3]

[1]Department of Pediatrics, Division of Critical Care Medicine, Northwestern University, Feinberg School of Medicine, [2]Center for Interdisciplinary Research in Pediatric Critical Illness and Injury, Children's Memorial Research Center, [3]Department of Pediatrics, Division of Neurology, Northwestern University, Feinberg School of Medicine, Chicago, IL, USA

Background and aims: Disruption of the cytoskeleton contributes to breakdown of the blood brain barrier (BBB) after traumatic brain injury (TBI). We have previously shown that myosin light chain kinase (MLCK) plays a pivotal role in the compromise of barrier function following acute lung injury (Proc Natl Acad Sci 2003, 100:6322; AJP Lung 2007, 292:1327). The role of MLCK in BBB dysfunction after TBI is not known.

Methods: Adult C57Bl6 mice were subject to midline closed skull injury or sham operation using a stereotactically guided pneumatic compression device (Lloyd et al., J Neuroinflammation 2008, 5:28). Coronal sections from each animal (n = 8 per group) were prepared at 4- 24hr 3- and 5d recovery. To quantify extravasation of macromolecules following TBI, immunohistochemical (IHC) staining for IgG and albumin was performed. To quantify changes in MCLK, the substrate MLC and phosphorylated MLC (p-MLC) IHC was performed and the expression quantified in digitized images by blinded observers. To determine the functional role of MLCK in the mechanisms leading to compromise of the BBB after TBI, mice were treated with an inhibitor of MLCK (ML-7) 30 minutes prior to TBI. After 24 hr recovery BBB breakdown, MLCK, MLC and p-MLC expression were quantified.

Purpose: We tested the hypothesis that MLCK is up-regulated following TBI, leading to breakdown of the BBB and extravasation of macromolecules into brain parenchyma.

Results: Breakdown of the BBB begins at 4hr and continues until 5d recovery. At each time point there were significant increases ($p< 0.01$ vs sham) in IgG and albumin in brain parenchyma at the impact site compared to sham controls. MLCK expression was increased compared to controls at 4hr, 24hr and 3d, with corresponding increases in p-MLC at 24hr and 3d ($p< 0.05$ vs sham). The substrate MLC was significantly reduced at 24 hr recovery ($p< 0.05$ vs sham). Inhibition of MLCK with ML-7 prevented both the breakdown of the BBB at 24 hr, as measured by albumin extravasation and the increase in MLCK in the injured animals.

Conclusions: Based on precedent for the important role of MLCK in the regulation of endothelial and epithelial barrier integrity in the lung, intestine and skin, we examined the role of MLCK in the mechanisms leading to breakdown of the BBB following TBI. Here, we show that expression of MLCK is increased after TBI, that this increase is associated with an increase in the enzyme product, pMLC, and with a decrease in the substrate MLC. Administration of an inhibitor of MLCK prior to TBI prevented both these changes as well as the increase in BBB permeability measured by extravasation of albumin. These findings support a role for MLCK in the mechanisms of BBB dysfunction following TBI. The effect of treatment with an inhibitor of MLCK implicates this pathway in the mechanisms by which TBI leads to breakdown of the BBB. Greater understanding of the mechanisms by which MLCK regulates BBB cytoskeletal integrity following TBI may advance the development of new therapeutic approaches to the prevention of cerebral edema.

123

Brain Poster Session: Neuroprotection

HEMOGLOBIN EXPRESSION IN NEURONS: DEPENDENCY ON PO_2 AND EPO

D.W. Schelshorn[1], **W. Kuschinsky**[1], A. Schneider[2], M.H. Maurer[2]

[1]Department of Physiology and Pathophysiology, University of Heidelberg, [2]Sygnis Bioscience, Heidelberg, Germany

Hemoglobin (Hb) is the major protein in red blood cells and transports oxygen from the lungs to the organs. In invertebrates, neuronal Hb appears to serve as intracellular storage molecule for oxygen.

We describe here:

1. the cellular and area- specific distribution of Hb expression,
2. the relationship between Hb expression and local oxygenation,
3. the induction of neuronal Hb expression by erythropoietin (EPO).

Ad 1: Immunohistochemistry shows a specific expression of Hb in neurons of the cortex, hippocampus, olfactory bulb, and cerebellum of the rodent brain, but not in astrocytes and oligodendrocytes. The neuronal Hb distribution is distinct from the neuroglobin expression pattern on both cellular and subcellular levels.

Ad 2: Mice were injected with pimonidazole (Hypoxyprobe-1), a marker substance suitable to detect local oxygen pressures below 10 mmHg. We verified this feature of pimonidazole by exposing neurons in culture to different degrees of hypoxia. With immunofluorescent double-staining (anti- Hb and anti-pimonidazole), we assessed the distribution of oxygen-deficient regions. A high pimonidazole staining which indicates a low pO_2 was found in the somata of neurons of the CA3 and partly of the CA1 region of the hippocampus, as well as in Purkinje cells of the cerebellum. These cells also displayed weak Hb signals. They were often located in direct neighborhood of cells that had strong Hb signals but no indication of low oxygen levels. These findings indicate a reciprocal relationship between Hb expression and hypoxia, Hb -positive neurons being higher oxygenated than Hb- negative neurons.

Ad 3: EPO exerts neuroprotective actions in the CNS. We therefore asked whether EPO might induce Hb expression in neurons and, in parallel, might reduce brain hypoxic areas. Mice were injected with a reported neuroprotective dose and treatment scheme of EPO (5000 IU/kg) 24 h before the onset of hypoxia (8% O_2) for 30 min. In hippocampal sections the area stained by pimonidazole was determined. The hypoxic area increased from 3.8 ± 2.6 % of the total hippocampus area during normoxia to 10.5 ± 2.0 % (mean ± SD) during hypoxia. The newly appearing hypoxic areas of pimonidazole binding encompassed both cells displaying weak as well as strong Hb signals. Hypoxia appeared in focally concentrated regions rather than evenly distributed throughout the hippocampus. EPO-treated mice showed a significantly reduced pimonidazole-positive area both under normoxic (0.3 ± 0.3 %) and hypoxic (6.0 ± 1.5 %, mean ± SD) conditions. At the same time, the immunoreactivity for Hb was elevated in EPO-treated animals. Thus, EPO induces neuronal Hb expression and reduces zones of hypoxia both under physiological and hypoxic conditions. We therefore propose a novel and promising mechanism for EPO action in the brain, i.e. counteraction of cellular hypoxia by upregulation of neuronal hemoglobin expression.

We conclude that 1. Hb is expressed specifically by neurons in the brain, 2. local Hb expression is

related to tissue oxygenation, 3. EPO can upregulate neuronal Hb expression resulting in an enhanced brain oxygenation under physiological and hypoxic conditions.

BIODISTRIBUTION AND RADIATION DOSIMETRY OF THE NK1 LIGAND GR-205171 DETERMINED FROM PAPIO ANUBIS WHOLE-BODY PET

K. Ridler[1], E.A. Rabiner[1], L. Kegeles[2], J. Castrillon[2], E. Hackett[2], M. Laruelle[1], M. Slifstein[2]

[1]Clinical Imaging Centre, Glaxosmithkline, London, UK, [2]Division of Translational Imaging, Dept of Psychiatry, Columbia University, New York, NY, USA

Background and aims: [^{11}C]GR-205171 ([2(^{11}C)-methoxy-5-(5-trifluoromethyl-tetrazol-1-yl)-benzyl]-

(2S-phenyl-piperidin-3S-yl)-amine) is a selective neurokinin 1 (NK_1) receptor PET ligand. Positron emission tomography (PET) was used to determine the whole body radiation dosimetry of [^{11}C]GR-205171, in 3 adult male baboons (Papio Anubis).

Methods: Three anaesthetized male baboons (Papio Anubis), weight 25.4 ± 2.3 kg) were examined on a Siemens Accel whole body scanner in 2D mode for 85 min following a bolus injection of [^{11}C]GR-205171 (185 ± 26 MBq). Subjects were scanned at 6 overlapping bed positions covering from head to mid-thigh. Organs with activity above background level were identified on the reconstructed PET images. Time activity curves were generated from sub-samples of these organs and area under the curve was estimated (Bq/cm^3*hr). These values were multiplied by organ volumes of a 70 kg mathematical phantom (Cristy and Eckerman 1987), normalized for body mass and injected dose to obtain residence times (hr). Residence times were used as input to the Olinda program (Stabin et al. 2005) to generate estimates of absorbed dose and Equivalent Dose (ED).

Results: Individual organ absorbed doses are presented in Table 1 (mSv/MBq). Effective dose was estimated at 8.72 ± 2.23 μSv/MBq. The dose limiting organ was the lung (5.54x10^{-2} mSv/MBq). For studies performed under RDRC, this would limit single study dose to a maximum of 888 MBq.

ORGAN	MEAN(SD)		ORGAN	MEAN(SD)		ORGAN	MEAN(SD)
Adrenals	3.46E-03(3.21E-05)		Kidney	1.48E-02(1.60E-03)		Spleen	2.31E-02(3.15E-03)
Brain	5.64E-03(1.21E-03)		Liver	1.10E-02(6.11E-04)		Testes	9.89E-04(2.67E-05)
Breasts	2.42E-03(1.71E-04)		Lungs	5.54E-02(2.15E-02)		Thyroid	2.86E-03(4.69E-04)
Gallbladder Wall	2.76E-03(4.74E-		Muscle	1.53E-03(2.95E-		Urinary Bladder	1.40E-03(5.09E-

	04)			04)		Wall	04)
Lower Large Intestine Wall	1.01E-03(6.03E-04)		Ovaries	1.15E-03(6.15E-04)		Uterus	1.12E-03(6.18E-04)
Small intestine	3.69E-03(2.41E-03)		Pancreas	3.25E-03(1.80E-04)		Total Body	2.79E-03(2.08E-05)
Stomach Wall	2.21E-03(2.92E-04)		Red Marrow	1.79E-03(1.68E-04)			
Upper Large Inetestine Wall	1.60E-03(5.98E-04)		Osteogenic Cells	1.85E-03(5.76E-04)		**Effective Dose Equivalent**	**1.21E-02(2.69E-03)**
Heart Wall	1.86E-02(4.47E-03)		Skin	1.01E-03(3.29E-04)		**Effective dose**	**8.72E-03(2.32E-03)**

[Radiation-Absorbed Dose Estimates (mSv/MBq).]

Conclusions: We estimated [^{11}C]GR-205171 radiation dosimetry from data acquired with whole-body PET in 3 non-human primates. The estimated effective dose was 8.72 ±2.23 μSv/MBq, within the range of carbon-11 labelled ligands. A 370MBq injection of [^{11}C]GR-205171 would result in an exposure of 3.2mSv (excluding exposure from accompanying transmission scanning).

High levels of absorbed radiation in the lung may be due to specific binding of [^{11}C]GSK-205171. Examination following a high dose of an NK_1 blocking compound, will be important, in assessing the effects of peripheral and central NK_1 blockade on estimated dosimetry figures.

References:

Cristy, M. and K. Eckerman (1987). ORNL Report ORNL/TM-8381 V1-V7. Oak Ridge, TN, Oak Ridge National Laboratory.

Stabin, M. G., R. B. Sparks, et al. (2005). Journal of Nuclear Medicine 46(6): 1023-1027.

125

Brain Poster Session: Epilepsy

P-GLYCOPROTEIN FUNCTION IN THE BLOOD-BRAIN BARRIER OF EPILEPTIC RATS

S. Syvänen[1], G. Luurtsema[2], C.F.M. Molthoff[2], A.D. Windhorst[2], M.C. Huisman[2], A.A. Lammertsma[2], R.A. Voskuyl[1], E.C.M. de Lange[1]

[1]Division of Pharmacology, LACDR, Leiden University, Leiden, [2]Nuclear Medicine and PET Research, VU University Medical Center, Amsterdam, The Netherlands

Objectives: It has been hypothesized that P-glycoprotein (P-gp) is responsible for drug resistance in epilepsy by hindering anti-epileptic drugs from penetrating the blood-brain barrier and reaching their targets inside the brain[1-2]. The objective of this study was to compare the brain distribution of (R)-[^{11}C]verapamil, a frequently used PET tracer for studying P-gp function[3-5], in naïve and epileptic rats and thus to investigate possible differences in P-gp function between these two groups.

Methods: Male Sprague-Dawley rats were treated with kainic acid to induce epilepsy (n=20) or with saline (n=20). At 1 week after treatment, each rat underwent a PET study with (R)-[^{11}C]verapamil. In half of the rats of each group, the P-gp inhibitor tariquidar was administered 20-30 minutes prior to the start of the (R)-[^{11}C]verapamil scan. Blood samples were withdrawn during the PET scan and analyzed with regard to tracer metabolism in plasma. Brain radioactivity concentrations, expressed as standardized uptake values (SUV) were compared between naïve and epileptic rats as well as between tariquidar treated and untreated rats.

Results: Differences in brain SUV uptake between naïve and epileptic rats were small. In both groups uptake of (R)-[^{11}C]verapamil in the brain was very low with SUV values ranging from 0.60 at the start of the 60 minutes scan to 0.15 at the end of the scan. Pretreatment with tariquidar resulted in an up to 10-fold increase in brain SUV in both naïve and epileptic rats. In the tariquidar treated rats there was a small tendency towards slower wash-out of verapamil from epileptic rat brains than from naïve rat brains. Plasma kinetics and metabolism of (R)-[^{11}C]verapamil were unaltered by both tariquidar treatment and epilepsy.

Conclusions: P-gp function in naïve and epileptic rats appeared to be similar. Therefore, this study did not confirm the hypothesis that P-gp plays a major role in limiting brain uptake of anti-epileptic drugs that are P-gp substrates. P-gp function, however, was investigated 1 week after induction of epilepsy. It cannot be ruled out that P-gp function may be altered at other time points after induction of epilepsy.

References:

1. Löscher W et al. (2002) J Pharmacol Exp Ther 301:7-14.

2. Brandt C et al. (2006) Neurobiol Dis 24:202-11.

3. Luurtsema G et al. (2005) Nucl Med Biol 32:87-93.

4. Bankstahl J et al. (2008) J Nucl Med 49:1328-35.

5. Bartels AL et al. (2008) Parkinsonism Relat Disord. 14(6):505-8.

Brain PET Oral 6: Neurodegenerative Disorders

IN VIVO DIAGNOSIS OF ALZHEIMER'S DISEASE BY MEANS OF [^{18}F]BAY 94-9172 AND PET

H. Barthel[1], J. Luthardt[1], M. Patt[1], E. Hammerstein[2], G. Becker[1], K. Hartwig[2], A. Schildan[1], S. Hesse[1], P. Meyer[1], J. Reischl[3], U. Hegerl[2], C. Reininger[3], B. Rohde[3], H.-J. Gertz[2], O. Sabri[1]

[1]Department of Nuclear Medicine, [2]Department of Psychiatry, University of Leipzig, Leipzig, [3]Bayer-Schering Pharma AG, Berlin, Germany

There is optimism that ß-amyloid (Aß) PET tracers may shift the time-point for accurate diagnosis of Alzheimer's disease (AD) from postmortem to antemortem. BAY 94-9172 is a new Aß-binding ^{18}F-labeled stilbene derivative currently in clinical development. Within the following the results of a proof of principle study investigating the ability of PET brain scanning with BAY 94-9172 to differentiate subjects with AD from healthy controls (HCs) are presented.

10 subjects with AD (DSM-IV and NINCDS-ADRDA criteria, age = 69±7yrs, Clinical Dementia Rating (CDR) score = 1-2, Mini-Mental State Examination (MMSE) score = 19±7, ApoE4: 6 positive), 10 age-matched healthy controls (HCs, MMSE score ≥ 28, CDR score = 0, ApoE4: 2 positive), as well as 3 patients with fronto-temporal dementia (FTD, Neary consensus criteria as well as MRI and/or [^{18}F]FDG findings compatible with FTD, age = 59-78yrs, MMSE score = 9-14, CDR score = 1-2, ApoE4: 1 positive) were included. Dynamic brain PET images (ECAT EXACT HR+, ~300MBq [^{18}F]BAY 94-9172 i.v., 3D mode, Neuroshield, correction for measured transmission, filtered back-projection) were acquired. The 70-90min post injection images were analyzed: 1) visually by three blinded experts, 2) by volume of interest (VOI) analysis: VOIs anatomically defined via MRI (1.5 Tesla, 3D T1w volumetric MPRAGE sequence) co-registration, resulting standard uptake value (SUV) ratios using the cerebellar cortex as reference region, 3) via voxelwise, single-case comparisons with a database created with the PET data from the 10 HCs (SPM2, cluster size > 30 voxel, $p < 0.001$).

Visual analysis revealed 9 of the 10 AD, but only 1 of the 10 HC brains to be positive for Aß ($p < 0.001$). In FTD, 2 of the 3 patients were rated positive for Aß. For all subjects, the frequency of ApoE4-positive genotypes was higher in the Aß-positive compared with the Aß-negative PET scans ($p=0.05$). When compared to these of the HCs, the SUV ratios in AD subjects were significantly higher in frontal (1.73±0.37 vs. 1.35±0.18, $p=0.0098$), anterior cingulate (1.72±0.36 vs. 1.41±0.15, $p=0.022$), posterior cingulate (1.79±0.48 vs. 1.36±0.13, $p=0.012$) and lateral temporal (1.49±0.30 vs. 1.24±0.10, $p=0.020$) cortices, as well as in caudate heads (1.49±0.30 vs. 1.19±0.13, $p=0.010$). Voxelwise analyses were in complete agreement with the results of the visual rating. Here, a newly developed Aß load index combining information on extent and severity of pathological tracer uptake was negatively correlated to the MMSE score ($r=-0.609$, $p=0.004$).

These results indicate that [^{18}F]BAY 94-9172 PET scanning has the potential to non-invasively provide accurate and quantitative measures of Aß load during life. As such, this new tracer may facilitate an antemortem diagnosis of AD. Further evaluation of the diagnostic efficacy of [^{18}F]BAY 94-9172 in global, multi-center trials is ongoing.

This trial is sponsored and supported by the Bayer-Schering Pharma AG.

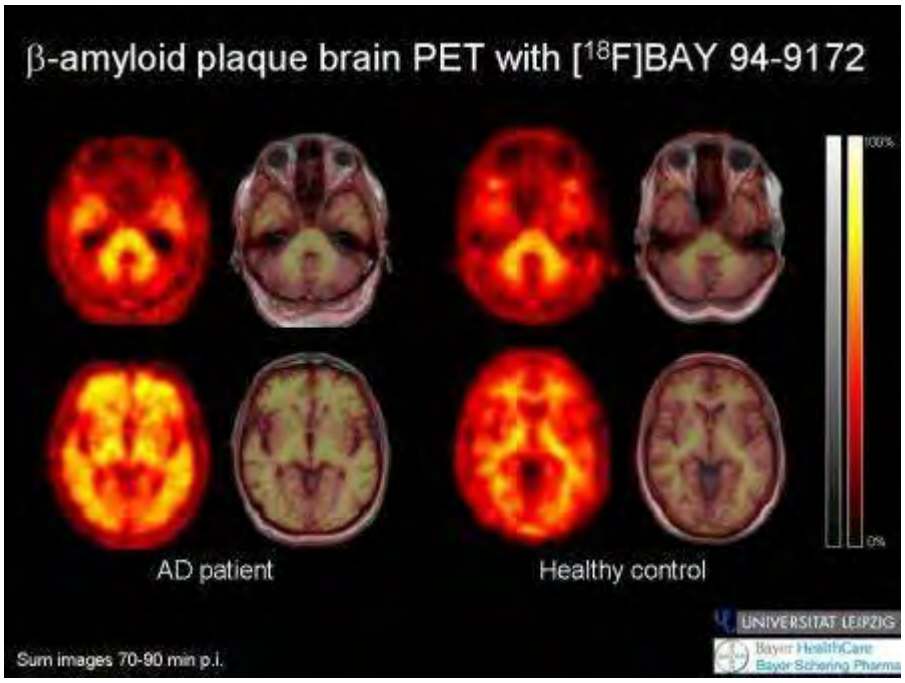

[Typical [18F]BAY 94-9172 PET images in AD and HC]

130

Brain PET Oral 1: PET Image Reconstruction and Processing

EVALUATION OF A 3D ITERATIVE RECONSTRUCTION ALGORITHM THAT ALLOWS FOR NEGATIVE IMAGE VALUES IN HIGH RESOLUTION PET STUDIES

F.H.P. van Velden[1], C. Comtat[2], J. Nuyts[3], A. Reilhac[4], A.A. Lammertsma[1], R. Boellaard[1]

[1]Department of Nuclear Medicine & PET Research, VU University Medical Center, Amsterdam, The Netherlands, [2]Service Hospitalier Frédéric Joliot (S.H.F.J.), Commissariat à l'Énergie Atomique, Orsay, France, [3]Katholieke Universiteit Leuven, U.Z. Gasthuisberg, Leuven, Belgium, [4]CERMEP, Bron, France

Background and aims: The High Resolution Research Tomograph (HRRT, CTI/Siemens) is a dedicated human brain positron emission tomography (PET) scanner. At present, all available 3D iterative reconstruction algorithms show bias in low count regions of short duration frames (10-60 s), hampering quantitative accuracy especially when using reference tissue models [1]. In a previous simulation study [2], a maximum-likelihood iterative reconstruction method that allows for negative image values (NEG-ML) [3] showed promising results with respect to bias reduction in low count regions. The goal of the present study was to evaluate quantitative accuracy of 3D ordinary-Poisson (using prompts and randoms) NEG-ML (NEG-OP) and its impact on kinetic analysis of HRRT data.

Methods: A homogeneous phantom, a 3D anthropomorphic human brain (Hoffman) phantom and dynamic [^{11}C]flumazenil human brain studies (n=5) were reconstructed using NEG-OP (15 iterations, 16 subsets). For comparison, reconstructions were also performed using standard 3D OP ordered subsets expectation maximization (OP-OSEM, 16 iterations, 16 subsets), recommended 3D ordered subsets weighted least squares (OSWLS, 7 iterations, 16 subsets) [1] and analytical 3D filtered-backprojection (3D-FBP). Bias was measured in low count frames, using a high count frame as reference. Human brain studies were analyzed using receptor parametric mapping, a basis function implementation of the simplified reference tissue model, with pons as reference tissue, providing binding potential (BP_{ND}) images. In addition, volume of distribution (V_T) and delivery (K_1) images were obtained using a basis function implementation of the standard single tissue plasma input compartment model.

Results: Using NEG-OP, bias in the homogeneous phantom was reduced to within 3% for short duration frames (OP-OSEM: < 4%, OSWLS: < 8%, 3D-FBP: < 1%), having the lowest coefficient of variation within the phantom (< 150%, OP-OSEM: < 410%, OSWLS: < 190%, 3D-FBP: < 1100%). For short duration frames of the Hoffman phantom, however, bias was still observed in both grey (< 9%, OP-OSEM: < 7%, OSWLS: < 9%, 3D-FBP: < 1%) and white (< 15%, OP-OSEM: < 21%, OSWLS: < 28%, 3D-FBP: < 1%) matter regions. Visually, NEG-OP showed less artifacts in V_T, BP_{ND} and especially K_1 images than the other methods. However, for both V_T and BP_{ND}, linear regression with fixed intercept against 3D-FBP showed slightly poorer slopes (0.87 and 1.20, respectively) than the other iterative methods (OP-OSEM: 0.92 and 1.12, OSWLS: 0.93 and 1.02). As 3D-FBP images were very noisy, no regression for K_1 images was possible.

Conclusions: Although NEG-OP is not free of bias, it does show bias reduction combined with low noise levels, resulting in improved K_1 images. As 3D-FBP reconstructions are very noisy, linear regression against 3D-FBP might not provide a fair comparison. Further studies are needed to fully assess the potential of the NEG-OP algorithm for HRRT reconstructions.

References:

[1] Van Velden et al. J Nucl Med. 2009; 50(1):72-80.

[2] Grèzes-Besset et al. IEEE NSS Conf Rec. 2007; 4:3009-3014.

[3] Nuyts et al. J Nucl Med. 2002; 43(8):1054-1062.

Acknowledgments: Financial supported provided by the Netherlands Organization for Scientific Research (NWO, VIDI Grant 016.066.309).

131

Brain Oral Session: Neurological Diseases

LONGITUDINAL µPET STUDY ON A TRANSGENIC RAT MODEL FOR HUNTINGTON DISEASE REVEALS PROGRESSIVE METABOLIC AND DOPAMINERGIC CHANGES

N. Van Camp[1], R. Boisgard[1], K. Siquier[1], J. Benoit[1], I. Blockx[2], F. Chauveau[1], F. Hinnen[1], B. Kuhnast[1], S. Von Hörsten[3], H. Nguyen[4], O. Riess[4], F. Dollé[1], A. Van der Linden[2], B. Tavitian[1]

[1]CEA/DSV/I2BM/SHFJ/LIME, Orsay, France, [2]University of Antwerp, Bio-Imaging Lab, Antwerpen, Belgium, [3]Friedrich-Alexander-Universität Erlangen-Nürnberg, Erlangen, [4]Eberhard-Karls-Universität Tübingen, Tübingen, Germany

Objectives: Huntington's disease (HD) is an autosomal dominant neurological disorder caused by an expansion of CAG repeats within the coding region of the HD gene (IT15). It is characterized by striatal degeneration, motor symptoms and complex neuropsychiatric alterations. Recently, von Hörsten et al. (2003) described the first transgenic rat model for HD with a slow onset and disease progression. We present here the first longitudinal µPET study on this model to characterize in vivo glucose metabolic changes and dopamine-2 receptor binding evolution.

Methods: Male homozygous transgenic (Tg) and wild type (WT) animals (12/12) were scanned at the age of 5, 10 and 15months with MRI (9T,Biospec,Bruker,Ettlingen) and µPET (Concorde Focus 220) using [^{18}F]FDG (65±9MBq) and [^{18}F]Fallypride (1.6±0.7nmol/kg) to study brain glucose metabolism and D_2-receptor binding. Tracers were injected one hour before a 30-minutes PET scan. For [^{18}F]FDG imaging, animals were fastened 24hours prior to the experiment and blood glycaemia was determined. During imaging, animals were anesthetised using isoflurane (2%) and body temperature was kept constant at 37°C. After image reconstruction, PET images were coregistered to the corresponding high-resolution MRI images using brainvisa/anatomist software. [^{18}F]FDG images were proportionally scaled while [^{18}F]Fallypride images were corrected for non-specific binding using the cerebellum as a reference region. Finally, SPM student t-tests between Tg and WT were applied for each age. Statistical maps ($p< 0.01$, minimum cluster size of 20pixels) were then displayed on the template images and further used to define volumes of interest on the PET images.

Results: At 5months of age we did not detect any differences in glucose metabolism, though D_2-receptor binding was significantly increased in Tg in the ventral striatum and parts of the olfactory bulb. At 10months, glucose metabolism was increased in Tg in the ventral striatum whilst D_2-receptor binding was significantly decreased in the ventral striatum and dramatically decreased in the olfactory bulb. Finally, at 15months of age, brain glucose metabolism was decreased in Tg animals, mostly in striatum and cortex, and D_2-receptor binding was decreased in the entire striatum and olfactory bulb.

Conclusions: The first neurodegenerative changes were observed at 10months of age for D_2-receptor binding, and brain glucose metabolism was decreased at 15months. Surprisingly, this neurodegeneration was preceded by increased D_2-receptor binding and brain metabolism starting from 5months, suggesting the existence of compensatory mechanisms before the appearance of clinical signs. Temporary compensation during the presymptomatic stage of HD has been observed previously (Nguyen et al.2006). Here, imaging studies revealed a high level of differences between Tg and WT in the ventral striatum starting as early as 5months, a region involved in the control of emotions, which might correspond to emotional disturbance patterns described in this model (Bode et al.2008). We also found significant changes at the level of the olfactory bulb, which corresponds to the observation that olfactory deficits occur at a very early stage of the disease in presymptomatic HD patients. These hypotheses will be further correlated with behavioral and histological findings on the Huntington rat model.

Acknowledgements: This study was funded in part by the EC-FP6-project DiMI(LSHB-CT-2005-

512146),EC-FP6-project EMIL(LSHC-CT-2004-503569),RATstream™(LSHM-CT-2007-037846),FWO.

132

Brain Oral Session: Traumatic Brain Injury: Metabolism

STABLE ISOTOPE COMPARISON OF CEREBRAL LACTATE AND GLUCOSE METABOLISM IN RESTING NORMAL CONTROL COHORTS AND TRAUMATICALLY BRAIN INJURED PATIENTS

T. Glenn[1], M. Horning[2], G. Brooks[2], N. Martin[1]

[1]Neurosurgery, University of California, Los Angeles, Los Angeles, [2]Integrative Biology, University of California, Berkeley, Berekely, CA, USA

Objectives: Traditional clinical hallmarks of severe traumatic brain injury (TBI) include reduced cerebral blood flow and cerebral metabolic rates for oxygen. Recent clinical studies of cerebral metabolism based on arterial-jugular venous difference measurements have shown that the brain takes up lactate during the acute period after traumatic brain injury (Glenn, 2003). Additionally, initial studies in TBI patients using [3-13C] lactate infusion showed that the brain oxidized the lactate (Glenn, 2007). To further elucidate the role of post-traumatic cerebral metabolism a normal volunteer cohort was studied in addition to TBI patients. We hypothesized that the injured brain will take up and oxidize more lactate than in the normal cohort.

Methods: Four severely injured TBI (age=37.9±11.2, all male) and 3 normal resting subjects (age=31.3±5.6, 2 male, 1 female) were consented for infusion studies. All TBI patients were simultaneously infused on days 5.86±2.0 with [6,6-D2]glucose and [3-13C]lactate followed the next day by [6,6-D2]glucose [1-13C]glucose. Normal subjects were infused with [6,6-D2]glucose and [3-13C]lactate. On all subjects, arterial and jugular venous blood samples, and expired breath were collected every 30 minutes for 3 hours. Isotopic enrichments for plasma samples were analyzed by GC/MS and breath IE's were analyzed by GC/IRMS. Cerebral blood flow was measured by the bedside 133Xenon clearance technique.

Results: Cerebral blood flow was significantly lower in TBI patients than in Normals (33.0±8.6 and 46.0±7.8 ml/100g/min., respectively, p=0.03). Mean arterial and jugular isotopic enrichments for lactate were significantly lower (p=0.047 and p=0.045 respectively) in TBI (0.024±0.013% and 0.020±0.011%) versus Normals (0.044±0.011% and 0.038±0.010%, respectively). Thus, whole body lactate turnover (Ra and Rd) showed a 100% increase as opposed to whole-body glucose turnover rates that increased only 20% following TBI compared to Normals. Cerebral glucose fractional extraction was not different from zero, but lactate fractional extraction ((Ea*Ca) - (Ev*Cv)/(Ea*Ca)) was significant and similar between TBI (11.7±5.2) and Normal (14.3±4.1). As well, during days 4-6 the CMR for lactate was similar between TBI (-0.03±0.2) and Normal (-0.7±0.18 mg/100g/min). However, following TBI, cerebral lactate oxidation (=[(13CO2v)(CVCO2)] - [(13CO2a)(CaCO2)*(CBF)]/Ea) was 3-fold higher following TBI (0.9 mg/100 g/min vs 0.25 mg/100g/min in Normals).

Conclusions: The normal resting human brain can take up and oxidize lactate. Following TBI, whole-body lactate production and removal were greatly increased as is tracer-measured cerebral lactate oxidation. In conclusion, this study shows that the injured brain utilizes fuels other than glucose and suggests that a metabolic fuel based therapy may be an effective aid to recovery.

References: Glenn TC, Kelly DF, Boscardin WJ, McArthur DL, Vespa PM, Oertel MF, Hovda DA, Bergsneider M, Hillered L, Martin N. Energy dysfunction as a predictor of outcome after moderate or severe head injury: indices of oxygen, glucose and lactate metabolism. J Cereb Blood Flow Metab Oct;23(10):1239-50, 2003 Glenn TC, Wallis G, Hirt D, Vespa P, Dusick J, Brooks G, Hovda D, Martin N. Lactate is oxidized by the human brain following traumatic brain injury. Brain '07, Osaka Japan BP46-3U, 2007.

133

BrainPET Poster Session: Brain Imaging: MRI/fMRI

SPATIOTEMPORAL INVESTIGATION OF THE BOLD AND CBV RESPONSE TO BRIEF SOMATOSENSORY STIMULATION IN AWAKE MARMOSETS

Y. Hirano[1], J. Liu[1], B. Stefanovic[2], A. Silva[1]

[1]CMU/LFMI, NINDS/NIH, Bethesda, MD, USA, [2]Sunnybrook Health Sciences Centre, Toronto, ON, Canada

Objectives: Understanding the spatiotemporal features of the hemodynamic response (HDR) to functional brain stimulation is essential to the proper application of fMRI to study brain function. Previously, we showed that the BOLD-, CBF-, and CBV-HDR to a single electrical pulse can be robustly detected in α-chloralose anesthetized rats (Hirano et al., ISMRM 2008), and that both spatial and temporal characteristics of such responses are fine enough to resolve the heterogeneity of fMRI amplitudes, onset times, and time-to-peak across the cortical layers. Here, we extend the work to investigate the spatial and temporal evolution of the BOLD- and CBV-HDR in awake nonhuman primates.

Methods: Adult male common marmosets were implanted head posts in the skull and secured to a head holder. fMRI experiments were performed at 7T by GRE-EPI with following parameters: TE/TR = 13/250 ms, acquisition bandwidth 200 kHz, nominal resolution = 400 x 400 x 2000 μm^3. To measure the HDR to somatosensory stimulation, a pair of contact electrodes was secured across each wrist and bilateral electrical stimulation (333 μs pulses, 2 mA amplitude, 64 Hz) was performed synchronized with the scanner. The stimuli consisted of individual epochs containing 1 or 256 electrical pulses (333 μs or 4-s stimulus lengths), respectively, repeated 128 times or 16 times. Before commencing the CBV-HDR, a maximum dose of 30 mg/kg of 30 nm iron oxide particles (MION) were injected intravenously to the animal.

Results: Robust BOLD- and CBV-HDRs were obtained in the primary and secondary somatosensory cortex (S1 and S2) before and after 20 and 30 mg/kg MION injection at 4-s stimulus (Figure). The amplitude increased (31% and 44 % increased at 30 mg/kg than 20 mg/kg in S1 and S2 respectively) with MION dosage. At 10 mg/kg MION and less, CBV-HDRs showed nonspecific responses and poor separability between S1 and S2 (data not shown). We concluded that 30 mg/kg of MION is a more appropriate dose to investigate spatiotemporal characteristics of the fMRI response. Using 30 mg/kg MION, we then proceeded to compare the CBV impulse response function (IRF) with previously acquired BOLD IRFs (data not shown). Both the BOLD and the CBV-IRF from S2 had stronger amplitude than the one from S1, in agreement with the notion that high order cortical processing is dominant in primates. We are currently analyzing the temporal features of the BOLD and CBV IRF in the marmosets.

Figure: BOLD and CBV activation maps at 4-s stimulation (64 Hz).

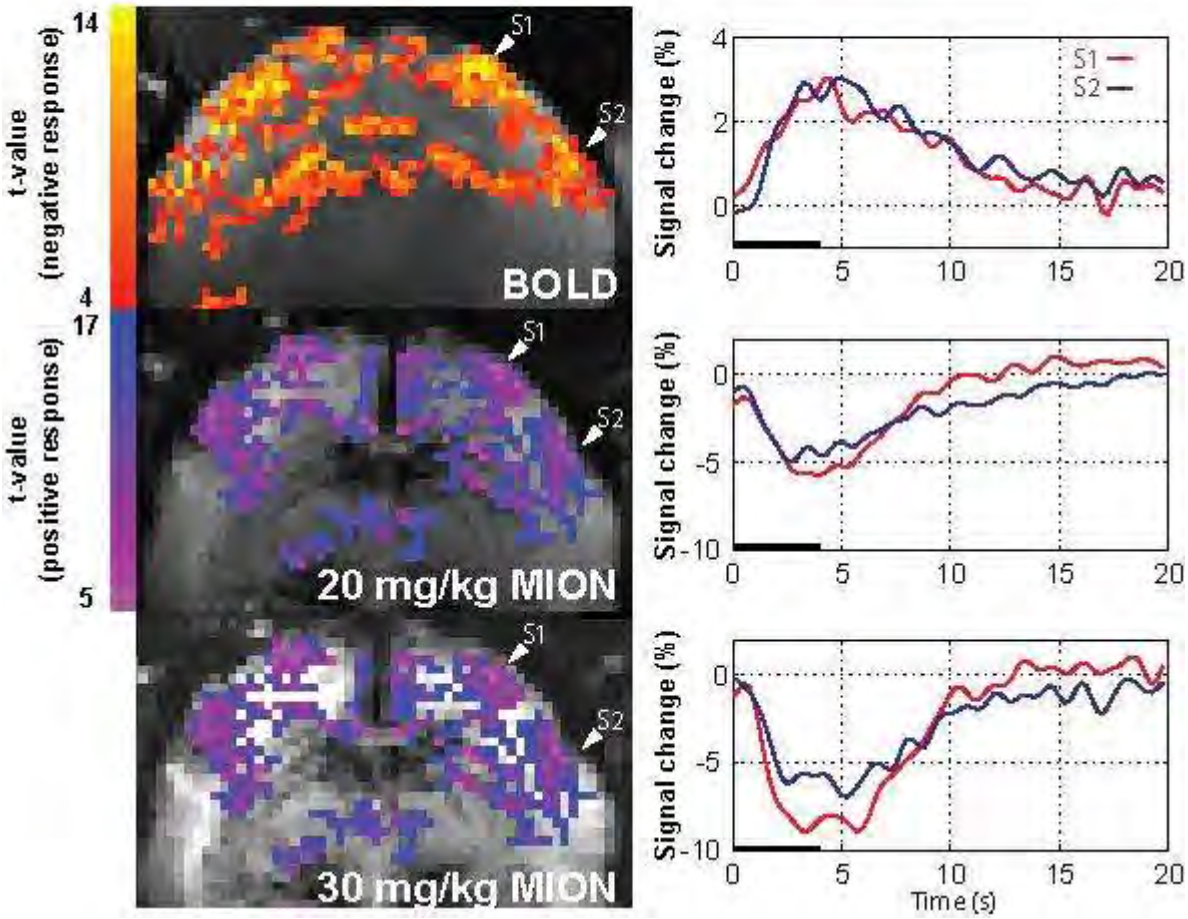

[Figure]

Conclusion: Robust CBV-HDR in S1 and S2 was observed after 30 mg/kg MION injection in awake marmoset. The refinement of this study will allow for a better understanding of the mechanisms of neurovascular coupling in unanesthetized primates and facilitate the applicability of animal fMRI studies to the investigation of human brain function.

135

Brain Oral Session: Neurovascular Unit

CHOLINERGIC MODULATION OF NEUROVASCULAR COUPLING IN THE RAT SOMATOSENSORY CORTEX

C. Sandoe, P. Fernandes, X. Tong, C. Lecrux, E. Hamel

Department of Neurology and Neurosurgery, Montreal Neurological Institute, McGill University, Montreal, QC, Canada

Background and objectives: Functional hyperemia, or neurovascular coupling, is the highly coordinated increase in cerebral blood flow (CBF) seen in areas of increased neuronal activity. Evidence suggests that the perfusion response is driven by the afferents to the target areas and, more importantly, by their local processing. The exact mechanisms by which this occurs, however, as well as the cell types and messengers involved, are still poorly understood. The cholinergic system is involved in many brain functions from memory to attention and arousal, and increasing acetylcholine (ACh) levels through basal forebrain (BF) stimulation leads to cortical activation. Particularly, increased cortical ACh broadens somatosensory cortex receptive fields and uncovers hidden ones (Lamour et al., J Neurophysiol 1988, 60:725-750), while reduced ACh levels after BF lesion decreases sensory stimulus-dependent plasticity and whisker stimulation-evoked functional activity (Juliano et al., PNAS 1991, 88:780-784; Jacobs et al., 1991, Brain Res 560:342-345), suggesting that cholinergic tone modulates thalamocortical sensory information processing. Here, we further investigated this role using CBF as an index of neurovascular coupling and c-Fos immunohistochemistry to identify the cellular basis of the modulation.

Methods: Endogenous brain ACh levels were increased with the ACh-enhancing drug linopirdine (10mg/kg, intraperitoneal), or decreased via intracerebroventricular injection of the selective cholinotoxin saporin (4μg/2μL). In all experiments, the whisker-to-barrel cortex pathway was used as a model of sensory input-induced CBF increase. Whiskers were mechanically stimulated and CBF was monitored by Laser Doppler flowmetry in urethane-anesthetized rats. Brains were then perfused and stained for neuronal activation using single (c-Fos alone) or double immunohistochemistry for c-Fos and markers of pyramidal cells or different GABA interneuron subtypes.

Results: Saporin treatment decreased cholinergic afferents to the cortex and decreased the CBF response to whisker stimulation (-27.8±1.7%, $p< 0.001$, n=18); this was accompanied by a decrease in stimulus-induced neuronal activation in the barrel cortex as detected with c-Fos immunostaining. In contrast, ACh increase via linopirdine treatment increased the CBF response to whisker stimulation (+30.8±1.9%, $p< 0.001$, n=6) without clearly altering the extent of c-Fos activation in the barrel cortex. Instead, a shift in the types of interneurons activated in specific layers of the somatosensory cortex seemed to occur.

Conclusions: Our results clearly support a role for ACh in the modulation of sensory input to the somatosensory cortex, showing that enhancing or decreasing cortical ACh neurotransmission had a direct impact on the neurovascular coupling response to thalamocortical afferent activation. Further, they suggest that this modulation may be due, in part, to a shift in the neuronal networks activated by the incoming stimuli, although a direct effect of ACh on neuronal electrical activity cannot be ruled out. These studies provide important insight into the modulation of sensory information processing by ACh. In addition, they may be of relevance to neurodegenerative conditions such as Alzheimer's disease, where a cholinergic deficit is observed, selected groups of interneurons are affected and neurovascular coupling is impaired.

Sponsored by CIHR, MOP-84209 (EH); Jeanne Timmins studentship (CS); and Heart and Stroke Foundation of Canada/Canadian Stroke Network postdoctoral fellowship (CL).

136

Brain Poster Session: Experimental Cerebral Ischemia: Blood Flow & Metabolism

BLOOD FLOW IN CORTICAL MICROVASCULAR NETWORKS AT NORMAL AND HIGH HEMATOCRIT

T.P. Santisakultarm[1], N. Cornelius[1], N. Nishimura[1], P.C. Doerschuk[1], W.L. Olbricht[2], A.I. Schafer[3], R.T. Silver[3], C.B. Schaffer[1]

[1]Biomedical Engineering, [2]Chemical and Biomolecular Engineering, Cornell University, Ithaca, [3]Department of Medicine, Weill Cornell Medical College, New York, NY, USA

Objectives: Cerebrovascular disease is a key contributor to cognitive degeneration [1], so it is critical to develop methods for detailed analysis of blood flow in cortical microvascular networks. Increases in hematocrit, as occur in polycythemia vera, can lead to decreased blood flow and may increase the chance for vascular occlusions [2]. In the brain, such impaired blood flow could lead to neurological damage. Here, we develop methods to study time-dependent blood flow throughout the cortical microcirculation in rodents with normal and high hematocrit.

Methods: We use in vivo two-photon excited fluorescence microscopy to image vascular topology and blood flow. A craniotomy is prepared over parietal cortex in an anesthetized mouse and covered with a glass window. Fluorescein-dextran is intravenously injected to label the blood plasma (Fig.1a). Blood flow velocity in arterioles, capillaries, and venules throughout the network is determined by tracking the motion of red blood cells within individual vessels [3]. An electrocardiogram is acquired simultaneously to determine the flow speed across the cardiac cycle (Fig.1b). Erythropoietin (EPO, 10 IU) is subcutaneously administered for five consecutive days to increase hematocrit from 44% to 52%.

Results: The change in flow speed across a cardiac cycle is apparent in arterioles on the brain surface, in capillaries deep within cortex, and even in surface venules, with decreasing modulation, respectively (Fig.1b). In the EPO-injected animals, average capillary flow speed is reduced by 32% as compared to controls ($p < 0.01$; EPO-injected: 127 vessels, 13 animals; Control: 111 vessels, 6 animals). In addition, the fraction of stalled capillaries in the top 350-µm of the cortex increased from 3% to 19% in high hematocrit animals ($p < 0.01$; EPO-injected: 357 vessels, 4 animals; Control: 405 vessels, 5 animals). The modulation of flow speed in arterioles due to a heart beat is decreased by 69% in mice with high hematocrit ($p < 0.0001$. EPO-injected: 22 vessels, 4 animals. Control: 32 vessels, 8 animals).

Conclusions: We have measured time-dependent cerebral blood flow in individual microvessels throughout the vascular hierarchy in normal and high hematocrit mice. Elevated hematocrit decreases blood flow and increases the fraction of stalled capillaries. These changes in cerebral microcirculation could lead to increased risk of stroke and neurodegeneration in disorders where hematocrit and blood viscosity is heightened.

References:

O´Brien, J.T., Vascular cognitive impairment. Am J Geriatr Psychiatry, 2006.

Segura, T., et al., Cerebral embolism in a patient with polycythemia rubra vera. Eur J Neurol, 2000.

Schaffer, C.B., et al., Two-photon imaging of cortical surface microvessels reveals a robust redistribution in blood flow after vascular occlusion. PLoS Biol, 2006.

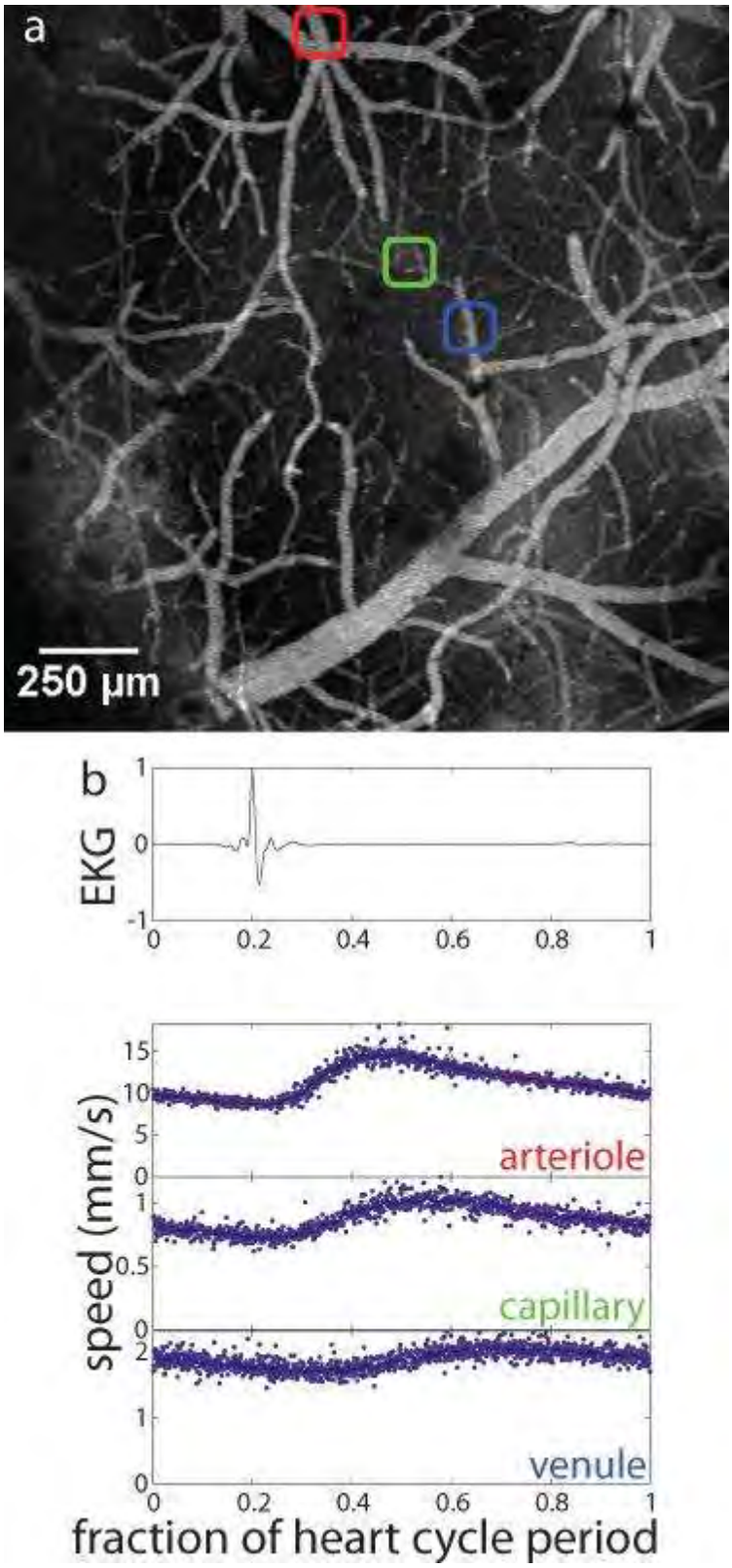

[Fig.1.]

Fig.1. Blood flow speed measured using in vivo two-photon excited fluorescence microscopy. (a) Vasculature at the brain surface. (b) Electrocardiogram-triggered flow speed in an arteriole, a capillary, and a venule.

137

Brain Oral Session: Experimental Cerebral Ischemia: Neuroprotection

DEFEROXAMINE REDUCES INTRACEREBRAL HEMORRHAGE-INDUCED BRAIN INJURY IN AGED RATS

Y. Hua[1], M. Okauchi[1], R. Keep[1], L. Morgenstern[2], T. Schallert[1], G. Xi[1]

[1]Neurosurgery, [2]Neurology, University of Michigan, Ann Arbor, MI, USA

Objectives: Deferoxamine (DFX) reduces brain edema, neuronal death and neurological deficits after intracerebral hemorrhage (ICH) in young rats(Hua et al 2006; Xi et al 2006). In the present study, we investigated whether DFX is effective on brain injury after ICH in aged rats.

Methods: There are two sets of experiments in this study. In the first set, male Fischer 344 rats (18-months old) had an intracaudate injection of 100-µl autologous whole blood. Sham rats only received a needle insertion. Rats were treated with DFX (10, 50 or 100 mg/kg, i.m.; n=9) or vehicle (n=12) 2 and 6 hours post ICH and then every 12 h up to 72 hours. Rats were sacrificed at day 3 for brain edema measurement. In the second set, rats were treated with DFX or vehicle 2 and 6 hours post ICH and then every 12 h for 7 days. Rats had magnetic resonance (MR) scans for T2 imaging eight weeks after ICH and were sacrificed for brain atrophy measurement. Forelimb placing score and corner turn score were assessed at four and eight weeks. Body weight and blood pressure were measured at 1, 3, 7, 14, 21, 28, 42 and 56 days after surgery. Body weight was expressed as % change in body weight using this formula: % change in body weight = (body weight on each time point-body weight before surgery)/body weight before surgery. Mean arterial blood pressure was measured using tail cuff plethysmography.

Results: ICH caused a marked increase in perihematomal water content in vehicle-treated rats (81.6±0.9 vs. 77.7±0.4% in sham control, $p< 0.01$). The systemic administration of 100 mg/kg DFX starting 2 hours after ICH reduced edema (80.3±0.6 vs. 81.6±0.9% in the vehicle-treated group; $p< 0.01$). DFX at doses 50 and 10 mg/kg also reduced perihematomal brain edema (80.4±0.5%, $p< 0.01$, and 80.7±0.9%, $p< 0.05$, respectively). DFX treatment did not change brain water content in the sham-operated rats. MR scans showed that DFX reduced ICH-induced ventricle enlargement. 50 and 100 mg/kg DFX also reduced ICH-induced ventricle enlargement, caudate atrophy and ICH-induced neurological deficits in aged rats. However, while 10 mg/kg DFX reduced ventricle enlargement and forelimb placing deficits, it did not reduce caudate atrophy and corner turn deficits.

During the long-term experiments, body weight and mean arterial blood pressure were monitored. DFX treatment did not affect the body weight change among the ICH groups. Also, in sham rats, there were no differences between DFX- and vehicle-treated groups.

Conclusions: These results indicate that DFX can reduce ICH-induced brain injury in aged as well as young rats and that a dose higher than 10 mg/kg is the optimal dose of DFX in this model.

References:

1. Hua Y, Nakamura T, Keep RF, Wu J, Schallert T, Hoff JT, Xi G (2006) Long-term effects of experimental intracerebral hemorrhage: the role of iron. J Neurosurg 104:305-12.

2. Xi G, Keep RF, Hoff JT (2006) Mechanisms of brain injury after intracerebral hemorrhage. Lancet Neurol 5:53-63.

138

Brain Oral Session: Experimental Cerebral Ischemia: Neuroprotection

EFFECTS OF CEREBRAL ISCHEMIA AND ISCHEMIC PRECONDITIONING ON NEURONAL HEMOGLOBIN

Y. He, Y. Hua, W. Liu, H. Hu, R. Keep, G. Xi

Neurosurgery, University of Michigan, Ann Arbor, MI, USA

Objectives: Recent studies have showed hemoglobin (Hb) is expressed in neurons (Ohyagi et al 1994). The presence of neuronal Hb and its high affinity for oxygen indicate it may have an important role in regulating oxygen hemostasis in neurons. On the other hand, it has been known that exogenous Hb is deleterious to the brain after brain hemorrhage (Xi et al 2006). The present study examined if cerebral ischemia or ischemic preconditioning (IPC) affects neuronal Hb levels in vivo and in vitro.

Methods: There were three parts to the in vivo study. In the first part, rats were subjected to 15 minutes of transient middle cerebral artery occlusion, an IPC stimulus, or sham operation (n=6, each group). In the second part, rats underwent a permanent middle cerebral artery occlusion (pMCAO) to induce brain injury or a sham operation (n=10, each group). In the third part, rats underwent a further pMCAO three days after IPC or sham operation (n=7, each group). All rats were killed 24 hours later for immunohistochemistry, Western blot analysis and real-time polymerase chain reaction (PCR). In vitro, primary cultured neurons and astrocytes were used for Western blotting and real-time PCR. Cultured neurons were exposed to 2 hours of oxygen-glucose deprivation with 22 hours of reoxygenation.

Results: We found that Hb is widely expressed in rat cerebral neurons but not astrocytes. Western blot analysis showed that Hb expression was significantly upregulated in the ipsilateral caudate and the cortical core of the middle cerebral artery territory after IPC. To further confirm the synthesis of Hb within the brain, quantitative real-time PCR was performed on rat brains subjected to IPC or sham operation. There was a 1.8±0.9 fold increase in HbA mRNA in the ipsilateral caudate and 2.6±1.2 fold increase in the ipsilateral cortical core sample in IPC-treated rats compared to shams ($p< 0.05$). HbB mRNA was also upregulated by 27.9±8.4 times in the ipsilateral caudate and 4.8±2.3 times in the ipsilateral cortical core compared to shams ($p< 0.05$). Hb levels also increased in more penumbral cortex and the contralateral hemisphere 24 hours after pMCAO, but expression in the ipsilateral caudate and cortical core area were decreased. Ischemic preconditioning modified pMCAO-induced brain Hb changes. Neuronal Hb levels in vitro were increased by 2 hours of oxygen-glucose deprivation and 22 hours of reoxygenation.

Conclusions: Our present study demonstrates that Hb is expressed in cerebral neurons, and that neuronal Hb is inducible after cerebral ischemia. An understanding of the mechanisms of induction of neuronal Hb after ischemia and the function of neuronal Hb should be helpful in seeking effective new treatment for stroke.

References:

1. Ohyagi Y, Yamada T, Goto I (1994) Hemoglobin as a novel protein developmentally regulated in neurons. Brain Res 635:323-7.

2. Xi G, Keep RF, Hoff JT (2006) Mechanisms of brain injury after intracerebral haemorrhage. Lancet Neurol 5:53-63.

139

Brain Poster Session: Experimental Stroke & Cerebral Ischemia

MRNA GRANULES FORM IN PENUMBRAL NEURONS FOLLOWING FOCAL ISCHEMIA

D. DeGracia, M.K. Lewis, N.N. Rizk, J.C. Dunbar

Department of Physiology, Wayne State University, Detroit, MI, USA

Objectives: Irreversible Translation arrest (TA) following global ischemia TA correlates with the delayed death of vulnerable neurons. Stroke, or focal ischemia, results in a pathophysiology that shares some features with, but has significant differences from, global ischemia. Stroke results in immediate necrosis of brain tissue, while a similar type of delayed neuronal death occurs in adjacent penumbral tissue. Others have shown that penumbral neurons undergo post-ischemic TA. We therefore sought to investigate if similar alterations to translation regulatory systems occur following focal ischemia as have been observed following global ischemia.

Methods: We evaluated markers of stress granules (SGs) and mRNA sequestration using double labeling immunofluorescence histochemistry (IC) and in situ fluorescent immunohistochemistry (FISH). Focal ischemia was produced using normothermic middle cerebral artery occlusion (MCAO) by suture occlusion of the distal MCA. Experimental groups (n=3-5/group) included 2hr MCAO + 24 hr reperfusion, 3hr ischemia only, and 4 hr ischemia only. Stroke volume was characterized by TTC staining. Slices from perfusion-fixed animals were double-labeled for poly-adenylated mRNAs (via FISH) and the following protein markers (via IC): PABP, S6, TIA-1, and TTP. In vitro and in vivo translation rates were measured by standard methods.

Results: 2 hr MCAO resulted in ipsilateral necrosis of striatal and cortical tissue at 24 hr reperfusion. At 3hr and 4 hr ischemia-only, pre-necrotic cells were shrunken and pycnotic but did not display evidence of changes in SG number or composition, or evidence of mRNA granulation. Neurons outside the core showed graded effects. Those adjacent to the core showed mRNAs granules that colocalized with PABP but not S6, TIA-1 or TTP. mRNA granules were most prominent in layer II cortical pyramidal neurons. The presence of mRNA granules correlated with decreased translation rates. Ipsilateral cortical neurons distal to the core and contralateral neurons did not show evidence of mRNA granules. The number of SGs compared to controls in penumbral neurons was a function of distance from the lesioned area on the ipsilateral side.

Conclusions: Neuronal necrosis occurred independent of morphological changes in translational machinery. Penumbral neurons showed graded effects with respect to mRNA granule formation. Our data suggests that mRNA granules contribute to the prolonged TA in penumbral neurons following focal cerebral ischemia as we have shown occurs after global cerebral ischemia.

140

Brain Poster Session: Cerebral Vascular Regulation

DEPTH-RESOLVED MICROSCOPY OF CEREBRAL BLOOD FLOW AND VOLUME DURING SOMATOSENSORY STIMULATION WITH DOPPLER OPTICAL COHERENCE TOMOGRAPHY

V. Srinivasan[1], S. Sakadzic[1], I. Gorczynska[2], A. Yaseen[1], J. Fujimoto[2], D. Boas[1]

[1]Photon Migration Imaging Laboratory, MGH/MIT/HMS Athinuola A. Martinos Center for Biomedical Imaging, Massachusetts General Hospital/Harvard Medical School, Charlestown, [2]Department of Electrical Engineering and Research Laboratory of Electronics, Massachusetts Institute of Technology, Cambridge, MA, USA

Objectives: Investigation of laminar differences in cerebral blood flow and volume during functional activation has been difficult due to the limited spatial resolution of techniques such as MRI and diffuse optical imaging. Recently two-photon microscopy has emerged as a useful tool for depth-resolved measurements of microvasculature during functional activation. However, in conventional two-photon microscopy penetration depths are limited to ~500 microns, simultaneous measurements at multiple cortical depths are difficult, and quantification of high velocities in diving arterioles can be challenging. Doppler Optical Coherence Tomography (OCT) is a new microscopy technique that potentially addresses these limitations. The objective of this study is to investigate Doppler OCT for measuring changes in cerebral blood flow and volume during functional activation.

Methods: Sprague Dawley rats (N=5) were prepared with cranial windows, identically to our previous preparations for two-photon microscopy.(1) Imaging was performed during forepaw stimulation (300 μs pulses at 3 Hz for 4 s with 0.5 mA-1.1 mA amplitude) while rats were under alpha-chloralose anesthesia. Rats were first imaged during forepaw stimulation using 2D optical intrinsic signal imaging (OISI) to determine the response area and to confirm physiological stability of the animal.

A spectral/Fourier domain OCT microscope was constructed for in vivo imaging of the rat cerebral cortex. Briefly the light source consisted of a Mai Tai Ti:Sapphire laser (Spectra Physics) operating at ~830 nm and spectrally broadened in a nonlinear UHNA3 fiber (manufactured by Nufern, distributed by Thorlabs). The axial (depth) resolution was approximately 4.5 microns in air (3.3 microns in tissue). A home-built spectrometer enabled an imaging speed of 22,000 axial scans per second and an axial imaging range of 2.5 mm in air. The transverse resolution was ~11 microns. OCT cross-sectional images were acquired repeatedly at a rate of 4 frames per second across 2 mm of cortical tissue for 8 seconds (1 s pre-stimulus, 4 s stimulus, and 3 s post-stimulus). Doppler OCT signals were extracted by high-pass filtering each OCT image along the transverse dimension, calculating a windowed autocorrelation function at each position, and performing a linear fit to the phase of the autocorrelation function. 25-30 repetitions were performed for the contralateral and ipsilateral forepaw, with 20 s between stimuli.

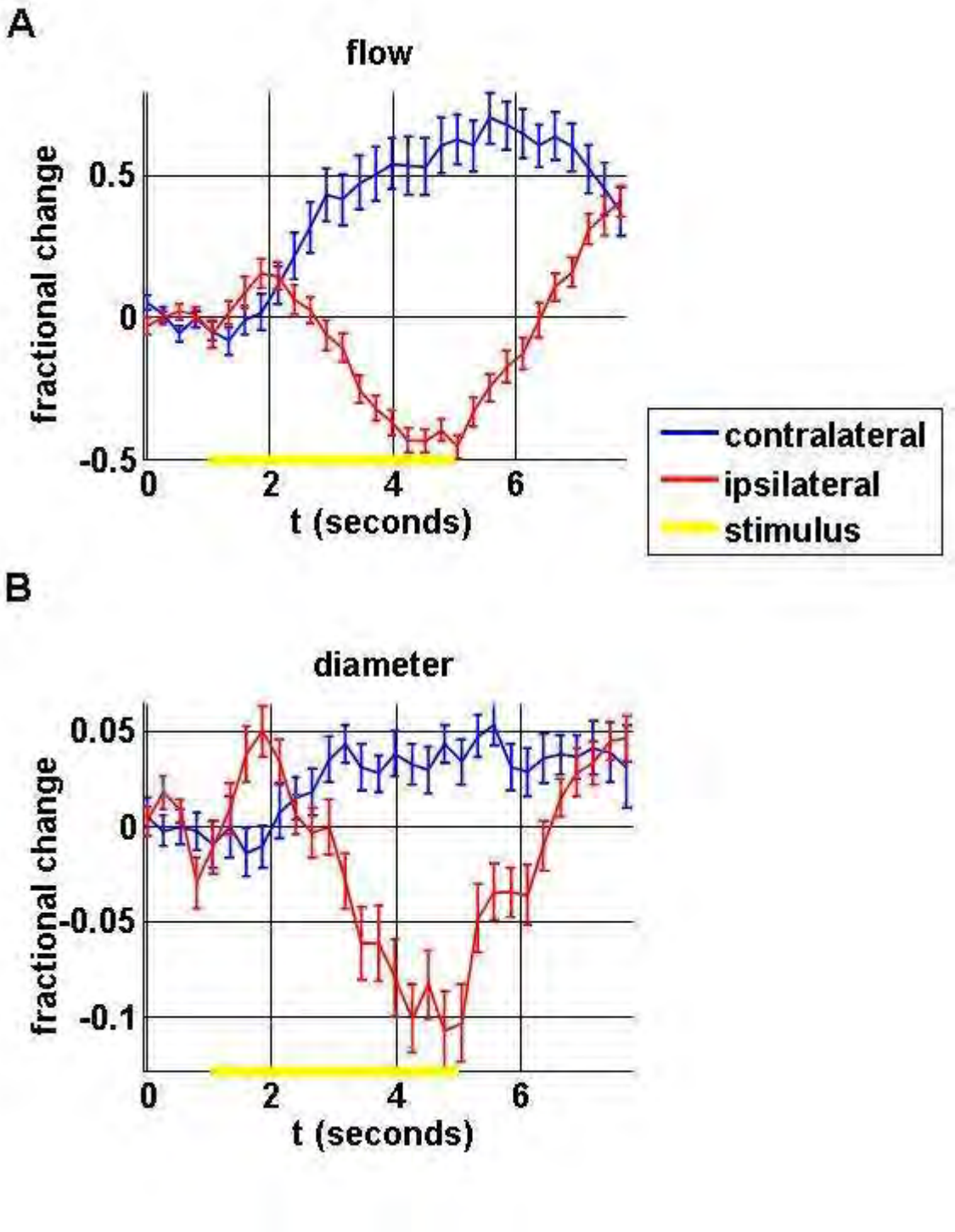

[Diving Arteriole during Functional Activation]

Results: Figure 1A shows fractional flow changes and Figure 1B shows fractional diameter changes of a single representative diving arteriole in the somatosensory cortex during contralateral (blue) and ipsilateral (red) stimulation.

Conclusions: Doppler OCT can simultaneously measure spatiotemporal characteristics of blood flow and volume over cortical depths of 1 mm. Therefore, Doppler OCT has potential as a research tool to understand neurovascular coupling mechanisms and elucidate the BOLD signal.

References: 1. A. Devor et al., J Neurosci 28, 14347 (Dec 31, 2008).

141

Brain Poster Session: Experimental Cerebral Ischemia: Global Ischemia

REDISTRIBUTION OF MRNA AFTER GLOBAL BRAIN ISCHEMIA AND REPERFUSION

J.T. Jamison, M.K. Lewis, J.J. Szymanski, D.J. De Gracia

Department of Physiology, Wayne State University, Detroit, MI, USA

Objective: Death of vulnerable neuron populations following global brain ischemia and reperfusion (I/R) correlates with irreversible translation arrest (TA), but the mechanisms of irreversible TA are not known. However, all post-ischemic neurons show a stress-induced TA, but translation recovery follows HSP70 translation in resistant neurons.

Methods: Here, we evaluated markers of translation and translation regulation including ribosomal protein S6, eIF4G, PABP, TIA-1, TTP, HuR, HSP70 by immunofluorescence histochemistry, and poly-adenylated [p(A)] mRNAs using fluorescent in situ hybridization in brain slices after [SRK1] 48 hr reperfusion following 10 min global brain ischemia. We assessed different combinations of staining pairs. Additionally we used co-immunoprecipitation to evaluate protein-mRNA interactions in post-ischemic brain homogenates, specifically at 8 hr reperfusion, when markers of TA show the greatest divergence. Normothermic I/R were performed by bilateral carotid artery occlusion (2VO) plus hypotension, and various durations of reperfusion between 1 and 48 hours. Brains were perfusion fixed and double labeled for various combinations of the above markers. Standard methods for co-immunoprecipitation were used [SRK2].

Results: We observed that p(A) mRNAs underwent redistribution from a homogeneous cytoplasmic pattern to a granular pattern during reperfusion. Granulation of the mRNA correlated precisely with TA as measured by in vivo radioactive amino acid incorporation. The “mRNA granules” colocalized with eIF4G and PABP, but not S6, TIA-1 or TTP. HuR colocalized to mRNA granules at 1hr reperfusion in resistant neurons, and only after 36 hr reperfusion in vulnerable neurons. Colocalization of HuR and mRNA granules correlated with HSP70 translation. IP of PABP co-precipitated GAPDH and HSP70 mRNA, whereas IP of HuR co-precipitated only HSP70 mRNA. Co-IP results validated the microscopy studies.

Conclusions: These results indicate that mRNAs are generally sequestered from 40S subunits following brain reperfusion, and that selective translation of stress induced messages occurs early in resistant areas but is delayed in vulnerable neurons. This delay likely plays a prominent role in irreversible TA and hence cell death.

143

Brain Poster Session: Translational Studies

CEREBRAL HEMODYNAMICS OF PRETERM INFANTS DURING POSTURAL INTERVENTION MEASURED WITH DIFFUSE CORRELATION SPECTROSCOPY AND TRANSCRANIAL DOPPLER ULTRASOUND

E. Buckley[1], N. Cook[2], T. Durduran[1,3], M. Kim[1], C. Zhou[1], R. Choe[1], G. Yu[1], D. Licht[4], J. Detre[3,4], J. Greenberg[5], H. Hurt[2], A. Yodh[1]

[1]Physics and Astronomy, University of Pennsylvania, [2]Neonatology, [3]Radiology, [4]Neurology, Hospital of the University of Pennsylvania, [5]Neurology, University of Pennsylvania, Philadelphia, PA, USA

Objective: Preterm infants are at significant risk of brain injury, in part due to their limited ability to regulate cerebral blood flow (CBF). A continuous monitor of CBF at the bedside could therefore be a valuable supplement for gathering information about a patient´s condition and for guiding treatment.

In this study, diffuse correlation spectroscopy (DCS), a continuous and non-invasive optical technique to measure blood flow, and transcranial Doppler ultrasound (TCD) were employed to monitor the cerebral hemodynamics of 4 preterm neonates during a 0 to 12° postural change on 9 different days.

Methods: The DCS instrument consists of a 785 nm source laser, a single mode detector fiber located on the tissue surface 1.5 cm from the source, and detection electronics to measure the light intensity autocorrelation function. Variations in the decay time of the autocorrelation function, which we refer to as the blood flow index (BFI) are related to blood flow in the tissue [1]. BFI was recorded on the forehead of each preterm infant at 7 Hz for 5 minutes at each head-of-bed angle (HOB) adjustment from 0 to 12° and was repeated 3 times.

For TCD, measurements of peak systolic, end diastolic, and mean velocities (PSV, EDV, and MV respectively) were obtained on the middle cerebral artery. Three data points were taken at each HOB angle before the bed was repositioned, and the HOB angle was elevated twice. DCS and TCD measurements were not taken at the same time.

Results: Figure 1 shows the relationship between baseline PSV and BFI for TCD and DCS data taken on the same day from the same patient. A significant correlation ($p< 0.05$) between PSV and BFI, as well as between MV and BFI, was discovered. Similar correlations were not found with BFI and EDV.

Both techniques showed no significant population averaged hemodynamic changes during HOB elevation as compared to HOB flat. In addition, no population averaged correlations between rCBF and relative ultrasound parameters were found (rCBF and rPSV, $r_s = 0.1$, $p > 0.05$; rCBF and rEDV, $r_s = 0.17$, $p> 0.05$; rCBF and rMV, $r_s = 0.1$, $p > 0.05$).

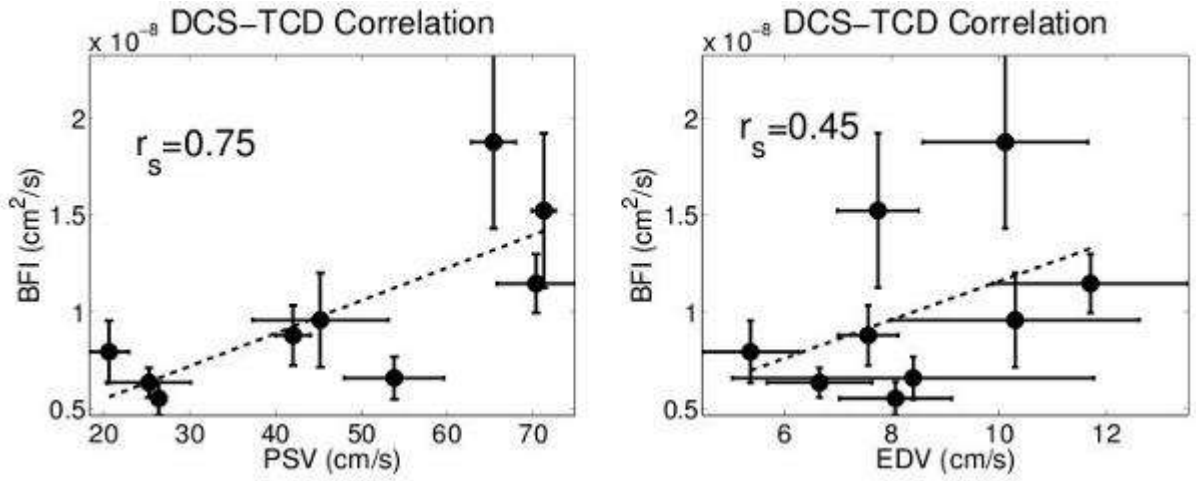

[Correlation Between TCD and DCS]

Conclusions: In summary, we have demonstrated the feasibility of DCS to continuously monitor changes in CBF in very low birthweight preterm infants. We also showed with DCS that when posed with a small HOB challenge, the infants maintained a constant CBF. This result was corroborated by findings from TCD measurements.

References: [1] D. A. Boas, L. E. Campbell, and A. G. Yodh. Scattering and imaging with diffusing temporal field correlations. Physical Review Letters, 75(9):1855-1858, 1995.

145

Brain Poster Session: Neonatal Ischemia

AGE-DEPENDENT EFFECTS OF GRADUAL CEREBRAL PERFUSION PRESSURE (CPP) DECREASE AND TEMPORARY CPP BREAKDOWN ON NEUROCHEMICAL RESPONSE IN SWINE

R. Bauer[1], B. Walter[2], K. Aisenpreis[1], J. Soukup[3], M. Eiselt[4], H. Fritz[5]

[1]Institute of Molecular Cell Biology, Friedrich Schiller University, Jena, [2]Department of Neurosurgery, Zentralklinik Bad Berka, Bad Berka, [3]Department of Anesthesiology and Intensive Care Medicine, Martin Luther University Halle-Wittenberg, Halle/Saale, [4]Institute of Medical Statistics, Computer Sciences and Documentation, Friedrich Schiller University, Jena, [5]Department of Anesthesiology and Intensive Care Medicine, Matha-Maria Hospital, Halle/Saale, Germany

Objectives: Compromised CPP appears as a main pathogenetic factor for disturbed brain functioning and resulting structural brain damage during ontogenesis. However, there is still a lack of knowledge on the age-dependent relation between the level of CPP reduction, which induces a critically reduced brain perfusion leading to excessive transmitter release and disturbed brain energy metabolism prone to initiate brain tissue damage cascades. Therefore, in newborn and juvenile pigs, we gradually reduced CPP up to a complete temporary breakdown and estimated the effects on brain oxidative metabolism as well as responses on extracellular glutamate (Glu), dopamine (DA), lactate (Lac) and lactate/pyruvate ratio (Lac/Pyr).

Methods: Experiments were performed in 8 newborn (PD13) and 11 juvenile pigs (PD51), anesthetized with 1.3% isoflurane in N_2O/O_2 and artificially ventilated. CBF was measured by colored microspheres, $CMRO_2$ and $CMR_{Glucose}$ were calculated. Intracranial pressure (ICP) was measured subcortically and two microdialysis probes were implanted bilaterally into the striatum. Extracellular DA, Glu, Lac and Lac/Pyr were estimated by HPLC with electrochemical detection and by enzymic fluorometric assays. For CPP manipulation, cisterna magna was punctured by a lumbar puncture needle and fixed in place for elective CSF (cerebrospinal fluid) infusion/withdrawal to control ICP. Furthermore, a cerclage of a plastic-coated wire was performed around the trunk of the pulmonary artery in order to apropriately adjust the vessel diameter for perfusion control resulting in ABP stabilization (in order to prevent Cushing response). Artificial CSF infusion was adjusted to induce consecutively a stepwise CPP decrease at four levels, beginning at 50 mmHg (CPP-50), followed by 40 mmHg (CPP-40), 30 mm Hg (CPP-30), and zero mmHg (CPP-0, ICP was always ~10-20 mmHg above ABP) for every 15 minutes. The recovery period was observed for 180 minutes.

Results: Whereas juvenile pigs showed a corresponding gradual decrease in CBF between stages CPP-50 and CPP-30, a significant CBF reduction occurred in newborn piglets not until stage CPP-30 ($P < 0.05$). At this stage of CPP reduction an alteration of brain oxidative metabolism occurred solely in juvenile pigs ($P < 0.05$). This was accompanied by DA and Glu elevation ($P < 0.05$). However, already at CPP-50, Lac and Lac/Pyr were elevated ($P < 0.05$). In contrast, newborn piglets showed mild elevation in Lac and Lac/Pyr not until stage CPP-30, whereas all other microdialysis parameters changed during the period of complete global brain ischemia at CPP-0. Complete global brain ischemia was confirmed by nearly complete suppression of ECoG activity. At this stage striatal DA and Glu reached the strongest elevation in juvenile pigs. Similar alterations were seen in newborn piglets, but the respective changes were markedly blunted ($P < 0.05$).

Conclusions: Lower limit of CBF autoregulation determines modifications in neurochemical parameters, clearly before $CMRO_2$ and $CMR_{Glucose}$ are reduced. Early indicators for mild to moderate hypoperfusion are evidently Lac, Lac/Pyr and DA elevation, but Glu appears to be an indicator for tissue ischemia. The immature brain generates a markedly diminished potential for excitotoxicity suggesting a substantial reason for blunted cerebral damage in consequence of gradual CPP impairment.

THE PROTECTIVE ROLE OF PGC-1α IN ISCHEMIA-INDUCED HIPPOCAMPAL NEURONAL INJURY

S.-D. Chen[1], T.-K. Lin[1], D.-I. Yang[2], S.-Y. Lee[1], C.-W. Liou[1], Y.-C. Chuang[1]

[1]Department of Neurology, Chang Gung Memorial Hospital-Kaohsiung Medical Center, Chang Gung University, Kaohsiung, [2]Institute of Brain Science, National Yang-Ming University, Taipei, Taiwan R.O.C.

Background and purpose: Transient global ischemia (TGI) is known to cause delayed hippocampal neuronal death. Excessive reactive oxygen species generation after TGI/reperfusion may contribute this TGI-induced hippocampal neuronal death. Activation of PGC-1α, a coactivator of peroxisome proliferator activated receptor gamma, is emerged as a master regulator in oxidative stress in hypoxic/ischemic condition. Uncoupling protein 2 (UCP 2) and superoxide dismutase 2 (SOD 2) are molecules important for counteracting excessive oxidative stress under certain circumstances including cerebral ischemia and may be regulated by PGC-1α. We studied hippocampal PGC-1α activation and the expression of UCP 2 and SOD 2 in a rat TGI model and explored if this signaling pathway is relevant to this delayed hippocampal neuronal death.

Methods: Rats were subjected to TGI by transient bilateral common carotid artery occlusion and systemic hypotension (mean arterial pressure to 35-40 mm-Hg) for 10 min followed by restoration of blood flow to normal level. Hippocampal proteins were extracted and subjected to western blot for PGC-1α, UCP 2 and SOD 2 expression. Oxidized protein of hippocampus under ischemic condition was examined at various time points after reperfusion. Anti-sense oligodeoxynucleotide (ODN) for PGC-1α is used to investigate the role of PGC-1α over UCP 2 and SOD 2 expression and the effect over oxidized protein of hippocampus and neuronal survival under TGI/reperfusion. Apoptosis-related DNA fragmentation were evaluated for outcome measurement after ischemia/reperfusion. Surviving CA1 neuronal cells were counted under light microscopy.

Results: PGC-1α expression increased in 1 to 4h after ischemia/reperfusion. UCP 2 expression increased in 4 to 48 h after ischemia/reperfusion. SOD 2 expressions increased in 4 to 48 h after ischemia/reperfusion. Increased oxidized protein of hippocampus under ischemic condition was detected at 1-24 h after reperfusion. Anti-sense ODN for PGC-1α pretreatment 24 h before TGI showed decreased PGC-1α, UCP 2 and SOD 2 expression which was accompanied by a heightened protein oxidation and enhanced hippocampal CA1 neuronal damage based on apoptosis-related DNA fragmentation.and the surviving neuronal counts.

Conclusions: This study may provide a molecular evidence for the PGC-1α/ UCP 2 and SOD 2 neuroprotective cascade in ischemic brain injury.

150

Brain Oral Session: Brain Imaging

A COMPARISON OF THE EVOLUTION OF THE ISCHAEMIC PENUMBRA IN THE SHRSP & WKY RAT USING DIFFUSION AND PERFUSION MRI

C. McCabe[1], W. Holmes[1], L. Gallagher[1], W. Gsell[2], D. Graham[3], A.F. Dominiczak[3], I.M. Macrae[1]

[1]Glasgow Experimental MRI Centre, Division of Clinical Neurosciences, University of Glasgow, Glasgow, [2]Biological Imaging Centre, MRC Clinical Sciences Centre, Imperial College London, London, [3]BHF Glasgow Cardiovascular Research Centre, Division of Cardiovascular & Medical Sciences, University of Glasgow, Glasgow, UK

Objectives: The stroke prone spontaneously hypertensive rat (SHRSP) is a highly pertinent model of human stroke with increased sensitivity to focal ischaemia [1]. The mechanisms underlying increased stroke sensitivity remain poorly understood. However, impaired collateral flow to penumbral tissue is thought to contribute. Our objective was to compare the size and fate of penumbral tissue in SHRSP and WKY.

Methods: Male SHRSP and WKY rats (12-16 weeks old, n=8) were anaesthetized (1-2% isoflurane in 70:30 N_2O:O_2), ventilated and the middle cerebral artery permanently occluded by the intraluminal filament technique. Diffusion-weighted (DWI) and perfusion-weighted (PWI) MRI was performed on a Bruker Biospec 7T/30 cm system with diffusion/perfusion mismatch used to define penumbral tissue.

PWI was run on a single slice within MCA territory using an arterial spin labeling (ASL) sequence. DWI revealed ischaemic damage. DWI and PWI were run every hour from 1 to 6 hours post MCAO. Apparent diffusion coefficient (ADC) and relative CBF (rCBF) maps were generated using Image J and thresholded using previously published values [2,3] to calculate mismatch area.

Results: By 1 hr post-stroke the ADC derived lesion volume was significantly larger in SHRSP compared to WKY (275 ± 75.2 vs 171 ± 29.2 mm^3; $P< 0.05$ unpaired t-test) and increased in both strains from 1-6 hrs (275 ± 75.2 to 330 ± 57 mm^3, SHRSP; 171 ± 29.2 to 253 ± 43 mm^3, WKY; $P< 0.05$ paired t-test between 1hr & 6hr). In contrast, perfusion deficit area was similar between strains at 1 hr (43.6 ± 9.7 vs 39.9 ± 6 vs mm^2) resulting in 59% less penumbra in SHRSP than WKY (Figure 1).

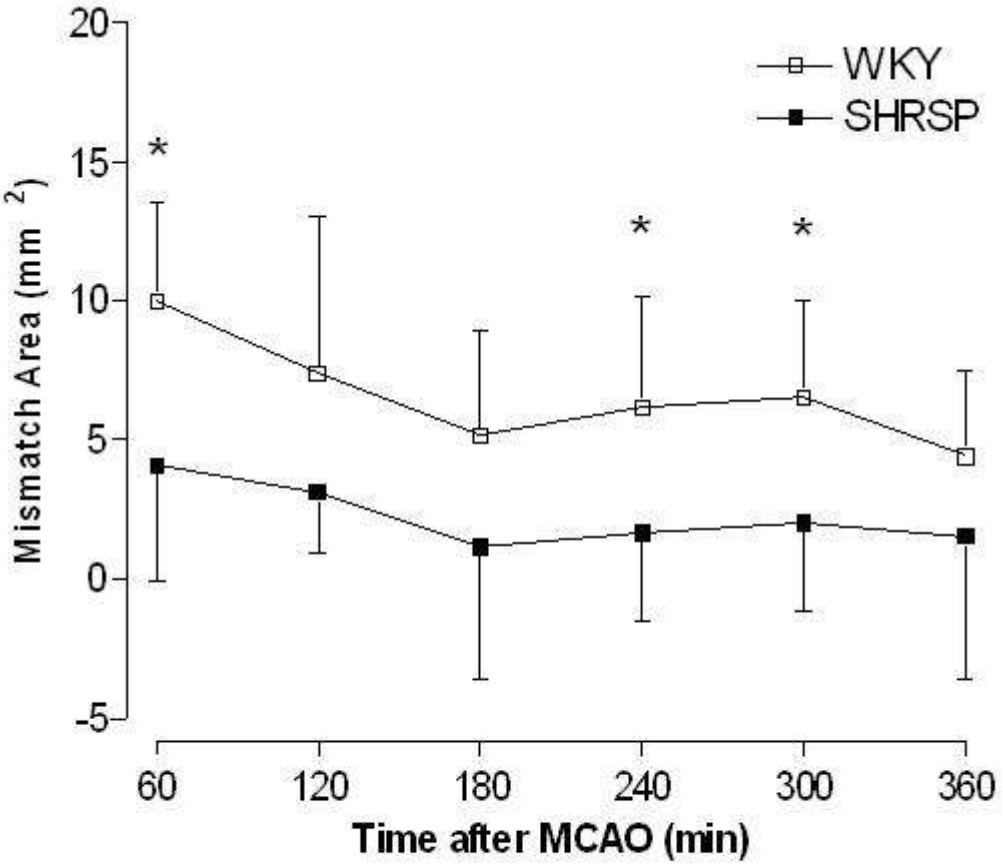

Figure 1. Temporal evolution of the mismatch area between the ADC and rCBF area in WKY and SHRSP rats following permanent MCAO. Data presented as mean±S.D, * indicates P<0.05 unpaired t-test (n=8 per group).

[Fig 1.]

The perfusion deficit remained unchanged in WKY (40.2 mm^2 at 6 hrs) but increased in SHRSP (to 48 mm^2, $P< 0.05$, paired t-test). In WKY 56% of penumbra was incorporated into the ADC lesion by 6 hrs. In SHRSP, the increase in both ADC lesion and perfusion deficit over time resulted in no overall change in the very small mismatch area.

Conclusions: The present study demonstrates 1. SHRSP have significantly more ischaemic damage and less penumbral tissue than WKY within 1 hour of stroke onset; 2. penumbral tissue is recruited into the ADC abnormality over time in both strains; 3. The expanding perfusion deficit in SHRSP predicts greater tissue at risk of infarction. These results could have important implications for the management of stroke patients with pre-existing risk factors such as hypertension and suggest ischaemic damage could progress at a faster rate and over a longer time in the presence of hypertension.

References:

[1] Jeffs B et al. Nature Genetics (1997) 16, 364-367.

[2] Meng X et al. Annals of Neurology (2004) 55, 207-212.

[3] Hoehn-Berlage M et al. JCBFM (1997) 17, 534-542.

ADMINISTRATION OF FISH OIL DURING PERINATAL PERIODS GREATLY RELIEVE THE BEHAVIORAL DEFICITS IN NEONATAL HYPOXIA-ISCHEMIA

Y. Gao[1,2], W. Zhang[1,2], H. Gao[1], W. Yang[1], H. Shen[1], G. Cao[1,2], J. Chen[1,2]

[1]State Key Laboratory of Medical Neurobiology, Fudan University, Shanghai, China, [2]Department of Neurology, University of Pittsburgh School of Medicine, Pittsburgh, PA, USA

Background: The development of the rodent models of neonatal hypoxia-ischemia brain injury is similar to what is observed in the human neonates suffering from hypoxia-ischemia encephalopathy. In spite of increased knowledge of its pathophysiology, we still lack effective strategy for neuroprotection. OMEGA-3 play an important role in many aspect of physical function such as synaptic transmission, cognitive development and memory-related learning. Fish oil is considered to be the major source of OMEGA-3, especially content high percentage of Eicosapentaenic acid (EPA) and Decosahexaenic acid (DHA). DHA is a critical component of brain membrane phospholipids and is necessary for the development of nervous system. EPA could inhibit the conversion of arachdonic acid (AA) into and prostaglandins, which is the main source of inflammation after brain injury, and is a potential antioxidant against ischemia brain injury. In this study, we determined the changes of OMEGA-3 in brain tissue after neonatal hypoxia-ischemia brain injury and investigated the neuroprotective effect of fish oil on the behavioral recovery after hypoxia-ischemia.

Methods: After being pregnant, rats were divided into two groups, one is given regular diet for rodent (RD group) and the other is supplied special diet containing 5% fish oil (FOD group), then both of them were given regular diets 14 days after gestation. Neonatal of 7 days old was suffered from hypoxia-ischemia brain injury, and Lipid analysis was performed respectively on 1 day or 7 days after this injury. Behavioral performance of gait walking, righting reflex, grid walking and water maze were also recorded after damage. All data are expressed as mean±SD, and statistic analysis was performed using SPSS tests, with $p < 0.05$ considered statistically significant.

Results: We found that, with the increase of AA, hypoxia-ischemia brain injury greatly reduced the concentration of DHA and EPA in brain tissue. Although only hypoxia could decrease the ratio of DHA and EPA to AA (from the normal ratio of 2.68±0.26 to 2.12±0.11, $P< 0.001$) 24hrs after hypoxia, but it raise to the normal level 7 days after H-I. On the other hand, Hypoxia-Ischemia cause long last decrease of this ratio (from 2.44±0.26 to 1.95±0.03, $P< 0.001$) fish oil treatment could maintain the high level of this ratio even after the hypoxia-ischemia (RD group: from the normal 2.68±0.26 to 2.04±0.32, 24hrs after H-I, $P< 0.01$; FOD group: from the normal 3.05±0.09 to 3.15±0.10, 24hrs after the damage, $P< 0.05$). The concentration of EPA in ipsilateral is extremely higher compared with sham in fish oil diet group 7 days after the injury (sham is 0.138±0.01%, H-I is 0.176±0.009% respectively, $P< 0.05$). Furthermore, fish oil apparently relieve the behavioral deficits in gait walking and righting reflex ($P< 0.001$), and improve the long term recovery in grid walking and water maze even 5 weeks after brain damage ($P< 0.05$).

Conclusions: These results suggest that supplementary of fish oil could ameliorate the brain damage and is beneficial to the behavioral recovery from hypoxia-ischemia brain injury.

159

Brain Poster Session: Neuroprotection

BRAIN ISCHEMIC POSTCONDITIONING EXERTS ITS NEUROPROTECTIVE EFFECT BY MODULATING ASIC1A AND NCX3 EXPRESSION IN THE ISCHEMIC PENUMBRA REGION

G. Pignataro, E. Esposito, O. Cuomo, R. Sirabella, R. Gala, P. Molinaro, G. di Renzo, L. Annunziato

Neuroscience, Federico II University of Naples, Naples, Italy

Background and aims: As clinical trials of pharmacological neuroprotective strategies in stroke have been disappointing, attention has turned to the brain´s own endogenous strategies for neuroprotection. Two endogenous mechanisms have been characterized so far, ischemic preconditioning and ischemic postconditioning. However, preconditioning as a strategy to attenuate the pathophysiological consequences of ischemia-reperfusion injury can be applied on pretreatment situations, such as protection before cardiac bypass surgery. A non-pharmacological neuroprotective strategy to be applied after ischemia onset, however, remains illusive. Based on recent studies on the heart (Yellon et al., 2002) and proof of principle experiments in the brain (Burda et al., 2006; Pignataro et al., 2006 and 2008; Wang et al., 2008; Zhao et al., 2006), a hypothesis has been offered that a modified reperfusion subsequent to a prolonged harmful ischemic episode may confer ischemic neuroprotection, a phenomenon termed postconditioning.

To study how this clinically relevant neuroprotective strategy exerts its effect many transcriptional mechanisms have been taken into consideration. In particular, the well known family of Mitogen Activated Kinases (MAPK) has been proposed as important mediator of this mechanism of neuroprotection.

Methods: Ischemic postconditioning has been induced in 8 weeks old SD male rats as previously described (Pignataro et al., 2008). Briefly, anaesthetized rats were subjected to 100 minutes of middle cerebral artery occlusion by intraluminal suture method. After 10 minutes of reperfusion, the filament was reintroduced and kept in situ for 10 more minutes. Protein and mRNA expression was evaluated at different time points by Western Blotting and RT-PCR, respectively.

Objectives: The main objective of this study was to evaluate the effect of MAPK activated by postconditioning on the expression of Acid Sensing Ionic Channels (ASIC) and Na^+/Ca^{2+} exchangers (NCXs). These two plasmamembrane proteins are expressed in the CNS and are able to control the intracellular Na^+ and Ca^{2+} homeostasis and involved in the progression of the ischemic lesion (Annunziato et al., 2004; Pignataro et al., 2004, 2008).

ASIC and NCX mRNA and protein expressions were investigated in the penumbra region of rats subjected to harmful ischemia or ischemic postconditioning and treated with specific MAPK inhibitors or with vehicle alone.

Results: Results of this study showed that NCX1, NCX3 and NCKX2 are up-regulated in those brain regions protected by postconditioning treatment, whereas ASIC1a expression is dramatically reduced in the same brain regions.

These changes in ASIC and NCX expression seem to be mediated by p-AKT. In fact, treatment with LY- 294002, a specific p-AKT inhibitor, was able to revert the postconditioning neuroprotective effect and to prevent variations in NCX and ASIC expression.

Conclusions: The results obtained in the present study indicate that NCX1, NCX3, NCKX2 and ASIC1a are involved in the neuroprotection mediated by p-AKT and elicited by ischemic postconditioning and may represent important targets in setting on a new strategy for stroke treatment.

160

BrainPET Poster Session: PET Acquisition and Processing

OFF-LINE MOTION CORRECTION METHODS FOR MULTI-FRAME PET DATA

J.E.M. Mourik, M. Lubberink, F.H.P. van Velden, A.A. Lammertsma, R. Boellaard

Nuclear Medicine & PET Research, VU University Medical Center, Amsterdam, The Netherlands

Background and aims: Patient motion during PET acquisition may reduce spatial resolution and alter time-activity curves, especially for small region of interests, thereby affecting outcome of tracer kinetic analyses. Currently, on-line optical motion tracking systems are available [1-2]. Although these systems show some important advantages, e.g. in-frame motion correction, there are also some drawbacks. First, old datasets, scanned without an on-line motion tracking system, cannot be corrected. Second, most on-line motion tracking systems require that PET data to be acquired in list-mode, which is not possible on older scanners. Third, application of these systems is not always possible due to limited view within the gantry in case of auxiliary equipment. Off-line (mathematical) motion correction methods do not have these disadvantages. Aim of the present study was to evaluate several off-line frame-by-frame motion correction methods for correcting patient motion.

Methods: Four different motion correction methods were evaluated. They differed in the way realignment parameters were derived, based on:

1. sum of first x frames of normal PET scan,
2. sum of first x frames of non-attenuation corrected PET scan,
3. attenuation map and
4. attenuation map divided by measured attenuation correction factors.

In method 2-4 realignment was included in a final image reconstruction process to correct for attenuation and emission mismatch as well. Two simulation studies were performed, based on [^{11}C]flumazenil and [^{11}C]PK11195 datasets, respectively. In both simulation studies kind (rotation, translation) and amount of motion were varied. Simulated PET scans were corrected for motion using all four correction methods. Next, optimal settings derived from the simulation studies were used to evaluate two clinical datasets each of [^{11}C]flumazenil, [^{11}C]PK11195 and [^{11}C]PIB. For the clinical datasets, volume of distribution (V_T) values, obtained with Logan analysis [3], were compared before and after motion correction.

Results: Optimal results were obtained when realignment parameters were based on method 2, where differences in regional V_T values were < 2.8% and < 3.5% for [^{11}C]flumazenil and [^{11}C]PK11195 simulation studies, respectively. In comparison, differences up to 22%, 62% and 46% were observed in regional V_T values for method 1, 3 and 4, respectively. For the clinical datasets, visual inspection revealed that motion was no longer visible after correction using these optimal settings. Differences in V_T of up to 433% before and after motion correction were found for the clinical data. Moreover, when no motion was present in the original (clinical) dataset, differences in V_T before and after motion correction were < 1.5±1.3%, indicating that method 2 can always be used without degrading quantitative accuracy.

Conclusions: When no optical tracking system is available or when old datasets have to be reanalyzed, the presented frame-by-frame motion correction method, using the sum of first x frames of non-attenuation corrected PET scans, provides a means to analyse data in which the patient has moved.

References:

[1] Goldstein et al. IEEE Trans.Med.Imaging 1997; 16:17-27.

[2] Bloomfield et al. Phys.Med.Biol. 2003; 48:959-978.

[3] Logan et al. Nucl.Med.Biol. 2000; 27:661-70.

Acknowledgments: Financial support provided by the Netherlands Organisation for Scientific Research (NWO, VIDI Grant 016.066.309).

161

Brain Poster Session: Cerebral Vascular Regulation

PREDICTIVE FACTORS OF CEREBRAL HYPERPERFUSION SYNDROME BEFORE AND IMMEDIATELY AFTER CAROTID ANGIOPLASTY AND STENT PLACEMENT

T. Iwata, T. Mori, **H. Tajiri**, M. Nakazaki

Shonan Kamakura General Hospital, Kamakura City, Japan

Objectives: To anticipate high risk of hyperperfusion syndrome (HPS) following carotid angioplasty and stent placement (CAS) is useful for perioperative management. The purpose of our retrospective study was to find predictors of HPS before and immediately after CAS and to investigate the utility of single-photon emission computed tomography (SPECT) and transcranial color-coded real-time sonography (TCCS) as predictors.

Methods: Included for analysis were patients:

1. who underwent elective CAS in our institution from July 2005 to March 2008,
2. with unilateral carotid stenosis,
3. who underwent ^{99m}Tc-ethyl cysteinate dimmer (^{99m}Tc-ECD) SPECT study before and immediately after CAS,
4. who underwent acetazolamide (ACZ) challenge test of ^{99m}Tc-ECD SPECT study before CAS and
5. who underwent TCCS study before and immediately after CAS.

Regional cerebral blood flow (rCBF) by using ^{99m}Tc-ECD SPECT and mean blood flow velocity (mBFV) in the middle cerebral artery (MCA) by using TCCS were examined before and immediately after CAS. Clinical HPS was defined as symptoms as follows:

1. throbbing ipsilateral frontotemporal or periorbital headache and
2. at least one symptom of temporary deterioration of consciousness level, focal seizure and hemiparesis.

Age, sex, degree of stenosis, hypertension (HT), hyperlipidemia (HL), diabetes mellitus (DM), asymmetry index (AI)=(rCBF in the affected hemisphere coupled with a carotid stenosis/rCBF in the contralateral hemisphere) before and immediately after CAS, AI change=(AI immediately after CAS－AI before CAS), AI ratio=(AI change/AI before CAS), regional activity-to-cerebellar activity (R/CE) ratio=(rCBF in the affected hemisphere coupled with a carotid stenosis/rCBF in the ipsilateral cerebellum hemisphere) before and immediately after CAS, R/CE ratio-change=(R/CE immediately after CAS－R/CE before CAS), R/CE ratio-ratio=(R/CE ratio-change)/(R/CE before CAS), CVR=[(post-ACZ rCBF－resting rCBF) /resting rCBF], MCA mBFV in the affected hemisphere before CAS and MCA mBFV ratio=(MCA mBFV immediately after CAS in the affected hemisphere/MCA mBFV before CAS in the affected hemisphere) were assessed.

Results: Eighty consecutive patients underwent CAS and ten of them presented HPS after CAS. In TCCS study, the dropout rate due to an insufficient acoustic temporal bone window was 20% (16/80).

Between HPS and non_HPS groups, there were significant differences in severe carotid stenosis, CVR and MCA mBFV in the affected hemisphere ($p< 0.05$: Mann-Whitney U test) in the preoperative items, and significant differences in AI after CAS, AI change, AI ratio, R/CE ratio after CAS, R/CE ratio-change, R/CE ratio-ratio and MCA mBFV ratio ($p< 0.05$: Mann-Whitney U test) in the postoperative items, although there were no significant differences in age, sex, HT, HL, DM, AI before CAS and R/CE before CAS. Logistic regression analysis showed that CVR [Odds ratio (95%CI); 0.674 (0.492-0.926), p=0.015] was the significant predictor among the preoperative items, and that MCA mBFV ratio [Odds ratio (95%CI); 9.696 (1.550-60.657), p=0.015] and R/CE ratio-change [Odds ratio (95%CI); 1.169 (1.018-1.342), p=0.027] were the significant predictors among the postoperative items.

Conclusions: Significant predictors of HPS were CVR before CAS, and MCA mBFV ratio and R/CE ratio-change immediately after CAS. SPECT and TCCS studies are useful to predict HPS.

EVALUATION OF RECONSTRUCTION BASED PARTIAL VOLUME CORRECTION

J.E.M. Mourik, M. Lubberink, F.H.P. van Velden, A.A. Lammertsma, R. Boellaard

Nuclear Medicine & PET Research, VU University Medical Center, Amsterdam, The Netherlands

Background and aims: The limited resolution of current clinical PET scanners results in incorrect estimation of true radioactivity, which is known as the partial volume effect. Different partial volume correction (PVC) methods exist [1]. One way is to correct for partial volume during reconstruction. Such a reconstruction based PVC method improves the spatial resolution by taking the point spread function of the scanner into account. The aim of present study was to assess the accuracy of reconstruction based PVC.

Methods: The NEMA NU2 image quality phantom with spheres of varying internal diameter (10, 13, 17, 22, 28 and 37 mm) was scanned on both HR+ (resolution: ~4.1 to 7.8 mm FWHM; CTI/Siemens) and HRRT (resolution: ~ 2.3 to 3.4 mm FWHM; CTI/Siemens) scanners. This phantom was used to obtain recovery (measured/true activity) of the spheres for the different reconstruction algorithms used. In addition, dynamic [^{11}C]flumazenil data (n=5), acquired on both scanners were used. HR+ data were reconstructed using normalization and attenuation weighted ordered subsets expectation maximization (NAW-OSEM, 4 iterations (i), 16 subsets (s)), NAW-OSEM smoothed with a 5 mm Gaussian filter (clinical standard) and a reconstruction based PVC method (PVC-OSEM, 4i, 16s) [2-3]. In addition, HRRT data were reconstructed using 3D ordinary Poisson (OP) OSEM (8i, 16s), OP-OSEM smoothed with a 6 mm Gaussian filter and a HRRT PVC algorithm (PVC OP-OSEM, 16i, 16s). For each reconstruction, parametric volume of distribution (V_T) images were generated using a basis function implementation of the standard single tissue compartment model [4].

Results: For the HRRT, good recoveries of the spheres were obtained for both standard OP-OSEM (0.84 to 0.97) and PVC OP-OSEM (0.91 to 0.98) for the HRRT. In addition, for the HR+, good recoveries were found for the PVC-OSEM reconstruction (0.84 to 0.94), which corresponded well with results of the standard HRRT OP-OSEM reconstructions. In contrast, much lower recoveries were found for standard NAW-OSEM 5 mm (0.42 to 0.86). In addition, for clinical data, good correspondence (slope: 1.00 ± 0.08; R^2: 0.95 ± 0.01) was found between HR+ PVC-OSEM and HRRT OP-OSEM derived V_T values, see also Figure 1.

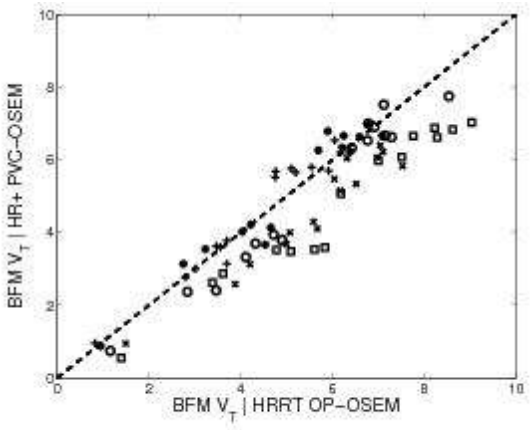

Figure 1 - HRRT OP-OSEM versus HR+ PVC-OSEM based regional BFM V_T values for 15 ROIs per subject (n=5)

[Figure 1]

Conclusions: The present study showed that HR+ image resolution using PVC-OSEM was comparable to the resolution of the HRRT scanner. Outcome of tracer kinetic analysis of HR+ studies reconstructed with PVC-OSEM correlated well with outcome of HRRT studies, indicating that reconstruction based partial volume correction yields quantitatively accurate images.

References:

[1] Boussion et al. Phys.Med.Biol. 2006; 51:1857-1876.

[2] Brix et al. Eur.J.Nuc.Med. 1997; 24:779-786.

[3] Mourik et al. NeuroImage 2008; 39:1041-1050.

[4] Gunn et al. NeuroImage 1997; 6:279-87.

Acknowledgments: Financial support provided by the Netherlands Organisation for Scientific Research (NWO, VIDI Grant 016.066.309.

CHARACTERISING THE RELATIONSHIP BETWEEN PLASMA PHARMACOKINETICS AND OCCUPANCY FOLLOWING SINGLE DOSE ALLOWS PREDICTION OF REPEAT DOSE OCCUPANCY

S. Abanades[1,2], J. van der Aart[1], J. Barletta[1], C. Marzano[1], G. Searle[1], J. Ahmad[1], S. Zamuner[3], V. Cunningham[1], E. Rabiner[1], M. Laruelle[4], R. Gunn[1,5]

[1]GSK, Clinical Imaging Center, [2]Dept. of Experimental Toxicology, Imperial College, London, UK, [3]GSK, CPMS, Verona, Italy, [4]GSK, Schizophrenia & Cognition DPU, Harlow, [5]Dept. of Engineering Science, University of Oxford, Oxford, UK

Objectives: PET receptor occupancy (RO) studies provide valuable information for dose selection and optimisation in clinical drug development. To date, occupancy data have mainly been analysed assuming a ´direct´ relationship between plasma drug concentration and RO, however, these models may fail to characterise a system which is not in equilibrium. A more comprehensive modelling approach to link the pharmacokinetics of a drug in plasma (PK) and RO using an ´indirect´ model is presented. The method is applied to predicting serotonin transporter (SERT) occupancy after repeat dosing (RD) of the SSRI duloxetine, from PET data acquired after a single dose (SD) of duloxetine.

Methods: Four healthy male volunteers were scanned 4 times with [^{11}C]DASB on a Siemens HiRez scanner: baseline, two time points following SD of 20mg duloxetine (times selected using an adaptive design in the interval 0-72h) , and once after RD (20mg dose given daily for 4 days). Duloxetine plasma concentration was measured throughout the study. Regions of interest (ROI) were delineated on a coregistered MR-T1 image for the striatum, thalamus and midbrain, with the cerebellum as the reference region. ROI were applied to the PET data to generate time activity curves and the simplified reference tissue model was used to derive regional estimates of binding potential (BP_{ND}) allowing for the calculation of RO in scans 2, 3 and 4. Plasma duloxetine data following SD was fitted to a one compartment model with a first order absorption rate constant to derive continuous duloxetine SD plasma data and predicted RD plasma data. An indirect PK/RO model was fitted to the measured SD PET occupancy data to characterize the relationship between PK and RO.

$$\frac{dRO(t)}{dt} = k_{on}\, C_P(t)\,\left(R_T - RO(t)\right) - k_{off}\, RO(t)$$

[Indirect PK/RO Model]

$C_P(t)$ is the duloxetine plasma concentration, k_{on} and k_{off} are the receptor association and dissociation rate constants, RO(t) is the RO time-course and R_T is the maximum RO. This model was used to predict the duloxetine RD occupancy by applying it to the predicted RD PK time-course.

Results:

	Single Dose		Repeat Dose		
Subject	**Time (h)**	**Measured RO**	**Time (h)**	**Measured RO**	**Predicted RO**
1	6.3	0.70	7.0	0.71	0.77
	26.1	0.49			
2	6.0	0.74	6.0	0.78	0.79
	26.3	0.49			
3	8.0	0.79	6.1	0.72	0.91
	32.0	0.72			
4	18.9	0.65	7.1	0.78	0.80
	44.0	0.43			

[Measured and Predicted RO for duloxetine at RD]

Mean injected activity=235.5+-49.9 MBq , Duloxetine plasma $t_{1/2}$=11.1+-3.6 h.

Conclusions: Characterizing the relationship between plasma PK and RO of a drug following SD allows for prediction of RD occupancy.

165

BrainPET Poster Session: Kinetic Modeling

QUANTIFICATION OF [^{11}C]FLUMAZENIL BINDING USING A REFERENCE TISSUE MODEL ON AN EXPERIMENTAL HIGH-RESOLUTION VERSUS A ROUTINE CLINICAL PET SCANNER

F.H.P. van Velden[1], B.N.M. van Berckel[1], R.W. Kloet[1], F.L. Buijs[1], N. Tolboom[1,2], S.P.A. Wolfensberger[1,3], G. Luurtsema[1], A.A. Lammertsma[1], R. Boellaard[1]

[1]Department of Nuclear Medicine & PET Research, [2]Department of Neurology, [3]Department of Psychiatry, VU University Medical Center, Amsterdam, The Netherlands

Background and aims: The High Resolution Research Tomograph (HRRT, CTI/Siemens) is a dedicated human brain positron emisson tomography (PET) scanner. To date, however, only a limited number of human brain studies have been performed using the HRRT, with most studies having been acquired on whole body PET scanners, such as the ECAT EXACT HR+ (CTI/Siemens). Previously, an excellent interscanner comparison (slope: 1.00-1.07, intercept fixed to origin) has been reported for an HRRT-HR+ test-retest study using plasma input models [1]. In reference regions, however, tracer concentrations are lower and, therefore, more prone to bias. The purpose of the present study was to quantitatively compare HRRT and HR+ scanners in case of a reference tissue model approach.

Methods: Seven healthy volunteers underwent two 60 min scans (one on each scanner) immediately following administration of 365±34 MBq [^{11}C]flumazenil. All data were histogrammed in 16 time frames with variable frame lengths (same on both scanners). Prior to each emission scan a transmission scan was acquired. HR+ studies were reconstructed using 2D filtered backprojection with Fourier rebinning followed by 5 mm FWHM Gaussian smoothing. HRRT studies were reconstructed using 3D ordered subsets weighted least squares (7 iterations, 16 subsets) [2]. Reconstructed HRRT images were also smoothed with a 6 mm FWHM Gaussian kernel to match image resolution with that of the HR+ scanner. Pharmacokinetic parameters were generated from time-activity curves, obtained for fourteen different anatomical regions from the dynamic emission frames. Binding potential (BP_{ND}) data were generated using a basis function implementation of the simplified reference tissue model [3].

Results: One subject showed patient motion (> 5 mm) on the HR+ scans and was excluded from comparisons. Another subject had been administered a relatively low dose in both scans (~311 MBq), causing unreliable reference region input curves (due to noise) and was therefore excluded. For the remaining subjects, BP_{ND} values derived from HRRT and HR+ scans showed excellent correlation ($r = 0.95\pm0.02$) with a slope of 1.04±0.15 (intercept fixed to origin), which reduced to 0.90±0.10 after resolution matching. Test-retest variability was 14.9±9.4% and 12.3±10.0% without and with resolution matching, respectively.

Conclusions: The somewhat lower values seen in HRRT studies versus those of the HR+ when using reference tissue rather than plasma input models might be due to low counts in the reference region, causing bias in HRRT reconstructions [2] and/or inaccuracies in attenuation and scatter corrections. Higher BP_{ND} values derived from HRRT scans prior to resolution matching indicate improved quantification due to a reduction in partial volume effects (consistent with [1,4,5]).

References:

[1] Van Velden et al. IEEE MIC Abstract 2008, M06-1.

[2] Van Velden et al. J Nucl Med. 2009; 50(1):72-80.

[3] Gunn et al. NeuroImage. 1997; 6(4):279-287.

[4] Van Velden et al. IEEE NSS Conf Rec. 2006; 5:3097-3099.

[5] Leroy et al. J Nucl Med. 2007; 48(4):538-546.

Acknowledgments: Financial supported provided by the Netherlands Organization for Scientific Research (NWO, VIDI Grant 016.066.309).

OXYGEN INHALATION DOES NOT MARKEDLY AFFECT CEREBRAL BLOOD FLOW DURING FOCAL ISCHAEMIA: POTENTIAL USE AS A PENUMBRAL IMAGING BIOMARKER

T. Baskerville[1], C. McCabe[1], J. Chavez[2], C. Santosh[3], M. Macrae[1]

[1]University of Glasgow, Glasgow, UK, [2]Wyeth Pharmaceuticals, Collegeville, PA, USA, [3]Southern General Hospital, Glasgow, UK

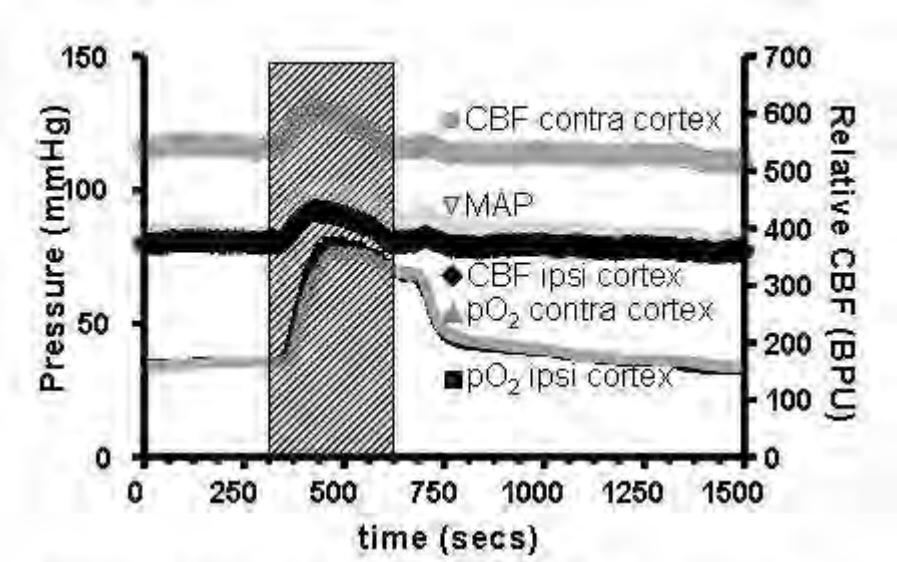

Figure: Relative MAP,CBF & pO_2 responses to hyperoxia (100% inhalation for 5 mins) in rats with MCAO. Data (n=6) were averaged before, during (hatched bar) and after oxygen challenge. Changes in MAP, CBF and pO_2 were analysed using paired t-test (where data were not normally distributed a Mann-Whitney test was applied). BPU=perfusion units.

[MAP, CBF and brain pO2 responses during hyperoxia]

In the UK stroke is the third leading cause of death and most common cause of severe disability. Identification of the ischaemic penumbra (potentially salvageable tissue) is a critical goal for stroke researchers. We have recently developed a novel MRI technique using inspired oxygen (100%) as a metabolic biomarker to characterise the penumbra (Santosh et al 2008). In order to determine the clinical utility of using 100% oxygen as an imaging biosensor, we investigated the effects of 100% oxygen inhalation on cerebral blood flow (CBF) and brain tissue oxygenation (pO_2) during stroke. Male Sprague Dawley rats (290-350g) were anaesthetised with 2% isoflurane, surgically tracheotomised, artificially ventilated (Air) and the middle cerebral artery permanently occluded (MCAO) by the intraluminal filament technique. Blood pressure was continuously monitored and blood gas analyses performed to ensure physiological stability. Oxyflo/oxylite probes were placed

stereotaxically into the ipsilateral (penumbral region of MCA territory) and contralateral cortex to record relative CBF and tissue pO_2. The following paradigm was used (90 mins post MCAO) to investigate the effect of hyperoxia: 5 mins air, 5 mins 100% oxygen and 15 mins air inhalation. Brain histology was carried out 2 hours after stroke to check probe placement in relation to ischaemic damage.Hyperoxia induced an increase in mean arterial blood pressure (MAP) of 13.7%±3.34 and 12.42%±4.81 for sham (n=6, P< 0.0001, paired t-test) and MCAO (n=6, P< 0.005, paired t-test) rats, respectively. During hyperoxia there was a small, transient increase in CBF in sham operated rats (ipsilateral; 4.94%±3.47, P=0.69, contralateral; 5.59%±2.46 P=0.58, Mann Whitney test) and in rats that underwent MCAO (ipsilateral; 8.7%±4.02, P=0.39 contralateral cortex; 6.67%±4.61, P=0.30, Mann Whitney test). This increase in CBF appeared to be a regulatory response to increased MAP during hyperoxia and was not statistically significant. In sham-operated animals concomitant recording of brain pO_2 showed that during hyperoxia, pO_2 levels increased ipsilaterally by 64.7%±9.80 (from 28.6 to 47.4mmHg, P< 0.01, paired t-test) and contralaterally by 86.9%±40.1 (from 29.8 to 54.2mmHg, P< 0.05, paired t-test). Similarly, following MCAO, tissue oxygenation levels rose by 89.44%±43.3 (ipsilateral, from 35.1 to 65.2mmHg) and 84.14%±50.2 (contralateral, from to 64.2mmHg) from baseline pO_2 values in response to hyperoxia. PO_2 increases during hyperoxia in the MCAO group were not statistically significant due to increased variability within this group. Thus, our data show that during hyperoxia MAP increases and there is a small increase in CBF along with a robust increase in brain tissue oxygenation. The data provide new insight into the effect of hyperoxia on local brain parameters and its potential clinical use as an imaging biomarker to identifying the penumbra in stroke patients.

Santosh et al. (2008). JCBF & METABOL. 2008 Oct;28(10):1742-53.

Grant support: Translational Medicine Research Collaboration with Wyeth Research.

THE EFFECT OF DES ACYL GHRELIN ON CORTICAL SPREADING DEPRESSION

J. Yonekura, J. Hamada, E. Kitamura, K. Koizumi, R. Masuda, M. Fukuda, S. Maruyama, F. Sakai

Neurology, Kitasato University School of Medicine, Sagamihara, Japan

Objectives: Cortical spreading depression(CSD) is a short-lasting depolarization wave which moves across the cortex accompanied by changes in cellular activity and in cerebral blood flow (CBF). CSD has been discussed as a possible mechanism for the aura phase of migraine. We have recently shown that orexin-A inhibits CSD in rats (in preparation). It's generally known that des acyl ghrelin indirectly increases orexin concentration in the brain . In the present study, we investigated the influence of des acyl ghrelin on the CSD induced in the rats.

Methods: Fifteen male Splague-Dawley rats (350-450g) (n=9;intracerebroventricular injection, n=6; intravenous injection) were anesthetized withα-chloralose and urethane, intubated, and ventilated mechanically. The right femoral artery was cannulated for measurement of blood pressure, and other physiological parameters were measured. CBF was continuously monitored by laser-Doppler flowmetry. The cortical DC-potential was measured by extracellular platinum electrode. The stainless tube with polyethylene resin was placed in the right lateral ventricle to administer des acyl ghrelin. Also, the right femoral vein was cannulated for intravenous administration of des acyl ghrelin. First, CSD was induced by dropping 3µl of 1M KCl on rat brain surface and DC-potential and CBF were measured continuously. Then, 2µl of 100pM of des acyl ghrelin in saline was injected in right lateral ventricle, and CSD was evaluated continuously. The mean value of CBF change was compared between pre and post injection. The average amplitude change of DC-potential was also evaluated in the same way. Also, the frequency of appearance of CSD was compared between pre and post injection. For statistical analysis, we used paired t-test.

Results: After the intracerebroventricular (i.c.v.) administration of des acyl ghrelin, the amplitude of DC potential was 26.5±4.9m V(mean±SEM) and there was no difference comparing with 28.4±4.1m V of before injection. Also there was no significant difference in the mean change of CBF (before injection: 92.2±9.1%, after injection of acyl ghrelin of i.c.v administration: 86.5±11.5%). But there was a significant decrease in the frequency of CSD (before i.c.v. administration: 10±3.3, after the i.c.v. administration: 6.1±2.0) ($p< 0.001$). After intravenous administration of des acyl ghrelin, the amplitude of DC potential was not changed(before: 16.7±0.9mV, after: 14.7±1.4mV). There was no difference between the mean change of CBF value (before: 80.3±2.3 %, after: 71.2±11.6%) by des acyl ghrelin intravenous administration ($p< 0.1$). There was a significant decrease in the frequency of CSD (before i.v. administration: 8.2±1.1, after the administration: 6.5±0.7) ($p< 0.05$). There was no difference in physiological parameters between pre and post administration of des acyl ghrelin.

Conclusions: Our study suggested that des acyl ghrelin inhibits frequency of CSD. CSD is known to occur during migraine aura. In the present study, it was suggested that des acyl ghrelin may give some influence on the pathogenetic mechanism of migraine aura. We have previously shown that orexin-A has some role in the regulation of CBF. It´s suggested that des acyl ghrelin indirectly increase orexin concentrations in the central nervous system and inhibits the frequency of CSD. This is the first report that evaluated the influence of des acyl ghrelin on CSD.

169

BrainPET Poster Session: Kinetic Modeling

ROBUST FITTING OF PET DATA TO IMPROVE ESTIMATION: APPLICATION TO A [^{11}C]-WAY-100635 STUDY

F. Zanderigo[1], R.T. Ogden[1,2], C. Chang[3], S. Choy[1], A. Wong[1], R.V. Parsey[1,2]

[1]Department of Molecular Imaging and Neuropathology, New York State Psychiatric Institute, [2]Department of Psychiatry, Columbia University, College of Physicians and Surgeons, New York, NY, [3]Department of Mathematical Sciences, New Jersey Institute of Technology, University Heights, Newark, NJ, USA

Objectives: In the analysis of PET time activity curves (TAC), model fitting is typical accomplished by minimizing the least squares (LS) criterion, which is known to be optimal for data having a Gaussian distribution, but not robust in the presence of outliers (e.g., subject head motion). In contrast, quantile regression (QR) provides robust estimates not heavily influenced by outliers [1]. In practice, when no influential points are present LS is used [2] otherwise QR performs better. Choosing a fitting method (QR or LS) to use on each TAC based only on that TAC may be termed the data adaptive (DA) approach. We apply our DA method to clinical PET TAC data. We expect that DA will result in reduced variance of estimating model parameters within groups of subjects thus enhancing the power to detect differences among different groups.

Methods: [^{11}C]-WAY-100635 TACs from 28 female and 21 male controls were modeled using a two-tissue constrained compartment model [3]. Both LS and DA were applied to estimate the radioligand distribution volume (V_T) in 13 regions of interest (ROI). Mean and standard deviation (SD) of V_T values estimated by LS ($mean_{LS}$, SD_{LS}) and DA ($mean_{DA}$, SD_{DA}), respectively, were calculated for each ROI within each group. Males and females were separated because females have ~20% higher binding than males ($mean_{LS}$ across ROIs and subjects: 3.84 vs. 3.17). The $mean_{DA}/mean_{LS}$ and SD_{DA}/SD_{LS} ratios were then calculated in each group and each ROI.

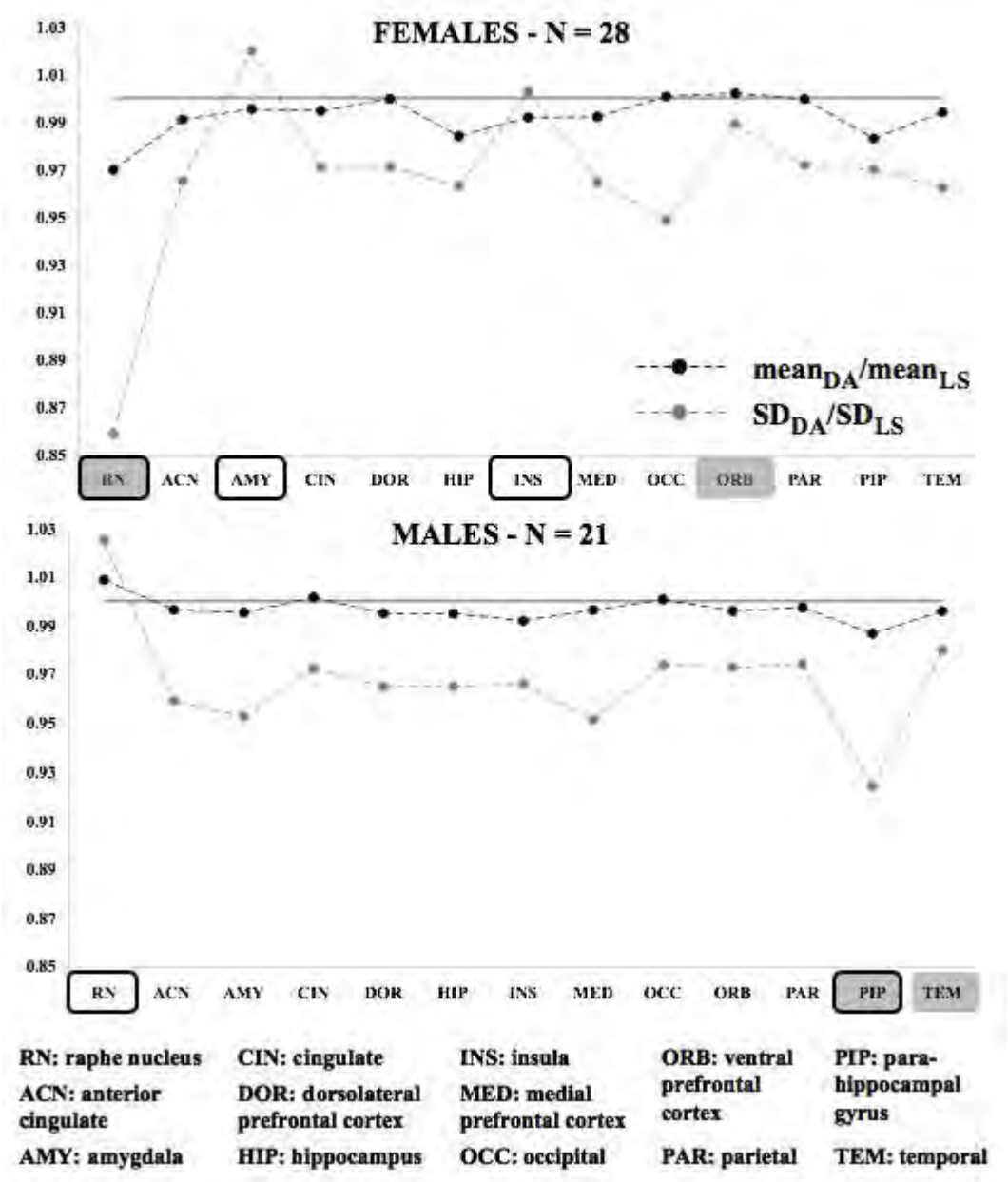

[Figure 1]

Results: For both the groups, Figure 1 reports the $mean_{DA}/mean_{LS}$ (black line) and SD_{DA}/SD_{LS} (gray line) ratios obtained in each ROI. Application of DA leads to a decrease in the SD of V_T estimates within females of 14.1% in the best (RN) and 1.1% in the worst case (ORB), respectively. At the same time, the $mean_{DA}/mean_{LS}$ ratios stay close to unity. In cases in which DA fails to improve the accuracy of estimated V_T (AMY, INS), the performance of the two approaches is comparable. Results obtained in males show a decrease in SD of 7.2% in the best (PIP) and 2% in the worst case (TEM), respectively. The $mean_{DA}/mean_{LS}$ ratios are closer to unity, and DA fails to improve the accuracy of estimated V_T just in one ROI (RN).

Conclusions: By reducing the variance of parameters estimates, the statistical power in group analysis and the sensitivity in occupancy studies are increased (i.e. the number of people to be

recruited for clinical trials is reduced). This can be implemented without the need for additional hardware and/or image registration algorithms to monitor and correct subject head motion.

References:

[1] Koenker and Bassett, Econometrica 46: 33-50, 1978.

[2] Cook, Technometrics 19: 15-18, 1977.

[3] Parsey, et al., J Cereb Blood Flow Metab 20: 1111-1133, 2000.

170

Brain Poster Session: Experimental Stroke & Cerebral Ischemia

BLOOD CELL MICRORNA EXPRESSION PROFILE OF NEUROLOGIC DISEASES: A PILOT MICRORNA ARRAY STUDY

D. Liu, Y. Tian, B. Ander, H. Xu, B. Stamova, F. Sharp

Department of Neurology and the M.I.N.D. Institute, University of California at Davis, Sacramento, CA, USA

MicroRNAs (miRNAs) are a recently discovered class of endogenous, small non-coding RNAs that regulate gene expression and have a critical role in many biological and pathological processes. Here we investigated the miRNA expression profile in blood cells after brain injuries. Adult rats were subjected to ischemic strokes, hemorrhagic strokes, sham surgeries, kainate-induced seizures, compared with controls. The blood cell miRNA expression patterns were assessed 24 hours later, using Taqman rodent miRNA arrays. Results showed that many miRNAs were upregulated and a few ones were downregulated at least twofold in blood cells after each experimental condition. miRNA response patterns were different for each condition. These results demonstrate the possible use of blood cell miRNAs as biomarkers and may be helpful to explain the results of our previous blood cell mRNA profile studies that many genes were downregulated of in these above conditions.

DOCOSAHEXAENOIC ACID COMPLEXED TO HUMAN ALBUMIN IS NEUROPROTECTIVE AFTER FOCAL CEREBRAL ISCHEMIA IN RATS: THERAPEUTIC WINDOW STUDY

L. Belayev, L. Khoutorova, K.D. Atkins, N.G. Bazan

Neuroscience, Louisiana State University, New Orleans, LA, USA

Introduction: We have previously shown that DHA complexed to human albumin (DHA-Alb) is markedly neuroprotective at relatively moderate-low doses compared with native human serum albumin (Alb) in the setting of focal cerebral ischemia in rat (Belayev et al, 2005). In this study, we defined the therapeutic window within which this therapy would confer neurobehavioral neuroprotection.

Methods: Physiologically controlled male Sprague-Dawley rats received 2 h middle cerebral artery occlusion (MCAo) by retrograde insertion of an intraluminal suture coated with poly-L-lysine (Belayev et al, 1996). The drug (DHA-Alb, 4 mg/kg or Alb, 25%, 0.5% of body weight), was administered i.v. at either 2, 3, 4 , 5, 6 or 7 h after onset of stroke (n=4-5 per group). Control group received saline at 1 h after onset of reperfusion. The neurological status was evaluated during occlusion (60 min), and on day 1, 2, 3 and 7 after MCAo; a grading scale of 0-12 was employed, as previously described. Seven days after MCAo, brains were perfusion-fixed and infarct volume was measured.

Results: The physiological variables were entirely comparable among all groups. There were no significant differences with respect to rectal and cranial temperatures, arterial blood gases or arterial blood glucose. Alb and DHA-Alb treatment, started at 2, 3 and 4 h after onset of stroke significantly improved neurological score compared to saline, but there was no significant difference between DHA-Alb and Alb groups. Rats given DHA-Alb at 5 and 6 h after onset of stroke neurobehavioral improvement, however, exceeded that of native ALB at 72 h (5 h, DHA-Alb: 5.9 ± 0.9 vs. Alb: 7.3± 0.6 and 6h, 3.4 ± 0.5 vs. 6.2 ± 1.1, respectively) and on day 7 (3 h, DHA-Alb: 4.2 ± 0.9 vs. 6.4 ± 0.5 and 4 h, 2.8 ± 0.5 vs. 5.8 ± 1.1, respectively, $p< 0.05$). There was no significant neurological improvement when treatment was delayed until 7 h. Total (cortical and subcortical) corrected infarct volume was significantly reduced by DHA-Alb treatment compared to Alb treated rats, even when initiated as late as 5 and 6 h after onset of stroke (50.3±14 and 29.2 ± 16 vs. 118.4 ± 23 mm^3, respectively). Cortical infarct volumes were also significantly reduced by treatment with DHA-Alb in the same 5 and 6 h groups compared to Alb (22.7±9 and 15.1 ± 4 vs. 66.9 ± 14.4 mm^3, respectively). Subcortical infarct areas and volumes were not significantly different between DHA-Alb and Alb groups.

Conclusions: The DHA-Alb complex affords high-grade neurobehavioral neuroprotection in focal cerebral ischemia, equaling or exceeding that afforded by native ALB, at considerably moderate doses. Even DHA-Alb therapy was initiated as late as 5 and 6 h after onset of MCAo, it improved the behavioral score and reduced infarct volume. This is clearly clinically advantageous in that moderate DHA-Alb doses would be expected to reduce the likelihood of acute intravascular volume overload and congestive heart failure sometimes induced when patients with compromised cardiovascular function are treated with high-moderate doses human albumin therapy.

174

Brain Oral Session: Neurological Diseases

SPATIAL PATTERNS OF LONGITUDINAL CHANGES IN AMYLOID DEPOSITION IN NONDEMENTED OLDER ADULTS

J. Sojkova[1,2], Y. Zhou[2], M. Kraut[2], J. Brasic[2], L. Ferrucci[1], D. Wong[2], S. Resnick[2]

[1]National Institute on Aging, National Institutes of Health, [2]Russell H. Morgan Department of Radiology and Radiological Sciences, Johns Hopkins Medical Institutions, Baltimore, MD, USA

Objectives: Cross-sectional studies of nondemented older adults suggest that amyloid deposition in the precuneus represents an early finding in the progression of Alzheimer's disease. In this longitudinal study, we investigate whether changes in retention of [^{11}C]PIB, a PET tracer that binds to β-amyloid, are detectable on a voxel-wise basis. We hypothesize that the spatial distribution of longitudinal changes in amyloid deposition will localize to regions of increased amyloid deposition observed in cross-sectional studies of nondemented older adults.

Methods: 24 nondemented participants (5 CDR=0.5; baseline age 79.2(8.1) years) in the Neuroimaging Substudy of the Baltimore Longitudinal Study of Aging had [^{11}C]PIB PET and volumetric MRI at baseline and again after a mean (SD) of 1.5 (0.5) years. Parametric images reflecting the distribution volume ratio (DVR), an index of [^{11}C]PIB specific binding to β-amyloid, were generated from [^{11}C]PIB dynamic PET using a simplified reference tissue model and a linear regression with spatial constraint algorithm (SRTM-LRSC) (Zhou et al., 2003, Neuroimage). The longitudinal changes in gray matter [^{11}C]PIB retention over time were analyzed using SPM5 ($p< 0.005$, spatial extent 100 voxels), adjusting for baseline age.

Results: In nondemented older adults, voxel-wise changes in amyloid deposition can be detected over a 1.5-year follow-up. Significant increases in amyloid deposition are seen in left precuneus (BA 19), right fusiform (BA 19) and right lingual gyri (BA 19); left superior frontal gyrus (BA 8), left orbitofrontal gyrus (BA11), and right medial frontal gyrus (BA 10) extending to right anterior cingulate gyrus.

Conclusions: In nondemented older adults, longitudinal changes in amyloid deposition occur in regions showing increased amyloid deposition in cross-sectional studies, specifically the precuneus region and the prefrontal cortex. Longitudinal changes in amyloid retention are detectable at the voxel level using the DVR images generated from [^{11}C]PIB dynamic images with SRTM-LRSC parametric imaging algorithm.

Support: This research was supported by the Intramural Research Program of the NIH, National Institute on Aging and N01-AG-3-2124.

175

Brain Poster Session: Inflammation

THE EFFECT OF PPAR-γ DURING STROKE RECOVERY IN THE DIABETIC OB/OB MOUSE

R. Kumari, L. Willing, S. Patel, **I. Simpson**

Neural - Behavioral Sciences, Hershey Medical Centre, Penn State University, Hershey, PA, USA

Background and aims: agonist to ameliorate stroke injury in genetically diabetic¸The diabetic patient is 2-6 times more likely to experience a stroke and the subsequent morbidity and mortality is substantially greater than a euglycemic individual. PPAR-γ agonists are very effective in normalizing hyperglycemia and are widely used in the treatment of type II diabetes. Hence, we tested the effect of darglitazone, a selective peroxisome proliferators gamma activated receptor (PPAR-γ ob/ob mice.

Methods: Male ob/+ and ob/ob mice received darglitazone (1mg/kg) in powdered chow or control chow for 7 days at 7 weeks of age. Blood glucose was measured before and on alternate days during treatment. Hypoxia/ ischemic (H/I) insults were induced in 8 week old ob/ob and ob/+ mice by the ligation of the right common carotid artery followed by systemic hypoxia (8% oxygen: 92% N_2) for 24 min. At 4, 8, and 24hr of recovery, blood samples were obtained by cardiac puncture for serum and plasma collection and measurement of corticosterone, cholesterol, triglycerides and VLDL. Brains were rapidly removed and frozen for histological examination, RNA isolation and in situ hybridization.

Results: Darglitazone significantly lowered the blood glucose level in ob/ob mice by day 3 and normalized elevated levels of triglycerides and VLDL in treated ob/ob mice, whereas cholesterol levels remained elevated. Hematoxylin and eosin staining was performed on brain sections at 24 hr of recovery and infarct area was measured. Darglitazone treatment dramatically reduced the infarct area in ob/ob mice compared to the untreated group (29.54 ± 12.29% to 3.32 ± 1.65%) but was without significant effect on ob/+ mice (12.96 ± 5.97% vs 7.65 ± 2.89%), n=6-8. Proinflamatory cytokines (IL-1ß, TNF-α, IL6), mRNA determinations as well as in situ hybridization of bfl1 (microglia) and GFAP (astrocytes) at various times of recovery suggests that darglizatone promotes an initial activation of microglia in the ob/ob mice resulting in a transient increase in bfl1 and TNFa expression to control levels at 4 hr of recovery, which were subsequently suppressed at 8 hr and 24 hr in ob/ob animals.

Conclusion: This study in ob/ob mice confirms our observations in the db/db mice that the microglial activation and proinflamatory responses are delayed and diminished in the diabetic animal and damage following H/I is greater. Moreover, treatment of the ob/ob mice with the PPAR-g agonist darglitazone, which restored euglycemia and lowered triglyceride levels, dramatically reduces infarct area in the diabetic mice. This reduction in infarct size was associated with an enhancement in the initial activation in microglial responsiveness to the ischemic insult, which appears to be associated with successful recovery. The challenge now is to determine whether this enhanced microglial response and the markedly reduced infarct are related and occur as a result of the restoration of euglycemia or to a specific interaction with darglitazone.

ANATOMICAL STUDY OF NORMAL VARIATIONS OF CIRCLE OF WILLIS IN 132 FETUSES, INFANTS AND ADULTS

S. Ansari[1], M. Dadmehr[2], B. Eftekhar[3], F. Nejat[2], S. Kamali Ardakani[2], S.M. Ghodsi[2], J.E. Heavner[4], B. Vidic[4], J. Mocco[1]

[1]Department of Neurosurgery, University of Florida, College of Medicine, Gainesville, FL, USA, [2]Department of Neurosurgery, Tehran University of Medical Sciences, Tehran, Iran, [3]Royal Hobart Hospital, Tasmania, TAS, Australia, [4]Health Science Center, Texas Tech University, Lubbock, TX, USA

Objective: Several studies have investigated the variations in the anatomy of each segment of circle of Willis whereas a few have addressed the variations of this arterial circle as a whole. In this study the entire circle of Willis and its variations were studied in a cohort of Iranian people and compared with previous reports.

Material and method: 132 brains of recently deceased Iranian people (102 adults and 30 fetuses and infants) were dissected and anatomic variations of the circle of Willis were observed. The dissection process was digitized for further studies. Using computer software (Osiris) the external diameters and length of the vessels were measured and the circle variations were classified. The variations of the circle as whole and segmental variations were compared with previous studies.

Results: Nearby 41% of the circles were symmetric. Uni-and bilateral hypoplasia of posterior communicating arteries (PcoAs) constituted the most common variation in our study which was similar to previous works. Aplasia of the precommunicating part of the anterior cerebral artery (A1) and the precommunicating part of the posterior cerebral artery (P1) were not observed. In 3.3% of fetuses and infants and 3% of adult instances both right and left posterior communicating arteries were absent. There was one case of anterior communicating artery (AcoA) aplasia in adult group which was not seen in fetus and infant instances. As a whole, there were no two identical circles regarding to their dimensions.

Conclusion: The anatomical variations discovered in Iranian circle of Willis in this current study were not significantly different to those of more diverse populations reported in the literature. On the whole, the frequencies of the different variants of the entire cerebral arterial circle and segmental variations were comparable with previous studies. The main differences between the fetal and adult disposition are the diameter of the PcoA and the circular part of the posterior cerebral artery.

177

Brain Oral Session: Blood Brain Barrier

NADPH OXIDASE FROM CIRCULATING INFLAMMATORY CELLS EXACERBATES INJURY IN EXPERIMENTAL STROKE

X. Tang[1,2], Z. Zheng[1], R. Giffard[2], M. Yenari[1]

[1]Neurology, UCSF SF VAMC, San Francisco, [2]Anesthesia, Stanford University School of Medicine, Stanford, CA, USA

NADPH oxidase (Nox2) is a major enzyme system which generates superoxide generation in inflammatory cells, but has recently been found in non inflammatory cells such as endothelial cells and neurons. Here we show that Nox2 contributes to experimental stroke, especially in circulating inflammatory cells. Experimental stroke was produced in mice by 2h transient middle cerebral artery occlusion (tMCAO) with an intraluminal suture model, followed by 22h reperfusion. Three different paradigms were studied:

1. Mice treated with the Nox2 inhibitor, apocynin (Apo, 2.5 mg/kg IV 30 min prior to reperfusion) or vehicle (Veh),
2. Nox2 deficient (X-CGD, deficient in the gp91 subunit) vs wildtype (Wt) mice, and
3. to determine whether Nox2 in circulating cells vs brain resident cells contribute to ischemic injury, bone marrow chimeras were generated by transplanting bone marrow from Wt or X-CGD into X-CGD or Wt, respectively.

Brains were assessed for infarct volume, hemorrhage, in situ $O^{\bullet-}$ detection, as well double labeling for $O^{\bullet-}$ in neurons (NeuN), endothelial cells (CD31) and microglia (CD11b). Brain tissue within peri-infarct regions was sampled for Western blots. Infarct size was reduced whether Nox2 was pharmacologically inhibited (by 37% vs vehicle, $P< 0.05$) or genetically absent (by 54% vs Wt, $P< 0.001$). This was also associated with reduced incidences of cerebral hemorrhage (17% vs. 58%, Apo vs Veh; 14% vs 58%, X-CGD vs Wt). After ischemia, most of the $O^{\bullet-}$ was generated by neurons, some microglia, and rare endothelial cells. $O^{\bullet-}$ was markedly reduced by Apo treatment and in X-CGD mice in all cell types (1% vs. 448%, Apo vs Veh; 11% vs 448%, X-CGD vs Wt). Apo treatment and X-CGD mice showed decreased MMP9 (40% vs. 86%, Apo vs Veh; 50% vs 86%, X-CGD vs Wt) and decreased loss of ZO-1(182% vs. 27%, Apo vs Veh; 48% vs 27%, X-CGD vs Wt). Infarcts in Wt mice who received Nox2 deficient marrow (40.1 ± 6.7 mm^3) were decreased significantly compared to either the Wt mice who received Wt marrow (100.4 ± 9.9 mm^3, $P< 0.01$) or X-CGD mice who received Wt marrow (74.5 ± 6.5 mm^3, $P< 0.05$). Furthermore, mice receiving Nox2 deficient marrow had smaller infarcts than X-CGD deficient mice transplanted with Wt marrow. We conclude that either pharmacologic or genetic inhibition of Nox2 leads to reduced brain injury and hemorrhage, and is correlated to decreased $O^{\bullet-}$ and MMP9 expression and prevents the loss of ZO-1. Nox2 originating from the circulating inflammatory cells contributes more to exacerbating experimental stroke than that of the brain resident cells.

A SARTAN DERIVATIVE WITH VERY LOW ANGIOTENSIN II RECEPTOR AFFINITY AMELIORATES ISCHEMIC CEREBRAL DAMAGE THROUGH ANTI-OXIDATIVE AND ANTI-INFLAMMATORY EFFECTS

S. Takizawa[1], E. Nagata[1], S. Takagi[1], T. Miyata[2]

[1]Division of Neurology, Department of Internal Medicine, Tokai University School of Medicine, Isehara, [2]Center for Translational and Advanced Research on Human Disease, Tohoku University Graduate School of Medicine, Sendai, Japan

Aims: Angiotensin II receptor blockers (ARBs) have been reported to protect the brain against ischemic damage, but their hypotensive effect limits clinical use because blood supply to the penumbra is decreased. We synthesized a novel ARB-derivative, R-147176, which is 6700 times less potent than olmesartan in AT_1 binding inhibition, and therefore has a less anti-hypertensive effect, but has marked inhibitory effects on oxidative stress and advanced glycation [1]. We evaluated the effect of R-147176, given orally or intravenously, on infarct volume in transient thread occlusion and photothrombotic models in rats. The anti-oxidative and anti-inflammatory properties were also investigated.

Methods: Transient focal ischemia was achieved through 2-hour thread occlusion of the middle cerebral artery following 7-day reperfusion in Male Sprague-Dawley rats (n=43) as described previously [2]. Coronal brain sections were stained with hematoxylin and eosin for the measurement of infarct volume, as well as immunohistochemically with ED-1 and TUNEL. Levels of oxidatively modified proteins and the content of pentosidine were quantified. Permanent ischemia was induced by photothrombotic occlusion of middle cerebral artery (n=16). Seven days later, infarct volume was measured from the sections stained with hematoxylin and eosin.

Results: R-147176, given orally or intravenously (10-30 mg/kg/day), significantly reduced infarct volume (Fig. 1B), albeit no influence on blood pressure lowering (Fig. 1A), in both ischemia models. R-147176 significantly reduced the numbers of ED-1-positive cells in the penumbra and TUNEL-positive cells in the infarcted cortex and penumbra, compared with the vehicle-treated control. Protein carbonyl formation in the brain in the R-147176-treated group was significantly reduced compared with that in the vehicle-treated group.

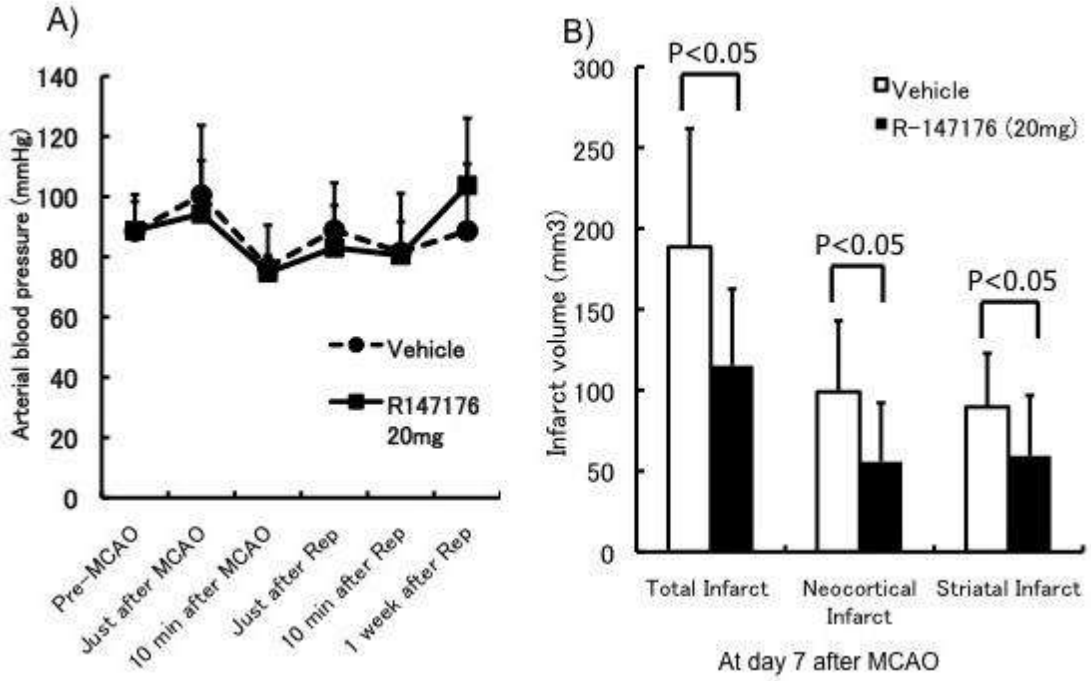

[Figure]

Conclusions: This ARB derivative, despite its significantly lower AT_1 receptor affinity and marginal anti-hypertensive effect, ameliorated ischemic cerebral damage through its anti-oxidative and anti-inflammatory effects. These findings may open a new avenue for the treatment of stroke.

References:

[1] Izuhara Y, et al. A novel sartan derivative with very low angiotensin II type 1 receptor affinity protects the kidney in type 2 diabetic rats. Arterioscler Thromb Vasc Biol 28: 1767-73, 2008.

[2] Takizawa S, et al. A novel inhibitor of advanced glycation and endoplasmic reticulum stress reduces infarct volume in rat focal cerebral ischemia. Brain Res 1183:124-37, 2007.

NOREPINEPHRINE TRANSPORTER OCCUPANCY BY ANTIDEPRESSANT IN HUMAN BRAIN MEASURED USING POSITRON EMISSION TOMOGRAPHY WITH (S,S)-[^{18}F]FMENER-D$_2$

M. Sekine[1,2], I. Hiroshi[1], R. Arakawa[1,2], M. Okumura[1,2], T. Sasaki[1], H. Takahashi[1], H. Takano[1], Y. Okubo[2], T. Suhara[1]

[1]Molecular Neuroimaging Group, Molecular Imaging Center, National Institute of Radiological Sciences, Chiba, [2]Department of Neuropsychiatry, Nippon Medical School, Tokyo, Japan

Objectives: Norepinephrine transporter (NET) is one of the main targets of antidepressants. Although serotonin transporter occupancy was reported to be over 80% at clinical doses of serotonin reuptake inhibitors (SSRIs) during the treatment of depression [1], NET occupancy by antidepressants in human brain has not been reported because of a lack of suitable radioligands for NET. (S,S)-[^{18}F]FMeNER-D$_2$ was recently developed as a radioligand for the measurement of NET binding with positron emission tomography (PET) [2,3]. In this study, we investigated the degree of NET occupancy by different doses of an antidepressant, nortriptyline, using PET and (S,S)-[^{18}F]FMeNER-D$_2$.

Methods: Six healthy males (age 22 - 39 yrs; mean ± SD, 30.5 ± 6.3 yrs) participated in this study. PET scans with (S,S)-[^{18}F]FMeNER-D$_2$ were performed before and after oral administration of a single dose of nortriptyline on separate days. The nortriptyline doses were 10 mg, 25 mg, and 75 mg in two subjects each. After a bolus i.v. injection of 188.9 ± 4.2 MBq of (S,S)-[^{18}F]FMeNER-D$_2$, scanning was performed for 0 - 90 min (1 min×10, 2 min×15, 5 min×10), followed by scanning for 120 - 180 min (10 min×6). Regions of interests were drawn on the thalamus and caudate in each PET image. The thalamus was used as target region, and the caudate as reference region. Areas under the curve (AUCs) of radioactivity in the target and reference regions were calculated for 120 - 180 min. The ratio of the thalamus-to-caudate AUCs minus 1 was used as the binding potential (BP_{ND}) for NET. NET occupancy was defined as the percentage reduction of BP_{ND}. Venous blood samples were obtained to measure the concentrations of nortriptyline just before injection of the tracer and at 180 min after. This study was approved by the Ethics and Radiation Safety Committee of the National Institute of Radiological Sciences, Chiba, Japan. After complete description of this study, written informed consent was obtained from all subjects.

Results: The mean NET occupancies by nortriptyline doses were 16.4 % at 10 mg, 33.2 % at 25 mg, and 41.1% at 75 mg, respectively. The mean plasma concentration of nortriptyline was 0 ng/ml at 10 mg, 23.7 ng/ml at 25 mg, and 50.5 ng/ml at 75 mg. Estimated ED_{50} (50% effective dose) was 76.8 mg of administration dose and 59.8 ng/ml of plasma concentration.

Conclusions: NET occupancy by nortriptyline corresponding to the administration dose and plasma concentration was observed. To determine the optimal administration dose of nortriptyline for patients with depression, the relation between therapeutic effects and NET occupancy needs to be investigated in further studies.

References:

[1] Meyer JH et al. Am J Psychiatry 2004; 161: 826-35.

[2] Takano A et al. Eur J Nucl Med Mol Imaging 2008; 35: 153-7.

[3] Arakawa R et al. J Nucl Med 2008; 49: 1270-6.

182

Brain Poster Session: Cerebral Vascular Regulation

RAPID CEREBRAL HEMODYNAMIC MODULATION DURING COMPLEX COGNITIVE FUNCTIONS: EVIDENCE OF TIME-LOCKED ASSOCIATIONS WITH AGE

D. Schuepbach, D. Hell

Psychiatric University Hospital, University of Zürich, Zürich, Switzerland

Objectives: There is evidence that age affects complex cognitive functions from a neuropsychological and neurophysiological perspective. Age related changes in neurovascular coupling have been also described (D'Esposito et al., 2003). We recently introduced cerebral hemodynamic modulation (Schuepbach et al., 2007), a means that assesses rapid changes of brain perfusion, to executive functions, and we found evidence of time-locked associations between rapid cerebral hemodynamic modulation and performance during those tasks. In the following functional transcranial Doppler (fTCD) investigation, we correlated rapid cerebral hemodynamic modulation during a variety of executive functions with age.

Methods: Subjects underwent executive tasks, namely the Wisconsin Card Sorting Test, a means of abstraction and cognitive flexibility, the Tower of Hanoi puzzle and the Stockings of Cambridge, which are considered as measures of planning. Bilateral fTCD measurements of the middle (MCA) and anterior (ACA) cerebral arteries were carried out during the tasks. Partial correlation analyses examined the linkage between rapid cerebral hemodynamic modulation and age during early phases of those paradigms, with gender and test performance as covariates.

Results: There were significant and inverse associations between early phases of rapid cerebral hemodynamic modulation in the MCA and age in executive tasks ($P < 0.05$), which were mostly observed during time intervals of 1-2s and 2-3s after the start of the paradigms. Older subjects showed significantly less increase of brain perfusion due to cognitive stimuli than younger participants. However, task performance was a significant cofounder in some tests.

Conclusions: These results suggest that there is a pattern of age related associations with cerebral hemodynamic modulation in the lateral hemispheres during complex cognitive functions suggestive of higher modulatory qualities in young age. Unsurprisingly, task performance attenuated some associations. Since there is evidence of time-locked associations between rapid cerebral hemodynamic modulation and performance during complex cognitive functions, the finding of age-related linkage with cerebral perfusion could be used as a marker of cognitive decline and as a tool for the development of cognitive enhancers for neuropsychiatric disorders such as schizophrenia or Alzheimer's disease.

References:

D'Esposito M, Deouell LY, Gazzaley A, 2003. Alterations in the BOLD fMRI signal with ageing and disease: a challenge for neuroimaging. Nature Review Neuroscience 4:863-872.

Schuepbach D, Weber S, Kawohl W, Hell D, 2007. Impaired rapid modulation of cerebral hemodynamics during a planning task in schizophrenia. Clinical Neurophysiology 118, 1449-1459.

183

Brain Oral Session: Neurological Diseases

CEREBRAL HYPOPERFUSION PRECEDES COGNITIVE DECLINE IN HYPERTENSIVE PATIENTS WITH ISCHEMIC WHITE MATTER LESIONS

K. Kitagawa[1], N. Oku[2], Y. Kimura[3], Y. Yagita[1], M. Sakaguchi[4], J. Hatazawa[3], S. Sakoda[1]

[1]Department of Neurology, Osaka University Graduate School of Medicine, Suita, [2]Hyogo College of Medicine Hospital, Nishinomiya, [3]Department of Tracer Kinetics and Nuclear Medicine, [4]Stroke Center, Osaka University Graduate School of Medicine, Suita, Japan

Background and aims: Vascular risk factors have been believed important for cognitive decline and dementia. Our purpose was to determine if cerebral hypoperfusion contriubutes to cognitive decline in hypertensive patients with deep white matter lesions.

Methods: We have enrolled 1065 non-demented patients with at least one cardiovascular risk factor or any history of cardiovascular events, who had underwent carotid ultrasonography to evaluate the severity of carotid atheroscleroisis from 2001 to 2005 in a hospital-based cohort study. Among them, twenty-seven hypertensive patients (age, 64.8±7.5 yr) with an evidence of cerebral small vessel disease in MRI underwent PET study with an 15[O]-labeled water injection for measurement of baseline cerebral blood flow and mini-mental state examination for cognitive function. Patients without significant arterial stenosis in MR angiography and carotid duplex ultrasonography were enrolled to focus on cerebral hemodynamics with cerebral small vessel disease. At an interval of three years, these patients underwent second MMSE test. Cognitive decline was defined as a drop of four points in 3 year.

Results: Baseline MMSE score was 27.5±1.9 (mean±SD). Carotid IMT was 0.94±0.18 mm. Six patients exhibited cognitive decline, and three of them were diagnosed as dementia. Baseline CBF in six patients with cognitive decline was significantly lower than that in the rest 21 patients (31.2±2.4 vs. 42.5±5.9 ml/100g/min, $P < 0.001$). Among two groups with and without cognitive decline in the follow-up period, no difference was observed in the baseline data of age, sex, education period, history of stroke, cardiovascular risk factor, the carotid IMT, MMSE score, severity of brain atrophy and white matter lesions.

Conclusions: Our prospective study shows that cerebral hypoperfusion is a significant predictor for future cognitive decline. Our results strongly support a hypothesis that cerebral hypoperfusion and vascular risk factors contribute to cognitive decline and incident dementia.

INTRACELLULAR CALCIUM LEVELS AND VASOCONSTRICTION INDUCED BY 5-CT AND S6C IN RAT AFTER CEREBRAL ISCHEMIA

H. Ahnstedt, R. Waldsee, L. Edvinsson

Clinical Sciences, Experimental Vascular Research, Lund University, Lund, Sweden

Objective: Middle cerebral artery occlusion (MCAO) in rat increases the contractile responses of the middle cerebral arteries (MCAs) induced by different vasoconstrictor mediators and decreases the blood flow that follows the brain ischemia. Previous studies have shown that there is up-regulation of endothelin type B (ET_B) receptors [1] after MCAO and up-regulation of 5-HT_{1B} receptors in MCAs after subarachnoid hemorrhage [2]. The objective of this study was to evaluate the intracellular calcium changes that occur during contraction induced by the 5-HT_1 receptor agonist 5-carboxamido-tryptamine (5-CT) and the ET_B receptor agonist sarafotoxin 6c (S6c) in rat MCAs after MCAO.

Methods: MCAO for 90 minutes and reperfusion for 48 hours in rat were followed by evaluation of ischemic brain damage by TTC staining and neurological examination. The MCAs were removed and mounted in sensitive myographs and the contractile responses to S6c or 5-CT were studied in the right MCA (stroke) and the left MCA (control). Intracellular calcium measurements using FURA-2 were applied on segments of MCAs and calcium changes and contraction were evaluated simultaneously.

Results: Brain damage calculations after MCAO confirmed a mean brain damage of 15.6 ± 1.9 %. The neurological deficit score, using an established scoring system of 0-5 to assess the neurological behavior of the animals [3], was about 4 at the time of reperfusion and 2 after 48 hours. Pharmacological results showed that S6c induced contraction in MCAO arteries (25.3 ± 11.3 %) but not in control arteries (4.1 ± 1.3 %) relative to 63.5 mM potassium contraction. The response to 5-CT decreased after MCAO; 53.2 ± 4.8 % in control arteries compared to 16.8 ± 8.4 % in MCAO arteries. The intracellular calcium concentration at resting level was 84.8 ± 17.2 nM; contraction induced by 5-CT and S6c increased the plateau calcium level (in nM) to 111.9 ± 22.4 and 130.3 ± 24.5, respectively.

Conclusion: Our data shows that MCAO results in increased contractile responses mediated by ET_B receptors. Contradictory to what have been seen after subarachnoid hemorrhage, cerebral ischemia results in decreased contractile responses induced by 5-CT. There was no significant change in the intracellular calcium handling between control arteries and MCAO arteries suggesting that altered contractile responses mediated by ET_B and 5-HT_1 receptors are not due to calcium itself.

References:

1. Stenman, E., et al. Stroke, 2002. 33(9): p. 2311-6.

2. Ansar, S., et al. Am J Physiol Heart Circ Physiol, 2007. 293(6): p. H3750-8.

3. Bederson, J.B., et al. Stroke, 1986. 17(3): p. 472-6.

185

Brain Oral Session: Traumatic Brain Injury

SNP IMPROVES CEREBRAL HEMODYNAMICS DURING NORMOTENSION BUT FAILS TO PREVENT SEX DEPENDENT IMPAIRED CEREBRAL AUTOREGULATION DURING HYPOTENSION AFTER BRAIN INJURY

W.M. Armstead[1], J.W. Kiessling[1], W.A. Kofke[1], M.S. Vavilala[2]

[1]Anesthesiology and Critical Care, Univ of Pennsylvania, Philadelphia, PA, [2]Anesthesia, Univ of WA, Seattle, WA, USA

Objectives: Traumatic brain injury (TBI) is a leading cause of morbidity and mortality in children and boys are disproportionately represented. Hypotension is common and worsens outcome after TBI because it can cause ischemia when cerebral autoregulation is impaired. Since CBF may contribute to neuronal cell integrity, optimal management of CPP for limiting tissue hypoxia at low CPP or edema at high CPP is a critical determinant of outcome after TBI. If decreased CBF after TBI worsens outcome, it was hypothesized that administration of a cerebrovasodilator, such as sodium nitroprusside (SNP), may improve CBF and cerebral autoregulation in a sex dependent manner.

Methods: CBF via microspheres, pial artery diameter, blood velocity via transcranial Doppler and intracranial pressure (ICP) were measured before and after fluid percussion brain injury (FPI, 2atm) in untreated and SNP (0.1mg/kg iv) pre- and post-injury treated (30 min) male and female newborn pigs during normotension and hypotension (blood withdrawal to decrease MAP by 45%). Autoregulatory index (ARI) = % change CVR / % change CPP where CVR = Vcerebral blood vessel / MAP-ICP.

Results: SNP (0.1 mg/kg iv) alone produced equivalent percent cerebrovasodilation in male and female piglets. Reductions in pial artery diameter, cortical and hippocampal CBF, and CPP concomitant with elevated ICP after FPI were greater in male compared to female piglets during normotension; this was blunted by SNP treatment pre- or post-FPI (-22 ± 2 and -11 ± 1% reduction in artery diameter in absence vs. -3 ± 1 and -6 ± 1% in presence of SNP, for male and female piglets). During hypotension, pial artery dilation was impaired more in the male (17 ± 1 vs 2 ± 1%) than the female (33 ± 1 vs 17 ± 1%) after FPI. However, SNP did not improve hypotensive pial artery dilation after FPI in the female (17 ± 1 vs 14 ± 2%) and paradoxically caused vasoconstriction after FPI in the male (2 ± 1 vs -9 ± 2%). Autoregulatory pial artery dilation during hypotension was unchanged by SNP in the absence of FPI (20 ± 2 vs 21 ± 2 % for the male). Papaverine induced pial artery vasodilation was unchanged by FPI and SNP, indicating that impairment of cerebral autoregulation by SNP is not an epiphenomenon. Cortical and hippocampal CBF, CPP, velocity, and ARI were unchanged during hypotension in sham pigs but decreased markedly during combined hypotension and FPI in male but less so in female pigs. However, SNP did not prevent reductions in CBF, CPP, middle cerebral artery flow velocity, or ARI during combined hypotension and FPI in either sex.

Conclusions: These data indicate that despite improved cerebral hemodynamics after FPI during normotension, normalization of CPP via decreased ICP with cerebrovasodilator administration does not restore CBF or autoregulation during hypotension after FPI. Indeed, CPP based therapy aggravates sex dependent loss of autoregulation after FPI. These data suggest that therapies directed at a purely hemodynamic increase in CPP will fail to improve outcome during combined injury of TBI and hypotension.

COMPARTMENTAL ANALYSIS OF [^{11}C]TEMOZOLOMIDE IN GLIOMAS AND NORMAL BRAIN TISSUE

R. Hinz[1], A. Saleem[2], C.S. Brock[3], J.C. Matthews[1], T. Jones[2], P.M. Price[2]

[1]Wolfson Molecular Imaging Centre, University of Manchester, [2]Academic Department of Radiation Oncology, Christie Hospital NHS Trust, Manchester, [3]Imperial College Healthcare NHS Trust, London, UK

Background and aims: This investigation presents a comparison of compartmental modelling with spectral analysis for the kinetic analysis of a radiolabelled anti-cancer drug [^{11}C]temozolomide aiming at resolving inconsistencies in previously reported results.

Methods: 15 glioma patients underwent paired dynamic PET scans for 90 min with [^{11}C]temozolomide on the brain tomograph ECAT 953B. 3D imaging data and arterial plasma input functions were acquired and regions of interest defined for the whole tumour, for a tumour area with high signal (tumour rim) and on contralateral normal brain tissue.

Purpose: Two previously published reports analysing these [^{11}C]temozolomide data with spectral analysis found that distribution volumes (VD) and plasma-to-tissue rate constants (K_1) could differ as much as an order of magnitude dependent on the treatment of the fractional tissue blood volume [1,2]. In an attempt to resolve these differences, we have characterised the kinetics of [^{11}C]temozolomide in gliomas and normal brain tissue with reversible compartmental models.

Results: Consistent with the previous reports [1, 2], the [^{11}C]temozolomide kinetics in normal brain tissue is adequately described by a one-tissue compartment model with a free blood volume term. In gliomas, an additional exponential was identified with spectral analysis. In line with this, the fit of the tumour tissue-time activity curves with a two-tissue compartment model and a free blood volume term was significantly better than the fit with the one-tissue compartment model.

Population mean...

The figure shows mean values with one standard deviation bars for K_1, VD and the mean residence time of the tracer in tissue (MRT) from our cohort of 15 subjects obtained with compartmental analysis. The population mean values for K_1 are in close agreement with those obtained with spectral analysis in [2], when the contribution from the blood volume was excluded, and are about an order of magnitude smaller than those in [1], where the blood volume term was erroneously included in the calculation of K_1. Contrary to the findings of VD_{normal}= 6.97 and VD_{tumour}= 54.4 in [1], our VD estimates are only slightly smaller than those reported in [2]. Consequently, the MRT estimates for normal tissue are slightly smaller than in [2], but in contrast to [1], clearly distinct to those obtained for tumour and tumour rim, respectively.

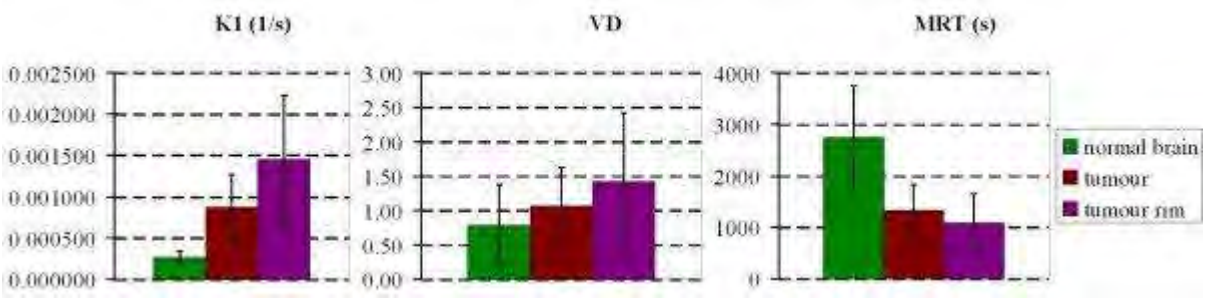

[Population mean +/- one standard deviation]

Conclusions: Compartmental modelling provides stable estimates of [^{11}C]temozolomide kinetic parameters compared to spectral analysis due to its ability to constrain the parameter space independent of the choice of a functional base, thus reducing variability. Consistent with earlier reports [1,2], the increase in K_1 best reflects the activity of the lesion suggesting changes of the [^{11}C]temozolomide blood-brain-barrier penetration in malignant disease.

References:

[1] Meikle SR et al. Cancer Chemother Pharmacol 42 (1998), 183-93.

[2] Rosso L et al. Cancer Res 69 (2009), 120-7.

187

Brain Poster Session: Neuroprotection

CLARIFICATION OF THE ANTI-STRESS EFFECTS OF ANGIOTENSIN II AT1 RECEPTOR BLOCKERS AND THEIR MECHANISMS OF ACTION

M. Honda[1,2], E. Sanchez-Lemus[1], J.M. Saavedra[1]

[1]Section on Pharmacology, National Institutes of Mental Health, NIH, [2]JSPS Research Fellow in Biomedical and Behavioral Research at NIH, NIH, Bethesda, MD, USA

Objectives: Peripheral administration of Angiotensin II (Ang II) AT_1 receptor blockers (ARBs) prevents the hypothalamus-pituitary-adrenal (HPA) axis stimulation during the psychological stress of isolation. We wished to determine, in models of acute psychological and physical stress, the effect of ARB administration on the HPA axis response and on the expression of brain Ang II receptors.

Methods: Adult male Wistar Hanover rats were treated for three days with s.c. administration of the ARB candesartan (1mg/kg/day), followed by 2hr restraint in plastic cylinders, a model of psychological stress, or by 2hr of immobilization to a metal board, a model of psychological and physical stress.

Results: Peripherally administered candesartan significantly blocked all brain AT_1 receptors including those in the PVN. There was increased plasma corticosterone, ACTH and aldosterone concentrations after restraint and immobilization stress. Candesartan did not prevent these increases. Both restraint and immobilization stresses increased AT_{1A} mRNA expression selectively in the PVN, and candesartan prevented this upregulation produced by restraint stress. Acute restraint stress increased benzodiazepine-1(BZ-1) binding in cingulate, frontal, parietal cortex. Candesartan blocked these increases in the frontal and layer IV of parietal cortex. In the pituitary gland, significant AT_{1A} mRNA increase and AT_{1B} mRNA decrease were observed after immobilization stress. In adrenal zona glomerulosa, AT_1 binding and AT_{1B} mRNA decreased after restraint or immobilization stress. In adrenal medulla, AT_{1A} and tyrosine hydroxylase mRNA increased after restraint and immobilization stress. However these changes were not prevented by ARB treatment.

Conclusions: Our results implicate ARBs in the PVN, pituitary and adrenal gland in the regulation of the response to psychological and physical stresses. There is a differential response of AT_1 receptor subtypes during stress. Our results suggest that the control of the HPA axis stimulation by ARBs depends on the type and intensity of the stress challenge. On the other hand, our findings about the BZ-1 binding in some cortical areas suggest that the anti-anxiety properties of ARBs are a general phenomenon common to isolation and restraint stress. Our observations support the hypothesis of limited anti-stress effects of ARBs, depending on the stress type, intensity and duration.

References:

1. Armando I, Carranza A, Nishimura Y, Hoe KL, Barontini M, Terrón JA, Falcón-Neri A, Ito T, Juorio AV, Saavedra JM (2001) Peripheral administration of an Angiotensin II AT_1 receptor antagonist decreases the hypothalamic-pituitary-adrenal response to isolation Stress. Endocrinology 142:3880-9.

2. Leong DS, Terrón JA, Falcón-Neri A, Armando I, Ito T, Jöhren O, Tonelli LH, Hoe KL, Saavedra JM (2002) Restraint stress modulates brain, pituitary and adrenal expression of Angiotensin II AT_{1A}, AT_{1B} and AT_2 receptors. Neuroendocrinology 75:227-40.

3. Saavedra JM, Armando I, Bregonzio C, Juorio A, Macova M, Pavel J, Sanchez-Lemus E (2006) A centrally acting, anxiolytic Angiotensin II AT_1 receptor antagonist prevents the isolation stress-

induced decrease in cortical CRF_1 receptor and benzodiazepine binding. Neuropsychopharmacology 31:1123-34.

4. Sanchez-Lemus E, Murakami Y, Larrayoz-Roldan IM, Moughamian AJ, Pavel J, Nishioku T, Saavedra JM (2008) Angiotensin II AT_1 receptor blockade decreases lipopolysaccharide-induced inflammation in the rat adrenal gland. Endocrinology 149:5177-88.

189

Brain Poster Session: Cerebral Vascular Regulation

LIPID-SOLUBLE CIGARETTE SMOKE PARTICLES UPREGULATE CONTRACTILE ENDOTHELIN TYPE B AND THROMBOXANE A2 RECEPTORS OF RAT MIDDLE CEREBRAL ARTERIES

H. Sandhu[1], C.B. Xu[1,2], L. Edvinsson[1,2]

[1]Department of Clinical Experimental Research, Glostrup Research Institute, Glostrup University Hospital, Glostrup, Denmark, [2]Division of Experimental Vascular Research, Institute of Clinical Sciences in Lund, University Hospital of Lund, Lund, Sweden

Objective: Cerebrovascular smooth muscle cells (SMCs) are associated with enhanced expression of endothelin type B (ET_B) receptor expression. Stroke is strongly associated with several cardiovascular risk factors; e.g. cigarette smoking, increase in low density lipoproteins (LDL), hypertension, inter alia (1). We examined the question if lipid-soluble cigarette smoke particles affect the expression of the contractile ET_B and thromboxane A2 (TP) receptors during organ culture; a method which mimics vascular receptor upregulation seen in cerebral ischemia (2).

Method: Kentucky Reference cigarettes are smoked with aid of vacuum and the smoke particles retrieved on a filter. These were dissolved in 1 ml dimethyl sulfoxide (DMSO) or in water. Fresh cotton filters soaked in DMSO or water were used as controls. Middle cerebral arteries (MCAs) - removed from adult male Sprague Dawley rats (body weight approximately 250 g) - are incubated for 24 h with 0.15 µl DMSO-soluble smoke particles (DSP), water-soluble cigarette smoke particles, DMSO or water. The MCAs are mounted in myographs and contractile responses to the ET_B specific receptor agonist sarafotoxin (S6c) or the TP specific receptor agonist U46619 are studied. Real time PCR and immunohistochemistry are used to semi-quantify the ET_B and TP receptor mRNA and protein levels, respectively.

Results: S6c does not elicit significant contraction of fresh artery segments; however, after organ culture for 24 h S6c induces marked vasoconstriction which does not differ if a small volume of DMSO or water is present during the organ culture (2). Addition of DSP to the organ culture increases the maximum of the S6c response; Emax from 60 ± 7 % in control DMSO or water, to 105 ± 10 % in DSP ($p< 0.05$). The water soluble smoke particles did not enhance the contraction. The Emax of the U46619 response also increased; from 112 ± 5 % in control to 148 ± 12 % in DSP ($p< 0.05$). Real time PCR showed that DSP upregulates both ET_B and TP receptor mRNA expression; thus suggesting an effect at the transcriptional level. Immunohistochemistry showed that the ET_B and the TP receptors are upregulated by the organ culture in the SMCs and not in the endothelium. Addition of DSP to the organ culture further upregulates this ET_B and TP receptor expression at the same location.

Conclusion: We demonstrate for the first time that lipid-soluble cigarette smoke particles but not water-soluble cigarette smoke particles or nicotine per se in smoking dosage (date not shown), enhance the SMC expression of ET_B and TP receptors. The ET_B and TP receptor mediated contractions are upregulated in the SMC and this occurs in parallel with enhanced expression of their mRNA levels. The in vitro organ culture model can be used to study the molecular signal pathways leading to upregulation of the contractile ET_B and TP receptors.

References:

(1) Bhatia M., et al. Cerebrovascular Diseases 20: 180-6, 2005.

(2) Henriksson M., et al. Stroke 34: 1479-83, 2003.

CEREBRAL BLOOD FLOW SIMULATION USING A VASCULAR GRAPH MODEL

J. Reichold[1], M. Stampanoni[2,3], A.L. Keller[4], A. Buck[5], P. Jenny[1], B. Weber[6]

[1]Institute of Fluid Dynamics, ETH Zurich, Zurich, [2]Swiss Light Source, Paul Scherrer Institut, Villigen, [3]Institute for Biomedical Engineering, University and ETH Zurich, Zurich, Switzerland, [4]Max Planck Institute for Biological Cybernetics, Tübingen, Germany, [5]Nuclear Medicine, University Hospital Zurich, [6]Institute for Pharmacology & Toxicology, University of Zurich, Zurich, Switzerland

Background and aims: This work aims at constructing a computational model that can faithfully predict cerebral blood flow (CBF) in realistic vascular networks. We propose a vascular graph (VG) model, based on simple fluid dynamic principles, that comprises an upscaling algorithm, which both reduces the computational cost and allows CBF simulations even when the discrete topology of the capillary bed is unknown.

Methods: The cerebral vasculature can be represented by a graph of resistive elements. Each vessel bifurcation or end-point is a vertex, the blood vessels themselves designate the graph's edges that connect pairs of vertices. By requiring mass conservation at the vertices and providing appropriate boundary conditions, the resulting linear system of equations can be solved to yield pressure and flow values for the entire graph.

This procedure has been thoroughly described for the analogous problem in electrical circuits (Weinberg, 1962), was adapted to vascular networks by Lipowsky and Zweifach (Lipowsky et al, 1974), and was recently extended by Boas and coworkers (Boas et al, 2008). We have further enhanced the model with focus on three-dimensionality and applicability to complex realistic vascular networks. By embedding the vasculature in a computational grid representative of brain tissue, the interaction between the two compartments can be captured in a truly three-dimensional fashion.

The proposed upscaling algorithm replaces the discrete topology of the capillary bed by a coarser-scale network with similar fluid dynamical properties. This is achieved by dividing the computational domain into sub-volumes for each of which effective conductance values of the capillary bed are computed.

Results: The VG model was applied to high-resolution angiography data of the rat cortex obtained with synchrotron radiation based x-ray microscopy (Weber et al, 2006). Our simulations reproduce the well-established finding that the dilation of an arteriole leads to an increase in CBF in the feeding vessel, as well as the capillary bed it irrigates and the corresponding draining veins. We also find that flow decreases in all other arterioles that supply that same region of the capillary bed. This decrease, however, is not as pronounced as the flow increase in the dilated vessel. Our simulations further suggest that the spatial specificity of a local dilation depends both on the cortical depth of the dilation site as well as the type of vessel (Duvernoy et al, 1981) whose diameter is modified.

Our simulations of occluded penetrating arterioles demonstrate that CBF recovers downstream of the occlusion with increasing number of bifurcations. Approximately 350 micron away from the occlusion site, the effect of the constriction is negligible. This distance is consistent with the spatial distribution of the penetrating arterioles and compares well with the recent findings of Nishimura and coworkers (Nishimura et al, 2007).

Conclusions: We have presented a modeling framework that can compute blood pressure and flow, as well as scalar transport and exchange between vasculature and tissue. The introduction of an upscaling algorithm extends the model's applicability to very large networks and eliminates the need for detailed knowledge of the capillary bed topology.

195

Brain Poster Session: Ischemic Preconditioning

CBF EFFECTS OF BRAIN PRECONDITIONING PRODUCED BY CORTICAL LESIONS

L. Zhao, T. Nowak

Department of Neurology, University of Tennessee Health Science Center, Memphis, TN, USA

Aims: Diverse phenomena of brain preconditioning have been described, including effects of brief focal ischemia or discrete cortical lesions to reduce infarct volume following subsequent middle cerebral artery (MCA) occlusion. Ischemic preconditioning has been associated with early CBF recovery in penumbra during the initial hours of subsequent permanent MCA occlusion that predicted eventual infarct volume (Zhao and Nowak, J. Cereb. Blood Flow Metab. 26:1128-1140, 2006). The current study examined CBF responses and peri-infarct depolarizations in brain preconditioned by a prior cortical cold lesion (CL).

Methods: Small cortical lesions were produced in male Spontaneously Hypertensive Rats (SHR) under isoflurane anesthesia by application of a 2 mm diameter liquid nitrogen-chilled metal probe to the thinned skull overlying MCA territory. Sham animals experienced surgical preparation without freezing. The following day rats were subjected to permanent focal occlusion of the MCA and ipsilateral common carotid artery. Infarct volumes were determined at 24 h in hematoxylin-eosin stained frozen sections. CBF was also monitored by C14-iodoantipyrine autoradiography at various time points after occlusion, or throughout the initial hours of occlusion by speckle contrast perfusion imaging with simultaneous electrophysiological recording.

Results: Edema-corrected infarct volumes were 116 ± 14, 113 ± 11 and 85 ± 14 cubic mm in Naïve, Sham and CL groups (mean ± SD; n= 9, 10, and 10), respectively, demonstrating the efficacy of preconditioning by prior lesions. The CBF deficit at 15 min after occlusion was unaffected by CL, but volumes of severely ischemic territory (CBF less than 30 ml/100g/min) at 3 h after occlusion were 130 ± 8, 113 ± 10 and 67 ± 19 cubic mm (n = 5, 4, and 7) in these groups, establishing a phenomenon of early CBF improvement identical to that previously observed after ischemic preconditioning. The magnitude of protection was independent of CL size in the range 2-8 cubic mm. Peri-infarct depolarizations were associated with propagated waves of hyperemia detected by perfusion imaging. These events were completely eliminated in animals with CL larger than 5 cubic mm. However, their incidence was also decreased in animals with smaller, still protective lesions to an extent comparable to that observed after sham surgery. Excluding rats with large lesions, median depolarization numbers during 4 h of occlusion in Naïve, Sham and CL groups were 7 (range 5-11, n = 5), 4 (range 1-5, n = 6) and 4 (range 3-5, n = 7), respectively.

Conclusions: Cortical lesions produce preconditioning mechanistically identical to that induced by prior ischemia, since both are associated with early CBF recovery. CL also reduces the number of peri-infarct depolarizations, although sham surgery had a comparable effect, indicating that such attenuation is not by itself sufficient for protection. The potential contribution of decreased depolarization number to subsequent CBF recovery and infarct volume reduction remains to be established.

196

Brain Oral Session: Cerebrovascular Regulation

THE EFFECT OF HEALTHY AGING ON CEREBRAL AND SYSTEMIC HEMODYNAMIC RESPONSES TO POSTURE CHANGE

B. Edlow[1], M. Kim[2], T. Durduran[2], E. Buckley[2], C. Zhou[2], G. Yu[2], M. Putt[3], A. Yodh[2], J. Greenberg[1], J. Detre[1]

[1]Neurology, University of Pennsylvania, [2]Physics and Astronomy, [3]Biostatistics, Univ of Pennsylvania, Philadelphia, PA, USA

Objectives: Studies of healthy subjects have demonstrated that the systemic response to posture change, the baroreceptor reflex, is impaired with aging (1). In addition, aging is associated with lower baseline cerebral blood flow velocities (2), lower baseline cerebral perfusion (3) and an increased incidence of orthostatic hypotension (4). The effect of healthy aging on cerebrovascular autoregulation, however, has yet to be fully elucidated. We used a novel, hybrid optical instrument to assess the impact of healthy aging on cerebral and systemic hemodynamics during posture change.

Methods: Diffuse Correlation Spectroscopy and Near-infrared Spectroscopy were used concurrently to measure relative cerebral blood flow (rCBF), total hemoglobin concentration (THC), microvascular oxyhemoglobin concentration (HbO_2), and deoxyhemoglobin concentration (Hb) in the frontal lobe cortex of 60 healthy subjects ranging from age 20 to 78. Subjects were studied for 5 minutes at each of the following sequential positions: head of bed (HOB) at 30˚, supine, standing, and supine. Noninvasive measurements of systemic hemodynamics, arterial oxygen saturation (O_2Sat) and end-tidal CO_2 ($EtCO_2$) were performed continuously. A linear mixed effects model was used to quantify the effects of posture and age on each hemodynamic parameter, with age treated as a continuous variable.

Results: The study population had a mean age of 42.3 years and was comprised of 28 men and 32 women. Mean body mass index was 24.7 kg/m^2, blood pressure 115.4/74.5 mmHg, heart rate (HR) 71.3 beats per minute, and $EtCO_2$ 39.4 mmHg. None of these baseline measurements varied significantly with age. Supine-to-standing posture change caused significant declines in rCBF ($p< 0.001$), THC ($p=0.002$), and HbO_2 ($p< 0.001$), and an increase in Hb ($p=0.001$) across the age continuum (See Table). Diastolic blood pressure (DBP, $p< 0.001$), mean arterial pressure (MAP, $p=0.018$), and HR ($p< 0.001$) increased, while $EtCO_2$ ($p< 0.001$) decreased upon standing. Aging was associated with a smaller magnitude of postural change in HR ($p=0.002$), $EtCO_2$ ($p=0.006$), and HbO_2 ($p=0.012$), but no difference in the postural change in rCBF ($p=0.287$).

Conclusions: Healthy aging does not alter postural changes in frontal cortical perfusion, despite age-related postural effects on HR, $EtCO_2$, and HbO_2.

References:

(1) Gribbin B,et al.Circ Res.1971;29:424-431.

(2) Krejza J,et al.Am J Roentgenol.1999;172:213-218.

(3) Matsuda H,et al.Stroke.1984;15:336-342.

(4) Shibao C,et al.Am J Med.2007;120:975-980.

Table. Postural Changes in Cerebral and Systemic Hemodynamics (N=60)

	HOB 30° to Supine	Supine to Stand	.Initial Supine to Recovery Supine
ΔrCBF, %	16.3 (5.1)*	-33.0 (5.4)*	8.1 (5.9)
ΔTHC, µmol/L	2.3 (1.0)*	-4.2 (1.3)*	1.6 (1.2)
ΔHbO_2, µmol/L	2.6 (0.9)*	-5.7 (1.0)*▼	1.2 (1.0)
ΔHb,µmol/L	-0.3 (0.3)	1.5 (0.4)*	0.4 (0.3)

[Table 1/1]

	HOB 30° to Supine	Supine to Stand.	Initial Supine to Recovery Supine
ΔMAP, mmHg	-4.0 (2.4)	7.5 (3.1)*	4.6 (2.2)*
ΔSBP, mmHg	-1.7 (3.1)	0.4 (4.2)	2.2 (2.9)▲
ΔDBP, mmHg	-4.0 (2.0)	11.9 (2.7)*	4.4 (1.7)*
ΔHR, bpm	0.1 (1.2)	20.1 (2.5)*▼	-4.0 (1.0)*
ΔO_2Sat,%	0.1 (0.4)	-0.2 (0.5)	-0.003 (0.4)
Δ$EtCO_2$,mmHg	0.5 (0.7)	-4.3 (0.9) *▼	0.1 (0.5)

[Table 1/2]

Data are expressed as mean (standard error)

*Significant change with new posture, P< 0.05

▲Larger magnitude of postural change with increasing age, P< 0.05

▼Smaller magnitude of postural change with increasing age, P< 0.05

197

Brain Poster Session: Neurologic Disease

PROTON (^{1}H) MAGNETIC RESONANCE SPECTROSCOPY OF AUTOSOMAL RECESSIVE CEREBELLAR ATAXIAS

I. Iltis[1], D. Hutter[1], K. Bushara[2], C. Gomez[3], G. Öz[1]

[1]Center for Magnetic Resonance Research, [2]University of Minnesota, Minneapolis, MN, [3]University of Chicago, Chicago, IL, USA

Objective: Friedreich's ataxia (FRDA) and ataxia with oculomotor apraxia type 2 (AOA2), the most frequent forms of autosomal recessive ataxias (1,2), exemplify the two main mechanisms that underlie these conditions (3). Therefore it is of interest to assess the metabolic and cellular alterations in these two diseases that represent different molecular pathways to neurodegeneration. Here, we investigated the neurochemical alterations in the brains of patients with FRDA and AOA2 by high field ^{1}H MRS.

Methods: Two patient populations and their respective age-matched control groups participated in this study: Eight patients with FRDA (5 F/ 3M, average age ± SD, 27 ± 9 years) and their controls (10 F/10 M, 26 ± 5 years), 8 patients with AOA2 (4 F/ 4 M, 38±9 years) and their controls (7 F/12 M, 36 ± 11 years). Neurochemical profiles of cerebellar hemispheres (volume, 4.9 ml) and vermis (6.3 ml) were measured at 4T using previously described data acquisition and analysis methods (5). Metabolite concentrations were corrected for the amount of cerebrospinal fluid (CSF) in each voxel.

Results: In the vermis, both patient groups exhibited a higher concentration of myo-inositol (AOA2 +44%, p< 0.0001, FRDA +12%, p=0.023) and a higher glutamine / glutamate ratio (AOA2 +35%, p=0.001, FRDA +31%, p=0.002) (Fig.). Disease-specific alterations were also identified: N-acetylaspartate (NAA) was significantly lower in the vermis in FRDA, while choline, creatine and glucose concentrations were increased in AOA2. In the cerebellar hemispheres, NAA concentrations were significantly lower in both patient groups, and glutamine / glutamate ratio was higher only in patients with AOA2. Significant atrophy was observed in the vermis of both patient groups, characterized by a higher CSF content (AOA2 vs. controls, 52 ± 13% vs. 11 ± 4%; FRDA vs. controls, 18 ± 5% vs. 11 ± 3%).

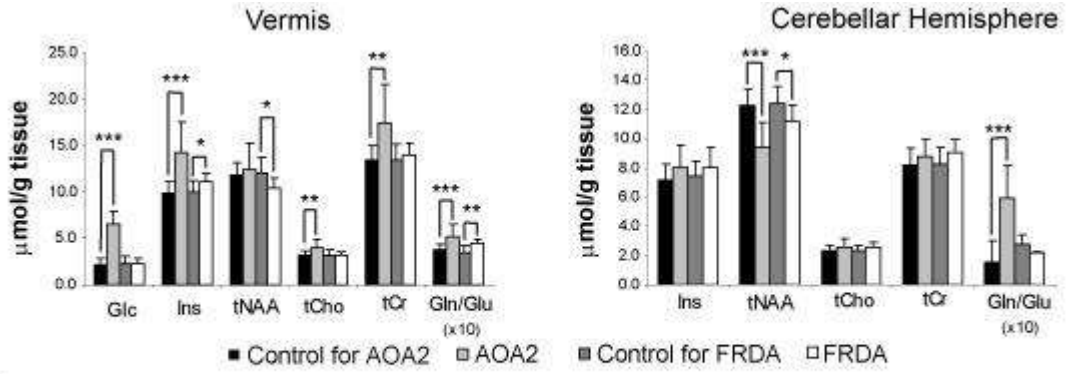

^{1}H Magnetic Resonance Spectroscopy of Autosomal Recessive Cerebellar Ataxias.
Glc, glucose; Ins, *myo*-inositol; tNAA, total N-acetylaspartate; tCho, total choline; tCr, creatine + phosphocreatine; Gln/Glu, glutamine over glutamate ratio. *, p < 0.05; **, p < 0.01; ***, p < 0.001.

[Quantification of Metabolites]

Conclusion: High level of myo-inositol is indicative of fibrous gliosis, described in post-mortem studies (6). Neuroaxonal loss is likely to be responsible for the lower NAA level observed in these patients, while an altered glutamine / glutamate ratio possibly indicates an alteration in neurotransmission. Disease- and region-specific alterations in the metabolic profile of the vermis and cerebellar hemispheres were identified in two populations of patients with cerebellar ataxias using ^{1}H MRS at 4T.

References:

1. Le Ber I, et al. Brain 2004;127:759-767.

2. Viau M, et al. Brain Res. 2005;1049:191-202.

3. Taroni F & DiDonato S, Nat Rev Neurosci, 5: 641, 2004.

4. Mascalchi M, et al. Radiology 2002;223:371-378.

5. Tkáč I, et al. Appl Magn Reson 2005;29:139-157.

6. Criscuolo C, et al. Neurology 2006;66:1207-1210.

Supported by Kory and Scott Tabor Ataxia Research Fund, NIH R21 NS056172, P41 RR08079, P30 NS057091, M01RR00400 and MN Medical Foundation.

Brain Poster Session: Experimental Stroke & Cerebral Ischemia

EFFECTS OF P-TYPE CALCIUM CHANNEL BLOCK ON NITRIC OXIDE PRODUCTION DURING CEREBRAL ISCHEMIA AND REPERFUSION IN MICE

T. Ohkubo, Y. Asano, K. Hattori, D. Furuya, T. Shimazu, H. Nagoya, M. Yamazato, Y. Ito, Y. Kato, **N. Araki**

Department of Neurology, Saitama Medical University, Saitama, Japan

Objectives: Nitric oxide (NO) plays an important role in the pathogenesis of neuronal injury during cerebral ischemia. P-type calcium channels are present in the brain. We investigated the effects of P-type calcium channel blocker on NO production during cerebral ischemia and reperfusion.

Methods: Twenty four C57BL/6 mice were used in the study. ω-Agatoxin-TK (0.5 μg/kg), P-type calcium channel blocker, was administered by intraperitoneal injection at 30 minutes before cerebral ischemia in 7 mice (ω-Aga group), and the drug was not administered in the remaining 17 mice (control group). The animals were anesthetized with 2% halothane and maintained with 0.5-1% halothane. NO production was continuously monitored by in vivo microdialysis. A microdialysis probe was inserted into the left striatum and perfused with Ringer's solution at a constant rate of 2 μl/min. After 2 hours equilibrium period, fractions were collected every 10 minutes. A laser Doppler probe was placed on the right skull surface. Global ischemia was produced by clipping both common carotid arteries using Zen clip for 10 minutes. The levels of nitrite (NO_2^-) and nitrate (NO_3^-) in the dialysate samples were measured by the Griess reaction.

Results:

1. Blood Pressure: No significant differences were observed between ω-Aga group and control group.
2. Cerebral Blood Flow (CBF) (Fig.1): CBF decreased to 3.7±2.0% (mean±SD) in ω-Aga group and 4.2±1.5 in control group during ischemia. After reperfusion, CBF transiently returned to baseline values and then gradually decreased significantly in both groups. In ω-Aga group, CBF at 30 minutes (65.4±27.7*%), 60 minutes (60.4±12.9*), 80 minutes (65.3±13.3*) and 120 minutes (67.3±12.1*) after reperfusion were significantly higher than those in control group (47.7±10.2, 50.2±10.1, 51.6±12.2, 55.5±13.1, respectively).
3. NO Metabolism (Fig.2): In ω-Aga group, the change rate of NO_2^- levels during ischemia (106.3±31.9*%), at 10 minutes (119.8±21.8*) and at 80 minutes (105.5±35.2**), and at 120 minutes (102.7±23.6*) after reperfusion were significantly higher than those in control group (80.4±23.5, 88.8±31.3, 60.5±21.6, 64.2±37.7, respectively). As for the change rate of NO_3^- levers, no significant differences were observed between the two groups. The change rate of total NO (NO_2^-+NO_3^-) levels at 80 minutes (147.9±34.6*), and at 120 minutes (143.2±22.1*) in ω-Aga group were significantly higher than those in control group (111.8±27.3, 108.5±39.0, respectively) [*: $p< 0.05$, **: $p< 0.005$].

Conclusions: The above data indicate that ω-Agatoxin-TK attenuates the decrease of cerebral blood flow following reperfusion and affects the NO production after reperfusion. Although it has been reported that N-type calcium channel blocker cilnicipine increased eNOS expression, the relationship between NOS and P-/Q-type calcium channel is not clear. These data suggest P-type calcium channel inhibition may exert the brain protective effect through the influence on cerebral blood flow and NO metabolism.

<Fig.1>

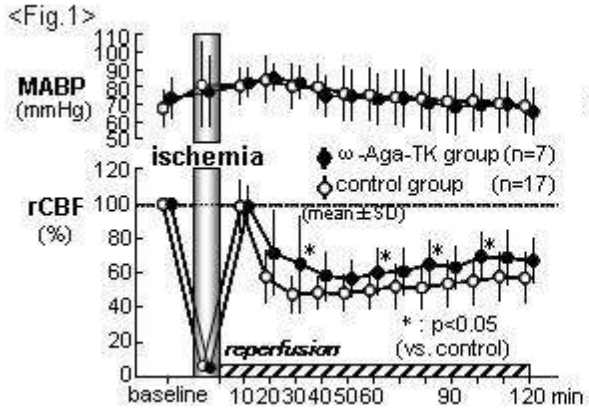

<Fig.2>

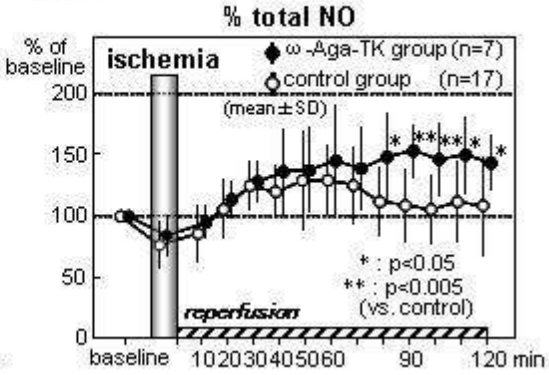

[effects of ω-agatoxin]

Brain Poster Session: Experimental Cerebral Ischemia: Vascular & Endothelial

ALPHA4-INTEGRIN INHIBITION IS NEUROPROTECTIVE AFTER EXPERIMENTAL BRAIN ISCHEMIA IN MICE

A. Liesz[1], S. Karcher[1], C. Sommer[2], R. Veltkamp[1]

[1]Neurology, University of Heidelberg, Heidelberg, [2]Neuropathology, University of Mainz, Mainz, Germany

Objectives: Inflammatory cascades play a detrimental role in the acute phase after ischemic stroke[1]. Invading inflammatory cells are an important source of proinflammatory cytokine release and secondary infarct growth[1,2]. Alpha4-Integrins are adhesion molecules on leukocytes. Blocking of these integrins by specific antibodies prevents the migration of leukocytes into the brain[3] which represents a potent therapy in experimental encephalomyelitis[4] and clinical multiple sclerosis[5]. Therefore, we investigated the effect of Alpha4-Integrin inhibition on brain ischemia outcome and its impact on postischemic brain inflammation and systemic immune parameters.

Methods: Permanent focal cerebral ischemia was induced by transtemporal middle cerebral artery occlusion (MCAO). Mice were treated 24h before MCAO with a single intraperitoneal dose of 300µg Anti-Alpha4-Integrin, controls received IgG2 isotype. Impact of antibody treatment on circulating lymphocyte counts was analyzed by flow cytometry. Infarct volume and behavioural deficits ("Corner Test", "Cylinder Test") were determined at several time points after MCAO. Brain cytokine expression was analyzed by RT-PCR, serum cytokine levels were measured by ELISA. Leukocyte brain invasion ($CD45^+$, $CD3^+$, $B200^+$, $DX5^+$, MPO^+ and $Foxp3^+$ cells) and microglial activation (IBA-1^+ cells) was determined by immunohistochemistry.

Results: Anti-Alpha4-Integrin treatment significantly reduced the infarct size 7d after MCAO (11±1.7 mm^3) compared to control treatment (14±1.9 mm^3, n=10 per group, $p< 0.01$). Correspondingly, behavioural assessment revealed a significantly improved outcome in the treatment group at 3d ($p=0.015$) and 7d ($p=0.012$) after MCAO. Anti-Alpha4-Integrin injection did not alter the number of circulating B-, T_{Helper}-, $T_{Effector}$- and NK-cells in the blood 3d after treatment compared to control mice. We investigated the brain invasion of diverse leukocyte subsets after ischemia, including T-, B-, NK-cells and neutrophilic granulocytes as well as the activation of resident IBA-1^+ microglial cells, in treated mice and control animals 5d after MCAO. Alpha4-Integrin inhibition significantly ($n=5$, $p< 0.05$) reduced cerebral expression of the proinflammatory cytokines TNF-alpha, IL-6 and Interferon-gamma at 24h and 3d after MCAO compared to controls. In contrast, expression of the neuroprotective, anti-inflammatory cytokines IL-10 and TGF-beta was not affected by the therapy. Furthermore, Anti-Alpha4-Integrin injection did not alter the serum concentrations of the main pro- and anti-inflammatory cytokines in naïve mice and at 24h and 5d after MCAO, respectively.

Conclusions: To our knowledge, this study shows for the first time that Alpha4-Integrin inhibition significantly reduces infarct size and behavioural deficits after experimental brain ischemia. The present data suggests that this neuroprotection is mediated by reduced cerebral neurotoxic cytokine release whereas systemic immune system function and cytokine homeostasis is not altered.

References:

1. Dirnagl, U. Inflammation in stroke: the good, the bad, and the unknown. Ernst Schering Res Found Workshop (2004).

2. Liesz, A., et al. Regulatory T cells are key cerebroprotective immunomodulators in acute experimental stroke. Nat Med (2009).

3. Rose, D.M., et al. Alpha4 integrins and the immune response. Immunol Rev (2002).

4. Yednock, T.A., et al. Prevention of experimental autoimmune encephalomyelitis by antibodies against alpha 4 beta 1 integrin. Nature (1992).

5. Polman, C.H., et al. A randomized, placebo-controlled trial of natalizumab for relapsing multiple sclerosis. N Engl J Med (2006).

200

Brain Poster Session: Neonatal Ischemia

EFFECTS OF NA^+/H^+ EXCHANGER ISOFORM 1 INHIBITOR CARIPORIDE ON CA1 PYRAMIDAL NEURONAL DEATH IN MOUSE MODEL OF HYPOXIC ISCHEMIC ENCEPHALOPATHY

P. Cengiz[1], K. Uluc[2], N. Kleman[2], P. Ferrazzano[1], D. Sun[2]

[1]Department of Pediatrics, University of Wisconsin, [2]Department of Neurological Surgery, University of Wisconsin, Madison, WI, USA

Background: Hypoxic ischemic encephalopathy (HIE) is an important cause of mortality, morbidity in neonates. Goal of this project is to investigate role of plasma membrane Na^+/H^+ exchanger isoform 1 (NHE-1) in neonatal HIE. NHE-1 is essential in regulation of pH_i. Its activity is stimulated upon acidosis after ischemia. We previously found that inhibition of NHE-1 is neuroprotective following focal cerebral ischemia in adult animals (Luo et al, 2005). However, it is unknown whether NHE-1 plays a role in immature brain damage following hypoxia ischemia (HI). We hypothesized that overstimulation of NHE-1 occurs in HI and inhibition of NHE-1 with cariporide (HOE 642) is neuroprotective.

Methods: Left common carotid arteries of P9 mice (C57/Blk6) were ligated under isoflurane anesthesia and 0.21% FiO_2. Animals recovered for 2 hours (h), exposed to 8% O_2 (balanced nitrogen) for 55 minutes (min) at 37°C and were grouped into 4 groups. Group I and III received saline injection intraperitoneally (i.p) 3 times as vehicle controls. Group II received HOE 642 (0.5 mg/kg i.p.) 10 min, at 24 h and 48 h after HI. Group IV received HOE 642 (0.5 mg/kg i.p.) 5 min prior to initiation of HI, and at 24 h and 48 h after HI. At 72 h after HI, the brains were transcardially fixed with 4% paraformaldehyde. Brain sections (70 μm) were prepared and stained with Fluoro-Jade. Number of Fluoro-Jade stained cells in the CA1 regions of hippocampus were compared between the vehicle control and HOE 642- treated animals. Neuronal damage was quantified using a scale (score 1: 0-200 , 2: 201-500, 3: 501-1000, 4:>1000 positively stained cells). Four slices for each brain were analyzed. Number of Fluoro-Jade positive cells per brain was averaged.

Purpose: To investigate whether pharmacological inhibition of NHE1 reduces hippocampal damage in neonatal mice and to investigate dose and administration interval of HOE 642 for neuroprotection following HI.

Results: Figure 1 shows, CA1 pyramidal neurons in vehicle control mice were positively stained with Fluoro-Jade (left panel, arrow) at 72 h following 55 min HI. In contrast, the HOE-treated mouse had few stained cells in CA1 region (right panel, *). ~ 30% reduction of Fluoro-Jade-positive cells was seen in HOE-treated brains (groups II and IV) (Table 1).

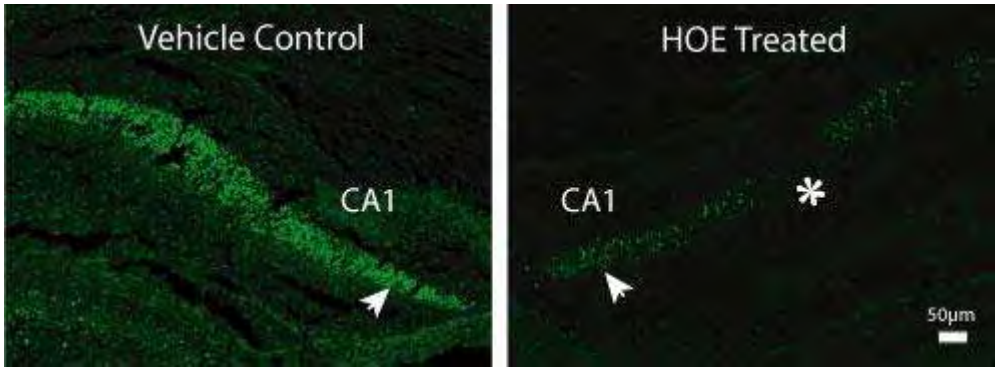

[Figure 1.]

	Score (mean ± S.D.)
Group I	2.7 ± 1.2
Group II	1.9 ± 1.1
Group III	2.0 ± 1.1
Group IV	1.9 ± 1.1

[Table 1. Neurological injury scores of the groups.]

Conclusions: This preliminary study demonstrated that inhibition of NHE-1 with HOE 642 following HI was neuroprotective in P9 mice suggesting that NHE-1 activity may contribute to delayed CA1 pyramidal neuronal cell death after neonatal HI.

202

Brain Poster Session: Hemorrhagic Transformation

INTRACRANIAL HEMORRHAGE IN MICE WITH ACUTE RISE IN BLOOD PRESSURE DURING CHRONIC HYPERTENSION

Y. Wakisaka[1], Y. Chu[1], J.D. Miller[1], G.A. Rosenberg[2], D.D. Heistad[1,3,4]

[1]Internal Medicine, University of Iowa, Iowa City, IA, [2]Neurology, University of New Mexico Health Sciences Center, Albuquerque, NM, [3]Pharmacology, University of Iowa, [4]VA Medical Center, Iowa City, IA, USA

Objectives: Acute as well as chronic hypertension (HT) is a risk factor for intracranial hemorrhage (ICH). We have developed new models of spontaneous ICH with acute, superimposed on chronic, hypertension. We tested the hypotheses that increases in oxidative stress and activation of matrix metalloproteinase (MMP)-9 are associated with, and may precede, spontaneous ICH during hypertension, and that susceptibility to ICH would be increased more by angiotenin-II (AngII) than by norepinephrine (NE) because of the pro-oxidant effects of AngII.

Methods: Chronic HT was produced in C57BL/6 mice with AngII-infusion and L-NAME. One week later, acute HT was produced in some chronic HT mice by daily subcutaneous injection of AngII (chronic/acute HT-AngII group) or NE (chronic/acute HT-NE group). Superoxide was measured in brain homogenates using lucigenin-enhanced chemiluminescence. MMPs levels were estimated by gelatin zymography and by in situ zymography.

Results: Systolic blood pressure (SBP) increased to 163±3 (mean±SE) mmHg 7 days after start of AngII-infusion and L-NAME. Injection of AngII transiently increased SBP in chronic/acute HT-AngII mice (ΔSBP: 57±4 mmHg). Eleven of 15 chronic/acute HT-AngII mice developed neurological signs after 15±1 days. ICH was demonstrated with histological examination. Only one of 15 chronic HT mice, without acute HT, developed ICH. Superoxide was low in control mice, increased in chronic HT mice (3.8±0.2 fold vs control), increased further in chronic/acute HT-AngII mice without ICH (6.5±0.6), and was highest in chronic/acute HT-AngII mice with ICH (11.4±1.2) (each, $p< 0.01$ vs control). NAD(P)H oxidase activity (superoxide after addition of 100μM NADPH) increased in parallel with changes in superoxide. RT-PCR revealed that Nox4 was upregulated and SOD2, SOD3, and catalase were downregulated in chronic/acute HT-AngII mice with and without ICH. Expression of several other pro- and anti-oxidant enzymes was unchanged. Changes in MMP-9 levels (gelatin zymography) also paralleled oxidative stress, with no changes in MMP-2 levels. In situ zymography showed that activated MMPs and an oxidative stress marker were co-localized on extracellular matrix and endothelium of cerebral vessels, especially in vessels that appeared to be associated with ICH. When chronic HT mice received injections of NE, SBP increased more than chronic/acute HT-AngII mice (ΔSBP: 68±3, $p< 0.01$), but incidence of neurological signs was less than in chronic/acute HT-AngII mice (40% vs 73%). Histological studies showed that chronic/acute HT-NE mice developed significantly fewer ICH than chronic/acute HT-AngII mice. Levels of oxidative stress and MMP-9 did not increase in chronic/acute HT-NE mice without ICH compared to those of chronic HT mice, and were significantly less than those of chronic/acute HT-AngII mice with and without ICH.

Conclusion: We have developed new models of ICH in mice with acute, superimposed on chronic, hypertension. AngII-mediated acute HT increased oxidative stress and levels of MMP-9, with increased propensity for ICH. Incidence and number of ICH were greater during AngII- than NE-induced acute HT, perhaps related to the extraordinary pro-oxidant effects of AngII. The findings suggest that acute HT induced by AngII, and less by NE, may play a critical role in spontaneous ICH during chronic HT.

COMBINING ELECTROPHYSIOLOGY WITH FMRI TO INVESTIGATE NEUROPHARMACOLOGICAL MODULATION OF BRAIN FUNCTION IN THE RAT

C. Martin[1], N. Sibson[2]

[1]Department of Physiology, Anatomy and Genetics, [2]Gray Institute for Radiation Oncology and Biology, University of Oxford, Oxford, UK

Background and aims: Functional brain imaging methods which exploit the neurovascular coupling of neuronal activity to changes in haemodynamics are increasingly applied to study the functional effects of neuropharmacological agents in both human and animal subjects. A problem is that neuroimaging signals such as the blood oxygen level dependent (BOLD) functional magnetic resonance imaging (fMRI) signal may be subject to multiple neuronal, neurovascular, haemodynamic and systemic effects of the drug under investigation. To address this, our understanding of the neurophysiological basis of functional imaging signals must be expanded to include the effects of altered neurotransmitter function (e.g. by experiment, clinical trial or disease) and differences across neuropharmacologically diverse cortical and subcortical structures. An effective approach for establishing relationships between fMRI responses and underlying neuronal activity is one in which both of these signals are measured concurrently. Achieving this within the MR environment is difficult due to distortion of electrophysiological signals by rapidly changing magnetic gradient fields. Here, we report the development of methodology for concurrent acquisition of fMRI and electrophysiological measures of neuronal activity in the rat. We use this method to investigate the effects of the serotonin releasing agent, fenfluramine, on both baselines and stimulus evoked responses.

Methods: Animals were anaesthetized with isoflurane, tracheotomised for artificial ventilation and cannulated for administration of drugs and monitoring of physiological parameters. Electrodes were constructed from carbon fibre bundles (diameter ~50microns) and inserted into the hindpaw sensorimotor cortex. Stimulating electrodes were inserted into the contralateral hindpaw. Imaging was performed on a 7-Tesla horizontal bore magnet. Anatomical scans to cover the whole brain were acquired using a T2-weighted fast spin-echo sequence (field of view 30X30mm, matrix size 128X128, slice thickness 0.5mm). Functional data were acquired using T_2*-weighted multi-echo gradient-echo sequences (effective TE 12ms, field of view 30 X 30 mm, matrix size 128 X 64, slice thickness 0.5mm). Fenfluramine (10mg/Kg) was injected intravenously after a period of baseline data acquisition. Analysis procedures to remove the MR artefacts from the data included an adaptive template-based artefact removal procedure and band-pass filtering.

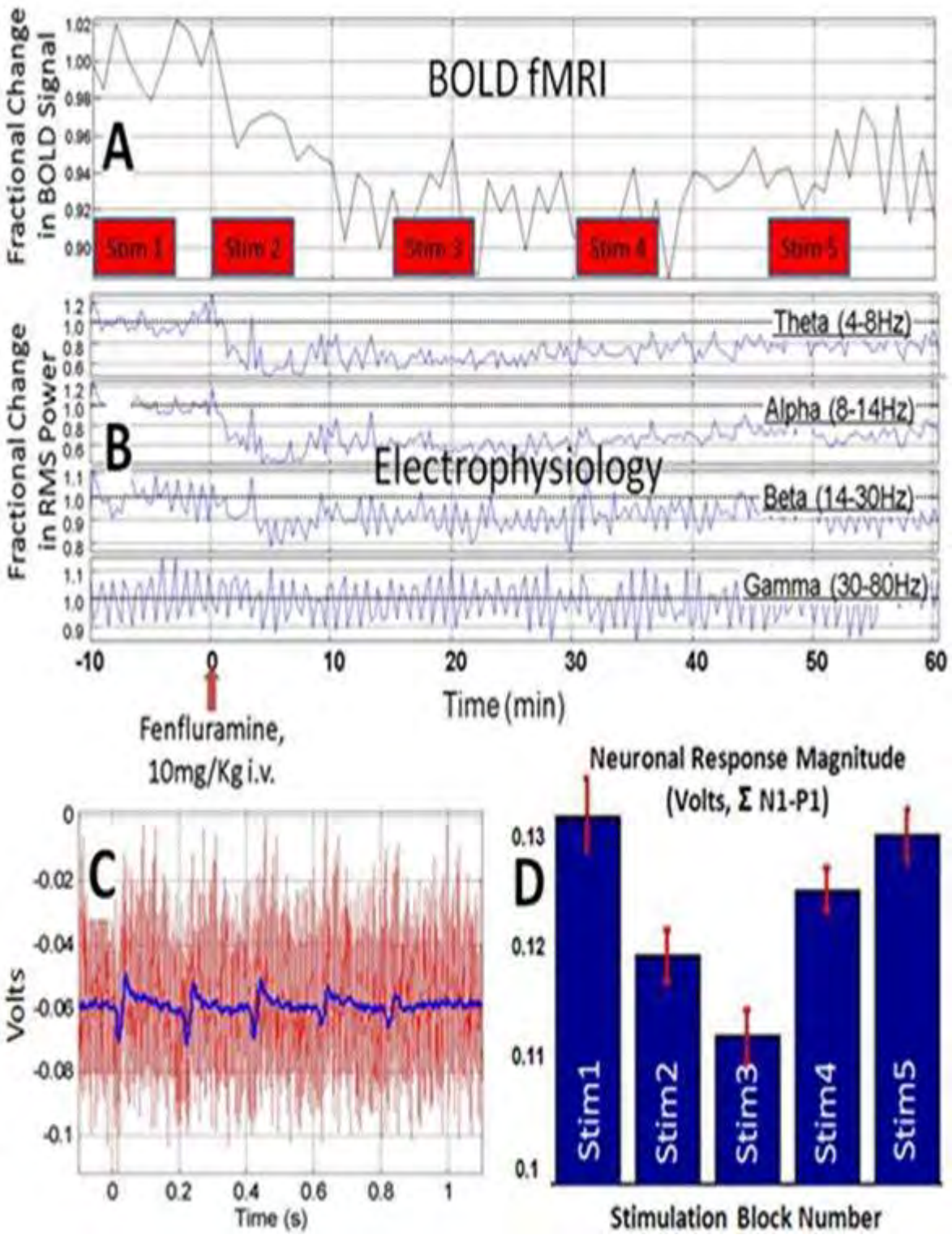

[Fig1]

Results and conclusions: We demonstrate that electrophysiological measures of both baseline and stimulation-evoked neuronal activity can be obtained concurrently with fMRI data acquisition. Fenfluramine administration produced simultaneous decreases in the BOLD fMRI signal (**A**) and in

EEG power fluctuations (**B**). Neuronal responses to hindpaw stimulation could be easily extracted from the data following processing to remove MR gradient artefacts (**C**: red - before processing, blue - after processing). Neuronal responses were also transiently attenuated by fenfluramine administration (**D**). These procedures will be used to investigate the effects of neuropharmaoclogical manipulation of neurotransmitter function on the relationship between neuronal activity and fMRI reponses. Methods for conducting experiments in awake animals are also being developed.

206

Brain Poster Session: Cerebral Vascular Regulation

EVALUATING CROSSTALK BETWEEN EPOXYEICOSATRIENOIC ACIDS (EETS) AND NEUROPEPTIDE SIGNALING IN NEUROGENIC VASODILATION

J. Iliff[1,2], N. Alkayed[1,2]

[1]Department of Anesthesiology and Peri-Operative Medicine, [2]Department of Physiology and Pharmacology, Oregon Health and Science University, Portland, OR, USA

Objectives: Epoxyeicosatrienoic acids (EETs) are vasodilator eicosanoids synthesized by P450 epoxygenases and metabolized by soluble epoxide hydrolase (sEH) [1]. We recently reported that the machinery for EETs synthesis and metabolism is present in perivascular vasodilator nerve fibers and associated ganglia innervating the rat middle cerebral artery. We have also found that EETs play a functional role in the regulation of cerebral blood flow (CBF) by these nerves [2, 3]. The vasomotor actions of these fibers have been attributed to the release of the neuropeptides vasoactive intestinal peptide (VIP) and calcitonin gene-related peptide (CGRP) [4]. We therefore set out to determine if EETs and neuropeptide signaling interact in the neurogenic regulation of CBF. In the present study, we evaluated the following potential modes of interaction between EETs and the vasodilator action of VIP and CGRP:

1. post-junctional potentiation of neuropeptide vasomotor action by EETs,
2. parallel and additive vasomotor effects of EETs and neuropeptides,
3. intracellular regulation of pre-junctional neuropeptide release by EETs, and
4. dependence of neuropeptide-evoked vasodilation upon endothelium-derived EETs.

Methods: CBF was monitored over front-parietal cerebral cortex in adult male Wistar rats by laser Doppler flowmetry (LDF). The neuropeptides VIP or CGRP (1 nmol/L - 1 μmol/L) were perfused over the pial surface via a closed cranial window and the LDF responses were measured in the presence and absence of 14,15-EET (100 nmol/L).

Results: VIP (n = 5) and CGRP (n = 5) evoked a concentration-dependent hyperemia in the cortex with EC_{50} values of 0.475 μmol/L and 6.64 μmol/L and with maximal values of 26 ± 7% and 22 ± 3% at 1 μmol/L concentration, respectively. In the presence of 14,15-EET, neither the EC_{50} nor the maximal CBF responses to VIP or CGRP were significantly altered.

Conclusions: These data suggest that neurogenic EETs do not act post-junctionally to potentiate the vasomotor action of the neuropeptides VIP or CGRP. Further studies will evaluate the other modes of interaction between neurogenic EETs and neuropeptide signaling. Resolving the interactions between these cerebral vasodilator signaling pathways may provide novel therapeutic options for the treatment of such pathological states as migraine, stroke and vasospasm after subarachnoid hemorrhage. Supported by NS44313 to NJA and a predoctoral NRSA to JJI.

References:

1. Spector AA, Norris AW: Action of epoxyeicosatrienoic acids on cellular function. Am. J. Physiol., Cell Physiol. 292, C996-1012 (2007).

2. Iliff JJ, Close LN, Selden NR, Alkayed NJ: A novel role for P450 eicosanoids in the neurogenic control of cerebral blood flow in the rat. Exp. Physiol. 92, 653-658 (2007).

3. Iliff JJ, Wang R, Zeldin DC, Alkayed NJ: Epoxyeicosanoids as mediators of neurogenic vasodilation in cerebral vessels. Am J Phsyiol Heart Circ Physiol (under review), (2008).

4. Hamel E, Perivascular nerves and the regulation of cerebrovascular tone. J. Appl. Physiol. 100, 1059-1064 (2006).

208

Brain Poster Session: Brain Imaging: Neurologic Disease

HEMODYNAMIC CHANGES FOLLOWING WINGSPAN STENT PLACEMENT - A QUANTITATIVE MAGNETIC RESONANCE ANGIOGRAPHY STUDY

S. Prabhakaran[1], K. Wells[2], M.D. Jhaveri[2], D.K. Lopes[3]

[1]Neurological Sciences, [2]Radiology, [3]Neurosurgery, Rush University Medical Center, Chicago, IL, USA

Background: Quantitative magnetic resonance angiography (QMRA) is a novel non-invasive imaging modality that combines time-of-flight MRA and phase-contrast imaging to provide anatomic visualization as well as blood flow measurements within arteries. No published data exists on the use of QMRA to assess hemodynamic changes following Wingspan stent placement for intracranial stenosis.

Methods: We retrospectively identified all patients at our institution who met the following criteria:

1. Wingspan stent placement for symptomatic >50% intracranial arterial stenosis;
2. baseline QMRA scan performed within 6 months prior to stent placement;
3. follow-up QMRA scan performed within 1 week following stent placement; and
4. high-quality QMRA images without motion artifact or technical errors.

Other socio-demographic, clinical, and imaging data were abstracted from medical charts. We compared volumetric flow rates (mL/min) pre- and post-stenting using paired t-tests. $P < 0.05$ was considered significant.

Results: Among 9 patients who met above criteria (mean age 65.8 years), lesions were located in the supraclinoid internal carotid arteries in 3 patients, the middle cerebral arteries in 3, and intracranial vertebrobasilar arteries in 3. The mean pre-treatment stenosis was 71.0 + 13.3%. The mean pre-treatment QMRA volumetric flow rate in the stenotic artery was 81.2 + 59.6 mL/min and increased to a mean of 133.3 + 21.5 mL/min ($P = 0.020$) or 64.2% after stenting. There was a strong positive correlation between change in volumetric flow rate and degree of stenosis prior to stenting ($r = 0.705$, $P = 0.034$). No correlation was seen between post-stent degree of stenosis and post-stent VFR or change in VFR. Total CBF, flow in non-stented vessels, and collateral flow in circle of Willis vessels did not significantly change.

Conclusion: We found that QMRA is a promising new non-invasive method for the measurement of cerebral hemodynamics following intracranial Wingspan stent placement. Larger prospective studies are needed to confirm our findings and increase our understanding of flow changes following endovascular interventions for intracranial stenosis.

IN VIVO SIMULTANEOUS FUNCTIONAL AND MORPHOLOGICAL BRAIN IMAGING USING INTEGRATED PET/MRI (IPET/MRI) SYSTEM IN SMALL ANIMALS

M. Imaizumi[1], S. Yamamoto[2], Y. Kanai[1], M. Tatsumi[1], H. Kato[1], I. Higuchi[1], M. Kawakami[3], M. Aoki[3], E. Shimosegawa[1], J. Hatazawa[1]

[1]Department of Nuclear Medicine and Tracer Kinetics, Osaka University Graduate School of Medicine, Suita, [2]Kobe City College of Technology, Kobe, [3]Hitachi Metals. Ltd., NEOMAX Company, Saga, Japan

Background and aims: Simultaneous measurements of positron emission tomography (PET) and magnetic resonance imaging (MRI) is a promising strategy for direct comparison of functional and morphological information. Therefore, development of PET/MRI is currently on-going for experimental researches and clinical applications. An integrated PET/MRI (iPET/MRI) system has been constructed that combines an optical fiber based MR-compatible PET with a low magnetic field permanent magnet MRI for small animals. Our aim is to investigate the feasibility of in vivo simultaneous imaging using the iPET/MRI system.

Methods: The iPET/MRI system consists of depth-of interaction block detectors made of LGSO, optical fibers (~80 cm), and position sensitive photomultiplier tubes for PET, and radio-frequency coil (φ 76 mm) and 0.3T Nd-Fe-B permanent magnet (Hitachi Metal, NEOMAX Co., Ltd) for MRI. To test this system, small animals (Wistar rat, Male, N=6~) were anesthetized by MR-compatible inhalation device with 1.5% isoflurane and injected approximately 37 MBq of ^{18}F-FDG with MR contrast medium intravenously. Simultaneous PET (list mode) and MR (fast low angle shot < FLASH> T1-weighted sequence, TR/TE=50/5 msec) imaging were performed 30-90 min after ^{18}F-FDG injection. During MRI acquisition, PET data were acquired in 3 axial positions by shifting the PET detector ring to cover ~5cm axial field of view.

Results: ^{18}F-FDG images showed high uptake in the brain, harderian glands, heart and kidneys, consistent with known distribution. In the cranium and cervical portions, MR images with contrast medium provided superior anatomic information such as cerebral basal ganglia, cerebellum, brainstem, spinal cord, oral cavity structures and cervical brown adipose tissue with excellent soft-tissue contrast. MR angiography depicted internal jugular vein, transverse sinus, superior sagital sinus, and superior and inferior vena cava. Simultaneous PET/MR images were obtained successfully without noticeable distortion in either PET or MR image sets. The excellent quality of these integrated images enables us to clearly identify small structures in the cranium of rats.

Conclusions: We confirmed that our iPET/MRI system can be used for in vivo simultaneous brain imaging of small animals.

Research support: Program for Promotion of Fundamental Studies in Health Sciences of the National Institute of Biomedical Innovations (No. 06-35).

210

BrainPET Poster Session: Molecular Brain Imaging: Clinical Applications

DECREASED NEUROKININ$_1$ (SUBSTANCE P) RECEPTOR BINDING IN PATIENTS WITH PANIC DISORDER: POSITRON EMISSION TOMOGRAPHIC STUDY WITH [^{18}F]SPA-RQ

Y. Fujimura[1], F. Yasuno[1], A. Farris[1], J.-S. Liow[1], M. Geraci[2], W. Drevets[2], D. Pine[2], S. Ghose[3], A. Lerner[1], R. Hargreaves[4], D. Bruns[4], C. Morse[1], V. Pike[1], R. Innis[1]

[1]Molecular Imaging Branch, [2]Mood and Anxiety Disorders Program, National Institute of Mental Health, Bethesda, MD, [3]Department of Psychiatry, UT Southwestern Medical Center, Dallas, TX, [4]Merck Research Laboratories, West Point, PA, USA

Objectives: Pain and stress in animals cause release the peptide neurotransmitter substance P, which binds to and causes internalization of neurokinin$_1$ (NK_1) receptors. Positron emission tomography (PET) can localize and quantify NK_1 receptors in brain using the non-peptide antagonist radioligand, [^{18}F]SPA-RQ. We sought to determine if patients with panic disorder have altered density of NK_1 receptors in brain because of their history of recurrent panic attacks. We also sought to determine if a drug-induced panic attack releases substance P in brain, as measured by decreased binding of [^{18}F]SPA-RQ.

Methods: PET scans with [^{18}F]SPA-RQ were performed in 14 patients with panic disorder and 14 healthy subjects. Of these two groups, 7 patients and 10 healthy subjects were scanned twice, once at baseline and once after injection of doxapram, a drug that induces panic attacks.

Results: NK_1 receptor binding in patients (n=14) compared to that in healthy subjects (n=14) was significantly decreased by 12-21% in all brain regions. Doxapram effectively produced panic attacks in 6 of 7 patients with panic disorder but only 2 of 10 healthy subjects. Doxapram caused no significant change of [^{18}F]SPA-RQ binding in either patients or healthy subjects.

Conclusions: Although induction of a panic attack has no significant effect on [^{18}F]SPA-RQ binding to NK_1 receptors, patients with panic disorder have widespread reduction of NK_1 receptor binding in brain. The potential importance of decreased NK_1 receptor binding in panic disorder could be explored in the future by measuring the effects of treatment and by comparison with other anxiety-related disorders.

References:

[1] Science 1998;281:1640-1645.

[2] Synapse 2007;61:242-251.

Disclosures: This research was supported by the Intramural Program of NIMH (project # Z01-MH-002852-01). R.H. and H.D.B. were employees of Merck Research Laboratories. Y.F. and F.Y. were supported by the JSPS Research Fellowship in Biomedical and Behavioral Research at NIH.

Figure legend: Decreased NK_1 receptor binding at baseline in patients compared to healthy controls. The distribution of receptor binding (BP_{ND}) in 14 patients and 14 healthy controls is shown for two brain regions (frontal and occipital).

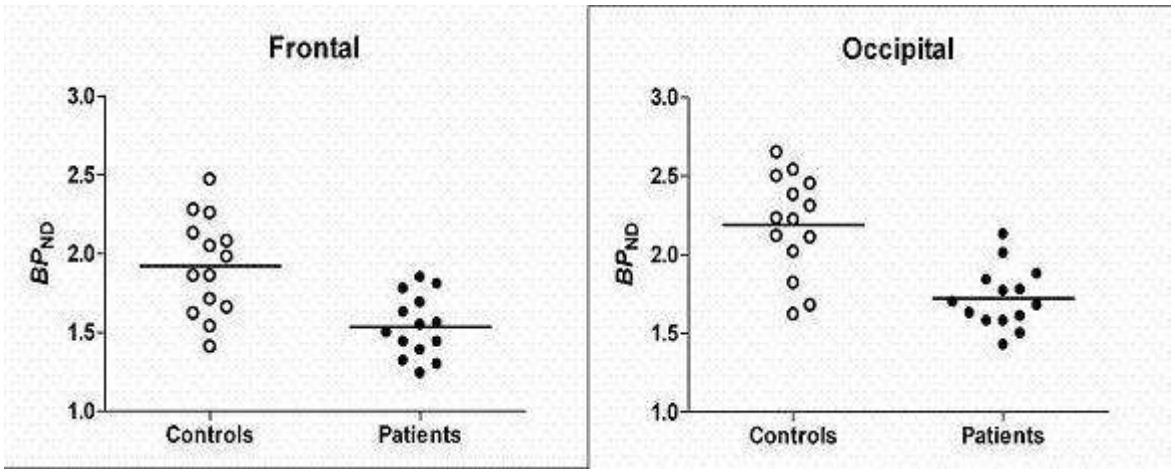

[Decreased Binding in patients with panic disorder]

211

BrainPET Poster Session: Molecular Brain Imaging: Clinical Applications

AN MRI BASED F18-FDOPA PET TEMPLATE OF THE RAT BRAIN

J. Chen[1], R.-S. Liu[2], J.-C. Chen[1]

[1]Department of Biomedical Imaging and Radiological Sciences, National Yang Ming University,
[2]National PET/Cyclotron Center, Taipei Veterans General Hospital, Taipei, Taiwan R.O.C.

Objectives: Parkinson disease (PD) is a well known neurodegenerative disease that suffers millions of people. The characteristics of this disease is a gradually loss of dopamine neurons in the midbrain, but its exact cause is still unknown. F-18-FDOPA radiopharmaceutical is commonly used with PET to assess presynaptic nigrostriatal dopaminergic function which is an important index for brain function evaluation. To facilitate quantitative analysis of PD animal model using animal PET, we would like to develop an MRI based F18-FDOPA rat brain PET template for neurodegenerative disease study in small animals.

Methods: Four male Sprague Dawley rats (body weight range, 350-400 g) were scanned by both the 7T microMR and the microPET R4®. To choose the best objective function for co-registration, a Micro Deluxe Phantom was adopted to do accuracy evaluation. For phantom analysis using Pmod 2.95, we designed five markers on the middle slice of a phantom image for evaluation and then performed evaluation in two ways. One is pre-rotated PET image 5 degrees about z axis. The other is not only pre-rotated PET image 5 degrees about z axis but also pre-translated 5 mm in the x direction. The pre-processing steps in SPM 5, i.e. realignment, coregistration, normalization and smoothing, were used to create a F18-FDOPA rat brain PET template.

Results: In phantom analysis, the distance deviations of the five markers in two evaluation cases with Normalized Mutual Information (NMI) method are between 0.05 and 0.22 mm and between 0.20 and 0.40 mm, respectively. Because these are all less than 1 mm as required, therefore, NMI method was chosen as the optimal objective function for inter-modality image registration. The MRI based F18-FDOPA PET template for normal male rat brain was generated for voxel based statistical analysis in SPM for small animal studies.

Conclusions: The MRI based small animal PET template can be used for accurate assessment of local brain function change in the PD rat model study.

References:

1. Schweinhardt P, Fransson P, Olson L, Spenger C, Andersson JL, A template for spatial normalisation of MR images of the rat brain, J Neurosci Methods. 2003 Oct 30;129(2):105-13.

2. Casteels C, Vermaelen P, Nuyts J, Van Der Linden A, Baekelandt V, Mortelmans L, Bormans G, Van Laere K., Construction and evaluation of multitracer small-animal PET probabilistic atlases for voxel-based functional mapping of the rat brain, J Nucl Med. 2006 Nov;47(11):1858-66.

TREATING FOCAL CEREBRAL ISCHEMIA WITH BDNF GENE DELIVERED BY RECOMBINANT HERPES-SIMPLEX-VIRUS VECTORS VIA INTRANASAL OLFACTORY PATHWAY IN RATS

G. Xu[1], X. Liu[2]

[1]Neurology, Department of Neurology, Jinling Hosptial, Nanjing University School of Medicine, [2]Jinling Hospital, Nanjing, China

Objective: Many growth factors such as brain-derived neurotrophic factor (BDNF) have been reported with effecacy of neurogenesis and neuroprotecton in amimal model of focal cerebral ischemia. But gene therapy for cerebrovascular disease in human still has many problems, of which lacking an effective delivery pathway to central nervous system (CNS) is a major hindrance for the clinical application of this promising strategy. This study was aimed to evaluate the feasibilty and efficacy of deliverying BDNF gene with recombinant herpes-simplex-virus vectors to CNS via intranasal olfactory pathway in rat with focal cerebral ischemia.

Method: Recombinant herpes-simplex-virus vector was constracted by deleting 6 viral genes, which included the coding sequence for an immediat early (IE) gene, ICP4. Focal cerebral ischemia was induced by middle cerebral artery occlusion (MCAO) with a nylon filament in Sprague-Dawley rats. MCAO rats were randomized into three groups: BDNF, eGFP and control. Six hours after MCAO, recombinant herpes-simplex-virus vectors carrying BDNF gene or enhanced green fluorescent protein (eGFP) gene, a marker gene, or the void vectors were administrated intranasally. Bromodeoxyuridine (BrdU) was injected intraperitoneally twice daily on the fifth and sixth days for the purpose of neurogenesis measurement. On the seventh day and forteenth day after MCAO, the cerebral infarct volumes, neurogenesis, expression of BDNF and eGFP were assessed. Neurological outcomes were serially assessed by the rotated test after MCAO.

Results: Rats in BDNF group scored higher in neurological function tests 7 and 14 days after MCAO compared with eGFP and control groups ($p< 0.05$). Rats administrated with BDNF gene has a trend of decreased infarct volume 14 days after MCAO compared with that of eGFP and control groups, but the differences did not reach the significant level ($P=0.065$). Histological detections revealed that expression of BDNF in hippocampus and temporal lobe were significantly enhenced 7 and 14 days after MCAO in BDNF group in contrast to eGFP and control groups ($p< 0.05$). Green fluorescence was also detected in hippocampus and temporal lobe of rats administrated with eGFP gene. The BrdU-positive cells in subventricular zone and hippocampus was significantly increased in BDNF gene treated rats than eGFP treated and control rats ($p< 0.05$).

Conclusions: Recombinant herpes-simplex-virus vectors administrated via intranasal olfactory pathway can efficiently delivering BDNF gene into CNS and expressing. BDNF gene therapy is efficacious in treating focal cerebral ischemia in rats.

Keywords: Brain-derived neurotrophic factor; Cerebral ischemia; Gene therapy; Intranasal administration; Rats.

215

Brain Poster Session: Brain Imaging: Neurologic Disease

MAPPING THE HEMODYNAMIC RESPONSE FUNCTION IN THE PRIMARY AUDITORY CORTEX UNDER NORMO- AND HYPERCAPNIA

K.C. Mazzetto-Betti[1], **R.F. Leoni**[2,3], O.M. Pontes-Neto[1], A.C. Santos[1], A.C. Silva[3], D.B. de Araujo[1,2]

[1]Department of Neurology, Psychiatry and Medical Psycology, FMRP - University of São Paulo,
[2]Department of Physics and Mathematics, FFCLRP - University of São Paulo, Ribeirão Preto, Brazil,
[3]Laboratory of Functional and Molecular Imaging, National Institute of Neurological Disorders and Stroke, National Institutes of Health, Bethesda, MD, USA

Introduction: The cerebrovascular coupling forms the basis of modern functional neuroimaging techniques, such as functional MRI (fMRI). However, it is not fully understood how fMRI maps obtained during focal cognitive studies of the brain depend on the baseline cerebral blood flow. The purpose of this study is to quantify the amplitude and temporal characteristics of the blood oxygenation-level-dependence (BOLD) response to an auditory stimulus during normo- and hypercapnia in healthy subjects.

Methods: 20 healthy volunteers participated of this study (mean age:23,6y, 13women). The protocol was composed by five intervals of a scrambled auditory stimulus (3 seconds each) intercalated by six intervals of rest (21 seconds each). Hypercapnia was achieved by a combination of air and CO_2, delivered via a valve device controlled by a computer software. End-tidal CO_2 ($ETCO_2$) was measured by a MR-compatible device (Veris MR, Medrad, Pittsburgh, PA, USA). Hypercapnic challenge was measured in three levels of $ETCO_2$ with respect to the basal condition of each subject: 5, 7, 10mmHg. MR images were acquired in a 3T scanner (Philips Achieva, The Netherlands). For each condition a series of 141 EPI volumes were acquired with the following parameters: TR=1000ms, TE=30ms, FA=90°, resolution=128x128, FOV=230mm, 21 slices, slice thickness=4mm. Image preprocessing consisted of slice time correction, temporal and spatial filtering (4mm), and motion artifact correction, using the Brain Voyager^{TM}QX (Brain Innovation, Maatrich, The Netherlands). An autoregressive method was applied to analyze four parameters of the HRF: onset, time-to-peak, full-width-at-half-maximum (FWHM) and amplitude. Statistical analysis was conducted in GraphPad Prism, and consisted of an ANOVA followed by a Bonferroni correction.

Results and discussion: Fig.1 shows the mean BOLD time-courses obtained at different CO_2 levels from all subjects. In agreement with previous work in the visual cortex [Cohen and Kim, 2002], the amplitude of the BOLD presented a significant decrease with increasing $ETCO_2$ ($p< 0.001$), presumably due a task-induced increase in CBF that is independent and additive to a CO_2-induced increase in resting CBF [Friston et al., 1990]. In addition, BOLD onset were longer for higher $ETCO_2$ ($p< 0.001$) [Cohen and Kim, 2002]. However, the other temporal parameters FWHM and time-to-peak were not significantly different between normocapnia and hypercapnia. This could be either due to the short stimuli (3s) employed here, which elicited brief BOLD responses in all cases, or due to a different cerebrovascular reactivity in auditory cortex relative to other areas of the brain.

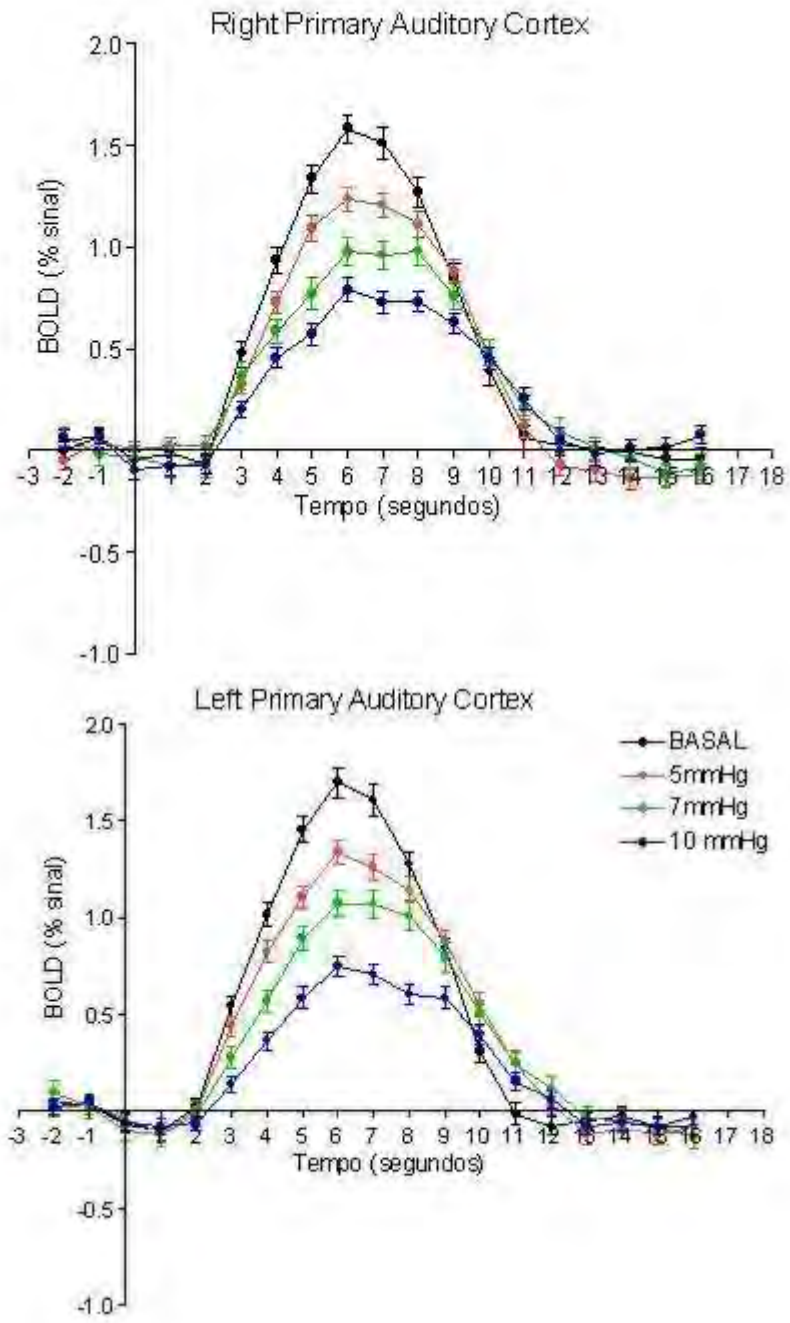

[Figure 1]

Conclusion: The amplitude and onset time of the BOLD response to brief auditory stimuli were significantly modulated by hypercapnia, providing useful information about the cerebrovascular reactivity of the auditory cortex in healthy volunteers, and opening up the possibility of using fMRI and hypercapnia to evaluate patients of different cerebrovascular diseases.

References:

1. Friston et al., JCBFM 1990; 10:458-466.

2. Cohen and Kim, JCBFM 2002; 22:1042-1053.

Brain Oral Session: Traumatic Brain Injury

TREATMENT OF ACUTE SUBDURAL HEMATOMA WITH ERYTHROPOIETIN: POTENTIAL OF SUBDURAL VERSUS SYSTEMIC APPLICATION

O. Kempski[1], M. Rahimi[1], M. Wähmann[1], H. Bächli[2], E. Güresir[3], A. Raabe[4], B. Alessandri[1]

[1]Institute for Neurosurgical Pathophysiology, University Medicine, Johannes Gutenberg-University of Mainz, Mainz, Germany, [2]Department of Neurosurgery, University Clinics of Basel, Basel, Switzerland, [3]Department of Neurosurgery, Johann Wolfgang Goethe -University, Frankfurt a.M., Germany, [4]Department of Neurosurgery, University Clinics, Inselspital Bern, Bern, Switzerland

Objective: Erythropoietin is a endogenous cytokine which production is induced under hypoxic conditions to increase erythrocyte concentration. Recently, receptors for EPO have also been discovered in the central nervous system and a neuroprotective function of EPO was found following traumatic brain injury. Trauma to the brain is often associated with acute subdural hemorrhage (ASDH) that worsens outcome of patients substantially. Despite early evacuation of the blood clot many patients still die or remain severely disabled. The goals of the present study were to evaluate the neuroprotective potential of EPO in the treatment of ASDH and to compare systemic versus subdural application.

Method: Sprague-Dawley rats were anesthetized with chloral hydrate and a catheter was placed in the tail artery and jugular vein. A craniotomy was prepared for the insertion of a L-shaped, blunted needle into the subdural space and closed with acrylic glue and dental cement. ASDH was produced by infusion of 400 µl unheparanized autologous venous blood (50 µl/min) into the subdural space. Ipsilateral CBF and contralateral ICP were monitored for at least 60 min and lesion volume was assessed 48 h after ASDH. Three separate experimental series were conducted:

1. Measurement of EPO concentration in the ipsilateral hemisphere 45 min after intravenous EPO injection. (n=3/group).
2. Neuroprotection by intravenous EPO treatment: NaCl or EPO (200, 2000, 20`000IU per animal, n=8-10/group) were injected i.v. at 30 min after ASDH 3) Neuroprotection by subdural EPO application: 60 min after ASDH the craniotomy was opened and the subdural blood evacuated.

After closing of the craniotomy 150 µl NaCl or EPO (0.02 / 0.2 / 2 / 200IU) were applied through a small burr hole directly onto the cortical surface (n=9/group).

Results: After injection of NaCl, EPO 200, 2000 and 20'000IU tissue concentrations of EPO reached 1.7±0.2, 11.7±0.2. 88.4±4 and 672±63 mIU/ml homogenate, respectively. In all series ICP and CBF values did not differ between groups during the entire monitoring period. Lesion volume after i.v. injection of NaCl or EPO (series 2) was 38.2±1.9 (NaCl), 28.8±2.8 (200IU), 24.2±1.3 (2000IU) and 46.5±4.7mm3 (20'000IU). EPO 200 and 2000IU reduced lesion volume significantly whereas 20'000IU was neurotoxic. ($p < 0.05$, one-way ANOVA with Student-Newman-Keuls post-hoc test). If EPO was applied subdurally (series 3) after evacuation of the blood clot a concentration of 0.02IU (11.2±6.2mm3) was sufficient to reduce lesion volume significantly when compared to NaCl (49.7±43.3mm3) whereas 200IU (173.2±114mm3) increased lesion volume significantly. No significance was found for comparison of NaCl- with 0.2IU (43.9±23mm3) and 2IU (67.9±31.1mm3, one-way ANOVA on ranks).

Conclusion: Brain damage due to acute subdural hematoma can be reduced by EPO with and without

evacuation of the subdural blood volume. The needed EPO concentration for neuroprotection is 10'000 times lower with subdural application. High concentrations of EPO were neurotoxic independent of the route of application. Thus, subdural dosing of EPO after surgery might be a cost effective treatment but EPO has to be managed carefully in patients in order to avoid adverse effects on lesion development.

217

Brain Poster Session: Brain Edema & Water Transport

BRAIN EDEMA AND TUMOURS CELLS OF CNS

T. Shah, T. Khan, M. Adil, V.V. Zinchuk

Neurology, Osh Medical Institute, Osh, Kyrgyzstan

The studying of differences of a tumoral cell from normal, in particular features of its duplication, represents to rational therapy of tumours. We propose a new approach to the prolifirative activity of tumours cells of cns with the developing brain edema. Studying changes of brain substances at tumours astrocyter, s lines, we recognised that tumours changes of its structural elements can influence. We worked on two groups of patients-operating and non operating. In group operating and non operating close and on a distance from a tumour, it was observed changes of nervous cells. Changes in grey substance of a brain, it was observed near to all tumour. These changes were more significant. Changes in cerebral water compartments were assessed by diffusion-weighted MRI with determination of the apparent diffusion coefficient (ADC). There were several lines of evidence indicating that changes in the properties of the peripheral nervous system. CT scans showed massive cerebral edema and development of obstructive hydrocephalus. With a help of a method tutoradiography appeared possible appilication and reception most complete estimations of these positions, is especial on an experimental material and on cultures of a fabrics. At the same time, we observed that the phagocytic figure and total number of cycling immune complexes decreased evidently. Marked alteration of quantitative correlations of T- and B-lymphocytes were observed. Due to the increase of peripheral blood lymphocytes with simultaneous evident reduction of the monocyte count (by 28%).

220

Lassen Award: Lassen Award Symposium

FUNCTIONAL AND STRUCTURAL SYNERGY FOR RESOLUTION RECOVERY AND PARTIAL VOLUME CORRECTION IN BRAIN PET

M. Shidahara[1], C. Tsoumpas[2], A. Hammers[2], N. Boussion[3], D. Visvikis[3], H. Ito[1], Y. Kimura[1], T. Suhara[1], I. Kanno[1], F. Turkheimer[2]

[1]Molecular Imaging Center, National Institute of Radiological Sciences, Chiba, Japan, [2]MRC Clinical Sciences Centre, Hammersmith Hospital, Imperial College London, London, UK, [3]INSERM, U650, Laboratoire de Traitement de l'Information Medicale (LaTIM), Brest, France

Objectives: Positron Emission Tomography (PET) has the unique capability of measuring brain function but its clinical potential is affected by low resolution and lack of morphological detail. The purpose of this study is to evaluate a wavelet synergistic approach that combines functional and structural information from a number of sources (CT, MRI and anatomical frequency-based atlases[1]) for the accurate quantitative recovery in PET imaging. When the method is combined with anatomical frequency-based atlases, the outcome is a functional volume corrected for partial volume effects of all the selected regions.

Methods: The proposed method is based on the multiresolution property of the wavelet transform[2]. First, the target PET image and the corresponding anatomical image are decomposed into several resolution elements. Secondly, high-resolution components of the PET image are replaced, in part, with those of the anatomical image after appropriate scaling. The amount of structural input is weighted by the relative high frequency signal content of the two modalities. Anatomical information was provided either by CT and MRI volumes or by a frequency-based anatomical atlas[1] whose regional intensity values were obtained by averaging the PET data for each ROI. Accurate simulations of a brain [^{18}F]FDG dataset based on Zubal brain phantom[3] were conducted to evaluate the accuracy of ROI values after resolution recovery. As anatomical information, three images (the measured MRI, CT and the segmented image) were used. The resolution-recovered images were compared with the true image of 10 ROIs. The proposed method was also applied to two clinical datasets from an Alzheimer disease patient with moderate atrophy ([^{18}F]FDG) and a young normal volunteer ([^{11}C]raclopride). Static images of these datasets were processed using both MRI and the Hammersmith frequency-based Atlas[1], and the results were compared.

Results: Simulation studies showed that resolution recovery with CT images, which contain minimum amount of tissue anatomy, did not improve resolution. The use of MRI images brought significant improvements in PET image resolution but improvements were maximized when atlas-based segmented images as anatomical references were used (**Fig-1A**). These results were replicated in the clinical data sets (**Fig-1B**).

Conclusions: The synergistic use of functional and structural data, and the incorporation of anatomical information in particular, generate morphologically corrected PET images of exquisite quality.

Reference:

[1] Hammers A, 2003, Hum Brain Mapp, 19, 224-47.

[2] Boussion N, 2006, Phys Med Biol, 51, 1857-76.

[3] Tsoumpas C, 2008, Med Phys, 35, 1299-309.

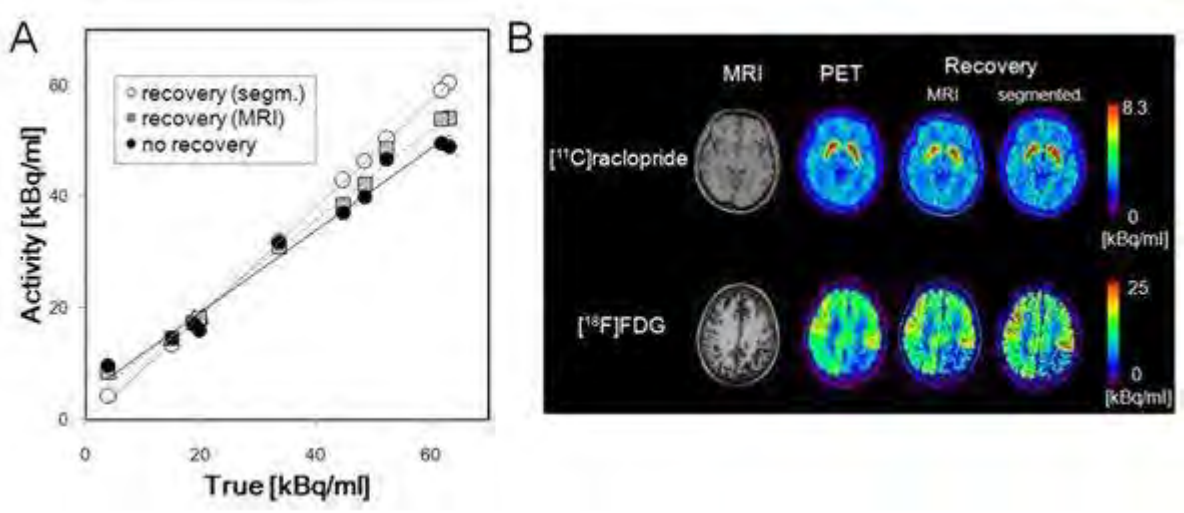

[Figure1]

Fig.1 (A) ROI comparisons of the simulated FDG images against true image (B) Original and resolution recovered images of a [^{18}F]FDG and [^{11}C]raclopride studies.

ERROR ANALYSIS OF DOPAMINE D_2 RECEPTOR OCCUPANCY STUDY WITH AGONIST LIGAND [^{11}C]MNPA

M. Shidahara[1], H. Ito[1], T. Otsuka[1], Y. Ikoma[2], C. Seki[1], F. Kodaka[1], R. Arakawa[1], H. Takano[1], H. Takahashi[1], Y. Kimura[1], I. Kanno[1], T. Suhara[1]

[1]Molecular Imaging Center, National Institute of Radiological Sciences, Chiba, [2]Department of Investigative Radiology, National Cardio-Vascular Center Research Institute, Suita, Japan

Objectives: Occupancy of dopamine D_2 receptors by antipsychotic drugs can be estimated from reduction in the observed binding potential (BP_{ND}). Because BP_{ND} varies widely in occupancy studies, accuracy of the measurement of wide range BP_{ND} should be confirmed. The purpose of this study is to investigate errors in quantitative analysis for estimating dopamine D_2 receptor occupancy by antipsychotics with agonist ligand [^{11}C]MNPA which has high affinity and selectivity to dopamine D_2 receptors[1].

Methods: Simulated TACs of [^{11}C]MNPA with several noise levels were generated to investigate the bias and variation of parameter estimates caused by the statistical noise for non-linear least square (NLS) fitting and a simplified reference tissue model (SRTM) methods. A dynamic tracer concentrations was consisted of three target conditions (K_1=0.44, k_2=0.067, k_3=0.02, 0.1 or 0.2, k_4=0.18), and a reference (K_1=0.44, k_2=0.067) with a dynamic frame (20sec × 9, 1min × 5, 2min × 4, 4min × 11, 5min × 6, totally 90min) and a measured input function from human study[1]. Three true BP_{ND} values were assumed; 1.111 (baseline), 0.556 (occupancy = 50%) and 0.111 (90%). Then Gaussian noise was added at the noise level 1%, 3%, 5%, 7% and 10%, and five hundred noisy data sets were generated for each[2]. The reliability of BP_{ND} estimated by NLS and a SRTM and the calculated occupancy, dependency of scan durations (32, 44, 60, 75 and 90min) for SRTM were investigated.

Results: For NLS and SRTM methods, the bias of estimated BP_{ND} values became larger as the noise level increased and these bias of BP_{ND} were larger than those of occupancy (**Fig. 1A** and **1B**). In the case of small BP_{ND}, the bias became larger. For SRTM method, reliable and unbiased occupancy estimates of [^{11}C]MNPA could be obtained by 60 min with the relative standard deviation remaining less than 10%. However, shorten scan duration depredate the quantification of very small binding potential (**Fig1C**).

Conclusions: Dopamine D_2 receptor occupancy by antipsychotics can be estimated precisely by SRTM method with an optimal scan duration with [^{11}C]MNPA.

Reference:

[1] Otsuka T, 2008, Neuroimage, 41, suppl. 2, T134.

[2] Ikoma Y, 2008, Neuroimage, 47, 43-50.

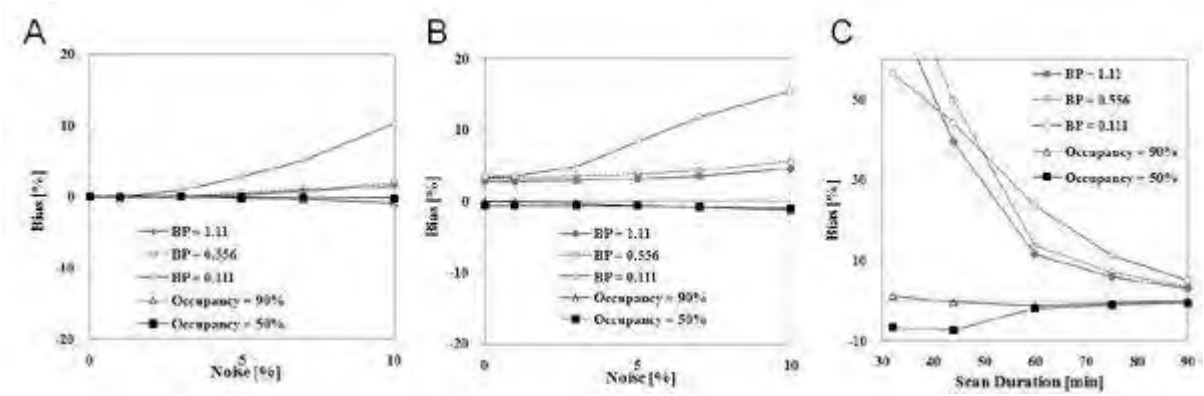

[Figure1]

Fig. 1 (A) Noise level dependency: Bias of BP and Occupancy estimated by NLS, (B) estimated by SRTM, (C) Scan Duration Dependency: Bias of BP and Occupancy at a 3% noise level estimated by SRTM.

Brain Poster Session: Epilepsy

AN IMPROVED METHOD TO MEASURE CEREBRAL P-GLYCOPROTEIN FUNCTION REVEALS CHANGES IN BRAIN UPTAKE OF (R)-[^{11}C]-VERAPAMIL FOLLOWING STATUS EPILEPTICUS IN RATS

J.P. Bankstahl[1], C. Kuntner[2], M. Bankstahl[1], T. Wanek[2], J. Stanek[2], M. Müller[3], O. Langer[2,3], W. Löscher[1]

[1]Institute for Pharmacology, Toxicology, and Pharmacy, University for Veterinary Medicine Hannover, Hannover, Germany, [2]Dept. of Radiochemicals and microPET Imaging, Austrian Research Centers, Seibersdorf, [3]Dept. of Clinical Pharmacology, Medical University of Vienna, Vienna, Austria

Objective: Multidrug efflux transporters like P-glycoprotein (Pgp) at the blood-brain barrier (BBB) are believed to play an important role in resistance to antiepileptic drug treatment. (R)-[^{11}C]verapamil (VPM) positron emission tomography (PET) can be used to measure Pgp function, but low brain uptake of VPM hampers the mapping of Pgp function in different brain regions. We investigated if this limitation can be overcome by Pgp modulation prior to PET imaging and if this method is suitable to quantify differences in Pgp expression after status epilepticus in rats, which we found in a previous study (Bankstahl and Löscher, 2008).

Methods: Two groups of naïve female Sprague-Dawley rats (n=12) underwent single VPM PET scans 2 h after intravenous administration of different doses of the third generation Pgp inhibitors elacridar or tariquidar. Radioactivity uptake in brain was expressed as the area under the time activity curve (AUC) normalized for injected ^{11}C-activity. A sigmoidal dose-response curve was fitted to AUC values measured after different inhibitor doses. To study regional differences of cerebral Pgp activity, paired VPM PET scans, before and after administration of tariquidar (3 or 15 mg/kg), were performed both in naïve rats and in rats 48 h after pilocarpine-induced status epilepticus.

Results: Inhibitor administration resulted in up to 10-fold increased VPM AUCs with ED_{50} values of 1.16 ± 0.12 mg/kg and 3.00 ± 0.24 mg/kg for elacridar and tariquidar, respectively. In the paired PET scans, the 15 mg/kg tariquidar dose uniformly increased radioactivity distribution across different brain regions as compared to baseline scans, both in naïve and epileptic rats. In epileptic but not in naïve rats, the 3 mg/kg tariquidar dose resulted in obvious regional differentiation of brain radioactivity distribution, with lowest uptake observed in cerebellum. Immunohistochemical staining demonstrated an almost 2-fold increase of Pgp labeling in the cerebellum of epileptic rats as compared to other brain regions.

Conclusion: Our data suggest that VPM PET in combination with administration of moderate doses of Pgp inhibitors can be used for the mapping of regional Pgp function in the brain. The current data will help to study changes in Pgp-function at the BBB in further models of epilepsy as well as in pharmacoresistant patients.

References: Bankstahl, J. P. und W. Löscher (2008). "Resistance to antiepileptic drugs and expression of P-glycoprotein in two rat models of status epilepticus." Epilepsy Research **82**(1): 70-85.

The research leading to these results has received funding from the European Community´s Seventh Framework Programme under grant agreement no. 201380 (EURIPIDES).

Brain Poster Session: Stem Cells & Gene Therapy

CHARACTERISATION OF NEURAL STEM CELLS FOR OESTROGEN IN VITRO: POTENTIAL FOR IMPROVING STEM CELL BASED THERAPY FOR STROKE

S. Patkar[1], R. Tate[1], M. Modo[2], R. Plevin[1], H.V.O. Carswell[1]

[1]SIPBS, University of Strathclyde, Glasgow, [2]Centre for the Cellular Basis of Behaviour, Kings College London, London, UK

Stroke is a problem for the ageing population. The ageing population is increasing but there is no licensed therapy for chronic stages of the disease. Stem cells are already known to have enormous potential to improve stroke outcome in the chronic stages (Miller, 2006) but we need to improve their integration in vivo. Evidence also suggests that the female hormone, oestrogen, enhances differentiation of neural stem cells (Brannvall et al., 2002). The long-term aim of the present study is to determine whether oestrogen can improve the success of neural stem cell grafting in experimental stroke. We used an immortalised temperature sensitive murine neural stem cell line, the Maudsley hippocampal stem cell line clone 36 (MHP36) because they proliferate only at low temperatures (33°C) in vitro, develop into mature neurons and glia on transplantation into the higher temperature brain (37°C) and cease dividing once matured reducing the chance of producing tumours. The short-term aim was to fully characterise the MHP36 for oestrogen receptors (ER) and the enzyme, aromatase, which synthesizes oestrogen.

The expression of aromatase (gift from J. Hutchison), ERalpha (Novachem) and ERbeta (gift from G. Greene, CO1531) protein in the MHP36 stem cells were investigated by immunofluorescene and Western blotting. In addition, reverse transcriptase PCR (RT-PCR) and the sequencing of amplicons were carried out to confirm the expression of each transcript of interest. Appropriate controls were used in each assay.

Undifferentiated MHP36 cells were shown to express aromatase using Western blots. Immunofluorescence staining revealed expression of aromatase in the cytoplasm and not in the nucleus (Fig.A, MHP36 cells stained for aromatase using Texas red, bar represents 20μM). Expression was confirmed by semi-nested RT-PCR. ERalpha was absent in the MHP36 stem cells when compared to positive control breast cancer cells MCF-7, which stained the nucleus for ERalpha using immunofluorescence and Western blotting, these results were confirmed by RT-PCR. On the other hand, ERbeta was observed to be expressed in the peri-nuclear membrane of the MHP36 cells using immunofluorescence (Fig.B, MHP36 cells stained for ERbeta with FITC, bar represents 20μM) and expression was confirmed by RT-PCR.

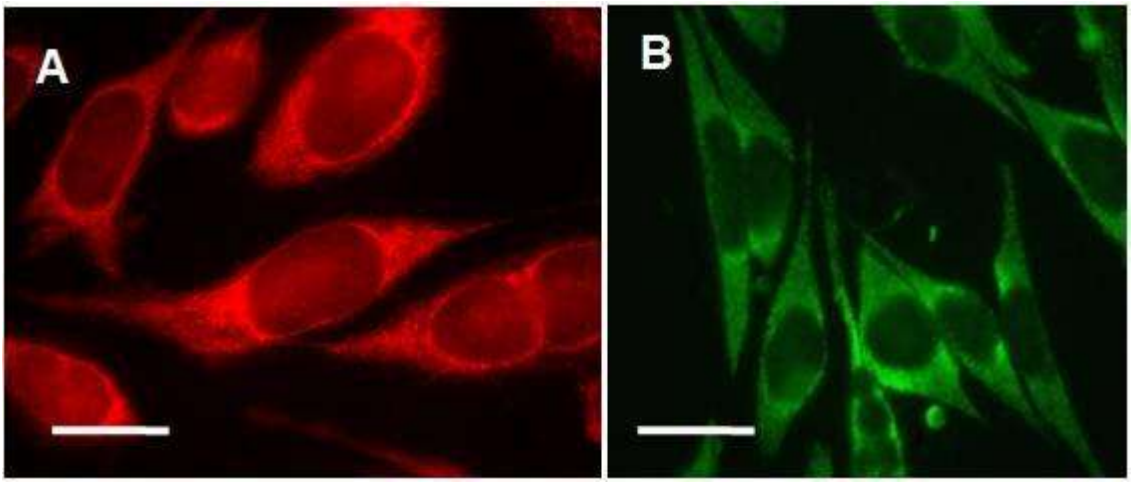

[Immunofluorescence staining for Aromatase and ERb]

We have thoroughly characterised the MHP36 cells for oestrogen and demonstrated for the first time that they express ERbeta and aromatase, but do not express ERalpha. This expression of aromatase and ERbeta by the cells is appealing, since the local endogenous production of oestrogen via aromatase by the MHP36 cells may help improve the integration, survival and differentiation of transplanted cells in vivo after experimental stroke, possibly mediating ERbeta activation which is the hypothesis for our next studies.

Brannvall K., Korhonen L. & Lindholm D., 2002, Molecular and Cellular Neurosciences, Volume 21, Issue 3, 512- 520.

Miller R.H., 2006, Brain Research, Volume 1091, Issue 1, 258.

Brain Oral Session: Blood Brain Barrier

SPECIES DIFFERENCES IN BRAIN UPTAKE OF THREE PET RADIOLIGANDS

S. Syvänen[1], Ö. Lindhe[2], M. Palner[3], B.R. Kornum[3], O. Rahman[4], B. Långström[4], G.M. Knudsen[3], M. Hammarlund-Udenaes[5]

[1]Division of Pharmacology, LACDR, Leiden University, Leiden, The Netherlands, [2]Uppsala Imanet, GE Healthcare, Uppsala, Sweden, [3]Neurobiology Research Unit, University Hospital Rigshospitalet, Copenhagen, Denmark, [4]Uppsala Applied Science Lab, GEMS PET Systems, GE Healthcare, [5]Department of Pharmaceutical Biosciences, Uppsala University, Uppsala, Sweden

Objectives: This Positron Emission Tomography (PET) study was designed to compare interspecies differences in brain uptake of three radiolabelled P-glycoprotein (P-gp) substrates; [^{11}C]verapamil, a calcium channel blocker which has been used extensively in PET[1-3]; [^{11}C]GR205171, a NK_1-receptor antagonist; and [^{18}F]altanserin, a $5HT_{2A}$-receptor antagonist.

Methods: The radioligands were prepared as previously reported[4-6] and administered as a fast bolus to all species at the start of the emission scan. Brain radioligand concentrations, expressed as standardized uptake values (SUV), and brain-to-plasma SUV ratios were compared; [^{11}C]verapamil in rats, guinea pigs and monkeys; [^{11}C]GR205171 in rats, guinea pigs, monkeys and humans; and [^{18}F]altanserin in rats, minipigs and humans. The effect of P-gp inhibition was investigated by administering cyclosporin A (CsA) 30 min prior to the radioligand bolus injection. Blood samples were withdrawn and analyzed using HPLC to determine the concentration and metabolism of unbound radioligand in plasma.

Results: Pronounced species differences were found in the brain SUV and brain-to-plasma SUV ratio of [^{11}C]verapamil, [^{11}C]GR205171 and [^{18}F]altanserin with higher brain distribution in humans, monkeys and minipigs than in rats and guinea pigs. For example, the brain-to-plasma SUV ratio of [^{11}C]GR205171 was almost 9-fold higher in humans compared to rats. The species differences were still present after P-gp inhibition although the increase in brain concentrations after P-gp inhibition was somewhat greater in rats than in the other species. Differences in plasma concentrations, plasma protein binding and metabolism did not explain the species-related differences.

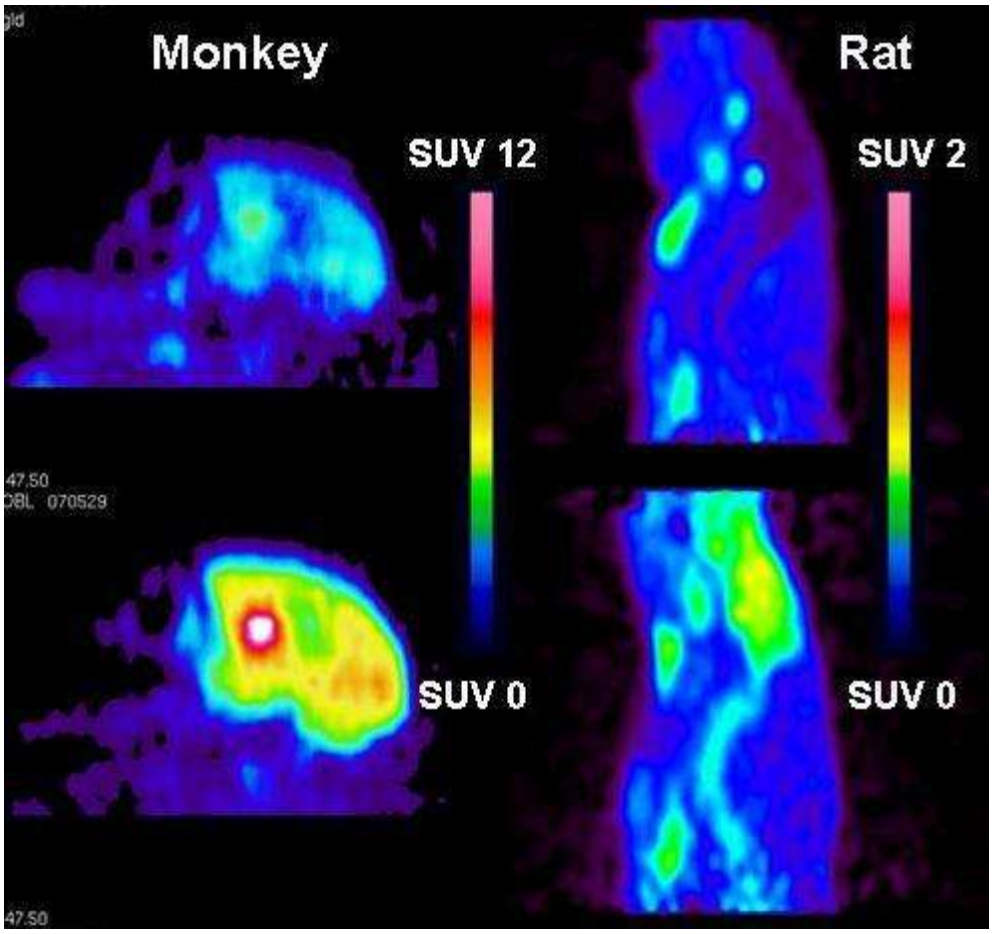

[[11C]GR205171 brain uptake]

Conclusions: The findings are important for the interpretation of drug delivery to the brain when comparing or extrapolating preclinical to human data. Compounds found to be P-gp substrates in rodents are likely to be substrates also in higher species, but sufficient blood-brain barrier permeability may be retained in humans to allow the compound to act on intracerebral targets.

References:

1. Hendrikse NH et al. (1999) Cancer Res 59:2411-2416,

2. Bart J et al. (2003) Neuroimage 20:1775-1782,

3. Sasongko L et al. (2005) Clin Pharmacol Ther. 77:503-514,

4. Lemaire C et al. (1991) J Nucl Med. 32:2266-2272,

5. Bergström M et al.(2000) Neuropharmacology 39:664-670,

6. Syvänen S et al. Neuroimage. 32:1134-1141.

Brain Poster Session: Spreading Depression

CARDIOVASCULAR RESPONSE TO ASPHYXIA DOES NOT CRITICALLY DEPEND ON GENERATION OF ANOXIC DEPOLARIZATION

F. Richter[1], A. Lehmenkühler[2], R. Bauer[3], H.-G. Schaible[1]

[1]Insitute of Physiology I/Neurophysiology, Friedrich Schiller University Jena, Jena, [2]Pain Inst. & Ctr. for Med. Education, Düsseldorf, [3]Institute of Molecular Cell Biology, Friedrich Schiller University Jena, Jena, Germany

Recently, we were able to exclude that transient asphyxia (up to 1 min) conditions the adult rat brainstem for spreading depression (SD). Rather superfusing the brainstem with artificial cerebrospinal fluid (ACSF) in which 75% of the chloride ions were replaced by acetate and to which 10 mM KCl and 10 mM tetraethylammonium (TEA) were added was suitable to condition the brainstem for SD. Brainstem SDs were accompanied by transient increases in regional blood flow in the brainstem, but not in cerebral cortex. Now we tested, whether a transient asphyxia:

i. can induce DC shifts resembling SD in the adult brainstem, and
ii. whether such DC shifts were accompanied by changes in regional blood flow or vegetative parameters.

Experiments were performed in 15 sodium thiopentone-anesthetized rats (100 mg/kg, i.p.), paralyzed with pancuronium bromide (2-4 mg/kg/h i.v.) and artificially ventilated. We recorded DC deflections at two sites in the brainstem close to the caudal trigeminal nucleus (lateral spacing 1 mm), and in the cerebral cortex. Both at the cerebral cortex and at the brainstem local blood flow was continuously recorded by Laser Doppler probes together with arterial blood pressure and heart rate. Blood gases and acid-base balance values were checked prior, during and after each period of asphyxia. Asphyxia was induced by stopping the respiratory pump.

In the native brainstem an asphyxia lasting about 50-60 s resulted in a negative DC deflection of 5.5±5.4 mV (n=10) (mean value±std. dev., respectively). Systemic arterial blood pressure (ABP) declined to 25.5±4.7% and heart rate to 55.3±21.3%. The regional blood flow in the brainstem decreased to 48.9±28.1% and in the cortex to 66.1±24.1% of baselines. During reoxygenation ABP and heart rate normalized, but blood flow increased transiently in the brainstem to 395.1±100.7%, and in cerebral cortex to 210.9±82.6%. Superfusion of the brainstem with acetate-TEA-KCl-ACSF did not alter blood gases and acid-base balance values. After this pretreatment, 1-min-asphyxia caused negative DC deflections in the brainstem reaching 25.4±6.5 mV (n=30), accompanied by reduced heart rates (45.2±21.5% of baseline) and ABP (43.8±16.4% of baseline). Accordingly, regional blood flow in the brainstem decreased to 71.7±33.1% and in cerebral cortex to 66.7±37.2%. During reoxygenation both heart rate and ABP normalized quickly, but similar as in controls, regional blood flow in the brainstem exceeded the baseline to 343.2±135.2% and in cerebral cortex to 225.5±95.1%. Systemic administration of MK-801 (3 mg/kg, i.p.) did neither influence the asphyxia-related DC shifts nor the observed changes in ABP, heart rate or regional blood flow.

In adult rats the conditioning of the brainstem with acetate-TEA-KCl-ACSF was a prerequisite to observe full-blown negative DC shifts during asphyxia. However, during transient asphyxia heart rate and ABP declined quantitatively similar whether anoxic depolarization was elicited or not. This was in contrast to spreading depression in the brainstem where DC shifts caused a transient increase in

regional blood flow in brainstem and in ABP [1]. Thus, the cardiovascular response to asphyxia does not critically depend on generation of anoxic depolarization.

[1] Richter et al., JCBFM 28, 2008, 984-994.

Brain Oral Session: Experimental Stroke and Cerebral Ischemia 1

AUTOLOGOUS BONE MARROW CELL ADMINISTRATION 24H FOLLOWING MCAO REDUCES BEHAVIORAL DEFICITS AND LESION SIZE IN A NOVEL LARGE ANIMAL MODEL

J. Boltze[1,2,3], A. Förschler[4,5], H. Barthel[6], B. Nitzsche[1], A. Dreyer[1], V. Zeisig[1], T. von Geymüller[1], C. Boltze[1], O. Sabri[6], D. Lobsien[5], A. Hoffmann[7], A. Reischauer[8], F. Emmrich[2,3,9], U. Gille[10]

[1]Neurorepair Research Group, Fraunhofer Institute for Cell Therapy and Immunology, [2]Institute for Clinical Immunology and Transfusion Medicine, [3]Translational Centre for Regnerative Medicine, Leipzig, [4]Department of Neuroradiology, University Hospital rechts der Isar, Technical University of Munich, Munich, [5]Centre for Diagnostic Radiology, [6]University Clinic of Nuclear Medicine, University of Leipzig, [7]Department of Anatomy, Histology and Embryology, Faculty of Veterinary Medicine, University of Leipzig, [8]Institute for Veterinary Pathology, University of Leipzig, [9]Fraunhofer Institute for Cell Therapy and Immunology, [10]VITA34 Inc., Leipzig, Germany

Objectives and background: The purpose of our study was to evaluate the therapeutic efficacy of autologous bone marrow cell (BMC) application in the sub-acute stage of stroke in large animals by long term behavioral phenotyping and multimodal brain imaging. The model itself was designed on close approximation to the situation of human stroke patients, potentially providing enhanced translational power for experimental protocols including cell therapies.

The promising therapeutic potential of BMC therapies for stroke has recently been demonstrated in numerous rodent trials. As many experimental protocols, showing promising results in small animal studies, failed in clinical trials, transfer to clinical application requires close-to-practice large animal models of stroke. We evaluated benefit of autologous BMC transplantation 24h upon stroke onset in a novel sheep model of focal cerebral ischemia which also allows for control of lesion size and subsequent functional deficits.

Methods: 30 adult rams weighting 51 to 104 kg were subjected to permanent middle cerebral artery occlusion (MCAO) for stroke induction. 100 mL of bone marrow were harvested from the iliac crest and BMCs were subsequently obtained by density centrifugation. A minimum of 4.0x10E6 cells gained per kilogram bodyweight (kgBW) was defined as inclusion criterion for cell treated subjects. Following baseline behavioral phenotyping, magnetic resonance imaging (MRI) and positron emission tomography (PET), 15 animals were randomly subjected to intravenous autologous nuclear BMC treatment 24h after MCAO. 15 sheep served as controls. Functional outcome was continuously observed by behavioral phenotyping. Lesion size development and brain atrophy were monitored by MRI as well as ^{15}O-water- and ^{18}F-Deoxyglucose PET performed at days 14 and 42 before brains were removed for further histological investigation (which is actually still ongoing).

Results: In 4 animals, less than 2.0x10E6 cells per kgBW were obtained. Those subjects were excluded from the treatment group, but also monitored by MRI for 42 days. In BMC treated animals (n=11), an enhanced functional improvement was observed as compared to control animals ($p< 0.01$). Despite a spontaneous tendency of motorfunction improvement, non-treated animals suffered from moderate to severe motor and sensory dysfunctions like ataxia, absent startle reflexes and spatial hemineglect for the entire observation period. MRI investigations showed similar lesion size in both groups at day 1 ($p=0.59$) and reduction of lesion size/hemispherical atrophy in cell treated rams 42 days upon MCAO ($p< 0.01$), but not at day 14. These findings could be confirmed by ^{15}O-water- and ^{18}F-Desoxyglucose PET ($p< 0.05$) and macroscopic pathological lesion volumetry ($p< 0.05$). Interestingly, transplantation of less than 4.0x10E6 BMCs failed to induce lesion size reduction. No tumor formation was observed upon BMC administration.

Conclusions: Autologous BMC administration 24h following stroke is safe and effective in sheep and

might therefore be evaluated as a novel treatment option for stroke in upcoming clinical trials. The study revealed first indications that the therapeutic effect is related to a cell-dose-dependent neuroprotection. However, further examinations are required to elucidate the role of neural replacement and/or activation of the endogenous restorative potential of the brain in this approach.

IMPACT OF CYTOKINES AND GROWTH FACTORS ON CONTRACTILE ENDOTHELIN RECEPTORS IN RAT CEREBRAL ARTERIES

E. Stenman, **H. Ahnstedt**, M. Henriksson, L. Edvinsson

Clinical Sciences, Experimental Vascular Research, Lund University, Lund, Sweden

Objective: Cerebral ischemia induces an increased endothelin receptor mediated contraction in rat cerebral arteries via enhanced expression of endothelin ET_B receptors in the smooth muscle cells [1]. The aim of the present study was to examine if growth factors and cytokines, well-known to be activated in cerebral ischemia [2], can influence the function and expression of cerebrovascular endothelin receptors.

Methods: Rat middle cerebral arteries (MCAs) were cultured for 24 h with or without tumor necrosis factor-α (TNF-α; 10 and 100 ng/ml), interleukin-1β (Il-1β; 10 and 100 ng/ml), platelet-derived growth factor (PDGF 10 and 100 ng/ml), epidermal growth factor (EGF; 20 and 100 ng/ml) or basic fibroblast growth factor (bFGF; 10 and 100 ng/ml). The MCAs were mounted in sensitive myographs and contractile responses were obtained for sarafotoxin 6c (ET_B receptor agonist) and endothelin-1 (in this case ET_A receptor agonist, due to ET_B receptor desensitization). The receptor mRNA levels were examined by real-time PCR.

Results: Culture of isolated MCA segments results in enhanced expression of ET_B receptors in the smooth muscle cells; a response also seen after cerebral ischemia. Here we found that TNF-α (100 ng/ml) and EGF (20 ng/ml) further enhanced the culture-induced expression of the ET_B receptor mediated contraction, while EGF (100 ng/ml) decreased the ET_B receptor mediated contraction. On the other hand bFGF induced an enhanced ET_A receptor mediated contraction while PDGF and Il-1β did not affect the endothelin receptor mediated contraction. Real-time PCR showed that neither TNF-α (100 ng/ml) nor EGF (20 ng/ml) influenced ET_B receptor mRNA after 24 hours of organ culture. Instead bFGF (10 ng/ml) increased the amount of ET_B receptor mRNA, which is in accordance with previous studies on cultured MCA smooth muscle cells [3]. The ET_A receptor mRNA levels were not affected by TNF-α (100 ng/ml), EGF (20 ng/ml) or bFGF (10 ng/ml).

Conclusion: The results suggest that TNF-α and bFGF may contribute to the up-regulated endothelin receptor mediated response seen in cerebral arteries after cerebral ischemia, while EGF has different impact on cerebrovascular endothelin receptors, depending on concentration. This mechanism could participate in the final formation of the brain infarct after cerebral ischemia.

References:

1. Stenman, E., et al. Stroke, 2002. 33(9): p. 2311-6.

2. Doyle, K.P., R.P. Simon, and M.P. Stenzel-Poore. Neuropharmacology, 2008. 55(3): p. 310-8.

3. Xu, C.B., E. Stenman, and L. Edvinsson. Biochem Pharmacol, 2002. 64(3): p. 497-505.

230

Brain Poster Session: Glial Functions

ASTROCYTES - THE KEY SENSORS OF O_2 TENSION IN THE BRAIN?!

T. Kulik[1], S. Aronhime[1], H.R. Winn[2]

[1]Neurosurgery, Mount Sinai School of Medicine, [2]Neurosurgery, Mount Sinai Hospital, New York, NY, USA

Background: Adenosine (Ado) is an endogenous purine nucleoside, whose level is markedly increased during hypoxia (1), causing an Ado 2a receptor mediated vasodilatation (2). The cellular source of Ado under hypoxic conditions remains elusive, but astrocytes have been implicated. They are a critical component of the glial-vascular unit: Interposed between neuron and cerebral blood vessels, they are strategically positioned to affect cerebral blood flow in response to neuronal activity.

Objective: We sought to determine if astrocytes produce Ado in response to changes in O_2 levels.

Methods: Primary, mixed cultures were established from the cerebral hemispheres of 1-3 day old Wistar rat pups. Cultures were purified based on differential adhesion after 5-7 DIV and a high purity of astroyctes (>90%) ascertained with GFAP/DAPI immunolabeling. Astrocytes were trypsinized after 11 DIV and attached to microcarrier beads kept in spinner flasks. After 23 DIV these flasks were flushed with N_2, and dissolved O_2 in medium measured continuously utilizing a fluorometric technique. Samples of supernatant were acquired at predetermined time intervals and given O_2 levels. Using solid phase extraction, samples were cleaned, the eluent nitrogen evaporated, reconstituted and submitted to HPLC analysis for adenine nucleotides. Compounds of interest were identified by retention time as well as wavelength spectrum, and confirmed by enzymatic peak-shifting techniques and spiking of samples.

Results: Levels of Ado rose rapidly from **25.2 nM ± 0.3 nM at normoxia** to **173.2 µM ± 94.5 µM at anoxia** (Figure). This increase represents a >10,000X elevation from baseline levels and was significant ($p< 0.005$). We derived the following equation: $y=0.39e^{1.27x}$ ($R^2=0.97$), where y = Ado concentration (M) and x = O_2 (mmHg).

Conclusion: Astrocytes release Ado in an O_2 tension dependant fashion. The rise in Ado concentration occurs rapidly. In addition, concentrations of Ado produced by astrocytes are similar to those found in the hypoxic brain (1) and are in the range which evokes vasodilatation of penetrating arteries (3). We would conclude that astrocytes may be the main source for vasoactive adenosine in the hypoxic brain.

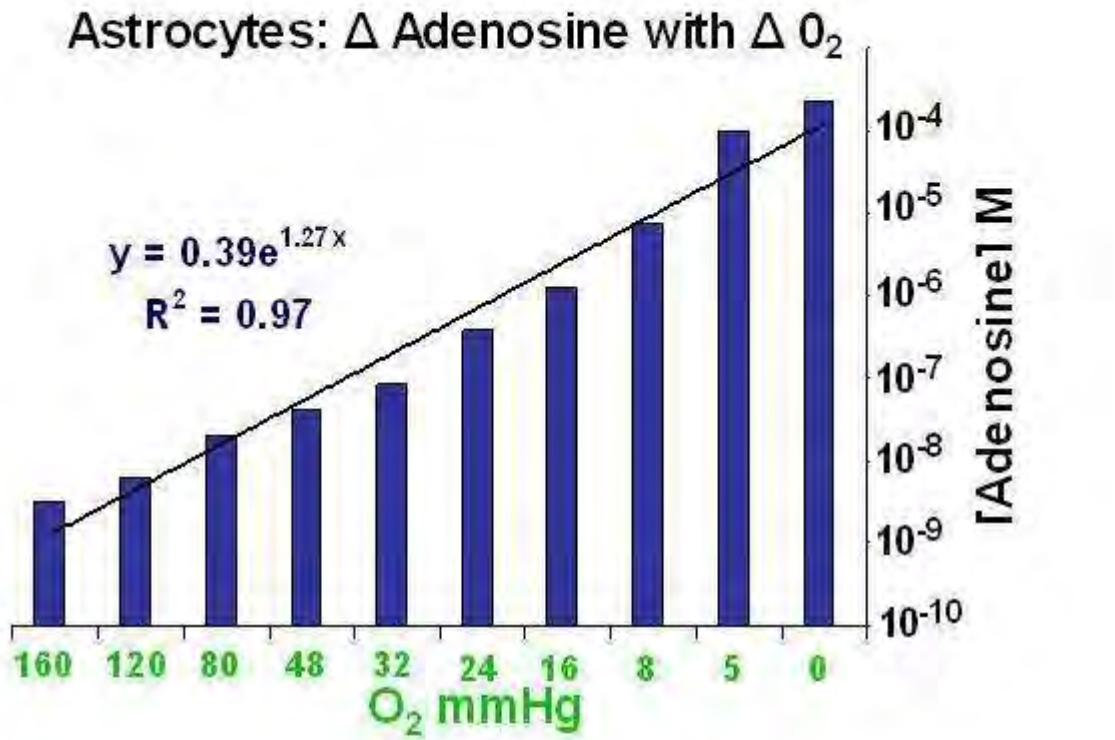

[Figure]

References:

1. Winn HR, Rubio R, Berne RM: Brain adenosine concentration during hypoxia in rats. Am J Physiol 241:H235-242, 1981.

2. Miekisiak G, Kulik T, Kusano Y, Chen J-F, Winn HR: Cerebral blood flow response in adenosine 2a receptor knockout mice during transient hypoxic hypoxia. J Cereb Blood Flow Metab 28(10):1656-64, 2008.

3. Ngai AC, Coyne EF, Meno JR, et al: Receptor subtypes mediating adenosine-induced dilation of cerebral arterioles. Am J Physiol Heart Circ Physiol 280:H2329-2335, 2001.

231

Brain Poster Session: Neurovascular Unit in Health & Disease

EFFECT OF DIFFERENT ANESTHETICS ON NEUROVASCULAR COUPLING

H. Radhakrishnan, K. Thakur, W. Wu, S. Ruvinskaya, J. Marota, D. Boas, **M.A. Franceschini**

Radiology / Martinos Center for Biomedical Imaging, Massachusetts General Hospital, Charlestown, MA, USA

Objective: In response to somatosensory stimulation, thalamic afferent activity in layer IV generates the first somatosensory evoked potential (SEP) component P1. This is followed by secondary activity in superficial layers (N1), and later by cortico-cortical interactions (P2 and N2).

The hemodynamic response following stimulation historically has been attributed to the initial neuronal activity in layer IV (P1). In (Franceschini 2008) we found N1 and P2 are better predictors of hemodynamic response than P1. Using alpha-chloralose as the anesthetic and parametric stimuli, we could not detect differences between N1 and P2. Here, modulating the electrical and hemodynamic responses with different anesthetics we could uncouple N1 and P2 and determine which SEP components more strongly correlate with the hemodynamic response.

Methods: We divided 40 male Harlan Sprague-Dawley rats into 6 groups, with different maintaining anesthetics: alpha-chloralose, isoflurane, pentobarbital, ketamine-xylazine, fentanyl-droperidol, and propofol. Simultaneous EEG (4 scalp electrodes) and Diffuse Optical Imaging (DOI) measurements (32 channel CW system) were obtained during event-related electrical forepaw stimulation. Electrical stimuli comprised 0.2 ms pulses with current < 0.2 mA (motor threshold), delivered at 3 Hz. In each rat we performed 10 twelve-minute runs, presenting stimuli with durations of 1, 3, 5, 7, 9, 11, and 13s with average ISI of 12s. Following the stimulation runs, we measured baseline blood flow (BF) and vascular reactivity to a hypercapnia challenge using Diffuse Correlation Spectroscopy (DCS) to evaluate differences between anesthetics.

The DOI and EEG data were analyzed as described in (Franceschini 2008). BF velocity was obtained as described in (Cheung 2001).

Results: SEP and hemodynamic responses were linear with stimulus duration, in agreement with (Ances 2000; Franceschini 2008; Martindale 2005; Ureshi 2004). For the GABAergic anesthetics used (alpha-chloralose, isoflurane, pentobarbital and propofol) we found the P2 SEP component could predict the hemodynamic responses statistically significantly better than P1 or N1. Rats anesthetized with Ketamine-Xylazine and Fentanyl showed pronounced N2 SEP responses; if this component was included as a linear regressor for all anesthetics, the P2-N2 hemodynamic prediction had a significantly larger R^2 and F-score than any other combination of SEP components.

Conclusion: Using these six anesthetics we could uncouple the N1 and P2 contributions to the hemodynamic response and determined that P2 and N2 cortico-cortical interactions drive hemodynamic responses, with the N2 negative SEP component driving vasoconstriction to counteract the vasodilatory role of P2. The different anesthetics exhibited significant differences in baseline BF, but BF always increased with hypercapnia. Including baseline BF as a regressor did not improve hemodynamic predictions, indicating that baseline BF minimally affects neurovascular coupling. Finally, neurovascular coupling appears unaltered by the type of anesthesia.

References:

Ances, B.M., et al. 2000. J Cereb Blood Flow Metab 20, 921-930.

Cheung, C., et al., 2001. Phys Med Biol 46, 2053-2065.

Franceschini, M.A., et al. 2008. Neuroimage 41, 189-203.

Martindale, J., et al. 2005. J Cereb Blood Flow Metab 25, 651-661.

Ureshi, M., et al. Neurosci Res 48, 147-153.

Brain PET Oral 5: In Vivo Pharmacology II: Serotonin

BRAIN SEROTONIN TRANSPORTER OCCUPANCY BY ORAL SIBUTRAMINE DOSED TO STEADY STATE: A PET STUDY USING ^{11}C-DASB IN HEALTHY HUMANS

P.S. Talbot[1], S. Bradley[2], C.P. Clarke[2], K.O. Babalola[3], A.W. Philipp[2], G. Brown[1], A.W. McMahon[1], J.C. Matthews[1]

[1]Wolfson Molecular Imaging Centre, University of Manchester, [2]Icon Development Solutions, [3]Division of Imaging Science & Biomedical Engineering, University of Manchester, Manchester, UK

Background and aims: Sibutramine HCl is a monoamine reuptake inhibitor prescribed in a dose of 10-15 mg/day as an appetite suppressant in the clinical management of obesity. In vitro and in vivo animal data suggest that efficacy is mediated by its metabolites desmethylsibutramine (M1) and di-desmethylsibutramine (M2) which have approximately 100-fold higher affinity for the 5-HT and norepinephrine reuptake transporters (SERT and NET, respectively) than the parent compound. However, there is a paucity of in vivo data in humans about mechanisms underlying:

i. clinical efficacy; and
ii. the dose-independent non-response observed in a significant minority of patients.

We present the first PET study investigating central actions of sibutramine at the SERT in humans.

Methods & purpose: 12 consenting, normal-weight, healthy males (mean age 40.7 yr; range 30-50 yr) completed a double-blind, placebo-controlled, balanced-order, within-subject crossover investigation of the central SERT occupancy (measured with ^{11}C-DASB) associated with sibutramine 15 mg/day dosed to steady state over 5 days. Exploratory secondary analyses investigated correlations between SERT occupancy and

i. plasma concentrations of sibutramine, M1 and M2;
ii. food intake as measured by a standardised test meal.

For the PET scans (2 per subject, on placebo and sibutramine), emission data were acquired for 100 minutes on the High Resolution Research Tomograph (HRRT) following i.v. injection of ^{11}C-DASB (498.5 ± 105.8 MBq [13.5 ± 2.9 mCi]); injected mass 4.5 ± 2.6 µg; radiochemical purity 96.7 ± 1.1%). For each subject, ROIs (putamen, caudate, thalamus and brainstem [BS]) were extracted from a T1-weighted MRI using an automated method. Binding potentials (BP_{ND}) were calculated by Logan reference tissue method, using cerebellum as reference region. SERT occupancy was defined as % change in BP_{ND} between placebo and sibutramine conditions.

Results: Mean ± SD baseline (placebo) BP_{ND} values across regions were: BS 0.60 ± 0.09; caudate 0.82 ± 0.24; putamen 1.22 ± 0.32; thalamus 1.25 ± 0.31. Mean occupancy across all regions and subjects was 30.0% ± 10.2% (range ~ 10% - 50%), with a significantly greater proportion of the variability across subjects (ANOVA 63%) than regions (8%). There was no significant relationship between SERT occupancy and plasma concentration of either parent sibutramine or M1, and a positive correlation (trend; p =0.09) between occupancy and M2. All subjects with significant appetite suppression (n = 5) had SERT occupancy in the upper range (~ 25-50%). Non-responders (n = 7) had

occupancy across the whole range. Very weak correlations were found between plasma concentrations and effect on appetite, mainly due to the high levels of variability in eating response across the group.

Conclusions: Our data would support the following:

i. SERT occupancy by clinical doses of sibutramine can be measured accurately by ^{11}C-DASB PET and is of modest magnitude compared to clinically effective doses of SSRI antidepressants (~ 80%);
ii. SERT occupancy is predominantly mediated by M2 in humans;
iii. SERT occupancy may be necessary but not sufficient for efficacy in humans, supporting preclinical data suggesting that the hypophagic effect of sibutramine requires the co-inhibition of both SERT and NET.

234

Brain Poster Session: Neuroprotection

INCREASING OMEGA-3 INTAKE WITH A DIET RAPESEED OIL-ENRICHED DIET PREVENTS FROM MIDDLE CEREBRAL ARTERY OCCLUSION INDUCED-DAMAGE

N. Blondeau[1,2], B. Delplanque[3], C. Gandin[1], G. Agnani[3], N. Simon-Rousseau[4], C. Heurteaux[1,2]

[1]Institut de Pharmacologie Moléculaire et Cellulaire, CNRS-UMR 6097, Valbonne, [2]University of Nice - Sophia Antipolis, Nice, [3]University of Paris Sud, Orsay, [4]ONIDOL, Paris, France

Objectives: Cardiovascular and cerebral diseases are major public Health concerns in Western countries, whose populations have a severe deficiency in omega-3 intake, especially in alpha-linolenic acid (ALA). This is described as risk factors of coronary heart disease and stroke. The primary cause of stroke is an impairment of local blood flow resulting in neurovascular unit damages. Until now none of acute and preventive pharmacological therapies that have been tested demonstrates the capacity to preserve both arterial and neuronal function. Nevertheless, several studies suggest beneficial effects of diets rich in seafood and vegetable oils in cerebral diseases. The aim of this work was to evaluate preventive strategy with ALA on cerebral ischemia investigating particularly whether diet enriched with rapeseed oil, rich in ALA could prevent the damage induced by middle carotid artery occlusion (MCAO).

Methods:

1. To induce focal ischemia, we used the MCAO model in mice described as the closest to human. This intraluminal suture technique reliably induces neurological deficits and hemispheric infarcts restricted to the territory of the MCA 24 hour after the onset of ischemia. The regional cerebral blood flow (CBF) was monitored by laser-Doppler flowmetry during ischemia and 15min after the filament withdrawal to assess the reperfusion level. Only animals whose cerebral blood flow during ischemia had decreased below 20% of the pre-ischemic level were selected for histological analyses. 24 hour post-ischemia, we quantified the infarct volume on serial brain slices stained with Cresyl violet and the survival rate.
2. ALA supplementation was performed either by an ALA injection (500µmol/kg) or by diet enriched with rapeseed oil (5, 10, 20%, provided by ONIDOL). As control, we used vehicle injection, palm oil enriched diet, lacking in ALA or regular diet (SAFE R03T-25).

Results: We had previously shown that single ALA injection preconditions the brain triggering tolerance in a rat model of global ischemia. We have now confirmed in mice that an ALA injection 3 days before a 60 min MCAO reduced by half the infarct volume 24 hour post-ischemia ($p < 0.05$) and an ALA level increase might be a preventive strategy against focal ischemia. This led us to introduce the consumption of rapeseed oil (5, 10, 20%) in long-term diets in mice. A 5% rapeseed enriched diet (Rape-SS5) had no effect on the infarct volume. In contrast a 10% diet (Rape-SS10) drastically reduced the infarct volume by 45% ($p < 0.01$) and a 20% rapeseed diet (Colza-SS20) by 30% (N.S). As control, a 5% palm oil diet, rich in palmitic acid failed to induce neuroprotective effects. Another parameter of evaluation, possibly of more importance concerns the reperfusion. 77,5% of the Rape-SS5 mice did not reperfused 30min after the filament withdrawal, contrary to the Rape-SS10 (33.3%). This outcome may not be interpreted as actual reduction of the infarct volume but may be essential in the prediction of the overall outcome.

Conclusion: Our results provide further evidence for a therapeutical value of alpha-linolenic acid enriched diet as preventive treatment of brain injury resulting from focal ischemia/reperfusion.

235

Brain Poster Session: Neurogenesis

BRAIN PLASTICITY AND ANTI-DEPRESSANT EFFECTS ARE VERSATILE POTENTIAL OF ALPHA-LINOLENIC ACID TO PROMOTE STROKE RECOVERY

N. Blondeau[1,2], D. Debruyne[1], M. Piens[3], C. Nguemeni[1], J.C. Plumier[3], R.H. Lipsky[4], A.M. Marini[5], C. Heurteaux[1,2]

[1]Institut de Pharmacologie Moléculaire et Cellulaire, CNRS-UMR 6097, Valbonne, [2]University of Nice - Sophia Antipolis, Nice, France, [3]Centre de Neurobiologie Cellulaire et Moléculaire, University of Liège, Liège, Belgium, [4]Department of Neurosciences, Inova Fairfax Hospital, Falls Church, VA, [5]Department of Neurology and Neuroscience Program, Uniformed Services University of the Health Sciences, Bethesda, MD, USA

Objectives: Prevention and treatment of stroke, a major public Health concern in Western countries, are major challenges in modern medicine. Besides mortality and devastating neurovascular unit damages, post-stroke depression (PSD) is a frequent psychiatric complication (prevalence of 30%). PSD increases mortality rates and worsen functional outcomes. We have previously demonstrated that alpha-linolenic acid (ALA), a polyunsaturated fatty acid reduces the ischemic damage by limiting glutamate-mediated neuronal death. We aimed to create a global strategy based on three sequential injections of ALA for stimulating brain responses and decreasing the post-stroke psychiatric complications to achieve the best functional recovery.

Methods:

1. The protective effects of three sequential injections of ALA as pre- or post-treatment against stroke were determined using the MCAO model in mice.
2. The effect of single or repeated ALA-injection treatment on neurogenesis was evaluated studying BrdU incorporation in the hippocampal Dentate Gyrus and by immunohistochemistry with fluorescent double-labeling.
3. Neuronal plasticity known to contribute to brain repair was evaluated measuring the expression of key proteins involved in synaptic functions, synaptophysin-1, VAMP-2, and SNAP-25 as well as proteins supporting glutamatergic neurotransmission, V-GLUT1 and V-GLU2, by Western blot.
4. To investigate the functional-anatomical relationship between ALA and neurogenesis/synaptogenesis, we studied BDNF expression by RT-PCR, Western blot and ELISA.
5. Neuroprotection, neurogenesis and synaptogenesis were also tested in vitro on neural stem cells and hippocampal cultures.
6. ALA treatment was tested in the Porsolt Forced Swim Test and Tail Suspension Test, that are commonly accepted to predict antidepressant efficiency of drugs.

Results: Three sequential injections of ALA enhanced protection. As a pre-treatment, it reduced by approximately 30% the post-ischemic infarct volume 24 hours post-MCAO. As post-treatment, it augmented neuronal survival rates by three-fold 10 days following ischemia. By themselves the three sequential injections of ALA increased neurogenesis 3 days after the end of the treatment. BrdU-positive cells increased by 1.5 in the ALA-injected mice as well as the number of neuronal progenitor cells Brdu-DCX positive by 50%. In the cortex, ALA treatment induced a parallel increase of synaptophysin-1 and VAMP-2, two vesicle-associated synaptic proteins and SNAP-25, their membrane-associated synaptic protein. It also increased the vesicular glutamate transporters V-

GLUT-1 and -2 (key factors of the glutamatergic neurotransmission efficacy). These ALA effects were correlated with an in vivo increase in BDNF protein levels, which was confirmed in vitro on neural stem cells and hippocampal cultures. Because BDNF has antidepressant activity, we tested whether chronic ALA treatment could produce antidepressant-like behavior. ALA-injected mice had significantly reduced measures of depressive-like behavior compared to vehicle-treated animals, suggesting another aspect of ALA treatment that could boost functional stroke recovery by reducing psychiatric complication.

Conclusion: The present work demonstrates that treatment of experimental stroke with repeated ALA-injections improves protection. Beside to acute vasodilation and excitotoxicity limitation ALA displays versatile potential like enhancement of neurogenesis, synaptogenesis and neurotransmitter transmission. From a clinical point of view, this “multi-target” effect of chronic ALA-treatment may represent a novel approach to stroke and subsequent PSD therapies.

236

Brain Poster Session: Blood-Brain Barrier

TOBACCO SMOKE: A CRITICAL ETIOLOGICAL FACTOR FOR VASCULAR IMPAIRMENT AT THE BLOOD-BRAIN BARRIER

L. Cucullo[1], T. Sathe[2], M. Hossain[1], V. Fazio[1], E. Rapp[3], D. Janigro[1,4]

[1]Cell Biology, [2]Cleveland Clinic, [3]Flocel Inc, [4]Molecular Medicine, Cleveland Clinic Lerner College of Medicine, Cleveland, OH, USA

Objectives: Tobacco smoke (TS) is a critical etiological factor for vascular impairment [1] and the pathogenesis and progression of a variety of neuroinflammatory diseases (e.g., Alzheimer's disease and multiple sclerosis [2,3]). However, the exact pathophysiology of TS at the brain microvascular level has yet to be unveiled. For this purpose, we first assessed the effect of chronic TS exposure on human brain microvascular endothelial (HBMEC) and monocytes (THP-1) cell cultures and then evaluated in vitro the physiological response to TS of a human BBB model. This was assessed under normal and pathological hemodynamic changes (flow-cessation/reperfusion). Since many vascular adverse effects of smoking are related to the exposure to reactive oxidative substances of which TS is highly enriched, we tested the hypothesis that a concomitant antioxidant (vitamins E and C) supplementation can protect the BBB.

Methods: A concentrated TS solution was prepared from 2R4F research cigarettes using a Borgwaldt RM2 apparatus. TS was quantified as puffs/mL (p/mL), and diluted to the desired concentration (0.008, 0.016, and 0.032 p/mL) prior use.

Vitamin E and C (Fischer Scientific) were diluted to a final physiological concentration of 40 and 80 μmol/l respectively.

The specific effects of TS on endothelial cells and monocytes were initially assessed in static culture systems (12 well plates). Cell morphology and viability were assessed via inverted light microscopy. The release of pro-inflammatory cytokines (TNF-α, IL-1β, and IL-6) and matrix metalloproteinases 2 and 9 was assessed by ELISA. The immune response of the endothelial and THP-1 cells was assessed by FACS.

The effect of tobacco smoke exposure on the BBB and the protective efficacy of vitamin E and C were assessed in a well established dynamic in vitro BBB model (DIV-BBB) that closely mimics the physiological characteristics and response of that in vivo [4].

Results: TS decreased endothelial cell viability only at high concentrations (≥0.016 puffs/mL) while not significantly affecting that of monocytes. At low concentration (0.008 puffs/mL) TS induced the expression of the vascular endothelial adhesion molecules VCAM-1, P-selectin and E-selectin, the differentiation of THP-1 cells into macrophages, the release of the pro-inflammatory cytokines TNF-α, IL-1β, and IL-6, and that of activated matrix metalloproteinase-2 and -9. In addition, TS worsened BBB failure after flow-cessation/reperfusion (Fc/Rp). The coadjuvant administration of physiological concentrations of either vitamin E or C significantly decreased the pro-inflammatory activity of TS and reduced the loss of BBB integrity after reperfusion in smoke-exposed BBB modules.

Conclusions: TS is a strong vascular inflammatory primer that directly affects the BBB endothelium and the immune cells and can significantly worsen the BBB damage caused by other vascular inflammatory insults. Our data also suggest that supplementation of antioxidant vitamins can significantly reduce this risk.

References:

1) Rahman, M. M. et al.; Curr. Vasc. Pharmacol. 2007; 5, 276-292.

2) Hawkes, C. H. et al.; Mult. Scler. 2007, 13, 610-615.

3) Almeida, O. P. et al.; Am. J. Geriatr. Psychiatry 2008, 16, 92-98.

4) Cucullo, L. et al.; J. Cereb. Blood Flow Metab 2008; 28(2),312-28.

238

Brain Poster Session: Neonatal Ischemia

SUPERFUSED NEONATAL RAT CEREBROCORTICAL SLICES DURING OXYGEN-GLUCOSE DEPRIVATION: $^{1}H/^{31}P$ NMR METABOLIC CHARACTERISTICS OF BIOENERGETIC PROTECTION BY MILD HYPOTHERMIA

J. Liu[1], M.J.S. Kelly[2], L. Litt[1]

[1]Department of Anesthesia and Perioperative Care, [2]Department of Pharmaceutical Chemistry, University of California San Francisco, San Francisco, CA, USA

Aims: Large clinical trials of asphyxiated human neonates have found that mild therapeutic (post-insult) hypothermia substantially improves neurological outcomes. Using an ex vivo rodent brain slice model and high resolution (14T) NMR determinations of Perchloric Acid (PCA) extracted metabolite concentrations, we asked if NMR metabolic profiles after oxygen-glucose deprivation (OGD), during and after mild hypothermia, could characterize bioenergetic impairment and recovery, accurately differentiating good from bad outcomes, thereby encouraging additional data taking for multivariate metabolomic analyses.

Methods: Experiments began with 20 superfused, respiring, 350μ cerebrocortical slices obtained from the same litter of 7-day old rat pups, using the IACUC-approved protocol in earlier studies (1). The superfusate, or oxyACSF, was a modified Krebs balanced salt solution and 10 mmol/L glucose (1). Bicarbonate buffering and oxygenation of oxyACSF was from continuous bubbling with (95% O_2)/(5% CO_2) gas mixture, resulting in constant PCO_2 (40 mmHg), PO_2 (600- 650 mmHg), pH (7.4), and temperature (37°C for normothermia; 32°C for 3 hrs of hypothermia followed by 60 min slow rewarming.) Thirty minute OGD experiments began after 3-hrs oxygenation with no change in the 10-15 ml/min flow, when oxyACSF was switched to ACSF with no glucose and a $PO_2 < 8$ mmHg (Ocean Optics oximeter) from 3 hrs of bubbling 100% N_2. In one group hypothermia began just before OGD, in another it began after 15 min of OGD. Five slices were removed: before starting OGD; at the end of OGD before restoring oxyACSF; at the end of hypothermia, or at the corresponding time during normothermia; and after 3 hrs more of normothermic recovery. Twenty-eight PCA metabolites were quantified with $^{1}H/^{31}P$ NMR analysis. Histology and immunohistology was used to examine slices removed at different times in the protocol.

Results: In slices where 3 hrs hypothermia began just before OGD, concentrations at the end of the experiment (after slow rewarming and 3 hrs normothermia) of 8 metabolites were significantly ($p< 0.05$) greater in hypothermia-treated slices, with the following (hypothermia treated group)/(normothermia treated group) ratios: alanine (1.6), acetate (1.32), NAA (1.8), GABA (1.65), glutamate (1.72), glutamine (2.14), and ATP (1.33). Because we had N=4, it is likely that more data will provide additional significant concentration differences. In additional experiments where the onset of 3 hrs hypothermia began 15 min after the start of OGD, final concentration ratios (hypothermia/normothermia) for the 8 metabolites were still significantly greater than 1. As expected, slow rewarming always caused significant changes in metabolite concentrations.

Conclusions: Finding metabolic/histologic protection when mild hypothermia starts both before and after OGD validates use of the neonatal brain slice model for mechanistic studies. The data are sufficiently accurate to proceed to metabolomic investigations. We are optimistic that metabolomic multivariate analyses will ultimately be able to distinguish and predict good and bad outcomes.

References: 1. Zeng J, Yang GY, Ying W, Kelly M, Hirai K, James TL, Swanson RA, Litt L. (2007) Pyruvate improves recovery after PARP-1-associated energy failure induced by oxidative stress in neonatal rat cerebrocortical slices. J Cereb Blood Flow Metab 27(2):304-15.

BLOOD-BRAIN BARRIER ABNORMALITIES IN PATIENTS WITH VASCULAR COGNITIVE IMPAIRMENT QUANTIFIED BY DYNAMIC CONTRAST-ENHANCED MRI

G. Rosenberg, S. Taheri, R. Sood, C. Gasparovic, J. Prestopnik, E. Edmonds, C. Ford, J. Adair

Neurology, University of New Mexico Health Sciences Center, Albuquerque, NM, USA

Background and aims: The incidence of vascular cognitive impairment (VCI) is increasing worldwide due to the aging of the populations. Progress in diagnosis and treatment of VCI has been impeded because of the heterogeneity of the illness and the overlap particularly in the early stages with other causes of impaired cognition. Several biomarkers have been used to identify pathological abnormalities in patient with VCI: proton magnetic resonance spectroscopy (^{1}H-MRS) showed reduced levels of N-acetylaspartate (NAA) in the white matter, suggesting ischemic changes, and elevated levels of albumin are found in the cerebrospinal fluid (CSF), suggesting BBB disruption.

Purpose: White matter damage is a prominent feature in small vessel form of VCI. Disruption of the blood-brain barrier (BBB) is proposed as a cause of the white matter damage. We used quantitative contrast-enhanced MRI to determine the role of the blood-brain barrier (BBB) in the white matter injury. We hypothesized that BBB abnormalities would be associated with reduced NAA and increased CSF albumin index.

Methods: To test the hypothesis we used dynamic contrast-enhanced MRI (DCEMRI) with Gadolinium-DTPA (Gd-DTPA) to quantify BBB permeability, ^{1}H-MRS to measure NAA, and lumbar puncture to obtain CSF to calculate the albumin index. Forty patients suspected to have VCI were recruited into the study along with 20 age-matched controls. A consensus diagnosis was made based on clinical findings, neuropsychological test results, and MRI.

Results: We recruited 40 patients with leukoaraiosis and symptoms suggstive of VCI. After evaluation 27 were diagnosed as VCI-no dementia (VCI-ND) (one had VCI-dementia), and 10 had leukoaraiosis with minimal findings (LEUK). Three patients could not be classified. From the controls, we established normal values for BBB permeabilty in white matter as $3X10^{-4}$ml/gm/min. We found increased BBB permeability over controls in 26 of the VCI patients ($p< 0.05$). Total permeability and intensity in localized regions of increased permeability were calculated and used for cluster analysis (R statistical package), which separated the VCI patients into three groups: low, mid, and high permeability. Those in the lower group were mainly LEUK, while the higher two groups were VCI-ND patients. Those in the mid and highest permeability groups had significantly lower NAA than the lowest BBB group ($p< 0.05$). Albumin index was highest in the high permeability group ($p< 0.05$). Patients (n=15) classified clinically as small vessel disease were more likely to be in the mid and high permeability groups.

Conclusions: Our results provide quantitative evidence using DCEMRI of an abnormality in BBB permeability in patients with VCI. Our results suggest that BBB permeability is an additional biomarker, complementing reduced white matter NAA and elevated CSF albumin index. One explanation for the increased permeability is that on-going inflammation causes secondary myelin damage. Another is that secondary damage occurs during tissue repair or angiogenesis. Long-term followup will identify a sub group of patients with progressive disease and abnormalities of the BBB suggestive of inflammation. Determination of the natural history of BBB abnormalities is now feasible and could aid clinical trials.

BRIEF FOCAL CEREBRAL ISCHEMIA INDUCES IL-1 β PROTEIN EXPRESSION IN RATS

X. Zhan, B. Ander, F. Sharp

Neurology, MIND/UC Davis, Sacramento, CA, USA

Objective: Transient ischemic attack (TIA) is a common cerebrovascular disorder. TIAs are under recognized, under reported and under treated though as many as a third of classical TIA patients eventually go on to have ischemic strokes (1). Our previous study demonstrated that 5 or 10 minutes of brief focal ischemia caused microinfarctions and an inflammatory response in rat brains (2). Since cytokines can contribute to the cellular damage and inflammatory response seen following a stroke, we hypothesized that the expression of cytokines might be increased following very brief focal ischemia that simulates TIAs occurring in humans.

Methods: Male Sprague-Dawley rats weighing 280-320 g (Charles River Labs, USA) were used in this study (n=12). Focal cerebral ischemia was produced by occluding the middle cerebral artery (MCA) using the intraluminal suture technique. Rats subjected to 5 min or 10 min of brief focal ischemia were allowed to survive 24 h. A stroke group receiving 2 hour focal ischemia was used to compare to the brief focal ischemia treatment. Sham-operated rats were subjected to the identical surgical protocol except that no suture was inserted. After a 24 h period of reperfusion, cortex and basal ganglia in the ischemic hemisphere were dissected and frozen at −70°C. Frozen tissues were homogenized in ice-cold buffer containing a complete protease inhibitor mixture. The homogenates were centrifuged at 14,000 x g for 30 min at 4°C, and the pellet was discarded. The protein (20 m g) in the supernatant was used for ELISA analysis for IL-1β, IL-6, TNF-α, and IFN-g . Data were calculated as fold changes and expressed as mean ± SE. One-way ANOVA was performed with a Student-Neuman-Keuls post hoc test. A p value of less than 0.05 was considered statistically significant.

Results: IL-1 β levels were increased significantly by 77.48 ± 0.94 ($p< 0.05$) fold, and 166.21 ± 0.47 ($p< 0.05$) fold at 24h following 10 min and 2 h of ischemia respectively. The increase (by 2.34 ± 0.22 fold) at 24h following 5min of ischemia was not significant. IL-6 levels were increased by 3.22 ± 0.42, 5.12 ± 0.46, and 6.81 ± 0.30 fold; IFN-g levels were increased by 1.62 ± 1.24, 1.88 ± 0.49, and 1.68±1.70 fold; TNF-α levels were increased by 0.73 ± 0.60, 2.56 ± 0.64, and 3.11 ± 0.34 fold at 24h following 5min, 10min, and 2hour ischemia respectively. The changes in IL-6, IFN-g , and TNF-a at 24h following 5min and 10 min of focal ischemia were not significant.

Conclusion Focal ischemia of 10 minutes duration, that simulates a TIA that occurs in humans, increases IL-1 β expression in brain 24 hours later. Thus, ischemia without infarction can increase this cytokine in brain.

Acknowledgments: Department of Neurology and MIND Institute, University of California at Davis; and supported in part by NS054652.

Reference:

(1). Rothwell, P.M., Buchan, A., Johnston, S.C., 2006. Lancet Neurol. 5, 323-331.

(2). Zhan X, Kim C, Sharp F.R. 2008. Brain Research. 1234, 183-197.

INCREASED CD36 AND INFLAMMATORY RESPONSE ARE INVOLVED IN EXACERBATED ISCHEMIC BRAIN INJURY IN DIABETIC CONDITION

E. Kim[1], A. Tolhurst[1], Y. Bao[1], S. Cho[1,2]

[1]Research/pre-clinic, Burke Medical Research Institute, White Plains, [2]Neuroscience, Weill Cornell Medical College, New York, NY, USA

Background and aims: Diabetes, a chronic pro-inflammatory state in periphery, is a predisposing risk factor for stroke. Recent studies indicate that CD36 is an inflammatory mediator that contributes to tissue injury in cerebral ischemia (Cho et al. 2005, Kim et al. 2008). Furthermore, the expression of CD36 is up-regulated in the presence of high glucose and implicated as a novel marker for insulin resistance. The purpose of the study is to determine whether CD36 and associated inflammatory responses are involved in ischemic injury in experimental diabetic conditions.

Methods: Experimental diabetic conditions in mice were established by feeding normal chow (ND) or diabetogenic diet (DD) for 8 weeks and administrating vehicle (veh) or streptozotocin (STZ) 3 week after commencing the diets. This approach results in four groups of mice: ND/Veh, DD/Veh, ND/STZ, and DD/STZ. Fasting blood glucose levels were measured 7 week of diet. Following week, mice were subjected to 30 min focal middle cerebral artery occlusion (MCAO) according to the methods previously described (Kim et al. 2008). Infarct volume (IV) and % swelling were measured in 3d-post ischemic brain. The expression of CD36, MCP-1, CCR2, TNFα, and IL-6 were compared between the most diabetic condition (DD/STZ) and ND/veh.

Results: Compared to ND/veh (32.8±2.6, n=19), blood glucose levels were significantly increased in ND/STZ (247.9±25.5, $p< 0.01$, n=20) and DD/STZ (331.3±45.8 $p< 0.01$, n=11). Accordingly, IV was also increased in ND/STZ (42.7±2.0 $p< 0.05$, n=12) and DD/STZ (54.8±1.5, $p< 0.01$, n=11) compared to ND/veh (32.8±2.6, n=20). The gene expression levels of inflammatory mediators were significantly elevated in the DD/STZ brain (CD36, 1.6±0.2; MCP-1, 2.1±0.2; CCR2, 1.7±0.2; TNFα, 1.4±0.1; IL-6, 2.0±0.4 fold vs ND/veh, $p< 0.05$, n=4-6). In addition, peritoneal macrophage CD36 protein expression was significantly increased in DD/STZ (2.1±0.5 fold vs ND/veh, $p< 0.05$, n=4-6).

Conclusions: The data demonstrate that diabetic condition exacerbates ischemic injury and increases the expression of inflammatory mediators in the brain/periphery. The study implicates that peripheral inflammatory status at the time of stroke and suggests an inclusion of risk factors in the experimental stroke models.

245

Brain Oral Session: Functional Brain Imaging

CONTRIBUTION OF DOPAMINE D1 AND D2 RECEPTORS TO AMYGDALA ACTIVITY

H. Takahashi, T. Otsuka, H. Takano, F. Kodaka, H. Kikyo, R. Arakawa, M. Miyoshi, M. Okumura, H. Ito, T. Suhara

National Institute of Radiological Sciences, Chiba, Japan

Objectives: To investigate the contribution of dopamine receptor subtypes to amygdala activation in human, we conducted a multimodal in vivo neuroimaging study in which dopamine D1 and D2 receptor bindings in the amygdala were measured with positron emission tomography (PET) and amygdala activation in response to fearful faces was assessed by functional magnetic resonance imaging (fMRI) in healthy volunteers.

Methods: Fourteen healthy male volunteers were studied. PET studies were performed on ECAT EXACT HR+. For evaluation of dopamine D1 and D2 receptors, [^{11}C]SCH23390 and [^{11}C]FLB457 were used, respectively. Dynamic scans were performed for 60.0 minutes for [^{11}C]SCH23390 and 90.0 minutes for [^{11}C]FLB457. Quantitative analysis was performed using the three-parameter simplified reference tissue model. The cerebellum was used as a reference region. Parametric images of BP_{ND} of [^{11}C]SCH23390 and [^{11}C]FLB457 were created. Amygdala activations in response to fearful faces were examined using fMRI. The fMRI were acquired with a 3.0 Tesla system. Data analysis was performed with the statistical parametric mapping software (SPM2). To conduct multimodality voxel-wise correlation analysis between BOLD signal and dopamine receptor binding, we used the biological parametric mapping (BPM) toolbox for SPM.

Results: Voxel-wise correlation analysis by BPM revealed that dopamine D1 binding in the amygdala was positively correlated with amygdala activation in response to fearful faces ($R>0.6$, $p< 0.015$), but dopamine D2 binding in the amygdala was not related to amygdala activation.

Conclusion: Dopamine D1 receptors might play a more vital role in enhancing amygdala response than dopamine D2 receptors when sensory inputs are affective.

References:

Casanova R, Srikanth R, Baer A, Laurienti PJ, Burdette JH, Hayasaka S, Flowers L, Wood F, Maldjian JA (2007) Biological parametric mapping: A statistical toolbox for multimodality brain image analysis. Neuroimage 34:137-43.

Inglis FM, Moghaddam B (1999) Dopaminergic innervation of the amygdala is highly responsive to stress. J Neurochem 72:1088-94.

Lammertsma AA, Hume SP (1996) Simplified reference tissue model for PET receptor studies. Neuroimage 4:153-8.

Rosenkranz JA, Grace AA (2002) Cellular mechanisms of infralimbic and prelimbic prefrontal cortical inhibition and dopaminergic modulation of basolateral amygdala neurons in vivo. J Neurosci 22:324-37.

TREATMENT WITH ANGIOTENSIN II RECEPTOR BLOCKER, OLMESARTAN, RECOVERS PROTECTIVE EFFECT OF CHRONIC MILD HYPOPERFUSION AFTERY MCA OCCLUION IN HYPERTENSIVE RATS

E. Omura-Matsuoka[1], **Y. Yagita**[2], T. Sasaki[1], Y. Terasaki[1], N. Oyama[1], Y. Sugiyama[2], S. Okazaki[2], K. Kitagawa[2]

[1]Cardiovascular Medicine, [2]Neurology, Osaka University Graduate School of Medicine, Suita, Japan

Objectives: We showed occlusion of unilateral common carotid artery (CCAO) for two weeks reduced infarct size after occlusion of middle cerebral artery (MCAO) in Wistar rats. The purpose of this study is to show whether CCAO for two weeks reduces infarct size after MCAO also in spontaneously hypertensive rats (SHR), and to clarify the effect of administration of angiotensin II AT_1 receptor blocker (ARB), olmesartan, in SHR.

Methods: < Wistar vs. SHR > In adult male Wistar rats (n=28) or SHR (n=18), each animal was anesthetized with halothane. Pre-CCAO group rats received the left CCAO and the left MCA was subsequently occluded permanently 2 weeks later (n=22). Sham group rats received only exposure of the left CCA and MCAO 2 weeks later (n=24)**.** The CBF change during MCAO was recorded by laser-Doppler flowmetry. Infarct size and neurological deficit were determined 2 days after MCAO.

< ARB on SHR > In adult male SHR, CCAO group rats received the left CCAO and were administered orally vehicle (VE) or olmesartan (OL) 5mg/kg per day for 13 days before the left MCAO. Sham group rats received only exposure of the left CCA and oral administration of VE or OL for 13 days before subsequent MCAO. They were devided into 4 groups; Sham-VE group (n=8), Sham-OL group (n=9), CCAO-VE group (n=10) and CCAO-OL group (n=10). The CBF change during MCAO, infarct size and neurological deficit were also evaluated.

Results: In Wistar rats, infarct size was significantly attenuated in pre-CCAO group (126.5 ± 111.0 mm^3) compared with sham group (328.8 ± 81.9 mm^3). Pre-CCAO group also showed better recovery in neurological findings than sham group. Cortical perfusion after MCAO was significantly preserved in pre-CCAO group (51.8 ± 10.8 %) compared with sham group (37.8 ± 8.5 %). However, in SHR, infarct size was almost identical between pre-CCAO and sham groups. Administration of olmesartan 5 mg/kg for 13 days reduced systolic blood pressure about 30 mmHg (Sham-VE; 197.0 ± 6.9 mmHg, CCAO-VE; 207.3 ±13.0 mmHg, Sham-OL; 169.9 ± 12.3 mmHg, CCAO-OL; 175.5 ± 16.9 mmHg). CCAO-OL group showed significant reduction of infarction volume (192.3 ± 70.6 mm^3) compared with Sham-VE (321.1 ± 54.8 mm^3), Sham-OL group (305.9 ± 54.4 mm^3) or CCAO-VE group (283.9 ± 65.2 mm^3). CCAO-OL group also showed best neurological score among 4 groups. Cortical perfusion after MCAO was significantly preserved in CCAO-OL group (33.9 ± 6.5 %) compared with Sham-VE group (22.7 ± 8.6 %) or CCAO-VE group (24.4 ± 9.1 %).

Conclusions: Chronic CCAO preserved cortical perfusion and attenuated infarct size after MCAO in Wistar rats, but the protective effect of CCAO was not found in SHR. In SHR, the administration of ARB after CCAO induced mild reduction of cerebral blood flow, reduction of ischemic insult and better neurological recovery. Administration of ARB for 2 weeks after CCAO induced ischemic tolerance also in SHR.

References:

1. Kitagawa K et al., Stroke, 36:2270-2274, 2005.

2. Todo K et al., Stroke, 39:1875-1882, 2008.

250

Brain Oral Session: Experimental Stroke and Cerebral Ischemia 2

EFFECTS OF TRANSCRANIAL NEAR-INFRARED LASER IRRADIATION ON CEREBRAL BLOOD FLOW IN MICE

H. Nawashiro[1], Y. Uozumi[1], S. Sato[2], S. Kawauchi[3], K. Shima[1], M. Kikuchi[3]

[1]Neurosurgery, National Defense Medical College, [2]Biomedical Information Sciences, National Defense Medical College Research Institute, [3]Medical Engineering, National Defense Medical College, Tokorozawa, Japan

Objectives: Photobiostimulation effects of near-infrared (NIR) laser irradiation have been known for almost forty years[1)]. Recently it has been reported that NIR laser irradiation is effective in cerebral ischemia in vivo and clinically[2)]. We examined the effect of 808 nm laser diode irradiation on CBF in mice. Furthermore, we examined the role of nitric oxide and a neurotransmitter, glutamate to regulate CBF in this animal model. The potential of NIR laser irradiation in the treatment of cerebral ischemia was also investigated.

Methods: Male C57BL/6J mice 9- to 11-weeks old and weighing 23 to 27 g (CLEA Japan, Inc, Tokyo, Japan) were used in the study. Under general and local anesthesia, an 808 nm CW diode laser (B&W Tek, Inc, Newark, DE) was applied to the left hemisphere transcranially. To determine the appropriate power density (PD) of NIR laser irradiation, we irradiated the laser with three different PD (0.8 W/cm^2; n=6, 1.6 W/cm^2; n=9, 3.2 W/cm^2; n=6), and measured the PD using a laser power meter with photodiode head (Laserstar; Ophir Optronics Ltd, Jerusalem, Israel) before and after every irradiation. CBF was measured in the cortex with a non-invasive and non-contact laser Doppler blood perfusion imager (PeriScan PIM II, PeriMed, Stockholm, Sweden). We measured directly nitric oxide in the brain tissue during NIR laser irradiation by an amperometric nitric oxide (NO)-selective electrode (IMN-111, Inter Medical, Nagoya, Japan). Furthermore, in N^g-nitro-L-arginie methyl ester hydrochloride (L-NAME) treated mice NO was also measured during NIR laser irradiation (n=4). To gain insight into potential mechanisms linking neurotransmission with CBF, effects of a non-competitive N-methyl-D-aspartate receptor blocker, MK-801 was investigated. To confirm the effect of pretreatment by NIR laser irradiation, we conducted the 1.6W/cm^2 NIR laser irradiation to the left hemisphere transcranially for 30 minutes before bilateral common carotid artery occlusion (BCCAO) (n=13). The control mice (n=13) were also subjected to 15-minute BCCAO without pretreatment by NIR laser irradiation.

Results: Transcranial NIR laser irradiation (1.6 W/cm^2 for 15 to 45 minutes, wavelength, 808 nm) increased local CBF by 30% compared to control value in mice. NIR laser irradiation also provoked a significant increase in cerebral NO concentration. Mice that received the broad-spectrum NO synthase (NOS) inhibitor, L-NAME did not show any CBF increase by NIR laser irradiation. Mice administered MK-801 showed immediate increase but loss of delayed increase in local CBF by NIR laser irradiation. Pretreatment by NIR laser irradiation improved residual CBF following bilateral carotid occlusion in mice.

Conclusions: Our data suggest that targeted increase of CBF is available by NIR laser irradiation and it is concerned in NOS activity and NO concentration. Besides, NIR laser irradiation may have a protective effect for transient ischemia.

References:

1) Hamblin MR: The role of nitric oxide in low level light therapy, Proc. of SPIE 6846 (2008) 684602.

2) Lampl Y, Zivin JA, Fisher M, et al: Infrared laser therapy for ischemic stroke: a new treatment

strategy Result of the NeuroThera effectiveness and safety trial-1 (NEST-1), Stroke 38 (2007) 1843-1849.

251

BrainPET Poster Session: Kinetic Modeling

BENEFIT OF PIXEL-BY-PIXEL DELAY CORRECTION FOR MEASUREMENT OF HEMODYNAMIC PARAMETERS IN PATIENTS WITH CEREBROVASCULAR DISEASE USING O-15 PET

H. Okazawa[1], T. Kudo[1], M. Kobayashi[1], M. Isozaki[2], Y. Arai[2], T. Tsujikawa[1], Y. Fujibayashi[1], T. Kubota[2]

[1]Biomedical Imaging Research Center, [2]Department of Neurosurgery, University of Fukui, Eiheiji-cho, Japan

Objectives: In calculation of regional cerebral blood flow (rCBF) using O-15 water PET, arterial input function is usually determined by arterial blood sampling, and delay of the input is corrected for radioactivity in the whole brain or at slice-by-slice levels. However, delay of the tracer is assumed to be different between the hemispheres in patients with unilateral arterial occlusive lesions. To calculate precise quantitative hemodynamic parameters, pixel-by-pixel estimation for delay of the tracer arrival time was performed and the delay map was applied for calculation of parameters.

Methods: Fifty-two patients (mean age=65±11y) with unilateral major cerebral arterial stenoocclusive disease underwent O-15 gas and water PET scans. All patients had occlusion or stenosis (>70%) in the internal carotid or middle cerebral arteries (MCA). For estimation of input function, arterial blood radioactivity was measured continuously using an automatic counter with a constant flow from the brachial artery. The delay of the input was estimated pixel-by-pixel and delay map of tracer arrival time was created. The 3-weighted-integral method was employed for calculation of rCBF and arterial-to-capillary blood volume (V_0) with pixel-by-pixel delay correction. Cerebral blood volume (CBV), oxygen extraction fraction (OEF) and cerebral metabolic rate of oxygen ($CMRO_2$) were also calculated from the O-15 gas PET scans using the bolus inhalation method, and asymmetry-index (AI) of these parameters were compared.

Results: Eleven patients showed ipsilateral significant increase in OEF (55.1±4.1 %) and all of them showed delay of tracer arrival and significant rCBF decrease (32.4±4.2 mL/100g/min) in the affected region compared to the contralateral hemisphere. The remaining 41 patients had OEF in normal range or slight increase as a global change and showed no differences in delay between the bilateral hemispheres. V_0 showed a slight decrease in the impaired hemisphere of patients with misery perfusion. AI for OEF (OEF-AI) was well correlated with those of delay (delay-AI) and CBF (CBF-AI). Correlation coefficient between OEF-AI and delay-AI ($r = 0.70$) was better than that between OEF-AI and CBF-AI ($r = 0.56$). The mean AI values for hemodynamic parameters in all patients were OEF-AI = 1.06±0.09, delay-AI = 1.05±0.06, 1/(CBF-AI) = 1.10±0.11, 1/($CMRO_2$-AI) = 1.05±0.08, CBV-AI = 1.02±0.16, and V_0-AI = 0.89±0.17. Patients with misery perfusion showed significantly higher OEF-AI (1.17±0.12, $P< 0.05$) and longer delay (0.34±0.19 sec, $P< 0.005$) as compared with patients with normal OEF.

Conclusion: Pixel-by-pixel estimation of tracer arrival time provided a delay map for regional differences and precise parametric values for evaluation of hemodynamic status in the patients with cerebrovascular disease. The delay image and delay-AI, correlated well with OEF change, would be able to estimate OEF elevation in impaired circulation in calculation of rCBF and V_0 images using O-15 water PET.

References:

[1] Ohta H, et al. J Cereb Blood Flow Metab 1996;16:765-780.

[2] Okazawa H, et al. J Nucl Med 2003;44:1875-1883.

[3] Okazawa H, et al. Eur J Nucl Med Mol Imaging 2007; 34: 121-129.

253

Brain Poster Session: Brain Imaging: Neurologic Disease

HYPOPERFUSION IN PARKINSON´S DISEASE ASSESSED BY ARTERIAL SPIN LABELING PERFUSION MRI

M. Fernández-Seara, **M. Aznárez-Sanado**, F. Loayza, F. Villagra, M. Pastor

Neuroscience, CIMA, University of Navarra, Pamplona, Spain

Objectives: Previous studies of cerebral perfusion in Parkinson´s disease (PD) without dementia have yielded conflicting findings, with some reporting no deficits, others describing hypoperfusion and others reporting hyperperfusion (1). Arterial spin labeling (ASL) is an excellent tool to obtain quantitative maps of cerebral blood flow (CBF) non-invasively. The objective of our study was to assess resting CBF abnormalities in a group of PD patients using ASL and statistical parametric mapping (SPM).

Methods: Twelve medicated patients without dementia (3 females, age range [46-76], UPDRS range [6-21], 10 with predominant right side affectation) and 11 healthy age-matched controls were scanned on a 3T Trio after signing written informed consent. ASL images were acquired using a technique that combined pulsed continuous ASL (2) with a background suppressed 3D GRASE sequence, modified to achieve late inflow delay (3), with parameters: labeling time=1.6 s and post-labeling delay=1.5 s. Scan time=6min. An anatomical dataset was also acquired. All data were analyzed using SPM5 and Matlab. Raw ASL images were realigned and co-registered to the anatomical dataset. Mean CBF maps were computed after subtraction of label and control images, based on a modified single compartment model (4), normalized to the MNI template and smoothed. Perfusion differences between patients and controls were assessed in a voxel-wise statistical analysis using two-sample t-test. Grand mean scaling to 50 ml/100g/min was included in the model. The significance level was set at $p< 0.05$ uncorrected for multiple comparisons, cluster size >50.

Results: Areas of hypoperfusion in the patients were (Fig.1): in the frontal lobes, bilaterally anterior prefrontal cortex and superior frontal gyrus; in the parietal lobe, right precuneus, bilaterally superior parietal lobules, left middle cingulate and posterior insula; in the temporal lobe, bilaterally middle temporal gyri with the larger cluster on left, the hippocampi, temporal poles and middle anterior temporal gyri; in the occipital lobe, left middle occipital gyrus; in the basal ganglia, right and left thalamus, left putamen tail and caudate nucleus, consistent with the predominantly right hemiparkinsonian affectation of our patient population. No regions of hyperperfusion were found.

Conclusions: The main areas of hypoperfusion found in the PD patients are known to be affected early during the disease course, such as the basal ganglia and their dopaminergic output, the prefrontal cortex. Other areas such as the middle temporal lobes surprisingly appear to be affected at a functional level before clinical manifestations are observed. Perfusion patterns in these areas could correlate with symptoms, especially cognitive changes that may be subclinical.

References:

1. Amorim, et al, 2007. Eur J Nucl Med Mol Imaging 34, 1455-1457.

2. Dai, et al. Magn Reson Med 60, 1488-1497.

3. Fernandez-Seara, et al, 2008. Proceedings of ISMRM, p. 3343.

4. Chalela, et al, 2000. Stroke 31, 680-687.

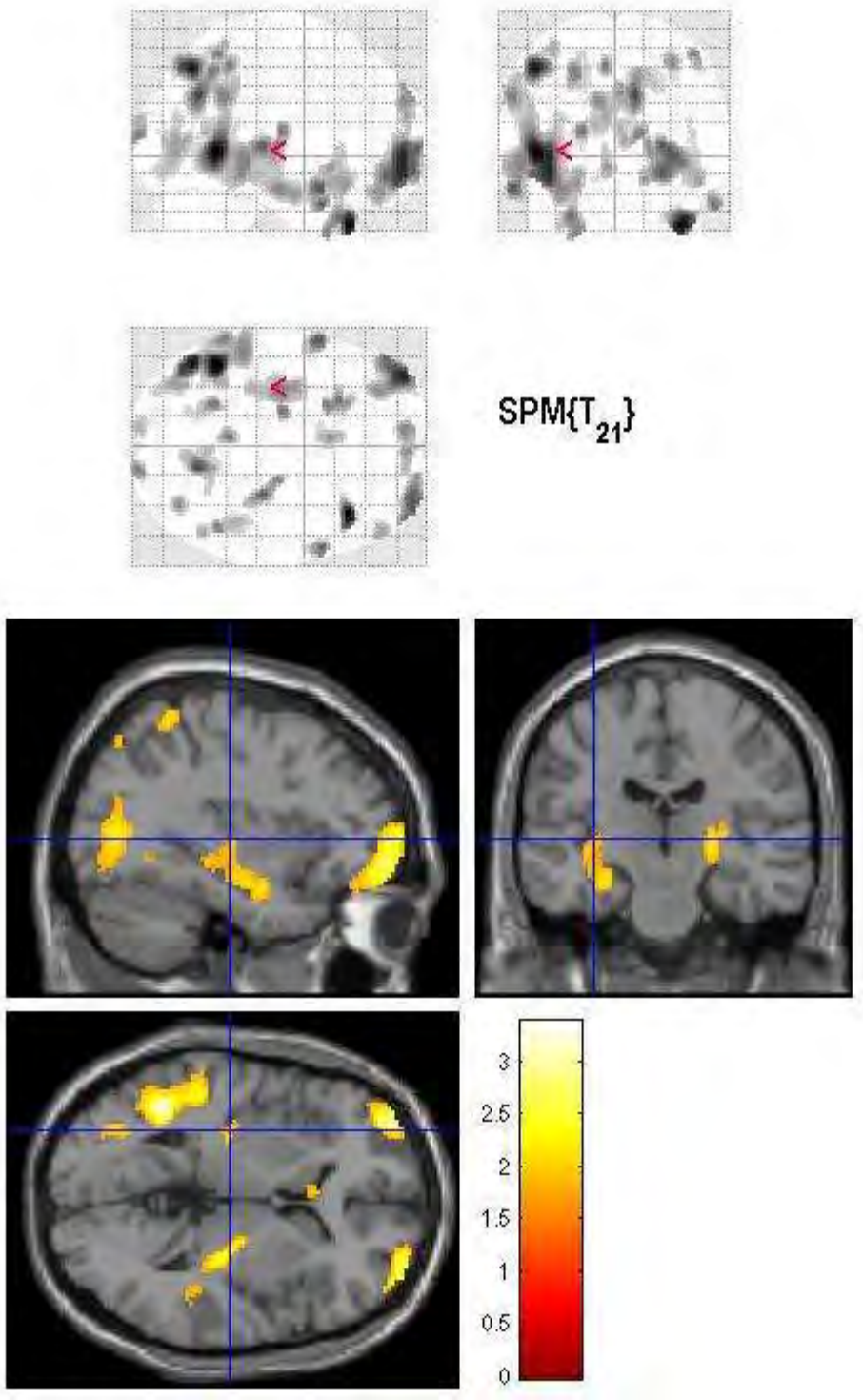

[Figure 1]

Brain Poster Session: Inflammation

RAPID INDUCTION OF CHEMOKINES IN GLIA CELLS CONTRIBUTES TO NEUTROPHIL RECRITMENT INTO CEREBROSPINAL FLUID IN EXPERIMENTAL KLEBSIELLA PNEUMONIAE MENINGOENCEPHALITIS

C.-T. Chiu[1,2], S.-Y. Chen[3], L.-L. Wen[4], H.-P. Pao[3], J.-Y. Wang[3]

[1]Neurosurgery, En Chu Kong Hospital, [2]Graduate Institutes of Medical Sciences, [3]Physiology, National Defense Medical Center, [4]Clinical Laboratory, En Chu Kong Hospital, Taipei, Taiwan R.O.C.

Klebsiella pneumoniae (K. pneumoniae) infection of the brain was less reported than in other organs, but an increase in incidence and morbidity has been noted in Taiwan. The incidence of death (> 30%) and long-term neurological sequelae remain high. We have previously demonstrated that glial cells are important cellular sources of proinflammatory cytokines in CSF in a rat of model of K. pneumoniae

meningoencephalitis. The CXC chemokines such as growth related oncogene (GRO, CXCL1) and macrophage inflammation protein-2 (MIP-2, CXCL2) are chemoattractant for neutrophils while CC chemokines such as monocyte chemotractic protein-1 (MCP-1, CCL2) are chemoattractant for monocytes. We found that the increases of WBC counts in CSF and blood were time-dependent. Leukocytosis was observed in CSF at 8 hrs after K.p-infectiont with a predominance of PMNs. The concentrations of GRO (CXCL1) and MIP-2 (CXCL2) in CSF are much higher than those in serum at 4 and 8 hr after K.p infection of the brain, suggesting a likely brain origin. After K.p. infection**,** the mRNA expression of chemokines (GRO, MIP-2, and MCP-1) in brain tissue increased significantly in a time-dependent manner. However, mRNA level of their receptors only showed slight changes with CXCR1 and CXCR2 mRNA level upregulated while the CCR2 mRNA expression rapidly suppressed compared to sham animals. Intracerebroventricular injection of reparixin (CXCR1 and CXCR2 antagonist) or vMIP-2 (viral macrophage inflammatory protein-2), a broad spectrum peptide antagonist of chemokine receptors, attenuated PMN recruitment into CSF. and also attenuated the elevated concentrations of GRO (CXCL1) in CSF and upregulation of gene expression of CXCR2, but not CXCR1, in brain tissue at 8 hr after K.p infection. Taken together, our results suggest a rapid induction of chemokines and chemokine receptors in glial cells, which may play a role in PMN recritment into CSF and and subsequent cell/tissue injury following K. pneumonia infection of CNS.

255

Brain Poster Session: Glial Functions

ASTROCYTES ARE NEUROPROTECTIVE AGAINST TRANSIENT FOREBRAIN ISCHEMIA IN CA3 HIPPOCAMPUS

S. Yamamoto, Y. Wang, T. Sakurai, S. Terakawa

Photon Med Res Ctr, Hamamatsu Univ Sch Med, Hamamatsu, Japan

Objective: The recent evidences suggest that the astrocytes participate in the excitatory neurotransmission. In the present study, we sought to determine the role of astrocytes in the process of delayed neuronal death (DND) following transient forebrain ischemia in rats.

Methods: In anesthetized SD rats (300 g), the studies were performed. Three days before 4-vessel occlusion (4VO), L-α-aminoadipic acid (L-αAAA, 2 mM, 10 μl), a gliotoxin, was injected by pressurized bolus into rt. CA3 hippocampus. Transient (10-min) forebrain ischemia was induced by 4VO, CBF was measured by laser-Doppler flowmetry, and intracellular Ca^{2+} concentration ($[Ca^{2+}]_i$) changes were examined by intravital fluorescence imaging using fluo3/AM, a Ca^{2+} indicator. To obtain the images, we employed the fiber-coupled confocal microscope, which is capable of observing confocal images inside the brain (1). In different animals, seven days after 4VO, numbers of residual neurons were counted on HE-stained slices. The results were compared among the control group (non-treated rats), the L-αAAA group (L-αAAA-injected rats), and the vehicle group (aCSF-injected rats).

Results: Three days after the injection, glial fibrillary acidic protein (GFAP) expression decreased in rt. CA3 of the L-αAAA-treated brains, indicating the reduction of astrocytes. 4VO decreased CBF (mean ± SD %) to 25 ± 18 in CA1 (n=6) and to 20 ± 11 in CA3 (n=6) of the control group, and to 28 ± 5 in CA3 of the L-αAAA group (n=5). They did not significantly differ among the groups. DND was remarkable, seven days after 4VO, in CA1 but not in CA3 of the non-treated brains (n=5) (Fig. 1). In rt. CA3 of the L-αAAA-treated brains (n=4), but not of the vehicle-treated brains (n=4), the comparable DND was noticed (Fig. 1). In the control group, the $[Ca^{2+}]_i$ increased in CA1 (n=6) upon 4VO and returned to the baseline level after 30-min reperfusion, although in CA3 (n=6) the increase was significantly ($p< 0.05$) less. Interestingly, in CA3, L-αAAA (n=5) but not vehicle (n=5) produced similar $[Ca^{2+}]_i$ increases to those in CA1 of the control group upon 4VO.

Conclusion: We observed that:

1. L-αAAA, a gliotoxin, decreased a number of astrocytes in CA3 three days later, but did not change CBF responses upon 4VO;
2. L-αAAA induced DND in CA3 seven days after 4VO, while without ischemia it did not induce it; and
3. L-αAAA produced similar calcium responses in CA3 upon 4VO to those observed in CA1, a vulnerable region.

These results suggested that astrocytes play neuroprotective roles in CA3 through suppressing $[Ca^{2+}]_i$ increase against ischemia/reperfusion.

Supported by the grant from MEXT #18053010 (SY).

Reference: 1) Sakurai T, Yamamoto S, Miyakawa A, et al. (2006) Fiber-coupled confocal microscope for real time imaging of cellular signals in vivo. Proc of SPIE 6088:608803-1 - 608803-6.

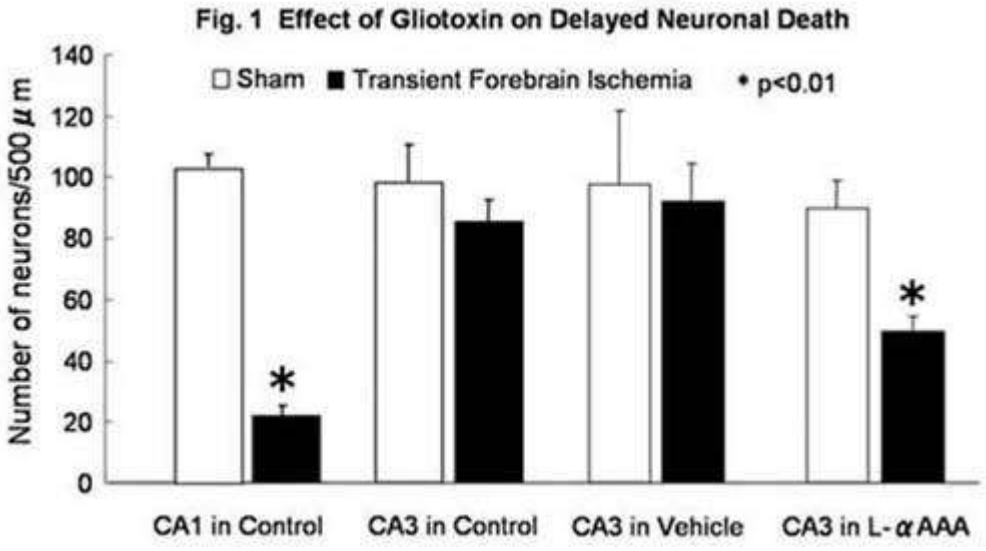
Fig. 1 Effect of Gliotoxin on Delayed Neuronal Death
□ Sham ■ Transient Forebrain Ischemia * p<0.01
Number of neurons/500 μm
140
120
100
80
60
40
20
0
*
*
CA1 in Control
CA3 in Control
CA3 in Vehicle
CA3 in L-αAAA

[Fig. 1]

Brain Oral Session: Cortical Spreading Depression

CLUSTERS OF CORTICAL SPREADING DEPOLARIZATIONS AFTER SUBARACHOID HEMORRHAGE MAY ADVANCE DELAYED CORTICAL ISCHEMIA VIA REDUCED O_2-SUPPLY AND INCREASED O_2-CONSUMPTION

B. Bosche[1,2], R. Graf[1], R.-I. Ernestus[2], C. Dohmen[3], T. Reithmeier[2], G. Brinker[2], A.J. Strong[4], J.P. Dreier[5], J. Woitzik[6,7]

[1]Max Planck Institut for Neurological Research with Klaus-Joachim-Zuelch-Laboratories of the Max Planck Society and the Faculty of Medicine of the University of Cologne, [2]Neurosurgery, [3]Neurology, University of Cologne, Cologne, Germany, [4]Department of Clinical Neuroscience, Institute of Psychiatry, King's College London, London, UK, [5]Departments of Neurology and Experimental Neurology, Charité Campus Mitte, University Medicine Berlin, Berlin, [6]Department of Neurosurgery, University Medicine Mannheim, Mannheim, [7]Department of Neurosurgery, Charité Campus Benjamin Franklin, University Medicine Berlin, Berlin, Germany

Objectives: The pathophysiology of delayed cortical ischemia (DCI) after subarachnoid hemorrhage (SAH) is poorly understood. It has recently been questioned whether vasospasm of large proximal arteries is the only cause for this life-threatening complication after SAH (Macdonald 2007, 2008), and DCI has been associated with clusters of cortical spreading depolarization (CSD) (Dreier 2006). In animal models, CSD is a well studied self-propagating wave of neuronal and astrocytic depolarization that can be associated with a biphasic response of cortical blood flow (Strong 2007, Sukhotinsky 2008) in penumbra and/or hypoxic conditions. In this study, we examined how clusters of CSD may promote DCI in human cerebral cortex after SAH.

Methods: Nine patients were prospectively recruited from two different neurosurgery centers (Cologne and Mannheim/Heidelberg, Germany). We used subdural electrocorticographic (ECoG) (Dreier 2006) and tissue oxygen pressure ($p_{ti}O_2$) spatiotemporal co-recordings. $P_{ti}O_2$ is predominantly correlated to local cerebral blood flow but also affected by tissue metabolism. We differentiate between "single" CSD (20%) and repetitive waves of CSD occurring within clusters (80%). We analyzed alterations of CSD-associated $p_{ti}O_2$ curve patterns (biphasic alteration, monophasic decrease or increase), the key features (baseline, minimum and maximum) as well as the specific phase durations and integrals.

Results: In a total recording time of 850 hours, 120 waves of CSD were found in eight of nine patients (~89%). CSD emerged predominantly between the fifth and seventh days after SAH. 53.2 % of CSDs were associated with clear $p_{ti}O_2$ alterations. We detected CSD within clusters occurring simultaneously with mainly biphasic $p_{ti}O_2$ responses comprising a primary hypoxic and secondary hyperoxic phase. Monophasic $p_{ti}O_2$ decreases were minor in number, however ~70% of them were detected in patients with MRI- or CT-proven DCI. The absolute number and the number/day of CSDs were positively correlated with the duration of the hypoxic phase of biphasic $p_{ti}O_2$ responses ($p=0.005$; $p=0.003$, respectively; Spearman's correlation) and the absolute number of CSDs was negatively correlated with the duration of the secondary hyperoxic phase ($p=0.008$). Eight of nine patients showed clusters of CSD. In five of them, four or more repetitive CSD with $p_{ti}O_2$ responses were detected and characterized by their specific order as 1st, 2nd, 3rd and 4th or higher rank within clusters. Analysis revealed that the primary hypoxic phase of the $p_{ti}O_2$ responses significantly increased over time within clusters ($p=0.011$, Friedman-test). We attribute these findings mainly to changes in local cerebral blood flow in the cortical microcirculation but also to augmented metabolism, both associated to CSD.

Conclusions: Our results indicate that clusters of CSD are involved in the reduction of O_2 supply and the increase of O_2 consumption, thereby promoting DCI, which may reveal a novel pathophysiological mechanism with clinical relevance after SAH.

References:

Macdonald RL et al. Nat clin prac neurol 2007.

Macdonald RL et al. Stroke 2008.

Dreier JP and Woitzik J et al. Brain 2006.

Strong AJ et al. Brain 2007.

Sukhotinsky I et al. J CBFM 2008.

ROBUST PET-MR IMAGE REGISTRATION METHODS FOR NON-HUMAN PRIMATES USING MUTUAL INFORMATION MEASURES

C. Sandiego, D. Weinzimmer, R.E. Carson

Yale University PET Center, New Haven, CT, USA

Objectives: Analysis of PET brain data from non-human primates (NHP) usually involves registration of PET and MR data. Typically, an early summed PET image (e.g., 0-10 min) provides high contrast between gray and white matter, important for a successful registration. However, kinetics and distribution vary dramatically between tracers, especially in studies involving pharmacological agents. This poses difficulties for PET-MR registrations, where algorithms sometimes fail due to relatively high activity outside the brain within the scanner field-of-view. The aim of this study is to develop a robust, automated method for PET-MR NHP registration for application to a wide variety of PET studies. The approach is to register different time periods of PET data to the MR and select the best transformation.

Methods: Forty-six PET datasets using five tracers were evaluated from rhesus monkey brains, acquired on the high resolution research tomograph (HRRT). T1-weighted MR images (M) were acquired on a 3T scanner, using an extremity coil. The PET-MR intrasubject registration was a two step process. First, the automated image registration (AIR) algorithm was used as an initialization step; this was followed by FLIRT (FSL) using normalized mutual information (NMI) to obtain the transformation. From each dynamic dataset, n=6 summed PET images, P_i, were created using different time intervals: 0-10, 0-30, 10-30, 30-60, 60-90, and 90-120 min. Using the registration algorithms between M and P_i, n transformations (T_i) were determined using each of the images P_i. The n transformations, T_k, k=1,…,n, were then applied to each PET summed image, P_i, i=1,…,n, to yield n^2 resliced PET images in MR space, $P_{ik}= T_k\{P_i\}$. Each P_{ik} was masked with a binary image created from the MR image to eliminate outside brain activity. NMI was then computed as a similarity measure between each resliced PET and the MR image due to the transformation applied, i.e., N_{ik}=NMI(M, P_{ik}) for j=1,...,n. To choose the optimal transformation, T*, the total NMI score was calculated across PET images ($S_k=\Sigma_i N_{ik}$) and T* was chosen as the transformation that provided the best S value. The quality of PET-MR registrations was assessed visually as either good or misregistered.

Results: Transforms from all time periods showed some misregistrations: $T_{0\text{-}10}$ (11%), $T_{0\text{-}30}$ (4%), $T_{10\text{-}30}$ (4%), $T_{30\text{-}60}$ (28%), $T_{60\text{-}90}$ (37%), and $T_{90\text{-}120}$ (65%). Low brain uptake (with respect to extra-brain uptake) and noisy images contributed to the poorer registrations. For the new method, the optimal transform T* varied across studies with respect to the selected time interval: $T_{0\text{-}10}$ (19.6%), $T_{0\text{-}30}$ and $T_{10\text{-}30}$ (28.3%), $T_{30\text{-}60}$ (15.2%), $T_{60\text{-}90}$ (6.5%), and $T_{90\text{-}120}$ (2.2%). For all studies evaluated, the chosen transform T* corresponded to an image designated as visually good.

Conclusions: A new method for automated PET-MR registration for NHP studies based on NMI measures is proposed, in order to handle the great variability in PET studies with different ligands. This initial evaluation suggests that the method is robust, i.e., no algorithm failures were detected. To further validate this approach, a more extensive quantitative evaluation must be performed with more tracers.

USING PET TO STUDY THE EFFECTS OF DEEP BRAIN STIMULATION OF THE SUBTHALAMIC NUCLEUS IN THE TREATMENT OF PARKINSONS DISEASE

J. Sidtis[1,2], M. Tagliati[3], D. Sidtis[1,4], V. Dhawan[5], D. Eidelberg[5]

[1]Geriatrics, Nathan Kline Institute, Orangeburg, [2]Psychiatry, New York University Medical School, [3]Neurology, Mount Sinai School of Medicine, [4]Speech Language Pathology and Audiology, New York University, New York, [5]Center for Neuroscience, Feinstein Institute for Medical Research, Manhasset, NY, USA

Background and aims: Bilateral high-frequency deep brain stimulation of the subthalamic nucleus (STN-DBS) has become a significant approach to the treatment of Parkinsons Disease (PD). However, the mechanism of action is still not well understood.

Methods: Seven subjects with bilateral STN-DBS underwent two sets of 12 H20 PET scans on separate days, once with the stimulators on at therapeutic settings, once with the stimulators off. For each session, there were 2 replications of a rest state and 5 speech tasks. In addition to the 12 scans, composite images were created from the initial 6 (first half) and the subsequent 6 scans (second half). Regions of interest encompassing each slice were applied to 59 slices. CBF was measured at 3 thresholds: maximum CBF, mean CBF of voxels at the upper 10% of activity, and mean CBF of all voxels (100%). Total CBF was calculated at 10% (mean CBF*10% voxels) and at 100% (mean CBF*100% voxels).

Purpose: The determination of global effects is critical to characterizing regional changes associated with specific tasks and specific neurological disorders. This study examined global effects of bilateral STN-DBS on CBF in subjects with ideopathic PD. This research is part of a larger study of the effects of PD and STN-DBS on regional CBF and speech.

Results: The effects of STN-DBS and time (first versus second half) were evaluated using nonparametric statistics to avoid assumptions about underlying distributions. In the ON condition, there were no significant effects of time. However, in the OFF condition, there were significant decreases from the first to second half of the scanning session for CBF max, and for total flow at 10% but not 100% (Wilcoxon Signed Ranks Test, $p < 0.03$). There were no significant ON-OFF effects for the first half of the study, but in the second half of the study OFF was significantly lower than ON for each measure (Wilcoxon Signed Ranks Test, $p < 0.03$).The time course of these declines was further examined by ordering the scans by their sequence during the scan session rather than task. As expected, there was no significant effect of sequence in the ON condition. In the OFF condition, there were significant declines for both CBF max (Chi-square = 23.64; $p = 0.014$) and CBF 10% (Chi-square = 26.03; $p = 0.006$).

Conclusions: CBF was stable when STN-DBS was ON, but CBF decreased over time in the OFF condition. The effects of STN-DBS have been considered in terms of specific changes in the basal ganglia, and on local field effects. These results demonstrate a third mechanism of action in STN-DBS: a global effect consisting of higher peak CBF. The changes in CBF associated with STN-DBS may reflect generalized increases in cortical excitability. This mechanism may play a role in therapeutic response, undesired side effects, or both. PET should play a significant role in understanding these effects [Supported by R01 DC007658].

261

Brain Oral Session: Functional Brain Imaging

HIV CAUSES PREMATURE AGING OF BRAIN FUNCTION

B. Ances[1], F. Vaida[2], J. Yeh[3], I. Grant[4], A. McCutchan[3], R. Ellis[5], R. Buxton[6]

[1]Neurology, Washington University School of Medicine, Saint Louis, MO, [2]Family and Preventative Medicine, [3]Medicine, [4]Psychiatry, [5]Neurosciences, [6]Radiology, University of California at San Diego, San Diego, CA, USA

Background and aims: Highly active antiretroviral therapy (HAART) has increased the prevalence of HIV infected older individuals (> 50 years old). A growing need has arisen to characterize the effects of aging and HIV infection. While the effects of aging and HIV have been studied in other organ systems, their interaction on brain function has not been investigated. We used non-invasive functional magnetic resonance imaging (fMRI) to measure the blood oxygen level dependent (BOLD) effect, cerebral blood flow (CBF), and calculated cerebral metabolic rate of oxygen consumption ($CMRO_2$) within HIV infected (HIV+) and HIV- controls. We hypothesized that HIV infection will confer a proaging effect on brain function due to ongoing viral induced inflammation and oxidative stress.

Methods: BOLD and CBF responses were obtained from 26 HIV+ subjects and 25 HIV- controls, from 20-62 years old, on a 3 Tesla General Electric scanner. All subjects underwent both mild hypercapnia and functional activation experiments. Mild hypercapnia provided a calibration method for calculating functional $CMRO_2$ changes. Functional activation consisted of a black and white radial checkerboard flickering at 8 Hz. Clusters of CBF activated voxels within the visual cortex (VC) were assessed. A Wilcoxon rank test investigated if differences in measured fMRI outcomes (baseline CBF, functional changes in CBF, BOLD, and $CMRO_2$) were present between HIV+ and HIV- subjects. The association and the interaction between fMRI measures, HIV status, and age were investigated using a multiple regression model.

Results: The median age for HIV+ subjects and HIV- controls was similar with no significant differences observed for either sex or education. Baseline CBF was reduced for both age ($p < 0.001$) and HIV status ($p < 0.001$). HIV infection was equivalent to a 15 year increase in age. Similarly, both age ($p = 0.005$) and HIV ($p = 0.01$) led to increases in functional CBF changes, with HIV infection equivalent to a 21 year increase in age. Functional BOLD changes decreased with age ($p = 0.001$) and HIV status ($p = 0.05$). HIV infection was equivalent to a 15 year increase in age dor functional BOLD changes. Calculated functional $CMRO_2$ changes ($p < 0.001$) increased with both age ($p < 0.001$) and HIV status ($p = 0.007$) with a significant interaction present ($p=0.001$).

Conclusions: Our results suggest that HIV infection accelerates aging effects on brain function. We hypothesize that these changes in brain function could be caused by ongoing inflammation and oxidative stress due to HIV**.** Functional CBF and $CMRO_2$ changes were elevated in HIV+ subjects compared to HIV- controls, possibly suggesting an element of increased metabolic requirements due to neuroinflammation. However, the coupling between CBF and $CMRO_2$ remained preserved suggesting that HIV infection does not alter the basic physiology between increased metabolic requirements and oxygen delivery.

PARAMETRIC MAPPING OF NK1 RECEPTOR BINDING USING [^{11}C]R116301

S. Wolfensberger, M. Yaqub, B. van Berckel, B. Windhorst, J. Leysen, A. Lammertsma, **R. Boellaard**

Nuclear Medicine & PET Research, VU University Medical Center, Amsterdam, The Netherlands

Purpose: NK1 receptors have been implicated in various neuropsychiatric disorders. [^{11}C]R116301 has been proposed as a PET tracer for visualizing and quantifying NK1 receptors in vivo. In previous studies, both simplified reference tissue models and tissue ratio methods have been used, in combination with a region of interest (ROI) approach. The purpose of this study was to determine the optimal method for parametric analysis of [^{11}C]R116301 binding.

Methods: Two dynamic PET studies were performed in 11 normal volunteers. Three subjects were scanned before and after a blocking dose of aprepitant and 8 subjects were scanned twice under baseline conditions (test-retest). Total scan duration was 90 minutes and for all subjects scans were separated by 5 hours. Data were analysed using striatum as region of interest and cerebellum as reference tissue. Parametric binding potential (BP_{ND}) images were obtained using receptor parametric mapping (RPM), a basis function implementation of the simplified reference tissue model (SRTM), five versions of a multi-linear reference tissue method (MRTM), and Logan graphical analyses with reference tissue input. In addition, striatum to cerebellum standardized uptake value ratio minus 1 (SUVr-1) for the time interval 60-90 minutes, an approximation for BP_{ND}, was evaluated. Results of all these methods were compared with BP_{ND} derived using SRTM. Finally, effects of shortening scan duration on BP_{ND} were evaluated.

Results: When comparing kinetic methods with SRTM, best performance was obtained with RPM (fitting for R_1, k_2 and BP_{ND}). This method showed high correlation (r^2 = 0.93 and 0.82, respectively), with acceptable bias (regression slopes 1.10 and 0.88, respectively). RPM also provided good test-retest variability (VAR = 10.1 ± 8.9% and 12.6 ± 5.5%, respectively) with good reliability (ICC = 0.78 and 0.86, respectively). Linearized methods, i.e. all MRTM versions and reference Logan, failed to provide accurate and precise estimates of BP_{ND}, probably due to the slow kinetics of this tracer. Surprisingly, SUVr-1 also showed high correlation with SRTM (r^2 = 0.96, regression slope = 0.85) with both excellent test-retest VAR (6.2% ± 3.07) and ICC (0.91). After reducing analysis time to 60 minutes, RPM correlation with 90 minutes SRTM remained high (r^2 = 0.87, regression slope = 0.90). There was, however, some decline in test-retest VAR (17.13% ± 14.79) and reliability (ICC = 0.62). In addition, there was only a small reduction in performance of SUVr-1 when the time interval was reduced to 80-90 minutes.

Conclusion: RPM is the optimal parametric method for quantifying [^{11}C]R116301 binding. It shows both good test-retest variability and reliability, and there is scope for reducing scan times. A simple tissue ratio method also holds promise for routine clinical applications.

263

Brain Poster Session: Brain Imaging: Neurologic Disease

THE REPRODUCIBILITY OF THE CALIBRATED BOLD IN HEALTH AND DISEASE

B. Ances[1], F. Vaida[2], R. Buxton[3]

[1]Neurology, Washington University in St. Louis, Saint Louis, MO, [2]Medicine, [3]Radiology, University of California at San Diego, San Diego, CA, USA

Background and aims: Reproducibility studies of blood oxygen level dependent (BOLD) functional magnetic resonance imaging (fMRI) are needed to understand basic physiology of neurovascular coupling as a single scan may be affected by a subject's performance, variations in scanner hardware, or biological factors. We assessed the reproducibility of calibrated BOLD fMRI in both HIV infected subjects (HIV+) and healthy controls (HIV-).

Methods: BOLD and cerebral blood flow (CBF) responses were obtained from 8 HIV+ subjects and 10 HIV- controls, from 20-45 years old, on a 3 Tesla General Electric scanner at two separate scanning sessions separated by at least 3 months. All subjects underwent calibrated BOLD studies consisting of both mild hypercapnia and functional activation experiments. Mild hypercapnia provided a calibration method for calculating functional $CMRO_2$ changes. Functional activation consisted of a black and white radial checkerboard flickering at 8 Hz. Clusters of CBF activated voxels within the visual cortex (VC) were assessed. The coefficient of variation (CV), a normalized measure of dispersion of a probability distribution, was determined for each calibrated BOLD measures outcome(functional changes in CBF, BOLD, and cerebral metabolic rate of oxygen consumption ($CMRO_2$)) within both HIV+ and HIV- subjects. A variance components random effects model was used for each fMRI variable.

Results: The median age for HIV+ subjects and HIV- controls was similar with no significant differences observed for either sex or education. For HIV- controls the intrasubject CV values for functional BOLD, CBF, and $CMRO_2$ were 8.8%, 10%, and 10.5% respectively. For these individuals total variability was greatest for functional $CMRO_2$ (47.3%) compared to either CBF (30.1%) or BOLD (16%). For HIV+ subjects, intrasubject variability was greater for each of the functional measures - 38.8% for CBF, 69.8% for BOLD, and 11.2% for $CMRO_2$. Total variability was also increased for HIV+ subjects for each of these fMRI measures (61% for CBF, 74.6% for BOLD, and 17% for $CMRO_2$).

Conclusions: HIV+ subjects have greater total variability than HIV- controls for measured functional changes in CBF and BOLD. In contrast, calculated functional $CMRO_2$ changes were less variable for HIV+ subjects compared to HIV- controls. A possible breakdown in neurovascular coupling may occur in HIV+ subjects.

265

Brain Poster Session: Cerebral Metabolic Regulation

MONITORING OXYGEN PARTIAL PRESSURE IN CEREBRAL MICROVASCULATURE WITH HIGH SPATIAL RESOLUTION USING PHOSPHORESCENCE LIFETIME IMAGING

M. Yaseen[1], V. Srinivasan[1], S. Sakadžić[1], S. Vinogradov[2], C. Ayata[3,4], D. Boas[1]

[1]Photon Migration Imaging Laboratory, MGH/MIT/HMS Athinuola A. Martinos Center for Biomedical Imaging, Massachusetts General Hospital/Harvard Medical School, Charlestown, MA, [2]Department of Biochemistry and Biophysics, University of Pennsylvania, Philadelphia, PA, [3]Stroke and Neurovascular Regulation Laboratory, Department of Radiology, Massachusetts General Hospital/ Harvard Medical School, [4]Stroke Service and Neuroscience Intensive Care Unit, Department of Neurology, Massachusets General Hospital/Harvard Medical School, Charlestown, MA, USA

Objective: Identifying changes in metabolic activity in brain tissue is important for gaining insight into functional activation, head trauma, and various neuropathologies such as stroke and Alzheimer's disease. Determining the distribution of oxygen in the cerebral vasculature is essential to the evaluation of metabolic activity. Currently, the most widely accepted techniques for measuring oxygen levels in vivo suffer from at least one of several possible limitations, including poor spatial resolution, the risk of physiological disruption resultant from an invasive measurement, or uncertainty associated with the fact that the technique does not provide a direct measure of O_2.

We have developed and tested a confocal optical imaging system to determine oxygen partial pressure (pO_2) in microvessels with high spatial resolution. The system quantifies pO_2 by measuring phosphorescence quenching of exogenous, O_2-sensitive dyes confined to blood plasma, such as Oxyphor R2. The phosphorescence lifetimes of these compounds vary with O_2 concentration as described by the Stern-Volmer equation. The technique, therefore, provides a minimally invasive, direct measurement of dissolved O_2 concentration in the cortical microvasculature.

Methods: The system's ability to perform lifetime imaging was evaluated by imaging heterogeneous phosphorescent phantoms. Theoretical calculations were also performed to determine the optimal imaging parameters to yield pO_2.

Experiments were performed to quantify pO_2 in cortical vessels of Sprague Dawley rats under a variety of conditions such as hypoxia, hyperoxia, and functional stimulation. The vessels were exposed through a sealed cranial window. After intravenously administering R2, the dye was excited using a low power, continuous wave 532 nm diode laser. An electro-optical modulator was used to control and gate the intensity of the excitation beam. Phosphorescence signal was collected through time-correlated single photon counting at a 50 MHz sampling rate using an avalanche photodiode. We developed custom software to control data acquisition and image processing. pO_2 was determined at select points of interest by binning the photon counts, fitting the phosphorescence decay profiles to an exponential decay, and subsequently using a calibration curve to relate lifetime measurement to pO_2.

Results: Figure 1 displays an image of merging cortical veins of a rat under normoxic conditions, collected by integrating the phosphorescence decay profiles at each pixel. The non-uniform brightness both between and within the vessels illustrates the heterogeneity of vascular pO_2 over short distances. By varying the fraction of inspired oxygen, changes in phosphorescence lifetime within the vessels are observed.

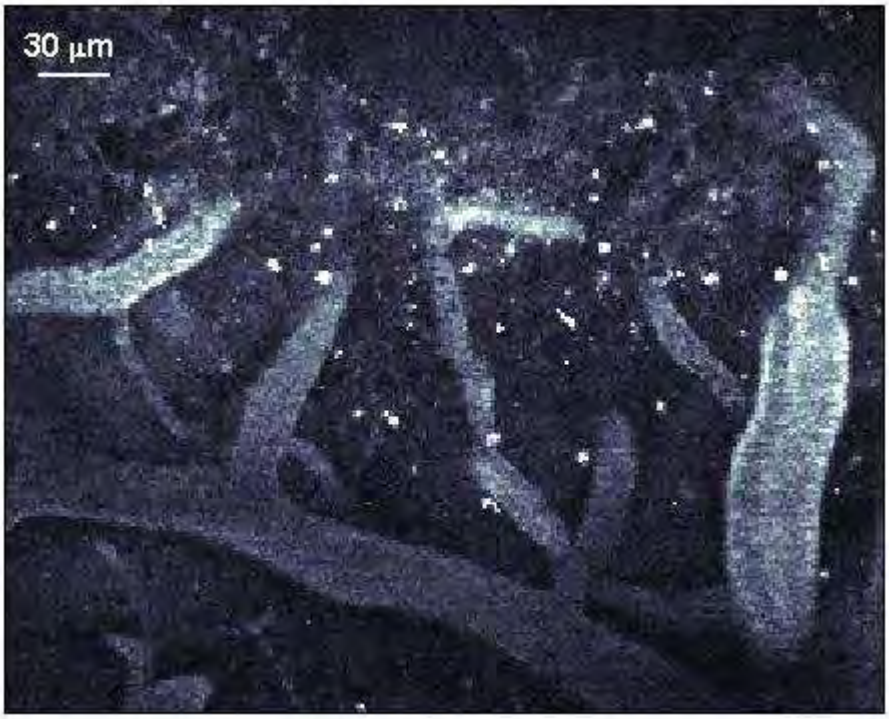

[Figure 1. Merging veins in rat cortex]

Conclusions: Our system demonstrates potential for characterizing spatial and temporal variation of cerebral pO_2 under several different physiological conditions. When coupled with simultaneous blood flow measurements, our system will allow for high-resolution quantification of cerebral metabolic rate of oxygen ($CMRO_2$), providing a better understanding of metabolic dynamics during functional stimulation and under various neuropathologies.

Brain Poster Session: Neonatal Ischemia

THE ROLE OF ACTIVATED MICROGLIA/MACROPHAGES IN NEONATAL FOCAL STROKE

Z. Vexler[1], J. Faustino[1], A. Klibanov[2], C. Jonhson[1], N. Derugin[3], M. Wendland[4]

[1]Neurology, University California San Francisco, San Francisco, CA, [2]University of Virginia, Charlottesville, VA, [3]Neurosurgery, [4]Radiology, University California San Francisco, San Francisco, CA, USA

Objectives: Studies in adult stroke models have demonstrated that pharmacologic strategies that limit macrophage accumulation/microglial activation are neuroprotective, suggesting that microglial cells contribute to injury induced by cerebral ischemia. Recent studies, however, showed that selective ablation of proliferating microglial cells exacerbates ischemic injury in the adult brain and that microglial cells can support neurogenesis, indicating beneficial properties of these cells. In the neonatal brain, macrophage accumulation is substantial both after hypoxia-ischemia and focal ischemic stroke but the relative contribution of activated microglia and invading macrophages in injury is unknown. We have previously reported that early after transient focal cerebral ischemia in neonatal rats macrophages are comprised of activated microglia rather than invaded macrophages (Denker et al, J. Neurochem. 2007). The aim of this study was to determine if depletion of microglial cells affects injury acutely after neonatal focal stroke.

Methods: Postnatal day 5 (P5) rats were injected with liposome-encapsulated clodronate or empty liposomes (3ul, intra-cortical). At P7, rats were subjected to a 3 hr middle cerebral artery occlusion (MCAO) and underwent diffusion-weighted MRI during occlusion for evidence of injury. Injured rats were sacrificed 24 hr post-reperfusion for measurements of injury volume (determined in 6 consecutive Nissl-stained coronal sections), densities of microglial cells in adjacent sections (Iba1 immunohistochemistry), and numbers of neurons with cleaved caspase-3. Cytokine concentrations (8-plex, IL1a, IL1b, TNF-a, IL-6, IL-18, CINC-1, MCP-1 and MIP-1) and degradation of a structural protein spectrin by caspase-3 and calpain (Westernn blot analysis) were measured in injured and contralateral cortex in separate groups of rats.

Results: Depletion of microglia by clodronate was confirmed in injured rats by lack of Iba1 staining whereas the expected pattern of ramified microglial cells in contralateral hemisphere and ameboid cells in injured tissue (Dingman et al, J. Neurochem. 2007) was observed in vehicle-treated rats. Injury volumes were not significantly different between clodronate-treated and vehicle-treated groups (51.1±7.4% and 54.8±8.3%, respectively, n=5-6 per group). Spectrin cleavage mediated independently by calpains and caspase-3 was profoundly increased in injured tissue in both groups, as was evident from Western Blot analysis (11-15 and 20-25 fold increase for calpain- and caspase-3 cleaved spectrin, respectively), but spectrin degradation was not significantly affected but clodronate treatment. Microglial depletion affected cytokine concentrations in contralateral hemisphere, IL-6 levels in particular. Surprisingly, in ischemic-reperfused tissue, the levels of IL1b, TNF-a, IL-6, CINC-1 and MCP-1 which were elevated by MCAO, remained unaffected and only the levels of MIP-1a were significantly reduced following microglial depletion.

Summary and conclusions: Our findings demonstrate that in neonatal rats depletion of microglial cells does not reduce injury size after focal ischemia-reperfusion, at least acutely. We are currently exploring whether depletion of microglial cells results in reduction of phagocytosis of apoptotic neurons and enhances injury over time.

NIH NS44025, AHA GIA 0855235F.

CORTICAL MICROHEMORRHAGES REDUCE STIMULUS-EVOKED CALCIUM RESPONSES IN NEARBY NEURONS

F.A. Cianchetti, N. Nishimura, C.B. Schaffer

Biomedical Engineering, Cornell University, Ithaca, NY, USA

Objectives: Microhemorrhages are a common feature of the aging cerebral cortex and increased incidence of such lesions appears to be correlated to cognitive dysfunction [1]. Here, we investigate the changes in the response of somatosensory neurons to a peripheral stimulus after hemorrhage of a nearby microvessel.

Methods: We use in vivo two-photon excited fluorescence microscopy to image vasculature as well as cell-resolved neural activity in the brain of urethane-anesthetized rats. Blood vessels are labeled with an intravenous injection of tetramethylrhodamine-dextran and neural activity is imaged using the calcium-sensitive fluorescent dye Oregon Green BAPTA, which is bulk loaded into cells in somatosensory cortex [2]. Astrocytes are labeled with surlforhodamine 101 [3] so that neurons and glia can be distinguished. We use 100-fs duration, ~1-μJ, 800-nm laser pulses to selectively injure a specifically targeted arteriole, leading to a 50 - 200-μm diameter hemorrhage [4]. We monitor intracellular calcium transients in response to an electric stimulus to the hind paw at baseline (Fig. 1a) and at 5 to 30 minutes after inducing a microhemorrhage for neurons and neuropil within 200 μm of the hemorrhage site (Fig. 1b).

Results: To characterize the neural response, we calculate the normalized fluorescence change, dF/F_0, over a 4-s window around the stimulus. An average response to 10 stimuli is determined for each neuron or region of neuropil. We then compare the amplitude of the average response at baseline (Fig. 1c) to that after a microhemorrhage (Fig. 1d). We find that the average amplitude of the calcium response drops to 50% of baseline after the microhemorrhage, while no change is observed in controls where no hemorrhage is induced ($p< 0.0001$, 30 (15) neurons and neuropil regions across 4 hemorrhaged (control) rats, t-test).

Conclusions: We have shown that a small hemorrhage in the brain adversely impacts the functionality of nearby neurons. In most of the cases we examined, the amplitude of the evoked neural response is significantly reduced, and in a few instances the response is eliminated completely. This decrease in neural response could play a role in the loss of cognitive function following brain microhemorrhages.

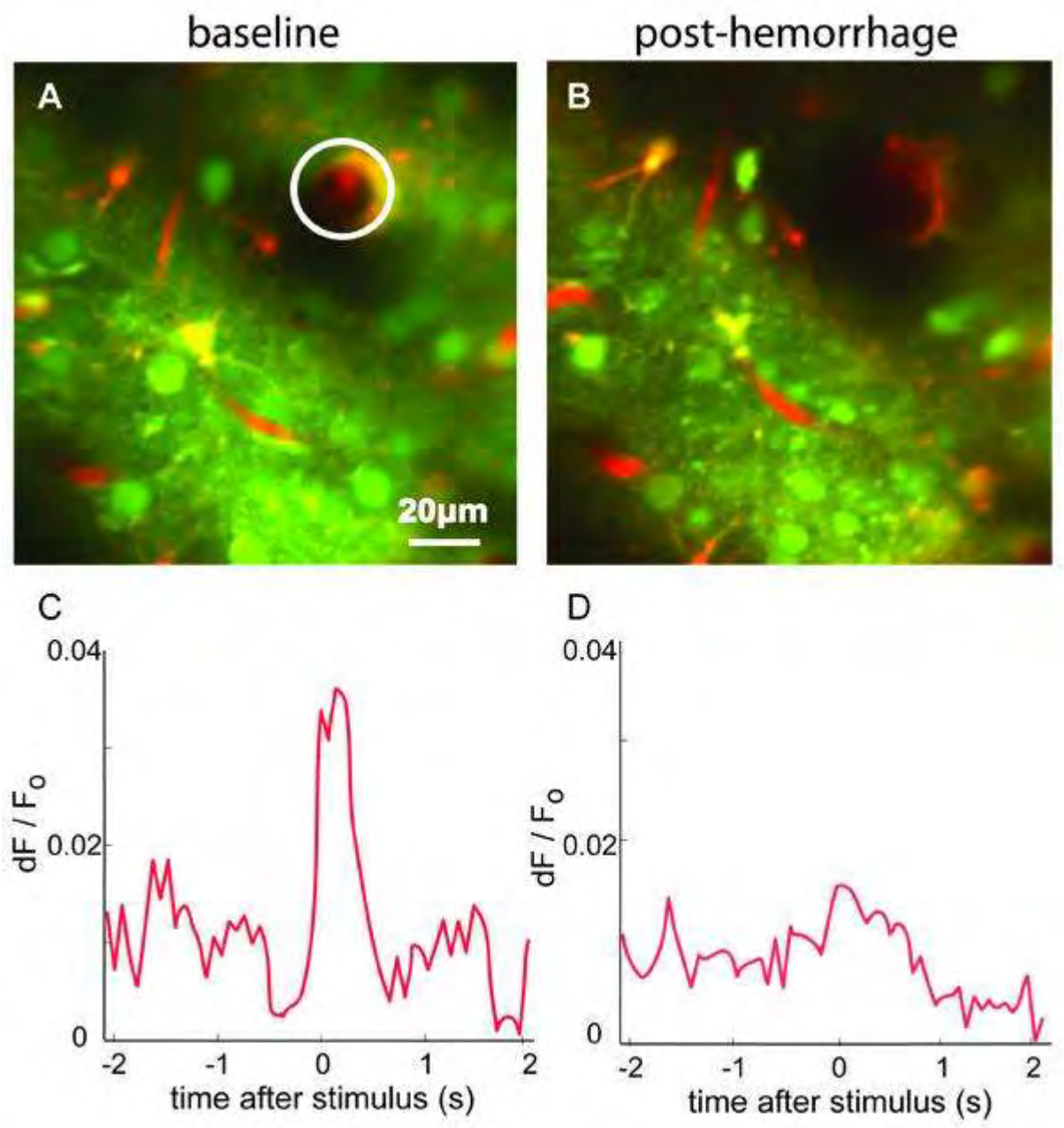

[Figure1]

Fig. 1: Two-photon imaging of stimulus evoked calcium dynamics after microhemorrhage. Blood vessels (red) and cell bodies (green) (a) before and (b) after triggering a hemorrhage in the target arteriole using femtosecond laser ablation (circle in(a)). Stimulus evoked calcium transients, before (c) and after (d) the microhemorrhage.

References:

[1] Cullen 2005, Cerebral Blood Flow Metabolism 25,1656.

[2] Stosiek 2003, Proc Natl Acad Sci USA. (2003) 100,7319.

[3] Nimmerjahn 2004, Nature Methods (2004) 1,31.

[4] Nishimura 2006, Nature Methods (2006) 3,99.

270

Brain Poster Session: Transcriptional Regulation

REGULATION OF CELL SURVIVAL RELATED GENES IN CEREBELLUM FOLLOWING HYPOXIA PRECONDITIONING

H. Xu, F. Sharp

Neurology Department and M.I.N.D Institute, University of California at Davis Medical Center, Sacramento, CA, USA

Objectives: Hypoxia Preconditioning (HP) in the brain is a well-known endogenous protective paradigm in which pre-exposure to sub-lethal hypoxia can protect the brain from injury due to lethal hypoxia or ischemia occurring 24 to 72 hours later (Gidday 2006). Though HP has been studied extensively, its mechanisms are still not understood. Since de novo gene transcription and protein expression are required for the hypoxia preconditioning, we have extended previous studies by performing whole genome expression profiling of individual brain regions of adult mice and carefully following the entire time course of hypoxia preconditioning.

Methods: Adult C57BL/6 male mice (8~9 weeks old) were exposed to systemic hypoxia (8% O2) for 3 hours and allowed to recover in normoxia for 24 hr. Animals were sacrificed and the brains were removed and dissected into individual brain regions at multiple time points during the 3hour hypoxia and subsequent 24hours of reoxygenation. Total RNA was purified and gene expression assessed with Affymetrix Mouse Expression 430 2.0 arrays. One-Way ANOVA with false discovery rate correction for multiple comparisons was used to identify differentially regulated genes. The differentially regulated genes were then subjected to a variety of bioinformatics analyses including functional annotation, pathway and promoter sequence analyses.

Result: Among the brain regions examined, cerebellum demonstrated the largest numbers of gene expression changes following hypoxia preconditioning. The greatest numbers of regulated genes in cerebellum were observed immediately after the 3hours of hypoxia and 1hour after reoxygenation. In contrast to the forebrain, where down regulation of gene expression predominated over up-regulation events during this time period, cerebellum exhibited a predominant up-regulation of genes following HP. Compared to hippocampus, substantially more genes involved in cell survival regulation were up-regulated in cerebellum during this time period. Besides hypoxia inducible factor (HIF), various nuclear receptor transcription factors were found to play important roles in regulating the unique gene expression response cerebellum after HP. Most notably, a novel group of genes regulated by transcription factor hepatic nuclear factor 4A (HNF4A) have been identified as being hypoxia responsive genes in cerebellum.

Conclusions: HP induces both time-dependent and region-dependent gene expression responses. The substantial number of unique genes regulated in cerebellum may be critical not only for the survival of the organism during systemic hypoxia, but also for the maturation of neuroprotection effect of HP. Region-specific transcription factors, including HNF4A, likely contribute to region specific genomic responses to hypoxia preconditioning.

References: Gidday JM. (2006) Cerebral preconditioning and ischaemic tolerance. Nat Rev Neurosci 7:437-448.

PRETREATMENT WITH ETHYL EICOSAPENTAENOIC ACID AMELIORATES ISCHEMIC BRAIN DAMAGE IN A RAT TRANSIENT FOCAL ISCHEMIA MODEL

M. Ueda, T. Inaba, Y. Nishiyama, S. Okubo, S. Suda, N. Kamiya, C. Nagata, H. Nagayama, Y. Katayama

Neurology, Nippon Medical School, Tokyo, Japan

Introduction: Long-chain n-3 polyunsaturated fatty acids, such as eicosapentaenoic acid (EPA) and docosahexaenoic acid (DHA), which are derived from marine products, have attracted considerable attention, because fish consumption is inversely related to stroke risk in a meta-analysis of cohort studies [1]. In addition, a recent clinical controlled trial has shown that ethyl EPA (EPA-E) reduces stroke recurrence in Japanese hypercholesterolemic patients [2]. The present study examined neuroprotective effects of EPA-E pretreatment using a rat transient focal ischemia model.

Methods: Under halothane anesthesia, 24 male Sprague-Dawley rats, weighing 250-300g, were subjected to 90 min focal ischemia using an intraluminal suture technique following an overnight fast. EPA-E (100mg/kg/day) or vehicle was orally administered once a day for seven days prior to ischemia induction. Rectal temperature was maintained at 37˚C during ischemia and up to 2 hrs after reperfusion, and physiological parameters, including arterial blood pressure, arterial blood gases and blood glucose level, were determined several times during the surgical procedures. In addition, cortical blood flow was monitored during ischemia and up to 2 hrs after reperfusion using Laser-Doppler flowmetry. Neurological scores were assessed based on hemiparesis and abnormal posture using grading scale [3] at 24 hrs after reperfusion, and then animals were decapitated (n = 7, each) or perfusion-fixed using 4% paraformaldehyde (n = 5, each) following blood examination for serum lipid profiles and fatty acid levels (EPA, DHA, gamma-linoleic acid, arachidonic acid). Infarct and edema volumes were determined using 2,3,5-triphenyltetrazolium chloride (TTC) stained brain sections (n = 7, each), and TUNEL staining and immunohistochemistry using antibodies against 8-hydroxydeoxyguanosine (8-OHdG) or 4-hydroxy-2-nonenal (4-HNE) were performed to examine apoptosis, oxidative DNA damage and lipid peroxidation (n = 5, each). Statistical significance was set at $p < 0.05$.

Results: All physiological variables were within normal limits. Serum EPA levels, but not others, were significantly increased in the EPA group than the vehicle group. Cortical blood flow was decreased to approximately 20% of baseline during ischemia without any statistical differences between the groups. EPA-E treated rats showed significant reduction in infarct and edema volumes, as well as significantly improved neurological scores, compared with the vehicle treated animals. Immunohistochemistry revealed significant decrease in numbers of 8-OHdG, 4-HNE and TUNEL positive cortical cells in the EPA group than the vehicle group.

Conclusion: The present study showed that pretreatment with EPA-E (100mg/kg/day) for 7 days ameliorated ischemic brain damage following transient focal ischemia without any cortical blood flow changes in rats, and that reduced oxidative stress might be involved in the neuroprotective mechanisms of EPA-E.

References:

[1] He K, et al.; Stroke 35, 1538-1542 (2004).

[2] Tanaka K, et al.; Stroke 39, 2052-2058 (2008).

[3] Amemiya S, et al.; Eur J Pharmacol 516, 125-130 (2005).

FENFLURAMINE DECREASES 5-HT_{1B} BINDING OF [^{11}C]AZ10419369 IN THE PRIMATE BRAIN

S.J. Finnema[1], A. Varrone[1], T.J. Hwang[1], B. Gulyás[1], E. Pierson[2], L. Farde[1], **C. Halldin**[1]

[1]Clinical Neuroscience, Karolinska Institutet, Stockholm, Sweden, [2]CNS Discovery, AstraZeneca, Wilmington, DE, USA

Objectives: We recently reported an initial PET-study using the selective serotonin 5-HT_{1B} receptor radioligand [^{11}C]AZ10419369 (Pierson et al., 2008). The 5-HT_{1B} receptor has a role in the modulation of synaptic serotonin release. The aim of the present study was to assess the sensitivity of [^{11}C]AZ10419369 binding to pharmacological manipulation of endogenous serotonin levels in cynomolgus monkeys.

Methods: A total of 12 PET measurements were conducted on six experimental days in four cynomolgus monkeys. On each day two measurements were performed using i.v. bolus administration of [^{11}C]AZ10419369. A baseline measurement was followed by a displacement measurement in which fenfluramine (1.0 or 5.0 mg/kg) was infused i.v. between 15 and 20 minutes after radioligand injection. The monkeys were anaesthetized with sevofluran (2-5%), except in two measurements where a mixture of ketamine and xylazine was used. Emission data were acquired for 123 minutes using the HRRT PET-system. The specific binding ratio was calculated as the ratio of the area under the curve (45-123 min) of the target region to the reference regions (cerebellum). The displacement effect was estimated as relative change (%) in specific binding ratio.

Results: Administration of fenfluramine had no evident effect on radioactivity in the reference region (cerebellum). After administration of fenfluramine (1.0 and 5.0 mg/kg), the respective binding ratios decreased in the occipital cortex by 33 ± 11% and 49 ± 19%, in striatopallidal complex by 18 ± 23% and 38 ± 9%, and in midbrain by 28 ± 18% and 49 ± 16%, respectively.

Conclusions: This preliminary study supports that the new 5-HT_{1B}-ligand [^{11}C]AZ10419369 is sensitive to endogenous serotonin levels in vivo. The radioligand may accordingly serve as a tool to further examine serotonin-related brain functions and psychiatric disorders, as well as effects of drugs on endogenous levels of serotonin in brain.

References: Pierson et al., NeuroImage 2008; 41 (3) 1075-1085.

RELATIONSHIP BETWEEN CEREBRAL OXYGEN EXCHANGE(COE) AND CEREBRAL BLOOD VOLUME(CBV) IN CHOPSTICKS OPERATION

N. Oka[1], K. Yoshino[1], S. Ishizaki[2], T. Kato[3]

[1]Graduate School of Media and Governance, [2]Department of Media and Governance, Keio University, Kanagawa, [3]Department of Brain Environmental Research, KATOBRAIN Co., Ltd., Tokyo, Japan

Background and aims: In rehabilitation medical treatment, evaluation by the brain activity has been widely accepted. Our previous research using near-infrared light imaging confirmed tendencies that an increase/decrease in COE (cerebral oxygen exchange) is related to a degree of task difficulty and performance improvement in sensory-motor cortical areas (BA6,4,3,1,2). In the prior research, it is known that the hand movements stimulate the sensory-motor cortical areas in the same side. Therefore, the relationship between COE and CBV (cerebral blood volume) in sensory-motor cortical areas by the same side movements was examined in this research.

Methods: Subjects were five normal adults (three males and two females) who use chopsticks by their right hands. The performance was evaluated by the number of small cube moved using chopsticks to a plate (10cm away) in one trial (15s). Tasks were right hand condition and left condition. One condition was composed of 20 trials. The measurement regions was determined to sensory motor cortical areas based on 10-20 international EEG methods. The analysis were performed in significant regions where COE changes (O-D values) were found between the tasks (t-test: $p < 0.05$). The relationships between COE and CBV were examined by the average using all trials.

Purpose: The purpose of this study was to examine the relationships between COE (oxyhemoglobin minus deoxyhemoglobin: O-D) and CBV (oxyhemoglobin plus deoxyhemoglobin: O-D) in the sensory motor areas on the same side as the hand.

Results: In right hand condition, COE did not increase ($0 < O\text{-}D$) but CBV increased ($0 < O+D$) in the right sensory-motor cortical areas. On the other hand, in left hand condition, COE increased ($O\text{-}D < 0$) and CBV decreased ($O+D < 0$) (Figure).

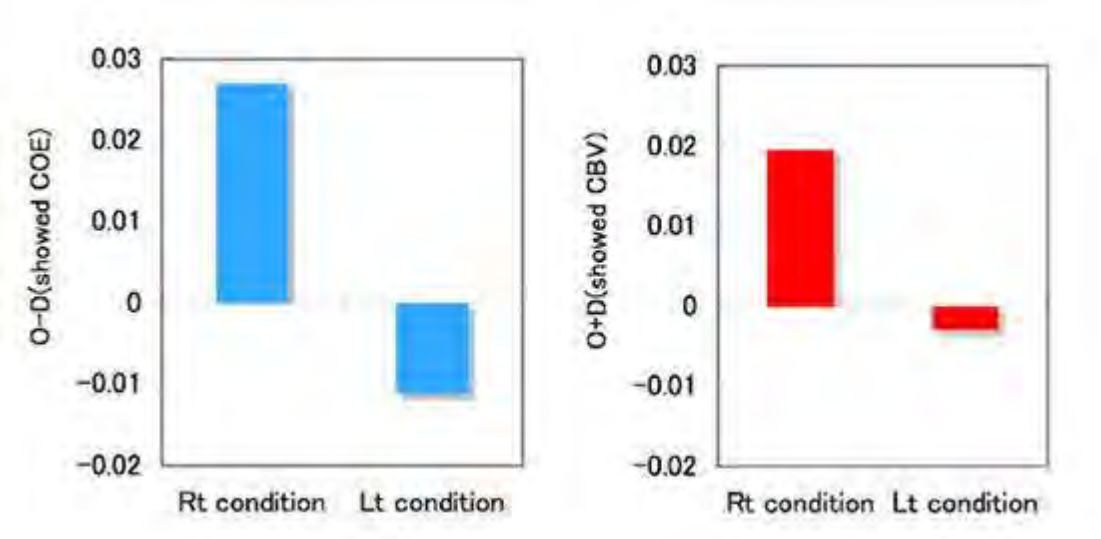

[Change of sensory-motor area in right hemisphere]

Conclusions: In this study, it was showed that CBV did not increase even if COE increased. This results suggested it is necessary to reconsider direct coupling regarding CBV increase as cortical activation.

STRIATAL DOPAMINERGIC FUNCTION DURING SPEECH PRODUCTION

K. Simonyan[1], P. Herscovitch[2]

[1]Laryngeal and Speech Section, NINDS/NIH, [2]PET Department, Clinical Center/NIH, Bethesda, MD, USA

Voluntary voice production for speech and song is a complex motor behavior controlled by the laryngeal motor cortex and its input and output structures, such as basal ganglia, thalamus and cerebellum. Neuroanatomical studies in non-human primates and neuroimaging studies in humans have shown that the putamen receives the strongest of all basal ganglia connections from the laryngeal motor cortex and is functionally active during voluntary voice production. Although the neuroanatomical and functional organization of the basal ganglia has been described, little is known about their neurotransmitter function during voluntary voice production in humans. The objective of this study, therefore, was to identify endogenous dopamine release during rest and speech production in healthy humans using PET with [^{11}C]raclopride (RAC).

Thirteen right-handed monolingual English-speaking subjects (mean age 54.8 years, 6F/7M) were studied. Subjects underwent a dynamic 100-min PET scan with RAC, which included 50-min rest and 50-min speech production (GE Advance tomograph). RAC was administered as a 1-min bolus followed by a constant infusion. A high-resolution MRI was obtained in all subjects. PET images were corrected for subject motion and registered to each individual MRI normalized to the Talairach-Tournoux space. Volumes of interest were defined on each MRI using macrolabels maps and transferred to the co-registered PET images. RAC binding potential (BP) was determined as a ratio of concentrations in the regions with (putamen and caudate nucleus) and without (cerebellum) specific binding from the three frames over 40-50 min at rest and eight frames over 60-100 min during speech production. The speech-induced effects on dopamine release were estimated as the percentage change from resting baseline of the RAC BP values during speech production and their statistical significance was assessed using two-tailed paired t-test ($p \leq 0.05$, corrected).

The baseline RAC BP values were 2.17±0.36 in right putamen, 2.34±0.35 in left putamen, 1.58±0.37 in right caudate nucleus and 1.55±0.41 in left caudate nucleus (mean ± SD). During speech production, RAC BP was significantly reduced by 10.7% in right putamen, 11.1% in left putamen, 11.7% in right caudate nucleus and 13.6% in left caudate nucleus (all $p < 0.0008$). Decreased RAC BP values in the putamen showed left-hemispheric lateralization during speech production ($p = 0.04$).

We have demonstrated, for the first time to our knowledge, endogenous release of striatal dopamine during speech production in healthy subjects. Its left-hemispheric lateralization is consistent with the observation of left-lateralized functional networks during voluntary voice production in humans, suggesting behavior-specific integration and adaptation of the dopamine system for motor control of voluntary voice production. These results are critical for understanding the central mechanisms of voluntary voice control in humans and would potentially help in elucidating the pathophysiology of motor control deficits in neurological voice and speech disorders.

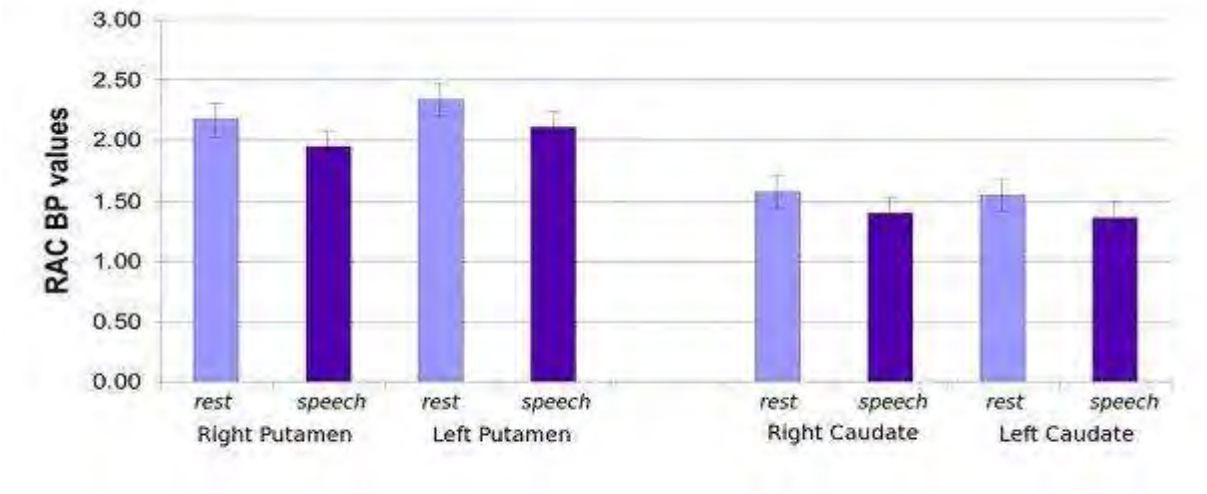

[RAC BP values]

BrainPET Poster Session: Brain Imaging: Stroke

PERFUSION INSTABILITY IN THE PENUMBRA INFLUENCES INFARCT PROBABILITY IN ACUTE ISCHEMIC STROKE PATIENTS

J.-M. Lee[1], H. An[2], A.L. Ford[1], K.D. Vo[3], A.M. Nassief[1], C.P. Derdeyn[3], W.J. Powers[4], W. Lin[2]

[1]Neurology, Washington University School of Medicine, Saint Louis, MO, [2]Radiology, University of North Carolina, Chapel Hill, NC, [3]Radiology, Washington University in St. Louis, St. Louis, MO, [4]Neurology, University of North Carolina, Chapel Hill, NC, USA

Objectives: It has been postulated that cerebral blood flow (CBF) and metabolism are unstable during the acute phase of cerebral ischemia. However, animal models which rely on fixed occlusions of cerebral vessels, do not allow study of this phenomenon; and human studies have largely relied on single measures during acute ischemia. In this study, we sought to serially examine MR-measured CBF during hyperacute ischemia in a cohort of stroke patients to assess the impact of CBF fluctuations on infarct probability.

Methods: Eight acute ischemic stroke patients were imaged at three time-points: 2.7 ± 0.8 hrs (tp1) and 6.2 ± 0.2 hrs (tp2) after symptom onset; and at 1 m (tp3) to delineate the region of the final infarct (FLAIR image). Six patients received intravenous tPA prior to tp1 while two patients did not. Dynamic susceptibility contrast method was used to obtain CBF. Measurements were normalized to the contralateral unaffected hemisphere. Co-registration and tissue segmentation were performed to align the timepoints and separate gray from white matter, respectively. Brain voxels were classified into CBF deciles at tp1, and further subclassified (based on tp2 measures of the same voxel) into voxels with increased CBF vs. without increased CBF. Probability of infarction (based on co-registered tp3 FLAIR images) was calculated for each decile and compared between tp1 alone and tp1 with increased CBF at tp2 vs. tp1 without increased CBF at tp2. These 3 groups were compared using a repeated-measure ANOVA with post-hoc Newman-Keuls test.

Results: Shown are ΔCBF maps from 2 patients (panel A, B), representing CBF changes between tp1 and tp2 (red increase, green no change, blue decrease). CBF showed significant variability from tp1 to tp2 in all patients. To examine if this CBF variability contributed to infarct probability, 3 probability curves were created and compared. The infarct probability of CBF deciles at tp1 was compared to:

1. that of the subset of voxels with increased CBF at tp2 vs.
2. that of the subset of voxels without increased CBF at tp2 (panel C).

A lower probability of infarction was predicted when tp2 CBF improvement (red triangles) was considered compared to considering tp1 data alone (black circles, $p < 0.05$); likewise, a higher probability of infarction was predicted when tp2 CBF non-improvement (blue squares) was considered compared to considering tp1 data alone (black circles, $p < 0.05$). Moreover, altered probabilities were most notable in the CBF ranges from 20-50%, which likely represent the theoretical penumbra.

Conclusion: CBF is highly dynamic during acute ischemia and impacts infarct probability, especially in the "penumbral range" of CBF (20-50%). These findings underscore the importance of dynamic changes in CBF during acute ischemia, and caution that single time-point imaging belies the complex physiology during acute ischemia.

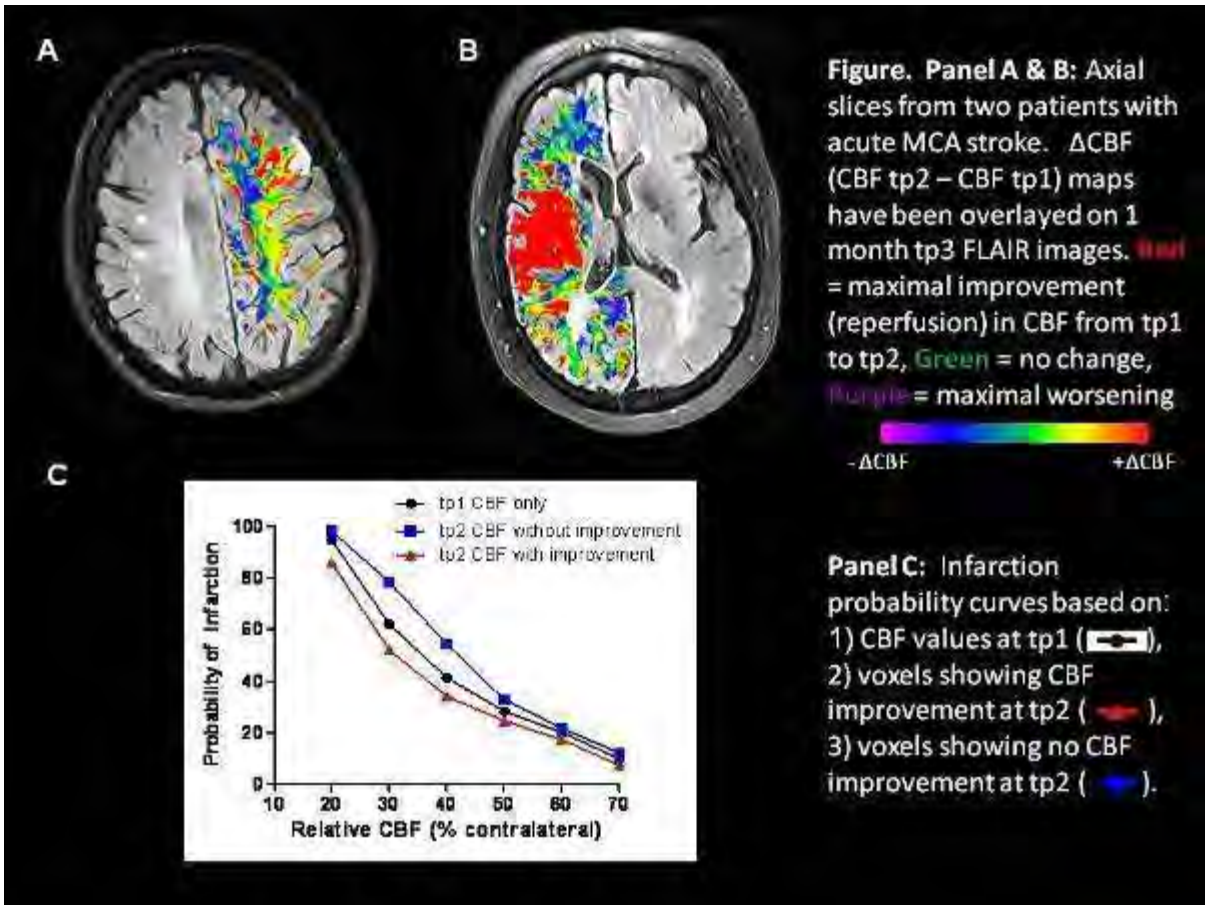
A
B
C
Figure. Panel A & B: Axial slices from two patients with acute MCA stroke. ΔCBF (CBF tp2 – CBF tp1) maps have been overlayed on 1 month tp3 FLAIR images. Red = maximal improvement (reperfusion) in CBF from tp1 to tp2, Green = no change, Purple = maximal worsening
-ΔCBF
+ΔCBF
tp1 CBF only
tp2 CBF without improvement
tp2 CBF with improvement
Probability of Infarction
Relative CBF (% contralateral)
Panel C: Infarction probability curves based on: 1) CBF values at tp1 ( ), 2) voxels showing CBF improvement at tp2 ( ), 3) voxels showing no CBF improvement at tp2 ( ).

[FIGURE]

COMPARISON OF MANUAL AND AUTOMATED METHODS FOR MEASURING STRIATAL D2 RECEPTOR BINDING IN PRIMARY DYSTONIA: A PET STUDY WITH [^{11}C]RACLOPRIDE

S. Peng[1], Y. Ma[1], M. Carbon[1], S. Bressman[2], V. Dhawan[1], D. Eidelberg[1]

[1]Center for Neurosciences, The Feinstein Institute for Medical Research, Manhasset, [2]Department of Neurology, Beth Israel Medical Center, New York, NY, USA

Objectives: Primary dystonia is one of genetic brain disorders resulting from dysfunction in the neurotransmission of dopamine D2 receptor systems. Brain imaging with PET has revealed different degrees of loss in striatal D2 receptor availability in subjects with DYT1 and DYT6 genotypes. Many analytical techniques have been proposed to quantify D2 receptor binding with various levels of complexities. The objective of this work was to evaluate the use of simplified approaches to evaluate loss in D2 receptor binding in dystonia gene carriers.

Methods: [^{11}C]raclopride (RAC) PET and MR images were acquired from 22 DYT1 gene carriers (age 52±15 yr), 12 DYT6 gene carriers (age 34±16 yr) and 11 normal controls (age 42±16 yr). MR scans were correlated with PET to define striatal volumes of interest (VOI) either manually in the native space or automatically following the spatial normalization into Talairach space. Binding indices in caudate and putamen were measured by distribution volume ratio (DVR) over 30-70 min or striatal-to-occiptal ratio minus 1 (SOR) at 60 min post injection. Differences in RAC binding among subject groups were evaluated statistically by using parameters computed from different analysis methods. Subject age was included as a covariate in the design of a multivariate general linear model.

Results: All analyses showed that striatal RAC binding in the DYT1 and DYT6 groups was reduced compared to normal mean (e.g. Figure 1). The reduction in the DYT6 group was 2-3 times larger than that in the DYT1 group, with the mean values predicted from the statistical model. DVR values from the manual analysis in the native space revealed that RAC binding decreased in the caudate ($F= 4.3$; $p< 0.02$) and the putamen ($F=4.9$; $p< 0.013$). On the other hand, SOR values from the manual analysis demonstrated almost twice as much decrease than DVR in RAC binding in the caudate ($F=19.3$; $p< 0.0001$) and the putamen ($F=18.4$; $p< 0.0001$). In addition, SOR values calculated from the automatic analysis yielded similar results as those from the manual analysis in the caudate ($F=17.8$; $p< 0.0001$) and putamen ($F=18.2$; $p< 0.0001$).

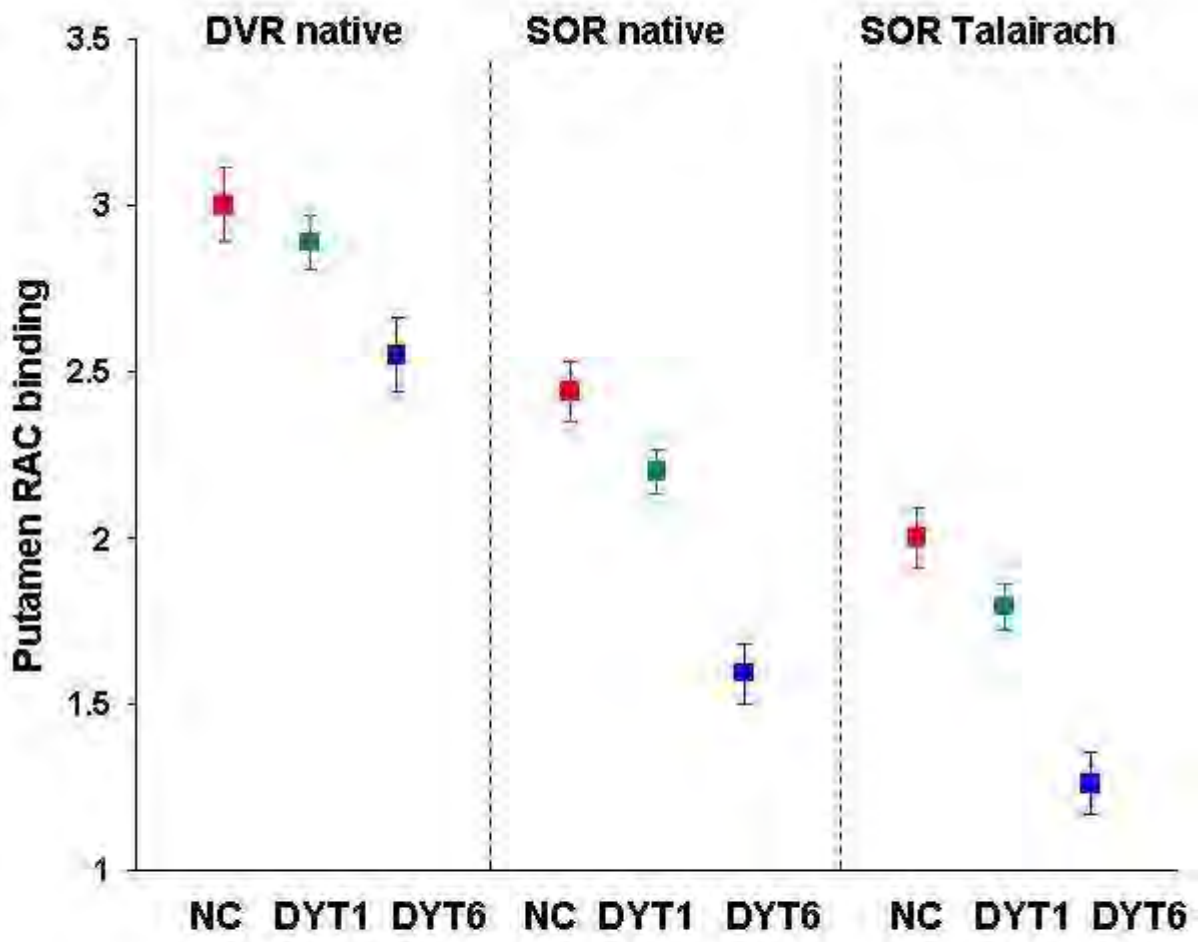

Reduction in striatal RAC binding in dystonia gene carriers. The graph shows the mean and standard error from age-corrected data in the native and standard space respectively.

[Figure 1. Dystonia v.s. normal control (NC)]

Conclusions: Analyses with different binding parameters and VOI strategies have revealed significant losses in striatal D2 receptor binding in dystonia gene carriers. The striatal-to-occipital uptake ratio obtained from a static frame is more sensitive in discriminating subject groups than the distribute volume ratio from dynamic data acquisition. This simple parameter can be computed automatically in the standard brain space to permit rapid brain mapping analysis on a VOI or voxel

basis. This method may be valuable in quantifying topographic evolution in D2 receptor availability in other neuropsychiatric disorders.

References: 1. Asanuma K et al. Decreased [^{11}C] raclopride binding in striatum in non-manifesting DYT1 carriers. Neurology 2005; 64(2):347-349.

SALT-INDUCED KINASE 1 REGULATED HISTONE ACETYLATION IN PRIMARY NEURONS AND ITS ROLE IN ANDROGEN-MEDIATED NEUROPROTECTION IN EXPERIMENTAL STROKE

J. Cheng, P. Herson, W. Zhang, P. Hurn

Oregon Health and Science University, Portland, OR, USA

Androgens alter experimental stroke outcomes in a dose- and androgen receptor- dependent manner. At physiological doses, both testosterone and its nonaromatizable metabolite dihyrdotestosteron (DHT) reduce infarct sizes after focal cerebral ischemia, and the protection is blocked by flutamide, a specific androgen receptor antagonist. Using microarray, we have previously shown that salt-induced kinase 1 (SIK-1) is induced by DHT in penumbral tissue after middle cerebral artery occlusion (MCAO). SIK1 belongs to the sucrose nonfermenting-1 protein kinase/AMP-activated protein kinase family and encodes a Ser/Thr kinase. In C. elegans, the homology of SIK-1 is believed to function as a histone deacetylase (HDAC) kinase, thus inhibiting HDAC activities and enhancing histone acetylation in neurons. The present study determined if SIK-1 is an important mediator of androgen neuroprotection in experimental stroke and acts by modulating histone acetylation. First, we confirmed by quantitative real-time PCR (qPCR) that SIK-1 was induced in the cortical and striatal penumbra of castrated male rats treated with DHT (15 mg/implant) at 6 and 12 h following MCAO, and SIK1 induction was lost with concomitant administration of flutamide (15 mg/pellet). To examine the involvement of SIK-1 in neuronal pathophysiology after ischemia, we constructed a lentivirus expressing small interference RNA (siRNA) with >70% knockdown efficiency on murine SIK-1 mRNA. Lentivirus-mediated SIK-1 knockdown significantly exacerbated neuronal cell death induced by oxygen and glucose deprivation (OGD) as determined by MTT assay and lactate dehydrogenase (LDH) release. At 22 h reoxygenation following 2.5 h OGD, MTT levels were decreased, and LDH release from damaged cells was increased in neurons infected with lentiviruses expressing SIK1 siRNA (MTT: 42 ± 7%; LDH: 65 ± 11%, n=4) as compared to control neurons without lentiviral infection (MTT: 68 ± 5%; LDH: 54 ± 11%) or neurons infected with empty virus (MTT: 78 ± 9%; LDH: 54 ± 11%) or virus expressing unfuctional siRNA (MTT: 86 ± 10%; LDH: 45 ± 9%). Consistent with the hypothesis that SIK-1 functions as a HDAC kinase and promotes histone acetylation, SIK-1 knockdown resulted in a decrease in baseline histone acetylation in primary neurons. However, HDAC inhibitor trichostatin A (TSA)-enhanced baseline histone acetylation level was not attenuated by lentivirus-delivered siRNA against SIK-1. In contrast, SIK-1 knockdown blunted TSA-elevated histone acetylation at 6 h reoxygenation following 2.5 h OGD and subsequently abolished the neuroprotection of TSA at 22 h reoxygenation. Our results suggest that DHT-induced post-ischemic expression of SIK-1, a novel neuroprotective gene in vitro, may contribute to androgen's neuroprotective properties at physiologically relevant levels and may act as an endogenous HDAC kinase.

IMAGING AND QUANTITATION OF CANNABINOID CB_1 RECEPTORS IN HEALTHY HUMAN BRAIN USING THE INVERSE AGONIST RADIOLIGAND [^{11}C]MEPPEP

G. Terry[1,2], J.-S. Liow[1], S. Zoghbi[1], **J. Hirvonen**[1], A. Farris[1], A. Lerner[1], J. Tauscher[3], J. Schaus[3], L. Phebus[3], C. Felder[3], C. Morse[1], J. Hong[1], C. Halldin[2], V. Pike[1], R. Innis[1]

[1]Molecular Imaging Branch, National Institute of Mental Health, Bethesda, MD, USA, [2]Department of Clinical Neuroscience, Psychiatry Section, Karolinska Institutet, Stockholm, Sweden, [3]Lilly Research Laboratories, Eli Lilly and Company, Indianapolis, IN, USA

Objectives: [^{11}C]MePPEP ((3R,5R)-5-(3-methoxy-phenyl)-3-((R)-1-phenyl-ethylamino)-1-(4-trifluoromethyl-phenyl)-pyrrolidin-2-one) is a positron emission tomography (PET) radioligand for imaging and quantifying cannabinoid CB_1 receptors that has been studied in rodents (Terry et al.) and monkeys (Yasuno et al.). The goals of this study were to compare the simple outcome measure of brain uptake (determined from 40 to 80 minutes) with distribution volume (determined from brain data and serial concentrations of parent radioligand separated from radiometabolites in plasma) in healthy human brain. Although our initial scans lasted for 150 minutes, we later extended the acquisitions to 210 minutes to ensure that time-independent measures of distribution volume were stable and well identified.

Methods: [^{11}C]MePPEP was studied in 16 subjects with 23 PET scans (643 ± 95 MBq) using a GE Advance camera (GE Healthcare). We examined the ability of [^{11}C]MePPEP to image and quantify CB_1 receptors by using the "gold standard" of serial measurements of unchanged parent in arterial plasma for up to 120 minutes and brain radioactivity for up to either 150 minutes (n = 8) or 210 minutes (n = 8) after injection. We examined the retest reliability (i.e., within subject variability) of our measurements by conducting test/retest studies (n = 7), as well as the intersubject variability (i.e., coefficient of variability = SD/mean) of our measurements.

Results: The brain uptake of [^{11}C]MePPEP was high (200 - 400% SUV) and relatively stable, which allowed images to be acquired for 210 minutes (Fig. 1). A two-tissue compartment model provided a better fit of the measured data than a one-tissue compartment model. Distribution volume (V_T) was well identified (5%) and provided stable values from 60 minutes until the end of 210 minutes of scanning. We observed a moderate intra- and intersubject variability of brain uptake (7% and 18%), and a higher intra- and intersubject variability of V_T (13% and 55%).

Conclusions: The distribution volume (V_T) of [^{11}C]MePPEP was well measured by the standard criteria of identifiability, time stability, and moderate retest variability. However, the intersubject variability of V_T for [^{11}C]MePPEP was much higher than that of the simple measure of brain uptake between 40 and 80 minutes in this small sample size. We do not know the true variability of CB_1 receptor density in this sample. Nevertheless, in comparison to brain uptake, we suspect that V_T is more accurate (since it corrects for exposure of the radioligand to the brain), but is less precise (because of the noise added by the plasma measurements and modeling analysis). Thus, both brain uptake and V_T should be used with caution in any clinical studies, since neither has both high accuracy and high precision.

References:

Terry G, et al. (2008) Neuroimage 41:690-698.

Yasuno F, et al. (2008) Neuropsychopharmacology 33:259-269.

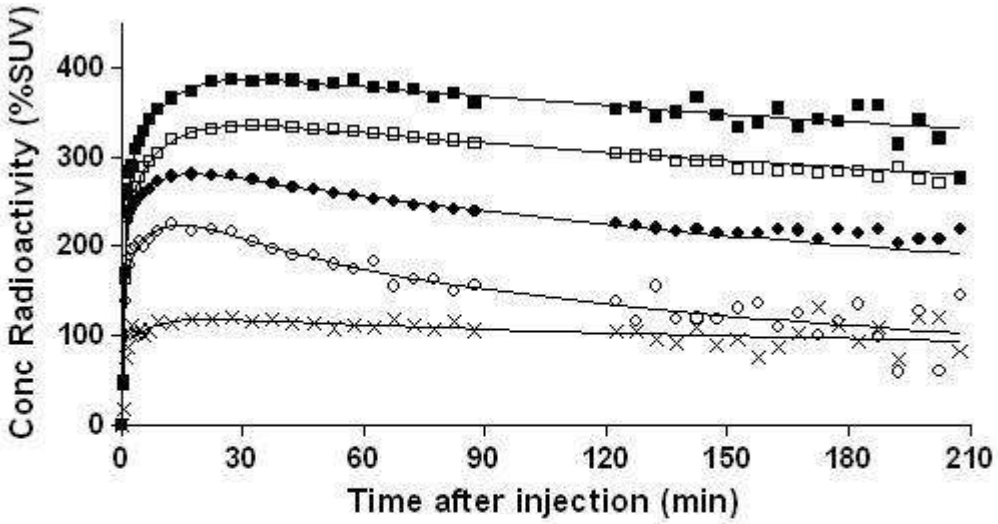

FIGURE 1. Time-activity curves of [^{11}C]MePPEP in brain. Measurements from the putamen (■), prefrontal cortex (□), cerebellum (●), pons (○), and white matter (x) were fitted with an unconstrained 2-tissue compartment model (–). Data from this subject is representative of all subjects. Conc = concentration.

[Time-activity curves of [11C]MePPEP in brain]

282

Brain Poster Session: Cerebral Vascular Regulation

CEREBROVASCULAR REACTIVITY AND CEREBRAL AUTOREGULATION: DISTINCT PHYSIOLOGICAL PROPERTIES?

E. Carrera[1], L. Lee[2], S. Giannopoulos[1], **R. Marshall**[1]

[1]Neurology, [2]Radiology, Columbia University Medical Center, New York, NY, USA

Background: Cerebrovascular reactivity testing (CVR) with CO2 challenge is used clinically as a measure of cerebrovascular reserve. Spontaneous, short time-frame, cerebral autoregulation (CA) can also be measured by determining correlations between simultaneous fluctuations of blood pressure and cerebral blood flow velocities. It is unknown, however, whether CVR measures the same physiological process as CA.

Methods: We prospectively studied CVR and CA in 20 healthy volunteers (mean age 32 ± 8, 15 men). CBFV was monitored continuously with transcranial Doppler over both middle cerebral arteries at a depth of 50-56mm using a standard headframe. Arterial blood pressure was continuously monitored using a non-invasive finger cuff. After 10 minutes monitoring at normocapnea, 5% CO2 was administered via facemask for 10 minutes. Using continuous, in-line capnometry, CVR was calculated as percent increase in MCA mean flow velocity (MFV) per mm Hg pCO2 during the inhalation period. Cerebral CA was determined by transfer function analysis to derive the phase shift between spontaneous ABP and CBFV fluctuations at 0.1 Hz.

Results: CO2 inhalation produced an average CVR of 2.85 ± 1.3%. A significant average decrease in phase shift occurred in response to CO2 inhalation, from 37.6 ±11.4 degrees to 21.0 ± 15.9 degrees ($p < .001$). However, there was no evidence of a significant correlation between CVR and CA change during CO2 inhalation (Pearson correlation coefficient = -0.248, $p = 0.32$), nor between CVR and baseline CA (Pearson = 0.341, $p = 0.17$), across individuals in our group.

Conclusion: Phase shift between ABP and CBFV is reduced during CO2 challenge, demonstrating a decrease in spontaneous CA with vasodilatation. Our finding that neither magnitude of CA change nor baseline CA correlated with the degree of CVR suggests that cerebrovascular reserve and CA measure distinct physiological properties. Further investigation into the relationship between these 2 components of cerebral hemodynamics is warranted to determine how best to make use of these measurements in pathological states where these properties may dissociate.

283

Brain Oral Session: Cerebrovascular Regulation

WHEN DOES ANGIOGENESIS ACCOMPANIED WITH RBC FLOW DEVELOP IN ISCHEMIC TISSUE AFTER PERMANENT MCA OCCLUSION IN C57BL/6J MICE?

M. Tomita[1], J. Tatarishvili[1], H. Toriumi[1], Y. Tomita[1,2], M. Unekawa[1], H. Hattori[1], N. Suzuki[1]

[1]Neurology, [2]Department of Preventive Medicine for Cerebrovascular Disease, Keio University School of Medicine, Tokyo, Japan

The time of angiogenesis in ischemic tissue may vary, depending upon levels of angiogenic factors (e.g., VEGF, FGFb, EGF, or TGF-b), or the degree of functional recovery (BBB or arterial regulation via muscles, glial sheathing and nerves). In this study, morphological development of new vessels and resumption of RBC flow after ischemia were targeted. Sixteen male C57BL/6J mice, 10 weeks old, under isoflurane anesthesia, with a closed skull window in the left parieto-temporal cortex, were observed every day after permanent MCA occlusion (sham-operated control n=8). The temporo-parietal area centering arteriolo-arteriolar anastomoses (AAA) between MCA and ACA were observed. FITC-labeled RBCs was injected into the tail vein at each day. The mouse head was fixed to a head holder with a landmark bar, so that long-term changes of the same microvasculature could be observed every day. A laser scanning confocal fluorescence microscope was used for RBC tracking and RBC velocity and number measurements with our software KEIO-IS2 (Matlab domain)(Tomita, M. et.al. Microcirculation 15:163, 2008). A halogen lamp (for general observation), laser beam at 488 nm (FITC for RBC) or at 533 nm (RITC for capillaries) was used as appropriate. The mouse was returned to the animal house after each day's experiment and brought back to the laboratory next day. This procedure was repeated for a week. Day 0-1: MCAO induced immediate RBC disappearance (anoxia) in the core ischemic region, and to a lesser extent in the penumbra near the AAA. However, since RITC (plasma indicator) filled capillaries, the capillaries were somehow patent immediately after occlusion, implying occurrence of RBC sieving or plasma skimming. Such plasma passage became impeded within a few hours in the core. Day 1-2: Fragments of microvessels and tissue debris were observed, with abundant macrophages which phagocytosed RITC that had leaked from the vessels. Day 3: We recognized newly built vessels, mostly immature capillaries and reconstructed veins, around the marginal zone of the infarction. As shown in the Figure A and B (a rough sketch), straight capillaries that sprouted from the arteriolo-arteriolar cut end connected with dilated and tortuous vessels. Figure C shows revascularization of remodeled veins and a reactive part with many modular protrusions. Labeled RBC were flowing the capillaries and remodeled veins, with unsteady motions. Day 7: Revascularization similar to that reported by Tomita Y et al. (J CBFM. 25:858, 2005) was observed in cerebral ischemic tissue by 7 day after MCAO in mice. The ischemic core appeared to be liquefied in all 8 mice. In conclusion, angiogenesis was apparent in the marginal zone as early as day 3 after MCA occlusion in mice.

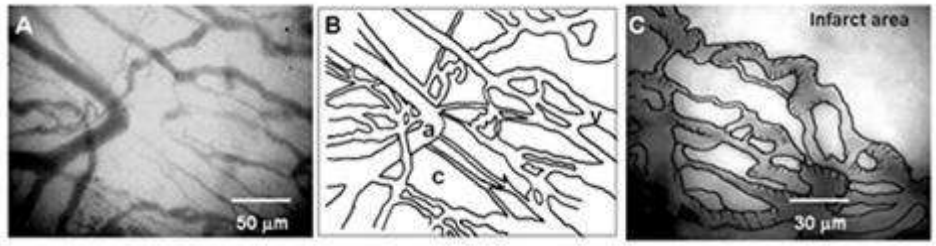

[Fig. 1]

UNBIASED LOGAN GRAPHICAL ANALYSIS USING THE RENORMALIZATION METHOD

H. Hontani[1], N. Hoshino[1], M. Naganawa[2], K. Sakaguchi[2], M. Sakata[3], K. Ishiwata[3], Y. Kimura[2]

[1]Department of Computer Science and Engineering, Nagoya Institute of Technology, Nagoya, [2]Molecular Imaging Center, National Institute of Radiological Sciences, Chiba, [3]Positron Medical Center, Tokyo Metropolitan Institute of Gerontology, Tokyo, Japan

Objective: The Logan Graphical Analysis (LGA) is used for imaging a distribution volume V_T. For LGA, we compute a set of $\{(x(t), y(t))\}$ from the measured time-activity curves in tissue (tTAC) and plasma (pTAC) to find a best-fitting line $y(t) = \alpha\, x(t) + \beta$. (Eq.1).

Here, x(t) and y(t) are defined as a ratio of an integrated pTAC over tTAC and an integrated tTAC over tTAC, respectively. As known[1] , linear regression (LR) underestimates V_T and its unbiased estimator is expected.

Renormalization Method (RM) [2] enables an unbiased maximum likelihood estimation under the existence of inhomogeneous noises both in x and y by successive evaluation of bias. In this study, the applicability of RM to LGA was investigated.

Methods: Let $X_t = (x(t),y(t),1)^T$ and $U=(u_1,u_2,u_3)^T$. Then, we can rewrite (Eq.1) as $X_t^T U = 0$, where $||U|| = 1$ and $V_T = -u_1/u_2$. Let C_t denote the covariance matrix of the noise of X_t. The maximum likelihood estimates of u_i minimize $J^{MLE}(U) = \sum_t W_t(U)\, (X_t^T U)^2$, where $W_t(U)=1/(U^T C_t U)$. Though, the perturbation theorem tells us that the estimates become biased.

RM removes the bias by iteratively minimizing $J^{REN}(U)$ instead of J^{MLE} : $J^{REN}(U) = \sum_t W_t(U)\, \{(X_t^T U)^2 - U^T C_t U\}$, where the last term compensates the bias. In RM, the covariance matrix C_t should be given, and it is unknown in advance. Thus, a set of voxel-based noisy TACs were simulated using physiologically plausible kinetic parameters, and the mean of C_t was calculated from the set of simulated TACs.

We applied RM and LM to synthesized tTACs and to real one of [^{11}C]SA4503-PET. For generating the synthesized data, we simulated a set of voxel-based tTACs using a measured pTAC and the rate constant of [^{11}C]SA4503 [3].

Results:

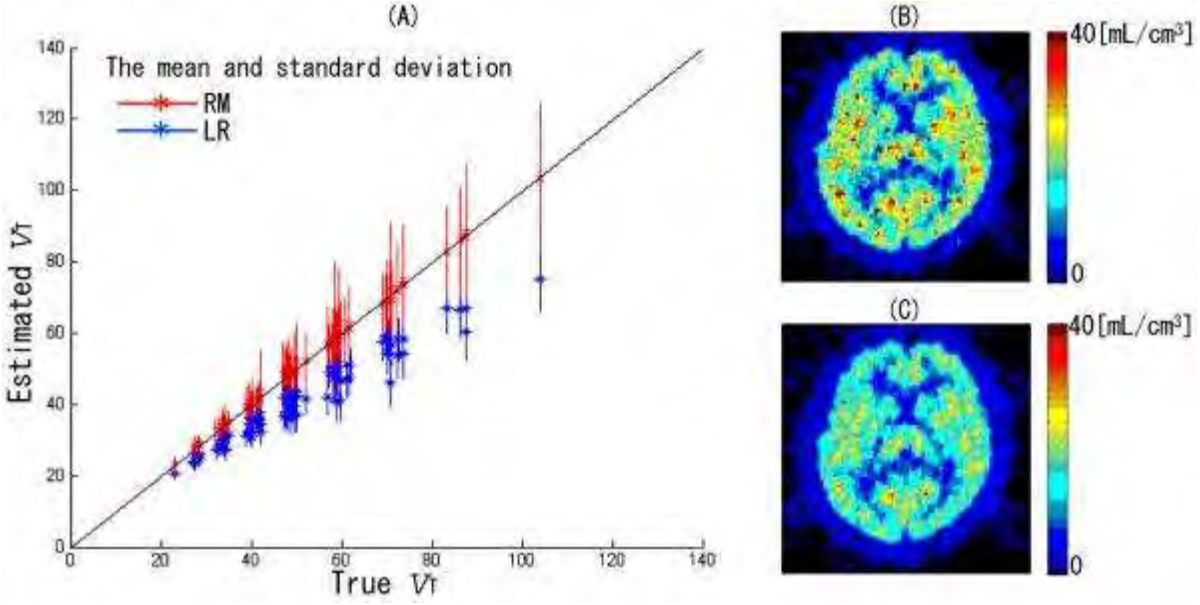

[Results]

The simulation results are summarized in Fig. (A). RM plotted in red was almost identical ($y=0.99x+0.23$, $r^2=1.00$), and LR plotted in blue showed the underestimation especially in large V_T ($y=0.70x+6.14$, $r^2=0.94$). The estimation of deviation was larger than that of LM. However, RM successfully suppressed the bias.

The figures (B) and (C) show the results of imaging of V_T obtained from the real data by RM and by LR, respectively. For the estimation, t* was set to be 15min post-injection. The computational time for RM was 10 min for 60 thousands voxels. RM gave brighter images than LR, and improved their contrast.

Conclusions: For computing unbiased estimates, we introduced RM. We estimated the average of each C_t based on simulations. Simulation results showed that RM suppresses the bias and has the potential to realize bias-free parametric imaging of V_T.

References:

[1] Slifstein et al., J Nucl Med, 41, 12, 2000.

[2] Kanatani, IEEE PAMI, 16, 3, 320-326, 1994.

[3] Sakata et al., NeuroImage, 35, 1-8, 2007.

Brain Oral Session: Cerebrovascular Regulation

FEASIBILITY OF MRI-BASED MEASUREMENTS OF CEREBROVASCULAR REACTIVITY IN AN ANESTHETIZED ANIMAL MODEL USING A CONTROLLED CEREBROVASCULAR CHALLENGE

J.D. Winter[1], S. Dorner[2], J. Fisher[3,4], G. Detzler[1], A. Kassner[1,5]

[1]Physiology and Experimental Medicine, The Hospital For Sick Children, [2]Thornhill Research Inc., [3]Department of Anesthesiology, University Health Network, University of Toronto, [4]Department of Physiology, [5]Department of Medical Imaging, University of Toronto, Toronto, ON, Canada

Objectives: Recent technological advances in the controlled manipulation of end-tidal partial pressure of CO_2 ($PetCO_2$) offer the ability to generate high-quality MRI-based maps of cerebrovascular reactivity (CVR) (1). Using this novel methodology, researchers have demonstrated potential for identifying reduced CVR in patients with cerebrovascular disease (2). However, to better understand the basis for CVR abnormalities, we need controlled investigations in animal models. The purpose of this study was to demonstrate the feasibility and repeatability of MRI-based measures of CVR in an anesthetized animal model using standardized and repeatable $PetCO_2$ manipulation.

Methods: We acquired blood-oxygen-level-dependent (BOLD) MRI data on a 1.5 T GE Signa MRI scanner using standard single-shot echo-planar imaging on three pigs (2 months of age). Imaging parameters included: echo time = 40 ms, repetition time = 2 s, field-of-view = 160 mm, resolution = 2.5 mm, slices = 16, slice thickness = 4.5 mm, volumes = 270 and acquisition time = 9 minutes. Animals were induced, orally intubated and mechanically ventilated. Anesthesia was maintained with a ketamine and midazolam infusion. The vascular stimulus consisted of four square-wave cycles of hypercapnia (~ 55 mmHg for 60 s) and normocapnia (~ 40 mmHg for 60 s). This was achieved using a computer-controlled gas delivery system in combination with a sequential gas delivery circuit (RespirAct™, Thornhill Research Inc., Toronto, Canada), which also continuously recorded $PetCO_2$ (1). To assess repeatability we acquired two data sets consecutively.

Data post-processing was performed offline using FSL and Matlab scripts. First, we matched the $PetCO_2$ and BOLD MRI time courses by estimating the time delay between $PetCO_2$ and whole-brain BOLD signal changes. Once in phase, we calculated CVR (% ΔMR signal/mmHg CO_2) on a pixel-by-pixel basis from the slope of the regression of % MR signal with $PetCO_2$. To compare the test-retest CVR data, we automatically identified grey matter regions from anatomical scans and extracted mean grey matter CVR. We assessed repeatability using the coefficient of variation (CV).

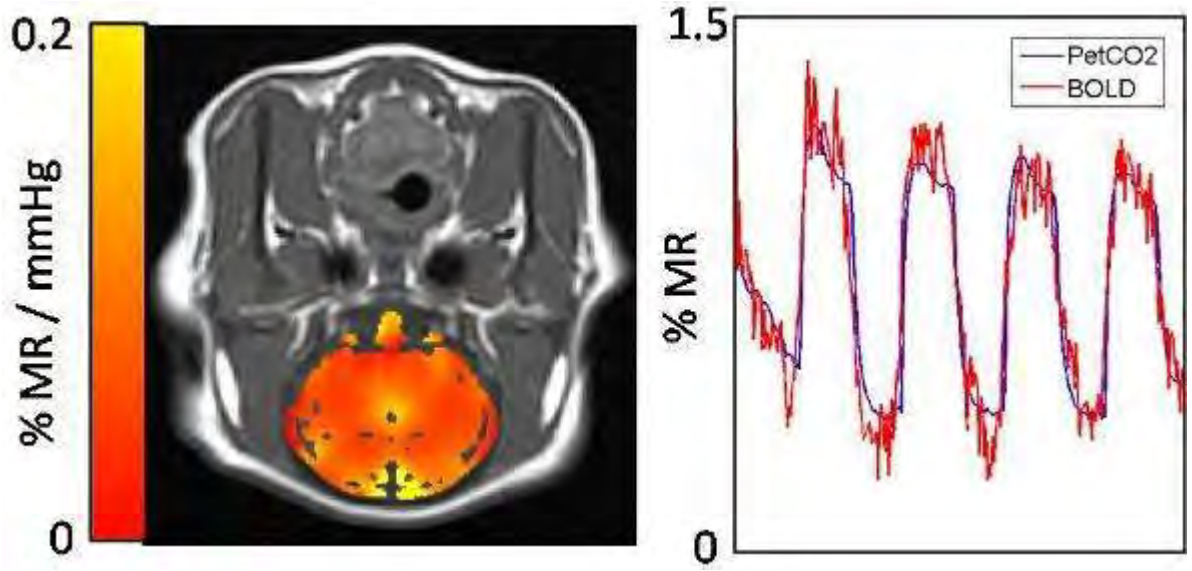

[Figure 1]

Results: Figure 1 provides a representative CVR map and the BOLD MRI time series for all grey matter overlaid with the fitted $PetCO_2$ model. Mean (± std. err.) grey matter CVR across all subjects was 0.064 ± 0.010 %MR/mmHg, and the mean CV was 8.9 ± 1.2 %.

Conclusions: Using controlled $PetCO_2$ manipulation we demonstrated the feasibility and repeatability of CVR measurements in a porcine animal model. To our knowledge, this is the first study to demonstrate CVR mapping in an anesthetized animal model using a controlled cerebrovascular stimulus, which may have implications for future animal studies investigating cerebrovascular impairment. Furthermore, we have illustrated the prospect of utilizing this CVR methodology in anesthetized human patients.

References:

1. Prisman E, et. al.,JMRI,27:185-91,(2008).

2. Mandell D, et. al.,Stroke,39:2021-8,(2008).

288

Brain Oral Session: Brain Imaging

PROBING PERFUSION WATER TRANSPORT BY ASL-QBOLD TECHNIQUE

X. He, M.E. Raichle, D.A. Yablonskiy

Mallinckrodt Institute of Radiology, Washington University School of Medicine, St. Louis, MO, USA

Objectives: Characterization of the distribution channels of pulsed arterial spin labeled (PASL) water among brain tissue compartments can provide important information on the dynamics of the transendothelial and transcytolemmal water transport and help in deciphering of PET and MRI perfusion experiments. Here we demonstrate that the recently proposed technique - quantitative BOLD (qBOLD) (1), that takes into consideration intrinsic MR relaxation properties of intravascular, intracellular and interstitial tissue compartments, allows effectively addressing these questions.

Methods: This study was approved by Washington University's IRB. All images were acquired on a Siemens 3T Trio MRI scanner. A hybrid of the FAIR (2) with QUIPPS (3) and GESSE (Gradient Echo Sampling of Spin Echo) (1,4) sequences was employed to acquire T2* attenuation curves from ASL-labeled water signal with inversion/labeling times TI between 1.2 and 2.2 sec. The MR ASL signal was modeled as originated from capillaries, interstitial space and intra-cellular space. The signals from interstitial space and intracellular space were characterized as exponentials with different T2* time constants (1). The signal from partially deoxygenated blood in capillaries was modeled as a "powder-type" (5), accounting for distribution of frequencies resulted from different capillary orientations with respect to the external B0 field.

Results:

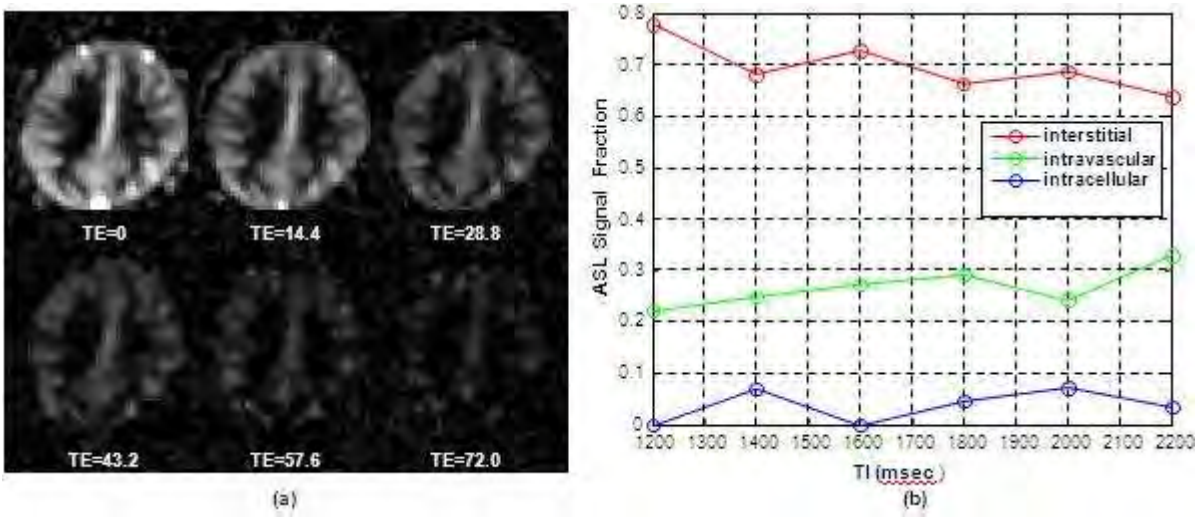

[Figure 1]

Figure 1a shows a representative set of ASL water images acquired with TI of 1400 ms and corresponding to different gradient echo times TE. Notice the T2* decay of the ASL signal. Averaged across nine studies, T2* for interstitial and intracellular labeled water were 109±24 and 50.7±7.7 ms, respectively. T2* for capillary water was 71±40 ms, consistent with its blood oxygenation level of 75%.

The time evolution of water fractions in different compartments is shown in Fig. 1b. The capillary fraction slightly increases with TI increasing. The dominant signal portion comes from the labeled

water in the interstitial (extravascular-extracellular) space, averaged around 70% and declining with TI increasing while the signal fraction from intracellular space is consistently lower than 10%.

Conclusions: In this study, the ASL labeled water has been used to probe the dynamics of the transendothelial and transcytolemmal water transport in normal human brain. Our results indicate that the extravascular labeled water in PASL experiment is mainly confined within the interstitial space implying a very slow dynamic transcytolemmal water transport (estimated apparent lifetime of intracellular water on the order of tens of seconds), consistent with PET tracer kinetic studies (6,7).

References:

1. He and Yablonskiy, MRM 57:p115;

2. Kim, MRM 35:p293;

3. Wong, et al, MRM 39:p702;

4. Yablonskiy, MRM 39:p417;

5. Sukstanskii and Yablonskiy, JMR 151:p107;

6. Larson, et al, JCBFM 7:p443;

7. Kassissia, et al, Cir Res 77:p1201.

289

Brain Poster Session: Blood-Brain Barrier

THE ROLES OF TISSUE INHIBITOR OF METALLOPROTEINASES 1 AND 2 DURING CEREBRAL ISCHEMIA-REPERFUSION INJURY

M. Gomi, M. Fujimoto, T. Aoki, M. Hayase, T. Marumo, M. Nishimura, Y. Takagi

Neurosurgery Department, Kyoto University, Kyoto, Japan

Background: Matrix metalloproteinases (MMPs) are zinc-dependent endopeptidases that are involved in a variety of cellular activities. Enhanced MMPs can cause vasogenic edema and hemorrhagic transformation after cerebral ischemia, and affect the extent of ischemic injury. Active and latent MMPs are stringently regulated by endogenous tissue inhibitor of metalloproteinase (TIMPs). We hypothesized that the endogenous TIMPs were essential to protect against blood-brain barrier (BBB) disruption after ischemia by regulating the activities of MMPs.

Materials and methods: C57BL/6 male mice, TIMP-1(-/-) mice and TIMP-2(-/-) mice were used. Cerebral ischemia was induced by using the standard intraluminal middle cerebral artery occlusion method.

Results: In Wild-type (WT) mice, TIMP-1 mRNA expression was quite low under normal conditions, and was gradually increased until 24 h after reperfusion. MMP-2 was up regulated at 3h, and MMP-9 was at 3 and 24h after ischemia. In TIMP-1(-/-) mice, MMP-9 protein expression and gelatinolytic activity were significantly more augmented after cerebral ischemia than those in WT mice at 24h. TIMP-2 gene deletion mice exhibited no significant difference in MMP expressions. Evans blue leakage was used to estimate the extent of postischemic vasogenic edema. In TIMP-1(-/-) mice and TIMP-2(-/-) mice, evans blue extravasation was significantly increased when compared with WT mice. We evaluated DNA fragmentation by TUNEL staining and cleaved caspase-3 expression. At 24h after ischemia, there was a significant increase of TUNEL-positive cells in the cerebral cortex in TIMP-1(-/-) mice and TIMP-2(-/-) mice compared with WT mice, but no change in the caudate putamen. The expression of cleaved caspase-3 in the cerebral cortex in TIMP-1(-/-) mice was significantly more enlarged than in WT mice. The infarct area was augmented in TIMP-1(-/-) mice than in WT mice at 24h after ischemia, but TIMP-2(-/-) mice also exhibited a slightly exacerbated infarct area although this difference did not reach statistical significance.

Conclusion: These results suggest that TIMP-1 inhibits MMP-9 activity and can play a neuroprotective role in cerebral ischemia.

TYPE III PHOSPHODIESTERASE INHIBITOR PROVIDE PROTECTIVE EFFECTS AGAINST POST-STROKE COMPLICATIONS THROUGH CELL SIGNALING PATHWAY OF CREB PHOSPHORYLATION

T. Urabe, N. Zhang, N. Miyamoto, T. Watanabe, Y. Ueno, Y. Tanaka, R. Tanaka, N. Nattori

Neurology, Juntendo University School of Medicine, Tokyo, Japan

Background and aims: The number of patients afflicted with cerebral infarction is on the increase at present and stroke is a leading cause of disability worldwide, with no effective clinical treatment that enhances recovery. Post-stroke cognitive impairment, depressive disorders, and pneumonia are recognized complications in such patients. The present study was designed to assess the neuroprotective mechanisms of an inhibitor of type III phosphodiesterase (PDE III-I, cilostaqzol), through signaling pathways, which lead to activation of transcription factor cyclic adenosine monophosphate (cAMP) responsive element binding protein (CREB) phosphorylation using rat chronic cerebral hypoperfusion model.

Methods: Adult male Wister rats (8-week-old) weighing 250-270 g underwent bilateral common carotid artery ligation (LBCCA). They were divided into the PDE III-I group (n=167) and the vehicle (control) group (n=167). Performance at the Morris water maze task and immunohistochemistry for 4-hydroxy-2-nonenal (HNE), GST-pi, Iba-1, phosphorylated CREB (p-CREB), Bcl-2, and cyclooxygenase (COX)-2 were analyzed at baseline and at days 3, 7, 14, 21, and 28 days after hypoperfusion. Elicited swallowing reflex, positive cultures of bacteria from the lung and immunohistochemistry for tyrosine hydroxylase (TH), substance P, and phosphorylated CREB (pCREB) were evaluated at baseline and at days 14, 28 and 42 after LBCCA. We also measured the levels of dopamine and substance P in the striatum.

Results: PDE III-I significantly improved spatial learning memory (6.8±2.3 sec; $P< 0.05$) at 7 days after hypoperfusion. Cilostazol markedly suppressed accumulation of HNE-modified protein and loss of GST-pi-positive oligodendrocytes in the cerebral white matter during the early period after hypoperfusion ($P< 0.05$). PDE III-I up-regulated p-CREB and Bcl-2 ($P< 0.05$), increased COX-2 expression, and reduced microglial activation in the early period of hypoperfusion. PDE III-I treatment significantly improved the swallowing reflex by shortening the latency to swallowing and increasing the numbers of swallows ($P< 0.05$) at 14 days of hypoperfusion. It decreased the positive culture of bacteria from the homogenized lung as well as the number of colony in the positive cultures. PDE III-I treatment markedly increased TH expression in the substantia nigra, and maintained dopamine (84.7±2.3 vs 79.2±4.1% control; $P=0.0512$) and substance P levels (86.6±7.9 vs 73.9±6.5% control; $P< 0.05$) in the striatum.

Conclusions: We have shown that PDE III-I provides protection against cerebral hypoperfusion-induced cognitive impairment and swallowing disturbance via white matter damage in a rat LBCCA model. The results suggest that PDE III-I has potential therapeutic and brain protective effects based on multi-target mechanism through cell signaling pathway of CREB phosphorylation, and may be helpful in the treatment of patients suffering from post-stroke complications.

REDUCTION OF CEREBRAL INFARCTION IN RATS BY BILIVERDIN ASSOCIATED WITH AMELIORATION OF OXIDATIVE STRESS

K. Deguchi[1], T. Yamashita[1], S. Nagotani[1], M. Takamiya[1], K. Tomiyama[2], N. Morimoto[1], M. Miyazaki[3], N.-H. Huh[3], A. Nakao[2], T. Kamiya[1], K. Abe[1]

[1]Department of Neurology, Okayama University, Okayama, Japan, [2]Department of Surgery, University of Pittsburgh, Pittsburgh, PA, USA, [3]Department of Cell Biology, Okayama University, Okayama, Japan

Background and aims: Biliverdin (BV), one of the byproducts of heme catalysis through heme oxygenase (HO) system, is a scavenger of reactive oxygen species. We hypothesized that BV treatment could protect rat brain cells from oxidative injuries via its anti-oxidant efficacies.

Methods: Cerebral infarction was induced by transient middle cerebral artery occlusion (tMCAO) for 90 min, followed by reperfusion. BV or vehicle was administered intraperitoneally immediately after reperfusion. The size of the cerebral infarction 2 days after tMCAO was evaluated by 2,3,5-triphenyltetrazolium chloride (TTC) stain. Superoxide generation 4 h after tMCAO was determined by detection of oxidized hydroethidine. In addition, the oxidative impairment of neurons were immunohistochemically assessed by stain for lipid peroxidation with 4-hydroxy-2-nonenal (4-HNE) and damaged DNA with 8-hydroxy-2′-deoxyguanosine (8-OHdG).

Results: BV treatment significantly reduced infarct volume of the cerebral cortices associated with less superoxide production and decreased oxidative injuries of brain cells.

Conclusions: The present study demonstrated that treatment with BV ameliorated the oxidative injuries on neurons and decreased brain infarct size in rat tMCAO model.

Fig. 1 TTC-stained coronal sections 2 days after tMCAO with or without BV treatment (A) and the quantitative analysis of infarct volume (B). Ve: vehicle controls, BV: biliverdin. (C) Immunohistochemistry for 4-HNE and 8-OHdG in the ischemic core lesion 4 h after tMCAO. (D) Note reduction of the number of stained cells in the BV-treated group compared with the vehicle-treated group (*$p < 0.05$, scale bars: 50 μm). SC: sham controls, Ve: vehicle controls, BV: biliverdin.

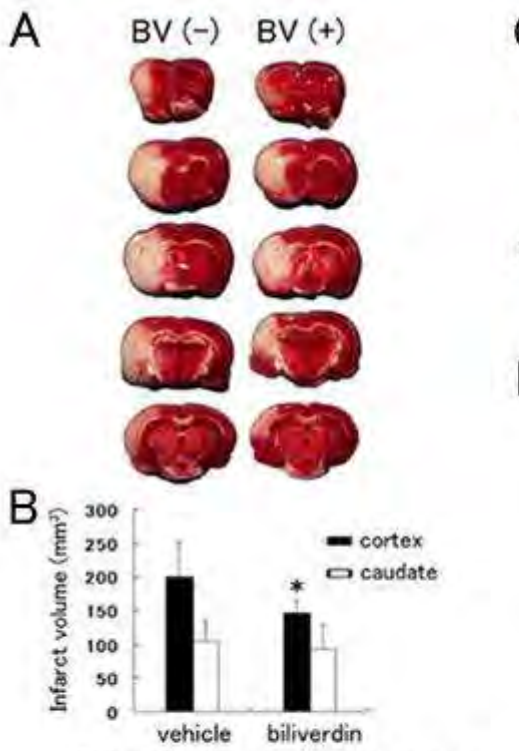

TTC stained coronal sections and the quantative analysis of infarction volume

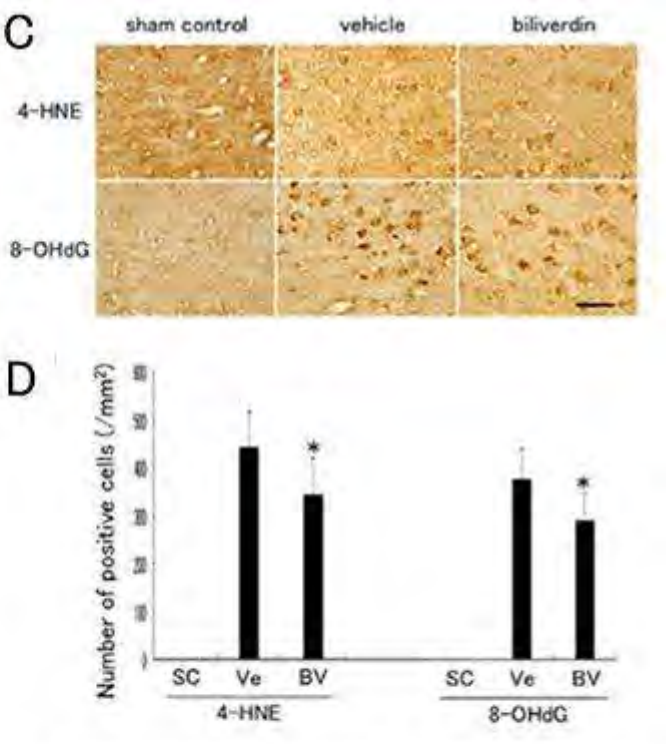

Immunohistochemistry for 4-HNE and 8-OHdG in the ischemic core lesion 4 h after tMCAO (C). and the quantitative analysis of the number of stained cells (D).

[Fig.1]

292

Brain Poster Session: Traumatic Brain Injury

LPS PRECONDITIONING ATTENUATES NEUROBEHAVIORAL DEFICITS FOLLOWING CONTROLLED CORTICAL IMPACT BRAIN INJURY IN MICE

L. Longhi[1], C. Perego[2], N. Sacchi[1], E. Zanier[2], F. Ortolano[1], N. Stocchetti[1], T. McIntosh[3], **M.G. De Simoni**[2]

[1]University of Milano, [2]Mario Negri Institute, Milano, Italy, [3]Media NeuroConsultants, Media, PA, USA

Background and aims: To date it is unknown whether traumatic brain injury could benefit from preconditioning stimuli. We tested the hypothesis that a low dose of lipopolysaccharide (LPS) that is known to act as preconditioning stimulus in models of hypoxia/ischemia[1] could attenuate the neurobehavioral sequelae of controlled cortical impact (CCI) brain injury.

Methods: C57/Bl6 mice (n = 12) were subjected to either intraperitoneal injection of LPS (0.1 mg/Kg)[1] or saline. Subsequently they were anesthetized with sodium pentobarbital (65 mg/kg) and subjected to CCI brain injury[2] at the following time points: 1, 3, 5, and 7 day-interval. Another group of mice received identical LPS injection, anesthesia and surgery, to serve as uninjured (sham-operated) controls. Neurobehavioral motor outcome was evaluated by a blinded investigator at 1 week postinjury by performing the Neuroscore[3].

Purpose: To evaluate the effects of LPS on functional outcome following CCI brain injury.

Results: All brain-injured mice showed a robust behavioral deficit at 1 week postinjury compared to sham-operated mice. Mice receiving LPS at either 3, 5 and 7 day-interval prior to CCI brain injury had a behavioral performance that was significantly better compared to that of mice receiving saline or LPS at 1 day-interval ($p < 0.01$ Kruskall-Wallis analysis of variance (ANOVA) followed by Mann-Whitney U test for individual comparison).

Conclusions: Our data show for the first time that the neurobehavioral sequelae of traumatic brain injury can be attenuated by a preconditioning stimulus.

References:

1. Rosenzweig HL et al. J Cereb Blood Flow Metab. 27(10):1663-74, 2007.

2. Longhi L et al. J Neurotrauma. 21(12):1723-1736, 2004.

3. Fujimoto ST et al. Neurosci. Biobehav. Rev. 28(4):365-378, 2004.

GELATIN-SILOXANE HYBRID SCAFFOLDS WITH VASCULAR ENDOTHELIAL GROWTH FACTOR INDUCES BRAIN TISSUE REGENERATION

M. Takamiya[1], H. Zhang[1], K. Deguchi[1], K. Tsuru[2], V. Lukic[1], T. Yamashita[1], S. Nagotani[1], S. Hayakawa[2], A. Osaka[2], T. Kamiya[1], K. Abe[1]

[1]Department of Neurology, [2]Biomaterial Laboratory, Okayama University, Okayama, Japan

Background and aims: In the brain after infarction or trauma, the tissue becomes pannecrotic and forms a cavity. In such situation, a scaffold is necessary to produce new tissue. In this study, we implanted a new porous gelatin-siloxane hybrid derived from gelatin and 3-(glycidoxypropyl) trimethoxysilane (gelatin-GPTMS) scaffolds into a brain defect, and investigated whether it makes a new brain tissue. In addition, vascular endothelial growth factor (VEGF) was added on gelatin-GPTMS scaffolds and its effect on tissue regeneration was examined.

Results: At 30 days after the implantation, the marginal territory of the scaffolds became occupied by newly formed tissue. Immunohistochemical analysis revealed that the new tissue was constituted by endothelial, astroglial and microglial cells, some of which were labeled for bromodeoxyuridine (BrdU). Addition of VEGF promoted numbers of these cells.

Conclusions: The present study demonstrated that combination of gelatin-GPTMS scaffolds and VEGF was preferable for brain regeneration.

Fig 1. Whole brain (A) and HE stained coronal brain section (B) with gelatin-GPTMS scaffold implantation. The hybrid scaffold (arrow heads) kept the integrity of brain shape (A, B). The inset in panel A shows the scaffold observed by scanning electron microscopy. Representative gelatin-GPTMS scaffold implanted coronal brain sections, without (C-a, and C-c) and with (C-b and C-d) VEGF. The panels C-c and C-d were from rectangles in panels C-a and C-b, respectively. The white dotted line indicates the boundary between the newly formed tissue and the original tissue (C-c and C-d). Panel C-e shows quantitative analysis of the newly formed tissue volume in the gelatin-GPTMS scaffold ($p^* < 0.05$).

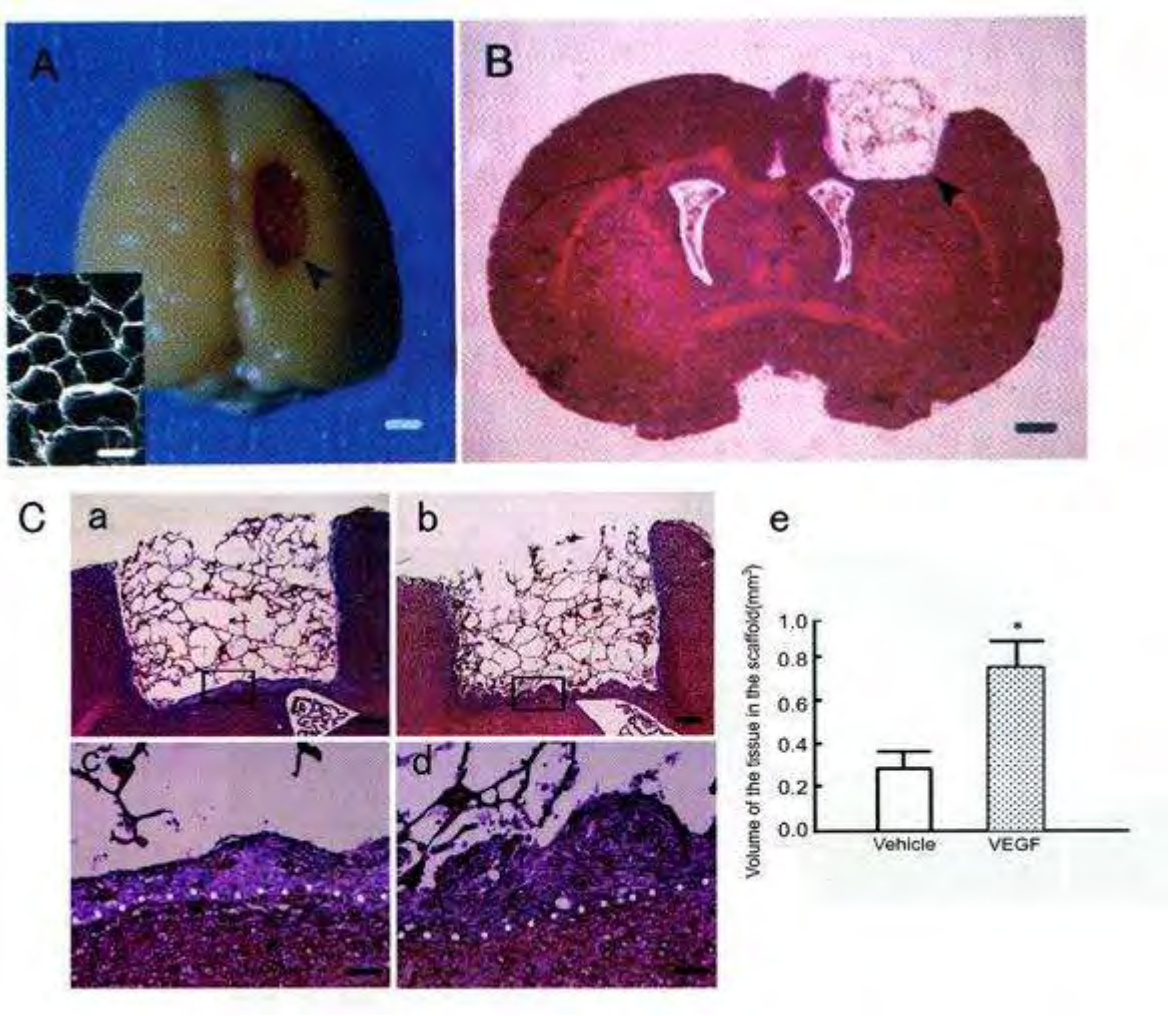
A
B
C
a
b
c
d
e
Volume of the tissue in the scaffold/(mm³)
1.0
0.8
0.6
0.4
0.2
0.0
Vehicle
VEGF
*

[Fig.1]

Brain Poster Session: Cerebral Vascular Regulation

FIBERED CONFOCAL FLUORESCENCE MICROSCOPY FOR IN VIVO STUDY OF CEREBRAL MICROCIRCULATION IN THE RAT: VASODILATORY EFFECTS OF THE PHYTOESTROGEN GENISTEIN

M. Castelló-Ruiz[1], J.B. Salom[1,2], J.M. Pradillo[3], M.C. Burguete[2], V.G. Marrachelli[1], G. Torregrosa[1,2], I. Lizasoain[3], E. Alborch[1,2]

[1]Centro de Investigación, Hospital Universitario La Fe, [2]Departamento de Fisiología, Universitat de València, Valencia, [3]Departamento de Farmacología, Facultad de Medicina, Universidad Complutense de Madrid, Madrid, Spain

Objectives: Conventional intravital fluorescence microscopy and confocal laser-scanning microscopy involve the positioning of a microscope objective on the cerebral microvascular field. A new image system combining confocal fluorescence microscopy with fiber optics, namely fibered confocal fluorescence microscopy (FCFM), replaces the microscope objective with a mini-optical probe (1). We sought to apply FCFM for the study of brain microcirculation in the rat and to assess the vasoactive effects of the phytoestrogen genistein, which effects relaxing isolated cerebral arteries and increasing laser-Doppler measured cerebral perfusion have been reported (2, 3).

Methods: Male Wistar rats (300 g) were anesthetized and the head fixed in a stereotaxic. A cranial window covering all the right parietal bone was drilled and the dura was removed. A ProFlex Z probe connected to the Laser Scanning Unit of a FCFM system (Cell-vizio, Mauna Kea Technologies) was positioned above the cortex. A bolus (700 μL) of 5-10 mg/mL FITC-dextran was injected through the left femoral vein to label plasma. Saline washed erythrocytes from a donor rat were labeled by incubating (2 h, 25°C) with 10 mg/mL FITC isomer I-Celite and injected into a receptor rat. Sodium nitroprusside (SNP, 10 μM) and endothelin-1 (1 μM) were topically administered to test for reactivity of pial vessels. Genistein (10 mg/kg) was infused directly into the brain circulation through the right carotid artery and through the femoral vein. Images were displayed, acquired and analyzed with an Apple computer fixed up with ImageCell software.

Results: Fluorescent labeling of the plasma with 10 mg/mL FITC-dextran allowed the visualization of surface corticoparietal microvessel networks including arterioles, venules and capillaries (Figure). Fluorescent labeling of erythrocytes with FITC isomer I-Celite allowed the visualization of circulating cells in the brain surface. Counterstaining of microvessels with 5 mg/mL FITC-dextran improved images of circulating erythrocytes in the brain vascular networks and their transit throughout capillaries. Topical SNP and endothelin-1 induced increases and reductions in microvessel diameter, respectively. Both intracarotid and intravenous infusion of genistein induced increases in the diameter of most but not all pial vessels. However, the intracarotid effect was immediate and higher in magnitude (70%) while the intravenous effect was delayed (6 min) and lesser in magnitude (50%).

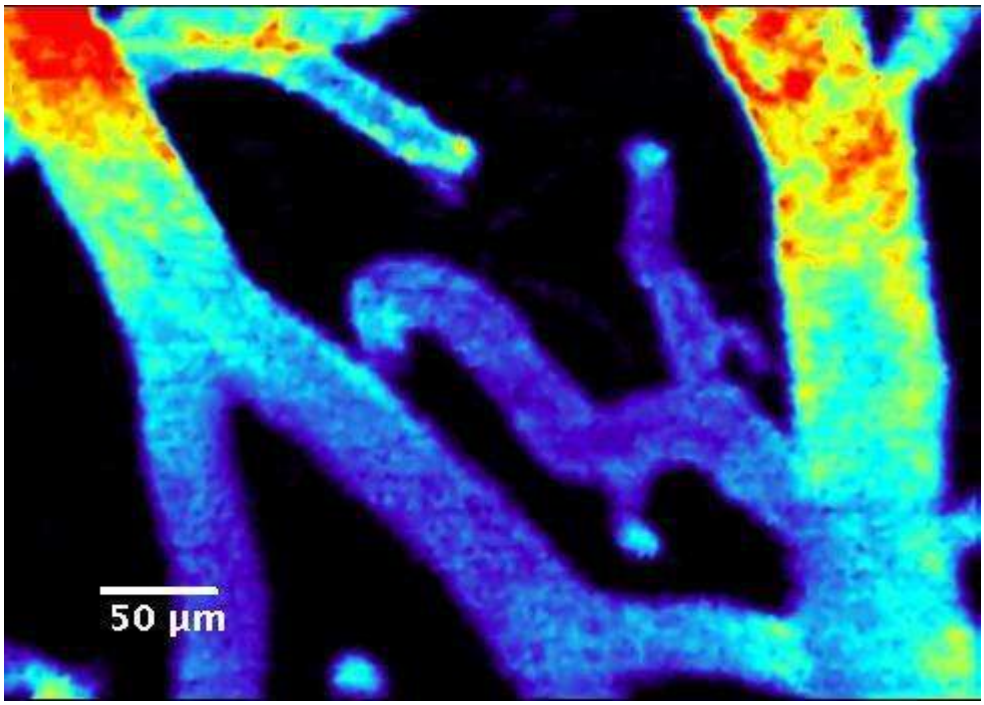

[Figure]

Conclusions: A new FCFM-based technique has been applied to in vivo study of cerebral microcirculation in the rat and it has proven appropriate to assess pial vessel vasoactivity and to observe the transit of blood cells. Vasodilatory responses to local and systemic genistein are in line with reported (3) increases in cerebral perfusion induced by this phytoestrogen.

References:

1. Laemmel et al (2004) J Vasc Res 41:400-11.

2. Torregrosa et al (2003) Eur J Pharmacol 482:227-34.

3. Salom et al (2007) Phytomedicine 14:556-62.

Supported by RETICS-RENEVAS from ISCIII (RD06/0026/0006).

300

Brain Poster Session: Experimental Cerebral Ischemia: In Vitro

EXPRESSION OF NUCLEOSIDE TRANSPORTERS IN RAT CORTICAL ASTROCYTES IN PRIMARY CULTURE: EFFECTS OF HYPOXIA AND GLUCOSE DEPRIVATION

Z. Redzic, S. Malatiali, M. Al-Bader

Department of Physiology, Faculty of Medicine, Kuwait University, Kuwait, Kuwait

Objectives: The objectives of this study were to explore the amount of mRNA for rat equilibrative nucleoside transporters (rENT) 1 and 2 and rat concentrative nucleoside transporter (rCNT) 1, 2 and 3 in rat cortical astrocytes in primary culture under normal conditions, after 1 hour exposure to hypoxia and inhibition of glycolysis (2% O_2, 5% CO_2 in N_2, 10 mM 2-deoxy-D-glucose (2-DG), 1 mM D-glucose) (ischemia group) and after 1 hour exposure to hypoxia and inhibition of glycolysis, followed by 1 hour exposure to normal conditions (5% CO2 in the air, 5 mM glucose, no 2-DG) (reperfusion group).

Methods: Primary cultures of cortical astrocytes were produced as explained (1). Real time polymerase chain reaction (PCR) was used to explore the amount of mRNA; the threshold cycles for target amplification (Ct) values were estimated for genes of interest and the difference between their Ct values and Ct values for the housekeeping gene glyceraldehyde 3-phosphate dehydrogenase (GAPDH) (ΔCt) was calculated. The quantification of gene expression and the significance of difference was estimated using the comparative ΔΔCt method, as described earlier (2).

Results: In rat cortical astrocytes, the Ct value of GAPDH did not differ between the control (20.34±0.51, n=5), ischemia (20.4±0.41, n=3, $p>0.05$) and reperfusion group (20.7±0.3, n=3, $p>0.05$). Therefore, this gene was used as the endogenous control. The data for ENTs and CNTs are presented in the Table 1, signs * and ** indicate $p< 0.05$ and $p< 0.01$ vs. control, respectively; according to the ΔCt values from the control group, mRNA for rENT1, rENT2 and rCNT2 was abundant, while the mRNA for rCNT1 was less abundant. The mRNA for rCNT3 was either absent or present at very low abundance, since the ΔCt values were close to the ΔCt values in negative controls (>20) in all experimental groups (not shown). One hour exposure to ischemic-like conditions leads to a significant increase in the amount of mRNA for rCNT1 and to a significant decrease in the amount of mRNA for rENT1. When exposure to ischemic-like conditions was followed by exposure to normal conditions (reperfusion group) there was an increase in the amount of mRNA for rENT2, a decrease in the amount of mRNA for rENT1 and further increase in amount of mRNA for rCNT1.

	Control group ΔCt±SD	$2^{-\Delta\Delta Ct}$	Range $[2^{-\Delta\Delta Ct+SD} - 2^{-\Delta\Delta Ct-SD}]$	Ischemia group ΔCt ±SD	$2^{-\Delta\Delta Ct}$	Range $[2^{-\Delta\Delta Ct+SD} - 2^{-\Delta\Delta Ct-SD}]$	Reperfusion groupΔCt ±SD	$2^{-\Delta\Delta Ct}$	Range $[2^{-\Delta\Delta Ct+SD} - 2^{-\Delta\Delta Ct-SD}]$
rENT1	3.15±0.48 (n=4)	1.00	0.58-2.81	5.66±0.58 (n=4)	0.25*	0.13-0.48	4.94±0.64 (n=4)	0.40*	0.29-0.56
rENT2	5.04±0.69 (n=5)	1.00	0.18-5.58	4.82±0.73 (n=4)	1.16	0.66-2.05	3.40±0.79 (n=4)	2.06*	1.43-2.96

rCNT1	15.49±0.32 (n=5)	1.00	0.75-1.33	13.91±1.19 (n=4)	2.98*	1.51-5.88	13.19±0.64 (n=4)	4.91**	3.54-6.80
rCNT2	1.72±0.57 (n=5)	1.00	0.16-6.25	2.35±0.31 (n=4)	0.85	0.10-7.02	2.33±0.89 (n=4)	0.33	0.13-0.70

[Relative expression of rENTs and rCNTs]

Conclusions: Exposure of rat astrocytes in primary culture to ischemia-like conditions and ischemia-reperfusion like conditions leads to a significant change in the amount of mRNA for nucleoside transporters.

References:

1. Parkinson FE and Xiong W (2004) Stimulus- and cell-type-specific release of purines in cultured rat forebrain astrocytes and neurons. Journal of Neurochemistry 88, 1305-1312.

2. Livak KJ and Schmittgen TD (2001) Analysis of relative gene expression data using Real Time quantitaive PCR and $2^{-\Delta\Delta Ct}$ method. Methods 25, 402-408**.**

301

Brain Oral Session: Functional Brain Imaging

INTERHEMISPHERIC FUNCTIONAL CONNECTIVITY CHANGES AFTER TRANSIENT FOCAL ISCHEMIA IN RAT BRAIN: A SERIAL RESTING-STATE FMRI STUDY

M.P.A. van Meer[1,2], K. van der Marel[1], K. Wang[3], W.M. Otte[1,2], J.W. Berkelbach van der Sprenkel[2], R.M. Dijkhuizen[1]

[1]Image Sciences Institute, University Medical Center Utrecht, [2]Rudolf Magnus Institute of Neuroscience, University Medical Center Utrecht, Utrecht, The Netherlands, [3]Institute of Automation, Chinese Academy of Sciences, Beijing, China

Objectives: Resting-state fMRI can identify the synchronization of spontaneous low-frequency fluctuations of the blood oxygenation level-dependent (BOLD) signal in the brain, indicative of functional connectivity (FC)[1]. Because no peripheral stimulation is required, resting-state fMRI is an ideal tool to study dynamics of changes in functional organization of different neuronal networks after brain injury. In this study we applied serial resting-state fMRI to assess changes within the sensorimotor network after unilateral stroke in rats.

Methods: Experimental stroke was induced by 90-min transient intraluminal occlusion of the right middle cerebral artery (tMCA-O) in adult male rats (n=14). Sensorimotor function was measured longitudinally by measuring neurological deficiency score (NDS) and adhesive removal time from the affected forelimb[2]. Structural MRI (T_2- weighted) and resting-state BOLD fMRI (T_2*-weighted gradient echo EPI) measurements were acquired before and at 3, 7, 21, and 70 days after stroke on a 4.7T MR system. Rats were ventilated with 1-2% isoflurane in air/O_2 (2:1). Animals were divided in two groups based lesion extent: Group I animals had only subcortical lesions (n=5); Group II animals had both cortical and subcortical lesions (n=9). Low-frequency BOLD fluctuations were band-pass filtered between 0.01 and 0.08 Hz. Lesioned tissue was excluded from the analysis. Interhemispheric FC was measured as the correlation coefficient r between low-frequency BOLD signals in ipsi- and contralateral S1fl (forelimb region of the primary somatosensory cortex) and its Fisher-transformed z'-value.

Results: The figure shows the temporal pattern of mean (+/-SD) interhemispheric FC between ipsi- and contralateral S1fl. At 3 days after stroke, interhemispheric FC was reduced in both groups. Group I animals demonstrated recovery of interhemispheric FC at 7 days after tMCA-O, which was accompanied by an improvement of neurological function and adhesive removal time. In Group II animals, however, interhemispheric FC remained reduced at 7 days, in parallel with lower sensorimotor function scores as compared to Group I animals. Partial recovery of interhemispheric FC in Group II was observed after 10 weeks, when behavioral scores had also improved.

Conclusions: This study shows that resting-state fMRI can be applied to study changes in FC in a rat stroke model. Acutely after stroke a decrease was detected in interhemispheric FC of bilateral S1fl, despite the absence of structural ischemic damage in the ipsilesional S1fl. Animals with only subcortical ischemic lesions showed relatively fast restoration of interhemispheric FC, whereas animals with both cortical and subcortical lesions showed delayed recovery. We found correspondence between the evolution of FC within the bilateral sensorimotor network and changes in sensorimotor scores, which suggests that resting-state fMRI provides a valuable method to study brain reorganisation in relation to functional recovery after cerebral injury.

References:

[1]Biswal et al., MRM 34 (1995):537-541.

[2]Van der Zijden et al., JCBFM 28 (2008):832-840.

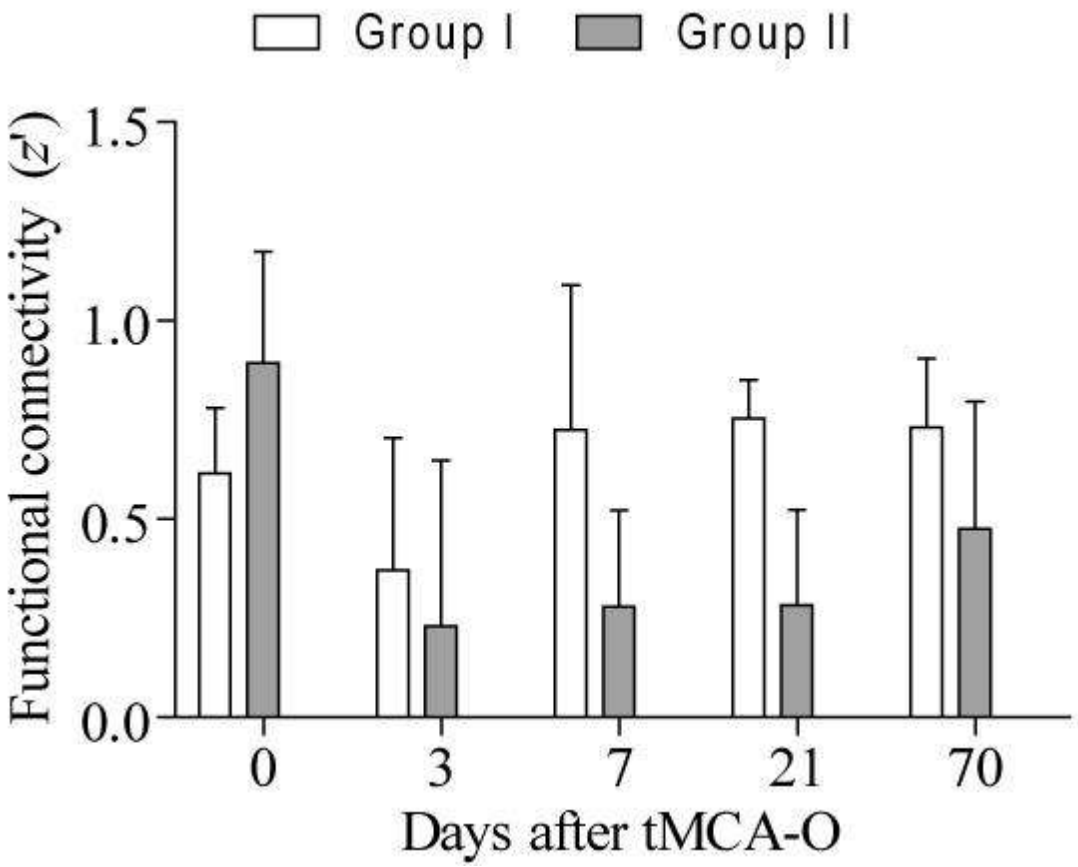

[Figure_RestState]

303

Brain Poster Session: Experimental Cerebral Ischemia: Vascular & Endothelial

ENHANCED CONTRACTILE RESPONSE OF VASCULAR CONTRACTILE RECEPTORS FOLLOWING DISTAL FOCAL PERMANENT OCCLUSION

M.N.P. Rasmussen[1], M. Hornbak[1], L. Edvinsson[1,2]

[1]Department of Clinical Experimental Research, Glostrup Research Institute, Glostrup University Hospital, Glostrup, Denmark, [2]Department of Medicine, Institute of Clinical Sciences, University Hospital of Lund, Lund, Sweden

Objectives: Previous investigations have revealed that cerebral ischemia is accompanied by changes in the receptor expression in cerebral vasculature. It has been shown that following experimental cerebral ischemia levels of the vasoconstrictors endothelin (ET), 5-hydroxytryptamine (5-HT) and angiotensin (Ang II) are increased[1, 2]. We have previously demonstrated a time-dependent up-regulation of the contractile ET_B, AT_1 and 5-HT_1 receptors in cerebral arteries following subarachnoid haemorrhage and transient middle cerebral artery (MCA) occlusion at both mRNA, protein and functional levels[3, 4]. This up-regulation leads to enhanced vasoconstriction and show correlation with reduction in regional cerebral blood flow (rCBF) and infarct volume. The present study was designed to investigate if small permanent vascular insult without visible ischemic damage leads to altered expressional profile of contractile receptors in the smooth muscle cells of the cerebral artery. To test the hypothesis we employed a model of focal permanent occlusion by ligation of the distal part of the MCA. This additionally gives us the opportunity to investigate vessel segments both upstream and downstream to an occlusion. The knowledge obtained from this study will further the understanding of how cerebral arteries participate in the events that take place following a stroke.

Methods: Focal permanent occlusion is obtained by a distal ligation of the MCA in male Wistar rats. Artery access is achieved by craniotomy and occlusion is verified by laser-Doppler[5]. Controls consist of un-ligated left MCA and sham operated rats. After 24 hours, MCA segments located upstream and downstream to the ligature are investigated for expressional changes of ET, AT and 5-HT receptors at protein (immunohistochemistry) and functional (myograph) level[6]. TTC stainings are performed to examine brains for ischemic damage.

Results: The contractile responses to S6c (selective ET_B agonist) and 5-CT (5-HT_1 agonist) are significantly stronger in the right occluded MCA (85.1 ± 27.2%, and 59.1 ± 9.4%, respectively) compared with the left MCA (11.8 ± 4.3% and 27.7 ± 6.7%, respectively), and for S6c also the MCA from sham operated rats (21.3 ± 9.7%) 24 hours after occlusion. Changes were observed in the vessel segments downstream to the occlusion and not in the upstream. TTC staining showed no indication of ischemic damage in any rat groups.

Conclusion: A small focal vascular occlusion without tissue ischemia leads to increased contractile function of ET_B and 5-HT_{1B} receptors. Since in the upstream segments, receptor expression was unaltered it does not appear as change in shear stress is the crucial factor. In addition, the changes seen in the downstream segments, without noticible tissue damage, indicate that it is not the ischemic condition per se which is responsible for an increased receptor expression/sensitivity.

References:

1. Barone FC, et al. J Cereb Blood Flow Metab 1994:14: 337-342.

2. Nishimura Y, Suzuki A. Clin Exp Pharmacol Physiol Suppl 1995:22: S99-101.

3. Ansar S, et al. Am J Physiol Heart Circ Physiol 2007:293: H3750-H3758.

4. Stenman E, et al. Stroke 2002:33: 2311-2316.

5. Rajanikant GK, et al. Stroke 2007:38: 3023-3031.

6. Maddahi A, Edvinsson L. BMC Neurosci 2008:9: 85.

305

Brain Poster Session: Neonatal Ischemia

ROUTINE DWI-MRI AS A BIAS-KILLER AND A RAT PUP-SAVER IN NEONATAL NEUROPROTECTION PRECLINICAL TRIALS

S. Fau[1,2], C. Po[3], P. Meric[3], C. Marlangue[1]

[1]NPA, UPMC CNRS UMR 7102, [2]NICU/PICU, Hopital d'Enfants A. Trousseau / APHP, Paris, [3]ICSN, CNRS, Gif-sur-Yvette, France

Objectives: Lack of internal validity in preclinical trials may lead to disappointing failures in clinical trials. Moreover biases may increase preexisting variability of animal models and consequently increase requested sample sizes.

In previous work we highlighted that our model of transient neonatal focal ischemia suffers from a poor reproductibility because of:

1. inconstant initial ischemia,
2. cases of poor reperfusion,
3. variability of the concerned arterial territory size.

This leads to high variance of the infarct size and finally increases required sample size. We make the hypothesis that post-reperfusion DWI-MRI allows to:

1. detect absence of initial ischemia,
2. detect poor reperfusion,
3. delineate the initial ischemic territory.

Our objective is to prove that routine DWI-MRI in our neuroprotection studies allows to remove biases and use less animals.

Methods: A neuroprotection study tested the effectiveness of the pananticaspase Q-VD-OPh to reduce the H48 infarct size in our model (1mg/kg IP directly after reperfusion). This model, performed in P7 Wistar rat pups, associates a permanent MCA occlusion with a transient CCA occlusion (50 minutes). Using previous data, requested sample size calculation leads to n=24 per group (α=0.05, 1-β=0.80, expected effect: 40% decrease of infarct size, bilateral test). Using a 7.4T, we performed ADC map and MR-angiography in each animal 10 minutes and 120 minutes after reperfusion. We evaluate postischemic edema on ADC maps ($V_{ADC}M_{10}$ and $V_{ADC}M_{120}$) by counting in ipsilateral hemisphere, pixels which ADC was < mean-2SD of the controlateral hemisphere ADCs. We named “artefacts” the animals presenting an absence of postischemic edema and/or a poor reperfusion at M10 post-reperfusion. Classical histology measurement of the infarct size (V_{HISTO}) was carried out at H48. We created two composite measurements using the ratios of final infarct size and postischemic edema sizes, respectively $V_{HISTO}/V_{ADC}M_{10}$ and $V_{HISTO}/V_{ADC}M_{120}$. We compared 4 various statistical analysis using the various measurement and including or not the “artefacts”, respectively: V_{HISTO} including “artefacts”, V_{HISTO} excluding “artefacts”, $V_{HISTO}/V_{ADC}M_{10}$ excluding “artefacts” and $V_{HISTO}/V_{ADC}M_{120}$ excluding “artefacts”.

Results: On 48 animals, 2 died, 20 didn't show any initial edema, 4 showed poor reperfusion. None of the four statistical analysis showed effectiveness of the Q-VD-OPh. A posteriori power was extremely

low when MRI was not used (0.16). A posteriori power was much higher when we associated use of composite criteria and exclusion of “artefacts”. It arose that, a posteriori, requested sample size (calculated with above conditions) decrease from 94 down to 9 per group.

Measurement/ Artefact	Vhisto/ Included	Vhisto/ Excluded	Vhisto/ VadcM10/ Excluded	Vhisto/ VadcM120/ Excluded
Vehicle (moy+/-SD)	7.2±7.3	11±5.1	54.5±17.3	62.5±14.8
Q-VD-OPh (moy+/-SD)	8.0±7.7	10.7±6.9	56.9±26.1	59.3±22
p(t-test)	0.71	0.91	0.80	0.69
a posteriori power	0.16	0.40	0.67	0.88
n per group in a future study	94	30	15	9

[Main results]

Conclusions: In neuroprotection studies using our model, routine DWI-MRI allows on the one hand to eliminate biases like absence of initial ischemia or poor reperfusion, and on the other hand to dramatically reduce the requested sample sizes.

307

Brain Poster Session: Neuroprotection

METFORMIN ATTENUATES TYPE 2 DIABETES-INDUCED BRAIN OXIDATIVE IMBALANCE

C. Carvalho[1], S. Correia[1], M. Santos[1], R. Seiça[2], P. Moreira[3]

[1]Center for Neuroscience and Cell Biology and Department of Zoology, University of Coimbra, [2]Faculty of Medicine, University of Coimbra, [3]Center for Neuroscience and Cell Biology, Coimbra, Portugal

Type 2 diabetes is a well known metabolic disorder that usually occurs in people over 30 years old and is characterized by a relative insulin deficiency and an insulin resistance that leads to a state of hyperglycemia. There is considerable evidence that many biochemical pathways adversely affected by hyperglycemia are associated with the generation of reactive oxygen species (ROS), ultimately leading to increased oxidative stress in a variety of organs including the nervous system. The brain is one of the most important targets for ROS, due to its high levels of polyunsaturated fatty acids, high oxygen consumption, high content in transition metals (e.g., Fe^{2+}) and poor antioxidant defenses. Metformin is a widely used drug for the management of type 2 diabetes. This oral antidiabetic agent is a biguanide derivative whose main actions are to reduce hepatic glucose production and increase glucose uptake. Due to these effects, metformin is considered an insulin sensitizer. Despite the success of this antidiabetic agent in the treatment of type 2 diabetes, its mechanisms of action remain unclear. Although some antioxidant properties have been attributed to metformin, the antioxidant action of this antidiabetic agent in brain tissue has not yet been evaluated. In this line, this study was designed to evaluate the effect of metformin treatment in the brain of diabetic Goto-Kakizaki (GK) rats (a nonobese, spontaneously type 2 diabetic model). For this purpose we compared brain homogenates obtained from untreated GK rats versus GK rats treated with metformin during a period of 4 weeks. Brain homogenates obtained from Wistar rats were used as control. Several parameters were analysed: lipid peroxidation [thiobarbituric acid reactive substances (TBARS) and malondialdehyde (MDA) levels] and protein oxidation (carbonyl groups) markers, H_2O_2 levels and non-enzymatic [reduced glutathione (GSH) and vitamin E] and enzymatic [glutathione peroxidase (GPx), glutathione reductase (GRed) and manganese superoxide dismutase (MnSOD)] antioxidant defenses. Compared to control rats, brain homogenates of GK rats presented a significant increase in the levels of MDA, GPx and GRed activities and a significant decrease in MnSOD activity supporting the idea that type 2 diabetes promotes an oxidative imbalance in brain tissue. However, metformin treatment normalized the majority of the parameters altered by diabetes. Besides its antihyperglycemic action, metformin induced a significant decrease in the levels of lipid peroxidation markers and GPx and GRed activities. Additionally, this antidiabetic agent promoted a significant increase in the levels of GSH and in the activity of MnSOD. These results indicate that metformin protects against diabetes-associated oxidative stress suggesting that metformin could be an effective neuroprotective agent.

Cristina Carvalho has a PhD fellowship from the Fundação para a Ciência e a Tecnologia (SFRH/BD/43965/2008).

308

Brain Poster Session: Cerebral Vascular Regulation

ANGIOGRAPHY AND VENOGRAPY OF BAT INTRACRANIAL VESSELS.ADAPTATION TO PROLONGED INVERSION

J. Ashaolu

Anatomy, University of Ilorin, Ilorin, Nigeria

Background and aims: Bat contend with prolonged inversion in their roosting colonies, and both inversion and valsalva maneuver in Man has been reported to increase intracranial pressure (Flanagan, 2001). The aim of this study is to verify if bats possess accessory drainage system(s) or arterial shunt(s) for regulating intra-cranial circulation.

Methods: 4 bats captured irrespective of sex weighing between 250-260g were divided into 2 groups of 2 each (A and B). The group A and group B bats were anaesthetized with chloroform and administered with 3mls Urografin (a radiographic contrast) through the left and right ventricles to study the venography and angiography respectively.

Purpose: To verify how bats contend with cranial hydrodynamics during inversion.

Results: X-ray images were taken and placed on a viewing box, and photographic records obtained for analysis showed that; the posterior vena cava was highly enlarged, the superior sagittal sinus communicated with the facial veins, the vertebral arteries have a midline origin that appears to emanate from the arch of aorta other than the origin from the subclavian artery, the vertebral arteries communicated by shunts with each other and, the common carotid arteries appear visually narrower compared to the vertebral arteries.

Conclusions: All these arterial and venous modifications suggest reasons for bats protection against increased intracranial pressure or increased hemodynamics when inverted in their roosting colonies.

References: Flanagan MF.(2001) The accessory drainage system: its role in humans and other mammals. Dynamic Chiropractic. Old Tappan, New Jersey. www.chiroweb.com/archives/19/26/04.html.

309

Brain Poster Session: Brain Edema & Water Transport

THE ROLE OF C-JUN N-TERMINAL KINASE IN A MOUSE MODEL OF INTRACEREBRAL HEMORRHAGE

D. Michel-Monigadon[1], V. Mottier[2], C. Bonny[3], **L. Hirt**[1]

[1]Laboratory of Neurology, Centre Hospitalier Universitaire Vaudois, [2]Institut de Biologie et de Morphologie, Université de Lausanne, [3]Xigen Pharmaceuticals, Lausanne, Switzerland

Background: Intracerebral hemorrhage (ICH) is a subtype of stroke characterized by a haematoma within the brain parenchyma resulting from blood vessel rupture and with a poor outcome. In ICH, the blood entry into the brain triggers toxicity resulting in a substantial loss of neurons and an inflammatory response. At the same time, blood-brain barrier (BBB) disruption increases water content (edema) leading to growing intracranial pressure, which in turn worsens neurological outcome. Although the clinical presentation is similar in ischemic and hemorrhagic stroke, the treatment is different and the stroke type needs to be determined beforehand by imaging which delays the therapy.

C-Jun N-terminal kinases (JNKs) are a family of kinases activated in response to stress stimuli and involved in several pathways such as apoptosis. Specific inhibition of JNK by a TAT-coupled peptide (XG-102) mediates strong neuroprotection in several models of ischemic stroke in rodents. Recently, we have observed that the JNK pathway is also activated in a mouse model of ICH, raising the question of the efficacy of XG-102 in this model.

Method: ICH was induced in the mouse by intrastriatal injection of bacterial collagenase (0,1U). Three hours after surgery, animals received an intravenous injection of 100µg/kg of XG-102. The neurological outcome was assessed everyday until sacrifice using a score (from 0 to 9) based on 3 behavioral tests performed daily until sacrifice. Then, mice were sacrificed at 6h, 24h, 48h and 5d after ICH and histological studies performed.

Results: The first 24h after surgery are critical in our ICH mice model, and we have observed that XG-102 significantly improves neurological outcome at this time point (mean score: 1,8 + 1.4 for treated group vs 3,4 + 1.8for control group, $p< 0.01$). Analysis of the lesion volume revealed a significant decrease of the lesion area in the treated group at 48h (29 + 11 mm^3 in the treated group vs 39 + 5 mm^3 in the control group, $p = 0.04$). XG-102 mainly inhibits the edema component of the lesion. Indeed, a significant inhibition of the brain swelling was observed in treated animals at 48h (14 + 13 % vs 26 + 9 % in the control group, $p = 0.04$) and 5d (-0,3 + 4.5 % vs 5,1 + 3.6 % in the control group, $p = 0.01$).

Conclusions: Inhibition of the JNK pathway by XG-102 appears to lead to several beneficial effects. We can show here a significant inhibition of the cerebral edema in the ICH model providing a further beneficial effect of the XG-102 treatment, in addition to the neuroprotection previously described in the ischemic model. This result is of interest because currently, clinical treatment for brain edema is limited. Importantly, the beneficial effects observed with XG-102 in models of both stroke types open the possibility to rapidly treat stroke patients before identifying the stroke subtype by imaging. This will save time which is precious for stroke outcome.

311

Brain PET Oral 1: PET Image Reconstruction and Processing

RADIOLIGAND DISCOVERY AND DEVELOPMENT THROUGH BIO-MATHEMATICAL MODELLING

Q. Guo[1], M. Brady[1], C. Salinas[2], R. Gunn[1,2]

[1]Dept of Engineering Science, University of Oxford, Oxford, [2]Clinical Imaging Centre, GSK, London, UK

Objectives: The development of PET radioligands for novel neuroreceptor, transporter and enzyme targets is a complex process. Traditional radioligand screening methods focus on lipophilicity and affinity, but these only partially identify the characteristics of a successful radioligand. We have developed a bio-mathematical modeling approach which also accounts for non-specific binding and kinetics, aiming to predict the in vivo performance of candidate radioligands from in silico / in vitro data. The performance of our method is evaluated on a dataset including in silico / in vitro and in vivo data for each compound (n=28).

Methods: The approach presented here uses a standard input function and a one tissue compartment model to approximate the in vivo behavior of ligands in both target and reference regions with a parsimonious parameter set (influx rate constant K_1, efflux rate constant k_2 and binding potential BP_{ND}) predicted from in silico / in vitro data. K_1 prediction is based on the Renkin-Crone model ($K_1=F\cdot(1-e^{-PS/F})$) with perfusion F, capillary surface area S, and incorporates a model to predict permeability P from lipophilicity and molecular volume. k_2 is predicted by $k_2=V_{aq\_T}\cdot K_1\cdot f_{ND}/V_{aq\_P}\cdot f_P$, under the assumption of passive diffusion, from K_1, apparent aqueous volumes in plasma V_{aq_P} and tissue V_{aq_T}, free fractions in plasma f_P and tissue f_{ND} measured using equilibrium dialysis assays. The model to predict BP_{ND} ($BP_{ND}=f_{ND}\cdot B_{max}/K_D$) uses target density B_{max} and affinity K_D measurements derived from in vitro homogenate binding assays and f_{ND}.The in vivo performance of a ligand is estimated using the coefficient of variation of BP_{ND} (%COV[BP_{ND}]) metric derived from Monte Carlo simulations. 28 compounds for 10 targets were evaluated using our method to predict their in vivo performance and subsequently validated against in vivo PET data in the Landrace Pig.

Results: The predicted K_1, k_2 and BP_{ND} values from in silico / in vitro data were consistent with the in vivo estimates (Pearson´s r_{K1}= 0.54, p_{K1}=0.001, r_{k2}=0.73, p_{k2}< 0.0001, and r_{BPND} =0.82, p_{BPND}< 0.0001). The prediction showed that widely accepted "good" ligands such as ^{11}C-Flumazenil had small %COV[BP_{ND}] values whereas "poor" imaging probes were identified with a higher value such as ^{11}C(R)-PK11195. The model´s ranking of the candidates within a specific target was generally consistent with historical decisions made on the in vivo PET data.

Compound	Target	ROI	K_1 in vivo (ml/g/min)	K_1 predicted (ml/g/min)	k_2 in vivo (min^{-1})	k_2 predicted (min^{-1})	BP_{ND} in vivo	BP_{ND} predicted	%COV [BP_{ND}]
^{11}C-Flumazenil	BDZ	Frontal Ctx	0.48	0.48	0.43	0.47	5.96	17.6	2.22

^{11}C-FLB-457	D2	Thalamus	1.27	0.39	0.16	0.19	1.21	9.62	2.11
^{11}C-Raclopride	D2	Striatum	0.46	0.62	0.41	0.61	1.88	0.45	6.81
^{11}C-FLB-457	D2	Striatum	1.24	0.39	0.16	0.19	12.6	137	18.6
^{11}C-Raclopride	D2	Thalamus	0.45	0.62	0.40	0.61	0.40	0.03	77.7
^{11}C-(R)PK11195	PBR	Frontal Ctx	0.33	0.16	0.05	0.06	0.55	0.17	10.7
^{11}C-GSK215083	5-HT6	Striatum	0.70	0.58	0.06	0.09	1.05	0.53	3.14
^{11}C-GSK000002	5-HT6	Striatum	0.31	0.52	NQ	0.02	0.08	0.13	17.4
^{11}C-GSK000003	5-HT6	Striatum	0.16	0.14	0.04	0.07	0.00	0.01	>100

[In vivo performance prediction for 7 compounds]

Conclusion: Bio-mathematical modelling can aid the radioligand discovery and development process and efficiently leverage large compound databases.

312

BrainPET Poster Session: Kinetic Modeling

COMPARISON OF IN VIVO KINETICS OF ^{18}F-FALLYPRIDE AND ^{11}C-FLB-457

N. Vandehey[1], J. Moirano[1], D. Murali[1], A.K. Converse[2], J. Engle[1], R.J. Nickles[1], J. Mukherjee[3], M. Schneider[4], J. Holden[1], **B. Christian**[1]

[1]Dept. of Medical Physics, [2]Waisman Laboratory for Brain Imaging and Behavior, University of Wisconsin - Madison, Madison, WI, [3]Department of Psychiatry & Human Behavior, University of California Irvine, Irvine, CA, [4]Harlow Center for Biological Psychology, University of Wisconsin - Madison, Madison, WI, USA

Objectives: ^{18}F-Fallypride (FAL) and ^{11}C-FLB-457 (FLB) are two commonly used PET radioligands for imaging extrastriatal dopamine D_2/D_3 receptors. Though both tracers provide excellent visualization of receptor binding in regions with low D_2/D_3 receptor density (e.g. cortex), there are differences in their in vivo kinetics that may affect sensitivity for measuring subtle changes in receptor binding. Focusing on regions of low binding, we made a direct comparison of the kinetics of FAL and FLB in the rhesus monkey.

Methods: Single scan, multiple-injection studies; which includes high, medium, and low specific activity injections, were performed on two male rhesus monkeys with both FAL and FLB using a microPET scanner. Arterial blood samples were taken and measured for both whole blood and parent compound in plasma, which were used as the input functions to the kinetic model. Dynamic ROI data drawn on the cerebellum, occipital cortex, thalamus, and substantia nigra were fit using a hot-cold compartment model in the COMKAT environment to obtain estimates of the transport (K_1,k_2) and binding (k_{on}, B_{max},k_{off}) parameters.

Results: Measurement of the plasma-tissue transport constants, K_1 and k_2 and their ratio, reveals that FLB (K_1=0.49±0.11, k_2=0.59±0.10, K_1/k_2 = 2.69±0.51) has a considerably higher free space distribution volume (K_1/k_2) than FAL (K_1=0.47±0.12, k_2=0.23±0.05, K_1/k_2 = 0.82±0.21) averaged over the regions, due to a reduced tissue to plasma efflux constant (k_2). Both tracers have comparable k_{off} values of 0.025 (FLB) and 0.023 (FAL) but FLB has a slightly higher rate of association (k_{on}= 0.087±0.02) compared to that of FAL (k_{on}= 0.070±0.02), yielding a lower equilibrium dissociation constant, K_D. Within the first injection period of these scans (up to 90 minutes), FAL reaches pseudo-equilibrium in regions of mid-to-low binding, but FLB does not. Input function analysis showed that FAL is retained at a higher concentration in plasma for a longer period of time than FLB, having a 3x higher concentration after 60 minutes.

Conclusions: These findings in the rhesus monkey are consistent with human data for free space distribution volume (K_1/k_2) [1,2]. The slightly higher affinity ($1/K_D$) of FLB may be advantageous for measurement of baseline cortical D_2/ D_3 binding, however the higher k_2 of FAL may enhance the sensitivity for detecting changes in endogenous dopamine release due to its higher rate of clearance out of the free space.

References:

(1) Asselin, M.-C., Montgomery, A. J., Grasby, P. M. & Hume, S. P. (2007). Quantification of PET studies with the very high-affinity dopamine D_2/D_3 receptor ligand [^{11}C]FLB 457: re-evaluation of the validity of using a cerebellar reference region. Journal of Cerebral Blood Flow & Metabolism; 27, 378-392.

(2) Mukherjee J, Christian BT, Dunigan KA, Shi B, Narayanan TK, Satter M, Mantil J. Brain imaging of ^{18}F-fallypride in normal volunteers: blood analysis, distribution, test-retest studies, and preliminary assessment of sensitivity to aging effects on dopamine D_2/D_3 receptors. Synapse. 2002; 46,170-88.

313

Brain Poster Session: Experimental Stroke & Cerebral Ischemia

AFFECTIVE AND COGNITIVE CONSEQUENCES OF SMALL CEREBRAL INFARCTS

G. Neigh, M. Shurte

Psychiatry & Behavioral Sciences, Emory University, Atlanta, GA, USA

Objective: Together, late-life major depression and subsyndromal depression rob more than 15% of the elderly population of personal happiness and exacerbate comorbid conditions (1). The most serious consequence of late-life depression is premature death due to increased mortality following myocardial infarction and stroke as well as an increased rate of suicide (2). Although the etiology of late-life depression is not fully understood, it is associated with vascular pathology. Silent cerebral infarcts (SCI) have been identified in over 50% of patients with late onset depression (3), and these lesions are associated with more severe symptoms (4), more hospital admissions for depression, and longer hospitalizations for depression (5). Due to the inherent limitations of human research, it is unknown whether vascular changes in the elderly are causative of depressive behaviors or an unrelated but co-occurring event. Because small cerebral infarcts have been repeatedly associated with increased occurrence and severity of symptoms of depression, the current work tests the hypothesis that small cerebral infarcts induce anxiety-like and depressive-like behaviors in a rat model.

Methods: Male rats (3 or 18 mos old) were anesthetized and microembolism or SHAM procedures were performed. Briefly, the left or right common carotid was exposed and microbeads (50um in diameter) were injected via a 30-G needle. After 14d of recovery from the procedure, rats were tested for both depressive-like and anxiety-like behaviors. Tests included: social interaction, elevated plus maze, open field, sucrose preference, and forced swim.

Results: Data indicate that rats that received microembolism infarcts demonstrate an increase in depressive-like behavior, as measured by deficits in sucrose preference and forced swim activity, as compared to SHAM operated rats. Results from the full panel of behavioral tests in both age groups will be presented. Analysis of the brain tissue from these rats will determine the role of lesion laterality and location in generation of behavioral changes.

Conclusions: The data collected to date indicate that experimental induction of small cerebral infarcts is sufficient to induce depressive-like behavior. This suggests that small cerebral infarcts may be one underlying cause of late life depression in the elderly population. A better understanding of the behavioral consequences of small cerebral infarcts will provide insight into the neurobiology of vascularly-induced behavioral changes and guide the development of novel treatment strategies.

References:

1. Katz IR, Streim J,Parmelee P: Prevention of depression, recurrences, and complications in late life. Prev Med 1994; 23:743-7502.

2. Gottfries CG: Late life depression. Eur Arch Psychiatry Clin Neurosci 2001; 251 Suppl 2:II57-613.

3. Fujikawa T, Yamawaki S,Touhouda Y: Incidence of silent cerebral infarction in patients with major depression. Stroke; a journal of cerebral circulation 1993; 24:1631-16344.

4. Yamashita H, Fujikawa T, Yanai I, et al: Clinical features and treatment response of patients with major depression and silent cerebral infarction. Neuropsychobiology 2001; 44:176-1825.

5. Yanai I, Fujikawa T, Horiguchi J, et al: The 3-year course and outcome of patients with major depression and silent cerebral infarction. Journal of affective disorders 1998; 47:25-30

BRAIN COOLING BY NOVEL INTRAVENTRICULAR CATHETER

R. Moomiaie-Qajar[1], G. Gould[1], D. Botta[2], J. Simmons[3], J. Elefteriades[4]

[1]Yale School of Medicine, [2]Surgery, Yale School of Medicine, New Haven, [3]CoolSpine LLC., Woodbury, [4]Surgery-Cardiac, Yale School of Medicine, New Haven, CT, USA

Background: The neuroprotective effects of hypothermia are well-known. We recently reported effective cooling of the spinal cord in a sheep model by a self-contained intrathecal catheter. In that study we sucessfully induced localized hypothermia of the spinal cord, thereby promising a potential modality for spinal cord protection during aortic aneurysn repair.

Purpose: The present study is designed to determine if cooling catheters in the lateral ventricles of the brain can effectively cool the cerebral spinal fluid (CSF) and thereby reduce brain temperature while maintaining systemic normothermia. In particular, it is unknown whether a cooling system can overcome the warming by the native cerebral blood flow.

Methods: The cooling catheter is a self-contained system that circulates a cold fluid and cools the CSF that circulates in the brain. The CSF in turn cools the surrounding brain by conduction. This cooling catheter was specifically designed for application to the lateral ventricles of the brain. Burr holes were made in the skull and the catheter was placed into the lateral ventricles using the standard method for placement of ventriculostomy catheter. The study was conducted in sheep because of their body mass is similar to adult humans. To monitor the cooling effect, four temperature probes were placed in the brain (left and right hemispheres of the brain in anterior and posterior locations to the ventricles).

Results: Five experiments were successfully completed (temperature probes modified after first experiment). In each animal, two cooling catheters were successfully placed into the lateral ventricles. The mean brain temperature for all sheep decreased to 34.5°C (mean) during the 3 hour cooling period. This represented a 9.7% reduction from the average baseline brain temperature of 38.2°C. During the cooling period, the cooling fluid was circulated through the catheter at a maximum rate of 50 ml per minute. The lowest achieved brain temperature during cooling was 26.7°C, which represented a 28.6% decrease from baseline. When cooling was stopped, the brain temperature readings equilibrated with the core temperature promptly. Post- mortem examination of the brains showed no significant morphologic changes under gross or histologic examinations.

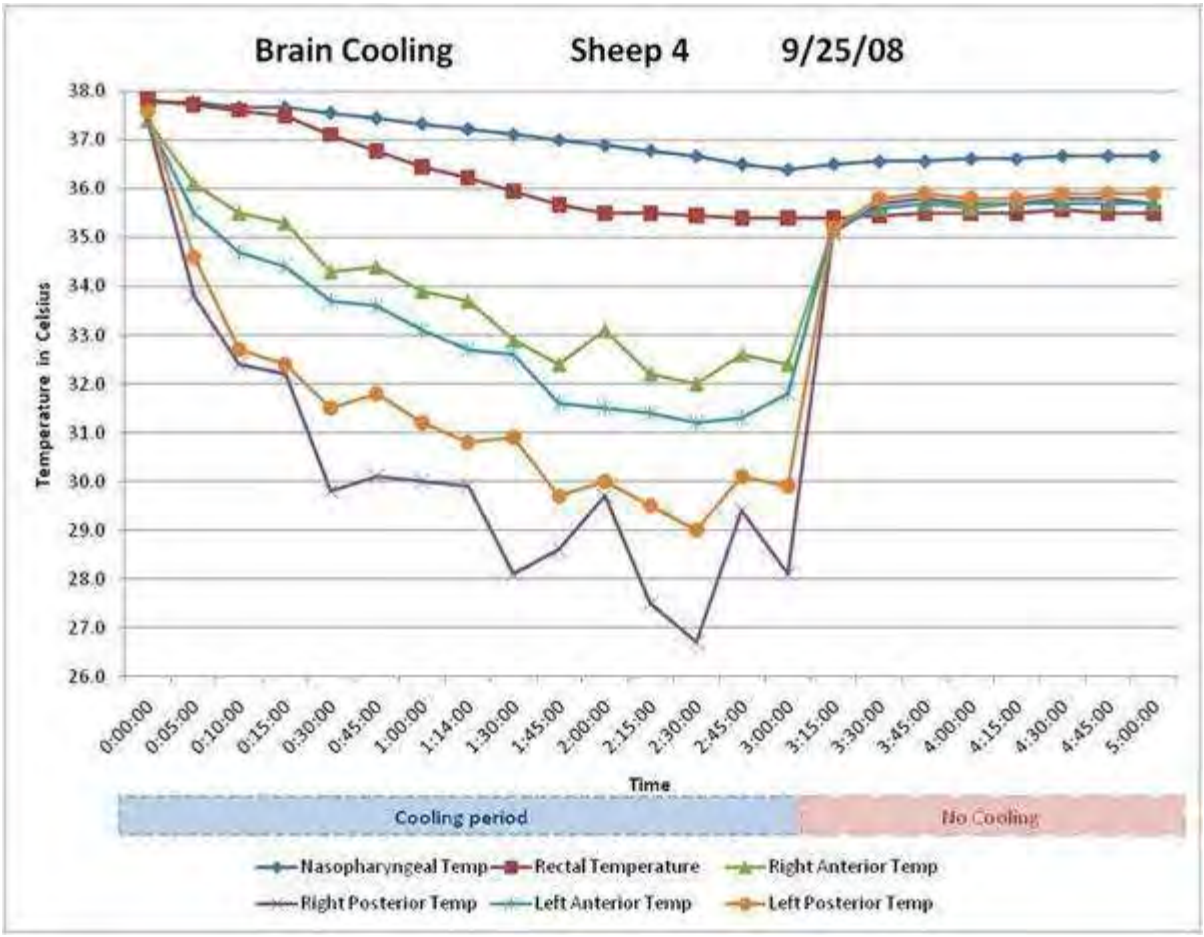

[CoolSpine Intraventricular Cooling Catheter]

Conclusion: Localized cooling of the brain to moderate hypothermic levels while maintaining relative systemic normothermia was demonstrated in an animal model with our intraventricular cooling catheters. This novel technique holds promise as an additional neuroprotection modality to mitigate brain injury in deep hypothermic circulatory arrest for aortic arch surgery as well as in traumatic brain injury and stroke.

317

BrainPET Poster Session: Kinetic Modeling

A NEW SPECTRAL ANALYSIS METHOD FOR MEASURING REGIONAL RATES OF CEREBRAL PROTEIN SYNTHESIS IN L-[1-^{11}C]LEUCINE PET STUDIES

M. Veronese[1], A. Bertoldo[1], S. Bishu[2], A. Unterman[2], G. Tomasi[3], C.B. Smith[2], K.C. Schmidt[2]

[1]Department of information Engineering, University of Padova, Padova, Italy, [2]Section of Neuroadaptation & Protein Metabolism, National Institute of Mental Health, Bethesda, MD, [3]Department of Diagnostic Radiology, Yale University, New Haven, CT, USA

Objective: Due to the limited spatial resolution of PET, a region of interest (ROI) likely contains a heterogeneous mixture of tissues. To date, however, we have been applying a homogeneous tissue kinetic model (HOM) for determination of regional rates of cerebral protein synthesis (rCPS) from L-[1-^{11}C]leucine PET data in humans [1]. Since Spectral Analysis (SA) [2] applies to heterogeneous as well as homogeneous tissues, it might be an alternative quantitative method. In this study, we developed and tested a new SA algorithm to estimate rCPS at the ROI level.

Methods: Because previous SA methods [2,3] did not consistently produce reliable estimates when applied to L-[1-^{11}C]leucine data, we developed a new SA iterative filtering (SAIF) method. SAIF uses prior information concerning irreversibility of trapping of the tracer as well as components that cannot be distinguished from blood; intermediate components are assumed to reflect tissue reversible compartments. Performance of SAIF was compared to previous SA methods [2,3] in simulation studies. Bias and precision (coefficient of variation (CV)) of the estimates were used as performance indices. We also compared three methods of analysis of L-[1-^{11}C]leucine PET data measured in 9 healthy male subjects:

1. SAIF;
2. HOM applied at the ROI level with a nonlinear least squares algorithm; and
3. HOM applied at the voxel level with a basis function method.

Goodness-of-fit was assessed by the weighted residual sum of squares.

Results: In simulation studies SAIF yielded the best fit, lowest bias (< 2%), and lowest CV (6%), compared with previous SA methods. In measured data, rCPS estimated with SAIF agreed with the average of rCPS values estimated by using HOM at the voxel level, but differed substantially from ROI-based rCPS estimated by HOM (Table). This is consistent with the presence of a greater degree of tissue heterogeneity in the ROI, compared to individual voxels, that is not accounted for with the homogeneous tissue kinetic model. In most regions CVs with SAIF were somewhat higher than when a fixed kinetic model was used, probably due to the increased number of parameters estimated with SAIF.

ROIs	Homogenous Model ROI analysis	Homogenous Model Voxel analysis	SAIF ROI analysis

Whole Brain	1.85 ± 0.10	1.61 ± 0.08	1.59 ± 0.13
Frontal Cortex	2.16 ± 0.13	1.90 ± 0.08	1.85 ± 0.11
Thalamus	1.72 ± 0.10	1.54 ± 0.09	1.49 ± 0.06
Corona Radiata	0.98 ± 0.07	0.84 ± 0.06	0.88 ± 0.08
Values are mean ± SD for 9 subjects			

[Table - rCPS (nmol g-1 min-1)]

Conclusions: SAIF demonstrated low bias and good precision. SAIF accounts for tissue heterogeneity, unlike HOM, and may be a useful and robust method for estimating rCPS at the ROI level.

References:

[1] Bishu S et al., JCBFM 2008, 28: 1502-1513;

[2] Cunningham VJ, Jones T, JCBFM 1993, 13:15-23;

[3] Turkheimer et al., JCBFM 1994, 14: 406-422.

Supported by IRP/NIMH/NIH.

PFC IMPROVES BRAIN OXYGENATION IN A RAT MODEL OF FOCAL CEREBRAL ISCHEMIA

G. Deuchar[1], D. Brennan[2], B. Condon[2], C. McCabe[1], C. Santosh[2], I.M. Macrae[1]

[1]Glasgow Experimental MRI Centre, Department of Clinical Neurosciences, University of Glasgow, [2]Institute of Neurological Sciences, Southern General Hospital, Glasgow, UK

Objective: With tissue hypoxia playing a central role in the regulation of cell death following stroke, supplementary oxygen has been postulated as a potential therapy to improve patient outcome (1). Perfluorocarbons (PFCs) are biologically inert compounds able to dissolve large amounts of gases including oxygen. We aimed to investigate whether hyperoxia and PFC could provide local conditions necessary for prolonged cell survival following stroke.

Methods: Male Sprague Dawley rats (n=10) were ventilated with air and 2% isoflurane. Focal cerebral ischemia was generated in a model of permanent middle cerebral artery occlusion (MCAO) by the intraluminal filament technique. Mean arterial blood pressure (MABP) was continuously measured and blood gases analysed to ensure physiological stability. Rats were placed in a stereotaxic frame and combined oxygen sensing and laser Doppler flow probes (OxyLite/OxyFlow, Oxford Optronix, UK) were inserted into both the ipsilateral (penumbral region of MCA territory) and contralateral cortex to measure brain tissue oxygenation (pO_2) and relative cerebral blood flow (CBF). Non-stroked rats were used as controls. Following a period of stabilization (air) the effect of hyperoxia (60% O_2) was investigated ~2 hours post MCAO. On stabilization of the response to 60% O_2 (~5mins), 1.5ml PFC was administered intravenously (0.25ml/min) with animal breathing 60% O_2.

Results: Basal brain pO_2 was lower in the ipsilateral cortex when compared to contralateral following MCAO (14.0±4.3mmHg vs 41.7±10.9mmHg, $P< 0.05$). In MCAO rats, hyperoxia alone resulted in significant increases from basal values in brain pO_2 in both the ipsilateral (97±20.4%, $P< 0.01$) and contralateral cortex (45.3±2.2%, $P< 0.05$). This effect was also evident in the corresponding cortex in control rats (increased by 93.3±16.6% and 73.7±11.6%, both $P< 0.01$). In contrast hyperoxia had no significant effect on CBF in either MCAO or control rats with hyperoxia while there were small transient increases in MABP (4.7±2.9% in MCAO, ns; 8.6±2.4% in control, $P< 0.05$).

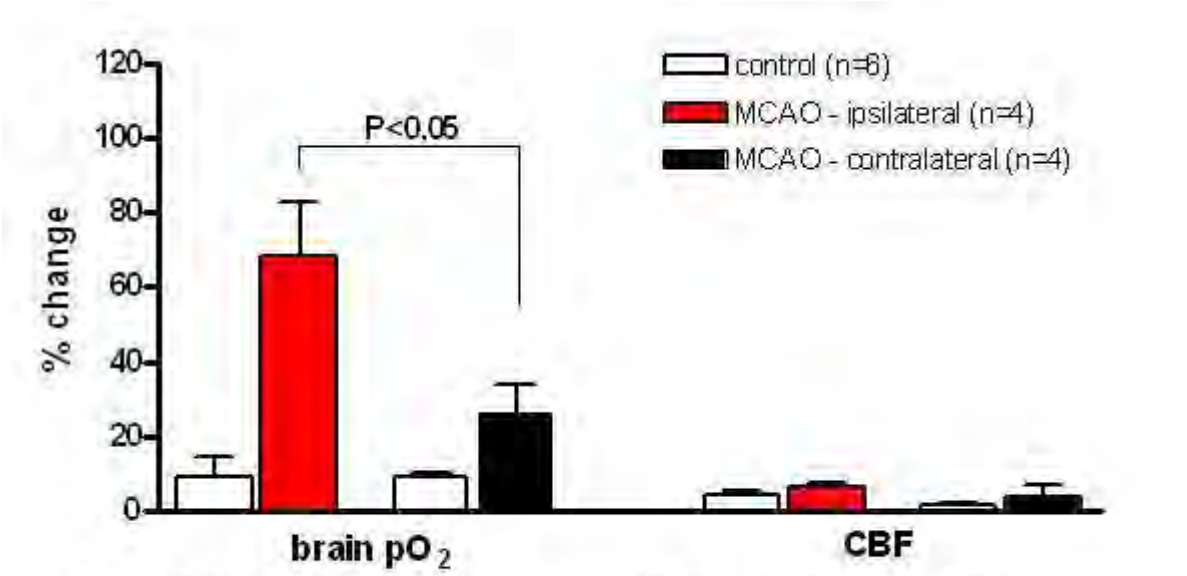

Figure 1. Effect of PFC on brain pO_2 and CBF while rat breathing 60% oxygen.

[Figure 1]

Figure 1 shows that PFC further increased brain pO_2 and to a greater extent in the ipsilateral cortex when compared to the contralateral in MCAO rats (68.4±14.4% vs 26.6±7.2%, P< 0.05). These effects were significantly greater when compared to the response in control rats where brain pO_2 was increased by 9.1±5.6% and 9.0±1.2% in the corresponding cerebral cortex. A small transient increase in CBF was evident during the first minute of PFC administration (Fig.1). During PFC administration there was also a transient increase in MABP in MCAO (18.8±5.8%) and control (11.9±1.2%) rats.

Conclusions: Our study further substantiates the potential of normobaric hyperoxia to provide conditions favourable for cell survival following stroke and suggests that PFC's may deliver additional oxygen to the ischemic penumbra thereby potentially prolonging the lifespan of this salvageable region of tissue following stroke.

References:

(1) Kim et al. Ann Neurol 2005. 57;571-5.

319

Brain Oral Session: Traumatic Brain Injury: Metabolism

MITOCHONDRIAL UNCOUPLING PROTEIN-4 POLYMORPHISMS ARE ASSOCIATED WITH DEPTH OF COMA AFTER TRAUMATIC BRAIN INJURY

J.L. Cousar[1], Y.P. Conley[2], A.A. Sarnaik[3], P.M. Kochanek[3], D.O. Okonkwo[4], R.S.B. Clark[3]

[1]University of Pittsburgh School of Medicine, [2]School of Nursing, University of Pittsburgh, [3]Critical Care Medicine, Safar Center for Resuscitation Research U. of Pittsburgh, [4]Neurological Surgery, University of Pittsburgh School of Medicine, Pittsburgh, PA, USA

Background and aims: Mitochondrial uncoupling proteins (UCP) are a family of anion-carrier proteins that allow controlled proton leak into the mitochondrial matrix, subsequently reducing membrane potential. UCP1 is found mainly in brown adipose tissue, whereas UCP2 and UCP4 are found in mitochondria within the central nervous system. UCP are thought to serve as key mediators in mitochondrial homeostasis and possibly neuronal function and synaptic transmission (1), and may protect against oxidative stress and calcium overload after brain injury (1-4). Recently it has been demonstrated that single nucleotide polymorphisms (SNP) of UCP genes are associated with schizophrenia and multiple sclerosis (5-7). However, there are no data examining the relationship between UCP polymorphisms and traumatic brain injury (TBI), the most common cause of death in children and young adults.

Methods: DNA samples collected from 177 adult patients (mean age 34±15 y; 83% male) with severe TBI were assayed for tagging SNP of UCP2 (rs660339) and UCP4 (rs3757241 and rs9381469). For each SNP, patients were dichotomized based on allele frequencies for multivariate logistic regression analysis to determine independent associations with initial Glasgow Coma Scale score (GCS), and Glasgow Outcome Score (GOS) assigned at 3-12 months (the last available GOS was used), adjusting for age and sex.

Purpose: To determine whether SNP of UCP2 and UCP4 genes are associated with relevant clinical variables after TBI.

Results: Frequencies for UCP2 at rs660339 were AA (16%), AG (50%), and GG (34%); UCP4 at rs3757241 were CC (61%), CT (36%), and TT (3%); and UCP4 at rs9381469 were AA (26%), AG (48%), and GG (27%). These frequencies were similar to published data available through the International HapMap Project, Public release #26, 2008-11-26. Both UCP4 polymorphisms, but not the UCP2 polymorphism, were independently associated with initial GCS. There was no association between any SNP and GOS.

UCP4 Polymorphism	Inital GCS (Median[Range])	Odds Ratio[5-95% Confidence Limits]	P
rs3757241	CC, 6[3-13] vs. CT/TT, 5[3-10]	1.243[1.021-1.512]	0.03
rs9381469	AG/GG, 5[3-10] vs. AA, 6[3-13]	0.818[0.674-0.994	0.04

[UCP4 Polymorphism and Glasgow Coma Scale Score]</i>

Conclusions: UCP4 is the most prevalent mitochondrial UCP in the brain. These data suggest that UCP4 polymorphisms are associated with initial depth of coma (as assessed by the GCS) after severe TBI, and are consistent with a role for UCP4 in neuronal activity (1) after brain injury. Further study is warranted. Support: NINDS NS38620/NS30318.

References:

(1) Andrews ZB, et al. Nat Rev Neurosci</i> 2005;6:829-40,

(2) Sullivan PG, et al. J Bioenerg Biomembr</i> 2004;36:353-6,

(3) Liu D, et al. Neuromolecular Med</i> 2006;8:389-414,

(4) Mattiasson G, et al. Nat Med</i> 2003;9:1062-8,

(5) Yasuno K, et al. Am J Med Genet B Neuropsychiatr Genet</i> 2007;144:250-3,

(6) Vogler S, et al. J Mol Med</i> 2005;83:806-11,

(7) Otaegui D, et al. Mult Scler</i> 2007;13:454-8.

MP4A PET IN MILD COGNITIVE IMPAIRMENT AND ALZHEIMER'S DISEASE

W.-D. Heiss[1], C. Haense[1], C. Hohmann[1], E. Kalbe[2], R. Krais[1], B. Bauer[1], B. Neumaier[1], K. Herholz[3]

[1]Max Planck Institute for Neurological Research with Klaus-Joachim-Zuelch-Laboratories of the Max Planck Society and the Faculty of Medicine of the University of Cologne, [2]Department of Neurology, University of Cologne, Cologne, Germany, [3]Wolfson Molecular Imaging Centre, University of Manchester, Manchester, UK

Background and aims: The radiolabeled acetylcholine analogue [11C]N-methyl-4-piperidyl acetate (MP4A) is a tracer for in vivo imaging of cerebral acetylcholine esterase (AChE) activity with positron emission tomography (PET). MP4A is hydrolyzed specifically by AChE whose activity is a marker of the integrity of cholinergic axons and cholinoceptive neurons in human cerebral cortex [1]. Previous preliminary studies indicate a general reduction of AChE activity in Alzheimer dementia (AD) and Mild Cognitive Impairment (MCI) [2]. We used [11C]-MP4A PET to investigate the functionality of the cholinergic system in healthy controls, MCI patients and AD patients.

Methods: MP4A PET was performed in 21 healthy controls (age 64.6±8.7 years), 20 patients with MCI (age 67.1±7.9 years, MMSE 27.2±1.6) and 15 patients with AD (age 66.1±7.9 years, MMSE 21.1±2.7). Subjects were free of cholinesterase inhibitors. A comprehensive neuropsychological battery was administered. Voxel based activity curves were obtained from Gauss filtered normalized frames and evaluated against putamen as reference. Afterwards parametric images of hydrolysis rate constant k3 were generated by non-linear least squares fits and analysed using standard atlas regions.

Results: All groups were comparable regarding age (Controls vs. MCI, $p=0.884$; Controls vs. AD, $p=1.00$; MCI vs. AD, $p=1.00$). Regions with the highest values of k3 in all three groups were amygdala, entorhinal cortex, hippocampus and precentral gyrus whereas in cuneus, precuneus, inferior parietal lobule and occipital cortex in all groups and additionally in temporal regions in MCI and AD patients the cortical AChE activity was lowest. The mean cortical k3 of controls was 0.084±0.008 min-1 which was significantly higher than in MCI patients (0.076±0.011 min-1, $p< 0.05$, reduction 9.58%) and in AD patients (0.066±0.009 min-1, $p< 0.01$, reduction 20.71%). The reduction of mean cortical k3 in AD compared to MCI (12.32%) was also significant ($p< 0.05$). Reduction of k3 in temporal regions was most pronounced. Hippocampus, amygdala and entorhinal also showed large k3 reductions in patients, but also high variance of values. Lower but still significant reductions were found for frontal regions and the cuneus.

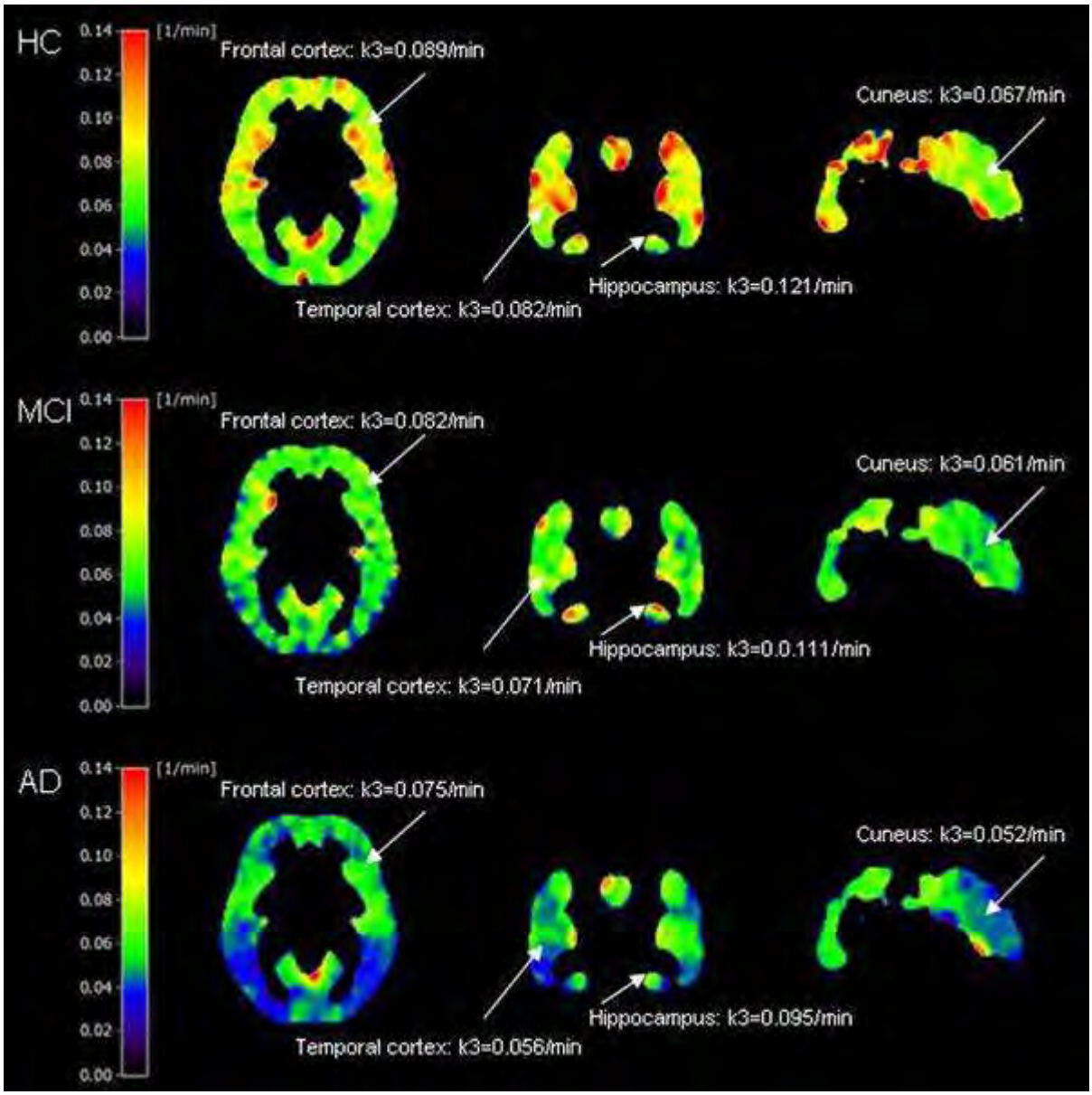

[Parametric images of [11C]-MP4A hydrolysis rates]

Conclusion: These results confirm impairment of the cholinergic system in AD which is even present to a lower degree in MCI. Since [11C]-MP4A PET allows a clear differentiation between groups it might be a valuable tool for early diagnosis of degenerative dementia.

Acknowledgements: This study was funded by the Marga and Walter Boll Foundation and the WDH Foundation.

References:

[1] Mesulam MM, Geula C (1991) Acetylcholinesterase-rich neurons of the human cerebral cortex: Cytoarchitecture and ontogenetic patterns of distribution. J Comp Neurol 306:193-220.

[2] Herholz K, Weisenbach S, Zuendorf G, Lenz O, Schroeder H, Bauer B, Kalbe E, Heiss WD

(2004) In vivo study of acetylcholine esterase in basal forebrain, amygdala, and cortex in mild to moderate Alzheimer disease. Neuroimage 21:136-143.

HUMAN BRAIN FUNCTIONAL ANALYSIS THROUGH PROPER ORTHOGONAL DECOMPOSITION DURING SINGLE WORD TRIAL

K. Oyama[1], T. Sugiura[1], T. Kato[2]

[1]Department of Mechanical Engineering, Keio University, Yokohama, [2]KATOBRAIN Co., Ltd., Tokyo, Japan

Objectives: The aim of this study is to make an indicator which reflects oxygen consumption in a capillary synchronized with neural activity and make a comparison of temporal changes of the index with those of hematocrit through analyses of hemoglobin changes measured on human scalp with near infrared light with application of a multivariate statistical technique.

Methods: We regarded time courses of oxygenated hemoglobin and deoxygenated hemoglobin obtained through single trial of a language task as time series data of coupled oscillators in mechanical systems. We divided the time courses into stimulus period and rest period and then applied proper orthogonal decomposition (POD), which can extract principal components from time series data, to each time period. Based on the assumption that increase in deoxygenated hemoglobin during stimulus reflects oxygen consumption in a capillary and increase in oxygenated hemoglobin after stimulus reflects oxygen supply, we obtained characteristic patterns of oxygen consumption and oxygen supply from stimulus time period and rest time period, respectively. Then we computed temporal changes in magnitude of two kinds of patterns based on the similarity to the representative patterns.

Results: Temporal changes of the index of cerebral oxygen exchange expressed by a ratio of the magnitude of oxygen consumption to that of oxygen supply are shown in Figure. The index reaches its maximum a few seconds after stimulus onset, showing deoxygenation in a capillary in early phase of neural activity and preceding increase in hematocrit, and gradually decreases the following seconds.

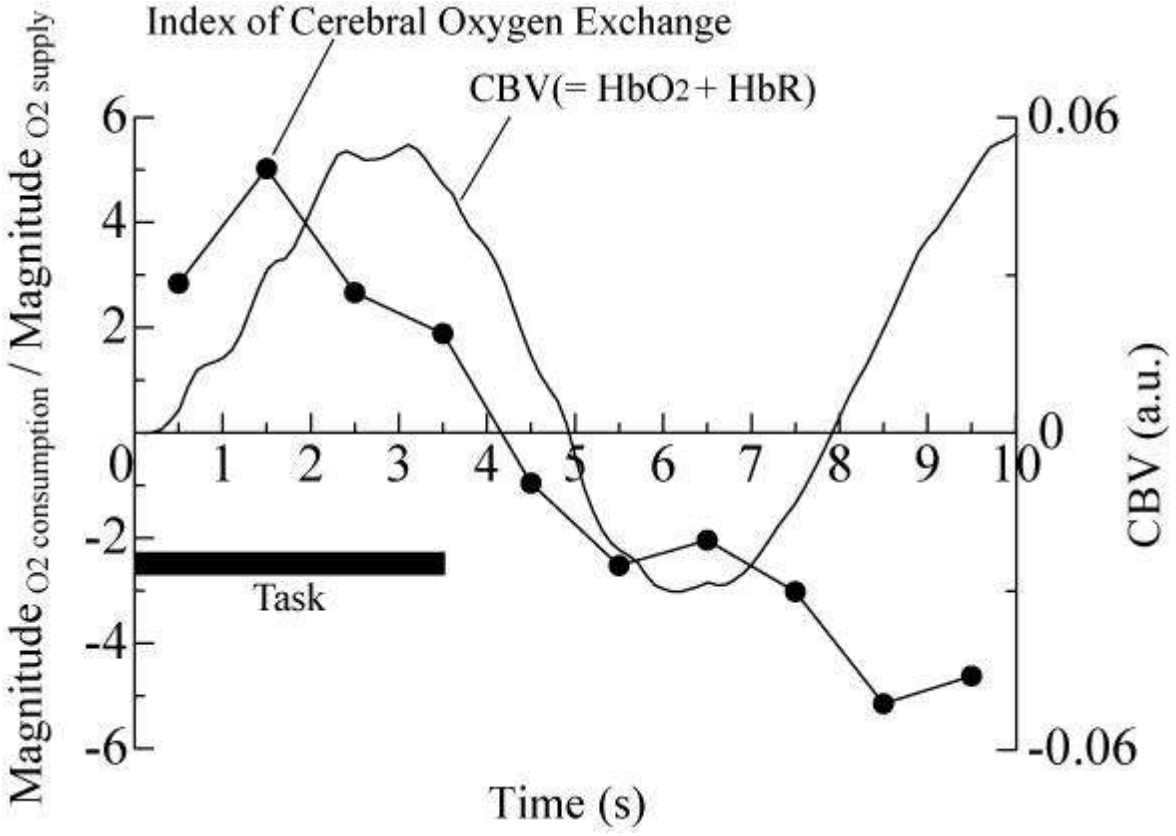

[Index of cerebral oxygen exchange]

Conclusions: We obtained an index of cerebral oxygen exchange synchronized with neural activity through application of POD to the time courses of oxygenated hemoglobin and deoxygenated hemoglobin. A comparison of changes of the index with those of hematocrit revealed a temporal difference between the two.

References:

T. Kato, 2004. Principle and technique of NIRS-Imaging for human brain FORCE: fast-oxygen response in capillary event, International Congress Series, 1270, 85-90.

Feeny B.F., Kappagantu R., 1998. On the Physical Interpretation of Proper Orthogonal Modes in Vibrations, Journal of Sound and Vibration, 211(4), 607-616.

323

Brain Poster Session: Neonatal Ischemia

MRI AND HISTOLOGICAL CHANGES CORRESPONDING TO DESCENDING CORTICOSPINAL TRACT DEGENERATION FOLLOWING NEONATAL HYPOXIC ISCHEMIC BRAIN INJURY AND ASSOCIATED BEHAVIORAL OUTCOME

S. Lama[1], M. Qiao[2], A. Ng[1], D. Barua[1], D. Kirk[1], T. Foniok[2], A. Kirton[3,4], U. Tuor[1,2]

[1]Medical Science, University of Calgary, [2]MR Technology, Institute for Biodiagnostics (IBD-West), National Research Council, [3]Pediatrics and Clinical Neurosciences, University of Calgary, [4]Pediatrics (Division of Neurology), Alberta Children's Hospital, Calgary, AB, Canada

Background and aims: Recently, clinical magnetic resonance imaging (MRI) studies have demonstrated acute diffusion weighted imaging (DWI) changes in the descending corticospinal tract (DCST), which includes motor fibres of the posterior limb of the internal capsule, cerebral peduncle, basis pontis and medullary pyramid (1,2). This has been attributed to possible early neuronal injury or Wallerian degeneration but the corresponding tissue correlates are currently not known. Crucial for improved diagnosis is the availability of an animal model with comparable MRI changes and in which the corresponding tissue changes of this pathological process can be determined and translated clinically.

Methods: Seven day old Wistar rat pups (n=29) were subjected to either sham surgery or unilateral cerebral hypoxia-ischemia produced by occlusion of the right common carotid artery under isoflurane anesthesia followed by exposure to hypoxia (3). At 24 and/or 48 hours following the hypoxia-ischemia, animals were anesthetized with isoflurane and T_2, Diffusion weighted images (DWI) and Apparent Diffusion Coefficients (ADC) maps of the brain were acquired using a 9.4T Bruker Biospin (Magnex) MR system. Animals were euthanized immediately post MRI or allowed to recover up to 4 weeks post insult. Behavioral outcome was assessed, 4 weeks post injury, using a modified neurological scoring system and cylinder test. Left-right hemispheric differences in T_2 relaxation times and ADC were compared using a paired t-test and to sham control values. Brains were processed and stained immunohistochemically with SMI 31 antibody for axonal phosphorylated neurofilaments.

Results: Quantitation of the T_2, DWI intensity and ADC changes demonstrated significant left-right differences along the DCST at 24h and 48h post injury (Fig. 1). Differences were most prominent in the cerebral peduncle and internal capsule (Fig. 2). SMI 31 staining of neurofilament within axons generally showed loss of staining ipsilaterally. Behavioral scores indicated deficits in the hypoxic ischemic animals in comparison to the sham controls.

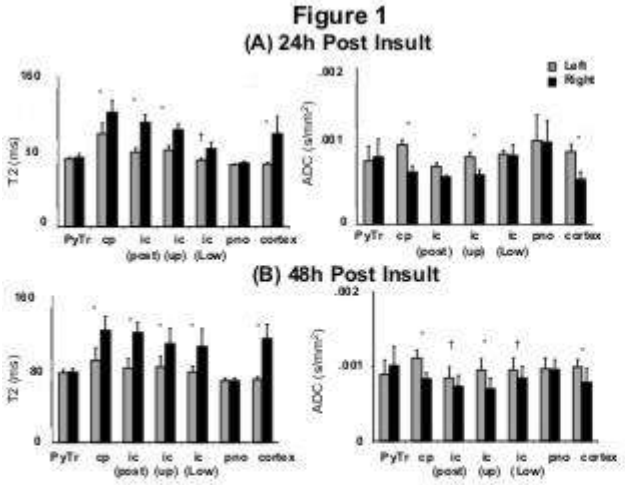

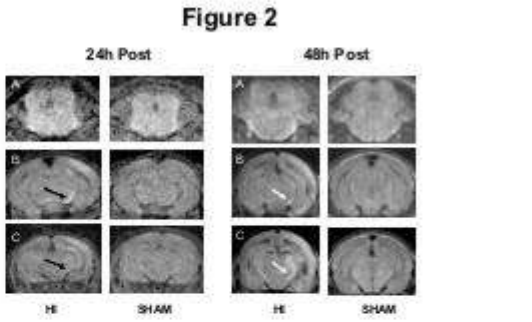

Fig 2 : Representative diffusion weighted images at the given times post suregary at medullary (A), pontine (B) and midbrain (C) levels. Arrows show cerebral peduncle and internal capsule of the DCST in B and C respectively.

Fig 1 : Mean T_2 or ADC in left or right (ipsilateral) regions of the DCST following either at 24h (**A**) or 48h (**B**) after a unilateral cerebral hypoxic ischemic insult. (* $p<0.001$, † $p<0.05$; Py Tr=Pyramidal tract, cp=Cerebral peduncle, ic=Internal capsule, post=posterior, pno=Pontine reticular nuclei oral)

[Figures 1 and 2]

Conclusions: CNS Wallerian degeneration detected histologically occurs in response to a substantial cortical injury caused by cerebral hypoxia ischemia and this can be detected by MRI in the form of T_2, DWI and ADC changes. This is accompanied by an observation of behavioural deficits in the hypoxic ischemic group. Our study provides evidence of a novel animal model to further investigate and help establish axonal degeneration as clinicopathological diagnosis non-invasively. (Supported by Heart and Stroke Foundation, Alberta and AHFMR/HBI Traineeship 2008).

Reference:

1. Kirton A,Shroff M, Visvanathan T, deVeber G, Stroke, (2007); 38(3):974-80;

2. Domi T, Kirton A, deVeber GA, Shroff M, Kouzmitcheva E, and MacGregor D; (2007) Stroke;

3. Meng S, Qiao M, Scobie K, Tomanek B, Tuor UI, Pediatr Res.(2006)59:554-9.

Brain Poster Session: Cerebral Metabolic Regulation

TWO-PHOTON MEASUREMENT AND MODELING OF NADH EMISSION CHANGES IN CORTEX DURING HYPOXIA, CORTICAL SPREADING DEPRESSION, AND FUNCTIONAL ACTIVATION

S. Sakadžić[1], V.J. Srinivasan[1], M.A. Yaseen[1], A. Devor[1,2], C. Ayata[3,4], D.A. Boas[1]

[1]Department of Radiology, MGH/MIT/HMS Athinuola A. Martinos Center for Biomedical Imaging, Massachusetts General Hospital, Harvard Medical School, Charlestown, MA, [2]Department of Neurosciences and Radiology, University of California at San Diego, San Diego, CA, [3]Stroke and Neurovascular Regulation Laboratory, Department of Radiology, [4]Stroke Service and Neuroscience Intensive Care Unit, Department of Neurology, Massachusetts General Hospital, Harvard Medical School, Charlestown, MA, USA

Objectives: Quantification of NADH changes in astrocytes and neurons during functional brain activation and pathological conditions provides critical insight in mechanisms of neurovascular coupling and brain metabolism [1-3]. Two-photon (2P) microscopy is becoming a tool of choice for in vivo measurement of NADH changes on the cellular level that is driving current progress in our understanding of astrocytic and neuronal metabolism [1,2,4]. However, the NADH emission spectrum is strongly attenuated by hemoglobin and in in vivo measurements the changes in NADH emission are affected by hemodynamic responses. We used modeling of excitation and emission light propagation based on microscopic 3D maps of rat cerebral vasculature to determine the effect of hemodynamic responses on detected NADH emission in 2P microscopy at various depths and conditions. The modeling procedure was then applied to evaluate the true NADH changes in our measurements during pathological changes and functional activation at different depths.

Methods: Two-photon imaging of the rat's cortex was performed through a sealed cranial window. Blood plasma and astrocytes were labeled with fluorescein-conjugated dextran (FITC) and Sulforhodamine101 (SR101), respectively. Simultaneous imaging of NADH fluorescence emission, astrocytes, and blood vessels was performed with three separate detectors in a commercial 2P microscope (Ultima, Prairie Technologies Inc.) using 740nm excitation wavelength. Imaging was performed during hypoxia, cortical spreading depression, and functional activation of the forepaw region. Based on the measured 3D map of the micro-vasculature we modeled the effect of blood volume and oxygen saturation changes on both excitation and emission of NADH fluorescence using ray tracing and Monte Carlo simulations.

Results: Based on the fluorescence excitation and emission propagation modeling we established a range of depths and distances from the cortical vessels of different diameter where the detection of the NADH emission is not significantly affected by the hemodynamic responses. We determined individual contributions of blood volume and oxygen saturation changes on detected NADH emission signal, and found that the blood volume changes are playing a dominant role. Changes in the detected signal of other dyes (SR101 and FITC) at all depths can also be used as valuable indicators of the hemodynamic response's influence on the NADH signal. Finally, light propagation modeling was applied to validate the measurements during pathological conditions and functional activation at different depths.

Conclusions: We developed a detailed excitation and emission light propagation modeling for 2P imaging of the NADH changes. The modeling was used to determine the hemodynamic response influence on measured NADH emission and it was applied to validate the NADH measurements during pathological conditions and functional activation. This study will help to improve the accuracy of in vivo 2P measurement of cortical metabolism. Analogous modeling can be used to assist 2P imaging of other fluorophores important for neuronal activation and brain metabolism such as calcium dyes and flavins.

References:

[1] Takano T. et al., Nat. Neurosci. 10, 754-762, 2007.

[2] Kasischke, K.A. et al., Science 305, 99-103 (2004).

[3] Turner, D.A. et al., Trends Neurosci. 30, 390-398, 2007.

[4] Iadecola C., Nedergaard M., Nat. Neurosci. 10, 1369-1376, 2007.

FUNCTIONAL MAGNETIC RESONANCE IMAGING IN UN-ANAESTHETIZED RATS USING A CHRONICALLY IMPLANTED SURFACE COIL

C. Martin[1], A. Kennerley[2], J. Berwick[2], N. Sibson[3], J. Mayhew[2]

[1]Department of Physiology, Anatomy and Genetics, University of Oxford, Oxford, [2]Department of Psychology, The University of Sheffield, Sheffield, [3]Gray Institute for Radiation Oncology and Biology, University of Oxford, Oxford, UK

Background and aims: Functional magnetic resonance imaging in animal models usually requires the use of anaesthetic agents. However, such agents interfere with normal neuronal, metabolic and haemodynamic function in addition to precluding the use of operant and behavioural experimental protocols. In light of this we have developed techniques to enable functional imaging studies to be repeatedly conducted in trained, restrained, un-anaesthetized rats. Chronic implantation of the surface coil and accurate repeated positioning of the subject in the scanner bore enabled acquisition of imaging data to commence within minutes of securing the animal. Using this methodology we have successfully recorded both local (whisker stimulation) and global (using hypercapnia) functional imaging responses in fully conscious animals over a period of several weeks.

Methods: Animals were gradually acclimatised to the noise of the scanner and increasing periods of restraint in a body harness for periods of up to 1 hour over a 3 week period prior to surgical preparation. Animals were then anaesthetized and a 15mm diameter surface transmit/receive coil (in-house design) was secured to the skull using plastic screws and cyanoacrylate. A cylindrical chamber protruded from the top of the coil and provided a means to secure the head during imaging. To enable electrical stimulation Teflon-coated tungsten microwires were implanted subcutaneously in the whisker pad and electrical connectors were positioned on the top of the head. Animals were allowed to recover for 72hrs prior to any imaging experiments. The apparatus is shown in **A**. Functional data were acquired from suitable coronal and oblique slices using a single shot MBEST Gradient Echo - Echo Planar Imaging sequence (B0 = 7, data matrix = 64*64, FOV = 30mm, slice thickness = 1mm, TR/TE=1000/12ms, flip angle 90^{o}). Stimuli consisted of 0.4mA, 2s, 40Hz bursts (0.3ms pulse width) and hypercapnia consisted of increasing the CO_2 concentration in inspired air (by means of directed air flow) to 5% for 1 minute. The BOLD signal was calculated as fractional change normalized by the mean of the one minute preliminary baseline signal.

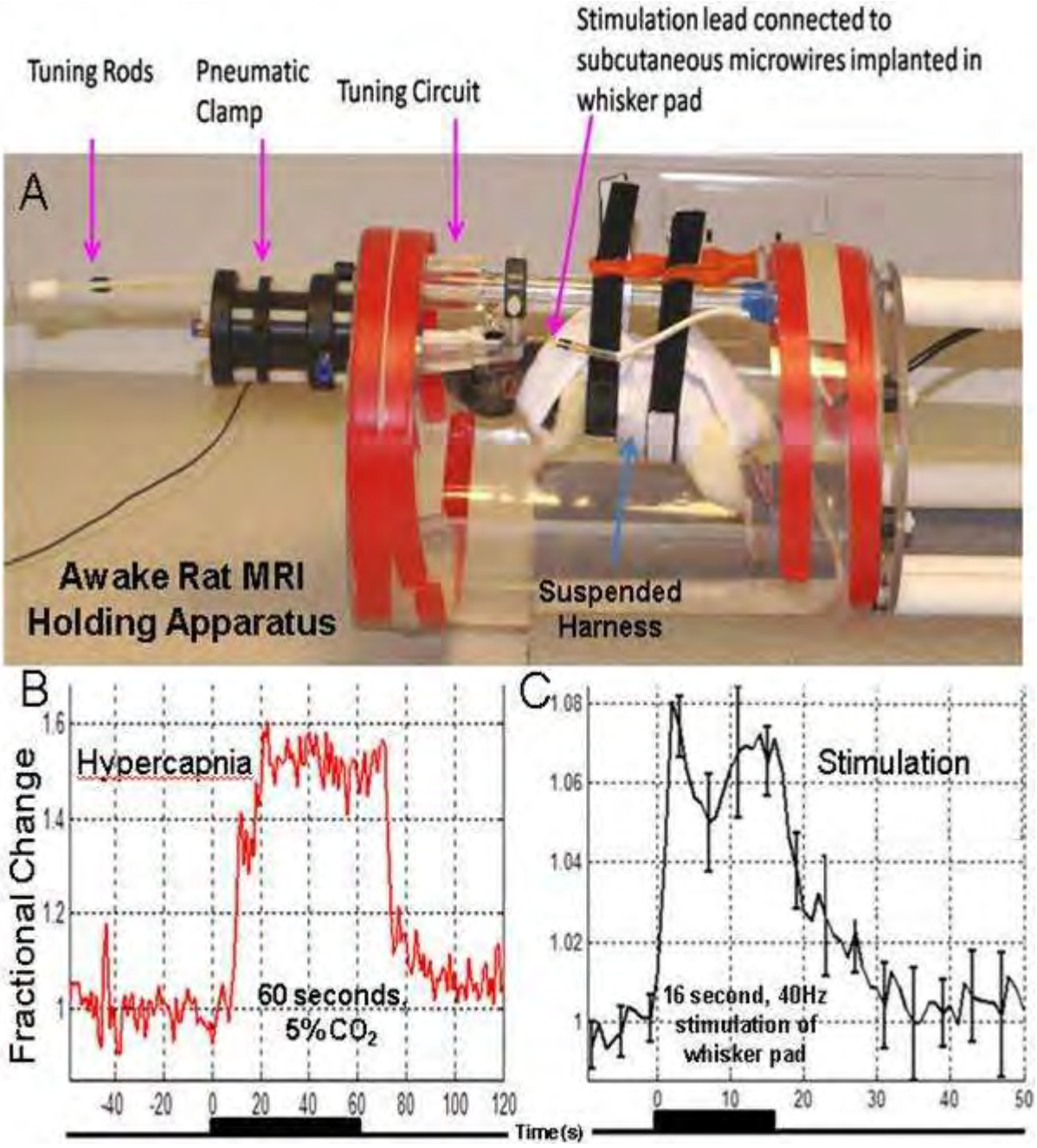

[Fig1]

Results and conclusions: We were able to successfully record BOLD fMRI responses to hypercapnia and whisker stimulation in awake rats. Hypercapnia produced large and rapid rises in BOLD signal amplitude **(B)**. Electrical stimulation of the whisker pad produced a reliable ~7% increase in BOLD signal in the corresponding barrel cortex **(C)**. Interestingly, responses to both hypercapnia and stimulation displayed faster temporal dynamics than have been reported previously in studies using anaesthetized animals. This methodology leaves the face and limbs free from obstruction, making possible a range of behavioural or sensory stimulation protocols. Further development of this animal model could enable traditional behavioural neuroscience techniques to be combined with modern functional neuroimaging.

326

Brain Poster Session: Experimental Cerebral Ischemia: Vascular & Endothelial

PRE AND POSTISCHEMIC ESTROGEN RECEPTOR EXPRESSION IN ISOLATED CEREBRAL MICROVESSELS AFTER ACUTE OR PROLONGED PERIODS OF HYPOESTROGENICITY

E. Zeynalov[1], C. Miyazaki[1], M. Littleton-Kearney[1,2]

[1]Johns Hopkins University School of Medicine, [2]Johns Hopkins University School of Nursing, Baltimore, MD, USA

Objectives: Estrogen receptors (ERs) in the brain modulate post-ischemic neo-vascularization, play a role in suppressing mitochondrial free radical formation, and may improve vasoreactivity in the brain in the presence of circulating estrogen. These effects are achieved when estrogen replacement therapy (ERT) is initiated early after loss of endogenous estrogen production, but after a time of prolonged hypoestrogenicity estrogen replacement therapy may be ineffective or even harmful relative to stroke prevention and treatment. It is unclear how short-term or prolonged estrogen deprivation effects ER expression in the healthy or postischemic cerebral microvasculature. The current study was designed to assess:

1. basal and
2. postischemic cerebral microvascular ER expression in estrogen depleted and in 17β-estradiol-treated rats after short-term or prolonged estrogen depletion.

Methods: Three groups of sexually mature female rats were used: ovariectomized (OVX), OVX plus early estrogen-treated (E2) and OVX plus delayed estrogen-treated (DE2). Estrogen treated rats were recovered for either 1 or 10 weeks postovariectomy then subcutaneously implanted with 17-β-estradiol pellets (0.05 mg). After 2 weeks of ERT rats were subjected to 15-min global 4 vessel occlusion ischemia and 3-h reperfusion. All surgical manipulations were performed under 1.5% isoflurane anesthesia, and all physiological variables were maintained within normal range. At the end of each experiment, blood was collected for estrogen levels, and brains were perfused and harvested for microvessel isolation. Each cortex was homogenized, then filtered 3 times through a 60-µm nylon mesh. Microvessel isolation purity was confirmed by microscopic imaging and ER protein expression was evaluated using Western blotting techniques. The band densities were quantified and expressed as a ratio to actin.

Results: Immunoblots for Von Willebrand Factor were used to confirm microvessel enrichment. ER-α expression was lower in the OVX (0.006±0.01) when compared to the E2 (0.183±0.15) and DE2 (0.192±0.10) groups. Early ischemia/reperfusion increased the microvascular ER-α expression in the OVX (0.358±0.12) group, but not in the E2 (0.111±0.05) or DE2 (0.190±0.03) groups. There were no differences in ER-β expression among groups under basal OVX 0.147±0.05; E2 0.093±0.07; DE2 0.139±0.07, or postischemic OVX 0.181±0.11; E20.084±0.06; DE2 0.152±0.08 conditions.

Conclusions: Compared to levels in healthy brain, transient global cerebral ischemia markedly increases ER-α expression in isolated cerebral microvessels of estrogen-depleted female rats. This effect is not observed in estrogen-treated rats regardless if ERT is initiated within 1 week or delayed for 10 weeks after ovariectomy. We conclude that the timing of ERT has no effect on basal or postischemic ER-α or ER-β expression. Further studies are needed to determine the mechanism of the difference between basal and postischemic ER-α expression in estrogen-depleted animals.

Brain Poster Session: Experimental Cerebral Ischemia: In Vitro

VESICULAR GABA TRANSPORTER (VGAT) IS CLEAVED BY CALPAINS UNDER EXCITOTOXIC CONDITIONS, GENERATING A NON-SYNAPTIC PROTEIN

J. Gomes[1], C. Melo[1], A. Inacio[2], L. Almeida[1], T. Wieloch[2], C. Duarte[1]

[1]Center for Neuroscience and Cell Biology and Department of Zoology, University of Coimbra, Coimbra, Portugal, [2]Wallenberg Neuroscience Center, Lund University, Lund, Sweden

Aims: Although GABA is the major inhibitory neurotransmitter in the CNS, and may be neuroprotective under excitotoxic conditions (1), it has been suggested that activation of $GABA_A$ receptors may contribute to cell damage due to chloride entry and consequent neuronal swelling (2,3,4). Recent findings showed that vesicular transporter expression directly regulates neurotransmitter release, controlling the quantal efficacy of synaptic transmission (5). Therefore, putative changes in VGAT protein levels during ischemia may affect GABAergic transmission and cell death. In this work we investigated the fate of VGAT in cultured neurons, subjected to excitotoxic conditions and in the ischemic brain.

Methods: Cultured hippocampal neurons were subjected to excitotoxic insults with glutamate. VGAT protein levels were determined by western blot, and gene expression was analysed by Real Time PCR. The cellular distribution of VGAT was visualized with immunocytochemistry. In vivo models used were: intrahippocampal injection of Kainate and transient Middle Cerebral Artery Occlusion (MCAO).

Results: We found that VGAT (58KDa) is cleaved upon glutamate stimulation of hippocampal neurons, in a biphasic manner, giving rise to a product of about 46KDa (tVGAT). About 40% of VGAT is cleaved within the first hour after glutamate stimulation, and 35% of the protein is cleaved 2-7h later. Truncated VGAT is stable for more than 24h. Under the same conditions, VGAT mRNA is downregulated, by a process of active mRNA degradation. Calpain I inhibition with ALLN or MDL28170 prevented the cleavage of VGAT in hippocampal neurons subjected to excitotoxicity. Inhibition of Caspases with Z-VAD-FMK did not affect glutamate-induced VGAT cleavage. VGAT cleavage was also observed in the cerebral cortex and striatum following transient Middle Cerebral Artery Occlusion (MCAO), a cerebral ischemia model. VGAT was also cleaved following intrahippocampal injection of kainate, a different model of in vivo excitotoxicity, but no effect was observed in transgenic mice overexpressing calpastatin, an endogenous calpain inhibitor. In vitro studies, using cerebrocortical synaptic vesicles and recombinant calpain I, also showed the cleavage of VGAT to the same product of about 46KDa. Immunoblot experiments using different antibodies against VGAT showed that calpain cleaves VGAT in the N-terminal region of the protein, giving rise to two similar truncated forms, at amino acid 52 and amino acid 60. Imunocytochemistry of GABAergic striatal neurons expressing GFP fusion proteins with VGAT or tVGAT proteins, showed that tVGAT immunoreactivity loses the synaptic localization, being homogenously distributed along the axons. This change in VGAT distribution was also observed with endogenous VGAT in glutamate stimulated hippocampal cultures.

Conclusions: Taken together, our results show that glutamate toxicity causes a down-regulation of VGAT, with a concomitant generation of a truncated VGAT, which is likely to affect GABAergic neurotransmission and may influence cell death, during ischemia.

References:

1. Kunjan et al, 2005, J. Neurochem. Res. 82, 665-673.

2. Inglefield and Schwartz-Bloom, 1998, J. Neurochem. 70, 2500-2509.

3. Katarzyma and Asla, 2000 J. Neurochem. 74, 2445-2454.

4. Allen et al. 2004, J. Neurosci. 24, 3837-3849.

5. Nathan et al, 2005, J. Neurosci. 25, 6221-6234.

Brain Poster Session: Neuroprotection

HISTOLOGICAL AND NEUROBEHAVIORAL OUTCOMES IN ISOFLURANE PRECONDITIONED ISCHEMIC MALE MOUSE BRAIN MAY BE DIHYDROTESTOSTERONE DOSE-SPECIFIC

W. Zhu[1], L. Wang[2], J. Palmateer[1], N. Libal[1], P. Herson[1], P. Hurn[1], S. Murphy[1]

[1]Anesthesiology & Peri-Operative Medicine, Oregon Health and Science University, Portland, OR, USA, [2]Neurology, Affiliated Drum Tower Hospital, Nanjing University, Nanjing, China

Objective: Isoflurane preconditioning (IsoPC) neuroprotection in experimental stroke is male-specific and testosterone-dependent.[1,2] Testosterone can be converted via 5α-reductase to the more potent androgen and pure androgen receptor agonist, dihydrotestosterone (DHT). We hypothesized that DHT would have similar or greater neuroprotective effects than testosterone on histological and neurobehavioral outcomes in IsoPC ischemic male brain.

Methods: C57BL/6 mice were castrated (CAST) and received no hormone or subcutaneous DHT pellets (0.5, 1.5, 5 mg) 7 days before preconditioning. Male and CAST + DHT mice were preconditioned for 4 hours with air (sham preconditioning, Sham PC) or 1.0% IsoPC 24 hours before 2 hours of middle cerebral artery occlusion. At 22 hours reperfusion, cortical and striatal infarct volumes (% contralateral structure) were determined by digital image analysis of coronal brain slices stained with 2,3,5-triphenyltetrazolium chloride. Based on infarct outcomes, the lowest neuroprotective DHT dose (0.5 mg) was used to assess neurobehavioral outcomes in sham PC and IsoPC CAST + DHT mice (n=13-15 per group) for 9 days following ischemia. Paw preference test (PPT), locomotor activity in the open field (OF), passive avoidance (PA) and novel object recognition task (ORT) were done to analyze forelimb asymmetry, spontaneous locomotor activity and cognitive function.

Results: IsoPC decreased infarct volumes in male and CAST + 0.5 DHT mice but had no effect in CAST, CAST + 1.5 DHT and CAST + 5 DHT groups (Table). Long-term behavioral assessment revealed that IsoPC in CAST and CAST + 0.5 DHT prevented impairment in PPT. In addition, 0.5 mg DHT in the absence of IsoPC improved PPT outcome. In contrast, IsoPC reduced impairment in ORT in CAST mice, but this effect was blocked in CAST + 0.5 DHT mice. OF and PA outcomes were equivalent among groups.

Experimental Groups	N	Cortical Infarct Volume (%)	Striatal Infarct Volume (%)
Sham PC Male	9	54 ± 5	96 ± 2
IsoPC Male	10	20 ± 7*	70 ± 6*
Sham PC CAST	9	55 ± 3	98 ± 3
IsoPC CAST	8	54 ± 4	100 ± 1
Sham PC CAST + 0.5 DHT	8	56 ± 2	103 ± 3
IsoPC CAST + 0.5 DHT	9	43 ± 4*	85 ± 3*
Sham PC CAST + 1.5 DHT	10	51 ± 5	97 ± 1
IsoPC CAST + 1.5 DHT	10	47 ± 2	94 ± 2
Sham PC CAST + 5 DHT	8	55 ± 4	94 ± 4
IsoPC CAST + 5 DHT	8	57 ± 2	89 ± 3

*p<0.05 compared to corresponding Sham PC

[Table]

Conclusions: Histological protection from IsoPC in experimental stroke is androgen-dependent, with intact males being protected and neuroprotection being lost in androgen-deficient CAST mice. Furthermore, IsoPC neuroprotection relative to histological outcomes is DHT-dependent and dose-specific, with IsoPC reducing infarct volumes only in CAST + 0.5 DHT mice and having no effect in CAST mice treated with higher DHT doses. However, IsoPC neuroprotection appears to be DHT-independent relative to neurobehavioral outcomes. Neurobehavioral studies showed that IsoPC minimized contralateral forelimb impairment in CAST mice regardless of 0.5 mg DHT treatment status. In addition, 0.5 mg DHT alone improved forelimb asymmetry regardless of preconditioning status. Finally, IsoPC improved cognitive function in CAST mice, with the effect being blocked by 0.5 mg DHT. Further studies are needed in ischemic male brain to clarify whether DHT has a causal or independent role in IsoPC neuroprotection relative to histological and neurobehavioral outcomes.

References:

1. Kitano et al. 2007. J Cereb Blood Flow Metab 27:1377-86.

2. Wang et al. 2007. Stroke 38:558.

330

Brain Poster Session: Blood-Brain Barrier

CYCLOOXYGENASE-1 AND 2 DIFFERENTLY MODULATE LIPOPOLYSACCHARIDE-INDUCED BLOOD-BRAIN BARRIER DISRUPTION VIA A MATRIX METALLOPROTEINASE MECHANISM

S. Aid[1], A.C. Silva[2], E. Candelario-Jalil[3], S.-H. Choi[1], G.A. Rosenberg[3], F. Bosetti[1]

[1]BPMS/ NIA, NIH, [2]Cerebral Microcirculation Unit, NINDS/NIH, Bethesda, MD, [3]Department of Neurology, University of New Mexico/ Health Sciences Center, Albuquerque, NM, USA

Objectives: Cyclooxygenases (COX) -1 and -2 play a key role in inflammation and are the pharmacological targets of non-steroidal anti-inflammatory drugs. We recently demonstrated that the expression of pro-inflammatory cytokines and chemokines is reduced in COX-1 null ($^{-/-}$) mice, and increased in COX-2$^{-/-}$ mice compared to their wild-type controls after intracerebroventricular (icv) lipopolysaccacharide (LPS) injection[1,2]. Since chemokines are involved in leukocyte recruitment into the inflamed brain, we hypothesized that COX-1 and COX-2 deletion will differentially modulate blood-brain barrier (BBB) permeability in response to LPS.

Methods: icv LPS (5 μg) was injected in COX-1 and COX-2 null and wild type mice. Twenty-four hours later, BBB permeability was quantified using gadolinium-enhanced magnetic resonance imaging (MRI). Gelatin zymography and fluorometric assay were used to measure the activity of matrix metalloproteinase (MMP)-9 and MMP-3, respectively. Gene expression level was assessed using quantitative real-time PCR.

Results: We found that LPS-induced BBB disruption was increased in COX-2$^{-/-}$ vs. their respective wild-type mice. In the hippocampus and cortex of LPS-treated mice, MMP-3 activity was significantly decreased in COX-1$^{-/-}$ mice, whereas in COX-2$^{-/-}$ mice the activity of both MMP-9 and MMP-3, known to mediate BBB breakdown, were increased. The gene expression of the leukocyte attracting chemokine CXCL10, the endothelial marker ICAM-1, and the macrophage marker CD45 were also found increased in the whole brain of COX-2$^{-/-}$ vs. COX-2$^{+/+}$ mice after LPS. The above genes, except for ICAM-1, were found decreased in the whole brain of COX-1$^{-/-}$ vs. COX-1$^{+/+}$ mice after LPS.

Conclusion: Altogether, these results indicate for the first time that COX-2$^{-/-}$ mice have increased BBB disruption in response to LPS and suggest that COX-2 selective inhibition may be detrimental to BBB integrity during inflammation.

References:

1. Aid et al. (2008) Journal of neuroinflammation 5:17.

2. Choi et al.(2008) FASEB J 22:1491-501. 3.

331

Brain Oral Session: Cortical Spreading Depression

INCREASED SUSCEPTIBILITY TO CORTICAL SPREADING DEPRESSION IN CADASIL MUTANT MICE

K. Eikermann-Haerter[1], Y. Wang[1], E. Dilekoz[1], J.F. Arboleda-Velasquez[2], S. Artavanis-Tsakonas[2], A. Joutel[3], M.A. Moskowitz[1], C. Ayata[1,4]

[1]Radiology, Massachusetts General Hospital, Harvard Medical School, Charlestown, [2]Cell Biology, Harvard Medical School, Boston, MA, USA, [3]Faculte de Medecine, Universite Paris 7-Denis Diderot, Paris, France, [4]Neurology, Massachusetts General Hospital, Harvard Medical School, Boston, MA, USA

Background and aims: Cerebral Autosomal Dominant Arteriopathy with Subcortical Infarcts and Leukencephalopathy (CADASIL) first manifests with migraine before the occurrence of recurrent strokes and vascular dementia. CADASIL has been linked to missense mutations (e.g., R90C) in the NOTCH3 gene exclusively expressed in vascular smooth muscle cells, which degenerate during the disease progress. Cortical spreading depression (CSD) is a transient neuroglial depolarization, which slowly propagates centrifugally once evoked when extracellular K^+ concentrations exceed a critical threshold. CSD is believed to underlie migraine aura. We have recently shown that human familial hemiplegic migraine mutations in $Ca_v2.1$ channel (i.e., neuronal mutation) enhance CSD susceptibility. Here, we tested whether CADASIL mutant mice (i.e., vascular mutation) overexpressing NOTCH3 R90C, and mice lacking the functional NOTCH3 protein (NOTCH3-KO), show altered CSD-susceptibility.

Methods: We determined CSD susceptibility by analyzing:

a. the electrical threshold for inducing CSD (single square pulses with increasing intensity on the occipital cortex), and
b. the frequency of repetitive CSDs induced by topical KCl (300 mM for 1h on the occipital cortex), in mechanically ventilated, physiologically monitored mice under isoflurane anesthesia.

CSDs were recorded from parietal and frontal cortex using glass micropipettes. Aquaporin4 (AQP4) expression was investigated by immunohistochemistry and Western blots in naïve brains. R90C transgenic mice were compared to non-transgenic mice as well as transgenic mice overexpressing WT human NOTCH3. NOTCH3-KO was compared to WT littermates.

Purpose: To test whether CADASIL mutations enhance CSD susceptibility.

Results: The electrical CSD threshold was significantly lower, and frequency of KCl-induced CSDs higher in R90C transgenic mice compared to WT. CSD speed was increased as well. NOTCH3-KO mice also displayed increased CSD frequency and propagation speed upon topical KCl, and this phenotype was even stronger than in R90C. No difference was detected in CSD susceptibility between male and female R90C mice. Senescence (22±5mo) partially reduced CSD susceptibility when tested in NOTCH3-KO. Subcortical recordings did not show striatal SD in any group. Interestingly, the water channel protein AQP4, predominantly expressed on astrocytic endfeet, ependyma and brain endothelium, was increased by two-fold in R90C brains suggesting a link between CSD susceptibility and brain water regulation.

Conclusion: In summary, our data show that the archetypal R90C CADASIL mutation enhances CSD

susceptibility, providing evidence for the first time that a vascular mutation can produce a migraine phenotype by increasing CSD susceptibility. This is the second gene to date associated with a human migraine syndrome that is shown to enhance CSD susceptibility.

Strain	Genotype	Gender	Threshold, µC	N	Frequency, #/h	N	Speed, mm/min
Notch3 R90C	WT	M	485 [98-65]	12	8±1	5	3.0±0.3
Notch3 R90C	WT	F	386 [161-114]	13	9±2	9	3.2±0.3
Notch3 R90C	TG	M	55 [2-55]*	13	12±1*	6	3.6±0.3*
Notch3 R90C	TG	F	25 [4-55]*	13	13±1*	7	4.3±0.5*
Notch3 KO	WT	M	-	-	9±2	8	-
Notch3 KO	KO	M	-	-	15±3*	8	-
Aged Notch3 KO	WT	M	-	-	9±2	8	3.0±0.3
Aged Notch3 KO	KO	M	-	-	13±1*	8	3.7±0.2*

[Table]

(Electrical threshold: median [interquartile range], others: mean±SD,*$p < 0.05$).

A CORTICAL REGION AND NEUROPATHWAY NECESSARY FOR READING CHINESE CHARACTERS REVEALED BY STRUCTURAL AND FUNCTIONAL MRI

C. Shan[1,2], T. Wang[1], R. Zhu[3], X. Zhao[3], Z. Lu[3], X. Zhou[3], X. Weng[2], B. Luo[3]

[1]Department of Rehabilitation Medicine, First Affiliated Hospital of Nanjing Medical University, Nanjing, [2]Laboratory for Higher Brain Function, Institute of Psychology, Chinese Academy of Sciences, Beijing, [3]Department of Neurology, First Affiliated Hospital, College of Medicine, Zhejiang University, Hangzhou, China

Objectives: To examine the crucial region and neural pathway necessary for Chinese logographic characters reading by using structural and functional MRI.

Methods: Three right-handed patients suffering from infarcts in the territory of the left posterior cerebral artery (PCA) were studied. All of them showed difficulties in naming familiar objects and people. Patient JXD was of inability to read aloud and comprehend Chinese characters without any other language deficits, i.e. pure alexia[1]. Patient CYH only had deficits in naming objects and people, his reading was normal, i.e. anomia. Patient KY could not understand written Chinese material because he made errors in recognizing the left part (i.e. radical) of a Chinese character, e.g. he read 秩(zhi4, order) as 铁(tie3, iron), read 银(yin2, silver) as 根(gen1, root), i.e. left hemiparalexia[2]. 3D-SPGR MRI scan and specific analysis software were used to overlap the lesions of three patients to distinguish the distinct lesions in pure alexia (JXD) and left hemiparalexia (KY). BOLD fMRI was adopted for JXD and CYH to reveal activations induced by Chinese characters reading. For KY, we used fMRI to demonstrate the activations to the Chinese characters presented in the left and right visual fields and made DTT (diffusion tensor tractography) examination to reveal the interruption of neuropathway (white matter).

Results: The analysis of 3D-SPGR MRI data reveals that the common lesions lie in the left medial ventral occipitotemporal cortex. JXD had additional lesions in the left lateral mid-fusiform cortex, where has been labeled as visual word form area (VWFA) by Cohen et al[3]. Compared with CYH, KY had additional lesion in the left splenium of corpus callosum. DTT confirms that the neuropathway through splenium was broken in KY. The fMRI results show Chinese characters activated CYH's left lateral mid-fusiform cortex (corresponding to VWFA) but not JXD's (see Fig 1). For KY, this area was activated only when Chinese characters were presented in his right visual field (RVF) (see Figure 1).

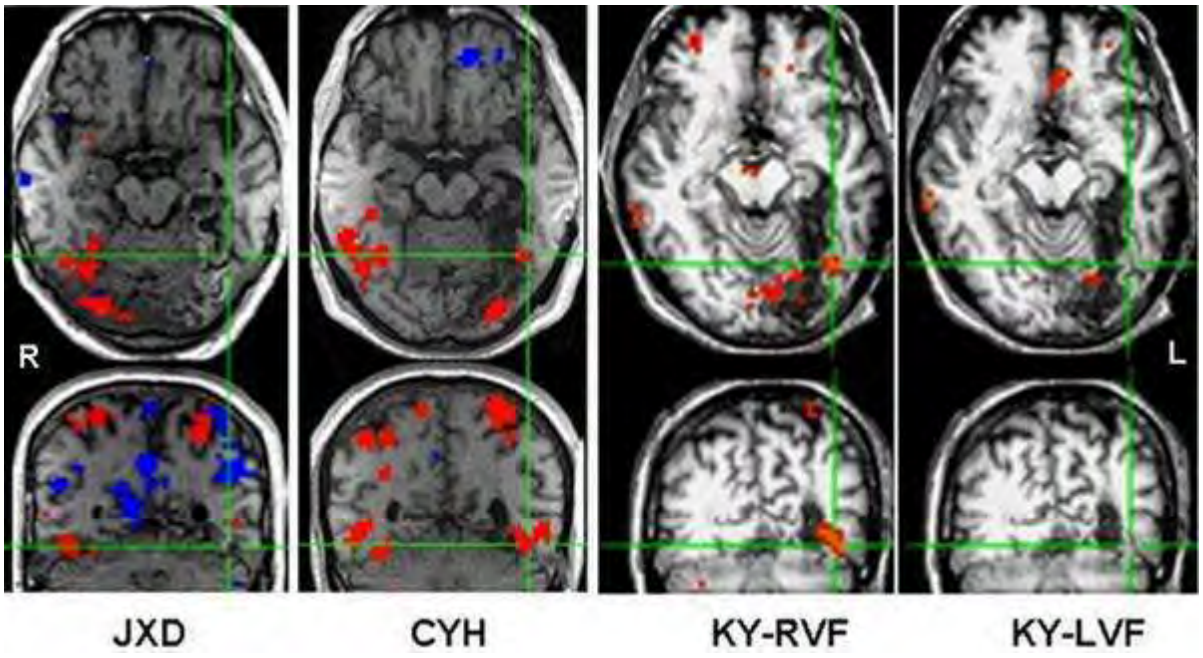

[Figure 1]

Fig. 1 The activations evoked by Chinese characters. The crosshair correspond to VWFA. (for JXD and CYH, TC: x=-43, y=-54,z=-12; for KY, TC: x=-38, y=-65, z=-1).

Conclusions: The left lateral mid-fusiform cortex is a crucial region for Chinese characters reading (recognizing). Therefore, the lesion in this area (JXD) may result in pure alexia. The neuropathway going through splenium of corpus callosum is necessary for transferring of visual information of Chinese characters from left visual field (right occipital cortex) to left VWFA. The infarction in this pathway (KY) can lead to alexia for characters/radicals in left visual field (left hemialexia or left hemiparalexia). Both the cortex and neuropathway crucial for Chinese logographic characters reading are similar to that of alphabetic word reading.

References:

1. Montant M, Behrmann M. Pure alexia. Neurocase, 2000, 6: 265-294.

2. Binder JR, Lazar RM, Tatemichi TK, Mohr JP, Desmond DW, Ciecierski KA. Left hemiparalexia. Neurology, 1992, 42: 562-569.

3. Cohen L, Dehaene S, Naccache L, Lehericy S, Dehaene-Lambertz G, Henaff MA, and Michel F. The visual word form area: Spatial and temporal characterization of an initial stage of reading in normal subjects and posterior split-brain patients. Brain, 2000, 123: 291-307.

Brain Poster Session: Spreading Depression

GABAPENTIN ACUTELY SUPPRESSES CORTICAL SPREADING DEPRESSION IN RATS

U. Hoffmann[1], C. Kudo[1,2], E. Dilekoz[1], M.A. Moskowitz[1], C. Ayata[1,3]

[1]Radiology, Stroke and Neurovascular Regulation Lab, Massachusetts General Hospital, Harvard Medical School, Charlestown, MA, USA, [2]Department of Dental Anesthesiology, Osaka University Graduate School of Dentistry, Osaka, Japan, [3]Neurology, Stroke Service and Neuroscience Intensive Care Unit, Massachusetts General Hospital, Harvard Medical School, Charlestown, MA, USA

Objectives: Cortical spreading depression (CSD), a slowly propagating wave of neuronal and glial depolarization, is the putative mechanism of migraine aura, and may trigger headache as well. It can be evoked in experimental animals when extracellular K+ concentration exceeds a critical threshold upon chemical or electrical stimulation. Spontaneously arising CSD-like depolarizations have recently been demonstrated in injured human brain as well. We have previously shown that migraine prophylactic agents (e.g., valproate) suppress CSD upon chronic treatment. It is not known whether this mechanism is shared by other migraine therapeutics as well. Gabapentin, an antiepileptic which also shows efficacy in migraine in preliminary studies, inhibits Cav2.1 channels (formerly the P/Q type) by binding the α2δ-1 subunit. Pharmacologic inhibition and gain-of function mutations in Cav2.1 channels, suppress and enhance CSD, respectively. Therefore, we tested the efficacy of gabapentin on CSD.

Methods: CSDs were recorded from parietal and frontal cortex using glass micropipettes in intubated and mechanically ventilated (70%N2O/30%O2) isoflurane-anesthetized rats. Gabapentin was administered as a single intravenous dose; CSD susceptibility was determined 1h after injection. In addition, gabapentin was administered chronically for 4 weeks in two divided daily oral doses; CSD susceptibility was determined ~2h after the last dose on the day of testing. Chronic valproate treatment (single daily intraperitoneal injections for 4 weeks) was used as a positive control. CSD susceptibility was determined by:

a. electrical threshold for inducing CSD (single square pulses with increasing intensity on the occipital cortex), and
b. the frequency of repetitive CSDs induced by topical KCl (1M for 1h on the occipital cortex).

Results: A single administration of gabapentin dose-dependently suppressed KCl-induced CSD frequency, and elevated the electrical CSD threshold. Chronic oral treatment using a lower dose was ineffective. Chronic valproate administration significantly reduced KCl-induced CSD frequency and elevated the electrical CSD threshold, as reported previously. CSD speed, duration and amplitude did not differ among groups.

Drug	Dose (mg/kg)	Route	Duration of treatment	Threshold (μC)	Frequency (#/h)	N
Vehicle	-	iv	single dose	250 [125-	15±2	8

				375]		
Gabapentin	100	iv	single dose	1600 [1000-1800]	12±3	7
Gabapentin	200	iv	single dose	800 [600-800]	10±2*	11
Vehicle (saline)	0.5 ml bid	po	4 weeks	600 [200-800]	14±2	14
Gabapentin	50 bid	po	4 weeks	400 [100-600]	14±3	16
Valproate	200 qd	ip	4 weeks	900 [650-1500]	9±2*	11

[Table 1]

Data are mean±SD or median [interquartile range]. bid, twice a day; qd once a day, *$p < 0.05$.

Conclusions: In summary, gabapentin dose-dependently suppressed CSD susceptibility as determined by two independent methods. Unlike other migraine prophylactic agents previously tested, chronic treatment was not required for efficacy, nor enhanced it. These data provide a potential mechanism for gabapentin action in migraine. Furthermore, because chronic treatment was not a prerequisite for efficacy, gabapentin, with its favorable pharmacokinetic and safety profile, may have a role in suppressing the CSD-like injury depolarizations shown to be detrimental in stroke, trauma and subarachnoid hemorrhage.

335

Brain PET Oral 3: Miscellaneous Targets

REGIONAL DIFFERENCES IN P-GLYCOPROTEIN FUNCTION AT THE HUMAN BLOOD-BRAIN BARRIER

M. Bauer[1], C. Wagner[1], R. Karch[2], T. Feurstein[1], K. Kletter[3], M. Zeitlinger[1], M. Müller[1], O. Langer[1]

[1]Clinical Pharmacology, [2]Medical Computer Sciences, [3]Nuclear Medicine, Medical University of Vienna, Vienna, Austria

Background and aims: P-glycoprotein (P-gp) acts at the blood-brain barrier (BBB) as an active cell membrane efflux pump for several endogenous and exogenous compounds. Recent animal data suggest regional differences of cerebral P-gp activity (Laćan et al., 2008). PET with the P-gp substrate (R)-[^{11}C]verapamil (VPM) can be used to measure cerebral P-gp function, but low brain uptake of VPM hampers the mapping of regional differences in P-gp function. This limitation can be overcome by P-gp modulation with moderate doses of P-gp inhibitors. The aim of this study was to assess regional P-gp function in humans before and after administration of the third-generation P-gp inhibitor tariquidar (TQD).

Methods: 5 healthy volunteers underwent paired VPM PET scans and arterial blood sampling, before and at 3h after i.v. administration of TQD (2 mg/kg body weight). VPM distribution volumes (DV) before and after TQD administration were calculated using a 4-rate-constant-2-tissue-compartment model. Parametric images depicting distribution volume (DV) differences between the 2 PET scans were generated using the pixel-wise Logan plot and analyzed by statistical parametric mapping (SPM5). TQD concentrations in venous plasma were quantified using liquid chromatography/mass spectrometry.

Purpose: The purpose of this study was to investigate P-glycoprotein function at the human blood-brain barrier in vivo.

Results: TQD administration resulted in significant increases (paired t-test) in whole-brain grey matter DVs and influx rate constants (K_1) of VPM across the BBB (DV=0.64±0.12 and 0.79±0.07, p=0.012; K_1=0.034±0.01 and 0.049±0.01, p=0.024, before and after TQD, respectively). A strong correlation was observed between TQD exposure in plasma and change in brain DV after administration of TQD (r=0.932, p=0.021). SPM analysis revealed significantly smaller DV increases in cerebellum, hippocampus, parahippocampus, enthorinal cortex, inferior temporal lobe, brain stem and cerebellum as compared to other brain regions, which points to increased P-gp expression and function in these regions.

Conclusion: TQD significantly increased brain distribution of VPM, due to increased influx. Regional differences in VPM DV changes in response to TQD treatment suggest regional variability of cerebral P-gp function, which might make some brain areas more resistant and others more vulnerable to the accumulation of P-gp substrates.

References:

Laćan G, Plenevaux A, Rubins DJ, Way BW, Defraiteur C, Lemaire C, Aerts J, Luxen A, Cherry SR, Melega WP (2008). "Cyclosporine, a P-glycoprotein modulator, increases [^{18}F]MPPF uptake in rat brain and peripheral tissues: microPET and ex vivo studies" Eur J Nucl Med Mol Imaging **35**(12): 2256-66.

The research leading to these results has received funding from the European Community´s Seventh Framework Programme under grant agreement no. 201380 (EURIPIDES).

Brain Poster Session: Translational Studies

NON-INVASIVE MEASUREMENTS OF CEREBRAL BLOOD FLOW WITH DIFFUSE OPTICS IN PATIENTS AFTER SEVERE HEAD INJURY

M.N. Kim[1], T. Durduran[1,2], S. Frangos[3], B.L. Edlow[4], E.M. Buckley[1], H. Moss[4], C. Zhou[1], G. Yu[1,5], R. Choe[1], E. Maloney-Wilensky[3], R.L. Wolf[2], J.H. Woo[2], M.S. Grady[3], J.H. Greenberg[4], J. Levine[3], A.G. Yodh[1], J.A. Detre[2,4], W.A. Kofke[3,6]

[1]Physics and Astronomy, [2]Radiology, [3]Neurosurgery, [4]Neurology, University of Pennsylvania, Philadelphia, PA, [5]Biomedical Engineering, University of Kentucky, Lexington, KY, [6]Anesthesiology and Critical Care, University of Pennsylvania, Philadelphia, PA, USA

Objectives: Patients suffering from severe head injury are a particularly challenging population clinically because of their heterogeneous condition and susceptibility to secondary injury. A continuous and non-invasive measure of microvascular CBF could help with individualizing care and alleviation of secondary injury. Current modalities for continuous monitoring provide only surrogate measurements of microvascular CBF, and some, like intracranial pressure, are invasive. We have developed and tested a novel, optical bedside monitor of microvascular CBF.

Methods: Six patients with traumatic brain injury (TBI), subarachnoid hemorrhage (SAH), or ischemic stroke were included in a validation study of diffuse correlation spectroscopy (DCS) against portable xenon-CT. CBF was measured continuously throughout two CT-scans: a baseline scan and a scan after pressor administration. Regions-of-interest under the DCS probes (placed bilaterally on the forehead) were drawn on the xenon-CT CBF maps, and CBF values were compared to values from DCS. Eleven TBI/SAH patients were recruited under a separate protocol to test DCS-CBF response to head-of-bed (HOB) elevation changes. DCS measured frontal cortical CBF while HOB position changed from 30^{o} to supine, each for 5 minutes. Results were compared against cerebral perfusion pressure (CPP) to assess cerebral autoregulation. Damaged autoregulation was defined as lack of correlation between CPP and CBF ($p>0.05$).

Results: Relative CBF measurements from DCS and xenon-CT comparing baseline and post-intervention values showed good correlation ($R=0.72$, $p=0.02$). Bland-Altman analysis comparing the two methods also showed good agreement. When HOB went from 30° to supine, CBF responses were highly variable both among patients as well as between hemispheres in a given patient. Figure below shows a CBF time-series with this type of discrepancy, in a 45-year-old male with subarachnoid hemorrhage from anterior communicating artery- and left anterior choroidal artery-origin aneurysms. Autoregulation is often damaged by neurotraumatic events, and the correlation ($p=0.03$) between this patient´s left hemisphere CBF and CPP may be interpreted as damaged autoregulation on that side. As a contrast, right hemisphere CBF did not correlate with CPP ($p=0.29$). Averaged over the entire population, we saw a insignificant CBF decrease (-1.1%+-7.8%) with head flat, but found that individual responses did significantly change from baseline CBF ($p< 0.05$).

Conclusions: We have validated DCS against Xenon-CT as a measure of local, microvascular CBF. We have also observed damaged cerebral autoregulation in patients after severe head injury which was confirmed by a large correlation between CBF and CPP during a simple intervention. Our results demonstrate the potential for DCS to provide continuous, non-invasive bedside monitoring of CBF for the purpose of CBF management and individualized care.

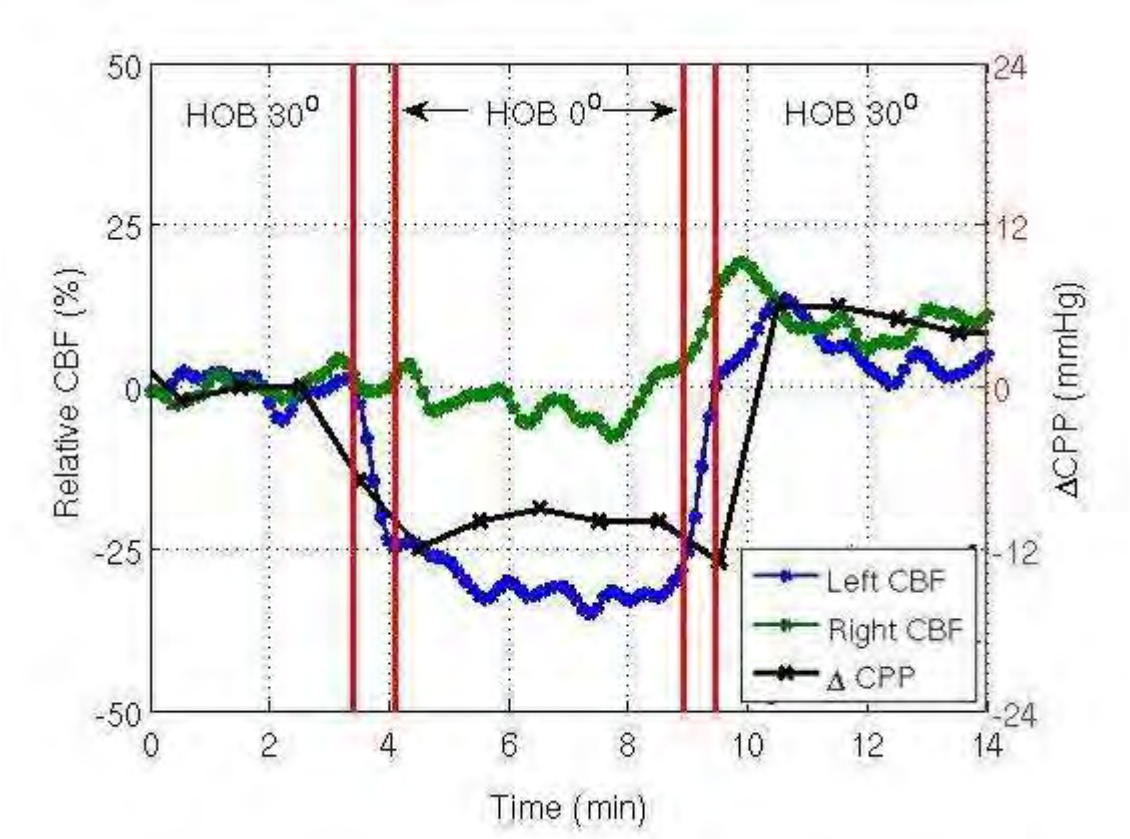

[Changes in CBF and CPP during HOB manipulation]

337

Brain Poster Session: Neuroprotection

PROGESTERONE PROMOTES A DOSE-SPECIFIC NEUROPROTECTIVE RESPONSE TO ISOFLURANE PRECONDITIONING IN ISCHEMIC OVARIECTOMIZED FEMALE MOUSE BRAIN

W. Zhu, N. Libal, P. Hurn, S. Murphy

Anesthesiology & Peri-Operative Medicine, Oregon Health and Science University, Portland, OR, USA

Objective: The response to isoflurane preconditioning (IsoPC) in focal stroke is sexually dimorphic, with male and ovariectomized female mice being protected by IsoPC, but IsoPC neuroprotection is lost in females and estradiol-treated ovariectomized mice (1, 2). We evaluated the progesterone (PROG) dose relationship in the ischemic sensitivity of IsoPC female mouse brain.

Methods: Young adult C57BL/6 female mice were ovariectomized (OVX) and received no hormone or subcutaneous PROG pellets (7.5 or 15 mg) 7 to 8 days before preconditioning and experimental stroke. Intact females, OVX, OVX + 7.5 mg PROG, and OVX + 15 mg PROG were preconditioned for 4 hours with air (sham preconditioning, Sham PC) or 1.0% IsoPC. Mice then underwent 2 hours of middle cerebral artery occlusion via intraluminal filament 24 hours after preconditioning. Laser-Doppler flowmetry (LDF) was used to monitor cortical perfusion. Brains were collected at 22 hours reperfusion. Cortical and striatal infarct volumes (% contralateral structure) were determined by digital image analysis of 2 mm thick coronal brain slices stained with 2,3,5-triphenyltetrazolium chloride.

Results: Relative LDF changes were equivalent among groups. In contrast to corresponding Sham PC groups, IsoPC increased cortical and striatal infarct volumes in intact females (Table). However, IsoPC decreased cortical and striatal infarct volumes in OVX and OVX + PROG (7.5 or 15 mg) mice, with the greatest reduction in infarction volumes being seen in OVX + 15 mg PROG group (Table).

Experimental Groups	N	Cortical Infarct Volume (%)	Striatal Infarct Volume (%)
Sham PC Female	14	34 ± 3	75 ± 5
IsoPC Female	14	52 ± 3*	98 ± 5*
Sham PC OVX	5	51 ± 2	108 ± 3
IsoPC OVX	6	24 ± 5*	58 ± 12*
Sham PC OVX + 7.5 mg PROG	6	45 ± 3	95 ± 7
IsoPC OVX + 7.5 mg PROG	6	23 ± 3*	57 ± 9*
Sham PC OVX + 15 mg PROG	5	42 ± 4	87 ± 11
IsoPC OVX + 15 mg PROG	5	12 ± 2*	31 ± 4*

*p<0.05 compared to corresponding Sham PC

[Table]

Conclusions: IsoPC worsened ischemic injury in young female mice, but ovariectomizing young females and thus significantly decreasing endogenous female sex steroid levels resulted in a neuroprotective response to IsoPC, suggesting that one or both female sex steroids (estradiol, progesterone) may be responsible for the response to IsoPC observed in young ischemic female brain.

Furthermore, progesterone promoted IsoPC neuroprotection in female ischemic brain in a dose-specific manner, with IsoPC reducing infarct volumes comparably in OVX and OVX mice treated with 7.5 mg progesterone but having the greatest neuroprotective effect in OVX mice treated with 15 mg progesterone. More studies are needed to further delineate the role of progesterone in the brain's response to IsoPC as well as determine the mechanisms underlying how progesterone might promote a protective response to IsoPC in female ischemic brain.

References:

1. Kitano et al. 2007. J Cereb Blood Flow Metab 27:1377-86.

2. Wang et al. 2008. J Cereb Blood Flow Metab 28:1824-34.

DISTRIBUTION OF TRANSFUSED BONE MARROW CELLS FOLLOWING ENDOTHELIAL DAMAGE OF A CORTICAL ARTERY

S. Yamada, H. Toriumi, H. Kimura, Y. Tomita, Y. Itoh, H. Hoshino, N. Suzuki

Department of Neurology, Keio University School of Medicine, Tokyo, Japan

Objective: Bone marrow cells (BMCs) are reported to supply "endothelial progenitor cells" as well as possible microglia and may be beneficial in treatment of cerebral infarction. To investigate possible repair function of BMCs transfused after endothelial damage in a cerebral artery, endothelial cells in a cortical artery were selectively injured and recruitment of BMC at the injured site was continually observed through cranial window in mice.

Methods: Endothelial injury was inflicted in a cortical branch of middle cerebral artery via photochemical reaction between systemically injected rose bengal and green laser light (wavelength: 540 nm, diameter: 150 micro m, power: 150 micro W) transilluminated through a cranial window for 150 seconds. BMCs were prepared from a C57BL/6 CAG-EGFP transgenic mouse, which express green fluorescent protein (GFP) under the control of a chicken beta-actin promoter and cytomegalovirus enhancer in all of the tissues except for erythrocytes and hair. The femurs and tibias were flushed with Hanks' buffered salt solution and BMCs were isolated with a separation medium (Lympholyte M). BMCs were transfused through tail vein 3 hours after endothelial damage. Distribution of BMCs was periodically observed through a cranial window with a confocal microscopy. Binding of fluorescein isothiocyanate (FITC)-labeled Ulex europaeus agglutinin 1 (UEA-1) lectin was used to identify endothelial cells.

Results: Vasospasm as well as thrombus formation was observed at the injured artery following rose bengal infusion / laser illumination, suggesting endothelial damage. Hemostasis was observed in cortical vessels peripheral to the injured artery. Major thrombus was degraded within several hours, starting recirculation in most cortical vessels. Immediately after transfusion, BMCs circulating through the cortical brain vessels was observed via cranial window. Some BMCs attached on the cortical vein and migrated to the parenchyma as well as to the subarachnoid space (Fig. The upper cell migrated through a vessel wall, whereas the lower cell stayed on the luminal surface. Movie will be presented). Most of the BMCs in the parenchyma were later identified as GFP/Iba-1 double-positive microglia by immunohistochemistry. Some cells stayed on the luminal surface of the cortical vein and elongated toward the direction of blood flow. In contrast, only a few GFP-positive cells adhered to the injured cortical artery. Circulating BMCs were observed as late as 7 days after infusion.

Conclusion: These results suggest that BMC transfused after endothelial damage does not contribute to endothelial repair, at least within 7 days. In contrast, most BMCs trapped in the brain vessels may migrate into the parenchyma and function as microglia.

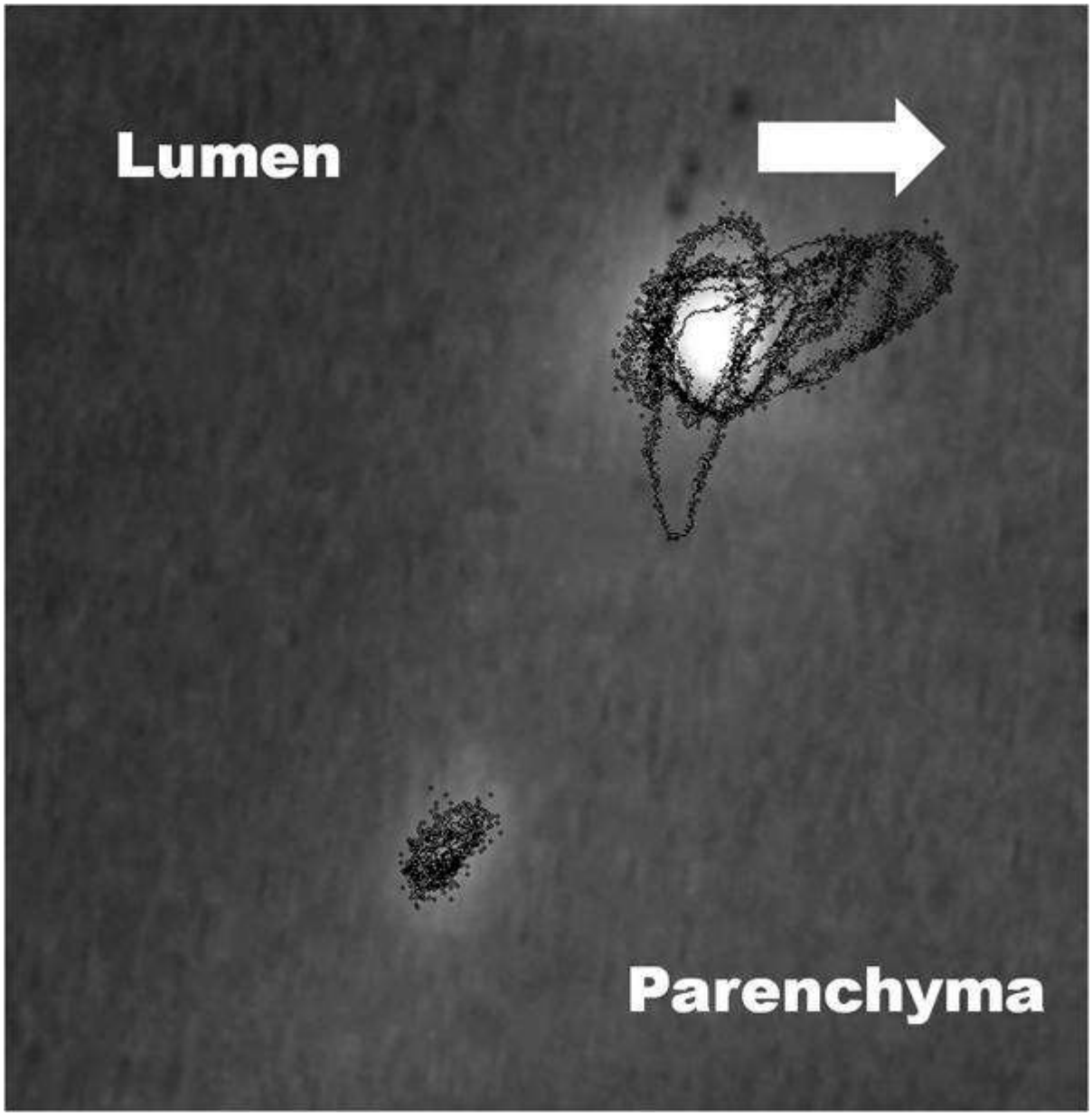

[Fig.]

340

Brain Poster Session: Cerebral Vascular Regulation

ROLE OF ADENOSINE 2A RECEPTOR (A2AR) IN AUTOREGULATION INDUCED BY ACUTE HYPOTENSION

Y. Kusano, **G. Echeverry**, G. Miekisiak, T. Kulik, H.R. Winn

Neurosurgery, Mount Sinai School of Medicine, New York, NY, USA

Objective: Adenosine is a potent vasodilator and is increased in brain during hypoxia, ischemia and with neuronal activation. During hypotension, some investigators note an increase in brain adenosine concentrations even within the autoregulatory range (1), whereas other investigators note an increase in brain adenosine levels only when MABP is decreased below the autoregulatory limit (2). The aim of this study is to evaluate the role of the A2aR during induced hypotension in mice.

Methods: Anesthetized and ventilated wild type (WT) and adenosine A2aR knockout (KO) mice (C57Bl/6) were used. Catheters were placed in femoral arteries for measurement of mean arterial blood pressure (MABP) and withdrawal of arterial blood as previously described (Miekisiak et all, 2008). MABP was lowered acutely by withdrawing arterial blood until reaching pre-determined target points within the autoregulatory range in mice (150-50mmHg). After 3 minutes, baseline MABP was restored. Cerebral blood flow (CBF) was measured using laser-Doppler flowmetery through the intact calvarium. Cerebral vascular resistance (CVR) was then computed from its relationship to flow and pressure. Preliminary studies measuring internal carotid artery pressure during hypotension confirmed that the changes in the femoral artery reflected the blood pressure at the base of the brain.

Results: In the A2aR KO animals (n=9), the change in CVR (0.37± 0.05, SEM) was significantly ($p < 0.05$) less than in the WT littermates (0.66± 0.03). Thus, during acute hypotension, autoregulation was significantly impaired in A2aR KO mice compared to WT (Fig).

Conclusions: These results suggest that the A2a receptor plays a significant role in autoregulation during acute hypotension.

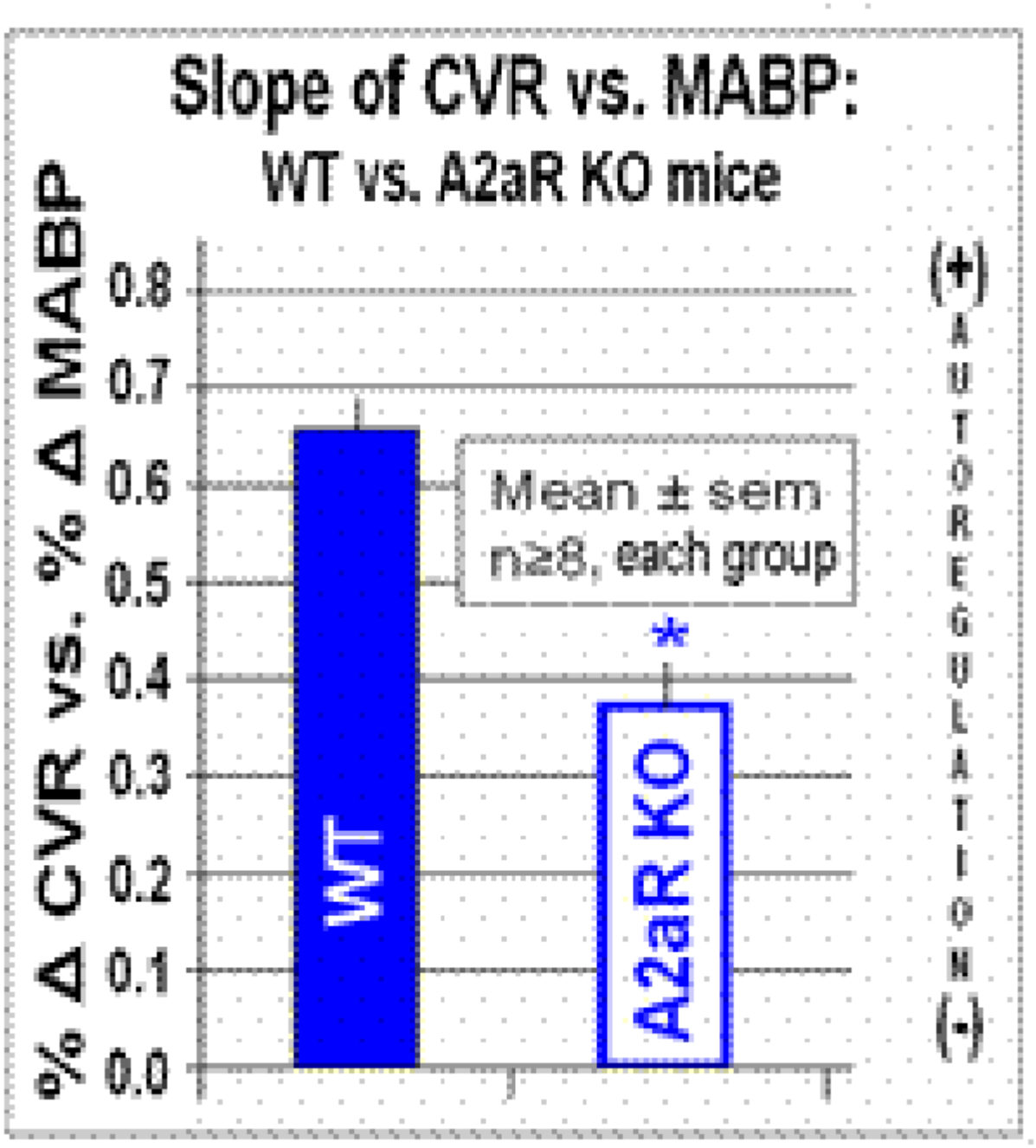

[Figure]

References:

1. Winn HR, Welsh JE, Rubio R, et al: Brain adenosine production in rat during sustained alteration in systemic blood pressure. Am J Physiol 239:H636-641, 1980.

2. Van Wylen DG, Park TS, Rubio R, et al: Cerebral blood flow and interstitial fluid adenosine during hemorrhagic hypotension. Am J Physiol 255:H1211-1218, 1988.

3. Miekisiak G, Kulik T, Kusano Y, et al: Cerebral blood flow response in adenosine 2a receptor knockout mice during transient hypoxic hypoxia. J Cereb Blood Flow Metab 28:1656-1664, 2008.

341

Brain Poster Session: Spreading Depression

FACILITATED SUBCORTICAL PROPAGATION OF CORTICAL SPREADING DEPRESSION IN FAMILIAL HEMIPLEGIC MIGRAINE TYPE 1 MUTANT MICE

K. Eikermann-Haerter[1], Y. Wang[1], M.D. Ferrari[2], A.M.J.M. van den Maagdenberg[2,3], M.A. Moskowitz[1], C. Ayata[1,4]

[1]Radiology, Massachusetts General Hospital, Harvard Medical School, Charlestown, MA, USA, [2]Neurology, [3]Human Genetics, Leiden University Medical Center, Leiden, The Netherlands, [4]Neurology, Massachusetts General Hospital, Harvard Medical School, Boston, MA, USA

Background and aims: Familial hemiplegic migraine (FHM) is a severe migraine variant. Characteristic are headaches, sometimes accompanied by transient but often severe motor deficits. FHM type 1 has been linked to missense gain-of-function mutations (e.g., S218L and R192Q) in the CACNA1A gene encoding the alpha1 subunit of neuronal $Ca_v2.1$ channels. FHM patients with the S218L mutation have a stronger clinical phenotype compared to those with R192Q mutation, and may develop seizures and coma in response to mild head trauma. Cortical spreading depression (CSD), the putative electrophysiological event underlying migraine, is a transient disruption of membrane ionic gradients and depolarization that slowly propagates across the cerebral cortex. Under favorable conditions, CSD can propagate into subcortical structures. We previously showed that FHM mutant mice exhibit increased susceptibility to CSD and its propagation into the striatum. Here we studied in detail the subcortical propagation of CSD into striatum, hippocampus, thalamus, brain stem and cerebellum in FHM type 1 mutant mice.

Methods: CSDs were induced every 15 minutes by brief topical KCl application on the occipital cortex in pentobarbital-anesthetized, mechanically ventilated ($70\%O_2/30\%N_2$), and physiologically monitored female R192Q or S218L knockin mice, and recorded simultaneously from subcortical structures and cortex using glass micropipettes. The spatial extent of subcortical SD propagation was studied by c-fos immunohistochemistry, 3 hours after 3 CSDs induced over 45 min.

Purpose: To study subcortical propagation pattern of spreading depression in FHM mutant mice.

Results: In S218L mice, CSD regularly propagated into striatum, hippocampus and thalamus, exhibiting an allele-dosage effect. When CSD propagated into thalamus, it did cross the midline and spread to the contralateral thalamus as well; spread into the contralateral cortex was not observed when tested in 3 mice. In R192Q mice, CSD often propagated into striatum (less frequently than S218L) but not into hippocampus or thalamus. None of the mutant strains showed brain stem or cerebellar SD. c-fos expression was upregulated in cortex, striatum, hippocampus (particularly dentate gyrus) and thalamus in S218L, and in cortex and striatum in R192Q mice.

Conclusions: In summary, FHM type 1 mutations facilitate subcortical propagation of CSD. Both S218L and R192Q strains show CSD propagation into striatum, the structure likely responsible for post-SD hemiparesis in mice. In addition, the S218L mutation facilitates CSD propagation into hippocampus as well as bilateral thalami, which are potential mechanisms for seizures and altered level of consciousness and coma in these patients.

Strain	Genotype	N	Striatum	Hippocampus	Thalamus

S218L	WT	6	32%/75%	0%/0%	0%/0%
S218L	HET	5	100%/100%	24%/100%	0%/0%
S218L	HOM	10	100%/100%	88%/100%	58%/86%
R192Q	WT	4	32%/100%	0%/0%	0%/0%
R192Q	HOM	4	71%/100%	0%/0%	0%/0%

[Table]

(N: # of mice tested. Data are expressed as % of CSDs / % of mice that show propagation into indicated subcortical structures)

PROTECTIVE EFFECTS OF LITHIUM SUPPLEMENTATION ON ALUMINIUM-INDUCED FUNCTIONAL AND STRUCTURAL ALTERATIONS IN RAT BRAIN

P. Bhalla, D.K. Dhawan

Department of Biophysics, Panjab University, Chandigarh, India

Background and aims: The present study was conducted to assess the role of lithium in conditions where aluminium (Al) toxicity leads to the chain of molecular events which can initiate and promote neurodegeneration.

Methods and purpose: To carry out the various investigations, Al was administered at a dose of 100mg/kg b.wt./day whereas lithium was supplemented in diet (1.1 g/Kg diet, daily) for the period of two months.

Results: Ca^{2+} ATPase activity was observed to be decreased in Al treated animals. Whereas, a significant increase in Ca^{2+} influx (via the voltage-operated calcium channels) and in the levels of cAMP were observed following Al treatment which were decreased with lithium co-administration. Further, a significant increase in the levels of phopholipase C ($PLC_{\acute{Y}1}$) was observed following Al treatment which was normalized following lithium supplementation. The nitric oxide synthase enzyme activity and the levels of L-citrulline were also found to be significantly increased in different brain regions (cerebrum and cerebellum) after Al treatment, which were significantly decreased following lithium supplementation. The DNA damage caused in the cell as a result of Al treatment was examined by single cell gel electrophoresis as well as DNA fragmentation studies and a significant increase in the DNA damage was observed which was found to be significantly improved upon lithium supplementation. Alterations in the neuronal histoarchitecture and ultra structure were also observed following Al treatment. Lithium supplementation greatly restored normalcy in the cerebrum and cerebellum layers with no loss of cerebral or purkinje cell layer as evident by light microscopy. Further, lithium supplementation to Al treated rats resulted in appreciably thwarting the ultrastructural changes with regard to integrity of the cells as a whole as well as the cell organelles as observed by transmission electron microscopy. The study demonstrates that lithium, an antidepressant drug, has the potential in containing or reversing the Al-induced functional and structural changes as evidenced by oxidative stress, DNA damage and altered calcium homeostasis as well as disordered signal cascade in experimental animals.

Conclusion: Al has been linked to neurodegeneration for decades and thus based on the neuroprotective effect of lithium in the brain in this animal system, we suggest that lithium should be considered and be exploited further for the prevention and therapy of brain disorders.

345

Brain Poster Session: Experimental Stroke & Cerebral Ischemia

DIFFERENTIAL CORRELATION OF P53 AND ROS DETERMINES HYPERGLYCEMIC ISCHEMIC BRAIN DAMAGE IN WILD-TYPE AND SOD2 HETEROZYGOUS KNOCKOUT MICE

S.L. Mehta[1], W. Chen[2], Y. Lin[3], P. Lolla[1], L. Cao[4], P.H. Chan[5], P.A. Li[1]

[1]Pharmaceutical Sciences/ BRITE, North Carolina Central University, Durham, NC, USA, [2]Department of Laser Therapy, Ningxia Medical University, Yinchuan, China, [3]University of Hawaii, Honolulu, HI, USA, [4]McMaster University, Ontario, ON, Canada, [5]Stanford University School of Medicine, CA, CA, USA

Objectives: Hyperglycemia negatively determines cerebral stroke outcome and indeed suggested to accelerate the infarction (Li et al., 2001, Muranyi et al., 2006), although the underlying mechanism is not clear. The reactive oxygen species (ROS) production is one of the critical factors implicated in the stroke pathogenesis and tumor suppressor protein, p53, has been linked to neuronal cell death and ROS levels. The objective of this study is to examine the expression of p53 and its association with ROS and ischemic brain damage under hyperglycemic condition in wild-type (WT) and manganese superoxide dismutase (SOD2) heterozygous knockout ($^{-/+}$) mice.

Methods: Male SOD2$^{-/+}$ and CD1 WT mice (24-26 g) were made hyperglycemic 30 min prior to middle cerebral artery occlusion (MCAO) with a single injection of glucose (25 %). Animals were killed at various times of reperfusion (0.5 to 24 hours) for assessment of brain damage, ROS production, p53 and cyclin G1 (CG1) protein levels**.**

Results: The results showed that hyperglycemia enhanced the ischemic brain damage in SOD2$^{-/+}$ mice. The damage was significantly greater in SOD2$^{-/+}$ as compared to WT and well correlated with the ROS production. The ROS production gradually and significantly increased in cortical and striatal area of WT mice, which was correlated with the elevation of p53 and survival factor, **CG1**. In contrast, ROS production showed abrupt elevation early during recirculation and decrease thereafter in SOD2$^{-/+}$ animals. Similarly, p53 and CG1 expression decreased in cortical and striatal area of SOD2$^{-/+}$ animals suggesting the down regulation of these factors in SOD compromised brain.

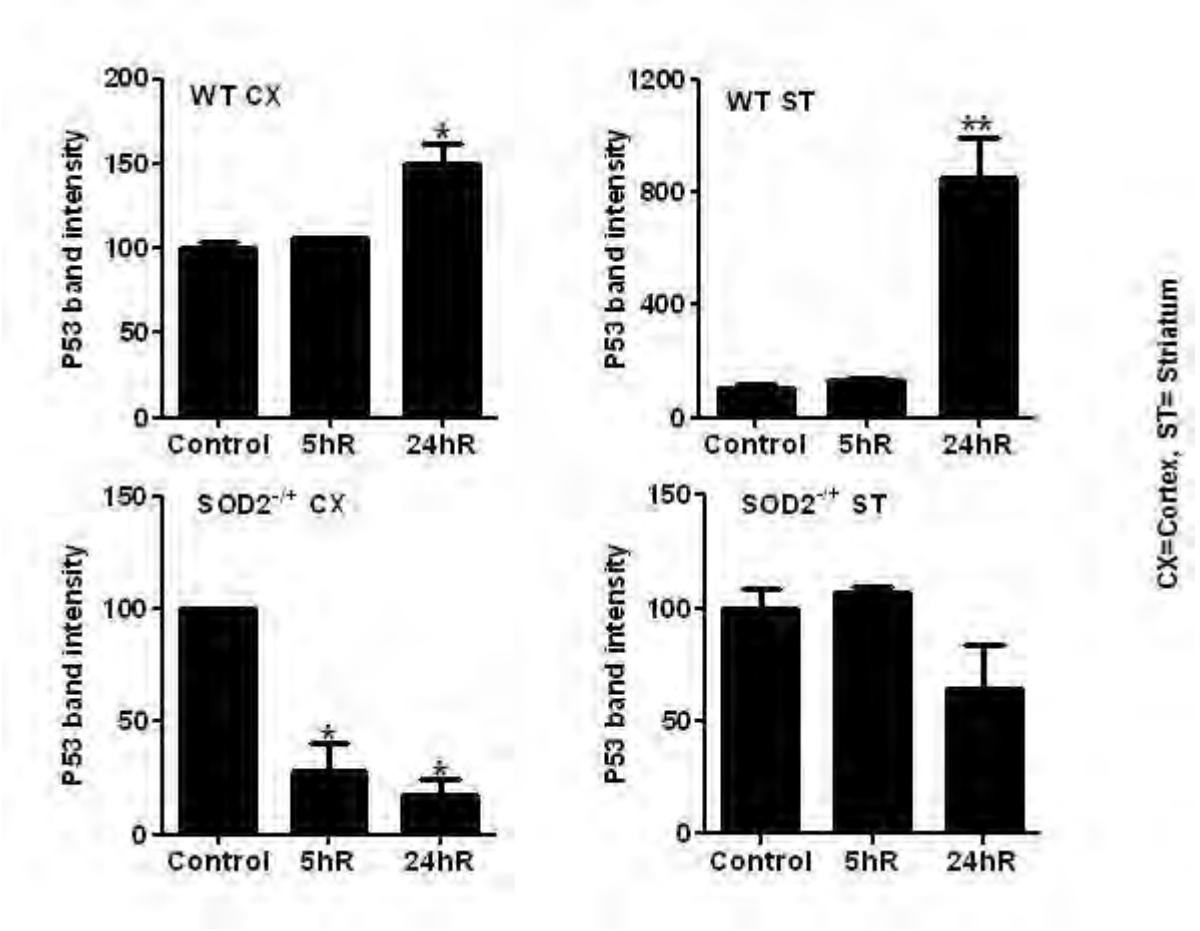

[p53 protein expression in cortex and striatum]

Conclusions: These results suggests that hyperglycemic ischemic brain damage is linked to ROS and p53 in WT, whereas, p53 plays no role in progression of damage in $SOD2^{-/+}$ animals. Thus, association of p53 and ROS appears to depend upon the severity of ischemic stress.

References:

Li PA, Rasquinha I, He QP, Siesjö BK, Csiszár K, Boyd CD, MacManus JP (2001) Hyperglycemia enhances DNA fragmentation after transient cerebral ischemia. J Cereb Blood Flow Metab 21:568-576.

Muranyi M, Ding C, He Q, Lin Y, Li PA (2006) Streptozotocin-induced diabetes causes astrocyte death after ischemia and reperfusion injury. Diabetes 55:349-355.

346

Brain Poster Session: Hemorrhagic Transformation

VASCULAR ADHESION PROTEIN-1 (VAP-1/SSAO) IS INVOLVED IN INTRACRANIAL HEMORRHAGIC COMPLICATIONS AFTER THROMBOLYSIS IN HUMAN STROKE

J. Montaner[1,2], M. Hernández-Guillamon[1], M. Solé[3], M. Parés[1], E. Cuadrado[1], T. Valente[3], L. Garcia-Bonilla[1], M. Ribó[2], M. Rubiera[2], C. Molina[2], J. Alvarez-Sabín[2], A. Rosell[1], M. Unzeta[3]

[1]Neurovascular Research Laboratory, [2]Neurovascular Unit, Department of Neurology, Vall d'Hebron Hospital, [3]Biochemistry and Molecular Biology, Neuroscience Institute, Autonomous University of Barcelona, Barcelona, Spain

Objectives: Vascular adhesion protein-1 (VAP-1) is a cell surface and soluble molecule that possesses semicarbazide-sensitive amine oxidase (SSAO) activity; which oxidatively deaminates primary amines (generating hydrogen peroxide, ammonia and the corresponding aldehyde) and plays a role in leukocyte transmigration through the inflamed vasculature. Leucocytes secrete proteases after tPA treatment contributing to BBB disruption. Therefore, we aimed to investigate for the first time the role of VAP-1 in hemorrhagic transformation (HT).

Methods: VAP-1/SSAO activity was determined radiochemically (pmol/min·mg protein) in 141 consecutive ischemic strokes involving the middle cerebral artery territory who received t-PA. Blood samples were obtained at baseline (pretreatment), in all patients. Hemorrhagic events were classified according to computed tomography (CT) criteria [petechial hemorrhagic infarctions (HI,1-2) and large parenchymal hemorrhages (PH,1-2 and remote PH)]. Brain CT scan was obtained at 24-48h or when a neurological worsening occurred. To calculate the sensitivity and specificity for VAP-1 values to predict brain bleedings a receiver operator characteristic (ROC) curve was configured. A replication study was conducted using cases from our plasma-library of t-PA treated patients [40 PH patients matched to 40 without HT]. Finally, SSAO/VAP-1 immunostaining of brain microvascular vessels was performed in 8 deceased stroke patients (2 without HT and 6 with HT). One of the cases with HT received thrombolytic treatment 3 days before death and the other cases suffered spontaneous hemorrhagic transformations. All brain samples were obtained within the first six hours after death.

Results: HT was present in 48 (34.3%) patients [21 (15%) HI-1, 11 (7.9%) HI-2, 10 (7.1%) PH-1, 3 (2.1%) PH-2 and 3 (2.1%) PH-R]. An increased baseline VAP-1 level was found among patients who later on develop a HT ($p< 0.001$). Moreover, the highest baseline VAP-1 level was found in patients with an ulterior PH and the lowest baseline VAP-1 level in those without HT (PH: 3.41 ± 1.07, non-HT: 2.48 ± 0.92 and HI: 2.79 ± 0.75; $p= 0.001$). For HT, VAP-1 (>2.7) was the main baseline predictor of HT appearance [OR 5.84 (2.16-15.80), p=0.001] and also hyperglycemia was independently associated to HT [OR 1.03 (1.007-1.05), p=0.008]. Baseline VAP-1 (>3.07) was the only predictor independently associated to PH appearance OR [8.94 (2.29-34.93), p=0.002]. In the subgroup of athrothrombotic strokes a cut-off of VAP-1= 3.12 had a 100% sensitivity and 100% specificity to identify PH. The replication study confirmed those results (data not shown). In the histological sub-study, brain samples with HT areas showed a strong SSAO/VAP-1 inmunostaining compared to the corresponding contralateral areas. SSAO/VAP-1 inmunostaining was associated with white blood cell extravasations and infiltration in those HT areas supporting our findings in the blood stream.

Conclusions: Baseline VAP-1 level predicts PH appearance after t-PA treatment. In the near future, VAP-1 determination might increase the safety profile for thrombolysis and anti-VAP-1 drugs might be combined with t-PA to prevent hemorrhagic complications.

Brain PET Oral 2: Novel Radiotracers and Modeling

PARAMETRIC METHODS FOR QUANTIFICATION OF [^{18}F]FP-ß-CIT STUDIES

R. Kloet[1], R. Boellaard[1], M. Ponsen[2], M. Yaqub[1], B. van Berckel[1], M. Lubberink[1], B. Windhorst[1], H. Berendse[2], A. Lammertsma[1]

[1]Nuclear Medicine & PET Research, [2]Deparment of Neurology, VU University Medical Center, Amsterdam, The Netherlands

Purpose: [^{18}F]FP-ß-CIT is a high affinity dopamine transporter (DAT) radioligand, which is of interest for studying the pathophysiology of Parkinson's Disease (PD). Recently it was shown that the simplified reference tissue model (SRTM)is the optimal method for quantifying [^{18}F]FP-ß-CIT data [1]. In this study performance of various SRTM based parametric methods and the impact of these methods on outcome of statistical parametric mapping (SPM) analysis were evaluated.

Methods: Dynamic 90 min [^{18}F]FP-ß-CIT scans were performed in 7 healthy (HC) and 6 PD subjects. Parametric binding potential (BP_{ND}) images were generated using various methods, such as reference Logan (Rlogan)[2], several multi-linear reference tissue methods without (MRTM0-2) and with (MRTM3,4)[3] fixing reference region washout constant (k_2'), receptor parametric mapping (RPM)[4], and SUVr (60-90 min) using cerebellum as reference region. Parametric methods were applied using different starting parameters, i.e. analysis starting time (t* = 2, 5, 20, 40, 50, 60 min) for Rlogan and MRTM variations or starting exponential for RPM (0.01, 0.005, 0.0025 min^{-1}), in order to first optimize performance of each method. Next, average striatum BP_{ND} derived from parametric data were compared with those obtained using SRTM applied to striatum time activity curves. Finally, parametric images with the best correlation, both before and after additional 5 mm FWHM Gaussian (G5) smoothing were used within SPM to determine the optimal method for detecting differences in [^{18}F]FP-ß-CIT binding between HC and PD.

Results: MRTM4 (t* = 20 min) and RPM (starting exponential = 0.0025 min^{-1}) showed best correlation (R^2=0.92, slope=0.87 and R^2=0.92, slope=0.90, respectively) of striatal BP_{ND} values with those obtained using SRTM. RPM (starting exponential = 0.01min^{-1}) showed best image quality and good correlation with SRTM, but showed bias (R^2=0.88, slope=0.40). Poor performance was seen for all other linearized methods (R^2< 0.6) and they were discarded for further analysis. SPM using G5 smoothed RPM BP_{ND} images, especially for starting exponential = 0.01 min^{-1}, provided best differentiation between PD and HC. Surprisingly, it was hardly possible to detect any differences in binding between these subject groups when SUVr images were used in the SPM analysis (see Table 1).

Conclusion: RPM outperformed all linearized methods investigated and is recommended for quantitative assessment of [^{18}F]FP-ß-CIT binding.

	ROI	Cluster level			Voxel level				
		Pcor-	KE	Puncor-	PFEW-	PFDR-	T	Z	Puncor-

		rected		rected	corr	corr			rected
SUVr (G5)									
RPM1 0.01 (G5)	left striatum	0.000	1668	0.000	0.000	0.000	20.83	6.28	0.000
RPM1 0.01 (G5)	right striatum	0.000	1356	0.000	0.000	0.000	15.63	5.78	0.000
RPM1 0.0025 (G5)	left striatum	0.000	855	0.000	0.001	0.001	13.70	5.55	0.000
RPM1 0.0025 (G5)	right striatum	0.000	647	0.000	0.128	0.004	8.63	4.66	0.000
MRTM4 20 (G5)	left striatum	0.000	1074	0.000	0.000	0.000	17.27	5.96	0.000
MRTM4 20 (G5)	right striatum	0.000	909	0.000	0.001	0.000	14.79	5.68	0.000

[Results SPM analysis in striatum]

References:

1. Yaqub et al. (2007) JCBFM 27: 1397-1406.

2. Logan et al. (1996) JCBFM 16: 834-840.

3. Ichise et al. (2003) JCBFM 23: 1096-1112.

4. Gunn, et al. (1997) Neuroimage 6: 279-28

SPATIO-TEMPORAL MAPPING OF NEUROTRANSMITTER ACTIVATION USING A LINEARIZATION OF THE PARAMETRIC NTPET MODEL

M.D. Normandin[1,2], R.D. Badgaiyan[3], E.D. Morris[1,2,4]

[1]Department of Radiology, Indiana University School of Medicine, Indianapolis, [2]Weldon School of Biomedical Engineering, Purdue University, West Lafayette, IN, [3]Division of Nuclear Medicine, Masschusetts General Hospital, Boston, MA, [4]Department of Biomedical Engineering, Purdue School of Engineering and Technology, Indiana University-Purdue University Indianapolis, Indianapolis, IN, USA

Objectives: We recently introduced [1], characterized [2], and validated [3] parametric ntPET (p-ntPET), a model for estimation of neurotransmitter kinetics from dynamic PET data. Here, we demonstrate voxel-by-voxel analysis with lp-ntPET, a linearization of the original model.

Methods: lp-ntPET extends the LSRRM [4] using basis functions to estimate the time course of neurotransmitter activation. The basis function that yields the best model fit is mapped to the optimal neurotransmitter response. Bases were chosen to allow estimation of response onset, peak time, and sharpness. This model includes four estimated parameters -- R_1, k_2 (interpreted in the two-tissue model sense), k_{2a} (apparent efflux rate in the one-tissue model sense), and response magnitude -- and is thus called lp-ntPET4.

Mathematical simplifications were considered to promote stable performance with noisy voxel data. Following the approach of SRTM2 [5] and MRTM2 [6], analysis was carried out using a global value for the reference region k_2. This model (lp-ntPET3) has three estimated parameters. The model was further simplified by fixing baseline BP (=$[k_2/k_{2a}]$-1) at each voxel according to prior analysis of pre-activation data. This model (lp-ntPET2) has two estimated parameters.

A human subject was injected with a bolus of [^{11}C]raclopride and scanned for 45 minutes. An emotional processing task hypothesized to elicit striatal dopamine release was initiated at 26 minutes. The dynamic data set was analyzed with lp-ntPET and subsequent simplifications as described above.

Results: Results of lp-ntPET4 analyses were variable and showed limited activation in striatum. Regions with high blood flow and low specific binding were prone to false positives. lp-ntPET3 and lp-ntPET2 indicated bilateral striatal activation with stronger responses in left vs. right caudate and putamen, consistent with results obtained using LSRRM. The onset of significant responses was generally synchronized with task initiation and peaked 1-2 minutes thereafter, in agreement with the anticipated response. Insignificant responses had little temporal coherence. Model simplifications reduced noise in the spatial distribution of activation, increased statistical power, and enhanced the temporal consistency of significant responses.

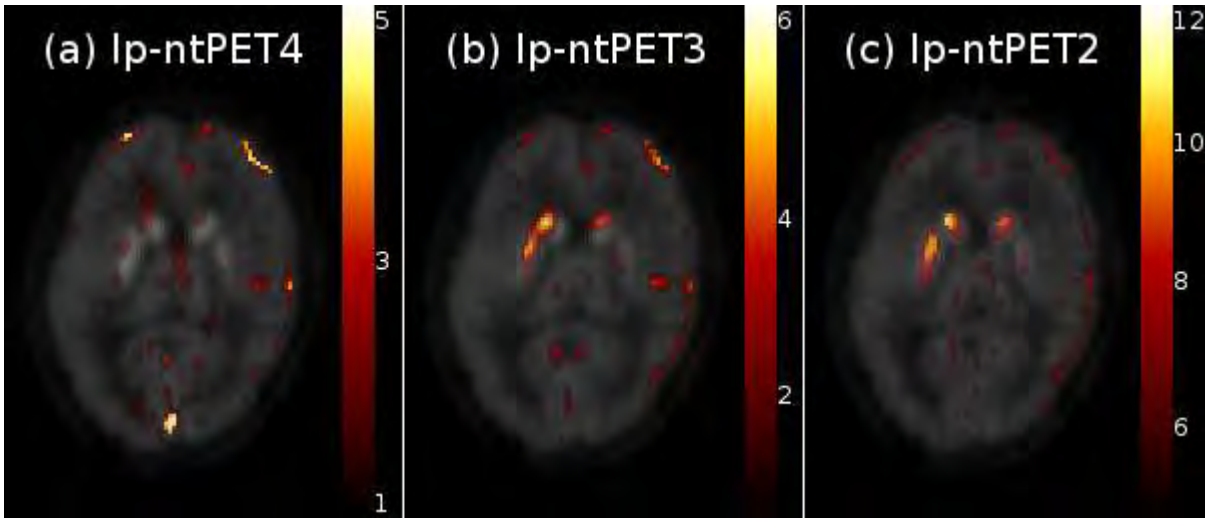

[Fig 1. Response t maps overlaid on emission image.]

Conclusions: The efficiency of lp-ntPET facilitates parametric image analysis, an intractable task for the computationally demanding p-ntPET. Simplifications of the lp-ntPET model improved the quality of results. Such simplifications are known to enhance precision at the expense of increased bias; simulation studies are under way to investigate this relationship for lp-ntPET.

References:

[1] Morris et al. (2005) Molecular Imaging Oct-Dec;4(4):473-89.

[2] Normandin and Morris. (2008) Neuroimage Feb 1;39(3):1162-79.

[3] Morris et al. (2008) Molecular Imaging and Biology Mar-Apr;10(2):67-73.

[4] Alpert et al. (2003) Neuroimage Jul;19(3):1049-60.

[5] Wu and Carson. (2002) Journal of Cerebral Blood Flow and Metabolism Dec;22(12):1440-52.

[6] Ichise et al. (2003) Journal of Cerebral Blood Flow and Metabolism Sep;23(9):1096-112.

Acknowledgements: Society of Nuclear Medicine Student Fellowship (MDN) and R21 AA015077 (EDM).

350

Brain Poster Session: Cerebral Metabolic Regulation

UNCOUPLING OF GLUCOSE UPTAKE IN NEURONS AND ASTROCYTES IN SOMATOSENSORY CORTEX IN VIVO

J. Chuquet, P. Quilichini, G. Buzsáki

Rutgers University, Newark, NJ, USA

Glucose is the primary energetic substrate of the brain and measurements of its metabolism are the basis of major functional cerebral imaging methods. Contrary to the dogmatic view that neurons are fueled solely by glucose in proportion to their energetic needs, recent in vitro and ex vivo analyses suggest that glucose preferentially feeds astrocytes. However, the cellular fate of glucose in the intact brain has not yet been directly observed. We have used a real-time method for measuring glucose uptake in astrocytes and neurons in vivo by imaging the trafficking of the non-hydrolysable glucose analog 6-NBDG using two-photon microscopy. During resting conditions we found that astrocytes and neurons both absorbed 6-NBDG at the same rate in the barrel cortex of the rat. However during intense neuronal activity triggered by whisker stimulation, astrocytes rapidly accelerated their uptake whereas neuronal uptake remained unchanged. Following the stimulation period, astrocytes returned to their pre-activation rates of uptake paralleling the neuronal rate of uptake. These observations suggest that glucose is metabolized primarily in astrocytes, supporting the hypothesis that astrocytes play a central role in the energetic fueling of neurons.

Brain Poster Session: Neurologic Disease

MULTIMODAL IMAGING OF THE HIPPOCAMPUS IN EARLY ALZHEIMER'S DISEASE

I. Yakushev[1], A. Gerhard[2], M. Lorscheider[1], I. Schermuly[1], H.-G. Buchholz[3], J. Albrecht[1], A. Hammers[4], M. Schreckenberger[3], A. Fellgiebel[1]

[1]Department of Psychiatry and Psychotherapy, University of Mainz, Mainz, Germany, [2]Wolfson Molecular Imaging Centre, The University of Manchester, Manchester, UK, [3]Department of Nuclear Medicine, University of Mainz, Mainz, Germany, [4]Division of Neurosciences and Mental Health, MRC Clinical Sciences Centre, Imperial College, London, UK

Objectives: Structural and functional disturbances of the hippocampus in early Alzheimer's disease (AD) have been consistently detected using various imaging modalities. Recently, functional magnetic resonance imaging (MRI) and neuroanatomical studies have provided evidence for a functional differentiation along the longitudinal axis of the hippocampus with the hippocampal head playing a crucial role in the formation of memories. Thus focussing on the hippocampal subdivisions, the objective of the present study was to investigate associations between different structural and functional imaging markers of hippocampal integrity and memory performance in early AD.

Methods: Global and regional hippocampal volumes, diffusivity, and glucose metabolism were quantified in 20 patients with early AD (MMSE 24.5±2.9, mean±SD) using structural MRI, diffusion-tensor imaging (DTI), and positron emission tomography with ^{18}fluorodeoxyglucose (FDG-PET). The study group included 11 subjects with mild Alzheimer's dementia and 9 subjects with amnestic mild cognitive impairment (MCI), who had an “Alzheimer-typical” FDG-PET finding. Such individuals were repeatedly shown to deteriorate to Alzheimer's dementia within 1-2 years (1,2). Regions-of-interest (ROIs) were placed manually onto the hippocampal head (HH), body (HB), and the whole hippocampus bilaterally. PET images were carefully corrected for partial volume effects taking into account both spill-in and spill-out effects. The measures from the different modalities were correlated for each ROI followed by correlations between the ROI values and scores on memory performance tests controlling for age. Finally, stepwise regression analyses with memory tests as dependent and ROI measures as independent variables were performed.

Results: In the whole group, the verbal delayed recall score correlated with mean diffusivity (MD) of the left HH ($r=-0.64$, $p=0.003$) and with the volume of the left HB ($r=-0.61$, $p=0.006$). Neither correlation retained the statistical significance when the analyses were restricted to the subgroup of MCI subjects. In the regression analyses, MD of the left HH was the only predictor of memory performance explaining 30.6% of the variance (model $p=0.007$). Glucose metabolism correlated with MD in the left HH only ($r=-0.48$, $p=0.038$). When the analyses were restricted to the subgroup of MCI subjects, the correlation appeared highly significant ($r=-0.90$, $p=0.003$).

Conclusions: The main finding of our study is the inverse correlation between performance on the verbal delayed recall test and diffusivity of the left HH. While the memory performance was also associated with the left HB volume, among the measures of three imaging modalities diffusivity of the left HH was the only predictor of verbal memory impairment in early AD. Furthermore, the correlation of the left HH diffusivity and glucose metabolism, which was especially pronounced in the subgroup of MCI subjects, indicates a close relationship between PET and DTI measures as early imaging markers of non-specific tissue damage. The lack of the association between hippocampal metabolism and memory performance is somewhat surprising, but is consistent with a recent report (3). We continue to work on the present study, introducing new variables and increasing the sample size.

References:

1) Chételat et al., 2003. Neurology 60:1374-7.

2) Mosconi et al., 2004. Neurology 63:2332-40.

3) Walhovd et al., in press. Neuroimage.

A MODEL OF RECURRENT STROKE: MRI AND HISTOLOGICAL CHANGES IN RATS SUBJECTED TO AN INITIAL MINOR AND SUBSEQUENT MODERATE INSULT

M. Qiao[1], Z. Zhao[2], P.A. Barber[2], D. Barua[2], T. Foniok[1], D. Kirk[3], S. Sun[2], **U.I. Tuor**[1,3]

[1]MR Technology, Institute for Biodiagnostics (West), National Research Council Canada, [2]Dept. of Neuroscience, [3]Experimental Imaging Centre, University of Calgary, Calgary, AB, Canada

Objectives: There is a high risk of recurrent stroke following a transient ischemic attack (TIA) or minor stroke [1,2]. Such patients would be ideal for treatment with neuroprotective agents after their initial insult. However, the cellular responses to a second stroke following an initial minor stroke are poorly understood. Indeed, animal models of recurrent stroke are lacking. The present study hypothesized that following a moderate stroke preceded by a minor stroke, the subsequent brain injury, examined with magnetic resonance imaging (MRI) and histological techniques, would either be exacerbated (if insults were additive) or reduced (if there was a pre-conditioning neuroprotective effect).

Methods: An initial mild transient focal cerebral ischemia was induced in rats by occluding the middle cerebral artery (MCAO) with a microclip for 40 min along with transient concurrent occlusion of both carotid arteries. Stroke severity was confirmed using MRI 2 days later and at three days a second moderate stroke was produced (60 min). Seven days later MRI and then histology was performed. Subgroups of animals (n=23) with either a single mild stroke, a single moderate stroke or a combination of mild and moderate stroke were compared. Brain injury was graded from 0-4 in 4 regions of an anterior section stained with hematoxylin and eosin (HE) providing a cumulative injury score. Sections were also stained for astrocytosis (GFAP) and microgliosis (ED1) immunohistologically.

Results: In rats 48hrs following a mild stroke, T2 maps appeared normal despite evidence of scattered cell death, modest increased GFAP labeling and no changes in ED1 or MAP2 (Fig. 1, 2). In contrast, MRI scans in rats with 60 min-MCAO had hyperintense areas in cortex corresponding to extensive cell death or infarction. Loss of MAP2 and GFAP staining were observed in the core of infarct with extensive labeling for ED1 and GFAP in the peri-infarct area. The recurrent stroke with a 40 min MCAO and a subsequent 60 min MCAO 3 days later resulted in a higher cumulative injury score than what was observed following a single mild MCAO (Fig. 2). Changes in MRI, MAP2, GFAP and ED1 tended to be greater than that observed in the group with a single moderate MCAO.

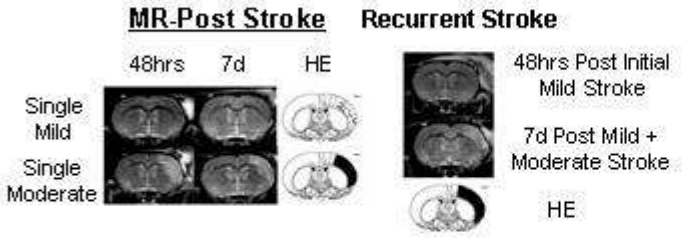

Fig.1. Changes in MRI and histology in the brains exposed to either a single middle cerebral artery occlusion (MCAO), a single moderate MCAO or a combination (recurrent) MCAO. T2 changes were shown as hyperintensity and solid black colour or dots showing tissue as infarct or scattered cell death, respectively.

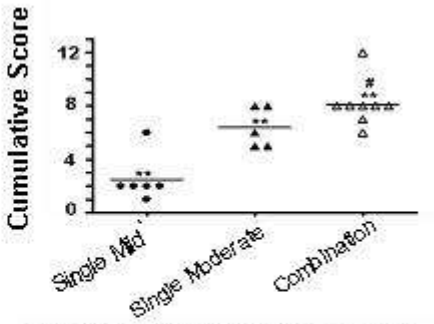

Fig 2. Cumulative histological score from the brains with either a single MCAO, a single moderate MCAO or a combination (recurrent) stroke. **P<0.01 vs the value of 0; #P<0.05 vs the single mild using a rank test.

[brain_09_06.jpg]

Conclusions: Unlike preconditioning studies, where periods of ischemia without permanent injury result in neuroprotection against a subsequent ischemic insult, we demonstrate that a minor stroke resulting in mild injury prior to a more substantial stroke could enhance the subsequent ischemic injury. This model of recurrent stroke should provide a valuable platform to test neuroprotective agents suitable for reducing stroke severity following a mild stroke or transient ischemic attack (Funded by CIRH).

References:

1. Hill et al. Neurology. 2004;62:2015-20.

2. Nguyen-Huynh MN, Johnston SC. Nat Clin Pract Cardiovasc Med. 2007 4:310-8.

353

Brain Poster Session: Experimental Cerebral Ischemia: Blood Flow & Metabolism

MILD INDUCED HYPERTENSION IMPROVES BLOOD FLOW VIA EXTERNAL CAROTID COLLATERALS IN COMBINED DISTAL MIDDLE CEREBRAL AND CAROTID OCCLUSION

I. Yuzawa[1], H.K. Shin[2,3], S. Sakadzic[4], D.A. Boas[4], H. Ay[5], C. Ayata[1,5]

[1]Stroke and Neurovascular Regulation Laboratory, Neuroscience Center, Massachusetts General Hospital & Harvard Medical School, Charlestown, MA, USA, [2]Division of Meridian and Structural Medicine, School of Oriental Medicine, Pusan National University, [3]MRC for Ischemic Tissue Regeneration, Pusan National University School of Medicine, Yangsan-si, South Korea, [4]MGH/MIT/HMS Athinuola A. Martinos Center for Biomedical Imaging, Department of Radiology, [5]Stroke Service and Neuroscience Intensive Care Unit, Department of Neurology, Massachusetts General Hospital, Harvard Medical School, Charlestown, MA, USA

Objectives: Mild induced hypertension (iHTN) improves cerebral blood flow (CBF) and decreases infarct size in isolated distal middle cerebral artery occlusion (dMCAO) in mice. The contributions of anterior (AComm) and posterior communicating (PComm) arteries, pial/dural anastomoses, and external (ECA) to internal carotid (ICA) collaterals to CBF improvement during iHTN are not known. We tested whether ECA collaterals augment CBF during iHTN in a model of dMCAO plus internal (ICAO) or common (CCAO) carotid occlusion in mice.

Methods: High spatiotemporal resolution laser speckle flowmetry was used to image CBF changes in 3 groups of mice (C57BL/6J): dMCAO alone (transtemporal clipping), dMCAO+ICAO, or dMCAO+CCAO. Each group was further divided into iHTN (phenylephrine to raise BP by 30%, starting 10 min after dMCAO) and saline (n=9 each). ICAO or CCAO was induced 10 min before dMCAO, and imaging was continued for 90 min. Indirect infarct volumes were measured 48h after ischemia using TTC-stained 1mm-thick coronal sections.

Results: Unilateral ICAO or CCAO significantly reduced CBF in both middle (MCA) and posterior cerebral artery (PCA) territories; anterior cerebral artery (ACA) territory flow was relatively preserved, consistent with a single confluent ACA in rodents. dMCAO led to larger CBF deficits in the presence of ICAO and CCAO compared to dMCAO alone. iHTN significantly decreased the area of severely ischemic cortex (≤20% residual CBF) during dMCAO (-46%). The efficacy of iHTN was diminished in the dMCAO+ICAO group (-34%), and abolished in the dMCAO+CCAO group (-14%), underscoring the importance of ECA collaterals. Consistent with this, iHTN reduced infarct volume in dMCAO+ICAO group (-64%) but not in dMCAO+CCAO (-6%). Examination of circle of Willis showed absent or hypoplastic ipsilateral PComm in >75% of C57BL/6J mice. Occasional presence of a PComm appeared to augment the efficacy of iHTN in this model.

Conclusions: Our data demonstrate that iHTN augments CBF mainly through ECA collaterals in the presence of ICAO in this mouse strain with poorly developed PComm. Therefore, iHTN may not be effective in patients with either ECAO plus ICAO, or CCAO, and an incomplete circle of Willis.

Group	Post-I/CCAO flow (ACA/MCA/PCA, %)		Area with ≤20% residual CBF (mm2)	Infarct volume (mm3)
dMCAO+ICAO	68±6 / 60±12 /	control	9.4 ± 1.3	19.1 ± 8.3

	57±6			
		iHTN	6.2 ± 2.1*	6.3 ± 1.4*
dMCAO+CCAO	72±9 / 52±6 / 48±7	control	12.2 ± 2.8	18.1 ± 3.6
		iHTN	10.5 ± 3.1	17.1 ± 2.2

[Efficacy of iHTN]

NORMOBARIC HYPEROXIA REDUCES THE NEUROVASCULAR COMPLICATIONS ASSOCIATED WITH DELAYED TISSUE PLASMINOGEN ACTIVATOR TREATMENT IN TRANSIENT FOCAL CEREBRAL ISCHEMIA

W. Liu[1], J. Hendren[1], X.-J. Qin[1], **K.J. Liu**[1,2]

[1]College of Pharmacy, [2]Department of Neurology, University of New Mexico, Albuquerque, NM, USA

Background and purpose: A major limitation of tissue plasminogen activator (tPA) thrombolysis for ischemic stroke is the narrow time window for safe and effective therapy.[1] Delayed tPA thrombolysis increases the risk of cerebral hemorrhage and mortality, which, in part, is related to neurovascular proteolysis mediated by matrix metalloproteinases (MMPs). We recently showed that normobaric hyperoxia (NBO) treatment reduces MMP-9 expression and blood brain barrier (BBB) disruption in the ischemic brain. [2, 3] Therefore, we hypothesized that NBO could increase the safety of delayed tPA thrombolysis in stroke.

Methods: Thirty six male Sprague Dawley rats were exposed to NBO (95%O_2) or normoxia (21%O_2) during 5-hr filament occlusion of the middle cerebral artery, followed by 19-hr reperfusion. Thirty min before reperfusion, saline or tPA were continuously infused to rats over 1 hr. Successful MCAO was confirmed with 2,3,5-triphenyltetrazolium chloride (TTC). Outcome parameters were neurological score, mortality rate, brain edema, hemorrhage volume and MMP-9. Hemorrhage was quantified with a hemoglobin spectrophotometry method. Edema was evaluated as hemispheric enlargement. MMP-9 was measured by gelatin zymography.

Results: Regardless of saline or tPA treatment, NBO-treated rats showed a relatively smaller infarct area on the TTC-stained brain section than normoxic rats. In normoxic rats, delayed tPA treatment at 4.5 hrs after stroke onset resulted in high mortality, more severe neurological deficits, increased hemorrhage volumes and augmented MMP-9 induction in the ischemic BBB microvasculature compared with saline. Rats treated with combined NBO and tPA showed significant reductions in tPA-associated mortality, brain edema, hemorrhage and MMP-9 augmentation, as compared with tPA alone.

Conclusions: These results suggest that early NBO treatment may represent an important strategy to increase the safety of delayed tPA thrombolysis in ischemic stroke.

Key words: Tissue plasminogen activator; cerebral hemorrhage; matrix metalloproteinases; oxygen; stroke.

Reference:

1. The national institute of neurological disorders and stroke rt-pa stroke study group. Tissue plasminogen activator for acute ischemic stroke. . N Engl J Med. 1995;333:1581-1587.

2. Liu S, Liu W, Ding W, Miyake M, Rosenberg GA, Liu KJ. Electron paramagnetic resonance-guided normobaric hyperoxia treatment protects the brain by maintaining penumbral oxygenation in a rat model of transient focal cerebral ischemia. J Cereb Blood Flow Metab. 2006;26:1274-1284.

3. Liu W, Sood R, Chen Q, Sakoglu U, Hendren J, Cetin O, Miyake M, Liu KJ. Normobaric hyperoxia inhibits nadph oxidase-mediated matrix metalloproteinase-9 induction in cerebral microvessels in experimental stroke. J Neurochem. 2008;107:1196-1205.

Brain PET Oral 6: Neurodegenerative Disorders

PRECLINICAL PREDICTORS OF PERFORMANCE OF AMYLOID-IMAGING TRACERS IN HUMANS

J.C. Price[1], W.E. Klunk[2], N.S. Mason[1], B. Lopresti[1], M.L. Debnath[2], M. Berginc[1], W. Bi[1], S.T. DeKosky[3,4], C.A. Mathis[1]

[1]Radiology, [2]Psychiatry, [3]Neurology, University of Pittsburgh, Pittsburgh, PA, [4]Neurology, University of Virginia, Charlottesville, VA, USA

Objectives: Desirable properties for amyloid-imaging tracers include good specific retention and rapid clearance of nonspecific binding (given sufficient initial brain entry). The difficulties involved in testing tracers in humans necessitate a robust preclinical protocol for predicting success in humans. Here we show the utility of measurements of in vitro binding affinity ($1/K_d$) and nonspecific clearance in animals for predicting relative performance of two amyloid-imaging tracers: PiB and a new [F-18]-labeled derivative, 2´F-PiB.

Methods: Two controls (CN: 75 yrs, 66 yrs, MMSE=30) and 1 Alzheimer´s disease (AD: 57 yrs, MMSE=28) subject were studied with PET (HR+ 10-15 mCi) over 90 (PIB) or 120 (2´F-PiB) min (no blood sampling). Anesthetized baboons were studied similarly (PiB: n=8; 2´F-PiB: n=4). Tissue uptake (SUV) and tissue ratios (SUVR) were computed (40-90 min) for frontal cortex (FRC) and cerebellum (CER: nonspecific uptake reference region). Computer simulations were performed to simulate AD time-activity curves for PiB and 2´F-PiB. Simulations utilized a legacy [1] PiB input function for an "average" AD subject and average (n=9) 2-tissue compartment AD PiB model parameters for FRC (K_1=0.254 $mL \cdot cm^{-3} \cdot min^{-1}$, k_2=0.122 min^{-1}, k_3=0.049 min^{-1}, k_4=0.017 min^{-1}) and CER (K_1=0.283 $mL \cdot cm^{-3} \cdot min^{-1}$, k_2=0.145 min^{-1}, k_3=0.012 min^{-1}, k_4=0.016 min^{-1}). Experimental values for in vitro K_d of 1.4 nM (PiB) and 5.5 nM (2´F-PiB) and the human PiB k_4 values (above) were used to estimate 2´F-PiB k_4 values.

Results: The 2´F-PiB k_4 values for AD FRC and CER were estimated to be 0.067 and 0.063 min^{-1}, respectively. The simulations predicted an AD PiB FRC SUV value that was 2.0-fold greater than that predicted for 2'F-PiB. This suggested that the specific retention of 2´F-PiB would be much lower than that of PiB. However, differences in nonspecific clearance could offset this effect when tissue ratios are calculated. This was examined via simulations for CER and in vivo baboon imaging data. The simulations predicted a PiB CER SUV value 1.6-fold higher than that for 2'F-PiB. This was consistent with PET data acquired in amyloid-free baboons for which the experimentally determined PiB CER SUV was 1.6-fold higher than that measured for 2'F-PiB. These results suggest that the PiB FRC SUVR would be ~1.3-fold greater that of 2'F-PiB (i.e., 2.0/1.6). The findings in humans were very consistent with these predictions. PET studies in the AD patient resulted in a PiB FRC SUV value that was 2.3-fold higher than that measured for 2'F-PiB, while the PiB CER SUV was 1.6-fold higher (and similar across all 3 subjects: 1.7±0.2). PET studies in the AD subject also yielded a PiB FRC SUVR value of 3.1, a value that was 1.4-fold higher than the 2´F-PiB FRC SUVR value of 2.2.

Conclusions: This comparison of experimentally-driven K_d simulations with animal studies of nonspecific clearance was robust relative to human in vivo PET data results and shows the value of experimentally-determined affinity and clearance in predicting in vivo performance of amyloid-imaging tracers in humans.

References: [1] Price JC et al, J Cereb Blood Flow Metab 2005, 25:1528-1547.

SEPARATING RECOVERABLE AND PERMANENT DAMAGE POST STROKE WITH CASL FMRI STRESS TESTING AND 18-FDG PET

G. Deutsch[1], J. O'Malley[1], R. Menon[2], V. Mark[3], B. Corbitt[1], H. Liu[1], J. den Hollander[4], J. Halsey[5]

[1]Radiology, Nuclear Medicine Division, University of Alabama at Birmingham, [2]Biomedical Engineering, [3]Rehabilitation Medicine, [4]Cardiology, [5]Neurology, University of Alabama at Birmingham, Birmingham, AL, USA

Introduction: Stroke typically results in neurometabolic activity defects in regions distal but functionally connected to the infarct, usually representing deafferentation effects of the lesion, a physiological phenomenon known as diaschisis. We tested a method of continuous arterial spin-labeled (CASL) perfusion MRI, during baseline and cerebrovascular stress, to identify and quantify regional activity reductions outside the lesion that should represent recoverable brain. 18-FDG PET was also performed to assist interpretation.

Materials and methods: We studied 6 patients (mean age 57, range 19-72 years) within 2-4 weeks post unilateral stroke involving the middle cerebral artery (MCA), with some variation in the extent of cortical and deeper white and gray matter involvement. MR Sequences: Patients and 22 controls were imaged on a 3T, Philips Intera scanner, using a transmit/receive head coil. Supratentorial slices covering cerebrum to cerebellum (single shot spin echo planar imaging; adiabatic-through-fast-passage labeling pulse) were acquired continuously in ascending order during resting-baseline and inhalation of 5% CO2. 18-FDG PET was performed on a GE 8-slice Discovery-LS PET-CT using intravenous injection of 10 mCi F-18 FDG and 3-D acquisition. Data Analysis: CASL data were stored as raw echo amplitudes and transferred for rCBF computations using custom software written in MATLAB™. Forty pairs of labeled and control images were motion corrected and averaged to produce a single set of perfusion images. Changes in rCBF were analyzed using an ROI method, a method for estimating relative functional versus anatomical defect size [Mountz, SemNucMed2003:33;56-76], and compared to controls with Statistical Parametric Mapping (SPM).

Results: Figure 1 depicts an angulated transverse section from a patient for T1 weighted MRI, CASL at rest and during CO2 stress, and 18-FDG PET. Figure 2 plots rCBF values and PET-18FDG as percent of mean in ROI segments formed by a cortical circumferential profile analysis. All patients showed a significant increase in rCBF between rest and stress and a reduction in the metabolic-to-anatomical “defect volume” (Table-1). The reduced defect volume quantifies an extended penumbra in the affected hemisphere. 18-FDG-PET showed reduction in activity distal to the infarct coinciding with the resting state rCBF reductions. Figure 3 shows SPM analysis of the case above compared to controls. Significant ($p < 0.01$) contralesional as well as ipsilesional hemispheric reductions are seen. Analysis of the CO_2 scan showed differences only within the lesion perimeter. Figure 4 shows absolute rCBF during rest and CO2 in one slice, with ROIs 7,8 improving most.

Discussion: The dramatic improvement in rCBF seen during CO2 stress outside the perimeter of the infarcted region strongly suggests primary neurometabolic reduction at rest and represents diaschisis or deafferentation effects. These regions also represent viable brain with recovery potential and probably account for some portion of the patients' current cognitive and motor deficits.

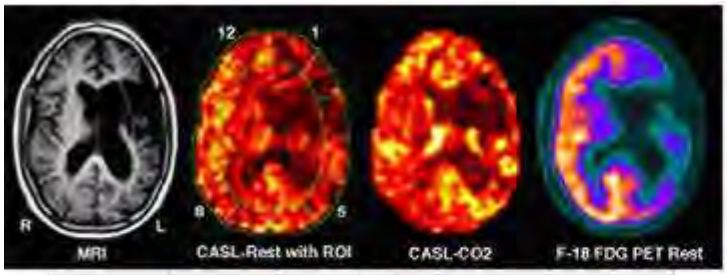

Fig 1 (left) Structural MRI, rCBF map at rest with ROI's drawn, rCBF map with CO_2, and FDG PET image at Rest

Fig 2 (below) CASL based rCBF values versus FDG PET at rest for 12 ROIs (% of mean activity)

Case	MRI lesion	rCBF Defect		PET
		Rest	CO_2	
1	15	31	20	-
2	5	18	9	16.3
3	19	45	26	39.8
4	18	41	30	68.0
5	18	38	26	60.8
6	27	49	31	69.5

Table 1: Lesion volumes (cc) from MRI; total rCBF defect (cc) calculated at rest and during CO_2 stress using CASL; and FDG-PET defect (cc) calculated at rest for 6 patients

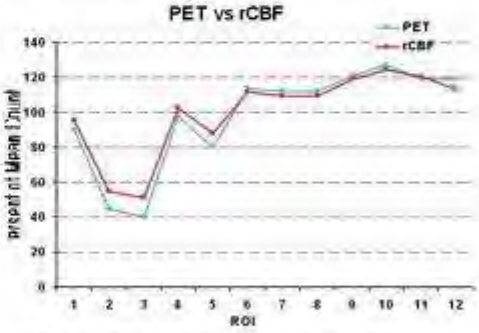

Fig. 3a Resting State Controls - Patient

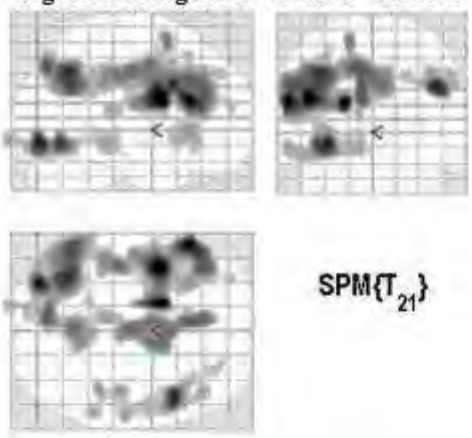

Fig 3b CO_2 Stress Contols - Patient

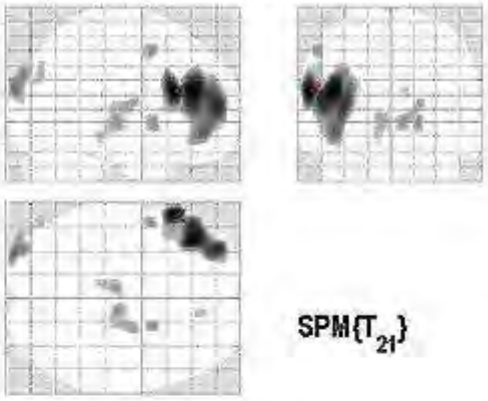

Fig 4a ROI Schematic

Fig 4b: rCBF (ml/100g/min) at rest

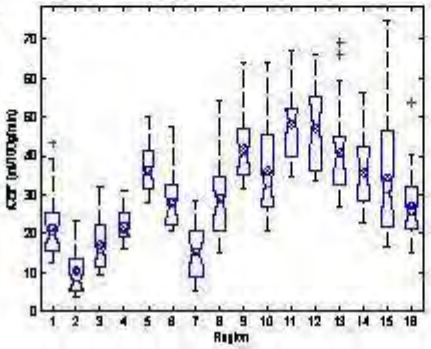

Fig 4c: rCBF (ml/100g/min) during CO2

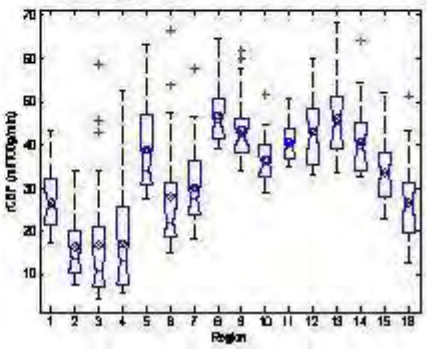

[Figure Layout]

SUBARACHNOID HEMORRHAGE INDUCES AUTOPHAGY

J.-Y. Lee[1,2], Z. Chen[1], S. Hu[1], O. Sagher[1], R.F. Keep[1], Y. Hua[1], G. Xi[1]

[1]Department of Neurosurgery, University of Michigan, Ann Arbor, MI, USA, [2]Department of Neurosurgery, University of Cologne, Cologne, Germany

Objectives: Aneurysmal subarachnoid hemorrhage (SAH) is a serious disease leading to high morbidity and mortality. The most death occurs within few days, and the exact mechanisms underlying brain injury during this early period following SAH are not fully identified (Cahill et al, 2006). Apoptotic cell death plays an important role in early brain injury after SAH. Recently, activated autophagy has been demonstrated in neurons exposed to intracerebral hematoma, hypoxia-ischemia, and traumatic brain injury. However, the role of autophagy is controversial. This study employed a modified endovascular perforation rat model to investigate whether autophagy pathway is involved in the early brain injury following SAH.

Methods: Male Sprague-Dawley rats were used. SAH was induced using endovascular perforation technique described by Bederson et al (1995) with slight modifications consisting of ICP-guided vessel perforation and temporarily occlusion of the ipsilateral ICA for 2 min. Sham-operated control rats underwent an identical procedure without vessel perforation (n=10). The rats were killed at Day 1 and 3 following SAH induction (n=10, each group). Microtubule-associated protein light chain-3 (LC3) and cathepsin-D were investigated by Western blot analysis and immunohistochemistry. Electron microscopy was performed to examine the ultrastructural changes of the neurons after SAH.

Results: LC3-II is one of the biochemical markers for autophagy. Although LC3-I could be detected in sham-operated control rats, the conversion of LC3-I to LC3-II was significantly increased in the ipsilateral frontobasal cortex at Day 1 and Day 3 ($P< 0.05$) following SAH induction. Cathepsin-D is a lysosomal enzyme important for degradation of altered cellular materials, and a significant elevated cathepsin-D expression could be demonstrated at Day 1 ($P< 0.01$) as well as on Day 3 ($P< 0.05$) compared to sham-operated control animals. Immunohistochemical study with antibody against cathepsin-D showed numerous positive stained neurons in deep layer of the frontobasal cortex. Under electron microscopy, double-membraned vacuoles were markedly accumulated in neurons at Day 1 following SAH.

Conclusion: This present study showed that the autophagy pathway is significantly activated in the acute phase after SAH. Further studies are needed to clarify the role of autophagy in SAH.

References:

Bederson JB, Germano IM, Guarino L (1995) Cortical blood flow and cerebral perfusion pressure in a new noncraniotomy model of subarachnoid hemorrhage in the rat. Stroke 26:1086-91.

Cahill WJ, Calvert JH and Zhang JH (2006) Mechanisms of early brain injury after subarachnoid hemorrhage. J Cereb Blood Flow Metab 26: 1341-53.

359

Brain Poster Session: Subarachnoid Hemorrhage

DEFEROXAMINE REDUCES EARLY BRAIN INJURY FOLLOWING SUBARACHNOID HEMORRHAGE

J.-Y. Lee[1,2], Y. He[1], O. Sagher[1], R.F. Keep[1], Y. Hua[1], G. Xi[1]

[1]Department of Neurosurgery, University of Michigan, Ann Arbor, MI, USA, [2]Department of Neurosurgery, University of Cologne, Cologne, Germany

Objectives: The treatment of subarachnoid hemorrhage (SAH) remains one of the major challenges. Despite advances in the diagnosis and treatment of aneurysms, the pathophysiological aspects following SAH are still poorly understood, and the therapeutic options in the acute phase are limited. Recent experimental studies in the setting of intracerebral hemorrhage in rats have demonstrated that deferoxamine, an iron chelator, reduced significantly brain edema and neuronal cell death leading to improved neurological outcome (Song et al, 2007). In this study, the effect of deferoxamine on early brain injury following SAH was examined.

Methods: Male Sprague-Dawley rats were used. SAH was induced using endovascular perforation technique described by Bederson et al (1995) with slight modifications consisting of ICP-guided vessel perforation and temporary occlusion of the ipsilateral ICA for 2 min. The rats were treated with either deferoxamine (100 mg/kg, i.p., given 2 h after hemorrhage followed by every 12 h) or vehicle (n=12, each group). Sham-operated control rats underwent an identical procedure without vessel perforation (n=12). The rats were killed at Day 1 following SAH induction for measurement of brain edema. To assess oxidative brain injury and neuronal cell death, heme oxygenase (HO)-1 expression was analyzed using Western blot analysis and Fluoro-Jade immunofluorescence staining was performed.

Results: Twenty-four hours following SAH induction, a significant increase in water content could be determined in ipsilateral cortex ($P < 0.05$) accompanied by significant upregulation of HO-1 expression ($P < 0.05$) in comparison with sham-operated control animals. Furthermore, diffusely distributed dying cells throughout the ipsilateral hemisphere could be observed at Day 1 following SAH induction. The treatment with deferoxamine resulted in significant decrease in brain edema ($P < 0.05$) and significant reduction in HO-1 expression ($P < 0.05$) as well as markedly less Fluoro-Jade positive labeled neurons.

Conclusion: Additionally to global ischemia, the excessive hemoglobin and iron overload play an important role in early brain injury following SAH. Acute treatment with deferoxamine ameliorates significantly hemoglobin-induced secondary brain lesions and therefore, could be a useful adjunct in the treatment of SAH.

References:

Bederson JB, Germano IM, Guarino L (1995) Cortical blood flow and cerebral perfusion pressure in a new noncraniotomy model of subarachnoid hemorrhage in the rat. Stroke 26:1086-91.

Song S, Hua Y, Keep RF, Hoff JT, Xi G (2007) A new hippocampal model for examining intracerebral hemorrhage-related neuronal death: effects of deferoxamine on hemoglobin-induced neuronal death. Stroke 38:2861-63.

360

Brain Poster Session: Oxidative Mechanisms

DOWN-REGULATION OF CASEIN KINASE 2 TRIGGERS ISCHEMIC NEURONAL DEATH VIA AKT INHIBITION AND ROS PRODUCTION AFTER OXIDATIVE INSULTS IN MICE

G.S. Kim, J.E. Jung, K. Niizuma, P.H. Chan

Department of Neurosurgery, Stanford University School of Medicine, Stanford, CA, USA

Objectives: Casein kinase 2 (CK2) plays a pivotal role in cell proliferation, cell cycle control and apoptosis by phosphorylating its various substrates (Pinna, 2002). But the role of CK2 and changes in its subunit levels and activity after oxidative insults in the brain are not well known.

Methods: In this study, we employed in vivo transient focal cerebral ischemia (tFCI) in models of 45-minute transient middle cerebral artery occlusion (Saito et al., 2003), subarachnoid hemorrhage (SAH) and in vitro oxygen glucose deprivation (OGD) to investigate the role of and changes in CK2 subunits following oxidative stress.

Results: We found that CK2 protein activity in the damaged cortex region from the ipsilateral hemisphere was reduced compared with the contralateral hemisphere (1 vs 0.7± 0.1, $p < 0.05$). Also, the protein levels of catalytic subunits CK2α and CK2α and phosphorylation of CK2β in the cortex region damaged by ischemic injury were markedly decreased 24 hours after ischemic injury and reperfusion (CK2α: 1 vs 0.35 ± 0.09, $p < 0.01$; CK2α′: 1 vs 0.44 ± 0.19, $p < 0.05$; pCK2β: 1 vs 0.3 ± 0.12, $p < 0.01$), whereas the regulatory subunit CK2β was not changed after ischemia and reperfusion as assessed by Western blotting. We also observed similar changes in the CK2 subunits in the SAH and OGD models, which are known to induce oxidative stress in neuronal cells. Immunofluorescent staining revealed that CK2α- and phospho-CK2β-positive cells were significantly diminished in the penumbra and ischemic core region in the injury area compared with the non-injured area. Treatment with MG132, a proteasome inhibitor, blocked CK2α down-regulation in a dose-dependent manner after tFCI and in the OGD model. The protein levels of CK2α in SOD1 transgenic mice did not decrease after ischemic injury compared with wild-type mice. CK2α-positive cells did not colocalize with cleaved poly(ADP-ribose) polymerase and terminal deoxynucleotidyl transferase-mediated uridine 5′-triphosphate-biotin nick end labeling in the injured cortex. Moreover, administration of a CK2-specific pharmacological inhibitor, tetrabromocinnamic acid (TBCA) (Pagano et al., 2007), into the ventricle facilitated neuronal cell death and increased infarct volume (Veh vs TBCA: 17.0% ± 7.24 vs 34.3% ± 12.8, $p < 0.05$) after tFCI by regulating AKT phosphorylation and reactive oxygen species production.

Conclusions: Oxidative stress induced by tFCI causes a reduction in CK2 activity via the loss of catalytic subunits α and α′ and CK2β phosphorylation, and this down-regulation of CK2 activity sensitizes neuronal cells to death after oxidative injury.

References:

Pagano, M. A., et al. (2007). Tetrabromocinnamic acid (TBCA) and related compounds represent a new class of specific protein kinase CK2 inhibitors. Chembiochem 8, 129-139.

Pinna, L. A. (2002). Protein kinase CK2: a challenge to canons. J Cell Sci 115, 3873-3878.

Saito, A., et al. (2003). Overexpression of copper/zinc superoxide dismutase in transgenic mice protects against neuronal cell death after transient focal ischemia by blocking activation of the Bad cell death signaling pathway. J Neurosci 23, 1710-1718.

DETERMINATION OF B_{MAX} AND K_D IN NON-HUMAN PRIMATES USING [^{11}C]GR103545, AN AGONIST PET TRACER FOR THE KAPPA OPIOID RECEPTORS

G. Tomasi[1], N. Nabulsi[1], D. Weinzimmer[1], M.-Q. Zeng[1], L. Blumberg[2], C. Brown-Proctor[2], Y.-S. Ding[1], R.E. Carson[1], Y. Huang[1]

[1]Yale University PET Center, New Haven, [2]Pfizer,Inc., Groton, CT, USA

Objectives: The k-opioid receptors are involved in depression and other mood disorders, as well as in dependency conditions such as obesity, alcoholism, heroin and cocaine abuse, but, despite their importance, they have not been systematically analyzed with PET. We employed a recently developed selective k agonist tracer ([^{11}C]GR103545, [1]), and performed a Scatchard study in rhesus monkeys with multiple tracer infusions to estimate the in vivo receptor concentration B_{max} and the dissociation constant K_d.

Methods: Three rhesus monkeys were employed in the study, performed with the Focus 220: 2 of them underwent 2 scans (baseline+self-block), the third was scanned 4 times (2 baseline and 2 self-block scans at different occupancy levels). The injected mass was 0.042±0.014 μg/Kg for baseline and ranged from 0.17 to 0.3 μg/Kg for the self-block studies. A Bolus+Infusion (B+I) protocol was employed with K_{bol} ranging from 100 to 200 minutes, and the cerebellum was used as reference region. Scan duration was 120 min. BP_{ND} of all ROIs was computed as $[(C_{ROI} / C_{CEREB}) -1]$, C_{ROI} and C_{CEREB} being the mean of the measured radioactivity concentrations from 90 to 120 min in a given ROI and in the cerebellum, respectively. In 4 of the 8 scans, plasma input functions were measured and a 2-tissue model was used to compute the volume of distribution in the cerebellum $V_{T,CEREB,}$ which was used to estimate the free to non-displaceable concentration ratio at equilibrium f_{ND} as $f_P / V_{T,CEREB}$. A standard Scatchard plot was used to estimate B_{max} and $K_{d,ND}=K_d/f_{ND}$. When $K_{d,ND}$ was allowed to vary among ROIs, results were very variable; therefore $K_{d\ ND}$ was constrained to be constant across ROIs.

Results: In all cases, a reasonable equilibrium was achieved from 90 to 120 min. Table 1 reports B_{max} estimates; the global $K_{d,ND}$ was estimated to be 5.83 nM. $K_{d\ ND}$ was alternatively computed for each ROI as (B_{max} / $BP_{ND\ BASEL}$) (fourth row of Table 1), $BP_{ND\ BASEL}$ being the mean across the 4 baseline scans. The mean and median of these estimates were 6.12 nM and 5.78 nM, respectively, in very good agreement with the common global estimate of 5.83 nM. In addition, K_d, computed as $K_{d\ ND}f_{ND}$, was 0.16 nM, in good agreement with the in vitro K_i value of 0.33 nM. Percentage standard errors (%SE) were high (>100%), partly due to large intersubject variability.

ROI	Brain-stem	Cingu-late	Frontal Cortex	Globus palli-dus	Insula	Occipital Cortex	Putamen	Tempo-ral Cortex	Thala-mus
Bmax(nM)	**2.7**	**7.4**	**3.8**	**8.2**	**7.5**	**2.7**	**15.1**	**3.9**	**2.8**
$BP_{ND,BASEL}$	0.3±0.2	1.3±0.3	0.7±0.2	1.3±0.4	1.3±0.2	0.5±0.2	2.2±0.8	0.5±0.1	0.7±0.1

±std dev									
$K_{d,ND}$ (nM) = B_{max}/BP_{ND}	7.6	5.6	5.5	6.4	5.6	5.8	6.9	5.8	5.9

[Results]

Conclusions: Use of a B+I protocol with the k-opioid receptor agonist tracer [^{11}C]GR103545 permitted the successful estimation of B_{max} and $K_{d\ ND}$ in vivo. The estimated value of 5.83 nM for $K_{d\ ND}$ was in good agreement with the in vitro measurement.

Reference: [1] Talbot PS et al.: 11C-GR103545, a radiotracer for imaging kappa-opioid receptors in vivo with PET: synthesis and evaluation in baboons. J Nucl Med (2005) 46(3):484-494.

362

BrainPET Poster Session: Molecular Brain Imaging: Clinical Applications

STUDY OF HUMAN EMOTIONAL PROCESSING USING MOLECULAR IMAGING

R. Badgaiyan[1,2], A. Fischman[2]

[1]Radiology, Massachusetts General Hospital & Harvard Medical School, [2]Shriners' Hospital for Children, Boston, MA, USA

Background and aims: Even though animal studies have implicated dopamine and noradrenaline in the processing of emotional memories, the role of these neurotransmitters in processing of human emotions is unclear. Clinical studies have however suggested that the processing is impaired in degenerative diseases of the basal ganglia. Since dopamine neurotransmission is dysregulated in these diseases, it could be critically involved in the processing. In this experiment, we used a molecular imaging technique to examine whether dopamine is released during processing of emotional memories in healthy volunteers.

Methods: The volunteers were asked to perform an emotional memory task after a dopamine receptor ligand was administered intravenously. Because endogenously released dopamine displaces its ligands from receptor sites, task-induced release of dopamine was detected and mapped by dynamically measuring the concentration of radiolabeled ligands. In this experiment, a specific dopamine receptor ligand ^{18}F-fallypride was used to study dopamine release in the brain. After a single intravenous administration of the ligand, volunteers were asked to perform an emotional memory task under a control and a test condition. The test condition was started 25 min after the ligand. In the control condition, which was started immediately after the ligand administration volunteers were asked to rate the intensity of emotions evoked by emotionally neutral words while in the test condition, they made similar rating for emotional words. The ligand concentration was dynamically measured at each voxel during the experiment, using an ECAT HR+ PET camera.

Results: Behavioral data indicated that emotional words presented in the test condition elicited more intense emotion. Additionally, most of these words retrieved emotional memories. Analysis of the PET data indicated that the rate of displacement of the ligand ^{18}F-fallypride increased significantly in the amygdala, medial temporal lobe and ventral prefrontal cortex. Increased rate of the displacement indicate that endogenous dopamine was released in these areas during processing of emotional memory. Interestingly, the fMRI studies have also implicated the same areas in the processing.

Conclusions: The results indicate that molecular imaging technique is a sensitive method to study neurochemistry of human cognition and that, dopamine mediates human emotional memory processing.

363

Brain Poster Session: Cerebral Metabolic Regulation

NEUROCHEMICAL AND PHARMCOLOGICAL STUDIES IN RAT MODEL OF DIET RESTRICTION-INDUCED ANOREXIA

T. Malik, D. Haleem

Neurochemistry and Biochemical Neuropharmacology Research Laboratory Biochemistry, Karachi University, Karachi, Pakistan

Anorexia nervosa (AN) patients exhibit extreme dieting, body weight loss and hyperactivity. The 5-hydroxytryptamine (5-HT; serotonin) system involved in the regulation of appetite and mood is the major neurotransmitter system of interest in research on AN. Pharmacological studies show that manipulations that tend to increase brain serotonin functions are anorexiogenic. The hypothesis of suppression of appetite through excessive release of 5-HT to receptors is not supported by data on subjects with clinical symptoms of AN as cerebrospinal (CSF) levels of 5-hydroxyindoleacetic acid (5-HIAA), a major metabolite of 5-HT, are reduced in AN patients and returned to normal in recovered patients. Loss of appetite in AN may simply follow self imposed dieting and diet restriction (DR). The hypothalamus is believed to be the site of the brain transducing satiety signals of serotonin. Studies on animal models show that excessive DR decreases 5-HT metabolism and synthesis in the brain and hypothalamus. The present lecture explains mechanism involved in DR-induced decreases of brain 5-HT. Possible role of regional 5-HT change in the elicitation of DR-induced deficits of behavior is discussed. Research on animal models of AN may help in developing strategies for the treatment of AN patients.

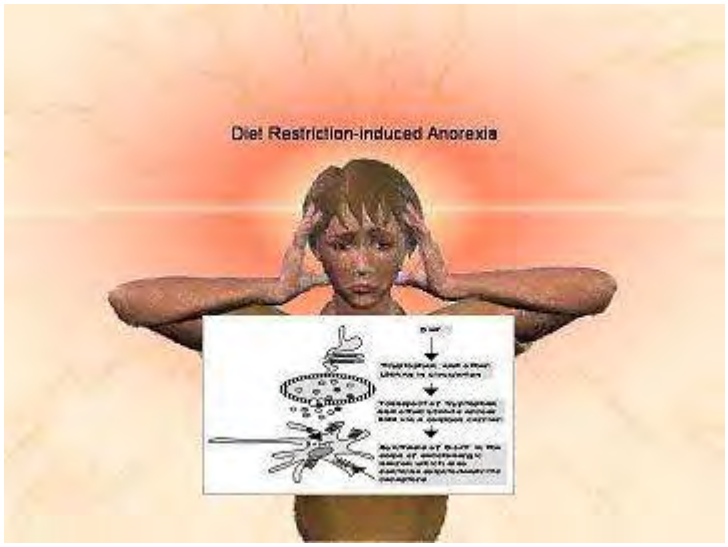

[Diet Restriction-induced Anorexia]

References:

1. D. J. Haleem, and S. Haider, NeuroReport., 7: 1153-1156 (1996).

2. S. Haider, and D. J. Haleem Med Sci Monit , 6: 1061-1067 (2000).

3. D. J. Haleem, Appetite, 52, 44-50 (2009).

Brain Poster Session: Angiogenesis

THE INSIGHT OF REVASCULARIZATION MECHANISM BASED ON ANGIOGENESIS AND ARTERIOGENESIS FROM THE EXPERIMENTAL AND CLINICAL WORKS IN MOYAMOYA DISEASE

H. Imai[1], M. Nakamura[1], C. Kubota[1], S. Puentes[1], A. Faried[1], Y. Yoshimoto[1], N. Saito[2]

[1]Department of Neurosurgery, Gunma University, Maebashi, [2]Department of Neurosurgery, Tokyo University, Tokyo, Japan

Objectives: We focused on unveiling the mechanism of revascularization after indirect bypass surgery, encephalo-myo-synangiosis (EMS) in moyamoya disease, which is progressive occlusive cerebrovascular disease of the internal carotid arteries (ICAs). This treatment is believed to form vascular anastomoses between the extracranial tissue and the brain to maintain blood flow to the ischemic tissue. However, the underlying mechanism is not completely understood. Research has concentrated on both experimental and clinical works for revascularization mechanism in terms of two types of vessel growth, angiogenesis and arteriogeneis.

Methods: Experiments: Fourteen miniature pigs underwent transcranial surgery for EMS after ICA occlusion. Animals were allowed to recover at 1 week (n=4) or 4 weeks (n=7) after EMS. Control group animals were treated in the same way without occlusion (n=3). MR imaging, angiography, and histopathology were performed. Patients: Total 29 hemispheres of 23 patients with moyamoya disease who were performed with angiography after direct or indirect bypass surgery were enrolled for the investigation. The eventual patterns of revascularization were categorized into 4 classes based on the dominancy of donor arteries.

Results: Experiments. One week after EMS, histopathology of both ICA occlusion and control groups showed the transplanted temporal muscle had adhered to the arachnoid via the fibrous coat where a number of newly formed small vessels (angiogenesis) in connective tissue were found. Four weeks after EMS, angiography and histopathology of ICA occlusion group showed the vascular anastomoses grew larger and more robust to construct patent anastomoses (arterogenesis) between the external carotid artery and the cortical arteries. In contrast, histopathology of the control group found cicatrized tissue of the fibrous coat. Patients: In cases of direct anasomosis, there are 4 hemispheres with dominant superficial temporal artery (STA) compared with EMS (STA>EMS), 7 hemispheres with dominant EMS compared with STA (EMS>STA). 5 hemispheres with nearly equal dominancy of both STA and EMS (STA=EMS), and 1 hemisphere without any anastomoses. In cases of indirect anastomosis, There are no hemisphere with (STA>EMS), 5 hemispheres with (EMS>STA), and 7 hemispheres with (STA=EMS).

Conclusions: The experiments disclosed functional revascularization for EMS required 2 distinct processes, angiogenesis and arteriogenesis (1). The angiogenesis is the initial step to generate the new vessels in the newly formed connective tissues, which resembles the process of wound healing associated with repair processes. However, the next step, arteriogenesis required specific and critical condition such as hypoperfusion of the cortex which boosts net forward flow from the donor artery to recipient pial artery due to the pressure gradient between the interconnecting arterial networks. Also clinical results showed EMS provide compensative blood supply via revascularization even in case of direct bypass as well as in indirect bypass surgery. EMS is reasonable surgical treatment for moyamoya disease because flexible revascularization developed adequately according with the requirement of blood supply in the ischemic lesion.

References:

1. M Nakamura, H Imai, K Konno et al. Experimental investigation of encephalo-myo-synangiosis

using gyrencephalic brain of the miniature pig: histopathological evaluation of dynamic reconstruction of vessels for functional anastomosis. J Neurosurg: Pediatrics (in press).

Brain Poster Session: Hemorrhagic Transformation

MRI SURROGATE MEASURES OF BLOOD-BRAIN BARRIER PERMEABILITY FOR THE PREDICTION OF HEMORRHAGIC TRANSFORMATION IN ACUTE ISCHEMIC STROKE

A. Kassner[1,2], S. Chen[2], R. Thornhill[1,2], W. Rammo[2], D. Mikulis[3]

[1]Physiology and Experimental Medicine, Hospital for Sick Children, [2]Medical Imaging, University of Toronto, [3]Medical Imaging, Toronto Western Hospital, Toronto, ON, Canada

Objectives: Therapeutic use of recombinant tissue plasminogen activators (rt-PA) in acute ischemic stroke (AIS) is currently limited to patients presenting ≤4.5h post-ictus, due to the increased risk of hemorrhagic transformation (HT) [1]. It has been shown that permeability MRI followed by tracer-kinetic modelling can be used to predict HT [2]. However, recent work suggests that information relating to blood-brain barrier permeability can be more rapidly extracted from the recirculation-phase of routine ´dynamic susceptibility contrast´ (DSC) MRI images [3-5]. Our purpose was to evaluate four distinct DSC parameters in discriminating between AIS patients who will proceed to HT and those who will not.

Methods: Eighteen AIS patients were examined < 6h post-ictus. All imaging was performed on a 1.5T clinical MRI system (GE Signa LX 12.0, Milwaukee, WI). DSC imaging consisted of a single-shot EPI scan with TR 1725ms, TE 31.5ms, FOV 240mm, matrix size 96×64, flip angle 90°, slice-thickness 5mm, 17 slices, and acquisition time 86s. Gadodiamide was injected as a bolus (Omniscan, GE, USA) at the initiation of DSC. HT was determined by follow-up CT or MRI 24-72h later. Data were analyzed offline. Two regions of interests (ROIs) were defined on diffusion-weighted MRIs, one within the infarct and another within the contralateral hemisphere and then copied to the equivalent DSC images. Mean values were recorded for each of the following four DSC parameters: relative-recirculation (´rR ´) [3], Peak Height [4], %Recovery of the ΔR_2^* v. time curve (%Recovery = 100 x (A-B)/A) [4]), and Slope of the ΔR_2^* v. time curve between 50-60s post-injection [5] (FIG.1). Data were grouped based on follow-up HT-status. For each parameter, differences between ROIs as well as between HT and non-HT patients were assessed using Wilcoxon matched pairs and Mann-Whitney U tests, respectively.

Results: Eight patients proceeded to HT. While the mean rR for infarcts was significantly greater than for contralateral ROIs (0.18±0.02 v. 0.08±0.01, P< 0.001), the converse was true for %Recovery (79±9 v. 91±3%, P< 0.001). The mean infarct rR for HT patients was significantly greater than for non-HT patients (0.22±0.06 v. 0.14±0.06, P< 0.001), while the mean %Recovery in HT patients was significantly lower than in non-HT patients (76±6 v. 82±11%, P< 0.05). No significant differences were detected with respect to Peak Height or Slope.

Conclusions: Both rR and %Recovery can be readily extracted from a standard 90s DSC data-set and each shows potential for delineating HT from non-HT infarcts.

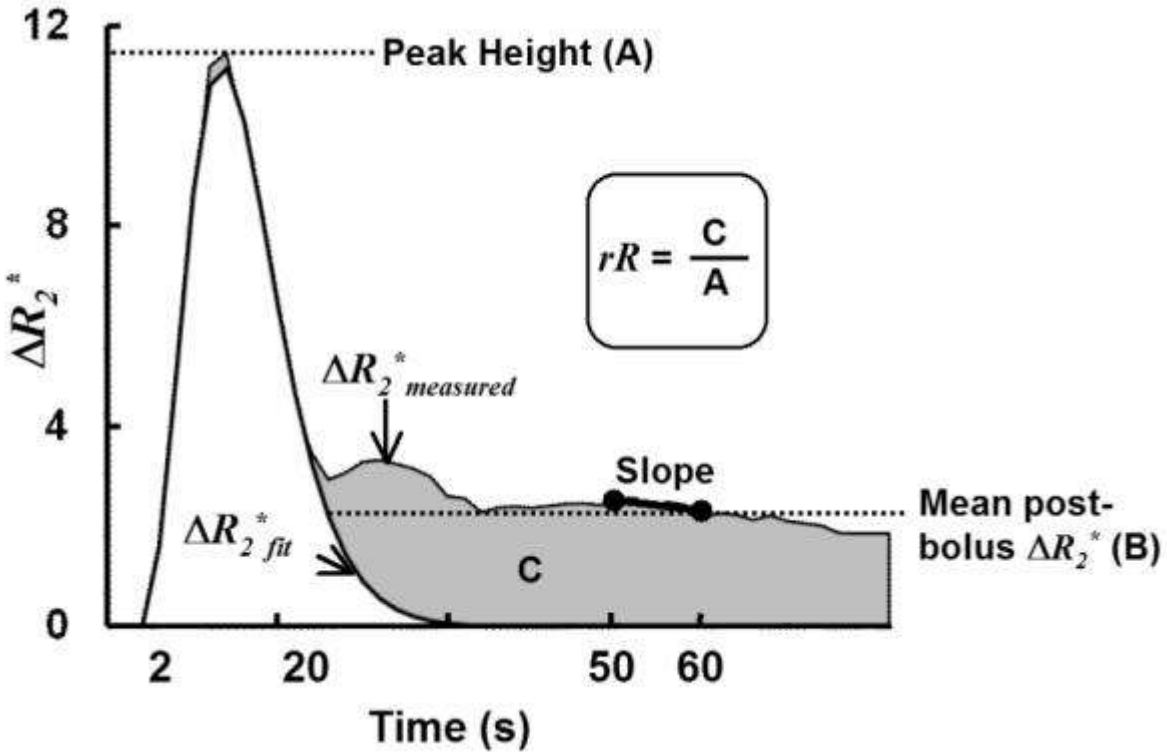

[Fig.1]

References:

[1] Hacke W et al. NEJM 2008;359:1317-1329.

[2] Kassner A. et al. AJNR 2005; 26:2213-2217.

[3] Kassner A. et al. JMRI 2000;103-113.

[4] Lupo JM. et al. AJNR 2005;26:1446-1454.

[5] Bang OY. et al. Ann Neurol 2007; 62:170-176.

Brain Poster Session: Brain Imaging: Neurologic Disease

EVALUATION OF FMRI MARKERS IN MILD COGNITIVE IMPAIRMENT

B. Zhu[1], B. Zhang[1], Y. Xu[2,3], M. Li[1], Z.-Z. Sun[2]

[1]Department of Radiology, [2]Department of Neurology, The Affiliated Drum Tower Hospital of Nanjing University Medical School, [3]Jiangsu Key Laboratory for Molecular Medicine, Nanjing, China

Objectives: To investigate alterations of advanced functional MRI such as proton magnetic resonance spectroscopy (^{1}H MRS) and apparent diffusion coefficient (ADC) value of diffusion weighted imaging (DWI) in mild cognitive impairment (MCI).

Methods: All experiments were conducted with a 1.5-T clinical MR image scanner (Philips Intera Master Medical Systems, Netherlands) with a standard quadrature head coil. MRS and DWI-ADC were administered to 13 patients with AD, 9 patients with MCI, and 13 controls(NINCDS/ADRDA criteria[1, 2]). ^{1}H-MRS were acquired with proton regional imaging of metabolites（PRIME）sequence. EPI sequence of DWI was adopted and b value was set to b_{min} (0 mm^2/s) and b_{max} (1000 mm^2/s). Alterations of NAA/Cr, mI/Cr and ADC value in hippocampus and temporoparietal region among groups were compared.

Results: NAA/Cr, mI/Cr and ADC value in hippocampus among AD, MCI patients and controls were significantly different ($P < 0.05$) (Fig. 1). AT a fixed specificity of 84.6%, the high sensitivity of 100% and 92.9% in differential AD and MCI from controls were concluded by combining the three indicators. The ROC plots illustrated the area under the curve of multi markers was biggest among the all four curves and the sensitivity of multi markers was highest.

Conclusion: New findings in this study were listed as follows:

1. The significant alterations of MRS-NAA, mI as well as DWI-ADC markers were found in MCI patients[1, 3, 4];
2. The changing extent of NAA and mI as well as DWI-ADC markers could be quantified;
3. The multi MRS and DWI markers in combination could improve the diagnostic value of fMRI in distinguishing MCI from the controls[4].

Alterations of NAA/Cr, mI/Cr and ADC in the hippocampus and the temporoparietal regions were helpful to clinical diagnosis in MCI. Furthermore, it had potential in predicting the progression of MCI to AD if we combined above multi indicators.

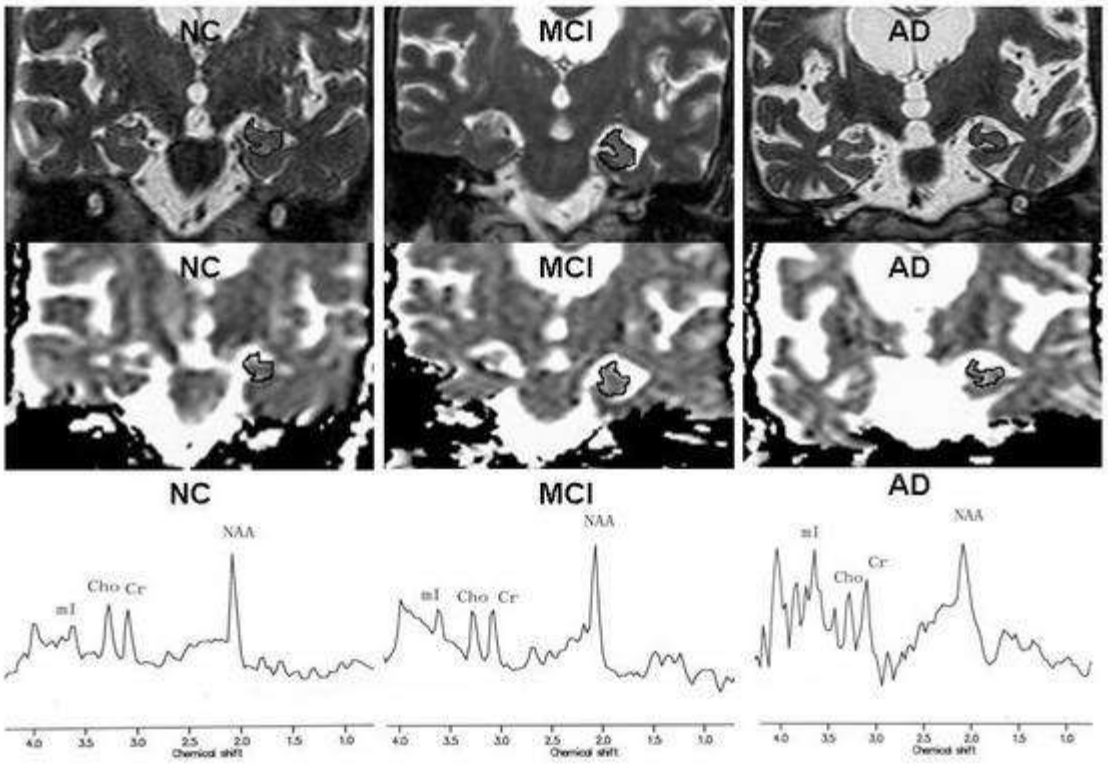

[Figure 1]

Fig. 1 Coronal T2WI and ADC map demonstrate tracings of the hippocampus and parahippocampal gyrus in a 73-year-old female control subject (left) , a 76-year-old female with MCI (middle) and a 71-year-old female with AD (right).

References:

1. Jones, R.S. and A.D. Waldman, 1H-MRS evaluation of metabolism in Alzheimer´s disease and vascular dementia. Neurol Res, 2004. 26(5): p. 488-95.

2. Blennow, K., M.J. de Leon, and H. Zetterberg, Alzheimer´s disease. Lancet, 2006. 368(9533): p. 387-403.

3. Kantarci, K., et al., DWI predicts future progression to Alzheimer disease in amnestic mild cognitive impairment. Neurology, 2005. 64(5): p. 902-4.

4. Kantarci, K., et al., Comparative diagnostic utility of different MR modalities in mild cognitive impairment and Alzheimer´s disease. Dement Geriatr Cogn Disord, 2002. 14(4): p. 198-207.

370

BrainPET Poster Session: Molecular Brain Imaging: Clinical Applications

CEREBRAL OXYGEN DIFFUSIVITY: A POTENTIAL MECHANISM OF UPPER LIMITATION OF OXYGEN EXTRACTION FRACTION IN ISCHEMIC CEREBROVASCULAR DISEASE

E. Shimosegawa, M. Imaizumi, H. Kato, J. Hatazawa

Department of Nuclear Medicine and Tracer Kinetics, Osaka University Graduate School of Medicine, Suita, Japan

Objectives: Cerebral oxygen extraction fraction (OEF) has upper limitation of around 65% even in the severely ischemic brain[1]. In a simplified model for oxygen diffusivity (D_c) from cerebral capillary bed to brain tissue, the OEF is defined as a function of cerebral blood flow (CBF) ($OEF = 1-\exp(-D_c/CBF)$)[2]. The model predicts that OEF would be close to 100% in severe ischemia when D_c is constant or increases with CBF reduction. We speculated that upper limitation of OEF is induced by D_c change in ischemic brain. We, therefore, investigated the relationships among OEF, CBF, cerebral blood volume (CBV), and D_c in patients with chronic ischemic cerebrovascular disease.

Methods: Twenty one patients (male:female=17:4, aged: 40~78 yr, mean age: 66.2±9.0 yr) with the unilateral intra-cranial steno-occlusive lesion and 12 normal volunteers (male:female=6:6, aged: 45~58 yr, mean age: 50.3±3.4 yr) underwent $H_2{}^{15}O$, $C^{15}O$, $^{15}O_2$ PET studies for measuring CBF, CBV, OEF, and cerebral metabolic rate of oxygen ($CMRO_2$). Recently developed high resolution (transverse and axial spatial resolutions of 3.5 and 5.0 mm in FWHM) and large Field-of-View (FOV, 260 mm axially) clinical PET scanner was used[3] (Shimadzu Co, Kyoto). Regions of interest (ROI) were placed on PET images for 23 brain regions in individual subject. Total of 483 and 276 regions were analyzed in patients and normal volunteers, respectively.

Results: In normal volunteers, mean CBF, CBV, OEF, and $CMRO_2$ were 50.5±21.3 ml/100ml/min, 2.76±0.79 ml/100ml, 35.9±5.6 %, 2.99±0.97 ml/100ml/min, respectively. In patients, mean CBF, CBV, OEF, $CMRO_2$ were 37.4±16.4 ml/100ml/min, 3.39±1.35 ml/100ml, 39.1±6.7 %, 2.57±0.77 ml/100ml/min, respectively. When OEF was plotted against CBF, the peak OEF was found to be 54 % at CBF of 20 ml/100ml/min. D_c showed a significant correlation with CBF ($D_c=0.40\times CBF+3.32$, $r=0.910$, $p<0.001$) and with CBV ($D_c=0.11\times CBF^3-2.17\times CBF^2+12.7\times CBF-1.70$, $r=0.368$, $p<0.001$).

Conclusions: The present study demonstrated that D_c is not a constant but variable depending on cerebral circulation. In the present simplified model, D_c is a function of cerebral capillary bed volume (CBV*) ($D_c=kr_{net}\times CBV^*$). Although CBV measured in the present method represented total CBV rather than CBV*, we found a significant correlation between D_c and CBV. Recent experimental study demonstrated that CBV* would passively decrease as CBF decrease[4]. We previously reported that total CBV severely decreased in ischemic core in acute stroke patients[5]. The mechanism responsible for upper limitation of OEF would be a restricted D_c due to capillary blood volume reduction in ischemic brain.

References:

1. Kanno I, et al. J Cereb Blood Flow Metab, 1988;8:227-235.

2. Hyder F, et al. J App Physiol, 1998;85:554-564.

3. Ibaraki M, et al. J Nucl Med, 2008;49:50-59.

4. Peppiatt CM, et al. Nature, 2006;443:700-704.

5. Hatazawa J, et al. Stroke, 1999;30:800-806.

371

Brain Poster Session: Cerebral Metabolic Regulation

ASSESSING THE QUANTIFICATION OF CMR_{O2} FROM BLOOD OXYGEN MEASUREMENTS

A. Vazquez, M. Fukuda, S.-G. Kim

Radiology, University of Pittsburgh, Pittsburgh, PA, USA

Objective: The metabolic rate of oxygen consumption (CMR_{O2}) is a direct index of brain function under resting and neurally active conditions. Although it was initially thought that CMR_{O2} does not change much with neural activity, studies have shown measurable increases with increased function [1-4]. CMR_{O2} is difficult to measure and most methods rely on its calculation from arterio-venous differences in blood oxygenation. Several assumptions are typically made to simplify this calculation:

1. the arterial blood is fully saturated,
2. the transport of oxygen from blood to tissue is rapid enough such that the average tissue oxygen tension is in equilibrium with the capillary oxygen tension, and
3. the changes in CMR_{O2} in mitochondria are rapidly equilibrated with the average tissue oxygen tension.

In this work, these assumptions are investigated.

Methods: For this purpose, the oxygen tension (P_{O2}) in a pre-penetrating arteriole and an emerging venule were measured using two oxygen probes (4μm tip diameter each) over the somato-sensory cortex of isoflurane anesthetized rats (n=6). Optical imaging (620nm light) was performed to map the somato-sensory area responding to electrical forepaw stimulation and target the placement of the probes. The tissue oxygen tension and regional cerebral blood flow (CBF) were also measured using an oxygen probe (30μm tip diameter positioned 300 μm in depth) and a LDF probe (450μm tip diameter), respectively. These measurements were recorded during forepaw stimulation (20s duration, 1.6mA, 1.0ms pulses at 3Hz, every 80s) under two experimental conditions: control and suppressed-CBF (achieved using a vasodilatory agent). Local field potential activity was measured using a metal electrode embedded in the tissue P_{O2} sensor to monitor electrical activity and ensure that there are no significant differences in the activity between experimental conditions.

Results: Under control conditions, stimulation induced a measurable, average increase in arteriolar P_{O2} from 77.9 to 88.4 mmHg, or from 87.6 to 90.9% in oxygen saturation (calculated using the Hill equation). As expected, tissue and venous P_{O2} increases were also observed with evoked stimulation. Under CBF-suppressed conditions, significant decreases in the tissue and venous P_{O2} responses were observed with forepaw stimulation. The time-to-20%-peak and time-to-80%-peak of the average tissue P_{O2} response were 1.4 s and 6.7 s, respectively. In addition, the lag between the venous and tissue P_{O2} responses was measured to range between 1.3 and 2.1 s based on their time-to-20%-peak and time-to-80%-peak.

Conclusions: Collectively, these findings show that a simple arterio-venous difference model may suffer from inaccuracies that depend on the volume encompassing the CMR_{O2} calculation and also on the temporal scale. For example, the CMR_{O2} baseline for these data was calculated to be 7.6 ml/min and stimulation increased CMR_{O2} by 17.5%; if the arterial P_{O2} is assumed to be 100 mmHg, the baseline CMR_{O2} would be 10.7 ml/min with a 13.6% increase with stimulation. In addition, the CMR_{O2} values over transition regions are generally overestimated.

References:

[1] Fox PT, et al., Science 241:462(1988);

[2] Shulman RG, et al., NMRBiomed 14:389(2001);

[3] Davis TL, et al., PNAS 95:1834(1998);

[4] Kim SG, et al., MRM 41:1152(1999).

QBASE: IMAGE DATABASE SYSTEM FOR MULTICENTER CLINICAL STUDIES WITH QSPECT PACKAGE

H. Watabe, T. Hayashi, T. Akamatsu, H. Iida

National Cardiovascular Center Research Institute, Suita, Japan

Objectives: QSPECT package has been developed for standardized calculation of quantitative CBF images using I-123 IMP[1] and is appropriate for multicenter clinical studies. It performs image reconstruction with attenuation and scatter corrections, and compute two CBF images of pre- and post-pharmacological stress from a single session of a SPECT scan in conjunction with twice-administration of I-123 IMP (Dual-Table IMP-ARG technique). It can handle data from several commercial SPECT cameras by obtaining additional calibration data. However, in multicenter studies, not only image calculation but also standardized visualization, analysis, and statistics of images are needed. It is also important to have well-designed and secure database system that can handle multi-modal data such as images, projection data, blood radioactivity, or patient information. We have developed QBASE, image database system for QSPECT package. The goal of QBASE is to develop secure and flexible image database system which includes anonymization, brain normalization for the multicenter clinical studies.

Methods: QBASE is written in Python language (http://www.python.org) and uses Web based user-interface. Access control mechanism is implemented for security. Relational database model is utilized to handle multiple studies, multiple sites and multiple files related to a patient. The data uploaded on the sever are first analyzed to determine file type and study attributes such as image modality, acquisition site, acquisition date, and a patient information. The data uploaded will be automatically anonymized. The CBF images will be able to normalized to a standard brain image using 12 parameters Affine transformation. Then, mean CBF and flow reserve values for whole brain, cerebellum, MCA, PCA, ACA regions[2] are automatically computed. Queries with several conditions are allowed to search the specific studies.

Results: A user uploaded the results of a I-123 IMP study to QBASE server and QBASE automatically determined acquisition conditions such as SPECT camera, collimator, and study duration. PET, MRI, X-ray CT images related to the study was also uploaded to the server. Additional study attributes such as PaCO2, Hct during the study can be attached. File lists belonged to the study was displayed on the web browser and by clicking the image name, the QBASE rendered the image, so the user could view and inspect the images. A table of the automatically determined regional CBF values was displayed and was able to be exported to CSV format data, which can be used further statistical analysis.

Conclusions: QBASE system was developed to support multicenter clinical studies with QSPECT package. The system was secure and flexible, and possible to fit several multicenter trials.

References:

[1] Kim et al. Neuroimage 33(4):1126-35 (2006).

[2] Kretschmann et al. "Cranial Neuroimaging and Clinical Neuroanatomy: Magnetic Resonance Imaging and Computed Tomography" (2003).

COMBINATION TREATMENT WITH ETHYL PYRUVATE AND ASPIRIN ENHANCES NEUROPTOTECTION IN THE POSTISCHEMIC BRAIN

S.-W. Kim[1], J.-H. Shin[1], J.-Y. Jeong[1], Y. Jin[1], I.-D. Kim[1], P.-L. Han[2], J.-K. Lee[1]

[1]Anatomy, Inha University School of Medicine, Inchon, [2]Nano Sciences and Brain Disease Research Institute, Ewha Womans University, Seoul, South Korea

Background and purpose: Ethyl pyruvate, acts as an anti-inflammatory molecule in various pathological conditions, including cerebral ischemia. Aspirin has been reported to confer neuroprotection to the ischemic brain, whose protective effect has been attributed to the anti-platelet action, NMDA- or Zn^{2+}-induced neurotoxicity aspirin also has direct neuroprotective effects, including NF-kB inhibition. In this study, we examined enhanced neuroprotective effects of combination treatment with ethyl pyruvate and aspirin in a rat cerebral ischemia model with middle cerebral artery occlusion (MCAO).

Methods: Male Sprague-Dawley rats were subjected to 1 h of MCAO. Ethyl pyruvate alone or in combination with aspirin was administered at various time points before or after MCAO. The changes in brain infarction, neurological deficits, microglia activation and pro-inflammatory cytokine expression were evaluated. Primary microglial cultures and primary cortical cultures were used to elucidate the underlying molecular mechanism of enhanced neroprotective effect of combination treatment.

Results: Ethyl pyruvate dose-dependently suppressed infarct volume in the post-ischemic brain, wherein intravenous administration of 5 mg/kg ethyl pyruvate 30 min after the occlusion reduced infarct volume to 34.5±15.5% ($n=6$, $p< 0.01$) of that of the untreated control. In combination with aspirin (5 mg/kg. i.v.), the neuroprotective effect was enhanced, resulting in 16.0±5.9% ($n=6$, $p< 0.01$) infarct volume. The time window for synergistic neuroprotection by ethyl pyruvate and aspirin extended to 9 h post-MCAO. The synergistic neuroprotection was accompanied by suppression of motor and other neurological deficits. Inflammatory processes were notably suppressed by the combination treatment in the postischemic brain and primary microglia cultures. wherein ethyl pyruvate and aspirin modulate NF-kB signaling differentially. Similar enhancement in neuroprotective effect and differential modulation of NF-kB signaling pathway was also observed in oxygen-glucose deprivation-treated primary cortical cultures.

Conclusions: Combination treatment of ethyl pyruvate and aspirin affords synergistic neuroprotection in the postischemic brain with a wide therapeutic window, in part via differential modulation of the NF-kB signaling pathway.

MAPPING DOPAMINERGIC DENERVATION IN PARKINSON DISEASE IN VIVO AND IN SITU: THE VISUALIZATION OF STRUCTURAL DETAILS BY CBV-WEIGHTED FMRI

C.-C.V. Chen[1], Y.-Y.I. Shih[1], K.-C. Mo[1], N.-W. Yao[1], Z.-J. Lin[1], C.-H. Huang[1], B.-C. Shyu[2], **C. Chang**[1]

[1]The Functional and Micro-magnetic Resonance Imaging Center, [2]Institute of Biomedical Sciences, Academia Sinica, Taipei, Taiwan R.O.C.

Background and aims: Striatal dopaminergic denervation is an important characteristic of Parkinson disease (PD). The damage is often evaluated by post-mortem immunohistochemistry (IHC), which in situ localizes the dopaminergic innervations in the brain tissues. Nevertheless, post-mortem techniques can not be applied to living organisms. To propose an approach that detects the structural details of dopaminergic denervation of PD in vivo and in situ, the cerebral blood volume (CBV)-weighted fMRI facilitated by the increased relaxivity with iron oxide nanoparticles (IRON) technique was employed. The CBV method is proposed for the following reasons. First, dopamine is a vasoactive neurotransmitter. Second, CBV responses can be a reflection of dopaminergic neurotransmission[1,2]. Since the resolution of the CBV images achieves the level of a pixel size of tens of microns, the CBV-weighted fMRI may be applicable in mapping striatal dopaminergic denervation in vivo and in situ in PD.

Methods: The Parkinsonian rats were lesioned ipsilaterally by infusing 6-OHDA into the right substantia nigra. A paradigm that activates the endogenous dopaminergic neurotransmissionthe, the nociceptive stimulation, was employed to induce the vasoactivity in the striatum so as to be detected by CBV-weighted fMRI[2]. Superparamagnetic iron oxide nanoparticles as a contrast agent were administered via the femoral vein at a dose of 30 mg Fe/kg. fMRI images were then captured using a 4.7-T Bruker Biospec spectrometer. Images were acquired using a FLASH sequence with a repetition time of 150 ms, echo time of 20 ms, field of view of 2.56 by 2.56 cm2, slice thickness of 1.5 mm, number of excitation of 1, acquisition matrix of 128 by 64 (zero-filled to 128 by 128), and temporal resolution of 9.6 s. Images were analyzed using a custom-built ISPMER data processing system.

Results: It was found that the intact striatum retained an integral CBV response whereas the lesioned straitum exhibited no CBV reactions in the denervation sites yet remaining responses in the residual dopaminergic fibers. The results indicate that CBV weighted fMRI detects the dopaminergic fiber lesion in PD with the acuity to differentiate the denervation from the spared innervations.

Conclusions: The preclinical findings strongly support the applicability of the CBV weighted fMRI as an in vivo and in situ mapping tool to evaluate the striatal dopaminergic denervation in PD.

References:

1.Choi JK, Chen YI, Hamel E, Jenkins BG (2006) Brain hemodynamic changes mediated by dopamine receptors: Role of the cerebral microvasculature in dopamine-mediated neurovascular coupling. Neuroimage 30:700-712. 2.Shih Y.Y.I., Chen C.C.V., Shyu B.C., Lin Z.J., Chiang Y.C., Jaw F.S., Chen Y.Y., and Chang C. (accepted) Journal of neuroscience, 2009.

Brain Poster Session: Brain Imaging: Neurologic Disease

EVALUATION OF APPARENT DIFFUSION COEFFICIENT (ADC) MAP BY USING IMAGE ANALYSIS SOFTWARE IN MILD COGNITIVE IMPAIRMENT (MCI)

B. Zhang[1], Y. Xu[2,3], B. Zhu[1], W.-H. Guo[4], J.-G. Zhang[4]

[1]Department of Radiology, [2]Department of Neurology, The Affiliated Drum Tower Hospital of Nanjing University Medical School, [3]Jiangsu Key Laboratory for Molecular Medicine, [4]Department of PET, The Affiliated Drum Tower Hospital of Nanjing University Medical School, Nanjing, China

Objectives: Measures of ADC can quantify the alterations in water diffusivity resulting from microscopic brain structural changes [1] in MCI and Alzheimer's disease (AD) patients. In this study, we investigated alterations on ADC values in MCI and AD patients and analyzed ADC maps by using Statistical Parametric Mapping (SPM). Furthermore we try to verify the accuracy of Brain Search (BS) software for ADC maps, designed by authors of this article, based on brain functional area automatic extraction method.

Methods: Scans were made on a 1.5-T clinical MRI scanner (Philips Intera Master Medical Systems, Netherlands) with a standard quadrature head coil. Conventional MRI and diffusion weighted imaging (DWI)-ADC was administered to 13 patients with AD, 9 with MCI, and 13 normal controls (NC) (NINCDS/ADRDA criteria[2]). The b values in DWI sequence were set at 0 mm2/s and 1000 mm2/s. The independent ADC map was analyzed by using BS and SPM, respectively. The significantly different functional brain areas among groups were recognized automatically as colorized coded areas by the software.

Results: ADC value in hippocampus among groups was significantly different ($P < 0.05$). The number of areas shown on the maps analyzed by using SPM was more than that identified by using BS. However, bigger areas and brightener color were found on the maps analyzed by using BS rather than by using SPM (Fig. 1). ADC values in the left limbic system were found significantly different among all groups when using both BS and SPM. Besides the left limbic system, other brain areas mapped are: the right Rectal Gyrus etc. between NC and MCI group; the right frontal lobe etc. between MCI and AD group; the right Inferior Frontal Gyrus etc. between NC and AD group.

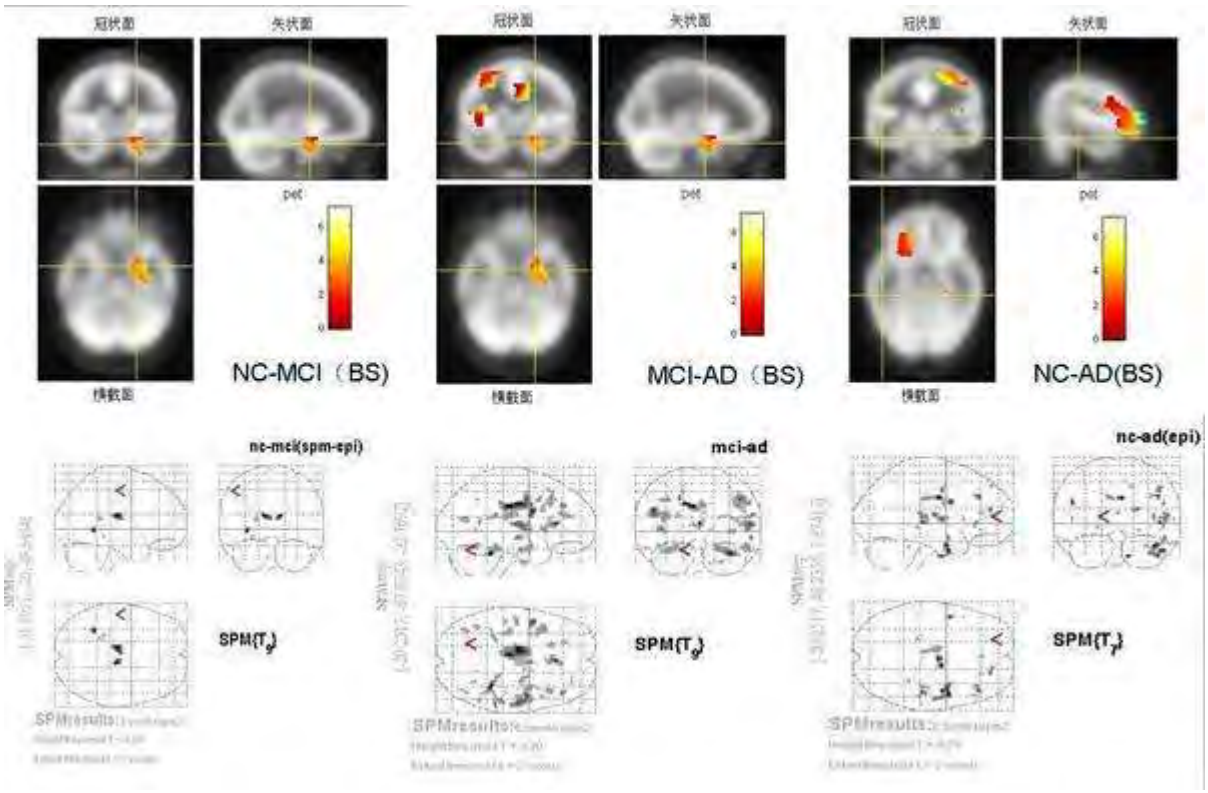

[Figure 1]

Fig. 1 Significantly different brain areas among AD, MCI patients and NC were shown, which were analyzed by BS (upper) and by SPM (lower), respectively.

Conclusion:

1. Alterations of ADC in the hippocampus are helpful to clinical diagnosis in MCI[1, 3].
2. Significantly different brain areas of ADC value are only located in the left limbic system, not in the right. And ADC values in the left limbic system and the right frontal lobe are significantly different among groups, which might be initial involvement in MCI[4].
3. Significantly different areas of ADC value, shown in an intuitive way, analyzed by using BS are helpful to find more obvious areas than SPM. We hope these new insights will take the analytic mapping of ADC value into diagnostic assessment in MCI and AD.

References:

1. Kantarci, K., et al., DWI predicts future progression to Alzheimer disease in amnestic mild cognitive impairment. Neurology, 2005. 64(5): p. 902-4.

2. Blennow, K., M.J. de Leon, and H. Zetterberg, Alzheimer´s disease. Lancet, 2006. 368(9533): p. 387-403.

3. Ackl, N., et al., Hippocampal metabolic abnormalities in mild cognitive impairment and Alzheimer´s disease. Neuroscience Letters. 384(1-2): p. 23-28.

4. Wang, L., et al., Changes in hippocampal connectivity in the early stages of Alzheimer´s disease: evidence from resting state fMRI. Neuroimage, 2006. 31(2): p. 496-504.

Brain Poster Session: Neurogenesis

NEUROGENESIS OF MOTOR NEURONS IN THE SPINAL CORD AFTER TRANSIENT ISCHEMIA

G. Takahashi[1], M. Sakurai[2], K. Tabayashi[1]

[1]Cardiovascular Surgery, Tohoku University Graduate School of Medicine, [2]Cardiovascular Surgery, Sendai Medical Center, Sendai, Japan

Objectives: Spinal cord injury after a successful operation on the thoracic aorta is a disastrous and unpredictable complication in humane beings. In an attempt to prevent this complication, various methods of spinal cord protection have been suggested, Because motor neurons in spinal cords have been thought not to replace after cell deaths. It has already shown that self-renewing stem cells do exist in discrete brain regions, including the dentate gyrus(DG) of the hippocampus and subependymal layer close to the subventricular zone (SVZ) of lateral ventricles. Recent studies have shown that adult neurogenesis is increased by an exogeneous neurotrophic factor supplement, seizures kindling an enriched environment and transient global ischemia, and is decreased by stress, excitatory amino acids, and adrenal steroids. On the other hand, motor neurons in anterior horns of spinal cord after transient ischemia has been thought to die with apoptotic change[1], and do not replaced after cell death. In the spinal cord, neurogenesis cannot be observed under physiologic condition. However, a different situation occurs after pathological spinal cord injury[2].

Because ischemic stroke often causes loss of the neural functions because of neural cell death, neurogenesis after ischemia should be important for compensation for and recovery of those functions. The stage of neurogenesis in the DG can be divided into three steps; 1 proliferation, 2 migration, 3 differantiation[3].

In the present study, we evaluate the three steps of neurogenesis in spinal cord after transient ischemia.

Materials and methods: Male domesticated white rabbits (Japan) were subjected to reproducible models for spinal cord ischemia. To evaluate the three steps of neurogenesis after ischemia, we used bromodeoxiuridine (BrdU), highly polysialylated neural cell adhesion molecule (PSA-NCAM), and neural molecular antigen (NeuN), and glial fibrillary acidic protein (GFAP), as markers for proliferation, migration, and differentiation, respectively.

Results: BrdU-labelled cells and PSA-NCAM-positive cells increased in the anterior horns of spinal cord at four days after ischemia. BrdU-labelled cells with PSA-NCAM expression were first detected in the spinal cord after 4 days of transient ischemia. A few of PSA-NCAM labeled cells with NeuN was detected after 7 days, however no PSA-NCAM-labelled with GFAP was detected.

Conclusions: Our results indicate that ischemic stress could stimulate the ability of neurogenesis even in spinal cord. Our findings will be important in developing therapeutic intervention to enhance endogenious neurogenesis after spinal cord ischemia.

References:

1. Sakurai M, F.N., Takizawa S, Abe K, Hayashi T, Shinohara Y, Nakazawa H, Tabayashi K, Induction of 3-L-nitrotyrosine in motor neurons after transient spinal cord ischemia in rabbits. J Cereb Blood Flow Metab., 1998. 18(11)1233-83.

2. Mikami Y, O.H., Sakaguchi M, Nakamura M, Shimazaki T, Okano HJ, Kawakami Y, Toyama Y, Toda M., Implantation of dendritic cells in injured adult spinal cord results in activation of

endogenous neural stem/progenitor cells leading to de novo neurogenesis and functional recovery. J Neurosci Res.,2004. 15(76)4: 453-65.

3. Sakurai M., Selective motor neuron death and heat shock protein induction after spinal cord ischemia in rabbits. J Thorac Cardiovasc Surg, 1997. 113(1): 159-64.

Brain Poster Session: Cerebral Vascular Regulation

LONG-TERM PROGNOSIS OF UNILATERAL CEREBROVASCULAR DISEASE WITH REDUCED ARTERIAL VASOREACTIVITY

M. Isozaki[1], Y. Arai[1], T. Kudo[2], M. Kobayashi[2], Y. Handa[1], T. Kubota[1], H. Okazawa[2]

[1]Department of Neurosurgery, [2]Biomedical Imaging Research Center, University of Fukui, Eiheiji-cho, Japan

Objectives: Impaired cerebral hemodynamics like misery perfusion is a high risk factor of subsequent ischemic stroke. The acetazolamide (ACZ) challenge test, which assesses cerebral vasoreactivity (CVR), has been reported to be useful to evaluate cerebral perfusion reserve and to predict the risk of cerebral hemodynamic impairment in patients with major cerebral arterial steno-occlusive disease. There are two types of CVR reduction, with or without decrease in baseline cerebral blood flow (CBF), and the former is considered overlapping significantly with a condition of miserly perfusion. The purpose of this study was to investigate the long-term prognosis of patients with preserved baseline CBF and reduced CVR measured with PET.

Methods: Twenty-nine patients with symptomatic unilateral major cerebral arterial occlusion or severe stenosis (>70%) in the internal carotid or middle cerebral arteries were involved in this study. They suffered from ipsilateral ischemic events, including transient ischemic attack (TIA) and minor complete stroke (modified Rankin scale 1 or 2). All patients underwent O-15 gas and water PET scans to measure CBF, oxygen extraction fraction (OEF), cerebral metabolic rate for oxygen ($CMRO_2$) and blood volume (CBV). All patients were followed at least 12 months and were medically treated for infarction and for underlying diseases such as hypertension, diabetes mellitus, and hyper-lipidemia during follow-up periods. The primary endpoint was stroke recurrence or death because of any diseases.

Results: Based on CVR values, 29 patients studied were divided into two groups of reduced CVR (N=16, 64±7y) and normal CVR (N=13, 57±9y). CVR values were 2.62±9.56 % in reduced CVR group and 25.2±11.4 % in normal CVR group. None of them showed significant decrease in baseline CBF in the ipsilateral hemisphere. There were no significant differences in CBF, CBV, OEF, $CMRO_2$ between the groups. Patients with normal CVR were followed up for 38.9±9.3 months and those with reduced CVR were followed up for 37.5±20.5 months. There were no significant incidences of TIA, minor stroke and death during the follow-up periods. One patient with normal CVR was dead because of a heart disease at 14 months after his PET study. Kaplan-Meier analysis and Mantel-Cox log-rank statistics showed that the incidence of ipsilateral stroke or death during follow-up periods was not significantly different between the two groups.

Conclusion: Patients with CVR reduction without decrease in baseline CBF showed no ischemic events during the follow-up period in this study, indicating these patients can be treated by medication for cerebral circulation and baseline diseases. The present long-term prognosis study showed the low risk of patients with sufficient cerebral perfusion at baseline condition even though they had a poor CVR in the affected territory.

References:

[1] Kuroda S, et al. Stroke 2001; 32: 2110-2116.

[2] Ogasawara K, et al. J Cereb Blood Flow Metab 2002; 22: 1142-1148.

[3] Okazawa H, et al. Eur J Nucl Med Mol Imaging 2007; 34: 121-129.

Brain Poster Session: Cerebral Vascular Regulation

AUTOREGULATION OF CEREBRAL BLOOD FLOW TO CHANGES IN ARTERIAL PRESSURE IN MILD ALZHEIMER´S DISEASE

A. Zazulia[1], **T. Videen**[1], J. Morris[1], W. Powers[2]

[1]Neurology, Washington University School of Medicine, St. Louis, MO, [2]Neurology, University of North Carolina, Chapel Hill, NC, USA

Background: Recent studies in transgenic mice overexpressing the amyloid precursor protein indicate that impaired autoregulation of cerebral blood flow (CBF) to changes in arterial pressure may be of critical importance in the development of pathological Alzheimer's disease (AD). Given the practical relevance of such a finding in guiding treatment of hypertension in the elderly, we designed this study to determine whether autoregulation is impaired in patients with AD.

Methods: Nineteen subjects aged 74±6 years with very mild (Clinical Dementia Rating [CDR] 0.5, n=15) or mild (CDR 1, n=4) AD, 74% of whom had treated mild-to-moderate hypertension, underwent ^{15}O-PET CBF measurements before and after mean arterial pressure (MAP) was lowered from 108±13 to 93±10 mm Hg with intravenous nicardipine infusion, PET imaging with the benzothiazole amyloid-imaging agent ^{11}C-PIB, and magnetic resonance imaging. Each subject's CBF and ^{11}C-PIB PET images were aligned, co-registered to a standard mean CBF image in Talairach atlas space, and masked to exclude non-cerebral structures. Bilateral hemispheric (global) CBF measurements were made using a mask in Talairach space restricted to brain between Z=+50 and Z=-10. CBF measurements were also obtained in regions of increased ^{11}C-PIB uptake (> 1.7 times uptake in cerebellar gray matter), in 0.56 cc spheres (10 mm diameter) in the anterior and posterior cortical borderzone regions of the middle cerebral artery territory, and in 3-20 cc regions of T2-weighted imaging defined leukoaraiosis.

Results: There was no significant difference in mean CBF before and after MAP reduction in the bilateral hemispheres (44.7±9.9 vs. 43.1±8.9 ml×100g^{-1}×min^{-1}, p=0.22), regions of increased ^{11}C-PIB uptake (48.6±14.3 vs. 45.8±12.6 ml×100g^{-1}×min^{-1}, p=0.09), cortical borderzones (42.8±11.0 vs. 40.8±9.5 ml×100g^{-1}×min^{-1}, p=0.11), and regions of leukoaraiosis (20.9±7.2 vs. 20.6±7.0 ml×100g^{-1}×min^{-1}, p=0.86). Differences in CBF among the four analyses are likely due to differences in the fraction of gray matter in the regions-of-interest.

Conclusions: The lack of significant change in CBF in bilateral hemispheres, cortical borderzones, or regions of high ^{11}C-PIB uptake or leukoaraiosis with a 10-15 mm Hg reduction in MAP suggests that there is neither a generalized nor local defect of autoregulation in AD.

381

Brain Poster Session: Neurogenesis

CHANGES IN CELL DEATH, GLIOSIS AND CELL PROLIFERATION/DIFFERENTIATION IN THE AMYGDALA FOLLOWING MYOCARDIAL INFARCTION

S.S. Yi[1], I.K. Hwang[1], K.-Y. Yoo[2], T.H. Han[3], C.H. Lee[2], S.Y. Lee[3], P.D. Ryu[3], M.-H. Won[2], Y.S. Yoon[1]

[1]Dept. of Anatomy and Cell Biology, College of Veterinary Medicine, Seoul National University, Seoul, [2]Dept. of Anatomy and Neurobiology, College of Medicine, Hallym University, Chuncheon, [3]Lab. of Veterinary Pharmacology, College of Veterinary Medicine, Seoul National University, Seoul, South Korea

Background and aims: Myocardial infarction (MI), also known as a heart attack, occurs when the blood supply to the heart is interrupted and finally this cause damage to myocardium. Recent studies showed that depression is frequently observed following MI, suggesting a link between heart disease and brain function. It has been reported that the neuronal death are occurred in the amygdala 72 h after 40 min coronary artery occlusion. The amygdala is a central component of the limbic system and plays a crucial role in behavioral responses to emotional stress.in recent study, new neurons are produced in the amygdala, piriform cortex, and adjoining inferior temporal cortex in adult primates. Although some researchers have demonstrated the neuronal death in the amygdala after MI, no studies have been reported on cell proliferation/differentiation and gliosis in the amygdala after MI in rats.

Methods: Induction of MI, Cresyl violet staining, Fluoro-Jade B (F-J B) histofluorescence staining and Immunohistochemistry for GFAP, Iba-1, Ki67 and DCX.

Purpose: In this study, we examined cell proliferation and neuroblast differentiation in the amygdala and morphological changes in astrocytes and microglia 2 weeks after MI, when behavioral signs compatible with depression are detected after cardiovascular events.

Results: In MI-operated group, cresyl violet positive neurons had condensed cytoplasm and Fluoro-Jade B-positive cells were detected. The cytoplasm of glial fibrillary acidic protein (GFAP) immunoreactive astrocytes and ionized calcium-binding adapter molecule 1 (Iba-1) immunoreactive microglia were hypertrophied and the processes in astrocytes and microglia were highly ramified and retracted in the amygdala. The number of Ki67 positive cells was significantly increased by 815% in MI-operated group compared to that in the sham-operated group. In addition, DCX immunoreactive neuroblast were abundant in the amygdala of MI-operated group.

Conclusions: The neuronal death, reactive gliosis and cell proliferation is promiment 2 weeks after MI. However, the neuronal differentiation is not detected this region. These results suggest that MI induce neuronal damage, reactive gliosis and proliferation of glia and neurons.

References:

1) Doetsch, F., García-Verdugo J.M., Alvarez-Buylla, A. J. Neurosci. 17 (1997), 5046-5061.

2) Frasure-Smith, N., Lespérance, F., Talajic, M. JAMA 270 (1993) 1819-1825.

3) Schmued LC, Hopkins KJ. Brain Res. 874 (2000) 123-130.

Brain Poster Session: Cerebral Vascular Regulation

SPATIAL VARIATION ANALYSIS OF THE PLASMA AND RED BLOOD CELL FLOW IN RAT SOMATOSENSORY CORTEX

H. Kawaguchi[1], K. Masamoto[1,2], T. Obata[1], I. Kanno[1]

[1]National Institute of Radiological Sciences, Chiba, [2]The University of Electro-Communications, Tokyo, Japan

Objectives: Spatiotemporal variations in the flow of fluorescently labeled plasma and red blood cells (RBCs) were characterized by calculating the locally-controlled arterio-venous transit times in the somatosensory cortex of rats from image acquired with confocal microscopy.

Methods: Sprague-Dawley rats (6-8w) were anesthetized with isoflurane (5% for induction and 1.3-1.5% for experiments), and an area (3x3mm^2) on the left parietal bone over the somatosensory cortex was removed to allow access to brain surface. The respiration rate was maintained at 0.87Hz with mechanical ventilation. For visualization of the cortical flow, a cocktail (0.02ml) of Qdot-605 (1μM used as a plasma marker) and FITC-labeled RBCs was injected into the external carotid artery at a rate of 2.23ml/min. The images of RBC and plasma flow were simultaneously obtained through a band-pass filter (500-590nm and 595-615nm, respectively) with confocal microscopy at an excitation of 488 nm. The frame rate was 14.2fps (interval of 70.4ms), the total measurement time 18 s (256 frames), and image size 512x512 pixels (FOV: 1.82x1.82mm^2). Average and standard deviation of the baseline intensity before arrival of the fluorescent markers was calculated several dozen frames from the start point of the measurements. The appearance time of the fluorescent markers was then measured by determining the earliest time point at which the intensity was greater than the average plus 2 SD on a pixel-to-pixel basis. To ensure no intensity overlap from neighboring pixels, spatial filtering was not used.

Results: Figure 1 shows a pixel-by-pixel map of the appearance time for the RBCs (a) and plasma marker (b). The pixel counts corresponding to vessels in the RBC map were 70-80% of that of the plasma map. The difference may be due to the rheological properties of RBCs and/or fluorescent wavelength-dependent differences in the optical properties of tissue, dyes, or detectors. The diameter of the detected vessels was observed to be greater in the plasma map than in the RBC map (1-2 pixels: 3.5-7.0μm), which agrees well with a previous report[1]. Veins of relatively large size (≥50mm) demonstrated a laminar flow, as seen by the spatial pattern of flow distribution in the upstream veins. A small difference in the appearance time between the plasma and the RBCs was observed for the arteries (-2 to 3 frames). In contrast, the veins had a longer appearance time for the plasma marker[O1] in comparison to that of the RBCs (-2 to 9 frames). The difference varied spatially across the venous network.

Conclusions: The spatial variation of plasma and RBC flows were successfully measured in this study. The present method can be used for the study of CBF regulation under various physiological conditions and local activations.

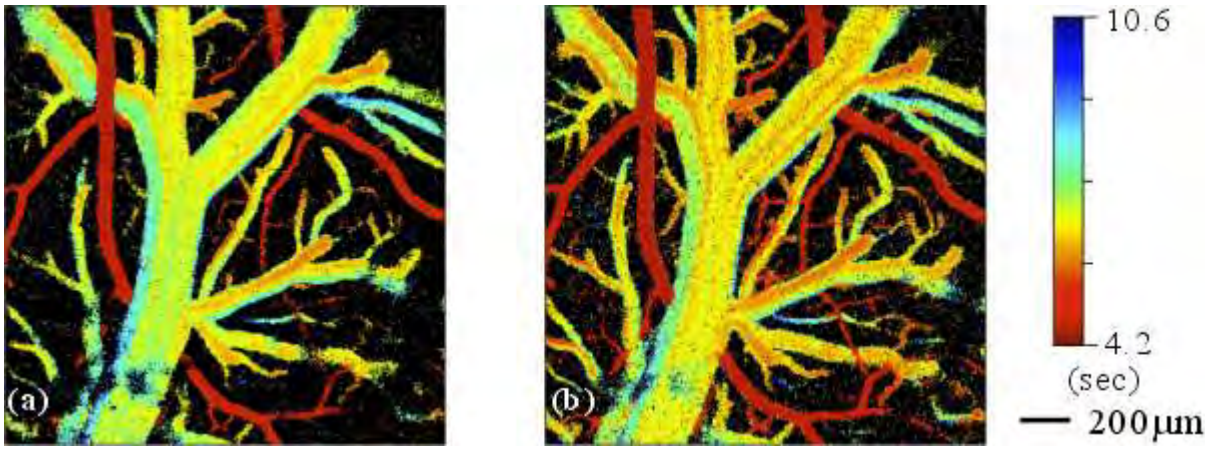

[Images of the appearance time of markers]

Reference:

[1] C. M. Rovainen et al, JCBFM, 13, pp.351-371, (1993).

CORRELATION BETWEEN INTRAINDIVIDUAL SEROTONIN TRANSPORTER AND SEROTONIN 1A RECEPTOR IN NORMAL MALE SUBJECTS: A POSITRON EMISSION TOMOGRAPHY STUDY

H. Takano, H. Ito, H. Takahashi, R. Arakawa, M. Miyoshi, F. Kodaka, T. Otsuka, T. Suhara

Clinical Neuroimaging Team, Molecular Neuroimaging Group, National Institute of Radiological Sciences, Chiba, Japan

Background and aims: The central serotonergic (5-HT) system is closely involved in regulating various mental functions associated with mood, anxiety, impulsive behavior etc. To date, several reports have addressed the comparison between pre- and postsynaptic functions of 5-HT (1, 2); however, these studies are limited in their applicability because of their small sample size. The aim of this study was to investigate the intraindividual relationship between 5-HTT and 5-HT_{1A} receptors using PET in a relatively large group of normal male subjects.

Methods: Dynamic PET scans were performed on 23 young, healthy males with both [C-11]DASB and [C-11]WAY-100635 to measure the binding of 5-HTT and 5-HT_{1A} receptors, respectively. A 2-parameter multilinear reference tissue model and a reference tissue model were used to calculate the binding potential (BP_{ND}) of [C-11]DASB and [C-11]WAY-100635, respectively, on a voxel-by-voxel basis, with the cerebellum as the reference region. All PET images were anatomically standardized to the template magnetic resonance image and smoothed with an 8-mm Gaussian filter using SPM2. Furthermore, the volumes-of-interest (VOIs), namely, the raphe nucleus, thalamus, striatum, parahippocampal gyrus, insula, temporal cortex, base of the frontal cortex, and the convexity of the frontal cortex were manually traced on the standardized and smoothed BP_{ND} images. Pearson's coefficient correlation was used to compare the bindings of both the tracers in the same VOIs; corrections for multiple comparisons among VOIs were not performed.

Results: The BP_{ND} values of each VOI are presented in Table (mean ± SD).

	DASB	WAY
Raphe Nuclei	2.46 ± 0.53	1.48 ± 0.46
Thalamus	1.67 ± 0.28	0.68 ± 0.28
Striatum	1.46 ± 0.17	1.38 ± 0.49
Parahippocampus	0.89 ± 0.16	5.13 ± 0.98
Insula	0.89 ± 0.09	5.26 ± 0.97
Anterior Cingulate	0.48 ± 0.09	4.1 ± 0.63
Temporal	0.25 ± 0.05	4.24 ± 0.79

Frontal base	0.26 ± 0.03	3.33 ± 0.64
Frontal convexity	0.24 ± 0.05	3.29 ± 0.58

[Table]

Pearson's correlation coefficient indicated significant inverse correlations between BP_{ND} of [C-11]DASB and that of [C-11]WAY-100635 in the insula ($r = -0.46$, $p = 0.028$), base side of the frontal cortex ($r = -0.47$, $p = 0.023$), and the convex side of the frontal cortex ($r = -0.46$, $p = 0.029$). No significant correlation was observed in other regions.

Conclusions: The distribution of 5-HTT and 5-HT_{1A} receptors in the brain was consistent with the findings of post-mortem studies. In addition, we found inverse correlations between BP_{ND} values of 5-HTT and 5-HT_{1A} in the insula and frontal cortex. These relationships might indicate a complementary nature between 5-HTT and 5-HT_{1A} functions in such regions. Further investigations are required to elucidate the relationship between the activity of the pre- and postsynaptic serotonergic system in relation to mental functions.

Reference:

1) Lundberg et al. Psychopharmacology, 195, 425-433, 2007.

2) Frey et al. Neuroimage, 42, 850-857, 2008.

385

Brain Poster Session: Neuroprotection

NEUROPROTECTIVE EFFECTS OF INDOLE-3-PROPIONIC ACID VIA REDUCING OXIDATIVE STRESS IN THE ISCHEMIC HIPPOCAMPUS

I.K. Hwang[1], S.S. Yi[1], K.-Y. Yoo[2], J.H. Choi[2], I.S. Lee[1], Y.S. Yoon[1], M.-H. Won[2]

[1]Dept. of Anatomy and Cell Biology, College of Veterinary Medicine, Seoul National University, Seoul, [2]Dept. of Anatomy and Neurobiology, College of Medicine, Hallym University, Chuncheon, South Korea

Background and aims: One of acceptable hypotheses is that cellular events involving reactive oxygen species (ROS) mediated oxidative damage may evoke neuronal damage. In normal condition, the ROS produced as by-products of mitochondrial electron transport chain are quenched by antioxidants and converted to non-toxic compounds by free radical scavenging enzymes. However, in aging and related neurodegenerative diseases, the accumulation of free radicals in tissues is found and can result in cell dysfunction and death. Since oxidative stress is frequently associated with mitochondrial dysfunction, antioxidants are able to penetrate intracellular compartments and ensure protection close to the ROS production site should exhibit a higher bioavailability than those remaining in the extracellular compartment or cytoplasmic membrane.Tryptophan-derived indole compounds have been widely investigated as antioxidants and as free radical scavengers. In these compounds, indole-3-propionic acid (IPA) is a deamination product of tryptophan and possesses a heterocyclic aromatic ring structure such as melatonin. It has been reported that IPA is equivalent to melatonin in scavenging free radicals and protecting against oxidative damage.

Methods: We used the progeny of male Monglian Gerbils (6 months of age). IPA (10mg/kg) treatment for 15 days before transient ischemia. After induction of transient forebrain ishcemia, we performed the the following activity to elucidate the protective effects of IPA; Spontaneous motor activity, Cresyl violet staining, Fluoro-Jade B (F-J B) histofluorescence staining, Immunohistochemistry for NeuN, GFAP, S-100, vimentin, Iba-1, Isolectin B4, HNE and 8-OhdG and Western blot for GFAP and Iba-1.

Purpose: There is no report on the effects of IPA against ischemic damage in vivo. In this study, therefore, we examined neuroprotective effects of IPA and its anti-oxidative effects in the hippocampus after 5 min of transient forebrain ischemia in gerbils.

Results: We investigated the neuroprotective effects of IPA against ischemic damage and anti-oxidative effects in the hippocampal CA1 region after 5 min of transient forebrain ischemia. The repeated oral administration of IPA (10 mg/kg) for 15 days before ischemic surgery protected neurons from the ischemic damage. In this group, the number of cresyl violet positive neurons in the CA1 was 56.8% compared to that in the sham group. In the vehicle-treated group, glial fibrillary acidic protein (GFAP)-, S-100- and vimentin-immunoreactive astrocytes, and Iba-1 and isolectin B4 (IB4)-immunoreactive microglia were activated 4 days after ischemia/reperfusion, whereas in the IPA-treated ischemic group, GFAP, S-100, Iba-1 and IB4 immunoreactivity was distinctly lower, but not in vimentin immunoreactivity, than those in the vehicle-treated ischemic groups. The administration of IPA significantly decreased 4-HNE, a marker for lipid peroxidation, levels in ischemic hippocampal homogenates compared to that in the vehicle-treated ischemic groups at various time points after ischemia/reperfusion. In addition, in the IPA-treated ischemic groups, DNA damage, using immunostaining for 8-hydroxy-2'-deoxyguanosine, in pyramidal neurons in the ischemic CA1 was significantly lower than that in the vehicle-treated ischemic groups.

Conclusions: IPA protects neurons from ischemic insult with deceases of lipid peroxidation and DNA damage in the ischemic hippocampal CA1 pyramidal neurons.

References:

1) Carney JM. 1986.Neurosci Lett 66: 127-130.

2) Bazan NG. 2005. Mol Neurobiol 32: 89-103.

387

Brain Poster Session: Neuroprotection

PRECONDITIONING OR POSTCONDITIONING WITH SEVOFLURANE CAN INDUCE NEUROPROTECTION AGAINST FOCAL CEREBRAL ISCHEMIA IN RATS

H. Wang[1], S. Lu[2], Q. Yu[1], H. Gao[2], W. Liang[1], J. Chen[2,3], **Y. Gao**[2]

[1]Dept of Anesthesiology, Huashan Hospital, Fudan University, [2]State Key Laboratory of Medical Neurobiology, Fudan University, Shanghai, China, [3]Department of Neurology, University of Pittsburgh School of Medicine, Pittsburgh, PA, USA

Background and purpose: The phenomenon of ischemic tolerance in the heart was first reported by Murry et al. in 1986,and that of ischemic preconditioning (PC) in the brain was reported by Kitagawa et al. four years later. Since then, studies on the mechanism and pharmacological agents to mimic ischemic preconditioning have been intense. Zhao et al. elucidated firstly that ischemic postconditioning could improve the outcomes of cardio ischemia/reperfusion insult in 2003. Recent data demonstrate that the PC effect of sevoflurane (Sevo), a comprehensively used volatile anesthetics clinically, is valid in vitro. It's unknown that the impact of Sevo pretreatment or post-administration in vivo and the precise mechanism. In this study, we preconditioned or postconditioned with Sevo to investigate the neuroprotective effect of Sevo against ischemic neuronal injury.

Methods: Male Sprague-Dawley rats were allocated to sham, vehicle, Sevo PC, Sevo postconditoning groups (n = 8-10/group). In the PC groups, the Sevo 1 and Sevo 2 groups received 0.5 or 1 minimum alveolar concentration (MAC) Sevo PC in air 30min/d after 15min equilibrium for 4 consecutive days, whereas postconditioning animals inhaled 1MAC Sevo in air once for 30min at 10min, 30min or 2h after reperfusion. Animals were subjected to focal ischemia for 60min by filament occlusion of the middle cerebral artery with the monitor of regional cerebral blood flow at 24h after Sevo pretreatment or before Sevo post-intervention. Rectal temperature was servo-controlled at 37 -38°C and physiological parameters were detected and maintained according to baseline status throughout the experiment. Neurologic assessment was performed 3 days after ischemia. The volume of cerebral infarction were determined by image analysis of cresyl voilet-stained coronal brain sections. Animals were euthanized at 0, 6, 12 and 24 h after reperfusion for detecting caspase3, caspase9 and apoptosis inducing factor (AIF) by immunofluorescence and Western blotting tests.

Results: Infarction volume was less in the Sevo 1and Sevo 2 groups (13.6±13.3% and 13.9±5.7 respectively, mean ± SD) than in vehicle group (46.6±9.3, $p < 0.01$and $p< 0.001$), but there were no significant difference between Sevo 1and Sevo 2 groups ($p>0.05$). In comparison with the vehicle, the post-administration of sevoflurane at 10min and 30min after reperfusion significantly decreased infarction volume (19.8±14.3, 26.4±18.3, $p < 0.05$). Similarly, the sevoflurane pre- and post-treatment at 10min and 30min after reperfusion groups demonstrated better neurologic function than the vehicle group ($p < 0.05$). Brains with ischemic insult without Sevo-treatment showed increase in caspase3, caspase9 and AIF, otherwise, Pre- or post-intervention with Sevo restored the levels of those factors.

Conclusion: The repeated preconditioning of sevoflurane may provide neuroprotection against focal cerebral ischemia in dose-independent manner and the effect of sevoflurane postconditioning is available in a short therapeutic window. Suppression of apoptosis responses may contribute to neuroprotection of sevoflurane.

A ROLE OF PHOSPHORYLATION OF CREB FOR NEURAL PROGENITOR CELLS IN THE SVZ AND PERI-INFARCT AREA

Y. Tanaka, N. Miyamoto, R. Tanaka, N. Hattori, T. Urabe

Neurology, Juntendo University School of Medicine, Tokyo, Japan

Background and purpose: We noted that transcription factor phosphorylation of cAMP response element-binding protein (CREB) is associated with a proliferation of neural progenitor cells (NPC) in the subventricular zone (SVZ) after ischemia. We examined whether acute focal ischemia induces neurogenesis and the expression of phosphorylation of CREB in the ischemic area.

Methods: Middle cerebral artery occlusion (MCAO) was administered to mice by filament insertion for 45 min and sacrificed at 24h, 72h and 7day after ischemia. 5-bromo-2-deoxyuridine (BrdU) was used to label proliferating cells and immunohistochemistry was performed.

Results: The numbers of BrdU/doublecortin (DCX) in the SVZ and the peri-infarct area significantly increased than contralateral side at 72h ($p< 0.05$). Phospho-CREB/DCX double-labeled cells also increased in the SVZ at 72h ($p< 0.05$). However, a small numbers of phospho-CREB/DCX double-labeled cells were seen from 72h to 7day in the peri-infarct area.

Conclusions: Our result showed that phosphorylation of CREB might play an important role in survival of newly generated NPCs in the SVZ and peri-ischemic area after MCAO.

389

Brain Poster Session: Inflammation

NEUROINFLAMMATION EXTENDS BRAIN TISSUE AT RISK TO VITAL PERI-INFARCT TISSUE: A DOUBLE TRACER [^{11}C]PK11195- AND [^{18}F]FDG-PET STUDY

M.A. Dennin[1,2], M. Walberer[1,2], H. Backes[2], B. Neumaier[2], G.R. Fink[1], M. Schroeter[1,2], R. Graf[2]

[1]Department of Neurology, University Hospital of Cologne, [2]Max-Planck-Institute for Neurological Research, Cologne, Germany

Background and aim: Focal cerebral ischemia elicits strong inflammatory responses involving activation of resident microglia and recruitment of peripheral monocytes/macrophages. These cells express peripheral benzodiazepine receptors (PBRs) and can be visualized by Positron Emission Tomography (PET) using [^{11}C]PK11195 that selectively binds to PBRs. Previous research suggests that transient ischemia in rats induces increased [^{11}C]PK11195 binding within the infarct core. We here investigated the expression of PBRs during permanent ischemia in rats.

Methods: Permanent cerebral ischemia in rats was induced by injection of macrospheres into the middle cerebral artery of Wistar rats (n=5). Multimodal in vivo imaging 7 days after ischemia comprised:

i. Magnetic Resonance Imaging to assess localization and extent of the infarcts,
ii. [^{18}F]-2-fluoro-2-deoxy-D-glucose ([^{18}F]FDG)-PET to characterize local cerebral glucose transport and metabolism and
iii. [^{11}C]PK11195-PET to detect overexpression of PBRs depicting neuroinflammation. Immunohistochemistry ex vivo verified ischemic damage and characterized extent and location of neuroinflammation.

Results: The rate constant K1 of [^{18}F]FDG was used to describe the transport of [^{18}F]FDG from blood into brain tissue as a surrogate marker for cerebral blood flow, and the rate constant Ki to assess [^{18}F]FDG metabolization. Based on those two parameters we identified four distinct regions of the ischemic brain. The “infarct core” was characterized by a significant decrease in [^{18}F]FDG transport (K1 = 0.042 ± 0.011 ml/ccm/min) compared to “contralateral cortex” (K1 = 0.099 ± 0.002 ml/ccm/min, $p < 0.01$) as well as by a significantly decreased [^{18}F]FDG metabolic rate constant (Ki = 0.009 ± 0.002 min^{-1}) compared to the contralateral side (Ki = 0.020 ± 0.003 min^{-1}, $p < 0.01$). Adjacent to the core, an “infarct margin” of tissue was defined as showing reduced [^{18}F]FDG transport of K1 < 0.08 ml/ccm/min, with a regular [^{18}F]FDG metabolic rate constant (Ki = 0.015 ± 0.002 min^{-1}). The “peri-infarct zone” adjacent to the infarct margin was characterized by preserved [^{18}F]FDG transport (K1 = 0.099 ± 0.009 ml/ccm/min) and an increased [^{18}F]FDG metabolic rate constant (Ki = 0.032 ± 0.003 min^{-1}) that was 60% higher than in the contralateral hemisphere (Ki = 0.020 ± 0.003 min^{-1}, $p < 0.01$). Increased [^{11}C]PK11195 binding (mean standard uptake value 1.93 ± 0.49) was found exclusively in this normo-perfused peri-infarct zone, co-localizing with the increase of the [^{18}F]FDG metabolic rate constant. Contrasting with previous data for transient ischemia, no [^{11}C]PK11195 binding was found in the infarct core. Overexpression of PBRs detected in vivo co-localized with the accumulation of activated microglia and macrophages assessed immunohistochemically.

Conclusion: These results suggest that after permanent focal ischemia, neuroinflammation occurs in the normoperfused peri-infarct zone together with increased energy demand. This combination of

inflammatory processes with metabolic disturbances is likely to put even normoperfused peri-infarct tissue at risk of secondary damage.

COMPARISON BETWEEN LECTIN-LIKE OXIDIZED LOW DENSITY LIPOPROTEIN RECEPTOR 1 EXPRESSION AND PREOPERATIVE ECHOGENIC FINDINGS OF VULNERABLE CAROTID PLAQUE

A. Saito[1], M. Fujimura[2], T. Inoue[2], H. Shimizu[1], T. Tominaga[1]

[1]Neurosurgery, Tohoku University, Graduate School of Medicine, [2]Neurosurgery, Konan Hospital, Sendai, Japan

Background and aims: Lectin-like oxidized low density lipoprotein 1 (LOX1) is an important cell surface receptor for the progression of atherosclerosis. LOX1 expressions in coronary atherosclerotic lesions and other systemic arterial plaques have been reported, however, the detail role of LOX1 in atherosclerotic formation of carotid plaques is unclear. Moreover, the relationships of LOX1 and atherosclerotic factors for the vulnerability of carotid plaque and preoperative echogenic findings have not been clarified.

Methods: LOX1, matrix metalloproteinase (MMP) -2, 9 and tissue inhibitor of MMP (TIMP)-2 expressions were immunohistochemically analyzed using carotid endarterectomy specimens obtained from 14 patients. Groups were divided into stable plaque group A and vulnerable plaque group B by preoperative echogenic findings of carotid plaques. Endothelial immunoreactive cells of LOX1 were calculated as endothelial index and the immunohistochemical findings of LOX1 and MMPs were compared between two groups.

Purpose: Our purpose is to clarify the relationship between LOX1 expression in carotid plaques and the vulnerable plaque formation comparing the LOX1 immunohistochemical expression in plaque specimen with the preoperative echogenic plaque findings.

Results: LOX1 was remarkably expressed, especially in smooth muscle cells in vulnerable plaque and colocalized in MMP-9 positive cells and apoptotic cells. All LOX1, MMP-2,9 and TIMP2 were remarkably expressed in the subendothelial layer in group B compared with group A. The endothelial LOX1 index was 63.75±4.92 in group A and 83.0±5.02 in group B ($p=0.02$). The endothelial MMP-2 index was 24.38±5.50 in group A and 32.83±6.79 in group B ($p=0.01$). The endothelial MMP-9 index was 46.13±6.31 in group A and 59.17±2.14 in group B ($p=0.002$). The endothelial TIMP-2 index had no significant difference between two groups ($p=0.14$).

Conclusions: LOX-1 expression was correlated to the echogenic findings of the vulnerability carotid plaques. LOX-1 may play an important role in the progression of vulnerable carotid plaque and might regulate vulnerable plaque formation in cooperation with MMPs and TIMP-2. Endothelial MMP-2 might suppress TIMP-2 activation in vulnerable plaques.

391

BrainPET Poster Session: Kinetic Modeling

K_3 IS A BETTER PARAMETER THAN BINDING POTENTIAL AS A QUANTITATIVE INDICATOR OF BETA AMYLOID BY [^{11}C]PIB PET

T. Ohya, K. Fukushi, H. Shimada, K. Sato, H. Shinoto, M. Miyoshi, S. Hirano, N. Tanaka, T. Ota, T. Irie

Molecular Imaging Center, National Institute of Radiological Sciences, Chiba, Japan

Aims: Quantitative measurement of beta amyloid (Aβ) in brain of Alzheimer diseases (AD) is necessary for monitoring the progression of the Aβ deposition and the efficiency of the Aβ immunotherapy. Though Logan-distribution volume ratio (DVR) is currently used for the diagnosis of AD by PET, DVR is not adequate as a quantitative indicator for Aβ, because it is a complex parameter. DVR is based on the assumption that K_1/k_2 is almost equal within whole brain. Thus, we noted the two parameters, k_3 and binding potential ($BP=k_3/k_4$), which are proportional indicators to the Aβ deposition, and examined their diagnosis power by clinical study. The stability of k_3 and BP as a quantitative indicator and the effect of k_4 condition on their stability were examined by simulation study.

Methods: Ninety minutes [^{11}C]PIB PET studies were performed in 22 volunteers with or without AD. The metabolite-corrected input function was measured in all cases. The PET data were analyzed by two-tissue compartment model with four kinetic parameters ($K_1 \sim k_4$). The t-test with two parameters (k_3, BP) between NC (N=10) and AD (N=12) groups was performed on Fine-SRT ROI (FUJIFILM RI Pharma Co.) (50 regions) and voxel ROIs, and their diagnosis power were compared by the number of the positive ROIs, where k_3 or BP significantly increased (t-test $P< 0.05$). In the Monte Carlo simulation study, tissue-time activity curves of NC and AD with statistical noise were made as follows. The three parameters were according to the typical NC or AD conditions from the clinical data: k_3 = .018 min^{-1}(NC), .040(AD), K_1 = 0.18 mL/g/min, k_2 =0.18 min^{-1} and input function were fixed. The simulations were performed under various k_4 conditions, and more than 2000 parameter results were obtained in each k_4 condition. The coefficient of variation (CV) of k_3 and BP were calculated from them.

Results: In the Fine-SRT ROIs study, the k_3 showed higher diagnosis power than BP to discriminate between NC and AD: 48 positive ROIs by k_3 and 40 ROIs by BP. Similar result was obtained with the parametric image for voxel-ROIs. From the simulation study, CVs of k_3 and BP were approximately the same under AD condition (k_3=.040, $k_4\approx$.025), whereas CV of k_3 was sufficiently lower than that of BP under NC condition (k_3=.018, $k_4\approx$.020) (Figure 1). These results supported the clinical result. The CV values of k_3 and BP were much dependent on the k_4 conditions, that is, BP became unstable when the k4 became smaller.

Conclusions: The k_3 may be a better quantitative indicator for Aβ monitoring than BP in the case of [^{11}C]PIB PET, though the selection of indicator for k_3 or BP is dependent on the k_4 value of the utilized PET tracer.

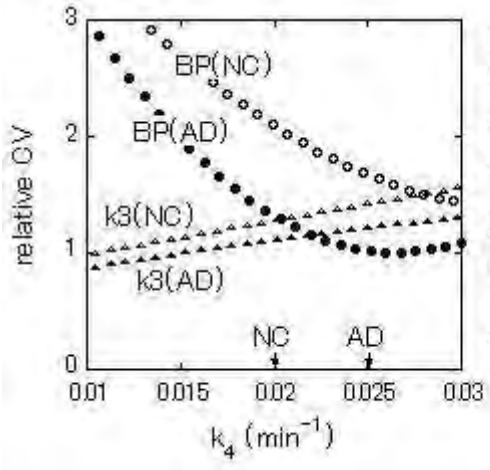

Figure shows the CV curves of k_3 and BP under various k_4 values at two k_3 values (NC=.018, AD= 040 min^{-1}). Arrows indicate mean k_4 values of NC and AD group in clinical study.

[Figure 1]

COORDINATED RESPONSE OF ARTERIAL NETWORKS INDUCED BY LOCAL STIMULATION IN ANESTHETIZED RAT SOMATOSENSORY CORTEX

K. Masamoto[1,2], T. Obata[2], I. Kanno[2]

[1]The University of Electro-Communications, Tokyo, [2]National Institute of Radiological Sciences, Chiba, Japan

Aim: To characterize the spatiotemporal dynamics of cerebrovascular networks induced by local stimulation, the cortical surface and intracortical vascular networks were imaged with confocal or multi-photon microscopy in the anesthetized rat somatosensory cortex.

Materials and methods: Sprague-Dawley rats (6-8w) were used for the experiments following an experimental protocol approved by the Institutional Animal Care and Use Committee. The animals were anesthetized with isoflurane (5% for induction and 1.3-1.5% for experiments), and endotracheal intubation was performed for mechanical ventilation. Catheters were placed into the femoral vein and artery for administration of fluorescent marker and arterial blood sampling, respectively. An area (3 mm x 3 mm) on the left parietal bone over the somatosensory cortex was removed. Arterial blood pressure, heart rate, and respiratory parameters were monitored throughout all experiments. Rectal temperature was maintained at 37ºC. For visualization of cortical vasculature, a bolus injection of Qdot 655 (1 μM, 0.2- 0.4 ml) was performed. The image of the cortical surface vessel was obtained with confocal microscopy with a 488-nm excitation, and the image of intracortical vessel was obtained with multi-photon microscopy at an excitation of 900 nm (~2.0 W at laser output) up to a depth of 0.6 to 0.8 mm from the cortical surface with a z-step of 0.01 mm. The image resolution in a x-y plane was 512 x 512 pixels, and a sampling rate was 13 frames per second. The artery and vein emerging from the parenchyma was identified by tracking pial arterial and venous networks, respectively. The cross-section diameter was measured at the focal point. The neural stimulation in the measured region was induced with electrical pulse (1.5 mA, 1.0-ms duration at 12 Hz) to contra-lateral side of forepaw. The stimulation trial was repeated with 8 times and averaged across all trials. The CBF response and somatosensory evoked potentials were also measured with laser-Doppler flowmetry (LDF) and a surface electrode, respectively, after the vascular imaging experiments.

Results and discussion: Stimulation-induced vasodilation was observed only for arterial side, whereas no detectable changes in the vascular diameter were obtained for the venous side. The time of onset of the arterial vasodilation (~0.5 sec) was in good agreement with the time-courses of CBF changes measured with LDF. The peak of dilation accounted for ~10% of resting vessel diameter. The arterial dilation started at the local point along the small arterioles, and spread into large upstream arteries located on the cortical surface. About 40% of arterioles that dive into the parenchyma showed vasodilation over the somatosensory area (FOV: 1.8 x 1.8 mm^2) where 15-20 penetrating arterioles were found. The penetrating arterioles that showed vasodilation was localized around the activated regions, although the upstream surface arteries respond globally. Further, the vasodilation of upstream arteries extended in a stimulus-dependent manner. These findings indicate that the branching point from parent surface arteries to the penetrating arterioles play a key role in controlling the spatial regulation of blood supply distribution in the intracortical regions where the energy demand locally varied depending on neural activity.

BRAIN DAMAGE AND FUNCTIONAL DEFICITS EVOLUTION FOLLOWING PERMANENT OR 3H-TRANSIENT ISCHEMIA IN MARMOSETS: STUDIES WITH BEHAVIORAL TESTS, MRI AND IMMUNOHISTOCHEMISTRY

E. Bihel[1], J. Toutain[1], P. Pro-Sistiaga[2], M. Bernaudin[1], S. Roussel[1], O. Touzani[1]

[1]UMR-CINAPS 6232, CERVOxy Team 'Hypoxia and Cerebrovascular Pathophysiology', CNRS, CEA, Université de Caen Basse Normandie and Université Paris Descartes, Caen, France, [2]Human Neuroanatomy Laboratory, Department of Health Sciences and C.R.I.B., School of Medicine, University of Castilla-La Mancha, Albacete, Spain

Objectives: Based on behavioral tests, magnetic resonance imaging (MRI) and immunohistochemistry, the aim of our study was to characterize, at both the acute and the chronic stages, the evolution of functional deficits and brain damage in the marmoset subjected to permanent or 3 hours transient ischemia induced by intraluminal occlusion of middle cerebral artery (MCAO)[1].

Methods: Six and five marmosets were subjected to transient (tMCAO) and permanent (pMCAO) intraluminal MCAO[1], respectively. During 45 days after the occlusion, a battery of behavioral tests has been performed weekly to quantify the sensorimotor deficits. These tests included neurological score, tactile simulation, hill and valley staircase, adhesive removal task, six tubes choice, and reaching up tube[2]. Each animal underwent 3 sessions of MRI (7T, Pharmascan; Bruker) at 60 min, 8 days and 45 days following MCAO. In each session, diffusion weighted imaging (DWI), T2 and T2*-MRI sequences were acquired. NeuN, GFAP and NeuN/BrdU labeling were undertaken at 45 days to assess neuronal loss, astrogliosis and neurogenesis, respectively.

Results: Behavior: Unilateral motor impairment of the contralateral forelimb and neglect of contralateral body side were observed in all subjects, with more severe deficit in pMCAO group. These deficits were long-lasting despite a partial recovery in tMCAO group. In pMCAO group, this partial recovery was significantly more delayed in most tests analyzed.

Brain lesion: MRI data showed that the lesion affected cortical and subcortical structures at the acute and sub-acute stages. At 60 min, the volume of the DWI lesion was not significantly different between tMCAO and pMCAO groups (298±165 mm³ and 208±116 mm³ respectively). At 8 days after the occlusion, the T2-MRI-defined lesion was larger in pMCAO group (462±348 mm³) compared to tMCAO group (123±86mm³ Mann Whitney test, p=0.04). At 45 days, a hyperintense signal in T2-MRI was visible in pMCAO group (28±22 mm^3) but not in tMCAO one. However, a hemispheric atrophy was observed in the two groups without statistically significant difference (4.8±1.7% and 3.1±1.5%, respectively for pMCAO and tMCAO). In the 3 sessions of MRI, T2* sequence did not revealed any cerebral hemorrhage.

Cellular reaction: NeuN and GFAP labeling revealed, at 45 days post-MCAO, a widespread neuronal loss and associated astrogliosis in the ipsilateral hemisphere in greater extend in pMCAO group. Compared to SHAM animals, those subjected to ischemia showed newly generated neurons, as attested by NeuN/BrdU double labeling, in the vicinity of the initial lesion, in particular in the caudate nucleus (Mann Whitney test p=0.06). However, no difference between pMCAO and tMCAO groups was noted.

Conclusions: The data show that intraluminal MCAO in the marmoset results in widespread brain damage and long-lasting functional deficits that can be reduced by reperfusion. Moreover, this work revealed the existence of a post-ischemic neurogenesis in this model. Altogether, the results show that this model of brain ischemia in the marmoset could be considered as suitable to test new therapies against stroke.

1. Freret T et al. (2008) J Cereb Blood Flow Metab; 28(4):786-96.

2. Marshall et al. (1996) Neurodegeneration; 5(3):275-86.

SIMPLIFIED QUANTIFICATION OF ADENOSINE A_{2A} RECEPTOR WITH [^{11}C]TMSX PET AND GRAPHICAL ANALYSES

M. Naganawa[1,2], M. Mishina[2,3], M. Sakata[2], K. Oda[2], K. Ishii[2], K. Ishiwata[2], Y. Kimura[1,2]

[1]Molecular Imaging Center, National Institute of Radiological Sciences, Chiba, [2]Positron Medical Center, Tokyo Metropolitan Institute of Gerontology, Tokyo, [3]Neurological Institute, Nippon Medical School Chiba-Hokusoh Hospital, Chiba, Japan

Objectives: [^{11}C]TMSX is one of the few available radioligands to quantify adenosine A_{2A} receptor (A2AR) [1]. Although A2ARs are rich in the basal ganglia and poor in other regions, [^{11}C]TMSX binds to not only classical A2ARs but also atypical sites. Therefore, it is difficult to find a reference region. In previous studies with arterial input function, we selected the centrum semiovale (CSO) as a reference region [2,3]. The purpose of this study was to investigate the availability of graphical analyses for human [^{11}C]TMSX studies with region of interest (ROI) analysis.

Methods: Seven healthy subjects were included in this study. The average dose was 570 ± 86 MBq and the specific activity was 39 ± 21 GBq/μmol. Dynamic PET scans were acquired for 1 hour with a SET-2400W (Shimadzu, Japan). A total of 25 ROIs was manually delineated on the summed PET image: CSO (reference), anterior and posterior putamen, caudate, midbrain, posterior cingulate, cerebral cortical areas, and cerebellum. The regional time-activity curves (TACs) were analyzed using one- and two-tissue compartment models (1T, 2T), Logan graphical analysis (LGA) and multilinear analysis (MA1) with a metabolite-corrected input function. TACs were also analyzed using reference Logan graphical analysis (LGAR). The clearance rate constant of the reference region (k_2') for LGAR was fixed to be 0.12 min^{-1}, the mean value from the 1T model. For all graphical methods, t* was set to be 20 min post-injection.

Results: Metabolism of [^{11}C]TMSX was very slow with parent fraction of 0.98 ± 0.01 at 3 min and 0.92 ± 0.05 at 60 min. The ROIs were well described by 2T model with a constraint of V_{ND} from the 1T estimation of CSO. The values of V_T ranged from 0.58 ± 0.16 (CSO) to 1.25 ± 0.29 mL/cm^3 (anterior putamen), with K_1 values of 0.068 ± 0.014 to 0.30 ± 0.07 mL/min/cm^3. The estimated V_T of graphical analyses and 2T matched well (V_T(LGA) = 0.99 V_T(2T) + 0.01 (r^2 = 0.99), V_T(MA1) = 1.01 V_T(2T) + 0.01 (r^2 = 0.99)). The estimated V_T in CSO was 5% higher in graphical analyses than in 1T model. As a result, the estimated BP_{ND} of LGA and MA1 showed smaller values compared with compartment model analysis (BP_{ND}(2T) = 0.83BP_{ND}(MA1) + 0.06 (r^2 = 0.92)). The LGAR provided similar results (BP_{ND}(LGAR) = 0.99BP_{ND}(MA1) - 0.01 (r^2 = 0.99)).

Conclusions: All graphical analyses provided similar estimates of V_T and BP_{ND} for ROI curves. This study suggests that LGAR is available for quantification of [^{11}C]TMSX ROI analysis. The difference of BP_{ND} values in graphical analyses and compartment analysis is due to the estimates of V_{ND} value. The suitability of CSO as a reference region should be further investigated and the noise-reduction method is required for LGAR imaging.

References:

[1] Ishiwata K, et al. JNM, 41:345-354, 2000.

[2] Naganawa M, et al. EJNM, 34:679-687, 2007.

[3] Svenningsson P, et al. Synapse, 27:322-335, 1997.

Acknowledgments: This work was funded by Grants-in-Aid for Scientific Research (B) No. 16390348, (C) No. 17590901 and No. 20591033 from JSPS.

RNAI-MEDIATED DOWNREGULATION OF BECLIN1 ATTENUATES FOCAL CEREBRAL ISCHEMIC INJURY AND ENHANCES NEUROGENESIS IN RATS

Y.-Q. Zheng, J.-X. Liu, X.-Z. Li

Research Center, Xiyuan Hospital, China Academy of Chinese Medical Sciences, Beijing, China

Objectives: Because autophagy appears to be occurring after cerebral ischemia, we tested the roles of Beclin 1-dependent autophagic way in focal cerebral ischemia in the rat middle cerebral artery occlusion model (MCAO).

Methods: Lentiviral vectors-associated RNA interference (RNAi) system was stereotaxically injected into the ipsilateral lateral ventricle to reduce Beclin1 expression. We than evaluated the ipsilateral infarct volume, autophagosomes formation, neurogenesis and apoptosis which might be modulated by Beclin1 RNAi.

Results: Beclin1 RNAi not only inhibited the autophagosomes formation but also repaired the ischemic injury in the ipsilateral hemisphere. On the 14th day after MCAO, Beclin-1 downregulation by RNAi increased the number of neural progenitor cells, newborn immature and mature neurons and reduced the apoptosis of immature striatal neurons in the surrounding ischemic core of ipsilateral hemisphere.

Conclusions: RNAi-mediated downregulation of Beclin1 improves outcomes after transient MCAO. This neuroprotective effect is likely exerted by inhibiting autophagy and apoptosis and enhancing neurogenesis.

A NOISE REDUCTION METHOD FOR GRAPHICAL ANALYSES WITH KL-EXPANSION DURING TRANSIENT EQUILIBRIUM CONDITION

K. Sakaguchi[1], M. Naganawa[1], M. Sakata[2], M. Shidahara[1], C. Seki[1], K. Ishiwata[2], Y. Kimura[1]

[1]National Institute of Radiological Sciences, Chiba, [2]Tokyo Metropolitan Institute of Gerontology, Tokyo, Japan

Objectives: Graphical analyses have advantages in unnecessary for the assumption of the number of compartments and fast computation. However, there is a large noise-induced bias or variability in the estimation of total volume of distribution (V_T) [1]. Principal component analysis based method (mPCA) was proposed for a noise reduction in Logan graphical analysis (LGA) [2], which might lead to a deformation of kinetics of time-activity curves (TACs). This study proposes a new noise reduction method for graphical analyses by Karhunen-Loève expansion (mKLE), which aims to maintain kinetics of voxel-based TACs.

Methods: mKLE is based on the assumption that the ratio of a TAC to the input function is approximately constant after a certain time (t*) (transient equilibrium condition). Then the TAC after t* can be represented by one basis function. The basis function is expressed as an axis which passes across the origin and minimizes the distance from TACs in feature space. mKLE was applied to a set of TACs to calculate the basis function. The noise-reduced TACs were obtained by projecting voxel-based TACs onto the basis function. mKLE was tested on human PET data of [^{11}C]TMSX, an adenosine A_{2A} antagonist radioligand [3]. Dynamic PET scans were acquired for 1 hour, and metabolite-corrected arterial input function was obtained. We tested 3 versions: without noise reduction and with mKLE or mPCA. The dynamic data were analyzed by LGA and multilinear analysis (MA1) to calculate the parametric V_T images. The regional mean value of V_T was calculated from the striatum drawn on the summed PET image. For all graphical methods, t* was set to be 30 min postinjection.

Results: Figure (A) shows a typical example of TAC from a voxel: an original TAC, the noise-reduced TACs by mKLE and mPCA, and the ROI-averaged TAC. The mKLE-estimated TAC agreed well with the ROI-averaged TAC. Figure (B) shows the V_T images from the same subject of Fig. (A). In the ROI-averaged TAC, the estimated V_T values of LGA and MA1 were the same as 1.23 mL/cm^3. The lowest value of V_T was given by LGA without noise-reduction (1.12 ± 0.17 mL/cm^3). Both mKLE and mPCA similarly improved V_T values estimated with LGA (1.23 ± 0.19 mL/cm^3 for mKLE, 1.24 ± 0.18 mL/cm^3 for mPCA). On the other hand, only mKLE improved V_T estimated with MA1 (1.24 ± 0.18 mL/cm^3), while mPCA caused overestimation and large variability (1.37 ± 3.21 mL/cm^3).

Conclusions: The experimental results suggest that the proposed method is promising for noise reduction of V_T imaging by graphical analyses.

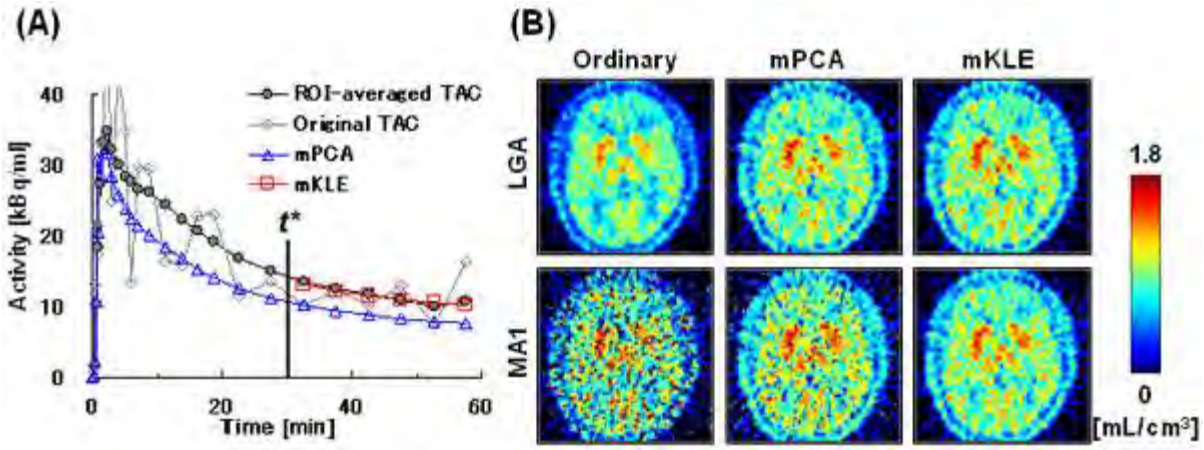

[Figure]

References:

[1] Slifstein, et al., J Nucl Med 41, 2083-2088, 2000.

[2] Joshi, et al., J Cereb Blood Flow Metab 28, 852-865, 2008.

[3] Ishiwata, et al., J Nucl Med, 41:345-354, 2000.

QUANTITATIVE ASSESSMENT OF DENSITY AND AFFINITY FOR DOPAMINE D_2 RECEPTORS WITH MULTIPLE INJECTIONS OF [^{11}C]RACLOPRIDE

Y. Ikoma[1,2], H. Watabe[1], T. Hayashi[1], K. Minato[2], H. Iida[1]

[1]Department of Investigative Radiology, National Cardiovascular Center Research Institute, Suita,
[2]Graduate School of Information Science, Nara Institute of Science and Technology, Ikoma, Japan

Objectives: Positron emission tomography with [^{11}C]raclopride is widely used to investigate the dopamine D_2 receptor system that is related with several neurological and psychiatric disorders in the brain. The dopamine D_2 receptor density (B_{max}) and affinity (K_d) can be determined using a graphical analysis based on Scatchard plot with PET scans [1,2]. However, in this estimation, multiple PET scans are required under variable specific activity of administered [^{11}C]raclopride, so that they are often obtained on separate day. To shorten the study period of B_{max} and K_d measurement, we have developed a multiple injection simplified reference tissue model (MI-SRTM) that provides the change of binding potential (BP) value from a single session of PET scanning in conjunction with multiple injections of [^{11}C]raclopride [3]. In this study, we established the method for estimating B_{max} and K_d with multiple-injection approach, and validated the proposed method by performing numerous simulations and studies on monkeys with PET and [^{11}C]raclopride.

Methods: In the simulation studies, to determine the injection protocol of our multiple-injection approach, time-activity curves (TACs) of the striatum and cerebellum were generated using plasma input function and two-tissue compartment 5-parameter model including K_1, k_2, k_{on}, B_{max}, and k_{off} for various mass of administered raclopride, and a relation between injected mass and BP estimated by MI-SRTM was investigated. Next, TACs were simulated with various B_{max} and k_{on} with proposed multiple-injection protocol. In these TACs, B_{max} and K_d were estimated by a graphical analysis of Scatchard plot, and estimated values were compared with true values. In the studies on three monkeys, PET scans were performed using PCA-2000A and three injections of [^{11}C]raclopride, and B_{max} and K_d were measured by the graphical analysis.

Results: In the simulation study with various injection mass, BP estimates became smaller as the injected mass increased. Based on this result, we planned a protocol for three injections with 50-minute intervals of 1.5, 10, and 30 nmol/kg raclopride so that the BP estimates would be high, middle, and small. Using this injection protocol, B_{max} and K_d could be estimated by the graphical analysis. Both of B_{max} and K_d were overestimated. However, in TACs with various K_d and fixed B_{max}, there was a good correlation between true and estimated K_d, and estimated B_{max} was constant. Meanwhile, in TACs with various B_{max} and fixed K_d, a good correlation was observed between true and estimated B_{max}, and there was little variation in estimated K_d. The estimation error became larger in the case where the K_d was larger or B_{max} was smaller. In the monkey studies, estimated B_{max} and K_d were about 32 and 16 pmol/mL, respectively, and both values were close to those previously obtained by the conventional method [2].

Conclusions: The dopamine D_2 receptor density and affinity could be estimated by 150-minute PET scan with three injections of [^{11}C]raclopride with 50-minute intervals.

References:

[1] Farde L et al., Science 231, 258-261, 1986.

[2] Doudet DJ et al., J Cereb Blood Flow Metab 23, 280-284, 2003.

[3] Watabe H et al., Neuroimage 31 (Suppl2), T73, 2006.

Brain Poster Session: Neuroprotection

THE EFFECT OF PDE3 INHIBITOR CILOSTAZOLE ON CRE ACTIVITY IN HUMAN NEURONAL CELL LINE

T. Sasaki[1], Y. Yagita[2], Y. Terasaki[1], E. Omura-Matsuoka[1], N. Ohyama[1], Y. Sugiyama[2], S. Okazaki[2], S. Sakoda[2], K. Kitagawa[2]

[1]Division of Stroke Center, Department of Internal Medicine, [2]Department of Neurology, Osaka University Graduate School of Medicine, Osaka, Japan

Background: Cilostazole is therapeutically approved as antiplatelet drug for use in patients with ischemic stroke. Recently, Cilostazole has been shown to have neuroprotective activities and inhibit white matter damage. Cilostazole generates various downstream biological activities. Among these pleiotropic effects, the activation of cAMP responsive element binding protein (CREB) - CRE cascade has been reported to contribute to their neuroprotective activity in animal model. In order to directly examine the relationship, we have chosen to utilize a cell culture-based assay using human neuronal cell lines.

Subjects and methods: We used M03.13 (human oligodendrocyte cell line), SH-SY5Y (human neuroblastoma cell line), and 1321N1 (human astrocyte cell mine). To directly detect the CRE transcription activity, we have transfected adeno-CRE reporter to these cell lines and measured the CRE activity using luciferase assays. M03.13 were cultured in DMEM + 10% fetal bovine serum (FBS) + antibiotics, and then replaced with the DMEM medium without FBS to differentiate to mature oligodendrocyte. SH-SY5Y were maintained in DMEM + 10% fetal bovine serum (FBS) including 10μM all-trans retinoic acid to differentiate to neuronal lineage. Cilostazole (1, 3, 10, 30μM), the type Ⅳphosphodiesterase (PDE) inhibitor rolipram (30μM), and adenylate cyclase activator forskolin (5μM) were administered for 24 hr.

Results: In M03.13, cilostazole significantly increased the CRE transcription activities with dose dependent manner. On the other hand, cilostazole did not significantly enhance the CRE activity in both SH-SY5Y and 1321N1, in contrast to be treated by rolipram and forskolin.

Conclusion: The effect of cilostazole on CRE activity was different between human cell types. Activation of cAMP-CREB signaling in oligodendrocyte by cilostazole may be one of the mechanisms of their protective effects and may have implications for therapeutic intervention to white matter damage via the activation of CREB-CRE signaling.

Brain Poster Session: Glial Functions

EFFECT OF S100B ON CELLULAR INJURY AND GLIAL ACTIVATION

A. Kleindienst[1], Z. Qu[2], C. Stadelmann[3], F. Hesse[1], I. Emtmann[1], M. Buchfelder[1]

[1]Dept. of Neurosurgery, University Erlangen-Nuremberg, Erlangen, [2]Dept. of Neurosurgery, [3]Dept. of Neuropathology, University of Göttingen, Göttingen, Germany

Objective: The supposed contrasting effects of S100B, the beneficial one in acute injury like traumatic brain injury (TBI), and the detrimental one in chronic injury and neurodegeneration like Alzheimer's disease, have been speculated to be due to a variation of the exposure to S100B. Studies in S100B transgenic mice suggest S100B to accelerate neuronal development (Shapiro et al., 2004). We demonstrated an exogenous S100B treatment to enhance hippocampal neurogenesis and to improve cognitive recovery following experimental TBI in the rat (Kleindienst et al., 2005). The purpose of the present study was to elucidate temporal and spatial effects of S100B on cellular injury, microglial and astrocyte activation in the same model of acute brain injury.

Methods: Following lateral fluid percussion injury in male Sprague-Dawley rats (n=32), we infused S100B (50ng/hr) or vehicle into the lateral ventricle for 7 days using an osmotic micro-pump. The animals were sacrificed on day 5 or 5 weeks post-injury, and 5mm sections, 100mm apart (bregma -3.3 to -5.6mm) were analysed histologically. Cell death was assessed using TUNEL and hematoxylin-eosin staining, activation of astrocytes was examined applying the glial markers GFAP and S100B, microglial activation by ED1 immunostaining, and axonal damage by APP.

Results: TUNEL-positive cells were present directly beneath the lesion site in vehicle and S100B-treated animals on day 5 post-injury (238±6 and 234±24 cells/mm2, respectively, n.s.), but not after 5 weeks. The intraventricular S100B infusion did not significantly affect the early (TBI $p=0.004$, TBI+S100B $p=0.036$) or late (TBI $p=0.039$, TBI+S100B $p=0.002$) axonal injury, but resulted in an unspecific microglial activation opposite to the injury site as documented by an increased ED1 expression (TBI+S100B $p=0.001$). After 5 weeks, both injury and S100B treatment resulted in an increased number of GFAP expressing cells in the corpus callosum (TBI $p=0.005$, TBI+S100B $p=0.003$, sham+S100B $p=0.005$), while in the hippocampal granular cell layer (GCL) this effect was only present in non-injured control animals ($p=0.048$). The S100B expression in the GCL was increased by a S100B treatment after 5 weeks, both in injured and non-injured animals ($p=0.017$ and $p< 0.001$).

Conclusion: In accordance to the participation of S100B in injury-induced cell proliferation, we found the S100B expression in the germinative area of the hippocampus on the lesion side to be significantly enhanced by an intraventricular infusion at 5 weeks post-injury. The S100B infusion in non-injured control rats provoked a symmetrically increased S100B expression and astrocytosis after 5 weeks. S100B did not exert an effect on early cell death or axonal injury. The significance of some delayed APP and ED1 accumulation and reactive astrocytosis has to be clarified by long-term experiments.

References:

Kleindienst, A., McGinn, M.J., Harvey, H.B., Colello, R.J., Hamm, R.J. and Bullock, M.R. (2005). Enhanced hippocampal neurogenesis by intraventricular S100B infusion is associated with improved cognitive recovery after traumatic brain injury. J Neurotrauma 22, 645-55.

Shapiro, L.A., Marks, A. and Whitaker-Azmitia, P.M. (2004). Increased clusterin expression in old but not young adult S100B transgenic mice: evidence of neuropathological aging in a model of Down Syndrome. Brain Res 1010, 17-21.

413

Brain Poster Session: Inflammation

PLATELET DEPLETION WITH AN ANTI-GPIB-ANTIBODY IMPROVES THE FUNCTIONAL OUTCOME AFTER FOCAL CEREBRAL ISCHEMIA IN MICE

S.M. Sonanini[1,2], S.M. Krieg[1,2], N. Plesnila[1,2,3]

[1]Department of Neurosurgery, [2]Institut for Surgical Research, University of Munich Medical Center - Großhadern, Munich, Germany, [3]Royal College of Surgeons in Ireland, Dublin, Ireland

Objectives: Following reperfusion from focal cerebral ischemia platelets adhere to the cerebrovascular endothelium. This interaction is mediated by interaction of the glycoprotein (GP) Ib receptor with endothelial von Willebrand factor (1) and occurs within the time window of post-ischemic cell death, i.e. 2-8 hours after reperfusion. The pathophysiological role of this interaction is yet unclear. Therefore the aim of the current study was to address the role of platelets for the development of reperfusion injury after experimental ischemic stroke.

Methods: C57/Bl6 mice (n=36) were randomized to 6 groups (n=6 each) and were subjected to 45 min of transient middle cerebral artery occlusion (tMCAO) (5). Complete blockade of GPIbα and >95% depletion of circulating platelets was achieved by intraperitoneal injection of 2 µg/g body weight of a monoclonal anti-GPIbα Fab antibody at reperfusion (t=0h) or 1, 3, 5 or 7 h thereafter (2). 24 h after tMCAO, functional outcome was evaluated by using a modified 19-point neurological severity score (NSS). Infarct volume, neuronal cell loss, and the degree of intracerebral haemorrhage (ICH) were quantified by Nissl staining.

Results: All treated groups showed an improved functional outcome after 24h as compared to controls, particularly groups R+5h and R+7h with a 55% and a 76% better NSS, respectively (R+5h: 6.3 ± 1.0; R+7h: 3.3 ± 0.3 vs. control: 13.9 ± 0.9; $p< 0.05$). Compared with controls, ischemic lesions were reduced by a maximum of 52% (R+7h) (R+0h: 30.4 ± 3.1 mm3; R+1h: 35.5 ± 2.5 mm3; R+3h: 31.7 ± 2.3 mm3; R+5h: 36.4 ± 3.9 mm3; R+7h. 25.7 ± 1.1 mm3 vs. control: 49.3 ± 1.7 mm3; $p< 0.05$). After 5 and 7h reperfusion less necrotic neurons could be observed (R+5h: 57.1 ± 12.4 cells; R+7h: 50.7 ± 6.9 cells vs. control: 144 ± 21.9 cells; $p< 0.05$). Despite functional and histological improvements a significant number of animals showed ICH (R+0h: n=2; R+1h: n= 3; R+3h: n=5; R+5h: n=2; R+7h: n=1 vs. control: n=0; $p>0.05$).

Conclusions: These data indicate that - despite the increased risk of ICH - blockade of GPIbα, a major platelet adhesion receptor, has an important impact on functional and histopathological outcome following reperfusion from focal cerebral ischemia. Thus, early inhibition of platelet adhesion with an GPIbα antibody may offer a novel treatment strategy for cerebral ischemia.

Reference list:

1. Andrews RK et al. IUBMB Life 56: 13-18, 2004.

2. Bergmeier W et al. Blood 95: 886-893, 2000.

3. del Zoppo GJ. Neurology 51: S9-14, 1998.

4. Kleinschnitz C et al. Circulation 115: 2323-2330, 2007.

5. Plesnila N et al. Proc Natl Acad Sci U S A 98: 15318-15323, 2001.

CEREBRAL SALT WASTING FOLLOWING SUBARACHNOID HEMORRHAGE: A RAT MODEL

S. Schlaffer[1], H. Tam[2], N. Sharma[2], J. Verbalis[2], M. Buchfelder[1], A. Kleindienst[1]

[1]Dept. of Neurosurgery, University Erlangen-Nuremberg, Erlangen, Germany, [2]Dept. of Medicine, Georgetown University, Washington, DC, USA

Objective: Aneurysmal subarachnoid hemorrhage (SAH) is associated with a high mortality and morbidity. Beside vasospasm, one third of patients will develop severe hyponatriemia, which has also been referred to as cerebral salt wasting (CSW). Both syndromes have been connected to the hypothalamic neuropeptide arginine-vasopressin (AVP). Utilizing in vivo microdialysis an established experimental model of SAH, we were able to demonstrate a central AVP release, which may contribute to pathophysiological events following SAH (Kleindienst et al., 2004). The present study is designed to examine CSW in experimental SAH.

Methods: In male Wistar rats (250-350 g), SAH was induced by injecting 150µl of autologous blood into the great cistern (SAH n=16). In a second group of rats, SAH was induced twice, 24 hours apart (double SAH n=12). Control rats underwent sham procedure (sham n=8). The rats were housed in metabolic cages, and the daily sodium excretion as well as sodium, osmolarity and AVP in serum were measured for 10 days. Statistical analysis was performed using the Mann Whitney rank sum test (SPSS software).

Results: Following SAH, sodium excretion was significantly increased on day 1 ($p=0.002$) and on day 4 ($p=0.026$) as compared to control rats (n=8). Serum sodium (141.5 mmol/l day 0, 142.0 mmol/l day 5) and serum osmolarity (303.5 mosmol/kg day 0, 307.2 mosmol/kg day 5) remained stable, while the initial increase of AVP normalized over the investigation period (46.99 pg/ml day 0, 8.14 pg/ml day 5). Following double SAH, rats suffered increased morbidity and lost significant weight, while natriuresis was not significantly altered.

Conclusions: The rat model of SAH by injecting blood into the great cistern is suitable for studying the pathophysiology of CSW. Increased natriuresis paralleled the time course of early and late vasospasm known in this model. Double SAH does not enhance natriuresis but resulted in increased morbidity and weight loss thereby interfering with the assessment of electrolyte and fluid balance.

References: Kleindienst, A., Hildebrandt, G., Kroemer, S.A., Franke, G., Gaab, M.R. and Landgraf, R. (2004). Hypothalamic neuropeptide release after experimental subarachnoid hemorrhage: in vivo microdialysis study. Acta Neurol Scand 109, 361-8.

416

Brain Poster Session: Experimental Cerebral Ischemia: Vascular & Endothelial

PROGRESSION OF PLATELET - ENDOTHELIUM INTERACTIONS AFTER ACUTE STROKE IN MICE

S.M. Sonanini[1,2], S.M. Krieg[1,2], S.W. Kim[3], N. Plesnila[1,2,3]

[1]Department of Neurosurgery, [2]Institute for Surgical Research, University of Munich Medical Center - Großhadern, Munich, Germany, [3]Royal College of Surgeons in Ireland, Dublin, Ireland

Objectives: Secondary to their function in haemostasis, platelets (Plt) are supposed to have pro-inflammatory properties (3) (4). As secondary neuronal damage after ischemia is accompanied by neuroinflammatory activity, especially leukocyte-endothelium-interactions (LEI) (2), the aim of the current study was to characterize the progression of Plt-activation and adhesion after focal transient cerebral ischemia.

Methods: For cerebral ischemia (I) C57/Bl6 mice were subjected to 45 minutes of occlusion of the middle cerebral artery (tMCAO). After 1, 3, 5, 12, or 24 h (n=6 each) of reperfusion (R) mice were anesthetized, intubated, and mechanically ventilated. Blood was harvested from donor mice by cardiac puncture and Plts were separated and stained with carboxyfluorescein diacetate succinimidyl ester (CFDA-SE). A total of 100x106 Plt were injected i.v. Plt-endothelium interactions (PEI) in cortical cerebral vessels of the ischemic penumbra were investigated by intravital fluorescence microscopy (IVM) for 2 h.

Results: Key physiologic parameters like body temperature, blood pressure, blood pH, pO2, and pCO2 were within the physiologic range during tMCAO and IVM. In sham operated animals only physiologic rolling of Plt along the cerebrovascular endothelium was observed (3.4 ± 1.0 Plt/100µm/min). After I/R a significant ($p< 0.05$) increase of TEI could be observed in postcapillary venules with a peak at R=5 h (rolling Plt: 12.97 ± 0.74 Plt/100µm/min; sticking Plt: 1.31 ± 0.17 Plt/100µm/min). In arterioles significant rolling Plt was already noticed 3h after ischemia (1.36 ± 0.24 Plt/100µm/min vs. sham: 0.19 ± 0.10 Plt/100µm/min). 12 and 24h after I/R PEI returned to baseline values.

Conclusion: Platelet-endothelium interactions (PEI) occur in the vessels of the ischemic penumbra during the time window of neuronal cell death (2-8 h after ischemia) and show the same time course as the adhesion of leukocytes (2). Since Plt do not only interact with the endothelium but also with leukocytes (4) our data suggest that Plt may be part of the inflammatory response which leads to reperfusion damage following cerebral ischemia (1).

Reference list:

1. Garcia JH et al. Am J Pathol 144: 188-199, 1994.

2. Kataoka H et al. J Cereb Blood Flow Metab 25: S91, 2005.

3. Weyrich AS et al. Trends Immunol 25: 489-495, 2004.

4. Zarbock A et al. Blood Rev 21: 99-111, 2007.

EFFECTS OF BETULINIC ACID IN A RAT MODEL OF CEREBRAL VENOUS ISCHEMIA

A. Heimann[1], K. Horiuchi[1,2], B. Alessandri[1], H. Li[3], O. Kempski[1]

[1]Institute for Neurosurgical Pathophysiology, Universitätsmedizin, Johannes Gutenberg-University, Mainz, Germany, [2]Department of Neurosurgery, Nara Medical University, Nara, Japan, [3]Department of Pharmacology, Johannes Gutenberg-University, Mainz, Germany

Background and aims: Betulinic acid, one of three triterpenoids which are isolated from traditional Chinese medical herbs, has been shown to up-regulate eNOS and to reduce the NADPH oxidase expression (J Pharmacol Exp Ther. 2007; 322(2):836-42). Furthermore betulinic acid sulfate is a potent inhibitor of the classical pathway of the complement system and a weak inhibitor of the alternative pathway (Bioorg Med Chem. 2007;15(10):3489-98). Thus, betulinic acid may be useful in the therapy of focal cerebral ischemia. Therefore this study was designed to investigate whether betulinic acid has neuroprotective potential in a rat model of focal venous ischemia.

Methods: 18 male Wistar rats were randomized into two groups, anaesthetized, intubated and ventilated. The tail artery was canulated for blood pressure monitoring and blood gas control. Regional cerebral blood flow (rCBF) was assessed by laser Doppler scanning and tissue impedance was measured to monitor cell swelling and cortical spreading depression in the ipsilateral hemisphere. After stable baseline conditions two adjacent bridging veins were occluded photochemically (2-VO). During the initial 75 minutes after 2-VO ten cortical spreading depressions were elicited by intracortical injection of 150 mM KCl as metabolic challenge. Vehicle (n=9; DMSO) or betulinic acid (n=9; 30 mg/kg b.w.) was administered for seven days by daily gavage, before animals were euthanatized for histological infarct evaluation (HE-staining).

Results: Body weight, arterial blood pressure and blood gases did not differ between the experimental groups. At baseline rCBF ranged between 50.01±6.3 LD-units (vehicle) and 42.32±6.8 LD-units (betulinic acid) and was significantly decreased after 2-VO to 44% and 50% of baseline, respectively (Fig.1 A). During the initial 75 minutes after 2-VO cortical spreading depressions occurred 12.7±0.7 times in the vehicle group and 12.4±1.3 times in the betulinc acid group (ns.). Quantitative histological evaluation showed a significant infarct reduction from 3.81±2.21 mm3 in the vehicle to 1.90±1.1 mm3 in the betulinc acid group (Fig. 1B).

Conclusion: Betulinic acid has a neuroprotective effect in a rat model of venous focal cerebral ischemia. The inhibition of the complement system is a possible mechanism of action, since in the same model a C-1 inhibitor also reduced infarct size (BrainRes 1999; 838:210-213). Further studies have to determine the degree of contribution of complement inhibition and NO production to the observed infarct reduction.

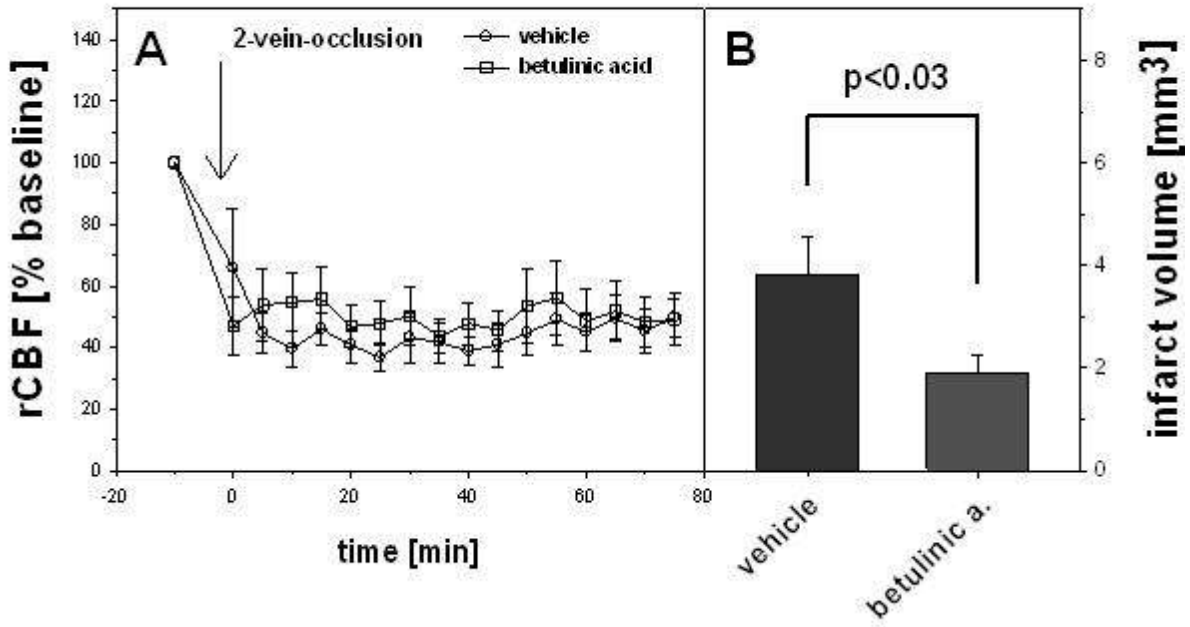
A
2-vein-occlusion
vehicle
betulinic acid
rCBF [% baseline]
time [min]
B
p<0.03
infarct volume [mm3]
vehicle
betulinic a.

[Fig 1.jpg]

Brain Poster Session: Neonatal Ischemia

PROTECTIVE EFFECTS OF PACAP AND VIP ON ISCHEMIA-SENSITIVE VASCULAR REACTIONS OF THE NEONATAL BRAIN

F. Bari[1], L. Lenti[1], A. Zimmermann[1], D. Kis[1], O. Oláh[1], G. Tóth[2], D. Busija[3], F. Domoki[1]

[1]Department of Physiology, [2]Department of Medical Chemistry, Faculty of Medicine, University of Szeged, Szeged, Hungary, [3]Department of Physiology and Pharmacology, Wake Forest University Health Sciences, Winston-Salem, NC, USA

Pituitary adenylyl cyclase activating polypeptide (PACAP) and vasoactive intestinal peptide (VIP) are structurally related peptides sharing at least partially the same receptors. Both neuropeptides are potent vasodilators of the cerebral circulation, and also, they are neuroprotective in numerous experimental models. Still, it is already evident that these two peptides are not completely identical in their action and each peptide activates multiple mechanisms. In piglets, PACAP38 dilates pial arterioles via cyclooxygenase (COX)-dependent mechanisms, while PACAP27-related vasodilation is insensitive to COX enzyme blockade (Lenti et al. 2007). The effect of VIP on the newborn pial vasculature has not been characterized yet. Impairment of cerebrovascular reactivity (CR) contributes to ischemia/reperfusion (I/R)-induced neuronal damage. However, neuroprotective mediators such as PACAP and VIP may be released from the neurovascular unit during I/R, which could reduce neuronal injury. In our present work we sought to characterize the VIP-induced vasodilation. Furthermore, we tested if PACAP and VIP preserve CR to endothelium- or neuron-dependent I/R-sensitive dilator responses. Pial arteriolar diameters were determined via the closed cranial window/intravital microscopy technique in anesthetized, ventilated piglets (1 day old, n=86). First, we tested the vasodilator potency of VIP (10^{-8}-10^{-6} M, topically) on the newborn pial vasculature. Prior to the repeated VIP application vehicle, the non-selective COX inhibitor indomethacin (5 mg/kg) or the selective COX-1 and COX-2 inhibitors SC-560 (1 mg/kg) and NS-398 (1 mg/kg) were administered intravenously. The involvement of nitric oxide synthase (NOS) was also evaluated using the NOS inhibitor N-omega-nitro-l-arginine methyl ester (L-NAME 15 mg/kg iv). In the second set of experiments vascular responses to hypercapnia (5-10% CO_2 ventilation) or topical N-methyl-D-aspartate (NMDA, 10^{-4} M) were measured before and after I/R. Prior to I/R, non-vasoactive doses of PACAP27, PACAP38 (10^{-8} M), VIP (10^{-9} M), or vehicle were applied onto the cortex. VIP evoked concentration-dependent, repeatable pial arteriolar dilation (15±3-69±8%*, mean±SEM, n=8, *p< 0.05) in our model. This vascular response was partially COX-1-dependent, since indomethacin and SC-560 abolished the vasodilation at the lowest VIP concentration (15±4 % and -1±3%* dilation before and after indomethacin, n=7); however, arteriolar responses remained intact when applying higher doses. I/R significantly attenuated hypercapnia- and NMDA-induced vasodilations that were both preserved by either PACAP27 or 38. For instance, post-ischemic CR to NMDA (vehicle vs. PACAP27, CR expressed as % of response before I/R, n=6-6) was 31±10 vs. 94±10%*, and CR to 10% CO_2 was 27±8 vs. 101±19%* (n=6-6). VIP also protected the CO_2-evoked response (88±13%* CR to 10% CO_2 after I/R, n=8), however, failed to preserve the NMDA-induced vasodilation after I/R (35±12% CR after I/R, n=6). In conclusion, VIP is potent vasodilator in the neonatal cerebral circulation by activating (at least at low concentration) COX-1-dependent pathways. PACAP- and VIP-induced neuroprotection is likely mediated in part by preservation of certain I/R-sensitive cerebrovascular mechanisms via at least partially different, specific ways of action.

Lenti L, Domoki F, Kis D, Hegyi O, Toth GK, Busija DW, Bari F. (2007) Pituitary adenylate cyclase-activating polypeptide induces pial arteriolar vasodilation through cyclooxygenase-dependent and independent mechanisms in newborn pigs. Brain Res 1165:81-88.

421

Brain Poster Session: Experimental Stroke & Cerebral Ischemia

CHANGE OF EXPRESSION OF OREXIN IN THE RAT BRAIN AFTER FOAL CEREBRAL ISCHEMIA

E. Kitamura, N. Kanazawa, S. Maruyama, J. Yonekura, R. Masuda, K. Koizumui, J. Hmada, F. Sakai

Kitasato University School of Medicine, Sagamihara, Japan

Objective: Orexin is known as a neuropeptide which controls feeding behavior, arousal or sleep behavior and has a function on maintenance of homeostasis. There are only few dozens of orexin containing neurons in hypothalamus. The orexinergic fibers are widely distributed in spinal cord and brain (1). Also orexin has some function on the brainstem neuronal nuclei related with the pathophysiological mechanism of migraine and brain ischemia (2,3). But the role of orexin in brain ischemia remains incompletely understood. In the present study, we investigated the expression of orexin in the rat brain after middle cerebral artery occlusion.

Methods: Twenty-eight male Sprague Dawley rats (350-500g) were anesthetized with isoflurane. An intraluminal occluder was made of 4-0 surgical nylon monofilament coated with silicone. An occluder was inserted through the left common carotid artery to occlude middle cerebral artery. At 120 min after the occlusion, the brain was recirculated. At 3(n=7), 6(n=7), 12(n=7) and 24h(n=7) after recirculation, rats were perfused with heparinized 0.1M PBS and Zamboni's fixative.After enucleating the brains, we soaked them in 30% sucrose for 3 days. 10-μm-thick frozen section stained with hematoxylin and eosin. And we used immunohistochemical staing. Double immunofluorescence labeling for orexin-A and MAP2 (Microtubule Associated Protein) was performed to investigate the expression of orexin in rat cortex and hypothalamus (primary antibody: anti orexin-A polyclonal rabbit antibody, anti MAP2 monoclonal mouse antibody). For statistical analysis, we used paired t-test.

Results: In all rats subjected to middle cerebral artery occlusion, an ischemic lesion was detected in the ipsilateral hemisphere on coronal sections stained with hematoxylin and eosin. In the cortex, there was no difference in the expression of orexin-A between ischemic hemisphere and contralateraral non ischemic hemisphere. In the hypothalamus, there was no significantly different in the number of neurons which expressed orexin-A at 3, 6 and 12h after recirculation. But at 24h recirculation, there was a significant difference in the number of neurons which expressed orexin-A in the hypothalamus. The number of neurons(36.7±19.6) which expressed orexin-A in the ischemic side was significantly larger comparing with the non-ischemic side (25.7±15.3)($p< 0.01$).

Conclusions: Our study suggested that at 24h after recirculation, in the hypothalamus, the number of the neurons which expressed orexin-A of the ischemic side was larger than that of the non ischemic side. Cortical spreading depression (CSD) was induced following focal brain ischemia. We have already shown that the intracerebroventricular administration of orexin inhibited CSD in the rat(in preparation). Given these reports, in the present study, it was suggested that orexin-A may give some influence on the pathophysiologial mechanism of focal cerebral ischemia.

References:

1. Cell. 1998 Feb 20;92(4):573-85.

2. Headache. 2007 Jun;47(6):951-62.

3. Neurosci Lett. 2002 May 10;324(1):53-6.

ROLE OF VASOPRESSIN V1A RECEPTORS FOR DEVELOPMENT OF SECONDARY BRAIN DAMAGE AFTER SUBARACHNOID HEMORRHAGE IN RATS

K. Hockel[1], K. Schöller[1,2], R. Trabold[1,2], N. Plesnila[1,2,3]

[1]Laboratory of Experimental Neurosurgery, Institute for Surgical Research, University of Munich Medical Center - Grosshadern, Ludwig-Maximilians-University, [2]Department of Neurosurgery, University of Munich Medical Center - Grosshadern, Ludwig-Maximilians-University, Munich, Germany, [3]Department of Neurodegeneration, Royal College of Surgeons in Ireland, Dublin, Ireland

Objectives: Mechanisms of early brain damage after subarachnoid hemorrhage (SAH) are poorly understood and mortality remains high. Arginine vasopressin (AVP) and its V1a receptores are involved in the development of secondary brain damage after traumatic brain injury (Trabold et al. 2009) and focal cerebral ischemia (Vakili et al. 2005). Thus, the aim of the present study was to investigate the role of AVP for brain edema formation, functional outcome and mortality following experimental SAH in rats.

Methods: Male Sprague-Dawley rats were anesthetized, intubated, and mechanically ventilated. SAH was induced using the filament perforation model. Mean arterial blood pressure (MABP), intracranial pressure (ICP), and regional cerebral blood flow (rCBF) were continiously recorded up to 60 minutes after SAH. Seconds prior to the insult animals received either a V1a receptor antagonist (V1880-1MG, 40 µg/kg bw i.v.) or vehicle (0.9% NaCl) for 3 hours. Brain water content was assessed by the wet and dry method 24 hours after SAH (n=8 per group). Functional deficits and mortality were analyzed over 7 days (n=10 per group). Plasma vasopressin concentration was determined at t=5, t=30 and t=120 minutes post SAH.

Results: Within 5 minutes after SAH plasma vasopressin increased 35-fold as compared to baseline ($p< 0.05$). Inhibition of V1a receptors prevented brain edema formation of the ipsilateral hemisphere ($p< 0.05$), resulted in a better neurological function ($p< 0.05$) and reduced 7-day mortality from 50% (vehicle group) to 20% ($p< 0.05$).

Conclusions: The present study shows that AVP is involved in the development of secondary brain damage after SAH via V1a receptors. The early systemic application of a V1a receptor antagonist lead to significantly reduced mortality and improved neurologic function, most likely due to reduced brain edema formation. Therefore V1a receptor antagonists may be potent novel drugs for the reduction of secondary brain damage after subarachnoid hemorrhage.

References:

Trabold R, Krieg S, Scholler K, Plesnila N (2009) Role of Vasopressin V(1a) and V(2) Receptors for the Development of Secondary Brain Damage after Traumatic Brain Injury in Mice. J Neurotrauma.

Vakili A, Kataoka H, Plesnila N (2005) Role of arginine vasopressin V1 and V2 receptors for brain damage after transient focal cerebral ischemia. J Cereb Blood Flow Metab 25:1012-1019.

423

Brain Poster Session: Neuroprotection

PROTECTIVE EFFECT OF HISPERIDIN ON TRANSIENT FOCAL CEREBRAL ISCHEMIA IN MALE WISTAR RATS

S. Raza, **F. Islam**

Dept of Toxicology, Hamdard University, New Delhi, India

Introduction: The adult brain consumes 3-4 ml O2/min per 100 g tissue, and this can represent up to 20% of all inhaled oxygen. When cerebral circulation is altered, oxygen consumption in the ischemic zone is dramatically reduced, thus inducing significant neuronal injury (Chan, 2001). .An imbalance between oxidant and antioxidant has been postulated to lead the neurodegeneration in cerebral ischemia-reperfusion injury(Mao-Tsun Lin, 2002).

Hypothesis: In this study, we examined whether Hisperidin, an antioxidant can prevent or slowdown neuronal injury in cerebral ischemia.

1. Lipid peroxidation.
2. Antioxidant enzymes activity.

Materials and methods: Animals were pretreated with oral Hisperidin (25 mg/kg for 15 days). The middle cerebral artery of adult male Wistar rats was occluded for 1 hr and reperfused for 22 h(Longa et.al.,1989).

Results: Hisperidin was found a good antioxidant in up-regulating the antioxidant status, lowering the TBAR's level and recovering results close to baseline.

Discussion: The activity of antioxidant enzymes and content of GSH was decreased significantly in MCAO group as compared with sham. The rats of MCAO+Hisperidin group have shown a significant protection in the activity of above-mentioned antioxidant enzymes and content of glutathione when compared with MCAO group. Increase in lipid peroxidation after MCAO in ipsilateral and contralateral hemisphere of brain was observed which was reduced by Hisperidin treatment.Further Histopathological changes and its attenuation in drug treated animal confirm the result.

Conclusion: These results suggest the neuroprotective potential of Hisperidin in cerebral ischemia and is mediated through its antioxidant activity.

Refrences:

1) El-Sayed el-SM, Abo-Salem OM, Abd-Ellah MF, Abd-Alla GM.J Biochem Mol Toxicol. 2008 Jul;22(4):268-73.Hesperidin, an antioxidant flavonoid, prevents acrylonitrile-induced oxidative stress in rat brain.

2) Longa EZ, Weinstein PR, Carlson S, Cummins R.Stroke. 1989 Jan;20(1):84-91.Reversible middle cerebral artery occlusion without craniectomy in rats.

3) Morita-Fujimura Y, Fujimura M, Yoshimoto T, Chan PH.Stroke. 2001 Oct;32(10):2356-61.Superoxide during reperfusion contributes to caspase-8 expression and apoptosis after transient focal stroke.

4) Yang CY, Lin MT.Stroke. 2002 Mar;33(3):790-4.Oxidative stress in rats with heatstroke-induced cerebral ischemia.

PRELIMINARY CLINICAL STUDY IN PATIENTS WITH HEMISPATIAL NEGLECT AFTER STROKE BY NEGLECT TEST BATTERY AND ^{99M}TC-ECD SPECT

Y. Yin, Y. Li, X. Li

Nuclear Medicine, No.1 Hospital of China Medical University, Shenyang, China

Objective: To explore the presence, clinical characters, anatomical foci in image, and mechanism of Hemispatial neglect (HSN), neglect test battery and SPECT rCBF imaging were performed on patients with stroke.

Methods: Thirty dextromanual patients who were diagnosed as having unilateral stroke clinically were recruited. A neglect test battery including line bisection test, star cancellation test and drawing test was performed on the subjects. The severity of neglect was measured on neglect tests. The lowest rCBF, the range with decreased rCBF, number of the foci with decreased rCBF, the flow deficit size and the total number of pixels in the foci were measured on SPECT rCBF imaging.

Results: Twenty-five patients were diagnosed as having HSN by the neglect test battery. Contralateral neglect (CN) and ipsilateral neglect (IN) were observed in both right and left hemisphere strokes. On SPECT images, the patients with neglect had decreased rCBF in the frontal cortex most often, parietal, occipital, temporal cortices second often, and basal ganglia and thalamus in some cases. The patients who had two or more regions damaged showed neglect more often and severe. The correlation coefficients between rCBF in the foci, the decreased percentage of rCBF of the foci and the severity of neglect were -0.119 ($p>0.05$) and 0.221 ($p>0.05$). The correlation coefficients between the range, number of foci, the flow deficit size, the total number of pixels of the foci and the severity of neglect were 0.537 ($p< 0.05$), 0.493 ($p< 0.05$), 0.561 ($p< 0.05$), 0.466 ($p< 0.05$), respectively. No difference between CN and IN on SPECT images reached statistical significance.

Conclusions: The severity of neglect did not correlate with rCBF and the decreased percentage of rCBF in the foci, while it was significantly correlated with the range, number of foci, the flow deficit size and the total numbers of pixels of the foci significantly. And the patients with CN and IN did not show any difference on the presence of HSN, the manifestation on the neglect test battery and SPECT images. HSN is the damage of multiple sites, with combined damage resulting in more severe neglect.

LOW-FREQUENCY ULTRASOUND (60 KHZ) WITH VARIED DUTY CYCLE: EFFECTS ON ISCHEMIC BRAIN TISSUE AND THE INNER EAR

P. Reuter[1], J. Masomi[1], H. Kuntze[1], I. Fischer[2], A.-O. Viertmann[1], J. Marx[1], K. Helling[2], C. Sommer[3], B. Alessandri[4], O. Kempski[4], M. Nedelmann[5]

[1]Neurology, [2]Department of Otolaryngology, [3]Neuropathology, [4]Insitute of Neurosurgical Pathophysiology, Johannes Gutenberg-University, Mainz, [5]Neurology, Justus-Liebig University, Giessen, Germany

Background and aims: The thrombolytic activity of ultrasound, but also the safety of ultrasound thrombolysis depends on variation of technical ultrasound parameters. In a recent in vitro study, a longer duration of the duty cycle [relationship of the on-phase to the total duration of an ultrasound pulse] was shown to improve thrombolytic efficacy of ultrasound (Meunier et al., 2007). The aim of our study was to examine the effect of different duty cycle settings in vivo on brain tissue after occlusion of the middle cerebral artery.

Methods: To investigate the effects of 60 kHz pulsed ultrasound, rats were transcranially treated following reperfusion of the middle cerebral artery (90 minutes after induction of ischemia by use of the suture model). The duty cycle was set at 20% and 80%, while keeping time average intensity constant. Analysis included measurement of infarct volume (TTC-staining) and functional-neurological evaluation. An additional group of healthy animals was insonated with the same ultrasound setup, and acoustically evoked potentials were measured to examine side effects on the auditory system.

Results: Ultrasound at short duty cycle setting resulted in a significant increase of the ischemic lesion volume compared to control animals. This negative side effect could not be detected in prolonged on-phase pulsation (resulting in reduction of energy spikes within the pulse). Furthermore, insonation resulted in a reduction of auditory function (reduction of the auditory threshold level up to 40 dB).

Conclusions: The results demonstrate that longer duty cycles not only positively influence the therapeutic effects but are also beneficial with regard to safety issues. The findings may serve as a basis for future developments of prototype therapeutic ultrasound devices. The study is first to describe side effects on the auditory system, which may further limit clinical utility of low frequency ultrasound in therapeutic applications. Further histological investigation of the tissue (brain and auditory system) may give more insight into the nature of the observed side effects.

References: J. M. Meunier, C. K. Holland, C. J. Lindsell, and G. J. Shaw. Duty cycle dependence of ultrasound enhanced thrombolysis in a human clot model Ultrasound Med Biol. 2007 April; 33(4): 576-583.

A NOVEL MODIFIED METHOD AND ITS CONFIRMATION OF INJECTION INTO CSF VIA THE CEREBELLOMEDULLARY CISTERN IN MICE

Y. Chen[1,2], A. Ito[1], N. Saito[1]

[1]Department of Neurosurgery, Faculty of Medicine, University of Tokyo, Tokyo, Japan, [2]Department of Neurosurgery, Sir Run Run Shaw Hospital, Medical College of Zhejiang University, Hangzhou, China

Background and aims: Central administrations of delivering drugs and chemotherapeutic agents are very difficult to be applied in mice related to the small size. Injection into the cerebellomedullary (CM) cistern is one of the options of central administrations. As its location is relatively fixed, it has potent advantantage than intraventricular administration under some pathological state, especially in supratentorial lesion models. We aimed to obtain a more accurate method for Injection into the CM cistern in mice.

Methods: We modified the method firstly introduced by Ueda et al. We choose the prone position with nape elevation and extension under inhalation anesthesia. The nape of the neck was incised at the midline. The hand-made curved tip of a 27 gauge dental needle was inserted into the cleft between the occiput and the atlas vertebra through the muscles and ligaments, being warranted on the line between sagittal suture and midline of nape. A volume of 6 μl methylene blue aqueous solution was injected slowly into the CM cistern to check accuracy. Mice were sacrificed 1 hour (n=8), 6 hours (n=6) or 24 hours (n=6) after injection.

Results: Twenty C57BL/6 mice were used to check our modified method and all succeeded without any serious vital or neurological deficits. The dye in the injection place and the intracranial distribution (CM cistern, ventral cisterns, trigerminal nerve and optic nerve roots) could be recognized within 6 hours after injection. The dye was disappeared in all places while being checked 24 hours after injection.

Conclusions: Our new method of injection into CM cistern is easy to be grasped and can become a common method to examine chemical substances' effects on central nerve system in mice. It is no use for dye injection along with the drug procedure for confirmation if mice were sacrificed beyond 6 hours after injection.

Brain Poster Session: Neuroprotection

NEUROPROTECTIVE EFFECTS OF METAPLEXIS JAPONICA ON GLOBAL AND FOCAL CEREBRAL ISCHEMIA RAT MODELS

D. Lee[1], N.R. Pandit[1], N. Jamarkattel[1], J.-G. Kim[2], M.-Y. Kim[1], M. Song[1], J. Park[2], D. Lim[1], J.Y. Kim[1], Y. Bu[1], H. Kim[1,2]

[1]Herbal Pharmacology, College of Oriental Medicine, Kyung Hee University, [2]Korea Institute of Science and Technology for East Medicine (KISTEM), Neumed Co. Ltd, Seoul, South Korea

Objectives: Metaplexis japonica (Apocynaceae) is a perennial herb, extensively used in traditional chinese medicine like consumptive disease, impotence, seminal emission, white vaginal discharge, agalactia, scroful. The purpose of our study was to evaluate the protective effect of M. japonica and its different fractions against in vitro and in vivo ischemia.

Methods: In the present study, we fractionated the 70% EtOH extract of M. japonica with different polarity solvents and administered the resulting fractions at a dose 100 mg/kg to the rats and subjected to the middle cerebral artery occlusion (MCAo) rat model and four-vessel occlusion (4-VO) model of global ischemia. Oxygen-glucose deprivation followed by reoxygenation was used to investigate the effects of M. japonica in neuronal cell line. We used the intraluminal suture method induced by the transient MCAo for 2 h followed by 24 h reperfusion in rats. After 24 h of MCAo, the infarction volume was measured by TTC staining. Functional effects of M. japonica and its fractions were investigated by Rota-rod and balance beam test 20 h after MCAo. 4-vessel occlusion was induced for 10 min followed by 7 d reperfusion.

Results: The effect on neuronal damage was measured 7 days after ischemia. Infarct volume after rats were subjected to 2 h MCAo and 24 h reperfusion was found as 33.0 ± 1.6% in vehicle treated group whereas M. japonica (30 and 100 mg/kg) showed 27.2 ± 3.6% and 16.1 ± 4.0% ($p < 0.01$), respectively. Hexane, EtOAc and BuOH fractions treated group showed 24.9 ± 5.2%, 12.6 ± 2.9% ($p < 0.001$) and 19.2 ± 4.2% ($p < 0.01$) infract volume respectively.

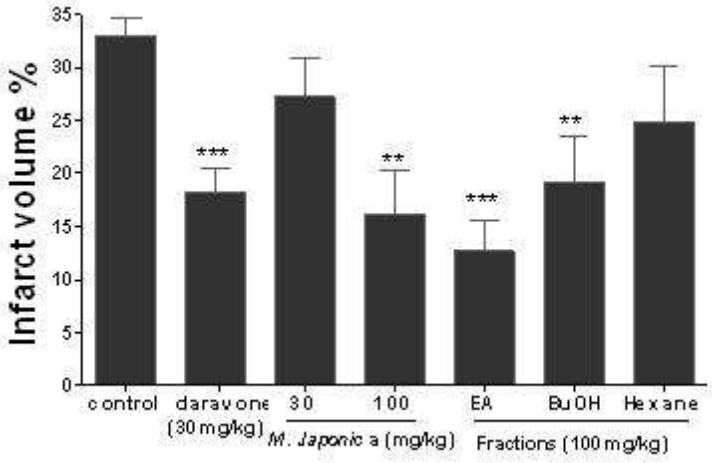

[Fig. 1.]

M. japonica at 300 mg/kg reduced hippocampal neuronal cell death by 13.03% as compared with a vehicle-treated group in 4-VO.

Conclusions: M. japonica and its fractions protected the hippocampal neuronal cell death, reduced brain damage and improved behavioral deficits in stroke rat model.

Acknowledgments: This work was supported by a grant (PF 0320201-00) from Plant Diversity Research Center of 21st Century Frontier Research Program (Ministry of Science and Technology, Korea), and by grants from the Second Stage of Brain Korea 21 Project (Ministry of Education, Korea).

References:

1) Zea Longa EL, Weinstein PR, Carlson S, Summins R. Reversible middle cerebral artery occlusion without craniectomy in rats. Stroke 1989; 20: 84-91.

2) Pulsinelli WA and Brierley JB. A new method of bilateral hemispheric ischemia in the unanesthetized rat. Stroke 1979; 10: 267-272.

Brain Poster Session: Brain Edema & Water Transport

THE EFFECTS OF PIOGLITAZONE TREATMENT ON THE REGULATIONS OF AQUAPORIN-4 AND ADIPONECTIN IN OLETF RATS

T. Shimazu[1], K. Takayanagi[2], H. Hasegawa[2], R. Suge[3], M. Ninomiya[4], J. Asakura[2], Y. Kato[4], M. Yamashiro[2], T. Mitarai[2], N. Araki[4]

[1]Neurology, Saitama Neuropsychiatric Institute, [2]Nephrology and Hypertension, Saitama Medical School, Medical Center, [3]Physiology, [4]Neurology, Saitama Medical University, Saitama, Japan

Objectives: Aquaporin (AQP), especially AQP-4 has been seen to be involved not only in the brain edema formation (1), but also in several disorders including trauma and cerebral ischemia. In addition, several preliminary studies have demonstrated that AQP-4 may be concerning with learning ability in rats with cognitive impairment. Recently, it is recognized that peroxisome-proliferators-activated receptor gamma (PPAR gamma) agonists improve disability of cognitive function in patients with early Alzheimer disease (2) and stroke in diabetes (3). We were interested in the possible effect of pioglitazone (PPAR-gamma agonist) on the expression of AQP-4 in deabetic brain. The Otsuka Long-Evans Tokushima Fatty (OLETF) rat, an outbred strain of Long Evans Tokushima Otsuka rat (LETO), lacks CCK-1 receptor and is an animal model of type-2 diabetes. It has been reported that the OLETF was selectively impaired learning ability, depending on types of learning.

Methods: OLETF and LETO (22 weeks age, male, n = 5 each) were used as subjects. Half of each group was administrated pioglitazone (20 mg/kg/day) orally. All subjects were sacrificed at 24-weeks old, and brains were removed. Plasma adiponectin levels were measured after 14days of treatment.

Brains were subdivided into four different parts, cortex, cerebellum, hippocampus and striatum. These samples were applied to RNA extraction or immunostaining. Total RNA was extracted by GITC method. Synthesized single strand cDNA was applied to real time PCR amplification with TaqMan probes. Results were analyzed by DCTmethod.

Results: AQP-4 expression in cortex of OLETF was greater than that of LETO, while effect of pioglitazone was not significant. In hippocampus, AQP-4 expression of OLETF was significantly increased comparing to LETO. Administration of pioglitazone attenuated the increase in AQP-4 expression in OLETF. Plasma adiponectin levels significant increased in OLETF rats with pioglitazone treatment.

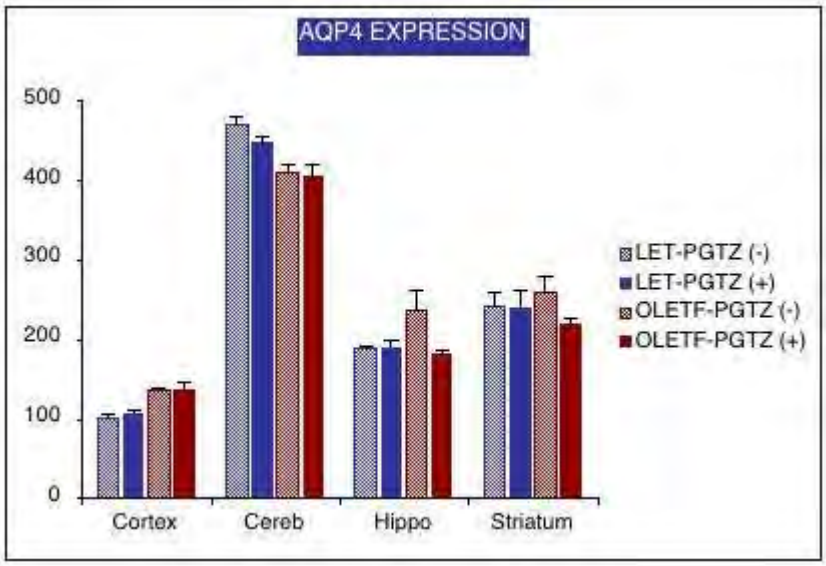

[AQP-4]

Conclusions: These results indicate that in the OLETF rats pioglitazone has an important role in the diabetes cognitive function treatment through the regulation of AQP-4 expression and adiponectin. In hippocampus the AQP-4 expression of OLETF may be related to be increased circulating adiponectin level in response to pioglitazone treatment.

References:

1. Taniguchi M, Yamashita T, et al. (2000): Brain Res Mol Brain Res 78, 131-137.

2. Watson GS., Cholerton BA., et al. (2005): The American Journal of Geriatric Psychiatry 13, 950-958.

3. Wicox R., Bousser MG., et al. (2007): Stroke 38, 865-873.

Brain Poster Session: Hemorrhagic Transformation

MULTIPARAMETRIC MRI OF PATHOPHYSIOLOGICAL PROCESSES INVOLVED IN HERMORRHAGIC TRANSFORMATION AFTER EMBOLIC STROKE IN SPONTANEOUSLY HYPERTENSIVE RATS

I.A.C.W. Tiebosch, R. Zwartbol, M.J.R.J. Bouts, R.M. Dijkhuizen

Image Sciences Institute, University Medical Center Utrecht, Utrecht, The Netherlands

Objectives: Risk of hemorrhagic transformation (HT) limits thrombolytic treatment against acute ischemic stroke. Elucidation and delineation of the pathophysiological basis of HT after stroke may lead to improvement of treatment strategies. Multiparametric MRI uniquely allows serial in vivo assessment of multiple pathophysiological processes involved in HT.[1] The goal of this study is to characterize MRI profiles of ischemic regions that develop HT in a clinically relevant model of embolic stroke in spontaneously hypertensive rats.

Methods: Spontaneously hypertensive rats (SHRs, n=17) were subjected to unilateral embolic ischemic stroke[2] as part of a large study on effects of combination treatment strategies. Researchers are blinded for treatment assignments. At 0-2 h, 24 h and 7 days post-stroke, tissue damage, perfusion status and blood-brain barrier (BBB) integrity were assessed with diffusion-, T_2-, T_2*-, perfusion- and post-contrast (Gadobutrol) T_1-weighted MRI.[3] After MRI at day 7, rats were sacrificed and brains were excised and sectioned. Regions with clear blood accumulation within the ischemic lesion were identified as HT areas. HT regions and non-HT areas within the lesion, as well as their contralateral counterparts, were outlined on the MR images. The temporal profiles of the T_2, T_2*, apparent diffusion coefficient (ADC), cerebral blood flow index (CBF_i), cerebral blood volume (CBV) and contrast leakage through the BBB were measured in these regions and satistically compared by a repeated measures one-way ANOVA with post hoc Student-Newman-Keuls testing ($P < 0.05$ was considered significant).

Results: Eleven SHRs completed the experimental protocol, of which five showed HT.

Acutely after stroke, ADC and CBF_i were significantly reduced in HT and non-HT areas. Contrast-enhanced T_1-weighted signal was significantly elevated in HT but not in non-HT regions.

After 24 h, ADC was still decreased in the entire ischemic lesion, while T_2, T_2* and contrast leakage had increased. In HT regions, T_2 elevation and contrast leakage were larger than in non-HT areas. In addition, CBV and CBF_i were considerably lowered in HT regions at this stage.

At day 7, when HT was identified histologically, T_2^* values were significantly lower in HT as compared to non-HT regions (but not as compared to contralateral). Also, contrast leakage remained strongly elevated in HT areas.

Conclusions: We found that HT after stroke in SHRs, particularly after 24 h, is associated with locally reduced perfusion, largely increased BBB leakage and substantial edema, indicative of severe ischemia. HT may be directly detected by T_2^* shortening[4], however in our study T_2^* in HT areas was considerably influenced by T_2^* prolongation due to edema formation. Nevertheless, HT was implied by a T_2^* drop between 24 h and 7 days, which was not the case for the non-HT regions. Our study confirms that multiparametric MRI allows characterization of pathophysiological processes involved in HT. Furthermore, MRI of perfusion status and BBB integrity may provide prognostic information on risk of HT after stroke.

References:

[1] Jiang et al., JCBFM 2002;22(5):559-568;

[2] Zhang et al., Brain Res 1997;766:83-92;

[3] Dijkhuizen et al. JCBFM 2001;33(8):2100-2104;

[4] Neumann-Haefelin, Neuroreport 2001;12:309-311.

Funding: Netherlands Heart Foundation (2005B156).

Brain Poster Session: Stem Cells & Gene Therapy

GENE EXPRESSION IN THE BRAIN AFTER INSONATION WITH ULTRASOUND: A COMPARISON BETWEEN EXPERIMENTAL AND DIAGNOSTIC ULTRASOUND PROBES

P. Reuter[1], A. Fabrizius[2], M. Nedelmann[3], J. Marx[1], B. Alessandri[4], O. Kempski[4], T. Hankeln[2]

[1]Neurology, [2]Molecular Genetics, Johannes Gutenberg-University, Mainz, [3]Neurology, Justus-Liebig University, Giessen, [4]Insitute of Neurosurgical Pathophysiology, Johannes Gutenberg-University, Mainz, Germany

Background and aims: Latest experimental and clinical studies could show that the use of diagnostic ultrasound (3 MHz) in addition to rtPA treatment successfully enhances thrombolysis cerebral vessel occlusion. However, a potential effect on gene expression is unknown, but should be considered for safety reasons.

The aim of this study was to examine the effects of ultrasound treatment on cerebral gene expression. For this purpose, three ultrasound probes of different frequencies (3 MHz diagnostic probe; 60 and 488 kHz experimental probes) were compared.

Methods: The brain of healthy rats was transcranially insonated with the above probes. For measuring the gene expression we extracted RNA of the cerebral cortex and transcribed the RNA into cDNA. After normalization to reference genes (GAPDH, actin, cyclophillin A, ARP and albumin) we measured expression of several candidate genes from different functional groups (major focus: apoptosis, angiogenesis, NO-metabolism, stress). Gene expression levels were determined by quantitative Real-Time RT-PCR (qPCR) assays.

Results: The measurement of mRNA-expression of selected genes with qPCR showed significant differences between insonated and non-insonated animals. As one example, insonation with the diagnostic ultrasound probe induced a doubled increase of gene expression of the pro-apoptotic gene bcl-2. Most of the regulations were detected after insonation with 488kHz ultrasound. We found an up to 3-fold change after 4 or 24 hours for 14 of the 24 studied genes compared to sham-insonated animals. Angiogenesis factors (Vegfa, Egfr, Egr1) showed a decreased expression. Fewest regulations were detected after insonation with the 60 kHz ultrasound probe (3 of 24 measured genes).

Conclusions: The results of this study indicate that not only histological changes can be observed after ultrasound treatment, but also changes of gene expression are detectable. Most of the changes were found after treatment with 488 kHz ultrasound. Further studies have to identify whether these changes have a positive or negative effect on the ischemic lesion. Additionally these findings give reasons to a global gene expression study.

431

Brain Poster Session: Cerebral Metabolic Regulation

EFFECT OF VALPROATE ON RAT CEREBRAL GLUTAMINE METABOLISM: A CARBON 13 CELLULAR METABOLOMIC APPROACH APPLICABLE TO DRUG DEVELOPMENT

M. El Hage, B. Ferrier, G. Baverel, G. Martin

Metabolys Inc., Lyon Cedex, France

Objectives: It is well established that glutamine metabolism plays a central role in brain functions; indeed, glutamine is both synthesized in astrocytes to detoxify glutamate and ammonia and metabolized in neurons for the provision of the neuromediators glutamate and GABA. The objectives of the present study were:

i. to provide a panoramic view of cerebral glutamine metabolism in brain slices in vitro and
ii. to evaluate this model and the cellular metabolomic approach as tools for drug research and development.

Methods: For this, slices prepared from rat brain hemispheres were incubated under appropriate conditions with 5 mM L-[3-^{13}C]glutamine in the absence and the presence of 1 mM valproate, a widely used antiepileptic drug. At the end of incubation, substrate removal and product formation were measured by both enzymatic and carbon 13 NMR spectroscopy methods.When combined with an original mathematical model of cerebral glutamine metabolism, the latter methods allowed to calculate fluxes through the enzymatic steps involved.

Results: In the absence of valproate, 3-^{13}C-glutamine was used as substrate at high rates by glutaminase but the glutamine removal measured enzymatically was much smaller than the 3-^{13}C-glutamine removal indicating that glutamine synthesis also occurred in astrocytes. Concomitant removal of the glutamate present at zero-time and 3-^{13}C-glutamate accumulation were also observed. The lactate found at zero-time was also used as substrate and only a small ^{13}C-lactate synthesis occurred. Small amounts of unlabeled alanine but not of pyruvate accumulated. GABA accumulation was found by both enzymatic and NMR measurements; GABA was found labeled mainly on its C3 (direct synthesis) and, to a very small extent, on its C2 (indirect synthesis). Accumulation of aspartate, labeled mainly on its C2 and C3 and, to a lesser extent, on its C1 and C4 was also observed. Labeling of glutamate and glutamine on carbons other than their C3 reveals that resynthesis of both amino acids occurred. Approximately half of the C3 of the 3-^{13}C-glutamine removed was released as CO_2.

In the presence of valproate, 3-^{13}C-glutamine removal was slightly inhibited, but net glutamine synthesis, glutamate accumulation and labeling, lactate removal and labeling as well as alanine accumulation remained unchanged. Aspartate accumulation and labeling on its C2 and C3 (but not on its C1 and C4) and GABA labeling on its C3 were decreased by valproate. The addition of valproate also diminished the production of $^{13}CO_2$.

Flux calculations indicate that valproate slightly inhibited flux through glutaminase and caused an accumulation of GABA by the direct pathway. It also inhibited fluxes through succinate semialdehyde dehydrogenase plus alpha-ketoglutarate dehydrogenase, succinate dehydrogenase, fumarase, malic enzyme, aspartate aminotransferase and pyruvate carboxylase. By contrast, valproate did not alter fluxes through alanine aminotransferase, lactate dehydrogenase, pyruvate dehydrogenase, citrate

synthase, aconitase, isocitrate dehydrogenase, glutamate dehydrogenase, glutamine synthetase and glycogen phosphorylase.

Conclusion: It is concluded that the model used in vitro and the cellular metabolomic approach employed are suitable for studying the beneficial and adverse interactions of drugs with brain energy and intermediary metabolism.

INFANT BRAINSTEM IS PRONE TO THE GENERATION OF SPREADING DEPRESSION DURING SEVERE HYPOXIA

M. Müller, M. Kron, M. Dutschmann, F. Funke

Zentrum Physiologie und Pathophysiologie, Universität Göttingen, Göttingen, Germany

Background and aims: Spreading depression (SD) resembles a concerted, massive neuronal/glial depolarization. Being associated with cerebropathology it is well studied in cortex and hippocampus. Brainstem tissue, however, is considered to be quite resistant to the generation of SD. Nevertheless, there have been recent in vivo studies showing that - upon proper preconditioning - SD can also be induced in the brainstem of rats [1,2]. We have now analyzed under which conditions hypoxic SD (HSD) can be induced in rat brainstem slices.

Methods: Acute brainstem slices (400 μm) were prepared from infant and adult rats and placed in an interface recording chamber (35-36°C). HSD was induced by severe hypoxia (95% N_2, 5% CO_2) and was followed by extracellular DC potential recordings and optical imaging of the intrinsic optical signal (IOS), complemented by monitoring extracellular K^+ changes and sharp-electrode recordings from single neurons.

Purpose: Detailed analysis of the spatiotemporal profile of HSD in acute rat brainstem slices.

Results: In brainstem slices (preconditioned by increasing extracellular K^+ to 8 mM) severe hypoxia triggered SD within a few minutes. The sudden HSD-related extracellular DC potential shift of approximately -20 mV showed the typical profile known from other brain regions and was accompanied by an IOS, i.e. an increase in light scattering within the tissue [3]. Spatiotemporal IOS analysis revealed that in infant brainstem, HSD was preferably ignited within the spinal trigeminal nucleus (Sp5) and spread out mostly medially invading the hypoglossal nucleus, the nucleus of the solitary tract (NTS), and occasionally the ventral respiratory group (VRG). The neuronal hypoxic depolarizations underlying the generation of HSD were massive, but incomplete. At the peak of HSD Sp5 neurons maintained a membrane potential of -35 mV. The propagation velocity of HSD (3.1±1.5 mm/min, n=17) and the extracellular K^+ peak level (49.5±19.4 mM, n=8) were less marked than in other brain regions. In adult brainstem HSD was mostly confined to the NTS. Its occurrence was facilitated by hypotonic solutions (15 mM NaCl omitted) but not by glial poisoning (5 mM fluoroacetate, 3-5 hours) or block of GABAergic and glycinergic synapses (20 μM bicuculline plus 0.5 μM strychnine, 20 min).

Conclusions: Brainstem tissue reliably generates propagating HSD episodes, which may be of interest for basilar-type migraine and brainstem infarcts. The preferred occurrence of HSD in the infant brainstem and its propagation into the VRG may be of importance for neonatal brainstem pathology such as sudden infant death syndrome.

Supported by the DFG (CMPB) and the BMBF (BCCN-Göttingen).

References:

(1) Richter F., Ruprecht S., Lehmenkühler A., Schaible H.G. (2003). Spreading depression can be elicited in brain stem of immature but not adult rats. J Neurophysiol 90: 2163-2170.

(2) Richter F., Bauer R., Lehmenkühler A., Schaible H.G. (2008). Spreading depression in the brainstem of adult rat: electrophysiological parameters and influences on regional brainstem blood flow. J Cereb Blood Flow Metab 28: 984-994.

(3) Müller M., Somjen G.G. (1999). Intrinsic optical signals in rat hippocampal slices during hypoxia-induced spreading depression-like depolarization. J Neurophysiol 82: 1818-1831.

OPTIMISATION OF SUPERVISED CLUSTER ANALYSIS FOR EXTRACTING REFERENCE TISSUE INPUT CURVES IN (R)-[^{11}C]PK11195 STUDIES

M. Yaqub[1], B.N.M. Berckel[1], A. Schuitemaker[2], R. Hinz[3], F.E. Turkheimer[4], A.A. Lammertsma[1], R. Boellaard[1]

[1]Nuclear Medicine and PET Research, [2]Neurology and Alzheimer Centre, VU Universite Medical Centre, Amsterdam, The Netherlands, [3]Wolfson Molecular Imaging Centre, University of Manchester, Manchester, [4]Neuroscience, Imperial College London, London, UK

Background and aims: (R)-[^{11}C]PK11195 is widely used for imaging activated microglia in the brain. To date, (R)-[^{11}C]PK11195 studies have primarily been analysed using reference tissue methods with one of the following reference tissues: cerebellum, grey matter cerebrum or automatic extraction by cluster analysis methods[1,2]. The aim of the present study was to further investigate performance of a recently published supervised cluster algorithm (SVCA)[1], including a new simplified reference tissue method (SRTM) with blood volume correction[3] and use of a reduced number of predefined kinetic classes[2] within SVCA to improve quantification.

Methods: (R)-[^{11}C]PK11195 data was taken from young healthy controls (YC), elderly healthy controls (OC) and Alzheimer's Disease patients (AD). Cerebellum (CER) and thalamus regions were defined manually in grey and white matter. In order to extract reference tissue curves, supervised cluster analysis methods were evaluated for 6 (SVCA6) [1] and 4 kinetic classes (SVCA4) [2]. CER input functions were also used for comparison. Kinetic analyses were performed using both SRTM with non-linear regression and a basis function implementation (RPM) of SRTM. RPM analysis was performed both with and without correction for fractional blood volume (V_B) using image derived blood input curves [3]. Data were also analysed using the reversible two tissue plasma input model with correction for fractional blood volume (2T4k). Thalamus was the region interest and parameters of interest were BP_{ND} for RPM/SRTM, and DVR-1 for 2T4k. DVR is the thalamus to reference tissue distribution volume of ratio. V_T using 2T4k were also evaluated for reference tissues.

Results: Averages (±SD) of reference tissue V_T showed comparable trends for CER (1.01±0.39, 0.85±0.32, 0.78±0.23; YC, OC, AD), SVCA4 (0.92±0.38, 0.68±0.26, 0.58±0.15) and SVCA6 (1.07±0.49, 0.84±0.37, 0.82±0.20) across subject groups.

Thalamus DVR-1 estimates were best using SVCA4 (0.14±0.14, 0.29±0.07, 0.44±0.32), second for CER (0.035±0.134, 0.047±0.049, 0.066±0.159) and poorest for SVCA6, showing higher values in OC (0.075±0.133) than in AD (0.008±0.167).

Without V_B correction, RPM and SRTM showed similar results. Overall, SVCA4 showed more plausible results than CER and SVCA6, i.e. better distinction between YC, OC and AD (Fig. 1), and better correlation with corresponding DVR-1 (R^2=0.47). Finally, for SVCA4 and SVCA6, RPM with V_B correction did not show significantly better results than without such a correction (Fig. 1).

Conclusions: Supervised cluster analysis with 4 kinetic classes is the method of choice for extracting reference tissue curves in [^{11}C](R)-PK11195 studies.

References:

[1] Turkheimer et al; J Nucl Med 2007;48:158-167.

[2] Boellaard et al; IEEE Nucl Sc & MIC, Dresden, 2008.

[3] Tomasi et al; J Nucl Med 2008;49:1249-1256.

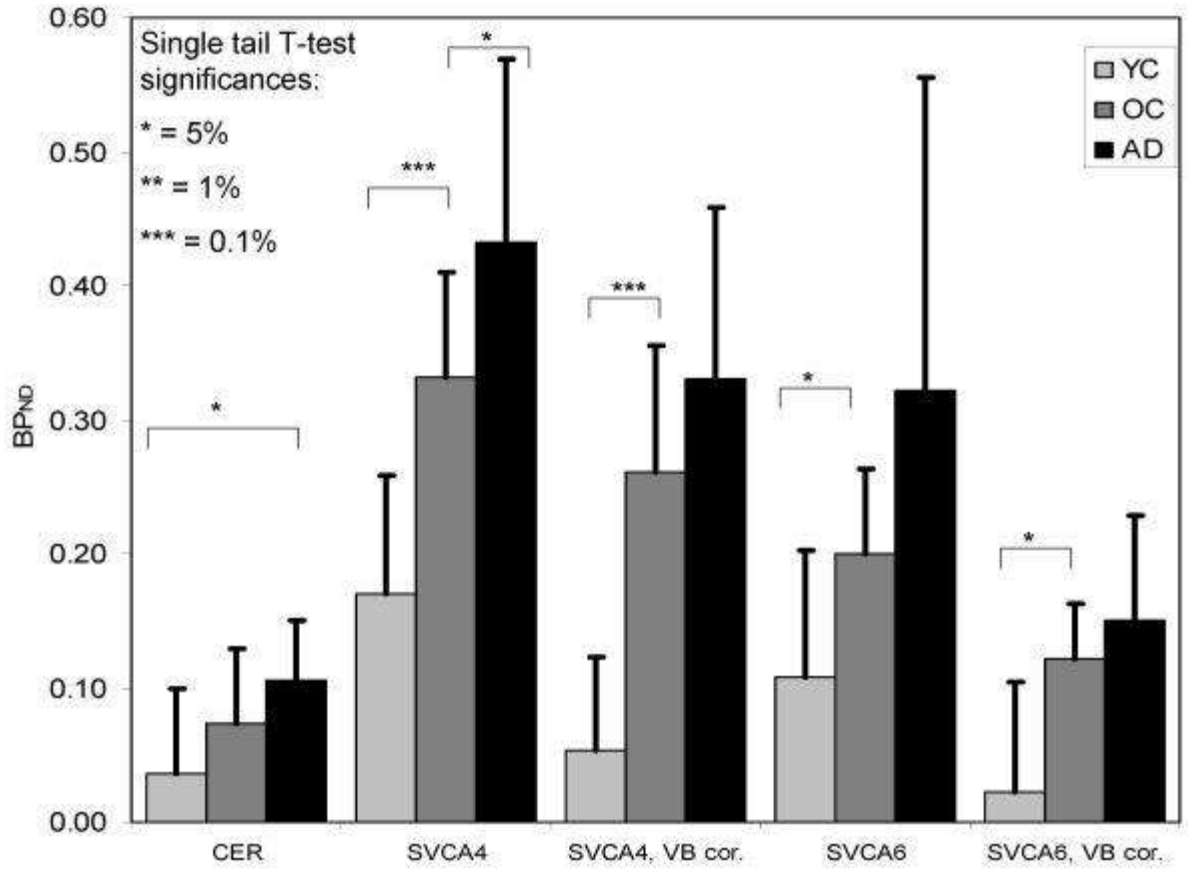

[Fig. 1]

Fig. 1: Thalamus BP_{ND} estimated using RPM, with and without a correction for V_B (VB cor.) and different reference tissue input curves (CER, SVCA4 and SVCA6).

DISTURBED K^+-CHANNEL ACTIVITY OF HIPPOCAMPAL CA1 NEURONS DURING CYANIDE-INDUCED ANOXIA IN A MOUSE MODEL OF RETT SYNDROME

M. Kron, M. Müller

Zentrum Physiologie und Pathophysiologie, Universität Göttingen, Göttingen, Germany

Background and aims: Rett syndrome is a neurodevelopmental disorder caused by mutations in the X-chromosomal MECP2-gene. $Mecp2^{-/y}$ knockout mice - a model of Rett syndrome - show an imbalance of inhibitory and excitatory synaptic transmission(1). Recently, we unveiled an enhanced hypoxia susceptibility of the hippocampus of $Mecp2^{-/y}$ mice which seems to arise from disturbed potassium fluxes(2). The present study aims to identify dysfunctional K^+-channels.

Methods: Experiments were conducted in acute hippocampal slices of $Mecp2^{-/y}$ and wildtype (WT) males (postnatal day 40). Sharp-electrode recordings were performed in CA1 pyramidal neurons to quantify changes in membrane potential and input resistance in response to 1 mM cyanide (chemical anoxia) under control conditions and in the presence of glibenclamide or charybdotoxin. Single-channel recordings were performed in inside-out and cell-attached patches.

Purpose: Identification of disturbed neuronal K^+-channels in Rett syndrome.

Results: Intracellular recordings did not reveal significant differences in pyramidal cell resting membrane potential (-56.7±3.8 mV vs. -58.7±12.1 mV) and input resistance (86±40 MΩ vs. 74.8±27.3 MΩ) between WT and $Mecp2^{-/y}$ pyramidal neurons. Cyanide elicited an initial hyperpolarization (-7.1±3.7 mV) and decreased the input resistance (-34%) in WT neurons. In $Mecp2^{-/y}$ neurons both the hyperpolarization and decrease in input resistance were dampened by ~50%. These initial responses were followed by a progressive (terminal) depolarization. In the presence of the BK-channel blocker charybdotoxin (10 nM), cyanide caused an initial depolarization in WT (5.1±3.8 mV) and Mecp2-deficient pyramidal neurons (4.5±4.8 mV). In WT neurons, the subsequent hyperpolarization became more pronounced (-10.2±5.5 mV) but remained unchanged in $Mecp2^{-/y}$ neurons. In the presence of the K_{ATP}-channel blocker glibenclamide (50-100 µM), cyanide caused an initial depolarization in WT (2.9±5.7 mV) that also occurred in $Mecp2^{-/y}$ pyramidal neurons (4.4±4.2 mV). The subsequent hyperpolarization was virtually unchanged in WT neurons but was detectable in only 55% of the recorded $Mecp^{-/y}$ neurons. To assess the modified function of K^+-channels during anoxia in more detail, single-channel analyses were performed. In cell-attached patches, cyanide caused a pronounced activation of a tolbutamide-insensitive intermediate-conductance (80 pS) K^+-channel in WT neurons, but only a moderate activation in $Mecp2^{-/y}$ neurons. Basic BK-channel properties were unchanged, but BK-channels became massively activated in $Mecp2^{-/y}$ neurons during the terminal depolarization.

Conclusions: The enhanced hypoxia susceptibility of the $Mecp2^{-/y}$ hippocampus seems to arise from disturbed K^+-channel function. As a result, the cyanide-induced hyperpolarization is weakened. Accordingly, during early hypoxia, the membrane potential is stabilized less efficiently. Also the ability to compensate pharmacological K_{ATP}-blockade during metabolic arrest seems impaired. The enhanced activation of the BK-channel in $Mecp2^{-/y}$ neurons may suggest more pronounced intracellular Ca^{2+}-rises during anoxia.

Supported by the DFG (CMPB).

References:

(1) Medrihan L, Tantalaki E, Aramuni G, Sargsyan V, Dudanova I, Missler M, Zhang W (2008).

Early defects of GABAergic synapses in the brain stem of a MeCP2 mouse model of Rett syndrome. J Neurophysiol **99**:112-121.

(2) Fischer M, Reuter J, Gerich FJ, Hildebrandt B, Hägele S, Katschinski D, Müller M (2009). Enhanced hypoxia susceptibility in hippocampal slices from a mouse model of Rett syndrome. J Neurophysiol, in press.

437

Brain Poster Session: Cerebral Metabolic Regulation

METABOLIC ROLE OF AQUAGLYCEROPORIN 9 IN ASTROCYTES

C. Guérin[1], J.-F. Brunet[1], N. Mastour[1], L. Regli[2], L. Pellerin[3], **J. Badaut**[1,4,5]

[1]Neurosurgery, Lausanne University Hospital, Lausanne, Switzerland, [2]Neurosurgery, University Medical Center Utrecht, Utrecht, Netherlands Antilles, [3]Physiology, Lausanne University, Lausanne, [4]Clinical and Fundamental Neurosciences, University of Geneva, Geneva, Switzerland, [5]Pediatrics, Loma Linda University, Loma Linda, CA, USA

Aim: Aquaglyceroporin-9 (AQP9) is a member of the Aquaporin channel family involved in water flux through plasma membranes and exhibits the distinctive feature of also being permeable to glycerol and monocarboxylates. AQP9 is detected in astrocytes and catecholaminergic neurons (Badaut et al. 2004). However, the presence of AQP9 in the brain is now debated after a recent publication claiming that AQP9 is not expressed in the brain (Rojek et al. 2007). Based on our results (Badaut et al. 2008), we have evidence of the presence of AQP9 in the brain and we further hypothesize that AQP9 plays a functional role in brain energy metabolism.

Methods: The presence of AQP9 in brain of OF1 mice was studied by RT-PCR and immunohistochemistry. To address the role of AQP9 in brain, we used commercial siRNA against AQP9 to knockdown its expression in 2 cultures of astrocytes from two distinct sources (from differentiated stem cells (Brunet et al. 2004) and primary astrocyte cultures). After assessment of the decrease of AQP9, glycerol uptake was measured using [H^3]-glycerol. Then, modifications of the astrocytic energy metabolism was evaluated by measurement of glucose consumption, lactate release (Pellerin and Magistretti 1994) and evaluation of the mitochondrial activity by MTT staining.

Results: AQP9 is expressed in astrocytes of OF1 mouse brain (mRNA and protein levels). We also showed that AQP9 mRNA and protein are present in cultured astrocytes. Four days after AQP9 siRNA application, the level of expression is significantly decreased by 76% compared to control. Astrocytes with AQP9 knockdown exhibit a 23% decrease of glycerol uptake, showing that AQP9 is a glycerol channel in cultured astrocytes. In parallel, astrocytes with AQP9 knockdown have a 155% increase of their glucose consumption without modifications of lactate release. Moreover, considering the observed glucose consumption increase and the absence of proliferation induction, the significant MTT activity increase (113%) suggests an increase of oxidative metabolism in astrocytes with AQP9 knockdown.

Discussion: The involvement of AQP9 in astrocyte energy metabolism adds a new function for this channel in the brain. The determination of the role of AQP9 in astrocytes provides a new perspective on the controversial expression of AQP9 in brain. We also suggest that AQP9 may have a complementary role to monocarboxylate transporters in the regulation of brain energy metabolism.

Financial support: SNF-3100AO-108001 and 31003A-122166, Novartis foundation.

References:

Badaut J et al.(2008) Induction of brain aquaporin 9 (AQP9) in catecholaminergic neurons in diabetic rats. Brain Res 1188:17-24.

Badaut J et al. (2004) Distribution of Aquaporin 9 in the adult rat brain: preferential expression in catecholaminergic neurons and in glial cells. Neuroscience 128:27-38.

Brunet JF et al.(2004) Early acquisition of typical metabolic features upon differentiation of mouse neural stem cells into astrocytes. Glia 46:8-17.

Pellerin L, Magistretti PJ.(1994) Glutamate uptake into astrocytes stimulates aerobic glycolysis: a mechanism coupling neuronal activity to glucose utilization. Proc Natl Acad Sci U S A 91:10625-10629.

Rojek AM, et al.(2007) Defective glycerol metabolism in aquaporin 9 (AQP9) knockout mice. Proc Natl Acad Sci U S A 104:3609-3614.

ADAPTIVE OPTIMAL DESIGN IN PET OCCUPANCY STUDIES

S. Zamuner[1], V.L. Di Iorio[1], J. Nyberg[2], R.N. Gunn[3,4], V.J. Cunningham[3], R. Gomeni[1], A.C. Hooker[2]

[1]Clinical Pharmacology Modelling & Simulation, Glaxosmithkline, Verona, Italy, [2]Div. of Pharmacokinetics and Drug Therapy, Dept. of Pharmaceutical Biosciences, Uppsala University, Uppsala, Sweden, [3]GlaxoSmithKline Clinical Imaging Centre, Imperial College - London, London, [4]Dept. of Engineering Science, University of Oxford, Oxford, UK

Objectives: The integration of positron emission tomography (PET) occupancy studies into clinical drug development plans provides a valuable tool for dose selection and optimization in man by accurately characterising the relationship between the time-course of plasma drug (PK) concentration and target receptor occupancy (RO)[1].

PET studies are typically conducted using a sequential adaptive design. An initial cohort of subjects is treated with an initial dose with scan times usually targeting the maximal plasma concentration and/or a lower concentration. The decision on sample size, dose and scan times for subsequent cohorts is derived from the analysis of previous data. The selection of informative doses and scan times remain critical issues for a precise and accurate characterization of the PK-RO relationship.

The purpose of this work is to define and evaluate the benefit of an adaptive-optimal PET experiment strategy for the selection of PET scan times and doses, over and above traditional PET study designs using simulated experimental data.

Methods: A population kon-koff model relating the plasma concentration of the drug and the PET binding potential (BP) was applied to generate the simulated data. Twelve subjects were considered and designs with 3, 4, and 6 adaptive steps were investigated. BP time-course data were simulated from the following designs: fixed designs (sampling schedule fixed at baseline, tmax and 24 hours post-dose), educated designs where sampling schedule was selected from an independent expert, and optimal designs. One hundred studies per design were simulated to test the performance of the adaptive/optimal algorithm.

In the proposed adaptive/optimal algorithm, dose and PET sampling times for the first cohort were fixed. This information was used to estimate the model parameter values. These values were used to select doses and PET scan times in the next cohort. For each subsequent cohort data from all previous cohorts were used as prior information to select doses and PET scan times.

Optimization was performed for two scenarios; scanning time only and scanning time and dose using a D-optimality criterion as implemented in the PopED software[2].

Results: A clear improvement in terms of bias (SME), precision (CV) and accuracy (RMSE) of the population estimates (kon and koff) was found when comparing fixed vs. educated vs. optimal designs. Unbiased mean estimates were found for the optimal designs; a great improvement in accuracy was found when comparing optimal vs. fixed designs (25-30 fold) and still a significant improvement was found when comparing optimal vs. educated designs (2-3 fold). Optimisation over both sampling times and doses compared with optimisation over only sample times provided slight improvements in accuracy and precision when the initial dose selection was not informative about the receptor binding time course.

Conclusions: These results indicate that adaptive optimal design of PET occupancy studies provides a reliable strategy for study design by optimally selecting doses and scan times which then allow for a more accurate assessment of the pk-occupancy relationship.

References:

[1] Lim, K.S, et al. Clin Pharmacol Ther. 81, 252-8 (2007).

[2] Foracchia, M. et al. Comput Methods Programs Biomed, 74, 29-46 (2004).

BrainPET Poster Session: Molecular Brain Imaging: Clinical Applications

WIDESPREAD MICROGLIA ACTIVATION IN RECENT ONSET SCHIZOPHRENIA

B. van Berckel[1,2], M. Yaqub[1], A. Schulte[3], M. Bossong[2], R. Boellaard[1], R. Kloet[1], A. Schuitemaker[4], N. van Haren[2], G. Luurtsema[1], B. Windhorst[1], W. Cahn[2], A. Lammertsma[1], A. Rozemuller[3], R. Kahn[2]

[1]Nuclear Medicine & PET Research, VU University Medical Center, [2]Psychiatry, Rudolf Magnus Institute for Neuroscience, [3]Pathology, [4]Neurology, VU University Medical Center, Amsterdam, The Netherlands

Objectives: Schizophrenia is a brain disease involving progressive loss of grey matter of unknown cause. Most likely, this loss reflects neuronal damage, which should in turn be accompanied by microglia activation. The aims of this study were to assess regional microglia activation in vivo using (R)-[^{11}C]PK11195 and PET, and to measure activated microglia in post-mortem brains of patients with schizophrenia.

Methods: For the PET study, ten patients with schizophrenia (age: 24 ± 2 years, 9 male) within five years of disease onset and ten healthy controls (23 ± 4 years, 7 male) were included. Dynamic (R)-[^{11}C]PK11195 scans (60 minutes) in 3D acquisition mode were performed using an ECAT EXACT HR+ (CTI/Siemens). Arterial blood was withdrawn continuously using an on-line detection system (Veenstra). At set times, discrete blood samples were taken to determine both plasma to whole blood ratios and parent (R)-[^{11}C]PK11195 fractions. All sinograms were corrected for dead time, tissue attenuation, decay, scatter and randoms, and were reconstructed using a standard filtered back projection algorithm and a Hanning filter with a cut-off at 0.5 times the Nyquist frequency. Subjects also underwent an MRI scan and MRI images were aligned to corresponding PET images to define various regions of interest (ROI) using an automatic procedure. (R)-[^{11}C]PK11195 PET scans were analyzed using a supervised cluster analysis method. This method was recently validated for analysis of (R)-[^{11}C]PK11195 data and yields binding potential (BP_{ND}) as outcome measurement[1].

In addition, a post-mortem study was performed. Autopsy was performed on the brains of ten patients with schizophrenia and without other neurological diseases (age between 18 and 72 years). Disease duration was much longer than 5 years. Brain tissue of frontal cortex was used for immunohistochemical evaluation of microglia and astrocytes (using HLADR and GFAP, respectively).

Results: Results of the PET study are shown in Table 1.

Region	Schizophrenia	Controls	Significance
Total Brain	0.093 ± 0.037	0.004 ± 0.035	<0.001
Cerebellum	0.256 ± 0.066	0.168 ± 0.049	<0.05
Hippocampus	0.034 ± 0.055	-0.063 ± 0.059	<0.05
Cingulate Ant	0.118 ± 0.052	0.042 ± 0.069	<0.05

Thalamus	0.207 ± 0.093	0.123 ± 0.050	<0.05
Sup Temp	0.154 ± 0.057	0.083 ± 0.065	<0.05
Parietal	0.134 ± 0.036	0.106 ± 0.068	ns
Occipital	0.282 ± 0.089	0.226 ± 0.076	ns
Striatum	0.100 ± 0.069	0.060 ± 0.062	ns

[Table 1: (R)-[11C]PK11195 BP-ND for various ROI.]

In the post-mortem study, an increase in the number of activated microglia cells and reactive astrocytes was seen in only 5 subjects. No relation with age was found.

Conclusion: There is widespread activation of microglia in recent onset schizophrenia.

EFFECT OF IMIDAPRIL ON CEREBRAL PRODUCTION OF NITRIC OXIDE DURING CEREBRAL ISCHEMIAN AND REPERFUSION IN MICE

H. Nagoya, T. Ohkubo, Y. Asano, K. Hattori, T. Shimazu, M. Yamazato, Y. Kato, Y. Ito, N. Araki

Neurology, Saitama Medical University, Saitama, Japan

Objectives: It is suggested that the angiotensin-converting enzyme (ACE) inhibitors shift the autoreguration curve to left, and has antiarteriosclerotic effects, and protectect against the cerebral ischemia. We investigated the effect of Imidapril on the cerebral nitric oxide production in the C57BL/6 mice in steady state and during ischemia and reperfusion.

Methods: Twenty male C57BL/6 mice were used: control group [n=10], and Imidapril group (Imidapril was administered 1mg/kg a day for two weeks) [n=10]. The animals were anesthetized with 2% halothane and maintained with 0.5-1% halothane. NO production was continuously monitored by in vivo microdialysis. A microdialysis probe was inserted into the left striatum and perfused with Ringer's solution at a constant rate of 2 µl/min. After 2 hours equilibrium period, fractions were collected every 10 minutes. A laser Doppler probe was placed on the right skull surface. Global ischemia was produced by clipping both common carotid arteries using Zen clip for 10 minutes. The levels of nitrite (NO_2^-) and nitrate (NO_3^-) in the dialysate samples were measured by the Griess reaction.

Results:

1. Mean blood pressure; There were no significant differences between the two groups before cerebral ischemia and during ischemia. The Imidapril group showed significantly lower BP than that of the control group after reperfusion.
2. Cerebral blood flow; There was no significant difference between the two groups.
3. NO_2^- : The level of NO_2^- in the Imidapril group [2.34 ± 0.71 µmol/ L(mean ± SD)] before ischemia was significantly higher than that of control group [1.35±0.47µmol/ L] ($p< 0.05$). There was no significant difference between the two groups during ischemia and after reperfusion. (Fig.1)
4. NO_3^- ; There was no significant difference between the two groups.
5. Total NO (NO_2^-+NO_3^-): The level of total NO in the Imidapril group [3.95 ± 1.13µmol/ L(mean ± SD)] before ischemia was significantly higher than that of control group [2.84 ± 0.85µmol/ L] ($p< 0.05$). (Fig.2)

Conclusion: This study suggests that Imidapril increases NO production in the baseline level (before cerebral ischaemia). As Imidapril increases the baseline level, it is difficult to analyze the effect of imidapril on the NO production during ischemia and reperfusion.

【Fig.1】

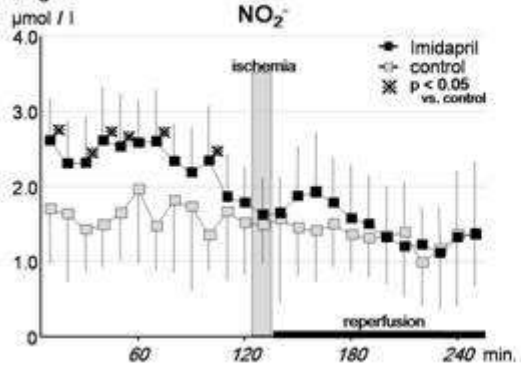

【Fig.2】

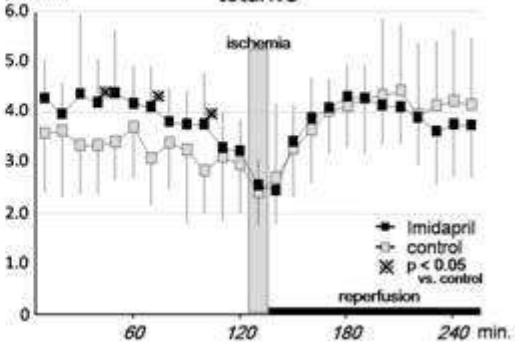

[production of nitric oxide]

EFFECT OF PTERYGOPALATINE ARTERIAL BLOOD FLOW CANNOT BE IGNORED IN A MOUSE MODEL OF INTRALUMINAL SUTURE MIDDLE CEREBRAL ARTERY OCCLUSION

Y. Chen[1,2], A. Ito[1], K. Takai[1], N. Saito[1]

[1]Department of Neurosurgery, Faculty of Medicine, University of Tokyo, Tokyo, Japan, [2]Department of Neurosurgery, Sir Run Run Shaw Hospital, Medical College of Zhejiang University, Hangzhou, China

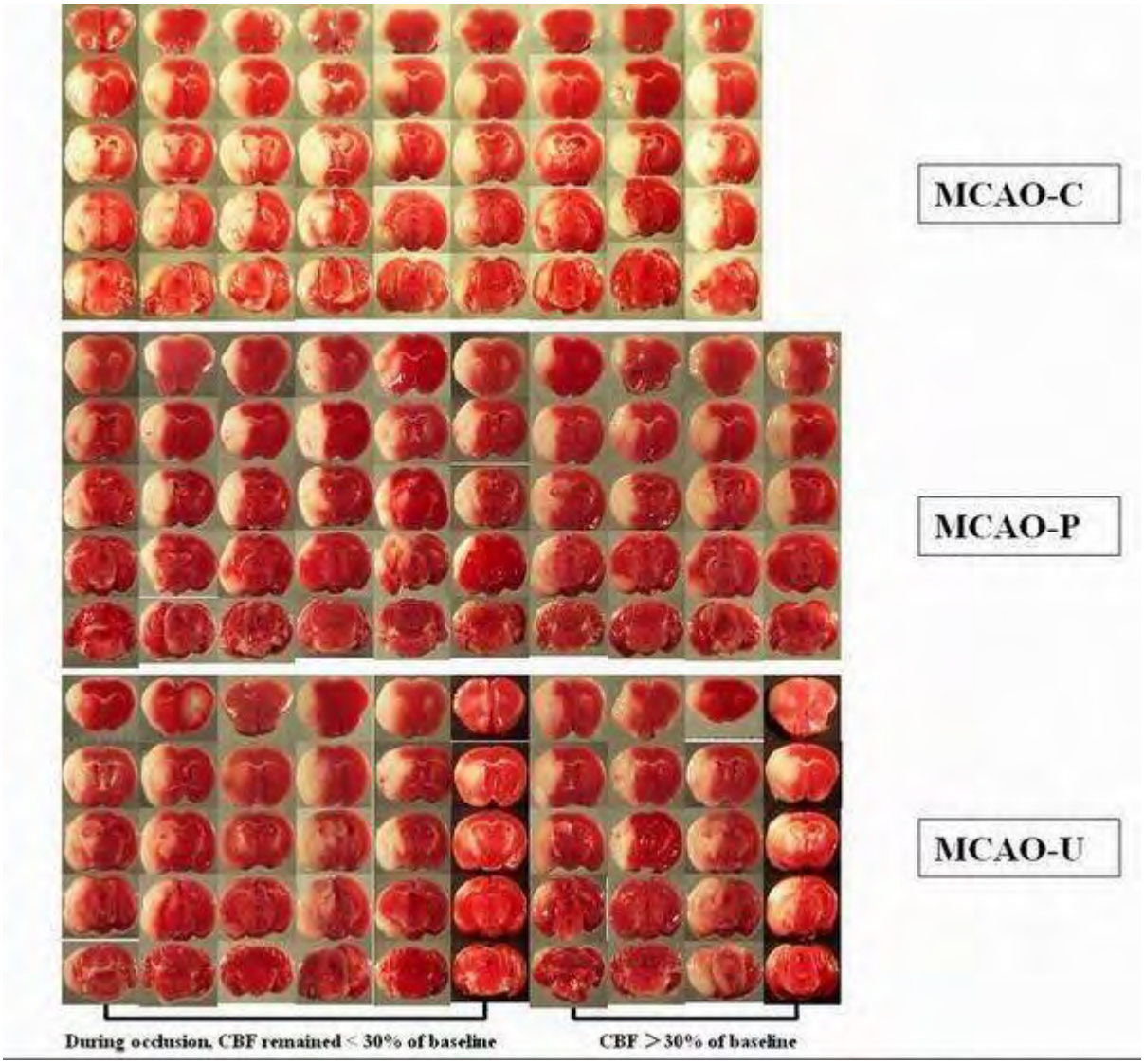

[Staining with TTC. All sections from 3 groups]

Background and aims: The mouse model of intraluminal suture middle cerebral artery occlusion (MCAO) is still associated with several issues, such as variability of infarction volume and survival. Collateral blood flow and surgical methods contribute to these problems. To produce MCAO in mice, the pterygopalatine artery (PPA) is not normally cut or blocked because of technical demands related

to the position of this artery and the size of the mouse. The effect of blood flow in the (PPA) in the mouse MCAO model was evaluated.

Methods: While producing mouse MCAO models using commercially available silicone-coated monofilaments, we temporarily occluded the common carotid artery (CCA) or PPA to determine whether cerebral blood flow (CBF) values, infarct size and the stability of the model would be affected.Forty male C57BL/6 mice were divided into 3 groups: MCAO with blocked CCA blood flow (MCAO-C; n = 12), MCAO with blocked PPA blood flow (MCAO-P; n = 16) and MCAO without either CCA or PPA blood flow blockage (MCAO-U; n = 12).

Results: The CBF values were significantly higher during occlusion in the MCAO-U than in the other two groups ($p < 0.001$). We stained whole brains from each group at 24 h after reperfusion with 2% 2,3,5-triphenyltetrazolium chloride. Although mean infarct volume did not obviously differ between the MCAO-U and other two groups, infarct volumes varied significantly more within the MCAO-U, than in the other two groups ($p < 0.05$).

Conclusions: Collateral circulation from the PPA to the brain significantly influences the mouse MCAO model, and cannot be ignored. An approximately consistent mouse MCAO model can be generated using commercially available silicone-coated sutures while blocking PPA blood flow during occlusion.

Brain Poster Session: Neonatal Ischemia

IL-10 OVEREXPRESSION BY NON-VIRAL GENE THERAPY AFTER EXCITOTOXIC NEONATAL BRAIN DAMAGE

P. Gonzalez[1], **L. Acarin**[1], H. Peluffo[2], A. Aris[3], A. Villaverde[3], B. Castellano[1], B. Gonzalez[1]

[1]Neuroscience Institute and Dept. Cell Biology, Physiology and Immunology, Autonomous University of Barcelona, Barcelona, Spain, [2]Pasteur Institute of Montevideo and Department of Histology and Embryology, Faculty of Medicine, UDELAR, Montevideo, Uruguay, [3]Institute of Biology and Biotechnology, Autonomous University of Barcelona, Barcelona, Spain

Background and aims: As a result of its strong anti-inflammatory nature, together with the well known involvement of inflammation in determining lesion outcome of central nervous system (CNS) pathologies, interleukin-10 (IL-10) has shown a great neuroprotective potential after adult CNS injuries. However, very little is known about its putative anti-inflammatory and neuroprotective role in the damaged immature CNS, where its specific particularities, suggest a differential scenario for IL-10 actions. Therefore, the aim of the present study was to evaluate the anti-inflammatory and neuroprotective potential of IL-10 overexpression after neonatal brain excitotoxic damage.

Methods: IL-10 overexpression was induced by means of non-viral gene therapy in NMDA-injected postnatal day 9 rat brain. Following several survival times ranging from 12 hours until 7 days post-lesion, samples were processed for PCR techniques, ELISA analysis, western blotting, histological techniques and double immunofluorescent labeling.

Purpose: Evaluate changes in lesion volume, neurodegeneration rate, astroglial and microglial activation, neutrophil infiltration, production of pro-inflammatory cytokines and expression inflammatory related enzymes induced by IL-10 overexpression after neonatal excitotoxicity.

Results: IL-10 overexpression increased lesion volume and the density of degenerating neurons at early survival times after the excitotoxic damage. In parallel, IL-10 treated animals displayed an increased density of microglia/macrophages and a reduced astroglial content of intermediate filament proteins like GFAP and vimentin. Moreover, IL-10 overexpression enhanced neutrophil recruitment to the brain parenchyma and production of inflammatory related enzymes such as cyclooxygenase-2 (COX-2) and inducible nitric oxide synthase (iNOS). Finally, IL-10 overexpression did not induce any variation in interleukin-1β and tumour necrosis factor α production but a slight increase in interleukin-6 content at later survival times.

Conclusions: IL-10 overexpression in the excitotoxically damaged postnatal rat brain is unexpectedly deleterious for lesion outcome and modulates the main associated inflammatory processes.

GREEN TEA (CAMELLIA SINENSIS) POTENTIATES EXTRAPYRMIDAL SYMPTOMS OF HALOPERIDOL: A STUDY IN RAT MODEL

T. Malik, D. Haleem

Neurochemistry and Biochemical Neuropharmacology Research Laboratory, Biochemistry, Karachi University, Karachi, Pakistan

Objectives: Schizophrenia, a psychiatric illness, has been treated with typical antipsychotic drug haloperidol (HAL). Although the treatment is associated with a high rate success but Extrapyramidal Symptoms (EPS) associated with the treatment is a serious limitation of the therapy. Some studies have suggested that oxidative stress induced during the metabolism of HAL is involved in the elicitation of EPS. The components of green tea (Camellia sinensis) have been demonstrated to have therapeutic efficacy in reducing oxidative stress. It has been reported that flavoniods of green tea have free radical scavenging properties thus antioxidant in nature. Therefore, it can be speculated that green tea may prevent the EPS induced by HAL.

Methods: In the cohort design of study we examined the efficacy of Green Tea Extract (GTE) (1g / L) on HAL (0.1g / kg) - induced EPS. Treatment was done for 5 weeks. Groups were tested for motor coordination on Rota-rod each week. Tardive Vacuous Chewing Movements (t VCMs) were also monitored by an observer blind to the treatment. The animals were scarified after 35^{th} hour of drug withdrawal. The brain samples from dorsal and ventral striatum were taken and analyzed by HPLC.

Results: We found that HAL - induced impairment of motor coordination were greater in GTE than water treated animals. The elicitation of t VCMs were also significantly greater in GTE treated animals. The metabolism of dopamine was greater in the Nuclease Accumbens (NA) in dorsal striatum of GTE plus HAL model than water plus HAL treated animals. The results suggest that increases of DA and metabolism in the dorsal striatum may be involved in the elicitation of greater EPS induced by HAL in GTE treated groups, conversely the levels of DA was decreased in the rest of the brain regions of GTE treated animals. It is suggested that an increase in DA metabolism observed in the Ventral Tegmental Area (VTM) of ventral striatum of GTE than water treated animals may potentiate schizophrenic symptoms.

Conclusion: Our results recommend that GTE intake may provoke more vulnerability to HAL - induced side effects and more likely to relapsed schizophrenic symptoms in patients treated with haloperidol. We suggest that patients on HAL therapy should avoid green tea. The mechanism by which green tea may potentiate HAL - induced EPS is discussed.

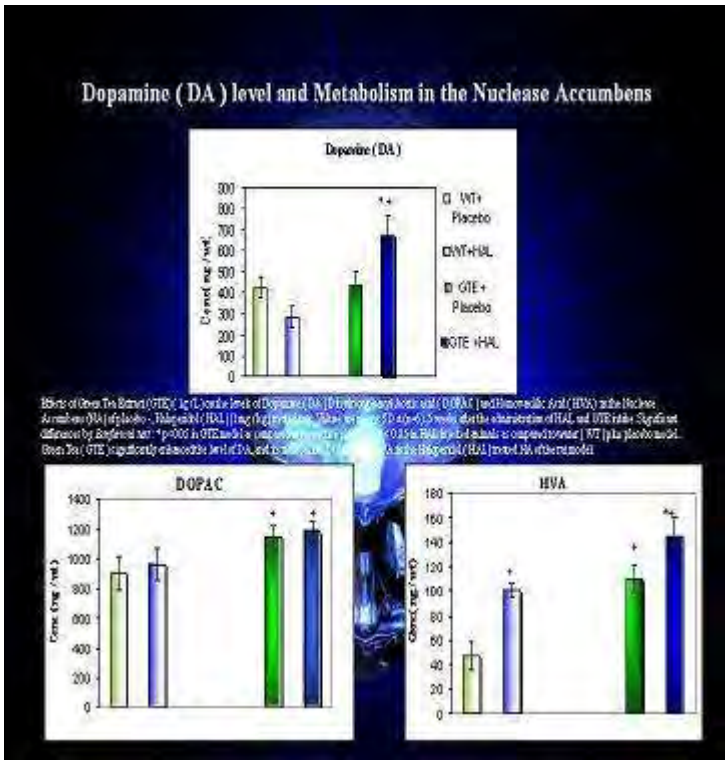

[Dopamine and Metabolism in the Nuclease Accumbens]

References:

1. Haleem, D.J., Samad, N. & Haleem, M.A. (2007). Reversal of haloperidol-induced tardive vacuous chewing movements and supersensitive somatodendritic serotonergic response by buspirone in rats. Pharmacol Biochem Behav, 87, 115-21.

2. Bishnoi, M., Chopra, K. & Kulkarni, S.K. (2008). Co-administration of nitric oxide (NO) donors prevents haloperidol-induced orofacial dyskinesia, oxidative damage and change in striatal dopamine levels. Pharmacol Biochem Behav.

3. Cho, H.S., Kim, S., Lee, S.Y., Park, J.A., Kim, S.J. & Chun, H.S. (2008). Protective effect of the green tea component, L-theanine on environmental toxins-induced neuronal cell death. Neurotoxicology, 29, 656-62.

HEMIN PROTECTS AGAINST PHOTOTHROMBOTIC CORTICAL ISCHEMIC INJURY IN MICE

J. You, H. Lee, S.J. Kim, C.D. Kim, W.S. Lee

Department of Pharmacology and MRCITR, Pusan National University School of Medicine, Yangsan, South Korea

This study aimed to investigate whether hemin can reduce mouse brain injury and facilitate the recovery following photothrombotic cortical ischemia in mice. Male C57BL/6 mice were anesthetized and systemically administered Rose Bengal. Permanent focal ischemia was induced in the medial frontal and somatosensory cortices by irradiating the skull with a cold light laser. Animals were treated with hemin and zinc protoporphyrin (ZnPP) 1 h after photothrombosis, and were sacrificed 24 h after ischemic insult. Hemin caused a significant reduction in the infarct size, the Evans blue extravasation index, and immunoreacitivities of PARP, but was without effect on HIF-1α expression, and furthermore induced a significant increase in the immunoreactivities of neuroglobin and heme oxygenase-1 (HO-1) in the ischemic region. These effects were reversed by co-treatment with ZnPP, a HO-1 inhibitor. It is suggested that hemin can facilitate the recovery following photothrombotic cortical ischemia via expression of neuroglobin and HO-1 proteins, and thereby indicating advantages in the therapeutic strategy for cerebral ischemia.

EFFECT OF THE RESVERATROL TREATMENT ON THE NA^+,K^+ -ATPASE ACTIVITY IN THE HIPOCAMPUS AND CORTEX OF GLOBAL CEREBRAL ISCHEMIA-EXPOSED RATS

F. Simão, A. Matté, C. Matté, F.M.S. Soares, A.T. Wyse, C.A. Netto, C.G. Salbego

Biochemistry, Federal University of Rio Grande do Sul, Porto Alegre, Brazil

Objectives: Cerebral ischemia causes an interruption of neuronal and glial oxidative metabolism and can lead to irreversible loss of brain function. Neuronal damage caused by global ischemia is associated with an imbalance in ionic (1). Na^+,K^+-ATPase is a membrane enzyme responsible for the active transport of sodium and potassium ions in the central nervous system, maintaining the ionic gradient necessary for neuronal excitability and regulation of neuronal cell volume (2). Resveratrol (RSV, trans-3,4,5-trihydroxystilbene) is a naturally occurring polyphenolic compound highly enriched in grapes, peanuts, red wine, and a wide variety of plants. RSV has been reported to elicit many cellular responses including cell cycle arrest, differentiation, and apoptosis, and it has antiinflammatory, antileukemic, neuroprotective, and antiviral properties (3). Previously we demonstrated that RSV was able to protect brain slices against lesion induced by oxygen and glucose deprivation (4). Here we investigated the effect of RSV treatment on the Na^+,K^+-ATPase activity in hippocampus and cerebral cortex of the rats submitted to global cerebral ischemia.

Methods: Global cerebral ischemia was induced in male wistar rats (300-350g) by four vessel occlusion for 10 min. Animal groups included in the study were: sham, sham plus RSV treatment, ischemic and ischemic plus RSV treatment (30 mg/kg i.p. for 7 days before ischemia). Neuronal injury was analyzed by Fluoro-Jade C and Nissl staining. The expression and activity of the Na^+,K^+-ATPase were measured in cortex and hippocampal homogenates by western blotting and by assaying the inorganic phosphate released from ATP, respectively. The effect of RSV on Na^+,K^+-ATPase was analyzed at 1 h, 24 h and 7days after global cerebral ischemia.

Results: Global cerebral ischemia induced a statistically significant decrease in the Na^+,K^+-ATPase activity in both, hippocampus and cortex, at 1h and 24h of reperfusion. Maximal decrease was observed 24 h after the ischemic damage. The decline in the Na^+,K^+-ATPase activity was prevented in the animals treated with RSV at 24 h of reperfusion. Our results indicate that global cerebral ischemia induced a significant alterations in the Na^+,K^+-ATPase activity in the hippocampus and cortex and RSV treatment prevented these changes in the Na^+,K^+-ATPase activity.

Conclusion: We suggest that the maintenance of Na^+,K^+-ATPase activity afforded by RSV could be related to cellular neuroprotection.

References:

(1) Siesjo BK, 1988. Crit. Care. Med. 16:954-962.

(2) Ericinska M and Silver IA, 1994. Prog. Neurobiol. 43:37-71.

(3) Virgili M and Contestabile A, 2000. Neurosci. Lett. 281:123-6.

(4) Zamin et al, 2006. Neurobiol. Dis. 24:170-182.

CHANGES IN PRESENCE AND ACTIVITY OF JNK ISOFORMS IN BRAIN MITOCHONDRIA OF RATS EXPOSED TO FOCAL CEREBRAL ISCHEMIA

Y. Zhao, T. Herdegen

Institute of Experimental and Clinical Pharmacology, University Hospital of Schleswig-Holstein, Campus Kiel, Kiel, Germany

Objectives: c-Jun N-terminal kinases (JNKs), a family of MAP kinases, are central mediators of apoptosis and neurodegeneration, but also of plasticity and regeneration. Current concepts suggest that it is the compartmentalisation rather than the mere substrate affinity which determines the physiological and pathological functions of individual JNKs. In contrast to the JNK mediated activation of pro-apoptotic Bcl-2 substrates, data on the presence and activation of JNK isoforms in mitochondria are rare. In the present study, we have analysed the localisation of JNK1, JNK2 and JNK3 isoforms in mitochondria isolated from ischemic cortices in rats exposed to transient middle cerebral artery occlusion (MCAO).

Methods: In male normotensive Wistar rats, the middle cerebral artery was occluded for 90 min followed by reperfusion. Two, 6 and 18 h after the onset of MCAO, the cortices from the ipsilateral hemisphere of rat brains were isolated for whole cell extraction, cytosol, nuclear and mitochondria isolation. The changes in protein levels of individual JNK isoforms were analysed by Western blots. Immunodepletion was used for the detection of individual phosphor-JNK isoforms.

Results: The mitochondrial preparations were free of cytoskeletal, nuclear and ER contaminations. The specificity of the used antibodies was demonstrated in preparations of brain mitochondria from JNK deficient mice. The majority of JNK is localized at the outer membrane or the adjacent space of the mitochondrion. In controls, all JNK isoforms were present in mitochondria with JNK1 as a dominant JNK isoform detected major carrier of a pronounced basal JNK activity. Following MCAO, the distribution pattern of JNKs in mitochondria completely changed. The presence and activity of JNK1 almost completely declined, whereas those of JNK3 and, to a minor extent, of JNK2 substantially raised. Complexes of MKK4:JNK1 were reduced, whereas complexes of MKK4:JNK3 and MKK7:JNK3 increased in rat brain mitochondria.

Conclusions: These data demonstrate that following cerebral ischemia, the basal physiological JNK1 activity in mitochondria is replaced by JNK2 and JNK3. JNK2 and JNK3 activity in mitochondria may be essential for the initiation of apoptosis and neurodegeneration and represent, therefore, a target for compartment-specific neuroprotective strategies.

BrainPET Poster Session: Brain Imaging: MRI/fMRI

CO-REGISTRATION OF T2*-WEIGHTED MRI WITH [^{14}C]-2-DEOXYGLUCOSE AUTORADIOGRAPHY TO VALIDATE DELINEATION OF THE ISCHAEMIC PENUMBRA

C. Robertson[1], C. McCabe[1], M.D.R. Lopez-Gonzalez[2], D. Brennan[2], L. Gallagher[1], W. Holmes[1], B. Condon[2], K. Muir[2], C. Santosh[2], I.M. Macrae[1]

[1]Glasgow Experimental MRI Centre (GEMRIC), University of Glasgow, [2]Institute of Neurological Sciences, Southern General Hospital, Glasgow, UK

Objectives: Accurate identification of the ischaemic penumbra is critical in determining whether stroke patients will benefit from thrombolysis and in the design of future clinical trials of potential neuroprotectants. We have recently developed a novel MRI technique that could potentially enable a more precise definition of the penumbra where 100% oxygen is used as a metabolic biotracer to detect tissue metabolism [1]. This 'oxygen challenge' (OC), has now been tested to validate that the penumbra, as defined by a T2* signal change during OC, equates with evidence of persisting tissue metabolism. This was achieved by co-registering T2* OC images with [^{14}C]-2-deoxyglucose (^{14}C 2-DG) autoradiograms, for determination of local cerebral glucose utilisation (LCMRglu) [2].

Methods: Male Sprague Dawley rats (300-323g, n=5) were anaesthetised (2% isofluorane), ventilated (Air) and the middle cerebral artery permanently occluded (MCAO) by the intraluminal filament technique. Imaging (6 coronal slices throughout MCA territory) was performed on a Bruker Biospec 7T/30 cm system. A T2 scan was generated as a neuroanatomical template for co-registration. Diffusion-weighted imaging (DWI) determined ischaemic damage and Perfusion-weighted imaging (PWI), using a continuous ASL technique, determined the perfusion deficit. A T2* weighted sequence was acquired during OC: 5 mins air, 5 mins 100% oxygen & 15 mins air inhalation. Following OC, rats were immediately administered an iv bolus of 125 µCi/kg ^{14}C 2-DG. MRI images were co-registered to corresponding ^{14}C 2-DG autoradiograms. Glucose utilisation was determined by optical density measurements (MCID v4) and MRI-defined regions of interest (ROI) were picked within cortical ischaemic core, contralateral cortex and penumbra, as defined by PWI/DWI mismatch.

Results: The mean (±SD) time to commence OC was 65±6 min following MCAO. OC induced a T2* signal increase of 1.26% in contralateral cortex. Within ischaemic core, LCMglu was reduced by 98.5% (relative to contralateral cortex) and OC induced a small 0.74% increase in T2*. In penumbra, a 35% increase in LCMRglu co-registered with the greatest (3.97%) increase in T2* signal change (Figure). Interestingly, hyperglycolysis (295% increase in LCMRglu) occurred within the boundary of the ADC lesion and corresponded with a 1.04% T2* signal increase.

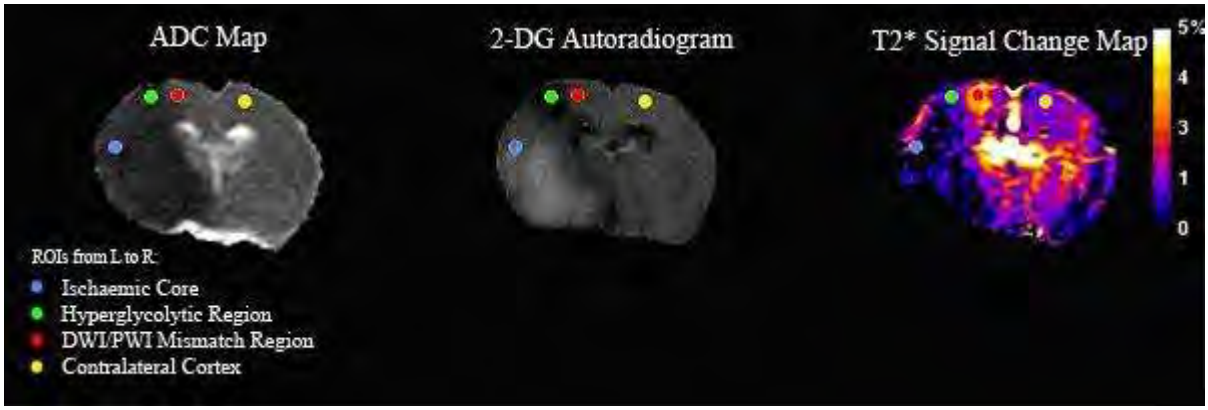

[Corresponding ROIs on co-registered images]

Conclusions: Co-registration of MRI and autoradiograms provides evidence that the area of greatest T2* signal increase, which fell within penumbra (defined by PWI/DWI) is metabolically active (as defined by LCMRglu). Negligible T2* signal change and glucose utilisation were recorded within ischaemic core. Hyperglycolysis which bordered the ADC lesion and coregistered with a lower T2* increase, may be indicative of anaerobic glycolysis.

Research supported by an MRC project grant and Capacity Building Studentship (to CR).

References:

[1] Santosh, C et al. J Cereb Blood Flow & Metab (2008) Oct;28(10):1742-53.

[2] Sokoloff, L et al. J Neurochem (1977) 28, pp 897-916.

TESTING THE PERFORMANCE OF ITERATIVE RECONSTRUCTION AT LOW STATISTICS VIA LISTMODE SUB-SAMPLING IN HIGH RESOLUTION BRAIN PET

M.D. Walker[1], P.J. Julyan[1,2], P.S. Talbot[1], J.C. Matthews[1]

[1]Wolfson Molecular Imaging Centre, The University of Manchester, [2]North Western Medical Physics, Christie Hospital NHS Trust, Manchester, UK

Background: It has been reported that the scatter correction on the HRRT PET scanner becomes erroneous for frames with low statistics [1]. Also reported is that iterative reconstruction (OP-OSEM) leads to significant bias for such frames [2]. This bias is problematic for dynamic PET scanning, and may be present on other scanners.

Objectives: This study investigates low-statistics induced bias for HRRT images. We test the hypothesis that the bias is a property of the image reconstruction, and not the result of performing scatter correction on data of low statistical quality.

Methods: Statistically independent, low-count replicates of listmode data ([40 replicates of 15 s, 840K NEC];[10 replicates of 60 s, 3360K NEC]) were created from a high statistics human dataset (391 MBq [^{11}C]-DASB, 600 s frame starting at 5 min. post injection, 33.6M NEC, 197M prompts, 40% randoms). This was achieved by sub-sampling the listmode data, creating replicates with equal expectation values but with independent noise. A scatter correction sinogram was calculated from each replicate. A second scatter correction sinogram was calculated by scaling the high-statistics (smooth) scatter correction sinogram. Each replicate was reconstructed with both scatter correction sinograms via OP-OSEM [3,4] (12 iterations, 16 subsets). The replicate images were summed and compared with the high statistics image. Bias was defined as the percentage difference between the summation image and the high statistics image. The inter-replicate voxel variance was also calculated.

Results: The regions investigated had adequately converged by the final iteration. Images generated at low-statistics showed significant differences compared to the high statistics image. The use of a scatter correction derived from high-statistics data did not reduce this difference, nor did it reduce the inter-replicate voxel variance. The low-statistics images exhibit a negative bias in regions of high tracer uptake (-17%, caudate head), and a positive bias in regions of low tracer uptake (+27%, ventricles).

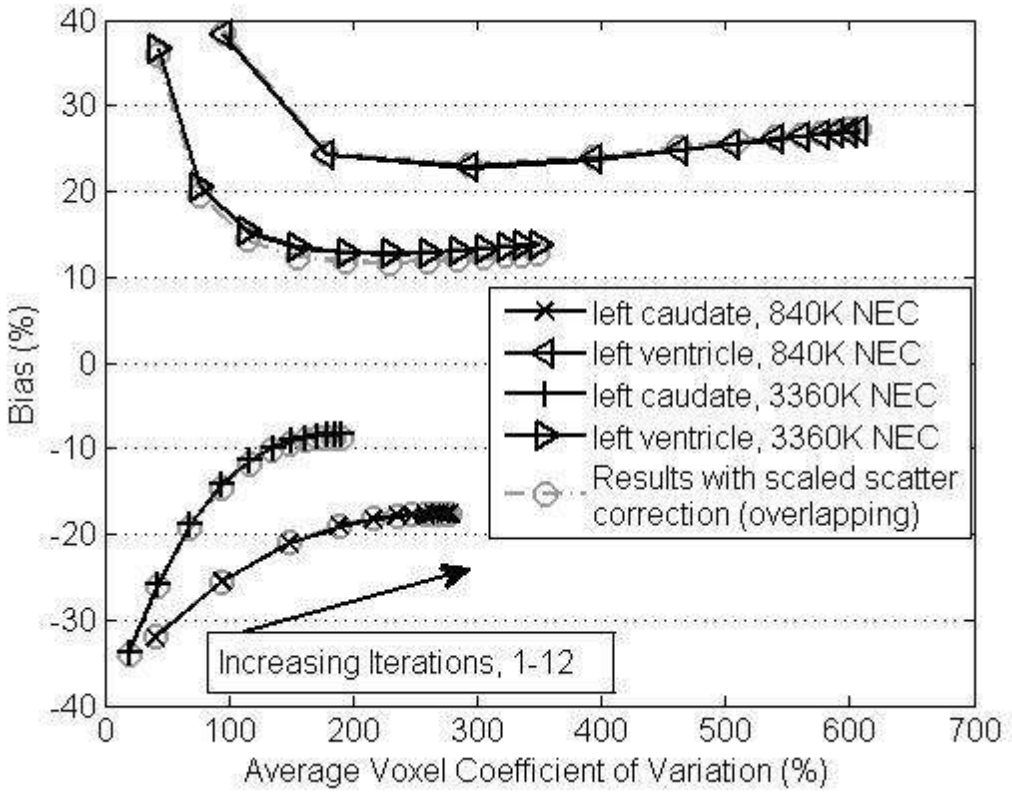

[Figure 1]

Figure 1. Bias and variance effects at low statistics, calculated by comparison of low statistics images ([15 s, 840K NEC];[60 s, 3360K NEC]) with a high statistics image ([600 s, 33.6M NEC]).

Conclusions: Bias can occur in low statistics frames using OP-OSEM reconstruction. Low and high statistic scatter corrections did not significantly alter the bias or variance. The observed bias is likely to be a property of the image reconstruction. Care must be taken in the use of iterative reconstruction with dynamic data.

References:

[1] Ju-Chieh C et al., IEEE Nuclear Science Symposium Conference Record 2007; pp 4475-4480.

[2] van Velden FHP et al., J Nucl Med 2009;50:72-80.

[3] Comtat C et al., IEEE Nuclear Science Symposium Conference Record 2004; pp 3492-3496.

[4] Hong IK et al., IEEE Trans Med Imaging 2007;26:789-803.

450

Brain Oral Session: Experimental Stroke and Cerebral Ischemia 1

INFLUENCE OF CHRONIC ARTERIAL HYPERTENSION ON THE EVOLUTION OF PERFUSION-DIFFUSION MISMATCH

A. Letourneur, S. Roussel, J. Toutain, M. Bernaudin, O. Touzani

UMR CI-NAPS 6232, CERVOxy Team 'Hypoxia and Cerebrovascular Pathophysiology', CNRS, CEA, Université de Caen Basse-Normandie and Université Paris Descartes, Caen, France

Objectives: Chronic arterial hypertension (CAH) increases the risk of stroke as well as the severity of the resultant lesion. In spite of this fact, arterial hypertension is rarely taken into consideration during preclinical investigations. To better define the therapeutic window in hypertensive subjects, the aim of our study was to analyse the impact of CAH on the spatio-temporal evolution of the ischemic lesion in the acute phase. Special attention was paid to the ischemic penumbra defined by the mismatch between perfusion and diffusion as visualised by magnetic resonance imaging (MRI).

Methods: Six sequential MRI examinations (7 Teslas, Bruker) were undertaken from 30 minutes up to 4 hours after intraluminal permanent Middle Cerebral Artery Occlusion (MCAO) in isoflurane-anaesthetised spontaneously hypertensive rats (SHR, n = 11) and their normotensive control rats (WKY, n = 12). Mean arterial pressure (MAP), heart rate, and blood gases were monitored throughout the experiment.

In each MRI session, Apparent Diffusion Coefficient (ADC) maps were generated based on echo planar images (Diffusion Weighted Imaging (DWI), repetition time (TR) = 3500 ms, echo time (TE) = 40.53 ms, matrix = 128x128). Perfusion Weighted Imaging (PWI) examinations have been realized using the first pass of a gadolinium chelate (Gradient Echo EPI; TR = 500 ms, TE = 10.32 ms, 120 repetitions, matrix: 256x256). The integrity of the blood brain barrier (BBB), the occurrence of haemorrhage and the status of major cerebral arteries were also imaged sequentially with specific sequences (respectively T1, T2*, Angiography). Animals were euthanized 24h later and infarct volume was measured.

Results: MAP, as measured in awake rats, was higher in SHR than in WKY (170±11 mmHg; 130±18 mmHg; $p < 0.001$). This difference in blood pressure was also seen in the anesthetised rats during MRI examination.

MRI studies showed that the ischemic lesion, defined by a significantly decreased ADC relative to the mean value of the contralateral hemisphere, was significantly larger in hypertensive rats than in normotensive ones at all the time points analysed (ANOVA followed by Fischer PLSD ($p< 0.005$ at each time)). Analysis of the mismatch between perfusion and diffusion interestingly showed that WKY displayed a significant penumbra up to 240 min post occlusion, whereas in SHR, the penumbra disappeared as soon as 60 min following the occlusion (Figure). MRI angiography confirmed MCAO in all animals. Neither major BBB disruption nor haemorrhage was observed irrespective of the strain studied.

Conclusion: Hypertensive rats present larger lesions and a rapid disappearance of the penumbra compared to normotensive ones. This suggests that even if a treatment is precociously administered, the ischemic damage will remain greater in hypertensive subjects. This supports the integration of CAH in pre-clinical studies relative to the treatment of stroke.

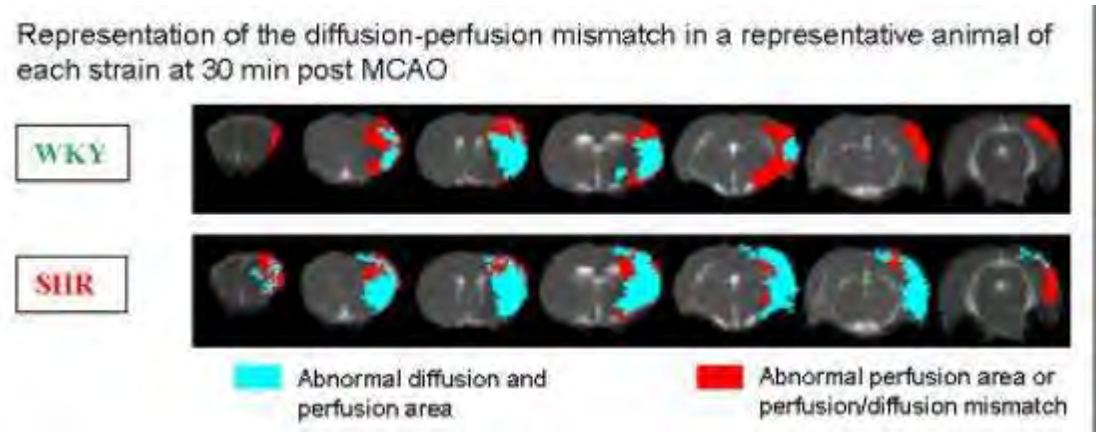
Representation of the diffusion-perfusion mismatch in a representative animal of each strain at 30 min post MCAO
WKY
SHR
Abnormal diffusion and perfusion area
Abnormal perfusion area or perfusion/diffusion mismatch

[Figure]

Brain Poster Session: Blood-Brain Barrier

INTRACAROTID INJECTION OF DEHYDROCHOLIC ACID (DHC) INDUCES CEREBRAL ISCHEMIA AND BLOOD BRAIN-BARRIER DISRUPTION

E.J. Kang[1,2], S. Major[1,2], D. Jorks[2], A. Friedman[3], J.P. Dreier[1,2]

[1]Center for Stroke Research Berlin (CSB), [2]Experimental Neurology, Charité - University Medicine Berlin, Berlin, Germany, [3]Faculty of Health Sciences, Ben-Gurion University, Beer-Sheva, Israel

Objectives: Intracarotid application of the bile salt DHC has been used to open the blood brain-barrier (BBB) in the ipsilateral hemisphere.[1,2] This observation has drawn attention as a possible means for therapeutic studies of drug delivery into the central nervous system (CNS). However, DHC's mechanism of action is unknown. Here we studied the effects of intracarotid application of DHC on regional cerebral blood flow (rCBF), intracortical direct current (DC) potential and extracellular potassium concentration ([K+]o) in a rat cranial window preparation.

Methods: Male Wistar rats (n = 6; 250-350 g) were anaesthetized with thiopental-sodium (100mg/kg, intraperitoneally), tracheotomised, and artificially ventilated. End-tidal CO_2 concentration was adjusted to approximately 35 mmHg. Body temperature was maintained at 38.0°C with a heating pad. Systemic arterial pressure was monitored via the left femoral artery. Evans blue was administered via the left femoral vein to evaluate BBB opening. The right external carotid artery was cannulated in a retrograde manner for intracarotid injection of DHC. An open parietal window was implanted to place two K^+-sensitive microelectrodes and a laser-Doppler flowmetry (LDF) probe. Epidural DC potential and rCBF were measured by an Ag/AgCl electrode and a second LDF probe at a closed frontal window.

Results: Intracarotid application of DHC (17.5%, 1ml) induced an increase of rCBF to 373 ± 90 % followed by a decrease to 33 ± 16 % after 65 ± 85 s in 5 of 6 experiments. A shallow increase of the [K+]o from 3.0 to 9.8 ± 6.3 mM started simultaneously with the decrease of rCBF typical of cerebral ischemia. This was accompanied by ictaform epileptic field potentials with an amplitude of -3.4 ± 2.3 mV, a spike duration of 64.8 ± 5.5 ms, and spike frequency of 1.2 ± 0.8 Hz in 5 experiments. Moreover, an increase of systemic arterial pressure accompanied the decrease of rCBF typical of a compensatory systemic hypertension. 45 ± 28 s after onset of the rCBF decrease we observed a sharp saddle-shaped negative intracortical DC shift of -20.3 ± 1.9 mV accompanied by a sharp rise of [K+]o to 49.1 ± 10.6 mM typical of cortical spreading depolarisation (CSD). The latency of this intracortical DC shift was 20 ± 20 s between the rostral and the caudal microelectrodes indicating a spread typical of CSD between them. The DC negativity and rise of [K+]o did not recover for an observation period of at least 60 min.

Conclusions: Spigelman et al.[1] previously described a BBB disruption in response to intracarotid DHC (17.5%, 1 ml) in the rat. No routine histology was performed. Here we show that this procedure induces prolonged cerebral ischemia. The BBB disruption may either be a direct effect of DHC or secondary to the ischemia. However, the procedure is not suitable for drug delivery into the CNS. Bile acids act as detergents. The ischaemia might be the consequence of severe damage to the cerebrovascular endothelium which will be investigated further.

References:

1. Spigelman et al. (1983) Neurosurgery 12:606-612.

2. Nita et al. (2004) Neurophysiology 92:1011-1022.

INVOLVEMENT OF CALCIUM-CALMODULIN DEPENDENT PROTEIN KINASE II ON ENDOTHELIN RECEPTOR EXPRESSION IN CEREBRAL ARTERIES OF RAT

R. Waldsee, S. Eftekhari, L. Edvinsson

Clinical Science, Experimental Vascular Research, Lund, Sweden

Objective: Experimental cerebral ischemia and organ culture of cerebral arteries result in enhanced expression of endothelin ET_B receptors in smooth muscle cells via increased transcription.(1, 2) The present study was designed to evaluate the involvement of calcium-calmodulin dependent protein kinase (CAMK) on the expression of endothelin receptors after organ culture.

Methods: Rat basilar arteries were incubated for 24 hours with and without the CAMK inhibitor, KN93. The contractile responses to endothelin-1 (ET-1; ET_A and ET_B receptor agonist) and sarafotoxin 6c (S6c; ET_B receptor agonist) were studied using a sensitive myograph. The mRNA levels of ET_A and ET_B receptors and of CAMKII were determined with real-time polymerase chain reaction (PCR) while the protein level was evaluated by semi-quantitative immunohistochemistry.

Results: The mRNA levels of CAMKII and of the ET_B receptor were increased during organ culture but there was no change in ET_A receptor expression. This effect was abolished by co-incubation with KN93. In functional studies, KN93 attenuated the S6c-induced contraction and to a minor degree the ET-1 induced response. This was confirmed at the protein level by immunohistochemistry where the endothelin receptors were found co-localised with CAMKII, in the smooth muscle cells. Phosphorylated extracellular signal-regulated kinase ERK1/2 was measured by immunohistochemistry. Incubation of arteries with KN93 decreased the level of pERK1/2. In addition, pERK1/2 co-localised both the endothelin receptors and CAMKII.

Conclusion: Our results show that the CAMK II is involved in the endothelin receptor regulation and interacts with the ERK1/2 pathway, resulting in enhanced receptors expression in rat basilar artery.

References:

1. Adner M, Geary GG, and Edvinsson L.. Acta Physiol Scand 163: 121-129, 1998.

2. Stenman E, Malmsjo M, Uddman E, Gido G, Wieloch T, and Edvinsson L. 33: 2311-2316, 2002.

MITOCHONDRIAL ROS PRECONDITIONING PROTECTS RAT BRAIN ENDOTHELIAL CELLS AGAINST GLUCOTOXICITY THROUGH HIF-1 ACTIVATION

S. Correia, M.S. Santos, P. Moreira

Center for Neuroscience and Cell Biology, Coimbra, Portugal

Endothelial dysfunction is a critical feature in the onset of the type 2 diabetes-induced vascular complications. It has been proposed that hyperglycemia, a hallmark of type 2 diabetes, is a major causal factor in the development of endothelial dysfunction in diabetic patients, which predisposes to several pathologies including vascular dementia and Alzheimer's disease. Accumulating evidence demonstrates that hypoxic preconditioning protects the brain against several types of deleterious/lethal insults through the induction of the transcription factor hypoxia inducible factor 1 (HIF-1). Furthermore, it has been reported that mitochondrial reactive oxygen species (ROS) are required for HIF-1 activation and stabilization. Thus, the aim of this study was to evaluate if mitochondrial ROS are able to protect brain endothelial cells against hyperglycemia through the activation of HIF-1. For this purpose, we pre-incubated rat brain endothelial cells (RBE4) with several mitochondrial modulators (rotenone, antimycin A and potassium cyanide). Using fluorimetric methods we observed that these mitochondrial modulators were able to increase mitochondrial ROS production without affecting cell viability (mitochondrial preconditioning). Furthermore, immunocytochemistry and Western blotting analyses revealed that these mitochondrial modulators also activated HIF-1 and its target genes, the vascular endothelial growth factor (VEGF) and glucose transporter 1 (GLUT-1). In addition, mitochondrial preconditioning protected RBE4 cells against deleterious effects induced by high levels of glucose (30 mM). Altogether, our results show that mitochondrial ROS preconditioning protects brain endothelial cells against high glucose levels through the activation of HIF-1. Exploring how mitochondrial manipulation activate adaptive responses mediated by HIF-1, may offer new avenues for the treatment of vascular endothelial dysfunction associated to several pathologies including neurodegenerative conditions.

This work is supported by the European Foundation for the Study of Diabetes / Servier.

Sónia Correia has a PhD fellowship from the Fundação para a Ciência e a Tecnologia (SFRH/BD/40702/2007).

PROTOPORPHYRIN IX INTERACTION WITH PERIPHERAL TYPE BENZODIAZEPINE RECEPTOR IN RATS

H. Ozaki, S. Zoghbi, J. Hong, V. Pike, R. Innis, M. Fujita

Molecular Imaging Branch, National Institute of Mental Health, Bethesda, MD, USA

Objectives: The major physiological porphyrin, protoporphyrin IX (PPIX), is well-known to bind to peripheral type benzodiazepine receptor (PBR) as one of the endogenous ligands [1]. The published K_i value of PPIX ranges from 0.015 to 19 μM, whereas the other porphyrins are less potent at PBR [1, 2]. The purpose of this study was to evaluate PPIX interaction with PBR in vivo using PET. We used 5-aminolevulinic acid (ALA) for this study because with its administration to rats, plasma concentration of PPIX is expected to become in the range of its K_i value for PBR [3].

Methods: Male Sprague-Dawley rats (about 320 g body weight) were divided into 3 groups (control, ALA- and PK 11195-pretreated groups: n=4, 4 and 3, respectively). ALA (200 mg/kg) was intravenously injected to animals 2 h before PET scans. This dose of ALA produces plasma and organ PPIX peak levels of 0.5 - 20 μM [3]. For comparison, a receptor saturating dose of PK 11195 (10 mg/kg) was intravenously administered 2 min before PET scans. In each animal, one 2 h PET scan of PBR was performed using N-acetyl-N-(2-[^{11}C]methoxybenzyl)-2-phenoxy-5-pyridinamine ([^{11}C]PBR28) and the HRRT device under isoflurane anesthesia. The time activity curves of the heart, kidney, liver, lung, skeletal muscle, parotid gland and spleen were drawn using individual regions of interest and then the area under the curve for each organ was calculated. In 2 animals of each of the 3 groups, more quantitative analysis was performed in brain by measuring total distribution volume using an unconstrained two-tissue compartment models and metabolite-corrected arterial input function.

Results: Control scans with [^{11}C]PBR28 showed high levels of uptake in the heart, kidney, lung and spleen. The ALA-pretreatment dramatically suppressed the normal uptake of radioactivities in the heart, lung and parotid gland (Figure 1, $p < 0.01$). However, there was no blocking effect in the kidney, liver, skeletal muscle and spleen (Figure 1). PK 11195 also blocked the radiotracer binding to PBR in the heart, kidney, lung, parotid gland and spleen (Figure 1, $p < 0.01$). In the brain, the distribution volume was decreased by both pretreatments. In all organs, blocking effect of 200 mg/kg of ALA was weaker than that of 10 mg/kg of PK 11195.

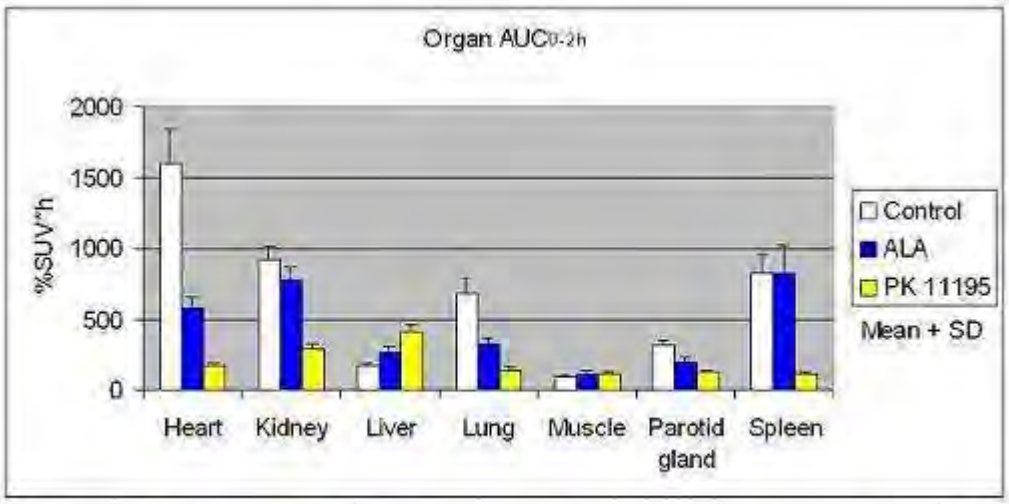

Figure1. Area under curve of each organ for 2 h after [11C]PBR28 injection in the control, ALA-pretreated and PK 11195-pretreated groups

[AUC of each organ]

Conclusions: PPIX reduced [^{11}C]PBR28 binding to PBR in rats although 200 mg/kg of PPIX was not enough for complete blocking. This study provides the first indication for the in vivo competitive binding of PPIX with a PET ligand at PBR. Since endogenous PPIX levels are high in porphyria, this disorder should demonstrate reduced target uptakes of the radiotracer as seen in the rats.

References:

[1] Molecul Pharmacol 34 (1988): 800-805.

[2] Biochem Biophys Res Commun 311 (2003): 847-52.

[3] J Photochem Photobio B: Biol 44 (1998): 29-38.

GLUTAMINE SYNTHESIS RATE IN THE HYPERAMMONAEMIC RAT BRAIN USING SIMULTANEOUS LOCALIZED IN VIVO ^{1}H AND ^{15}N MRS

C. Cudalbu[1], B. Lanz[1], F. Morgenthaler[1], Y. Pilloud[1], V. Mlynárik[1], R. Gruetter[1,2]

[1]Laboratory for Functional and Metabolic Imaging (LIFMET), Ecole Polytechnique Fédérale de Lausanne (EPFL), Lausanne, [2]Departments of Radiology, Universities of Lausanne and Geneva, Lausanne and Geneva, Switzerland

Objectives: Glutamine synthetase is a critical step in the glutamate-glutamine cycle, the major mechanism of glutamate neurotransmission and is implicated in the mechanism of ammonia toxicity. ^{15}N MRS is an alternative approach to ^{13}C MRS in studying glutamate-glutamine metabolism. ^{15}N MRS studies allow to measure an apparent glutamine synthesis rate (Vsyn) which reflects a combination of the glutamate-glutamine cycle activity (Vnt) and net glutamine accumulation. The net glutamine synthesis (Vsyn-Vnt) can be directly measured from ^{1}H NMR. Therefore, the aim of this study was to perform in vivo localized ^{1}H MRS interleaved with ^{15}N MRS to directly measure the net glutamine synthesis rate and the apparent glutamine synthesis rate under ^{15}N labeled ammonia infusion in the rat brain, respectively.

Methods: ^{1}H and ^{15}N MRS data were acquired interleaved on a 9.4T system (Varian/Magnex Scientific) using 5 rats. $^{15}NH_4Cl$ solution was infused continuously into the femoral vein for up to 10h (4.5mmol/h/kg) (1). The plasma ammonia concentration was increased to 0.95±0.08mmol/l (Analox GM7 analyzer). ^{1}H spectra were acquired and quantified as described previously (2). ^{15}N unlocalized and localized spectra were acquired using the SIRENE sequence (3); and quantified using AMARES and an external reference method (4). The metabolic model used to analyze the total Gln and 5-^{15}N labeled Gln time courses is shown on Fig 1a.

Results: Glutamine concentration increased from 2.5±0.3mmol/kg to 15±3.3mmol/kg whereas the total glutamate concentrations remained unchanged (Fig. 1b). The linear fit of the time-evolution of the total Gln from the ^{1}H spectra gave the net synthesis flux (Vsyn-Vnt), which was 0.021±0.006µmol/min/g (Fig. 1d). The 5-^{15}N Gln peak (-271ppm) was visible in the first and all subsequent scans, whereas the 2-^{15}N Gln/Glu peak (-342ppm) appeared after ~1.5h (Fig. 1c). From the in vivo 5-^{15}N Gln time course, Vsyn=0.29±0.1µmol/min/g and a plasma NH_3 fractional enrichment of 71±6% were calculated. Vnt was 0.26±0.1µmol/min/g, obtained assuming a negligible Gln efflux (5). Vsyn and Vnt were within the range of ^{13}C NMR measurements (6).

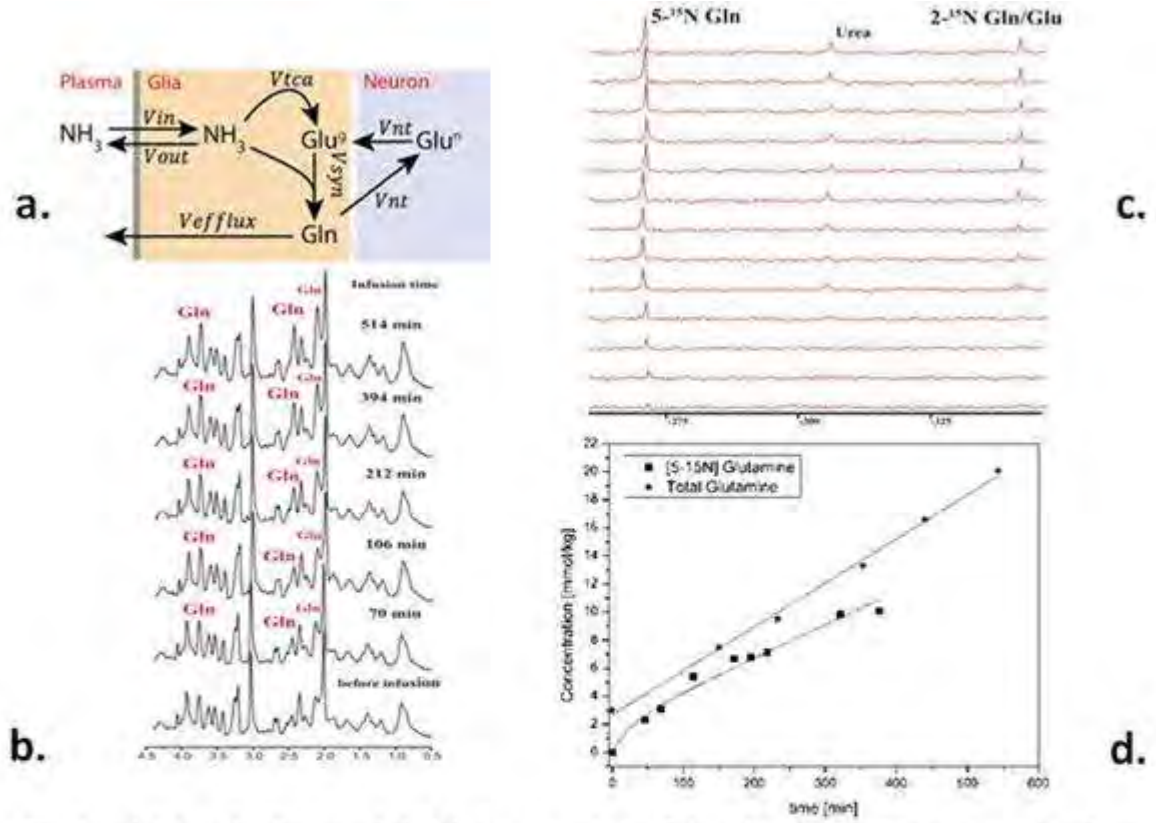

Fig 1: a) Metabolic model; b) One series of *in vivo* ^{1}H spectra acquired at 9.4T in the rat brain; c) A series of in vivo unlocalized ^{15}N spectra acquired at 9.4T in the rat brain at different time points (from bottom to top: 23, 47, 69, 115, 173, 193, 218, 321, 376, 398, 420, 463, 529min). The ^{15}N chemical shifts were referenced to nitromethane; d) The time courses and corresponding fits of total Gln and 5-^{15}N Gln from one rat.

[Fig. 1]

Conclusion: The combination of ^{1}H and ^{15}N NMR allowed for the first time a direct and localized measurement of Vnt and apparent glutamine synthesis rate. Vnt is approximately one order of magnitude faster than the net glutamine accumulation.

References:

[1] Kanamori K et al., NMRBiomed 1993;6:21.

[2] Mlynarik V et al., JMagnReson 2008;194:163.

[3] ChoiI Y et al., MagnResonMed 2000 ;44 :387.

[4] Gruetter R, et al., MagnResonMed 1991;20:327.

[5] Kanamori K et al., BiochemJ 1993 ;293 :461.

[6] Sibson NR et al, ProcNatlAcadSci 1997;94:2699.

[11C]-CIMBI5: A NOVEL 5-HT2A AGONIST PET TRACER

A. Ettrup[1], M. Palner[1], N. Gillings[2], K. Någren[2], L.K. Rasmussen[3], S. Keller[2], M. Sibomana[2], M. Begtrup[3], J. Madsen[2], G.M. Knudsen[1]

[1]Neurobiology Research Unit and Center for Integrated Molecular Brain Imaging (CIMBI), [2]PET and Cyclotron Unit, Copenhagen University Hospital, Rigshospitalet, [3]Department of Medicinal Chemistry, Faculty of Pharmaceutical Sciences, University of Copenhagen, Copenhagen, Denmark

Objectives: Receptor agonist PET tracers have a better potential than antagonist tracers to reflect displacement under endogenous neurotransmitter release, however, only antagonistic PET tracers targeting the 5-HT_{2A} receptor are currently known. The aim of this study was to validate a novel 5-HT_{2A} agonist PET tracer in the pig brain.

Methods: The high-affinity 5-HT_{2A} receptor selective agonist N-(2-[^{11}C-OCH_3]methoxybenzyl)-2,5-dimethoxy-4-iodophenethylamine ([^{11}C]-INBMeO, [^{11}C]-CIMBI5) was radiolabelled by methylation of the N-Boc-protected precursor using [^{11}C]methyl triflate and subsequent deprotection with TFA. In five Danish Landrace pigs, [^{11}C]-CIMBI5 was given as IV bolus injection, and the pigs were subsequently PET scanned with a HRRT camera. Three of the pigs were scanned a second time, now under treatment with the 5-HT_{2A} receptor antagonist ketanserin (3 mg/kg bolus, 1 mg/kg*hour infusion). Total activity in full blood, plasma, and radioactive metabolites were measured throughout the scan using HPLC.

Results: Compared to cerebellum [^{11}C]-CIMBI5 showed a high cortical uptake, and the time activity curves confirmed significantly higher uptake in cortex compared to cerebellum showing a ratio ($AUC_{cortex}/AUC_{cerebellum}$) of approximately 1.4. Following ketanserin pre-treatment, the cortical binding of [^{11}C]-CIMBI5 was reduced to cerebellar levels. In the radio-HPLC analysis, we found a lipophilic radioactive metabolite building accounting for up to 20% of the total activity in plasma and maintaining stable levels after 20 minutes and throughout the scan.

Conclusions: The novel agonist PET tracer [^{11}C]-CIMBI5 distributes in the brain in a pattern compatible with the known 5-HT_{2A} receptor distribution, and its binding is displaceable by ketanserin. Thus, [^{11}C]-CIMBI5 is a promising candidate for human 5-HT_{2A} PET scanning, although the relatively high cerebellum binding, indicative of a high non-specific binding, may compromise the possibility to detect changes in [^{11}C]-CIMBI5 binding following changes in extracellular 5-HT levels. Therefore, changing the ^{11}C-labeling site to eliminate the lipophilic metabolite or changing the chemical structure to alter lipophilicity may optimize the signal-to-noise ratio and thus improving the potential of [^{11}C]-CIMBI5 for future clinical use.

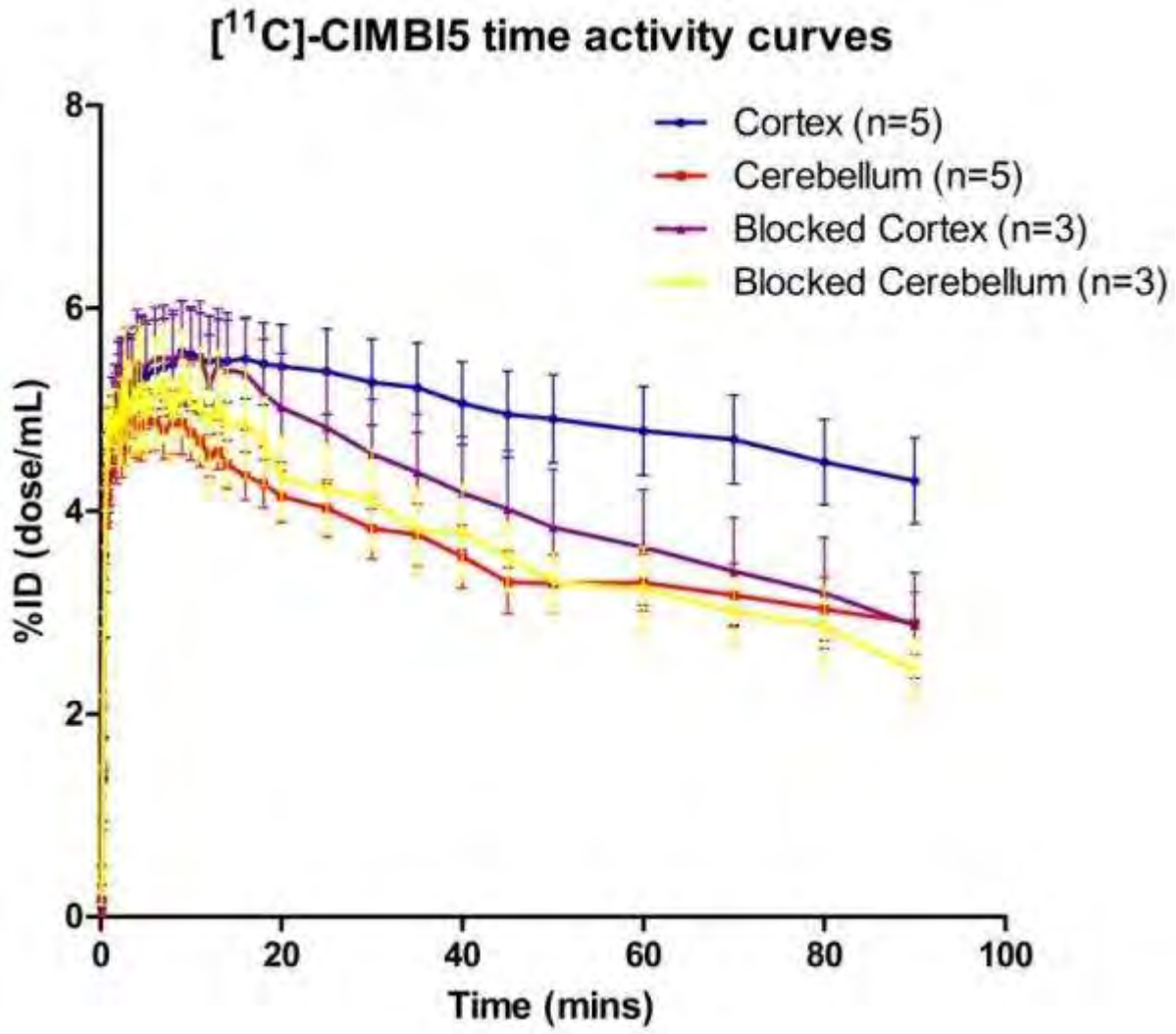

[[11C]-CIMBI5 time acitivity curves]

PHNO IN VIVO AFFINITY FOR D2 AND D3 RECEPTORS: A PET STUDY IN RHESUS MONKEYS

J.D. Beaver[1], J.D. Gallezot[2], N. Nabulsi[2], D. Weinzimmer[2], T. Singhal[2], M. Slifstein[3], R.N. Gunn[1], M. Laruelle[4], Y.-S. Ding[2], Y. Huang[2], R.E. Carson[2], E.A. Rabiner[1]

[1]GSK, Clinical Imaging Center, London, UK, [2]Yale University PET Center, New Haven, CT, [3]Columbia University, New York, NY, USA, [4]GSK, Schizophrenia & Cognition DPU, Harlow, UK

Objectives: We previously used SB-277011 (a D_3 selective antagonist) and [^{11}C]PHNO PET in non-human primates to determine the proportion of [^{11}C]PHNO BP_{ND} attributable to D_3 and D_2 components. Additional data from the same subjects using SB-277011 with [^{11}C]raclopride and [^{11}C]fallypride were also used to estimate the relative regional density of D_3 and D_2 receptors. These data implied that in vivo [^{11}C]PHNO has a ~20-fold higher affinity for D_3 relative to D_2 [1, 2]; however, this method of estimating the regional density of D_3 and D_2 receptors assumes that [^{11}C]raclopride and [^{11}C]fallypride are non-selective for D_2 over D_3. Here we used an independent method, that does not rely on these assumptions, to test directly the affinity of [^{11}C]PHNO for D_3 and D_2 receptors.

Methods: Two rhesus monkeys were scanned four times each on a Focus 220 PET scanner. 54±26 MBq of [^{11}C]PHNO was injected using a bolus-plus-infusion protocol (K_{bol} = 50 min) over 120 minutes. Infusion rates varied from 0.032 to 2.1 μg/kg/hr. Images were reconstructed with FORE/FBP. The concentration of non-displaceable [^{11}C]PHNO was assumed to be uniform in the brain at equilibrium (t >= 90 min), and was estimated in the cerebellum. Scatchard plots were drawn for selected regions of interest and analyzed using 1- (1S) and 2-site (2S) models, from which K_d/f_{ND} and B_{max} parameters were estimated. For the 2S model, the two K_d/f_{ND} values were assumed to be identical across brain regions.

Results: Using a 1S model, K_d/f_{ND} estimates were highest in the caudate (CN, 14 and 5 nM for subjects 1 and 2, respectively) and putamen (PU, 9 and 7 nM for subjects 1 and 2, respectively), intermediate in the pallidum (GP, 3 nM for both subjects) and lowest in the substantia nigra (SN, 0.3 and 0.5 nM for subjects 1 and 2, respectively). Using a 2S model, the D_3 K_d/f_{ND} for subjects 1 and 2 was 0.2 and 0.8 nM, respectively, whereas the D_2 K_d/f_{ND} was 13 and 6 nM, respectively. The D_3 BP_{ND} comprised ~65% of the total BP_{ND} in GP and >95% in SN. The D_2 BP_{ND} comprised >80% of the total BP_{ND} in the CN and PU.

Conclusions: This study provides the first direct evaluation of PHNO in vivo affinity. Our findings demonstrate a ~20-fold selectivity of [^{11}C]PHNO for D_3 over D_2 receptors, confirming our previous findings established using SB-277011 with [^{11}C]PHNO, [^{11}C]raclopride and [^{11}C]fallypride [1, 2]. The D_3 BP_{ND} proportion of the total BP_{ND} observed in the present study is also consistent with the previous data acquired using SB-277011 (i.e., 95% in SN, 72% in GP, 24% in CN and 10% in PU). Understanding PHNO affinity at the D_3 and D_2 sites allows the estimation of regional D_3 receptor distribution in vivo.

References:

[1] Rabiner, E.A. et al., (In press) Synapse.

[2] Rabiner, E.A. et al., (2008) Neuroimage Vol 41 (Suppl. 2), T39.

COMPARISON BETWEEN BOLD AND CBV FLUCTUATIONS USING PARTIAL DIRECTED COHERENCE IN RAT BRAINS DURING REST

W.H. Shim[1], K.Y. Baek[1], B. Rosen[2], J.S. Jeong[1], Y.R. Kim[2]

[1]Bio&Brain Engineering, KAIST, Daejeon, South Korea, [2]Radiology, Martinos Center for Biomedical Imaging/Massachusetts General Hospital, Charlestown, MA, USA

Objectives: Recently, low frequency vascular fluctuations during rest and functional connectivity analyses of fMRI have been introduced as one of the potential methods to effectively assess brain dynamics [1]. However, most of resting state fMRI connectivity studies has been limited to the investigation of MRI signal changes based on blood oxygen level-dependence (BOLD). Since BOLD is an indirect signal based on the mixture of multiple physiologic parameters, we hypothesize that understanding underlying vascular parameter is important and perhaps more informative for displaying direct brain dynamics. In the current study, we specifically compared BOLD resting state fMRI fluctuations with CBV signals using partial direct coherence (PDC) analyses.

Methods: Three normal healthy Sprague-Dawley rats (~300g) were used for the BOLD and CBV acquisition (Gradient Echo Planar Imaging: TR/TE=1000/12.89ms; FOV=2.5*2.5cm2; five contiguous 1mm slices;Recording time=10 min). ROIs were placed over the regions as motor cortex (M1& M2), primary sensory areas (S1fl), secondary somatosensory cortex (S2), caudate putamen (CPu) and thalamus area (TA). Each ROI time course was detrended to the second order and bandpass-filtered between 0.01 and 0.3 Hz. Functional connectivity between ROIs in both BOLD and CBV were calculated by partial directed coherence (PDC).

Results:

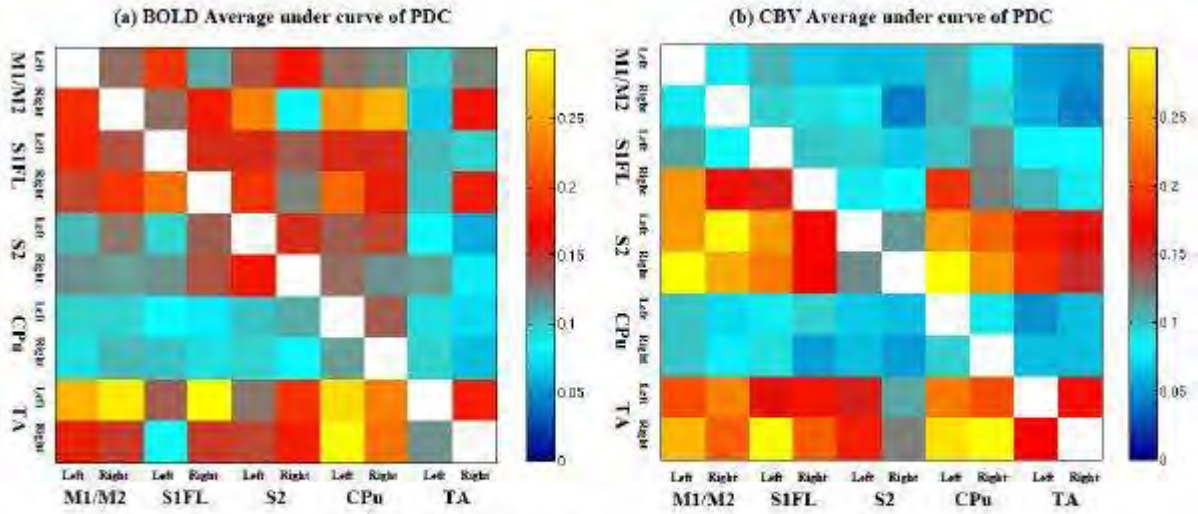

Fig. 1. Average under curve of PDC distribution tables for BOLD(a) and CBV(b).

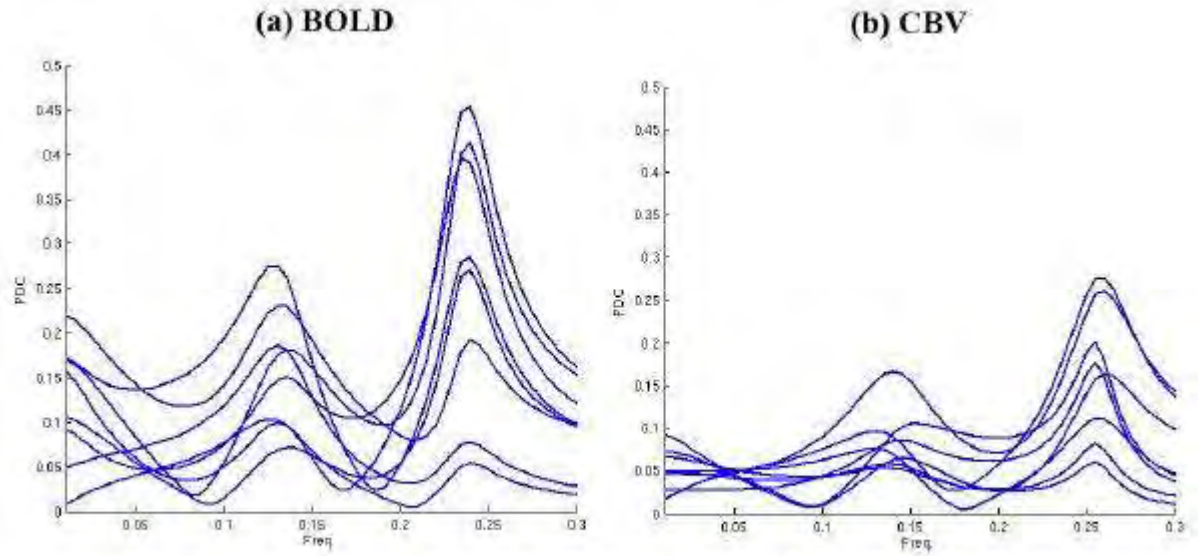

Fig 2. Partial directed coherence from M1/M2, CPu to TA.

[Partial directed coherence result.]

Fig.1 shows distribution tables of average PDC values, average area under the curve between 0.01 and 0.3 Hz in frequency domains. Both BOLD and CBV show similar functional influences from M1&M2 to TA and from CPu to TA. The directional BOLD interactions among M1&M2, S1fl and S2 and the functional pathways from CPu to M1&M2, S1fl and S2 were different from those found in CBV. Specifically, we found directional causality from M1&M2 to S2 and from CPu to S2 in CBV. Within significant PDC pathways (e.g., from M1/M2, CPu to TA: Fig. 1), the PDC spectra across frequency displayed similar patterns between BOLD and CBV, in which distinctive frequency peaks appeared near both 0.12 Hz and 0.24 Hz in both BOLD and CBV time courses (Fig. 2).

Conclusions: Even though both BOLD and CBV seem to have similar frequency bands responsible for communicating between the brain regions, two methods reveal different causality networks, especially in M1&M2- and CPu-related areas. To support our PDC results, we also applied the Granger-causality analysis method to our data. The Granger-causality results were variable according to the autoregressive model order; however, the directional functional connectivities between ROIs were similar to our PDC results in most cases. We speculate that the differences between BOLD and CBV might be caused by metabolic efficiency difference in resting states or the baseline vascular conditions. The findings warrant future studies for understanding the relationship between underlying vascular parameter and blood oxygen level-dependence in functional connectivity analysis.

References: [1] FT Sun, et al. (2004) Neuroimage,21, 2, 647-658.

Brain Poster Session: Cerebral Metabolic Regulation

BRAIN GLUTAMATERGIC ACTIVITY AND EAC CELL DEVELOPMENT: EFFECT OF CAFFEINE

M.K. Poddar, A. Mandal

Department of Biochemistry, University of Calcutta, Kolkata, India

Brain is thought to function normally under equilibrium condition in the interaction of inhibitory and excitatory neurotransmitters, γ-amino butyric acid (GABA) and glutamate respectively. The excitation and inhibition homeostatic balance is known to alter by exogenous and endogenous factors that may alter due to stress or some pathological conditions including neoplastic transformation[1]. Such changes in neuronal function bring about alteration at the biochemical and physiological levels including endocrine and immune systems. It is well known that centrally active drugs interacts with different types of CNS activities, whose actions having clinical values in animals including human depending on their (drugs) dosages, toxicity, duration of exposure as well as their efficacy. Caffeine (plant alkaloid, 1,3,7-trimethyl xanthine), present in coffee, is one of the CNS stimulant having significant place in modern medicine due to its worldwide consumption and high bio potency. It (caffeine) also acts as chemopreventive, antioxidant and anticancer agent[2]. It is biochemically as well as pharmacologically acts as an adenosinergic antagonist[2]. Recent-past observation from our laboratory has shown that caffeine attenuates the EAC cell progression through reversal of EAC cell-induced dysfunction of gonadal hormones, suppression of specific and nonspecific immune response, diminution of antioxidant activity and induction of central GABA-ergic activity[2]. Since glutamatergic and GABA-ergic systems interact each other[3] and adenosine, the inhibitory neurotransmitter through its receptors plays a modulatory role on glutamatergic activity[4], the present authors are interested to study the effect of long-term consumption of caffeine on brain glutamatergic activity during the development of Ehrlich ascites tumor cells in adult albino female mice of Swiss strain (25-30 gm). In the present study animals were treated either with caffeine (20mg/kg/day, p.o) for 22-27 consecutive days or inoculated with EAC cells (5×10^6 cells/ ml, i.p) and allowed to develop for 10-15 days or animals bearing EAC cells were treated with caffeine for 22-27 consecutive days. Control animals were treated with corresponding vehicle(s) under similar conditions. Development of EAC cells in mice impaired the whole brain GABA/glutamate-glutamine cycle regulation along with a significant reduction in central glutamatergic activity [by measuring the steady state levels of glutamine, glutamate and GABA; enzyme activities of glutamic acid decarboxylase, GABA-transaminase, glutaminase and glutamine synthetase along with the specific binding of glutamate receptor (using ^{14}C-glutamate) including the kinetic parameters, maximum binding (Bmax) and binding affinity (1/Kd)]. Although caffeine consumption (20mg/kg/day, p.o) for 22-27 consecutive days did not change the central glutamatergic activity, its consumption during EAC cell development retarded EAC cell growth and also restored/attenuated the EAC cell-induced inhibition of brain glutamatergic activity. These results therefore, suggest that long-term consumption caffeine may reduce the development of EAC cells through the attenuation/restoration of EAC cell-induced inhibition of central GABA-glutamate regulation and its activity in mice.

References:

1. Levinson JN, El-Husseini A., Molecular Pain, 1:12, 2005.

2. Mandal A, Poddar MK. Planta Medica 74: 1779, 2008.

3. Lasse KB et al., J Neurochem 98:641, 2006.

4. Ciruela F et al., J Neurosci 26:2080, 2001.

Supported by University of Calcutta, Kolkata & University Grants Commission, New Delhi, India.

ENDONUCLEASE G DOES NOT PLAY AN OBLIGATORY ROLE IN PARP-ACTIVATED CELL DEATH AFTER TRANSIENT FOCAL CEREBRAL ISCHEMIA

J. Zhang[1], Z. Xu[1], K. David[2], X. Li[1], K. Kibler[1], T.M. Dawson[2], V.L. Dawson[2], R.C. Koehler[1]

[1]Department of Anesthesiology/Critical Care Medicine, [2]The Institute for Cell Engineering, Johns Hopkins University, Baltimore, MD, USA

Objectives: Activation of poly (ADP-ribose) polymerase (PARP) and subsequent translocation of apoptosis-inducing factor (AIF) contribute to neuronal injury from NMDA, oxygen-glucose deprivation, and stroke. In C. elegans, an analog of endonuclease G (Endo G) has been implicated in the DNA fragmentation induced by translocation of AIF to the nucleus. The present objective was to investigate if Endo G plays an obligatory role in the PARP dependent injury from middle cerebral artery occlusion (MCAO).

Methods: Endo G knockout and wild type (WT) mice were used to investigate the function of Endo G gene. Using isoflurane anesthesia, 90 minutes of MCAO was performed with the intraluminal filament technique. After 72 hours of reperfusion, infarct volume was analyzed. In some groups, saline vehicle or DR2313, a PARP inhibitor, was infused intravenously before MCAO (1 ml/kg; 10 mg/kg), at reperfusion (1 ml/kg; 10 mg/kg), and through the first 4.5 h of reperfusion (1 ml/kg/h; 10 mg/kg/h).

Results: Infarct volume was not different between male WT (47±6% of hemisphere; ±SD) and Endo G knockout (49±8%) mice or between female WT (37±16%) and Endo G knockout (35±9%) mice. Latex casts indicated a similar arterial distribution in WT and knockout mice, and a similar diameter of the posterior communicating artery. Furthermore, the reduction in laser-Doppler flux during MCAO was not different between WT and knockouts. When male mice were treated with DR2313, infarct volume was decreased to a similar extent in WT mice (saline = 44±14%; DR2313 = 22±16%) and in Endo G knockout mice (saline = 57±15%; DR2313 = 22±17%). The decrease in laser-Doppler flux was not influenced by DR2313 infusion.

Conclusion: These data demonstrate that Endo G is not required for the pathogenesis of transient focal ischemia in either male or female mice. Because the injury in Endo G null mice remains dependent on PARP, as demonstrated by tissue rescue with a PARP inhibitor, Endo G is not obligatory for executing PARP-dependent injury during stroke.

Brain Poster Session: Neuroprotection

ROSUVASTATIN PROTECTS CULTURED CORTICAL NEURONS AGAINST OXYGEN-GLUCOSE DEPRIVATION AND GLUTAMATE EXCITOTOXICITY

F. Domoki[1], B. Kis[2], T. Gáspár[3], F. Bari[1], J.A. Snipes[3], D.W. Busija[3]

[1]Department of Physiology, University of Szeged, Szeged, Hungary, [2]Department of Radiology Brigham and Women's Hospital, Harvard Medical School, Boston, MA, [3]Department of Physiology and Pharmacology, Wake Forest University Health Sciences, Winston-Salem, NC, USA

Objectives: Statins are known to exert pleiotropic effects unrelated to the inhibition of cholesterol biosynthesis. We examined if rosuvastatin (RST) preserved viability of cultured neurons after oxygen-glucose deprivation (OGD) and glutamate (L-glut) excitotoxicity.

Methods: Primary rat cortical neurons were isolated from E18 rat fetuses (Kis et al. 2003). Cultures 5-7 days in vitro (DIV) were treated with RST and/or mevalonate, geranylgeranyl pyrophosphate (GGPP), and cholesterol for 1-3 days. On 8 DIV, the cultures were exposed to 3h OGD or L-glut (200 mM, 1h). Neuronal viability was determined 24h after completion of the experiments. Additional experiments were performed to determine whether perillic acid, a non-specific inhibitor of both geranylgeranyl transferase GGT 1 and Rab GGT, and the GGT 1-specific inhibitor, GGTI-286, would reproduce the neuroprotective effect of RST.

Results: Three-day pretreatment with RST (5 μM) increased neuronal survival after OGD from 44±1% to 82±2%*, and after L-glut (0.5 μM RST) from 56±1% to 89±4%* (% of untreated controls, mean±SEM, n=24-96, *p< 0.05). One-day RST treatment was not protective against either stress. RST-induced neuroprotection against OGD was abolished by mevalonate coapplication; however, RST-induced protection against L-glut was not sensitive to mevalonate. These data indicate that inhibition of 3-hydroxy-3-methyl-glutaryl-coenzyme A (HMGCoA) reductase is involved in the mechanism of protection against OGD but not L-glut. The neuroprotective effect of RST against OGD was also abolished by GGPP but not by cholesterol coapplication, and was replicated by perillic acid but not by GGTI-286. RST and perillic acid but not GGTI-286 reduced neuronal ATP and membrane Rab3a protein levels, and they reduced post-OGD reactive oxygen species (ROS) levels determined with fluorescent detection of hydroethidin-ethidium conversion. Neuronal glutathione (GSH) and antioxidant protein (Mn superoxide dismutase (SOD), CuZnSOD, GSH peroxidase, catalase) levels were unaffected by RST. In RST-treated neurons, L-glut-evoked increases in intracellular Ca^{2+} levels - determined with Fluo4 AM fluorescence/confocal microscopy - were reduced by ~50%, and similar reduction in L-glut-induced ROS generation was observed.

Conclusions: RST elicits delayed preconditioning-like neuroprotection in cultured neurons against OGD and L-glut excitotoxicity. However, the mechanism of protection is markedly different against the two stresses. The neuroprotective mechanism of RST against OGD involves inhibition of HMGCoA reductase leading to depletion of GGPP and decreased geranylgeranylation of proteins which are probably not isoprenylated by GGT 1. Reduced neuronal ATP levels and ROS production after OGD may be directly involved in the mechanism of neuroprotection. In contrast, RST-induced neuroprotection against excitotoxic stress appears to be independent of HMGCoA reductase inhibition. Instead, L-glut results in reduced neuronal Ca^{2+} influx and subsequent reduction in ROS generation in RST-treated neurons that can contribute to the neuroprotection.

Grant support: National Institute of Health (HL30260, HL65380, HL77731), National Scientific Research Fund of Hungary (OTKA K68976, K63401). Ferenc Domoki was supported by tthe János Bólyai Research Scholarship of the Hungarian Academy of Sciences.

Reference: Kis B, Rajapakse NC, Snipes JA, Nagy K, Horiguchi T, Busija DW. (2003) Diazoxide induces delayed pre-conditioning in cultured rat cortical neurons. J Neurochem 87:969-980.

DEVELOPMENT OFDPET, A PET TECHNIQUE TO MEASURE THE DIFFUSION OF DRUGS AFTER DIRECT DELIVERY TO THE BRAIN

R.W. Sirianni[1], W.M. Saltzman[2], R.E. Carson[1,2]

[1]Diagnostic Radiology, [2]Biomedical Engineering, Yale University, New Haven, CT, USA

Objectives: Active agents have been delivered directly to the brain to treat or better understand diseases in the fields of substance abuse, mental illness, neurodegenerative disorders, brain cancer, ischemia and epilepsy, yet the spatial gradients that result from local delivery are not always known. Methods have been developed to measure drug transport parameters in vitro through use of brain slices or extracted tissue elements, however, these methods do not capture the full complexity of transport in living tissue, where the diffusion of drugs occurs in parallel with binding and uptake by cells, elimination and degradation. Methods used to measure drug distribution in vivo are too invasive to apply to humans and therefore cannot monitor the effectiveness of drug delivery in clinical studies. In these studies, we developed a method for non-invasive measurement of the diffusion of radiotracers with Positron Emission Tomography (PET). This diffusion-PET (dPET) system will eventually be used to characterize the spatial distribution of radiolabeled drugs or drug-polymer delivery systems after direct delivery in vivo.

Methods: The rate of movement of bound (C_b)and free drug (C_f) from a point source may be expressed in two partial differential equations that are a function of radial position (r), time (t), the diffusion coefficient (D), and a source term that accounts for non-diffusional processes such as binding, uptake or elimination. A numerical solution for the total detectable concentration of drug can be generated by assuming uniform distribution of first-order elimination (k_2) and reversible binding to cells (k_{on}, k_{off}). dPET data were simulated in Matlab by accounting for (1) decay, (2) counting statistics, and (3) resolution (1.5mm). Multiple data fitting trials were performed via least-squares to obtain an estimate for D in the presence of varying levels of binding and elimination. For initial in vitro tests, a point source of [18F]FDG(5-50ul, < 200uCi) was introduced into an agarose tissue phantom. Data were collected on the microPET Focus 220 for 1-6 hours, reconstructed via OSEM methods, and image data were analyzed to obtain an estimate of the diffusion coefficient.

Results: In modeling simulations, diffusion coefficients were accurately estimated for low molecular weight drugs subject to diffusion (D=0.06 mm^2/min), elimination (k_2=0.1 min^{-1}) and reversible binding (k_{on}=0.3min^{-1} and k_{off}=0.075min^{-1}). Assuming 20% pixel-noise, accurate estimates of D_{eff} were produced for both [18F] and [11C] in a 30min simulation (D_{fitted}=0.060±0.0024 and 0.057±0.0030, respectively, n=10).

Initial measurements of the [^{18}F]FDG diffusion in an agarose brain phantom resulted in estimates of D (0.034 and 0.071mm^2/min) near its theoretical value (0.052mm^2/min). We expect that optimization of the infusion technique (eg, preventing backflow) will improve parameter estimates.

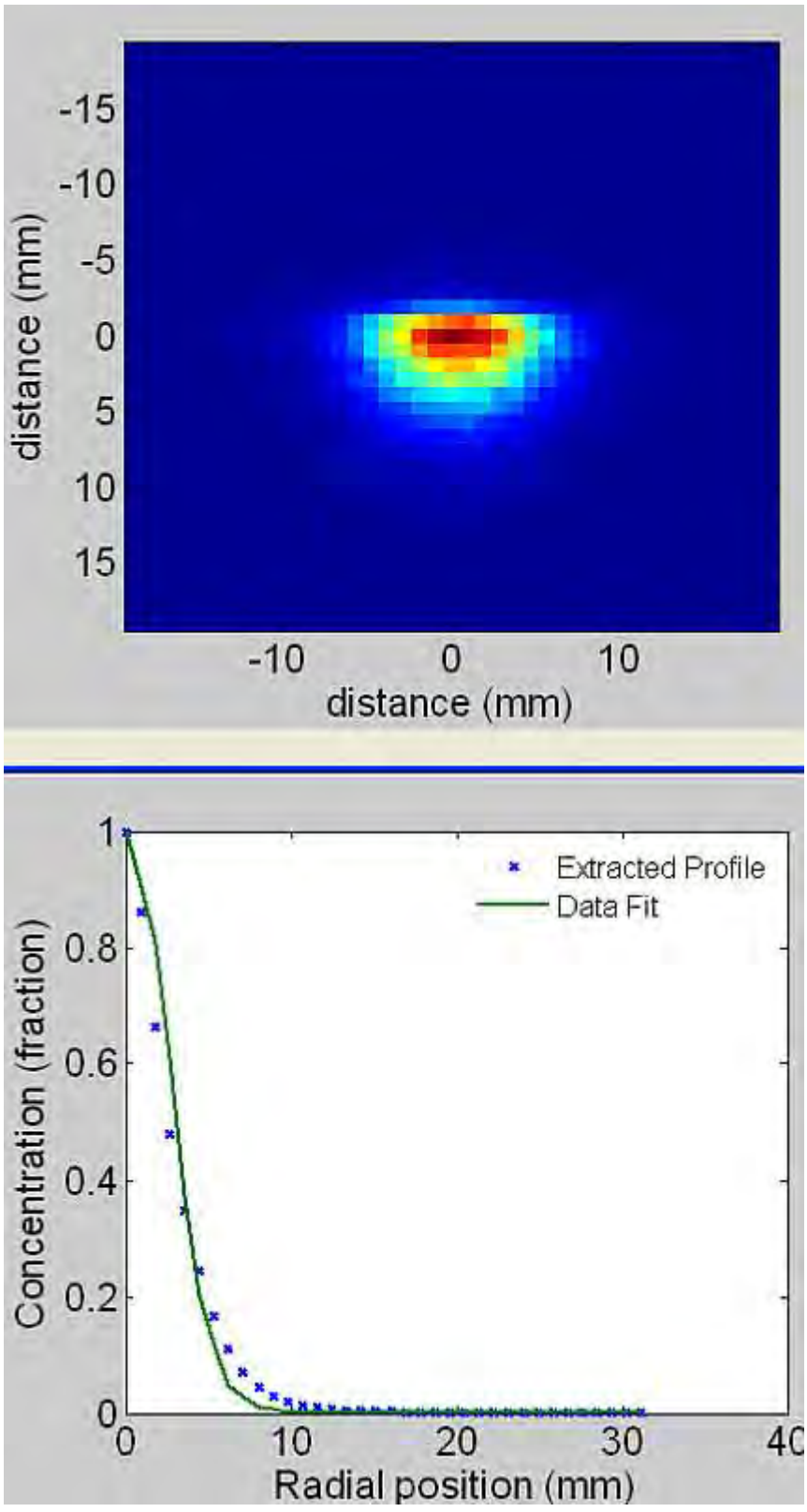

[Sample In Vitro Data]

Conclusion: Data-fitting experiments and preliminary in vitro measurements demonstrated the

feasibility of using PET to measure the distribution of radiolabeled drugs after direct delivery to the brain. The studies described here provide the basis for the next step in the development of dPET, i.e., the measurement of tracer diffusion in vivo, and suggest that dPET is a viable method to measure the spatial distribution of radiolabeled drugs in the brain.

Brain Poster Session: Spreading Depression

CORTICAL SPREADING DEPRESSION RECOVERY IS MODULATED BY TISSUE PERFUSION PRESSURE RATHER THAN OXYGENATION

I. Sukhotinsky[1], J. Xu[1], J.R. Sims[1], **C. Ayata**[1,2]

[1]Stroke and Neurovascular Regulation Laboratory, [2]Stroke Service and Neuroscience Intensive Care Unit, Massachusetss General Hospital/Harvard Medical School, Boston, MA, USA

Background and aims: We have recently shown that hypotension markedly prolongs the DC shift duration during CSD, while hypoxia under normotensive conditions had a much more modest effect, suggesting that perfusion pressure is a more important determinant of CSD recovery than tissue oxygenation. We hypothesized that the prolongation of DC shift during hypotension is due to tissue hypoxia, and tested whether normobaric hyperoxia restored the DC shift duration in hypotensive rats, and whether induced hypertension shortens the DC shift duration in normoxic rats.

Methods: Urethane-anesthetized rats were intubated and mechanically ventilated. Arterial blood pressure, gases and pH were monitored. CSD was induced by topical KCl (1M) application, and recorded using intracortical glass microelectrodes. Associated CBF changes were recorded by laser Doppler flowmetry. Absolute tissue partial pressure of O_2 (p_tO_2) was measured by phosphorescence lifetime using an intracortical electrode (OxyLite, Oxford Optronics). Experimental conditions were:

i. normoxic normotension,
ii. normoxic hypotension,
iii. hyperoxic hypotension,
iv. hyperoxic normotension, and
v. normoxic hypertension.

Hypotension was achieved by controlled blood withdrawal, hypertension by intravenous phenylephrine infusion (PHE, 2 mg/ml, 3 ml/h), and normobaric hyperoxia by inhalation of 100% O_2. Data are mean±SD. Conditions (i), (ii), (iii), and (iv) were studied within the same rat and compared among each other, while (v) was studied in a separate group of rats and data before and after PHE were compared. *$p< 0.01$ vs. control.

Purpose: To test whether normobaric hyperoxia restores the DC shift prolongation during CSD under hypotensive conditions.

Results: Normoxic hypotension doubled the DC shift duration compared to normoxic normotensive rats, and transformed the CBF response by unmasking an initial hypoperfusion as reported previously. Normobaric hyperoxia normalized baseline p_tO_2 in hypotensive animals, but failed to restore the DC shift duration or the CBF response. Normobaric hyperoxia did not alter the DC shift duration or CBF response in normotensive animals either. Normoxic hypertension significantly increased baseline CBF (breakthrough hyperemia) and shortened the DC shift duration by ~30% without changing the peak hyperemia during CSD.

Experimental Condition	BP (mmHg)	paO2 (mmHg)	ptO2 (mmHg)	CBF (%)	DC Duration (sec, at half amplitude)		DC Amplitude (mV)		N
(i)	89±15	115±21	15±4	101±2	25±3		28±3		10
(ii)	45±4	118±19	10±4	83±10	50±14*		29±5		10
(iii)	43±6	388±47	15±4	72±35	51±17*		27±5		10
(iv)	91±9	409±31	-	106±31	24±2		26±4		6
					before	after	before	after	
(v) PHE	165±15	116±40	-	312±98	25±5	17±2*	25±3	24±2	6

[Results]

Conclusion: Our data suggest that blood pressure is a critical determinant of CSD recovery and the CBF response to CSD. Hyperoxia did not reverse the hypotensive prolongation of CSD despite normalized p_tO_2, suggesting that the mechanism does not involve tissue hypoxia. Instead, the initial hypoperfusion and diminished hyperemia during CSD may play a role in delaying the DC shift recovery in hypotensive rats. The data also suggest that hypotension may be detrimental to tissue outcome in stroke, subarachnoid and intracerebral hemorrhage, and traumatic brain injury, where injury depolarizations have been observed.

469

Brain Poster Session: Experimental Stroke & Cerebral Ischemia

POTASSIUM DISTURBANCES AT THE 'ISCHEMIC EDGE' IN RAT EXPERIMENTAL FOCAL ISCHEMIA

A. Kharlamov[1], V.E. Yushmanov[1], S.C. Jones[1,2,3]

[1]Anesthesiology, [2]Anesthesiology and Neurology, Allegheny-Singer Research Institute, [3]Radiology, Univ of Pittsburgh, Pittsburgh, PA, USA

Aims: Maximum changes of sodium (1), MAP2 (2), water and K^+ (3,4) and transient BBB disruption (5) occur at the edge of the ischemic core after experimental focal ischemia. These phenomena may be related to higher levels of 'trickle' blood flow that result in greater degrees of swelling in the peripheral areas of the ischemic core. Here we hypothesize that the 'ischemic edge' (IE) differs depending on position (dorsal or ventral) and ischemic model.

Methods: Experimental focal ischemia was induced by MCA transection and bilateral common carotid artery or suture occlusion in 14 Sprague-Dawley rats (isoflurane/N_2O) for 2.5-5 h. Brains were sectioned for quantitative K^+ histochemistry and micro-punched using our previous procedures (4). 2D images of brain K^+ concentration, $[K^+]_{br}$, were used to extract $[K^+]_{br}$ profiles along the cortical ribbon using MCID software and to provide in the one suture model animal a 3D image of $[K^+]_{br}$ in the entire brain.

Results: There were prominent decreases in $[K^+]_{br}$ in all animals at the edges of the ischemic core. The frequency distribution of $[K^+]_{br}$ at these edges showed a bimodal distribution with peaks at 85 and 103% of ischemic core $[K^+]_{br}$ with the minimum at 92.5%. An IE was defined by having a $[K^+]_{br}$ less than this 'trough' value. In the MCAT animals, the distances from the edge of the normal cortex to the dorsal and ventral IE regions were 2.1±0.1 mm and 2.6±0.2 mm, respectively ($p=0.041$, unpaired t-test).

From the suture model animal, a 3D reconstruction from K^+-stained coronal slices (IE with $[K^+]_{br}< 56$ mM in yellow) in the figure indicates that the IE completely surrounds the ischemic core but that the rostral IE (right) is narrower than the caudal IE (left).

Conclusions: We conclude from 2D evidence that the low level of $[K^+]_{br}$ which defines the dorsal IE is closer to normal cortex than the ventral IE, suggesting lower dorsal collateral potential. The 3D study suggests that there are differences between IE characteristics due to the model of ischemia. The low K^+ in the IE is not normally recognized as a feature of ischemic pathology, and its characteristics and their relation to the associated exaggerated progression of ischemic pathology are important unexplored concepts that need further study. These characteristics of the IE displace the notion that the ischemic region is homogeneous and progresses towards infarct at an equal rate. This concept has diagnostic and therapeutic implications based upon a potentially enhanced understanding of ischemic pathology.

Support: NIH-NS030839.

References:

1. Jones et al. (2006) Stroke 37:883-888.

2. Dawson et al. (1996) JCBFM 16:170-174.

3. Kato et al. (1987) Exp Neurol 96:118-126.

4. Kharlamov et al. (2007) JCBFM 27(S1):BP53-7W.

5. Jones et al. (2007) JCBFM 27(S1):PBO5-9.

[QM68_Projection of Stack_4.jpg]

470

Brain Oral Session: Traumatic Brain Injury: Metabolism

BLOOD-INDUCED, BUT VOLUME-INDEPENDENT CHANGES OF BRAIN EDEMA, TISSUE DEATH AND GLUCOSE METABOLISM AFTER ACUTE SUBDURAL HEMATOMA

B. Alessandri[1], H. Bächli[2], A. Heimann[1], M. Behzad[1], M. Schreckenberger[3], H.-G. Buchholz[3], **O. Kempski**[1]

[1]Institute for Neurosurgical Pathophysiology, University Medicine, Johannes Gutenberg-University of Mainz, Mainz, Germany, [2]Department of Neurosurgery, University Clinics of Basel, Basel, Switzerland, [3]Department of Nuclear Medicine, University Medicine, Johannes Gutenberg-University of Mainz, Mainz, Germany

Objective: Traumatic brain injury is often accompanied by acute subdural hemorrhage (ASDH). Underneath the ASDH ischemic and metabolic changes are induced which worsen outcome of patients dramatically. Despite early surgical intervention, i.e. evacuation of the blood volume, many patients die or remain severely disabled. Besides the blood volume, additional factors from extravasated blood may play a role in lesion development. In order to separate blood from volume induced effects:, we compare the effects of a subdurally infused blood volume with the same volume of paraffin oil (no blood components) on their effects on acute and chronic pathophysiological parameters.

Method: Sprague-Dawley rats were anesthetized with chloral hydrate and a catheter was placed in the tail artery and jugular vein. A craniotomy was prepared for the insertion of a L-shaped, blunted needle into the subdural space and closed with acrylic glue and dental cement. ASDH was produced by infusion of 300 µl unheparanized autologous venous blood or paraffin oil (50 µl/min) into the subdural space. Three different experiments were carried out:

1. Effects on MAP, ICP, CPP during 40 min and on histological damage 48 h after subdural infusion of blood or paraffin oil (n=8/group).
2. Acute and chronic effects of blood or paraffin oil on brain edema: Brains were removed either 2, 24 or 48 h after subdural infusion. Brain water content was measured by the wet-dry weight method (n=6-8/group).
3. Acute glucose metabolism by means of PET using [18F]-deoxyglucose: FDG activity was measured 2 h after blood or paraffin oil infusion.

Values were normalized for injected FDG activity and body weight. Values were analyzed either by calculating an ipsi-to-contralateral ratio of cortical and subcortical regions of interest (ROI) or by categorizing all voxels into low-high normalized FDG activity.

Results: Blood and paraffin oil produced almost identical changes of MAP, ICP, CPP and CBf during the 40 min monitoring after subdural infusion. However, 2h after injury glucose metabolism, was significantly reduced by blood in the cortical, but not in the subcortical ROI. Voxel-by-voxel analysis also showed significantly more voxels with lower activity in the blood infusion group than in the paraffin oil group. Ipsilateral brain water content was not affected at 2h, but differred significantly between groups at 24h ((80.3±1.2%) vs. 79.0±0.2%, $p< 0.05$) and at 48h (80.7±1.2% vs. 78.9±0.5%), $p< 0.05$ post-injury. Blood produced also a significantly larger brain damage (48.1±23.0 mm3 vs. 21.1±11.8 mm3, $p< 0.02$).

Conclusion: Despite the same volume of blood and paraffin oil produced similar acute changes in

ICP, CPP and CBF glucose metabolism underneath the infusion site was more reduced with blood than with paraffin oil at 2h post-injury followed by larger brain swelling and lesion volume 48h after injury. Thus, lesion development after ASDH is not only determined by the blood volume, but in part also by blood constituents.

ELECTROCONVULSIVE THERAPY INDUCES ALTERATIONS IN DOPAMINE RECEPTOR AND TRANSPORTER BINDING IN THE STRIATUM OF HEALTHY AND MPTP-LESIONED NON-HUMAN PRIMATES

A.M. Landau[1,2], M.M. Chakravarty[1], S. Jivan[2], A.P. Zis[2], A. Gjedde[1], D.J. Doudet[1,2]

[1]PET Center and Center of Functionally Integrative Neuroscience, Aarhus University Hospital, Aarhus, Denmark, [2]Medicine/Neurology, University of British Columbia, Vancouver, BC, Canada

Objectives: Parkinson's disease (PD) is a progressive neurodegenerative disorder. Depression is one of the most disabling co-morbidities associated with PD and both PD and depression are poorly treated in advanced patients. Electroconvulsive therapy (ECT), a form of electric brain stimulation, is one of the most effective therapies used to treat depression and has additional beneficial effects on the motor symptoms of PD. Little is known about the mechanisms of action of ECT in PD patients. Rodent studies do not allow long-term longitudinal studies of regional changes in monoamine neurotransmission and ethical concerns reduce the feasibility of performing extensive longitudinal studies in human PD subjects. The aim of this work is to explore the neural mechanisms underlying the therapeutic effects of ECT, focusing on dopaminergic neurotransmission in the lesioned and unlesioned striatum of non-human primates.

Methods: The 1-methyl-4-phenyl-1,2,3,6-tetrahydropyridine (MPTP) neurotoxin was used to induce hemi-parkinsonism (unilateral lesion) in 4 rhesus monkeys and full parkinsonism (bilateral lesion) in 3. Six monkeys were left unlesioned. ECT was performed under anaesthesia using a clinical ECT device. Electrodes were placed bilaterally and 6 ECT treatments were administered over a 3 week period. Animals received a PET scan before the initiation of ECT treatment and then 24-48 hours, 1 week and 6 weeks after the end of the course of ECT. Monkeys were scanned using SCH23390, a dopamine D1 receptor ligand; raclopride, a dopamine D2 receptor antagonist; and methylphenidate, which binds to the dopamine transporter (DAT). PET data were coregistered to an average MR from 12 different monkeys and binding potentials were determined using the Logan model for the 30-60 minute time period of the scan. Left and right sides of each brain region were averaged in unlesioned and bilaterally lesioned monkeys; whereas sides were kept separate for the analysis in unilaterally lesioned monkeys.

Results: In unlesioned monkeys, ECT induced a significant increase in dopamine D1 and a decrease in dopamine D2 receptor binding in the striatum. DAT binding increased at 24-48 hours and 1 week following the final ECT treatment but returned to baseline levels by 6 weeks. In full PD and the lesioned side of hemi-PD monkeys, no effects were observed in DAT binding and, like in unlesioned monkeys, increases in D1 binding were again observed. Decreases were still observed in raclopride binding of D2 receptors in full PD monkeys.

Conclusion: These data are in agreement with studies in unlesioned and parkinsonian rodents showing increases in dopamine D1 receptor binding in response to ECT. Effects of ECT on D2 receptors and DAT have not been previously investigated. Better understanding of the mechanism of action of ECT may lead to refinements in its clinical therapeutic applications in depression and PD.

References:

Strome, E.M. et al., Biol Psychiatry 57 1004-1010, 2005.

Strome, E.M. et al., J Psychiatry Neurosci 32: 193-202, 2007.

Collins, D.L. et al., J Comp Assis Tom 18(2):92-205, 1994.

Logan, J. et al., J Cereb Blood Flow Metab 16:834-840, 1996.

Brain Oral Session: Traumatic Brain Injury

FULL CONTACT KARATE INCREASES SERUM LEVELS OF S-100B, & NSE, BIOCHEMICAL MARKERS OF BRAIN TISSUE DAMAGE

M. Graham[1], P. Ryan[1], P. Evans[2], B. Davies[3], J. Baker[4]

[1]The Newman Centre for Sport and Exercise Research, Newman University, Birmingham, [2]Department of Endocrinology, Royal Gwent Hospital, Newport, [3]Health and Exercise Science Research Unit, University of Glamorgan, Cardiff, [4]Division of Sport, University of the West of Scotland, Glasgow, UK

Objectives: Mild brain injuries (MBI) are usually defined by an initial unconsciousness limited to 30 minutes, a Glasgow coma score between 13 and 15, the absence of intra-cranial lesion on computerised tomography (CT) and a post-traumatic amnesia period between 1 and 24 hours (Kosakevitch-Ricbourg, 2006). Neurobiochemical markers of brain damage have increased in interest in both experimental and clinical neurotraumatology (Raabe et al., 1999). The aim of the study was to analyse whether technical knockouts (TKOs) or kicks to the head (KTH) in full contact karate elicited significantly greater increased serum concentrations of biochemical markers of brain tissue damage, than kicks to the body (KTB).

Methods: Twenty four full contact karate practitioners were divided into three groups: TKO, (n=6, mean ± SD, age 33.5 ± 3.8 years), KTH (n=6, mean ± SD, age 27.3 ± 7.8 years), and KTB (n=12, mean ± SD, age 28.2 ± 6.5 years). The TKO and KTH groups both received direct kicks to the head, while group KTB received only blows to the body. Blood samples were taken before and immediately after combat for analysis of S-100B and neurone specific enolase (NSE).

Results: Significant increases in serum concentrations of S-100B ($p< 0.05$) were encountered before and after combat in the TKO group (0.16 ± 0.25 vs 0.42 ± 0.39) and after combat in groups TKO and KTH compared with KTB (0.42 ± 0.39 vs 0.32 ± 0.14 vs 0.12 ± 0.16, $\mu g.L^{-1}$) and significant increases in NSE before and after combat in the TKO group (11.9 ± 5.9 vs 20.2 ± 11.4 $ng.ml^{-1}$).

Conclusions: Head kicks in full contact karate are sufficient enough to cause biochemically discernible damage of brain tissue. The severity of traumatic brain injury is associated with the early post-traumatic release of protein S-100B and NSE (Herrmann et al., 1999) and their early kinetics after traumatic brain injury reflect a different type of intracranial pathology as demonstrated in cranial CT and have become an extremely sensitive prognostic marker (Korfias et al., 2006).

References:

Kosakevitch-Ricbourg, L. Clinical scoring scales for brain injury. Rev Stomatol Chir Maxillofac. 2006; 107: 211-217.

Raabe, A., Grolms, C., Sorge, et al. Serum S100B protein in severe head injury. Neurosurgery. 1999; 45: 477-483.

Herrmann, M. 1999. Protein S-100B and neuron specific enolase as early neurobiochemical markers of the severity of traumatic brain injury. Restorative Neurology and Neuroscience. 14: 109-114.

Korfias, S., Stranjalis, G., Boviatsis, E., et al. Serum S-100B protein monitoring in patients with severe traumatic brain injury. Intensive Care Med. 2007; 33: 255-260.

OPTIMIZATION OF CEREBRAL BLOOD FLOW BY INTRA-AORTIC BALLOON PUMP COUNTERPULSATION DURING MANAGEMENT OF NEUROGENIC PULMONARY OEDEMA ASSOCIATED WITH SUBARACHNOID HAEMORRHAGE

M. Hachemi[1], C. Di Roio[1], S. Tixier-Wulf[1], A. Terrier[1], E. Bonnefoy-Cudraz[2], F. Dailler[1]

[1]Department of Neurocriticale Care, [2]Department of Cardiac Intensive Care, Hospices Civiles de Lyon, Lyon, France

Introduction: Neurogenic pulmonary oedema (NPE) is a well recognised complication of subarachnoid haemorrhage (SAH) and severe traumatic brain injuries. The incidence of NPE was reported to be 6% in a series of 457 patients with SAH [1]. NPE is characterized as an acute, protein-rich lung oedema occurring shortly after cerebral injury. NPE may compromise haemodynamics, decrease cerebral blood flow and increase cerebral vasospasm which increases the morbidity of SAH. Yet, the precise pathogenetic mechanisms remain unclear, but the role of a sympathetic storm may be the most important cause.

Patients and methods: We report two patients with neurogenic pulmonary oedema and cardiac failure after subarachnoid haemorrhage treated with intra-aortic balloon pump counterpulsation (IABP) therapy.

Results:

- Case 1: A 51 year old man was admitted to the cardiac intensive care unit for cardiac arrest with pulmonary edema. Coronarography was normal. CT scan showed an extensive SAH with intraventricular haemorrhage and secondary hydrocephalus. Initial Glasgow coma scale was 3 (Hunt & Hess grade V). Cerebral angiography showed an aneurysm of the anterior communicant artery. Chest radiograph showed frank pulmonary oedema. Echocardiography showed acute severe left ventricular dysfunction (ejection fraction (EF) 25%) associated with left ventricular apical ballooning (takotsubo-like myocardial dysfunction). The PaO2/ FIO2 ratio was 75 on admission. Despite conventional treatment (mechanical ventilation, dobutamine) IABP was necessary to treat cardiac failure and pulmonary edema. Four hours after the insertion of IABP, PaO2/ FIO2 ratio was 315. Left ventricular EF reached 50% 12 hours after insertion. The IABP was removed after 17 hours. Despite embolization of the aneurysm and treatment of intracranial hypertension by decompressive craniectomy, the patient death occurred at day 8.

- Case 2: A 46 year old woman was admitted in ICU for SAH (Hunt & Hess grade IV). Her medical past history included diabetes, hypertension, coronaropathy (EF 50%) and she was treated with clopidogrel and acetyl salicilyc acid. Ten hours after admission, she developed arterial hypotension and pulmonary edema (cardiogenic and neurogenic). PaO2/ FIO2 ratio was 150. At day two, despite conventional therapy (mechanical ventilation and high dose of dobutamine, norepinephrine, epinephrine), EF was less than 20%. IABP was inserted to optimize haemodynamic function. Three hours after the insertion of the IABP, infusion of dobutamine, norepinephrine, epinephrine was stopped. Then the IABP was removed after four days. The patient was extubated at day 13, and was discharged of the ICU at day 18 with EF 45% and a good cardiac and neurologic outcome.

Conclusions: These two cases illustrate the potential usefulness of the intra-aortic balloon pump counterpulsation as an adjunctive therapy in neurogenic pulmonary edema and cardiac failure after subarachnoid haemorrhage.

Reference: [1]Solenski NJ, Haley EC Jr, Kassell NF, Kongable G, Germanson T, Truskowski L, et al. Medical complications of aneurysmal subarachnoid hemorrhage: a report of the multicenter,

cooperative aneurysm study. Participants of the Multicenter Cooperative Aneurysm Study. Crit Care Med 1995; 23: 1007-17.

475

Brain Poster Session: Blood-Brain Barrier

HUMAN BRAIN IMAGING AND RADIATION DOSIMETRY OF [^{11}C]-N-DESMETHYL-LOPERAMIDE, A POSITRON EMISSION TOMOGRAPHIC RADIOTRACER TO MEASURE THE FUNCTION OF P-GLYCOPROTEIN

N. Seneca[1,2], S.S. Zoghbi[2], J.-S. Liow[2], W. Kreisl[2], P. Herscovitch[3], K. Jenko[2], R.L. Gladding[2], A. Taku[2], V.W. Pike[2], R.B. Innis[2]

[1]Clinical Research & Exploratory Development, F. Hoffmann-La Roche Ltd., Basl, Switzerland, [2]Molecular Imaging Branch, NIMH, [3]PET Department, Clinical Center/NIH, Bethesda, MD, USA

P-glycoprotein (P-gp) is a membrane-bound efflux pump that limits the distribution of drugs to several organs of the body [1]. At the blood-brain barrier, P-gp blocks the entry of both loperamide and its metabolite N-desmethyl-loperamide (dLop) and thereby prevents central opiate effects. Animal studies have shown that [^{11}C]dLop, in comparison to [^{11}C]loperamide, is a promising radiotracer because it generates negligible radiometabolites that enter brain [2,3].

Objectives: The purposes of this study were to determine if [^{11}C]dLop is a substrate for P-gp at the blood-brain barrier in humans and to measure the distribution of radioactivity in the entire body so as to estimate radiation exposure.

Methods: Brain PET scans were acquired in four healthy subjects for 90 min and included concurrent measurements of the plasma concentration of parent radiotracer. Time-activity data from the whole brain were quantified using a one-tissue compartment model to estimate the rate of entry (K_1) of radiotracer into brain. Whole-body PET scans were acquired in eight healthy subjects for 120 min.

Results: Brain imaging. After injection of [^{11}C]dLop, the concentration of radioactivity in brain was low (~15% SUV) and stable after ~20 min. In contrast to the low uptake in brain, pituitary and choroid plexus accumulated high concentrations of radioactivity about 650% and 280% SUV, respectively. Similar to brain, uptake in the pituitary and choroid plexus was relatively rapid and stable until the end of the scanning session. Plasma concentration of [^{11}C]dLop declined rapidly over time, but the percentage composition of plasma was unusually stable, with parent radiotracer constituting 85% of total radioactivity after ~ 5 min. The rate of brain entry was very low (K_1 = 0.009 ± 0.002 mL×cm^{-3}×min^{-1}). Whole-body imaging. As a measure of radiation exposure to the entire body, the effective dose of [^{11}C]dLop was 7.8 ± 0.6 mSv/MBq.

Conclusions: The low brain uptake of radioactivity is consistent with [^{11}C]dLop being a substrate for P-gp in humans and confirms that this radiotracer generates negligible quantities of brain-penetrant radiometabolites. The low rate of brain entry (K_1) is consistent with P-gp rapidly effluxing substrates while they transit through the lipid bilayer. The current data reports baseline brain uptake of [^{11}C]dLop in healthy humans and future studies after P-gp blockade will further confirm that [^{11}C]dLop is acting as an active substrate for P-gp in humans. Based on our animal studies which showed that brain uptake of [^{11}C]dlop was high after inactivation of P-gp by either genetic knockout or pharmacological inhibition [2-4], we hope to translate these animal studies to humans. The radiation exposure of [^{11}C]dLop is similar to that of many other ^{11}C-radiotracers. In conclusion, [^{11}C]dLop is a promising radiotracer to study the function of P-gp at the blood-brain barrier, where impaired function would allow increased uptake into brain.

References:

1. Fromm MF. Trends Pharmacol Sci. 2004;25: 423-429.

2. Zoghbi SS, et al. J Nucl Med. 2008;49(4): 649-656.

3. Lazarova N, et al. J Med Chem. 2008; 9;51(19):6034-43.

4. Liow, et al. J Nucl Med. 2008; In press.

THERAPEUTIC WINDOW OF ARGININE VASOPRESSIN V_1 RECEPTOR INHIBITION FOLLOWING TRANSIENT FOCAL CEREBRAL ISCHEMIA IN MICE

S.W. Kim[1,2], R. Trabold[2], N. Plesnila[1,2]

[1]Royal College of Surgeons in Ireland, Dublin, Ireland, [2]Laboratory of Experimental Neurosurgery, Department of Neurosurgery and Walter-Brendel-Center for experimental Medicine, University of Munich Medical Center - Grosshadern, Ludwig-Maximilians-University, Munich, Germany

Objectives: Previously we showed that inhibition of arginine vasopressin (AVP) V_1 but not V_2 receptors have beneficial effects following experimental stroke when treatment was initiated before the onset of ischemia (1). Since such a pre-treatment protocol has no clinical relevance, the current study was designed to investigate the therapeutic window of AVP V_1 receptor inhibition following transient cerebral ischemia.

Methods: Male C57/BL6 mice were subjected to 60 minutes occlusion of the middle cerebral artery by an intraluminal filament (MCAo) followed by 23 hours of reperfusion. 15, 75, 180, or 360 minutes after MCAo, 500 ng of the AVP V_1 receptor antagonist [deamino-Pen(1), O-Me-Tyr(2), Arg(8)]-vasopressin were injected into the left ventricle (n=8 each). Twenty-four hours after MCAo infarct volume and brain edema formation were quantified. Mortality and neurological function were evaluated in separate groups over 7 days.

Results: Mice treated with the AVP V_1 receptor antagonist immediately after the MCAo had less brain edema ($p< 0.01$) and 42% smaller infarct volumes as compared to vehicle treated animals ($p < 0.05$). This neuroprotection resulted in significantly improved mortality and neurological function ($p < 0.05$). Although brain edema formation was also reduced when treatment started up to 75 minutes after MCAo no further beneficial effects were observed on the other assessed parameters.

Conclusions: Together with our previous results (1) the current findings demonstrate that vasopressin V1 receptors play an important role in the pathophysiology of ischemic stroke, most likely through the inhibition of brain edema formation. Therefore inhibition of AVP V1 receptors may have a particularly high clinical potential when applied shortly before or after reperfusion, e.g. in patients receiving thrombolytic therapy by rtPA.

1. Vakili A, Kataoka H, Plesnila N. Role of arginine vasopressin V_1 and V_2 receptors for brain damage after transient focal cerebral ischemia. JCBFM. 2005; 25(8):1012-9.

COGNITIVE AND EMOTIONAL CHANGES IN THE BEHAVIOR OF RATS AFTER OCCLUSION OF THE ANTERIOR CEREBRAL ARTERY

H. Mertgens, G. Mies, R. Graf, H. Endepols

Max Planck Institute for Neurological Research, Cologne, Germany

Objectives: The anterior cerebral artery (ACA) supplies cingulate and frontal cortical regions in both humans and rats. Ischemic lesions in the ACA territory of humans impair cognitive functions and reduce incentive drive. We studied in a rat model of ACA occlusion (ACAo) loss and recovery of function longitudinally over one year using various behavioral paradigms.

Methods: ACAo (n=8) or sham operation (n=2) was performed in male Lister hooded rats by stereotactic injection of the vasoconstrictor endothelin-1 (ET-1; 150 pmol in 0.3 µl phosphate buffer) or vehicle. To analyze functional outcome, we carried out behavioral tests, which assess decision-making during foraging (food-carrying task), anxiety (elevated plus maze), spatial working memory (spontaneous alternation in the Y-maze), exploratory behavior (open field), working memory (object recognition task) and attentional set-shifting (bowl-digging task). In order to set up a longitudinal study, these tests were carried out before, a week after (early testing phase) and a year after ACAo (late testing phase). Behavioral data were finally correlated with MRI (T2) and PET (^{18}F-fluorodesoxyglucose) assessments of structural and metabolic alterations.

Results: Early after ACAo, rats carried less food pellets in the food-carrying task ($F(9, 126) = 2.62$, $p=0.012$), moved more slowly ($F(2, 126) = 35.1$, $p< 0.001$), went on fewer trips ($F(2, 126) = 5.8$, $p=0.015$) than before and showed jagged movement patterns. The number of pellets per trip increased with distance between food and cage before but no longer after ACAo ($F(9, 126) = 5.9$, $p< 0.001$). All these changes remained constant after one year. In the elevated plus maze, lesioned animals spent more time on the open arms than before ACAo ($F(2, 28) = 8.3$, $p=0.003$). Arm alternation rate in the spontaneous alternation task decreased from 83 % to chance level in the early measurements but recovered to 77.6 % after one year. Locomotor activity in the open field stayed constant in all testing phases apart from early impairment of homebase-behavior ($F(2, 56) = 210.3$, $p< 0.001$), which recovered considerably after one year. Object recognition was not impaired in both testing phases after ACAo and rats showed no side preference but behavioral changes like decreased rearing ($F(2, 23) = 5.9$, $p=0.013$). Attentional set-shifting did not change after ACAo. Behavioral changes in the elevated plus maze and in the open field after ACAo correlated with metabolic impairment (PET) of the anterior cingulate cortex, prelimbic regions, septum, piriform cortex and the hippocampus. Behavioral impairments in the food carrying task correlated with structural lesion size (MRI) of the anterior cingulate cortex, prelimbic areas, the septum, and with ventricular enlargement.

Conclusion: Like in humans, ischemic lesions in the ACA-territory of rats cause cognitive and emotional deficits. These deficits are correlated with metabolic and/or structural loss. One year after occlusion, some functions recover spontaneously, while others remain impaired.

FROM MEDIUM TO ULTRA HIGH FIELD MR-BRAINPET

H. Herzog, N.J. Shah

Forschungszentrum Juelich, Juelich, Germany

Objectives: Hybrid MR-PET scanning which allows simultaneous measurements of the two modalities will lead to new horizons for multi-parametric imaging observed by modality specific features in regard to functions and anatomy. Here, we report on a project at the Forschungszentrum Jülich where two hybrid MR-PET scanners constructed by Siemens and dedicated for human brain studies are being installed, one at 3T MRT and the other at 9.4T MRT.

Methods: The 3TMR-PET consists of a commercial MRI MAGNETOM Tim-Trio and a newly developed PET detector with avalanche photodiodes (APD) as readout electronics rather than magneto-sensitive photomultiplier tubes. The PET detector, called BrainPET, with an outer diameter of 60 cm fits in the MR bore. It consists of 32 copper shielded cassettes each with six compact detector modules. The detector front-end has 12 x 12 LSO crystals of 2.5 x 2.5 x 20 mm^3 which are read out by an array of 3 x 3 APDs. Each cassette is linked by a 10 m long cable to the filter plate of the MRI room the data acquisition electronics on the outside. A combined transmit/receive RF coil is placed inside the BrainPET.

The 9.4T magnet is a newly developed centre piece of a whole-body scanner and has a bore size of 90 cm and a weight of 57 t. To perform brain MRI within the ultra-high magnetic field a new multi-channel transmit system is being implemented. New sequences to study nuclei such 23Na, 17O, and 19F have been developed. Adaption and testing of the BrainPET to the 9.4T MR environment is planned. Some preliminary tests of the BrainPET concerning resolution, scatter fraction, count rate performance, and image quality were carried out in the 3TMR-PET. Currently, the 9.4T instrument is producing MRI images; the adaption of the BrainPET is due to commence shortly.

Results: The tangential resolution (FWHM) was about 2.4 mm (r = 0 to 5 cm) in a central transversal plane with r = 0 to 5 cm, whereas radial resolution ranged from 2.1 mm to 5.5 mm. Within the 15 central image planes the axial resolution was 2.5 ± 0.2 mm at r = 0 cm and 3.1 ± 0.2 mm at r = 5 cm. When images of a cylindrical phantom with three cold rods were OSEM3D reconstructed and attenuation corrected, a scatter fraction of 27% was found in the air filled rod. Using a 25 cm long cylinder of 20 cm diameter filled with 18F the peak prompt-minus-delayed count rate was 680000 cps at 50 kBq/ml. Furthermore, first tests of possible interferences of the BrainPET towards the 3T MRT yielded only minimal changes of the MR performance.

Conclusions: After first promising tests with the 3TMR-PET further detailed tests will be performed and the experiences will be transferred to the 9.4TMR-PET.

480

Brain Poster Session: Glial Functions

ACTIVATION OF ASTROCYTES BY ALBUMIN IS MEDIATED BY P38 MAPK AND ERK, BUT NOT JNK, -DEPENDENT PATHWAYS

H. Ralay-Ranaivo[1,2], M. Wainwright[1,2]

[1]Department of Pediatrics, Division of Neurology, Northwestern University, Feinberg School of Medicine, [2]Center for Interdisciplinary Research in Pediatric Critical Illness and Injury, Children's Memorial Research Center, Chicago, IL, USA

Background and aims: Albumin, which may infiltrate brain parenchyma after compromise of the blood brain barrier, has been implicated in the evolution of neurologic injury and mechanisms of epileptogenesis. Astrocytes are activated in response to neurologic insults and contribute to the mechanisms of repair, neurologic injury, or susceptibility to subsequent neurologic injury. The contribution of albumin to astrocyte activation is not well understood. This study aims to determine the effect of albumin on astrocyte injury, activation and release of inflammatory markers. Here, we tested the hypothesis that specific mitogen activated protein kinase (MAPK) pathways (p38 MAPK; extracellular signal-regulated protein kinase, ERK; and c-Jun N-terminal kinase, JNK) selectively regulate astrocyte responses to albumin.

Methods: Enriched astrocytes were cultured from neonatal rat brains and treated with 0.1mM bovine serum albumin. Astrocyte activation was quantified by serial measurements of the pro-inflammatory cytokine IL-1β, S100B, iNOS, and the nitric oxide metabolite, nitrite. Cell injury was quantified by lactate dehydrogenase (LDH) release. MAPK activation was quantified by Western blotting. The level of the regulatory chemokine fractalkine (FKN) produced by astrocytes in response to albumin was measured by ELISA. To distinguish the specific contribution of p38MAPK, ERK or the JNK pathway to each of these albumin-induced responses, cells were treated with specific MAPK inhibitors (SB203580, PD98059, and SP600125).

Purpose: To determine the specific MAPK pathways which regulate cell injury, cytokine release, chemokine release and increase in NO in astrocyte responses to albumin.

Results: After 24 hr exposure, albumin induced an increase in the release of LDH, consistent with cell injury. Albumin induced a significant increase in the levels of the inflammatory markers IL-1β and nitrite released in the media as well as the level of iNOS in the cell lysates. Notably, levels of S100B levels were decreased under the same conditions, while levels of the chemokine FKN were increased by treatment with albumin. Albumin activated all MAPKs, producing increases in the levels of phosphorylated p38 MAPK, ERK, and JNK as early as 30min. The increase in LDH and the decrease in S100B produced by albumin were not dependent on MAPK activation. In contrast, inhibition of p38MAPK and ERK pathway, but not JNK partially attenuated the albumin-induced increases in IL-1β, nitrite and FKN.

Conclusions: Albumin activates all MAPKs in cultured astrocytes. Exposure to albumin is both cytotoxic to astrocytes and induces markers of glial activation including both IL-1β and iNOS. In response to albumin, astrocytes produce divergent response in levels of S100B (decreased) and FKN (increased). Of these responses, the increase in the pro-inflammatory cytokine IL-1β and the increase in nitrite are MAPK-dependent, mediated by p38MAPK and ERK, not JNK. These findings identify a role for specific MAPK signaling pathways in the mechanisms of astrocyte activation produced by albumin and implicate these pathways in the protective and pathologic responses to albumin in the CNS.

LEUKOCYTE ADHESION TO CEREBRAL ENDOTHELIUM IS SUFFICIENT TO INDUCE POST-ISCHEMIC CELL DEATH

S.W. Kim[1,2], H. Kataoka[3], N. Plesnila[1,2]

[1]Royal College of Surgeons in Ireland, Dublin, Ireland, [2]Laboratory of Experimental Neurosurgery, Department of Neurosurgery and Walter-Brendel-Center for Experimental Medicine, University of Munich Medical Center - Grosshadern, Ludwig-Maximilians-University, Munich, Germany, [3]The Department of Neurosurgery, Kyoto University Graduate School of Medicine, Kyoto, Japan

Objectives: Despite the fact that leukocytes are known to play a pivotal role in brain damage after cerebral ischemia, the pathomechanism of leukocyte-induced cell death is not well understood. The aim of the current study was to investigate the temporal and causal relationship between leukocyte-endothelium interactions (LEI), leukocyte migration into brain parenchyma, and neuronal cell death following reperfusion from focal cerebral ischemia.

Methods: ICAM-1$^{-/-}$ or C57BL/6 mice were subjected to permanent middle cerebral artery occlusion (MCAo) or 60 minute MCAo followed by 23 hours of reperfusion. LEI were examined by intravital fluorescent microscopy 40, 60, 90 and 120 minutes after permanent ischemia and 4, 4.5, 5, 5.5 and 6 hours after reperfusion following transient ischemia. Animals were sacrificed 12 h after onset of permanent ischemia and 24 hours after the onset of transient ischemia for determination of infarct volume and tissue leukocyte counts.

Results: Deletion of Intercellular Adhesion Molecule-1 (ICAM-1), a leukocyte adhesion molecule, reduced leukocyte adhesion to cerebral endothelium by 30% ($P< 0.05$) and decreased the infarct volume by 48% ($P< 0.05$), but did not affect the number of leukocytes in the brain parenchyma.

Conclusions: Our results suggest that the transmigration of leukocytes into post-ischemic brain may not be directly related to neuronal cell death as previously anticipated but that already the intravascular interaction of leukocytes with the cerebral endothelium may be sufficient for the induction of post-ischemic cell death. Further studies will be necessary to identify the transendothelial signaling pathways responsible for this novel phenomenon.

Brain Poster Session: Brain Imaging: Neurologic Disease

A COMPARISON OF GREY MATTER DENSITY IN RESTLESS LEGS SYNDROME PATIENTS AND MATCHED CONTROLS, USING FSL-VBM

R. Comley[1], S. Cervenka[2], S. Palhagen[3], G. Panagiotidis[4], J. Matthews[5], R. Lai[6], C. Halldin[2], L. Farde[2], T. Nichols[1], B. Whitcher[1]

[1]Clinical Imaging Centre, GlaxoSmithKline, London, UK, [2]Dept of Clinical Neuroscience, Karolinska Institutet, [3]Dept of Neurology, [4]Dept of Laboratory Medicine, Karolinska University Hospital Huddinge, Stockholm, Sweden, [5]School of Cancer and Imaging Sciences, The University of Manchester, Manchester, [6]Discovery Medicine, GlaxoSmithKline, Harlow, UK

Objectives: Restless legs syndrome (RLS) is a common neurological disorder where the pathophysiology is incompletely understood. To date two studies have used voxel-based morphometry (VBM) to examine grey matter density (GMD) in RLS. Increased GMD in medicated RLS patients compared to controls was reported in the pulvinar (Etgen, 2005; n=51), but was not replicated in unmedicated patients (Hornyak, 2007; n=14), instead slightly increased GMD in the ventral hippocampus and orbitofrontal gyrus was observed. We performed VBM on data from 16 unmedicated RLS patients and 16 matched controls using FSL-VBM.

Methods: 16 RLS patients naïve to dopaminergic drugs and 16 age and sex matched controls received structural T1 weighted MR scans (mean age 55 SD ± 7 and 56 ± 8 years respectively; symptom duration 27 ± 12 years; IRLS score 18.5 ± 3.9). Images were acquired using a 1.5T GE Signa system with a T1 and T2-weighted protocol. T1 images were reconstructed using a 256x256x156 matrix with an original resolution of 1.02x1.02x1mm. For 3 subjects the original z-axis resolution was 1.2mm and in one case 1.5mm. Structural data was analysed using FSL 4.1. Briefly, brain-extraction (with optic nerve and eye clean up) was performed; images were segmented and GM partial volume images aligned to the MNI152 template (affine registration, followed by nonlinear registration); images were then averaged to create a study-specific GM template; native GM images were then non-linearly re-registered to that template; images were then modulated (to correct for local expansion or contraction) by dividing by the Jacobian determinant of the warp field and smoothed with an isotropic Gaussian kernel (σ = 4mm). Voxelwise GLM was applied using permutation-based non-parametric testing, correcting for multiple comparisons across space, using age and gender as covariates.

Results: Data quality checks with performed and no anatomical pathologies or data processing outliers were discovered. We could not reject the null hypothesis of no difference in GMD between the two groups (voxel-wise significance: no significant voxels at $p< 0.05$ (FDR corrected); $p=0.89$ (FWE corrected)). Further the distribution of t-values was found to be symmetric and centred about zero, evidence against false negatives due to data anomalies.

Conclusions: We found no evidence of differences in GMD between healthy controls and unmedicated RLS sufferers using a sample size similar to previous literature. This further raises the possibility that previous differences seen by Etgen et al were either spurious, or related to treatment induced effects. We saw no suggestion of the increases in GMD (ventral hippocampus and orbitofrontal gyrus) seen by Hornyak et al, in a similar patient population (although only 11 of those patients were drug naïve). In the present study a well controlled data set was analysed with an advanced automated image analysis technique, we have found no structural correlate of RLS.

References:

Etgen T, et al. Bilateral thalamic gray matter changes in patients with restless legs syndrome. Neuroimage. 2005 Feb 15;24(4):1242-7.

Hornyak M, et al. Voxel-based morphometry in unmedicated patients with restless legs syndrome. Sleep Med. 2007 Dec;9(1):22-6.

FSL-VBM: http://www.fmrib.ox.ac.uk/fsl/fslvbm/index.html.

483

Brain Oral Session: Neonatal Ischemia

CEREBRAL OXYGEN METABOLISM (CMRO2) REACTIVITY TO HYPERCAPNIA IN NEONATES WITH SEVERE CONGENITAL HEART DEFECTS MEASURED WITH DIFFUSE OPTICS

T. Durduran[1,2], M.N. Kim[2], E.M. Buckley[2], C. Zhou[2], G. Yu[2], R. Choe[2], S.M. Durning[3], S. Mason[4], L.M. Montenegro[5], S.C. Nicholson[5], M.E. Putt[6], R.A. Zimmerman[7], J. Wang[1], J.H. Greenberg[8], J.A. Detre[1,8], A.G. Yodh[2], D.J. Licht[4]

[1]Radiology, [2]Physics and Astronomy, University of Pennsylvania, [3]Division of Respiratory Therapy, [4]Divison of Neurology, [5]Division of Anesthesiology and Critical Care, Children's Hospital of Philadelphia, [6]Department of Biostatistics & Epidemiology, University of Pennsylvania, [7]Division of Neuroradiology, Children's Hospital of Philadelphia, [8]Neurology, University of Pennsylvania, Philadelphia, PA, USA

Objectives: Optical, "diffuse correlation spectroscopy" (DCS) is a novel technology for non-invasive transcranial CBF monitoring. When hybridized with "near-infrared spectroscopy" (NIRS) to measure cerebral oxy-, deoxy- and total-hemoglobin (HbO_2, Hb, THC), the instrument permits calculation of cerebral metabolic rate of oxygen extraction ($CMRO_2$). DCS was previously validated against arterial spin labeled perfusion MRI in neonates with severe congenital heart defects. In this study, we estimate changes of $CMRO_2$ in this population due to hypercapnia.

Methods: A DCS/NIRS instrument with a MRI compatible optical probe was used to measure thirty-three neonates (22 hypoplastic left heart syndrome, 11 transposition of the great arteries) who were scheduled for cardiopulmonary bypass. All patients were full term at birth (37 to 42 weeks). All were prepared for surgery with protocolized ventilation and anesthesia (Fentanyl 5-10μg/kg, pancuronium 0.2 mg/kg). Vital signs including blood pressure, electrocardiogram, pulse oximetry and end-tidal CO_2($EtCO_2$) were continuously monitored. After confirmation of normocapnia (pCO_2=40-45mmHg) by arterial blood gas sampling baseline data was acquired for 10 minutes. CO_2 was then added to the gas mixture to achieve an $FiCO_2$ of 2.7% as measured by capnometry. Conventional anatomic MRI sequences were obtained while the gases were equilibrating (15minutes). Continuous optical data was acquired throughout the procedure. At the end of this period, arterial blood gas samples were drawn to confirm higher $PaCO_2$. Oxygen extraction fraction (OEF) was estimated from NIRS data assuming a compartmentalized model for the vasculature and baseline values for microvascular blood oxygenation and volume. $CMRO_2$ was then calculated as the product of OEF and CBF using a standard model.

Results: Mean (±standard error) changes in CBF of 59±6%, HbO_2 of 11.0±1.1μM, Hb of -2±0.4μM, THC of 9.4±1.1μM, $CMRO_2$ of 130±7% and $EtCO_2$ of 21±2 mmHg were observed (Figure 1), and vascular reactivity was calculated to be 4.2±1.6 %CBF/mmHg . All changes were significant ($p< 0.05$).

Conclusions: CBF-CO_2 reactivity was intact and consistent with literature values of 1.5-9% CBF change/mmHg[1-3]. Calculated $CMRO_2$ increased significantly with hypercapnia in most patients, though the magnitude of this change depended on assumed baseline values. This increase persisted when assumed values were varied across a (wide) physiological range. This finding contrasts with the common understanding that, in healthy persons, $CMRO_2$ is unaffected by hypercapnia. The observed increase in $CMRO_2$ in neonates with congenital heart disease suggests that baseline $CMRO_2$ may be reduced in response to very low CBF (10.2±0.8 ml/min/100g), and supports the notion that hypercapnia may be neuroprotective. The next phase of this study will employ an improved NIRS instrument and algorithm to reduce the number of required assumptions.

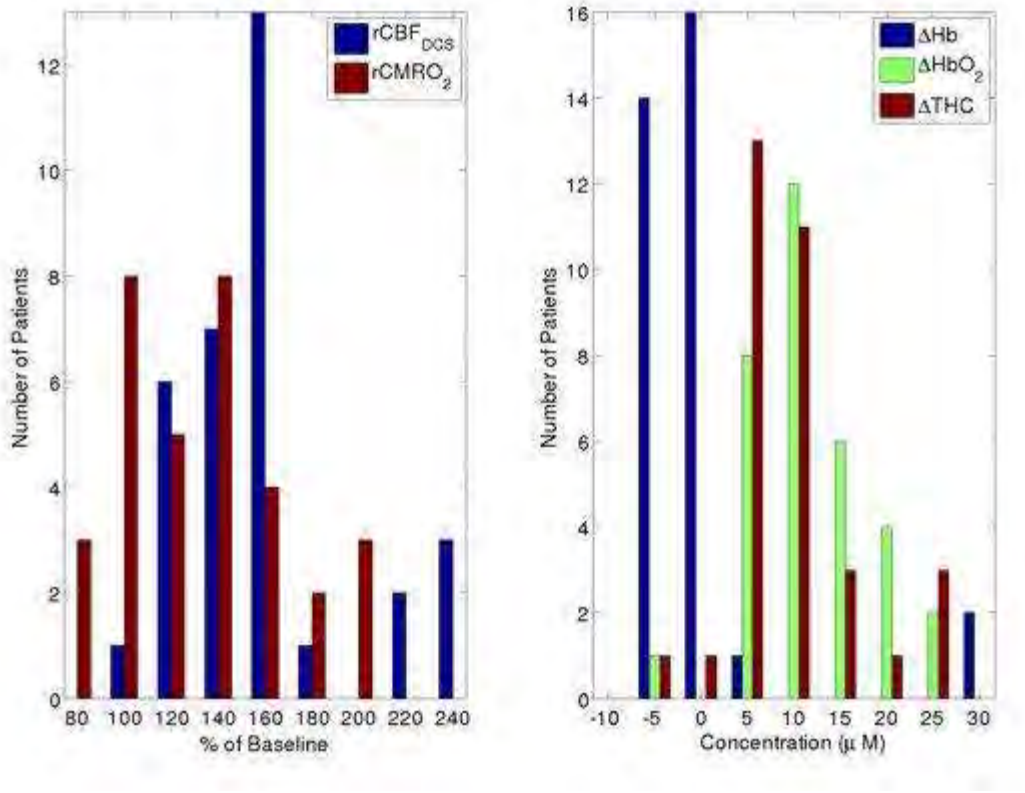

[Figure 1]

References:

1. Pryds et al.Journal of Pediatrics,115,638,1989.

2. Levene et al.Pediatr Res,24,175, 1988.

3. Greisen et al. Acta Paediatr Scand,76,394,1987.

CYTOCHROME P450 EXPRESSION AT THE HUMAN BLOOD-BRAIN BARRIER: FOCUS ON CYP3A4 AND ITS ROLE IN CARBAMAZEPINE BRAIN METABOLISM

C. Ghosh[1], M. Hossain[1], J. Gonzalez-Martinez[2,3], L. Cucullo[1], D. Janigro[1,3], N. Marchi[1]

[1]Cell Biology, Cleveland Clinic Lerner College of Medicine, [2]Neurological Surgery, Cleveland Clinic, [3]Molecular Medicine, Cleveland Clinic Lerner College of Medicine, Cleveland, OH, USA

Objectives: Drug delivery to the brain may be hampered by the overexpression of multiple drug resistance proteins in blood-brain barrier (BBB) endothelial cells [1,3,4]. We hypothesized that BBB endothelial cells may also act as a metabolic barrier or as a system capable of pro-drug transformation. Thus, while cytochrome P450 (CYPs) iso-enzymes play a major role in the metabolism of AED in the liver, it is not clear whether these enzymes are also functionally expressed in human BBB endothelial cells and possibly involved in drug response or resistance [2,4].

Methods: Primary endothelial cultures were obtained from brain specimens of patients affected by drug resistant epilepsy (EPI-EC) and resected aneurisms domes (ANE-EC). A human-derived cell line of brain microvascular endothelial cells was used as controls (HBMEC). Transcript levels of CYPs were assessed by cDNA microarrays[5]. Results were confirmed by immunohistochemistry on resected epileptic brain tissue. In vitro, control EC were exposed to laminar flow and the levels of CYP3A4 evaluated. HPLC analysis was performed to assess the functional relevance of CYPs BBB expression on carbamazepine metabolism.

Results: EPI-EC and ANE-EC displayed up regulated mRNA levels for Cyp3A4, Cyp2J2, Cyp4A11, Cyp2E1 and Cyp11b compared to control. An increased mRNA level of CYPs was paralleled with an increase in drug-transporter transcripts. Laminar flow induced mRNA levels of a broad spectrum of enzymes: Cyp33, Cyp2J2, CARS-Cyp, Cyp4A11, Cyp2C9, Cyp3A4, Cyp2E1, Cyp11b, Cyp2A6, Cyp1B1 and Cyp2C. Among these enzymes, Cyp3A4, Cyp2C9, Cyp2A6 and Cyp2J2 are involved in the metabolic conversion of AEDs. In particular, CYP3A4 levels were increased in EPI and ANE endothelial cells and up-regulated by shearing forces [5]. Immunohistochemical analysis confirmed BBB expression of CYP3A4 in dysplastic human epileptic brain while CYP3A4 was lower in specimens of well organized cortex. In vitro, CYP3A4 expression positively correlated with the extent of carbamazepine metabolism.

Conclusions: Our results reveal the functional expression of P450 enzymes at the human BBB. Among these enzymes, the levels of CYP3A4 determined the amount of CBZ metabolized. These results reveal a novel powerful molecular mechanism of AED metabolism by the BBB.

References:

1) Dombrowski SM, Desai SY, Marroni M, Cucullo L, Goodrich K, Bingaman W et al. Overexpression of multiple drug resistance genes in endothelial cells from patients with refractory epilepsy. Epilepsia 2001;42:1501-6.

2) Ghersi-Egea JF, Walther B, Perrin R, Minn A, Siest G. Inducibility of rat brain drug-metabolizing enzymes. Eur.J.Drug Metab Pharmacokinet. 1987;12:263-5.

3) Cucullo L, Hossain M, Rapp E, Manders T, Marchi N, Janigro D. Development of a humanized in vitro blood-brain barrier model to screen for brain penetration of antiepileptic drugs. Epilepsia 2007;48:505-16.

4) Marchi N, Hallene KL, Kight KM, Cucullo L, Moddel G, Bingaman W et al. Significance of MDR1 and multiple drug resistance in refractory human epileptic brain. BMC Med. 2004;2:37.

5) Desai SY, Marroni M, Cucullo L, Krizanac-Bengez L, Mayberg MR, Hossain MT et al. Mechanisms of endothelial survival under shear stress. Endothelium 2002;9:89-102.

485

Brain Poster Session: Subarachnoid Hemorrhage

EFFECTS OF INHIBITION OF THE MYOSIN-LIGHT-CHAIN KINASE ON BRAIN-EDEMA FORMATION AFTER SUBARACHNOID HEMORRHAGE IN MICE

S. Feiler[1], C. Ricken[2], H. Luhmann[3], K. Engelhard[2], C. Werner[2], C. Kuhlmann[3], N. Plesnila[1,4], S. Thal[2]

[1]Department of Neurosurgery and Walter Brendel Center for Experimental Medicine, University of Munich Medical Center - Grosshadern, Ludwig-Maximilians-University, Munich, [2]Department of Anesthesiology, [3]Institute for Physiology und Pathophysiology, Johannes Gutenberg-University, Mainz, Germany, [4]Royal College of Surgeons in Ireland, Dublin, Ireland

Objectives: The precise mechanisms leading to blood-brain-barrier (BBB) breakage and vasogenic brain edema formation after the subarachnoid hemorrhage (SAH) are still unknown. Recent studies suggest that the contractile apparatus of endothelial cells may contribute to the disruption of the BBB. In an in-vitro BBB model hypoxia activated the myosin light chain kinase (MLCK) of cerebral endothelial cells. This mediated a contraction and change in conformation of the endothelial cytoskeleton and resulted in increased permeability of the BBB. Increased phosphorylation of the myosin light chain (MLC) may therefore contribute to impaired integrity of the BBB^2 after cerebral insults. The aim of this study was therefore to investigate the role of MLCK on brain edema formation after experimental SAH.

Methods: Male C57/Bl6 mice (23 to 25 g body weight) were studied and cared for prior to and at all stages of the experiments in compliance with the institutional guidelines and regulations of the Animal Care Committee of the District Government of Rheinland-Pfalz. Mice were put under anesthesia with medetomidin, midozolam, fentanyl, intubated, and mechanically ventilated. After preparation of the left bifurcation of external and internal carotid artery, a blunted 5/0 monofilament suture was introduced into the ECA and was advanced into the ICA under control of cerebral blood flow and ICP until perforation of the circle of Willis. Afterwards all wounds were closed and anesthesia was terminated by antagonisation with flumacenil, naloxon and atipamezol. The mice were randomly assigned (n=8 per experimental group) with allocation concealment to either the specific MLCK inhibitor ML-7 (1 mg/kg body weight) or vehicle (normal saline solution). Treatment was injected intraperitoneally 1 hour before and 6 hours after SAH induction. 24 hours after SAH the brain edema, ICP and neurological outcome were measured. Data are presented as mean±SD.

Results: 24 hours after SAH brain water content was significantly reduced by 1.2% in comparison to the control group (81±0.6% in the control group). The average ICP was 10±2 mmHg in comparison to 18±2 mmHg in the control group. A significantly improvement of neurological outcome was present in mice treated with ML-7 as compared to vehicle treatment (2±1 points vs. vehicle: 6.5±4).

Conclusions: In the present study we demonstrated, that inhibition of the myosin light chain kinase reduced brain edema formation, decreased ICP, and improved neurological outcome following SAH. In vitro data indicate that these effects are caused by reduced permeability and improved stability of the BBB. Accordingly, the activation of MLCs could be the underlying mechanism leading to the opening of the BBB after SAH. Therefore our study suggests that MLCs inhibitors may represent a novel class of drugs suitable for the treatment of post-hemorrhagic brain edema.

486

Brain Oral Session: Brain Imaging

MR-DERIVED OXYGEN METABOLIC INDEX (OMI) PREDICTS GRAY MATTER INFARCTION BETTER THAN ADC DURING THE HYPER-ACUTE PHASE OF ISCHEMIC STROKE

A.L. Ford[1], H. An[2], K.D. Vo[3], A.M. Nassief[1], C.P. Derdeyn[3], W.J. Powers[4], W. Lin[2], J.-M. Lee[1]

[1]Neurology, Washington University School of Medicine, Saint Louis, MO, [2]Radiology, University of North Carolina, Chapel Hill, NC, [3]Radiology, Washington University in St. Louis, St. Louis, MO, [4]Neurology, University of North Carolina, Chapel Hill, NC, USA

Objectives: Distinguishing "reversibly" from "irreversibly" injured brain tissue during acute brain ischemia could potentially extend the current therapeutic window for interventions by individualizing treatment decisions. Prior PET studies have suggested that cerebral metabolic rate of oxygen utilization ($CMRO_2$) is a good predictor of tissue viability in acute ischemic stroke. More recent studies have suggested that MR-measured diffusion- and perfusion-weighted sequences may be able to determine tissue viability. We have developed a novel MR-imaging approach to measure oxygen metabolic index (OMI), a parameter closely related to $CMRO_2$. In a cohort of ischemic stroke patients, we directly compared the ability of OMI and ADC, measured within 3.5 hours of symptom onset, to predict brain tissue destined to die or remain alive at 1 month.

Methods: Eight ischemic stroke patients were imaged within 2.7 ± 0.8 hours of stroke symptom onset. Six patients received intravenous tPA prior to the scan while two patients did not. Dynamic susceptibility contrast method was used to measure cerebral blood flow (CBF), and a previously validated asymmetric spin echo sequence was used to provide a measure of oxygen extraction fraction (OEF). OMI was derived from the product of CBF and OEF. All measurements were normalized to the contralateral unaffected hemisphere. Co-registration and tissue segmentation were performed to align timepoints and separate gray from white matter, respectively. Histograms were constructed to demonstrate the relative frequency of OMI (or ADC) values for tissue destined to die or survive on 1 month FLAIR imaging. ROC analyses were performed to quantify the ability of the parameter to distinguish alive and dead tissue. Areas under the ROC curves (AUC) of the two parameters were compared using paired t-tests.

Results: Representative 3-hour OMI, 3-hour ADC, and 1 month FLAIR maps are shown for a patient with acute right middle cerebral artery infarction (see Fig). Histograms show relative frequency of 3-hour OMI (or ADC) values for "dead" voxels at 1 month (red curve) and "alive" voxels at 1 month (green curve). The accuracy of OMI and ADC for separation of dead and alive tissue was quantified using ROC analysis. For gray matter, mean AUC for OMI was 0.78 ± 0.10 compared to mean AUC for ADC, 0.72 ± 0.09 ($p = 0.01$). For white matter, mean AUC for OMI was 0.73 ± 0.09 compared to ADC, 0.73 ± 0.09 ($p = 0.5$). For whole brain tissue, mean AUC for OMI was 0.75 ± 0.09 compared to ADC, 0.73 ± 0.08 ($p = 0.12$).

Conclusions: Hyper-acute measures of OMI were a better predictor of gray matter death than ADC and an equally accurate predictor of white matter death. Thus, MR-OMI shows promise as a potential MR imaging approach to delineate the core of an evolving infarction.

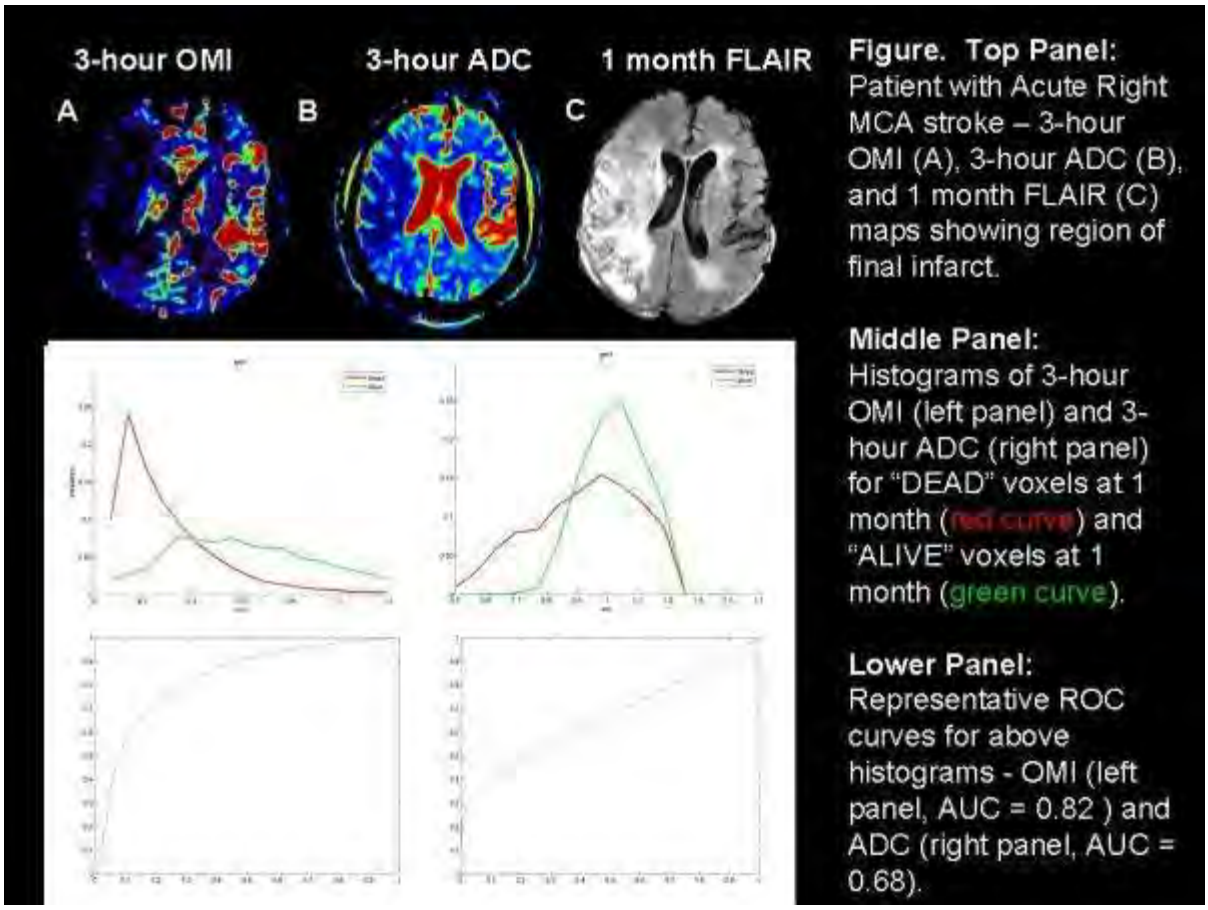
3-hour OMI
3-hour ADC
1 month FLAIR
A
B
C
Figure. Top Panel: Patient with Acute Right MCA stroke – 3-hour OMI (A), 3-hour ADC (B), and 1 month FLAIR (C) maps showing region of final infarct.
Middle Panel: Histograms of 3-hour OMI (left panel) and 3-hour ADC (right panel) for "DEAD" voxels at 1 month (red curve) and "ALIVE" voxels at 1 month (green curve).
Lower Panel: Representative ROC curves for above histograms - OMI (left panel, AUC = 0.82) and ADC (right panel, AUC = 0.68).

[Figure]

BrainPET Poster Session: Radiotracers and Quantification

KINETIC MODELLING OF A SLOW RADIOLIGAND: [^{11}C]GR205171 BINDING TO NK1 RECEPTORS BEFORE AND AFTER ADMINISTRATION OF CASOPITANT

V.J. Cunningham[1], E.A. Rabiner[1], S.A. Fernandes[2], R.N. Gunn[1,3], R. Gomeni[4], S. Zamuner[4]

[1]GlaxoSmithKline Clinical Imaging Centre, Imperial College, London, UK, [2]Discovery Medicine, Neurosciences Centre for Excellence In Drug Discovery, GlaxoSmithKline, Verona, Italy, [3]Dept. of Engineering Science, Oxford University, Oxford, UK, [4]Clinical Pharmacology, Modeling & Simulation, GlaxoSmithKline, Verona, Italy

Objectives: The PET radioligand, [^{11}C] GR205171, is a high affinity, selective NK1-receptor antagonist that has been used in vivo to characterise NK1-receptor binding in rhesus monkeys[1,2] and in humans[3].The kinetic behaviour of this radiotracer varies significantly across brain regions, consistent with the known distribution of NK1-receptors, but, because of slow kinetics, care is required in the selection of a PET model suitable for estimation of the correspondingly wide range of regional binding potentials[3]. Casopitant is a selective NK1 antagonist currently in development for prevention of chemotherapy-induced and postoperative nausea and vomiting. As part of a study in humans to develop a pharmacokinetic-receptor occupancy (PK-RO) model for Casopitant, the suitability of several compartmental models for the estimation of [^{11}C]GR205171 NK1 receptor binding was investigated in baseline scans and following administration of Casopitant.

Methods: Eight healthy male volunteers entered and completed a study to estimate the brain NK-1 RO following Casopitant. All subjects had 2 PET scans, at baseline and 24 hrs following a single dose of 2.5, 5, 20, 50, or 120 mg Casopitant. [11C]GR205171 was administered as an intravenous bolus. Arterial blood was collected throughout the scans and plasma samples were assayed for radiolabelled metabolites, enabling generation of arterial plasma parent input functions (IF). Eight regions of interest (ROI) were defined in each subject. Several modelling approaches were compared. One and two-tissue compartmental models, with reversible and irreversible kinetics and IF, and a reference tissue model with cerebellum as input were applied to each ROI in each individual scan independently. Finally analyses using compartmental models with simultaneous estimation of multiple regions sharing common parameters across regions and/or across regions and across scans within subjects, were applied.

Results: Analyses confirmed cerebellum as a reference region, albeit with two apparent tissue compartments. Estimates of RO at higher doses of Casopitant were consistently high (>85%) for all models. However there was variation between models in RO estimates at lower doses, reflecting different biases and stability. Models were compared on the basis of goodness of fit criteria, consistency of parameter estimates between regions and subjects, and on the pharmacological reasonableness of observed differences in the estimated rate constants. The most robust and consistent estimates were obtained using shared parameter models.

Conclusions: [^{11}C]GR205171 has slow kinetics, in the context of an ^{11}C PET scan, which presents difficulties in the accurate estimation of the receptor dissociation rate constant (k_4), and hence leads to significant variability in the estimation of low RO. A shared parameter model which assumes that kinetic differences between regions and scans is attributable only to differences in plasma clearance (K_1) and the association rate constant (k_3), but with k_4 and other parameters being the same across regions and scans, enhances the stability of the RO estimate and was considered most suitable for the analysis of [^{11}C]GR205171 human PET studies.

[1] M. Bergstrom et al, Neuropharmacology 39 (2000) 664-670.

[2] S. Zamuner et al, Nucl. Med. Biol. 29 (2002) 115-123.

[3] V. Cunningham et al, Int. Congress Series 1265 (2004) 12-24.

488

Brain Oral Session: Experimental Cerebral Ischemia: Neuroprotection

REDUCTION OF ACTIVATION OF MICROGLIA/MACROPHAGE CONFERS NEUROPROTECTION FOLLOWING INTRACEREBRAL HEMORRHAGE

M. Xue, V.W. Yong

Clinical Neurosciences and Hotchkiss Brain Institute, University of Calgary, Calgary, AB, Canada

Objectives: Microglia, the resident immune cells of the CNS, become activated following CNS injuries including intracerebral hemorrhage (ICH). Correspondingly, monocytes from the circulation migrate into areas of CNS injury to become macrophages. These activated cells are often called "microglia/macrophage" since it is difficult to differentiate between them in situ using immunohistochemistry. Activated microglia/microphages are capable of releasing numerous cytotoxic mediators such as matrix metalloproteinases, free radicals, chemokines and cytokines, but they can also produce neurotrophic factors such as NGF, FGF and BDNF. The degree of activation of microglia/macrophage is often correspondent with the extent of resulting pathology, and it is uncertain whether the microglia/macrophage reaction promotes or reduces the evolving pathology. We tested the hypothesis that the activation of microglia/macrophages promotes neuronal injury in the acute period after ICH and that inhibiting their activity attenuates brain injury and improves outcomes following ICH.

Methods: 10-µl of autologous blood obtained from tail was introduced into the right striatum of adult male mice (7-9 weeks old) to produce ICH injury. C57/B6 wildtype mice were used to evaluate the time course of brain injury from 1-7 day(s). We determined the area of brain damage and the extent of neuronal death and microglia/macrophage activity. We also used transgenic CD11b thymidine kinase (CD11b-TK) mice where proliferating microglia/macrophages were removed by ganciclovir treatment. These mice were killed at 3 days after ICH injury and brain sections were stained for various parameters.

Results: We found that ICH injury resulted in activation of microglia/macrophages through 1-7 day(s) of insult. The area of brain damage peaked at 2-3 days; the number of dying neurons peaked at 1-3 days, while the activation of microglia/macrophages peaked at 3-4 days. These findings led us to choose day 3 for further studies. We found that the activation of microglia/macrophages was significantly reduced in CD11b-TK transgenic mice with ganciclovir treatment after ICH compared to various injury control groups, including wildtype mice with ganciclovir treatment after ICH. Correspondingly, the area of brain damage and the extent of neuronal death were also reduced in CD11b-TK mice with diminished microglia/macrophage activity. Ongoing work with pharmacological deactivators of microglia will be presented at the meeting.

Conclusions: Activation of microglia/macrophages in the early periods after ICH promotes brain injury. These results shed light on the advent of new medications for ICH patients, including microglia deactivators.

Brain Poster Session: Transcriptional Regulation

STAT3 REGULATES THE TRANSCRIPTION OF THE MOUSE MN-SOD GENE AS A NEUROPROTECTANT IN CEREBRAL ISCHEMIC REPERFUSION

J.E. Jung, G.S. Kim, P. Narasimhan, P.H. Chan

Department of Neurosurgery, Stanford University School of Medicine, Stanford, CA, USA

Objectives: Cerebral ischemic reperfusion increases superoxide anion O_2^- from mitochondria in the brain (Chan, 1996). These mitochondrial anions are rapidly removed by manganese superoxide dismutase (Mn-SOD), a primary mitochondrial antioxidant enzyme. Mn-SOD scavenges superoxide radicals and its overexpression provides neuroprotection following cerebral ischemia and reperfusion (Maier et al., 2006). Mice with Mn-SOD deficiency exhibit large infarct volume after ischemic reperfusion (Kim et al., 2002). However, the mechanism underlying the regulation of Mn-SOD expression and its role in neuroprotection after ischemic reperfusion are still unclear. In this study, we identified the signal transducer and transcriptional activator 3 (STAT3) as a transcriptional factor of the mouse Mn-SOD gene and elucidated the novel mechanism for O_2^- generation from mitochondria via a decrease in Mn-SOD expression by STAT3 deactivation after transient focal cerebral ischemia (tFCI).

Methods: We employed in vivo tFCI by way of 45 mins of transient middle cerebral artery occlusion, and in models of 2.5 h of oxygen glucose deprivation/24 h of reoxygenation in vitro. We cloned and constructed 1779 bp length of mouse Mn-SOD promoter containing STAT3 putative binding motifs in 5′ flank of mouse Mn-SOD gene. This clone was ligated with pGLU vector and then used in a luciferase assay for analysis of transcription activity of Mn-SOD promoter.

Results: We found that Mn-SOD expression is rapidly down-regulated (50% reduction, $p < 0.05$) by reperfusion in the cerebral ischemic brain. Interestingly, we also found that STAT3 is usually recruited into the putative STAT3 binding sites of the mouse Mn-SOD promoter and up-regulates the transcription of the mouse Mn-SOD gene in the normal mouse brain. It was revealed that STAT3 is highly phosphorylated at Y705 in the normal mouse brain. However, at early post-reperfusion periods after tFCI, STAT3 is significantly dephosphorylated (60-70% reduction, $p < 0.05$) and the recruitment of STAT3 into the promoter of Mn-SOD is completely diminished. In addition, the transcriptional activity of the mouse Mn-SOD gene was significantly reduced (70% reduction, $p < 0.05$) in primary cortical neurons whose STAT3 activity is disrupted by STAT3-specific siRNA. Moreover, we found that STAT3 deactivated by reperfusion induces the accumulation of O_2^- (50-60% increase, $p < 0.05$) from mitochondria through a reduction in the Mn-SOD expression caused by the loss of STAT3 activity under reperfusion as well as neuronal cell death (50-70%, $p < 0.05$). We also found that Mn-SOD is a direct target of STAT3 in reperfusion-induced neuronal cell death using SOD2 (-/+) heterozygous knockout mice.

Conclusion: Our study demonstrates that STAT3 is a novel transcriptional factor of the mouse Mn-SOD gene and is a pivotal mediator in the generation of reactive oxygen species, which trigger neuronal cell death from mitochondria after cerebral ischemic injury.

References:

1. Chan PH (1996) Stroke 27:1124-1129.

2. Maier CM et al. (2006) Ann Neurol 59:929-938.

3. Kim GW et al. (2002) Stroke 33:809-815.

This work was supported by National Institutes of Health grants P50 NS014543, RO1 NS025372, RO1 NS036147, and RO1 NS038653.

490

Brain Oral Session: Functional Brain Imaging

FUNCTIONAL BOLUS-TRACKING ARTERIAL SPIN LABELING: A NEW APPROACH TO QUANTITATIVE FMRI

M. Kelly[1], C. Blau[1], O. Gobbo[1], K. Griffin[2], J. Jones[2], C. Kerskens[1]

[1]Trinity College Institute of Neuroscience, Trinity College Dublin, [2]School of Medicine, University College Dublin, Dublin, Ireland

Objectives: The alterations in the BOLD signal when cerebral blood flow, volume and vascular structure change (due to aging and or neurovascular disease) are relatively unknown. This presents a considerable obstacle when interpreting BOLD fMRI studies (D'Esposito et al, 2003). The purpose of this study is to develop a new quantitative fMRI technique, bolus-tracking arterial spin labelling (ASL) fMRI, which provides a quantitative assessment of the blood perfusion of an activated brain region. The technique was used to quantify changes in both the mean and capillary transit time (MTT and CTT) during neuronal activation in the rat brain.

Methods: A Fokker-Planck equation that describes the distribution of labelled arterial water in the brain during ASL experiments was derived (Kelly et al, 2009). A bolus-tracking ASL sequence was designed to provide concentration-time curves that represent the passage of a bolus of labelled arterial water through the ROI (graph). Wistar rats (n=6) were sedated with medetomidine, which has been shown to provide suitable conditions for fMRI studies in rats (Weber et al, 2006). Electrical stimulation of the right forepaw resulted in neuronal activation in the left primary somatosensory cortex forelimb (S1FL) region.

The left and right S1FL regions were selected as the activated and control ROI respectively. The solution to the Fokker-Planck equation for the boundary conditions describing the bolus-tracking ASL experiment was fitted to the concentration-time curves (graph). The MTT and CTT were calculated from the first and second moments of the resultant curve respectively (Meier & Zierler, 1954; Kim & Kim, 2006).

Results: The graph shows the concentration-time curves fitted to the Fokker-Planck model for the control and activated ROIs. The mean MTT and CTT were 1.87s ± 0.18s and 1.65s ± 0.06s respectively for the control ROI. For the activation ROI, the mean MTT and CTT were reduced to 1.68s + 0.2s and 1.37s ± 0.17s respectively. This represents a statistically significant difference ($p < 0.01$) between the activated and control ROI for both transit times.

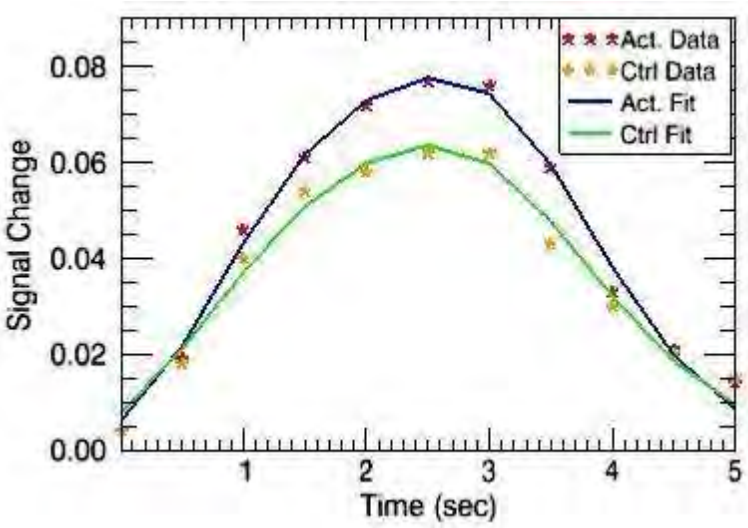

[Model fitted to data for activated and control ROI]

Conclusions: We have developed a new fMRI technique that quantifies the change in MTT and CTT during neuronal activation. The measured decrease in MTT during neuronal activation was expected, as flow to an activated region is known to increase, MTT is proportional to 1/Flow and CTT is proportional to $1/Flow^2$. The technique offers the potential to longitudinally monitor changes in these parameters during neuronal activation due to increasing age or disease progression.

References:

D'Esposito et al, Nature Neuroscience, 2003, vol.4, pp. 863-872.

Kelly et al, Physics in Medicine and Biology, 2009, article in press.

Kim & Kim, Magnetic Resonance in Medicine, 2006, vol.55, no.5, pp1047-1057.

Meier & Zierler, Journal of Applied Physiology, 1954, vol.6, pp731-744.

Weber et al, NeuroImage, 2006, vol.29, no.4, pp1303-1310.

INFLAMMATORY SIGNALING VIA BRADYKININ RECEPTORS CONTRIBUTES TO THE DEVELOPMENT OF SECONDARY BRAIN DAMAGE AFTER SUBARACHNOID HEMORRHAGE IN MICE

K. Schöller[1,2], S. Feiler[2], S. Anetsberger[2], N. Plesnila[1,2]

[1]Department of Neurosurgery, University of Munich Medical Center - Grosshadern, Ludwig-Maximilians-University, [2]Insitute for Surgical Research, University of Munich Medical Center-Grosshadern, Ludwig-Maximilians-University, Munich, Germany

Objectives: The kallikrein-kinin system is involved in inflammatory signaling after traumatic brain injury and cerebral ischemia via bradykinin B_2 receptors. The current study was conducted to clarify the role of both bradykinin receptor subtypes (B_1 and B_2) for the development of secondary brain damage after experimental subarachnoid hemorrhage (SAH).

Methods: 6-8 week old C57/Bl6 mice (controls) and bradykinin B_1- and B_2-receptor knock-out (-/-) mice were anesthetized, intubated and mechanically ventilated. The SAH was induced by endovascular puncture. Intracranial pressure (ICP, parenchymal probe) and cerebral blood flow (CBF, Laser-Doppler flowmetry) were continuously measured from 15 minutes before until 15 minutes after SAH. 24 hours after SAH ICP measurement was repeated and animals were subsequently sacrificed to quantify the brain water content. Mortality, neurological function and postoperative weight gain was quantified over a period of 7 days after SAH.

Results: ICP and CBF did not differ between groups in the first 15 minutes after SAH. 24 hours after SAH, however, ICP ($p< 0.05$) and brain water content ($p< 0.05$ B_2-/-) was reduced in bradykinin receptor knock-out animals compared to controls. 7-day mortality was 43%, 71% ($p< 0.05$ vs. controls), and 14% ($p< 0.05$ vs. controls) in control, B_1-/-, and B_2-/- mice, respectively. The neurological function was significantly better in B_2-/- mice ($p< 0.05$) compared to control and B_1-/- mice on the first postoperative day. B_2-/- animals also exhibited a better weight gain on postoperative day 4 whereas the B_1-/- group showed a lesser weight gain from postoperative 3 through 7 compared to control animals ($p< 0.05$).

Conclusions: An inflammatory response mediated by bradykinin B_2 receptors contributes to the development of secondary brain damage after SAH. Thus, pharmacological inhibition of B_2 receptors might be a future candidate for the treatment of post-hemorrhagic cerebral edema.

THE ROLE OF MOLECULAR INTERACTIONS IN THE PATHOGENESIS OF ALZHEIMER'S DISEASE: COULD NANOTECHNOLOGY PUT A STOP TO IT?

A. Nazem[1], **G.A. Mansoori**[2]

[1]Mashhad University of Medical Sciences, Mashhad, Iran, [2]Chemical and Bio Engineering & Physics, University of Illinois at Chicago, Chicago, IL, USA

Background and aims: The current medical approach toward Alzheimer's disease (AD) is to lower the symptoms associated with it. However, the need for therapeutic agents to halt the irreversible progression of the disease process is completely palpable through scientific community. Designing such therapeutic agents is not attainable without a complete knowledge of the underlying molecular mechanisms and the chemical structures of the involved molecules in the pathologies under survey.

Nanosciences and technology are a new area of scientific revolution, promising drastic breakthroughs in medical diagnostic and therapeutic approaches. The potentials of this new field, however, are not clear for most of clinical scientists. In this project we aim to show these potentials for Alzheimer´s disease treatment on a strong foundation of AD molecular mechanisms.

Methods: We first reviewed the molecular mechanisms involved in the pathogenesis of AD. For this purpose we include original research articles published between years 2000 and 2008, from journals with impact factor greater than 3. We then classify the various steps into three major categories: predisposing processes, pathogenetic processes and protecting mechanisms. Afterwards we scrutinize the potential of nanotechnology building blocks and complex systems in ceasing the pathogenetic processes.

Purpose: Our fiest objective in this article was to reach a unifying picture of the various molecular mechanisms involved in AD pathogenesis. Based on these mechanisms, we present the applications of nanotechnology building blocks and complex nano-systems that are potentially capable of stopping the AD pathology.

Results: Some nanotechnology building blocks, nanoparticles and complex nanosystems, are suggesting shortcuts to the treatment of AD. These nanoscience based systems are biologically functional. Designing these nanoscale agents have been recently provided by nanotechnology.

Conclusions: Through nanotechnology it would be possible to design targeted drug delivery systems, against different culprit molecules in AD pathogenesis. However, further research is needed to examine the biological compatibility of nanotechnology products.

APPLICATION OF CORTICAL THICKNESS MAPPING ASSESSED BY MRI TO FUNCTIONAL [^{18}F]-FLUMAZENIL-PET EXAMINATIONS

C. la Fougere[1,2,3], S. Grant[1], E. Schirrmacher[1], R. Schirrmacher[3], A. Evans[3], A. Thiel[1]

[1]Lady Davis Institute, McGill University, Montreal, QC, Canada, [2]Department of Nuclear Medicine, University of Munich Medical Center - Grosshadern, Ludwig-Maximilians-University, Munich, Germany, [3]Montreal Neurological Institute, McGill University, Montreal, QC, Canada

Objective: Most voxel-based morphometry (VBM) MRI-studies of gray matter volume tacitly assume that changes in gray matter density also represent changes in neuronal density. We propose a strategy to directly assess this relationship using high-resolution [^{18}F]-Flumazenil PET as neuronal density marker and surface based cortical thickness (SCT) mapping. In contrast to VBM methods, which provide relative gray matter densities, SCT-mapping bears the advantage of providing a direct quantitative index of cortical morphology. This metric captures the distance between the white matter surface and the gray CSF intersection based on a geometric definition; the output is a scalar value measured in millimeters.

Methods: Anatomical MRI's (Siemens Sonata 1.5 T) with 1 mm isotropic resolution were acquired for SCT measurements in four normal hemispheres. Images were registered into standardized stereotaxic space using a 12-parameter linear transformation, corrected for non-uniformity artifacts, segmented into white matter, gray matter, cerebrospinal fluid by means of CIVET-software. CIVET operates based on the notion that each vertex of the white matter surface is closely related to its gray matter surface counterpart; SCT can thus be defined as the distance between these linked vertices. Dynamic PET measurements (60 min) were acquired on a high-resolution dedicated brain-scanner (Siemens, HRRT) after injection of 370 MBq of [^{18}F]-Flumazenil as slow bolus over 60 s. The dataset was normalized, corrected for attenuation and scatter, and then iteratively reconstructed into an image volume consisting of 207 transaxial image planes with a voxel size of 1.22 mm. The PET volume was transformed into stereotaxic space using the parameters derived from MRI. Voxel-wise parametric maps of the non displaceable binding potential ($BP_{ND} = k_3/k_4$) of FMZ were calculated by the method of Logan using the white matter TAC as a reference tissue input. The average SCT and BP_{ND} of [^{18}F]-Flumazenil in each vertex were calculated in predefined cortical regions (frontal, parietal, mes. and lat. temporal, occipital cortex, cingulum and central region).

Results: Average global BP_{ND} and SCT were 7.7±2.2 and 3.1±0.3 with ranges from [4.0 - 11.4 and 2.5 - 4.0] respectively. A significant positive relationship between BP_{ND} and SCT was found for the regions of the cortical convexity (frontal, parietal, lateral occipital and central cortex, r=0.98, p=0.07). In the lateral and mesial temporal cortex SCT was higher than would be expected from BP_{ND} in this region (SCT 3.2±0.31 mm, BP_{ND}= 8.3± 2.11mm) and in the primary visual cortex SCT was much lower than BP_{ND} (BP_{ND}=8.6, SCT=2.5, r=0.08).

Conclusion: The proposed strategy of combining high-resolution PET and SCT-mapping suggests that for the greatest part of the convexity cortex, BP_{ND} of [^{18}F]-Flumazenil and SCT are highly correlated. This means that variability of cortical thickness might mainly be explained by variation in density of neuronal structures in those regions. However certain brain regions, especially on the mesial brain surface and in the temporal lobe do not seem to follow this relationship. Findings from morphometry studies in these areas should thus be interpreted cautiously with respect to conclusions on changes in the density of underlying neuronal structures.

Brain Poster Session: Neuroprotection

POST-SYNAPTIC SIGNALING COMPONENTS AND CAVEOLIN-1 DECREASE WITH AGE IN MEMBRANE/LIPID RAFTS AND SYNAPTOSOMAL MEMBRANE FRACTIONS ISOLATED FROM MURINE BRAINS

B.P. Head[1], J. Bonds[1], D.M. Roth[1], J. Peart[2], H.H. Patel[1], P.M. Patel[1]

[1]Anesthesia, VA/UCSD, San Diego, CA, USA, [2]Heart Foundation Research Center, Griffith University, Goldcoast, QLD, Australia

Objective: Spines/synaptic densities decreases in aged brains (1,2). Recent work has demonstrated that membrane/lipid rafts (MLRs) are essential for the development and stabilization of synapses and that synaptic residents involved in neurotransmission and neurotrophic signaling (e.g., NMDARs, AMPARs, Trk receptors, p75NTR, SFKs), are compartmentalized to MLRs and that their expression and localization to these discrete microdomains is dependent upon the cholesterol binding/scaffolding protein caveolin (Cav) (3-8). MLRs, enriched in cholesterol, glycosphingolipids, and sphingomyelin, are essential for development/stabilization of synapses. We have previously demonstrated that Cav-1 expression is necessary for NMDAR-mediated signaling and neuroprotection against oxygen-glucose deprivation (OGD) in primary neurons in vitro (3). We therefore assessed whether there exists age-related changes in synaptic signaling components within MLRs and synaptosomes (Syn).

Methods: Sucrose density fractionation methods were used to isolate MLRs and Syn from hippocampi of wild type (WT) C57BL/6 mice [young (Yg, 3-6 months), mature (Mt, 12 months), and aged (Ag, 24 months)] and Cav-1 KO mice (Yg). For MLRs, tissue was homogenized in 150 mM sodium carbonate (pH 11.0), and mixed with 1 mL of 80% sucrose to generate 2 mL of 40% sucrose. Above the 40% layer, 6 mL of 35% and 4 mL of 5% sucrose were layered and centrifuged at 175,000 g for 3 h at 4°C. Samples were removed in 1 ml aliquots and MLRs were found in buoyant fractions 4-5 (5/35% interface). For isolation of synaptosomes, tissue was homogenized in 5 ml of solution A (0.32 M sucrose, 0.5 mM CaCl2, 1 mM NaHCO3, 1 mM MgCl2) containing protease and phosphatase inhibitors and then centrifuged for 10 min at 1000 g at RT to remove large debris. Supernatant was layered onto 4 ml of 1.2 M sucrose and centrifuged at 160,000 g for 15 min. Synaptosomes (interface between the 1.2 M/0.32 M) were mixed with 4 ml of 0.32 M sucrose, layered onto 4 ml of 0.8 M sucrose, and centrifuged at 160,000 g for 15 min to yield a pellet enriched in synaptosomes. Pellet was resuspended in 1 ml of lysis buffer containing protease and phosphatase inhibitors and used for immunoprecipitation (IP) and/or immunoblot analysis.

Results: PSD-95 (post-synaptic density marker), the ionotropic glutamate receptors NMDAR2A (NR2A), NR2B, AMPAR, and Cav-1 were detected in MLRs from Yg brains, with less detection in MLRs from Mt and Ag brains. Cav-1 and PSD-95 IPs of MLRs showed a decrease in NR2A, NR2B, AMPAR, PSD-95 and Cav-1 in both IPs from Mt and Ag MLRs compared to Yg. There was also a significant decrease in PSD-95, NR2A, NR2B, and Cav-1 in Syn and PSD-95 IPs of Syn with age. Hippocampi Syn from Cav-1 KO mice (Yg) showed reduced PSD95, NR2A, and Cav-1 compared to WT (Yg).

Conclusions: These data indicate that Cav-1 expression and its ability to organize signaling complexes may be a key determinant of age-related changes in synaptic signaling in addition to changes that result from certain neurological disorders (i.e., Alzheimer's, Parkison's, and Prion disease).

Brain Poster Session: Neuroprotection

TRPM2 CHANNELS CONTRIBUTE TO MALE-SPECIFIC CORTICAL NEURON CELL DEATH FOLLOWING OXYGEN-GLUCOSE DEPRIVATION

P.S. Herson, S. Verma, Y.-F. Yang, E. Oyarazabel, P.D. Hurn

Department of Anesthesiology and Peri-Operative Medicine, Oregon Health & Sciences University, Portland, OR, USA

Objective: Excessive production of reactive oxygen species (ROS), termed oxidative stress, is a major contributor to ischemia-induced neuronal cell death in vitro and in vivo. Data from our group and others have demonstrated that oxidative stress activates the transient receptor potential-M2 (TRP-M2) non-selective cation channel resulting in cell death (1,2), suggesting that TRPM2 may participate in ischemia-induced neuronal cell death. However, no direct link between TRPM2 channel activation and ischemic neuronal death has been established. Therefore, we examined the effect of genetic and pharmacological inhibition of TRPM2 channels on neuronal survival in vitro following oxygen-glucose deprivation.

Methods: Male and female neurons were cultured separately from cortex of embryonic day 18 (E18) C57BL/6 mice. The TRP inhibitors, 2-Aminoethoxy diphenyl borate (2-APB), N-(p-Amylcinnamoyl)anthranilic acid (ACA) or clotrimazole were applied to the culture medium 20 min. prior to OGD and maintained throughout OGD and re-oxygenation (ReOX). Cortical cultures were infected with 3rd generation pseudo-type lentivirus containing shRNA, or empty vector, and expressing green fluorescent protein (GFP) by applying 1-2 µl virus (>10^6 infective particles/mL) directly to the culture media (1 mL). Cells were visualized by fluorescent microscopy (infected cells green). Forty-eight hoursafter transduction, cultures were exposed to oxygen-glucose deprivation (OGD) for 2 hours after which normoxia was re-established in culture media(ReOx)**.** Cell death was assayed 24 hours after ReOx by detecting the release of lactate dehydrogenase (LDH) and cell survival assayed using colorimetric assay of MTT conversion to formazan.

Results: Exposure to the TRP inhibitor 2-ADP (100 µM) significantly protected male cortical neurons from injury, decreasing cell death from 17.3±2.3% (n=3) to 7.1±1.8% (n=3; $P< 0.05$). In contrast, the application of 2-ADP had no effect on survival of female cortical neurons (n=2). Similar results were obtained with two additional TRP channel inhibitors, clotrimazole and ACA. Infection of cultures with shRNA lentivirus produced efficient knockdown of TRPM2 as determined by quantitative RT-PCR, and resulted in significantly reduced male neuronal cell death, decreasing from 28.9±4.5% (n=7) to 18.3±6.5% (n=7). No further neuroprotection was observed in male neurons infected with shRNA and additionally exposed to TRP channel inhibitors. Consistent with TRP inhibitor data, no protection was observed in female neurons infected with TRPM2 shRNA lentivirus.

Conclusions: Sexual dimorphism in ischemic injury after stroke is well documented and the effect of sex steroids in outcome has been well established. Using sex-specific cortical neuronal cultures, we report a gender-specific role for TRPM2 channel activation in neuronal damage following in vitro ischemia. These data indicate that differential TRPM2 channel regulation following ischemia contributes to sex-specific outcome and that inhibition of TRPM2 channels may provide a novel neuroprotective strategy for improving stroke outcomes in men.

References: 1. Herson PS & Ashford ML (1997) J. Physiol. 501.1, 59-662. 2. McNulty S & Fonfria E (2005) Pflugers Arch. 451, 235-42.

PIXEL-BY-PIXEL ANALYSIS OF DUAL CONTRAST-ENHANCED MRI RESULTS IN EXPERIMENTAL STROKE

T. Nagaraja[1], R. Paudyal[2], K. Karki[2], J. Ewing[2], J. Fenstermacher[1], R. Knight[2]

[1]Anesthesiology, [2]Neurology, Henry Ford Health System, Detroit, MI, USA

Introduction: Digitized image acquisition and analysis enables precise localization of regional variations of brain responses to injury and treatments. Only a few studies, however, have reported results employing such techniques in experimental stroke [1,2]. In this study, generalized estimating equations (GEE) analysis was applied to data on blood-brain barrier (BBB) damage obtained from a rat model of transient cerebral ischemia by employing magnetic resonance imaging (MRI) with two contrast agents of different sizes.

Methods: Male Wistar rats (~300 g; n=6) were subjected to focal cerebral ischemia using suture occlusion of the right middle cerebral artery for 3 hour followed by reperfusion via suture withdrawal. Contrast agents, gadolinium-diethylenetriaminepentaacetic acid (Gd-DTPA; ~0.6 kDa) and Gd-DTPA linked to bovine serum albumin (Gd-BSA; 68 kDa) were synthesized. Status of the BBB at 21 hours of reperfusion was assessed first by Gd-DTPA-MRI and then by Gd-BSA-MRI in a 7 Tesla magnet. Offline image processing was performed to localize contrast enhancing areas and construct maps of blood-to-brain influx constant (K_i) using Patlak plots [1]. The mean K_i values from these maps were used to perform correlation analysis of the vascular permeability measured by MRI for the two contrast agents. Finally, the entire set of pixel-by-pixel correlations in all ROIs were analyzed by a generalized estimating equation (GEE) technique [3,4], using the R software package geepack [4].

Results: The larger contrast agent Gd-BSA enhanced to a smaller extent than the smaller Gd-DTPA, but was contained within the latter region. It was assumed, therefore, that regions with Gd-BSA enhancement represented areas of common enhancement for both agents and were chosen as regions of interest (ROI) for further analysis. The comparison of mean values of Gd-DTPA with Gd-BSA from such ROI yielded a correlation of $R = 0.36$ with $P < 0.40$). In contrast, the GEE analysis performed on the longitudinal data associated with 6 clusters corresponding to the 6 ROIs chosen yielded a correlation of $R = 0.32$ with $P < 0.002$.

Conclusion: The simple mean comparison indicated that the K_i values were poorly and insignificantly correlated. The GEE analysis, however, showed that despite the poor correlation between the means, there was a significant relationship between the two measures. Thus, it may be possible to investigate the distribution of vascular pore sizes via the slope of the relationship between the transport constants of the two different-sized contrast agents, rather than via their mean values alone.

References:

1. Ewing JR et al. Magn Res Med 50:283-292 (2003).

2. Wu C et al. Computer Methods and Programs in Biomedicine 78:75-86 (2005).

3. Yu MC, Dunn OJ. Educ Psychol Measur 42:987-1004 (1982).

4. Ulrich H et al. Statistical software 15:1-11 (2006).

Grant support: Supported by NIH 1RO1NS38540, 1RO1HL70023 and AHA 0270176N, 0635403N.

Brain Poster Session: Neuroprotection

INVOLVEMENT OF HIF PATHWAY IN THE PROTECTIVE MECHANISMS OF AGED GARLIC EXTRACT IN ISCHEMIA

C.D. Gomez-Martinez[1], **P. Aguilera**[2], M. Espinoza-Rojo[3], P.D. Maldonado[2], A. Ortiz-Plata[4], M.E. Chanez-Cardenas[2]

[1]Universidad Autonoma de Guerrero, [2]Patologia Vascular Cerebral, Instituto Nacional de Neurologia y Neurocirugia, [3]Laboratorio de Biologia Molecular, Universidad Autonoma de Guerrero, [4]Neuropatologia, Instituto Nacional de Neurologia y Neurocirugia, Mexico, Mexico

Ischemia and reperfusion generate oxidative stress hence the use of antioxidants diminish disease progression. Aged garlic extract (AGE) is an odorless garlic presentation with antioxidant properties. In middle cerebral artery occlusion (MCAO) model in rats the administration of AGE at the onset of reperfusion (R) significantly reduced the size of the infarct area. The treatment with AGE prevented the increase in nitrotyrosine positive cells and the decrease in antioxidant enzymes activity induced by MCAO. Several antioxidant compounds like vitamin E and quercetin decrease damage induced by ischemia partially through the hypoxia inducible factor (HIF) pathway. In order to determine if this pathway is involved in the protective mechanism of AGE, we evaluated the expression of HIF-1 alpha and its target genes hemooxygenase-1 (HO-1) and glucose transporter 1 and 3 (GLUT-1 and-3).

Methods: Rats were subjected to MCAO for 2 h, treated with 1.2 mL/kg/i.p. of AGE at the beginning of reperfusion (R) and sacrificed after 2 h (2I/2R group). Brain damage was determined measuring the infarct area by 2,3,5-triphenyltetrazolium chloride staining and evaluating motor impairment (1). Total RNA was obtained from frontoparietal cortex and concentration was determined spectrophotometrically. Five micrograms of RNA were used to synthesize the cDNA. TaqMan probes were used for detection of HIF-1alfa, HO-1, GLUT-1 and -3 mRNA. 18S ribosomal RNA was used as an internal control. Amplification was performed utilizing an ABI PRISM 7500 sequence detection system from Applied Biosystems. Data were calculated utilizing the DCt method. Data are expressed as mean-fold change ± S.D. and analyzed by one-way analysis of variance (ANOVA) followed by a post hoc Tukey test (SPSS 13.0). $P< 0.05$ was considered statistically significant.

Results: AGE reduced the infarct area in 2I/2R+AGE group by 70%. However, this treatment itself was not associated with a noticeable improvement in the neurological outcome. HIF-1 alpha mRNA in 2I/2R group (0.62±0.04-fold) showed an increase with the AGE treatment (1.84±0.12-fold). After this result we decided to analyze the response of HIF-1 target genes HO-1, GLUT-1 and -3. HO-1 mRNA showed an increase after 2I/1R and 2I/2R (16.23±4.19 and 48.93±20.70-fold respectively). 2I/2R+AGE group did not induce any significantly change (61.24±18.35-fold). After 1 h R, GLUT mRNA increased (GLUT-1, 2.43±0.77 and GLUT-3, 3.16±0.48 -fold) and returned to basal level after 2 h R (GLUT-1, 1.03±0.33 and GLUT-3, 1.33±0.15 fold). AGE treatment after 2 h R induces an increase in GLUT-3 mRNA in control+AGE and 2I/2R+AGE groups (6.62±2.95 and 3.44±1.42 -fold, respectively).

Conclusions: The increase observed in HO-1 and GLUT-1 mRNA in the 2I/1R group could be associated to the HIF-1 alpha protein stabilization or by activation of other transcription factors as part of brain endogenous protective mechanisms. Interestingly, HIF-1 alpha and GLUT-3 mRNA was increased by AGE treatment. Since HIF-1 alpha and its target genes could contribute to the establishment of tolerance in the brain, it is possible that AGE is contributing to protect brain through the activation of this pathway.

1. Longa, E.Z. et al.1989. Reversible middle cerebral artery occlusion without craniectomy in rats. Stroke 20, 84-91.

500

Brain Oral Session: Neurovascular Unit

EXCESSIVE OXYGEN SUPPLY DOES NOT CHANGE CEREBRAL BLOOD FLOW RESPONSES TO INCREASED NEURONAL ACTIVITY

U. Lindauer[1,2], C. Leithner[2], H. Kaasch[2], B. Rohrer[2], G. Royl[2], N. Offenhauser[2], M. Füchtemeier[2], M. Kohl-Bareis[3], U. Dirnagl[2]

[1]Department of Neurosurgery, Technical University Munich, Munich, [2]Experimental Neurology, Charité - University Medicine Berlin, Berlin, [3]Department of Mathematics and Technology, University of Applied Sciences Koblenz, Remagen, Germany

Introduction: Neuronal activation leads to an increase in regional cerebral blood flow (rCBF) and blood oxygenation (rCBO). Several mechanisms of oxygen metabolism induced delivery of vasoactive substances have been discussed to couple neuronal activity and metabolism to blood flow in the brain. It was suggested that during cellular activity oxygen consumption locally increases which causes deoxygenation of hemoglobin and release of nitric oxide (NO) a) from deoxygenised hemoglobin (Stamler et al., 1997), b) due to nitrite reduction by deoxyhemoglobin (Gladwin et al., 2000), or c) due to activation of purinergic P2y-receptors at vascular endothelial cells during deoxygenation-induced ATP release from erythrocytes (Dietrich et al., 2000). According to these elegant models of combined oxygen and vasodilator release, blood flow would be directly matched to tissue oxygen demands.

Methods: We measured rCBF and rCBO responses to increased neuronal activity induced by functional stimulation or cortical spreading depression (CSD) under hyperbaric hyperoxygenation (3 or 4 ATA, FiO2 1.0) in the anesthetized rat. During hyperbaric hyperoxygenation oxygen supply to tissue is entirely provided through physically dissolved oxygen and no deoxygenation of hemoglobin occurs. Laser Doppler flowmetry combined with optical microfiber-spectroscopy was performed using a cranial window preparation (dura mater intact) in rats to measure relative changes in rCBF (functional activation, CSD) and rCBO (functional activation). Averaged rCBF and rCBO responses to electrical forepaw stimulation (3 Hz, 16 s stimulation period; 3ATA: n=8; 4ATA: n=5) or CSD (only LDF, elicited by 160-180mM potassium at a small remote burr hole; 3ATA:n=6; 4ATA: n=5) were recorded under normobaric normoxia and compared with responses during hyperbaric hyperoxygenation at 3 or 4 ATA. Neuronal activity was measured by recording somatosensory evoked potentials (functional activation study) or direct current potentials (CSD study).

Results: Hyperbaric hyperoxygenation increased arterial pO2 to > 2000 mmHg and cerebral hemoglobin saturation within the microcirculation to 100%. Resting blood flow as well as functional activation- or CSD-induced neuronal activity did not change compared to baseline conditions at normobaric normoxia. During forepaw stimulation, the deoxy-Hb decrease normally occurring during functional activation disappeared. The rCBF responses to functional activation as well as to CSD did not change under hyperbaric hyperoxygenation compared with control responses under baseline conditions.

Discussion: Our results suggest that rCBF regulation during physiological neuronal activation as well as during the much stronger metabolic stimulus of CSD involves other mechanisms than oxygen metabolism-dependent delivery and release of vasoactive mediators during deoxygenation of hemoglobin.

501

Brain Poster Session: Neuroprotection

ISCHEMIA CAUSES DELAYED AND SUSTAINED REMOVAL OF FUNCTIONAL SYNAPTIC SK2 CHANNELS

P.S. Herson[1], D. Allen[1,2], M. Kuroiwa[1], C. Bond[2], J. Maylie[3], R. Lujan[4], J.P. Adelman[2]

[1]Department of Anesthesiology and Peri-Operative Medicine, [2]Vollum Institute, [3]Department of Obstetrics and Gynecology, Oregon Health & Sciences University, Portland, OR, USA, [4]Departmento de Ciencias Medicas, Universidad de Castilla-La Mancha, Albacete, Spain

Objective: We have shown that synaptic SK2 channel activity in CA1 neurons dampens glutamate-mediated excitability and Ca^{2+} influx through NMDAr (1), and that the induction of long term potentiation (LTP) results in the immediate endocytosis of synaptic SK2 channels from potentiated CA1 spines (2). In addition, our recent data indicates that pharmacological enhancement of SK channel activity protects CA1 neurons against cerebral ischemia induced by cardiac arrest and cardiopulmonary resuscitation (CA/CPR). Therefore, we utilized electrophysiology and immuno-EM techniques to examine the effect of CA/CPR on synaptic SK channels.

Methods: C57BL/6 male mice underwent 8 min. CA/CPR, as described previously (3). For electrophysiology experiments, transverse hippocampal slices were prepared using our published protocols (2). Current-clamp recordings were obtained to record excitatory post-synaptic potentials (EPSPs) from visualized CA1 neurons, with solutions; ACSF solution (mM): 119 NaCl, 2.5 KCl, 1 NaH2PO4, 26.2 $NaHCO_3$, 1.3 $MgCl_2$, 2.5 $CaCl_2$, 10 Dextrose, and aerated with 95% O_2/5% CO_2; SR95531 (5 μM) and CGP55845 (2 μM) present to reduce $GABA_A$ and $GABA_B$ contributions, respectively; Internal pipette solution (mM): 140 KMeSO4, 8 NaCl, 1 MgCl2, 10 HEPES, 2 Mg-ATP, 0.4 Na2-GTP, and 20 μM EGTA, pH 7.3. Post-embedding immunohistochemistry and electron microscopy (immuno-EM) were performed as described previously (2) and radial distance from the post-synaptic density (PSD) was analyzed.

Results: The effect of ischemia on synaptic SK2 channels was examined by recording evoked subthreshold EPSPs from CA1 neurons in acute hippocampal slices. Blocking SK2 channels with apamin significantly increased the amplitude of EPSPs in slices from mice taken 15 minutes after CA/CPR (197±28% (n=4) of baseline; $P< 0.05$) equivalent to the effect of apamin in sham-operated control mice (196±29% (n=9); $P< 0.05$). The effect of apamin was significantly reduced at 3 hours post CA/CPR (129±4% (n=4); $P< 0.05$ compared to Sham controls), and reduction observed at 3 hrs was prevented by injection of mice with a protective dose of 1-EBIO (16 mg/kg) 30 min. prior to CA/CPR (190±12% (n=3); $P< 0.05$ compared to CA/CPR+vehicle). We performed immuno-EM labeling to determine the precise sub-spine distribution of SK2 channels in hippocampal slices from sham mice and 3 hr after CA/CPR. Analysis of radial distance revealed that SK2 immunogold particles were predominantly observed in the synapse (PSD) in sham mice (80%) and that 3 hr after CA/CPR very few SK2 immunogold particles were observed in the PSD (8%), while most were observed to be intracellular within spines (92% > 20 nm from PSD).

Conclusions: The electrophysiology data presented indicates that CA/CPR causes a functional loss of synaptic SK2 channels at a time-point between 15 min. and 3 hr. of resuscitation. Consistent with this functional data, post-embedding immuno-EM data shows that CA/CPR causes endocytosis of synaptic SK2 channels. Therefore, our data indicates that ischemia causes a physical and functional loss of synaptic SK2 channels, which may underly the increased sensitivity to excitotoxicity of hippocampal CA1 neurons.

References:

1. Ngo-Anh TJ etal. (2005) Nat Neurosci 8:642-649.

2. Lin MT etal. (2008) Nat Neurosci 11:170-177.

3. Kofler J etal. (2004) J Neurosci Methods 136:33-44.

502

Brain Poster Session: Neurogenesis

MODULATION OF FATE DETERMINANTS OLIG2 AND PAX6 IN RESIDENT GLIA EVOKES SPIKING NEURONS RECEIVING SYNAPTIC INPUT AFTER MILD BRAIN ISCHEMIA

K. Gertz[1], G. Kronenberg[1], G. Cheung[2], A. Buffo[3], H. Kettenmann[2], M. Götz[3], M. Endres[1]

[1]Experimental Neurology, Charité - University Medicine Berlin, [2]Max Delbrück Center for Molecular Medicine, Berlin, [3]Institute for Stem Cell Research, Helmholtz-Center, Munich, Germany

Background: Although in vitro studies suggest that non-neurogenic regions of the adult central nervous system potentially contain multipotent parenchymal progenitors, neurons are clearly not replaced in most brain regions after injury. The transcription factors Olig2 and Pax6 play largely opposing roles in determining progenitor cell fate in neurosphere culture as well as in the adult mammalian central nervous system in vivo. We have previously demonstrated that after cerebral ischemia astrocytes expressing enhanced green fluorescent protein (eGFP) under control of the GFAP promoter predominantly adopt a complex electrophysiological phenotype. Importantly, the majority of GFAP-eGFP+ cells are also Olig2-immunoreactive. Therefore, we here explored Olig2 antagonism and Pax6 overexpression in a model of mild transient brain ischemia to re-direct endogenous resident progenitors proliferating in situ toward a neuronal fate.

Methods: 129/Sv wildtype mice were subjected to 30 minutes of filamentous middle cerebral artery occlusion (MCAo) followed by reperfusion. 48 hours later, retroviruses containing either only GFP, Olig2-VP16-IRES-GFP to interfere with Olig2 function, or Pax6-IRES-GFP were injected stereotaxically into the ischemic lesion core, i.e. the lateral striatum. Animals were killed at 10 and 17 days after MCAo for further immunohistological and electrophysiological analysis.

Results: Cells transduced with the control vector showed complex glial membrane properties and did not express Doublecortin (DCX). By contrast, DCX+ cells emerged reproducibly both after repression of Olig2 and after overexpression of Pax6. Similarly, after modulation with fate determinants cells expressed Na+ currents to a higher percentage at both time points after MCAo. After infection with the control virus cells did not elicit action potentials, but we were able to detect action potentials after repression of Olig2 and after overexpression of Pax6. Commonly, we observed a single action potential during the depolarizing pulse, but in some cases more than one action potential was observed. After Pax6 transduction we also observed spontaneous current events.

Conclusion: Therapeutic gene transfer via retroviral vectors into the ischemic lateral striatum resulted in a significant number of infected cells differentiating into immature DCX+ neurons with Na+ currents capable of generating single action potentials. Our study demonstrates that resident glia can be re-programmed toward functional neuronal differentiation following brain injury in vivo, including specifically synaptic integration. Our present data provide proof-of-principle evidence that resident cells proliferating in ischemic gray matter can be recruited into functional neuronal differentiation, a crucial first step toward neurorepair.

503

BrainPET Poster Session: PET Acquisition and Processing

HIGHLY DETAILED ANATOMICALLY ACCURATE 3D BRAIN PHANTOMS FOR PET WITH 3D PRINTING

M.A. Miller, G.D. Hutchins

Department of Radiology, Indiana University School of Medicine, Indianapolis, IN, USA

Objectives: The quantitative capabilities of positron emission tomography, coupled with targeted radiotracers, are leading to the application of this technology as a neuroimaging biomarker with increasing frequency. Neuroimaging based biomarker studies are now being incorporated into multicenter trials using PET imaging systems with varying intrinsic performance and stability characteristics. . Phantom studies are usually performed in order to evaluate the system performance and variability among PET imaging sites used in a given study. An ideal phantom would precisely model the shape and activity distribution of the brain. A commonly used brain phantom is the Hoffman 3D phantom [1]. While this phantom is very well suited for some types of measurements, the apparent activity distribution in the phantom depends on the resolution of the camera making it difficult to use in addressing quantitative issues that require the full resolution of modern PET cameras. Our objective is to develop a method for manufacturing phantoms that accurately model realistic anatomy and are not dependent on imaging system performance.

Methods: We have developed a method of creating phantoms using rapid prototyping technology (3D printing). The system allows us to create phantoms based on any geometric model, including those derived from high resolution anatomical images. The method consists of incorporated radioactive tracer as a dye in the printing system of a powder-based rapid prototyping system. We use a Z Corp Z510 3D printer [Z Corporation, Burlington, MA]. Printing with 0.18 mm slice thickness at 600 dpi, our custom software allows us to accurately place activity throughout phantom volumes as large as 254 × 356 × 203 cm3. Software that uses digital atlases as input allows us to specify the activity concentration at the level of individual voxels.

Results: Printed activity distributions are linearly variable and reproducible to better than 2%. We have printed and imaged human brain phantoms based on the SPL human brain atlas [2,3] and rat brain phantoms based on the Paxinos and Watson atlas [4].

Conclusions: We have developed a practical method for making complex radioactive phantoms that model realistic anatomy at resolutions well below current or anticipated PET resolutions. Further development will produce phantoms with long lived isotopes. We intend to create a phantom library that models the distributions of [18F]FDG and [11C]PIB for a patient at multiple stages of Alzheimer Disease. This library will allow us to effectively image the same patient longitudinally on multiple scanners at multiple sites, providing us with detailed data on PET reproducibility and variability.

Supported by the Indiana Genomics Initiative (INGEN). INGEN is supported in part by Lilly Endowment, Inc.

References:

[1] E. J. Hoffman et al. IEEE Trans Nucl Sci 1990; 37: 616-620.

[2] M. E. Shenton et al, in Biomedical Visualization, 1995.

[3] R. Kikinis et al, IEEE Trans Vis Comp Graph 1996; 2: 232-241.

[4] G. Paxinos and C. Watson, “The Rat Brain in Stereotaxic Coordinates”, 4th Ed., Academic Press, 1998.

504

Brain Poster Session: Traumatic Brain Injury

TRAUMATIC INJURY INDUCES CELL-SPECIFIC SHIFTS OF BRANCHED CHAIN AMINO ACID METABOLISM IN RAT BRAIN

M. Ren[1], G. Xing[2], W. Watson[3], A. Verma[3], J.T. O'Neill[1]

[1]Pediatrics, Uniformed Services University of the Health SciencesServices, [2]Psychiatry, [3]Neurology, Uniformed Services University of the Health Sciences, Bethesda, MD, USA

Background: Traumatic brain injury (TBI) is associated with a primary immediate insult and secondary cascades of biochemical processes that can result in delayed cell death. Secondary injury of TBI presents an opportune therapeutic target for neuroprotection, but very rarely have potential research agents and techniques proven clinically beneficial making the search for novel agents all the more urgent. We suspect metabolism of branched chain amino acids (BCAAs) leucine, isoleucine, and valine could modify these injurious cascades. A further understanding of these pathways could lead to potential manipulation as a potent therapeutic strategy. Normally BCAAs are not only substrates for protein synthesis but are also essential for transamination reactions that yield an ammonium group which can buffer CNS glutamate and GABA levels. Transamination of BCAAs produces their branched chain keto-acid (BCKA) counterparts, which can be metabolized as bioenergetic fuels via the mitochondrial BCKA dehydrogenase (BCKD) complex. The BCKD is tightly regulated by BCKD kinase (BCKDK) and is inactivated upon phosphorylation. In response to pathological conditions the metabolism of BCAAs may adapt multiple roles for cell and tissue preservation.

Objectives: To assess modification of BCAA metabolic pathways by analyzing their associated enzymes (transaminase, dehydrogenase and kinase) and thereby determine the likely pathway BCAAs follow in response to traumatic injury. We also examined the activation state of BCKD in response to stress of primary cultured rat neurons and astrocytes.

Methods: Our TBI model was controlled cortical impact (CCI) in rats. CCI was induced with a penetration width of 6 mm, depth of 2.5 mm, and velocity of 4 m/s. Brains were analyzed at 4 hr, 1 d, 3 d and 7 d post TBI with immunohistochemistry, RT-PCR and western blot. Neurons and astrocytes were studied as primary cultures and analyzed for BCKD and pBCKD before and after metabolic stress.

Results: We found BCAA transaminases as well as BCKDK decreased 29 and 10%, respectively ($p < 0.05$), 4 h following CCI. BCKDK then increased by 200% ($p < 0.05$) by 3 days. The overall level of pBCKD increased 1 day (~ 100%, $p < 0.05$) after CCI. Immunohistochemical analysis demonstrated that pBCKD localized within neurons under normal conditions. However, following CCI, pBCKD dramatically increased in astrocytes, yet decreased in neurons. In rat brain primary culture, we found 2 fold ($p < 0.05$) higher basal levels of BCKD in neurons than in astrocytes while the pBCKD levels were similar. When the astrocyte cultures were challenged with TGF-β there was a marked increase (125%, $p < 0.05$) in pBCKD levels, while neuronal cultures treated with glutamate demonstrated decreased (69% $p < 0.05$) in pBCKD levels.

Conclusions: Our findings demonstrate significant differences in the activation state of BCKD in neurons and astrocytes under normal and pathological conditions. Our results suggest reactive astrocytes may shift BCKAs away from mitochondrial utilization resulting in greater concentrations to supply neurons with more energy substrate after brain insults. Funded by NIH grant NS37814, and DoD grants MDA-905-02-2-0005 and MDA905-03-2-0001 (A.V. PI).

505

Brain Poster Session: Experimental Cerebral Ischemia: Global Ischemia

PERK ACTIVATION FOLLOWING GLOBAL BRAIN ISCHEMIA IS INDEPENDENT OF UNFOLDED PROTEINS

T. Sanderson[1], M. Deogracias[1], K. Nangia[1], J. Wang[1], R. Kumar[1,2]

[1]Emergency Medicine, [2]Physiology, Wayne State University, Detroit, MI, USA

Objectives: Transient global brain ischemia results in death of neurons in the CA1 hippocampus. Following ischemia, protein synthesis is inhibited throughout the entire brain. Most neurons eventually recover translational competence, however the CA1 never recovers. Protein synthesis is inhibited by phosphorylation of eIF2α. Following endoplasmic reticulum (ER) stress, eIF2α is phosphorylated by PERK. The prevailing dogma is that accumulation of newly synthesized (unfolded) proteins cause activation of PERK, eliciting the unfolded protein response (UPR). Activated PERK then phosphorylates eIF2α. However, it has never been directly demonstrated that unfolded proteins activate PERK after brain ischemia. We hypothesized that accumulation of unfolded proteins in the ER after global brain ischemia causes PERK activation, phosphorylation of eIF2α, and subsequent inhibition of protein synthesis. To assay this, we inhibited protein synthesis before ischemia to empty the ER of newly synthesized proteins. We theorized that in the absence of unfolded proteins, PERK would not be activated by ischemia/reperfusion.

Methods: m. The sections were incubated with primary antibodies for phosphorylated PERK (p-PERK), phosphorylated eIF2α (p-eIF2α), and neuronal nuclei (NeuN). AlexaFluor conjugated secondary antibodies were used. Images were obtained on a Leica LSM510 confocal microscope, under a 63X objective. A series of 10 optical sections were taken 0.35µm in the z-plane and stacked into z-stacks of 3.5µm. Protein synthesis was inhibited by intrahippocampal injection of anisomycin 90 minutes prior to ischemia. Anisomycin injection was verified with methylene blue. To assay in vitro protein synthesis, hippocampal homogenates were incubated with 100µM amino acids except methionine and cysteine and 1.5µCi[35S]-methionine/cysteine. Long Evans rats were subjected to 8 minutes of global brain ischemia utilizing bilateral carotid occlusion/hypotension. After 10 minutes of reperfusion, rat brains were fixed, cryoprotected, frozen and cryosectioned at 8

Results: Tracer dye showed that anisomycin was injected into the CA1 hippocampus. Anisomycin-injected hippocampal homogenates had a 99% inhibition of protein synthesis compared to vehicle-injected homogenates. Triple-label immunofluoresence in sham-operated animals showed minimal detectable p-PERK and p-eIF2α colocalizing with CA1 neuronal fluorescence. Ischemia and 10 minutes reperfusion resulted in an increase in p-PERK and p-eIF2α in CA1 neurons. Treatment of sham-operated control animals with anisomycin showed results similar to sham-operated controls. Interestingly, ischemia/reperfusion plus anisomycin had a similar increase in p-PERK and p-eIF2α to untreated ischemia/reperfused animals.

Conclusions: Protein synthesis was effectively inhibited with anisomycin. The average ER translocation time of proteins in CA1 hippocampal neurons is under 30 minutes. Therefore, administration of anisomycin 90 minutes before the onset of reperfusion results in an ER devoid of proteins undergoing folding. If unfolded proteins were involved in PERK activation, we would expect no PERK phosphorylation when the ER is emptied of unfolded proteins. Interestingly, we found that PERK was phosphorylated in the CA1 region even with anisomycin treatment. This suggests that the prevailing dogma for PERK activation is incorrect in the setting of brain reperfusion. Specifically, unfolded proteins do not activate PERK during brain ischemia or reperfusion. Further studies will be needed to discover the mechanism of PERK activation during brain reperfusion.

506

Brain Oral Session: Experimental Stroke and Cerebral Ischemia 2

INCREASED ACTIVITY OF SMALL CONDUCTANCE CALCIUM-ACTIVATED POSTASSIUM CHANNELS DECREASE HIPPOCAMPAL NEURONAL DAMAGE FOLLOWING GLOBAL CEREBRAL ISCHEMIA IN ADULT MOUSE

P.S. Herson[1], D. Allen[1,2], T. Nakano[1], J.P. Adelman[2], M. Kuroiwa[1]

[1]Department of Anesthesiology and Peri-Operative Medicine, [2]Vollum Institute, Oregon Health & Sciences University, Portland, OR, USA

Objective: We recently demonstrated that small conductance calcium-activated potassium (SK) channels function as endogenous negative modulators of NMDA-receptors in hippocampal CA1 neurons (1), leading us to hypothesize that treatments resulting in increased SK channel activity would protect neurons against ischemia-induced damage by decreasing NMDA receptor mediated excitotoxicity. Therefore, we examined the survival of CA1 neurons following cardiac arrest and cardiopulmonary resuscitation (CA/CPR)-induced ischemia in male mice in which SK activity has been increased either genetically (SK2-over expression; SK2 OE) or pharmacologically with 1-EBIO. In addition, we examined the SK2 knockout mice (SK2 KO).

Methods: C57BL/6 WT, SK2 KO and SK2 OE mice underwent 8 min. CA/CPR, as described previously (2). WT male mice were administered the SK channel agonist, 1-EBIO (16 mg/kg, intraperotineal (ip) injection), 30 min. prior to CA/CPR and given a subsequent boosting injection 6 hr. after resuscitation. Three days after CA/CPR, brains were removed, embedded in paraffin and 6 μm coronal sections serially cut. Sections were stained with hematoxylin and eosin (H&E) for analysis of damaged neurons. The entire length of the CA1 region of the hippocampus was counted in three levels (100 μm apart) beginning from -1.5 mm bregma and the percentage of damaged neurons calculated for each brain. The investigator who analyzed neuronal damage was blinded to the treatment group. A separate group of mice received a femoral artery catheter for continuous monitoring of blood pressure and obtaining blood samples at 10 minutes prior to arrest and at 30 minutes post-resuscitation for measurement of arterial blood gases, pH, sodium, potassium, lactate and glucose levels.

Results: The absence of SK2 channels (SK2 KO) appears to exacerbate CA1 neuronal damage following CA/CPR, increasing neuronal death by ~30% (from 36.9±6.5% (n=10) for control, to 50.6±7.3% (n=8)). In contrast, SK2-OE mice were significantly protected following CA/CPR, decreasing neuronal damage by ~70%, to 10.5±5.2% (n=7; $P< 0.05$). Similarly, the administration of 1-EBIO significantly reduced CA1 neuronal damage, from 62.4±8.6% (n=9) for vehicle to 33.9±8.9% (n=9; $P< 0.05$) for 1-EBIO treated mice. Physiological parameters, including arterial blood gases, pH, sodium, potassium, lactate and blood glucose was not significantly affected by 1-EBIO administration. CPR time and epinephrine dose used for resuscitation in each group was not different.

Conclusions: The current data indicates that genetic over-expression or 1-EBIO-mediated pharmacological enhancement of synaptic SK2 channel activity increases CA1 neuron survival following ischemic insult. Therefore, SK2 channels represent a new therapeutic target for neuroprotection following cerebral ischemia.

References:

1. Ngo-Anh TJ et al. (2005) Nat Neurosci 8:642-649.

2. Kofler J et al. (2004) J Neurosci Methods 136:33-44.

507

Brain Poster Session: Traumatic Brain Injury

LOW DOSE AT1 INHIBITION IMPROVES NEUROLOGICAL OUTCOME AND REDUCES SECONDARY BRAIN DAMAGE 24 HOURS AFTER BRAIN TRAUMA IN MICE

R. Timaru-Kast, C. Ricken, K. Engelhard, C. Werner, S.C. Thal

Department of Anesthesiology, Johannes Gutenberg-University, Mainz, Germany

Objectives: The intrinsic renin-angiotensin system is capable to modulate brain injury. Angiotensin II receptor type 1 (AT1) mediates vasoconstriction, apoptosis and neuroinflammation, increasing secondary brain damage. Whereas angiotensin II receptor type 2 (AT2) triggers vasodilatation, anti-inflammation and neuro-proliferation that may offer protection [1]. A recent study demonstrated a down-regulation of AT1 after controlled cortical impact (CCI) while AT2 was up-regulated temporarily [2]. The present study explores the potential neuroprotective effect of AT1 inhibition on secondary brain damage after CCI. The first goal of the study is dosage finding of the specific AT1 antagonist candesartan. Secondly the time window for the effective dose of candesartan was investigated.

Methods: C57Bl6 mice were anesthetized with fentanyl, midazolam and medetomidine, subjected to a pneumatic brain trauma on the right parietal cortex (CCI) and randomly assigned to different treatment groups: Study I: vehicle solution (Na_2CO_3), low (0.1 mg/kg), medium (0.5 mg/kg) or high dose (1 mg/kg) candesartan (n=8 each group, s.c. injection 30 min post CCI). Study II: application time points for candesartan 30min, 1h, 2h or 4h after CCI (n=7 at each time point), or vehicle (n=3 at each time point). Contusion volume was measured in Nissl stained sections 24 hours after CCI. In both studies, the primary lesion (PrimL) was quantified in a separate set of animals 15 min after CCI (n=8 and 7, respectively). Neurological outcome was assessed 24 h after CCI in Study II by Neurological Severity Score (NSS).

Results:

Study I: 24h after CCI contusion volume increased from 24 mm^3 (PrimL) to 41 mm^3 (vehicle). Low dose candesartan significantly reduced injury compared to vehicle (25 mm^3, $p< 0.05$), while medium and high dose candesartan did not significantly change lesion volume (35 and 36 mm^3, respectively).

Study II: NSS revealed a reduction of neurofunctional deficits in animals treated with low dose candesartan at all application time points. Contusion volume increased from 22 mm^3 (PrimL) to 47 mm^3 (vehicle). At all application time points contusion volume was markedly reduced by app. 40%, when compared to vehicle (33 mm^3, 36 mm^3, 34 mm^3 and 37 mm^3 for 30min, 1h, 2h and 4h, respectively; $p< 0.05$).

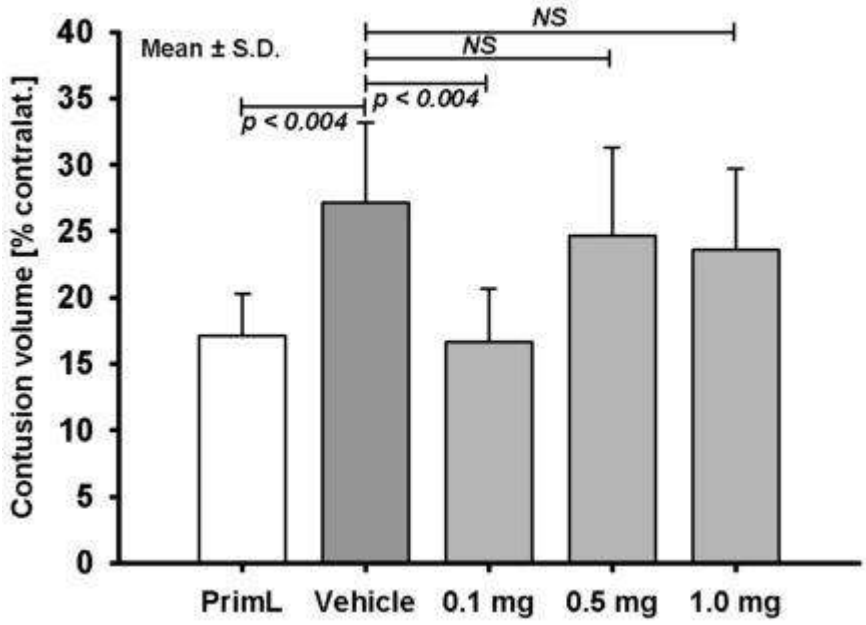

[pic1]

Conclusions: The present study demonstrates that low dose candesartan reduces neurofunctional impairment and secondary brain damage when applied for up to 4 hours after experimental brain trauma. Possible mechanisms are:

1. direct vascular effects of AT1 receptor inhibition, i.e. increased cerebral blood flow by arterial vasodilatation, and
2. a shift of intracerebral angiotensin II action from AT1 mediated pro-apoptotic and inflammatory to AT2 mediated neuroproliferative and protective effects.

In accordance with previous ischemic stroke studies [3], higher doses candesartan failed to reduce lesion volume. Beneficial effects of high dose AT1 inhibition may be abolished by systemic side effects, e.g. reduction of mean arterial blood pressure. However, low dose AT1 inhibition is a promising therapeutic strategy to prevent secondary brain damage.

References:

[1] Li J, et al. FASEB J 2005; 19(6):617-9.

[2] Thal et al. Anesthesiology. 2007: Abst CD A1555.

[3] Brdon J, et al. J Hypertension 2007; 25:187-96.

508

Brain Poster Session: Stem Cells & Gene Therapy

IMMUNE-MEDIATED EFFECTS OF GRAFTED HUMAN EMBRYONIC STEM CELLS-DERIVED NEURAL STEM CELLS IN PEDIATRIC HYPOXIC-ISCHEMIC BRAIN INJURY MODEL

M. Daadi, A. Arac, Z. Li, G. Sun, J. Wu, G. Steinberg

Stanford University School of Medicine, Stanford, CA, USA

Ischemic brain injury in newborn infants represents a major cause of cerebral palsy, mental retardation and epilepsy. Currently, there are no effective interventions to improve the chronic sequelae of perinatal asphyxia. Stem cell-based therapy has the potential to replace the necrotic tissue caused by hypoxia-ischemia (HI) and to restore function. Promising preclinical studies in experimental stroke models have demonstrated the efficacy of stem cells derived from various sources, including bone marrow, cord blood and central nervous system. In most of these studies, grafted animals showed some degree of functional recovery. Although, these findings are promising, little is known about how stem cell transplantation therapy achieves these outcomes. It is generally believed that non-neural cells, such as those derived from bone marrow or cord blood, exert a neurotrophic effect on ischemia-injured tissue and do not survive for long-term in the grafted site. While neural stem cells are thought to provide cell replacement and neurotrophic support of the lesioned area. In the present study, we sought to determine how the inflammatory and cellular immune responses are modulated after stroke and transplantation of human neural stem cell progeny (hNSCs), derived from human embryonic stem cells (hESCs) in the rat model of neonatal HI.

The hNSCs were isolated from the hESCs and perpetuated using serum free media supplemented with epidermal growth factor, basic fibroblast growth factor and leukemia inhibitory growth factor. To generate the model of neonatal HI, seven-day-old rats were subjected to permanent ligation of the left carotid artery, followed by one and half hours in a hypoxic chamber (8%O2 and 92%N2, at 37°C). The newborns were divided into HI vehicle and HI transplant groups. Twenty-four hours after the induction of HI, animals were grafted with single cell suspension of hNSCs (4.5 x 105) into 3 sites in the forebrain. The animals were evaluated 5 weeks after transplantation for their sensorimotor skills in the cylinder and in the rotarod tests.

Our results showed that during the fifth week after transplantation, HI transplanted animals significantly improved in their use of the contralateral impeded forelimb ($P< 0.05$). The hNSC grafts significantly ameliorated the locomotor deficits in the rotarod test ($P< 0.05$). To evaluate potential effects on the immune system, the cellular composition of peripheral immune system was evaluated using flow cytometric analysis. Our data demonstrated that stroke induced a 3-fold increase in the CD3+, CD4+ T-cells and no significant changes in the CD8+ and CD11b+ cells in the blood and other peripheral systems of vehicle group. Graft treated animals manifested a significant decrease ($P< 0.05$) in the CD3+, CD4+ T lymphocytes, suggesting an anti-inflammatory effect. Post-mortem histopathological analysis of grafted hNSCs identified with a human-specific nuclear marker, demonstrated good survival, dispersion and differentiation in the stroke-damaged tissue. Interestingly, the transplanted animals showed a 2-fold increase in Iba1+ microglia with no apparent infiltration or reaction against the grafts. These preliminary results suggest that the peripheral immune system is modulated by hNSCs transplants and that microglia could play a neurotrophic role in HI-transplanted brains.

510

Brain Poster Session: Experimental Cerebral Ischemia: In Vitro

DOWNREGULATION OF KV4.2 CHANNELS BY NR2B-CONTAINING NMDA RECEPTORS IN CULTURED HIPPOCAMPAL NEURONS

Z. Lei, P. Deng, Y. Li, **Z. Xu**

Indiana University School of Medicine, Indianapolis, IN, USA

Objective: Somatodendritic Kv4.2 channels mediate transient A-type potassium currents (IA), and play critical roles in controlling neuronal excitability and modulating synaptic plasticity (1). Our previous studies have shown a downregulation of Kv4.2 and IA caused by activation of NMDA receptors (2). Our previous studies have shown a NMDA-dependent downregulation of Kv4.2 and IA. NMDA receptors are wildly believed to be heteromeric complexes of NR1A combined with NR2A-NR2D (3). NR2A- and NR2B-containing NMDA receptors have opposite role on excitotoxic neuronal injury (4). Here, we investigate the involvement of NR2A- and NR2B-containing NMDA receptors in glutamate modulation of Kv4.2 and IA in cultured hippocampal neurons.

Methods: Primary neuronal cultures were prepared from the hippocampus of E18 embryos (5). The neurons were treated on DIV18. The expression levels of Kv4.2 were analyzed by Western blotting, the cellular distributions of Kv4.2 were detected by immunostaining, and the properties of IA currents were measured by whole-cell voltage clamp recording.

Results: Bath application of glutamate caused a reduction in total Kv4.2 protein levels and Kv4.2 clusters, and produced a hyperpolarized shift in the inactivation curve of IA. The effect of glutamate on Kv4.2 and IA was inhibited by pretreatment of specific NR2B antagonists. In contrast to the predominant expression of NR2A-containing NMDA receptors at synapse, NR2B-containing NMDA receptors is wildly believed to be the predominant NMDA receptors expressed at extrasynaptic sites in mature hippocampal neurons in vitro (6). We found that, like bath application of glutamate, selective activation of extrasynaptic NMDA receptors caused a reduction in total Kv4.2 protein levels and Kv4.2 clusters. In contrast, specific stimulation of synaptic NMDA receptors had no effect on Kv4.2. In addition, the influx of Ca2+ was essential for extrasynaptic modulation of Kv4.2.

Conclusions: These results demonstrate that the downregulation of Kv4.2 and IA induced by glutamate is mediated by the activation of NR2B-containing receptors, which might be associated with NR2B-mediated NMDA responses, such as excitotoxic neuronal death.

References:

1. Birnbaum, S. G., Varga, A. W., Yuan, L. L., Anderson, A. E., Sweatt, J. D., and Schrader, L. A. (2004) Physiological reviews 84, 803-833.

2. Lei, Z., Deng, P., and Xu, Z. C. (2008) Journal of neurochemistry 106, 182-192.

3. Dingledine, R., Borges, K., Bowie, D., and Traynelis, S. F. (1999) Pharmacological reviews 51, 7-61.

4. Liu, Y., Wong, T. P., Aarts, M., Rooyakkers, A., Liu, L., Lai, T. W., Wu, D. C., Lu, J., Tymianski, M., Craig, A. M., and Wang, Y. T. (2007) J Neurosci 27, 2846-2857.

5. Lei, Z., Ruan, Y., Yang, A. N., and Xu, Z. C. (2006) Neuroscience letters 407, 224-229.

6. Tovar, K. R., and Westbrook, G. L. (1999) J Neurosci 19, 4180-4188.

Supported by NIH grant NS38053 and AHA grant 0655747Z, AHA0526007Z, AHA0425689Z, AHA0630172N, AHA0710027Z, AHA0825810G.

512

Brain Oral Session: Neonatal Ischemia

THERAPEUTIC ADMINISTRATION OF PLASMINOGEN ACTIVATOR INHIBITOR-1 PREVENTS HYPOXIC-ISCHEMIC BRAIN INJURY IN NEWBRONS

D. Yang[1], N. Nemkul[1], D. Lawrence[2], D. Lindquist[3], **C.-Y. Kuan**[1]

[1]Pediatrics, Division of Neurology, Cincinnati Children´s Hospital Medical Center, Cincinnati, OH, [2]Internal Medicine, University of Michigan, Ann Arbor, MI, [3]Radiology, Cincinnati Children´s Hospital Medical Center, Cincinnati, OH, USA

Objectives: Neurovascular proteases, including the matrix metalloproteases (MMPs) and plasmniogen activators (tPA and uPA), have important pathological functions in adult brains, but their roles in perinatal cerebrovascular diseases are less certain. In the Rice-Vannucci model of neonatal cerebral hypoxia-ischemia (HI), the induction of MMP-9 activity only occurred after the onset of much irreversible brain damage. In contrast, we recently showed that cerebral HI rapidly induces the parenchymal tPA activity in immature brains, suggesting that tPA may be an early mediator of neonatal HI brain injury (Adhami et al., 2008). The objectives of the present study are twofold. First, we wish to determine whether inhibition of the brain tPA and uPA activity with plasminogen activator inhibtor-1 (PAI-1) prevent MMP-9 activation after HI in newborn brains. Second, does brain infusion of PAI-1 have an overall therapeutic efficacy?

Methods: P7 Wistar rat pups were challenged by the Rice-Vannucci model of neonatal cerebral HI (unilateral carotid artery-ligation plus 90-min 10% oxygen). After the HI insult, animals received intracerebroventricle (ICV) injection of saline or PAI-1. The brain protein samples were prepared at 4 and 24 hrs of recovery for biochemical analysis, including plasminogen activator (tPA/uPA) activity assay, MMP zymogram, and occludin-immunoblot. Magnetic Resonance Imaging (MRI) analysis, including T2, apparent diffusion coefficient (ADC) and diffusion tensor imaging (DTI), were also performed at 24 hours of recovery. The extents of brain damage in saline- or PAI-1-injected animals were compared after 7 days of recovery to determine dose-response curve and therapeutic window of the PAI-1 treatment.

Results: We found that the PAI-1 treatment greatly reduced tPA and uPA activities at both 4 and 24 hrs, and blocked MMP-9 induction at 24 hrs of recovery. PAI-1 therapy also prevented HI-induced extravasation of immunoglobulins and degradation of the BBB-associated proteins. Moreover, the PAI-1 treatment decreased the extent of brain edema, cortical cell death, and white-matter oligodendrocyte degeneration at 24-48 hrs of recovery based on multiple biochemical, MRI, and histological assays. Finally, PAI-1 treatment provided a dose-dependent preservation of brain tissues at 7 days of recovery, and the therapeutic window is at least 4 hrs after HI.

Conclusion: Activation of the brain parenchymal PA system precedes and is required for MMP-9 induction in the experimental (Vannucci) model of neonatal HI brain injury. Overall, PAI-1 therapy protects against HI-induced BBB damage and brain edema in immature brains. Future studies are warranted to test whether a similar pathological mechanism also occurs in infants diagnosed with hypoxic-ischemic encephalopathy.

References: Adhami F, Yu D, Yin W, Schloemer A, Burns KA, Liao G, Degen JL, Chen J, Kuan CY (2008) Deleterious effects of plasminogen activators in neonatal cerebral hypoxia-ischemia. Am J Pathol 172:1704-1716.

513

Brain Poster Session: rt-PA

RT-PA PLUS HYPOTHERMIA REDUCES COMPLICATIONS OF RT-PA TREATMENT

X. Tang[1], L. Liu[1,2], M. Koike[1], M. Yenari[1]

[1]Neurology, UCSF SF VAMC, San Francisco, CA, USA, [2]Tiantan Hospital, Beijing, China

Both mild hypothermia and recombinant tissue plasminogen activator (rt-PA) have been shown to have beneficial effects in outcome from clinical brain ischemia. However, the benefits of rt-PA treatment are tempered by cerebral hemorrhage and blood brain barrier (BBB) disruption. Since coagulation and fibrinolytic pathways can be affected by temperature, the safety of hypothermia in combination with rt-PA is unknown. This study explored whether mild hypothermia plus rt-PA treatment is feasible in a model of focal cerebral ischemia. Male C57/BL6 mice were subjected to transient middle cerebral artery occlusion (MCAO) for 1 or 2 h using an intraluminal suture, followed by 24 h reperfusion. In the first study, mice were cooled to 33°C immediately after occlusion for 2 h followed by rt-PA treatment (10 mg/kg, IV: 10% bolus, and the remainder over 30 min) begun 3 h post occlusion (TH, n=12), and compared to rt-PA treatment at normothermia (TN, n=14) and no treatment (NN, n=6). Because brain hemorrhage is thought to occur during the reperfusion phase, we conducted a second study where both interventions were started upon reperfusion. TH (n=6): rt-PA plus hypothermia (33°C), TN (n=5): rt-PA treatment at normothermia (37°C), NN (n=6): MCAO at normothermia and no rt-PA, NH (n=8): hypothermia but no rt-PA. Infarct volumes were measured, and the extent of cerebral hemorrhage was evaluated by counting the number of faces from 5 sequential blocks with any visible hemorrhage (maximum # of faces=5). Ischemic brain samples were also assessed for endogenous tPA and PAI-1 levels using immunohistochemistry and Western blot. rt-PA treatment itself did not affect infarct size in this model (Exp. 1 & Exp. 2: TN vs. NN, N.S.), but hypothermia did (Exp. 2: NH (78.1±8.9 mm^3) vs. NN (152.1±8.6 mm^3), $P< 0.05$), even with the addition of rt-PA (Exp. 1: infarct volume was reduced by 34% in TH vs. TN, $P< 0.05$; Exp. 2: infarct volume was reduced by 48.9% in TH vs. TN, $P< 0.05$). Hemorrhage patterns were similar in both experiments; thus, the data for Exp. 2 are presented. Administration of rt-PA at normothermia increased the amount of cerebral hemorrhage (TN: 4.7 ± 0.3 faces, NN: 1.2±0.6, TH: 1.4 ± 0.4, $P< 0.001$), while hypothermia reduced it to levels similar to that seen in MCAO without rt-PA treatment. Furthermore, the combination of hypothermia and rt-PA treatment did not increase brain hemorrhage compared to hypothermia alone (TH: 1.4 ± 0.4 vs. NH: 0.7 ± 0.3, NS). Both Western blots and immunohistochemistry showed that endogenous tPA expression was reduced in hypothermic mice, whereas PAI-1 was not changed by temperature. Combination therapy with mild hypothermia and rt-PA, whether administered sequentially or simultaneously, should be safe, and may even reduce complications of rt-PA treatment.

A NOVEL ADENOVIRAL VECTOR FOR GENE THERAPY AGAINST CEREBRAL ISCHEMIA

S. Hou, D. Huang, A. Desbois

Institute for Biological Sciences, National Research Council Canada, Ottawa, ON, Canada

Background and aims: Viral vector-mediated gene therapy represents a promising approach to treat human neurological diseases. Among the many gene delivery vectors, replication defective adenoviral vectors have been widely used as an effective tool to express therapeutic genes in the brains of rodent models of human neurological diseases including cerebral ischemia. Needless to say, the development of an array of selective gene targeting vectors is vital for the future success of any therapeutic attempts aimed at protecting neurons in the diseased brains. However, selective gene expression in neurons is still a challenge. To this end, we have developed a expression vector which is capable of expressing gene products selectively in neurons under the regulation of hypoxia.

Methods: We have developed several expression vectors using a combination of neuron restrictive silencer elements (NRSEs), hypoxia responsive elements (HREs) and CMV minimal promoter (CMVmp). These elements were packaged into replication defective adenovirus to target gene expression selectively in neurons in a hypoxia-regulated manner. Neuronal selectivity and responsiveness to hypoxia of the constructed novel vectors were determined empirically in both neural cell lines, primary cerebellar granule neurons (CGNs) and in neonatal mouse brain under hypoxia.

Results: The construct p5HRE-3NRSE exhibited not only the highest level of reporter gene expression in neuronal cells, but also in an oxygen concentration-dependent manner when compared with all other constructs. As expected, this construct did not elicit reporter gene expression in non-neuronal cells including human HEK293A and HT29 cells, rat NRK cells, mouse 3T6 cells and 3T3 L1 cells. The construct was packaged into a replication defective adenoviral vector (Ad/5HRE-3NRSE). Remarkably, in response to hypoxia, Ad/5HRE-3NRSE showed strong gene expression in primary CGNs (12-fold induction compared with normoxia), but not in glial cells. Double immunostaining with antibodies against the reporter gene product luciferase and a neuron-specific marker protein, such as MAP-2, confirmed the specificity and inducibility of this construct in neurons. Preliminary in vivo studies using these vectors in a neonatal hypoxia mouse brain confirmed selective gene expression in neurons in response to hypoxia.

Conclusions: Taken together, further refinement of this vector may lead to the development of a useful tool for targeting gene delivery and therapy for stroke research and therapeutics.

515

Brain PET Oral 6: Neurodegenerative Disorders

PRESERVED SEROTONERGIC PROJECTIONS BUT WIDELY REDUCED BRAIN SEROTONIN 2A RECEPTORS IN PATIENTS AND IN A MOUSE MODEL OF ALZHEIMER'S DISEASE

L. Marner[1,2], A. Ettrup[1,2], P.V. Jensen[1,2], V.G. Frokjaer[1,2], J. Kalbitzer[1,2], S. Lehel[3], W.F.C. Baaré[2,4], S. Aznar[1,2], G.M. Knudsen[1,2], S.G. Hasselbalch[1,2,5]

[1]Neurobiology Research Unit, University Hospital Rigshospitalet, [2]Center for Integrated Molecular Brain Imaging, [3]PET and Cyclotron Unit, Copenhagen University Hospital Rigshospitalet, [4]Danish Research Center for Magnetic Resonance, University Hospital Hvidovre, [5]The Memory Clinic, Copenhagen University Hospital Rigshospitalet, Copenhagen, Denmark

Background and aims: Post mortem studies suggest serotonergic dysfunction in Alzheimer's disease (AD), and serotonin 2A (5-HT_{2A}) receptors are globally reduced early in the disease(1). The objective of the study was to investigate serotonin transporters (SERT) as a measure of serotonergic projections(2) in patients with AD and in a mouse model of amyloid plaque deposition.

Methods: We included 12 patients (mean age 73.7 ±7.6 years, 8 males) with Alzheimer's disease (average MMSE of 24, range 19-26) and 11 healthy age-matched subjects (mean age 72.5 ±6.8 years, 6 males). Subjects were investigated with a 90 min dynamic [^{11}C]DASB-PET to measure SERT and a 40 min steady-state [^{18}F]altanserin-PET to measure 5-HT_{2A} receptors. Partial volume correction was applied to correct for atrophy.

For autoradiography, we included 42 mice, of which 21 were APP/PS1 transgenic mice with increased age-related amyloid load but no pronounced cell death. The mice were 4, 8, or 11 months old, corresponding to pre-, mid- and late-plaque stages. Using [^{3}H]-escitalopram, we quantified levels of SERT in the hippocampus, and in the same mice, 5-HT_{2A} levels were assessed in hippocampus, prefrontal and somatosensory cortices using [^{3}H]MDL100907.

Results: In AD patients, SERT binding was 34% (p=0.0003) lower in the hippocampus, while cortical regions and midbrain were unaffected (figure 1). The 5-HT_{2A} receptors were markedly reduced (25-66%) in AD patients in most regions (figure 1). In the 8 and 11 month old transgenic AD mice SERT binding was normal in hippocampus and 5-HT_{2A} binding in somatosensory and prefrontal cortices was decreased in 8 months (p=0.06) and 11 months (p=0.01) old mice by 7-19%.

Conclusions: We showed a marked decrease in 5-HT_{2A} receptor binding in patients with AD and in the APP/PS1 mice. This suggests that the decreased 5-HT_{2A} binding may be associated with amyloid deposition. The SERT binding was unaffected in most cortical regions and in midbrain, suggesting that the serotonergic projections and the neuron bodies in dorsal nucleus raphe are intact. The SERT reduction in hippocampus in patients could be secondary to the neuron death taking place in hippocampus of AD patients(3) and not reported in the transgenic mice.

References:

1. S. G. Hasselbalch et al., Neurobiol. Aging. 29, 1830 (2008).

2. K. Nielsen et al., Synapse. 59, 270 (2006).

3. M. J. West, et al., Neurobiol. Aging. 25, 1205 (2004).

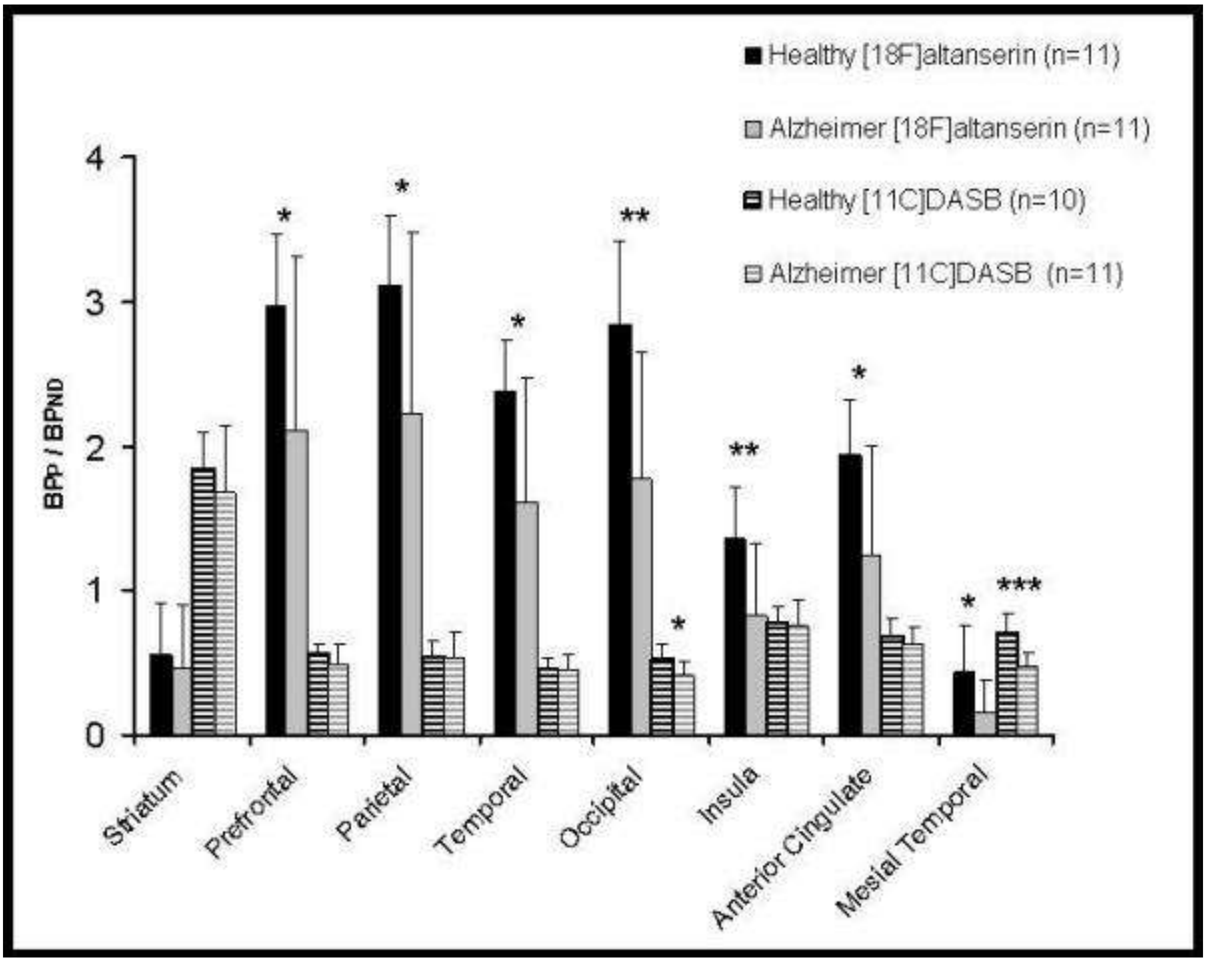
Healthy [18F]altanserin (n=11)
Alzheimer [18F]altanserin (n=11)
Healthy [11C]DASB (n=10)
Alzheimer [11C]DASB (n=11)
BPP / BPND
4
3
2
1
0
*
*
*
**
*
**
*
*
***
Striatum
Prefrontal
Parietal
Temporal
Occipital
Insula
Anterior Cingulate
Mesial Temporal

[Figure]

517

Brain Poster Session: Brain Imaging: Neurologic Disease

NEUROBIOLOGICAL EFFECTS OF ATYPICAL ANTIPSYCHOTICS AND COGNITIVE REMEDIATION THERAPY IN FIRST EPISODE SCHIZOPHRENIA

J.J. Furtner, A.O. Pintsov, G. Kasprian, G. Sachs, D. Prayer

Medical University of Vienna, Vienna, Austria

Background and aims: Cognitive deficits contribute to the disability of schizophrenic patients. These deficits, especially related to working memory tasks seem to be correlated with a dysfunction of the prefrontal cortex. The aim of this study is to examine whether the cognitive dysfunction of schizophrenics may be detected using f-MRI (n-back test) and whether an improvement may be shown after atypical antipsychotics in combination with cognitive therapy.

Methods: f-MRI was used during performance of the n-back working memory task (one-back test) to assess working memory in a total of 8 cases. A baseline fMRI examination was performed in 6 drug-naïve patients who met the DSM-IV criteria for schizophrenia and in 2 healthy controls. After the baseline fMRI examination patients were randomly assigned into different cohorts. To date there has been 1 patient in the first cohort who received only atypical antipsychotics while 2 patients in the second cohort received atypical antipsychotics in combination with cognitive therapy.

The f-MRI examination was repeated after 4 weeks of therapy in 3 patients. MR-imaging was performed on a 1.5 Tesla superconducting unit in conjunction with an 8-element Sense Head-Coil. Data was processed by using the standardized analyzing software package Brainvoyager (Brain Innovation, Netherlands).

Purpose: Purpose of this study is to examine the cognitive dysfunction of schizophrenic patients using a working memory task (n-back test) during f-MRI examination and to investigate if atypical antipsychotics in combination with cognitive therapy are more beneficial than medication only.

Results: In the baseline f-MRI examination all schizophrenics showed an exaggerated physiological response, especially in the right dorsolateral prefrontal cortex in comparison with the healthy controls. This hyperactivational state can be interpreted as a prefrontal dysfunction in terms of a greater effort being required to perform a one-back working memory task.

Those patients, who received atypical antipsychotics in combination with cognitive therapy showed a greater reduction of activation after 4 weeks (Fig.1) than the patient who received antipsychotics only. Thus one might expect that cognitive therapy in schizophrenic patients may improve prefrontal cortex dysfunction.

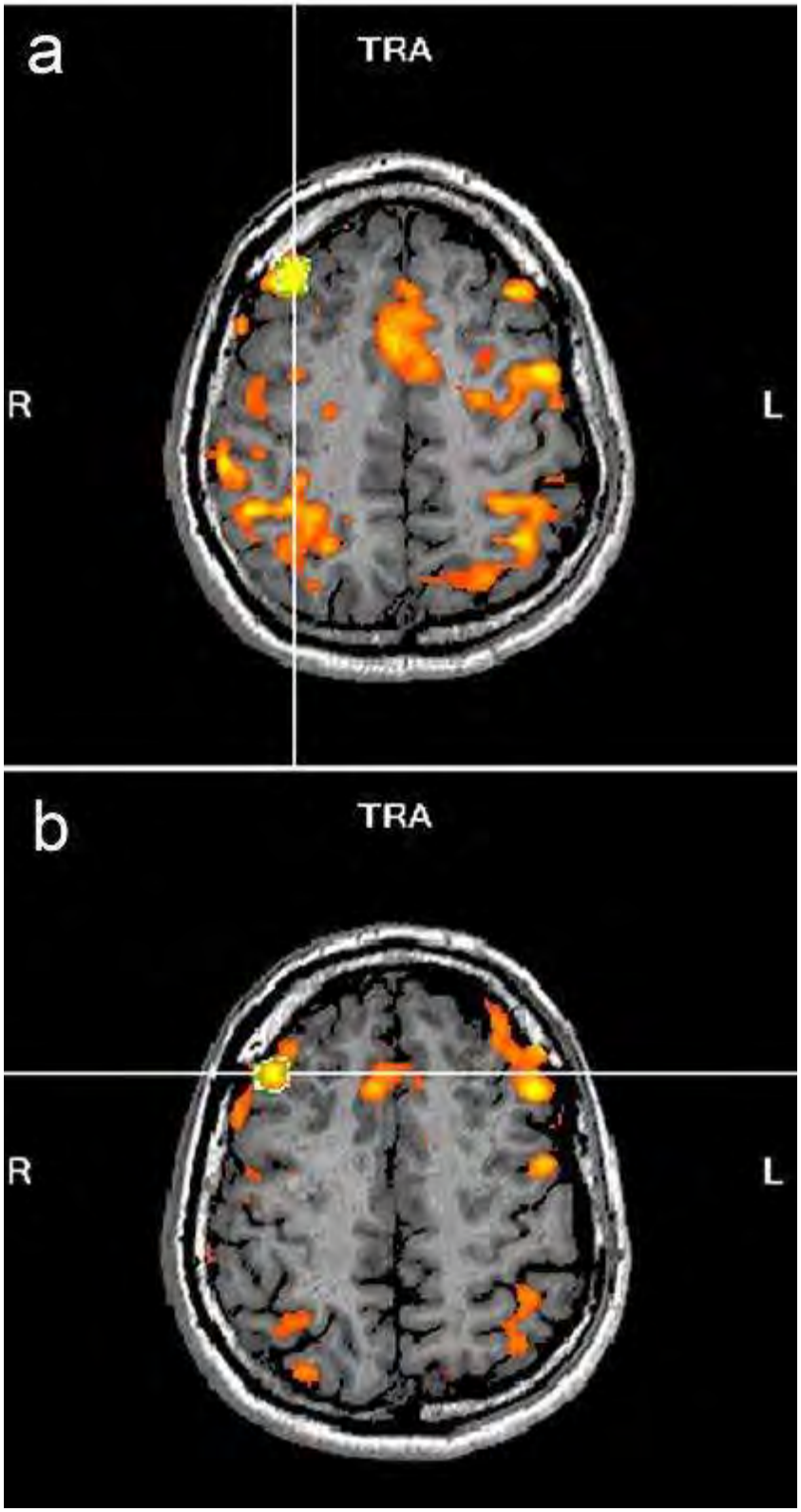

[Figure 1]

Conclusions: Once proved in a larger number of patients, these results might help deciding which therapy (pharmacological/ psychotherapeutical/ combined) will be beneficial. Furthermore, cognitive

outcome might be a predictor for social performance and fMRI data might be used as a marker for certain aspects of the disease.

Figure1: f-MRI results during performance of the n-back working memory task of a) a drug naïve schizophrenic patient and b) the same patient 4 weeks later after a combinated therapy of atypical antipsychotics and cognitive therapy. The picture shows the hyperactivation in the right dorsolateral prefrontal cortex in a drug naïve schizophrenic patient and the decrease of activation in the same cortical area after therapy.

518

Brain Poster Session: Blood-Brain Barrier

FLAIR OF EARLY BBB DISRUPTION IN ACUTE EXPERIMENTAL STROKE

E. Henning, A. Martin, S. Warach, L. Latour

Stroke Diagnostics and Therapeutics Section, NINDS/NIH, Bethesda, MD, USA

Introduction: In acute stroke patients, extravasation of Gd-contrast appears hyperintense on FLAIR in CSF spaces such as the sulci and lateral ventricles. This observation is thought to be indicative of early blood-brain barrier (BBB) disruption and has been associated with reperfusion, hemorrhagic transformation, and worse clinical outcome. Unfortunately, the mechanisms of barrier disruption and movement of Gd-contrast to the CSF space remain poorly understood and cannot be investigated in the clinic. In this study, we employed FLAIR to identify the same phenomenon early after experimental stroke in spontaneously hypertensive rats (SHR).

Methods: N=10 male SHR, 360±10 grams, were divided into two groups. Group 1 (N=5) received 50±6 minutes of right middle cerebral artery occlusion (MCAO) followed by reperfusion. Group 2 (N=5) received sham surgery. Imaging was performed using a 7.0T/30cm imaging spectrometer equipped with ±45 G/cm gradients. DW-EPI and GRE were performed at baseline (30-minutes post-MCAO). DW-EPI, GRE, T_2, and FLAIR imaging were performed at 30-minutes, 1 hour, and 1.5 hours post-reperfusion. At 1 hour and 1.5 hours post-reperfusion, Gd-DTPA (0.2ml @ 0.5 mol/L, i.v.) was administered. Additional FLAIR images were acquired 10 and 20 minutes post-contrast for assessment of Gd-DTPA extravasation. VOIs were drawn on ADC maps for stroke volume calculation and on FLAIR images at baseline for delineation of the lateral ventricles and healthy parenchyma. VOIs drawn on FLAIR were projected to post-reperfusion time points in order to track any observed signal enhancement.

Results: Lesion volume at baseline was 260±20 mm^3. At 30-minutes post-reperfusion, lesion volume decreased significantly to 50±20 mm^3 ($p< 0.01$). This decrease continued through 1 hour (14±7 mm^3, $p< 0.01$) and 1.5 hours (9±6 mm^3, $p< 0.01$) post-reperfusion. There was no difference in FLAIR signal at baseline between stroke and sham groups for the contralateral ($p=0.28$) and ipsilateral ($p=0.32$) ventricles. At 1 hour post-reperfusion (~2 hours after stroke onset), there was significant post-contrast FLAIR signal enhancement for the ipsilateral ventricle (2.31±1.04, $p< 0.01$) in comparison to sham (0.58±0.04). There were no differences for the contralateral ventricle ($p=1.00$). These findings were consistent at 1.5 hours post-reperfusion. Additional FLAIR enhancement was observed in N=1 animal in the parenchyma and N=1 animal in the meninges, both ipsilateral to stroke.

Conclusions: In this study, we have shown that FLAIR permits delineation of barrier disruption as early as 1 hour post-reperfusion following acute experimental stroke. These observations are identical to what has been observed in the clinic and are within the time frame of tPA administration. The methods presented herein provide an avenue to investigate:

1. Gd extravasation as a marker of BBB disruption;
2. the relationship between Gd extravasation, reperfusion, tPA, and hemorrhagic transformation;
3. novel therapies targeting the BBB.

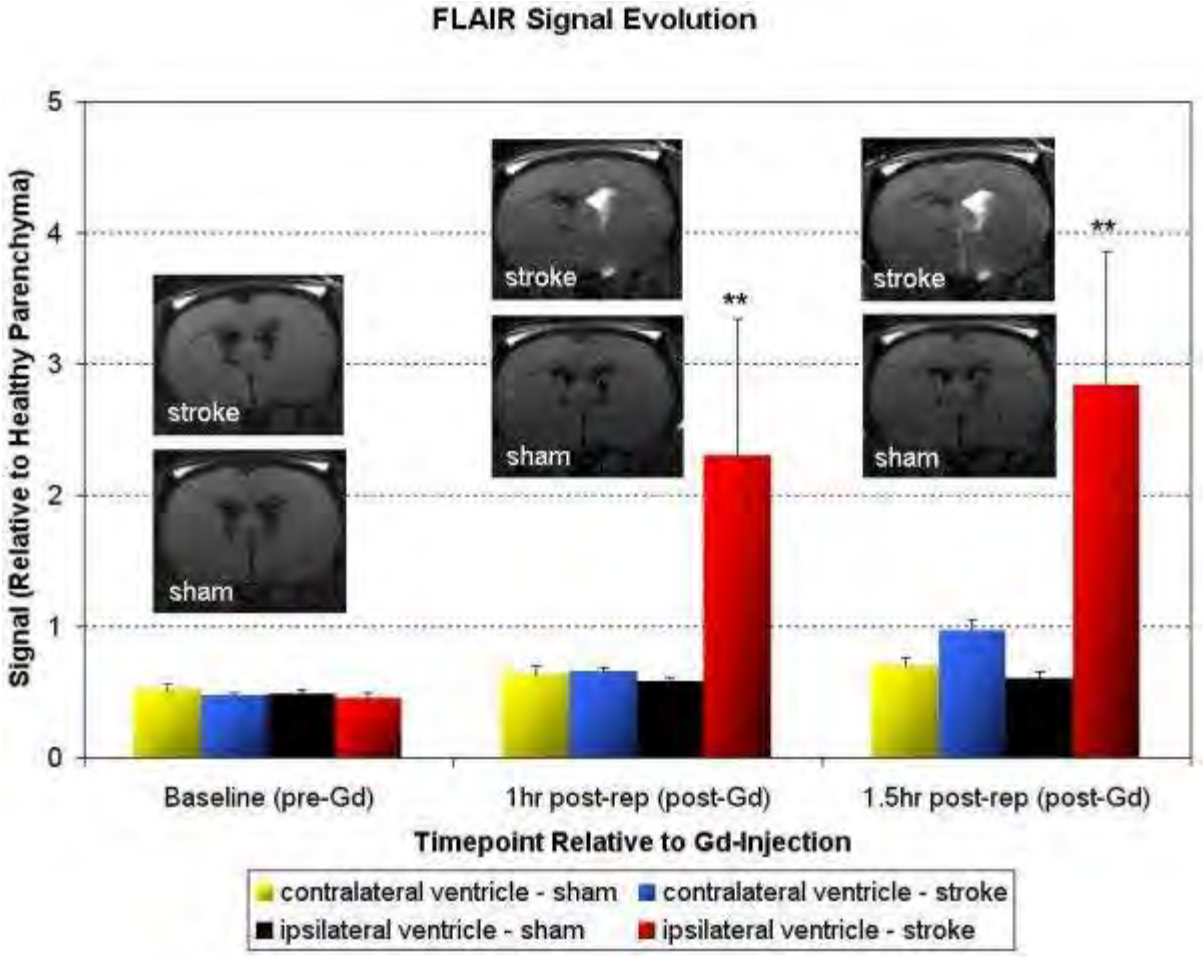
FLAIR Signal Evolution
Signal (Relative to Healthy Parenchyma)
5
4
3
2
1
0
stroke
sham
stroke
sham
stroke
sham
**
**
Baseline (pre-Gd)
1hr post-rep (post-Gd)
1.5hr post-rep (post-Gd)
Timepoint Relative to Gd-Injection
contralateral ventricle - sham
contralateral ventricle - stroke
ipsilateral ventricle - sham
ipsilateral ventricle - stroke

[Figure 1]

520

BrainPET Poster Session: Molecular Brain Imaging: Clinical Applications

PET IMAGING OF CEREBRAL GLUCOSE METABOLISM DURING EXECUTIVE FUNCTION IN NORMAL RHESUS

A.K. Converse, J.M. Moirano, J.A. Larson, K.V. Kronenfeld, T.R. Oakes, J.E. Holden, C.F. Moore, M.L. Schneider

University of Wisconsin, Madison, WI, USA

Objectives: To better understand executive function, we wished to identify regions of the primate brain activated by a reversal task that involves attention, working memory, and goal directed behavior. A priori, we expected to find activations in anterior cingulate gyrus, prefrontal cortex, and nucleus accumbens.

Methods: Adult normal rhesus macaques (Macaca mulatta, n=10) were injected with 2-[F-18]fluoro-2-deoxy-D-glucose (FDG) and placed in the Wisconsin General Test Apparatus to perform a Reversal task and, in a different session, a sensorimotor matched Control task for 30 minutes. Performance, as indicated by the number of correct trials, was recorded in the Reversal session. Following the behavior, the subjects were anesthetized with ketamine, maintained on isoflurane, and scanned by positron emission tomography (PET). Coincidence events were chosen so data for each individual corresponded to the same time frame post injection in each condition and were sorted into static sinograms. Images were reconstructed by filtered back projection with attenuation and scatter correction and aligned to template regions of interest (ROIs). The fractional difference in whole brain normalized radioactivity was calculated between the Reversal and Control scans for various bilateral ROIs and voxel-wise. Additionally, the total correct score was correlated against this measure of glucose metabolism alteration.

Results: Examining the group mean over all 10 subjects, no ROI exhibited significant metabolic alteration. However, task performance correlated positively with metabolic increases in putamen ($p_{unc}< 0.01$) and thalamus ($p_{unc}< 0.05$, 2-tail t, 10-2 d.f.). This ROI result was supported by the correlation map, which showed task performance positively correlated with metabolic increases in right putamen and posterior thalamus ($p_{unc}< 0.005$, 2 tail t test, 10-2 d.f.). Two subjects showed particularly low task performance, namely 1 and 3 correct trials as compared to a range of 8-35 for the remaining 8 subjects. Post hoc analysis of the group means without these two subjects showed activation of the lateral prefrontal cortex ROI ($p_{unc}=0.016$, 2-tail t, 8-1 d.f.), and, in the activation map, a significant positive cluster in the neighborhood of medial superior frontal gyrus in the coronal plane containing anterior commissure ($p_{corr}=0.023$, 2-tail t, 8-1 d.f., corrected for multiple comparisons and cluster extent, $t>3$, $k=501$ mm^3).

Conclusions: FDG PET imaging of normal rhesus macaques suggests positive correlations between executive function task performance and glucose metabolism in putamen and thalamus. In high performing subjects, task-related increases in glucose metabolism were observed in prefrontal cortex.

This work was supported by NIH AA12277.

522

Brain Oral Session: Experimental Stroke and Cerebral Ischemia 1

DISTINCT ADVANTAGES OF RECOMBINANT HUMAN VERSUS PLASMA DERIVED C1-INHIBITOR IN BRAIN ISCHEMIC INJURY

E.R. Zanier[1], R. Gesuete[1], F. Orsini[1], C. Storini[1], A. Fantin[1], M. Stravalaci[1], H. Vietsch[2], B. Ziere[2], M.L.M. Mannesse[2], M. Gobbi[1], M.G. De Simoni[1]

[1]Mario Negri Institute, Milano, Italy, [2]Pharming Technologies B.V, Leiden, The Netherlands

Background and aims: C1-inhibitor (C1-INH) is an endogenous multifaced anti-inflammatory molecule, known to act as inhibitor of complement and kinin systems. We have previously shown that C1-INH has potent neuroprotective properties in mouse models of cerebral ischemia and traumatic brain injury, where plasma-derived (pd) C1-INH attenuated acute neurobehavioral deficits, anatomical damage, and neurodegeneration. However pdC1-INH had a narrow therapeutic window, since no protective effects were observed when it was administered 1 hour after the onset of acute brain injury (1-5).

Methods: We evaluated the effects of the recently available recombinant human C1-INH (rhC1-INH), administered intravenously to C57Bl/6 mice undergoing both transient and permanent ischemia, on infarct volume and neurodegeneration. We then compared the localization of rhC1-INH and pdC1-INH in the ischemic brain tissue by immunohistochemistry and confocal analysis and evaluated their binding profiles using Surface Plasmon Resonance (SPR). Having found a selective binding of rhC1-INH to MBL we explored the susceptibility of mannose binding lectin (MBL) deficient mice to transient ischemia.

Puropose: To explore the efficacy and the therapeutic window of rhC1-INH and to investigate its possible mechanism of action in comparison with that of pdC1-INH.

Results: rhC1-INH markedly reduced cerebral damage when administered up to 18h from the beginning of transient ischemia and up to 6h after permanent ischemia, thus showing a surprisingly wide therapeutic window. We found that rhC1-INH was confined to cerebral vessels while pdC1-INH diffused into the brain parenchyma. Furthermore rhC1-INH, which has a different glycosylation pattern, showed a different binding profile. In particular, rhC1-INH, but not pdC1-INH, binds MBL with high affinity thus revealing a novel target of C1-INH action. Finally a significantly lower susceptibility to ischemic damage was observed in MBL-/- compared to WT mice.

Conclusions: rhC1-INH, which possesses a distinct glycosylation pattern and binding profile, is superior to the corresponding plasmatic protein in the protection against cerebral injury. This may possibly be due to a direct binding to MBL deposited on endothelial cells early after ischemia thus preventing lectin-complement pathway activation and providing a long lasting protection towards ischemic damage. The surprisingly wide time-window of efficacy of rhC1-INH represents a crucial aspect for the possible therapeutic use of this drug in the treatment of stroke. Noteworthy, C1-INH is already used in humans for the therapy of C1-INH deficiency.

References:

De Simoni MG et al. Neuroprotection by complement (C1) inhibitor in mouse transient brain ischemia. J Cereb Blood Flow Met. 2003.

De Simoni MG et al. The powerful neuroprotective action of C1-inhibitor on brain ischemia reperfusion injury does not require C1q. Am J Pathol. 2004.

Storini C et al. C1 inhibitor protects against brain ischemia-reperfusion injury via inhibition of cell recruitment and inflammation. Neurobiol Disease. 2005.

Storini C et al. Selective inhibition of plasma kallikrein protects brain from reperfusion injury. J Pharmacol Exp Ther. 2006.

Longhi L et al. C1-inhibitor attenuates neurobehavioral deficits and reduces contusion volume after controlled cortical impact brain injury in mice. Crit Care Med. 2009.

523

Brain Poster Session: Cerebral Vascular Regulation

GABA AND GLUTAMATE MEDIATE THE NEUROVASCULAR COUPLING RESPONSE TO WHISKER STIMULATION PARTLY VIA ARACHIDONIC ACID DERIVATIVES

P. Fernandes[1], A. Kocharyan[1], C. Lecrux[1], E. Vaucher[2], E. Hamel[1]

[1]Laboratory of Cerebrovascular Research, Montreal Neurological Institute, McGill University, [2]École d'Optométrie, Université de Montréal, Montréal, QC, Canada

Background and aims: Previously, we demonstrated that increases in cortical cerebral blood flow (CBF) induced by whisker stimulation occurred concurrently with cortical activation of COX-2 pyramidal cells and specific subsets of GABA interneurons (Fernandes P et al., Brain07, Abstract #BO12-3). Here, we investigated the contribution of glutamate, GABA and neuroglial components in this evoked CBF response using pharmacological blockade of receptors and/or astroglial synthetic pathways.

Methods: Increases in cortical CBF during whisker deflection (20 sec, ~10Hz) were measured in the contralateral barrel cortex by laser Doppler flowmetry at baseline and after intracisternal (i.c., 3µl of a 10^{-4}M, pH 7.4 buffered solution) injection of vehicles, antagonists of NMDA (MK-801), GABA-A (picrotoxin), epoxyeicosatrienoic acid (EET) (14,15-EEZE) receptors, inhibitors of prostaglandin synthetic enzyme cyclooxygenase-2 (COX-2) (NS-398) and of the EET synthetic enzyme P450 epoxygenase (MS-PPOH). The evoked CBF response was recorded in urethane-anesthetized rats following administration of these pharmacological compounds either alone or in combination, with 4 to 10 rats used per group. The femoral artery was cannulated for continuous monitoring of blood gases and blood pressure, and body temperature was measured throughout the experiments, with no differences observed among groups. Changes in CBF were compared by repeated-measures analysis of variance (ANOVA) or by one-way ANOVA for three groups.

Results: Vehicles had no effect on the CBF response evoked by whisker deflection when compared to baseline. As expected, MK-801 decreased the CBF response (-53.1±6.8%, $p< 0.001$) (Gsell et al., J Neurosci 2006, 26:8409-8416). Similarly, picrotoxin significantly reduced the CBF response (-39.1±3.9%, $p< 0.001$), and combined blockade of NMDA and GABA-A receptors demonstrated a significant additive inhibitory effect (-73.1±5.3%, $p< 0.01$). In agreement with a recent study (Liu et al., 2008, Am J Physiol Heart Circ Physiol, 295:H619-H631), inhibition of EETs synthesis with MS-PPOH or antagonism of the EET receptor with 14,15-EEZE diminished the perfusion response (-43.3±4.1%, $p< 0.001$ and -32.8±5.6%, $p< 0.01$, respectively). Their combined administration resulted in a significant additive effect on the CBF response (-62.4±5.8%, $p< 0.01$). In contrast, the combined administration of MS-PPOH with MK-801 or picrotoxin did not result in a greater effect than using MS-PPOH alone, suggesting a common route of action. The CBF response was reduced by COX-2 inhibition (-46.3±3.9%, $p< 0.001$), and the combined administration of NS-398 and picrotoxin had an additive inhibitory effect on the CBF response (-59.6±5.7%, $p< 0.01$).

Conclusions: These results show the interplay between pyramidal cells, GABA interneurons, and astrocytes in the regulation of CBF in the rat whisker barrel cortex. Together, the data indicate that:

i. both glutamate and GABA are involved in the perfusion response to whisker stimulation, and
ii. they act in parallel to activate the synthesis of arachidonic acid metabolites from the EET and/or prostaglandin pathways, some of these mediators being synthesized and released by astrocytes.

Overall, the data indicate that inhibitory and excitatory cells in the somatosensory cortex contribute to the neurovascular coupling response to thalamocortical afferents, and that astrocytes can be intermediaries for both types of neurons.

Supported by CIHR grant (MOP-84209, EH).

NEUROMETABOLIC ORIGIN OF FLAVOPROTEIN AUTOFLUORESCENCE SIGNAL IN THE CEREBELLAR CORTEX

W. Gao[1], K. Reinert[2], X. Wang[1], C. Gang[1], T. Ebner[1]

[1]Neuroscience, Univ of Minnesota, Minneapolis, MN, [2]Neurology, Systemic Neuroscience Inst., Univ. of Pittsburgh, Pittsburgh, PA, USA

Objectives: Flavoprotein autofluorescence imaging in the cerebellar cortex in vivo revealed that stimulation of the parallel fibers evokes a beam-like optical response consisting of an initial, brief increase in fluorescence (light phase) followed by a longer duration decrease (dark phase). In addition, off-beam parasagittal bands of decreased fluorescence are evoked due to feedforward inhibition of Purkinje cells and interneurons by molecular layer inhibitory interneurons (Reinert et al 2004; Gao et al 2006). The present experiments examined the cellular and metabolic origins of these three response components. The astrocyte-neuron lactate shuttle hypothesis (Pellerin and Magistretti 1994) states that during excitatory neurotransmission, the astrocytes that are activated by glutamate transporters glycolytically convert glucose to lactate and transport that lactate to neurons to fuel mitochondrial oxidative phosphorylation. We hypothesized that the light phase is neuronal and the dark phase is glial.

Methods: In the anesthetized mouse, mitochondrial flavoprotein autofluorescence (Reinert et al 2004) was used to image the responses to parallel fiber stimulation in the cerebellar cortex in vivo. Pharmacological manipulations were used to selectively block glutamatergic synaptic transmission, glial activation or glycolysis. Field potential recordings were used to assess for the status of the parallel fiber-Purkinje cell circuit.

Results: Parallel fiber stimulation evokes a beam like response and intersecting inhibitory bands. First, blocking neuronal synaptic transmission using a cocktail of glutamate receptor blockers (DNQX, D-APV and LY367385) selectively suppressed both the light phase and the inhibitory bands. The dark phase was largely intact. Preventing glial activation with the glial glutamate transporter blocker, DL-TBOA, abolished the dark phase. These findings imply a neuronal origin for the light phase and a glial origin for the dark phase. Second, substituting the glycolytic products pyruvate or lactate for glucose in the bathing solution selectively abolished the dark phase and the light phase remained unchanged, demonstrating that dark phase is primarily due to glycolysis and light phase oxidative metabolism.

Conclusions: Together these results establish that the light phase evoked by parallel fiber stimulation is due to oxidative metabolism of lactate in neurons driven by excitatory glutamate transmission. Conversely, the dark phase is primarily due to increased glycolytic metabolism in glia following neuronal oxidative metabolism. The inhibitory bands are primarily neuronal and are due to energy saving. These findings provide strong in vivo support for the astrocyte-neuron lactate shuttle hypothesis.

References:

Pellerin L, Magistretti PJ. Glutamate uptake into astrocytes stimulates aerobic glycolysis: a mechanism coupling neuronal activity to glucose utilization. Proc Natl Acad Sci U S A. 91(22):10625-9, 1994.

Reinert KC, Dunbar RL, Gao W, Chen G, Ebner TJ. Flavoprotein autofluorescence imaging of neuronal activation in the cerebellar cortex in vivo. J Neurophysiol 92: 199-211, 2004.

Gao W, Chen G, Reinert KC, Ebner TJ. Cerebellar cortical molecular layer inhibition is organized in parasagittal zones. J Neurosci 26: 8377-8387, 2006.

Brain Poster Session: Neuroprotection

TRANSIENT FOCAL CEREBRAL ISCHEMIA ACTICATES CALPAIN TO CLEAVE COLLAPSIN RESPONSE MEDIATOR PROTEINS

S. Hou[1], S. Jiang[1], B. Zurakowski[1], A. Desbois[1], J. Kappler[2]

[1]Institute for Biological Sciences, National Research Council Canada, Ottawa, ON, Canada, [2]Institut für Physiologische Chemie, Rheinische Friedrich-Wilhelms-Universität Bonn, Bonn, Germany

Background and aims: Calpains belong to a highly conserved family of calcium-dependent proteases which cleave a large number of substrates including cytoskeletal elements such as spectrins, and important regulatory proteins such as CDK-5 and collapsin mediator proteins (CRMPs). In the central nervous system, calpains are widely expressed and their activities are modulated by an endogenously-expressed inhibitory protein, calpastatin. Calpain activity can be inhibited by synthesized inhibitors, such as ALLN and calpeptin, which also provide potent neuroprotection against excitotoxicity. CRMPs are important brain-specific proteins with distinct functions during normal development and under disease conditions. CRMPs, also referred to as TOAD-64 (turned on after division 64 kDa), Ulip (UNC-33-like protein) or DRP (dihydropyrimidinase-related phosphoprotein), are a family of five cytosolic proteins discovered a decade ago with a role in collapsing and repelling growth cones. CRMPs can mediate the collapse of growth cones through the regulation of actin and tubulin cytoskeletons. In the present study, we provided evidence to show that all CRMP family members are targeted for cleavage by calpain activated in ischemic mouse brain.

Methods: All procedures for cerebral ischemia produced by middle cerebral artery occlusion (MCAO) using C57/black mice were approved by the local Animal Care Committee. Under temporary isofluorane anesthesia, mice were subjected to MCAO using an intraluminal filament as previously described. After 1 h of MCAO, the filament was withdrawn, blood flow restored to normal by laser Doppler flowmetry and wounds sutured. Animals were sacrificed after 24 h of reperfusion. Brain infarction was measured and brain tissues were subjected to protein extraction for Western blotting, and immunostaining analyses to determine changes of CRMPs.

Results: Among the five CRMPs, the expressions of CRMP1, CRMP3 and CRMP5 were the most abundant in the cerebral cortex and that all CRMPs were targeted for cleavage by ischemia-activated calpain. Subcellular fractionation analysis showed that cleavage of CRMPs by calpain occurred not only in the cytoplasm but also in the synaptosomes isolated from ischemic brains. Moreover, synaptosomal CRMPs appeared to be at least one fold more sensitive to cleavage compared with those isolated from the cytosolic fraction in an in vitro experiment, suggesting that synaptosomal CRMPs are critical targets during cerebral ischemia-induced neuronal injury. Finally, the expression of all CRMPs was co-localized with TUNEL positive neurons in the ischemic mouse brain which further supports the notion that CRMPs may play an important role in neuronal death following cerebral ischemia.

Conclusions: Collectively, these studies demonstrated that CRMPs are targets of calpains during cerebral ischemia and they also highlighted an important potential role that CRMPs may play in modulating ischemic neuronal death.

528

Brain Poster Session: Experimental Stroke & Cerebral Ischemia

INHIBITION OF THE SODIUM/HYDROGEN EXCHANGER IS NEUROPROTECTIVE AFTER FOCAL CEREBRAL ISCHEMIA: A SMALL ANIMAL MRI STUDY

P. Ferrazzano[1], A. Shi[2], N. Manhas[2], E. Hutchinson[3], E. Meyerand[3], D. Sun[2]

[1]Pediatrics, [2]Neurosurgery, [3]Medical Physics, University of Wisconsin School of Medicine and Public Health, Madison, WI, USA

Objectives: After focal cerebral ischemia, over-stimulation of the Na+/H+ exchanger isoform 1 (NHE1) causes a loss of Na+ ionic homeostasis and contributes to cell swelling and ischemic injury. Recently, inhibition of NHE1 has been shown to be neuroprotective in in vitro and in vivo ischemic injury. However, the therapeutic window for NHE1 inhibition, the time-course of infarct evolution after transporter inhibition, and the neuroprotective effects of NHE1 inhibition on white matter injury and cytotoxic edema formation, are difficult to assess using traditional methods. Small animal MRI provides an ideal means to study this complex physiology following cerebral ischemia and NHE1 transporter inhibition.

Methods: Transient focal cerebral ischemia was induced by a filament occlusion of the middle cerebral artery (MCAO) in wild-type controls (NHE1+/+), NHE1 deficient mice (NHE1+/-), and NHE+/+ mice treated with the NHE1 inhibitor Cariporide (HOE). In the HOE treated animals, 0.5 mg/kg was initially administered IP 30 minutes prior to the onset of reperfusion (Rp), and the same dose was repeated at 24 h and 48 h Rp. T2 and diffusion weighted imaging was performed over the 72 hours following reperfusion on a Varian 4.7 Tesla small animal MRI scanner. Diffusion-weighted spin-echo images (DWI) and T2-weighted fast spin-echo images were acquired in 12 contiguous axial slices with a field of view of 17x17mm and a slice thickness of 1mm. High resolution Diffusion Tensor Imaging (DTI) was performed on fixed brain specimens to evaluate white matter injury.

Results: The T2 images demonstrate excellent resolution and anatomic detail. A T2 lesion was first visible at 6 h Rp, and evolved over the following 24-72 h. The lesion seen in NHE1+/- mice and HOE treated mice was significantly smaller at all time points, suggesting neuroprotection in these animals. The size and extent of this T2 lesion correlated well with the infarction seen on TTC staining. At 1 h Rp, DWI revealed a lesion that was not visible on conventional T2 images, and that correlated well with the final infarct size seen at 72 h on T2 images and histology. High resolution DTI Mean Diffusivity Maps also demonstrated a smaller lesion in NHE1+/- animals which spared the cortex. Moreover, Fractional Anisotropy Maps revealed injury to the corpus callosum in NHE1+/+ animals but not in the NHE1+/- animals. Taken together, the DTI results suggest white matter integrity is maintained in the NHE+/- animals.

Conclusion: Small animal MRI is a useful measure for evaluating the evolution of injury after cerebral ischemia. T2 images correlate closely with histology, and DWI is a sensitive early marker of ischemic injury. Our MRI studies demonstrate that genetic and chemical inhibition of NHE1 is neuroprotective in this mouse model of transient focal cerebral ischemia.

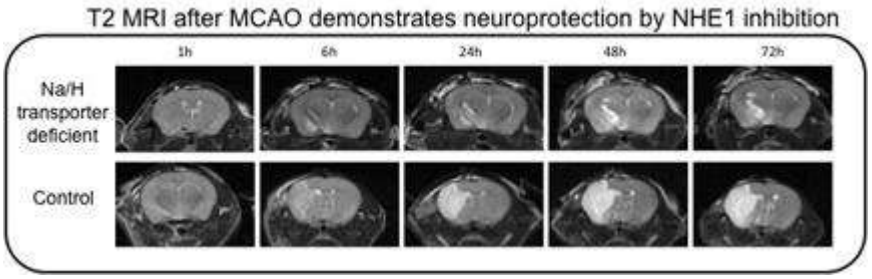

[T2 MRI]

Brain PET Oral 5: In Vivo Pharmacology II: Serotonin

THE SEROTONIN 4 RECEPTOR PET-LIGAND [11C]SB207145: SENSITIVITY TO OCCUPANCY BY UNLABELED LIGAND AND TO ENDOGENOUS SEROTONIN

L. Marner[1,2], N. Gillings[2,3], K. Madsen[1,2], D. Erritzoe[1,2], W. Baaré[2,4], C. Svarer[1,2], S.G. Hasselbalch[1,2], G.M. Knudsen[1,2]

[1]Neurobiology Research Unit, University Hospital Rigshospitalet, [2]Center for Integrated Molecular Brain Imaging, [3]PET and Cyclotron Unit, Copenhagen University Hospital Rigshospitalet, [4]Danish Research Center for Magnetic Resonance, University Hospital Hvidovre, Copenhagen, Denmark

Background and aims: The serotonin 4 (5-HT_4) receptor is involved in learning and memory and is a potential target for treatment of Alzheimer's disease and depression. [^{11}C]SB207145 has emerged as a useful radiotracer for quantitative PET-imaging of the cerebral 5-HT_4 receptors in humans[1]. In this study we investigate the in vivo affinity, K_D^{app}, and the radiotracer´s susceptibility to changes in endogenous serotonin.

Methods: Sixteen healthy subjects (age-range 20-45 years, 8 males) underwent a 2-hour dynamic [^{11}C]SB207145 PET examination. Two scans were performed on the same day in 13 subjects, of which seven received pharmacological challenges consisting of a 3-day blockage of the 5-HT_{1A}autoreceptors by a partial agonist/beta-adrenoceptor antagonist, pindolol, and a 60-min infusion of the selective serotonin reuptake inhibitor, citalopram, initiated about 30 min prior to the second injection of [^{11}C]SB207145. Volumes of interest were delineated automatically on coregistered 3T magnetic resonance images and time-activity curves were extracted. Modeling of BP_{ND} was performed using simplified reference tissue model with cerebellum as reference region.

The concentration of free unlabelled ligand (F) was estimated from the cerebellar time activity curve (40-110 min) as the mean radioactive concentration in cerebellum divided by the specific radioactivity. The bound ligand (B) was estimated as the difference between radioactive concentration in striatum and cerebellum divided by the specific radioactivity.

Results: The range in amount of injected unlabelled ligand enabled the estimation of a population-based K_D^{app} of 1.2 ±0.53 nM (±SE) as the negative inverse slope of a scatchard plot (figure). Subsequently, the receptor occupancy (O) was estimated for each individual as: $O=F/(F+K_D)$ and the BP_{ND} was subsequently individually corrected by dividing by 1-O. An upper limit of 0.028 mg/kg (70 kg subject: 2.0 mg) of [^{11}C]SB207145 per PET examination should ensure a receptor occupancy below 5%.

The occupancy was higher in females (11.9%) compared to the males (6.6%) ($p=0.046$) that had a larger body distribution volume. Thus, we found a sex difference in non-corrected BP_{ND} ($p=0.02$), which disappeared when correcting for occupancy. In spite of a significant increase in plasma prolactin level throughout the pharmacologically challenged scans as proxy for increased cerebral serotonin levels, BP_{ND} was unaltered in all tested regions (caudate nucleus, lentiform nucleus, insula, and hippocampus).

Conclusions: [^{11}C]SB207145 is a valuable tool for non-invasive quantification of 5-HT_4 receptors in the human brain. Due to its relatively high receptor affinity, K_D^{app}=1.2, and to a relatively low protein binding (f_P=0.25), a production with a relatively high specific radioactivity is required. The ligand is insensitive to acute changes in cerebral serotonin levels, which is an advantage when subjects are investigated under circumstances with possible fluctuations in the serotonin levels.

References: [1]Marner,L. et al. J Nucl Med 2007;48 (Supplement 2):159P.

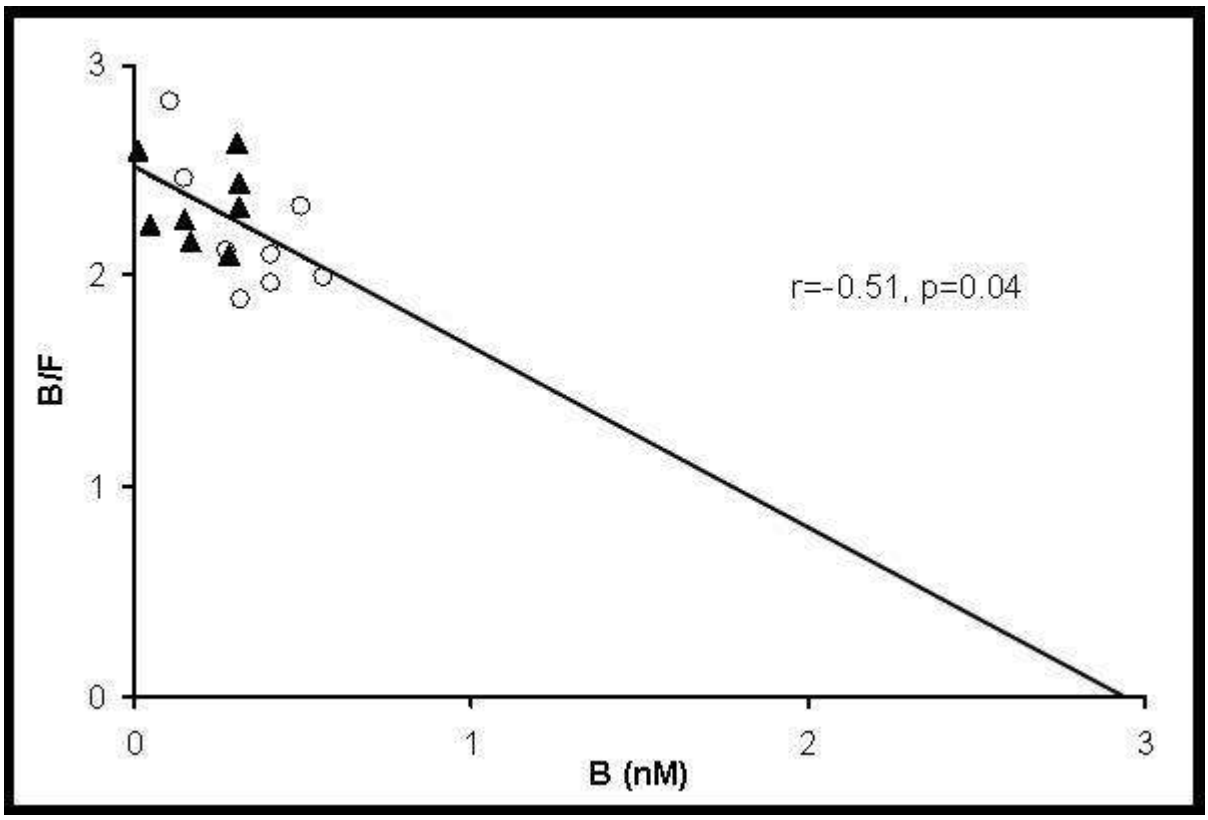

[Figure]

CANDESARTAN IMPROVES AUTOREGULATION OF LOCAL CORTICAL CEREBRAL BLOOD FLOW DURING HAEMORRHAGIC HYPOTENSION WHILE ENALAPRILAT DOES NOT

O.B. Paulson[1,2], S.T. Sigurdsson[1,3], A. Høj Nielsen[3], S. Strandgaard[3]

[1]Neurobiology Research Unit, Copenhagen University Hospital, Rigshospitalet, [2]Danish Research Center for Magnetic Resonance, Copenhagen University Hospital, Hvidovre, [3]Department of Nephrology, Copenhagen University Hospital, Herlev, Copenhagen, Denmark

Objectives: The renin-angiotensin system (RAS) maintains a tone in the cerebral resistance vessels, which can be influenced by RAS blockers. Several ACE-inhibitors (ACEi) have this effect. The beneficial effects of angiotensin II receptor blockers (ARBs) on stroke incidence and outcome in clinical trials might be related to this haemodynamic effect. Bradykinin is a potent endothelium dependent vasodilator which is broken down by ACE. Treatment with ACEi thus increases bradykinin levels. The present study investigated the effect of the ARB candesartan, the ACEi enalaprilat and the bradykinin antagonist HOE 140 on the lower limit of autoregulation of local cortical cerebral blood flow (CBF) compared to controls.

Methods: The study was carried out in 4 groups of Sprague-Dawley rats in general anaesthesia with isofluran and N_2O. Temperature and $PaCO_2$ were kept stable. Both femoral arteries and veins were cannulated. A craniotomy was made over one hemisphere, leaving the dura intact. CBF was measured continually on the surface of the brain with laser Doppler technique before and after intravenous injection of candesartan (0,2 mg/kg), enalaprilat (2 mg/kg) or the bradykinin antagonist Hoe 140 (4 nmol and then 2 nmol every 20 minutes). Blood pressure was stabilised with nor-epinephrine, and subsequently gradually reduced by controlled bleeding.

Results: The lower limit of CBF autoregulation (mean ±1 SD) in the candesartan group was 38 ± 7 mmHg in the enalaprilat group 51 ± 7 mmHg, in the Hoe 140 group 52 ± 6 mmHg and in the control group 44 ± 4 mmHg. There was a statistically significant difference between all groups except between the enalaprilat group and the control group.

Conclusion: A shift of the lower limit of local cortical CBF towards lower pressure is an effect that in clinical settings might be advantageous. Candesartan in the present acute experiment caused such a shift and it is surprising that enalaprilat did not, contrary to other ACE-inhibitors in earlier studies Results of combination treatment with ARBs and Hoe 140 and ACEi and HOE 140 are under way.

Brain Poster Session: Neuroprotection

CRITICAL ROLE OF SERINE-SPECIFIC PHOSPHORYLATION IN THE ACTIVATION OF HSP27 AND ITS NEUROPROTECTIVE EFFECT AGAINST ISCHEMIC NEURONAL INJURY

R. Stetler[1,2,3], G. Cao[1,2,3], G. Yanqin[3], F. Zhang[1,2], S. Wang[1,2], Z. Weng[1], P. Vosler[1], L. Zhang[1], J. Chen[1,2,3]

[1]Neurology, University of Pittsburgh School of Medicine, [2]Geriatric Research, Education and Clinical Center, Veterans Affairs Pittsburgh Health Care System, Pittsburgh, PA, USA, [3]State Key Laboratory of Medical Neurobiology, Fudan University School of Medicine, Shanghai, China

Background and aims: Other than thrombolytic therapy, an effective neuroprotective treatment for stroke is currently unavailable. Abnormal activation of cell death programs likely contributes to the pathogenesis of ischemic brain injury, as suppression of apoptosis via alteration of signaling pathways of death program promotes neuronal survival and improves functional recovery in rodent stroke models. HSP27 is a member of the small heat shock protein family, a group of ubiquitous stress proteins that are expressed in virtually all organisms. The expression of HSP27 is induced in the brain after cerebral ischemia, and overexpression of HSP27 has been found to be a potent neuroprotective molecule. In addition to its known function as a protein chaperone, recent studies suggest that HSP27 has apoptosis-suppressing effects in many cell death models, including ischemia. In nonneuronal systems, HSP27 gains anti-apoptotic properties after undergoing serine-specific phosphorylation. We have recently demonstrated that HSP27 interacts with and suppresses activated ASK1 via the N-terminal region of HSP27 and the kinase domain of ASK1. The N-terminal region of HSP27 contains critical serine residues required for phosphorylation; however, the precise mechanism underlying the effects of HSP27 phosphorylation on neuroprotection against ischemic insults is not fully understood.

Methods: In order to address the effects of HSP27 phosphorylation on neuroprotection against ischemic insults, we have used both an in vitro cortical culture model (oxygen/glucose deprivation) as well as the in vivo transient focal ischemia model. We created a transgenic mouse line overexpressing either wildtype HSP27 or an HSP27 phosphorylation mutant where three critical serine residues (at positions 15, 78 and 82) were mutated to alanines to yield a non-phosphorylatable mutant (HSP27-ala). Assessment of ASK1 activity, activation of downstream kinases, mitochondrial cell death signaling and cell survival were compared between transgenic strains and wildtype mice.

Purpose: In this study, we sought to determine if phosphorylation of HSP27 is required for inhibition of ASK1 activity and cell death signaling following cerebral ischemia.

Results: We have found that tg-HSP27 mice, but not tg-HSP27-ala mice, exhibit decreased infarct area following focal cerebral ischemia. Wildtype tg-HSP27 undergoes rapid phosphorylation and shifts to lower molecular weight oligomeric structures following ischemic injury, whereas the non-phosphorylatable mutant tg-HSP27-ala shifts to larger oligomers. The overexpression of HSP27 was neuroprotective in cortical cultures exposed to OGD, but HSP27-ala had no effect on cell survival. HSP27, but not HSP27-ala, physically interacted with activated ASK1 and suppressed downstream kinase signaling and mitochondrial cell death signaling following ischemic insults. In a cell-free system, neither purified recombinant HSP27 nor HSP27-ala was capable of inhibiting activated ASK1; however, when phosphorylated in vitro, phospho-HSP27 effectively inhibited ASK1 activity in a dose-dependent manner.

Conclusions: Our results suggest that phosphorylation of HSP27 is required for neuroprotection and suppression of ASK1 activity following ischemic injury. The interaction between phosphorylated HSP27 and activated ASK1 demonstrates a novel mechanism of HSP27 neuroprotection and provides

a tangible basis for the development of small molecule inhibitors targeting ASK1 activity based on an HSP27 phosphorylation-specific structure.

IN VITRO QUANTIFICATION OF MGLUR5 IN PONS AND CEREBELLUM OF HUMAN BRAIN USING [^{3}H]ABP688

L. Minuzzi[1], M. Diksic[2], S. Gauthier[3], R. Quirion[4], P. Rosa-Neto[1]

[1]Translational Neuroimaging Laboratory - MCSA, Douglas Hospital, [2]Department of Neurology and Neurosurgery, [3]McGill Centre for Studies in Aging, Douglas Hospital, [4]Department of Psychiatry, Douglas Hospital, McGill University, Montreal, QC, Canada

Objectives: Metabotropic glutamate receptor type 5 (mGluR5) has been associated to the memory processing and also to several neuropsychiatric disorders. The radiopharmaceutical [^{11}C]ABP688 has been showed to be a suitable PET ligand for measuring in vivo mGluR5 in animals and humans. However, despite the favourable kinetic, arterial blood sampling is required, implicating in technical limitations for PET imaging. The objective of the present study is to quantify the total number of mGluR5 in two regions of human brain that are potentially devoid or with markedly low receptors in order to provide a reference region for PET analysis. In vitro quantitative autoradiography was carried out using [^{3}H]ABP688 in human cryosections of pons and cerebellum in comparison to a mGluR5-rich region hippocampus.

Methods: Frozen human brain section of hippocampus, pons and cerebellum from five healthy controls were cryosectioned at 20 µm. Saturation binding study was carried out according to the method described by Hintermann et al. (2007) with some modifications. Briefly, the tissue was pre-incubated for 20 min in buffer containing 30 mM Na HEPES, 110 nM NaCl, 5 mM KCl, 2.5 mM $CaCl_2$ and 1.2 mM $MgCl_2$ (pH 7.4). The brain sections were then incubated for one hour in the presence of [^{3}H]ABP688 (74 Ci/mmol) at a range of concentrations from 0.125 to 8 nM. Non-specific binding was determined with addition of 10 µM MPEP. The slides were washed (3 x 5 min) in cold buffer, dipped in ice-cold distilled water and dried. The sections along with autoradiographic standards were exposed for five days to phosphor imaging plates. The B_{max} and KD of [^{3}H]ABP688 were calculated by saturation binding analysis.

Results: Binding of [^{3}H]ABP688 showed a heterogeneous and displaceable distribution in human tissue. Hippocampus (CA1) presented higher density of receptors (Bmax 1.31 ± 0.07 pmol/mg of tissue). Sections of pons and cerebellum showed markedly lower Bmax (0.08 ± 0.01 and 0.09 ± 0.01 pmol/mg, respectively) in comparison to hippocampus (ratio 1:15). Dissociation constant (KD) of pons and cerebellum were identical 0.4 ± 0.2 nM, whereas hippocampus revealed KD of 1.5 ± 0.2 nM.

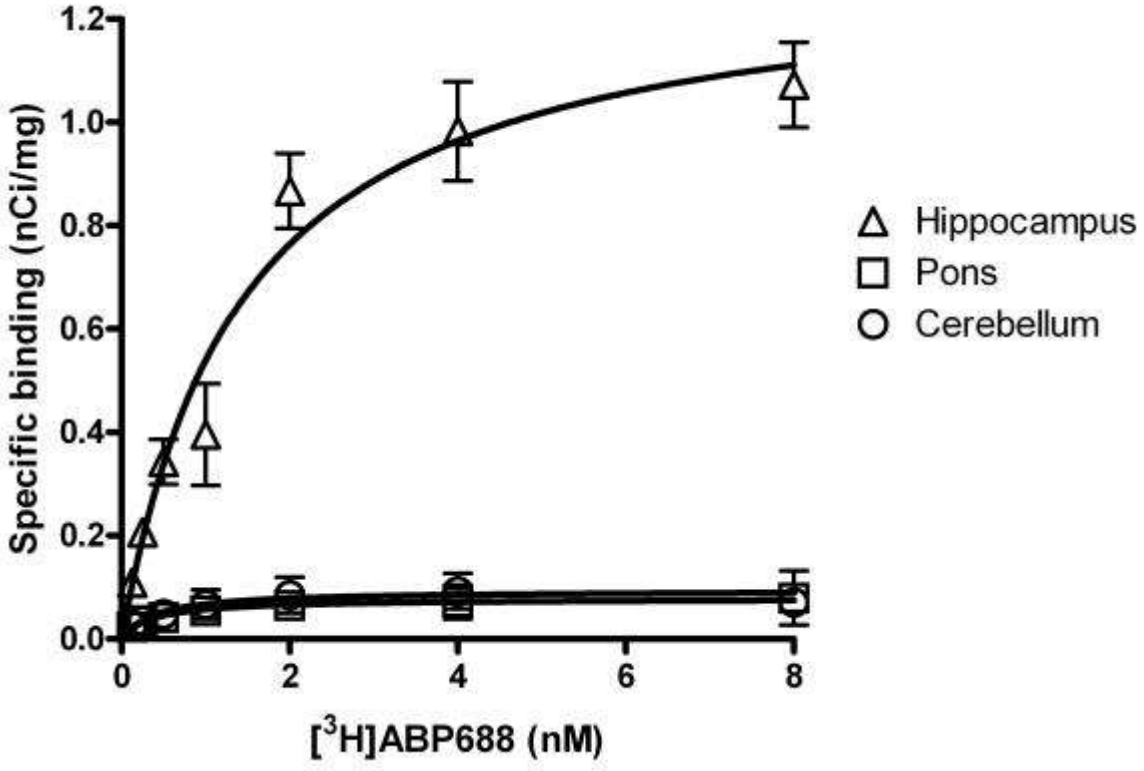

[Saturation Binding of [3H]ABP688 in Human Brain]

Conclusions: Saturation binding parameters in human tissue were similar to values found previously in rat brain using the same radioligand. Although pons and cerebellum showed presence of mGluR5, the distinctly lower amount of receptors suggests that they can be used as reference region for in vivo quantification of mGluR5 in humans.

References:

1. Ametamey, S. M., V. Treyer, et al.(2007). Human PET studies of metabotropic glutamate receptor subtype 5 with 11C-ABP688. J Nucl Med 48(2):247-52.

2. Hintermann, S., I. Vranesic, et al.(2007). ABP688, a novel selective and high affinity ligand for the labeling of mGlu5 receptors: identification, in vitro pharmacology, pharmacokinetic and biodistribution studies. Bioorg Med Chem 15(2):903-14.

538

Brain Poster Session: Inflammation

ROLE OF NADPH OXIDASE IN POST-ISCHEMIA BRAIN INFLAMMATION: A TEMPORAL PROFILE STUDY

H. Chen[1], P. Chan[1,2,3]

[1]Department of Neurosurgery, [2]Department of Neurology and Neurological Sciences, [3]Program in Neurosciences, Stanford University School of Medicine, Palo Alto, CA, USA

Objectives: In response to ischemia, the brain transcribes and expresses inflammation proteins, which activate downstream pathways and cause further detrimental effects [1]. SOD1 transgenic mice showed significantly less NF-kB-pathway activation, which suggests oxidative stress is important for the brain inflammation process after cerebral ischemia [2]. NADPH oxidase (NOX) is a resource of reactive oxygen species generation in the brain after cerebral ischemia [3]. Previous studies have revealed that NOX inhibition is neuroprotective after focal ischemia[4]. However, the role of NOX in greatly developed inflammation is not clear. Our hypothesis is that NOX is involved in the post-ischemic inflammation process and that inhibition of NOX will ameliorate inflammation and delayed infarction.

Methods: We subjected wild-type (WT) mice, $gp91^{phox}$-/- (gp91 KO) mice, and NOX inhibitor apocynin-treated mice (Apo) to 60 or 75 min of focal ischemia followed by 3 h, 24 h, 3 d and 7 d of reperfusion. We measured the brain infarction volume, inflammation-related pathways and protein expression (COX-2, ICAM-1, ERK), inflammation cell infiltration (neutrophils and microglia), and cytokine mRNA levels (IL-1b, IL-6, iNOS).

Results: There was a significantly higher infarction volume at 3 d than at 24 h of reperfusion, which indicates a continuous evolution of cell death that leads to delayed, larger infarction. In addition, a larger area of infarction was observed in the WT mice than in the Apo and gp91 KO mice at both 24 h and 3 d of reperfusion. Furthermore, the WT mice exhibited higher mortality than the gp91 KO mice at 7 d of reperfusion. At 3 h of reperfusion, there was little ICAM-1 and COX-2 protein expression. However, at 24 h of reperfusion, ICAM-1 and COX-2 expression increased and was more significant in the WT mice than in the Apo and gp91 KO mice. An ELISA revealed more neutrophil infiltration in the WT mice than in the gp91 KO or apocynin-treated mice, and there was abundant microglia activation at 24 h of reperfusion in the WT mice. The inflammation cytokine gene expression studies showed that at 24 h of reperfusion, only IL-1b mRNA levels increased by 2.3 fold. However, at 72 h of reperfusion, the levels of IL-1b, IL-6 and iNOS mRNA all were significantly increased. Furthermore, inhibition of NOX alleviated increases in the cytokine mRNA level. Oxidative stress is known to be involved in neuronal death via ERK signaling focal ischemia. We hypothesize that ERK signals are involved in gp91 KO-mediated neuronal protection. At 24 h of reperfusion, there was significantly more ERK phosphorylation in the WT mice than in the Apo and gp91 KO mice.

Conclusions:

1. The brain exhibits post-ischemic temporal patterns of inflammation progress, with minimal inflammation at 3 h and a robust inflammation process at 1 to 3 d of reperfusion.
2. NOX activation contributes to the progress of post-ischemic inflammation and subsequent delayed brain damage.

References:

1. Barone & Feuerstein. J Cereb Blood Flow Metab. 1999, 19:8192: Song et al., J Cereb Blood Flow

Metab. 2007, 27:7643: Bedard & Krause. Physiol Rev. 2007; 87:2454: Walder et al., Stroke 1997; 28: 2252.

539

Brain Oral Session: Neonatal Ischemia

PROLONGED DECREASE IN CEREBRAL BLOOD FLOW FOLLOWING A TRANSIENT SEVERE HYPOXIA IN LATE GESTATION FETAL SHEEP

A. Baburamani[1], E. Yan[2], D. Walker[1]

[1]Physiology, Monash University, [2]National Trauma Research Institute, The Alfred Hospital, Melbourne, VIC, Australia

Background: Transient hypoxic and/or asphyxic episodes are major contributors to brain injury in the developing fetus. Brain regions susceptible to hypoxic injury may associate with the degree of perturbation of regional cerebral blood flow (RCBF) during and after such insults.

Aim: To determine changes of global and RCBF in late gestation fetal sheep where transient systemic asphyxia was induced by complete umbilical cord occlusion (UCO) for 10 min.

Methods: At 124-127 days gestation (term 147 days), fetal sheep underwent surgery for implantation of catheters and the placing of an inflatable cuff around the umbilical cord. UCO (n=4) was induced by inflating the cuff for 10 min, while for control fetuses (n=5) the cuff was not inflated. An ultrasonic crystal probe was placed directly above the sagittal sinus to measure blood flow velocity (SSbfv). Mean arterial blood pressure (MAP) and heart rate (HR) were also measured throughout the experiment. At 130-132 days, differently colored microspheres were injected to determine RCBF at -1, +1, +5, +10, and +24 h with respect to UCO or sham manoeuvre.

Results: During the 10 min UCO, MAP increased and peaked at 2 min and then fell becoming hypotensive, until the cuff was released. Bradycardia was observed for the duration of the UCO. MAP and HR had returned to the basal levels by +30 min. SSbfv followed the changes of MAP during the UCO, but it remained significantly below normal values for up to +12 h before returning to the pre-UCO level. Before UCO, blood flow to various brain regions was between 200-300 ml/min/100g tissue. UCO significantly decreased blood flow to all brain regions (brainstem, grey matter, white matter, diencephalon, cerebellum, hippocampus, striatum, subventricular white matter) at +1 h, +5 h and +10 h post-UCO. The greatest falls of RCBF occurred in the midbrain, frontal and occipital cortex (-164%, -155%, -177%, respectively). At 24 h after UCO, blood flow to all brain regions was not different from the pre-UCO (-1 h) values.

Conclusions: A 10 min severe fetal hypoxia induced transient changes in MAP and HR, but prolonged decreases in RCBF for up to 10 h, and significant persistent reduction in SSbfv for up to 12 h following UCO. This study has validated SSbfv as a sensitive and reliable measurement for determining cerebral blood flow when compared to the direct measurement by microspheres. It is unclear if the prolonged decrease of cerebral blood flow is concomitant with depressed cerebral metabolism, or dissociation of cerebral blood flow and metabolism. However, it is notable that it occurs despite recovery of fetal systemic physiological parameters, suggesting that currently-used clinical observations of fetal well-being would not be able to detect the prolonged derangement of cerebral perfusion.

Brain Poster Session: Migraine

ANTIMIGRAINE EFFECTS OF AN L/N-TYPE CA^{2+} CHANNEL BLOCKER CILNIDIPINE IN THE RAT

R. Masuda, J. Hamada, K. Koizumi, J. Yonekura, E. Kitamura, F. Sakai

Department of Neurology, Kitasato University School of Medicine, Sagamihara, Kanagawa, Japan

Objectives: Migraine is a recurrent neurovascular disorder characterized by throbbing headache associated with nausea, vomiting, photophobia and phonophobia. The pathogenesis of migraine is still unclear, but both of trigeminovascular system and cortical spreading depression (CSD) are thought to have some role on the pathogenesis of migraine. At present, some migraine preventive drugs such as valproate, topiramate, amitriptyline and propranol inhibit CSD in rat. On the other hand, cilnidipine is a Ca^{2+} channel blocker with suppressive effects on L- and N-type Ca^{2+} channels. It is known that N type Ca^{2+} channels are localized at the presynaptic terminals of the neurons and some L/N-type Ca^{2+} channel blocker have antinociceptive effect and neuroprotective effect. The aim of this study is to clarify the antimigraine effect of cilnidipine in two types of migraine model rat.

Methods: (For nasociliary nerve (NCN) stimulation model) 5 male Sprague-Dawley rats, weighing 350-500g, were anesthetized with isoflurane, and ventilated mechanically with 30% O2. Parietal cortical blood flow (CoBF) was continuously monitored with the Laser-Doppler flowmeter. The NCN - a cerebrovascular branch of the trigeminal nerve in the rat - was approached from the orbit. NCN was stimulated electrically near its entrance to ethmoidal foramen through a bipolar platinum electrode with an electrical stimulator (2.3 V, 0.5 ms duration, 10 Hz, 30 sec stimulation). CoBF were measured during and after electrical stimulation of NCN under intraperitoneal injection of 2.0 ml saline (control) followed by cilnidipine, (100 μg/kg in 2.0 ml saline).

(For CSD model) A hydrogen electrode was placed in the open parietal cranial window to measure Direct current potential (DCP) after placement of Laser-Doppler flowmeter CSDs were triggered with an application of 1M KCL solution with the volume of 3μl through another open cranial window. DCP and CoBF were measured after application of KCL for 60min under intraperitoneal injection of 2.0 ml saline followed by cilnidipine.

The CoBF data were analyzed by one-way ANOVA and Dunnett's multiple comparisons and CSD data were analyzed by paired-T test.

Results: In NCS stimulation model, CoBF was maximally increased upon electrical NCN stimulation in control. This increase was significantly suppressed after the administration of cilnidipine ($P < 0.05$). In CSD model, cilnidipine significantly attenuated the number of CSD from 6.2 to 5.0 ($P < 0.05$).

Conclusions: Cilnidipine attenuated the blood flow increase upon NCS stimulation and number of CSD after KCl application. It is suggested that L/N-type Ca^{2+} channel blocker might have a potential of antimigraine prophylactic drug.

Reference:

[1] Suzuki N, Fukuda M, Dobashi K, Maruyama S, Kitamura A, Sakai F; J Cereb Blood Flow Metab 21: S249 (2001).

[2] Murakami M, Nakagawasai O, Fujii S, Kameyama K, Murakami S, Hozumi S, Esashi A, Taniguchi R, Yanagisawa T, Tan-no K, Tadano T, Kitamura K, Kisara K; Eur J Pharmacol 419: 175-81(2001).

[3] Yonekura J, Hamada J, Kitamura E, Koizumi K, Masuda R, Fukuda M, Sakai F; Kitasato Med J 38: 81-4(2008).

541

Brain Poster Session: Subarachnoid Hemorrhage

RAF INHIBITION PREVENTS ACTIVATION OF PRO-INFLAMMATORY MEDIATORS IN CEREBRAL ARTERIES AFTER SUBARACHNOID HEMORRHAGE

A. Maddahi, S. Ansar, L. Edvinsson

Clinical Science, Experimental Vascular Research, Lund University, Lund, Sweden

Objective: Late cerebral ischemia that is developed 4-15 days after subarachnoid hemorrhage (SAH) is a major cause of morbidity and mortality (1). Inflammatory mediators have been shown to be involved in the development of cerebral ischemia via activation of the mitogen-activated protein kinase (MAPK) pathway (2). In the present study, we hypothesize that treatment with a specific raf inhibitor will prevent the cerebral ischemia involving suppression of the inflammatory responses.

Methods: SAH was induced by injecting 250 µl autologous blood into the prechiasmatic cistern. Two groups of treated animals were intracisternally injected with a specific raf inhibitor (SB-386023-b) at 6 h or 12 h after the induced SAH. After 48 h the cerebral arteries were harvested and activation of the inflammatory and extracellular matrix-related genes (inducible nitric oxide synthase (iNOS), metalloproteinase 9 (MMP-9), tissue inhibitor of metalloproteinase 1 (TIMP1), interleukin 6 (IL-6) and interleukin-1beta (IL-1ß) and the extracellular signal regulated kinase 1/2 (ERK1/2) were investigated by immunofluorescence staining and real-time PCR. In addition, the CBF was examined by an auto radiographic technique.

Results: The level of MMP-9, TIMP1, iNOS, IL6 and IL-1ß proteins were upregulated in the wall of the basilar artery after SAH. The enhanced expression of MMP-9, TIMP1 and IL-1ß were located in the smooth muscle cells while iNOS and IL6 were located in both smooth muscle cells and endothelium as verified by colocalization studies. In addition, we demonstrated that SAH dramatically increases the phosphorylation level of ERK1/2 in the smooth muscle cells and reduces the cerebral blood flow (CBF) in the rat. In vivo treatment with a raf inhibitor given at 6 h but not after 12 h after SAH prevented the SAH induced upregulation of matrix metalloproteinase (MMPs), proinflammatory cytokines and ERK1/2 proteins and normalized CBF.

Conclusion: Treatment of signal-transduction at 6 h injection with a specific raf inhibitor prevents the enhanced expression of proinflammatory mediators and extracellular matrix-related genes seen after SAH. This suggests a novel approach towards treatment of inflammation associated with SAH.

References:

1. Ansar s, vikman p, Nielsen M, Edvinsson L. Am J Physiol Heart Circ Physiol. 2007 Dec; 293(6):H3750-8. Epub 2007 Sep 14.

2. Dumont, A. S., Dumont, R. J., Chow, M. M., Lin, C. L., Calisaneller, T., Ley, K. F., Kassell, N. F., & Lee, K. S. (2003) Neurosurgery **53,** 123-133; discussion 133-125.

ORAL METHYLPHENIDATE (RITALIN) DISPLAYS HIGH POTENCY TO BLOCK NOREPINEPHRINE TRANSPORTERS: A PET STUDY WITH (S,S)-[11C]MRB IN HEALTHY SUBJECTS

Y.-S. Ding[1], J. Hannestad[2], B. Planeta-Wilson[1], J.-D. Gallezot[1], S.-F. Lin[1], J. Ropchan[1], D. Labaree[1], W. Williams[2], R. Carson[1], C. van Dyck[2]

[1]Diagnostic Radiology, [2]Psychiatry, Yale University School of Medicine, New Haven, CT, USA

Objectives: ADHD is a major psychiatric disorder with onset in childhood that continues into adulthood. The neurochemical mechanisms of ADHD are poorly understood. Methylphenidate (MP, Ritalin), the most commonly used drug for the treatment of ADHD, significantly blocks dopamine (DA) transporters at 60 mg oral dose (Volkow et al., 1998); however, MP binds to the norepinephrine transporter (NET) with a higher inhibitory effect in vitro on NE uptake than on DA uptake (IC_{50} 37.7 vs. 193 nM). We report the first PET imaging study in healthy subjects using (S,S)-[^{11}C]methylreboxetine (MRB), a promising NET ligand, to determine the duration and magnitude of NET occupancy by oral MP.

Methods: For the duration study, 4 scans were performed on 3 days, with subjects receiving placebo or oral MP (40 mg) 75, 150, and 225 min before a scan. For the occupancy study, each subject had 4 PET scans after oral administration of single-blind placebo or MP 2.5 mg, 10 mg, and 40 mg. After injection of ^{11}C-MRB (740 MBq), 2 h list mode data were acquired with the HRRT. Parametric non-displaceable binding potential (BP_{ND}) images were computed using the multilinear reference tissue model (MRTM2) with occipital cortex as the reference region. Regions of interest (ROIs) from the AAL template were analyzed; small regions, such as locus coeruleus (LC), brainstem, hypothalamus, and thalamic subnuclei, were also defined. BP_{ND} and IC_{50} values were estimated.

Results: From the duration study, there was no significant difference in the BP_{ND} values at 75 min compared to 150 or 225 min; thus, we chose 75 min as the timing for the occupancy study. In the occupancy study, BP_{ND} was reduced by MP in a dose-dependent manner in all NET-rich regions. The avg. IC_{50} was 10 mg (range 6-15 mg, across all subjects [n = 6] and all ROIs [9]). At 40 mg MP, complete displacement was observed in LC, raphe and hypothalamus, whereas, 50-70% displacement was achieved in thalamus and its subnuclei.

Conclusions: Oral MP reached peak NET occupancy at approx. 75 min (duration at least 3 hours), occupying NET in a dose-dependent manner. Our data indicate that oral MP significantly blocks NET at clinically relevant doses; more importantly, these results demonstrate an IC_{50} for oral MP at NET (~0.14 mg/kg) comparable to that previously reported at DAT (0.25 mg/kg), strongly suggesting a crucial role of NET in the treatment and pathophysiology of ADHD.

References: Volkow ND, et al., Am J. Psychiatry 155:1325-1331 (1998).

543

Brain Oral Session: Experimental Stroke and Cerebral Ischemia 1

TRANSPLANTATION OF HUMAN NEURAL PROGENITOR CELLS INDUCES AXONAL PLASTICITY IN THE HOST BRAIN AFTER STROKE

R.H. Andres[1], N. Horie[1], G. Sun[1], H. Shichinohe[1], E. McMillan[2], C.N. Svendsen[1,2], B.T. Schaar[1], T.M. Bliss[1], G.K. Steinberg[1]

[1]Department of Neurosurgery and Stanford Stroke Center, Stanford University, Stanford, CA, [2]The Waisman Center, University of Wisconsin - Madison, Madison, WI, USA

Objectives: Cell transplantation therapy using human neural progenitor cells (hNPCs) has emerged as a promising new experimental treatment approach for stroke. However, many questions regarding the mode of action of the transplanted cells remain unanswered. In addition to directly replacing lost cells, transplanted hNPCs might enhance endogenous repair mechanisms that occur after cerebral ischemia. In the present study, we addressed the hypothesis that grafted hNPCs enhance axonal plasticity in the host brain after stroke and tried to elucidate the underlying mechanisms by functionally testing whether hNPCs secrete factors that enhance axonal plasticity in vitro.

Methods: hNPCs derived from the fetal cortex were grown as neurospheres. hNPCs or buffer were transplanted into the ischemic cortex of NIH Nude rats 7 days after distal middle cerebral artery occlusion (dMCAO). Five weeks post-transplantation, animals were injected with the anterograde axonal tracer biotinylated dextran (BDA) into the contralesional cortex and sacrificed 2 weeks thereafter. The extent of axonal sprouting towards the lesioned cortex from the contralateral side was quantified in different brain regions by confocal image analysis.

To investigate the underlying mechanisms of axonal plasticity in vitro, cortical and striatal progenitor cells were isolated from E14 rat embryos and grown as dissociated cultures. Indirect co-culture with hNPCs was performed during days 3-7 in vitro, and immunodepletion studies were carried out with either neutralizing antibodies against vascular endothelial growth factor (VEGF) and thrombospondin (TSP)-1/2, or Slit-neutralizing soluble ROBO-Fc chimeras. Species-matched antibody isotypes were used as controls. Axons were visualized by staining for neurofilament and axonal outgrowth was quantified using automated high-throughput image analysis software.

Results: hNPC-grafted rats showed significantly greater extension of BDA-labeled host axons from the contralateral hemisphere towards the damaged cortex after dMCAO than controls ($p< 0.05$). This finding correlated with neurological recovery in the vibrissae-elicited forelimb placing test ($p< 0.05$).

Indirect co-culture of cortical and striatal progenitor cells with hNPCs resulted in enhanced axonal outgrowth after 5 days in culture ($p< 0.01$). This effect was partially abolished when neutralizing antibodies against VEGF or TSP-1/2 were present ($p< 0.01$). Neutralization of Slit by exposure of the cultures to ROBO-Fc resulted in similar effects ($p< 0.01$).

Conclusions: In sum, our findings suggest that transplanted hNPCs significantly enhance axonal rewiring from the contralesional side after stroke. VEGF, TSP-1/2, and Slit were identified as at least partially responsible mediators of these effects in vitro. Understanding how transplanted hNPCs augment host brain plasticity might help us to improve cell transplantation approaches for stroke.

Brain Poster Session: Neuroprotection

CART INHIBITS NEUROTOXIC EFFECT OF Aβ BY AFFECTING Aβ METABOLISM AND Aβ-INDUCED OXYGEN STRESS IN VIVO AND IN VITRO

Y. Xu[1], L. Zhang[1], F.N. Niu[2], H. Jiang[1]

[1]Department of Neurology, The Affiliated Drum Tower Hospital of Nanjing University Medical School, [2]Department of Neurology, Drum Tower Hospital of Nanjing Medical University, Nan Jing, China

Background and aims: The accumulation and deposition of Amyloid β protein (Aβ) (neuritic plaques) in the brain are the key pathological features of Alzheimer´s disease (AD) even through its mechanism has not been completely understood. β-site amyloid precursor protein cleaving enzyme (BACE1) cleaves the amyloid precursor protein (APP) to promote Aβ generation while neprilysin (NEP) functions as one of the most important Aβ degradation proteases. Current therapeutic guideline on AD includes blocking Aβ overproduction and its neurotoxicity such as oxygen stress. Our previous work indicated that CART (cocaine and amphetamine regulated transcript) had neuroprotection on stroke. The aims of this study are:

1. To further investigate the neuroprotective role of CART on AD through inhibiting neurotoxicity induced by Aβ in vitro and in vivo.
2. To explore a potential mechanism of the neuroprotection by CART.

Methods: Aβ treats primary cortex neurons as an AD model in vitro. B6C3-Tg APP transgenic mouse serves as an AD model (10 months old) in vivo. Then CART or vehicle was injected into mouse lateral ventricles in APP mouse. CART was added into the primary neurons 24h after Aβ treatment 24h. Neuronal viability or neuronal cell death was assayed by MTT or Fluorescence Activated Cell Sorter (FACS) analysis. Learning/memory impairment of the mice was tested by Water maze behavioral test. The levels of mRNAs or proteins from cells and brains were measured by real time PCR or Western blot. Mitochondrial depolarization and reactive oxygen species (ROS) production were measured by fluorescence Microscopy and FACS analysis.

Results: Neuronal survival by MTT after 24 Aβ treatment was higher in CART-treated cultures (0.279±0.039, n=3, each in triplicate) compared to vehicle-treated cultures (0.199±0.029 n=3 in triplicate, $p< 0.05$). Similar results were obtained using FACS analysis. Water maze behavioral test indicated that CART administration shortened the mean escaping latency of the APP mice compared to vehicle-treated mice from 67.91±19.45 to 59.33±17.95 (n=10 per group, $p< 0.05$). CART suppressed mRNA and protein expression of BACE1 and Aβ, while increased expression of NEP in the cortex and hippocampus of APP brain (BACE1 mRNA from 0.215± 0.013 to 0.139±0.019; BACE1 protein from 1.210 ±0.015 to 0.723±0.022; Aβ mRNA from 0.237± 0.022 to 0.119±0.038; Aβ protein from 1.068± 0.122 to 0.661±0.093; NEP mRNA from 0.579±0.028 to 0.721±0.013; NEP protein from 0.059±0.014 to 0.075±0.034. $p< 0.05$). Finally, CART reduced Mitochondrial depolarization and ROS induced by Aβ (from 5806.33±51.67 to 4999±22.73, $p< 0.05$).

Conclusions: The findings suggest that CART is an important neuroprotectant against neurotoxicity induced by Aβ in vitro and in vivo. The mechanism of this neuroprotection is in part linked to reducing overproduction by affecting on generation, degradation of Aβ and blocking oxygen stress toxicity of Aβ. Thus, CART and its mechanism of action may serve as a novel therapeutic strategy against AD-related brain damage.

References: Role of cocaine- and amphetamine-regulated transcript in estradiol-mediated neuroprotection. Xu Y, Zhang W, Klaus J, et al. Proc Natl Acad Sci U S A. 2006 Sep 26;103(39):14489-94. Epub 2006 Sep 13.

MONITORING OF INTRA-ARTERIALLY ADMINISTERED BONE MARROW MONONUCLEAR CELLS IN RAT TRANSIENT FOCAL ISCHEMIA MODEL USING MRI

N. Kamiya[1], M. Ueda[1], H. Igarashi[2], Y. Nishiyama[1], S. Suda[1], Y. Katayama[1]

[1]Department of Internal Medicine, Devision of Neurology, Nippon Medical School, Tokyo, [2]Center for Integrated Human Brain Science, Brain Research Institute, University of Niigata, Niigata, Japan

Background and aims: We had reported that transplantation of bone marrow mononuclear cells (BMMCs) via carotid artery, but not via femoral vein immediately after reperfusion had neuroprotective effect in rat transient ischemic model. We revealed the difference of the protective effect determined by the number of the cells in brain at the acute stage of ischemia. To reveal the mechanisms of neuroprotective effect, the present study was designed to monitor the distribution of transplanted BMMCs in brain in process of time on rat transient focal ischemia model. It is impossible to monitor cells histologicaly on one rat in time course, because we need to euthanize rat to make brain slices. Using MRI system, we can scan brain and monitor administrated cells repeatedly.

Methods: 12 Male Sprague-Dawley rats, weighing 250-300g, were used in the study. Bone marrow was obtained autologously from the right femur of each animal, and BMMCs were isolated prior to ischemia using density-gradient centrifugation method. BMMCs were labeled with SPIO (super paramagnetic iron oxide) using electroporation method. Rats were then subjected to transient (90 min.) left middle cerebral artery (MCA) occlusion followed by 1x 10^7 BMMCs administration via the ipsilateral carotid artery (IA group) immediately after reperfusion. Control rats underwent the same procedure but received vehicle injection (Vehicle group). At 1 hour, 24 hours and 7 days after reperfusion, we underwent MRI study (3d gradient T2*) on every rats. After the final MRI, rats were decapitated and brains were carefully removed. Paraffin-embedded brain blocks were cut into 20 μm-thick coronal sections at 2 mm intervals to obtain six slices. Sections were stained with Berlin Blue to identify iron of transplanted cells and with hematoxylin and eosin (HE) to measure infarct volume.

Results: SPIO labeled BMMCs showed negative contrast enhancement in MRI corresponding to histological finding. Administrated cells distributed over the left MCA perfusing lesion at 1hr (figure) and decreased in process of time. Infarct volume significantly reduced in IA group than vehicle group. MRI study also revealed that administered cells were distributed within the ipsilateral hemisphere at 1hr, and that the cells were decreased in number thereafter. BMMCs tended to accumulate around ischemic lesion.

Conclusions: The present study established in vivo monitoring of transplanted SPIO-labeled BMMCs using MRI in process of time. The present data confirm significant neuroprotection following transient focal ischemia by autologous BMMCs administered intra-arterially, immediately after reperfusion in rats.

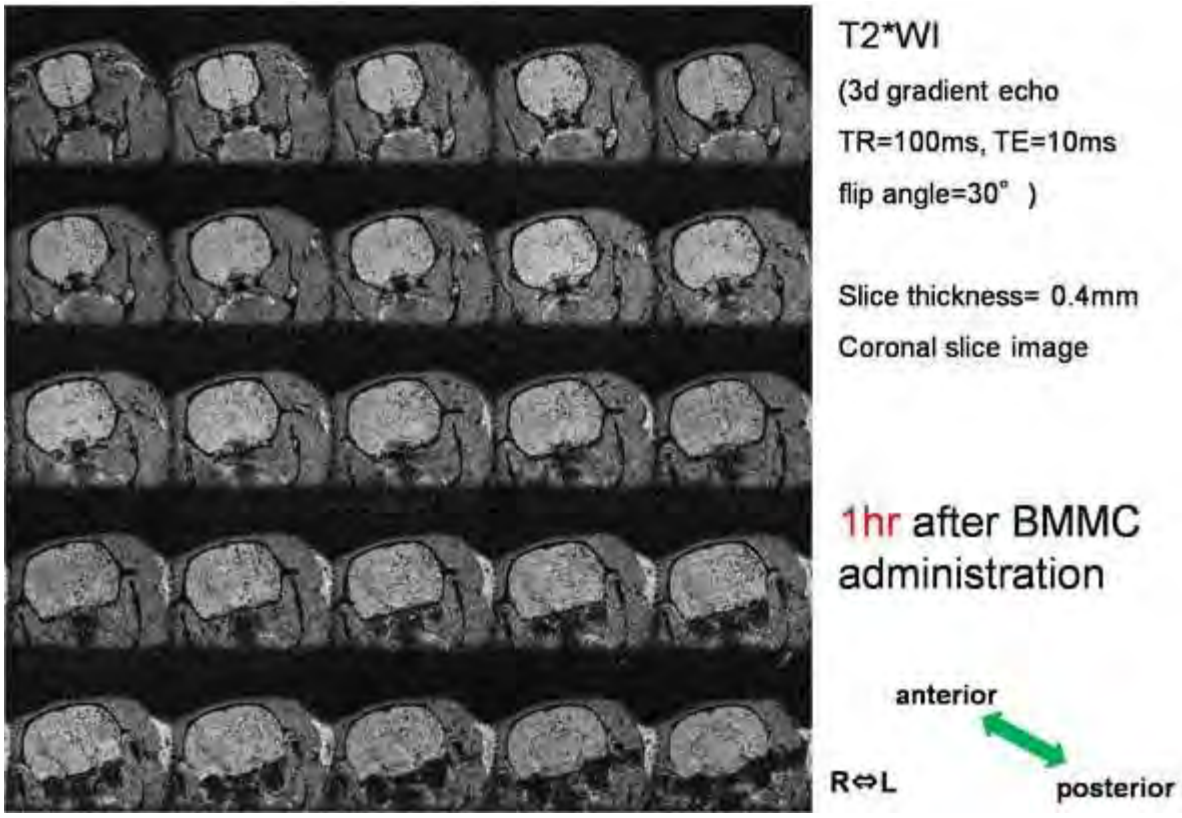
T2*WI
(3d gradient echo
TR=100ms, TE=10ms
flip angle=30°)
Slice thickness= 0.4mm
Coronal slice image
1hr after BMMC administration
anterior
R⇔L
posterior

[figure]

546

Brain Poster Session: Cerebral Vascular Regulation

ROLE OF ENDOTHELIN IN IMPAIRED RESPONSES OF CEREBRAL ARTERIOLES DURING TYPE 1 DIABETES MELLITUS

D. Arrick, G. Sharpe, H. Sun, W. Mayhan

Cellular/Integratvie Physiology, University of Nebraska Medical Center, Omaha, NE, USA

Previous studies have suggested that endothelin-1 may contribute to vascular abnormalities during a variety of disease states, including Type 1 diabetes mellitus. Endothelin-1 may contribute to structural and functional abnormalities of the blood vessels, and may also regulate the expression of other growth factors and cytokines to influence vascular function. However, there is a lack of information regarding the precise role of endothelin-1 in altered NOS-dependent responses of cerebral arterioles during Type 1 diabetes. Thus, our goal was to determine whether acute inhibition of endothelin-1 receptors (BQ-123) could influence NOS-dependent responses of cerebral arterioles in diabetic rats. We measured diameter of pial arterioles in nondiabetic and diabetic (STZ; 50 mg/kg) rats in response to eNOS- and nNOS-dependent (ADP and NMDA) and -independent (nitroglycerin) agonists before and during treatment with BQ-123. In addition, we measured superoxide production by cerebral cortex tissue obtained from nondiabetic and diabetic rats. We found that eNOS- and nNOS-dependent dilation of pial arterioles was impaired in diabetic compared to nondiabetic rats. In addition, treatment with BQ-123 restored impaired responses of cerebral arterioles in diabetic rats towards that observed in nondiabetic rats. Further the production of superoxide anion by cortex tissue was increased in diabetic rats when compared to nondiabetic rats. We suggest that endothelin-1 may contribute to impaired responses of cerebral arterioles during Type 1 diabetes. We speculate that endothelin receptor antagonism may be a potential therapeutic tool for the treatment of cerebrovascular dysfunction observed in diabetic subjects.

K3 IMAGING OF [11C]PIB PET USING THE THREE-PARAMETER ESTIMATION IN THE SHORT SCAN-TIME (TPESS) METHOD

H. Shimada[1,2], K. Fukushi[3], K. Sato[1], H. Shinotoh[1], M. Miyoshi[1], S. Hirano[1], N. Tanaka[1], T. Ota[1], H. Ito[1], S. Kuwabara[2], T. Irie[3], T. Suhara[1]

[1]Department of Molecular Neuroimaging, Molecular Imaging Center, National Institute of Radiological Sciences, [2]Department of Neurology, Chiba University, [3]Molecular Probe Group, Molecular Imaging Center, National Institute of Radiological Sciences, Chiba, Japan

Background and aims: Quantitative analysis of amyloid imaging agents may be necessary for assessment of the longitudinal changes in amyloid deposition and effects of anti-amyloid therapy on brain amyloid deposition in patients with Alzheimer's disease (AD). The 2-tissue compartment 4-parameter (2T-4k) model analysis of reversible ligands, however, needs long scanning period such as 90 to 120 min. It is often difficult to perform PET scans without head movements in such long scanning period and measure the plasma input function accurately with carbon-11 labeled ligands, resulting in unstable and inaccurate estimates of parameters. In [11C] PIB PET, our simulation study showed that the brain time activity curve is almost independent on k4 during the first 30 min, and thus k3, the bimolecule association rate (konBmax, min-1), could be estimated in the first 30 min by three-parameters model analysis excluding k4 parameter. Deliberately ignoring k4 stabilizes k3 estimates in the first 30 min. Here we call this method as the three-parameter estimation in the short scan-time (TPESS) method. In this study, we compared the TPESS method with the conventional 2T-4k model analysis by making k3 images in both methods.

Methods: Participants were 12 patients with AD (mean age: 70.0 +/- 9.6 years; male/female: 5/7; MMSE: 20.2 +/- 4.2) and age-matched 11 healthy controls (mean age: 65.2 +/- 12.4 years; male/female: 3/8; MMSE: 28.0 +/- 2.2). A dose (about 370 Mq) of [11C]PIB was intravenously injected and sequential PET scans were performed for 90 min with arterial blood sampling. Kinetics of [11C]PIB in 90 min were analyzed using the 2T-4k compartment model analysis and the TPESS method, in which the scan duration for analysis was shortened to 30 min. K3 values, an index of amyloid deposition, were compared between AD group and healthy control group in both methods, and SPM5 analysis was performed.

Results: There was the extensive increase in k3 values in AD compared with normal controls both in the 2T-4k model analysis and the TPESS method ($p < 0.01$, FDR corrected). The increase in k3 was more extensive and significant in the TPESS method. Mean cortical k3 values in control and AD groups were 0.0238 +/- 0.0077 and 0.0414 +/- 0.0273 in the 2T-4k model analysis, and 0.0125 +/- 0.0034 and 0.0263 +/- 0.0089 in the TPESS method respectively.

Conclusions: The TPESS method yields similar SPM analysis results as in 2T-4k compartment model analysis. This TPESS method is timesaving and thus applicable to clinical AD research.

ACUTE NICOTINE EFFECTS ON THE DISTRIBUTION OF NICOTINE α4β2 AND DOPAMINE D2/D3 RECEPTOR PET RADIOTRACERS

J. Mukherjee, K. Kasabwala, R. Kant, S. Pandey, C. Constantinescu, R. Coleman, M.-L. Pan, P. Parekh

Psychiatry and Human Behavior, University of California-Irvine, Irvine, CA, USA

Objectives: Nicotine, a major constituent in tobacco exhibits addictive properties by virtue of its interaction with nicotinic receptors (nAChR) including the α4β2 subtype. This interaction releases dopamine in the striatum. Using PET radiotracers for α4β2 nAChR (^{18}F-nifene) and dopamine D2/D3 receptors (^{18}F-fallypride (FP) and ^{18}F-desmethoxyfallypride (DMFP)) we have evaluated acute effects of nicotine in rodents using MicroPET on the two receptor systems.

Methods: Imaging was done using an Inveon MicroPET scanner. ^{18}F-Nifene, ^{18}F-FP and ^{18}F-DMFP were synthesized as previously reported. Sprague Dawley rats (400-600 g) anesthetized with isoflurane were used for PET studies. Radiotracers (0.8 to 1 mCi) were given iv. Test-retest was carried out to evaluate reproducibility. Rats were imaged for 90 mins (for ^{18}F-nifene and ^{18}F-DMFP) and 150 mins (for ^{18}F-FP) and binding potential (BP_{ND}) were measured. Post-^{18}F-nifene nicotine challenge (0.3 mg/kg, free base) was used to measure reversibility and nicotine occupancy was measured using various doses (0.02 to 0.50 mg/kg) injected 15 mins before ^{18}F-nifene. Nicotine (0.3 mg/kg) was coinjected with ^{18}F-FP and ^{18}F-DMFP to measure potential dopaminergic effects. Data was analyzed using ASIPRO and PMOD. For ex vivo studies, animals were sacrificed for autoradiographic analysis of brain sections using Optiquant imaging system.

Results: ^{18}F-Nifene binding to thalamic and other brain regions was consistent with the α4β2 nAChR distribution. Test-retest values for the thalamus varied less than 5% (BP_{ND} =1.30, n=3 rats, using reference cerebellum (CB)), confirming reliability of ^{18}F-nifene binding. Post-injection of nicotine (0.3 mg/kg, +30 min) rapidly displaced specifically bound ^{18}F-nifene indicating >90% occupancy. Low dose nicotine (0.02 mg) reached about 50% occupancy. ^{18}F-FP binding to D2/D3 receptors gave BP_{ND} values of dorsal striata (DST)=15; ventral striata (VST)=11; and with nicotine values were 20 and 12.5, respectively. ^{18}F-DMFP binding to D2/D3 receptors in striata (ST) gave BP_{ND} of 1.8 (without nicotine) and 2.9 (with nicotine). Ex vivo studies revealed similar effects in the case of ^{18}F-FP, while ^{18}F-DMFP binding exhibited ≈20% reduction (0.5 mg/kg nicotine) in VST when internal capsule as reference.

Conclusions: Nicotine dose-dependently occupies α4β2 nAChR and saturates receptors at 0.3 mg/kg. Although little or no effect on cerebral blood volume or flow to the ST by nicotine has been reported (Gozzi et al., 2006; Tanabe et al., 2008) delivery of dopamine D2/D3 receptor tracers, ^{18}F-FP and ^{18}F-DMFP to ST was significantly increased, with a net increase in measured BP_{ND}. Nicotine has been shown to marginally increase dopamine levels in the nucleus accumbens and other brain regions (Shearman et al., 2008) and therefore the increase in delivery and BP_{ND} is unlikely due to greater D2/D3 receptor availability. Recently, ^{18}F-FP has been used in heavy smokers and a small decrease in D2/D3 receptor availability was observed in the putamen. Further analyses are underway to delineate the effect of nicotine on ^{18}F-FP and ^{18}F-DMFP.

References:

1. Gozzi A, et al., Neuropsychopharm., 31: 1690-1703 (2006).

2. Shearman E., et al., Brain Res. Bull., 76:626-639 (2008).

3. Tanabe J, et al., Neuropsychopharm., 33:627-633 (2008).

4. Fehr C, et al., Am. J. Psychiatry, 165:507-514 (2008).

Research Supported by NIH R01 AG029479 and R01EB006110.

EVALUATION OF SENSITIVITY OF KINETIC MACRO-PARAMETERS TO CHANGES IN [^{18}F]FLUORODOPAMINE STORAGE AND METABOLISM IN THE STRIATUM

K. Matsubara[1,2], H. Watabe[2], Y. Ikoma[1,2], T. Hayashi[2], K. Minato[1], H. Iida[2]

[1]Lab. of Technology of Radiological Science, Nara Institute of Science and Technology, Ikoma,
[2]Department of Investigative Radiology, National Cardiovascular Center, Suita, Japan

Objectives: Dopa utilization and dopamine retention in the striatum can be investigated by [^{18}F]F-dopa PET study. [^{18}F]fluorodopamine synthesized from [^{18}F]F-dopa is stored in the intracellular vesicles or metabolized to [^{18}F]FDOPAC and [^{18}F]FHVA, which can diffuse out of brain tissue. In other hand, several approaches has been proposed to analyze [^{18}F]F-dopa PET data to obtain kinetic macro-parameters such as K, V_d, and k_{loss} which represent the net kinetics of [^{18}F]F-dopa as above [1, 2].

It was reported that reduction for dopamine storage and acceleration for dopamine metabolism to DOPAC and HVA occur in brain of patients with Parkinson's disease [3, 4]. According to these findings, we hypothesized that the parameter sensitive to the storage reduction and metabolic acceleration might be a good index for diagnosing Parkinson's disease. For the evaluation of sensitivity for estimated macro-parameter to change for dopamine storage and metabolism, we simulated the tissue time-activity curves (TACs) under variable change in dopamine storage or metabolism using a model describing the detail pathway of dopamine kinetics in tissue involving storage to the vesicle and metabolism to DOPAC and to HVA (Figure). We estimated macro-parameters from these TACs by conventional analytical methods and evaluated sensitivity of these parameters.

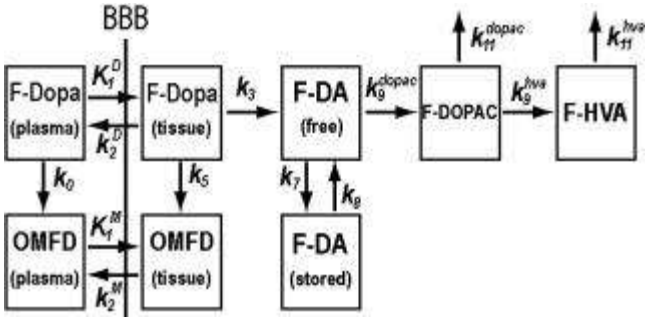

[Figure: model with the detail pathway]

Methods: First, we generated a standard TAC as normal condition, which mimics actual striatal TAC obtained by 120 min [^{18}F]F-dopa PET scan in normal monkey (macaca fascicularis, body weight:3.8 kg). Input function for F-dopa and OMFD obtained from blood sampling and metabolite analysis were used. Second, we simulated TACs with increasing or decreasing rate constants for dopamine storage (k_7) or metabolism to DOPAC (k_9^{dopac}). Third, simulated TACs were analyzed by conventional graphical analysis, Patlak and Logan analysis, and multilinear method proposed by Kumakura et al. [2]. Finally, for evaluation of sensitivity, difference between macro-parameters for a standard and altered TAC, which is defined as %change, were calculated.

Results: In case to decrease k_7 or increase k_9^{dopac}, %change of k_{loss} estimated by the multilinear

method was the largest among the macro-parameters (64.4 % for k_{loss} and 21.6 - 37.2 % for other parameters in case that k_7 decrease by 80% to standard condition).

Conclusion: Our results suggest that k_{loss} estimated by the multilinear analysis has better performance to detect changes in dopamine storage and metabolism sensitively than other macro-parameters. These findings agree with those in previous clinical study in Parkinson's disease [2, 5].

References:

[1] Martin, W. R., et al., 1989, Ann. Neurol. 26, 535-542.

[2] Kumakura, Y., et al., 2006, J. Cereb. Blood Flow Metab. 26, 358-370.

[3] Lotharius, J. and Brundin, P., 2002, Hum. Mol. Genet. 11, 2395-2407.

[4] Pifl, C. and Hornykiewicz, O., 2006, Neurochem. Int. 49, 519-524.

[5] Kumakura, Y., et al., 2005, J. Cereb. Blood Flow Metab. 25, 807-819.

Brain Poster Session: Neuroprotection: Hypothermia

THE EFFECT OF FNK PROTEIN AND HYPOTHERMIA COMBINED THERAPY ON RAT FOCAL BRAIN ISCHEMIA MODEL

M. Sakurazawa[1], K. Katsura[1], M. Saito[1], S. Asoh[2], S. Ohta[2], Y. Katayama[1]

[1]Department of Internal Medicine, Division of Neurology, Nephrology and Rheumatology, Nippon Medical School, Tokyo, [2]Department of Biochemistry and Cell Biology, Institute of Development and Aging Sciences, Nippon Medical School, Kawasaki, Japan

Objective: We previously reported that PTD-FNK protein has a strong neuroprotective effect on rat focal brain ischemia models[1)]. FNK protein is derived from antiapoptotic protein Bcl-x_L by substituting three amino acids artificially and thereby gains a higher anti cell death activity. FNK protein was fused with PTD (protein transduction domain) of the HIV/Tat protein to be able to pass through cell membranes and it was shown to be transduced to neuronal cells rapidly. The aim of this study is to investigate the effect of PTD-FNK protein and hypothermia combined therapy on cerebral infarction.

Methods: Eight-week-old SD rats were subjected to a 90min middle cerebral artery occlusion (MCAO). Focal ischemia was produced by intraluminal occlusion of the left MCA with a nylon monofilament. Rats were divided into 4 groups:

1. 37°C Vehicle administration,
2. 37°C PTD-FNK administration,
3. 35°C Vehicle administration, and
4. 35°C PTD-FNK administration.

PTD-FNK protein was intravenously administered 60min after the induction of MCAO. Hypothermia (35°C) was applied during 90min MCAO. At 24hr after MCA occlusion, the brain was removed and sliced into six coronal sections. All six sections were stained with 3% of 2,3,5-triphenyltetrazolium chloride and the volume of infarction was measured.

Results: Infarct volumes were significantly reduced in groups of 2) (142.5±49.1mm^3), 3) (81.5±35.0mm^3) and 4) (77.2±60.9mm^3) against group 1) (190.6±50.4mm^3). We failed to find significant difference of infarct volumes between group 3) and 4).

Conclusions: In this study we failed to show an additional protective effect with PTD-FNK protein administration compared to hypothermia alone therapy. If the hypothermia therapy is enough protective as shown in this study, it may be hard to get additional protective effect with additional therapy. Besides, possibility of reduced transduction of PTD-FNK into neuronal cells during hypothermia might influence the results.

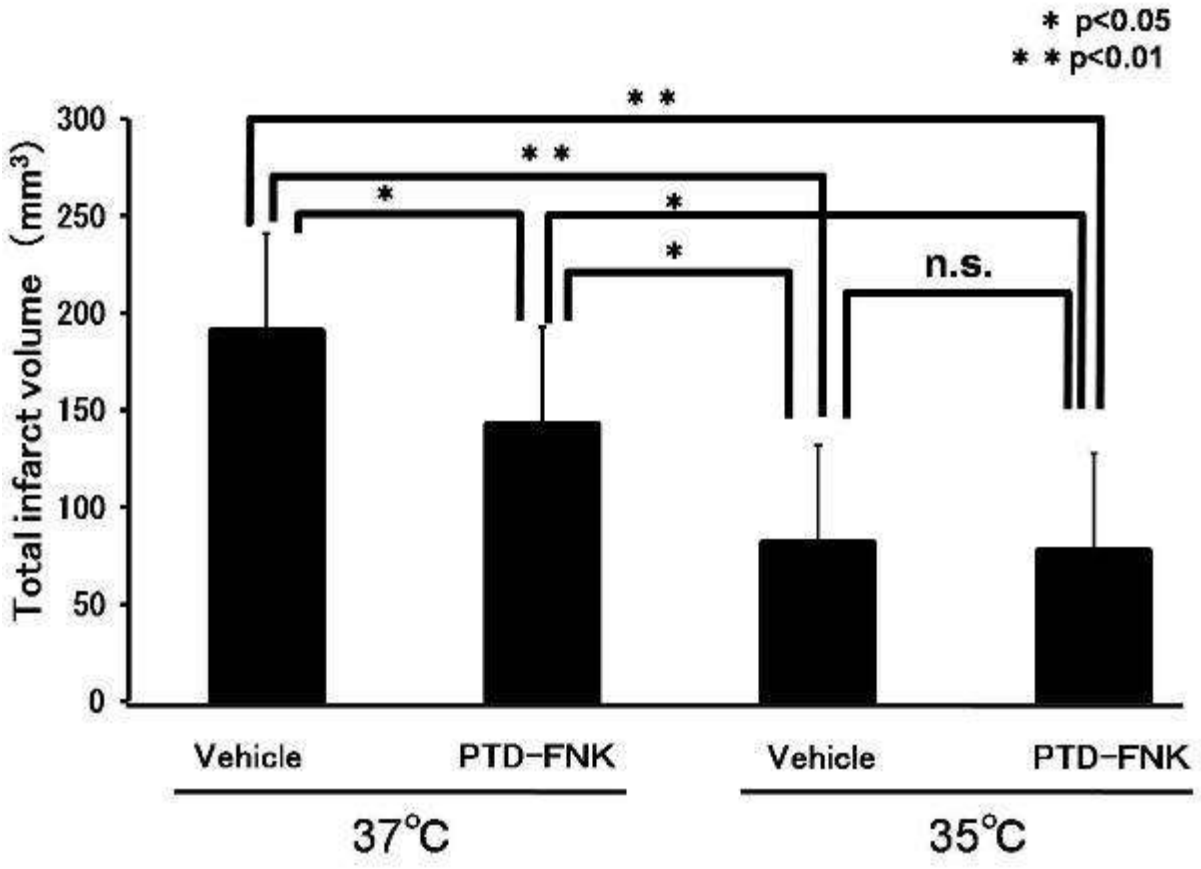

[figure1]

Reference: 1) J.Neurochem. (2008) 106, 258-270.

553

Brain Poster Session: Neuroprotection

NEUROTOXIC ROLES OF MICROGLIAL NF-KAPPAB AND $P2Y_{12}$ IN AN IN VITRO ISCHEMIA MODEL

C. Webster[1], H. Ma[1], R. Giffard[2], **M. Yenari**[1]

[1]Neurology, UCSF-SFVAMC, [2]Anesthesia and Neurosurgery, Stanford University School of Medicine, San Francisco, CA, USA

Following cerebral ischemia insults, microglia, brain immune cells, have been shown to become activated, initiating a complex inflammatory cascade via the key inflammatory player, nuclear transcription factor kappa B (NFkappaB), which plays a dual role in neuroprotection as well as exacerbating neurotoxicity. There is evidence that NFkappaB is activated by extracellular nucleotides, which have been shown to be generated by cells following necrotic insults such as ischemia. Here, we aim to establish the role of microglial NFkappaB as neurotoxic or neuroprotective following the in vitro ischemic model, oxygen glucose deprivation (OGD). Furthermore, $P2Y_{12}$, a G-protein coupled purinergic receptor that is activated by extracellular ATP or ADP, also the target for the anti-coagulant drug clopidogrel, has been shown to be involved in microglial chemotaxis following injury, and may activate NFkappaB via the G-protein coupled PKC pathway. Thus, we investigate the role of $P2Y_{12}$ in microglial migration and neuron cell death following OGD. To determine the role of microglia following in vitro ischemia, we co-cultured microglial cells or primary microglia with neurons and astrocytes (1:10:10) or microglia plus neurons (1:10), as well as astrocyte/neuron (1:1) and neuron only mixtures, and subjected these mixed cell cultures to OGD and reperfusion (as previously described) or control conditions, and measured neuron viability via MAP-2 ELISA. When microglial cells (either BV2 or primary) were co-cultured with both astrocytes and neurons, they increased neuron cell death following OGD two-fold ($n=6$, $p< .05$) relative to cultures of neurons alone, neuron/astrocyte, neuron/microglial cells, or no OGD controls. We also show that knocking down either NFkappaB (p65 or p50) or $P2Y_{12}$ in microglial cells, via siRNA transfection, significantly protected neurons in the triple culture model (neurons, BV2, astrocytes) following OGD compared to control triple cultures exposed to OGD ($n=6$, p50 $p< .05$, p65 $p< .05$, $P2Y_{12}$ $p< .05$). Furthermore, microglial cells in the triple cultures formed clusters around neurons and astrocytes following OGD with a four fold higher cluster score compared to their no OGD controls ($n=6$, NFkappaB p65 $< .01$, $P2Y_{12}$ $p< .01$). This data taken together suggests that astrocytes are required for microglial mediated neuron cell death following in vitro ischemia, and that the NFkappaB pathway in microglia, which seems to involve the purinergic receptor $P2Y_{12}$, significantly contributes to microglial migration toward injured neurons, and neurotoxicity in this model.

EFFECT OF PLANT EXTRACTS ON ISCHAEMIA AND REPERFUSION INDUCED CEREBRAL INJURY

R. Shri, K.S. Bora, S. Arora

Phamaceutical Sciences and Drug Research, Punjabi University, Patiala, India

Stroke is the third leading cause of death (1,2).

Stroke is the rapidly developing loss of brain functions due to a disturbance in the blood vessels supplying blood to the brain. This can be due to ischemia or due to a hemorrhage.

Ischemic stroke is a syndrome characterized by rapid onset of neurological injury due to interruption of blood flow to the brain (3). Free radicals have been implicated in cerebral ischemia and reperfusion-induced neuronal injury (4, 5). Levels of antioxidant enzymes fall during ischemia while free radical production increases during reperfusion. Many synthetic anti-oxidants have shown neuroprotective effect in ischemia and reperfusion-induced cerebral injury (6, 7). Naturally occurring plant contents such as phenolic compounds, carotenoids, ascorbic acid, thiols, and tocopherols have also shown anti-oxidant activity (8, 9).

Objective: The present study has been designed to investigate the neuroprotective effect of extracts of two plants possessing antioxidant activity viz Allium cepa and Ocimum basilicum on Ischemia and Reperfusion induced cerebral ischemia in Swiss albino mice.

Methods: Global cerebral ischemia was induced by bilateral carotid artery occlusion for 10 min followed by reperfusion for 24 h (10). Cerebral infarct size was estimated using triphenyltetrazolium chloride (TTC) staining (11). Elevated plus maze was employed to estimate short term memory. Degree of motor incoordination was evaluated using inclined beam walking test. Mitochondrial Thiobarbituric acid reactive substances (TBARS) assay was employed as an index for oxidative stress.

Results: Global cerebral ischemia followed by reperfusion produced a significant impairment in short term memory, motor coordination and a significant increase in TBARS. Pretreatment with methanolic extract of outer scales and edible portion of A.cepa (100 and 200mg/kg, p.o.) and methanolic and ethyl acetate extracts of leaves of O.basilicum (100 and 200mg/kg, p.o.) reduced cerebral infarct size, attenuated impairment in short term memory and motor coordination along with a marked decrease in mitochondrial TBARS. The effect was more significant with methanolic extract of outer scales of A.cepa and ethyl acetate extract of leaves of O.basilicum.

Conclusions: Pretreatment with test extracts may scavenge reactive oxygen species and consequently attenuate ischaemia and reperfusion induced cerebral injury.

References:

1) Whisnant JP. Stroke 1984;15:160.

2) Del Zoppo GJ, Wagner S, Tagaya M. Drugs 1997;54:9.

3) Baker K, Marcus CB, Hirffman K, Kruk H, Malfory B, Doctrow SR. J Pharmacol Exp Ther 1998;284:215.

4) Gilgun-Sherki Y, Rosenbuam Z, Melamed E, Offen D. Pharmacol Rev 2002;54:271.

5) Globus M, Alonsa O, Dietrich WD, Busto R, Ginsbeg MD. J Neurochem 1995;65:1704.

6) Horakova L, Ondre Jickova O, Bachrata K, Vajdova M. Gen Physiol Biophys 2000;19:195.

7) Iwashita A, Maemot T, Nakada H, Shima I, Matsuoka N, Hisajima H. J Pharmacol Exp Ther 2003;307:961.

8) Yang J, Meyers KJ, Heide JV, Liu RH. J Agric Food Chem 2004;52:6787.

9) Ames BN, Shigenaga MK, Hagen TM. Proc Natl Acad Sci U S A 1993;90:7915.

10) Himory N, Watanabe H, Akaike N, Kurasawa M, Itoh J, Tanaka Y. J Pharmacol Methods 1990;23:1117.

11) Bochelen D, Rudin M, Sauter A. J Pharmacol Exp Ther 1999;288:653.

Brain Poster Session: Inflammation

FAS LIGAND MEDIATED ACTIVATION OF NF-KB AND MIR-155 PATHWAY IN EXPERIMENTAL ISCHEMIA

X. Zhang[1], Y. Xu[1], F.N. Niu[2]

[1]Department of Neurology, The Affiliated Drum Tower Hospital of Nanjing University Medical School, [2]Department of Neurology, Drum Tower Hospital of Nanjing Medical University, Nan Jing, China

Background and aims: Inflammatory response accompanying apoptosis is one of the main pathological changes in ischemic brain injury. CD95 (Fas) and its natural ligands, CD95 ligand (Fasl), is involved in the pathological effect. Previous studies indicated that Fas ligation was a major cause of secondary inflammatory reaction in the penumbra after stroke through the activation of nuclear factor kB (NF-kB). MiR-155 is a NF-kB depend small non-coding RNAs whose target gene might be TNF-α. The activation by TNF-α leads to apoptosis and inflammation which form a lethal threshold and course neuron cell to die in penumbra. Fasl mutation mice (gld mice) were strongly resistant towards stroke-induced damage. However, its mechanism has not been completely understood. The aim of this study is to explore wether a potential mechanism of the neurotoxicity by Fasl is through activation of the NF-kB and miR-155 pathway. Deficiency of Fasl and its reaction in stoke may serve as a novel therapeutic strategy for stroke.

Methods: Gld and wild type (WT) mice were subjected to 2 hours MCAO and sacrificed at 24 hours of reperfusion. Brains were then removed, stained with 2,3,5-triphenyltetrazolium chloride (TTC) for infarct size measurement or dissected and quickly frozen for real time PCR and western blot analysis. In the in vitro model of neuronal oxygen-glucose deprivation (OGD), we pretreated neuron with MG-132, an inhibitor of NF-kB. Real-time PCR of miR-155 were performed according to standard protocols. The protein expression of TNF-α was assayed by Western blot.

Results: In vivo, total infarct size at 24 hours after MCAO in gld mice (15.02±5.22%) was significantly smaller than WT mice (24.19±5.59%, n=6 per group, $p< 0.05$). Real time PCR revealed that the miR-155 and TNF-α were down-regulated in the cortex of brain in gld mice compared to that of WT mice at 24 hours after MCAO (miR-155 decreased by 0.75±0.04 fold as compared to WT mice, TNF-α decreased from 1.15±0.13 to 0.80±0.04, $p< 0.05$). In vitro, neuronal viability after 24 hours were also significantly higher in gld (40.07±9.85%, n=3 in triplicate) than WT neurons (24.95±7.89%, n=3 in triplicate, $p< 0.05$), and miR-155 and TNF-α were also down-regulated in gld neuronal cell as in vivo. However, the levels of miR-155 remained unchanged following OGD treatment if pretreated with MG-132, suggesting that miR-155 was clearly dependent on the level of NF-kB activity. Furthermore, pretreatment with anti-miR-155 resulted in decreased expression of TNF-a in primary neurons after OGD in WT but not gld animals.

Conclusions: Our results indicated that deficiency of FasL inhibited the secondary inflammatory injury of stroke-related damage through the regulation of NF-kB and miR-155. These results offer new approaches in stroke treatment.

References:

1. Jia J, Guan D, Zhu W, et al. Estrogen inhibits fas-mediated apoptosis in experimental stroke. Exp Neurol. 2009, 215(1):48-52.

2. Jeyaseelan K, Lim KY, Armugam A. MicroRNA expression in the blood and brain of rats subjected to transient focal ischemia by middle cerebral artery occlusion. Stroke. 2008,39(3):959-966.

557

Brain Poster Session: Subarachnoid Hemorrhage

EFFECT OF CLAZOSENTAN ON MICROTHROMBOSIS AFTER EXPERIMENTAL SUBARACHNOID HEMORRHAGE

G. Chen, J. Ai, **R.L. Macdonald**

Neurosurgery, St. Michael's Hospital, University of Toronto, Toronto, ON, Canada

Background: Although clinical studies suggest clazosentan, a synthetic endothelin A receptor (ET_A) antagonist, attenuates development of cerebral vasospasm after subarachnoid hemorrhage (SAH), its effect on the secondary pathophysiological changes after SAH has not yet been investigated. Accumulating evidence has demonstrated that SAH-induced microthrombosis plays a role in the pathogenesis of delayed cerebral ischemia after SAH. To date, however, few studies focused on treatment of microthrombosis after experimental SAH.

Purpose: The purpose of this study was to determine the impact of clazosentan on the microthrombi formation after SAH in rats.

Methods: Adult male Sprague Dawley rats were divided into four groups:

1. control saline injected group (n = 6);
2. SAH group (n = 6);
3. SAH + vehicle group (n = 8) and
4. SAH + clazosentan group (n = 8).

SAH was induced by injection of 0.3 ml fresh arterial, non-heparinized blood into the prechiasmatic cistern over 20 seconds with a syringe pump. In SAH + clazosentan group, clazosentan was administered as an intravenous bolus of 1 mg/kg 1 hour after SAH and maintained at a constant infusion of 1 mg/kg/h with osmotic pump via the jugular catheter for 7 days. Brain samples were excised after perfusion fixation for further determinations at 7 days after SAH. Cross-sectional area of middle cerebral artery, basilar artery, and anterior cerebral artery was measured. Microthrombosis was evaluated by hematoxylin and eosin and fibrin (ogen) immunostaining.

Results: Clazosentan prevented vasospasm 7 after SAH ($p < 0.01$). The number of microthrombi was significantly higher in both cerebrum and cerebellum 7 days after SAH in the SAH and control SAH + vehicle groups ($p < 0.01$). Clazosentan decreased formation of microclots in this SAH model, and the number of microthombi-rich animals was decreased significantly in SAH + clazosentan group compared with SAH or SAH + vehicle groups ($p < 0.01$).

Conclusion: Clazosentan attenuated cerebral vasospasm and alleviated the microthrombosis in the late phase of SAH in this prechiasmatic blood injection SAH model.

558

Brain Poster Session: Subarachnoid Hemorrhage

ALTERATION IN VOLTAGE-DEPENDENT CALCIUM CHANNELS IN DOG BASILAR ARTERY AFTER SUBARACHNOID HEMORRHAGE

R.L. Macdonald, E. Nikitina

Neurosurgery, St. Michael's Hospital, University of Toronto, Toronto, ON, Canada

Background and aims: It is widely believed that nimodipine does not decrease vasospasm after subarachnoid hemorrhage (SAH), despite the prominent role of voltage-dependent calcium channels (VDCC), which it blocks, in contracting cerebral arteries. VDCC in large cerebral arteries have never been characterized, however, to determine why this is.

Methods: We characterized VDCC currents in smooth muscle cells from normal basilar artery and compared them to currents from cells obtained during vasospasm 7 days after SAH in dogs (n=14-17 dogs per group). Whole cell currents were evoked by step-depolarizations from holding potential (V_h) of -50 or -90mV in 10mM barium.

Results: Depolarization from V_h=-90mV revealed currents with features of high (HVA, classically L-type) and low-voltage activated (LVA, classically T-type) VDCC with 25 of 147 cells having LVA current forming more than 50% of the maximal current and absent LVA current in another 25 cells. Other cells had mixtures of currents. Activation thresholds, deactivation kinetics and activation/inactivation taus also suggested 2 VDCC currents and demonstrated window current through LVA VDCC at physiological membrane potentials. In SAH cells, VDCC currents had lower peak amplitude than control cells and displayed dramatic reductions in voltage dependence of inactivation that caused corresponding reductions in calculated window current to less than 10% of control.

Conclusions: These novel data document the presence of LVA VDCC in basilar artery, which are typically less sensitive to nimodipine. Second, the marked reduction in window current suggests that even if calcium influx through VDCC initiates vasospasm, SAH may reduce VDCC current, rendering vasospasm less sensitive to VDCC antagonists.

559

Brain Poster Session: Experimental Cerebral Ischemia: Vascular & Endothelial

INTRAMICROVASCULAR BEHAVIOR OF PLATELETS IN MURINE BRAIN AFTER SUBARACHNOID HEMORRHAGE EXAMINED BY INTRAVITAL FLUORESCENT MICROSCOPY

N. Tanahashi[1], T. Saitoh[2], K. Hattori[1], N. Araki[3]

[1]Neurology, Saitama International Medical Center, Saitama Medical University, Hidaka City, [2]Neurosurgery, Medical Center, Saitama Medical University, Kawagoe City, [3]Neorology, Saitama Medical University, Iruma-gun, Japan

Background and aims: The mechanisms of early brain injury after subarachnoid hemorrhage (SAH) are not fully understood. We examined platelet behavior in cerebral microvessels of a murine model of subarachnoid hemorrhage using intravital fluorescence microscopy.

Methods: We induced SAH using endovascular sutures in 16 C57BL/6J mice. Twelve mice underwent sham operations (n = 12). A cranial window was prepared in the right parietal region. Platelets obtained from donor mice were labeled with a fluorescent dye (carboxyfluorescein iodoacetate succinimidyl ester; CSFE) in vitro. Labeled platelets were intravenously administered at 3 hours after SAH and then platelet behavior in the brain microvessels was observed using intravital fluorescence microscopy.

Results: Platelet rolling and adhesion were observed in the cerebral microvessels of SAH mice. We found significantly more platelets rolling in the pial veins (1712 ± 840/mm^2/30 sec) and arteries (244 ± 299/mm^2/30 sec) of SAH than in those of sham operated mice (904 ± 979 and 15 ± 26/mm^2/30 sec, respectively; $P < 0.01$). Similarly, significantly more platelets adhered to the pial veins (81±44/mm^2) and arteries (30 ± 45/mm^2) of SAH than sham operated mice (56 ± 79 and 3 ± 6/mm^2, respctively; $P < 0.01$) More rolling platelets were identified in the pial veins than arteries f the SAH group (1712 ± 840 vs. 244 ± 299/mm^2/30 sec; $P < 0.05$). More platelets adhered to pial veins than to those in pial arteries but the difference did not reach significance. We classified the SAH mice into two groups based on the severity of hemorrhage and compared platelet numbers and behavior. More platelets were rolling and adhesive in the group with severe, than with mild SAH, but the difference did not reach significance ($P < 0.01$). Intravascular microthrombus formation in the pial veins occasionally resulted in vessel occlusion in mice with severe SAH.

Conclusions: Platelets apparently became activated in murine cerebral microvessels and interacted with the endothelium during the acute phase of subarachnoid hemorrhage resulting in cerebral microcirculatory disturbance.

560

Brain Poster Session: Inflammation

SMALLER CEREBRAL INFARCT SIZE IN FEMALES VERSUS MALES IS REPERFUSION-DEPENDENT AND ASSOCIATED WITH LESS INFLAMMATION AND NOX2-CONTAINING INFILTRATING T LYMPHOCYTES

V.H. Brait[1], K.A. Jackman[1], H. Diep[1], B.R.S. Broughton[1], A.K. Walduck[2], G.R. Drummond[1], C.G. Sobey[1]

[1]Pharmacology, Monash University, Clayton, [2]Pharmacology, The University of Melbourne, Parkville, VIC, Australia

Background and aims: Infarct size is typically smaller in females than in males following cerebral ischemia-reperfusion, the underlying mechanisms of which are not well understood. The aims of this study were:

1. to test the importance of reperfusion in the protection of females following ischemic stroke, and
2. to assess the involvement of local inflammation and the peripheral immune system.

Methods: In male (n=99) and female (n=91) C57Bl6/J mice, cerebral ischemia was induced by middle cerebral artery occlusion (MCAO) for 0.5 h followed by reperfusion for 23.5 h (ischemia-reperfusion; I-R). Control mice were subjected to sham surgery. In order to assess the importance of reperfusion, in some mice MCAO was maintained for 24 h with no reperfusion (I-NR). Brains were used to quantitate infarct volume, or for western blotting or immunofluorescence, and blood and spleens were removed for fluorescent activated cell sorting analysis or T lymphocyte proliferation assays. We assessed whether outcomes after cerebral I-R were associated with changes in expression of the pro-inflammatory proteins Nox2, cyclooxygenase-2 (Cox-2), or vascular cell adhesion molecule-1 (VCAM-1) protein, differences in circulating lymphocyte and splenocyte populations, or T lymphocyte function.

Results: After I-R, males had a larger infarct volume than females (55±11 vs. 24±6 mm^3, n=7-8; $P< 0.05$), whereas there was no gender difference following I-NR (88±11 vs. 88±9 mm^3, n=8-9). Expression of Nox2, Cox-2 and VCAM-1 was each significantly increased in the ischemic hemisphere of males after I-R, but was unchanged in females. Immunofluorescence studies indicated more Nox2 protein and T lymphocytes (CD3+) in the infarct zone in males than in females following I-R, and revealed Nox2 to be largely co-localized with CD3. In the spleen, there were significantly lower levels of T and B lymphocytes following I-R in both males and females, whereas preliminary studies indicated no significant change in circulating lymphocyte levels in either gender. In addition, T lymphocyte proliferation in vitro was not different between males and females following I-R.

Conclusions: Thus, following cerebral ischemia the smaller cerebral infarct volume observed in females is reperfusion-dependent. Furthermore, less brain inflammation occurs in females than males, and is associated with less infiltration of Nox2-expressing T lymphocytes into the brain in females after I-R. We speculate that Nox2-derived superoxide from infiltrating T lymphocytes contributes to the greater infarct volume in males versus females following cerebral I-R.

562

Brain Poster Session: Cerebral Vascular Regulation

VASCULAR RESPONSE IN MICE DEFICIENT IN THE POTASSIUM CHANNEL, TREK-1

K. Namiranian, E.E. Lloyd, S.P. Marrelli, R.M. Bryan

Anesthesiology, Baylor College of Medicine, Houston, TX, USA

Objective: TREK-1 is a member of a recently discovered family of ion channels termed two-pore domain potassium channels (K_{2P}). The K_{2P} channels were discovered by searching for genes with homology to the highly conserved potassium-selective pore domain. In the nervous system, TREK-1 is reported to be involved with neuroprotection, depression, and the mechanism of action of volatile anesthetics. However, its role in the cardiovascular system is not completely understood. We aim to investigate the role of TREK-1 in cardiovascular system and we hypothesized that TREK-1 is involved with regulating the response of vascular elements to vasodilators and vasoconstrictors.

Methods: Since there are no specific blockers or activators for TREK-1, a knockout (KO) mouse line was generated by replacing the first two coding exons of TREK-1 with a neomycin/beta-galactosidase cassette. Reverse transcriptase-PCR was used to detect the expression of TREK-1 mRNA. Vascular responses were measured by monitoring the artery diameter in isolated basilar arteries (BA) and isolated perfused middle cerebral arteries (MCA), both pressurized at 75mmHg. Vascular reactivity in aorta was measured in isolated aortic rings attached to a force transducer. The cardiac function was evaluated by Doppler ultrasound, and blood pressures were measured invasively in carotid artery and left ventricle via an arterial catheter.

Results: TREK-1 mRNA was found in mouse heart and all arteries studied (aorta, femoral, renal, mesenteric, middle cerebral and basilar) with the exception of the carotid artery. TREK-1 KO mice are viable and fertile and do not show any gross abnormality. TREK-1 mRNA was not detected in any of the tissues sampled from KO mice. The cardiac function and blood pressure were similar in TREK-1 KO and WT mice (n=5). In the perfused pressurized MCA, phenylephrine (0.1 to 100 μM) induced similar constriction (n=9), and luminal application of ATP (10 and 100 μM) elicited similar endothelium-mediated dilation in WT and KO littermates (n=12). The NO and EDHF component of the ATP-dilation were also similar in WT and KO mice. Acetylcholine (10 μM)-mediated dilations in BA of KO mice were not different from wild-type (WT) mice, either before or after inhibition of nitric oxide synthase (n=5-6). Linoleic acid (LA, 10 μM and 100 μM), an activator of TREK-1 and Ca-activated K channels (BK_{Ca}), dilated endothelin-constricted BA of WT and KO mice to similar extents. However, after selectively blocking BK_{Ca} with penitrem A, the dilation to LA in BA from KO mice was reduced 19±5%, while it was not affected in WT (n=6). This suggests that part of LA-induced dilation is mediated via TREK-1.

Conclusions: Since the studied vascular responses and cardiac function were not altered in the absence of TREK-1, this channel seems to be dispensable for cardiovascular system. Direct activation of TREK-1 dilates cerebral arteries; therefore TREK-1 may be a therapeutic target for designing vasodilators for the pathological conditions where blood flow is disturbed.

INCREASED CORTICAL INFARCT AFTER TRANSIENT ISCHAEMIC STROKE IN MICE LACKING THE IP RECEPTOR FOR PROSTACYCLIN

S. McCann[1], C. Roulston[1], G. Dusting[1,2]

[1]Bernard O'Brien Institute of Microsurgery, [2]Department of Surgery, University of Melbourne, Melbourne, VIC, Australia

Background and aims: Prostacyclin is a vasodilator, platelet anti-aggregatory and cytoprotective prostanoid generated mainly via the cyclooxygenase-2 (COX-2) pathway. Both enzyme and metabolites in the brain are up-regulated following stroke as part of the inflammatory cascade. While inhibition of COX-2 reduces brain damage following ischaemic stroke, prostacyclin treatment also has documented protective actions. The recent withdrawal of selective COX-2 inhibitors rofecoxib and valdecoxib due to an increased risk of adverse cardiovascular events has highlighted the need to re-examine the role of COX-2 products in the search for new therapies. We have investigated whether endogenous prostacyclin plays a role in the brain damage following transient ischaemic stroke.

Methods: Prostacyclin receptor-deficient mice (IP-/-; n = 7) on an apolipoprotein-E-deficient background were compared to control littermates with functional IP receptor (IP+/+; n = 5) after occlusion of the middle cerebral artery (2 h) by intraluminal filament. Cerebral blood flow was monitored during stroke using laser Doppler flowmetry. Infarct area and volume were calculated using MCID image analysis of unstained brain sections. Following stroke, brain oedema was estimated using MCID images and superoxide generation was examined using dihydroethidium (DHE) fluorescence.

Results: Following 24 h reperfusion, infarct volume was increased in the cerebral cortex of IP-/- mice (44.6 ± 9.6 mm^3) compared with IP+/+ littermates (10.0 ± 4.4 mm^3; $P < 0.01$). There was no difference in infarct size in the striatum. There was no difference between groups in cerebral blood flow changes during stroke. Brain oedema tended to be increased in IP-/- mice but this was not significant. Compared to the appropriate contralateral control and to IP+/+ mice (90 ± 5%), stroke affected cortical brain regions of IP-/- mice exhibited an increase in DHE-detected superoxide (122 ± 3%). An increase in DHE fluorescence was detected in the ischaemic penumbra of both genotypes.

Conclusions: The increased infarct size and oxidative stress in IP-/- mice indicates that endogenous prostacyclin signaling exerts a protective effect on cortical neuronal survival after transient stroke, but the mechanisms remain to be clarified.

HYPERINTENSE VESSEL SIGN ON FLUID-ATTENUATED INVERSION RECOVERY IMAGES ASSOCIATES WITH OCCLUDED MIDDLE CEREBRAL ARTERY

T. Kono[1], H. Naka[2], S. Aoki[1], H. Ueno[1], T. Ohshita[1], E. Nomura[2], T. Ohtsuki[1], T. Kohriyama[1], S. Wakabayashi[3], M. Matsumoto[1]

[1]Neurology, Hiroshima University Hospital, [2]Neurology, [3]Neurosurgery, Suiseikai Kajikawa Hospital, Hiroshima, Japan

Objectives: Hyperintense vessel sign (HVS)[1)] that MRI shows as high intensity signal on fluid-attenuated inversion recovery (FLAIR) images is as useful as diffusion-weighted images for early detection of an occluded artery. The aim of this study is to evaluate the frequency of HVS appearance and the following disappearance under whether the occluded vessel being reperfused or not.

Methods: From retrospective case series between January 2004 and March 2007 in Suiseikai Kajikawa Hospital, we selected the patient of ischemic stroke undergoing both 1.5T MRI DWI/ FLAIR images and MR angiography within 24 hours of onset. Patients with symptomatic stenosis or occlusion in M1 segment of the middle cerebral artery (MCA) were included and divided into either cardioembolic infarction or large vessel disease according to the Trial of ORG 10172 in Acute Stroke Treatment (TOAST) classification. The extent of stenosis of M1 segment in each patient was classified into the 3 grades as follows: mild (signal reduction), severe (focal signal loss with the presence of distal MCA) and occlusion. The second MRI was performed if medical doctors permitted for necessary. The 2 neurologists assessed every images independently.

Results: A total of 42 patients were enrolled (25 men, 33-93 years old; median age 70 years old). The interval from onset to the first MRI was 33 min - 21 h; median 3 h 35 min. The pathogenesis of ischemic stroke was either cardiogenic embolism (n=21) or large vessel disease (n=21). HVS was detected in 37 patients (88%), and was present in all (100%) of the 21 patients with cardioembolic infarction, that consisted of 19 “occlusion” and 2 “severe stenosis” by the grade. In contrast, 16 (76%) of the 21 patients with large vessel disease had positive HVS; all (100%) of 11 “occlusion” and 4 (44%) of 9 “mild to severe stenosis” showed positive HVS. Not only cardioembolic infarction but also large vessel disease showed positive HVS without statistical difference (p=0.41).The second MRI was obtained in 22 patients on the median 4 days after the first MRI. HVS disappeared in 11 (85%) of 13 patients under MCA recanalization, while it disappeared in 1 (11.1%) out of 9 if MCA failed to recirculate (OR 44.0, 95% CI: 3.08-655, p=0.03).

Conclusions: A positive HVS associated with occluded MCA (M1) on cardioembolic infarction or large vessel disease and disappearance of HVS correlated with reperfusion of the once occluded MCA. HVS could be as useful for early detection of MCA occlusion and recanalization well as MRA.

References: 1. Toyoda K, et al. Fluid-attenuated inversion recovery intraarterial signal: an early sign of hyperacute cerebral ischemia. AJNR Am J Neuroradiol.2001; 22: 1021-9.

568

Brain Poster Session: Traumatic Brain Injury

CONTROLLED CORTICAL IMPACT INDUCES EXPRESSION OF ACID-SENSING ION CHANNEL 2A IN MOUSE BRAIN

C. Goodman[1], M. Van[2], H. Saucedo Crespo[2], C. Robertson[2]

[1]Pathology, [2]Neurosurgery, Baylor College of Medicine, Houston, TX, USA

Background and aims: Acid-sensing ion channel (ASIC's) are ligand gated cation channels that open and flux sodium and calcium in response to increased proton concentration. In the periphery, these channels play a role in the detection of tissue ischemic injury, but they are also expressed in the central nervous system where their physiological role is unclear. ASIC's are up-regulated in ischemia and they may potentiate tissue damage in ischemia induced acidosis - a process that has been designated “acidotoxicity.” ASIC knock-out animals are resistant to cerebral ischemia and there are numerous molecules capable of blocking these channels with beneficial effect. Since acidosis is a common neurochemical finding in traumatic brain injury, we examined the ASIC expression in experimental focal traumatic brain injury.

Methods: Under general anesthesia, C57BL6/J mice were exposed to moderate controlled cortical impact (CCI). ASIC 2a gene expression was ascertained by reverse transcription polymerase chain reaction (RT-PCR) and protein levels were measured by Western blotting at 2, 24, 48 and 72 hours in the injured and uninjured cerebral hemispheres.

Results: No change in ASIC protein levels was seen at 2 hours but by 24 hours there was increased protein concentrations on the injured side. By 48 and 72 hours, the ASIC protein levels were equal on injured and uninjured sides. Gene expression was increased at 2 hours after CCI but by 24 hours expression was equal on both sides.

Conclusions: ASIC 2a expression is rapidly increased in cerebral cortical tissue injured by controlled cortical impact. The rapidity of the increased expression is similar to that seen in ischemia but the expression is more transient in CCI. Acidosis is a common neurochemical feature of ischemic and traumatic brain injury; therefore, increased expression of these channels may play a role in the evolution of traumatic brain injury and the increased vulnerability of injured cerebral tissue to secondary injury. Studies in ischemic injury suggest that the ASIC's are potential therapeutic targets and the present study indicate that pharmacological modulation of these channels might also be useful in traumatic brain injury. Amiloride class drugs as well as several invertebrate neurotoxins are potent ASIC blockers that may have therapeutic potential in managing acidotoxicity in ischemia and traumatic brain injury.

References:

1. Xiong, Z.G., et al., Acid-sensing ion channels (ASICs) as pharmacological targets for neurodegenerative diseases. Curr Opin Pharmacol, 2008. 8(1): p. 25-32.

2. Simon, R. and Z. Xiong, Acidotoxicity in brain ischaemia. Biochem Soc Trans, 2006. 34(Pt 6): p. 1356-61.

3. Johnson, M.B., et al., Global ischemia induces expression of acid-sensing ion channel 2a in rat brain. J Cereb Blood Flow Metab, 2001. 21(6): p. 734-40.

Research funding support from the National Institutes of Health P01 Grant #NS38660 is gratefully acknowledged. All experiments were performed under appropriate approved institutional animal use protocols.

570

Brain Poster Session: rt-PA

SIGNIFICANCE OF CLINICAL-DIFFUSION MISMATCH IN HYPERACUTE CEREBRAL INFARCTION

I. Deguchi, H. Takeda, D. Furuya, K. Hattori, H. Nagoya, Y. Kato, T. Fukuoka, N. Tanahashi

Neurology, Saitama Medical University Internatinal Medical Center, Saitama, Japan

Background and aims: In recent years, patient selection for intravenous tissue plasminogen activator (t-PA) based on clinical-diffusion mismatch (CDM) has been closely examined. Here, we investigated the relationship between prognosis and CDM in patients with hyperacute cerebral infarction within three hours of onset and compared CDM to diffusion-perfusion mismatch (DPM).

Methods: Of 122 patients with hyperacute cerebral infarction who visited the hospital within three hours of onset from April 2007 to November 2008, subjects were 85 patients with cerebral infarction in the anterior circulation who underwent head MRI diffusion weighted image (DWI)/magnetic resonance angiography (MRA) (51 men and 34 women with an average age of 74±10 years). Of these, CT perfusion (CT-P) was performed in 17 patients. CDM-positive cases were subdivided into ≥8 National Institute of Health Stroke (NIHSS) and ≥8 Alberta Stroke Program Early CT Score-DWI (ASPECTS-DWI) groups. CDM-negative cases were subdivided into ≥8 NIHSS and < 8 ASPECTS-DWI groups. Other patients were classified as belonging to the < 8 NIHSS group.

Results: Of the 35 CDM-positive cases, t-PA infusion was performed in 11 patients, and the modified Rankin Scale (mRS) score at 90 days after onset for these patients was clearly better when compared to the 24 patients who did not receive t-PA infusion. Of the nine CDM-positive cases, there were five DPM(+) cases and four DPM(-) cases, and a discrepancy was confirmed between CDM and DPM. In all DPM(+) cases, MRA confirmed lesions in major intracranial arteries.

Conclusions: In hyperacute cerebral infarction, CDM was useful for predicting the enlargement and progression of infarcts and determining whether to perform t-PA. By combining CDM and MRA findings (presence or absence of lesions in major intracranial arteries), it is also possible to more accurately ascertain the indications for t-PA in hyperacute phase cerebral infarction, and this may be used instead of DPM.

Brain Poster Session: Neonatal Ischemia

EMPIRICAL STUDY OF INTRA-UTERO FETAL CARDIAC INTERVENTION OF NEAR-TERM FETAL LAMB

Y.-M. Hua[1], K.-Y. Zhou[1], X.-Q. Shi[1], Y.-B. Wang[1], Z. Zheng[1], Q. Zhu[2]

[1]Pediatric Cardiology Department, [2]Department of Ultrasound Cardiography, The Second West China Hospital of SiChuan University, Chengdu, China

Objective: To evaluate the feasibility of analogous intrauterine fetal cardiac intervention in near-term fetal lambs.

Methods: Nine bigeminal pregnant ewes in latter 2nd-trimester and early 3rd- trimester were taken into the study of fetal cardiac intervention. Observated the end-results of after-procedure gestation. Evaluated histopathologic changes of brain, lung and liver in fetal and newborn lambs.

Results: While cardiocentesis the fetal lambs' heart rate decreased transiently and there exited bigeminal premature ventricular contractions in two procedures. Blood glucose and lactic acid were found increaseing significantly after procedure (P< 0. 05). During procedure fetal electrolyte kept stabilization. 3/9 ewes executed after fetal intervention, the ewes which come to full-term delivery and prematurity were both 3/9. The fetuses after-procedure were delivered through vagina and alive. The surfaces of the fetal chest were without inflammation and scar formation. Histological examination of brains, lungs and livers from both control and test groups demonstrated that all fetal lambs' brains were normal except that only one brain tissue of the test group showed mild pathologic change and all fetal lambs' lungs were normal. Immunohistochemisty of fetal brain showed there exited mild nerve cells apoptosis in three fetal brain with TUNLE. The fetal hepatic PAS staining showed great consumption of hepatic glycogen during fetal cardiac intervention, which could be re-accumulation in following gestation.

Conclusion: Intra-utero fetal cardiac intervention in near-term fetal lambs is of feasibility in some extend, further research needed to be done about this question.

References:

1. Mäkikallio K, McElhinney DB, Levine JC,et al.Fetal aortic valve stenosis and the evolution of hypoplastic left heart syndrome: patient selection for fetal intervention.Circulation 2006;113(11):1401-52.

2. Galindo A, Gutiérrez-Larraya F, Velasco JM, et al.Pulmonary balloon valvuloplasty in a fetus with critical pulmonary stenosis/atresia with intact ventricular septum and heart failure.Fetal Diagn Ther 2006;21(1):100-43.

3. Tworetzky W, Marshall AC.Fetal interventions for cardiac defects.Pediatr Clin North Am 2004;51(6):1503-13, vii4.

4. Wilkins-Haug LE, Benson CB, Tworetzky W, et al.In-utero intervention for hypoplastic left heart syndrome--a perinatologist´s perspective.Ultrasound Obstet Gynecol 2005;26(5):481-65.

5. Ikai A, Riemer RK, Ramamoorthy C, et al.Preliminary results of fetal cardiac bypass in nonhuman primates.J Thorac Cardiovasc Surg 2005;129(1):175-816.

6. Fok WY, Leung TY, Tsui MH, et al.Fetal hemodynamic changes after amniotomy.Acta Obstet Gynecol Scand 2005;84(2):166-97.

7. Wood CE, Giroux D.Central nervous system prostaglandin endoperoxide synthase-1 and -2 responses to oestradiol and cerebral hypoperfusion in late-gestation fetal sheep.J Physiol 2003;549(Pt 2):573-818.

8. Eghtesady P, Sedgwick JA, Schenbeck JL, et al.Maternal-fetal interactions in fetal cardiac surgery.Ann Thorac Surg 2006;81(1): 249-559.

9. Meuli M, Meuli-Simmen C, Hutchins GM, et al.In utero surgery rescues neurological function at birth in sheep with spina bifida.Nat Med 1995;1(4):342-710.

10. McClaine RJ, Uemura K, McClaine DJ, et al.A description of the preterm fetal sheep systemic and central responses to maternal general anesthesia.Anesth Analg 2007;104(2):397-406.

573

Brain Poster Session: Blood-Brain Barrier

HSP70 OVEREXPRESSION ATTENUATES ISCHEMIA-INDUCED DISRUPTION OF TIGHT JUNCTION PROTEINS FOLLOWING EXPERIMENTAL STROKE

Z. Zheng, J.Y. Kim, **M.A. Yenari**

UCSF-SFVAMC, San Francisco, CA, USA

Background and aims: We previously showed that microglia potentiate ischemic injury to blood brain barrier (BBB) components, and that overexpression of Hsp70 protects against stroke, in part, through an anti-inflammatory mechanism. Recent studies indicate that increases in BBB permeability following brain ischemia may be associated with alterations in neurovascular proteolytic activity, particularly thought the matrix metalloproteinases (MMPs). In this study, we evaluated the effects of Hsp70 overexpression on several BBB-related tight junction proteins in a previously validated transient middle cerebral artery occlusion (tMCAO) model in Hsp70 transgenic mouse (Tg). To determine whether this effect is mediated through Hsp70 expression within the brain or within circulating cells, we also studied bone marrow chimeras, where wildtype (Wt) mice received bone marrow from Tg mice (Tg chimera) or Wt mice as a control.

Methods: The mice were subject to 2 h brain ischemia, followed by 24 h reperfusion. IgG immunostaining was used to assess BBB integrity. Tight junction proteins, claudin-5, collagen 4 and ZO-I were assessed in cortical tissue ipsilateral to MCAo by using western blots and semi-quantitative densitometry was performed on digitized images using Taphone software.

Results: Increases in parenchymal IgG immunoreactivity were observed in both Wt and Tg mice, indicating the disruption of BBB, but the area and intensity of IgG immunostaing among transgenic mice were significantly decreased compared to wt mice, even when normalized to infarct size ($p< 0.01$). Similar patterns were observed in the bone marrow chimeras, with decreased BBB disruption in the Tg chimeras. Marked reduction of claudin-5, ZO-1 was evident in Wt mice. In contrast, Tg transgenic mice and Tg chimeras showed significant preservation of claudin-5 and ZO-1 proteins ($p< 0.05$). There were trends showing less disruption of collagen 4 in Tg mice and Tg chimeras, but this did not reach statistical significance.

Conclusions: Our data suggest that Hsp70 overexpression attenuates exacerbation of BBB permeability through the conservation of tight junction proteins, claudin-5 and ZO-1, and this effect appears to be mediated by Hsp70 overexpression in circulating leukocytes.

Brain Poster Session: Neuroprotection

BRAIN LIPID PEROXIDATION, RADICAL SCAVENGING EFFECTS AND ANTITUMOR ACTIVITY OF TAIWANESE BOTANY - YY-24 ON HUMAN GLIOBLASTOMA CELLS

L.L. Yang[1], Y.W. Yu[1], W.T. Huang[2]

[1]Department of Pharmcognosy, College of Pharmacy, Taipei Medical University, Taipei, [2]Division of Hemato-oncology/Chi-Mei Medical Center, Tainan, Taiwan R.O.C.

In the nervous system, reactive oxidative species (ROS) can cause neurodegenerative disorders, like Alzheimer's disease (AD), Huntington's diease (HD), Parkinson's disease (PD), amytrophic lateral sclerosis (ALS) and ataxia telangiectasia. Overproduction of ROS results in oxidative stress that can be an important mediator of damage lipids, proteins, and nucleic acids. Antioxidants prevent cellular damage by scavenging and inhibition of free radicals and prevention of pathologies. Oxidative stress has been implicated in the pathogenesis, including aging, atherosclerosis, diabetes mellitus, chronic inflammation and cancers. Gliomas are the most common type of primary brain tumor. Nearly two-thirds of gliomas are highly malignant lesions that account for a disproportionate share of brain tumor-related morbidity and mortality. Despite many technologic advances in neuroimaging, neurosurgery, and radiation therapy, there has been little improvement in survival for patients with malignant glioma. Approximately 17,000 primary brain tumors are diagnosed every year, and of those, about 60% are gliomas. Tumors of gliol origin such as glioblastoma multiforme comprise the majority of human brain tumors. In this paper, 30 kinds of Taiwanese Botany extracts were isolated from herbal medicine in our laboratory and their effects on 2,2-Diphenyl-1-picrylhydrazyl (DPPH) radical scavenging, superoxide anion radical scavenging, superoxide anion radical inhibition, ferrous ions chelating activities, ferric ion reducing antioxidant power (FRAP), lipid peroxidation, cell proliferation and potential cytotoxicity. The level of lipid peroxidation (LPO) was expressed as thiobarbituric acid reactive substances (TBARS). LPO product of $MDA(TBA)_2$ was induced by ferrous chloride and ferrous ammonium sulfate respectively on Wistar rat liver mitochondria and brain homogenate. Otherwise, the human malignant glioblastoma cell lines of GBM 8401 (astrocytoma-glioblastoma, grade III) and U-87 MG (astrocytoma- glioblastoma, grade IV) were used. We established screening program employing the 4,5-dimethylthiazol-2-yl)-2,5-diphenyltetrazolium bromide (MTT) reduction assay system utilizing human malignant glioblastoma cells. One of the most potential compounds, YY-24 exhibited a significantly antioxidant and brain homogenate lipid peroxidation. It had exhibited a dose dependent and time dependent manner in human malignant glioblastoma cells. The IC_{50} value of YY-24 after 24 hours were 175.03 ± 9.88 and 200.00 ± 0.02 μg/ml in GBM 8041 and U-87 MG, respectively. In addition, we had observed the apoptotic bodies in GBM 8401 and U-87 MG. YY-24 may medicate the cytotoxicity via apoptosis in GBM 8401 and U-87 MG. Furthermore, we well evaluated the mechanism of apoptosis by western blot in the future.

REDUCED ISCHEMIC INJURY IN HSP110/105 GENE KNOCK-OUT MICE AFTER FOCAL CEREBRAL ISCHEMIA

T. Marumo[1], J. Nakamura[2], M. Fujimoto[1], K. Nozaki[3], K. Nagata[2], Y. Takagi[1]

[1]Department of Neurosurgery, Kyoto University Graduate School of Medicine, [2]Department of Molecular and Cellular Biology, Institute for Frontier Medical Sciences, Kyoto University, Kyoto City, [3]Department of Neurosurgery, Shiga University of Medical Science, Otsu City, Japan

Background and aims: Hsp 110/105 belongs to the HSP110 heat shock protein family, which is a subgroup of the HSP70 family. In mammals, Hsp110/105 is constitutively expressed but exhibits particularly high levels in the brain. It has recently been shown that both Hsp110/105 and Hsp70 are elevated after cerebral ischemia. To study the role of this protein in vivo, we used hsp110/105 knock-out (KO) mice and investigate the effect of reduced Hsp110/105 levels on focal cerebral ischemia.

Methods: There are no histological and morphological differences in Hsp110/105 KO mice and their WT littermates. Hsp110/105 KO and wild-type mice were subjected to 30 minutes of transient middle cerebral artery occlusion followed by reperfusion for 24 hours. The infarct volume and neurological scores were measured and compared.

Results: The infarction volume and neurological deficit scores were significantly ($P< 0.05$) reduced in hsp110/105 KO mice compared with wild-type controls.

Conclusions: These results demonstrate that hsp110/105 KO mice are resistant to ischemic injury.

NEUROPROTECTION BY HUMAN UMBILICAL MESENCHYMAL CELLS TRANSPLATATION AFTER EXPERIMENTAL TRAUMATIC BRAIN INJURY

K.-F. Huang[1,2], C.-W. Hsu[3], Y.-S. Fu[4], J.-Y. Wang[3]

[1]Neurosurgery, Tzu Chi General Hospital, [2]Medical Sciences, [3]Physiology, National Defense Medical Center, [4]Anatomy, National Yang-Ming University, Taipei, Taiwan R.O.C.

Neuronal transplantation has provided a promising approach for treating traumatic brain injury (TBI). Human umbilical mesenchymal cells (HUMCs) have been suggested to promote survival of degenerating neurons after parkinsonism.

The purpose of this study was to evaluate the potential for survival, migration, differentiation and functional improvement of HUMCs transplanted into a rat model of TBI. Cortical impact injury (CCI) was produced in pentobarbitol-anaesthetised rats using a pneumatic piston with a 2.5-mm metal tip through a 5 mm parietal bone craniotomy and at a velocity of 4m/sec and a 2mm deformation depth below the dura. HUMCs isolated from Wharton´s jelly of the umbilical cord were injected into the ipsilateral or contralateral hippocampus of adult male rats 2 days following CCI. The animals were evaluated for neurological deficits using adhesive removal and rotorod tests at 1, 4, 7, 14 days and 1, 2, 3 months after transplantation. The animals were sacrificed at 1, 2 and 3 months after transplantation for immunohistochemistry evaluation. To study the proliferation and phenotypic differentiation of HMSCs, brain sections were immunostained for cell proliferation markers (bromodeoxyuridine. BrdU), or neuronal (NeuN), microglial (OX-42) and astrocytic (glial fibrillary acidic protein) markers. Behavioral testing revealed improvements in the rotorod test in ipsilateral HMSC-treated rats. The transplanted HMSCs successfully survived and migrated into injured brain and were preferentially localized around the injury site. Our results suggest that HMSCs have the potential for treatment of traumatically injured nervous system.

EFFECT OF RISPERIDONE ON HIGH-AFFINITY STATE OF DOPAMINE D2 RECEPTOR; A PET STUDY WITH [C-11]MNPA

F. Kodaka[1,2], H. Ito[1], H. Takano[1], H. Takahashi[1], R. Arakawa[1], M. Miyoshi[1], M. Okumura[1], T. Otsuka[1], K. Nakayama[2], T. Suhara[1]

[1]Department of Molecular Neuroimaging, Clinical Neuroimaging Section, National Institute of Radiological Sciences, Chiba, [2]Department of Psychiatry, Jikei University School of Medicine, Tokyo, Japan

Objectives: Early in vitro studies have revealed that dopamine D2 receptors (D2 receptors) have two interconvertible affinity states for endogenous dopamine, referred to as high- and low-affinity state [1]. [C-11]-(R)-2-CH3O-N-n-propylnorapomorphine ([C-11]MNPA), a newly developed D2 receptor agonist ligand, is more sensitive to displacement by endogenous dopamine than [C-11]raclopride in the primate brain[2]. For this reason, [C-11]MNPA represents a promising radioligand for positron emission tomography (PET) imaging of the high-affinity state of the dopamine D2 receptor. Risperidone, which is well known as a serotonin-dopamine antagonist and a commonly prescribed antipsychotic to alleviate positive symptoms of schizophrenia, acts as an antagonist against dopamine D2 receptors. While the occupancy of dopamine D2 receptors by risperidone has been measured by PET with conventional D2 receptor antagonist ligands such as [C-11]raclopride and [C-11]FLB457, little is known about its pharmacological behavior against the high-affinity state of D2 receptor because those conventional D2 receptor antagonist ligands are sensitive to both the high- and low-affinity state of D2 receptor. Here, we measured D2 receptor occupancy of [C-11]MNPA and [C-11]raclopride after oral administration of risperidone to evaluate its pharmacological action against the high-affinity state of D2 receptor.

Methods: PET studies were performed on eleven healthy men (21-39 years) under resting condition and oral administration of a single dose of risperidone (0.5-2.0 mg) on separate days. In each condition, PET scans using [C-11]raclopride and [C-11]MNPA were performed sequentially. For each PET study, the binding potentials (BPs) in the striatum were calculated by reference tissue model method with use of the cerebellum as reference region. The occupancy of dopamine D2 receptors was then calculated from the BP values of resting and drug challenge conditions. Relations between dopamine D2 receptor occupancy and the administered dose of risperidone were analyzed for each radioligand.

Results: The occupancies of dopamine D2 receptors in [C-11]raclopride and [C-11]MNPA studies ranged from 24% to 70% and from 22% to 66% in the striatum, respectively. The occupancy of [C-11]raclopride was positively correlated with that of [C-11]MNPA ($r = 0.72$, $P = 0.012$). The relation between dopamine D2 receptor occupancy and the dose of risperidone (dose-occupancy curve) with [C-11]raclopride and [C-11]MNPA was positive and logarithmically fitted ($r = 0.85$ for [C-11]raclopride, $r = 0.69$ for [C-11]MNPA). ED50 values calculated from the dose-occupancy curves with [C-11]raclopride and [C-11]MNPA were 0.98 mg and 1.03 mg, respectively.

Conclusions: The positive correlation of occupancies between both [C-11]raclopride and [C-11]MNPA studies and similar ED50 values of both studies indicate that risperidone blocks both high- and low-affinity state of dopamine D2 receptors in a similar dose-dependent manner.

References:

[1] Sibley DR, De Lean A. J Biol Chem 1982; 257(11): 6351-6361.

[2] Seneca N, Finnema SJ. Synapse 2006; 59(5): 260-269.

581

Brain Poster Session: Experimental Stroke & Cerebral Ischemia

EFFECT OF CLOPIDOGREL ON LASER INDUCED THROMBUS FORMATION IN MOUSE BRAIN MICROVASCULATURE OBSERVED BY INTRAVITAL FLUORESCENCE MICROSCOPY

T. Fukuoka[1], K. Hattori[1], N. Araki[2], N. Tanahashi[1]

[1]Neurology, Saitama International Medical Center, Saitama Medical University, Hidaka City, [2]Neurology, Saitama Medical University, Iruma-gun, Japan

Background and aims: We developed an apparatus of laser induced thrombus formation in murine brain microvasculature instantaneously. The purpose of this study was to observe the effect of clopidogrel on the process of laser induced thrombus formation and platelet behavior in the brain microvasculature of mice using intravital fluorescence microscopy.

Methods: C57 BL/6J mice (N=13) were anesthetized with chloral hydrate; their heads were fixed with a head holder, and a cranial window was made in the parietal region. Platelets were labeled in vivo by intravenous administration of carboxylfluorescein succinimidylester (CFSE). In six mice, clopidogrel (100mg/kg) was administered orally for two days before experiment. Seven mice were used as control. Laser irradiation (1000 mA, DPSS laser 532 nm, TS-KL/S2; Sankei) was spotted for 4 sec on pial arteries to induce thrombus formation. Labeled platelets and thrombus were observed continuously with a fluorescence microscope.

Results: After laser irradiation to the pial artery, complete occlusion rate in control group 60%(12/20 vessels) was significantly higher (P< 0.01) compared to clopidogrel group 20%(5/25 vessels)(Figure 1). All occluded vessels except one were recannalized within 1-2 min. Area of platelet thrombus at 30 min after laser irradiation in the control group (358±256 mm) was significantly (P< 0.05) larger than that of clopidogrel group (209±128 mm)(Figure 2).

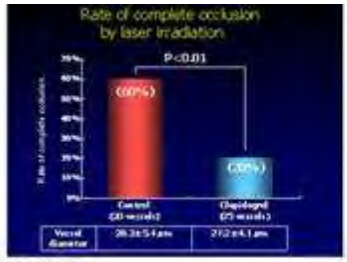

Figure 1

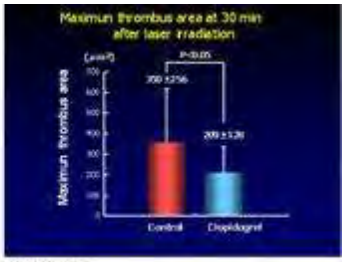

Figure 2

[ ]

Conclusions: Clopidogrel significantly inhibited laser induced thrombus formation in pial arteries of mice.

582

Brain Poster Session: Stem Cells & Gene Therapy

OVEREXPRESSION OF HUMAN DOWN SYNDROME CANDIDATE REGION 1 (DSCR1) GENE IMPROVES OUTCOME FOLLOWING CEREBRAL ISCHEMIA-REPERFUSION IN MICE

C.G. Sobey[1], K.R. Martin[2], M.A. Pritchard[2], V.H. Brait[1]

[1]Dept of Pharmacology, [2]Dept of Biochemistry, Monash University, Clayton, VIC, Australia

Background and aims: Down syndrome results from the trisomy of chromosome 21. The Down syndrome candidate region 1 (DSCR1) gene, recently renamed RCAN1, is found on chromosome 21. DSCR1 protein is highly expressed in the brain (Ermak et al, 2001), and following middle cerebral artery occlusion (MCAO) in mice DSCR1 mRNA and protein was found to increase in the peri-infarct region (Cho et al, 2008). The aim of this study was to investigate the effects of overexpression of DSCR1 on outcome following stroke.

Methods: DSCR1 transgenic (Tg) mice were produced by the overexpression of the human DSCR1 gene, only in cells that normally express DSCR1, on a C57Bl6/J X CBA background. Cerebral ischemia was induced by MCAO for 0.5 h followed by reperfusion for 23.5 h (ischemia-reperfusion; I-R) in age-matched groups of 8-14 week old male DSCR1 Tg (n=14) and wild-type (Wt; n=9) mice. MCAO was confirmed by a sudden drop in regional cerebral blood flow (rCBF; ~75%), measured by a laser-doppler flow probe positioned over the region perfused by the MCA. Control mice were subjected to sham surgery. After 24 h, neurological impairment was assessed (neurological score and hanging wire test) and %rCBF re-measured. Brain infarct and edema volume were then measured in thionin-stained coronal sections.

Results: After I-R, Tg mice had significantly less neurological impairment than Wt mice, with a lower neurological score (2.4±0.3 vs. 3.9±0.1; $P< 0.05$) and a longer hanging-wire time (38±5 vs. 9±3 seconds; $P< 0.0001$). %rCBF at 24 h was significantly higher in Tg than Wt mice (73±10 vs. 33±7 % pre-ischemia; $P< 0.01$). After I-R, Tg mice had a significantly smaller subcortical infarct volume than Wt mice (15±2 vs. 32±5 mm^3; $P< 0.01$). In addition, total infarct volume tended to be smaller in Tg than Wt mice (26±5 vs. 36±6 mm^3, n=9-14; $P=0.26$). Furthermore, edema volume was smaller in Tg than Wt mice (17±3 vs. 31±6 mm^3; $P< 0.05$).

Conclusions: Thus, overexpression of DSCR1 in mice improves outcome following cerebral I-R. Further studies are required to establish the mechanisms behind this improved recovery, and the relevance for individuals with Down syndrome.

References:

Cho, K-O., Kim, Y.S., Cho, Y-J. & Kim, S. Y. (2008). Upregulation of DSCR1 (RCAN1 or Adapt78) in the peri-infarct cortex after experimental stroke. Experimental Neurology, 212, 85-92.

Ermak G., Morgan T.E. and Davies K.J. (2001). Chronic overexpression of the calcineurin inhibitory gene DSCR1 (Adapt78) is associated with Alzheimer's disease. J. Biol. Chem, 276, 38787-38794.

CARBAMYLATED ERYTHROPOIETIN (I-125-CEPO) AS POTENTIAL RADIOTRACER FOR IMAGING NEUROPROTECTION IN CEREBRAL ISCHEMIA

A. Thiel[1,2], P. Rosa-Neto[1], E. Schirrmacher[3], H. Schipper[1,2], R. Schirrmacher[2,3]

[1]Neurology & Neurosurgery, McGill University, [2]Neurological Sciences, SMBD Jewish General Hospital and Lady Davis Institute for Medical Research, [3]Cyclotron Unit, McConnell Brain Imaging Centre, Montreal, QC, Canada

Objectives: Erythropoietin (EPO) and its derivatives have recently been shown to be neuroprotective in animal models of stroke, trauma and encephalitis (1) as wll as in a pilot study in human stroke (2). This neuroprotective effect is thought to be mediated by the Epo-ßc-heteroceptor complex which is expressed in low concentration in the normal brain but is up-regulated in situations where the brain is in need for neuroprotection (3). This study seeks to demonstrate that uptake of I-125-labelled carbamylated EPO (CEPO), a derivative which is neuroprotective but not erythropoietic, can be detected in ischemic brain tissue using ex-vivo autoradiography in a permanent rat middle cerebral artery occlusion (MCAO) model.

Methods: In experiment 1 male Sprague-Dawley (SD) rats were injected with 1.25µg of I-125-CEPO and sacrificed at 0.5,1,2,3 and 4h after injection. Radioactivity in blood-samples was measured as well as in 7 consecutive slices of the forebrain using autoradiography. In experiment 2 male SD-rats underwent a permanent right MCAO-occlusion procedure (4) and were injected with I-125-CEPO1, 2 and 3 hours after onset of ischemia. All animals were sacrificed 2h after injection and blood-radioactivity as well as tissue radioactivity were measured using the same procedures as in control animals. Standardized uptake values (SUV) were calculated for both hemispheres and within a standard region- of-interest (ROI) placed within the maximum tracer uptake and a contralateral mirror ROI.

Results: In control animals, elimination of radioactivity from the blood followed a two-parameter exponential decay function with an elimination half-life of 1.7 h. Tracer activity in the brain followed the same kinetic. No focal uptake outside blood vessels was observed. Mean global SUV was 0.0024 +/- 0.00140 g/µl. An increase of radiotracer activity in the ischemic hemisphere was observed in the MCAO animals. This accumulation was highest when the tracer was injected 3h post ischemia onset. This increase in the ischemic hemisphere was 30% of global uptake. In a standard ROI placed in the activity maximum within the ischemic hemisphere, an increase of 90% relative to the unaffected mirror ROI was found 3h after onset of ischemia (ipsilateral SUV_{MAX} = 5.66e-3 g/µl; mean contralateral SUV = 2.59e-3 +/- 0.734e-3., see figure).

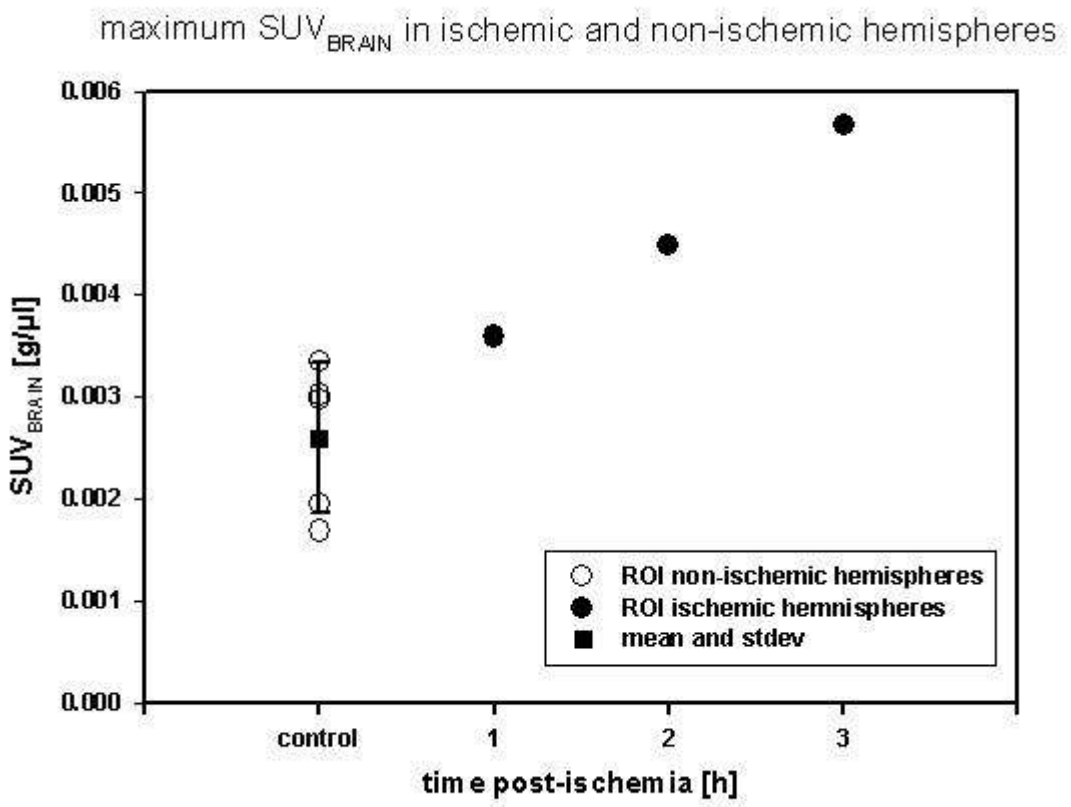

[figure1]

Conclusion: We demonstrate binding of I-125-CEPO in the ischemic hemisphere 3h after onset of ischemia. No significant binding was observed In control animals up to 4h after tracer injection. This study demonstrates the feasibility of using macromolecular substances to image neuroprotective systems and provides important data for the development of PET-based in vivo imaging methods for the EPO-receptor.

References:

(1) Brines M, Cerami A. Nat Rev Neurosci. 2005; 6:484-494.

(2) Ehrenreich et al. Mol Med. 2002; 8:495-505.

(3) Leist M, et al. Science. 2004; 305:239-242.

(4) Bela yev L, et al. Stroke. 1996; 27:1616-23.

ENDOTHELIUM-DEPENDENT RELAXATION AND ANTIOXIDANT EFFECTS BY G PROTEIN-COUPLED RECEPTOR GPR30 AGONISTS IN RAT CAROTID ARTERIES

B.R.S. Broughton, A.A. Miller, C.G. Sobey

Department of Pharmacology, Monash University, Clayton, VIC, Australia

Background & aims: Recent studies have identified that the novel membrane estrogen receptor, G protein-coupled receptor GPR30, is present in blood vessels. However, the potential role(s) of GPR30 in the vasculature remains unknown. We therefore examined whether putative agonists of GPR30 may possess vasorelaxant and antioxidant effects similar to those reported for estrogen.

Methods: Using wire myography we assessed both endothelium-dependent and -independent relaxation responses to the GPR30 agonists, G-1 and 5408-0877 (1 nM - 10 μM), in U46619-precontracted common carotid arteries from Sprague Dawley rats. Acetylcholine (ACh, 3 μM) was used to verify the presence or absence of an intact endothelium and all relaxations were expressed as a % of the response to sodium nitroprusside (SNP, 10 μM). Furthermore, we tested the effect of G-1 (10 μM) on NADPH (100 μM)-stimulated superoxide production by rat carotid and cerebral (pooled middle cerebral and basilar) arteries using lucigenin (5 μM)-enhanced chemiluminescence. Specific immunofluorescence was also used to confirm GPR30 expression in the arterial wall.

Results: We found that G-1 induces a concentration-dependent relaxation in carotid arteries from both males (e.g. 42 ± 8% at 10 μM; N = 6) and females (32 ± 7% at 10 μM; N = 6). Similarly, 5408-0877 induced a concentration-dependent relaxation in arteries from males (e.g. 35 ± 10% at 10 μM; N = 6) and females (34 ± 11% at 10 μM; N = 6). Overall, ACh relaxed carotid arteries by 87 ± 2%. Interestingly, G-1- and 5408-0877-induced relaxation was abolished by endothelium removal. In addition, NADPH-stimulated superoxide production was ~30-40% lower in carotid and cerebral arteries treated with G-1 versus untreated arteries. Furthermore, GPR30 immunoreactivity was observed in endothelium and vascular smooth muscle cells of carotid arteries from both genders.

Conclusions: In summary, this is the first study to assess the vascular effects of GPR30 agonists. Our data suggest that GPR30 is expressed throughout the vascular wall and receptor activation elicits endothelium-dependent relaxation of the carotid artery in male and female rats. In addition, activation of GPR30 reduces levels of NADPH oxidase-derived superoxide in carotid and cerebral arteries. Thus, these vasorelaxant and antioxidant properties of GPR30 are consistent with this receptor being a potential therapeutic target in the cerebral circulation during vascular disease.

585

Brain Poster Session: Experimental Stroke & Cerebral Ischemia

CHRONIC TWO PHOTON IMAGING OF DENDRITE DYNAMICS AFTER MICROHEMORRHAGE OF SINGLE PENETRATING ARTERIOLES USING FEMTOSECOND LASER ABLATION

J. Zhou, N. Rosidi, N. Nishimura, C. Schaffer

Biomedical Engineering, Cornell University, Ithaca, NY, USA

Objectives: Clinical evidence indicates that a higher incidence of microhemorrhages is linked to the development of dementia [1], suggesting that small hemorrhages may damage nearby neurons. In addition previous work has shown that occlusions of microvessels can lead to neural pathology such as shriveling of dendrites into nodules ("blebbing") [2]. Here we use two-photon excited fluorescence (2PEF) imaging of mice expressing YFP in neurons to determine whether hemorrhage of cortical penetrating arterioles (PA), without cessation of blood flow, leads to dendrite damage.

Methods: We prepared chronic glass-covered craniotomies in five adult transgenic mice expressing YFP in a subset of cortical pyramidal neurons [3]. 2PEF microscopy was used to visualize blood vessels labeled by intravenous injection of Texas-red dextran and YFP-labeled neurons (Fig. 1a). Microhemorrhages were produced by rupturing individual, specifically targeted PA using tightly-focused femtosecond laser pulses (Fig. 1b) [4]. Image stacks were taken at baseline and immediately, 1 hour, and 1, 3, and 7 days after the microhemorrhage. Dendrite morphologies were classified to identify signs of degeneration.

Results: The laser ablation used to cause the hemorrhage consistently caused the immediate blebbing of dendrites in an approximately 40 +/- 20 μm (mean +/- std. dev.) diameter region surrounding the target vessel (Zone1). After triggering vascular rupture, expanding blood plasma and red blood cells pushed the nearby dendrites outward as the targeted vessel bled, forming a sphere of approximately 120 +/- 40 μm diameter (Zone 2). Fluorescently-labeled plasma and diffuse red blood cells also penetrated into the tissue beyond this central sphere to a diameter of about 350 +/- 60 μm (Zone 3). As red blood cells and plasma are cleared away over days, the damaged and displaced dendrites in Zone 2 returned and blebbing was reduced. We observed no significant changes in dendrite morphology in Zone 3 at any time point in 10 out of 11 hemorrhages (Fig. 1 d, e, and f).

Conclusions: Chronic two-photon imaging of dendrites reveals that the pressure of blood entering the parenchyma after a microhemorrhage displaces and damages nearby dendrites, with some recovery after a few days. Surprisingly, dendrites further away from the target vessel that are exposed to blood plasma did not show signs of significant dendrite pathology acutely or out to one week post hemorrhage.

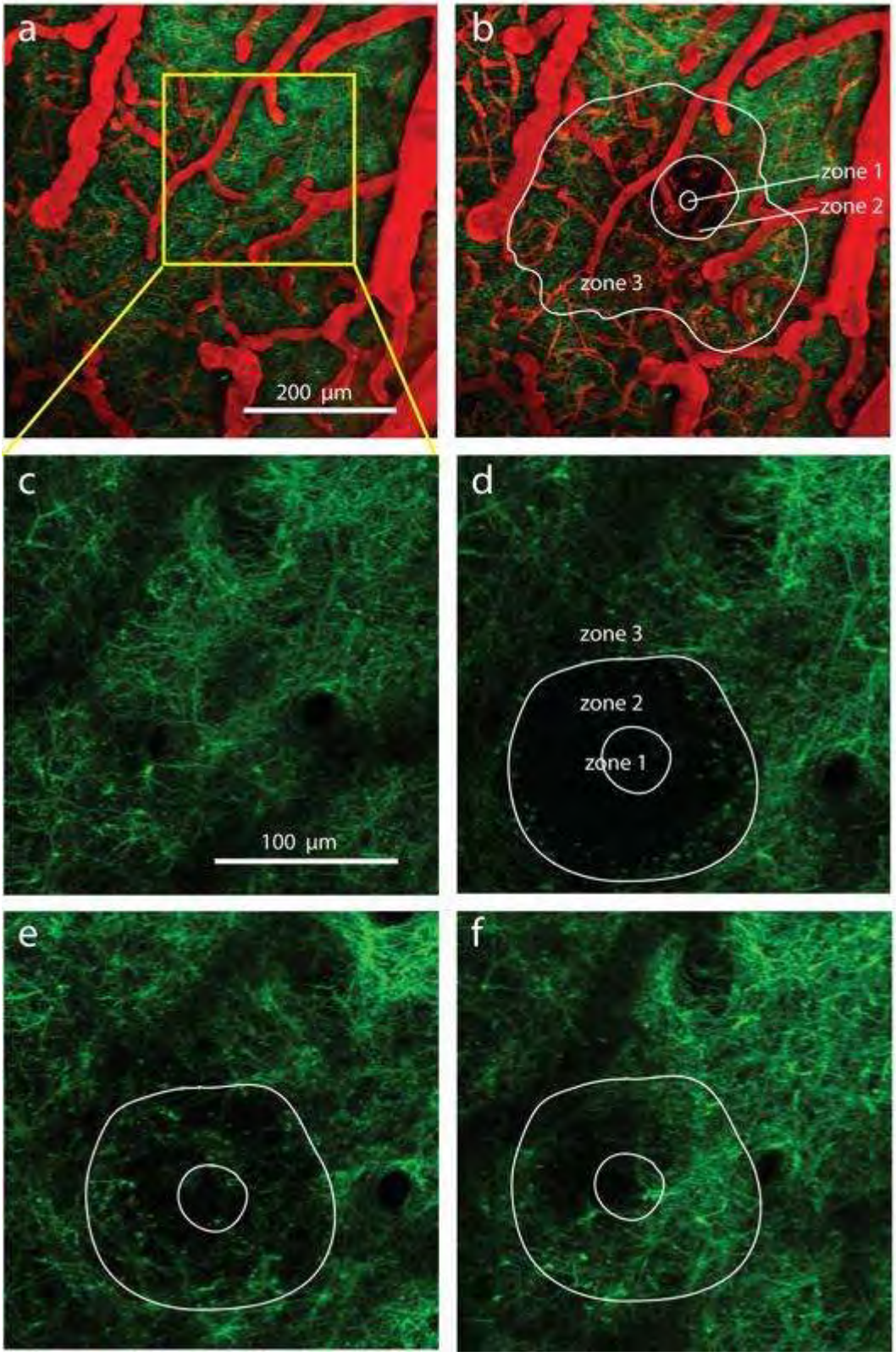

[Dendrite dynamics after microhemorrhage]

Fig. 1. 2PEF imaging of dendrites (green) and blood vessels (red) (a) before and (b) after

microhemorrhage. Dendrites (c) before, (d) immediately after, (e) 1 day and (f) 7 days after hemorrhage.

References:

1. Cullen KM, et al. J. Cere. Blood Flow Metab. (2005) 25, 1656.

2. Zhang S, et al. J. Neuro. (2005) 25, 5333.

3. Feng G, et al. Neuron (2000) 28, 41.

4. Nishimura N, et al. Nature Methods (2006) 3, 99.

586

BrainPET Poster Session: Brain Imaging: Stroke

DTI-PARAMETERS OF CORTICO-SPINAL TRACT INTEGRITY IN SUBACUTE SUBCORTICAL STROKE

B. Radlinska[1,2], S. Ghinani[1,2], I. Lepert[3], A. Thiel[1,2]

[1]Neurology & Neurosurgery, McGill University, [2]Neurological Sciences, SMBD Jewish General Hospital and Lady Davis Institute for Medical Research, [3]MR Imaging Unit, McConnell Brain Imaging Centre, Montreal, QC, Canada

Objectives: Studies investigating motor recovery after stroke have employed functional imaging to describe recovery related changes in functional cortical networks. The role of white matter damage for post-stroke recovery is less well understood. With diffusion tensor imaging (DTI), it became possible to image fiber tracts in the living human brain. The objective of this study is to determine to which extend different DTI parameters like fiber tract volume (FTV) and fractional anisotropy (FA) reflect damage to the corticospinal tract (CST) in subcortical stroke and how they are related to clinical symptoms.

Methods: We investigated 8 right-handed patients with first subcortical ischemic infarct affecting the CST within 10 days after stroke, as well as 5 age matched controls. DTI was performed on a 3T Siemens Trio scanner using a single-shot echo-planar sequence and parallel reconstruction. 64 x 2 diffusion weighted images were acquired using isotropically spaced diffusion encoding directions and a b value of 1000 s/mm^2 and a total of 2 images with b=0 s/mm^2 respectively. In the stroke hemispheres, fibers were traced retrogradely from a standardized seed region in the cerebral peduncle through the infarct using a deterministic algorithm (1,2). In non-affected hemispheres an identical seed region was used and tracts were traced through the posterior limb of the internal capsule. Mean FA within the tracts and FTV were compared within and between the groups and related to clinical severity (NIH scale). Tract portions above and below the level of the infarct/internal capsule were investigated separately.

Results: CST was successfully traced in both the affected and non-affected hemispheres of patients as well as in all controls. There were no significant differences in mean TVA and FA between left and right CST of controls (TVA_{LEFT} 11200 +/- 3034.263mm^3, TVA_{RIGHT} 10480 +/- 1885mm^3; FA_{LEFT} 0.499 +/- 0.0298, FA_{RIGHT} 0.494 +/- 0.0379). The CST volume of patients was significantly reduced on the affected side ($TVA_{AFFECTED}$ 4726 +/- 1660mm^3, $TVA_{NON\text{-}AFFECTED}$ 9896 +/- 3144mm^3, $P \leq 0.001$). Mean FA was also reduced in the affected CST ($FA_{AFFECTED}$ 0.425 +/- 0.0501, $FA_{NON\text{-}AFFECTED}$ 0.466 +/- 0.0310, $P \leq 0.10$). Furthermore, affected tracts in patients were significantly diminished in volume ($FTV_{AFFECTED}$ 4726 +/- 1660mm^3, $FTV_{CONTROL}$11200 +/- 3034 mm^3, $P < 0.01$) and FA ($FA_{AFFECTED}$ 0.425 +/- 0.0501, $FA_{CONTROL}$ 0.499 +/- 0.298, $P < 0.05$) relative to controls. This decrease in tract mean TVA and FA was significant both above ($P \leq 0.001$) and below ($P < 0.05$) the infarct within the patient group. The differences in TVA and FA were the same above and below the infarct. A loose correlation between FA and NIH score was found ($r=-0.73$, $P=0.1$).

Conclusions: Subcortical ischemic infarcts of the CST within 10 days of stroke onset significantly affect both mean CST volume and mean FA. Both parameters are significantly decreased within the stroke patients as well as relative to age matched controls independent of initial clinical symptom severity. The extent of FTV and FA decrease is the same along the entire CST.

References:

1. Mori S, et al. Ann Neurol 1999; 45:265-269.

2. Tuch DS, et al. Neuron 2003; 40(5):885-95.

587

Brain Poster Session: Neuroprotection

IGF-1 ATTENUATES ESTROGEN-MEDIATED NEUROTOXICITY IN A STROKE INJURY MODEL IN ACYCLIC FEMALE RATS

F. Sohrabji, A. Selvamani

Neuroscience and Experimental Therapeutics, Texas A&M Health Science Center, College Station, TX, USA

Previous work from our lab has shown that middle cerebral artery occlusion (MCAo) results in a larger cortical-striatal infarct in acyclic (reproductive senescent) females as compared to mature adult females that have normal, but lengthened, estrous cycles. Moreover, estrogen treatment to ovariectomized senescent females significantly increased infarct size, while estrogen replacement to ovariectomized mature adult females was neuroprotective. In order to understand the dimorphic role of estrogen in the mature adult and senescent brain, we examined reproductive age-related changes in IGF-1, a peptide that has been shown to:

a. be neuroprotective in stroke models,
b. decrease with advancing age and
c. downregulated by estrogen treatment in older females.

We found that circulating levels of IGF-1 were reduced in reproductive senescent females and further reduced by estrogen at both ages. We therefore tested whether IGF-1 administered to reproductive senescent females immediately after MCAo would decrease tissue damage in this group. Estrogen-treated and estrogen-deprived senescent females were subject to endothelin-1 mediated MCA occlusion and simultaneously infused with IGF-1 via a cannula implanted in the ventricle. At 7 days post-MCAo, animals were terminated and their brains analyzed for infarct size by TTC staining. As we reported previously, estrogen treatment increased infarct size in this group, while IGF-1 treatment completely abolished estrogen mediated neurotoxicity. Interestingly, IGF-1 treatment had no effect on the control (no estrogen) group, which suggests that IGF-1 interacts with estrogen to improve cell survival in the cortex. This is further supported by our second study where mature adult females were infused with the IGF-1 antagonist, JB-1. Here, too, JB-1 had no affect on the control (no estrogen) group, but abolished estrogen's neuroprotective effect on infarct size in this group. Cross-talk between estrogen and IGF-1 signaling pathways have been implicated in other adult neurodegenerative disease models and may also be implicated in stroke injury. Our findings support the hypothesis that aging- and estrogen-related changes in IGF-1 might be responsible for the significantly higher cortical damage in the reproductive senescent rats compared to their mature adult counterparts, and the disparate actions of estrogen in younger versus older females.

588

Brain Poster Session: Experimental Stroke & Cerebral Ischemia

LASER IRRADIATED THROMBUS FORMATION AND PLATELET BEHAVIOR IN MOUSE BRAIN MICROVASCULATURE OBSERVED BY INTRAVITAL FLUORESCENCE MICROSCOPY

K. Hattori[1], T. Fukuoka[1], N. Araki[2], N. Tanahashi[1]

[1]Neurology, Saitama International Medical Center, Saitama Medical University, Hidaka City, [2]Neurology, Saitama Medical University, Iruma-gun, Japan

Background and aims: Platelet behavior and thrombus formation in the microvasculature of the brain has not been fully investigated due to methodological difficulties. Photothrombosis using filtered light and a potent photosensitizing dye was occasionally applied to make vessel occlusions. However, the method is not satisfactory due to reproducibility, weak power etc. We developed an apparatus of laser induced thrombus formation in mouse brain microvasculature.

Purpose: The purpose of this study was to observe the process of laser irradiated thrombus formation and platelet behavior in the brain microvasculature of mice using intravital fluorescence microscopy.

Methods: C57 BL/6J mice (N=21) were anesthetized with chloral hydrate; their heads were fixed with a head holder, and a cranial window was made in the parietal region. Platelets were labeled in vivo by intravenous injection od carboxylfluorescein succinimidylester (CFSE). Laser irradiation (1250 mA, DPSS laser 532 nm, TS-KL/S2;Sankei) was spotted for 2-4 sec on pial microvessels to induce thrombus formation. Labeled platelets and thrombus were observed continuously with a fluorescence microscope.

Results: After laser irradiation to the pial artery, thrombus formed along the vessel wall immediately, and platelets accumulated on the surface of the thrombus leading to vessel occlusion and extended to the lesion of branch artery followed by spontaneous recannalization within 1-2 min (Figure). Fragmentation of thrombus was occasionally seen. Platelet adhesions to irradiated area were seen thereafter.

Laser irradiation to pial veins induced thrombus formation faster than that of pial arteries and occluded pial veins were hardly recannalized.

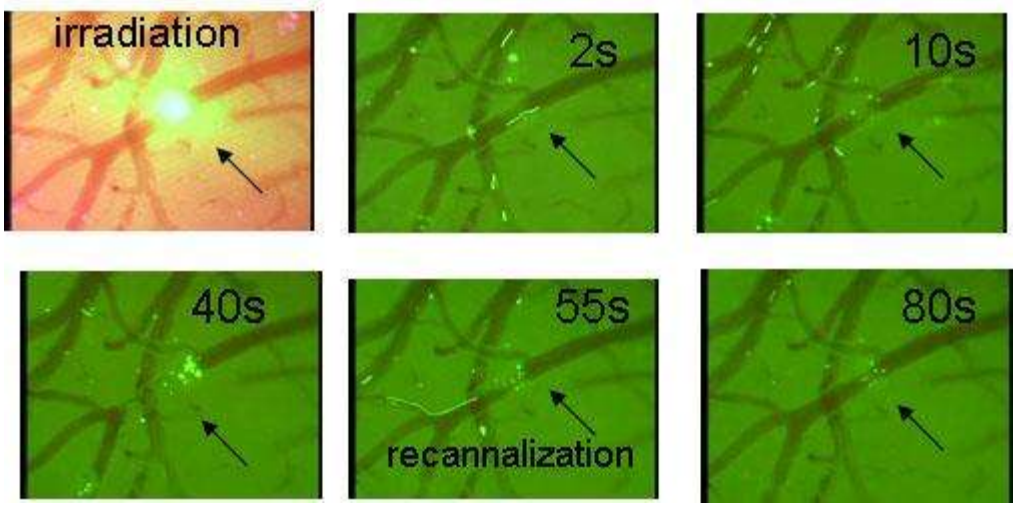

[Figure]

Conclusions: Laser irradiated thrombus formation is a promising method by which to investigate the pathophysiology of the interaction between platelets and endothelial cells.

589

Brain Poster Session: Stem Cells & Gene Therapy

NEURAL INDUCTION OF PERICYTE PROGENITOR CELLS FROM HUMAN PERIPHERAL BLOOD MONONUCLEAR CELL CULTURES

K.-H. Jung, K. Chu, S.-T. Lee, J.-S. Sunwoo, J.-J. Bahn, H.-K. Park, M. Kim, S.K. Lee, J.-K. Roh

Seoul National University Hospital, Seoul, South Korea

Background: Pericytes are located around vessels and contribute to vascular maintenance and vascular regeneration. It has long been suggested that pericytes may have stem/precursor cell potential. Our recent study has identified neural progenitor cells in peripheral blood mononuclear cells (PBMNCs) of acute stroke patients. However, there are still unsolved issues about the nature of circulating neural progenitors. Given that pericytes respond to injury, and regenerate the tissue, we hypothesized that neural progenitor cells outgrown from in vitro culture of PBMNCs might be tissue or bone marrow-derived pericyte progenitor cells (PPCs).

Methods: PBMNCs were isolated from the peripheral blood of 32 acute stroke patients, and 35 controls with risk factor-only. The fraction of pericytes in PBMNCs was measured using flow cytometry with anti-PDGFRβ or anti-NG2 antibodies. We investigated the association between characteristics of circulating PPCs and stroke phenotypes. We also developed the efficient protocols for mobilization, isolation, expansion, and neural induction of circulating PPCs.

Results: The fraction of circulating PPCs in PBMNCs was higher in acute stroke patients than control. These progenitor cells could be more efficiently isolated from acute stroke patients with greater NIHSS scores than risk factor-only group, suggesting that the circulating progenitor cells might be one marker of systemic resilience to ongoing tissue damage. PPCs could be efficiently mobilized by pharmacological stimulation, expanded ex vivo under hypoxia condition, and differentiate into a variety of neural cells under appropriate media conditions.

Conclusion: The feasibility of extracting and culturing PPCs in large numbers suggests that such autologous cells will be useful for applications ranging from basic research to cell-based therapy. Neural induction of PPCs from autologous peripheral blood makes them valuable candidates for transplantation therapy.

Brain Poster Session: Neuroprotection

BRAIN LIPID PEROXIDATION, RADICAL SCAVENGING EFFECTS AND ANTITUMOR ACTIVITY OF TAIWANESE BOTANY - YY-07 ON HUMAN GLIOBLASTOMA CELLS

Y.W. Yu[1], W.T. Huang[2], L.L. Yang[1]

[1]Department of Pharmcognosy, College of Pharmacy, Taipei Medical University, Taipei, [2]Division of Hemato-oncology/Chi-Mei Medical Center, Tainan, Taiwan R.O.C.

In the nervous system, reactive oxidative species (ROS) can cause neurodegenerative disorders, like Alzheimer's disease (AD), Huntington's disease (HD), Parkinson's disease (PD), amytrophic lateral sclerosis (ALS) and ataxia telangiectasia. Overproduction of ROS results in oxidative stress that can be an important mediator of damage lipids, proteins, and nucleic acids. Antioxidants prevent cellular damage by scavenging and inhibition of free radicals and prevention of pathologies. Oxidative stress has been implicated in the pathogenesis, including aging, atherosclerosis, diabetes mellitus, chronic inflammation and cancers. Gliomas are the most common type of primary brain tumor. Nearly two-thirds of gliomas are highly malignant lesions that account for a disproportionate share of brain tumor-related morbidity and mortality. Approximately 17,000 primary brain tumors are diagnosed every year, and of those, about 60% are gliomas. Tumors of gliol origin such as glioblastoma multiforme comprise the majority of human brain tumors. In this paper, 30 kinds of Taiwanese botany extracts were isolated from herbal medicine in our laboratory and their effects on 2,2-Diphenyl-1-picrylhydrazyl (DPPH) radical scavenging, superoxide anion radical scavenging, superoxide anion radical inhibition, ferrous ions chelating activities, ferric ion reducing antioxidant power (FRAP), lipid peroxidation, cell proliferation and potential cytotoxicity. The level of lipid peroxidation (LPO) was expressed as thiobarbituric acid reactive substances (TBARS). LPO product of MDA $(TBA)_2$ was induced by ferrous chloride and ferrous ammonium sulfate respectively on Wistar rat liver mitochondrias. and brain homogenates. We established screening program employing the 4,5-dimethylthiazol-2-yl)-2,5-diphenyltetrazolium bromide (MTT) reduction assay system utilizing the human malignant glioblastoma cell lines of GBM 8401 (astrocytoma-glioblastoma, grade III) and U-87 MG (astrocytoma- glioblastoma, grade IV) cells. One of the most potential compounds, YY-07 exhibited a significantly antioxidant and brain homogenate lipid peroxidation inhibition. It had also exhibited a dose dependent and time dependent manners in human malignant glioblastoma cells. The IC_{50} value of YY-07 after 24 hours were 81.09 ± 1.26 and 83.75 ± 2.17 μg/ml in GBM 8041 and U-87 MG, respectively. In addition, we had observed the apoptotic bodies in YY-07 treated GBM 8401 and U-87 MG. YY-07 may medicate the cytotoxicity via apoptosis in GBM 8401 and U-87 MG. Furthermore, we well evaluated the mechanism of apoptosis by western blot in the future.

FITC-LABELED RBC TRACKING IN ARTERIOLO-ARTERIOLAR ANASTOMOSES IN CONTROL STATE AND DURING ISCHEMIA AFTER MCA OCCLUSION IN MICE

H. Toriumi, J. Tatalishvili, M. Tomita, Y. Tomita, H. Hattori, M. Unekawa, N. Suzuki

Department of Neurology, School of Medicine, Keio University, Tokyo, Japan

Purpose: In arteriolo-arteriolar anastomoses (AAA) between MCA and MCA, blood had been hypothesized not to be actually flowing (watershed area) caught between two opposing arterial pressures, and only in occasions of one artery closure flow would get started as collaterals. To test this hypothesis we examined flow in AAA employing labeled RBC.

Methods: FITC-labeled RBC flow in AAA through a closed cranial window in 16 anesthetized C57BL/6J mice was examined in control state and after MCA occlusion (MCAO) employing a high speed camera laser scanning confocal fluorescence microscopy (Tomita et al., Microcirc 15, 163 (2008).

Results: When tracking RBC movements in AAA in control state, we noticed a paradoxical flow as shown in Figure 1: top panel, in which blood entered into an AAA from both MCA and ACA sides. The opposing blood flows collided at a meeting point and in some cases disappeared. White arrows indicate the direction of the flows. At the meeting point blood apparently sank into a hole of the origin of the penetrating arteriole, which was, mort of cases, not to be seen from above. Without FITC-labeled RBCs the confluent flow to the vertical direction had been missed. We found abundant such hidden “T-junctions” in AAAs; almost 2-3 per an AAA. However, dually fed confluent T-junction was only one per AAA. As shown in middle and bottom panels of Figure 1, dually fed junction was not fixed in position, but functionally liable to change from one to another with given hemodynamic conditions. Upon MCA occlusion, RBC flow immediately stopped at the MCA side but blood subsequently started to move to the retrograde direction towards MCA. The blood was supplied apparently from ACA. Figure 2 is a microphotograph in which 2 branches of MCA were seen where blood flow direction had been from top to bottom in control state. However, upon MCAO flow reversed in the right branch in all 7 cases studied ($p < 0.05$).

The blood apparently came from ACA through AAA, moved retrogradely towards the MCA stem and then branched off to supply to the left branch (arrows) with a great delay. When viewed from RBC velocities and numbers in capillaries in the ischemic tissue MCAO induced immediate RBC disappearance in the core ischemic region, and to a lesser extent in the penumbra near the AAA. Thus, unlike a general concept of “watershed”, the local blood flow near AAA was rather preserved. In preliminary experiments, we observed that AAAs became a center to develop collateral channels and key locations of angiogenesis in the marginal zone of ischemia.

Conclusions: In AAA blood was flowing even in control state towards a T-junction which was dually supplied both from MCA and ACA. The T-junction was functionally liable to change to a next T-junction. The so called watershed area near AAA appeared to be well supplied.

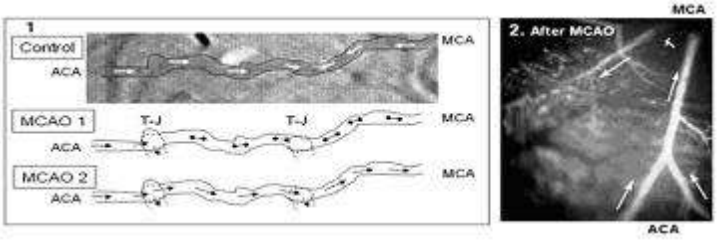

[Fig.1]

593

Brain Poster Session: Cerebral Vascular Regulation

SUSTAINED DILATION OF PIAL ARTERIOLES BY ARGINASE INHIBITION DURING PROLONGED MIDDLE CEREBRAL ARTERY OCCLUSION

S. Cao, D. Berkowitz, R. Koehler

Anesthesiology/Critical Care Medicine, Johns Hopkins University, Baltimore, MD, USA

Objectives: Administration of L-arginine (1) or endothelin antagonists (2,3) has been reported to increase intraischemic cerebral blood flow during middle cerebral artery (MCA) occlusion (MCAO). These observations raise the possibility that nitric oxide (NO) production is submaximal because of limited arginine availability and that reduced NO production promotes endothelin release during MCAO. In peripheral vessels, arginase activity can limit arginine availability for NO production (4). To determine if arginase activity limits vasodilation during MCAO, the diameter of pial arterioles in the ischemic border region was measured during cranial window superfusion with the arginase inhibitor ABH, [2(S)-amino-6-boronohexanoic acid]. Results were contrasted with those obtained by administration of L-arginine or the endothelin-A receptor antagonist BQ-610.

Methods: In isoflurane-anesthetized and mechanically ventilated rats, cranial windows were constructed over the MCA border region for measurement of pial arteriolar diameter. MCAO was produced for 2 h by the intraluminal filament technique.

Result: MCAO initially produced 38±9% (±SD) dilation that gradually subsided to 12±11% at 2 h of MCAO in the MCA border region in a control group superfused with artificial cerebrospinal fluid (n=8). Similar results were obtained in another control group with no cranial window superfusion. With superfusion of 1 μM of ABH throughout MCAO, the initial dilation of 38±10% was largely sustained (32±18%; n=6) at 2 h MCAO. With intravenous infusion of L-arginine (4 mmol/kg/h for 20 min + 2 mmol/kg/h for remainder of experiment), initial dilation after MCAO (40±14%) was better maintained at 2h MCAO (25±13%, n=7) than in a control group (initial dilation 37±8%; 7±15% at 2 h; n=9). Likewise, superfusion of 3 μM of BQ610 during MCAO prevented the loss of pial arteriolar dilation (32±7% to 32±15%; n=8) compared to a control group superfused with vehicle (0.02% DMSO; 34±4% to 5±10%; n=9). Intravenous injection of BQ610 (0.5 μmol/kg; n=5) at 90 min of MCAO increased laser-Doppler flow in the cortical border region from 43±19% to 69±20% of pre-ischemic baseline, thereby demonstrating that flow can be increased at a time when pial arterioles have a diminished dilation. Furthermore, intravenous injection of ABH (dose in 3μmol/kg; n=4) at 90 min of MCAO increased LDF from 41±28% to 76±44% of pre-ischemic baseline, thereby indicating that an arginase inhibitor was as effective as an endothelin antagonist in improving perfusion in the border region. Mean arterial blood pressure and blood gases were unchanged in all groups.

Conclusion: These results indicate that both arginase activity and endothelin-A receptor activation contribute to the gradual loss of pial arteriolar dilation in the ischemic border region during prolonged MCAO. We speculate that increased arginase activity decreases endothelial NO production, which then leads to increased release of endothelin.

References:

1. Morikawa et al. Stroke. 1994; 25:429-35.

2. Patel et al. J Cereb Blood Flow Metabol. 1996; 16: 950-8.

3. Zhang et al. Brain Res. 2005; 1045: 150-6.

4. Santhanam et al. Circ Res. 2007; 101:692-702.

Brain Poster Session: Spreading Depression

'NORMAL' AND 'INVERSE' NEUROVASCULAR COUPLING TO CORTICAL SPREADING DEPOLARIZATION (CSD) IN THE HUMAN BRAIN

S. Major[1,2,3], J. Woitzik[4], C. Drenckhahn[1,2,3], J.A. Hartings[5], M. Fabricius[6], A.J. Strong[7], J.P. Dreier[1,2,3]

[1]Neurology, [2]Experimental Neurology, [3]Center for Stroke Research (CSB) Berlin, [4]Neurosurgery, Charité - University Medicine Berlin, Berlin, Germany, [5]Neurosurgery, University of Cincinnati, Cincinnati, OH, USA, [6]Clinical Neurophysiology, University of Copenhagen, Glostrup Hospital, Copenhagen, Denmark, [7]Neurosurgery, King's College, London, UK

Background: CSD is a wave of neuronal depolarization which propagates in the cortex at a rate of ~3 mm/min. It induces vasodilation in healthy tissue. Hence, regional cerebral blood flow (rCBF) increases in response to CSD, a process termed 'normal' neurovascular coupling. Only after the neuronal repolarization, the vasodilation is followed by mild vasoconstriction resulting in spreading oligemia. The opposite of this 'normal' neurovascular response, termed 'inverse' neurovascular coupling, occurs when there is local dysfunction of the microvasculature. With 'inverse' coupling, severe microvascular spasm instead of vasodilation is coupled to CSD (Dreier et al. [1998] J. Cereb. Blood Flow Metab., 18, 978-990). The resulting spreading perfusion deficit in turn prolongs the neuronal depolarization (as reflected by a prolonged negative shift of the direct current (DC) potential) since the oxygen-/glucose deprivation further reduces ATP availability. Thus, in animal experiments, a prolonged negative cortical DC shift, the defining electrophysiologic feature of 'inverse' neurovascular coupling, indicates that the hypoperfusion is significant enough to produce a mismatch between neuronal energy demand and supply. Accordingly, the term 'cortical spreading ischemia' describes the CSD-induced initial perfusion deficit when it leads to a prolonged negative cortical DC shift. Here we studied the occurrence of 'normal' and 'inverse' coupling in aneurysmal subarachnoid hemorrhage (aSAH) patients.

Methods: A prospective study was performed in thirteen patients with aSAH using subdural opto-/electrodes for simultaneous laser-Doppler flowmetry and DC-electrocorticography (DC-ECoG) combined with measurements of tissue partial pressure of oxygen ($ptiO_2$). CSDs occurring in temporal clusters and in isolation were analyzed separately. Of each patient the isolated CSD with the longest ECoG depression period was analyzed here.

Results: Twelve patients showed isolated CSDs with a propagation velocity of 2.1 (1.8, 2.9) mm/min. The DC potential showed a negative shift of -10.8 (-9.7, -13.7) mV (duration: 153 [123, 283] s). Four of 12 CSDs analyzed displayed 'normal' neurovascular coupling since the predominant response was the initial hyperemia (257 (211, 311)% lasting for 689 (512, 812) s) followed by spreading oligemia to 92 (79, 102)%. Another three of the 12 CSDs did not show any significant change in level of rCBF. This behavior was rated as neurovascular 'uncoupling'. 'Inverse' coupling was observed in the remaining 5 of 12 isolated CSDs and was characterized by the following:

i. the DC potential change preceded the initial hypoperfusion by 65 (16, 83) s;
ii. rCBF fell to 59 (31, 62)% lasting for 118 (88, 265) s;
iii. the local hypoperfusion propagated with the cortical DC potential negativity in the tissue at a rate of 3.5 (1.6, 3.5) mm/min.

Linear regression found that the durations of the initial hypoperfusion and the cortical DC potential negativity were significantly correlated ($R=0.92$, $P< 0.001$, $n=8$). Moreover, linear regression

demonstrated a significant correlation between initial changes in level of rCBF and $ptiO_2$ in response to CSD (R=0.84, P=0.019, n=7).

Conclusion: Similar to animal experiments, 'normal' and 'inverse' coupling occur in the human brain. Thus, 'inverse' coupling is identified as a novel human disease mechanism and potential target for therapeutic intervention.

600

Brain Poster Session: Ischemic Preconditioning

HYPOXIC PRECONDITIONING REDUCES HYPOXIA-ISCHEMIA-INDUCED CELL PROLIFERATION IN THE RAT SUBVENTRICULAR ZONE

N. Jones[1], L. Kardashyan[2], P. Beart[2]

[1]Pharmacology, School of Medical Sciences, University of New South Wales, Sydney, NSW,
[2]Howard Florey Institute, The University of Melbourne, Melbourne, VIC, Australia

Objectives: Preconditioning with mild hypoxia and the hypoxia-mimetic compounds desferrioxamine (DFX) and cobalt chloride ($CoCl_2$) have been shown to have protective actions against a subsequent hypoxic-ischaemic (HI) brain insult. These treatments alone are not sufficient to cause neuronal injury, but can induce changes in gene expression and intracellular signalling pathways. The expression of the hypoxia-inducible transcription factor (HIF-1) (1) and several HIF-1 target genes (2) are up-regulated after preconditioning with hypoxia and mimetics in neonatal rat brain. Interestingly, many HIF-1 target genes (including erythropoietin and VEGF) have been shown to increase cell proliferation in the brain (3). We have investigated whether preconditioning treatments that can increase HIF-1 have long lasting neuroprotective actions and alter cell proliferation up to 5 weeks after an HI insult.

Methods: Sprague Dawley rats (postnatal day 6 (p6)) were exposed to preconditioning with hypoxia (3h, 8% oxygen), normoxia (3h, room air) or injected with DFX (200mg/kg, i.p.) or $CoCl_2$ (60mg/kg, i.p.). On p7, all pups were subjected to HI or sham surgery. Bromodeoxyuridine (BrdU, 50mg/kg, i.p) was injected twice daily for 3 days following surgery and was used to examine cell proliferation. At 5 weeks after HI insult, brains were collected for imunohistochemical and histological processing.

Results: Hypoxia, DFX and $CoCl_2$ preconditioning all significantly reduced the extent of brain injury after HI insult as measured using Nissl staining and MCID analysis. Cell proliferation was examined using immunohistochemistry for BrdU and cell counts were obtained from the subventricular zone (SVZ). HI alone significantly increased (by 106%) the number of BrdU positive cells in SVZ compared to sham operated controls. Preconditioning with hypoxia and DFX performed 24h prior to HI, reduced cell proliferation in SVZ by 28% and 33%, respectively, compared to animals which received HI alone. CoCl2 preconditioning had no effect on HI-induced cell proliferation in the SVZ. Interestingly, treatment with DFX alone, significantly increased the number of BrdU positive cells in SVZ compared to controls by 172%.

Conclusions: Modulation of HIF-1 and its target genes is likely to be involved in the brain plasticity and neuroprotective effects conferred by preconditioning with hypoxia, DFX and $CoCl_2$ in neonatal rat brain.

References:

(1) Bergeron et al (2000) Role of hypoxia-inducible factor-1 in hypoxia-induced ischemic tolerance in neonatal rat brain. Ann Neurol. 48: 285-96.

(2) Jones & Bergeron (2001) Hypoxic preconditioning induces changes in HIF-1 target genes in neonatal rat brain. J Cereb Blood Flow Metab. 21: 1105-14.

(3) Sharp & Bernaudin (2004) HIF1 and oxygen sensing in the brain. Nature Rev. Neurosci. 5: 437-48.

SONIC HEDGEHOG ATTENUATES BRAIN INFARCTION IN RAT FOCAL ISCHEMIA

D.-I. Yang[1], S.-S. Huang[2]

[1]Institute of Brain Science, National Yang-Ming University, Taipei, [2]Department of Pharmacology, Chung Shan Medical University, Taichung, Taiwan R.O.C.

Objective: Sonic hedgehog (Shh), a morphogen well known for its critical roles in embryonic development, has recently been shown to carry protective effects against ischemia/reperfusion. Shh gene therapy protected against myocardial ischemia by triggering expression of multiple trophic factors and engendering tissue repair in the adult heart (Kusano et al., 2005). Shh is also a critical factor in the pathophysiology of tissue injury induced by ischemia/reperfusion in liver (Tuncer et al., 2007) and kidney (Ozturk et al., 2007). In this study, we test whether topical application of the biologically active N-terminal domain of sonic hedgehog (Shh-N) may exert protective effects against ischemic insults in a rat model of middle cerebral artery occlusion (MCAO).

Methods: Male Sprague-Dawley rats were subjected to MCAO for 60 min. At the onset of reperfusion, fibrin glues (20 microliter) containing Shh-N and/or its inhibitor cyclopamine (CPM) were applied to the ipsilateral cortices. After reperfusion for 7 days, animals were sacrificed and brains removed for triphenyl tetrazolium chloride (TTC) staining. Data are expressed as Mean±S.E.M. Results shown were derived from combination of at least three independent experiments.

Results: Shh-N at 100, 300, and 1000 ng/ml substantially attenuated brain infarction caused by MCAO. The control animals treated with vehicle alone (0.1% BSA) exhibited infarct volumes of 139.5±23.0 mm^3 (N=7). Application of Shh-N at 30 ng/ml was without effects (150.4±23.2 mm^3; N=6). However, Shh-N at 100 ng/ml (62.94±20.3 mm^3; N=7, $P< 0.05$), 300 ng/ml (75.3±13.4 mm^3; N=8, $P< 0.05$), and 1000 ng/ml (47.5±19.1 mm^3; N=7, $P< 0.01$) significantly reduced the extent of cerebral infarction. Furthermore, while Shh-N at 300 ng/ml reduced infarct volumes (84.0±7.4 mm^3 in Shh-N-treated rats, N=14, versus 136.8±21.0 mm^3 in control rats with BSA only, N=11, $P< 0.01$), co-treatment of its pharmacological inhibitor CPM (10 micromolar) completely abolished this effect (84.0±7.4 mm^3 in Shh-N-treated rats, N=14, versus 170.2±20.1 mm^3 in rats with Shh-N plus CPM, N=7, $P< 0.001$). CPM alone was without effects in attenuating brain infarction (179.6±9.6 mm^3, N=7).

Conclusion: Shh may exert neuroprotective effects in cerebral ischemia in addition to its established roles in neural development. Pharmacological activation of signal transduction pathways downstream of Shh may therefore carry therapeutic potential in ischemic stroke.

References:

1. Kusano et al., 2005. Sonic hedgehog myocardial gene therapy: tissue repair through transient reconstitution of embryonic signaling. Nat Med 11:1197-1204.

2. Ozturk et al., 2007. Nitric oxide regulates expression of Sonic hedgehog and hypoxia-inducible factor-1alpha in an experimental model of kidney ischemia-reperfusion. Ren Fail 29:249-256.

3. Tuncer et al., 2007. Interaction of L-arginine-methyl ester and Sonic hedgehog in liver ischemia-reperfusion injury in the rats. World J Gastroenterol 13:3841-3846.

602

Brain Oral Session: Functional Brain Imaging

SPATIOTEMPORAL COMPLEXITY IN THE HAEMODYNAMIC RESPONSE TO SOMATOSENSORY STIMULATION IN THE UN-ANAESTHETIZED RAT

C. Martin[1], J. Berwick[2], A. Kennerley[2], Y. Zheng[2], J. Mayhew[2]

[1]Department of Physiology, Anatomy and Genetics, University of Oxford, Oxford, [2]Department of Psychology, The University of Sheffield, Sheffield, UK

Background and aims: Blood oxygen level dependent (BOLD) signals are used in functional magnetic resonance imaging (fMRI) to localize and quantify task-dependent changes in brain activity. As the BOLD signal is an indirect marker of neural activity, characterization of both the spatial and temporal haemodynamic response functions (changes in cerebral blood flow, volume and oxygen consumption) are critical for the accurate interpretation of functional imaging data. Our goal in this study was to use optical imaging spectroscopy (OIS) in a previously developed un-anesthetized rat model to extend current understanding of the spatiotemporal haemodynamic changes that underlie both positive and negative BOLD signals. OIS measures changes in the spectrum of remitted light from brain tissue which can be compared to known absorption spectra in order to calculate changes in haemoglobin concentration and oxygenation.

Methods: Under surgical anaesthesia the skull was exposed and a section overlying somatosensory cortex was thinned to translucency. An imaging chamber was then placed over the thinned region of skull and secured with skull screws and dental cement. To deliver electrical stimulation to the awake animals, Teflon coated tungsten microwires were chronically implanted into the contralateral whisker pad and fed subcutaneously to a connector adjacent to the imaging chamber. The animals were treated with an analgesic and left to recover for 3-5 days. For each imaging experiment, trained animals were placed into a harness and to reduce head movements, a pneumatically operated clamp secured the implanted imaging chamber and therefore the head. A medical endoscope was used to provide both illumination of the cortex and transmission of the remitted images to a digital camera. Stimulation consisted of a 16-second, 5Hz pulse train (0.4mA) with an individual pulse width of 0.3ms. The spectral analysis of remitted images produced 2-D maps, over time, of changes in oxyhaemoglobin (HbO_2), deoxyhaemoglobin (Hbr) and total haemoglobin (HbT) concentration (**A**).

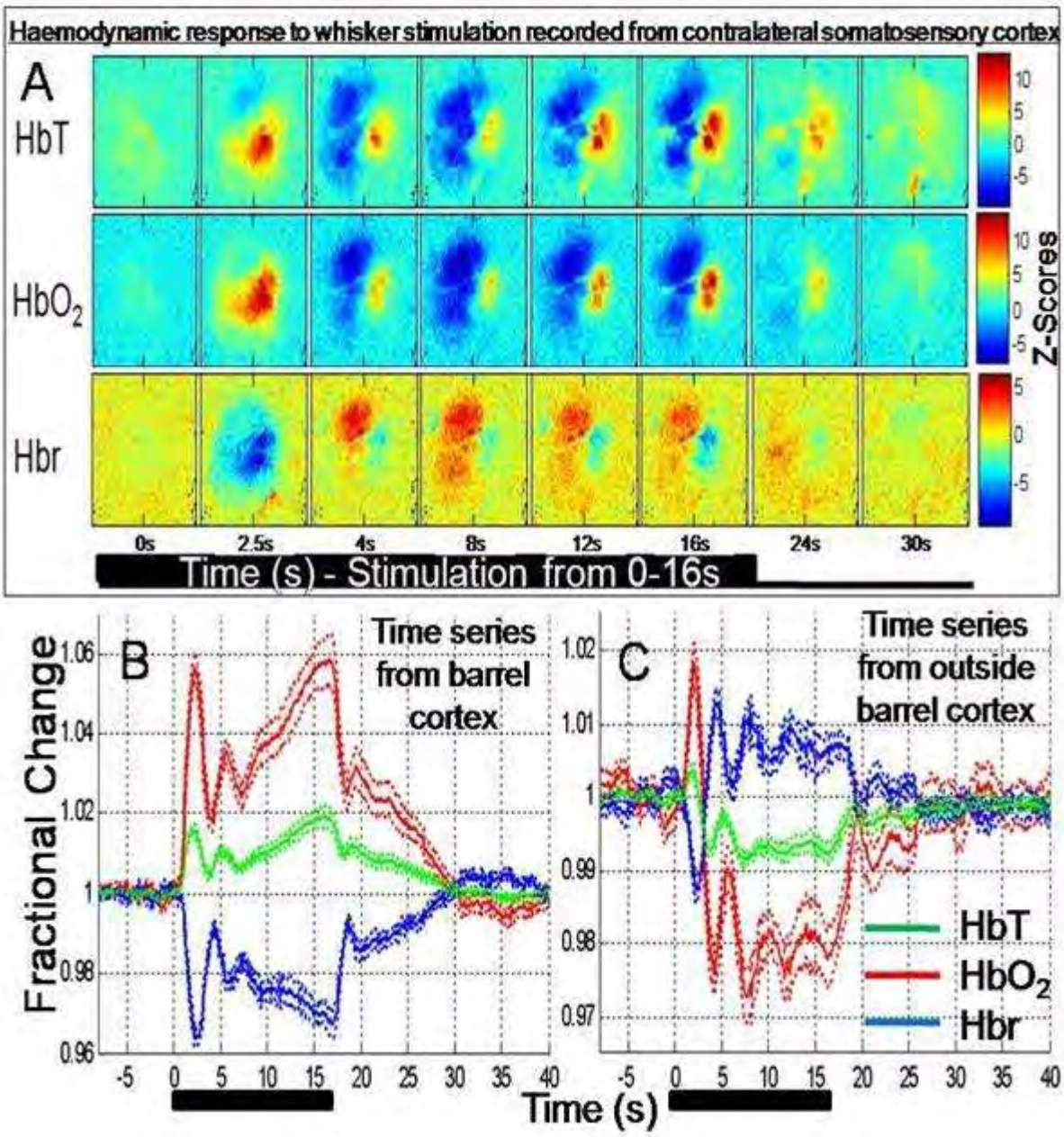

[Fig1]

Results and conclusions: The main finding of this study was that monotonic stimulation of the contralateral whisker pad in awake rats led to a complex spatiotemporal haemodynamic response in cortex. In addition to regions exhibiting a haemodynamic response predictive of a positive BOLD signal (increased HbO_2 & HbT, decreased Hbr - **A&B**), large regions of somatosensory cortex displayed an inverted haemodynamic response (decreased HbO_2 & HbT, increased Hbr) that is predictive of a negative BOLD signal (**A&C**). The magnitude and spatial extent of these signals varied during the stimulation period and furthermore, some regions of cortex were characterised by 'biphasic' haemodynamic changes, where initial signal increases in response to stimulation onset were followed by below baseline signal decreases as stimulation continued (**C**). These findings may have important implications for our understanding of the haemodynamic changes that underlie positive and negative BOLD signals.

DEVELOPMENT OF STEADY-STATE METHOD COMBINING BOLUS AND INCRESCENT INJECTION WITH A MULTI-PROGRAMMING SYRINGE PUMP

M. Kobayashi[1], Y. Michibata[2], R. Maruyama[1], Y. Higaki[3], Y. Kiyono[1], T. Kudo[1], T. Tsujikawa[1], Y. Yoshii[1], A. Waki[1], K. Kawai[1,3], Y. Fujibayashi[1], **H. Okazawa**[1]

[1]Biomedical Imaging Research Center, University of Fukui, [2]Faculty of Engineering, University of Fukui, Fukui, [3]Graduate School of Medical Science, Kanazawa University, Kanazawa, Japan

Objectives: Multipoint arterial blood sampling after radiotracer injection is usually required for precise quantification on PET study. When multiple scans are required in the same animal, however, the number of blood sampling is limited because of small blood volume in animals. In this study, we developed a new tracer injection method to apply the $H_2{}^{15}O$ steady-state (SS) method which needs only a few blood sampling points to measure cerebral blood flow (CBF).

Methods: We designed a program for $H_2{}^{15}O$ injection combining bolus and slowly increscent (B/I) injection manner to reduce time for achieving an equilibrium of blood radioactivity in the $H_2{}^{15}O$ SS method. In this program, $H_2{}^{15}O$ was injected rapidly for 45 sec to fill the dead volume of injection tube and increase blood radioactivity, followed by gradual administration to compensate decay of ^{15}O radioactivity in the blood. Efficacy of the program of $H_2{}^{15}O$ B/I injection to achieve fixed radioactivity was evaluated using a dose meter. Then, eight rats were studied with a small animal PET scanner. Small catheters were inserted into the femoral artery for blood sampling and the femoral vein for $H_2{}^{15}O$ administration. Before emission scans, a transmission scan was performed for 60 min using $^{68}Ge/^{68}Ga$. Six-minute list-mode PET scans were initiated at intravenous administration of 555 MBq/ml $H_2{}^{15}O$ using the B/I injection program with the syringe pump. Arterial blood was sampled every 1 min during PET scans. Fifteen minutes after the $H_2{}^{15}O$ PET scan, N-isopropyl-p-[^{125}I]-iodoamphetamine (^{125}I-IMP) was injected in the same rat and arterial blood was withdrawn at a constant rate for 10 min after tracer administration using the syringe pump. The rat brain was immediately removed and exposed to imaging plate for autoradiography. We selected similar 3 slices from $H_2{}^{15}O$ PET and ^{125}I-IMP autoradiography images. Regions of interest (ROIs) were placed at whole brain on the slices in each radiotracer image. CBF from $H_2{}^{15}O$ SS method and that calculated from ^{125}I-IMP-autoradiography based on microsphere model were compared.

Results: The radioactivity of $H_2{}^{15}O$ administered by the B/I injection program achieved equilibrium at approximately 20 MBq in a dose meter. In the rat study, radioactivity concentration of $H_2{}^{15}O$ rapidly achieved equilibrium in the blood and brain at approximately 2 min after administration (Figure). Correlation of the CBF values of $H_2{}^{15}O$ (48.6±5.8 mL/100g/min) using SS method and those of ^{125}I-IMP (48.8±5.8 mL/100g/min) was excellent ($y=0.99x+0.21$, $R^2=0.98$).

Conclusion: The SS method with the B/I injection is useful for CBF measurement on small animal study and can be applied for animal and human PET studies using many radiotracers with short half life.

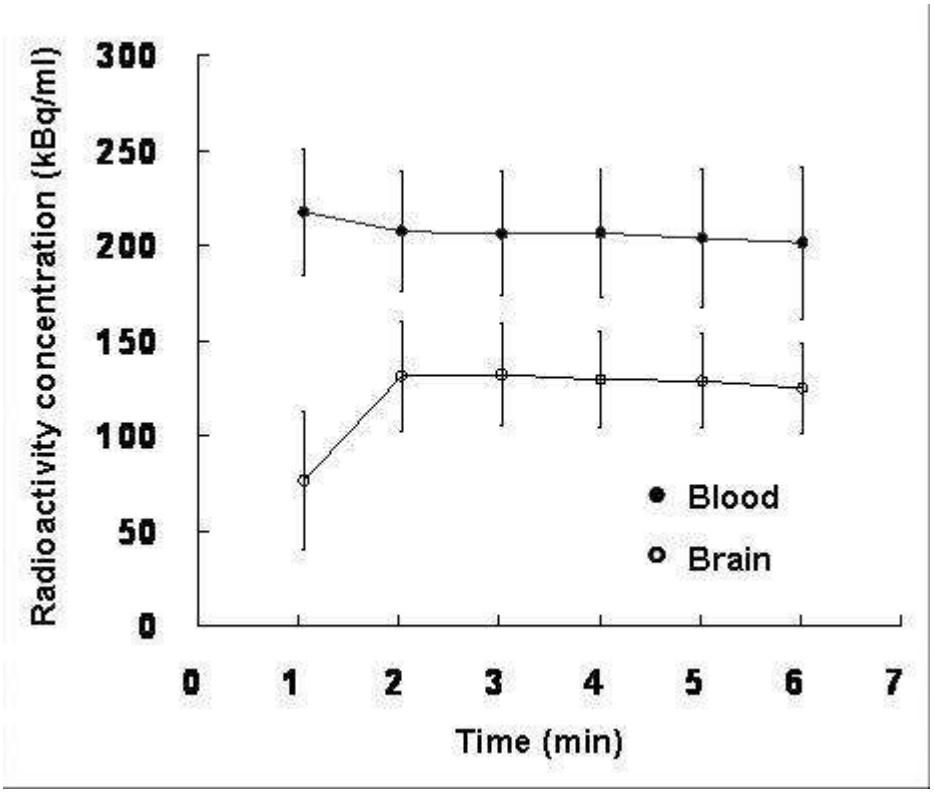

[Radioactivity concentration in blood and brain]

LONGITUDINAL MRI CHARACTERIZATION OF STROKE IN ISCHEMIA TOLERANT RATS

J. Artmann[1], M. Weller[2], E. Wong[3], **S. Wegener**[2]

[1]Neurology, University and ETH Zurich, [2]Neurology, University Zurich, Zürich, Switzerland, [3]Radiology and Psychiatry, University California San Diego, La Jolla, CA, USA

Objectives: The individual vulnerability to ischemia has a significant impact on tissue damage and outcome in stroke patients. Therapeutic interventions could be much better tailored to the patient if information about the individual resistance to ischemic injury was available. Tolerance to ischemia can be induced experimentally by "preconditioning". One preconditioning model that has been used to render the brain more tolerant to ischemia is the injection of 3-nitroproprionic acid (3NPA), a respiratory chain inhibitor. We used longitudinal MRI in adult rats to characterize how preconditioning with 3NPA affects the development of a stroke lesion and if a typical "MRI signature" of preconditioned tissue can be extracted from these data.

Methods: Adult Wistar rats received i.p. injections of 20 mg/kg 3NPA or saline and were subjected to transient (60 min) middle cerebral artery occlusion (MCAO) three days later. MR images were acquired during the occlusion (day 0) and after reperfusion (days 1, 4, 14). Quantitative CBF maps were obtained using flow-sensitive alternating inversion recovery (FAIR) arterial spin labeling with the QUIPSSII modification. In addition, diffusion-weighted (DWI) images, T1 and T2 maps and anatomical T2w images were obtained. Functional deficits were assessed at each time point using a modified neurologic deficit scale. Brains were analyzed using immunofluorescence and immunohistochemical techniques.

Results: At 15 min after insertion of the occluding device, the extent of the initial lesion on apparent diffusion coefficient (ADC) maps was similar between groups. Over the next 30 min of MCAO, however, there was a remarkable ADC recovery in the 3NPA group (Figure 1). During MCAO, preconditioned animals had fewer voxels with severely compromised CBF than controls. CBF on the unaffected side was lower in the 3NPA group during ischemia. A similarly low CBF was also found in 3NPA- preconditioned animals without stroke (data not shown). On day 14, infarcts were smaller and functional deficits less severe in the 3NPA group. However, rescue of neurons on the ischemic side was incomplete in 3NPA animals. There were no signs of tissue necrosis similar to controls, but in the ipsilateral striatum and layers II-III of the somatosensory cortex, selective neuronal death, gliosis and a mild inflammatory infiltrate were detected.

Conclusions: Even with a large initial lesion on ADC maps, tissue recovery was substantial in 3NPA-preconditioned animals. This was associated with a better functional outcome. On MRI, the 3NPA group showed higher intra-ischemic residual CBF, rapid intra-ischemic ADC recovery, less structural damage over time (depicted on fractional anisotropy, T2-w and T1-w images) and lower CBF values on the unaffected hemisphere. The latter could indicate vascular/metabolic adjustments of ischemia tolerance. Thus, MRI might have the potential to discriminate ischemia tolerant from vulnerable brains.

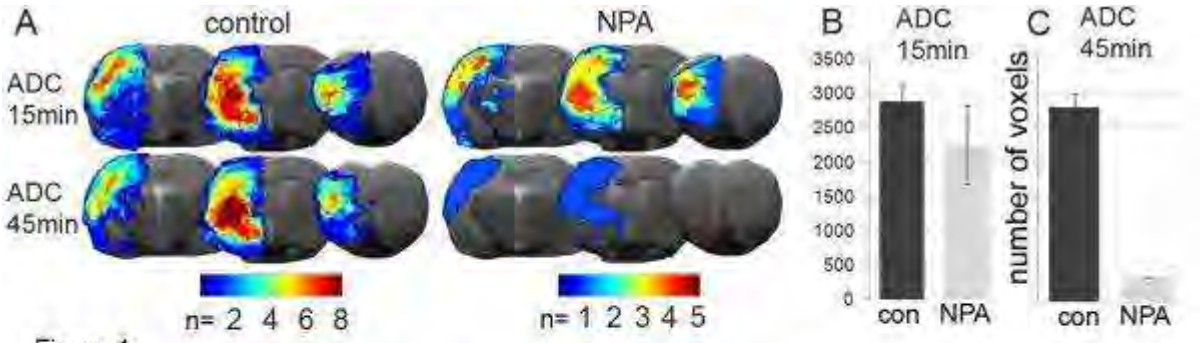

Figure 1:
A) Masks of the ischemic lesion from individual animals of the control or NPA-preconditioned group generated from ADC maps acquired 15 (upper panel) or 45 (lower panel) minutes after the onset of MCAO. Masks are overlaid onto anatomical (T2w) images.Regions of overlap between individual masks are color coded. While the ischemic area is similar 15 and 45 min after onset of the vascular occlusion in controls, there is a dramatic recovery in the NPA group.
B and C) Number of voxels with a significantly reduced ADC in both groups (mean +/- SE of mean). While the lesion depicted on ADC maps is of similar size 15 min after start of the occlusion (B), it is much smaller in NPA treated animals at 45 min.

[Figure 1]

605

Brain Poster Session: Experimental Stroke & Cerebral Ischemia

EFFECTS OF CILNIDIPINE ON NO PRODUCTION AND ISCHEMIC CHANGE OF HIPPOCAMPAL CA1 NEURONS DURING CEREBRAL ISCHEMIA AND REPERFUSION IN MICE

Y. Kato, T. Ohkubo, Y. Asano, K. Hattori, T. Shimazu, M. Yamazato, H. Nagoya, Y. Ito, **N. Araki**

Neurology, Saitama Medical University, Saitama, Japan

Introduction: Cilnidipine, an L/N-type Ca^{2+} channel blocker, has been reported to suppress ischemic brain injury in several animal models. The present study investigates the effects of cilnidipine on nitric oxide (NO) production and ischemic change of hippocampal CA1 neurons during forebrain ischemia and reperfusion.

Methods: Male mice (cilnidipine group; n=9, control group; n=17) were anesthetized by inhalation of halothane. NO production was continuously monitored by in vivo microdialysis. Microdialysis probes were inserted into the left striatum and were perfused with Ringer's solution at a constant rate 2µl/min. A laser Doppler probe was placed on the right skull surface. After 2 hours equilibrium period, fractions were collected every 10 minutes. Forebrain cerebral ischemia was produced by clipping both common carotid arteries using Zen clip for 10 minutes. Before 30 minutes of ischemia, 50 µg/kg of cilnidipine was intraperitoneally administered. Levels of nitric oxide metabolites, nitrite (NO_2^-) and nitrate (NO_3^-), in the dialysate were determined using the Griess reaction. (2) Analysis of hippocampus CA1 neurons: Two hours after the start of reperfusion, animals were perfused with 4% paraformaldehyde. Hippocampal CA1 neurons were analyzed into three phases (severe ischemia, moderate ischemia, survive), and the ratio of the number of surviving neurons was calculated (survival rate). (3) Brain sections were immunostained with an anti-nNOS antibody. To determine the fractional area density of nNOS-immunoreactive pixels to total pixels of the whole field, the captured images were analyzed. Mann-Whitney U test was used for group comparisons.

Results:

1. Blood Pressure [Fig.1]: Cilnidipine group showed significantly higher blood pressure than that of control group before the administration of cilnidipine, but blood pressure of both groups become almost same when ischemia started.
2. Cerebral Blood Flow (CBF) [Fig.1]: There were no significant differences in CBF during ischemia. CBF of cilnidipine group (64.2 ± 14.0) was significantly higher than that of control group (49.0 ± 11.6) in 80 minutes after the start of reperfusion.
3. NO Metabolism: 1) NO_2^- (% change): The level of NO_2^- in cilnidipine group was significantly higher than that of control group during ischemia (87.6 ± 35.0 vs. 65.3 ± 18.7 %) and in 10 minutes (104.6 ± 51.0 vs. 77.9 ± 19.4) after reperfusion. 2) NO_3^- (% change): There were no significant differences in the level of NO_3^- between cilnidipine and control group.
4. Survival rate in hippocampus CA1 area: There were no significant differences between the both groups.
5. nNOS activity: The percentage of nNOS-immunoreactive pixels to whole area in cilnidipine group (0.84 ± 0.16 %) was significantly lower than that of the control group (1.96 ± 0.53 %).

Conclusion: These data suggest that cilnidipine may improve CBF by activating eNOS rather than nNOS.

<Fig. 1>

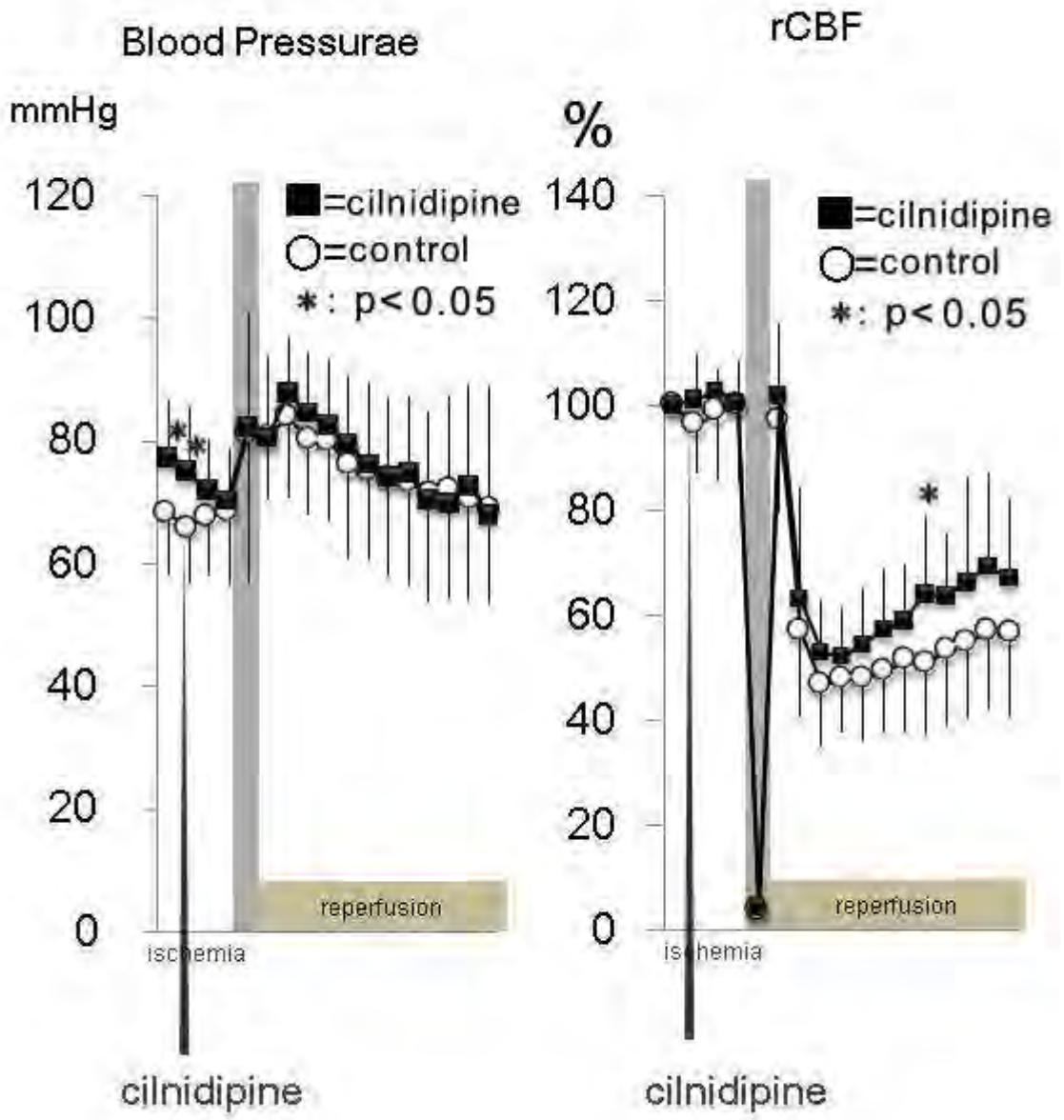
Blood Pressurae
mmHg
120
100
80
60
40
20
0
■=cilnidipine
○=control
*: p<0.05
reperfusion
ischemia
cilnidipine
rCBF
%
140
120
100
80
60
40
20
0
■=cilnidipine
○=control
*: p<0.05
reperfusion
ischemia
cilnidipine

[Fig. 1]

607

Brain Poster Session: Experimental Stroke & Cerebral Ischemia

IDENTIFICATION OF EARLY METABOLIC MARKERS OF VARIOUS DEGREES OF ISCHEMIA IN THE MOUSE BRAIN BY LOCALIZED ^{1}H MAGNETIC RESONANCE SPECTROSCOPY

C. Berthet[1], H. Lei[2,3], R. Gruetter[2,3], **L. Hirt**[1]

[1]Neurology, CHUV, [2]LIFMET, EPFL, [3]Radiology, UNIL, Lausanne, Switzerland

Objectives: Magnetic resonance (MR) imaging and spectroscopy (MRS) allow the establishment of the anatomical evolution and neurochemical profiles of ischemic lesions. The aim of the present study was to identify markers of reversible and irreversible damage by comparing the effects of 10-min middle cerebral artery occlusion (MCAO), mimicking a transient ischemic attack, with the effects of 30-min MCAO, inducing a striatal lesion.

Methods: ICR-CD1 mice were subjected to 10-minutes (n=11) or 30-minutes (n=9) endoluminal MCAO by filament technique at 0h. The regional cerebral blood flow (CBF) was monitored in all animals by laser-Doppler flowmetry with a flexible probe fixed on the skull with < 20% of baseline CBF during ischemia and >70% during reperfusion. All MR studies were carried out in a horizontal 14.1T magnet. Fast spin echo images with T_2-weighted parameters were acquired to localize the volume of interest and evaluate the lesion size. Immediately after adjustment of field inhomogeneities, localized ^{1}H MRS was applied to obtain the neurochemical profile from the striatum (6-8 microliters). Six animals (sham group) underwent nearly identical procedures without MCAO.

Results: The 10-min MCAO induced no MR- or histologically detectable lesion in most of the mice and a small lesion in some of them. We thus had two groups with the same duration of ischemia but a different outcome, which could be compared to sham-operated mice and more severe ischemic mice (30-min MCAO). Lactate increase, a hallmark of ischemic insult, was only detected significantly after 30-min MCAO, whereas at 3h post ischemia, glutamine was increased in all ischemic mice independently of duration and outcome. In contrast, glutamate, and even more so, N-acetyl-aspartate, decreased only in those mice exhibiting visible lesions on T_2-weighted images at 24h.

Conclusions: These results suggest that an increased glutamine/glutamate ratio is a sensitive marker indicating the presence of an excitotoxic insult. Glutamate and NAA, on the other hand, appear to predict permanent neuronal damage. In conclusion, as early as 3h post ischemia, it is possible to identify early metabolic markers manifesting the presence of a mild ischemic insult as well as the lesion outcome at 24h.

608

Brain Poster Session: Cerebral Metabolic Regulation

GAMMA OSCILLATIONS IN THE HIPPOCAMPUS ARE ASSOCIATED WITH HIGH OXYGEN CONSUMPTION

O. Kann[1], C. Huchzermeyer[1], R. Kovács[1], S. Wirtz[2], M. Schuelke[2]

[1]Neurophysiology, [2]Neuropediatrics, Charité-Universitätsmedizin Berlin, Berlin, Germany

Background and aims: Fast neuronal network oscillations in the gamma range (30-80 Hz) have been implicated in complex brain functions such as sensory processing and memory formation, and they might be associated with high energy demands.

Methods: We applied local field potential recordings, oxygen sensor microelectrodes, fluorescence imaging techniques (NAD(P)H, FAD) and pharmacology.

Purpose: We explored the fundamental relationships between gamma oscillations and mitochondrial functions (oxygen consumption, mitochondrial redox state) in hippocampal slice preparations.

Results: Activation of cholinergic receptors in hippocampal slices by acetylcholine evokes robust and persistent gamma oscillations and is associated with high oxygen consumption. Both findings are more prominent in subfield CA3 as compared to CA1 and the dentate gyrus. Moreover, gamma oscillations are associated with significant changes in mitochondrial redox state and are highly sensitive to decreases in interstitial partial oxygen pressure (pO_2).

Conclusions: Our data suggest that gamma oscillations are highly energy consuming and require a strong functional performance of neuronal mitochondria. This might explain the exceptional vulnerability of complex brain functions under pathological conditions.

609

Brain Poster Session: Inflammation

DIFFERENTIAL MODULATION OF THE CELLULAR IMMUNE SYSTEM IN A MOUSE MODEL OF INTRACEREBRAL HEMORRHAGE

S. Illanes, A. Liesz, R. Veltkamp

Neurology, University of Heidelberg, Heidelberg, Germany

Background and purpose: A stroke-induced immunodeficiency syndrome encompassing innate and adaptive immune cells develops in murine large ischemic stroke models[1]. Intracerebral hemorrhage (ICH) accounts for 15% of acute stroke, and is associated with high mortality and morbidity rates[2]. Experimental studies have identified a number of immunological factors that are involved in the pathophysiology of ICH, including leukocyte brain infiltration, initiation of the complement cascade and microglial activation[3]. However, there are no present studies characterizing the systemic immune response after experimental ICH. Our objective was to analyze lymphocytes subpopulation in blood and lymphatic organs in an experimental model of intracerebral hemorrhage (ICH) in mice.

Methods: In C57Bl/6 mice, ICH was induced by injection of 10µl (n=17), 30µl (n=17) or 50µl (n=17) of blood in the left striatum. Sham operation (n=17) served as control group. Differential leukocyte counts were performed in blood. Lymphocytic subpopulations were further characterized by FACS in blood, spleen, lymph node, and thymus day 3 after ICH. We compared absolute numbers of T_{helper} cells ($CD3^+CD4^+$), $T_{effector}$ cells ($CD3^+CD8^+$), B cells ($B220^+$), $T_{regulatory}$ cells ($CD4^+CD25^+Foxp3^+$) and NK cells ($PanNK^+$).

Results: Blood lymphocyte subpopulations were reduced in ICH compared to Sham, with a reduction of 5.7% (p=0.79) in the 30µl-ICH group and a reduction of 64% (p=0.19) in the 50µl-ICH group. In spleen the total number of splenocytes had an increase of 10.7% (p=0.27) in the ICH-30µl group and a significant reduction of 55% (p=0.0026) of the total splenocytes number compared to Sham in the ICH-50µl group. In thymus we found a reduction in the thymocyte counts number of 17.9% (p=0.11) in the 30µl-ICH group and a significant reduction of 68% (p=0.0001) in the 50µl-ICH group. The most remarkable findings were seen for the $T_{regulatory}$ cells with an increase number of 57.3% (p=0.0001) compeering to Sham in the 30µl-ICH group in spleen, 270.4% (p=0.0001) in thymus and 23.5% (p=0.15) in lymph nodes. However in the 50µ-ICH group the $T_{regulatory}$ cells were similar to Sham values in spleen, thymus and lynph nodes.

Conclusion: Hemorrhage size is a major determinator of post-stroke systemic immune modulation. Different Intracerebral blood volumes have a different impact on lymphocyte subpopulations, tending to induce proinflammatory reaction in mild and moderate hemorrhage size and a severe immunosuppression in large hemorrhagic stroke.

References:

1. Dirnagl U, et al. Stroke. 2007.

2. Dennis MS, el al. Stroke 1993.

3. Wasserman JK, et al. Eur J Neurosci. 2008.

LACK OF CAPILLARY DILATATION DURING FUNCTIONAL HYPEREMIA IN BICUCULLINE-INDUCED EPILEPTIC FOCI

F. Fernández Klett[1,2], N. Offenhauser[1], U. Dirnagl[1,3], J. Priller[2], U. Lindauer[1,3]

[1]Experimental Neurology, [2]Neuropsychiatry and Molecular Psychiatry, [3]Center for Stroke Research, Charité-Universitätsmedizin Berlin, Berlin, Germany

Background and aim: The spatial extent of the functional hyperemia associated with local increases in cerebral neuronal activity is determined by the architecture of the vascular arterial tree and the disposition of flow control structures. CNS capillaries are invested with pericytes, cells with contractile properties that may actively partake in the control of flow. Our aim was to test whether a dilatatory response of capillaries is substantial to the development of functional hyperemia.

Methods: We have used beta-actin-GFP mice, in which endothelial cells and pericytes can be fluorescently imaged, to assess dynamic vessel diameter and flow changes by means of in vivo two-photon microscopy. To elicit local transient increases in neuronal activity, we inserted a micropipette in the parietal cortex filled with the GABA-receptor antagonist bicuculline, which lead to the development of brief, recurring bursts of neuronal spike activity (inter-ictal spikes, IIS). We categorized cortical vessels into pial, penetrating and precapillary arterioles or capillaries based on location, diameter, and vessel wall morphology. Planar time-lapse images of these vessels (5-9 Hz) were collected simultaneously to IIS to measure rapid diameter changes. Subsequently, we performed line scans of the vessel lumen to trace IIS-associated changes in red blood cell (RBC) velocity.

Results: In total, the responses of 17 pial, 13 penetrating and 35 precapillary arterioles and 60 capillaries from 8 mice were studied. Mean±SD diameter and RBC velocity of the different segments were: pial art.: 14.0±4.8, 6.9±2.6; penetrating art. 14.7±4.0, vel. n.a.; precapillary art. 7.5±1.7, 2.8±1.3; capillaries 4.6±1, 0.6±0.4 (μm and mm/s, respectively). The average dilatatory response of pial, penetrating and precapillary arterioles reached maximally 2.4±.3.3%, 3.4±3.5% and 2.3±5% over pre-IIS values, respectively (~2s after IIS). Average RBC velocity in capillaries increased maximally by 10.6±12% over pre-IIS values. In contrast, no dilatation was observed in capillaries, measured at points immediate to pericytes (0.1±2.5% over pre-IIS diameter, measured at time of maximum RBC velocity increase). No significant difference was observed in the rise time of neither diameter nor RBC velocity response between different vessel types.

Conclusions: We hypothesized that, if a dilatatory response would originate in capillaries and then travel upstream to larger vessels, capillary vasoactivity would be emphasized in a context of brief neuronal activation. Bicuculline induced IIS are charachterized by robust yet brief neuronal spiking bursts, each lasting typically < 500 ms. However, no involvement of capillaries in the dilatatory response could be detected. Precapillary arterioles seem therefore to be the finest vessels determining the spatial extent of functional hyperemia in mice. Previous reports of capillary dilatation during hypercapnia or sustained functional stimulation are likely to represent passive dilatation of capillaries due to increased perfusion pressure effected at upstream arterioles.

CILOSTAZOL IMPROVES COGNITIVE FUNCTION BY ENHANCING VASCULOGENESIS AND NEUROGENESIS IN CA1 HIPPOCAMPUS IN A MOUSE MODEL OF TRANSIENT GLOBAL ISCHEMIA

H.K. Shin[1,2], H.R. Lee[2], D.H. Lee[3], K.W. Hong[2], C.D. Kim[2]

[1]Division of Meridian and Structural Medicine, School of Oriental Medicine, Pusan National University, [2]MRC for Ischemic Tissue Regeneration, Pusan National University, [3]Department of Obstetrics & Gynecology, School of Medicine, Pusan National University, Yangsan-si, South Korea

Objectives: Cilostazol (6-[4-(1-cyclohexyl-1H-tetrazol-5-yl)butoxy]-3,4-dihydro-2-(1H)-quinolinone) increases intracellular cyclic AMP levels by inhibiting type III phosphodiesterase. It has been recently suggested that cilostazol has a beneficial effect in the treatment of transient focal cerebral ischemic injury. Neovasculogenesis improves tissue microenvironment around the hippocampal CA1 injured ischemic area as a vascular niche and favors the proliferation and differentiation of neuronal precursor cells. We aimed to investigate whether vasculogenesis is enhanced in the hippocampus CA1 area in response to transient global ischemic injury under treatment with cilostazol, and whether reappearance of CA1 neurons is associated with recovery of deficit hippocampal-dependent spatial learning and memory.

Methods: To determine the optimal duration of bilateral common carotid arterial occlusion, C57BL/6 mice were subjected to global cerebral ischemia for various duration of time. The degree of hypoxia was assessed in the injured tissue using Hypoxyprobe^{TM}-1 kit. We chose occlusion of 20-min duration to produce global cerebral ischemia. C57BL/6 mice were treated with cilostazol (10 mg/kg/day, intraperitoneally) and histologically evaluated at 7, 14 and 28 days after the global ischemia.

Results: 20-min of global cerebral ischemia resulted in remarkable neuronal damage in CA1 areas compared with sham-operated animals and cilostazol (10 mg/kg/day, intraperitoneally) significantly reduced neuronal damage in the CA1 region. Treatment with cilostazol increased expression of brain-derived neurotrophic factor (BDNF), endothelial nitric oxide synthase (eNOS) and vascular endothelial growth factor (VEGF) in the brain. Stromal cell-derived factor-1α (SDF-1α) protein expression was significantly upregulated in the cilostazol-treated group at 14 days after ischemia, which was colocalized with CD31. To determine the effects of cilostazol on cell proliferation, BrdU was administered twice daily on day 1 to 3 after transient global ischemia. At 14 days after ischemia, BrdU-positive cells as well as BrdU and CD31 double-positive cells were greatly increased in cilostazol-treated groups. The escape latency was significantly increased in the vehicle group from 3 to 21 days after global ischemia when compared with the sham-operated group in Morris water maze task. The prolonged latency induced by global ischemia was significantly shortened by administration of cilostazol.

Conclusions: In summary, cilostazol showed beneficial effects promoting vascularization in the hippocampus area by upregulation of BDNF, eNOS, VEGF and SDF-1α and preserving the CA1 hippocampal region, thereby resulting in improvement of spatial learning memory in mice subjected to transient global ischemia. Enhancement of vascularization by cilostazol can be a valuable therapeutic option for the neurologic functional recovery after stroke.

This work was supported by the Korea Research Foundation Grant (KRF-2008-314-E00477, Shin) and the MRC program of MOST/KOSEF (R13-2005-009, Kim).

NR2A SUBUNIT PLAYS A CRUCIAL ROLE ON ISCHEMIC TOLERANCE IN CULTURED CORTICAL NEURON

Y. Terasaki[1], T. Sasaki[1], Y. Yagita[2], S. Okazaki[2], Y. Sugiyama[2], N. Oyama[1], E. Omura-Matsuoka[1], S. Sakoda[2], K. Kitagawa[2]

[1]Division of Stroke Center, Department of Internal Medicine, [2]Department of Neurology, Osaka University Graduate School of Medicine, Suita, Japan

Objectives: Based on the calcium-glutamate hypothesis, it has been emphasized that N- methyl D-aspartate (NMDA) glutamate receptor plays an important role of calcium influx to neuron. Clinically, the antagonist of glutamate receptor such as MK-801 proved ineffective. Recently, the difference between the subtypes of NMDA glutamate receptor was reported to affect downstream signal transduction and cell survival. Neuroprotective effect by ischemic tolerance has been reported to associate with up-regulation or down-regulation of various gene expressions. However the detailed mechanism is not fully clarified. The activation of a transcriptional factor, cyclic AMP response element binging protein (CREB), signaling contributes to a neuroprotective effect and phosphorylation of CREB serine 133 has been reported in ischemic tolerance. Within last decade, it has been reported that NR2A, a subunit of synaptic NMDA glutamate receptor, stimulated CREB function. We examined CRE transcriptional activity and the association with the subtypes of NMDA receptor and CREB phosphorylation in ischemic tolerance.

Methods: Primary cortical neuronal cultures were prepared from 16-day-old Wistar rat embryos and used 10 to 12 days in vitro. To examine whether ischemic tolerance was induced, cells were exposed to lethal 180-minute oxygen-glucose deprivation (OGD) 1 to 48 hr after sublethal 45-minute OGD. Neuronal death was quantified by measurement of lactate dehydrogenase (LDH) released by dead neurons into the bathing medium. The expression of transcriptional factor, total CREB and phosphorylated CREB was assessed by Western blotting. To evaluate cyclic AMP response element (CRE) gene expression, cells were transfected by adenovirus-CRE reporter and the luciferase activities were assayed after stimulation using a Dual-Glo luciferase assay system. To elucidate the role of CREB phosphorylation in ischemic tolerance, inhibition of that was performed with an adenovirus-dominant negative CREB mutant in which the phosphorylation site at serine 133 was changed to alanine (CREB-S133A). To evaluate whether NR2A was associated with induction of ischemic tolerance, NR2A-specific antagonist NVP-AAM077 was added to the bath medium between sublethal and lethal OGD. Additionally, we examined whether the treatment of bucuculline to block GABA receptors and stimulate NR2A induced ischemic tolerance. Whether cross tolerance was induced, glutamate (50μM) or hydrogen peroxide (50μM) was administered 24 hr after sublethal OGD.

Results: Ischemic tolerance was induced to be exposed to lethal 180-minute OGD 24 hr after sublethal 45-minute OGD. The protective efficacy of preconditioning persisted for 12 to 48 hr after sublethal OGD. After sublethal OGD p-CREB protein expression and CRE luciferase activity were upregulated. When cells were transfected by CREB-S133A, CRE luciferase activity was not upregulated and ischemic tolerance was lost. Next, we examined whether NR2A was associated with ischemic tolerance. To add NVP-AAM077 to the bath medium, the effectiveness of ischemic tolerance was lost. The administration of bucuculline enhanced CRE luciferase activity and induced ischemic tolerance. This neuroprotective effect of preconditioning could be also seen in other lethal injuries such as glutamate and hydrogen peroxide.

Conclusions: To obtain ischemic tolerance, it is important that neuroprotective signals through NR2A subunit of NMDA glutamate receptor induce phosphorylation of CREB protein and CRE transcriptional activity.

615

Brain Poster Session: Experimental Cerebral Ischemia: Global Ischemia

CHRONIC CEREBRAL HYPOPERFUSION MODEL IN MICE

C. Kudo[1,2], K. Eikermann-Haerter[1], I. Yuzawa[1], T. Qin[1], C. Liu[3], Y. Gu[1], H. Niwa[2], C. Waeber[1], M.A. Moskowitz[1], J.R. Sims[1,4], C. Ayata[1,4]

[1]Stroke and Neurovascular Regulation Laboratory, Department of Radiology, Massachusetts General Hospital/Harvard Medical School, Charlestown, MA, USA, [2]Department of Dental Anesthesiology, Osaka University Graduate School of Dentistry, Suita, Osaka, Japan, [3]Martinos Center for Biomedical Imaging, Department of Radiology, [4]Stroke Service and Neuroscience Intensive Care Unit, Department of Neurology, Massachusetts General Hospital/Harvard Medical School, Charlestown, MA, USA

Background and aims: Chronic cerebral hypoperfusion occurs in the setting of severe intracranial or cervical artery disease, or intrinsic microvasculopathies such as chronic hypertension, diabetes and amyloid angiopathy. Periventricular white matter changes are often associated. Bilateral common carotid ligation model used in rats to create chronic cerebral hypoperfusion is not suitable for mice due to severe ischemia and premature death. Recently, a bilateral carotid stenosis model has been developed by placing steel coils around common carotid arteries (Shibata M., Stroke 2004). We performed a detailed hemodynamic, histopathological, MRI, and neurological characterization of this new model in mice.

Methods: We used C57Bl/6 mice (24-29g, male) due to the frequently incomplete circle of Willis. Under brief isoflurane anesthesia, steel coils (inner diameter: 0.18mm, total length: 2.5mm, Sawane Spring Co., Japan) were placed around both common carotid arteries. Cerebral blood flow (CBF) was monitored by laser Doppler flowmetry (LDF) during coil placement. Absolute CBF was measured 1d or 28d after coil placement using ^{14}C-iodoantipyrine technique (IAP). Cerebrovascular reserve was determined by measuring hypercapnic hyperemia (5% CO_2) using laser speckle flowmetry. Neurological deficits were characterized by water-maze test at 28d. Ventricular enlargement was assessed by MRI. At time of sacrifice, mice were perfused with carbon black to examine circle of Willis anatomy. Brains were cryosectioned and stained by hematoxylin/eosin (routine histopathology), luxol fast blue (myelin), and glut-1 immunohistochemistry (microvascular architecture).

Purpose: Hemodynamic, histopathological, morphometric, and neurological characterization of bilateral carotid stenosis in mice.

Results: Cortical CBF decreased by ~30% bilaterally after coil placement, as measured by LDF. A similar reduction in absolute CBF was detected in structures supplied by carotid arteries (cortex, striatum, corpus callosum, hippocampus, dorsal thalamus) but not in cerebellum or brain stem, using IAP 1d after coil placement. At 28d, absolute CBF was restored to normal levels in all brain regions. Although the proportion of mice with posterior communicating arteries (PComm) was unchanged, the diameters of existing PComm were significantly larger in coiled mice at 28d. Capillary diameters were ~10% larger in cortex without a change in capillary length-density, while in striatum capillary length-density was decreased by ~30% without a change in capillary diameter. Consequently, cerebrovascular reserve in cortex was normal when tested 28d after bilateral carotid stenosis. Morphometric (MRI) and histopathological analyses showed an increase in ventricular volume suggesting brain atrophy. Brain myelin content was reduced by ~25% at 28d. Scattered microinfarcts were observed in striatum and cortex associated with neuronal loss and gliosis. Mice with bilateral carotid stenosis performed worse in spatial learning acquisition as tested by the water-maze test.

Conclusions: Our data suggest that bilateral carotid stenosis (coil) technique leads to relatively mild hypoperfusion and loss of cerebrovascular reserve that are restored within 4 weeks by posterior

communicating artery and capillary remodeling. Associated myelin loss, occasional microinfarcts and gross brain atrophy are likely responsible for the neurological deficits. The model may be suitable to investigate the pathophysiology of chronic cerebral hypoperfusion implicated in intracranial or cervical artery stenosis, as well as vasculopathies.

Lassen Award: Lassen Award Symposium

HYPERPERFUSION AND CHANGES IN VASOREACTIVITY AFTER ISCHEMIC STROKE: IMPLICATIONS FOR TISSUE RECOVERY

S. Wegener[1], M. Weller[1], E. Wong[2]

[1]Neurology, University Zürich, Zürich, Switzerland, [2]Radiology and Psychiatry, University California San Diego, La Jolla, CA, USA

Objectives: Hyperperfusion (or "luxury perfusion") after stroke has been observed early after reperfusion in patients as well as experimental models. While restoration of blood flow is the prerequisite for tissue recovery after stroke, it can have deleterious effects leading to reperfusion injury. There is still uncertainty about the phenomenon of post-stroke hyperperfusion: is it an indicator of a favorable outcome for the affected tissue, or is it part of the reperfusion injury cascade?

Methods: 8 Wistar rats were subjected to transient (60 min) middle cerebral artery occlusion (MCAO). MR images were acquired during the occlusion (day 0) and after reperfusion (days 1, 4, 14). Quantitative cerebral blood flow (CBF) maps were obtained using flow-sensitive alternating inversion recovery (FAIR) arterial spin labeling with the QUIPSSII modification. In order to get an estimate of vasoreactivity, CBF was measured in room air or in 5%CO_2 added to the anesthetic gas on days 4 and 14. In addition, diffusion-weighted (DWI) images, T1 and T2 maps and anatomical T2w images were obtained.

Results: During the vascular occlusion, CBF was significantly reduced in the ipsilateral MCA territory. On day 1, CBF had completely recovered, and most animals had a slight increase in CBF compared to the contralateral side in the formerly ischemic area. Hyperperfusion was much more pronounced and more localized on days 4 and 14. On vasoreactivity maps (CBF_{Co2}- CBF_{air}), the signal was low on day 4, while vasoreactivity had returned to baseline values or was even overshooting on day 14 (Figure 1). On individual images co-registered to the T2w images on day 14, the MR areas with hyperperfusion on days 4 and 14 could be mapped to the infarct border zone, while changes in vasoreactivity took place in more widespread areas throughout infarct core and border. In infarcts with cystic transformation on day 14, vasoreactivity remained depressed.

Conclusions: In a longitudinal MRI series after MCAO in rats, we observed late (>24h) hyperperfusion in the reperfused tissue, with a maximum on day 4. Hyperperfusion occurred mainly in tissue voxels in the infarct border. This could indicate the beginning of vascular adaptation processes in the infarct periphery. Vasoreactivity was depressed on day 4 in the ischemic area, but recovered towards day 14. Interestingly, there were areas of increased vasoreactivity on day 14 in almost all animals. Depressed vasoreactivity on day 4 could reflect the long lasting impact of stroke on endothelial function; furthermore, immature blood vessels are known to have less vasodilatory capacity. The reason for the overshooting vasoreactivity on day 14 remains open. We are currently analyzing brain slices for changes in the density and distribution of blood vessels, tissue damage and inflammatory infiltrate in the areas indicated on MRI.

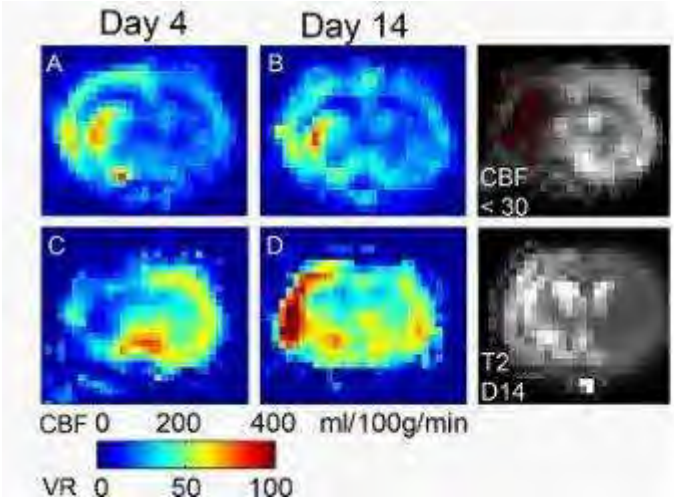

Figure 1: A, B: Averaged CBF maps acquired on days 4 and 14. C, D: Averaged Vasoreacivity (VR) maps (CBF $_{Co2}$- CBF $_{air}$) from days 4 and 14. On the right panel, voxels with CBF values below 30 ml/100g/min are overlaid onto the averaged d0 CBF map. Below is the averaged T2 map from d14.

[Figure 1]

619

Brain Poster Session: Migraine

OREXIN A ATTENUATES VASODILATATION BY TRIGEMINAL STIMULATION

K. Koizumi[1], R. Masuda[1], M. Fukuda[2], S. Tsukahara[3], J. Yonekura[1], S. Maruyama[4], N. Kanazawa[1], J. Hamada[1], F. Sakai[1]

[1]Neurology, [2]Allied Health Sciences, Kitasato University, Sagamihara, [3]Neurology, Sagamidai Hospital, Zama, [4]Laboratory Animal Science, Kitasato University, Sagamihara, Japan

Introduction: The orexin has been studied for recent 10 years and reported that it has several physiological functions, sleep, feeding, nociception, autonomic system. And orexinergic fiber is known to project from neurons of lateral hypothalamus area (LH) to central nerves system, including PAG, dorsal raphe, locus coeruleus, spinal cord, which involve in the trigeminal pain transmission and pain control system in migraine attack. Clinically, migraine patients often experience that migraine could be induced either by lack of sleep or too much sleep, yet sleep may relieve headache. In migraine with aura patients, plasma orexin A level was decreased (1). Another in vivo study reported that orexin 1 receptor stimulation by orexin A inhibits neurogenic dural vasodilatation (2). Accordingly orexin system is likely to be involved in migraine pathogenesis. In order to elucidate the exact involvement of orexin system in the pathophysiology of migraine, we investigated the effect of orexin A administration on the activation of trigeminovascular system in rats.

Methods: Five male Sprague-Dawley rats, weighing 350-400 gram, were anesthetized with isoflurane, and ventilated mechanically with room air. Parietal cortical blood flow (CoBF) on the right side was continuously monitored with the Laser-Doppler flow meter system. The nasociliary nerve (NCN) - a cerebrovascular branch of the trigeminal nerve in the rat - was carefully approached from the orbit in the right side. The post-ganglionic nerves from the pterygopalatine ganglion were gently eliminated from the ethmoidal foramen (EF). NCN was stimulated electrically near its entrance to EF through a bipolar platinum electrode with an electrical stimulator (6-28 μA, 0.5 ms duration, 10 Hz, 30 sec stimulation). CoBF were measured during and after electrical stimulation of NCN under intravenous injection of 1.0 ml saline followed by orexin A (30 μg/kg in 1.0 ml saline).

Results: CoBF was significantly increased upon electrical NCN stimulation during 60 seconds from the initiation of stimulation in control state. This increase was suppressed after orexin A administration in 60 seconds from the stimulation. The amount of blood flow increase when orexin A was given was significantly less than the control data.

Conclusion: Orexin A attenuated the blood flow increase upon trigeminal nerve stimulation. It is hypothesized that orexin system palys some role on modulation of cerebral blood flow and orexinergic dysfunction induces vasodilatation in migraine attack.

References:

[1] Yonekura J. Kanazawa N, Hamada J. Sakai F ; Kitasato Med J 2008 38:77-80.

[2] Holland PR, Akerman S, Goadsby PJ ; J Pharmacol Exp Ther. 2005 Dec;315(3):1380-5.

622

Brain Oral Session: Brain Imaging

RNA INTERFERENCE AGAINST AQUAPORIN-4 DECREASES THE APPARENT DIFFUSION COEFFICIENT IN THE NORMAL BRAIN

J. Badaut[1,2,3], S. Ashwal[1], A. Adami[1], B. Tone[1], R. Recker[1], B. Ternon[3], A. Obenaus[1,4,5]

[1]Department of Pediatrics, Loma Linda University School of Medicine, Loma Linda, CA, USA, [2]Clinical and Fundamental Neurosciences, University of Geneva, Geneva, [3]Neurosurgery, Lausanne University Hospital, Lausanne, Switzerland, [4]Radiology, [5]Radiation Medicine, Loma Linda University School of Medicine, Loma Linda, CA, USA

Aim: Diffusion weighted magnetic resonance imaging (MRI) is now widely used in human brain diagnosis (Obenaus and Ashwal 2008). To date molecular mechanisms underlying changes in Apparent Diffusion Coefficient (ADC) signals remain poorly understood. AQP4, localized to astrocytes, is one of the most highly expressed cerebral AQPs (Badaut et al. 2002). AQP4 is involved in water movement within the cell membrane of cultured astrocytes (Nicchia et al. 2003). We hypothesize that AQP4 contributes to water diffusion and underlying ADC values in normal brain.

Methods: We used an RNA interference (RNAi) protocol in vivo, to acutely knockdown expression of AQP4 in rat brain and to determine whether this was associated with changes in brain ADC values using MRI protocols as previously described (Badaut et al. 2007). RNAi was performed using specific small interference RNA (siRNA) against AQP4 (siAQP4) and a non-targeted-siRNA (siGLO) as a control. The specificity and efficiency of the siAQP4 were first tested in vitro in astrocyte and hippocampal slice cultures. In vivo, siRNAs were injected into the rat cortex 3d prior to MRI acquisition and AQP4 was assessed by western blot (n=4) and immunohistochemistry (n=6). Histology was performed on adjacent slices.

Results: siAQP4 application on primary astrocyte cultures induced a 76% decrease in AQP4 expression after 4 days. In hippocampal slice cultures; we also found a significant decrease in AQP4 expression in astrocytes after siAQP4. In vivo, injection of non-targeted siRNA (siGLO) tagged with CY3 allowed us to show that GFAP positive cells (astrocytes) were positively stained with CY3-siGLO, showing efficient transfection. Western blot and immunohistochemical analysis showed that siAQP4 induced a ~30% decrease in AQP4 expression without modification of tissue properties or cell death. After siAQP4 treatment, a significant decrease in ADC values (~50%) were observed without altered of T2 values.

Conclusions: Together these results suggest that AQP4 reduces water diffusion through the astrocytic plasma membrane and decreases ADC values. Our findings demonstrate for the first time that astrocytic AQP4 contributes significantly to brain water diffusion and ADC values in normal brain. These results open new avenues to interpretation of ADC values under normal physiological conditions and in acute and chronic brain injuries.

References:

Badaut J, et al. (2007) Temporal and Regional Evolution of Aquaporin-4 Expression and Magnetic Resonance Imaging in a Rat Pup Model of Neonatal Stroke. Pediatr Res 62:248-254.

Badaut J, et al. (2002) Aquaporins in brain: distribution, physiology, and pathophysiology. J Cereb Blood Flow Metab 22:367-378.

Nicchia GP, et al.. (2003) Inhibition of aquaporin-4 expression in astrocytes by RNAi determines alteration in cell morphology, growth, and water transport and induces changes in ischemia-related genes. Faseb J 17:1508-1510.

Obenaus A, Ashwal S. (2008) Magnetic resonance imaging in cerebral ischemia: Focus on neonates. Neuropharmacology 55:271-280 .

Statement of financial support: Supported by the Swiss Science Foundation (FN 3100AO-108001 and 31003A-122166), Swissheart Foundation, Novartis Foundation, Department of Pediatrics Research Fund, NASA Cooperative Agreement NCC9-149.

CHARACTERISTICS OF ADULT PATIENTS WITH MOYAMOYA DISEASE IN CHINA AND SIGNIFICANT INCREASE OF CEREBRAL BLOOD FLOW POST ENCEPHALO-DURO-ARTERIO-SYNANGIOSIS (EDAS)

L. Duan, Z. Li, W. Yang, P. Xian, W. Shi, J. Feng, R. Zong, F. Zhao, Z. Zhang

Department of Neurosurgery, Affiliated 307 Hospital, Academy of Military Medical Sciences, Beijing, China

Objective: To describe the clinical features and the efficacy of encephalo-duro-arterio-synangiosis (EDAS) in adult patients with Moyamoya disease (MMD) in China.

Methods: Data from 312 patients aged ≥18 with DSA/MRA confirmed MMD in our hospital between December 2002 and September 2008 were retrospectively reviewed. All patients underwent EDAS and were followed up for at least 3 Month (median 26-month). 83 cases were accepted DSA examination and 171 cases were repeated PET after operation 3-6 month.

Results: Majority of our adult patients presented with cerebral ischemia (173 case with infarction 55.4%, 76 case with TIA 24.4%) with the rest of 63 patients with cerebral hemorrhage (20.2%). After EDAS, neurological signs and symptoms were significantly improved in 219 out of 249 with ischemia. There was no rebleeding case in the haemorrhage group. PET examinations showed that post-operative cerebral blood flow was increased clearly on 138 of the 171 patients (80.7%). Post-operative DSA examinations revealed a revascularization on 66 of the 83 hemispheres (79.5%). Logistic regression analyze show the females and younger have better revascularization.

Conclusions: Largest case collection in our hospital so far demonstrated that adult patients in China with moyamoya disease present with different clinical features compared with other countries. There are significant higher incidence of cerebral infarction (55.4% vs. 14.9% in Japan). EDAS is also an effective surgical treatment in adult MMD patients in terms of clinical improvement and radiological evidence by DSA for revascularization and PET for increased brain blood flow.

625

Brain PET Oral 3: Miscellaneous Targets

AGE AND GENDER AFFECT 5-HT$_4$ RECEPTOR BINDING: A BRAIN PET STUDY IN HEALTHY VOLUNTEERS WITH [^{11}C]SB207145

K. Madsen[1,2], W.-J. Neumann[1,2], L. Marner[1,2], M. Haahr[1,2], N. Gillings[3], W. Baaré[2,4], S.G. Hasselbalch[1,2], G.M. Knudsen[1,2]

[1]Neurobiology Research Unit, Rigshospitalet, [2]Center for Integrated Molecular Brain Imaging, [3]PET and Cyclotron Unit, Rigshospitalet, [4]Danish Research Center for Magnetic Resonance, Hvidovre Hospital, Copenhagen, Denmark

Objectives: 5-HT$_4$ receptors are of clinical relevance due to their involvement in memory and learning and their presumed ability to reduce the pathological accumulation of cerebral β-amyloid in Alzheimer's disease (AD). The aim of this study was to investigate the effects of age and gender on 5-HT$_4$ receptor binding in both the high-binding region striatum, the global neocortex, and 3 cortical regions of importance for memory, learning and AD.

Methods: A bolus injection of [^{11}C]SB207145 was followed by a 2-hour dynamic PET scan in a GE Advance scanner in 30 healthy volunteers (16 men, mean age 44.4 years range 19.9-86.2). Volumes of interest (VOIs) were delineated automatically on co-registered 3T MRIs. Partial volume (PV) corrected time-activity curves were extracted from the VOIs, including gray matter voxels only, and BP_{ND} was modeled with SRTM. BP_{ND} in 5 VOIs were investigated for gender differences and correlation to age.

Results: Although non PV corrected BP_{ND} correlated negatively with age in some regions, when correcting for atrophy, we found positive correlations in the high-binding region striatum (R=0.3818, p=0.0373), in the dorsolateral prefrontal cortex (R=0.42, p=0.0208, see figure), and a tendency was found in the posterior cingulate gyrus (R=0.3378, p=0.0679). No correlations were found in the global neocortex or in the hippocampus.

Using age as a covariate, gender differences in PV corrected BP_{ND} were only found in the striatum, where a tendency for 6.8% higher BP_{ND} in women was found (p=0.068). In a post hoc analysis, this difference was driven by putamen, which was 8.3% higher in women (p=0.0355).

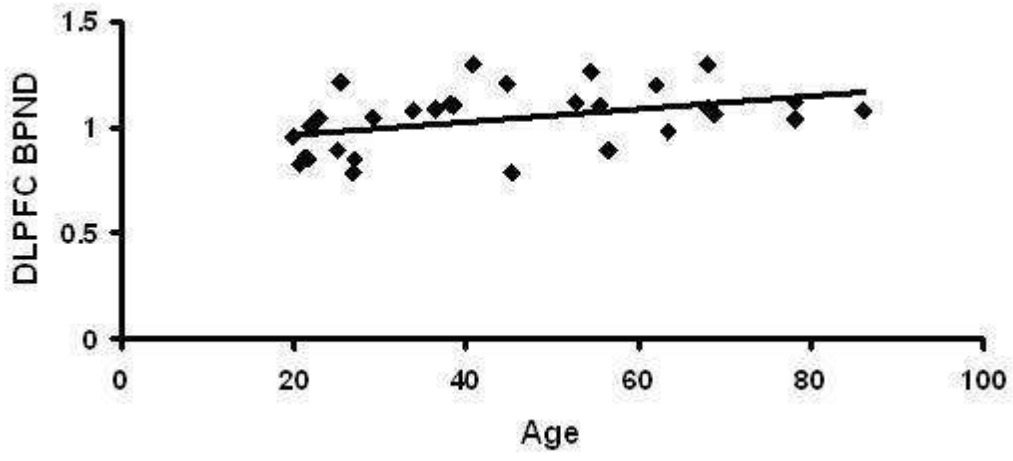

[Increase of 5HT4 receptors in DLPFC with age]

Conclusions: To our knowledge, this is the first time an increase of 5-HT receptors with age has been found. The up-regulation of 5-HT_4 receptors with age could be a compensation for a lower serotonergic tone with age. It is highly interesting that the cortical increase with age is seen in the regions affected by the highest β-amyloid accumulation in studies with ^{11}C-PIB PET in AD.

A localized gender difference of 8.3% is somewhat surprising, as most receptors do not show gender differences. However, depression and anxiety are more prevalent in females.

Brain Poster Session: Experimental Cerebral Ischemia: Vascular & Endothelial

ENDOTHELIAL DYSFUNCTION ABROGATES THE BENEFICIAL EFFECTS OF NORMOBARIC HYPEROXIA ON CEREBRAL PERFUSION AND TISSUE OUTCOME AFTER FOCAL CEREBRAL ISCHEMIA

H.K. Shin[1,2], P.L. Huang[3], K.W. Hong[2], C.D. Kim[2], C. Ayata[4]

[1]Division of Meridian and Structural Medicine, School of Oriental Medicine, Pusan National University, [2]MRC for Ischemic Tissue Regeneration, Pusan National University, Yangsan-si, South Korea, [3]Cardiovascular Research Center and Cardiology Division, [4]Department of Neurology and Radiology, Massachusetts General Hospital & Harvard Medical School, Charlestown, MA, USA

Background and aims: Improving brain tissue oxygenation via 100% O_2 inhalation is a potential therapeutic strategy in acute stroke. We have previously showed that normobaric hyperoxia (NBO) improves cerebral blood flow (CBF) and ameliorates tissue injury in focal ischemia. However, the mechanism of improved CBF and its contribution to tissue protection are unclear. One potential mechanism for hyperoxia to augment CBF is by enhancing endothelial nitric oxide synthase (eNOS) function in ischemic cortex. Stroke often occurs in individuals with vascular risk factors associated with endothelial dysfunction (e.g., hyperlipidemia). It is, therefore, possible that the efficacy of NBO in acute stroke is diminished in patients with endothelial dysfunction.

Methods: The spatiotemporal evolution of ischemic CBF deficit was studied during 60 min distal middle cerebral artery occlusion (dMCAO) using high resolution laser speckle flowmetry noninvasively through intact skull in eNOS knockout ($eNOS^{-/-}$) and hypercholesterolemic ApoE knockout ($ApoE^{-/-}$) mice (20-30g, male). $ApoE^{-/-}$ were fed high-fat "western" diet for 8 weeks starting at 4 weeks of age. Normoxic mice (30% O_2) were compared to NBO mice (100% O_2). The area of severe CBF deficit (≤20% residual CBF) was measured by thresholding. 47h after reperfusion, indirect infarct volume was measured using TTC staining.

Purpose: To test whether eNOS function is critical for the neuroprotective effects of NBO.

Results: The area of severely ischemic cortex was significantly larger in $eNOS^{-/-}$ compared to wild type (WT) controls, and remained larger throughout the imaging period (75 min). In WT mice NBO (15 min after dMCAO) significantly improved CBF and reduced the area of ischemic cortex by ~45% compared to normoxic WT (n=8 and 11, respectively), as previously reported. In $eNOS^{-/-}$ mice, however, NBO had the opposite effect: the area of CBF deficit rapidly and markedly increased after NBO (42% increase vs. normoxic $eNOS^{-/-}$, $p< 0.01$; n=5 and 9, respectively). In WT mice, NBO decreased infarct volume (indirect method) by ~45% compared to normoxic WT. In contrast, NBO increased infarct volume by ~10% in $eNOS^{-/-}$ compared to normoxic group ($p>0.05$). As in $eNOS^{-/-}$ mice, NBO rapidly increased the area of CBF deficit by ~30% in $ApoE^{-/-}$ compared to normoxic group (n=5 and 9, respectively; $p< 0.05$). The neuroprotective effect of NBO was also diminished in $ApoE^{-/-}$ compared to WT (~35% reduction in infarct volume vs. normoxic $ApoE^{-/-}$, $p>0.1$).

Conclusions: The beneficial effects of NBO on both ischemic tissue perfusion and outcome are abolished by endothelial dysfunction, suggesting that the neuroprotective effects of NBO are critically dependent on eNOS function. These data have direct implications for patient care, and suggest that while may improve tissue perfusion and outcome in younger stroke patients, it may be detrimental in older patients with multiple vascular risk factors associated with severe endothelial dysfunction. Current and future clinical trials of NBO in acute stroke need to address this issue by subgroup analyses.

This work was supported by the Korea Research Foundation Grant (KRF-2008-314-E00477, Shin),

the MRC program of MOST/KOSEF (R13-2005-009, Kim) and NIH (NS055104, Ayata; NS048426, Huang).

627

Brain Poster Session: Experimental Stroke & Cerebral Ischemia

HISTOLOGICAL AND MRI CHARACTERISTICS OF EXOFOCAL POSTISCHEMIC NEURONAL DEATH, FOLLOWING MIDDLE CEREBRAL ARTERY OCCLUSION IN MICE

V. Prinz[1,2], G. Kronenberg[1,2,3], C. Leithner[1], K. Gertz[1,2], M. Balkaya[1,2], S. Mueller[2], H. Hoertnagle[4], M. Endres[1,2]

[1]Klinik und Poliklinik für Neurologie, [2]Center for Stroke Research Berlin (CSB), [3]Klinik und Hochschulambulanz für Psychiatrie und Psychotherapie, Campus Benjamin Franklin, [4]Institut für Pharmakologie und Toxikologie, Charité - Universitätsmedizin, Berlin, Germany

Objectives: Cerebral ischemia in the territory of the middle cerebral artery (MCA) can induce delayed neuronal death remote to the primary lesion in the ipsilateral substantia nigra (SN). Nigral histopathological changes occur days to weeks after the initial event. However, the mechanisms leading to exofocal postischemic neuronal death (EPND) in the SN are complex and poorly understood. Especially the fate of dopaminergic neurons is discussed controversially.

Using a mouse model of mild stroke, we investigated the time-course and characteristics of EPND using sequential magnetic resonance imaging (MRI) and subsequent immunohistochemistry.

Methods: 129/SV mice were subjected to 30 min. of filamentous MCA occlusion and followed up by MRI on day 1, 4, 5, 7, 14, 21 and 28 post ischemia. At day 28, animals were sacrificed and immunohistochemistry was performed to investigate histopathological changes in the ipsilateral SN, compared to the contralateral side. Additional groups of animals were exposed to 30 min. of MCA occlusion and sacrificed 1, 4, 5, 7, 14 and 21 days after reperfusion for histological evaluation of the SN. MRI was performed on the respective day of sacrifice. A subset of animals was exposed to 30 min. of MCA occlusion and cerebral dopamine levels were measured using high pressure liquid chromatography (HPLC), 90 days post ischemia.

Results: On day 1, T2 weighted imaging showed high signal intensity in the striatum, but no changes in the ipsilateral SN. Likewise, diffusion weighted imaging (DWI) and T2 mapping did not reveal any changes in the SN. On days 4 and 5, T2 weighted imaging showed high signal intensity in the ipsilateral SN, accompanied by an increased T2 value ($p < 0.05$) and a decrease in the apparent diffusion coefficient ($p < 0.05$). These alterations persisted until day 7, but were no longer detectable at later time points.

Compared to the contralateral side, the density of NeuN and tyrosine hydroxylase (TH) positive cells in the ipsilateral SN decreased significantly over time, starting as early as day 7 post ischemia. Consequently, striatal dopamine levels were significantly decreased.

Conclusions: Secondary neuronal degeneration in the SN occurs within days after striatal ischemia and is characterized by a marked neuronal loss, including dopaminergic neurons. In our studies, transient MRI changes in the SN, indicating cellular edema, are of predictive value for the occurrence of EPND, as they are observed prior to histological cell loss.

Together with the striatum the substantia nigra forms a unique dual projection system, which is of high importance for behavioral and motor functions. We speculate that EPND may be responsible for neurological impairment that cannot be correlated to the primary ischemic lesion. In particular, EPND of dopaminergic neurons in the midbrain (SN and ventral tegmental area) may play an important role for impaired motor function and emotional sequelae.

Our findings provide a mouse model to further elucidate mechanisms of EPND that might be targeted for the development of novel therapeutic approaches for the prevention of EPND following stroke.

NEUROPROTECTIVE EFFECTS OF D-ALLOSE, RARE SUGAR, AGAINST CEREBRAL ISCHEMIA/REPERFUSION INJURY IN RATS

T. Nakamura[1], O. Miyamoto[2], F. Lu[1], N. Okabe[1], N. Kawai[3], T. Tamiya[3], T. Itano[1]

[1]Neurobiology, Kagawa University Faculty of Medicine, Miki, [2]Physiology, Kawasaki Medical University, Kurashiki, [3]Neurological Surgery, Kagawa University Faculty of Medicine, Miki, Japan

Objectives: Rare sugars have received increasing attention in recent years for a variety of usages such as low calorie carbohydrate sweeteners and bulking agents. D-alllose, an aldo-hexose, is one of the exceptions among rare sugars whose biological function have been suggested. The scavenging activity of D-allose was examined using electron spin resonance (1). The present study investigates anti-oxidative effects of D-allose on ischemic damage.

Methods: Animal protocols were approved by the Animal Committee of Kagawa University Faculty of Medicine. Male Sprague-Dawley rats, each weighing 250 to 350 g, were used for all experiments. Rats were subjected to temporary middle cerebral artery occlusion (MCAO) for 1 hour under pentobarbital anesthesia. D-allose was intravenously infused during occlusion and further 1 hour after reperfusion (100 or 400 mg/kg). Sections were stained with hematoxylin and eosin, and measured brain damage (infarction and atrophy volume) 1 week after MCAO. In another set of rats, apurnic/apyrimidic abasic sites (AP-sites) and 8-hydroxy-2'-deoxiguanosine (8-OHdG), oxidative stress markers (2), were investigated 24 hours after MCAO to clarify anti-oxidative effect of D-allose.

Results: All physiological variables were measured immediately before and 30, 70 min after ischemia. Blood glucose, pH, pCO_2, pO_2, and mean arterial blood pressure were within the normal range. These variables were not influenced by D-allose administration. Brain damage was significantly decreased by administration of 400 mg/kg of D-allose compared with vehicle group ($P < 0.05$, Figure 1). However, there were no significant changes in the 100 mg/kg of D-allose treatment group. The DNA oxidation markers, AP-sites and 8-OHdG, were increased in ipsilateral cortex compared with sham ipsilateral cortex 24 hours after MCAO ($P < 0.05$). D-allose (400 mg/kg) treatment significantly reduced both DNA oxidation markers ($P < 0.05$).

Conclusions: D-allose suppressed brain damage and the oxidative DNA injury markers in the brain after MCAO. These results suggest that D-allose is a potential therapeutic agent for cerebral ischemia. They may act by reducing the oxidative stress caused by the cerebral ischemia/reperfusion.

References:

(1) Murata et al. J Biosci Bioeng 96: 89-91, 2003.

(2) Nakamura et al. Stroke 39: 463-469, 2008.

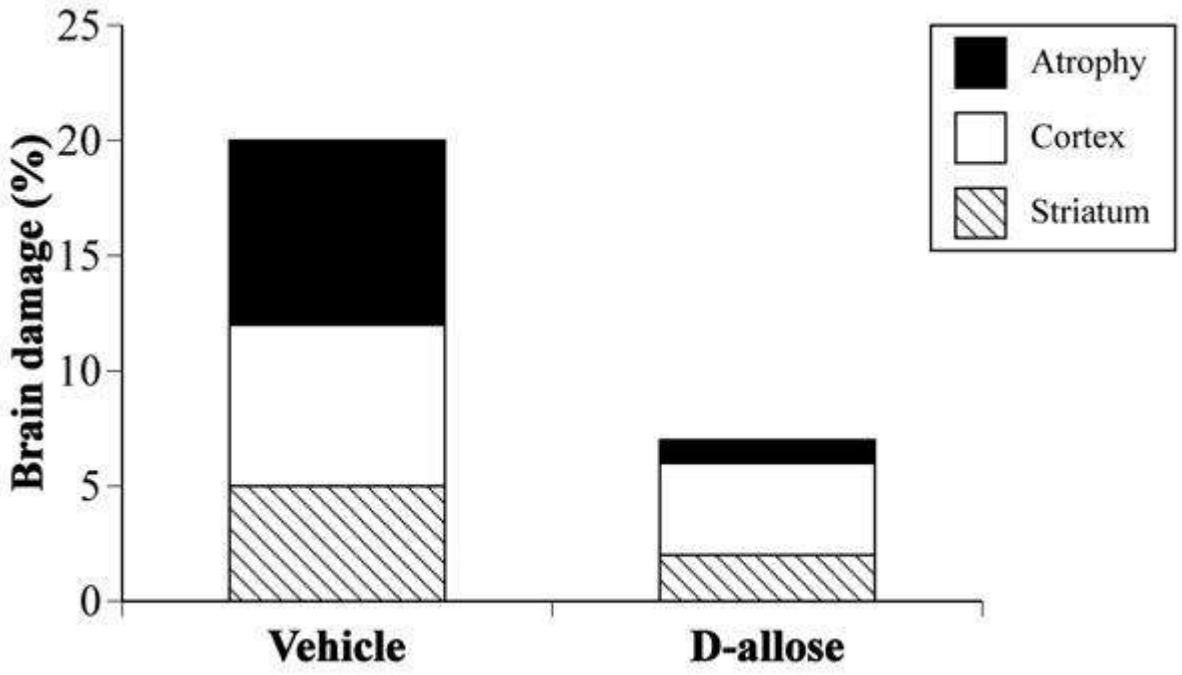

[Figure 1]

Figure 1. Bar graphs demonstrating the significant effect of D-allose treatment (400mg/kg iv.) on brain damage (infarction atrophy volume) following MCAO ($P < 0.05$, Vehicle vs. D-allose, $n = 5$ in each group).

Brain Oral Session: Traumatic Brain Injury

TEMPORAL EXPRESSION OF AQP4 AND NEUROIMAGING IN A JUVENILE RAT MODEL OF TRAUMATIC BRAIN INJURY

A. Obenaus[1,2,3], A. Adami[3], B. Ternon[4], B. Tone[3], D. Spagnoli[1], R. Recker[3], S. Ashwal[3], **J. Badaut**[3,4,5]

[1]Department of Radiation Medicine, [2]Radiology, [3]Pediatrics, Loma Linda University School of Medicine, Loma Linda, CA, USA, [4]Neurosurgery, Lausanne University Hospital, Lausanne, [5]Clinical and Fundamental Neurosciences, University of Geneva, Geneva, Switzerland

Aim: Traumatic brain injury (TBI) in infancy and childhood is a cause of death and a permanent disability. Young animals have more brain water than adult animals and typically the juvenile brain swells more than the adult brain after TBI. However, therapeutic treatments for juvenile TBI (jTBI) are typically based on adult physiology. Aquaporin 4 (AQP4), a water channel, is a possible therapeutic candidate, but, its involvement in juvenile brain swelling has not been studied. The aim of this study was to determine the level of AQP4 expression and compare it to edema formation serially measured using MRI after jTBI.

Methods: A jTBI rat model (P17d) utilized controlled cortical impact (CCI) using a 1 mm blunt tip piston to induce the trauma directly on the cortex. MRI was performed at 1, 3, 7 and 28 days after jTBI (see Badaut et al. 2007). AQP4 immunolabeling was evaluated on tissue slices corresponding to the MRI acquisitions. AQP4 staining was quantified using an infrared-scanner (LiCor) and was examined using epifluorescence microscopy. Values were quantified in 4 regions of interest (ROIs): ipsilateral cortex (under the impact), ipsilateral striatum and contralateral cortex and striatum.

Results: Significant decreases in ADC and increased T2 values were observed at 24h after CCI in all ROIs corresponding to the degree of edema formation. At 72 hours ADC values normalized while T2-values remained significantly elevated suggesting edema resolution. In the lesion area, the number of neurons was decreased and GFAP staining was increased at 3d, corresponding to development of gliosis. Significantly increased AQP4 in the lesion was coincident with the normalization MRI changes at 3 and 7d. However, increased AQP4 expression was also observed in the astrocytic end-feet in contact with blood vessels distant to the site of CCI. At 28 days AQP4 expression normalized throughout the brain except at the lesion site where AQP4-ir and ADC-values were still elevated.

Conclusion: AQP4 induction was increased during the period of active edema resolution in the lesion and peri-lesional region as we have previously observed in a stroke model (Badaut et al. 2007). In adult TBI, decreased AQP4 expression has been observed in the first days after trauma (Ke et al. 2001). Our findings strongly suggest that traumatic pathological mechanisms are different between young and adult animals. Our findings should be considered in the future development of new drugs acting on AQPs that potentially could be used to treat edema formation in children with TBI.

Financial support: Supported by the Swiss Science Foundation (FN 3100AO-108001 and 31003A-122166), Swissheart Foundation, Novartis foundation, Department of Pediatrics Research Fund, NASA Cooperative Agreement NCC9-149.

References:

Badaut J, Ashwal S, Tone B, Regli L, Tian HR, Obenaus A. (2007) Temporal and Regional Evolution of Aquaporin-4 Expression and Magnetic Resonance Imaging in a Rat Pup Model of Neonatal Stroke. Pediatr Res 62:248-254.

Ke C, Poon WS, Ng HK, Pang JC, Chan Y. (2001) Heterogeneous responses of aquaporin-4 in

oedema formation in a replicated severe traumatic brain injury model in rats. Neurosci Lett 301:21-24.

630

Brain Poster Session: Oxidative Mechanisms

NADPH OXIDASE ACTIVITY IS HIGHER IN CEREBRAL VERSUS SYSTEMIC ARTERIES OF FOUR ANIMAL SPECIES: ROLE OF NOX2

A.A. Miller[1], G.R. Drummond[1], T.M. De Silva[1], A.E. Mast[1], H. Hickey[2], J.P. Williams[3], B.R. Broughton[1], C.G. Sobey[1]

[1]Department of Pharmacology, Monash University, [2]Department of Pharmacology, Melbourne University, [3]Howard Florey Institute, Melbourne, VIC, Australia

Objectives: Reactive oxygen species (ROS) such as superoxide and hydrogen peroxide serve as important cell signalling molecules for the regulation of normal vascular function. Moreover, a wealth of evidence suggests that excessive generation of vascular ROS plays a key role in the pathogenesis of several vascular diseases such as hypertension and stroke. NADPH oxidases are now believed to be a major physiological source of ROS within cerebral and systemic vasculatures. We previously reported that NADPH oxidase activity is profoundly greater in intracranial cerebral versus systemic arteries of the rat (Miller et al., 2005). In the present study we firstly confirmed our finding in rats and then tested whether the activity of NADPH oxidase is also greater in intracranial cerebral arteries than in systemic arteries of other animal species, i.e. mouse, rabbit and pig. Secondly, using Nox2 deficient mice we evaluated the involvement of Nox2-containing NADPH oxidase in any such regional differences.

Methods: NADPH (100 μmol/L)-stimulated superoxide production by basilar (BA), middle cerebral (MCA) and common carotid (CA) arteries, and thoracic aorta (AO) from rat (Sprague Dawley, n=6), mouse (C57Bl/6J, WT, n=68; and Nox2-/-, n=17), rabbit (New Zealand White, n=6) and pig (Sus scrofa, n=6) was measured using lucigenin (5 μmol/L)-enhanced chemiluminescence. Basal superoxide and hydrogen peroxide production by mouse cerebral arteries (pooled BA and MCA), AO and CA, was measured using L-012 (100 μmol/L)-enhanced chemiluminescence and Amplex Red fluorescence, respectively. Protein expression of Nox2 and superoxide dismutase (SOD) isoforms 1-3 in mouse cerebral arteries (pooled BA and MCA), AO and CA was measured using Western Blotting. Confocal immunofluorescence was used to localize Nox2 in mouse MCA, AO and CA.

Results: In rats, WT mice, rabbits and pigs, NADPH-stimulated superoxide production by cerebral arteries was up to 40-fold greater than in AO and CA (n=3-12, $P< 0.05$). In WT mice, basal superoxide and hydrogen peroxide production by cerebral arteries was ~9-fold and ~2.5-fold higher (n=4-10, $P< 0.05$), respectively, than AO and CA, and was associated with ~40% greater expression of Nox2 (n=4, $P< 0.05$). By contrast, SOD1, SOD2 and SOD3 protein expression did not differ between artery types (n=6-8). Nox2 immunofluorescence was localized to the endothelium, and to a lesser extent the adventitia of MCA, AO and CA and appeared to be more intense in the endothelium of MCA than AO or CA (n=3). In Nox2-/- mice, NADPH-stimulated superoxide production was reduced by ~35% versus WT mice (n=5, $P< 0.05$), whereas Nox2 deletion did not affect superoxide production in AO or CA.

Conclusions: In summary, the findings of this study reveal that NADPH oxidase activity is greater in intracranial cerebral versus systemic arteries of several animal species. Furthermore, we provide evidence that higher cerebrovascular Nox2 activity may, in part, account for these regional differences.

References: Miller AA, Drummond GR, Schmidt HHHW & Sobey CG (2005) NADPH oxidase activity and function is profoundly greater in cerebral versus systemic arteries. Circ Res 97: 1055-1062.

CORTICAL AMYLOID LOAD AND GLUCOSE METABOLISM IN ALZHEIMER'S DISEASE AND MILD COGNITIVE IMPAIRMENT WITH [11C]PIB- AND [18F]FDG-PET IMAGING

S. Hatashita, H. Yamasaki

Shonan Atsugi Hospital & Clinic, Atsugi, Japan

Objective: The aim is to investigate the deposition of amyloid plaques by carbon 11-labeled Pittsburgh Compound B ([11C]-PIB) in the brains with dementia (Alzheimer's type, AD) and mild cognitive impairment (MCI). We clarify the relationship between cerebral amyloid load and glucose metabolism.

Method: Forty-three patients with AD, 49 with MCI and 80 healthy control (HC) were studied. All 172 patients underwent 60-min dynamic [11C]-PIB PET and 15-min static [18F]-FDG PET. [11C]-PIB data was acquired from 35-60 min after injection. Regions of interest (ROI) were defined on co-registered MRI and used in the analysis of the PET data. Distribution volume ratios (DVR) of PIB retention were determined using Logan graphical analysis (cerebellar gray as reference region). [18F]-FDG PET images were extracted using 3 dimensional stereotactic surface projections (3D-SSP) by a Z-score on a pixel-by-pixel basis. Quantitative analysis for [18F]-FDG used the standardized uptake value ratio (SUVR) values of cortical regions.

Result: All of 43 AD patients (MMSE: 19.6±4.6, CDR: 0.87±0.57) had a robust increase of PIB binding in the anterior and posterior cingulate, precuneus, frontal, parietal, lateral temporal cortical areas (typical PIB AD-pattern). The mean value of DVR in whole cortical areas was the highest among all groups (2.43±0.56, $P< 0.01$). On FDG PET 3D-SSP images, twenty (46%) of 43 AD patients with PIB AD pattern showed a significant reduction of cortical glucose metabolism in temporo-parietal, frontal, and precuneus cortices (classic metabolic AD-pattern). The mean value of FDG SUVR in cortical areas was the smallest (0.91±0.05, $P< 0.01$). However, increased PIB bindings did not correlate to comparable metabolic decreases in any of cortical areas. Of the 49 MCI patients (MMSE: 27.3±1.8, CDR: 0.5), twenty-seven showed AD like patterns of amyloid deposition similar to AD (DVR: 2.16±0.30, $P< 0.01$) whereas the remaining 22 patients had no PIB retention in cortical areas. Three (11%) of 27 MCI PIB positive patients had the hypometabolic AD-pattern and five (18%) showed hypometabolism only in posteior cingulate gyrus and precuneus on FDG images. The values of DVR in cortical areas were not correlated with FDG SUVR. In the precuneus, however, increased PIB retention was significantly related to the decreased glucose metabolism in MCI group, but not in the AD group ($r=-0.23$, $P< 0.05$). Seven of 84 HC had the PIB retention in cortical areas (DVR: 1.92±0.27, $P< 0.01$), but did not show the hypometabolic AD-pattern or hypometabolism in the precuneus.

Conclusion: The [11C]-PIB PET determines cortical amyloid load at different stage of AD, but the pattern of cortical amyloid deposition is not identical to hypometabolic pattern that seen in the [11C]-PIB PET. This amyloid plaque formation is not directly responsible for cerebral glucose metabolism in cortical regions.

CA^{2+} CHANGES IN ASTROCYTES AND NEURONS OF MICE PRIMARY SOMATOSENSORY CORTEX IN RELATION TO ACTIVITY-DEPENDENT RISES IN CEREBRAL BLOOD FLOW

B.L. Lind, M. Lauritzen

Department of Neuroscience and Pharmacology, University of Copenhagen, Copenhagen N, Denmark

Activity-dependent rises in cerebral blood flow are robust markers of neuronal activity in functional imaging studies, but it is still incompletely understood how the vascular signals are produced. Specifically, it is unknown to what extent vascular mediators from astrocytes or neurons contribute to the local vasodilatation, but it is believed that local cerebrovasodilatation is closely linked to Ca^{2+} rises in neurons and or astrocytes. The aim in this study was to investigate Ca^{2+} dynamics in mouse sensory cortex in relation to local evoked vasodilatation.

Mouse sensory barrel cortex was activated by stimulation of the contralateral infraorbital nerve (IO). The 8 weeks old male mice were anaesthetized with ketamine and xylazine while prepared surgically, and α-chloralose during the experiment. End-inspiratory CO_2 and blood pressure were monitored continuously. CBF responses were monitored through a cranial window using Laser-Doppler flowmetry (n=4), and Ca^{2+} imaging was carried out in vivo using a 2- photon microscope (n=8) (Leica SP-5). The Laser-Doppler probe was placed just above the craniotomy, and microelectrodes were inserted into layers 2/3 in the right whisker cortex. In 2-photon experiments we used 2 types of fluorescent dyes: Rhod2, which was surface loaded and entered astrocytes, and Oregon Green Bapta which was bulk-loaded using extracellular microinjections in the cerebral cortex. The cranial windows were covered with agar and a cover-glass was positioned before imaging. IO stimulation was done at stimulation intensity of 1.5mA, in trains of 5-45s at 1Hz.

Stimulation produced clear local CBF responses concomitantly with a local field potential (LFP). IO stimulation also increased intracellular Ca^{2+} levels in both neurons and astrocytes. The Ca^{2+} response consisted of a low-frequency positive oscillation that lasted for as long as the stimulation, and of shorter peaks of 0.1-0.2 s following every stimulation, superimposed on the low-frequency signal. Astrocytes and neurons appeared to respond within the same narrow time frame. Ca^{2+} responses comprised of a rapid increase followed by a slower downslope, and based on the current data it was not possible to define a difference in Ca^{2+} dynamics of cell bodies of astrocytes and neurons. In conclusion, activity-dependent rises in CBF were accompanied by rises in both astrocytic and neuronal Ca^{2+} during activation of rat cerebral cortex in response to somatosensory stimulation. This may point to both astrocytic and neuronal sources of local cerebrovasodilators in response to activation.

633

Lassen Award: Lassen Award Symposium

EXCESSIVE SUPEROXIDE PRODUCTION AND ENDOTHELIAL DYSFUNCTION IN CEREBRAL ARTERIES OF ATHEROSCLEROTIC MICE ARE DUE TO ENHANCED ACTIVITY OF NOX2-CONTAINING NADPH-OXIDASE

A.A. Miller, T.M. De Silva, C.P. Judkins, H. Diep, G.R. Drummond, C.G. Sobey

Department of Pharmacology, Monash University, Melbourne, VIC, Australia

Objectives: Despite the absence of atherosclerotic lesions, endothelial dysfunction occurs in cerebral arteries of atherosclerotic mice. Although such changes are proposed to result from oxidative stress, the contributing molecular mechanisms are unknown. Here, we have tested the hypothesis that enhanced superoxide (O_2^-) production by Nox2-containing NADPH oxidase leads to impaired endothelial function in cerebral arteries of high fat-fed apolipoprotein E-deficient ($ApoE^{-/-}$) mice.

Methods: All mice were fed a high fat diet (21% fat and 0.15% cholesterol) from 5 weeks of age for 7-14 weeks. Cerebral arteries (pooled middle cerebral and basilar) were isolated from C57Bl6/J wild-type (n=13), $ApoE^{-/-}$(n=26), Nox2 deficient ($Nox2^{-/-}$; n=10) and novel $Nox2^{-/-}/ApoE^{-/-}$ (n=23) mice. Basal O_2^- production by cerebral arteries was measured using L-012 (100 μmol/L)-enhanced chemiluminescence. Endothelial function was assessed in isolated cannulated middle cerebral arteries using a perfusion myograph via the vasoconstrictor response to the nitric oxide synthase inhibitor, N-nitro-L-arginine methyl ester (L-NAME; 100 μmol/L).

Results: Plasma total cholesterol levels of wild-type (n=6), $ApoE^{-/-}$ (n=9) and $Nox2^{-/-}/ApoE^{-/-}$ (n=10) mice were 13±0.2, 83±16, and 97±12 mmol/L, respectively. En face oil red O staining showed that there were no atherosclerotic lesions in aortae of wild-type mice (n=13). In $ApoE^{-/-}$ mice, aortic lesions were prominent (~9% of total aortic surface, n=13) but no lesions were observed in the cerebral arteries. O_2^- production was elevated in cerebral arteries from $ApoE^{-/-}$ (35±5 x 10^3 counts/mg; n=14, $P< 0.05$) versus wild-type (16±2 x 10^3 counts/mg; n=11) and Nox2-/- (10±2 x10^3 counts/mg; n=6) mice. However, in $Nox2^{-/-}/ApoE^{-/-}$ mice, cerebral artery O_2^- production was not elevated (11±1 x10^3 counts/mg; n=17). The magnitude of L-NAME-induced contractions of isolated middle cerebral arteries from $ApoE^{-/-}$ mice (Δ diameter = -13±4 %; n=6, $P< 0.05$) was < 50% of that in wild-type mice (-34±2 %; n=6), whereas in $Nox2^{-/-}/ApoE^{-/-}$ (-33±10 %; n=6) mice endothelial function was comparable to that in wild-types. By contrast, similar constrictor responses to high K^+ (124 mM) were observed in wild-type (-59±4 %), $ApoE^{-/-}$ (-60±5 %), and $Nox2^{-/-}/ApoE^{-/-}$ (-65±3 %) mice. In the presence of the O_2^- scavenger, tempol (1 mM), endothelial function was similar in $ApoE^{-/-}$ (-25±5 %) and wild-type (-24±3 %) mice.

Conclusions: In summary, excessive O_2^- production and endothelial dysfunction occur in cerebral arteries of atherosclerotic mice even in the absence of lesions. Furthermore, we report for the first time that these changes appear to be exclusively due to increased activity of Nox2-containing NADPH oxidase.

NEUROPROTECTIVE AND ANTI-INFLAMMATORY EFFECTS OF HISTONE DEACETYLASE INHIBITION BY VALPROATE IN TRAUMATIC BRAIN INJURY

H. Rhinn[1], V. Escriou[1], D. Sherman[1], E. Ake[2], M. Plotkine[2], **C. Marchand-Leroux**[2], V. Besson[2]

[1]U640, [2]Pharmacology of Cerebral Circulation, EA2510, Paris Descartes University, Paris, France

Objectives: TBI leads to a deleterious neuroinflammation evidenced by oedema, cytokines production, matrix metalloproteinases (MMP) activation and leukocytes infiltration. As many inflammatory mediators are regulated at the transcriptional level, a pleiotropic action on their transcription may afford a massive anti-inflammatory effect. Histone deacetylases (HDAC) are a family of enzymes removing acetyl groups from histones and nuclear components such as transcription factors, which make them playing a central role in the transcription modulation. Recently, valproic acid (VPA), a well-known drug largely used for the treatment of seizures and bipolar mood disorders, has been reported to inhibit HDAC causing hyperacetylation[1]. So we hypothesized that VPA could promote beneficial effects on deleterious consequences induced by TBI.

Methods: Male Swiss mice (28-32g) anaesthetized under 2% halothane, were submitted to TBI using a weigh-drop device (50g weight), as previsouly described[2]. Mice were given VPA (300 mg/kg) or its vehicle (0.9% NaCl) intraperitoneally 5 minutes after TBI as this dose inhibits HDAC activity demonstrated by an increase of histone H3 acetylation[3]. The neurological deficit was assessed by grip score measuring the length of time (in seconds) that mice remained on the string in some manner (using one or more paws, tail, tail plus paws), for a maximum of 30 seconds. In addition, during these 30-second period, the string test, scoring from 0 (severely impaired) to 5 (normal), evaluated the way mice could hang and move on the string. Cerebral oedema was determined by measuring brain water content (BWC) using the wet weight-dry weight technique. Levels of mRNA of 5 inflammatory mediators (interleukin-1β, chemokine receptor CCR2, MMP9 and 12, P-selectin) and the one of the chaperone protein HSP70 were quantified by quantitative RT-PCR. The effect of VPA on HDAC activity was evaluated by immunohistochemistry of acetylated histone H3.

Results: Uninjured mice had a grip score of 30±0.00s and a string score of 5.0±0.00 at 24 hours. At 24 hours post-TBI, the grip and string scores were markedly decreased in vehicle-treated mice (grip: 19.4±3.03s, $P< 0.01$; string: 1.0±0.30, $P< 0.001$) showing a neurological deficit. VPA-treated mice showed an improved grip (25.7±2.00s, $P< 0.05$) and string (2.5±0.52, $P< 0.05$) scores after TBI, demonstrating a neurological recovery-promoting effect. The BWC of uninjured mice was 79.6±0.11%. TBI induced an increase in the BWC (80.2±0.18%, $P< 0.05$) showing cerebral oedema. Treatment with VPA reduced the post-traumatic increase in BWC (79.7±0.16%, $P< 0.05$) demonstrating an anti-oedematous effect. The increase in levels of mRNA encoding for IL-1β, CCR2, MMP9 and 12, P selectin observed after TBI were reduced by VPA ($P< 0.001$). Moreover, VPA increased levels of post-traumatic mRNA of HSP70 ($P< 0.01$).

Conclusion: Our data show that VPA promotes neurological recovery and anti-oedematous effects after TBI. Beneficial effects induced by VPA are mediated, at least in part, through inhibition of HDAC, induction of HSP70 and reduction of levels of mRNA of 5 inflammatory mediators.

References:

1. Phiel et al., 2001, J. Biol. Chem. 276, 36734-36741.

2. Hellal et al., 2003. J. Neurotrauma. 20 (9), 841-851.

3. Ren et al., 2004. J. Neurochem. 89, 1358-1367.

TEMPLATE BASED ATTENUATION CORRECTION FOR BRAIN MR-PET SCANNERS

E. Rota Kops, **H. Herzog**

Institute of Neuroscience and Medicine, Forschungszentrum Juelich, Juelich, Germany

Objectives: A primary prerequisite that positron emission tomography is regarded as a quantitative imaging procedure is its ability to correct sufficiently for attenuation. While in dedicated PET scanners attenuation correction is usually based on measured transmission data, in the new combined MRI-PET scanners the attenuation coefficients must probably be obtained with help of the anatomical T1-weighted images. This work investigates template based attenuation correction (TBA) of PET scans, the procedure of which was described in a previous report [1], in comparison to conventional PET based attenuation data (PBA).

Methods: Several templates were created. Inputs for these templates were gender specific attenuation maps recorded by PET transmission scans as well as a female CT image converted into linear attenuation coefficients in cm^{-1} at 511 keV [2]. For the gender specific attenuation maps we used four male and four female transmission images and registered non-linearly three of them to the fourth. Furthermore, we took all eight images and registered non-linearly seven of them to a male eighth or to a female eighth. Finally, averages of these four registered groups were calculated resulting in four transmission based attenuation templates txAT (4mAT and 4fAT, 8mAT and 8fAT), for which the corresponding MR templates were obtained in the same way. The converted female CT image and its corresponding MR image built a CT based attenuation template (ctAT). Following the procedure described elsewhere [1], PET scans of 5 male and 5 female subjects of an ongoing study were attenuation corrected using the five groups of ATs and the reconstructed emission data were compared to PET images which were attenuation corrected using the conventional PBA data. Regions of interest (ROI) were drawn in cortical and subcortical relevant areas. Relative differences between PBA and the TBA images were calculated and averaged over all ROI and over each group.

Results: While in case of ATs, which have been created by referring to a female image, the means were positive with very similar standard deviations (4fAT: 1.04±3.73%, 8fAT: 0.13±3.57%, ctAT: 1.86±3.50%), the corresponding values obtained with ATs, which have been referred to a male image, showed a slight underestimation (4mAT: -2.84±3.63%, 8mAT: -2.46±3.52%). Between the mixed gender (8fAT: 0.13±3.57% and 8mAT: -2.46±3.52%) and the gender-related templates (4fAT: 1.04±3.73%, 4mAT: -2.84±3.63%, and ctAT: 1.86±3.50%) no significant differences could be found.

Conclusions: The presented results show that the mixed gender templates (8fAT and 8mAT) as well as the gender-related templates (4fAT, 4mAT, and ctAT) are appropriate for attenuation correction in a MR-BrainPET scanner.

References:

[1] Rota Kops E. et al, IEEE San Diego 2006.

[2] Burger C. et al, Eur J Nucl Med 2002; 29:922-927.

NEUROPROTECTIVE EFFECT OF CEFTRIOXONE IN A MODEL OF VENOUS ISCHEMIA

A. Heimann[1], T. Inui[1,2], B. Alessandri[1], K. Frauenknecht[3], C. Sommer[3], O. Kempski[1]

[1]Institute for Neurosurgical Pathophysiology, Universitätsmedizin, Johannes Gutenberg-University, Mainz, Germany, [2]Department of Neurosurgery, Nara Medical University, Nara, Japan, [3]Department for Neuropathology, Universitätsmedizin, Johannes Gutenberg-University, Mainz, Germany

Background and aims: The glutamate transporter GLT-1 removes glutamate from the extracellular space. Recently it has been shown that the beta-lactam antibiotic Ceftriaxone (CTX) increases the expression of GLT-1. It is controversial, however, whether the upregulation of GLT-1 has an neuroprotective effect in the ischemic penumbra. Thus, the aim of the study was first of all to investigate whether CTX reduces the infarct volume in a rat model of venous ischemia. A second experiment was designed to examine whether CTX pretreatment has an effect on glutamate (NMDA, AMPA) and GABA receptors.

Methods: In the first set of experiments 29 male Wistar rats were randomized into four groups. All animals were pre-treated either with saline (vehicle; n=7) or with 200 mg/kg/d (CTX; n=11) for five days. In two further groups GLT-1was inhibited by intraventricular injection of dihydro-kainate 30 min before induction of focal venous ischemia (CTX+DHK; n=6; vehicle+DHK; n=5). The animals were anaesthetized, intubated and ventilated. Blood pressure and blood gases were monitored and regional cerebral blood flow (rCBF) was assessed by laser Doppler scanning on the ipsilateral parietal cortex. Focal ischemia was induced by photochemical occlusion of two adjacent bridging veins (2-VO: see Crit Care Med 2003, 31: 2495-2501). The brains were removed 2 days after 2-VO and infarct volume was assessed by quantitative morphometry (HE-staining). In the second set of experiments 10 native rats (without ischemia) were pretreated with CTX (200mg/kg/d) or vehicle for 5 days before the brains were removed and immediately frozen for later evaluation for receptor density of NMDA, AMPA and GABA receptors using in-vitro autoradiograhy.

Results: Mean arterial blood pressure, rectal and brain temperature and blood gases remained normal in all groups. There was no difference in rCBF at baseline (42.21±16.4 LD-units), it decreased identically after 2-VO in all groups by approx. 50% (Fig. 1A). The infarct volume was 8.21 mm3 in the vehicle group. CTX pre-treatment resulted in a significant infarct reduction to 5.53 mm3 (Fig. 1B). After inhibition of GLT-1 transporter by dihydro-kainate the infarct size was 12.3 mm3 in the vehicle+DHK and 9.3 mm3 in the CTX+DHK group, respectively. Thus, both groups had significantly bigger infarcts than CTX treated subjects. In the second set of experiments quantitative in vitro receptor autoradiograpy did not show any differences for NMDA, AMPA and GABA receptors between the CTX/saline pre-treated native rats without ischemia.

Conclusion: CTX has a neuroprotective potential without changing glutamate receptors density. This effect can be abolished by GLT-1 inhibition, indicating that the up-regulation of glutamate transporter GLT-1 is one mechanism of action.

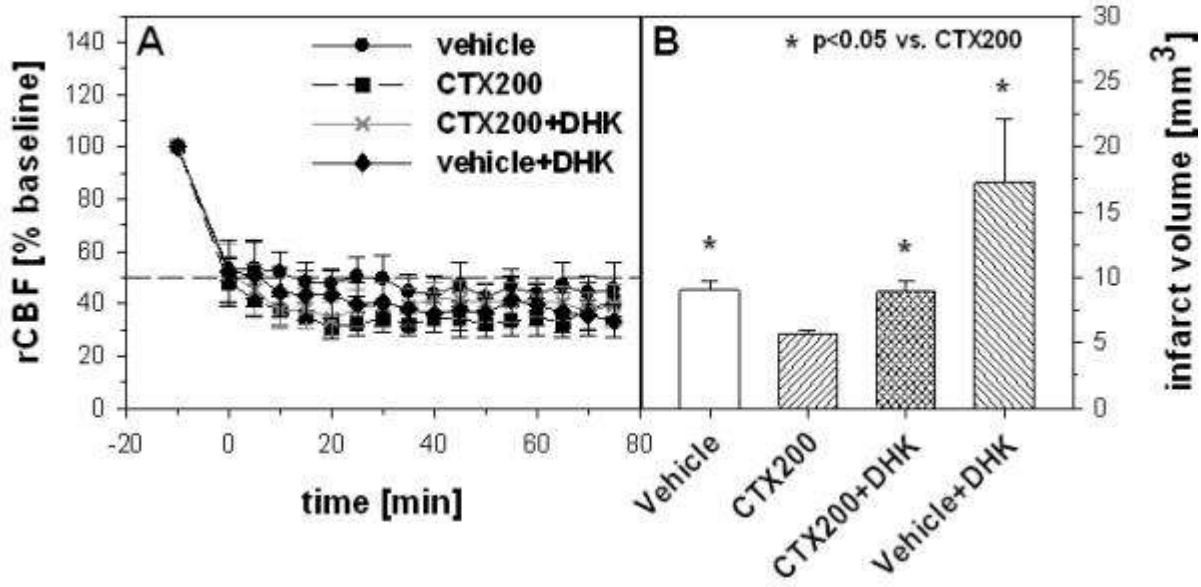
A
B
vehicle
CTX200
CTX200+DHK
vehicle+DHK
* p<0.05 vs. CTX200
rCBF [% baseline]
time [min]
infarct volume [mm3]
Vehicle
CTX200
CTX200+DHK
Vehicle+DHK

[Fig 1.jpg]

638

Brain Poster Session: Stem Cells & Gene Therapy

INTRAVENOUS COADMINISTRATION OF SMOOTH MUSCLE AND ENDOTHELIAL PROGENITOR CELLS ENHANCES ANGIOGENESIS IN FOCAL PERMANENT CEREBRAL ISCHEMIA IN MICE

N. Deroide[1], L.R. Nih[1], C. Déan[2], M. Clergue[1], B.I. Lévy[1], J.-S. Silvestre[1], G. Tobelem[2], N. Kubis[1]

[1]Unité INSERM 689, Hôpital Lariboisière, [2]Institut Vaisseaux Sang, APHP Hôpital Lariboisière, Paris, France

Objectives: Extensive evidences indicate that angiogenesis plays a key role in stroke recovery. Strong cooperation between endothelial and smooth muscle cells is required for the formation of a mature functional vascular network. Therefore, we assessed whether therapy based on coadministration of smooth muscle progenitor cells (SMPCs) and endothelial progenitor cells (EPCs) isolated from human cord blood enhances angiogenesis and neurogenesis, in a murine model of focal permanent cerebral ischemia.

Methods: Ischemia was induced in adult male C57Bl6 mice by the thermocoagulation of the middle cerebral artery (MCA). SMPCs ($0.5x10^6$), EPCs ($0.5x10^6$), SMPCs+EPCs ($0.25x10^6$+$0.25x10^6$) or phosphate-buffered saline (PBS) were intravenously administered 24 hours post-MCA occlusion (n=6-8/group). To assess proliferation, BrdU (100 mg/kg, i.p.) was injected 4 and 2 hours before sacrifice on day 7 post-MCAo. Infarct volume was measured by histomorphological analysis of Cresyl Violet stained sections. Blood-brain barrier (BBB) permeability was quantified using Evans Blue extravasation. Vascular area, cell proliferation and proliferating cell phenotype were determined in ischemic and peri-ischemic areas, using co-immunostaining with antibodies against doublecortin, laminin, CD31 and BrdU.

Results: Infarct volumes were not significantly different (7.09 ± 2.97, 6.83 ± 3.16, 6.70 ± 2.48 mm^3) for SMPCs, EPCs, SMPCs+EPCs-treated groups respectively, compared to the PBS group (6.01 ± 2.39 mm^3). However, the vascular area in the infarct was significantly increased in all treated groups with SMPCs, EPCs or EPCs+SMPCs, in the same range, compared to controls (+17.4%±8%, +19.4%±5.2% and +17.3%±3.6%, respectively, $p< 0.05$). Phenotypical vascular differences were evidenced between groups. SMPCs-treated mice showed an immature disorganized and dilated vasculature, EPCs-treated mice showed more numerous small vessels, whereas SMPCs+ EPCs-co-treated mice showed more mature and numerous vessels. The number of co-labelled BrdU-CD31 positive cells was significantly increased in all treated groups, compared to PBS but more markedly for the EPCs- and SMPCs+EPCs co-treated mice: 14.7±1.2/ROI (controls), 22.7±1.5/ROI (SMPCs), 33.3±3.2/ROI (EPCs) and 35.0±1.4/ROI (SMPCs+EPCs) ($p< 0.002$), indicating angiogenesis in this area of intense remodelling. In addition, the number of peri-infarct BrdU-positive cells was higher only in the SMPCs+EPCs-treated group (3-fold) compared to the three other groups ($p< 0.002$), but no neurogenesis was evidenced in this group. Despite vascular remodelling, we found no significant difference in BBB permeability at day 7 (111.67%±39,8%, 111.39%±31.1%, 114%±19%) for SMPCs, EPCs, SMPCs+EPCs-treated group respectively, compared to the PBS group.

Conclusions: Co-administration of human cord blood smooth muscle and endothelial progenitor cells triggers vascular remodelling and angiogenesis in the infarct and intensive cell proliferation in the peri-ischemic area in cerebral ischemia in mice. Whether, neurological deficit is improved remains to be determined.

639

Brain Poster Session: Cell Signaling

MAPK SIGNALLING PATHWAY REGULATE CEREBROVASCULAR RECEPTOR EXPRESSION IN HUMAN CEREBRAL ARTERIES

S. Ansar[1,2], E. Nilsson[1], O. Nilsson[3], H. Säveland[3], L. Edvinsson[1,2]

[1]Clinical Sciences, Division of Experimental Vascular Research, Lund University, Lund, Sweden, [2]Clinical Experimental Research, Glostrup Research Institute, Glostrup University Hospital, Glostrup, Denmark, [3]Neurosurgery, Lund University Hospital, Lund, Sweden

Objectives: Stroke is a serious disease and the third leading cause of death worldwide. During the last two decades substantial efforts have been made to understand the intracellular mechanisms involved in ischemia-induced cerebral damage and to develop drugs that protect the brain from damage once a stroke has occurred. However, despite extensive research, few therapies have been proven effective in the clinic so far.

Cerebral ischemia is multifactorial and we have before demonstrated upregulation of contractile endothelin-1 (ET), angiotensin (Ang II) and 5-hydroxytryptamine (5-HT) receptors in the major cerebral arteries from experimental focal and global ischemia, via enhanced transcription and translation. Previous studies have shown that inhibitors of the mitogen-activated protein kinases (MAPK) can diminish the ischemic area and contractile cerebrovascular receptors after experimental cerebral ischemia. Here we hypotheses that there is an upregulation of contractile cerebrovascular receptors after 48 h of organ culture in human cerebral arteries and this upregulation occur via the MAPK ERK1/2 pathway and can be inhibited by the MEK1/2 inhibitor U0126.

Methods: Human cerebral arteries were obtained from patients undergoing intracranial tumor surgery. The vessels were divided into segments and incubated for 48 h with or without the MEK1/2 inhibitor U0126. The vessels were then examined by using in vitro pharmacological methods. The contractile responses to ET-1 (ET_A and ET_B receptor), AngII, 5-carboxamidotryptamine (5-CT) and U46619 (Thromboxane (TP) receptor agonist) were investigated.

Results: After organ culture of the cerebral arteries the contractile responses of the ET-1, AngII and TP receptors were enhanced in comparison with data for fresh human arteries. However, 5-CT induced decreased contractile responses after organ culture as compared to fresh arteries. Incubation with the MEK1/2 inhibitor U0126 diminished the maximum contraction elicited by application of ET-1, Ang II and U46619 in human cerebral arteries considerably compared to control (organ culture). In addition, the MEK1/2 inhibitor decreased the contractile response to 5-CT. Statistical analyses were performed with Kruskal-Wallis non-parametric test with Dunn´s post-hoc test, where $P< 0.05$ was considered significant. Data are expressed as mean ± s.e.m.

Conclusion: This is the first study to demonstrate that there is a clear association between human cerebrovascular receptor upregulation via transcription involving activation of the MAPK pathway after organ culture. Inhibition of the MAPK pathways attenuated the vasoconstriction mediated by ET, AT and TP receptors in human cerebral arteries after organ culture. These results indicate that MAPK inhibition is a novel target for treatment of cerebrovascular disorders.

640

Brain Poster Session: Experimental Stroke & Cerebral Ischemia

NO PRODUCTION, HYDROXYL RADICAL METABOLISM AND ISCHEMIC CHANGE OF HIPPOCAMPAL CA1 DURING CEREBRAL ISCHEMIA AND REPERFUSION IN AT2KO MICE

Y. Ito[1], T. Ohkubo[1], Y. Asano[1], K. Hattori[1], T. Shimazu[1], M. Yamasato[1], H. Nagoya[1], Y. Kato[1], M. Horiuchi[2], M. Iwai[2], **N. Araki**[1]

[1]Neurology, Saitama Medical University, Saitama, [2]Molecular Cardiovascular Biology and Pharmacology, Ehime University, Graduate School of Medicine, Ehime, Japan

Introduction: It is reported that an angiotensin II type2 (AT2) receptor is up-regulated during cerebral ischemia, and the ischemic area induced by MCA occlusion was significantly larger in AT2 receptor knock out (AT2KO) mice than in wild type [1]. It is also suggested that AT2 receptor stimulation may protect brain tissue during cerebral ischemia. The purpose of this study is to investigate the nitric oxide production, hydroxyl radical metabolism and ischemic change of hippocampal CA1 during cerebral ischemia and reperfusion in AT2KO mice.

Methods:

1. AT2KO mice [n=5] and control mice (C57BL/6 mice [n=6]) were anesthetized by halothane. Both NO production and hydroxyl radical metabolism were continuously monitored by in vivo microdialysis. Microdialysis probes were inserted into the bilateral striatum. The in vivo salicylate trapping method was applied for monitoring hydroxyl radical formation via 2,3 dihydroxybenzoic acid (2,3-DHBA), and 2,5 dihydroxybenzoic acid (2,5-DHBA). A Laser Doppler probe was placed the skull surface. Blood pressure, blood gases and temperature were monitored and maintained within normal ranges throughout the procedure. Forebrain cerebral ischemia was produced by occlusion of both common carotid arteries for 10 minutes. Levels of nitric oxide metabolites, nitrite (NO_2^-) and nitrate (NO_3^-), in the dialysate were determined using the Griess reaction.
2. CA1 neurons: Hippocampal CA1 neurons were analyzed into three phases (severe ischemia, moderate ischemia, survive), and the ratio of the number of surviving neurons was calculated (survival rate).
3. Brain sections were immunostained with an anti-nNOS antibody. To determine the fractional area density of nNOS-immunoreactive pixels to total pixels of the whole field, the captured images were analyzed. Mann-Whitney U test was used for group comparisons.

Results:

1. Blood Pressure: AT2KO group (82.1 ± 10.4mmHg; mean ± SE) showed significantly higher blood pressure than that of the control group (68.0 ± 13.2), 50-10 minutes before ischemia, and 10 minutes after the start of reperfusion ($p< 0.05$).
2. Cerebral Blood Flow (CBF): No significant differences were obtained between the groups.
3. Nitric oxide metabolites (NO_2^- & NO_3^-): There were no significant differences between the groups.
4. Hydroxyl radical metabolites: 1) 2,3-DHBA; AT2KO group (99.1 ± 3.87%) showed significantly lower than that of control group (107.1 ± 7.41) 20 minutes after the start of reperfusion ($p< 0.05$) **(Fig.1)**. 2) 2,5-DHBA; There were no significant differences between the groups.

5. Survival rate in CA1 area: There were no significant differences between the groups.
6. nNOS activity: There were no significant differences between the groups.

Conclusion: These in vivo data suggest that AT2 receptor may be closely related to the hydroxyl radical metabolites in striatum following ischemia and repurfusion.

Reference: 1. Iwai et al. Possible Inhibition of focal cerebral ischemia by angiotensin II type 2 receptor stimulation. Circulation 2004; 110: 843-848.

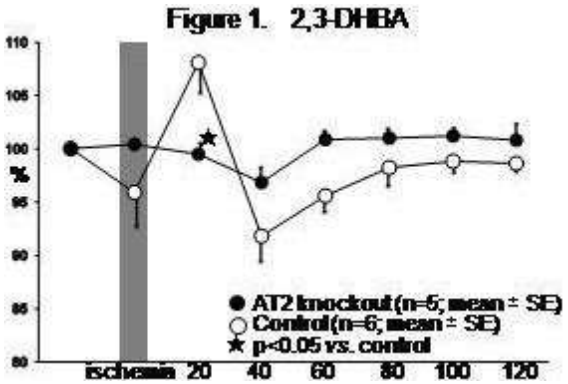

[BRAIN09]

641

Brain Poster Session: Inflammation

PIOGLITAZONE DOWN-REGULATES INTERLEUKIN-1β AND UP-REGULATES INTERLEUKIN-1 RECEPTOR ANTAGONIST IN THE PERI-INFARCT FRONTOPARIETAL CORTEX OF RATS EXPOSED TO CEREBRAL ISCHEMIA

J. Culman, T. Glatz, I. Stöck, P. Gohlke, Y. Zhao

Institute of Experimental and Clinical Pharmacology, University Hospital of Schleswig-Holstein, Kiel, Germany

Objectives: Interleukin-1 (IL-1) upon binding to the IL-1 receptor I (IL-1RI) activates the transcription of a number of pro-inflammatory cytokines and neurotoxic mediators which exert deleterious effects and exacerbate neuronal injury after ischemic stroke. Interleukin-1 receptor antagonist (IL-1ra) is the natural antagonist which inhibits the effects of IL-1 on target cells. A number of studies have demonstrated that systemic or central treatment with the peroxisome-proliferator-activated receptors gamma (PPARγ) agonists ameliorates brain injury after cerebral ischemia. We studied the effects of pioglitazone, a selective PPARγ agonist, applied intracerebroventricularly (ICV) on the expression of IL-1β, IL-1RI and IL-1ra in the peri-infarct frontoparietal cortex of rats exposed to cerebral ischemia.

Methods: Pioglitazone (3 nmol/h) or vehicle (controls) were infused ICV via osmotic minipumps in male Wistar rats, over a 5-day period before, and 24 or 48 h after transient middle cerebral artery occlusion (MCAO) for 90 min. The induction of IL-1β, IL-1RI and IL-1ra in the frontoparietal cortex adjacent to the ischemic core was studied by immunohistochemistry and Western blot at both time points after MCAO. Cortical cell cultures were used to ascertain the role of the PPARγ in the regulation of IL-1ra expression in neurons.

Results: Activation of cerebral PPARγ reduced the infarct size at both time points (by 37% and 32%, respectively). Pioglitazone infused ICV abolished IL-1β protein levels and decreased the number of IL-1 beta positive cells in the frontoparietal cortex adjacent to the ischemic core, the expression of the IL-1RI was not affected. Pioglitazone up-regulated IL-1ra protein in the peri-infarct cortical tissue and increased the numbers IL-1ra positive cells in this area at both time points after MCAO. In primary cortical cell culture, the selective PPARγ antagonist, GW-9662, failed to reverse the pioglitazone-induced up-regulation of IL-1ra protein, indicating that this effect was not mediated by PPARγ.

Conclusions: The activity of the IL-1 system depends on the balance between IL-1 and its antagonist, IL-1ra. Inhibition of IL-1β expression und the up-regulation of IL-1ra by pioglitazone shifted the balance between agonist/antagonist ligands towards reduction of post-ischemic inflammation. The suppression of post-ischemic inflammation in brain tissue limits the progression of ischemic injury and improves the recovery from ischemic stroke.

Brain Poster Session: Cell Signaling

UNRAVELING TLR-4 MEDIATED SIGNAL TRANSDUCTION PATHWAYS ACTIVATED IN GLIA AND THE INHIBITORY ACTIONS OF UNFRACTIONED HEPARIN

R. Gorina[1], A. Chamorro[2], A.M. Planas[1]

[1]Cerebral Ischemia and Neurodegeneration, IIBB (Institute of Biomedical Research)-CSIC - IDIBAPS, [2]Stroke Unit, Neurology Service, Hospital Clinic, Barcelona, Spain

Objectives: Inflammation is regarded as a target for the treatment of stroke (1). Heparin exerts beneficial effects in brain ischemia (2,3) that can be in part mediated by its anti-inflammatory properties (4). Innate immune responses mediated by toll-like receptor-4 (TLR-4) are involved in ischemic brain damage (5,6). In this study we examined the putative anti-inflammatory effect of heparin following activation of TLR-4.

Methods: Astrocyte-enriched cultures from rat cortex were exposed to the TLR-4 agonist LPS in the presence or absence of heparin. Activation of signal transduction pathways was examined, and small interference RNA (siRNA), blocking antibodies, or inhibitory drugs were used to demonstrate the involvement of various molecules.

Results: LPS induced the expression of inflammatory mediators, such as vascular cell adhesion molecule-1 (VCAM-1), cyclooxygenase-2 (COX-2), tumor necrosis factor-alpha (TNFα), interferon-gamma inducible protein-10 (IP-10) and monocyte chemoattractant protein-1(MCP-1). Activation of TLR-4 by LPS induced nuclear factor-kappa B (NFkB) activation within the first hour, as demonstrated by proteasome-dependent IkBalpha degradation and nuclear translocation of the p65 subunit of the NFkB complex. In addition, LPS caused phosphorylation (Tyr701) of signal transductor and activator of transcription-1 (Stat1), but this effect was delayed for 2h. Then, activation of Stat-1 dependent gene transcription was observed (e.g. suppressors of cytokine signalling-1 (SOCS-1) and IL-15 mRNA). LPS-induced pStat1 was mediated by Jak1; it was dependent on previous activation of NFkB, on new protein synthesis, and on release of a soluble factor to the medium. Heparin did not prevent NFkB activation or the expression of several target genes induced by LPS, in spite that this has been described in other cell types (7). However, heparin strongly inhibited the Jak1/Stat1 pathway. In addition, LPS induced a rapid activation of extracellular signal regulated kinase-1/2 (ERK1/2) that was partially inhibited by heparin, it was independent of NFkB and on new protein synthesis, but it was fully prevented by antioxidants. The Stat1 activation after LPS reported above was also dependent on ERK1/2 phosphorylation. We have evidences supporting that signaling through TNFα after LPS is involved in ERK1/2 activation, and that heparin interferes with this process.

Conclusions: The results show that oxidative stress induced by LPS caused early ERK1/2 phosphorylation that indirectly participated in delayed Stat1 tyrosine phosphorylation, and heparin interferes with these processes. Therefore, TLR-4 activation induces a complex pattern of intracellular and extracellular signaling that is, at least in part, cell-type dependent, and that heparin can interfere with the inflammatory cascade and specifically attenuate certain proinflammatory responses.

References:

1. Chamorro & Hallenbeck, 2006; Stroke 37:291-3.

2. Cervera et al., 2004; J Neurosci Res 77:565-72.

3. Chamorro, 2006; Stroke 37:3052-3.

4. Lever R, Page CP, 2002; Nat Rev Drug Discov. 1:140-8.

5. Caso et al., 2007; Circulation 115:1599-608.

6. Kilic et al., 2008; Neurobiol Dis 31:33-40.

7. Hochart et al., 2006; Br J Haematol 133(1):62-7.

Acknowledgement: Supported by the Spanish Ministry of Education and Science (CICYT) and by the European Community´s Seventh Framework Programme (FP7/2007-201, grant n° 201024, European Stroke Network).

INTRAVENOUS ADMINISTRATION OF AUTOLOGOUS MESENCHYMAL STEM CELLS DERIVED FROM BONE MARROW INTO STROKE PATIENTS

K. Houkin[1], O. Honmou[1], T. Matsunaga[2], S. Ishiai[3], S. Waxman[4], J. Kocsis[4]

[1]Neurosurgery, [2]Fourth Department of Internal Medicien, [3]Rehabilitation, Sapporo Medical University, Sapporo, Japan, [4]Neurology, Yale University School of Medicine, New Haven, CT, USA

Background: Intravenous injection of mesenchymal stem cells (MSCs) prepared from adult bone marrow has been reported to ameliorate functional deficits in several CNS diseases in experimental animal models. Bone marrow cells can be enriched in MSCs by selecting for plastic-adherent cells. MSCs will grow to confluency in appropriate culture conditions as flattened fibroblast-like cells. Although MSCs may be present in different proportions in the stromal cell fraction of various species, MSCs have a distinct cell surface antigen pattern including $SH2^+$, $SH3^+$, and $CD34^-$, and methodologies have been established to culture human MSCs in very high purity. Although human MSCs have been clinically used for several diseases, it is still uncertain whether MSCs may have therapeutic benefits on stroke patients.

Objectives: The objectives of this study were to examine feasibility and safety of cell therapy using culture-expanded autologous MSCs in twelve stroke patients. This study was a phase I clinical trial.

Methods: Twelve (male and female) patients aged >/=40 years with stroke were enrolled. Bone marrows from the stroke patients were obtained by aspiration from the posterior iliac crest after informed consent was obtained; the subject's consent was obtained according to the Declaration of Helsinki, and this study was approved by the Institutional Review Board at Sapporo Med. Sch. where the cells were isolated and transplanted. Bone marrow was plated in plastic tissue culture flasks, and the adherent cells were cultured in appropriate medium in a humidified atmosphere of 5% CO_2 at 37°C. After reaching confluency, they were harvested and cryopreserved until use. On the day of infusion cryopreserved units were thawed at the bedside in a 37°C water bath and injected intravenously into patients over 30 min. All patients were monitored closely during and within 48 h of MSC injections. Oxygen saturation, temperature, blood pressure, pulse and respiratory rate were carefully monitored before and after injection. Patients also had chest films before and after MSC injection. Patients had carefully been followed for 12 months.

Results: Human bone marrow-derived MSCs were successfully isolated from bone marrow aspirate from all 12 stroke patients, and all were successfully culture-expanded. Serial evaluations showed no adverse cell-related, serological, or imaging-defined effects.

Conclusions: In patients with cerebral infarcts, the intravenous administration of autologous MSCs appears to be feasible and safe, and merits further study as a therapy that may improve functional recovery.

USE OF RESIDUE CONSTRAINTS AND STOCHASTIC PROPERTIES OF NOISE IMPROVES THE ACCURACY OF PERFUSION INFORMATION RECOVERED FROM DYNAMIC CONTRAST MR/CT

N. Fitzgerald[1], F. O'Sullivan[1], G. Newman[2]

[1]University College Cork, Cork, Ireland, [2]Albert Eistein Research Centre, Philadelphia, PA, USA

The application of residue analysis for quantification of the haemodynamic parameters flow, volume and mean transit time for perfusion CT/MR is well established. This technique requires the use of deconvolution of the acquired dynamic data to estimate the residue function (R) which by definition takes a positive and monotone decreasing shape. Reconstruction of R provides estimates of each parameter. In the case of MRI, the raw signal intensity is well approximated by Rician statistics. The standard approach to estimation involves logarithmic transformation and deconvolution by truncated singular value decomposition. At low signal to noise this approach may not be efficient. A maximum likelihood deconvolution method involving an iterative re-weighted non-linear least squares algorithm incorporating residue function constraints has been developed. Simulation studies are presented to evaluate improvements in parameter estimates achieved by this approach relative to the standard deconvolution method. The results show that over a range of realistic signal to noise values, significant improvements in estimation accuracy are achieved (10-20% in flow and mean transit time). The method is applied to perfusion MRI data and smoothed parametric maps based on arterial input selected by shape driven segmentation are presented.

Supported by the Irish Health Research Board.

NEAR-INFRARED SPECTROSCOPY IN PRIMARY AND SECONDARY MOTOR AREAS IN SELF-PACED VERSUS EXTERNALLY CUED MOTOR TASKS

C. Drenckhahn[1,2,3], J. Steinbring[2,3], J. Duemmler[3], M. Kohl-Bareis[3,4], J.P. Dreier[1,2,3]

[1]Experimental Neurology, [2]Neurology, Charité, Universitätsmedizin Berlin, [3]Berlin Neuroimaging Center, Berlin, [4]RheinAhrCampus, University of Applied Sciences Koblenz, Remagen, Germany

Objectives: During the last years the application of near-infrared spectroscopy (NIRS) was studied in different setups to monitor cerebral oxygenation and perfusion in critical ill patients. However, NIRS still is not evaluated to be used as a validated bedside method and to influence clinical assessment and therapeutic decisions.

Methods: Using NIRS in human healthy subjects we investigated alterations in deoxy-hemoglobin (Hbdeoxy) concentrations as an indirect parameter for a hemodynamic response in the primary motor cortex (M1) and the supplementary motor area (SMA). M1 and SMA were measured simultaneously. 16 strongly right-handed volunteers underwent different finger tapping tasks which are known to be associated with increase in cerebral blood flow in M1 and SMA. The tasks were designed as blocks of 20s or single repetitive finger tapping either self-paced or externally triggered. 8 light sources and 7 detectors were positioned over the left M1 and the SMA covering an area of 12.5x7.5 cm. Time course and amplitude were analysed for the concentration of Hbdeoxy. For spatial analysis, the recording points with significant decrease in Hbdeoxy were determined.

Results: We detected a circumscribed decrease in Hbdeoxy at two different locations corresponding to SMA and M1 during functional activation. Significant changes in Hbdeoxy were located within an area of ~10 cm2 in projection on M1 and ~15 cm2 in projection on SMA, respectively. Both, M1 and SMA showed significantly higher shifts in Hbdeoxy following self paced movements demonstrating a higher level of activation due to planning and initiating in the self-paced task compared to the externally cued task (-2.81x10-5 vs. -2.22x10-5 mmol/l in M1, -1.63x10-5 vs. -1.25x10-5 mmol/l in SMA). In SMA the decrease of Hbdeoxy was significantly more accentuated following right hand movements compared to the increase during the left hand task (-3.4x10-5 vs. -2.2x10-5 mmol/l). This might indicate a more pronounced vascular response due to functional activation of the dominant hemisphere.

Conclusions: NIRS still has to be validated prior to its routine use as a non-invasive bedside tool in a clinical setup. Our data shows a reproducibility of NIRS compared to more complex methods like fMRI, PET or perfusion CT.

COGNITIVE FUNCTION AND INTELLIGENCE RELATED TO SEROTONERGIC NEUROTRANSMISSION: A BRAIN PET STUDY IN YOUNG HEALTHY VOLUNTEERS WITH ^{11}C-DASB

K. Madsen[1,2], D. Erritzoe[1,2], G. Zornhagen[2,3], E.L. Mortensen[2,3], G.M. Knudsen[1,2], S.G. Hasselbalch[1,2]

[1]Neurobiology Research Unit, Rigshospitalet, [2]Center for Integrated Molecular Brain Imaging, [3]University of Copenhagen, Copenhagen, Denmark

Objectives: Studies of central serotonergic activity in healthy volunteers have indicated that long-term memory and executive functions are sensitive to manipulations. Diseases involving the serotonin system often also involves cognitive dysfunction. However, only few PET serotonin studies have involved cognitive research in healthy volunteers. In this study was a positive correlation hypothesized between regional BP_{ND} of the serotonin transporter (SERT) and intelligence, primarily in left hemisphere regions.

Methods: A bolus injection of ^{11}C-DASB was followed by a 90 min dynamic PET scan in a GE Advance scanner in 32 healthy volunteers (25 males, mean age 25.8 years, range 20-37). Volumes of interest (VOIs) were delineated automatically on co-registered 3T MRIs. Time-activity curves were extracted from the VOIs' gray matter voxels, and BP_{ND} was modeled using Ichise's MRTM2 method.

Long term memory was measured with Rey Auditory Verbal Learning Test and Rey's Complex Figure. Executive function was measured with Trail Making B Test and Stroop. General intelligence was measured with The Danish Adult Reading Test (DART), and The Word and Number Test (WNT) (N=24). Educational years were scored. Correlations were performed in 4 bilateral fronto-striatal VOIs with age and day-light hours as covariates.

Results: A positive correlation was found between WNT and BP_{ND} in left caudate (R=0.586, p=0.0026, see figure), right caudate (R=0.578, p=0.0398), left ventrolateral prefrontal cortex (R=0.495, p=0.0139), a tendency was found in left dorsolateral prefrontal cortex (R=0.366, p=0.0784), but none in putamen. A positive correlation was also found between education years and left caudate (R=0.438, p=0.012) and a tendency was found in right caudate (R=0.526, p=0.096). No correlations between regional BP_{ND} and DART, specific memory and executive function tests were found. All p-values are uncorrected.

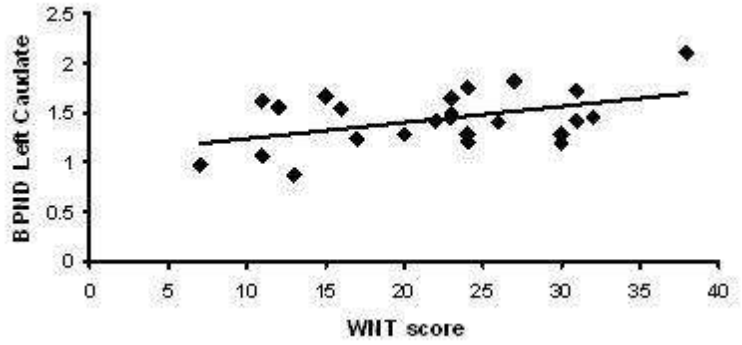

[SERT binding in left caudate in relation to WNT]

Conclusion: Our results showed a positive correlation between SERT binding primarily in the left hemisphere regions and intelligence measured with WNT. This was supported by same the pattern for education years found in caudate. Our results indicate that a putative link between the SERT level and general intelligence must be mediated through other mechanisms than mere memory and executive functions. However, an efficient 5-HT reuptake system seems to be of importance for general intelligence.

650

Brain Oral Session: Cortical Spreading Depression

LOCAL DYNAMIC METABOLIC RESPONSE TO SPONTANEOUS SPREADING DEPOLARISATIONS IN THE PENUMBRA OF THE ACUTELY INJURED HUMAN BRAIN

D. Feuerstein[1], A. Manning[2], P. Hashemi[3], M. Fabricius[4], A.J. Strong[2], M.G. Boutelle[3]

[1]Bioengineering, Imperial College London, [2]King's College Hospital, [3]Imperial College London, London, UK, [4]Glostrup University Hospital, Copenhagen, Denmark

Objectives: It has become clear that spreading depolarisations (SD) occur spontaneously in patients with acute traumatic or ischaemic brain injury [1]. They are waves of transient electrical depolarisations that propagate from the core of the injury to the surrounding compromised tissue. Although there is extensive evidence that SDs severely disrupt local cerebral blood flow [2] and metabolism [3] in animal models of stroke, little is known about the metabolic response to SD in the human brain.

Here we have used online rapid sampling microdialysis (rsMD) in human penumbral tissue to quantify the dynamic metabolic response to SDs detected by electrocorticography (ECoG).

Methods: In 10 patients selected for craniotomy, a clinical microdialysis (MD) probe, along with a 6-electrode subdural strip for the ECoG signal, was inserted under direct vision into the immediate vicinity of the injured cortical tissue. It was perfused with artificial cerebrospinal fluid at 2μL/min. The dialysate was assayed electrochemically using rsMD [4]. Glucose and lactate levels were thereby continuously measured at 1-minute intervals for up to five days following craniotomy. The rsMD data were analyzed and subsequently correlated to the SD events separately identified according to their ECoG signature [5].

Results: Metabolic changes were resolved in 90 identified SD events. The dialysis changes typically consisted of a rise in lactate peaking at +173.5 +/-29.6 μM and a drop in glucose down to -120.79 +/-13.2 μM relative to baseline values. The dialysis levels remained different from baseline values at 20 minutes after the SD event being 68.7+/-25.8 μM above baseline for lactate and 69.5+/-11.1 μM below baseline for glucose. In all patients the glucose concentrations did not recover their initial levels before the onset of the following SD, thus resulting in a progressive drop in extracellular glucose concentrations as measured by microdialysis.

Conclusions: These results agree well with experimental findings using rsMD [6]. The progressive fall in dialysate glucose suggests that the frequent occurrence of SD events leads to a failure of glucose supply to meet the energetic demand for the repolarisation of the cells. This could compromise the viability of the tissue and hence lead to further expansion of the lesion.

References:

[1] Strong et al., Current Opinion in Critical Care, 2007, 13:126-133.

[2] Strong, et al., Brain, 2007;130:995-1008.

[3] Hopwood et al., J Cerebral Blood Flow Metabolism, 2005;25:391-401.

[4] Parkin, et al., J Cerebral Blood Flow Metabolism, 2005;25:402-413.

[5] Fabricius et al., Brain, 2006; 129:778-790.

[6] Hashemi et al., J Cerebral Blood Flow Metabolism, 2009; 29:166-175.

651

Brain Poster Session: Experimental Stroke & Cerebral Ischemia

EFFECTS OF REHABILITATION ON BEHAVIORAL RECOVERY AND NEURONAL DAMAGE: A PET STUDY WITH ISCHEMIC BRAIN MODEL OF MONKEY

H. Tsukada[1,2], D. Fukumoto[1], H. Ohba[1], S. Nishiyama[1], T. Kakiuchi[1]

[1]Central Research Laboratory, Hamamatsu Photonics K.K., Hamamatsu, [2]CREST, Saitama, Japan

Objective: Rehabilitation by physiotherapist is one the essential treatments for patients suffered by cortical ischemic insult to recovery from movement inability. The rehabilitation started from acute phase has been well known to be more effective than that started from chronic phase. Although this suggests the existence of "critical period" for the recovery from the ischemic damage, the neurochemical mechanisms have not been clarified yet. In this study, we applied the monkey stroke model with occlusion/reperfusion of middle cerebral artery (MCA) (1, 2) to assess the effects of start timing of rehabilitation on behavioral recovery and neuronal damage.

Methods: Twenty mail young adult cynomolgus monkeys (Macaca fascicularis) were subjected to the study. Occlusion of right hemisphere MCA with surgical clip was performed under isoflurane anesthesia. After MCA occlusion for 3 hrs, the clip was removed for reperfusion of blood flow through the MCA. The effects of occlusion and reperfusion in MCA was confirmed by PET measurements with [^{15}O]gas. Rehabilitation as well as behavioral performance test was conducted with "apple test", where monkeys had to pick up small pieces of apple by right or left hand separately through small right or left window at the cage front door. Rehabilitation with "apple test" was started 4, 7 and 14 days after ischemic insult, and [^{11}C/^{18}F]Flumazenil-PET was performed before (normal), 1 and 28 days after the insult.

Results: When rehabilitation started 4 and 7 days after ischemic insult, behavioral performance was significantly recovered compared with control monkeys without rehabilitation. In contrast, when rehabilitation started 14 days after the insult, no significant recovery was observed. Neuronal damages determined with [^{11}C/^{18}F]Flumazenil-PET indicated that the ratio of mildly damaged area was significantly reduced when rehabilitation started 4 and 7 days after ischemic insult, while no significant changes in the damaged area when started 14 days after the insult.

Conclusion: We have reported that this stroke monkey model is useful for the assessment of neuroprotective reagent (3, 4). These results with behavioral performance task and PET imaging suggest that this animal model is also useful for the clarification of neurochemical mechanisms of rehabilitation, showing that the "critical period" might exist between 7 and 14 days after the ischemic insult in the stroke model of monkeys.

References:

1) H. Takamatsu, et al., Detection of reperfusion injury using positron emission tomography in a monkey model of cerebral ischemia, J. Nucl. Med. 41 (2000) 1409-1416.

2) H. Tsukada, et al., Transient focal ischemia affects the cAMP second messenger system and coupled dopamine D_1 and 5-HT_{1A} receptors in the living monkey brain: a PET study using microdialysis, J Cereb Blood Flow Metab 24 (2004) 898-906.

3) H. Takamatsu, et al., FK506 attenuates early ischemic neuronal death in a monkey model of stroke, J Nucl Med 42 (2001) 1833-1840.

4) K. Umemura, et al., Positron emission tomographic study of the neuroprotective effect of TRA-418, an anti-platelet agent, in a monkey model of stroke, J Nucl Med 46 (2005) 1931-1936.

Brain Poster Session: Spreading Depression

EVOLUTION OF CORTICAL SPREADING DEPRESSION IS ALTERED BY AGING AND CHRONIC CEREBRAL HYPOPERFUSION

E. Farkas[1], L. Lenti[1], L. Kemény[1], T.P. Obrenovitch[2], F. Bari[1]

[1]Department of Physiology, Faculty of Medicine, University of Szeged, Szeged, Hungary, [2]Division of Pharmacology, School of Life Sciences, University of Bradford, Bradford, UK

Objectives: Cortical spreading depression (CSD) are propagating waves of cellular depolarization that are associated with classical migraine and acute brain lesions. Aging and chronic cerebral hypoperfusion (CCH) compromise neural integrity and cerebrovascular regulation, yet their effect on CSD generation has not been established. Our objective was to determine the impact of age and CCH on the evolution of experimentally induced CSD and corresponding changes of cerebral blood flow (CBF).

Methods: Adult male Wistar rats were divided into 3 groups. Group 1 consisted of 2 month-old naïve animals. Groups 2 and 3 underwent either sham-operation (SHAM) or permanent, bilateral common carotid artery occlusion (2VO; a widely used model for CCH), under chloral-hydrate anesthesia (400 mg/kg, i.p.) at the age of 6-8 weeks, and survived for 6 months after 2VO onset. In all animals, two craniotomies were created on the right parietal bone (5 mm apart) under halothane anesthesia (in N_2O:O_2=2:1), at the age of 2 months (group 1, n=6) or 8 months (group 2, n=6; and group 3, n=5). The rats were freely breathing during surgery and subsequent data acquisition. Mean arterial pressure was monitored continuously through a catheter inserted into the left femoral artery. The anterior open cranial window incorporated a glass capillary electrode for the recording of EEG and direct current (DC) potential, and a laser Doppler probe for the monitoring of cortical CBF. The posterior craniotomy was used to trigger CSD by the application of 1M KCl, which was left in the window after the first application, and refreshed every 15 min during recording. The variables were continuously acquired for 2h. Each experiment was terminated by cardiac arrest, achieved by the injection of 1 ml air through a venous line in the left femoral vein.

Results: The frequency of CSD generation seen on the EEG recording as silencing of the signal was significantly lower due to aging (group 1: 9±6.0/2h, group 2: 2±1.0/2h group 3: 3±2.0/2h, median±stdev, Kruskall-Wallist test: $p< 0.033$*). The occurrence of CSD was progressively more frequent toward the end of the 2-h recording period in all 3 groups. The degree of CSD-associated hyperemia showed an age-related tendency to decrease (group 1: 53±7.4%, group 2: 47±8.7%, group 3: 48±10.4%, mean±s.e.m.). The sudden, transient drop of CBF typically preceding the CSD-associated hyperemia was less prominent in the older rats, especially under CCH (1st CSD: group 1: -34±9.5%, group 2: -20±6.1%, group 3: -13±4.8%, mean±s.e.m.).

Conclusions: This study so far demonstrates that K^+-induced CSD evolve less likely in older than in younger adult rats, implying a reduced sensitivity or higher threshold for CSD elicitation with aging. The impact of aging and CCH appears most obvious on the CSD-associated changes in CBF, which probably points to a less dynamic regulation of cerebrovascular reactivity. These findings prompt further analysis of CSD evolution in the aging brain, since CSD is known to occur during and after acute cerebrovascular events (e.g. subarachnoid hemorrhage, stroke), which are conditions more prevalent in later life.

Supported by the Hungarian Scientific Research Fund (OTKA; nr. K63401).

OLIGODENDROGENESIS AFTER CHORNIC CEREBRAL HYPOPERFUSION IN MOUSE

N. Miyamoto[1], Y. Tanaka[1], K. Yatomi[2], Y. Ueno[1], R. Tanaka[3], N. Hattori[1], T. Urabe[1]

[1]Department of Neurology, [2]Department of Neurosurgery, Juntendo University School of Medicine, Tokyo, [3]Department of Neurology, Juntendo Urayasu hospital, Chiba, Japan

Background and purpose: Cerebrovascular white matter (WM) lesions are observed in aging and stroke and constitute the core pathology of Binswanger disease, a form of subcortical vascular dementia. These WM lesions are believed to be responsible for cognitive impairment and are caused by chronic cerebral hypoperfusion. The neuropathological changes in these lesions are characterized by diffuse demyelination, the loss of the axons, and gliosis, but the process leading to these changes remains unclear. The rat model of chronic cerebral hypoperfusion is accompanied by cognitive impairment and cholinergic deficits and is used most widely. However, genetic studies are hampered because of limited accessibility to molecular technologies using knockout or transgenic animals. Within 5-7 years, a mouse model of chronic cerebral hypoperfusion was established. In this study, we induced white matter lesions in a mouse chronic cerebral hypoperfusion model, and then tested the capability of tissue regeneration in the lesioned area after ischemia using bromodeoxyuridine (BrdU) and a series of neuronal and glial markers.

Methods: Rats underwent on narrowing the bilateral CCAs with microcoils (BCAS, n=20). 5-Bromodeoxyuridine (BrdU, 50mg/kg) was injected for analysis of newly generated cells in white matter. Immunohistochemistry for BrdU, glutathione S transferase-pi (GST-pi), platelet derived growth factor receptor-α (PDGFR-α), and single stranded DNA (ssDNA) were analyzed at pre-operation, 7, 14 and 28 days after hypoperfusion.

Result: The white matter lesions were progressed in time dependent manner in KB staining. Newly generated BrdU-positive cells were transiently increased at 7days after ischemia then decrased. Oligo progenitor cells labeled by PDGFR-α in white matter significantly increased in time dependence after ischemia compared with pre-operation ($p< 0.01$). However, more mature oligodendrocyte labeled by GST-pi in white matter transiently increased in early period, but decreased in later period compared with pre-operation ($p< 0.01$). Moreover, apoptotic cells were increased in time dependent manner.

Conclusion: Our result indicated that chronic cerebral hypoperfusion transiently promoted generation of oligo progenitor cells, but white matter lesion were progressed because of decreasing mature oligodendrocyte and increasing apoptotic cell death. Moreover, the mouse, which is readily amenable to gene knockout and manipulation and has advantages in cognitive evaluation, can be a model of subcortical vascular dementia suited for pathogenetic analysis.

655

Brain Poster Session: Subarachnoid Hemorrhage

CEREBRAL ISCHEMIA ENHANCES VASCULAR THROMBOXANE RECEPTOR EXPRESSIONS

S. Ansar[1,2], C. Larsen[2], L. Edvinsson[1,2]

[1]Clinical Sciences, Division of Experimental Vascular Research, Lund University, Lund, Sweden, [2]Clinical Experimental Research, Glostrup Research Institute, Glostrup University Hospital, Glostrup, Denmark

Objectives: Cerebral ischemia remains the key cause of morbidity and mortality after subarachnoid hemorrhage (SAH) with a pathogenesis that is still poorly understood. Several studies have shown an increased thromboxane biosynthesis in patients with cerebral ischemia. We hypothesise that SAH induces changes in cerebrovascular receptor expression and function, which might influence the development of late cerebral ischemia. In previous studies have we revealed an upregulation of contractile endothelin type B (ET_B), angiotensin type 1 (AT_1) and 5-hydroxytryptamine 1B ($5\text{-}HT_{1B}$) receptors after SAH and temporal middle cerebral artery occlusion. The aim of the present study was to examine the involvement of thromboxane A_2 receptors (TP) in the pathofysiology of cerebral ischemia after SAH in cerebral arteries.

Methods: SAH was induced by injecting 250 µl blood into the prechiasmatic cistern. Two days after the SAH, basilar arteries (BA) and middle cerebral arteries (MCA) were harvested and contractile responses to the TP receptor agonist U46619 were investigated with myographs. In addition, the contractile responses were examined after pretreatment with the TP receptor antagonist GR3219b. The TP RNA levels were analyzed by quantitative real-time PCR. The global and regional cerebral blood flow (CBF) was quantified with an autoradiographic technique.

Results: SAH resulted in enhanced contractile responses to U46619 as compared to sham in BA and MCA. The TP receptor antagonist GR3219b abolished the enhanced contractile responses to U46619 observed after SAH. The TP receptor mRNA levels were elevated after SAH as compared to sham. Global and regional CBF was significantly reduced in SAH as compared to sham operated rats. Statistical analyses were performed with Kruskal-Wallis non-parametric test with Dunn´s post-hoc test, where $P< 0.05$ was considered significant. Data are expressed as mean ± s.e.m.

Conclusion: The results demonstrate for the first time that SAH induces upregulation of TP receptors both at functional, and mRNA levels. These results suggest a role for the TP receptors in the pathogenesis of cerebral ischemia after SAH.

THE EFFECTS OF ITERATIVE DECONVOLUTION PARTIAL-VOLUME CORRECTION ON BETA-AMYLOID PET

B. Thomas[1], L. Thurfjell[2], J. Rinne[3], S. Ourselin[4], B. Hutton[1]

[1]Institute of Nuclear Medicine, University College London, London, [2]Medical Diagnostics R&D, GE Healthcare, Amersham, UK, [3]Turku PET Centre, Turku, Finland, [4]Centre for Medical Image Computing, University College London, London, UK

Objectives: To investigate the effects of partial-volume (PV) correction on the discrimination between Alzheimer´s disease (AD) patients and healthy aging controls (HC) using novel amyloid imaging candidate [11C]-AH110690[1].

Methods: The effect of partial-volume correction (PVC) was assessed using data from a previously acquired study. Nine AD patients and nine HC underwent a baseline and 12-month [11C]-AH110690 PET scan (Siemens ECAT EXACT HR+) and T1 MRI.

PV correction was applied using the Van-Cittert (VC) iterative deconvolution technique. A position-invariant point spread function (PSF) of 5.1mm full-width at half-maximum (FWHM) was used for PVC, based on measurement.

Standardised Uptake Value Ratio (SUVr) images of both the PV corrected and uncorrected data were created by normalising summed images (50 - 70 minutes post-injection) using cerebellar grey matter as a reference region. The summed images were rigidly registered to the patient MR and spatially normalised to Montreal Neurological Institute (MNI) space. The summed images were then warped to MNI space using the parameters from the MR-MNI normalisation and smoothed by 8mm. Statistical Parametric Mapping (SPM5) analysis was carried out on the cohort. Two-sample t-tests, AD > HC, were performed on the uncorrected and PV corrected data. P-values were corrected for multiple comparisons using False Discovery Rate (FDR) (p=0.03) with an extent threshold of k=25 voxels.

Results: The VC deconvolution tends to amplify noise during subsequent iterations of the scheme. All images reached the stopping criteria at 30 iterations or fewer. Partial volume correction for each of the PET images of matrix size 128 x 128 x 63 took less than 2 minutes on an AMD Athlon XP 1700+ with 1792MB RAM and running Windows XP.

The SPM group analysis between Alzheimer's patients and control subjects detected significant clusters in the frontal (No-PVC p=0.021, PVC p=0.016) and parietal lobes (No-PVC p=0.018, PVC p=0.014). Both clusters increased in size after PVC (frontal +9.03%, parietal +3.26%). The total number of clusters detected increased from 25 to 37 with PVC.

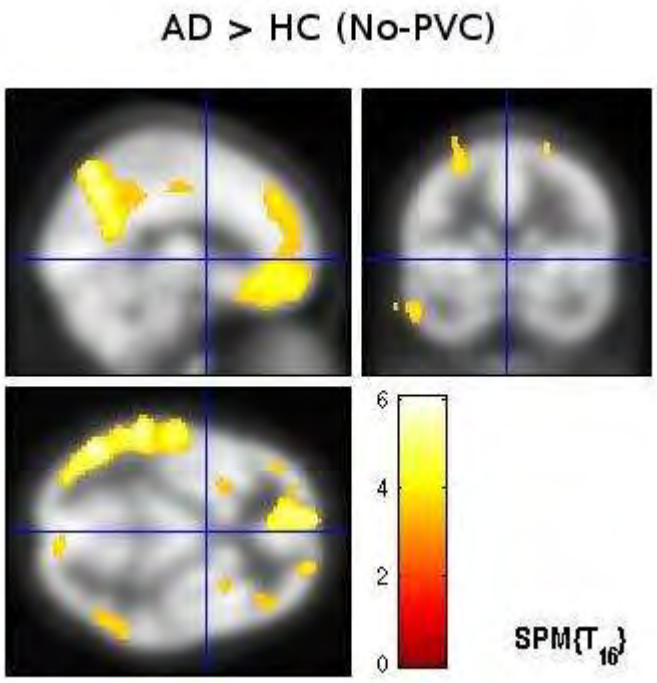

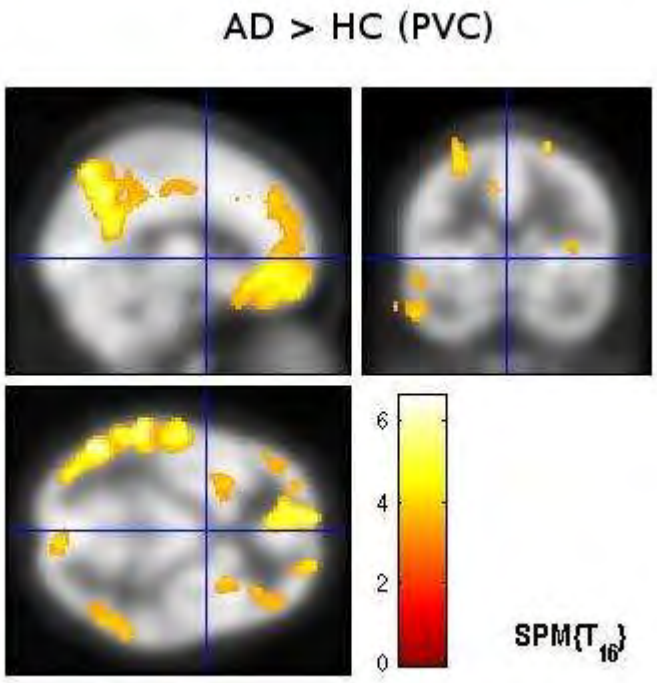

[SPM analysis with and without PV correction.]

Conclusions: This work has shown that the application of partial-volume correction increases the spatial extent of significant clusters using SPM analysis. The appearance of small clusters in the PV corrected image, absent from the uncorrected image, suggests that PV correction improves discrimination.

References:

- Juha O Rinne, Ian A Wilson, Lennart Thurfjell, Kjell Någren, Olof Solin, Pertti Lehikoinen, Juha Koikkalainen, Jyrki Lötjönen, Sargo Aalto, Kirsi Virtanen, Marita Kailajärvi, Mika Scheinin, Gill Farrar, ´Follow-up study of a new brain amyloid tracer, 11C-labelled 3'-F-PIB ([11C]AH110690)´, in Alzheimer's disease, Submitted.

- Jussi Tohka & Anthonin Reilhac (2008), ´Deconvolution-based partial volume correction in Raclopride-PET and Monte Carlo comparison to MR-based method´, NeuroImage 39(4), 1570-1584.

[1]In subsequent studies the compound is referred to as GE-067.

657

Brain Poster Session: Traumatic Brain Injury

COMBINATION THERAPY WITH FENOFIBRATE AND SIMVASTATIN ON DELETERIOUS CONSEQUENCES INDUCED BY TRAUMATIC BRAIN INJURY

X.R. Chen, T. Beziaud, M. Plotkine, **C. Marchand-Leroux**, V. Besson

Pharmacology of Cerebral Circulation, EA2510, Paris Descartes University, Paris, France

Objectives: We[1] and others[2] have demonstrated that fibrates and statins, exerted neuroprotective and pleiotropic effects in experimental models of traumatic brain injury (TBI). As combination of statins and fibrates synergistically enhanced peoxisome proliferator-activated receptor (PPAR) α activation, we hypothesized the combination of both class of drugs exert more important and/or prolonged beneficial effects in TBI than each one alone. In this study, we examined the effect of the combination of fenofibrate and simvastatine on the consequences of TBI.

Methods: TBI was induced by lateral fluid percussion of the temporoparietal cortex on male Sprague-Dawley rats (300-330 g), as previously described[1]. Sham-operated rats underwent the same surgery except for percussion. Simvastatin at 37.5mg/kg, 50 mg/kg fenofibrate, and its combination or its vehicle (water containing 0.5% methylcellulose) were administrated by gavage 1 and 6 h after brain injury. At 24, 48 h, 3 and 7 days after TBI, a neurological assessment was done by 2 tests: one for reflexes and sensorimotor responses (ranging from 0=worst to 9=best), and the second untitled beam walking test for motor coordination (ranging from 0=worst to 4=best). Then rats were killed, and brain lesion was measured at 7 days post-injury.

Results: TBI led to a decrease in the neurological score at 24 h post-injury ($p< 0.001$) demonstrating a neurological deficit that persisted at 48 h ($p< 0.001$). Rats treated with fenofibrate ($p< 0.05$), simvastatin ($p< 0.01$) or their combination ($p< 0.05$) showed an increase in the neurological scores at 24 h (fenofibrate: $p< 0.05$; simvastatin: $p< 0.01$;combination: $p< 0.01$) showing a neurological recovery. Even if monotherapies had no more effects on the neurological score at 48 h post-TBI and later, combination still showed an improvement of the neurological score until, at least, 7 days after TBI ($p< 0.01$) demonstrating a longest neurological recovery promoting effect. At 48 h and later after injury, rats receiving the combination showed an improvement of the beam walking score ($p< 0.05$) whereas monotherapies had no effects. TBI induced a brain lesion of 83±8 mm^3 that was reduced by treatment with the combination (36±12 mm^3, $p< 0.05$), whereas both monotherapies did not reduce it (fenofibrate: 62±20 mm^3; simvastatin: 65±22 mm^3).

Conclusions: Evidence that fenofibrate combined with simvastatin promote long-lasting beneficial effects on neurological recovery and lesion provides a strong basis for the use of this combination for TBI treatment.

References:

1. Chen et al., 2007, J. Neurotrauma, 24 (7): 1119-1131.

2. Lu et al., 2007, J. Neurotrauma, 24 (7):1132-1146.

659

BrainPET Poster Session: Radiotracers and Quantification

C-FIBRE LTP IS ASSOCIATED WITH DYNAMIC CHANGES IN OPIOID NEUROTRANSMISSION IN THE BRAIN

T. Hjornevik[1], B. Schoultz[2], J. Gjerstad[3,4], G. Henriksen[2,5], F. Willoch[1,6]

[1]Dept. of Anatomy & CMBN, University of Oslo, [2]Dept. of Chemistry, University of Oslo, [3]National Institute of Occupational Health, [4]Dept. of Molecular Bioscience, University of Oslo, Oslo, Norway, [5]Nuklearmedizinische Klinik and Poliklinik, Klinikium rechts der Isar, Technical University Munich, Munich, Germany, [6]Dept. of Radiology, Aker University Hospital, Oslo, Norway

Objectives: Neuronal events leading to development of long-term potentiation (LTP) in the nociceptive pathways may be a cellular mechanism underlying hyperalgesia. Opioid receptors control the descending modulatory system to the spinal cord, and play an important role in anti-nociception. In the present study, we examine how induction of spinal LTP affects the supraspinal opioidergic system.

Methods: All animals were for the following experiments anesthetized with isoflurane gas. The left sciatic nerve was given a high-frequency conditioning stimulation (HFS) to induce LTP (5 trains/1 s, 100 Hz, 1 ms pulses, 10 s intervals):

1. Spinal field potential recordings. Field potentials were recorded from neurons at depths of 100-300 µm from the surface of the spinal cord (n=6).
2. PET measurements.

PET studies were performed in parallel. Data was acquired (Inveon, Siemens) for 60 min after i.v. injection of [^{11}C]PEO, a u- and k-OR tracer. All rats (n=8) underwent the first day a rest study without any intervention. The other day tracer acquisition was performed 2.5 hrs after HFS conditioning. The data was 3DRP reconstructed and binding potentials (BP_{ND}) were calculated using a reference tissue model (MRTM0) in PMOD (PMOD Technologies Ltd., Zurich, Switzerland). Statistical comparisons between baseline and stimulation condition were performed with SPM5 (Wellcome Department of CognitiveNeurology, Institute of Neurology, London, UK) after anatomic standardization to an average PET uptake template. Level of significance was set at $p< 0.05$. The result image (HFS>baseline) was registered to a 2-D digital version of the Rat Brain atlas by Paxinos and Watson (2005), and statistical values were extracted from predefined volumes of interest (VOIs).

Results: An increase in C-fibre response and reduced C-fibre threshold were observed following sciatic nerve HFS throughout the observation time of 3 hours. Increased PEO binding was observed ipsilaterally in the amygdala, hippocampus, somatosensory cortex, and the superior colliculus. In addition, significant increased signal was located bilaterally in the nucleus accumbens, caudate putamen, and the hypothalamus.

Conclusions: The data shows that HFS applied to the sciatic nerve lead to a long lasting C-fibre LTP representative for hyperalgesia. Concomitantly, HFS was associated with a regional increased opioid receptor availability that is interpreted as reduced opioid tonic activity. The involved structures, amygdala in particular, are part of a pain modulatory circuitry. Therefore, a reduced descending opioid, anti-nociceptive activity may be related to the observed C-fibre LTP and associated abnormal pain states, such as hyperalgesia. Furthermore, the dynamic changes in opioid neurotransmission in

the limbic structures may connect the findings with an affective-emotional response to the applied noxious stimulus.

References: Paxinos G & Watson C, The Rat Brain in Stereotaxic Coordinates, Elsevier Academic Press, 2005.

ROLE OF BRAIN TYPE FATTY ACID BINDING PROTEIN IN THE TRANSIENT BRAIN ISCHEMIA

T. Kato[1], H. Yoshioka[1], Y. Owada[2], M. Sugita[1], T. Yagi[1], T. Wakai[1], H. Kinouchi[1]

[1]Neurosurgery, University of Yamanashi, Chuo, [2]Anatomy, Yamaguchi University Graduate School of Medicine, Yamaguchi, Japan

Objectives: It has been generally accepted that hippocampal neurogenesis does occur in matured mammals, especially after various injuries such as ischemia. The mechanism of this phenomenon is not clearly elucidated yet, but the radial glia cells, known as neuronal stem cells, are considerd to be involved. On the other hand, brain-type fatty acid-binding protein (B-FABP), a family of intracellular lipid-binding proteins, has been observed in radial glia cells of the adult animals and it has been considered to grow and protect neurons. Since there were no previous studies concerning to the neuroprotective and neurogenetic properties of the B-FABP, in this study, we investigate the distribution of expression and the extent of delayed neuronal death concomitant with the neurogenesis to determine whether this protein possesses neuroprotective and/or neurogenetic properties in the adult mouse using B-FABP knock-out (BKO) mice (Owada Y. Eur J Neurosci. 25: 175, 2006) comparing to the wild type.

Materials and methods: The transient forebrain ischemia (20 min bilateral carotid artery ligation and recirculation) models were prepared using C57BL/6 mice under generalized anesthesia and body temperature were maintained 37°C. We have evaluated and compared the difference between wild type and BKO regarding the expression and distribution of B-FABP together with the extent of the neuronal cell death, which was classified into 4 groups according to the survived cell numbers in the hippocampus: 76% or more; grade 1, 75-51%; grade 2, 50-26%: grade 3, 25% or less; grade 4, after 3 and 8 days after ischemia. In addition, we have assessed the neurogenesis in the the subgranular zone (SGZ), which is a part of the dentate gyrus of hippocampus by multi-labeled immunohistochemical staining with B-FABP, BrdU, Nestin, NeuN and GFAP.

Results: The upregulation of B-FABP expression was observed only in the wild type 3days after ischemia. Delayed neuronal death of the hippocampal CA2 region was significantly increased in the BKO group (grade 3.1) than the wild type (grade 1.9, $p< 0.05$). With regard to the neurogenesis, most of the BrdU positive cells were copositive to the Nestin and some of them were concurrently positive to the GFAP. The number of the BrdU positive cells in SGZ of the wild type animals significantly increased (584.2+/-185.1/ mm^2) in comparison with that of BKO (32.8+/-92.6 / mm^2, $p< 0.05$) 8 days after ischemia. Besides, Nestin was detected in the BrdU positive cells after 28 days after ischemia.

Conclusions: This study suggests that the B-FABP has neuroprotective and neurogenetic effect against transient forebrain ischemia. In addition, the specific expressions of B-FABP indicated that it is essential element for proliferation of radial glia and differentiation to the neuronal cells.

ASSESSMENT OF THE NEUROPROTECTIVE POTENTIAL OF AN ISOFLAVONE-ENRICHED DIET IN ISCHEMIC STROKE ASSOCIATED WITH HYPERTENSION IN RATS

G. Torregrosa[1,2], M. Castelló-Ruiz[1,2], M.C. Burguete[2], J.B. Salom[1,2], J.V. Gil[3], **T. Jover-Mengual**[2], O. Hurtado[4], M.A. Moro[4], E. Alborch[1,2]

[1]Centro de Investigación, Hospital Universitario La Fe, [2]Departamento de Fisiología, [3]Departamento de Medicina Preventiva y Salud Pública, Universidad de Valencia, Valencia, [4]Departamento de Farmacología, Facultad de Medicina, Universidad Complutense de Madrid, Madrid, Spain

Objectives: We and others have recently demonstrated that high-soy diets improve stroke outcome in rats undergoing either transient or permanent middle cerebral artery occlusion (MCAO) (1, 2, 3). We have also shown that the pure soy-derived isoflavone, genistein, limits the consequences of ischemic stroke when given at early stages (4). As hypertension is the main ethiopathogenic factor associated with stroke, the present study was carried out to determine whether the neuroprotective action of high-soy diet takes place also in ischemic stroke associated with hypertension in rats.

Methods: Just weaned (by about 50 g and 21-day old) male normotensive (WKY) and hypertensive (SHR) rats were allowed to grow with either soy-based high-isoflavone (468 µg/g diet) (high-IF) or isoflavone-free [IF(0)] diets. Therefore, four experimental groups were established: high-IF WKY (n=10), IF(0) WKY (n=8), high-IF SHR (n=11), and IF(0) SHR (n=12). Eight weeks later, transient focal cerebral ischemia (90 min) was induced by MCAO following the intraluminal thread technique. Cerebro-cortical laser-Doppler flow (cortical perfusion, CP), arterial blood pressure (ABP), core temperature, P_aO_2, P_aCO_2, pH and glycemia were mesured before (basal), during (ischemia) and after (reperfusion) MCAO. Neurological examination and infarct volume measurements (2,3,5-triphenyltetrazolium chloride) were carried out 3 days after the ischemic insult.

Results: CP values at the ischemia stage decreased to 28%-47% of the basal values. After 90 min. of MCAO, the thread was removed and CP began to increase to a sustained plateau amounting 112%-191% of the basal values. Neither intraischemic nor postischemic CP values were significantly different among the four groups. As to ABP, no significant changes were shown neither among the three intervals (basal, ischemia and reperfusion) nor among the four groups. Overall, during the ischemia period both PaO_2 and pH decreased, $PaCO_2$ increased, and glucose did not change. During the reperfusion period all the altered values tended towards basal values. Neither basal, ischemia or reperfusion values of the four parameters were significantly different among the four groups. At 3 days reperfusion, neurological scores (median with its minimum and maximum values) were: 2[0-8] (high-IF WKY group), 3[2-4] (IF(0) WKY group), 3[2-5] (high-IF SHR group), and 3[2-5] (IF(0) SHR group). As to the infarct volume (percentage of the whole hemisphere), the corresponding values were: 15.7±7.7%, 15.5±6.9%, 23.8±9.2%, and 25.3±9.4%. Statistical analysis showed no differences in neurological impairment or infarct volume among the four experimental groups.

Conclusions: Under the reported experimental conditions, the high-isoflavone diet does not reduce the impact of ischemic stroke associated with hypertension, in terms of both neurological impairment and infarct volume. The current results do not confirm the neuroprotective effects of the high-isoflavone diet previously reported in normotensive male Wistar rats, what means that the rat strain could have a great influence in the study of the impact of dietary interventions in experimental stroke.

References:

1. Burguete et al., 2006. Eur J Neurosci 23:703-710.

2. Lovekamp-Swan et al., 2007. Neuroscience 148:644-652.

3. Schreihofer et al., 2005. Am J Physiol Regul Integr Comp Physiol 289:R103-R108.

4. Castelló-Ruiz et al., 2008. Int J Stroke 3(Suppl. 1):166.

(Supported by RETICS-RENEVAS and grant PI06/0981, ISCIII)

663

BrainPET Poster Session: Molecular Brain Imaging: Clinical Applications

HEMODYNAMIC COMPROMISE IDENTIFIED BY OXYGEN EXTRACTION FRACTION RESPONSE (OEFR) TO ACETAZOLAMIDE IN STROKE PATIENTS WITH LARGE ARTERY OCCLUSION

M. Jumaa[1], M. Hammer[1], K. Uchino[1], S. Zaidi[1], R. Lin[1], V. Reddy[1], H. Kuwabara[2], D. Sashin[3], Y.-F. Chang[4], N. Vora[5], T. Jovin[1], L. Massaro[1], J. Billigen[1], H. Yonas[6], **E. Nemoto**[7]

[1]Neurology, University of Pittsburgh School of Medicine, Pittsburgh, PA, [2]Radiology, Johns Hopkins University, Baltimore, MD, [3]Radiology, University of Pittsburgh School of Medicine, [4]Neurosurgery, University of Pittsburgh School of Medicine, Pittsburgh, PA, [5]Neurology and Psychiatry, St. Louis University School of Medicine, St. Louis, MO, [6]Neurosurgery, University of New Mexico, Albuquerque, NM, [7]Radiology, University of Pittsburgh, Pittsburgh, PA, USA

Background: Hemodynamic compromise identified by cerebrovascular reserve (CVR) and oxygen extraction fraction (OEF) in stroke patients with large artery occlusion is an independent predictor of stroke risk ranging from 27 to 57%. However, comparison of both methods indicates that the sensitivity of CVR is substantially greater than OEF in detecting hemodynamic compromise which may be because CVR includes a vasodilator challenge with acetazolamide as opposed to OEF made in the resting state. We hypothesized that the response of OEF (OEFR) to an acetazolamide challenge would better correlate with CVR than OEF. We examined the correlation between CVR and OEFR to acetazolamide in stroke patients with large artery occlusion.

Methods: Stroke patients with large artery occlusion (internal carotid or middle cerebral artery) were studied by positron emission tomography (PET) using $H_2{}^{15}O_2$ (water) for cerebral blood flow (CBF) and $^{15}O_2$ (gas) for cerebral metabolic rate for oxygen before and after acetazolamide. CVR was calculated as: CVR (%) = [(CBFa-CBFb)/CBFb] X 100; where: CBFb = CBF before acetazolamide, CBFa = CBF after acetazolamide. OEF response (OEFR) was similarly calculated as: OEFR (%) = [(OEFa-OEFb)/OEFb]X100; for the entire middle cerebral artery territory of each hemisphere.

Results: There was a highly significant (P=0.0001) negative linear correlation between CVR and OEFR indicating increasing ischemic stress (Figure). Hemispheres from three patients showed a positive OEFR.

Discussion: A positive OEFR in response to a cerebrovascular challenge definitively indicates hemodynamic compromise and eliminates the problem of deciding on the absolute threshold for OEF to signify hemodynamic compromise. A negative OEFR reflects sufficient cerebrovascular reserve relative to oxygen demand.

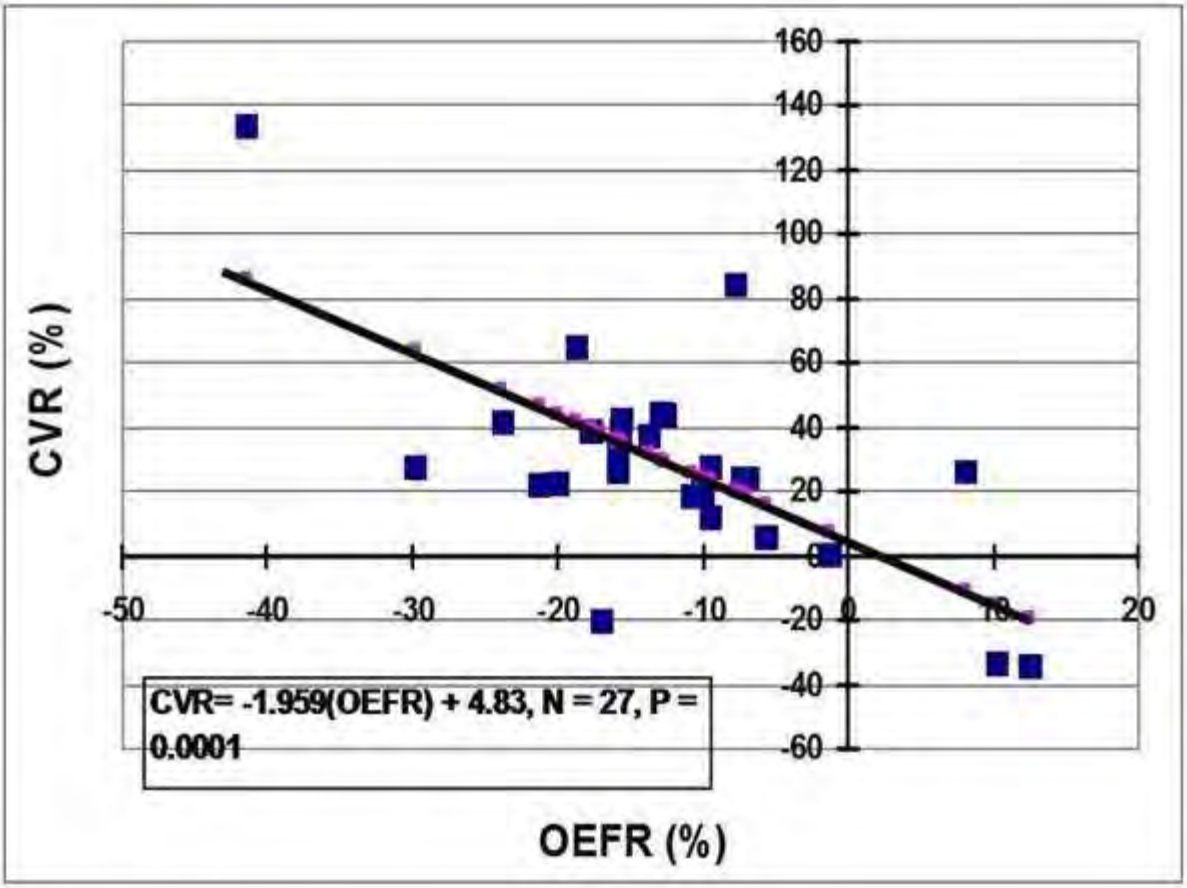
160
140
120
100
80
60
40
20
0
-20
-40
-60
-50
-40
-30
-20
-10
0
10
20
CVR (%)
OEFR (%)
CVR= -1.959(OEFR) + 4.83, N = 27, P = 0.0001

[CVR_OEFFig]

NEW STRATEGY FOR K3 QUANTIFICATION OF REVERSIBLE PET TRACERS

K. Sato[1,2], K. Fukushi[1], **N. Tanaka**[1,3], H. Shimada[1], H. Shinotoh[1], S. Hirano[1], T. Ota[1], M. Miyoshi[1], T. Ohya[1], T. Irie[1]

[1]Molecular Imaging Center, National Institute of Radiological Sciences, [2]Department of Psychiatry, Teikyo University Chiba Medical Center, Chiba, [3]Department of Neurosurgery, Tokyo Woman's Medical College Daini Hospital, Tokyo, Japan

Objectives: In recent years, reversible ligands are actively performed in the neuroreceptor PET studies. Full compartment analysis with nonlinear least squares (NLS) algorithm based on tissue 2-compartment reversible model is generally impractical, because the computation is time consuming and parameter estimation is uncertain due to excessive number of parameter. In this study, pre-equilibrium phase, where tissue time-radioactivity curve (TAC) is almost independent of k4, was appropriately extracted from total dynamics of reversible tracer. Time-radioactivity data was then analyzed by NLS analysis with three-parameter to precisely determine k3 value, which is of greatest physiological interest.

Methods: The properties of this method were explored by Monte-Carlo simulation. To reflect the real situation, parameters and input function referred the experimental results of [^{11}C]Pittsburgh Compound-B (PIB), the ligand for beta-amyloid imaging, in human study. Here, partial diiferential derivative of TAC with respect to each parameter was defined as the sensitivity of parameter. Difference (delta) was practically used in place of partial differentiation, and squares residual error was remarked, since the NLS algorithm includes the minimization of sum of squares error. Figure shows the sensitivity curve representing squares residual of TAC, $(\text{delta TAC})^2$ with respect to delta k for typical TAC of [^{11}C]PIB. Our method requires time reduction in data analysis for the contribution of k4 in TAC to be ignored. However, analysis time must be long enough for precise k3 estimation. Considering this trade-off based on sensitivity curve, the appropriate pre-equilibrium phase was determined. The time length necessary for this situation is about 30 min.

Results: In the simulation, k3 values were precisely calculated by early phase analysis with CV of 5 to 10%. Significant minus-bias of around -30% (-25% to -35%) that related to disregard of k4 was shown in k3 estimates. Nevertheless, the underestimates were comparable in degree, across 1 order of magnitude of k3 values, from 0.010 to 0.100 min^{-1}. Additional examination of k3 change in the clinical follow-up study showed relatively small bias in the ratio of k3 change (0 to -20%) compared to those in k3 value itself. Once the method was developed, it was pilot tested on the study with [^{11}C]PIB.

Conclusions: In the pre-equilibrium phase analysis, the advantages of precise k3 measurement and significantly shortened scan duration time were provided by giving up the calculation of k4 that is rather of little interest and is essentially difficult to quantify. The new method includes the optimization of time range for k3 estimation, referring to the sensitivity curve. Though this method is more suitable for the reversible tracer with relatively small k4, many reversible tracers are applicable to this method.

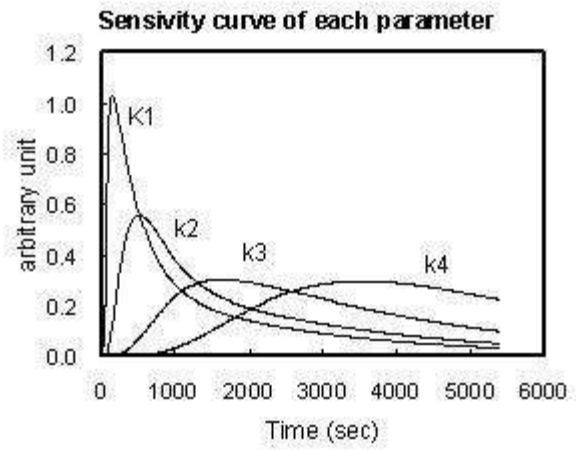
Sensivity curve of each parameter
1.2
1.0
0.8
0.6
0.4
0.2
0.0
arbitrary unit
K1
k2
k3
k4
0
1000
2000
3000
4000
5000
6000
Time (sec)

[Figure 1]

CORRELATIONS BETWEEN IMMUNE INFLAMMATORY PROCESSES IN ATHEROSCLEROSIS AND THE BIOELECTRICAL ACTIVITY AND HEMODYNAMICS OF THE BRAIN

S. Kuznetsova, V. Kuznetsov, **I. Palamarchuk**

Cerebrovascular Pathology, Institute of Gerontology AMS Ukraine, Kyiv, Ukraine

Background: That the patients with cerebral atherosclerosis show the dysfunction of brain structures, vascular tone disorders and reduced overall speed of cerebral hemodynamics and that the atherogenesis represents a process of immune and inflammatory disturbances is the common knowledge (del Zoppo GJ, 2008, Caplan LR 2008, Ross R 1999, Libby P, 2002).

Our recent investigations have been focused on the neuroimmune reactions in the patients with cerebral atherosclerosis. We found the imbalance of main lymphocyte subpopulations, the high level of circulating immune complexes and the high activity of autoimmune reactions in response to neuro antigens (S.M. Kuznetsova, M.I. Lisiany and I.S. Palamarchuk, 2008).

The above phenomena seem to be related with transcranial duplex density of atherosclerotic plaques and the dominant hemisphere of functional and cerebral hemodynamic disorders. We decided to look into this problem at a more specific angle of view, namely, to study immune changes in atherosclerosis and at CNS dysfunction.

Objective: The pattern of correlations between immune inflammatory processes and brain bioelectrical activity/hemodynamics in cerebral atherosclerosis (CA).

Methods: The study involved the group of CA patients, altogether 15 men and women at age range 50 to 65 years. Ten age-matched healthy subjects made the control group. EEG was recorded on Neurofax EEG 1100k (Nihon Kohden, Japan); extra- and transcranial scanning of major head and neck arteries (EN VISIOR, Philips); immunological investigation using monoclonal antibodies (Sorbent Service, Russia; Becton Dickinson, USA).

Results and discussion: The EEG recordings evidenced for diencephalic disturbances in both hemispheres, with signs of central-parietal-limbic and reticular structures dysfunction being noted for right hemisphere. In the CA patients, median frequency of the EEG spectrum in the right occipital-parietal leads correlated with the pulse index value (2.44±0.13) in the basilar artery ($r = -0.65$, $p < 0.05$) and with an increased adhesive activity of the neutrophils ($r = -0.66$, $p < 0.05$). Pulse index in the basilar artery correlated with the level of circulating immune complexes (117.0±31.04 in nominal units) of the blood ($r = -0.65$, $p < 0.05$). Total frequency of the EEG spectrum in the right central leads correlated with the level of antibodies to NSE ($r=0.55$, $p < 0.05$) and with LBFV in the left ICA ($r=0.80$, $p < 0.05$). Theta rhythm power in the right occipital leads correlated with LBFV in the right ICA ($r=0.61$, $p < 0.05$) and with the level of sensibilization of the neutrophils to the main myelin protein ($r=-0.56$, $p < 0.05$).

Conclusion: There exist statistical correlations in cerebral atherosclerosis between cerebral hemodynamics and neuroimmune indices and the bioelectric activity of the brain. The brain bioelectrical activity in the right hemisphere correlates with the high activity of autoimmune reactions (the adhesive activity of the neutrophils, the level of sensibilization of the neutrophils to the main myelin protein, the antibodies to NSE) in the patients with cerebral atherosclerosis.

667

Brain Poster Session: Experimental Stroke & Cerebral Ischemia

IN VIVO MONITORING OF TISSUE VIABILITY AND LESION GROWTH IN FOCAL CEREBRAL ISCHEMIA IN RATS USING ^{201}TLDDC SMALL-ANIMAL SPECT

U.H. Schröder[1], O. Großer[2], H. Amthauer[2], H. Scheich[3], K.G. Reymann[1], J. Goldschmidt[3]

[1]PG Neuropharmacology, Leibniz-Institut for Neurobiology, [2]Clinic for Radiology and Nuclear Medicine, Otto-v.-Guericke University, [3]Auditory Learning & Speech, Leibniz-Institute for Neurobiology, Magdeburg, Germany

In vivo monitoring of lesion size and lesion growth in focal cerebral ischemia in rodents is usually done using magnetic resonance imaging. But the diffusion- and perfusion-weighted images obtained with MRI cannot provide direct information on tissue viability in acute cerebral ischemia. In particular, it has remained highly controversial whether or to what degree irreversible damage in the ischemic core can be detected using diffusion weighted imaging.

We here introduce a novel method for in vivo monitoring of tissue viability and lesion growth in focal cerebral ischemia in rodents. The method is based on high-resolution SPECT-imaging of brain potassium metabolism using the thallium isotope ^{201}Tl as a tracer.

We induced cerebral ischemia in rats by endothelin-mediated reversible occlusion of the middle cerebral artery. After induction of ischemia rats were intravenously injected with the lipophilic chelate complex ^{201}thallium diethyldithiocarbamate (^{201}TlDDC) and the time course of the ^{201}Tl distribution was monitored with a dedicated small-animal SPECT/CT-scanner. In addition, we used a histochemical technique - a modified Timm-technique or autometallographic method - for mapping, with cellular resolution, the thallium distribution in the brain.

We provide evidence, using the histochemical technique and in vivo monitoring of ^{201}Tl redistribution, that Tl^+ is released from TlDDC into the brain extracellular space, from which neurons and glial cells take up the tracer. Upon MCAO induction we find, with SPECT-imaging as well as with thallium autometallography, a core region, in which Tl^+-uptake is reduced to background levels. This core region expands over time and can be monitored with submillimeter spatial resolution in vivo using small-animal multipinhole SPECT-imaging.

We conclude from these findings that ^{201}TlDDC small-animal SPECT can be used for in vivo monitoring of tissue viability and lesion growth in cerebral ischemia. ^{201}Tl has been used for more than three decades as a tracer for SPECT-imaging of myocardial viability in humans. Tl^+ is a well-established K^+-analogue, and K^+-uptake as well as the maintenance of intra- to extracellular K^+-gradients are closely linked to cellular viability. The use of ^{201}Tl for imaging brain potassium metabolism, however, was limited due to the poor blood-brain barrier K^+-permeability. Application of ^{201}TlDDC, from which $^{201}Tl^+$ is released after bypassing the blood-brain barrier, makes it possible to use ^{201}Tl for SPECT-imaging of tissue viability in the brain in the same manner as has been done previously in myocardial imaging.

Small-animal multipinhole SPECT-imaging can be performed at higher spatial resolution than small-animal PET-imaging. In addition, due to the long half-life of ^{201}Tl (73h) the spatiotemporal patterns of ^{201}Tl redistributions can be monitored, depending on the dose injected, over a period of about three days after a single injection of ^{201}TlDDC. ^{201}TlDDC small-animal SPECT is a convenient metabolic imaging technique that offers substantial advantages over both PET and MRI in assessing tissue viability in rodent models of cerebral ischemia in vivo.

669

Brain Poster Session: Experimental Stroke & Cerebral Ischemia

ANTERIOR CEREBRAL ARTERY OCCLUSION IN RATS: 1-YEAR FOLLOW-UP OF STRUCTURAL AND METABOLIC ALTERATIONS USING MRI AND μPET

H. Endepols, H. Backes, G. Mies, R. Graf

Max Planck Institute for Neurological Research, Cologne, Germany

Objectives: The anterior cerebral artery (ACA) supplies the medial portions of frontal lobes and superior medial parietal lobes in humans. ACA strokes are rare (approx. 3%), but lead to severe cognitive impairments and reduced incentive drive. In this study we evaluated interactions of structural and metabolic loss and recovery of function over one year using a rat model of ACA occlusion (ACAo).

Methods: In eight male Lister hooded rats the vasoconstrictor endothelin-1 (ET-1; 150 pmol in 0.3 µl phosphate buffer) was injected stereotactically near the anterior pericallosal part of the ACA. Two sham operated controls were injected with phosphate buffer. We used ^{15}O-H_2O-µPET to measure cerebral blood flow (CBF) before and 45 min after ACAo, ^{18}F-fluorodeoxyglucose (^{18}F-FDG)-µPET to measure regional brain glucose metabolism before, 1 h, 28 days, 90 days, and 360 days after ACAo, and MRI (T2 maps) to determine structural changes 24 h, 28 days, 90 days, and 360 days after ACAo. A correlation analysis (Pearson test) was performed between ^{15}O-H_2O-µPET and metabolic as well as structural data.

Results: Early measurements: ^{15}O-H_2O-µPET 45 min after ET-1 injection showed a massive reduction of cerebral blood flow in areas supplied by the ACA, including anterior cingulate cortex, prelimbic region, olfactory bulb, and septum. This was reflected by edema and ventricular enlargement seen in T2 maps 24 h after ACAo. ^{18}F-FDG-µPET 1 h after ACAo revealed a strong metabolic reduction in the olfactory bulb, but not in the other ACA territory areas. Additionally, metabolic deficits could be seen in the piriform region of three animals. In controls, a reduction of CBF was observed as well, but it did not cause lasting metabolic and structural lesions.

Late measurements: While there was a partial metabolic recovery in the olfactory bulb, metabolism progressively decreased in the anterior cingulate cortex, prelimbic region, and septum. MRI scans revealed further ventricular enlargement and cyst formation in the ACA territory and the piriform region.

^{15}O-H_2O-µPET in the ACA territory was inversely correlated to early ^{18}F-FDG-µPET. A positive correlation was found between ^{15}O-H_2O-µPET and ^{18}F-FDG-µPET at day 28, but not with later measurements. In contrast, ^{15}O-H_2O-µPET correlated positively with structural lesion size (MRI) at 24 h, day 28, and day 90. Metabolic and structural losses in the piriform region were not correlated to ^{15}O-H_2O-µPET.

Conclusions: Metabolic lesions in the ACA territory follow different time courses after ET-1 induced ACAo. Metabolic reduction in the olfactory bulb is fast, followed by partial recovery, whereas it progresses over time in prelimbic, cingulate, and septal regions. The inverse correlation between early CBF and early metabolic scans indicates that in regions of mild ischemia, metabolic reduction develops faster than in severely affected areas. Early CBF reduction correlates well with structural changes (edema and cyst formation) for up to day 90, but neither structural nor metabolic outcome after 360 days can be predicted by early CBF measurements. The piriform lesion occurring in three out of eight animals does not seem to be caused by ischemia and might represent secondary degeneration.

EFFECTS OF A CHRONIC EXPOSURE TO NICOTINE: A STUDY IN BABOON BY USING A MULTI-INJECTION PET STUDY WITH [^{18}F]FLUORO-A-85380

M. Bottlaender, N. Miro-Bernie, M.-A. Peyronneau, F. Dolle, S. Bourgeois, F. Hinnen, S. Goutal, W. Saba, J. Delforge, H. Valette

CEA, DSV, I2BM, Service Hospitalier Frederic Joliot, Orsay, France

Introduction: A particular feature of nicotinic acetylcholine receptors (nAChR) is that chronic exposure to nicotine induces a higher level of nicotine binding, termed up-regulation. The mechanism through which nicotine induces nAChR up-regulation is complex and not fully clarified to date. This feature has been evidenced in cells expressing nAChRs, rodents, monkeys and in humans. In the development of our program to study tobacco addiction, we aimed at studying in vivo this up-regulation. For this purpose, one Papio anubis baboon received nicotine continuously (Alzet osmotic minipumps) for 6 months. At various times (15 days, 2,3,4 and 6 months), the minipumps were removed and the baboon underwent, two or three days later, a multi-injection PET experiment.

Methods: The compartment model describing the fluoro-A-85380 kinetics is the usual non-equilibrium non-linear model. It includes four compartments and seven parameters. The PET protocol included three injections: a tracer injection of [^{18}F]fluoro-A-85380 (time 0), a partial saturation injection (90 min) obtained by a simultaneous injection of labelled and unlabelled fluoro-A-85380 (35 nmol), and a saturation injection (180 min) by a large amount of only unlabeled fluoro-A-85380 (1500 nmol). Measurements of plasma nicotine concentration during PET experiments allowed performing a correction, if needed (concentration > 1 ng/mL), by introducing in the model the nicotine kinetics. The nicotine parameters were set to values estimated in a previous study (Bottlaender, NeuroImage 2008). This method allowed to simulate the effect of residual nicotine concentration in the brain, to correct the ligand kinetic and therefore to estimate the ligand parameters without significant bias.

Results: During nicotine administration, the mean plasma nicotine concentration was 10 to 20 ng/ml. The estimation of nicotinic receptor concentration in thalamus remained unchanged: 4.66 ± 0.58 pmol/ml from 15th day to 6th month versus control: 4.87 pmol/ml, and 4.44 pmol/ml after three weeks of weaning. In contrast, the estimated K_dV_r, was twice smaller, 0.24 ± 0.07 nM, than the control value: 0.61 nM. After three weeks of weaning, K_dV_r returned to control value (0.63 nM). The estimates of the other model parameters were not disturbed by the chronic nicotine administration. However, this present approach can be used mainly in receptor-rich regions because difficulties in estimating all model parameters in receptor-poor regions.

This observed variation in nicotinic receptor affinity is in agreement with the usual response to the administration of an agonist, which induces conformational changes from low to high affinity state of the nAChR (Edelstein, Biol.Cybern., 1996). In contrary to published data, an up-regulation of nAChR in thalamus is not observed. However, our results are in agreement with one in vitro study (Vallejo J Neurosci. 2005).

Conclusion: Other previous studies in smokers had shown an increase of distribution volume and/or binding potential (Staley, J Neurosci. 2006; Mukhin;. J Nucl Med. 2008). Our results are in agreement with these findings, but show that this increase is only a consequence of an affinity change, all the other parameters, including the nicotinic receptor concentration, remaining unchanged.

Acknowledgments: This research was supported by grant from 'Canceropole, Ile-de-France, projet PL026'.

Brain Poster Session: Oxidative Mechanisms

REACTIVE OXYGEN SPECIES GENERATION AND BCL-2 DOWNREGULATION MEDIATED APOPTOSIS IN HUMAN GLIOMA U87 CELLS BY DEMETHOXYCURCUMIN

R. Kumar, P.M. Luthra

Dr. B R Ambedkar Center for Biomedical Research, University of Delhi, Delhi, India

Objective: In efforts to find novel approaches to inhibit proliferation and induce apoptosis in human glioma cells, we examined the action of naturally occurring compound demethoxycurcumin on human glioma U87 cell line. The protooncogene Bcl-2 inhibited reactive oxygen species (ROS) production and prevented apoptosis by regulating the cellular redox potential [1-3]. In this work, demethoxycurcumin induced ROS generation and Bcl-2 downregulation mediated apoptosis in human glioma U87 cells has been studied.

Methods: Apoptosis in U87 cells was induced by treating the cells with or without demethoxycurcumin (12.5 µg/ml and 25 µg/ml) for 2, 4, 6, 12, 24 and 48 h. The net intracellular generation of ROS was assessed by dichorofluorescein diacetate (H_2DCF-DA). Proliferation inhibition, chromatin condensation and DNA fragmentation was carried by MTT assay, nuclear staining and DNA ladder method respectively. Bcl-2 protein expression was measured by western blotting. The distribution of cells in the different phases of the cell cycle was carried by flow cytometery.

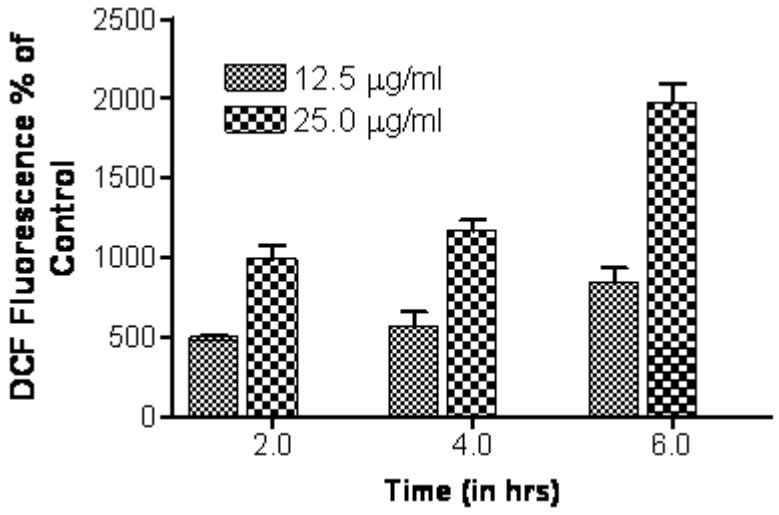

[ROS generation by demethoxycurcumin]

Figure. 1. ROS production during demethoxycurcumin-induced apoptosis. Human glioma U87 cells were exposed to 12.5 µg/ml and 25 µg/ml Demethoxycurcumin for 2, 4 and 6h. ROS production was detected H_2DCFH-DA selective for H_2O_2. The results were presented as a percentage of the fluorescence intensity compared with the control sample.

Results: Demethoxycurcumin exhibited high level of ROS generation in U87 cells in dose and time dependent manner (Figure. 1) and was associated with collapse of mitochondrial membrane potential ($\Delta\Psi m$), proliferation inhibition, chromatin condensation and DNA fragmentation and reduced expression of Bcl-2. In cell cycle analysis demethoxycurcumin showed G2/M arrest at 12.5 µg/ml

concentration after 24 h treatments, however at 48 h significant increase in sub-G1 apoptotic fraction was observed.

Conclusions: We have demonstrated for the first time that the induction of apoptosis associated with ROS production and down regulation of Bcl-2 in glioma U87 cells is mediated through demethoxycurcumin, meriting its further evaluation in vivo.

References:

1. D.J. Kane, T.A. Sarafian, R. Anton, H. Hahn, E.B. Gralla, J.S. Valentine, T. Ord and D.E. Bredesen. Bcl-2 inhibition of neural death: decreased generation of reactive oxygen species. Science 262 (1993) 1274-1277.

2. D.W. Voehringer, BCL-2 and glutathione: alterations in cellular redox state that regulate apoptosis sensitivity. Free Radic. Biol. Med. 27 (1999), 945-950.

3. J. Yang, X. Liu, K. Bhalla, C.N. Kim, A.M. Ibrado, J. Cai, T.I. Peng, D.P. Jones, X. Wang, Prevention of apoptosis by bcl-2: release of cytochrome c from mitochondria blocked. Science 275 (1997) 1129-1132.

REAL-TIME TRACKING OF CEREBRAL BLOOD FLOW DURING ARTERIAL OCCLUSION BY NEAR-INFRARED SPECTROSCOPY

K.M. Tichauer[1], J.T. Elliott[1,2], J.A. Hadway[1,3], T.-Y. Lee[1,2,3], K. St. Lawrence[1,2]

[1]Imaging Division, Lawson Health Research Institute, [2]Medical Biophysics, University of Western Ontario, [3]Imaging Research Laboratories, Robarts Research Institute, London, ON, Canada

Objectives: Cerebral aneurysms are a major risk factor for hemorrhagic stroke and are present in 3-6% of the population. An established treatment of aneurysms is the surgical placement of an aneurysm clip; however, the technique is associated with a significant risk of intraoperative stroke due to the need for temporary vessel occlusion during the clipping procedure. Minimizing the incidence of stroke requires continuous monitoring of cerebral blood flow (CBF) to ensure adequate perfusion to the affected arterial territory.

Using an indicator-dye dilution method, near-infrared spectroscopy (NIRS) could be used to measure CBF during surgery (1); however, measurements can only be repeated, on average, every ten minutes. Tsuji et al. demonstrated that a change in the difference between cerebral oxy- and deoxy-hemoglobin concentrations (ΔHbDiff) could be used to track changes in CBF during hypotension (2). The purpose of the present study was to investigate the accuracy of ΔHbDiff to changes in CBF caused by occlusion of the carotid arteries in piglets.

Methods: Experiments were conducted on piglets (< 1 week) that were anesthetized with isoflurane. Vascular occluders were placed around both carotid arteries and a cannula was inserted into an ear vein for administration of the NIRS contrast agent, indocyanine green (ICG). Following surgery, ΔHbDiff data were collected continuously during 10 minute intervals of no occlusion, single carotid occlusion, and bicarotid occlusion. Blood flow was then restored by deflating the occluders and the procedure was repeated. At the 2 minute mark of each interval, a bolus injection of ICG was administered to measure absolute CBF for comparison with ΔHbDiff at each level of perfusion.

Results: Eight piglets were studied (4 males, 4 females: 3.5 ± 0.9 days, 1.9 ± 0.1 kg). A statistically significant correlation was observed between ΔHbDiff and CBF for each piglet (average $R^2 = 0.986 \pm 0.016$, $p < 0.05$), although the slope of the regression had a coefficient of variation of 0.43. Figure 1 shows the relationship between HbDiff and CBF across all animals (mean ± SD). The large error bars for the CBF measurements was primarily due to inter-subject variability.

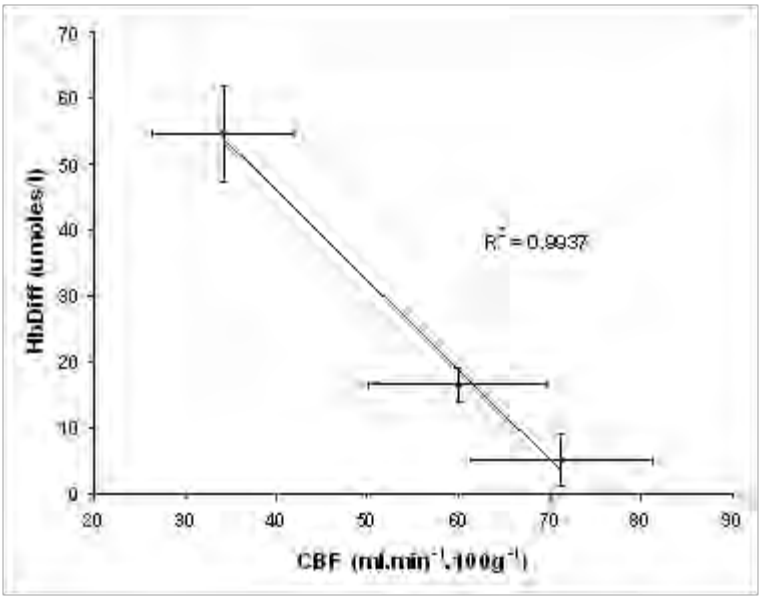

[Figure 1: HbDiff vs CBF]

Conclusions: The strong correlation between ΔHbDiff and CBF demonstrates the potential of using ΔHbDiff to continuously monitor blood flow during aneurysm surgery. Combining ΔHbDiff with NIRS measurements of CBF provides a means of determining if perfusion deficits during surgery drop below ischemic levels. The variability in the regression slope is likely due to differences in cerebral blood volume and total hemoglobin concentration between animals and is currently under investigation by our group.

References:

1) Brown et al. Pediatr Res 02;51:564.

2) Tsuji et al. Pediatr Res 98;44:591.

BEHAVIORAL TESTS TO REVEAL LONG-TERM FUNCTIONAL BENEFIT OF POTENTIALLY NEUROPROTECTIVE COMPOUNDS IN CEREBRAL ISCHEMIA IN MOUSE

V. Beray-Berthat, M. Frechou, B. Coqueran, M. Plotkine, **I. Margaill**

Pharmacology of Cerebral Circulation EA2510, Paris Descartes University, Paris, France

Objectives: All compounds showed neuroprotective in models of ischemia on the basis of short-term reduction in infarct volume have failed in clinical trials. Therefore a better evaluation of therapeutic strategies including long term behavioral outcome is needed[1]. In this context, the present study aimed to select sensorimotor tests that show long lasting deficits after cerebral ischemia in mouse.

Methods: Male Swiss mice (27-30g) anesthetized with ketamine and xylazine hydrochloride (50mg/kg and 6mg/kg ip respectively) underwent intraluminal occlusion of the left middle cerebral artery (n=23). Sham-operated mice (n=11) and non operated mice (n=7) were also included in the study. Behavioral tests were assessed at day 2 after ischemia and once a week until day 56 after the surgery. The neurological score evaluates sensorimotor reflexes. Beam walking tests assess the capacity of the mouse to walk on beams of different wide (1, 2 and 3 cm) and beam balance tests the ability to balance on a rectangular or a cylindrical beam. The pole test values the capacity of the mouse to go down a vertical wooden pole. For the chimney test, the mouse has to back up a vertical glass tube. The grip test measures the time during which the mouse hang on a horizontal string and the string test evaluates the way the mouse grips and moves on the string. Adhesive removal test measures the time to remove adhesives put on each forepaw. The circle test values the ability and rapidity of the mouse to exit concentric circles of different diameters.

Results: Whatever the time after surgery, the grip test and the beam balance test on the rectangular beam did not reveal any deficit after ischemia. In all the other tests, animals exhibited a deficit on day 2 after ischemia. An early functional recovery (before day 9) was observed for the chimney test, the string test and the balance beam test on the cylindrical beam. The neurological score, the beam walking tests, the pole test, the adhesive removal test and the circle test revealed a deficit up to 56 days.

Conclusions: In conclusion, among our battery, five tests are able to reveal long-term sensorimotor deficits. These tests appear of particular interest to screen strategies relevant for the treatment of clinical stroke.

References: 1. Stroke Therapy Academic Industry Roundtable (STAIR) 1999, Stroke 30:2752-2758.

ACCURATE MEASUREMENT OF ARTERIAL INPUT FUNCTION DURING FDG PET USING A BETA MICROPROBE

G. Warnock[1], C. Lemaire[1], X. Langlois[2], A. Luxen[1], A. Plenevaux[1]

[1]Centre de Recherches du Cyclotron, Universite De Liege, Liège, [2]Johnson & Johnson Pharmaceutical Research & Development, Division of Janssen Pharmaceutica N.V., Beerse, Belgium

An accurate arterial input function is essential for many kinetic models with PET and beta microprobe data. This includes functional data such as glucose metabolism, measured using FDG, and receptor binding using radioligands. The usual method for determining input function is manual blood sampling at specific time points followed by counting of the radioactivity in a given volume. However, the measurement of input function via arterial blood sampling generally has poor time resolution and can lead to significant blood loss in small rodents.

Beta microprobe systems have recently become commercially available as an affordable alternative to PET. These systems utilise implantable probes consisting of a small (0.25-1mm) scintillation crystal bonded to a fibre optic cable, which can be stereotactically located in a specific region of the rodent brain. Scintillation in the crystal is carried by fibre optic to a photomultiplier tube from which a time-activity curve is generated.

Pain et al (2004) used two beta microprobes to measure input function with one probe directly in the femoral artery. However, in this method the activity in surrounding tissues influenced the accuracy of the input function. Weber et al (2002; 2003) used an arteriovenous shunt and coincidence counter to measure input function while using beta microprobes in the brain. We have combined these two techniques to accurately measure FDG input function with high temporal resolution (1 second) and no loss of blood. Using our apparatus a beta microprobe is placed directly in the blood flow of an arteriovenous shunt. The bi-exponential conversion for FDG described by Weber et al (2002; 2003) can then be used to generate the arterial plasma input function. Via the shunt it is also possible to infuse tracer or treatment compounds, and to continuously measure blood pressure.

We have used our apparatus to measure input function in beta microprobe studies of the brain, and furthermore have combined the measurement of input function in this way with PET scanning in rats. Our method for the measurement of input function will be extended to further studies with additional radioligands. Thus, kinetic modelling can be carried out without the need for a reference region or less accurate estimation of input function.

References:

Pain F et al. J Nucl Med. 2004; 45:1577-1582.

Weber B et al. Eur J Nucl Med. 2002; 29:319-323.

Weber B et al. J Cereb Blood Flow Metab. 2003; 23:1455-1460.

Brain Poster Session: Mitochondria

NS1619 INDUCES IMMEDIATE PRECONDITIONING IN NEURONS AGAINST GLUTAMATE ECITOTOXICITY VIA ROS GENERATION BUT NOT BK_{CA} CHANNEL ACTIVATION

D. Busija[1], T. Gáspár[1], L. Lenti[2], P. Katakam[1], J. Snipes[1], F. Domoki[2], F. Bari[2]

[1]Physiology and Pharmacology, Wake Forest U Health Sciences, Winston-Salem, NC, USA,
[2]Department of Physiology, University of Szeged, Szeged, Hungary

Objectives: Activation of ATP-sensitive potassium (K_{ATP}) channels in the inner mitochondrial membrane has been shown to protect cultured neurons and brain against lethal insults by inducing immediate and delayed preconditioning (Stroke 30:2713, 1999; Brain Res. Rev. 56:89, 2007; Adv. Drug Del. Rev. 16:1471, 2008). It has been reported recently that the large conductance calcium activated potassium (BK_{Ca}) channel is present in the mitochondria of neurons and its activation with NS1619 has been reported to induce preconditioning. NS1619 is the most commonly used BK_{Ca} agonist. However, our recent study has questioned the role of functional mitochondrial BK_{Ca} channels in delayed neuronal preconditioning (J. Neurochem. 105:1115, 2008). On the other hand, BK_{Ca} channels might be involved in immediate preconditioning, but this possibility has never been explored. The objectives of our present experiments were:

1. to determine whether the BK_{Ca} channel opener NS1619 induces immediate preconditioning in cultured rat cortical neurons; and
2. to elucidate the role of BK_{Ca} channels in immediate preconditioning.

Methods: Primary cortical neurons were isolated from E18 Sprague-Dawley rat fetuses and studied at 7-9 days in culture.

Results: NS1619 (25-200 μM) increased reactive oxygen species (ROS) generation and depolarized mitochondria in a dose dependent manner, but neither was inhibited by BK_{Ca} channel antagonists. Furthermore, we could not detect the presence of the pore forming subunit of the BK_{Ca} channel in isolated mitochondria using commercially available antibodies while this subunit was present in brain lysates. One-hour treatment with NS1619 followed by washout of the drug induced protection against glutamate excitotoxicity (200 μM for 60 min). Neuronal viability 24 h after glutamate exposure was 58.45±0.95% for untreated cells. However, NS1619 at 50 μM increased viability to 78.99±0.90%*; NS1619 at 100 μM increased viability to 86.89±1.20%*; and NS1619 at 150 μM increased viability to 93.23±1.23%*; mean±SEM; *$p< 0.05$ vs. untreated cells; n=12-24). Viability of neurons exposed to only NS1619 was ~100%. Administration of the PI3-kinase inhibitor wortmannin, the PKC blocker chelerythrine, the MAP kinase antagonist PD98059, the ryanodine receptor inhibitor dantrolene, and the BK_{Ca} channel blockers iberiotoxin and paxilline were unable to antagonize the neuroprotective effects. In contrast, eliminating ROS with a scavenger during NS1619 application effectively blocked the development of preconditioning. Finally, treatment with NS1619 reduced the calcium load and ROS surge upon glutamate exposure.

Conclusions: Our results indicate that NS1619 is a potent inducer of immediate (current study) and delayed (previous study) neuronal preconditioning, and the protective effect is dependent on ROS generation but independent of the activation of BK_{Ca} channels. Since NS1619 has been shown to inhibit the mitochondrial electron transport chain, it seems likely that this effect may be the source of increased ROS and the resultant preconditioning. Our collective studies indicate that mitochondrial depolarization and subsequent protein kinase activation without ROS generation following selective

activation of mitochondrial K_{ATP} channels (J. Cereb. Blood Flow Metab. 28:1090, 2008) as well enhanced mitochondrial ROS release independent of potassium channel activation are both capable of protecting neurons against a variety of lethal stresses through distinct mechanisms. Suppported by NIH grants.

Brain Poster Session: Experimental Stroke & Cerebral Ischemia

SYNAPTIC DYSFUNCTION FOLLOWING RECURRENT HYPOGLYCEMIA IN DIABETIC RATS MAY CONTRIBUTE TO INCREASED ISCHEMIC DAMAGE

K. Dave[1], I. Saul[1], R. DeFazio[1], A. Raval[1], M. Perez-Pinzon[1], A. Pileggi[2]

[1]Neurology, [2]DRI, University of Miami, Miami, FL, USA

Objectives: Stroke and heart disease are the most serious complications of diabetes accounting for more than 65% of the mortality among diabetics (1). Hyperglycemia is one of the factors responsible for a worse outcome following stroke in diabetics (2). However, intensive therapy targeted to blood glucose control was able to delay onset and retard the progression of secondary complications of diabetes. The major side effect of intensive therapy in both type 1 and type 2 diabetics is recurrent hypoglycemic episodes (RH). The aims of the present study were:

1. to determine if RH episodes exacerbate cerebral ischemic damage and
2. to evaluate synaptic function following RH.

Methods: Streptozotocin (Stz)-induced diabetic rats were used as an animal model. Global cerebral ischemia was induced by tightening the carotid ligatures bilaterally following hypotension for 8 min. We determined the extent of neuronal death at 7 days of reperfusion in CA1 hippocampus following global cerebral ischemia in control, Stz-induced diabetic, insulin treated Stz-diabetic (ITD), and RH (two hypoglycemic episodes / day for 5 days). Hypoglycemia was defined as ~55-65 mg / dl blood glucose. Pre-ischemic synaptic function was measured in acute hippocampal slices. General population measurements of excitatory post-synaptic field potentials (fEPSP) were recorded with NaCl-filled glass micropipettes inserted into the stratum radiatum of the CA1 hippocampal subfield, and the Schaffer collaterals were electrically stimulated with bipolar tungsten electrodes.

Results: Following ischemia, in Stz-diabetic rats only 18% of pyramidal neurons survived as against 62% in control group ($p< 0.001$). Insulin treatment decreased ischemic damage by 41% ($p< 0.001$) as compared to the diabetic group. RH rats had 34% ($p< 0.05$) and 41% ($p< 0.001$) more damage as compared to ITD or control group, respectively. To determine if increased ischemic damage in RH group was due to synaptic dysfunctions, first we measured fEPSP amplitudes at different stimulation intensities as an index of synaptic strength in hippocampal slices. No significant difference was detected between ITD (15 slices from 4 animals) and RH (13 slices from 4 animals) groups. Next we examined paired pulse plasticity as an index of use-dependent synaptic plasticity. We observed that the ratio of fEPSP amplitudes following second pulse and first pulse was lower by 17% ($p< 0.02$) in RH group (ratio 1.69±0.08, 13 slices from 4 animals) as compared to ITD group (ratio 2.03±0.04, 15 slices from 4 animals) when the duration between two pulses was 50 ms. No significant differences were noted when duration was 25, 75, 150, 300 or 400 ms.

Conclusion: We are first to demonstrate that RH in diabetic animals exacerbates cerebral ischemic damage. Results also suggest that synaptic dysfunction following RH may be responsible for increased ischemic damage. These data indicate that recurrent hypoglycemic episodes may be an unexplored but important factor responsible for increased ischemic damage in diabetes.

References:

1) Biller and Love. Med Clin North Am, 77, 1993, 95.

2) Chopp et al. Stroke, 19, 1988, 1383.

3) Leese et al. Diabetes Care, 26, 2003, 1176.

Support: AHA (0735106N) and S.J. Glaser Research Grant.

Brain Poster Session: Experimental Stroke & Cerebral Ischemia

AROMATASE AND ABC1 ALTERATION IN ISCHEMIC HIPPOCAMPI OF MEGESTROL ACETATE TREATED-RATS

P. Kelicen[1], M. Cincioglu[1], S. Ugur[2]

[1]Department of Pharmacology, Hacettepe University, Faculty of Pharmacy, [2]Department of Vaccine, Serum and Experimental Animals, Refik Saydam Hıfzıssıhha Center, Ankara, Turkey

Objectives: Brain aromatase has been shown to be increased in expression after experimental stroke (Carswell et al, 2005). The present study investigated whether or not brain aromatase and ABC1 expressions were altered by aromatase inhibitor treatment (Megestrol acetate) after an experimental global brain ischemia produced by bilateral carotid artery occlusions plus systemic hypotension (BCAO + ht). Hippocampal cytosolic extracts were subjected to immunoblot analysis using anti-aromatase and anti-ABC-1. Global ischemia after cardiac arrest, intraoperative hypoxia/hypotension, or hemorrhagic shock is one of the causes of brain injury, resulting in severe neurological and neurobehavioral deficit. Since neurodegeneration can be protected by local aromatase expression and estrogen synthesis can be neuroprotective in the ischemia/reperfusion, aromatase may be a potential target to study reperfusion injury after brain ischemia. The expression of aromatase, an essential component of the aromatase cytochrome P450 (P450 arom; CYP 19) protein and the enzyme that catalyzes the biosynthesis of estrogens from androgenic precursors, is increased in the brain after injury or neurodegenerative disease, suggesting that, aromatase may be involved in neuroprotection (Negri-Cesi et al., 1996). The blood-brain barrier is a natural diffusion barrier, which expresses active carriers extruding drugs on their way to the brain back into the blood against concentration gradients. Whereas these so-called adenosine triphosphate-binding cassette (ABC) transporters prevent the brain entry of toxic compounds under physiological conditions, they complicate pharmacotherapies in neurological disease. Recent observations in animal models of ischemic stroke showed that some of the the prototypes of ABC transporters are upregulated on brain injury, deactivation of this carrier considerably enhancing the accumulation of neuroprotective compounds. We investigated the expression of aromatase and ABC1 proteins using Western blotting in rat hippocampus after transient global ischemia + hypotension (BCAO+jvht).

Methods: Transient two vessel occlusion global ischemia plus hypotension was produced. Briefly, SD male rats (250-280 g) were anesthetized and body temperature maintain within the normal range (37.0-37.5 °C), throughout the experiment. The femoral artery was exposed and catheterized to allow continuous recording of mean arterial blood pressure (MABP). Bilateral common carotid arteries were temporarily occluded (CAO), and blood was gradually withdrawn from the jugular vein to reduce the MABP to 35-45 mm Hg (ht). After 10 min of ischemia, the arterial clips were removed; the withdrawn warmed shed blood was reinfused to restore normotension. Hippocampi were homogenized and applied to immunoblotting.

Results and conclusion: Protein expressions of aromatase and ABC1 were observed in both control and damaged tissues. Immunoblot analysis demonstrated that aromatase and ABC1 expressions enhanced in the damaged (BCAO+jvht) hippocampi after 1 week reperfusion. Aromatase inhibitor megesetrol acetate treatment (30 days, p.o.; 20 mg/kg/day) decreased both aromatase and ABC1 levels in damaged hippocampi suggesting that ABC1 could be involved in the signal transduction cascade regulated by aromatase.

References:

Carswell et al., 2005. J Steroid Biochem Mol Biol. 96(1):89-91.

Negri-Cesi et al., 1996. J Steroid Biochem Mol Biol. 58(5-6):455-66.

This work is supported by Hacettepe University Research Foundation Project no: 02 02 301 009 ; approved by the ethical committee at H.U. (2002/63-5).

KINETIC PARAMETERS OF BAY 94-9172 BINDING TO ß-AMYLOID IN HUMAN BRAINS COMPUTED FROM PET DATA

G. Becker[1], H. Barthel[1], M. Patt[1], J. Luthardt[1], A. Seese[1], E. Hammerstein[2], B. Eggers[3], C. Reininger[4], B. Rohde[4], U. Hegerl[2], H.-J. Gertz[2], O. Sabri[1]

[1]Department of Nuclear Medicine, [2]Department of Psychiatry, University Hospital Leipzig, [3]Arzneimittelforschung Ltd., Leipzig, [4]Bayer-Schering Pharma AG, Berlin, Germany

Objectives: BAY 94-9172 is an ^{18}F-labeled stilbene derivative with a high affinity and specificity for β-amyloid in vitro. In early phase clinical development the visual assessment of BAY 94-9172 PET brain scans has demonstrated convincing diagnostic accuracy in the differentiation between subjects with Alzheimer's disease (AD) and healthy volunteers (HV) [Rowe et al., Lancet Neurol 2008, Barthel et al., J Nucl Med 2008]. Modeling of the kinetics of this PET tracer provides parameters by which direct quantification of brain ß-amyloid load can be acheived. The potential for these parameters for distinguishing between AD subjects and HVs was investigated.

Methods: After intravenous administration of 300MBq BAY 94-9172, the PET brain imaging was performed in 7 AD patients and 10 age-matched HVs using an ECAT EXACT HR+ system in 3D-acquisition mode. 23 frames were acquired from 0-90 min post injection. In each subject imaged, kinetic modeling was applied to the volume of interest (VOI) based tissue-activity curves generated for 25 brain regions (anatomically defined via MRI co-registration) using a per subject metabolite-corrected arterial input-function. Total distribution volume (DV) and binding potential (BP) = k3/k4 and k3 were used to characterize specific binding. Both standardized uptake value ratio (SUVR) and distribution volume ratio (DVR) were computed using the cerebellar cortex as a reference region.

Results: All cortical regions and the cerebellar cortex need two tissue compartments to be described adequately. All investigated parameters were significantly higher in ADs compared to HVs e.g. in frontal cortex (DV: 11.3±3.5 vs 7.2±1.3, p=0.004; BP: 3.2±1.3 vs 1.6±0.3, p= 0.002; k3= 0.059±0.029 vs 0.028±0.005, p=0.004), parietal cortex (DV: 10.2±2.3 vs 7.2±1.2, p=0.004; BP: 3.0±1.0 vs 1.6±0.2, p= 0.0004; k3= 0.049±0.022 vs 0.028±0.006, p=0.01) and posterior cingulate cortex (DV: 11.7±3.1 vs 7.5±1.2, p=0.002; BP: 3.4±1.3 vs 1.7±0.2, p= 0.001; k3= 0.062±0.029 vs 0.027±0.007, p=0.002). When the cerebellar cortex was used as a reference region (DVR, SUVR) results were highly significant ($p < 0.0001$) for all three regions, too.

Conclusions: Kinetic modeling of BAY 94-9172 brain PET images provides absolute quantification of brain ß-amyloid load which may be valuable for early disease detection and for monitoring the effect of amyloid modifying therapy.

References: The trial is sponsored and supported by the Bayer-Schering Pharma AG.

Brain Poster Session: Cerebral Vascular Regulation

OLMESARTAN CAN MAINTAIN NORMAL FUNCTION OF ENDOTHELIAL NITRIC OXIDE SYNTHASE IN THE BRAIN MICROVESSELS IN SPONTANEOUSLY HYPERTENSIVE RATS

N. Oyama[1], Y. Yagita[2], T. Sasaki[1], E. Omura-Matsuoka[1], Y. Terasaki[1], Y. Sugiyama[2], S. Okazaki[2], S. Sakoda[2], K. Kitagawa[2]

[1]Division of Stroke Center, Department of Internal Medicine, [2]Department of Neurology, Osaka University Graduate School of Medicine, Suita, Japan

Introduction: The endothelial nitric oxide synthase (eNOS) is important for cerebrovascular homeostasis and the reduction in bioactivity of eNOS leads to the dysfunction of cerebrovascular endothelium with subsequent decreased cerebral blood flow (CBF) and deteriorated ischemic stroke outcome. The accumulating evidence indicates that increased blood pressure diminished eNOS expression and impaired brain endothelial function. However, the influences of hypertension to the eNOS activity in the brain microvessels are still not fully understood. The present study is aimed to investigate whether hypertension can affect the phosphorylation of eNOS protein and antihypertensive agent can be useful to preserve eNOS function in the brain microvessels.

Methods: Five- or 10-week-old male Wistar rats or spontaneously hypertensive rats (SHRs) were used for experiments. We measured blood pressure by the tail-cuff method. Five-week-old SHRs were treated orally with olmesartan (0.02% RNH-6270) or vehicle for 5 weeks. Total and Ser1177-phosphorylated eNOS protein in the brain cortex were evaluated using Western blots. To assess the contribution of eNOS to maintaining CBF, we monitored CBF in the brain cortex by laser-Doppler flowmetry after intravenously administered L-N^5-(1-iminoethyl)ornithine (L-NIO; 20mg/kg), a relatively selective eNOS inhibitor. Measurements of the cerebrovascular response to L-NIO were expressed as the percentage change of the baseline.

Results: Mean blood pressures of 5-week-old SHRs (97.5±13.8 mmHg) were within normal range and were similar to those of 5- and 10-week-old Wistar rats (93.2±9.2 and 98.7±6.0 mmHg). In contrast, mean blood pressures in 10-week-old SHRs were higher (154.7±11.8 mmHg). The ratio of phospho-eNOS/total eNOS protein in 5-week-old SHRs was not significantly different from that in Wistar rats, whereas it was significantly lower in 10-week-old hypertensive SHRs ($P< 0.05$). Five weeks treatment of olmesartan suppressed the elevation of blood pressure in SHRs (93.2±7.6 mmHg) compared with vehicle treated SHRs (154.0±11.7 mmHg). Phosphorylation of eNOS protein was significantly enhanced in SHRs treated with olmesartan than with vehicle ($P< 0.05$). Phosphorylation level of eNOS was not different from that in age matched normotensive Wistar rats (Figure). In SHRs treated with olmesartan or vehicle, L-NIO infusion decreased CBF and reached a minimum at 5-10 minutes after starting infusion. At 5 minutes after administration, response to L-NIO in olmesartan treated SHRs (13.4±3.7%) was significantly higher than in vehicle treated SHRs (7.5±3.5 %) and similar to that in Wistar rats (13.2±5.3 %).

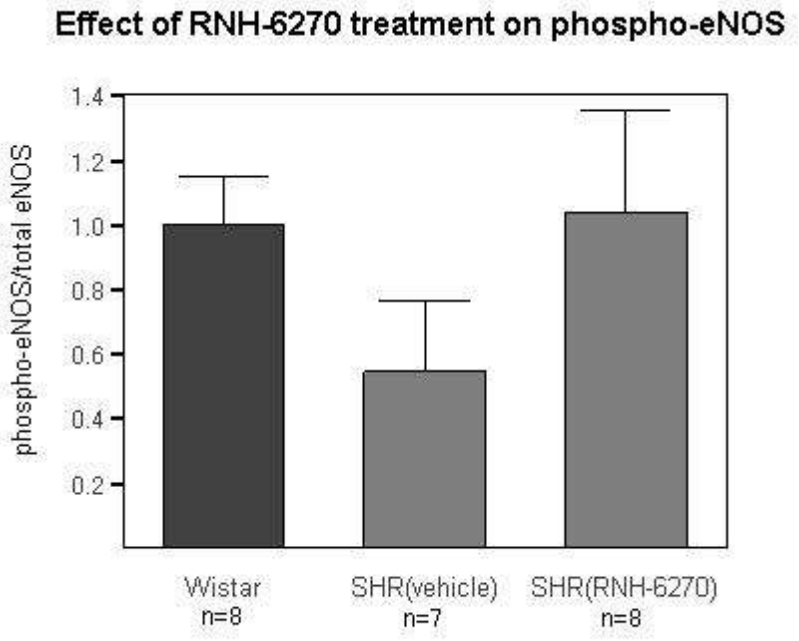

[Figure]

Conclusions: Activated eNOS expression in the brain was decreased in hypertensive SHRs. Olmesartan inhibited the elevation of blood pressure and preserved eNOS activity in SHRs. Additionally the contributions of activated eNOS to maintaining CBF were also preserved in olmesartan treated SHRs. Our findings indicate that antihypertensive agent such as olmesartan may help to preserve brain eNOS function against hypertension.

685

Brain Oral Session: Neonatal Ischemia

EFFECT OF THE CANNABINOID AGONIST WIN 55212-2 ON REMYELINATION AND NEUROGENESIS AFTER NEWBORN RAT BRAIN HYPOXIA-ISCHEMIA

D. Fernandez-Lopez[1], J.A. Martínez-Orgado[2], I. García-Yébenes[1], R. Cañadas[1], O. Hurtado[1], M.A. Moro[1], I. Lizasoain[1]

[1]Pharmacology, Complutense University of Madrid, [2]Neonatology, Alcorcón Hospital Foundation, Madrid, Spain

Background and purpose: Cannabinoids have emerged as interesting neuroprotective agents which efficacy has been proven in several animal models of acute and degenerative CNS diseases (1) . More recently, the endocannabinoid system has also been involved in the modulation of the proliferation, survival and differentiation of neural stem cells and progenitors (2), as well as in the prevention of oligodendrocyte cell degeneration and death under pathological conditions (3;4).

The CB1 and CB2 cannabinoid receptor agonist WIN 55212-2 (WIN) has shown a neuroprotective effect after experimental newborn brain hypoxia-ischemia (HI) (5), but its possible effects on the remyelination, proliferation and neurogenesis in this animal model remain unexplored. The main purpose of this work is to test the potential effect of the treatment with WIN in the aforementioned processes, which ocurrence strongly determine the long-term functional outcome after newborn brain HI.

Methods: 7-day old (P7) Wistar rat were submitted to unilateral permanent section of the common carotid artery, followed by the exposure of the rat pups to 90 minutes of hypoxia (8% O_2/92% N_2). The pups were administered either WIN (1mg/kg i.p.) or vehicle twice daily for 7 days after HI, and BrdU (50 mg/kg i.p.) twice daily from days P12 to P14 (5 to 7 days after HI). The immunohistochemical density of myelin binding protein (MBP) was measured at the end of the treatment period in several white matter areas. The total number of $BrdU^+$ cells in the ipsilateral SVZ was estimated using unbiased stereology at 7, 14 and 28 days after HI. Finally, the number of neuroblasts (Dcx^+ and $BrdU^+/Dcx^+$ cells) was quantified in the adjacent striatum 14 and 28 days after HI.

Results: HI induces a significant decrease of the density of MBP 24 hours after the insult. The treatment with WIN enhanced the recovery of the density of MBP in the ipsilateral external capsule 7 days after HI, reaching values similar to those observed in the non-injured hemisphere.

The total number of $BrdU^+$ cells in the ipsilateral SVZ was significantly higher in the WIN-treated animals than in the non treated animals (182570±11049 Vs 144373±7877, $p< 0.01$) at the end of the treatment with WIN (P14). The presence of double-positive cells for BrdU and Dcx in the adjacent striatum at P21 was higher in the WIN-treated animals, suggesting that some of the $BrdU^+$ cells observed in the SVZ after the treatment with WIN might have migrated and adquired the neuroblast phenotype at P21.

Conclusions:

1. WIN 55212-2 facilitates the remyelination of the injured white matter 7 days after HI.
2. WIN 55212-2 transiently increases the proliferation of neural stem cells in the ipsilateral SVZ 7 days after HI, as well as the presence of newly-generated neuroblasts in the injured striatum 14 days after HI.

Reference list:

(1) Mechoulam R et al., Trends Mol Med 2002; 8(2):58-61.

(2) Galve-Roperh I et al., Neuroscientist 2007; 13(2):109-114.

(3) Docagne F et al.,Mol Cell Neurosci 2007; 34(4):551-561.

(4) Molina-Holgado E et al., J Neurosci 2002; 22(22):9742-9753.

(5) Fernandez-Lopez D et al, Pediatr Res 2007; 62(3):255-260.

PRETREATMENT WITH THE HEME-OXIGENASE INHIBITOR ZINC PROTOPORPHYRIN-IX 24H BEFORE ISCHEMIA ENHANCES INFLAMMATION AND INCREASES INFARCT VOLUME

I. Pérez de Puig, R. Gorina, A. Martín, S. Rojas, T. Santalucía, A.M. Planas

Brain Ischemia and Neurodegeneration, Institute of Biomedical Research (IIBB)-CSIC-IDIBAPS, Barcelona, Spain

Objectives: Heme-oxygenase (HO) is an enzymatic system responsible for heme degradation[1]. Two HO isoenzymes have been described: an inducible form, HO-1, and a constitutive form HO-2. HO-1 mediates the anti-inflammatory effects of IL-10[2]. Expression of HO-1 is induced in focal brain after ischemia[3-5], and several lines of evidence suggest that it exerts a protective action against ischemic damage[6,7]. However, other findings suggest that HO-1 expression may be harmful [8]. Zinc proto-porphyrin-IX (ZnPP) is a naturally occurring compound that acts as a competitive inhibitor of HO. ZnPP has negative effects in several inflammatory conditions. However, previous studies showed that administration of ZnPP 30 min prior to transient middle cerebral artery occlusion (MCAO) or shortly after reperfusion, is protective against ischemic damage [9,10]. An inhibitory action of ZnPP on IL-1beta has been reported and may underlie the beneficial effects of ZnPP [11]. Here we tested whether systemic administration of ZnPP induced the expression of proinflammatory cytokines in the brain and whether the time of administration affected the outcome of cerebral ischemia.

Methods: We used a model of permanent MCAO with craniotomy in adult male FVB mice. ZnPP was given i.p. either 24h (ZnPP-24h) or 30 min (ZnPP-0.5h) before ischemia. The time course expression of TNF-alpha, IL-1beta, and HO-1 mRNA before and after ischemia was examined. Neutrophil infiltration was assessed with myeloperoxidase, and infarct volume was measured at day 4.

Results: ZnPP-0.5h reduced infarct volume, in agreement with previous reports. In contrast, ZnPP-24h had the opposite effect as it significantly increased infarct volume. Systemic administration of ZnPP specifically induced IL1beta and HO-1 mRNA expression in the control brain at 24h, but not at 0.5h. Therefore, the ZnPP-24h group, but not the ZnPP-0.5h group, had higher IL1beta and HO-1 than vehicle group at the time that ischemia was induced. The expression of TNF-alpha, IL1beta and HO-1 mRNA was increased at 4h and 8h postischemia. At the latter time points, the ZnPP-24h group showed noticeably higher TNF-alpha mRNA expression than the vehicle group, and exacerbated neutrophil infiltration also.

Conclusions: These findings evidence that ZnPP had dual effects depending on the time of administration. The negative effect of ZnPP-24h is likely mediated by exacerbation of the proinflammatory burden driven by ischemia.

References:

1. Lee & Chau, 2002; Nat Med 8: 240-46.

2. Ryter et al., 2006 ; Physiol Rev 86:583-650.

3. Koistinaho et al., 1996; Eur J Neurosci 8:2265-72.

4. Nimura et al., 1996; Mol Brain Res 37:201-8.

5. Fu et al., 2006; Neurol Res 28:38-45.

6. Panahian et al., 1999; J Neurochem 72:1187-203.

7. Moreira et al., 2007; J Cereb Blood Flow Metab 27:1710-23.

8. Matsuoka et al., 1999; J Cereb Blood Flow Metab 19:1247-55.

9. Kadoya et al., 1995; Stroke 26:1035-8.

10. Zhao et al., 1996; Stroke 27:2299-303.

11. Yamasaki et al., 1992; Neurosci Lett 142:45-7.

Acknowledgement: IP has has a predoctoral fellowship from AGAUR (Generalitat de Catalunya). Supported by the Spanish Ministry of Education and Science (CICYT) and by the European Community´s Seventh Framework Programme (FP7/2007-201, grant n° 201024, European Stroke Network).

DOES ENDOTHELIN-1 INDUCE CORTICAL SPREADING DEPOLARIZATION (CSD) VIA A DIRECT EFFECT ON THE VASCULATURE?

A.I. Oliveira-Ferreira, D. Milakara, D.V. Jorks, M. Alam, S. Major, J.P. Dreier

Center for Stroke Research Berlin, Charité - Universitätsmedizin Berlin, Berlin, Germany

Objectives: Endothelin-1 (ET-1) has attracted increasing interest since its discovery by Yanagisawa in 1988. Recognized as a neuropeptide with neurotransmitter/neuromodulator functions, ET-1 is also a potent vasoconstrictor. Moreover, it potently induces CSD in vivo. ET-1 has been related to several pathophysiogical states including subarachnoid hemorrhage, ischemic stroke and traumatic brain injury. The mechanism by which ET-1 induces CSD is not fully understood. Possibly ET-1-induced vasoconstriction leads to ischemia which causes CSD. Here we further analyzed whether ET-1-induced CSD is preceded by significant pial vasoconstriction and characterized pH changes and electrocorticogram (ECoG).

Methods: We used a two cranial window model in rats (n=11). ET-1 was brain topically applied in one window at 100nM and 1μM. A second window served as control. DC/AC-ECoG and laser-Doppler flowmetry were used to detect CSD. The pial arterioles were imaged onto a camera to assess whether significant vasoconstriction precedes ET-1-induced CSD. In the sequence of consecutive recorded images we marked our region of interest (ROI) at the right angle to the longitudinal axis of a pial arteriole. A single ROI is a line represented in MATLAB as a diagram with curves for the red, green and blue channels, where the x-axis represents length in pixel and the y-axis brightness. The blood vessel led to a clean valley with low noise in the green channel. The square root of absorbance between two inflection points was used to calculate the diameter value and diameter change over time. In another six experiments we recorded the pH changes associated with ET-1-induced CSD using pH-sensitive microelectrodes (comparison with CSDs in five control experiments).

Results: We observed a cluster of recurrent CSDs starting from the ET-1 superfused window and propagating to the control window. The cluster was associated with a negative DC shift of -2.6±2.2mV on which transient negative DC shifts of CSDs were riding. This was accompanied by a positive DC shift of 0.9±0.9mV in the control window superimposed with transient negative DC shifts. ET-1 induced significant vasoconstriction in large, medium and small pial arterioles before the first CSD (Wilcoxon Signed Rank Test). The magnitude of vasoconstriction was significantly more pronounced in medium and small compared to large arterioles (Repeated Measures ANOVA with Bonferroni Post-hoc test, Figure). Only in the presence of ET-1 a pH reduction to 7.20±0.07 preceded the sharp alkaline shift of the CSD in all experiments. The sharp alkaline shift coincided with the negative DC shift of CSD.

Conclusion: The pattern of the DC potential changes, the arteriolar constriction and pH reduction prior to the first cluster of CSDs support the notion that ET-1 induces CSDs due to its vasoconstrictive action. Our data may have implications for clinical conditions ranging from migraine to subarachnoid hemorrhage and ischemic stroke.

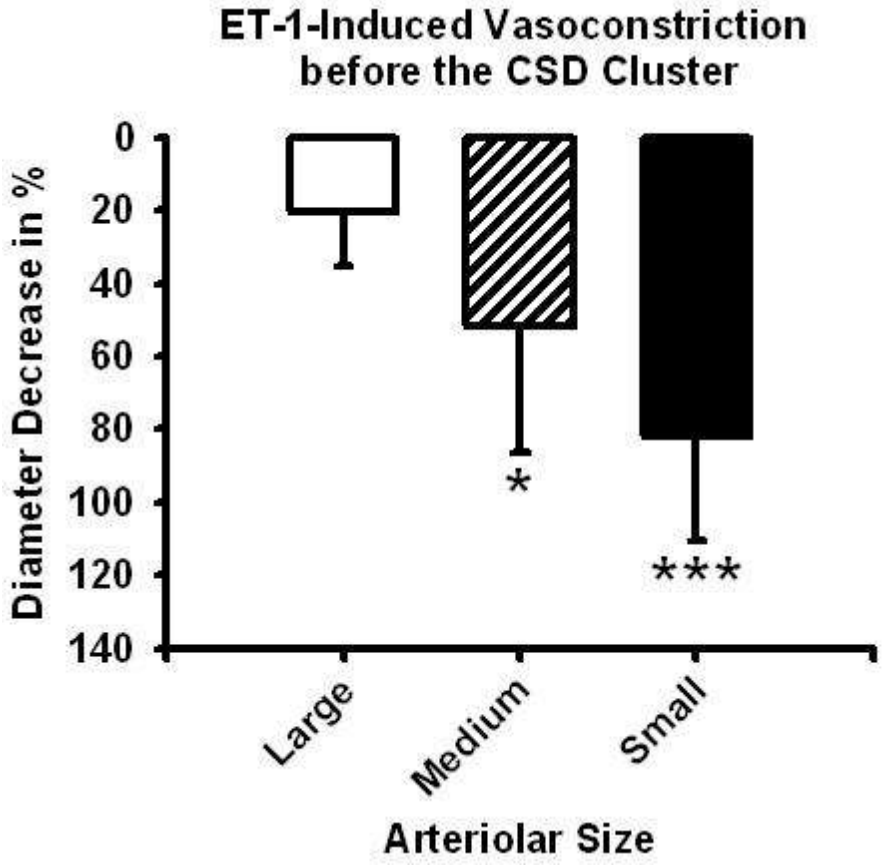
ET-1-Induced Vasoconstriction
before the CSD Cluster
Diameter Decrease in %
0
20
40
60
80
100
120
140
*
***
Large
Medium
Small
Arteriolar Size

[Figure]

688

Brain Oral Session: Neurovascular Unit

INFLUENCE OF INTRACRANIAL PRESSURE ON NEUROVASCULAR COUPLING: CLARIFYING MECHANISMS OF THE BOLD POST-STIMULUS UNDERSHOOT

M. Füchtemeier[1], N. Offenhauser[1], C. Leithner[1], J. Steinbrink[1], M. Kohl-Bareis[2], U. Dirnagl[1], U. Lindauer[1], G. Royl[1]

[1]Department of Experimental Neurology, Charité Universitätsmedizin Berlin, Berlin, [2]University of Applied Sciences Koblenz, RheinAhrCampus Remagen, Remagen, Germany

Objectives: Functional MRI (fMRI) with BOLD (blood oxygen level dependent) localizes activated brain areas non-invasively and is based on local vascular hyper-oxygenation during neuronal activation. However, the hemodynamic mechanisms of the underlying neurovascular coupling are still poorly understood. Therefore, the interpretation of the BOLD-signal is difficult. Which aspects can be attributed to passively occuring vascular effects and which aspects show the actual neuronal activation? Placed in the center of this discussion is the BOLD post-stimulus undershoot, a regularly seen transient hypooxygenation after the end of a stimulation period. Three main mechanisms have been introduced as explanation for the BOLD post-stimulus undershoot:

1. A neuronal inhibition follows immediately after cessation of the stimulus. Tight neurovascular coupling induces a cerebral blood flow (CBF) decrease leading to a transient relative increase of deoxy-Hemoglobin (deoxy-Hb) (Hoge et al., 1999).
2. After recovery of the CBF response, transient metabolic processes restore a steady-state equilibrium. These processes sustain an elevated cerebral metabolic rate of oxygen (CMRO2) that increases deoxy-Hb (Lu et al., 2004).
3. The BOLD post-stimulus undershoot is due to a temporal CBF / cerebral blood volume (CBV) mismatch.

After stimulus cessation, CBV returns to baseline values slower than CBF. The post-arteriolar compartment dilates passively during CBF elevation due to its compliance, similar to a balloon (Buxton et al., 1998) or windkessel (Mandeville et al., 1999). This dilated compartment stores CBV locally. After constriction of the feeding arterioles, this local CBV storage deoxygenates. We addressed these hypotheses by studying the effect of elevated intracranial pressure (ICP) on neurovascular coupling.

Methods: In anesthetized Wistar rats, a plastic catheter was positioned inside the cisterna magna. Over the somatosensory cortex, a closed cranial window was implanted. Using laser Doppler flowmetry and optical spectroscopy, CBF, deoxy-Hb, CBV and CMRO2 were measured, interleaved by blocks of 30s of electrical forepaw stimulation (monitored by somatosensory evoked potentials). In between stimulation blocks, intracranial pressure was adjusted to four different levels (3.5, 7, 14, 28 mmHg) by infusion of artificial cerebro-spinal fluid.

Results: During ICP elevation, the amplitude of the deoxy-Hb post stimulus overshoot (correlate of the BOLD post-stimulus undershoot) was reduced and close to zero. Surprisingly, elevated ICP also reduced deoxy-Hb decrease during activation. At an ICP of 28 mmHg the deoxy-Hb signal was even reversed. Time courses of CBF and CBV showed a trend towards less mismatch in the post-stimulus period (CBF returning to baseline values faster than CBV). CMRO2 in the post stimulus period was not elevated.

Conclusions: Our data shows that the deoxy-Hb post stimulus overshoot is caused by a passively occuring flow-volume mismatch rather than by metabolic afterload or neuronal inhibition. In addition, elevated ICP impaired, and even reversed the activity-induced deoxy-Hb decrease. Therefore, BOLD-fMRI might not be a reliable brain mapping method in states of ICP elevation.

689

Brain Oral Session: Experimental Stroke and Cerebral Ischemia 1

IMPACT OF GENETIC VARIANT OF BDNF (VAL66MET) POLYMORPHISM ON STROKE-INDUCED NEOVASCULARIZATION

L. Qin[1], R. Ratan[1,2], E. Kim[1], F. Lee[2], **S. Cho**[1,2]

[1]Burke Medical Research Institute, White Plains, [2]Weill Cornell Medical College, New York, NY, USA

Objective: The extent of angiogenesis affects stroke outcome and recovery. Brain derived neurotrophic factor (BDNF), a widely expressed neurotrophin in the mammalian nervous system, plays a key role in angiogenesis. BDNF is shown to promote endothelial cell survival and revascularization in ischemic limbs and newly described as a mediator of angiogenesis in ischemic tissue (Kermani and Hempstead, 2007). Recently, a common single nucleotide polymorphism (SNP) in the pro-domain of the bdnf , that leads to a methionine (Met) substitution for valine (Val) at codon 66 (Val66Met) has been identified in human. The mutation is associated with altered brain anatomy and memory and deficits in regulated BDNF secretion (Chen et al., 2006; Egan et al., 2003). By using mice with genetic knock-in of the humanized bdnf variant in both allele ($BDNF^{Met/Met}$) and wild type ($BDNF^{Val/Val}$), this study investigates the impact of genetic variant of BDNF (Val66Met) polymorphism on stroke outcome and stroke-induced neovascularization.

Methods: Male $BDNF^{Met/Met}$ and $BDNF^{Val/Val}$ (10-12 week old) mice were subjected to 30 min middle cerebral artery occlusion (MCAO) using an intraluminal thread method (Cho et al., 2005). Mice were killed 3/7 days after stroke. Brain sections were used for quantification of infarct volume. Enzyme-linked immunoadsorbant assay (ELISA) was used to evaluate the protein level of BDNF. Double fluorescence immunohistochemistry of CD31 (endothelial cell marker) and Ki-67(cell proliferation marker) was performed to visualize proliferating endothelial cell (neovascularization).

Results: Infarct volume (IV) and hemispheric swelling assessed 3 days after ischemia revealed no statistical difference between the strains ($BDNF^{Val/Val}$ vs $BDNF^{Met/Met}$, IV: 36.9±4.2, 27.7±5.4 mm^3; Swelling: 11.5±2.7, 7.9±3.5%, n=9-15). However, stroke-induced BDNF secretion was significantly reduced in $BDNF^{Met/Met}$ brain at both 3 and 7 days post-ischemia ($BDNF^{Val/Val}$ vs $BDNF^{Met/Met}$: 3d, 79.8±19.3, 42.8±14.6 pg/mg. 7d, 52.5±19.3, 30.9±8.8 pg/mg. n=5-10). The decreased BDNF secretion in $BDNF^{Met/Met}$ mice was associated with less neovascularization at 3 days post-ischemia (See figure, $BDNF^{Val/Val}$ vs $BDNF^{Met/Met}$, 13.6±2.2, 8.2±1.7 cell/mm^2).

Conclusion: The data demonstrate that stroke-induced BDNF secretion is not involved in the acute infarct development and BDNF secretion deficits in $BDNF^{Met/Met}$ mice is associated with reduced stroke-induced neovascularization. The study implicate translational approach that aim at reversing BDNF secretion deficits to promote stroke-induced angiogenesis. (Supported by NIH HL82511 and Burke Foundation).

References:

1. Kermani P, Hempstead B. Brain-derived neurotrophic factor: a newly described mediator of angiogenesis. Trends Cardiovasc Med. 2007, 17:140.

2. Chen ZY, Jing D, Bath KG, Ieraci A, Khan T, Siao CJ, Herrera DG, Toth M, Yang C, McEwen BS, Hempstead BL, Lee FS. Genetic variant BDNF (Val66Met) polymorphism alters anxiety-related behavior. Science. 2006, 314:140.

3. Egan MF, Kojima M, Callicott JH, Goldberg TE, Kolachana BS, Bertolino A, Zaitsev E, Gold B,

Goldman D, Dean M, Lu B, Weinberger DR. The BDNF val66met polymorphism affects activity-dependent secretion of BDNF and human memory and hippocampal function. Cell. 2003, 112:257.

4. The class B scavenger receptor CD36 mediates free radical production and tissue injury in cerebral ischemia. Cho S, Park EM, Febbraio M, Anrather J, Park L, Racchumi G, Silverstein RL, Iadecola C. J Neurosci. 2005, 25:2504.

Brain Poster Session: Glial Functions

SELENOPROTEIN S PROTECTS ASTROCYTES AGAINST ISCHEMIA-INDUCED APOPTOSIS

N. Fradejas Villar, D. Pastor Herrera, S. Mora-Lee, P. Tranque, S. Calvo

Medical Sciences, University of Castilla-La Mancha, Albacete, Spain

Objectives: Astrocytes are involved in maintaining brain integrity in conditions of disease and injury (1) and are thought to confer neuroprotection during brain ischemia (2). Since the molecular mechanisms involved in the astrocyte response to ischemia are not yet completely understood, our work is aimed to ascertain the relevance of the endoplasmic reticulum stress response in the astrocyte injury caused by ischemia. (3) Specifically, the work presented here was devoted to analyze the functions of Selenoprotein S (SEPS1) (4) in the astrocyte response to ischemia and ER-stress inducers, as this protein is involved in the retrotranslocation step of ER stress (5).

Methods: Differential display technique was used to uncover the genes whose expression was modified in cultured astrocytes subjected to oxygen and glucose deprivation (OGD) as an in vitro model of ischemia. Northern-blot and qRT-PCR were used to quantify Selenoprotein S expression levels. Selenoprotein S downregulation was reached by means of a specific siRNA. Cell viability was analyzed by the MTT method and flow cytometry of Annexin V/ propidium iodide stained astrocytes.

Results: Differential display analysis of astrocytes exposed to OGD uncovered the upregulation of Selenoprotein S gene during ischemia. Subsequent Northern blot and quantitative RT-PCR studies showed that OGD-induced Selenoprotein S mRNA increase was maximum after 4-hour and returned to control levels following reoxygenation. Astrocyte treatment with thapsigargin or tunicamycin also induced a significant increase of Selenoprotein S expression, indicating that this gene is expressed in astrocytes in the context of the ER-stress response.

siRNA technology was used to assess astrocytic Selenoprotein S functions. This approach caused a prominent diminution of Selenoprotein S expression which had a strong deleterious effect on astrocyte viability, decreasing survival to 4-hour OGD by 40%. In agreement with Selenoprotein S functions on ER-stress response, astrocyte survival to thapsigargin or tunicamycin treatment was also intensely diminished by Selenoprotein S siRNA.

In summary we can conclude that Selenoprotein S activation during ischemia has protective functions in astrocytes that might be related to the activation of retrotranslocation machinery.

References:

1. Nedergaard,M. and Dirnagl,U. (2005). Role of glial cells in cerebral ischemia. Glia 50, 281-286.

2. Li, L., Lundkvist,A., Andersson,D., Wilhelmsson,U., Nagai,N., Pardo,A.C., Nodin,C.,Stahlberg,A., Aprico,K., Larsson,K., Yabe,T., Moons,L., Fotheringham,A., Davies,I.,Carmeliet,P., Schwartz,J.P., Pekna,M., Kubista,M., Blomstrand,F., Maragakis,N., Nilsson,M.,and Pekny,M. (2008). Protective role of reactive astrocytes in brain ischemia. J. Cereb. Blood Flow Metab 28, 468-481.

3. Benavides, A., Pastor, D., Santos, P., Tranque, P., & Calvo, S. (2005). CHOP plays a pivotal role in the astrocyte death induced by oxygen and glucose deprivation. Glia, 52, 261-275.

4. Gregory V. Kryukov, Sergi Castellano, Sergey V. Novoselov, Alexey V. Lobanov, Omid Zehtab, Roderic Guigó, Vadim N. Gladyshev. (2003). Characterization of mammalian selenoproteomes. Science 300(5624):1439-43.

5. Ye Y, Shibata Y, Yun C, Ron D, Rapoport TA (2004) A membrane protein complex mediates retro-translocation from the ER lumen into the cytosol. Nature 429: 841-847.

691

Brain Poster Session: Cerebral Vascular Regulation

DYNAMIC CEREBRAL AUTOREGULATION AND CHANGE OF CEREBRAL BLOOD FLOW VELOCITY IN BOTH MCAS IN ACUTE ISCHEMIC STROKE DURING EXTERNAL COUNTERPULSATION

L. Xiong, J.H. Han, X.Y. Chen, T. Leung, Y. Soo, H. Leung, K.S. Wong

Department of Medicine & Therapeutics, The Chinese University of Hong Kong, Hong Kong, Hong Kong S.A.R.

Objectives: The presence or absence of cerebral autoregulation (CA) is critical for maintenance of stable cerebral blood flow. Serial transcranial Doppler ultrasonography (TCD) monitoring cerebral blood flow during external counterpulsation (ECP) may provide more information on the status of dynamic CA(dCA) after acute stroke onset.This study investigates whether dynamic cerebral autoregulation assessed from mean blood pressure (MBP) and mean cerebral blood flow velocity (CBFV) change from baseline during ECP is impaired after acute ischemic stroke onset; whether there is an effect of time course in the dynamic autoregulatory impairment within the acute and subacute stage of ischemic stroke.

Methods: Nineteen unilateral acute ischemic stroke patients with large artery disease and fourteen healthy controls were enrolled. A course of 35 daily one-hour sessions of ECP were applied to each patient within 7 days of symptom onset and controls. Admission National Institutes of Health Stroke score of the patient was 7±2. During ECP treatment, bilateral middle cerebral arteries (MCAs) were monitored by TCD to evaluate cerebral blood flow on day 3, 5, 7, 10, 14, 18, 21, 24, 28, 35 and 60 after stroke onset in stroke patients and on the first ECP session in controls. Beat to beat heart rate, continuous finger systolic and diastolic blood pressure and cerebral blood flow velocities of MCAs were obtained before, during and after ECP by means of Task Force Monitor.

Results: In stroke patients, the greatest increase of mean CBFV in the relevant MCA was noted at day 7 which was 4.1% from baseline and then gradually decreased till day 60. The greatest increase of mean CBFV in the irrelevant side was noted at day 18 which was 6.4% from baseline and then gradually decreased till day 60.MBP increased at every measurement points during ECP. At each measurement points, the differences in the magnitude of change from baseline in both mean CBFV and MBP were significant between patients and controls ($p< 0.05$).

Conclusions: Mean CBFV increased along with mean BP increase in bilateral MCAs, indicating a global impairment in dynamic cerebral autoregulation during the acute and subacute stage of acute ischemic stroke. The impairment of dCA would last 2 to 3 weeks after acute ischemic stroke onset.

References:

1. Kirkness CJ. Cerebral blood flow monitoring in clinical practice. AACN Clin Issues 2005;16:476-487.

2. Eames PJ, Blake MJ, Dawson SL, et al. Dynamic cerebral autoregulation and beat to beat blood pressure control are impaired in acute ischaemic stroke. J Neurol Neurosurg Psychiatry 2002; 72(4): 467-472.

3. Dawson SL, Panerai RB, Potter JF. Serial changes in static and dynamic cerebral autoregulation after acute ischaemic stroke. Cerebrovasc Dis 2003;16(1):69-74.

4. Immink RV, Van Montfrans GA, Stam J, et al. Dynamic cerebral autoregulation inacute lacunar and middle cerebral artery territory ischemic stroke. Stroke 2005; 36:2595-2600.

5. Reinhard M, Roth M, Guschlbauer B, et al. Dynamic cerebral autoregulation in acute ischemic stroke assessed from spontaneous blood pressure fluctuations. Stroke 2005; 36:1684-1689.

Brain Poster Session: Spreading Depression

PROPAGATION PATTERNS OF PERI-INFARCT DEPOLARIZATION AROUND ISCHEMIC FOCI IN RAT BRAIN ASSESSED BY LASER SPECKLE FLOWMETRY

T. Kumagai[1], H. Nakamura[1], M. Walberer[2], S. Vollmar[1], M. Sué[1], H. Endepols[1], G. Mies[1], M. Schroeter[2], R. Graf[1]

[1]Max-Planck-Institute for Neurological Research, [2]Department of Neurology, University of Cologne, Cologne, Germany

Objectives: Cortical spreading depression (CSD) and peri-infarct depolarization (PID) contribute to infarct expansion, however, the temporal and spatial aspects of this process are not fully elucidated. Alterations of cerebral blood flow (CBF) coupled to CSD/PID can be measured as a surrogate to assess CSD/PID propagation patterns in the surrounding of ischemic foci. We here studied CBF using Laser speckle flowmetry (LSF) in the cerebral cortex of rats in an embolic (macrosphere) stroke model.

Methods: In 6 male isoflurane anesthetized Wistar rats, a catheter was inserted into the left internal carotid artery. The left cranial bone was exposed (about 11mm x 6mm) and thinned to a thickness transparent enough to measure indicative CBF using LSF (CBF_{LSF}). The LSF system (laser diode & detecting camera) was placed over the exposed area to acquire images at a rate of 40 frames/min. TiO_2 macrospheres (diameter 0.335mm) were injected through the catheter until a detectable CBF_{LSF} change occurred. CBF_{LSF} recording was continued for up to 5 hours. Post-experimental evaluations of LSF images allowed three-dimensional spatial processing of CBF_{LSF} changes over time to assess hemodynamic patterns around the ischemic core. Spatiotemporal patterns of CBF_{LSF} changes were analyzed in 25 regions of interest (ROI: 1.4x1.4 mm) covering the whole field of view over frontal, parietal and temporal lobes.

Results: In 5 out of 6 rats, macrospheres caused occlusion of the middle cerebral artery (MCAo), and in 1 rat occlusion of the anterior cerebral artery (ACAo). In MCAo, the ischemic territory varied to some extent in size and location. In all rats, CSD/PID was observed after arterial occlusion. 1-3 minutes after the initial CBF_{LSF} decrease caused by the injection of macrospheres, the first one or two CSD/PID waves propagated radially or concentrically outwards starting from a primary ischemic center. These first waves seemed to act almost like a “switch” that consecutively left a not well differentiated ischemic center behind and established an ischemic core with clearer borders than those seen in the primary center. Subsequent waves of CSD/PID showed variable patterns depending on the severity of the developing ischemia: In cases of severe ischemia, waves of CSD/PID emerged at the rim of the ischemic core and propagated circumferentially along the rim. In cases of moderate to mild ischemia, in contrast, waves of CSD/PID emerged at multiple foci within a wide zone surrounding the ischemic core, and appeared as a rather chaotic pattern of CSD/PID propagation. This pattern was particularly pronounced in the single case of ACAo.

Conclusion: The results indicate that depending on the severity of CBF reduction variable patterns of CSD/PID propagation develop in the surrounding of ischemic lesions including concentric, multifocal and circumferential appearance. It is conceivable that the various CSD/PID patterns serve as one mechanism of infarct maturation.

Brain Oral Session: Neurovascular Unit

A MATHEMATICAL MODEL OF THE NEUROVASCULAR COUPLING SUGGESTING BOTH VASODILATION AND VASOCONSTRICTION

Y. Zheng[1], Y. Pan[1], S. Harris[1], S. Billings[2], D. Coca[2], J. Berwick[1], A. Kennerley[1], D. Johnston[1], J. Mayhew[1]

[1]Psychology, [2]Automatic Control and Systems Engineering, University of Sheffield, Sheffield, UK

Objectives: To investigate the coupling between neural activity and cerebral blood flow (CBF), a linear dynamic mathematical model was developed from data obtained using concurrent electrophysiology and laser Doppler flowmetry in rodent barrel cortex.

Methods: Urethane anesthetised Hooded Lister rats were used (200-300g). Electrophysiological recordings were made using a 16-channel electrode probe (NeuroNexusTechnologies) coupled to a data acquisition device (TDT, Florida) with a custom-written Matlab interface. The electrode was inserted normal to cortical surface under to a depth of 1,500μm. The evoked field potentials were used to obtain spatio-temporal estimates of the major current sources and sinks within the cortical layers. Time series of the layer IV current source density (CSD) sink were used as the incoming neural activity. The LDF probe (PeriFlux 5010, Perimed, Stockholm, 780nm illumination, 0.25mm separation) was placed as close to the electrode as possible.

Electrical stimulation of the whisker pad was delivered at 5Hz with intensity 1.2 mA and an individual pulse width of 0.3 ms. Each trial consists of a stimulus conditioning block of variable duration (2, 8 and 16s) followed by a probing block of 1s. The interval between the two blocks of stimulation also varies (0.6, 1, 2, 3, 4, 6 and 8s). Each trial lasted 60s, and was repeated 10 times per animal. Data were averaged over 10 animals.

Results: We show that the time series of CBF can be represented mathematically as two components: one increases with increased neuronal activity, while the other decreases. The dynamics of the two time series differ, and the summation of the two components provides excellent predictions of the measured CBF time series, shown in Fig.1. The CSD (blue) was normalised with respect to its first pulse, and the changes in CBF (green) was normalised with respect to its mean value during the control condition 4s prior to stimulus onset. The length of the conditioning block is 16s, with a resting gap of 8s between the conditioning and the probing blocks. Significantly, the mathematical model can predict the 'overshoot and plateau' characteristics often observed in the haemodynamic responses during the onset period of the stimulation, as well as the delayed return-to-baseline characteristics present in the haemodynamic response.

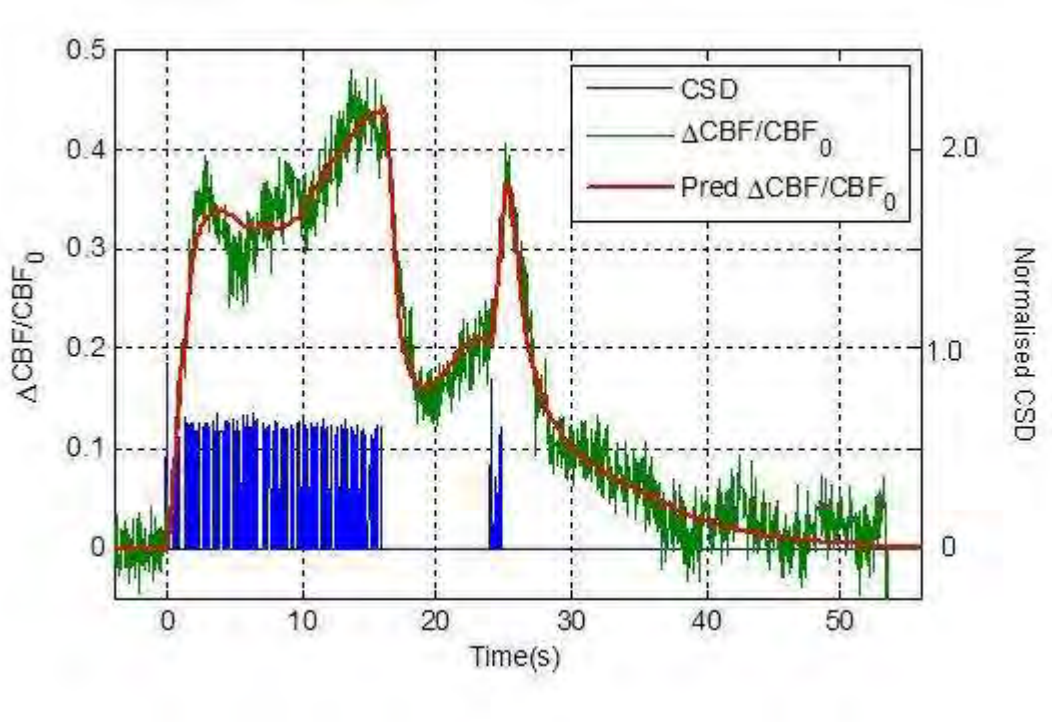

[Figure 1]

Conclusions: We hypothesise that the two model components of CBF changes are mediated by arterial volume changes produced by vasodilation and vasoconstriction following changes in stimulation induced neural activity.

The model structure corroborates the finding that neuronal activation evokes both vasodilation and vasoconstriction, and demonstrates the possible involvement of both vasomotor responses in the regulation of CBF (Metea and Newman 2006, Iadecola and Nedergaard 2007).

References:

Iadecola and Nedergaard (2007) Nature Neuroscience, 10(11): 1369-1376.

Metea and Newman (2006) J Neuroscience, 26(11): 2862-2870.

BAICALIN CAN PROMOTE NEURONAL DIFFERENTIATION VIA MODULATING JAK/STAT3 AND MASH1 PATHWAYS IN RAT NEURAL PROGENITOR CELLS

J. Shen[1,2]

[1]School of Chinese Medicine, [2]Research Centre of Heart, Brain, Hormone & Healthy Aging, University of Hong Kong, Hong Kong, Hong Kong S.A.R.

Objectives: Baicalin, a flavonoid isolated from the root of Scutellaria baicalensis G, has been proved to protect neural cells from oxidative injury. Whether Baicalin could promote neurogenesis is unknown yet. In this study, we hypothesized that Baicalin could stimulate neurogenesis by promoting the differentiation of neural progenitor cells. To verify the hypothesis, we investigated the effects of Baicalin on the proliferation and differentiation of neural progenitor cells.

Methods: Neural progenitor cells were prepared from cortex of embryonic E16 Sprague Dawley rats. The dissociated cells were seeded at a density of 1×10^5cells/ml in a DMEM/F12, replenished with 2% B_{27}, recombinant human basic fibroblast growth factor, and epidermal growth factor. The cells were then cultured with a differentiation medium contained DMEM/F12 (1:1) replenished 2% B_{27}, 5% fetal bovine serum for 14 days. Different concentrations of Baicalin (1, 2, 10, 20 mM) were added into the cultured medium. The newly formed neurons were identified by co-staining with BrdU, anti-Tublin b-III (Tuj1), anti-microtubule associated protein-2 (MAP-2) and 4', 6'-diamidino-2-phenylindole (DAPI) whereas the formation of glial cells conformed by co-staining with BrdU and anti-glial fibrillary acidic protein (GFAP). Fluorescent imaging was visualized with a fluorescence microscope system (Leica DMIL). To explore the mechanisms of Baicalin promoting neuronal differentiation of neural progenitor cells, we investigated the expressions of p-Stat3 and Mash1 with western blot and Q-PCR analysis.

Results: Fluorescent studies showed that Baicalin treatment promoted the neural progenitor cells to differentiate into neurons but inhibited the formation of glial cells. Western blot analysis and Q-PCR study showed that Baicalin dose dependently down-regulated the expression of p-Stat3 but up-regulated Mash1.

Conclusion: Baicalin could promote neurogenesis instead of astrogliogenesis of neural progenitor cells, which is mediated by suppressing Jak/Stat3 pathway and activating Mash1 gene expression.

Acknowledgement: This study was support by a Seed Fund for Applied Research, University of Hong Kong and a Seed Fund for Basic Research, University of Hong Kong.

WHEN HYPOTHERMIA MEETS HYPOTENSION AND HYPERGLYCEMIA: THE DIVERSE EFFECTS OF ADENOSINE 5'-MONOPHOSPHATE ON CEREBRAL ISCHEMIA IN RATS

F. Zhang[1,2], S. Wang[1], Y. Luo[3,4], X. Ji[3,4], E.M. Memoto[5], J. Chen[1,2]

[1]Neurology and Center of Cerebrovascular Disease Research, University of Pittsburgh, [2]Geriatric Research, Educational and Clinical Center, Veterans Affairs Pittsburgh Health Care System, Pittsburgh, PA, USA, [3]Cerebrovascular Diseases Research Institute, Xuanwu Hospital of Capital Medical University, [4]Key Laboratory of Neurodegenerative Diseases, Ministry of Education, Beijing, China, [5]Radiology, University of Pittsburgh, Pittsburgh, PA, USA

Objectives: Mild hypothermia renders potent neuroprotection against acute brain injury (Karibe et al 1994; Maier et al 1998). Recent reports demonstrate that adenosine 5'-monophosphate (AMP), a natural molecule of ATP catabolism, plays a role in thermoregulation and induces hypothermia in mice (Swoap et al 2007; Zhang et al 2006). This study therefore sought to determine whether AMP induces hypothermia in rats and to study its collective effects on focal cerebral ischemia induced by two-hour MCAO.

Methods: AMP was dissolved in normal saline and intraperitoneally injected into rats. Cerebral ischemia was induced by two-hour middle cerebral artery occlusion followed by reperfusion (Karibe et al 1994). Core body temperature, physiological parameters, blood gas and blood electrolytes were monitored. Western blots were performed to detect AMPK expression and phosphorylation.

Results: Intraperitoneal injection of AMP induced hypothermia in a dose-dependent manner (Fig. A). Four mmol/kg AMP induced promising mild hypothermia for 2.5 hours. Unexpectedly, AMP-induced hypothermia failed to reduce infarct volume after brain ischemia in rats; instead, it exaggerated the ischemic damage, indicated by an increased infarct volume as well as increased rates of hemorrhagic transformation, seizure and animal death (Fig. B&C). Physiological parameter monitoring revealed that AMP causes bradycardia and profound hypotension (Fig. D), leading to cerebral hypoperfusion. Furthermore, AMP administration resulted in severe hyperglycemia (Fig. E), metabolic acidosis and hypocalcemia. Additionally, western blots demonstrated early dephosphorylation and degradation of AMP-activated kinase in ischemic cortexes in AMP-treated rats (Fig. F).

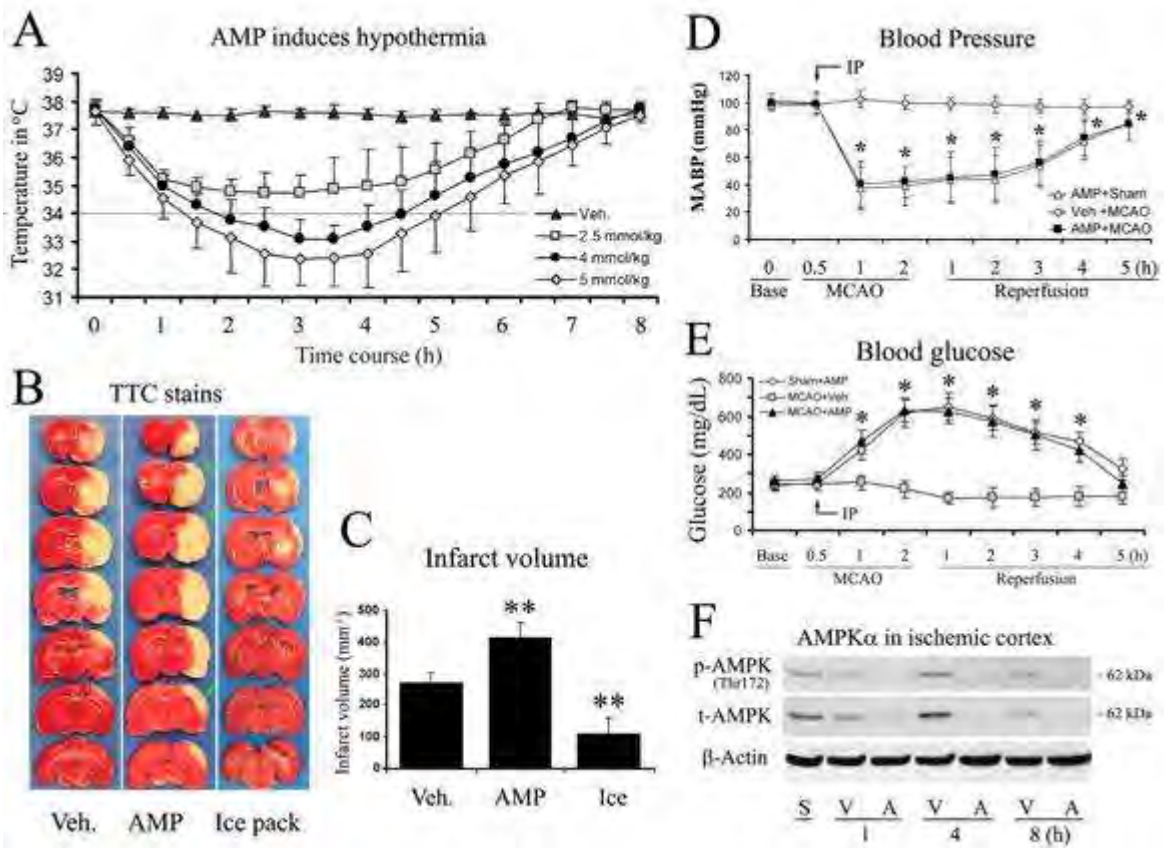

[Figure]

Conclusions: Our findings suggest that AMP induces hypothermia in rats, probably via limiting cellular access to glucose. However, the potential neuroprotection of AMP-mediated hypothermia against ischemia was overwhelmed by the detrimental effects of hypotension and hyperglycemia, thus making AMP an unlikely agent for inducing hypothermia to protect brain against ischemic injury.

References:

Karibe H, Chen J, Zarow GJ, Graham SH, Weinstein PR (1994) Delayed induction of mild hypothermia to reduce infarct volume after temporary middle cerebral artery occlusion in rats. J Neurosurg 80:112-9.

Maier CM, Ahern Kv, Cheng ML, Lee JE, Yenari MA, Steinberg GK, Kirsch JR (1998) Optimal Depth and Duration of Mild Hypothermia in a Focal Model of Transient Cerebral Ischemia : Effects on Neurologic Outcome, Infarct Size, Apoptosis, and Inflammation. Stroke 29:2171-80.

Swoap SJ, Rathvon M, Gutilla M (2007) AMP does not induce torpor. Am J Physiol Regul Integr Comp Physiol 293:R468-73.

Zhang J, Kaasik K, Blackburn MR, Lee CC (2006) Constant darkness is a circadian metabolic signal in mammals. Nature 439:340-3.

COMBINED FMRI AND METABOLIC VOLTAMMETRY IN VIVO: UNDERSTANDING THE NEUROCHEMICAL BASIS OF FUNCTIONAL IMAGING SIGNALS

N. Sibson[1], S. Mchugh[2], J. Lowry[3]

[1]Gray Institute for Radiation Oncology and Biology, [2]Department of Experimental Psychology, University of Oxford, Oxford, UK, [3]Department of Chemistry, National University of Ireland, Maynooth, Ireland

Objectives: The use of functional magnetic resonance imaging (fMRI) in both basic and clinical neuroscience is rapidly expanding. However, although advances have been made in correlating fMRI responses with the underlying neuronal activity, the fact remains that this technique does not directly measure neuronal activity but associated haemodynamic (and metabolic) events. Moreover, a constant relationship between neuronal, haemodynamic and metabolic processes across different brain regions is frequently assumed, despite substantial differences in neuronal architecture. Only by fully understanding the relationship between these parameters will we be able to fully utilise functional neuroimaging. Therefore, we must find a way of correlating fMRI data, which largely reflects the haemodynamic component, with neural and/or metabolic information. Long-term in-vivo electrochemistry (LIVE) enables real-time measurement of brain metabolites[1]. In this study we have developed methods for simultaneous fMRI and tissue oxygen measurements via LIVE for direct correlation of metabolic and haemodynamic factors.

Methods: Animals (n=3) were anaesthetised with 1.8% isoflurane in 70%N_2O:30%O_2, and a carbon fibre electrode (CFE) implanted into the right motor cortex (Bregma -1.5mm). Two further electrodes (auxiliary and reference) were implanted in the same cortical hemisphere (Bregma +3.5 and +4.5mm). Changes in O_2 concentration at the recording CFE were monitored using constant potential amperometry, with the CFE held at -900 mV (vs reference CFE). A multi-echo gradient echo imaging sequence was used to obtain blood oxygenation level dependent (BOLD) fMRI data: flip angle = 20º; TR = 27.3ms; TE = 7, 14, 21ms. Mean echo images were calculated from the individual echo images. Both BOLD and voltametric data were acquired continuously. Following a baseline period of 2min, oxygen content of the inspired gases was either reduced (0% O_2) for 30sec or increased (50%, 70% or 100% O_2) for 1 min. This paradigm was repeated 3 times for each condition.

Results: As shown in the figure, tissue O_2 measurements and BOLD responses obtained simultaneously demonstrated close correlation during complete oxygen removal (100% N_2O; between dotted lines); BOLD data taken from ROI in region of recording CFE. Both measurements showed a slightly delayed, but marked negative response on elimination of inspired O_2, owing to increased deoxyhaemoglobin levels (BOLD) and decreased tissue oxygen. Conversely, when the inspired oxygen was increased positive changes in both the BOLD and tissue oxygen signals were observed.

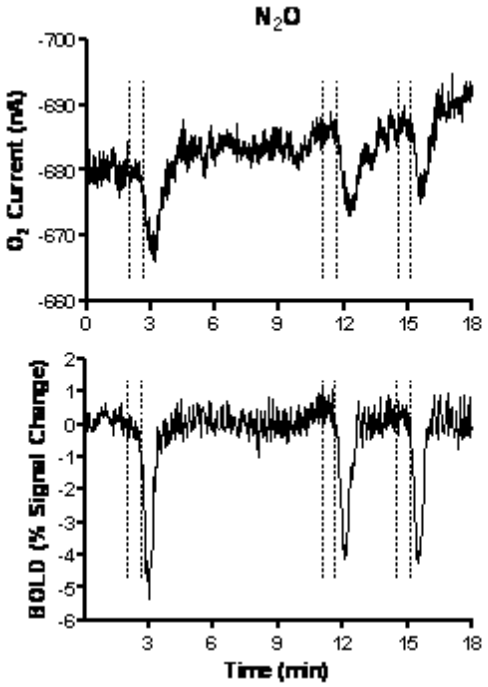

[fig]

Conclusions: Our findings demonstrate the feasibility of obtaining real-time metabolite information during fMRI acquisition. Although demonstrated here for oxygen measurements, the same LIVE technology can be applied to the measurement of many different neurochemicals, thus enabling comprehensive investigation of the relationship between fMRI signal changes and the underlying neurochemistry.

References: 1. O´Neill, R.D. ,Lowry, J.P., Voltammetry in vivo for chemical analysis of the living brain., in Encyclopedia of Analytical Chemistry. 2000, 676-709.

PJ34, A POLY(ADP-RIBOSE) POLYMERASE INHIBITOR, REDUCED TISSUE PLASMINOGEN ACTIVATOR-INDUCED HEMORRHAGE AFTER PERMANENT CEREBRAL ISCHEMIA IN MICE

M. Haddad, M. Plotkine, **I. Margaill**

Pharmacology of Cerebral Circulation EA2510, Paris Descartes University, Paris, France

Objectives: Tissue plasminogen activator (tPA) remains the only pharmacological treatment for acute ischemic stroke. However the increased risk of intracerebral hemorrhage after tPA largely contributes to limit its widespread use. tPA-induced hemorrhage seems to be related to the capacity of the thrombolytic to up-regulate matrix metalloproteinase-9 known to degrade the basal membrane components of blood vessels (Tsuji et al., 2005). Furthermore in a model of cerebral ischemia, the poly(ADP-ribose) polymerase (PARP) inhibitor 3-aminobenzamide was shown to reduce brain MMP-9 overexpression (Koh et al., 2005). In this context, we investigated whether the potent PARP inhibitor, PJ34 (N-(6-oxo-5,6-dihydrophenanthridin-2-yl)-2-(N,N-dimethylamino-acetamide), affected the rate of hemorrhage due to tPA therapy in a model of permanent cerebral ischemia.

Methods: Ischemia consisted in an intravascular occlusion of the left middle cerebral artery in male Swiss mice (30g) anesthetized with i.p. ketamine (50mg/kg) and xylazine hydrochloride (6mg/kg). Mice received either recombinant tPA (rtPA, Actilyse®, 10mg/kg, i.v. 6h after the onset of ischemia as a 10% bolus followed by an infusion over 30 min) or a combination of rtPA with the same protocol and PJ34 (3- 6 or 12 mg/kg, i.p. just after and 4 hours after the onset of ischemia). Control ischemic animals received the vehicle of rtPA and PJ34 (saline) with the same protocol. The neurological deficit (evaluated by a grip and a string test), infarct volume and intracerebral hemorrhage (counted on twelve 20-µm-thick coronal brain slices) were assessed 48 hours after ischemia.

Results: The rt-PA-treated ischemic mice showed a significant increased score of intracerebral hemorrhage compared to saline-treated ischemic mice (83 ± 10 versus 50 ± 8, $P< 0.05$). PJ34 reduced rt-PA-induced aggravation of hemorrhagic score at 3 mg/kg (37 ± 7, $P< 0.01$) and 6 mg/kg (52 ± 11, $P< 0.05$). PJ34 at 3 mg/kg also significantly improved the score in the string test ($P< 0.05$) and tended to reduce the deficit in the grip test ($P = 0.07$). Whatever the dosage, PJ34 had no effect on the infarct volume.

Conclusions: The present study demonstrates that PARP inhibition prevents rtPA-aggravation of both intracerebral hemorrhage and neurologic deficit. Thus PARP inhibition could be a valuable strategy to optimise tPA thrombolysis in stroke.

References:

Tsuji et al. (2005) Stroke, 36 :1954-1959.

Koh et al. (2005) Toxicology, 214 : 131-139.

CONTRALATERAL FOREPAW STIMULATION INCREASES THE INCIDENCE OF HYPEREMIC FLOW TRANSIENTS IN FOCAL ISCHEMIA IN THE RAT

J. Luckl[1], W. Baker[2], Z.-H. Sun[1], A. Yodh[2], T. Durduran[3], J.H. Greenberg[1]

[1]Department Neurology, [2]Department of Physics and Astronomy, [3]Department of Radiology, University of Pennsylvania, Philadelphia, PA, USA

Objectives: The possible neuroprotective effect of contralateral forepaw stimulation in temporary focal ischemia has been previously demonstrated (1), although its mechanism is still unclear. In the present study we tested the hypothesis that forepaw stimulation also exerts neuroprotection in permanent ischemia and we made an attempt to elucidate its mechanism by monitoring the cerebral ischemia with bispectral (laser speckle and intrinsic (OIS)) optical imaging.

Methods: Sprague-Dawley rats were prepared using isoflurane for occlusion of the right distal MCA and CCA. A 6x6 mm area centered 3 mm posterior and 4 mm lateral to Bregma was thinned for laser speckle and OIS (540/580/610 nm) imaging. The MCA was occluded by photothrombosis (2) and the CCA permanently ligated. Ten minutes after occlusion the left forepaw was stimulated (3 Hz, 2 mA) for two hours in a continuous loop: 4 secs stimulus, 3 secs rest. Both the core and cranial temperature were maintained at 37.5 C. Nine circular regions-of-interests (ROIs, 0.2 mm in diameter) were evenly spaced on the speckle contrast image avoiding vessels for the analysis of peri-infarct flow transients, blood flow and metabolic changes. Both the sham (n=6) and forepaw stimulated animals (n=6) underwent neurological examinations 24 h after ischemia (3) at which point all animals were sacrificed and the brains removed for determination of infarct size.

Results: Physiological variables were normal and not different between groups. The averaged residual flow after occlusion was between 40-58% of baseline in both groups in ROIs representing the peri-ischemic area between ACA and MCA. Similarly, there was no difference in residual flow (26-33%) between groups over the ischemic cortex. Both the neurological (sham: 3.5±1.6, stimulated: 4.2 ±1.3), and the histological (sham: 124±43, stimulated: 156±45,) examination did not show significant differences between groups. However, the averaged number of hyperemic flow transients were significantly higher in the forepaw stimulated animals (sham: 3.5±2.2, stimulated: 7.0±2.3; p=0.021). The propagation of the flow transients were multi-directional and confined mostly to the ACA-MCA watershed zone. In one case the propagation was bi-directional and in another case a hyperemic, low frequency oscillation could be seen over a well circumscribed part of the ischemic cortex. The flow transients were accompanied by changes in the concentration of oxy- and deoxyhemoglobin with some heterogeneity across animals and across regions. Hyperperfusive flow transients were usually accompanied by increases in oxyhemoglobin which sometimes remained elevated even when blood flow normalized, whereas hypoperfusive flow transients were followed by longer-lasting decreases in oxyhemoglobin, all suggesting changes in oxygen metabolism during the flow transients.

Conclusions: Although 2-hour forepaw stimulation had no positive effect on the outcome in chronic ischemia, forepaw stimulation appears to have a biological effect on the ischemic hemisphere by modulating/increasing the number of flow transients. The detailed analysis of combined speckle and OIS imaging give us a better insight into the propagation of peri-infarct flow transients and infarct evolution.

References:

(1) Burnett et al., Stroke 37:1327-1331, 2006.

(2) Margraf et al., Stroke 24:286-293, 1993.

(3) De Ryck et al., Stroke 20:1383-1390, 1989.

699

Brain Poster Session: Experimental Stroke & Cerebral Ischemia

PLATELET ACTIVATING RECEPTOR NULL MUTATION RENDERS NEURONS MORE SENSITIVE TO MCAO INDUCED TOXICITY

S. Whitehead[1,2], S. Jiang[1], J. Slinn[1], A. Aylsworth[1], S. Hou[1,2], S. Bennett[2]

[1]Institute for Biological Sciences, National Research Council of Canada, [2]Biochemistry, Microbiology and Immunology, University of Ottawa, Ottawa, ON, Canada

Objectives: Platelet-activating factor (PAF, 1-O-alkyl-2-acetyl-sn-glycero-3-phosphocholine) is a family of potent lipid second messengers generated through the cPLA$_2$/LPCAT lipid remodeling pathway. PAFs possess a wide range of biological functions including pro-inflammatory and neuromodulatory effects within the CNS [1]. Under normal physiological conditions, PAFs play a role in long-term potentiation in learning and memory dependent upon interaction with the G-coupled receptor platelet activating factor receptor (PAFR) [2]. Increased PAF metabolism is linked to neuronal death in ischemia, seizure, and AIDS dementia. PAF signal transduction, however, can be either neurotoxic or neuroprotective[3;4] depending upon the identity and degree of saturation of the sn-1 ether-linked alkyl chains of individual isoforms and the expression pattern of PAFR in target neurons[5;6]. Moreover, PAF-induced neuronal apoptosis can be triggered independently of PAFR with PAFR activation protecting neurons from the toxic effects of specific PAF isoforms. It is not known whether neurons are more sensitive to cell death following ischemia in the absence of the PAFR.

Methods: To address this, PAFR+/+ and PAFR-/- mice were subjected to a 1 h middle cerebral artery occlusion (MCAO) followed by 24h of reperfusion. In vitro studies involved primary cortical neurons and cerebellar cortical neurons (CGNs) from PAFR+/+ and PAFR-/- pups to oxygen glucose deprivation (OGD) followed by reperfusion. Rescue experiments involved the re-expression of PAFR by means of adenoviral infection into the CGNs from PAFR-/- mice.

Results: Here, we show that mice lacking the PAFR developed larger infarct sizes following ischemia-reperfusion injury suggesting a role for PAFR in neuroprotection. To confirm that PAFR null mutation protects neurons in vitro, we subjected primary cortical neurons and CGNs from PAFR+/+ and PAFR-/- pups to OGD followed by reperfusion. Our results demonstrated that neurons from PAFR-/- mice are more sensitive to OGD-induced cell death than cells generated from PAFR+/+ littermates. Restoration of PAFR expression by means of adenoviral infection into the CGNs from PAFR-/- mice rescued the PAFR-/- neurons from OGD-reperfusion induced neurotoxicity.

Conclusions: Overall these results clearly demonstrate the neuroprotective role of PAFR following cerebral ischemia reperfusion injury.

References:

1. S. M. Prescott, G. A. Zimmerman, D. M. Stafforini, T. M. McIntyre, Annu.Rev.Biochem. 69, 419-445 (2000).

2. C. Chen, J. C. Magee, V. Marcheselli, M. Hardy, N. G. Bazan, J.Neurophysiol. 85, 384-390 (2001).

3. N. G. Bazan, B. Tu, E. B. Rodriguez de Turco, Prog.Brain Res 135, 175-185 (2002).

4. A. A. Farooqui and L. A. Horrocks, Neuroscientist. 12, 245-260 (2006).

5. C. Brewer et al., J.Neurochem. 82, 1502-1511 (2002).

6. S. D. Ryan et al., J Neurochem 103, 88-97 (2007).

IMAGE-BASED MATHEMATICAL MODELLING FOR ISCHEMIC STROKE

Q. Li, S. Payne

University of Oxford, Oxford, UK

Objectives: Our aim is to construct a mathematical model of ischemic stroke that can be coupled with imaging data obtained from subjects who are still within the 'window of opportunity' for treatment in order that likely stroke outcome can be predicted and clinical decision making improved. We intend to build a new global phenomenological model of ischemic stroke from the cellular level to the voxel level, split into sub-models representing the underlying independent sub-systems.

Methods: The sub-models used here are based on the cell state, necrosis, toxin level, apoptosis, OEF and ATP, similar to the model proposed by [1] but including ATP dynamics and fully-coupled flow-metabolism behaviour. The cell can die in either necrotic or apoptotic fashion, the former being dependent upon cell state, the latter upon the energy available and a necrotic threshold. A point-based model approach was used as the physiological variables are regarded as functions of time only: hence any diffusive behaviour is neglected at this stage. Suitable parameter values were chosen, based on experimental data in the literature [2].

Results: The temporal behaviour of the six state variables is shown in Figure 1:

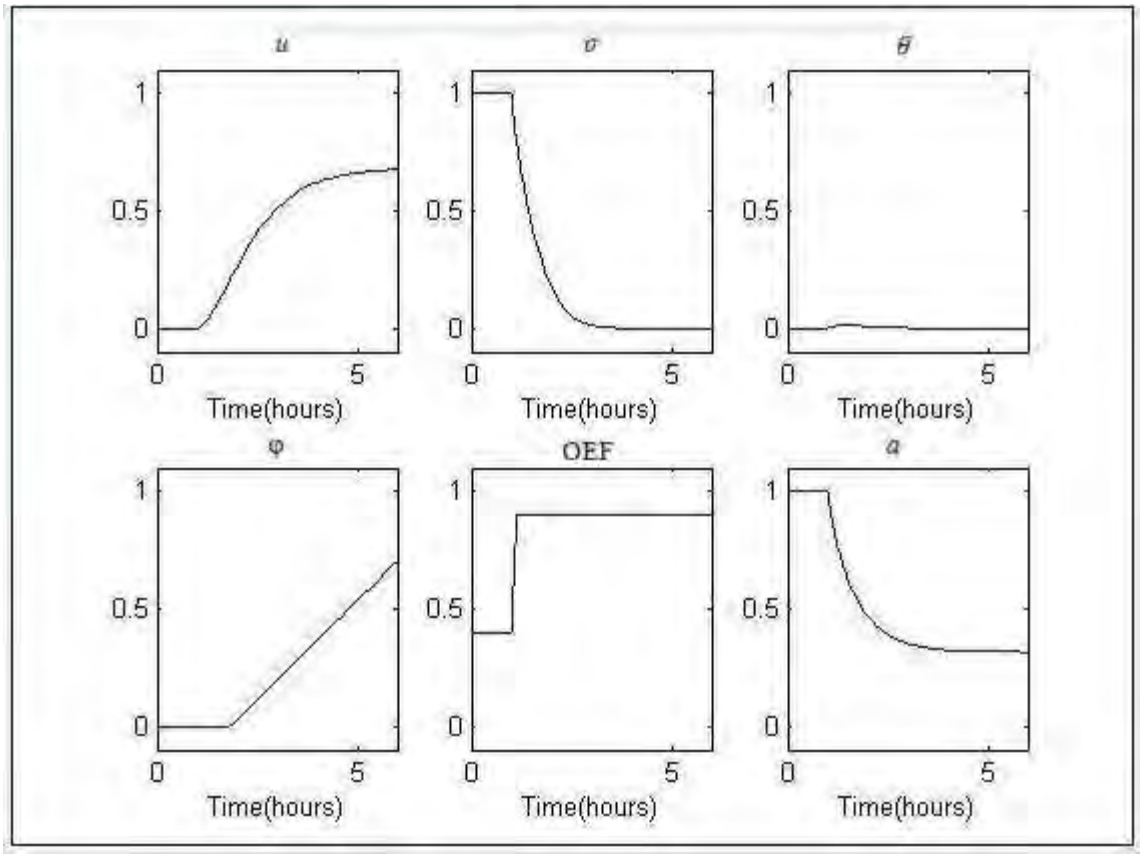

[Figure 1]

CBF has been reduced from 100% to 25% of baseline at a time of hour. The cell state (u) increases gradually from healthy (0) to partially impaired (0.7), as the necrosis state (σ) decreases from 1 to 0;

there is only a brief build-up of toxins (θ) during the transient as OEF increases. ATP (a) decreases from 1 to 0.3 and the apoptosis state (φ) does not reach 1. In this case, cell death occurs by necrosis: however, for different fractional cut-offs of CBF, cell death can occur by apoptosis. (Results not shown here).

Conclusions: The model proposed here mimics the different types of cell death occurring in a very simple manner: it is found that there is threshold phenomenon in the model, which affects the behaviour considerably, although the cut-off fraction of CBF can affect the type of cell death occurring. Despite the promising results shown here, there remains much further work to be done in terms of interpreting the cellular level behaviour and improving our modelling of the flow-metabolism coupling. Given the availability of imaging data, which has the potential to give spatially-resolved CBF and OEF, this model has the potential to form a basis for a clinically-based decision making tool.

References:

[1] E. Grenier, et al. (2008). 'A phenomenological model of the growth of the necrotic area in ischemic stroke'. Mathematical and Computer Modelling. In Press.

[2] M. Dronne, et al. (2008). 'A modelling approach to explore some hypotheses of the failure of neuroprotective trials in ischemic stroke patients'. Progress in Biophysics and Molecular Biology 97(1):60-78.

703

Brain Poster Session: Neuroprotection: Hypothermia

A CLINICALLY RELEVANT, PRECISE, AND NONINVASIVE MODEL OF THERAPEUTIC HYPOTHERMIA IN THE RAT

A. Lagina[1], K. Reed[2], R. Kumar[3], **J. Sullivan**[3]

[1]Emergency Medicine, [2]MS III, [3]Emergency Medicine and Physiology, Wayne State University, Detroit, MI, USA

Objectives: Hypothermia is neuroprotective after brain ischemia. Therapeutic hypothermia after resuscitation from cardiac arrest is increasingly used in the clinical setting, and may soon find wider clinical application in focal ischemic stroke. Experimental models of hypothermia range from rudimentary (placing the animal in a "cold room") to extremely elaborate. The state-of-the-art is described by DeBow and Colbourne: an implanted brain telemetry system is used to cybernetically control an array of heaters, misters and fans to maintain awake, freely-moving animals at target temperatures. Such systems, while effective and experimentally robust, are extremely costly, and do not model clinical practice. Therapeutic hypothermia is usually instituted via water-cooled extracorporeal systems in conjunction with sedation, and with monitoring of body core temperatures instead of brain temperatures. We undertook the development of a clinically relevant model of therapeutic hypothermia for use in the rat.

Methods: Veterinary warming blankets (Mul-T-Pads) were purchased from Gaymar, resized for the rat, and re-sealed with a heat-sealer (Scotchpak). The pad was fitted to a gel transfer cooling tank (Multi-Temp III, Amersham). Male Sprague-Dawley rats (N=5) were subjected to 2h focal brain ischemia under isoflurane/N_2O via MCAO technique. Thermocouples (Physitemp) monitored brain, temporalis and rectal temperatures. Brain thermocouples were stereotactically implanted in the MCA distribution bilaterally. Mean arterial pressure, heart rate and blood glucose were monitored by arterial catheter. Hypothermia was instituted at the onset of reperfusion with an initial tank temperature of 15 C. Animals were sedated with lorazepam during the 4h hypothermic interval. Animals were reperfused for seven days, and brains were taken to cresyl violet staining to assess stroke volume.

Results: This system proved to be highly responsive and practical, allowing for exquisite brain and core temperature control. Target temperature (32 C rectal) was attained by 35 minutes in all animals. Thereafter, core temperature was easily maintained to within 0.5 C with minimal adjustments of tank temperature and blanket position. Differences between ischemic and contralateral brain temperatures were negligible. Brain temperatures were closely approximated by temporalis temperature, even during rewarming, when brain temperatures rose more slowly than core temperatures. Arterial pressure, heart rate and glucose did not undergo significant fluctuations. Animals tolerated the procedure well and survived the 7-day reperfusion interval. Cresyl violet staining demonstrated appropriate placement of thermocouples and decreased stroke volumes compared to ischemic sham-hypothermia controls.

Conclusions: The system described here is an inexpensive, easily constructed and clinically relevant model of therapeutic hypothermia in the rat. Animals can be quickly taken to target temperature and maintained for long intervals. Disadvantages include the inability to use this system in non-sedated, freely-moving animals, although we are compelled to point out that therapeutic hypothermia is not performed in non-sedated, freely-moving patients. The entire apparatus can be constructed for about $3000 (including the tank). As temporalis temperature closely and accurately parallels brain temperature in this model, the use of invasive brain temperature monitoring could be deferred in preclinical studies.

References: DeBow S, Colbourne F. Brain temperature measurement and regulation in awake and freely moving rodents. Methods 30 (2003) 167-171.

704

Brain Poster Session: Cerebral Vascular Regulation

CEREBRAL HEMODYNAMIC RESPONSE OR EXCITABILITY IS NOT AFFECTED BY SILDENAFIL

C. Kruuse[1], A.E. Hansen[2], H. Larsson[3], M. Lauritzen[4], E. Rostrup[3]

[1]Dept. of Neurology, [2]Functional Imaging Unit and Dept of Radiology, [3]Functional Imaging Unit and Dept Clinical Physiology and Nuclear Medicine, [4]Dept. of Clinical Neurophysiology, Glostrup Hospital, University of Copenhagen, Glostrup, Denmark

Objective: Sildenafil (Viagra ®), a selective inhibitor of the cyclic guanosine monophosphate (cGMP) hydrolyzing phosphodiesterase5 enzyme (PDE5) is currently used for treatment of erectile dysfunction and pulmonary hypertension and recently suggested for use in post-stroke treatment. Sildenafil induces headache and migraine. Such headache induction may be caused by generally increasing either the excitability of neurons or the cerebrovascular response to external stimuli or both. Previously no effect of sildenafil on large cerebral arteries has been found in healthy subjects. Sildenafil administration and modulation of cGMP breakdown might increase the response to visual stimulation stimuli and give rise to an increased or prolonged cerebral response to visual stimulation and hypercapnia.

Methods: In 13 healthy females (23 ±3 year, 70.3±6.6 kg) the effect of sildenafil on a visual (reversing checkerboard) and a hypercapnic (6 % CO_2 inhalation) response was evaluated using blood oxygen level dependent (BOLD) imaging (3.0 T MR scanner). On separate occasions visual evoked potential (VEP) measurements (latency (P100) and maximal amplitude) were performed. Measurements were applied at baseline and 1 and 2 hours after ingestion of 100 mg sildenafil. Blood pressure, heart rate and side effects including headache were obtained.

Results: Ten of twelve subjects experienced headache on the day of MR investigations and nine of twelve on the day of VEP investigation. There was no significant difference between days. Sildenafil did not affect VEP amplitude or latency (P100). Both hypercapnia and visual stimulation elicited strong and consistent responses in each volunteer. However, the BOLD response to visual stimulation or CO_2 inhalation did not change after sildenafil administration.

Conclusion: In conclusion, sildenafil induces mild headache without potentiating a neuronal or local cerebrovascular visual response or influencing a global cerebrovascular response to CO_2 inhalation. Although sildenafil did induce a mild headache a generally increased neuronal response or an increased vascular reactivity appeared not to be involved in the pain process. The data further implies that sildenafil and subsequent augmentation of intracellular cGMP, does not in itself modulate the hypercapnic response in healthy subjects.

706

Brain Poster Session: Neonatal Ischemia

NEUROPROTECTIVE EFFECTS OF ACID-SENSITIVE ION CHANNEL INHIBITOR PSALMOTOXIN-1 IN SELECTIVELY VULNERABLE PUTAMEN AFTER HYPOXIA-ISCHEMIA IN NEWBORN PIGLET

Z. Yang[1], E. Carter[1], L. Marttin[2], R. Koehler[1]

[1]ACCM, [2]Pathology, Johns Hopkins University, Baltimore, MD, USA

Background and purpose: Acidosis is thought to play an important role in cerebral ischemic injury. Psalmotoxin-1 (PcTX), an inhibitor of Ca^{2+}-permeable acid-sensing ion channel 1a (ASIC1a), has been shown to reduce infarct volume in adult focal ischemia models (1). Here, we tested the hypothesis that PcTX attenuates neuronal damage in a global model of neonatal hypoxic-ischemic (H-I) encephalopathy.

Methods: Anesthetized piglets were subjected to 40 min hypoxia (9.8% O_2) followed by asphyxic cardiac arrest. Groups received intracereboventricular injections of artificial cerebrospinal fluid (aCSF), PcTX (1 µg in 50 µl aCSF) 20 min before H-I (PcTX pre-treatment) or PcTX 30 min after H-I (PcTX post-treatment). To contrast the role of ASIC1a with NMDA receptors in this model, another group received an intravenous injection of the NMDA antagonist MK-801 (1mg/kg) 20 min before H-I. Animals were survived 4 days for histology or 3 hours for measurements of nitrotyrosine immunoreactivity, as a marker of protein nitration, and protein carbonyl formation, as a marker of oxidative modification of proteins.

Results: At 4 days of recovery from H-I, viable neurons in putamen were markedly increased from 20 ± 5% (±SD; n=6) of sham surgical controls with aCSF injection to 47 ± 10% (n=7) with PcTX pre-treatment, which was similar to the 45 ± 18% value obtained with MK-801 pre-treatment (n=7). However, no significant protective effect was found with PcTX post-treatment (27 ± 17%, n=7). Pre-treatment with PcTX also resulted in improved recovery of neurological deficits on day 4 (aCSF = 40 ± 12; PcTX = 19 ± 13; maximum = 154). Arterial blood pressure, blood gases, and temperature were similar among groups. Immunoblots (n=6 per group) of putamen at 3 h of recovery indicated that PcTX pretreatment reduced ischemic-induced protein nitration (PcTX 1.37 ± 0.21 vs aCSF 2.4 ± 0.30 fold of sham+aCSF, $p< 0.05$) and protein carbonyl formation (PcTX 1.37 ± 0.21 vs aCSF 1.65 ± 0.27 fold of sham+aCSF, $p< 0.05$).

Conclusion: PcTX pre-treatment decreased nitrative and oxidative damage and protected striatal neurons from ischemic death in immature brain. The role of ASIC1a channels appears to be at least as important as that of NMDA receptors during H-I. In contrast to efficacy after reperfusion in adult transient focal ischemia (1), post-treatment with PcTX did not show obvious protection, possibly because of early recovery of tissue acidosis after resuscitation in neonatal hypoxia-ischemia.

Reference: 1. Pignataro et al. Brain 2007; 130:151-8.

QUANTITATIVE VERSUS QUALITATIVE OEF IDENTIFICATION OF HEMODYNAMIC COMPROMISE IN STROKE PATIENTS WITH LARGE ARTERY OCCLUSION

R. Lin[1], K. Uchino[1], S. Zaidi[1], V. Reddy[1], M. Jumma[1], H. Kuwabara[2], D. Sashin[3], Y.-F. Chang[4], N. Vora[5], M. Hammer[1], T. Jovin[1], L. Massaro[1], J. Billigen[1], H. Yonas[6], E. Nemoto[3]

[1]Neurology, University of Pittsburgh School of Medicine, Pittsburgh, PA, [2]Radiology, Johns Hopkins University School of Medicine, Baltimore, MD, [3]Radiology, [4]Neurosurgery, University of Pittsburgh School of Medicine, Pittsburgh, PA, [5]Neurology and Psychiatry, St. Louis University School of Medicine, St. Louis, MO, [6]Neurosurgery, University of New Mexico Health Sciences Center, Albuquerque, NM, USA

Objectives: The Carotid Occlusion Surgery Study (COSS) uses qualitative oxygen extraction fraction (OEF) by the count rate hemispheric ratio method to identify hemodynamic compromise in symptomatic stroke patients with internal carotid occlusion is a proven independent predictor of increased stroke risk and is being used to evaluate the efficacy of bypass surgery in reducing stroke risk compared to best medical therapy. COSS represents a major improvement over the previous study that failed to show efficacy of bypass surgery. However, our earlier study indicated that quantitative OEF alone may not accurately indicate hemodynamic compromise which may be more problematic with qualitative OEF. We determined the agreement between qualitative OEF as measured in COSS and quantitative OEF in identifying hemodynamic compromise in stroke patients with unilateral internal carotid occlusion.

Methods: Fourteen stroke patients with unilateral internal carotid occlusion were studied by positron emission tomography measurements of quantitative and qualitative oxygen extraction fraction (OEF) with $^{15}O_2$ gas and $H_2{}^{15}O$ water for brain oxygen uptake and blood flow. The qualitative COSS OEF ratio method uses seven two cm diameter volumes of interest placed over the middle cerebral artery (MCA) territory with a threshold ratio of 1.13 (ipsilateral/contralateral) to indicate ischemic stress. For quantitative OEF, the entire MCA territory of each hemisphere was analyzed with an OEF threshold of 50%. The higher of the two quantitative OEF values was included in the plot for each patient for comparison with the COSS OEF ratio method. Patients with bilateral occlusion were excluded.

Results: Three of the 14 patients were identified in hemodynamic compromise by the qualitative COSS ratio method and three by quantitative absolute OEF values >50% (Figure). However, they were different patients. Patients with quantitative OEF>50% had COSS OEF ratios ranging from 0.8 to 1.10 whereas patients with COSS OEF ratios >1.13 had absolute OEF values ranging from 30 to 47%.

Conclusion: Qualitative OEF by the COSS count rate ratio method does not identify the same patients in hemodynamic compromise as those identified by quantitative OEF.

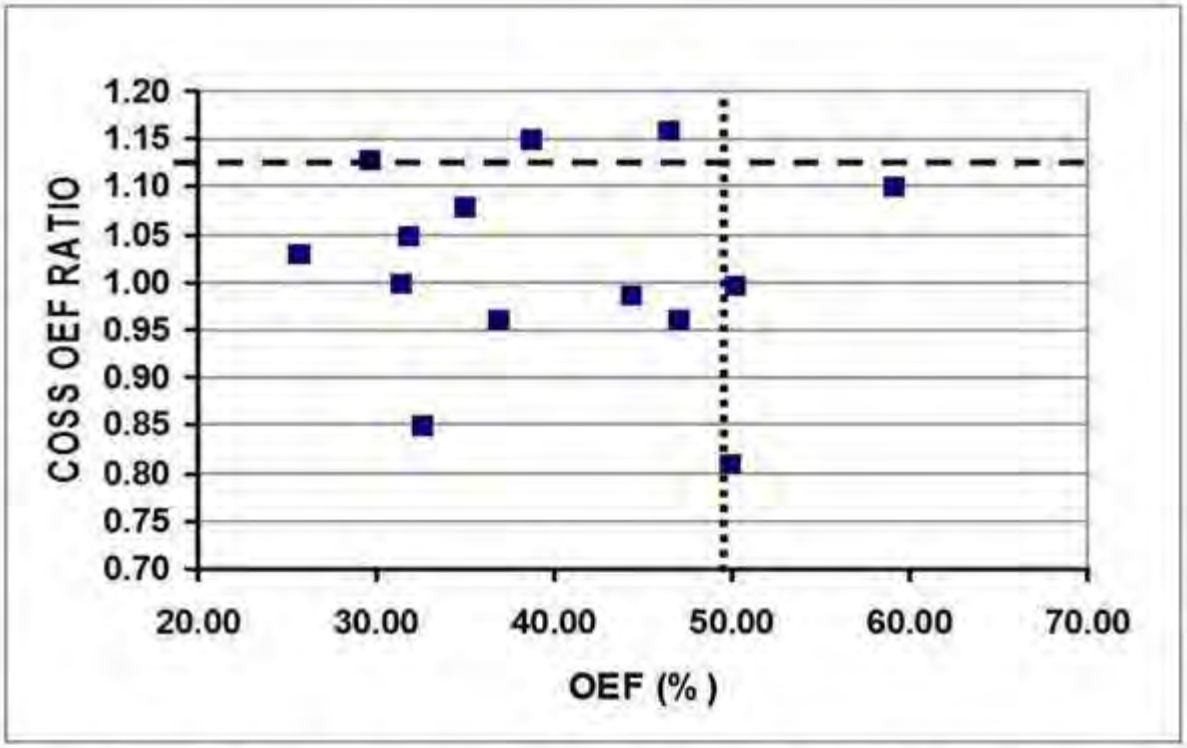

Figure Legend: Carotid Occlusion Surgery Study (COSS) qualitative OEF ratio versus quantitative OEF hemispheres with highest quantitative OEF in 14 stroke patients with unilateral internal carotid occlusion.

[COSS_QUOVADISFig]

Brain Poster Session: Experimental Cerebral Ischemia: Blood Flow & Metabolism

EARLY REGIONAL CHANGES OF CEREBRAL BLOOD FLOW IN AN EMBOLIC STROKE MODEL EVALUATED BY SEQUENTIAL PET

M. Walberer[1,2], **M.A. Dennin**[1,2], H. Backes[2], H. Endepols[2], B. Neumaier[2], R. Graf[2], M. Schroeter[1,2]

[1]Department of Neurology, University Hospital of Cologne, [2]Max-Planck-Institute for Neurological Research, Cologne, Germany

Objectives: The "macrosphere model" of focal cerebral ischemia mimics arterio-arterial embolism of atherosclerotic plaque material - a leading etiology of human stroke. Moreover, this model easily allows for a remote vessel occlusion within the Positron Emission Tomography (PET) scanner. Here we characterize the temporal and spatial dynamics of evolving focal ischemia in the macrosphere model in vivo using $[^{15}O]H_2O$-PET.

Methods: Polyethylene tubing was inserted into the internal carotid artery of 4 Wistar rats prior to placing the animals in a micro-PET scanner. Injection of four TiO_2 macrospheres (diameter 0.335mm) into the internal carotid artery induced middle cerebral artery occlusion (MCAO). One vehicle injected animal served as control. $[^{15}O]H_2O$-PET before as well as 5, 30, and 60 min after MCAO was used to assess the temporal dynamics of cerebral blood flow (CBF, measured as SUV $[^{15}O]H_2O$) without changing the animal's position in the scanner. A volume of interest (VOI) analysis covering the entire brain (126 cubic VOIs, 2x2x2mm) was used for a detailed evaluation of the spatial patterns of ischemia over time. 24 hrs after MCAO, ischemia was verified using ex vivo histology.

Results: Histologically, after MCAO all rats showed ischemic damage of the fronto-temporal and tempo-parietal cortex as well as the striatum; paramedial and occipital cortex were not involved. As expected, injection of saline alone did not induce ischemia. Measuring changes in CBF over time in vivo, we observed the development of an ischemic core between 5 to 30 minutes after ischemia induction. Surrounding VOIs showed hypo-, normo- or even hyperperfusion in this time interval. Between 30 to 60 minutes following MCAO, no further relevant changes in CBF occurred. Interestingly, the dynamics of CBF development over time seemed to be a more accurate predictor of the further fate of the respective VOI than static CBF values at either time point.

Conclusion: Sequential $[^{15}O]H_2O$-PET is a method to study the dynamics of early CBF alterations following embolic occlusion. In the macrosphere model, ischemia was evolving rapidly. Functionally relevant alterations in CBF occurred between 5 to 30 minutes after onset of stroke. Direct characterization of blood flow in novel stroke models using $[^{15}O]H_2O$-PET provides the basis for further multimodal imaging studies and facilitates the identification of primarily unaffected tissue accessible to therapeutic interventions.

709

Brain Poster Session: Oxidative Mechanisms

INTERACTION OF CAVEOLIN-1, CHOLESTEROL AND NITRIC OXIDE SYNTHASES IN HYPOXIC HUMAN SK-N-MC NEUROBLASTOMA CELLS

J. Shen[1,2]

[1]School of Chinese Medicine, [2]Research Centre of Heart, Brain, Hormone & Healthy Aging, University of Hong Kong, Hong Kong, Hong Kong S.A.R.

Objectives: Interaction between nitric oxide (NO) and caveolins appears to be a potential cellular signal pathway in ischemic brain injury. To elucidate the interaction of NO and caveolins in hypoxic neural cells, we investigated the expressions of caveolin-1 and caveolin-2 and NO production in human SK-N-MC neuroblastoma cells exposed to different periods of hypoxia.

Methods: Human neuroblastoma SK-N-MC cells were grown as a monolayer in minimum essential medium (MEM, Sigma) supplemented with fetal bovine serum (10%, v/v), glutamine (10mg/ml) and antibiotics (penicillin and streptomycin, 10mg/ml). For hypoxic treatment, confluent monolayers in multiple-well plates were placed in a modular incubator chamber. The cells were consistently incubated with 2% O_2 plus 5% CO_2 balanced with N_2 gas for 8, 15, 24 and 36 hrs at 37 ℃ respectively. To understand the interactions of caveolin-1, cholesterol and nitric oxide synthases in the hypoxic SK-N-MC cells, the cells were treated with different reagents to change the contents of NO and cholesterol.

Results: The expression of caveolin-1 mRNA and protein was transiently upregulated by 15 hrs of hypoxia but downregulated by 24 hrs or longer exposure to hypoxia, whereas the expression of caveolin-2 mRNA down-regulated by hypoxia. In normoxic SK-N-MC cells, both S-Nitroso-N-acetyl-DL-penicillamine (SNAP, NO donor) and 3-morpholinosydnonimine (SIN-1, peroxynitrite donor) up-regulated the expression of caveolin-1. Moreover, in the SK-N-MC cells exposed to 15 hrs of hypoxia, pretreatments of N^G-nitro-L-arginine methyl ester (L-NAME, a non-selective NOS inhibitor), 1400W (a inducible NOS inhibitor) or FeTMPyP (a peroxynitrite decomposition catalyst) attenuated the increase of caveolin-1 expression, but there were no obvious changes in the expression of caveolin-1 by incubation of 7-nitroindazole (7-NI, a selective neural NOS inhibitor) and l-N5-(1-iminoethyl)-ornithine (L-NIO, a selective endothelial NOS inhibitor). Meanwhile, hypoxia treatment induced intracellular cholesterol accumulation. Pretreatments of methyl-β-cyclodextrin (MCD) and methyl-β-cyclodextrin-cholesterol (MCD-CHOL) and oleic acid inhibited and enhanced the expression of caveolin-1 respectively. Those results suggest that the upregulation of caveolin-1 could be associated with iNOS-induced reactive nitrogen species production and lipid accumulation in the hypoxic neural cells. Furthermore, we compared the expression of eNOS, iNOS, and nNOS and NO production in wild-type and caveolin-1 over-expressed SK-N-MC cells after 15 hrs of hypoxia treatment. Exposure to 15 hrs of hypoxia inhibited eNOS expression but induced iNOS expression and NO production in the wild-type cells. However, over-expression of caveolin-1 prevented the loss of eNOS but downregulated the expression of iNOS and inhibited NO production.

Conclusion: The results suggest that augmentation of caveolin-1 in response to hypoxia stimulation could be a physiological regulating mechanism to inhibit iNOS-induced NO production. Overall, the complex interactions of reactive nitrogen species and caveolin-1 could be an important signal pathway in the modulation of NO production in hypoxic neural cells.

Acknowledgement: This work was supported by Hong Kong RGC GRF grant No. 7495/04M and No. 7748/08M.

REDUCED CEREBROVASCULAR REACTIVITY TO CO_2 INDUCED BY HYPERTENSION AND AGE: AN ARTERIAL SPIN LABELING STUDY IN RATS

R. Leoni[1,2], F.F. Paiva[1], D.B. de Araujo[2], A.C. Silva[1]

[1]Cerebral Microcirculation Unit - NINDS, National Institutes of Health, Bethesda, MD, USA,
[2]Department of Physics and Mathematics, University of Sao Paulo, Ribeirao Preto, Brazil

Introduction: The effect of hypertension on cerebrovascular autoregulation is of great interest, as hypertension is a major factor for stroke [1]. Previous studies have shown that hypertension impairs cerebral autoregulation in both humans and animals, but few have investigated the compounding effect of age. In the present study we used the arterial spin labeling (ASL) MRI technique to quantify CBF and CO2 reactivity in spontaneously hypertensive rats (SHR) at different ages.

Methods: Six SHR (N=2, 2 month old; N=4, 10 month old) were anesthetized under isoflurane (5% induction, 1.5% maintenance), orally intubated and mechanically ventilated in a 2:2:1 mixture of medical air, nitrogen, and oxygen. Experiments were performed in a horizontal 7T/30cm magnet (Bruker-Biospin, Billerica, MA). A home-built, transmit-only birdcage volume RF coil, 12cm internal diameter, and a commercially-built, receive-only 4-element surface coil array (Bruker-Biospin), were used for all image acquisition. For ASL, a small home-built figure-8 shaped labeling coil [2] was positioned under the neck of the animal. Hypercapnia was achieved by adding 1.5%, 3%, 5%, 6% and 10% CO_2 to the inhaled gas mixture. Single-shot ASL echo-planar images were obtained using TR/TE=10000/28ms, FOV=3.2x3.2cm, matrix=64x64, slice thickness=2mm, labeling time=8800ms, and post-labeling delay=994ms. Arterial blood gases were sampled at the end of each CO_2 level through a PE-50 catheter inserted into the right femoral artery. Significant differences across the data were tested with a Student's t-test.

Results: Contrary to a previous study [3], at normocapnia ($PaCO_2$ < 42mmHg), whole brain CBF values in old rats ($82 \pm 19 ml^{-1} \times g^{-1} \times min^{-1}$) were significantly lower than in young rats ($111 \pm 25 ml^{-1} \times g^{-1} \times min^{-1}$, $P < 0.05$). Addition of CO_2 significantly increased CBF in both young and old rats (fig.1a). Fig. 1b shows the mean CO_2 reactivity curves as a function of the $PaCO_2$. At normocapnia, the CO_2 reactivity in old rats ($2 \pm 1 ml \times 100g^{-1} \times min^{-1} \times mmHg$) was significantly lower than in young rats ($4 \pm 2 ml \times 100g^{-1} \times min^{-1} \times mmHg$, $P < 0.03$) [3], due to the impairment in vasomotor response induced by age, particularly when combined with hypertension [4]. However, at hypercapnia, the CO_2 reactivity values were identical in both groups and quickly approached zero for $PaCO_2$ > 60mmHg (fig.1b). CBF saturation was observed at $PaCO_2$ levels greater than 50mmHg (corresponding to 6% and 10% CO_2 levels) in both groups of rats [5] (fig. 1a).

Conclusions: The investigation of cerebral perfusion under normo- and hypercapnia showed a significant contribution of age in attenuation of both whole brain CBF as well as the cerebrovascular CO_2 reactivity in spontaneously hypertensive rats.

References:

[1] Liebeskind DS, Stroke 2003, 34:2279-84.

[2] Silva AC et al, MRM 1995;33:209-214.

[3] Tamaki K et al., Gerontology 1995;41(1):11-7.

[4] Ibarra et al., Arch Med Res 2006; 37:334-341.

[5] Duong et al., Magn Reson Med 2001; 45:61-70.

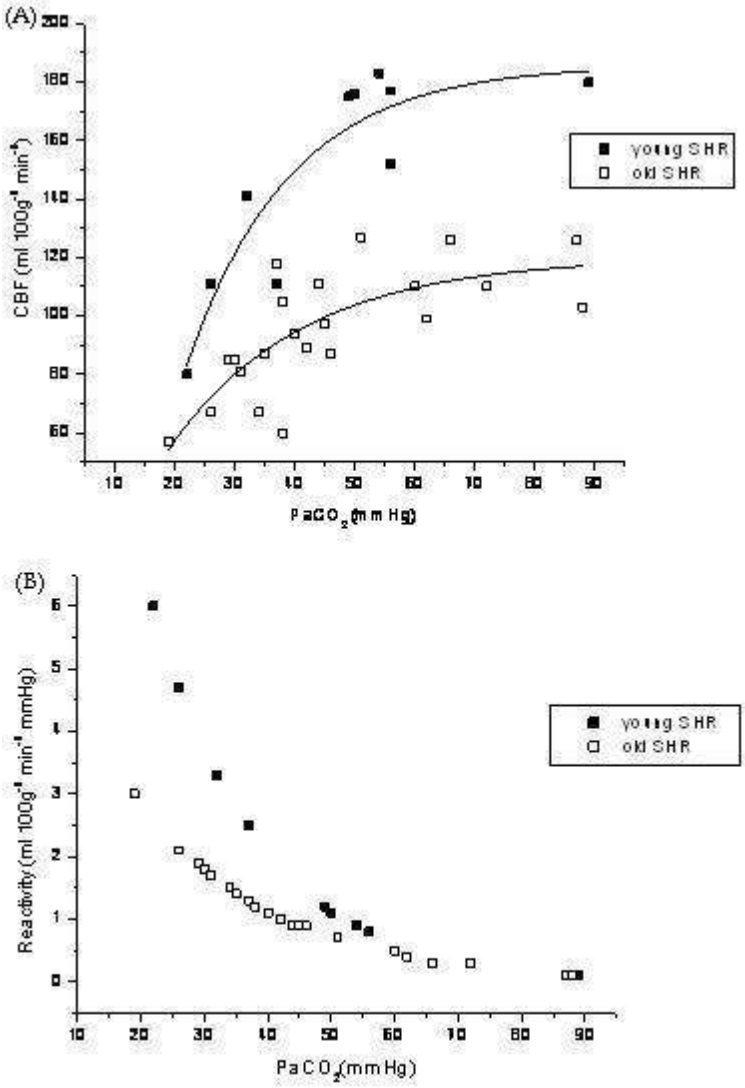

Figure 1: CBF and cerebrovascular CO2 reactivity in young and old spontaneously hypertensive rats (SHR).

[Figure 1]

711

BrainPET Poster Session: Brain Imaging: Stroke

A ASERIE OF STUDIES ON THE SECONDARY DEGENERATION IN THALAMUS-CORTEX TRACTS AFTER THALAMIC INFARCTION WITH DFFUSION TENSOR IMAGING

Z. liang[1], J. Zheng[1], X. Mo[1], C. Qin[1], Y. Wu[1], S. Jiang[1], Y. Dai[2], S. Li[1], J. Zeng[3]

[1]Department of Neurology, [2]Department of Radiology, Guangxi Medical University, Nanning, [3]Department of Neurology and Stroke Centre, Sun Yat-Sen University, Guangzhou, China

Background and aims: The secondary degeneration in pyramidal tracts after stroke have been demonstrated by animal experiments, atopsy examinations and diffusion tensor imaging. From our previous studies, a subcortical infarct may result in retrograde and anterograde degeneration of pyramidal tracts, moreover the degeneration of pyramidal tracts may hampered the neurological covery. However, the secondary degeneration in thalamus-cortex tracts (TCT) after thalamic infartion and its clinical significance still to be determined.

Methods: Eighteen patients with a recent thalamic infarct underwent three DTIs at first week (W1) and the fourth week (W4) as well as the twelfth week (W12) after onset. Eighteen age- and gender-matched controls underwent DTI one time. Mean diffusivity (MD) and fractional anisotropy (FA) were measured. Neurological deficit, motor deficit and life independence were assessed with NIH Stroke Scale, Fugl-Meyer scale and Barthel index respectively 2 hours before each DTI examination. To reveal the secondary degeneration in TCT, Mean diffusivity (MD) and fractional anisotropy (FA) were measured at thalamus, the TCT at corona radiata and centrum semiovale levels.

Results: Fourteen of the patients had some degree of sensory disturbance. From patients' colour encoded images, a deficit signal was observed on thalamic primary lesion, and along the TCT at corona radiata and centrum semiovale levels(Figure 1). FA values of thalamic primary lesion, ipsilateral TCT on corona radiata and centrum semiovale levels decreased significantly from W1 to W12 progressively ($P < 0.01$, respectively). The NIH Stroke Scale decreased, Fugl-Meyer scale and Barthel index increased significantly over the time ($P < 0.01$, respectively). The absolute values of percent reduction of FA value in ipsilateral TCT correlated positively to the degree of sensory disturbance.

Conclusions: The progressive anterograde degeneration in TCT revealed by DTI. may be responsible for persistent sensory disturbance.

712

Brain Poster Session: Cell Signaling

NITRIC OXIDE PRODUCTION INDUCED BY HYPOXIA MODULATES HIF-1 ALPHA EXPRESSION IN CULTURED ASTROCYTES THROUGH INTERACTION WITH SUPEROXIDE

Q. Chen, **W. Liu**, X. Sun, K. Liu

College of Pharmacy, University of New Mexico, Albuquerque, NM, USA

Objectives: Ischemic stroke results in cerebral tissue hypoxia, and increased expression of hypoxia-inducible factor (HIF) is critically implicated in ischemic tissue damage. Understanding the mechanisms of HIF-1alpha regulation has been an important research focus[1]. Nitric oxide (NO) and superoxide generation are increased under hypoxia/ischemic conditions[2,3], and each of them has been independently shown to regulate HIF-1alpha expression under several pathological conditions. In this study, we investigated the cross-affects of these two radicals on the expression of HIF-1 alpha in hypoxic astrocytes.

Methods: Immediately after the change of oxygen-free medium, astrocytes were placed into a humidity and air-tight chamber, which was flushed with 5%CO_2/95%N_2 for 15 min, then sealed and kept under 37°C for another 145 min. NO concentration in the conditioned medium was measured with the inNO-T nitric oxide measurement system using the amino-700 sensor; intracellular superoxide production was analyzed by fluorescence staining; HIF-1 alpha expression was measured with western blot.

Results: 2 hr-hypoxia remarkably increased HIF-1alpha protein levels in astrocytes, which was accompanied by increased NO and superoxide production. Decreasing superoxide with NAC, NADPH oxidase inhibitor (DPI), or SOD mimetic (MnTMPyP) decreased hypoxia-induced HIF-1 alpha protein expression, and increased NO production. NO synthase (NOS) inhibitor L-NAME alone inhibited superoxide generation as well as hypoxia-induced HIF-1alpha protein expression, however, it increased HIF-1apha protein in the presence of superoxide scavengers. Moreover, NO scavenger PTIO increased hypoxia-induced HIF-1 alpha protein expression and superoxide production. Incubation of astrocytes with peroxynitrite, the product of NO and superoxide reaction, did not change the expression of HIF-1 alpha protein expression under hypoxia condition.

Conclusion: These results suggest that superoxide critically contributes to hypoxia-induced HIF-1alpha protein stabilization under hypoxic condition. More importantly, our results indicate that hypoxia-induced NO generation may represent an endogenous mechanism for limiting the over-reaction to hypoxia stress by inhibiting HIF-1alpha protein expression.

Key words: Hypoxia, nitric oxide, superoxide, hypoxia-inducible factor-1 alpha.

References:

1. Lee JW, Bae SH, Jeong JW, Kim SH, and Kim KW. Hypoxia-inducible factor (HIF-1)alpha: its protein stability and biological functions. Exp Mol Med 36: 1-12, 2004.

2. Becher LB, Hoek TL, Shao ZH, Li CQ, and Schumacker P. Generation of superoxide in cardiomyocytes during ischemia before reperfusion. Am J Physiol Heart Circ Physiol 277:2240-2246, 1999.

3. Shen J., Lee W., Li Y., Lau C. F., Ng K. M., Fung M. L. and Liu K. J. Interaction of caveolin-1, nitric oxide, and nitric oxide synthases in hypoxic human SK-N-MC neuroblastoma cells. J Neurochem 107, 478-487, 2008.

713

Brain Poster Session: Cerebral Vascular Regulation

EXOGENOUSLY ADMINISTERED NITRIC OXIDE DOES NOT RECOVER THE ATTENUATION OF THE CBF RESPONSE TO SOMATOSENSORY STIMULATION AFTER NNOS INHIBITION

B. Piknova[1], A.N. Schechter[1], **A.C. Silva**[2]

[1]Molecular Medicine Branch, NIDDK/NIH, [2]Cerebral Microcirculation Unit, NINDS/NIH, Bethesda, MD, USA

Introduction: Since its discovery for over two decades ago, nitric oxide (NO), a small lipid-soluble gas molecule, has been shown to play critical roles in a wide variety of physiological functions. Of particular interest is the study of the role of NO in the signaling mechanisms linking local neuronal activity to brain hemodynamics [1]. Previously we have shown that pharmacological inhibition of the neuronal nitric oxide synthase (nNOS) enzyme induced uncoupling between neuronal and hemodynamic responses to functional activation of the somatosensory pathway in a-chloralose anesthetized rats [2]. In the present study, we investigate whether systemic administration of NO donors restores the attenuation of the functional CBF response produced by inhibition of nNOS.

Methods: The experiment was conducted on seven α-chloralose anesthetized Sprague-Dawley rats. The MRI experiments were carried out on a 7 T/30cm magnet (Bruker-Biospin, Billerica, MA). A dynamic arterial spin labeling (DASL) echo-planar imaging sequence (TR/TE 250/15 ms; 400x400x2000 μm3) was used to measure CBF and BOLD responses prior to and following an i.p. bolus (50 mg/kg) of 7-nitroindazole (7-NI, an in vivo inhibitor of nNOS), and after subsequent IV administration of the NO donor sodium nitroprusside (SNP, continuous IV infusion of 1.5uM solution in PBS to achieve low nmolar levels of NO in blood). The functional paradigm comprised 60 epochs of 10s off/5s on/15s off blocks, with the stimulation parameters 2mA, 0.3-ms, 3 Hz.

Results: Inhibition of nNOS significantly decreased both the CBF and the BOLD responses ($p< 0.05$) without affecting the resting CBF, as previously reported [2]. However, the NO-donor SNP had no effect in recuperating the attenuation of the CBF response (Fig. 1a, $p>0.05$). Interestingly, SNP did recover some of the BOLD response attenuation (Fig. 1b, $p< 0.05$).

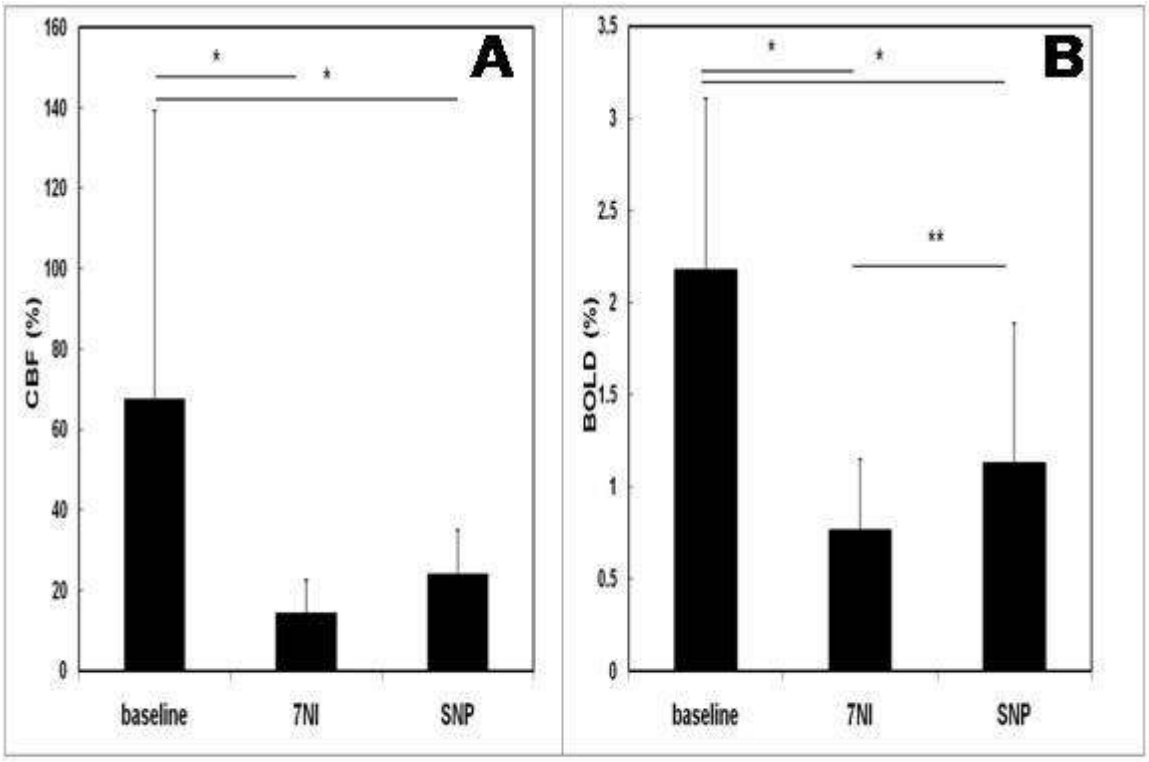

Fig. 1: CBF (A) and BOLD (B) responses to somatosensory stimulation after 7NI and SNP administration.

[Figure 1]

Conclusions: Our present study brings further experimental evidence for the critical role of NO as a mediator of the neurovascular coupling. The fact that exogenously administered NO did not recover the attenuation of the CBF response produced by nNOS inhibition is consistent with the notion that nNOS-derived NO is an obligatory mediator of functional hyperemia in the brain. The differential effects of NO on the BOLD response is suggestive of an influence of NO on the activity of cytochrome oxidase [3], that may change the BOLD x CBF relationship. Further studies are necessary to address the effects of NO on O_2 extraction and metabolism.

References:

[1] Iadecola C, Trends Neurosci 1993, 16(6):206:214.

[2] Stefanovic B. et al., JCBFM 2007, 27:741-754.

[3] Brown CG 2001, Biochim Biophys Acta 1504:46-57.

CEREBROVASCULAR RESERVE AND OXYGEN EXTRACTION FRACTION OF WHITE MATTER HYPERINTENSITIES IN STROKE PATIENTS WITH LARGE ARTERY OCCLUSION

S. Zaidi[1], K. Uchino[1], R. Lin[1], H. Kuwabara[2], D. Sashin[3], Y.-F. Chang[4], M. Hammer[1], V. Reddy[1], T. Jovin[1], N. Vora[5], M. Jumaa[1], L. Massaro[1], J. Billigen[1], H. Yonas[6], E. Nemoto[3]

[1]Neurology, University of Pittsburgh School of Medicine, Pittsburgh, PA, [2]Radiology, Johns Hopkins University School of Medicine, Baltimore, MD, [3]Radiology, [4]Neurosurgery, University of Pittsburgh School of Medicine, Pittsburgh, PA, [5]Neurology and Psychiatry, st. Louis University School of Medicine, St. Louis, MO, [6]Neurosurgery, University of New Mexico Health Sciences Center, Albuquerque, NM, USA

Objectives: Cerebral white matter hyperintensities (WMH) are associated with stroke, stroke risk factors, and dementia and are believed a consequence of hypoperfusion and arteriolar disease. We compared the relationship between cerebrovascular reactivity (CVR) and oxygen extraction fraction (OEF) as a measure of ischemic stress in periventicular and subcortical WMH lesions in stroke patients with large artery occlusive disease.

Methods: Seventeen stroke patients with large artery occlusions were studied by positron emission tomography using $^{15}O_2$ (gas) and $H_2{}^{15}O$ (water) for cerebral blood flow (CBF) and cerebral metabolic rate for oxygen before and after acetazolamide challenge for cerebrovascular reserve (CVR). WMH volumes (cm^3) were quantified by thresholding on coregistered MRI images in subcortical and perventricular zones of each hemisphere. CVR and oxygen extraction fraction (OEF) for WMH volumes were computed and only those with paired CVR and OEF values were used in linear regression analysis.

Results: A significant ($P< 0.0007$) linear inverse relationship between CVR and OEF after acetazolamide was observed for WMH revealing a progressive increase in OEF as CVR decreases reflecting a progressive decrease in CVR with an increase in OEF and ischemic stress (Figure). A negative linear relationship between CBF ($P=0.07$)and CMRO2 ($P=0.02$) and WMH volume suggests that WMH volume is related to reduced CBF, CMRO2 and CVR to increased ischemic stress.

Conclusions: The linear, negative relationship between CVR and OEF suggests that WMH regions vary in their level of ischemic stress which is related to reduced perfusion, metabolism and CVR and do not necessarily represent infarction.

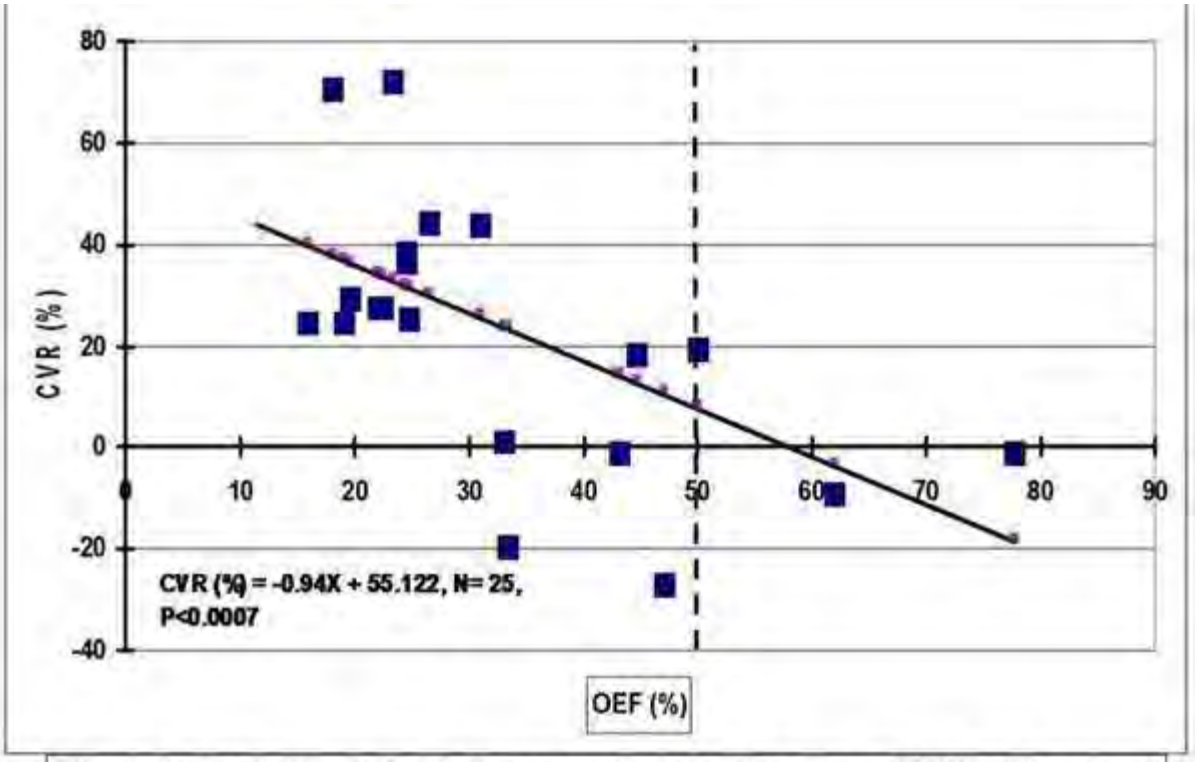

Figure Legend: Correlation between cerebrovascular reserve (CVR) and oxygen extraction fraction (OEF) in white matter hyperintensities reflecting decreasing CVR with increasing ischemic stress.

[WMHFig]

Brain Poster Session: Cerebral Vascular Regulation

CEREBROVASCULAR INSULIN RESISTANCE

P. Katakam[1], F. Domoki[1,2], L. Lenti[1,2], T. Gáspár[1], J. Snipes[1], D. Busija[1]

[1]Physiology and Pharmacology, Wake Forest University Health Sciences, Winston-Salem, NC, USA, [2]Department of Physiology Faculty of Medicine, University of Szeged, Szeged, Hungary

Objectives: Insulin resistance is a major risk factor for cerebrovascular and neurological diseases; however, cerebrovascular actions of insulin have never been studied. We determined the effects of insulin on vasoreactivity of rat cerebral arteries (CA). In addition, we studied the impact of metabolic insulin resistance associated with aging and obesity on vascular insulin sensitivity in young and aged Sprague-Dawley (SD) rats as well as obese (ZO) and lean (ZL) Zucker rats.

Methods: Videomicroscopy measured the intraluminal diameter of isolated cerebral arteries and laser Doppler studies estimated the cerebral blood flow in anesthetized rats. We also determined the mRNA and protein expression with PCR and western blot experiments. We estimated the intracellular calcium, nitric oxide (NO) and reactive oxygen species (ROS) in cultured rat cerebral microvascular endothelial cells (CMVECs) using fluorescence microscopy.

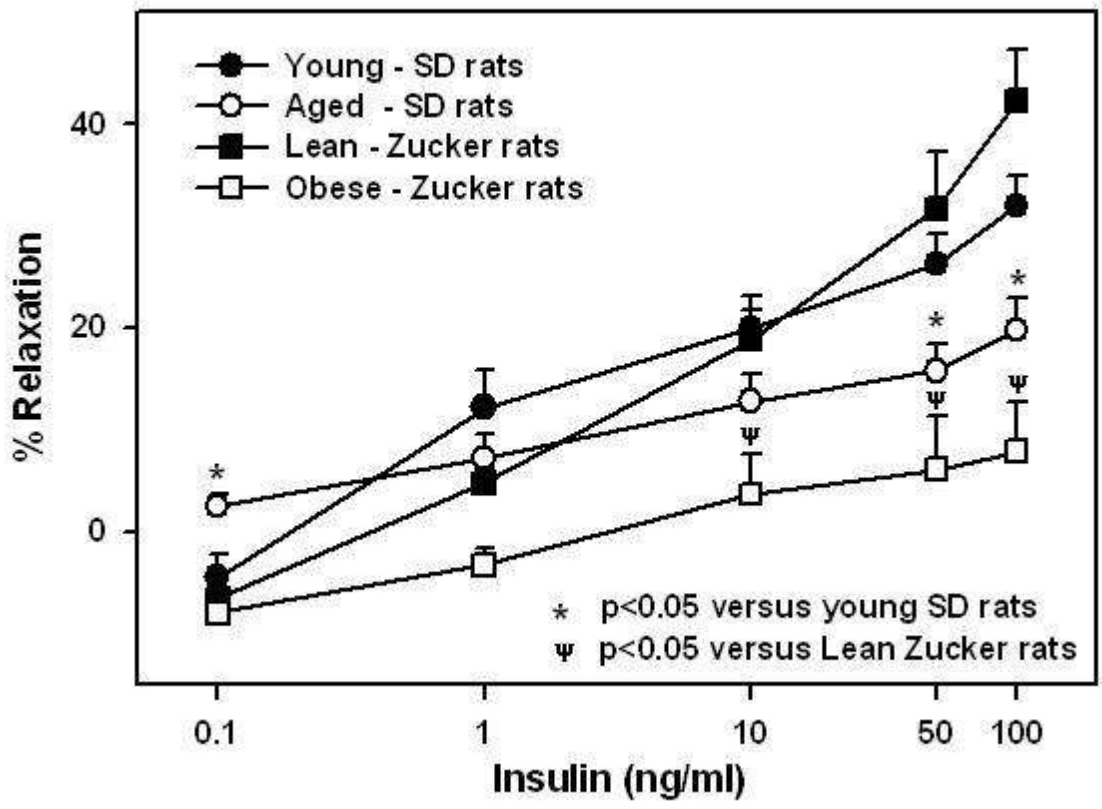

[Cerebrovascular Responses to Insulin]

Results: CA showed a dose-dependent biphasic response to insulin with initial vasoconstriction

followed by vasodilation. Insulin also increased cortical blood flow in vivo. Endothelial denudation abolished vasodilation to insulin. Inhibition of K^+ channels (K_{Ca}, SK_{Ca}, IK_{Ca}, K_{ir}, K_v and K_{ATP}), NO synthase (NOS) and cytochrome P450 (CP450) diminished insulin-induced vasodilation. Scavenging of ROS or inhibition of ROS generation abolished the vasoconstriction to insulin. Inhibition of cyclooxygenase, however, abolished vasoconstriction and enhanced vasodilation to insulin. Inhibition of endothelin-type A receptors enhanced the vasodilation while endothelin type B receptor blockade diminished vasodilation. PCR and immunblot studies identified insulin receptor mRNA and protein in the cerebral arteries. Insulin treatment resulted in phosphorylation of Akt. Fluorescence studies of CMVECs showed that insulin increased intracellular calcium influx; and enhanced generation of NO and ROS. Notably, aged SD rats and ZO rats with insulin resistance exhibited reduced insulin-induced vasodilation compared to controls (young SD rats and ZL rats) . Inhibition of NOS/inducible NOS and inhibition of ROS production or scavenging of ROS improved vasodilation in ZO rats suggesting that increased superoxide production possibly by NOS uncoupling contributed to reduced vasodilation.

Conclusions: For the first time, we identified the insulin receptors in cerebral arteries. Further, insulin induced biphasic cerebrovascular response; vasoconstriction is mediated by ROS, endothelin and vasodilation is mediated by endothelium, K^+ channels, NO and CP450 metabolites. Age and obesity induced metabolic insulin resistance is accompanied by cerebrovascular insulin resistance indicated by diminished vasodilation to insulin. In summary, oxidative stress resulting from enhanced NADPH oxidase activity and NOS uncoupling contribute to vascular insulin resistance and reduced vasoreactivity to insulin.

Support: NIH grants HL-030260, HL-065380, HL-07773.

717

Brain Poster Session: Cerebral Vascular Regulation

DYNAMIC MONITORING OF CEREBRAL COMPLIANCE USING TRANSCRANIAL DOPPLER ULTRASONOGRAPHY

E. Carrera, D.-J. Kim, G. Castellani, C. Zweifel, P. Smielewski, J.D. Pickard, M. Czosnyka

Clinical Neurosciences, Cambridge, Cambridge, UK

Objectives: Recent studies have suggested that the compartmental compliances of the brain may be assessed using MRI. However, no technique is currently available to continuously monitor the compliances of the cerebral arteries or of the CSF compartment. The goals of the present study are:

1. to develop a new computational method for continuous assessment of compartmental compliances using the relationship between the pulsatile components of cerebral arterial blood volume (CaBV), arterial blood pressure (ABP) and intracranial pressure (ICP);
2. to determine the compartmental compliances in normal subjects, in patients with unilateral carotid stenosis and in those with traumatic brain injury (TBI).

Methods: We included 21 normal subjects, 20 patients with unilateral carotid stenosis and 10 with TBI and transient increase in ICP (plateau waves of ICP). All patients had a continuous monitoring of blood flow velocities (using transcranial Doppler) and ABP (noninvasively or directly from the radial artery). ICP was monitored using intraparenchymal microtransducers. Using a mathematical model, we estimated the CaBV extracted from the CBFV waveform. The arterial compliance (Ca) was calculated as the ration between pulse amplitudes of CaBV and ABP of and, in TBI patients, intracranial compliance (Ci) was estimated as the ratio between pulse amplitudes of CaBV and ICP (Ci). Changes in compliances were monitored during hypo and hypercapnia in normal subject and in those with carotid stenosis, and during plateau waves in TBI.

Results: In normal subjects, Ca was significantly lower during hypocapnia ($p< 0.001$), wheras there was only a trend toward a lower Ca during hypercapnia, ($p=0.06$) suggesting that the compliances of cerbral arteries are significantly affected by vasoconstriction but less by vasodilatation induced by CO2 changes. In patients with carotid stenosis, Ca was significantly lower on the stenotic side during normocapnia ($P< 0.001$), hypercapnia ($P< 0.001$) and hypocapnia ($P=0.007$). Furthermore, Ca reactivity reflecting the changes in Ca with changes in CO2 was significantly lower on the stenotic side ($P=0.03$) during reduction of PaCO2. During plateau waves, occurring with concomitant massive vasodilatation, ICP increased ($P=0.001$) but ABP remained constant ($P=0.5$). Similarly, the pulse amplitude of ABP remained constant ($P=0.5$) whereas the pulse amplitudes of ICP and CaBV increased ($P=0.001$) reflected by an increased in Ca ($P=0.001$) and a concomitant decrease in Ci (see Figure).

Conclusion: This method shows that continuous monitoring of changes in brain compartmental compliances may be feasible using monitoring of ABP, CBFV and ICP. In patients with carotid stenosis, Ca and its reactivity to CO2 changes were lower on the affected side whereas, plateau waves induced an increase in Ca coupled with a decrease in Ci.

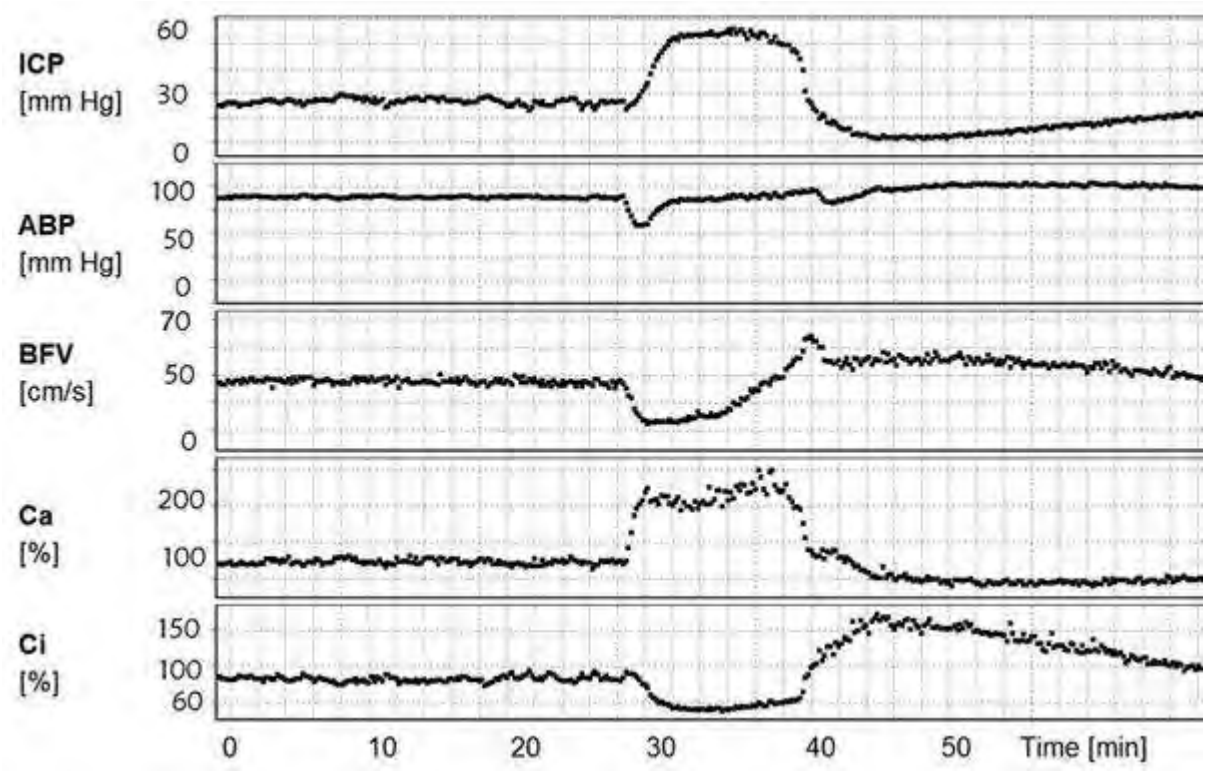

[Figure]

Monitoring of ICP, ABP, BFV, brain arterial (Ca) and intracerebral (Ci) compliances during plateau wave of ICP in a TBI patient.

BrainPET Poster Session: Brain Imaging: MRI/fMRI

FAST BOLUS-TRACKING FUNCTION MAGNETIC RESONANCE IMAGING (FMRI) IN MEDETOMIDINE-SEDATED RATS USING INTRAVASCULAR TRACER

C.W. Blau[1], M. Kelly[1], K.M. Griffin[2], J.F.X. Jones[2], C.M. Kerskens[1]

[1]Trinity College Institute of Neuroscience, Trinity College Dublin, [2]School Medicine and Medical Science, Dublin, Ireland

Objectives: Using a recently described animal model for fMRI (1) that has potential for longitudinal studies, we investigated the feasibility of using a commercial MRI contrast agent to detect neuronal activation. We show that neuronal activation can not only be easily detected using our method, but that information about the hemodynamic response can be gleaned over and above that provided by blood-oxygen level-dependent (BOLD) fMRI.

Methods: MRI Images of rat primary somatosensory cortex were obtained using a 7Tesla Bruker BioSpin scanner with purpose-built transmit and receive coils. T1-weighted images of the coronal slice of interest were acquired using a fast gradient echo sequence (echo time 3.5ms, repetition time 11.0ms, matrix 64x64, 1 average, 120 repetitions, acquisition time 60s). Male Wistar rats (n=4) were placed in the scanner under sedation with a continuous subcutaneous infusion of medetomidine (1) and electrically stimulated using 5ms duration, 5Hz, 3V pulses via electrodes connected to the forepaw, enabling unilateral stimulation of the associated cortical area. Shortly after initiation of stimulation and during acquisition of images, a bolus of meglumine gadopentate was injected via a tail-vein. The resulting images were evaluated using a software script in IDL language, and bolus transit curves calculated for the active and contralateral regions.

Results: The temporal activation pattern of select primary somatosensory cortical neurons was clearly visible on subtraction maps (see figure), and regions of activation selected from these maps showed a significant difference in both signal amplitude and time-to-peak of bolus arrival between activated and contralateral regions ($P < 0.01$, Student's t-test). Second moment is also significantly ($p < 0.05$) greater in the activated region. The outcome of analysis and deconvolution of the signal in the activated region with respect to contralateral control regions will be shown.

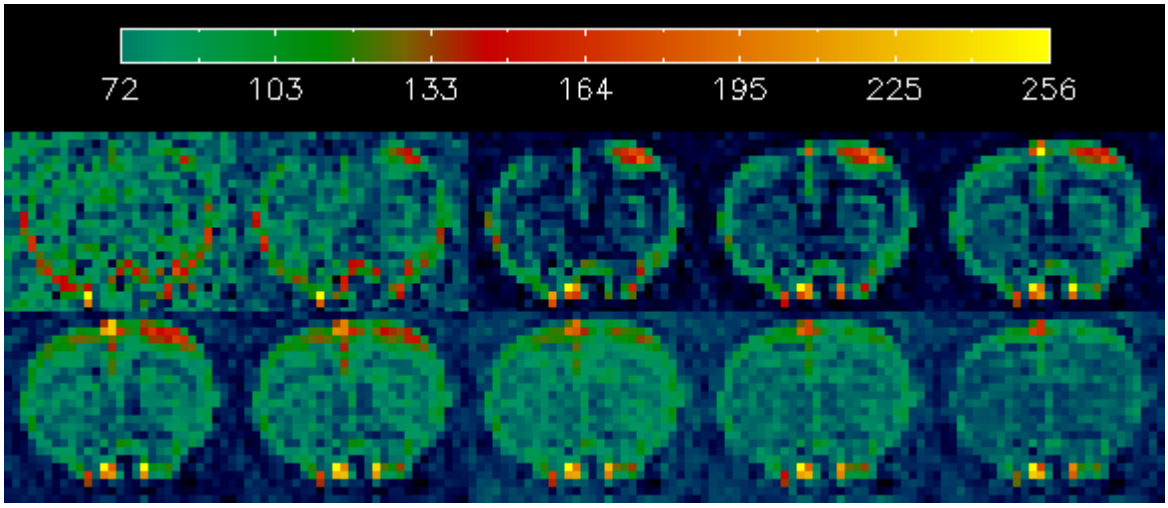

[Figure 1: Time evolution of neuronal activation]

Time evolution of neuronal activation of rat somatosensory cortex; subtraction images from images acquired 500ms apart.

Discussion: First moments of drug passage are generally thought to reflect mean transit time (MTT) through the entire vasculature, whilst the second moment has been hypothesized to represent micro-vascular topology (2) and this has been applied to other animal models to determine microflow heterogeneity (3). Our results show that the activation response causes a measurable increase in both flow rate and heterogeneity, which can be characterized further due to the fine temporal resolution of our method. The method shows promise for longitudinal studies in which changes in activation response could be repeatedly sampled over time. In conclusion, we present a novel method for both visualizing neuronal activation and quantifying the associated vascular response.

References:

(1) Weber et al. 2006, Neuroimage 29(4):1303:10.

(2) Weisskoff et al. 1993 Magn Res Med 29: 553-8.

(3) Tomita el al.2002, J Cereb Bl Fl Metab 22:663-9.

PROSPECTIVE INVESTIGATIONS ON THE SECONDARY DEGENERATION OF CORTICOSPINAL TRACTS IN CERVICAL SPINAL CORD FOLLOWING CEREBRAL INFARCT WITH DIFFUSION TENSOR IMAGING

J. Zeng[1], **Z. liang**[2], Z. Zhang[3], F. Wang[1], L. Li[1], Q. Hou[1]

[1]Department of Neurology and Stroke Centre, Sun Yat-Sen University, Guangzhou, [2]Department of Neurology, Guangxi Medical University, Nanning, [3]Department of Radiology, Sun Yat-Sen University, Guangzhou, China

Objective: To investigate the secondary degeneration of corticospinal tracts in cervical spinal cord following a recently cerebral infarct with diffusion tensor imaging(DTI), as well as its potential impact on neurological recovery.

Methods: 26 patients with a focal cerebral infract at unilateral posterior limb of internal capsule, corona radiata or at brainstem underwent DTI and evaluations with the NIH Stroke Scale (NIHSS), the Fugl-Meyer motor scale (FM) and the barthel index (BI) 3 times at the first week (W1), the fourth (W4) and twelfth week (W12) after stroke onset respectively. 26 gender and age match healthy volunteers underwent DTI three time at same time piots. The DTI parameters of Mean diffusivity (MD) and fractional anisotropy (FA value) were measured at cervical spinal cord and initial lesion (posterior limb of internal capsule, c corona radiata or at brainstem). The comparisons of DTI parameters between patient groud and controls were used t test, and the comprision of DTI parameters of patient group from the three time pionts were used competed data analysis of variance. Spearman correlation analysis was used to assess the association between the absolute value of percent change [((W12 - W1) / W1) × 100%] of FA values and of clinical scores.

Results: Compared to the controls, the FA values of contralateral side corticospinal tracts in cervical spinal cord in patients significantly decreased at every time point repectively($P < 0.01$). In patients group, the FA values of of contralateral side corticospinal tracts in cervical spinal cord decreased progressively from W1 to W12 ($P< 0.01$), but no significant modification of MD was observed. The absolute value of percent reduction of FA value of of contralateral side corticospinal tracts in cervical spinal cord in patients associated negatively with the absolute value of percent change of NIHSS and FM ($P< 0.05$), but not with the absolute value of percent change of BI ($P> 0.05$).

	n	W1	W4	W12
NIHSS	26	13.26±3.03	9.66±2.45	5.25±2.25
Fugl-Meye	26	28.35±2.25	50.25±2.32	73.38±3.55
BI	26	40±6.43	58.18±3.26	75.25±4.75

[Table 1 The clinical scores of patients in the thr]

Conclusions: The secondary degeneration of corticospinal tracts resulted from cerebral infarction

may extend to cervical spinal cord. The secondary degeneration of corticospinal tracts in cervical spinal cord may exist and progress at lest three months, and hamper the process of neurological recovery.

DESIGN, CONSTRUCTION, AND TESTING OF RF COIL AND ANIMAL BODY HOLDER FOR SIMULTANEOUS PET/MRI IMAGING OF RAT BRAIN

L.A. Lopas, J.M. Moirano, K.N. Kurpad, S.A. Hurley, A.K. Converse

University of Wisconsin-Madison, Madison, WI, USA

Background and aims: Recent advances in technology have allowed for simultaneous Positron Emission Tomography (PET) and Magnetic Resonance Imaging (MRI) experiments. Our goal is to compare and validate several different techniques for measuring quantitative regional cerebral blood flow (rCBF) using a simultaneous PET/MRI system in rats. This synthesis of existing technologies raises new pragmatic concerns. Due to space limitations we could not use a standard animal RF coil and head holder. Using an eight section birdcage RF coil schema, we constructed a system that integrates into the RF coil the necessary PET requirements and a stereotactic device that will reliably and repeatably position the rat brain with respect to the PET insert.

Methods: The RF coil is made of acrylic tubing, 51mm OD, 44mm ID, and 56 mm in length. Blunt and tapered 6mm threaded rods serve as ear bars. 19mm slots were cut into the coil allowing a U-shaped tooth bar holder to be fixed in place. A 17 mm wide tooth bar adjusts to fit the subject and can be locked in place by a screw at the bottom of the U of the tooth bar holder. In an effort to limit positron annihilation photon attenuation caused by the RF coil, minimal material was used throughout construction.

Because the position sensitive avalanche photodiodes (PSAPD) of the PET insert need to be kept at -10°C for optimal performance, we designed an insulated body holder to keep the subject at 37°C. To accomplish this, the body holder will shield the subject from the cooling system for the PSAPD while allowing for warm air to be blown on the subject. The body holder will be comprised of two half-cylinders that can be securely fitted together during the scan. This design allows for easy set up and positioning of the subject and the lines running to and from the subject.

Results: Initial scans were performed on a 4.7T (300 MHz) Varian MRI scanner (Palo Alto, CA). A 33mm diameter 30mL cylindrical saline phantom was scanned to demonstrate good coil uniformity and signal to noise ratio. In vivo scans of a rat brain were performed and uniformity was verified using a flip angle calibration method. From these results, we expect the RF coil to provide good coverage of the rat brain and accurate quantitative imaging results.

Conclusion: We have constructed an integrated RF coil/head stereotactic device and are working on a body holder that meets the unique requirements of simultaneous PET/MRI studies. Phantom scans have demonstrated the reliability and effectiveness of our design. Future work will include incorporation of PET/MRI fiducials and heating of the subject.

Brain Oral Session: Experimental Cerebral Ischemia: Neuroprotection

BEYOND POST-STROKE DEPRESSION: EFFECTS OF DELAYED CIPRAMIL TREATMENT ON SECONDARY EXOFOCAL POSTISCHEMIC DEGENERATION AND LONG-TERM STROKE OUTCOME

G. Kronenberg[1,2,3], M. Balkaya[1,2], V. Prinz[1,2], K. Gertz[1,2], S. Ji[1,2], H. Hoertnagl[4], C. Waebert[5], R. Stumm[6], **M. Endres**[1]

[1]Neurology, [2]Center for Stroke Research Berlin, [3]Dept Psychiatry Campus Benjamin Franklin, [4]Institute of Pharmacology and Toxicology, Charite - Universitaetsmedizin Berlin, Berlin, Germany, [5]Stroke and Neurovascular Regulation Laboratory, Massachusetss General Hospital/Harvard Medical School, Charlestown, MA, USA, [6]Institute of Pharmacology and Toxicology, Otto-v.-Guericke University, Magdeburg, Germany

Objectives: Post-stroke depression (PSD) is the most frequent neuro-psychiatric complication of stroke, affecting up to 50% of stroke survivors. Moreover, PSD has severe adverse effects on functional recovery and on longer-term survival. Despite its great clinical and therapeutic relevance, PSD remains underresearched. This may be partly due to the fact that suitable animal models are lacking and existing models are poorly characterized. Here, we set out to validate our well-defined stroke paradigm of 30 min middle cerebral artery occlusion (MCAo) in the mouse as a potential model to study pathogenetic mechanisms underlying the development of PSD and how these are impacted by psychopharmacotherapy.

Methods: 129/SV mice were subjected to either sham operation or MCAo/reperfusion. A subset of animals was treated with selective serotonin reuptake inhibitor (SSRI) citalopram starting seven days after induction of stroke. Behavioral assessment was begun at 14 weeks after MCAo and included sucrose consumption, spontaneous locomotor activity, the novelty-suppressed feeding paradigm, the elevated plus maze, the light-dark box as well as Porsolt's test. Animals were killed at 16 weeks after MCAo and brains harvested for further histological and biochemical evaluation. The primary lesion was delineated using NeuN staining. Accumulation of microglia in the ischemic striatum was quantified using activated microglia marker Iba1. The integrity of the mesolimbic dopaminergic pathway was probed using tyrosine hydroxylase (TH) immunohistochemistry and in situ hybridization. Dopamine levels were measured with HPLC. Striatal dopamine transporter density was examined using autoradiography.

Results: Following left-sided MCAo, animals reproducibly developed an 'affective' phenotype characterized by anhedonia, increased anxiety and despair. By contrast, right-sided MCAo was not associated with a depression-related phenotype but resulted in hyperactivity. Subacute citalopram administration reversed the behavioral alterations of left MCAo confirming pharmacological treatment validity of our model. Across groups (left MCAo, sham, treatment with either vehicle or citalopram) we observed a significant negative correlation between striatal dopamine levels and the latency to feed in the novelty-suppressed feeding test. Similarly, striatal dopamine levels showed a strong positive correlation with time in the lit compartment of the light-dark box and with the latency to float in Porsolt's test. MCAo caused significantly reduced dopamine and dopamine transporter levels in ischemic striatum in parallel with a reduced number of TH+ neurons in the ipsilateral midbrain. Delayed citalopram treatment largely attenuated all of these effects. Moreover, citalopram treatment reduced the size of the primary lesion along with the number of activated microglia in the ischemic striatum.

Conclusions: We here describe a reliable experimental model of post stroke depression. Our results highlight the significance of the mesolimbic dopaminergic pathway for the development of affective stigmata in this paradigm. Subacute treatment with SSRI citalopram not only reversed depressive behaviors, but also reduced the size of the primary ischemic lesion and prevented secondary exofocal

postischemic degeneration of midbrain dopaminergic neurons. Neuroprotection against secondary neuronal injury mechanisms may also underlie the clinical benefits of antidepressant therapy after stroke regarding both functional recovery and survival.

Brain Poster Session: Oxidative Mechanisms

IMPORTANT ROLE OF NADPH OXIDASE IN STRIATAL NEURONAL INJURY AFTER SEVERE TRANSIENT GLOBAL ISCHEMIA IN MICE

H. Yoshioka[1,2], K. Niizuma[1], M. Katsu[1], N. Okami[1], G.S. Kim[1], P. Narasimhan[1], H. Kinouchi[2], P.H. Chan[1]

[1]Neurosurgery, Stanford University School of Medicine, Stanford, CA, USA, [2]Neurosurgery, University of Yamanashi, Chuou, Japan

Objectives: Reactive oxygen species (ROS) have been implicated in neuronal injury after cerebral ischemia.[1] NADPH oxidase has been well characterized in immune cells to produce mainly ROS as superoxide radicals for host defense. The oxidase is a complex enzyme that consists of the membrane subunit cytochrome b_{558} ($gp91^{phox}$ and $p22^{phox}$) and multiple cytosolic subunits ($p47^{phox}$, $p67^{phox}$, $p40^{phox}$, and Rac-1). Upon stimulation, the cytosolic subunits migrate to the plasma membrane, whereby a functional complex generating ROS is formed. Recent studies suggest that NADPH oxidase can serve as a major source of ROS in the central nervous system[2,3]; however, the roles of NADPH oxidase in neuronal death after transient global cerebral ischemia (tGCI) are not well understood. We hypothesized that oxidative stress generated by NADPH oxidase in ischemic brain cells could lead to neurovascular injury. The purpose of the present study is to test this hypothesis in a newly developed model of tGCI in mice.

Methods: $Gp91^{phox}$-/- (gp91 KO) mice with a C57BL/6 background and their respective wild-type (Wt) littermates were subjected to tGCI by bilateral common carotid artery occlusion (BCCAO) for 22 min (we chose this timing because preliminary studies have shown reproducible striatal damage without high mortality). Ischemic neuronal injury was evaluated in the striatum 3 days after ischemia by cresyl violet staining. Western blot analyses of samples from the striatum were performed to investigate the expression and translocation of NADPH oxidase subunits. Localization of NADPH oxidase was examined by double immunofluorescence. For the detection of oxidative protein damage after ischemia, the carbonyl groups introduced into proteins were measured.

Results: Striatal neurons of the Wt mice 3 days after 22 min of BCCAO showed severe damage with high reproducibility in this model. Western blot analysis showed the upregulation of $gp91^{phox}$ and an increase in the cytosolic subunits ($p47^{phox}$, $p67^{phox}$, Rac-1) in the membrane fraction after ischemia. A double immunofluorescent study revealed that $p67^{phox}$-positive cells colocalized with neuron-specific nuclear protein or lectin-positive cells in the striatum, suggesting NADPH oxidase expressed in neurons and vascular endothelial cells. The carbonyl groups introduced into proteins by oxidative stress increased after ischemia in the Wt mice, and this increase was suppressed in the gp91 KO mice. Furthermore, striatal neuronal injury was significantly reduced in the gp91 KO mice compared with the Wt mice.

Conclusions: These results suggest an important role for NADPH oxidase in ROS production and striatal neuronal death after severe transient forebrain ischemia. We propose that NADPH oxidase is a therapeutic target for neurovascular damage in ischemic stroke.

References:

1. Chan PH. Reactive oxygen radicals in signaling and damage in the ischemic brain. J Cereb Blood Flow Metab. 2001; 21:2-14.

2. Infanger DW, Sharma RV, Davisson RL. NADPH oxidases of the brain: Distribution, regulation, and function. Antioxid Redox Signal. 2006; 8: 1583-1596.

3. Sun GY, Horrocks LA, Farooqui AA. The roles of NADPH oxidase and phospholipases A_2 in oxidative and inflammatory responses in neurodegenerative diseases. J Neurochem. 2007; 103: 1-16.

725

Brain Oral Session: Neonatal Ischemia

COMPARISON OF INDEPENDENT TECHNIQUES FOR MEASURING CEREBRAL VENOUS OXYGENATION IN NEONATES

K.M. Tichauer[1], J.T. Elliott[1,2], J.A. Hadway[1,3], T.-Y. Lee[1,2,3], K. St. Lawrence[1,2]

[1]Imaging Division, Lawson Health Research Institute, [2]Medical Biophysics, University of Western Ontario, [3]Imaging Research Laboratories, Robarts Research Institute, London, ON, Canada

Objectives: Measurement of the cerebral metabolic rate of oxygen ($CMRO_2$) by near-infrared spectroscopy (NIRS) requires knowledge of cerebral venous oxygenation. In previous studies from our group, venous oxygenation was calculated from the cerebral concentration of deoxy-hemoglobin (HHb) and assuming the cerebral blood volume (CBV) is comprised of 25% arterial blood and 75% venous blood [1]. However, a study in sick children suggested that the arterial-to-venous ratio varies substantially from patient to patient [2]. The purpose of the present study was to compare our HHb technique of measuring cerebral venous oxygenation with two alternate NIRS techniques - the partial venous occlusion [3] and head tilt [4] methods - that do not rely on assumptions of blood compartment ratios. Measurements were obtained over a range of arterial blood oxygenation levels in piglets and cerebral venous blood samples were collected for gold standard measurements of cerebral venous oxygenation.

Methods: Experiments were conducted on piglets (< 1 week) that were anesthetized with isoflurane. Cannulae were inserted through a burr hole in the skull into the superior sagittal sinus and into an ear vein for administration of the NIRS contrast agent, indocyanine green. Following surgery, cerebral venous oxygenation was measured using the three independent NIRS techniques at fraction of inspired oxygen levels of 50%, 21%, and 10%. The HHb technique relied on normalizing the NIRS measurement of HHb by the CBV, which is determined using an indicator-dye dilution method [1]. The second and third techniques required measuring changes in cerebral blood oxygenation following either partial venous occlusion of the jugular veins or a 15° negative head tilt - actions that resulted in cerebral oxygenation changes from only the venous compartment.

Results: Data were collected from nine piglets (5 males, 4 females: 2.8 ± 1.1 days, 1.8 ± 0.1 kg) over a sagittal sinus oxygenation range of 12-90%. Similar statistically significant correlations ($p < 0.05$) were observed for all three NIRS calculations of venous oxygenation compared to corresponding superior sagittal sinus blood oxygenation ($R^2 = 0.71$, slope = 1.01 for the HHb technique; $R^2 = 0.77$, slope = 0.74 for the partial venous occlusion technique; and $R^2 = 0.72$, slope = 0.82 for the head tilt technique).

Conclusions: The statistically significant correlations between all NIRS techniques and the gold standard suggest that each technique could be used interchangeably for measuring $CMRO_2$. The agreement between the techniques also suggests that the assumed 25:75 ratio of arterial-to-venous blood used by the HHb technique is reasonable in the newborn piglet; however, the partial venous occlusion and head tilt techniques have the advantage of not relying on this assumption, which could be beneficial to clinical studies. The advantage with the HHb technique is that it does not require any manipulation of the patient and, as such, might be associated with a higher success rate. Future clinical studies are needed to assess this assertion.

References:

1. Brown, D.W. Pediatr Res, 2003;54(6):861-7.

2. Watzman, H.M. Anesthesiology, 2000;93(4):947-53.

3. Yoxall, C.W. Pediatr Res, 1995;38(3):319-23.

4. Skov, L. Pediatr Res, 1993;33(1):52-5.

INCREASED CEREBRAL OXYGEN METABOLISM WITH METABOLIC SYNDROME ASSOCIATED RISK FACTORS

K. Uchino[1], R. Lin[1], S. Zaidi[1], H. Kuwabara[2], D. Sashin[3], Y.-F. Chang[4], M. Hammer[1], V. Reddy[1], T. Jovin[1], N. Vora[5], M. Jumaa[1], L. Massaro[1], J. Billigen[1], H. Yonas[6], E. Nemoto[3]

[1]Neurology, University of Pittsburgh School of Medicine, Pittsburgh, PA, [2]Radiology, Johns Hopkins University School of Medicine, Baltimore, MD, [3]Radiology, [4]Neurosurgery, University of Pittsburgh School of Medicine, Pittsburgh, PA, [5]Neurology and Psychiatry, St. Louis University School of Medicine, St. Louis, MO, [6]Neurosurgery, University of New Mexico Health Sciences Center, Albuquerque, NM, USA

Objectives: The constellation of cardiovascular risk factors including hypertension, diabetes, obesity and dyslipidemia are metabolic syndrome (MetS) associated risk factors for cardiovascular disease and stroke which may also affect cerebral blood flow (CBF), vascular reactivity and oxygen metabolism ($CMRO_2$).

Methods: Volunteers (n=15) free of vascular disease 59 ± 15 (mean ± SD) years of age were studied by quantitative positron emission tomography (PET) CBF, $CMRO_2$ and oxygen extraction fraction (OEF) before and after acetazolamide (15 mg/kg, i.v.). Magnetic resonance angiography of the brain and neck excluded subclinical cerebrovascular disease and MRI coregistration was used to define the entire hemispheric middle cerebral artery territories. Subjects with one or more of MetS risk factors or medicated were classified with MetS risk factors. Increased OEF threshold was set at 50% based on previous studies.

Results: Eight of ten subjects with MetS risk factors had OEF >50%. None of the five without risk factors had OEF >50%. The presence of MetS risk factors was highly correlated with OEF >50% by Fisher's exact test ($p< 0.007$). The increase in OEF was significantly ($P< 0.001$) correlated with $CMRO_2$ (Figure). Increased OEF was not associated with compromised acetazolamide cerebrovascular reactivity.

Discussion: Although the subjects with OEF >50% did not meet strict MetS criteria, the absence of high OEF in those without these risk factors reinforces the significance of this association. The observation of increased OEF and $CMRO_2$ with normal or even exaggerated CVR provides interesting insights into the mechanisms of MetS associated risk factors as they relate to stroke risk.

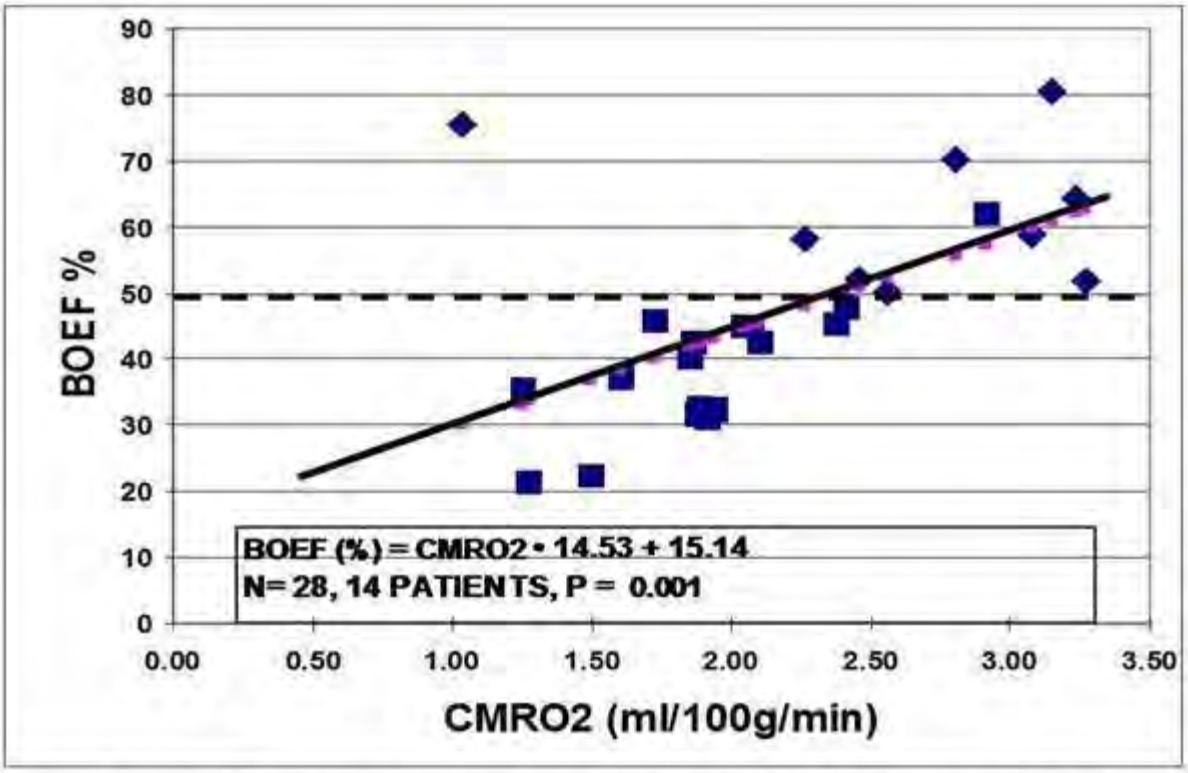

Figure. Baseline OEF and CMRO2 in 14 subjects. One subject with MetS risk factors not included had CMRO2 of 8-9 ml/100g/min and OEF of 56% and 62%. Triangles = subjects with MetS risk factors.

[MetSfig]

ASTROCYTE SURVIVAL TO ISCHEMIC DAMAGE REQUIRES AN INTACT MTOR/S6 KINASE PATHWAY

M.D. Pastor, N. Fradejas, P. Tranque, S. Calvo

School of Medicine University Castilla-La Macha Spain, Albacete, Spain

Astrocytes functions are crucial for CNS homeostasis, as they provide trophic, metabolic and antioxidant supports to neurons and play protective functions during brain damage (Li et al.2008). In order to identify genes involved in the astrocyte response to ischemia, we performed mRNA differential display using astrocytes subjected to oxygen and glucose deprivation (OGD). We detected a robust downregulation of S6 kinase 1 (S6K1) mRNA that was accompanied by a sharp decrease in protein level and activity. The main goal of this work was thus to analyze the functions of this kinase during brain ischemia.

Methods: To carry out this objective we used both in vitro and in vivo models of ischemia and S6K deficient mice. Cell viability and ROS production were measured by flow cytometry. Quantitative RT-PCR, Western blot and immunoprecipitation were used to analyze the expression levels of S6K and several pro- or antiapototic factors.

Results: Our data indicate that S6K protects astrocytes against in vitro ischemia, since OGD-induced apoptosis was increased by the combined deletion of S6K1 and S6K2 genes. Moreover, treatment with rapamycin, that inhibits S6K activity by acting on its upstream regulator mTOR, also incremented astrocyte injury caused by OGD. Among the mechanisms potentially involved in the increased damage observed in S6K-/- astrocytes, we have observed a defect in BAD inactivation by phosphorylation at its Ser136. In addition, the expression of the anti-apoptotic factors Bcl-2 and Bcl-xL was significantly decreased in astrocytes lacking S6K, suggesting that this kinase is involved in maintaining the balance between pro- and antiapoptotic factors under stress conditions. Besides, ischemia-induced reactive oxygen species accumulation was much more prominent in S6K-/- astrocytes while pretreatment with the antioxidant N-acetyl-L-cysteyne completely abrogated OGD-induced S6K-/- astrocyte death, suggesting that S6K regulates oxidative metabolism. Finally, when the effects of S6K on in vivo ischemia were analyzed following permanent middle cerebral artery occlusion, we observed that both, infarct volume and mice mortality were increased in S6K-/- mice. In summary, our results indicate that S6K confers protection against ischemia through the regulation of astrocyte ROS and pro- and antiapoptotic factors.

Reference: Li, L., A. Lundkvist, D. Andersson, U. Wilhelmsson, N. Nagai, A. C. Pardo, C. Nodin, A. Stahlberg, K. Aprico, K. Larsson, T. Yabe, L. Moons, A. Fotheringham, I. Davies, P. Carmeliet, J. P. Schwartz, M. Pekna, M. Kubista, F. Blomstrand, N. Maragakis, M. Nilsson, and M. Pekny. 2008. Protective role of reactive astrocytes in brain ischemia. J.Cereb.Blood Flow Metab 28:468-481.

DIPYRIDAMOLE CONFERS PROTECTION IN ACUTE FOCAL CEREBRAL ISCHEMIA IN THE RAT

L. Garcia-Bonilla, V. Sosti, M. Hernandez-Guillamon, A. Rosell, J. Montaner

Neurovascular Research Laboratory, Institut de Recerca Vall d'Hebron, Barcelona, Spain

Dipyridamole (DP) is a platelet inhibitor that has been previously shown to have antithrombotic benefit in the prevention of stroke, particularly when combined with low dose of aspirin. Recent experimental studies have reported as well that pre-treatment with DP promotes anti-inflammatory, antioxidative and neuroprotective effects in cerebral ischemia. We aimed to determine whether post-treatment with DP, an experimental paradigm more close to clinical stroke therapy, can also exert neuroprotection. Male Sprague-Dawley rats (n=48) were anesthetized with isoflurane and subjected to 120 min (group 1) or 90 min (group 2) of transient middle cerebral artery occlusion (MCAo). Reperfusion was allowed during the 24h or 48h follow-up (group 1 and 2, respectively). Animals were treated at the onset of reperfusion with either i.v. DP (100 mg/Kg) or vehicle. Rats in group 2 also received vehicle or DP dose (60 mg/Kg) orally at 24h and 36h after MCAo. DP was detected by fluorospectrometry 40 min after administration in treated rats (190 ±30 microg/mL, mean ± SE). The concentrations found in plasma (1.52 ±0.44 microg/mL, mean ± SE) and in the ischemic rat brain homogenates (2.34 ±0.30 microg/mL, mean ± SE) after 24h were higher than the DP effective concentration (1 microg/mL). Primary endpoints were infarct volume, evaluated using 2,3,5-triphenyltetrazolium chloride staining, and neurological outcome measured at 60 min, 24h and 48h following MCAo. DP treated animals subjected to 120 min MCAo showed a significantly neurological improvement at 24h when compared with neurological score after 60 min of occlusion (p= 0.0006). A slight non-significant trend in the infarct size was observed compared to the vehicle-treated group (24.5% vs. 29.19%, p=0.6282). However, when a shorter period of ischemia (90 min) and a long-lasting DP treatment were conducted, a significant reduction in the infarct volume was observed (7.9% vs. 24.4%, p= 0.0381). That was accompanied with a significant improvement in the neurological score (p=0.0065). DP protects from ischemic injury when given after MCA occlusion, suggesting that development of new acute therapies based on or combined with DP treatment might be beneficial for stroke patients.

Brain Oral Session: Traumatic Brain Injury: Metabolism

DIFFUSE OPTICAL MONITORING OF CEREBRAL HEMODYNAMICS IN PIGLET WITH TRAUMATIC BRAIN INJURY

C. Zhou[1], S.A. Eucker[2], T. Durduran[1,3], G. Yu[1,4], J. Ralston[2], S.H. Friess[2], R.N. Ichord[5], S.S. Margulies[2], **A.G. Yodh**[1]

[1]Physics and Astronomy, [2]Bioengineering, [3]Radiology, University of Pennsylvania, Philadelphia, PA, [4]Wenner-Gren Research Lab, Center for Biomedical Engineering, University of Kentucky, Lexington, KY, [5]Neurology, Children's Hospital of Philadelphia, Philadelphia, PA, USA

Objectives: Traumatic brain injury (TBI) is a leading cause of childhood morbidity and mortality in the United States, with an annual rate of approximately 200 per 100,000 children requiring hospitalization [1]. An understanding of the conditions of oxygen supply and consumption, and measurement of blood flow after traumatic brain injury is therefore important for clinical applications. In this study, we explored the feasibility of two diffuse optical techniques, diffuse reflectance spectroscopy (DRS, [2, 3]) and diffuse correlation spectroscopy (DCS, [4, 5]), for continuous, non-invasive measurement of cerebral blood flow and blood oxygenation through the intact scalp and skull in a newborn piglet traumatic brain injury model [6] at the bedside.

Methods: Eighteen anesthetized 3-5 day old female piglets (n = 18) were used for the study. Cerebral hemodynamic changes, including relative oxy-, deoxy- and total hemoglobin concentrations ($rHbO_2$, rHb and rTHC respectively), blood oxygen saturation (StO_2) and relative cerebral blood flow (rCBF), were quantified using DRS and DCS continuously and non-invasively before injury and up to 6 hours after the injury. Fluorescent microspheres (FM) were used to validate against rCBF measurements with DCS at discrete time points.

Results: A strong linear correlation was observed between the rCBF measurements with DCS and FM techniques ($R = 0.89$, $p < 0.00001$). Compared to pre-injury levels, rHb, $rHbO_2$ and rTHC increased 67 ±13% ($p = 0.0006$), 24 ±13% ($p = 0.1$) and 41 ±11% ($p = 0.005$) respectively immediately after injury and continued increasing over the next six hours (Figure 1A-C). StO_2 dropped significantly immediately post-injury (52 ±3%, $p = 0.02$), maintained this reduction at 30 minutes post-injury (54 ±2%, $p = 0.009$), but gradually normalized to pre-injury levels (Figure 1D). rCBF decreased significantly to 50 ±6% of pre-injury level ($p = 0.00003$) immediately after injury and continued at that level over the six hours (Figure 1E). Diffuse optical techniques were robust for the entire six hours measured after injury, were sensitive to spontaneous, transient physiological events, such as apnea, cardiac arrest and hypertonic saline infusion and were consistent with vital physiological recordings, including mean arterial blood pressure, arterial oxygen saturation and heart rate.

Conclusions: The investigation corroborates potential of the optical methods for bedside monitoring of pediatric and adult human patients in the neuro-intensive care unit.

References:

[1] Fisher MD (1997) Crit Care Nurs Q 20:36-51.

[2] Villringer A, Chance B (1997) Trends Neurosci 20:435-442.

[3] Gibson AP, Hebden JC, Arridge SR (2005) Phys Med Biol 50:R1-R43.

[4] Boas DA, Campbell LE, Yodh AG (1995) Phys Rev Lett 75:1855-1858.

[5] Boas DA, Yodh AG (1997) J Opt Soc Am A-Opt Image Sci Vis 14:192-215.

[6] Raghupathi R, Margulies SS (2002) J Neurotrauma 19:843-853.

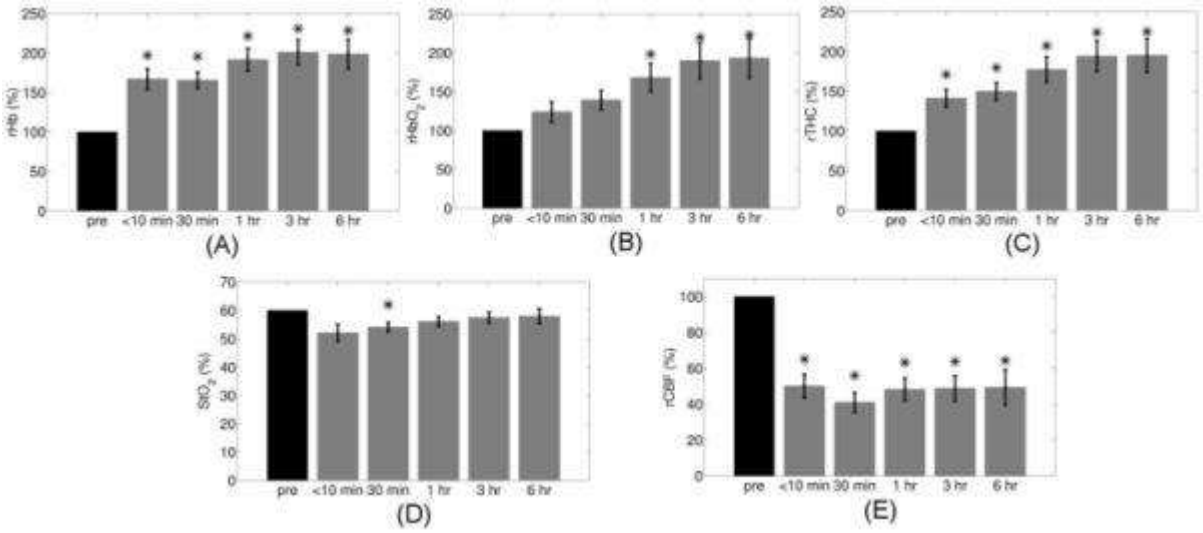

[Figure 1. Average injury effects.]

Brain Poster Session: Oxidative Mechanisms

MEASUREMENTS OF GLIAL METABOLIC FLUXES WITH ^{11}C-ACETATE USING POSITRON EMISSION AND AN ADAPTED NMR-BASED METABOLIC MODELING APPROACH

B. Lanz[1], M.T. Wyss[2,3], B. Weber[2,3], A. Buck[2], R. Gruetter[1,4,5]

[1]Laboratory of Functional and Metabolic Imaging, Ecole Polytechnique Fédérale de Lausanne, Lausanne, [2]PET Center, Division of Nuclear Medicine, University Hospital Zurich, [3]Institute of Pharmacology and Toxicology, University of Zurich, Zurich, [4]Department of Radiology, University of Lausanne, Lausanne, [5]Department of Radiology, University of Geneva, Geneva, Switzerland

Objectives: Acetate brain metabolism has the particularity to occur specifically in glial cells. Labeling studies, using acetate labeled either with ^{13}C (NMR) or ^{11}C (PET), are governed by the same biochemical reactions and thus follow the same mathematical principles. In this study, the objective was to adapt an NMR acetate brain metabolism model to analyse [1-^{11}C]acetate infusion in rats.

Methods: Brain acetate infusion experiments were modeled using a two-compartment model approach used in NMR[1,2,3]. The [1-^{11}C]acetate labeling study was done using a beta scintillator[4]. The measured radioactive signal represents the time evolution of the sum of all labeled metabolites in the brain. Using a coincidence counter in parallel, an arterial input curve was measured. The ^{11}C at position C-1 of acetate is metabolized in the first turn of the TCA cycle to the position 5 of glutamate (fig.1a). Through the neurotransmission process, it is further transported to the position 5 of glutamine and the position 5 of neuronal glutamate. After the second turn of the TCA cycle, tracer from [1-^{11}C]acetate (and also a part from glial [5-^{11}C]glutamate) is transferred to glial [1-^{11}C]glutamate and further to [1-^{11}C]glutamine and neuronal glutamate through the neurotransmission cycle.

Results: The standard acetate two-pool PET model describes the system by a plasma pool and a tissue pool linked by rate constants. Experimental data are not fully described with only one tissue compartment (fig.1b).The modified NMR model was fitted successfully to tissue time-activity curves from 6 single animals, by varying the glial mitochondrial fluxes and the neurotransmission flux Vnt.

A glial composite rate constant $Kgt^g=Vgt^g/[Ace]_{plasma}$ was extracted. Considering an average acetate concentration in plasma of 1 μmol/g[5] and the negligible additional amount injected, we found an average $Vgt^g=0.08\pm0.02$ (n=6), in agreement with previous NMR measurements[1].

The tissue time-activity curve is dominated by glial glutamate and later by glutamine (fig.1b). Labeling of neuronal pools has a low influence, at least for the 20 minutes of beta-probe acquisition. Based on the high diffusivity of CO_2 across the blood-brain barrier, $^{11}CO_2$ is not predominant in the total tissue curve, even if the brain CO_2 pool is big compared with other metabolites, due to its strong dilution through unlabeled CO_2 from neuronal metabolism and diffusion from plasma.

Conclusion: The two-compartment model presented here is also able to fit data of positron emission experiments and to extract specific glial metabolic fluxes. ^{11}C-labeled acetate presents an alternative for faster measurements of glial oxidative metabolism compared to NMR, potentially applicable to human PET imaging. However, to quantify the relative value of the TCA cycle flux compared to the transmitochondrial flux, the chemical sensitivity of NMR is required. PET and NMR are thus complementary.

References:

1. R.A.de Graaf, etal.,NMR.Biomed.16:339(2003).

2. R.Gruetter, etal.,Am.J.Physiol.Endocrinol.Metab.281:100(2001).

3. K.Uffmann, etal.,J.Neurosci.Res.85(13):3304(2007).

4. M.T.Wyss etal.,J.Cereb.Blood Flow Metab.29:44(2009).

5. N.Cetin, etal.,Neurochem.Int.5:359(2003).

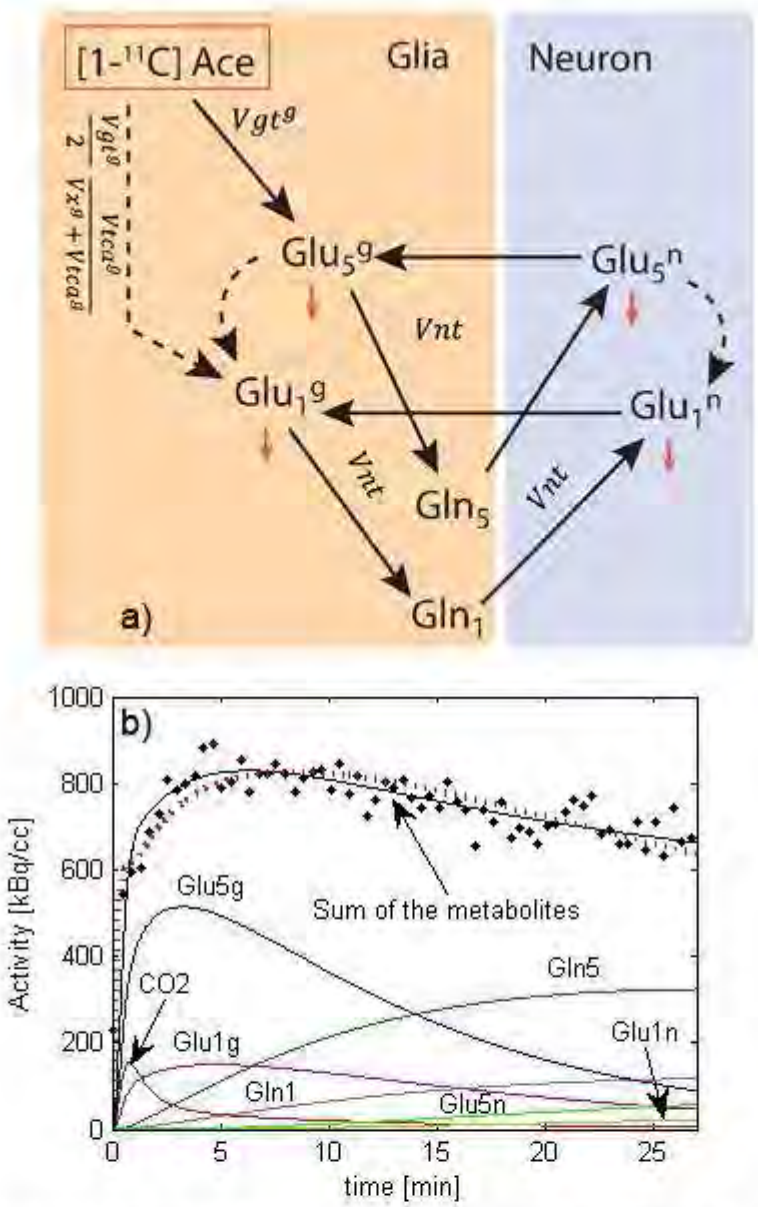

Fig.1: a) Brain metabolic model used for [1-^{11}C]acetate infusion experiment. A similar model [2] was used for ^{13}C NMR studies following [2-^{13}C]acetate infusion, with adapted label positions (i.e. glutamate and glutamine C4 followed by C3). The dotted arrows show the fluxes taking place in the second turn of the TCA cycle. The orange arrows show the loss of label into CO_2.

b) Typical fit of beta-probe data to the sum of the metabolites described in the model of figure1 a). The colored lines show the respective contribution of each metabolite to the total measured radioactivity. The red dotted line represents the fit with a standard two-pool model.

[Figure 1]

731

Brain Poster Session: Experimental Cerebral Ischemia: In Vitro

CELL TYPE SPECIFIC EFFECTS OF EXCITOTOXIC INSULT AND ENERGY LIMITATION ON CULTURED HIPPOCAMPAL NEURONS AND ASTROCYTES

S. Kahlert, **G. Reiser**

Institut für Neurobiochemie, Medizinische Fakultät, Otto-von-Guericke Universität, Magdeburg, Germany

Objectives: A characteristic of acute neurodegeneration after stroke is the massive increase in extracellular glutamate concentration. The ATP level gradually recovers with increasing distance from the core. In the penumbra, the region surrounding the core, the cellular energy is reduced due to reduced oxygen and glucose supply and increased extracellular glutamate concentration. The aim of the present study was to elucidate the question why neurons are much more affected by such adverse situations than the neighboring astrocytes.

Methods: To understand the mechanism of selective vulnerability of neurons we made a direct side by side comparison of rat hippocampal astrocytes and neurons in culture. We measured cytosolic Ca^{2+}, mitochondrial potential, ROS generation, cytosolic ATP and NADH level (1,2). The cells, which were observed during kinetic measurements, were localized after immunofluorescence staining with NeuN and GFAP for a unequivocal identification of the cell types.

Results: Glutamate triggers massive Ca^{2+} influx in both neurons and astrocytes. Maximal Ca^{2+} loads were 5 to 6 times above basal level. However, both cell types could significantly remove the glutamate - triggered cytosolic Ca^{2+} load in the prolonged presence of glutamate. The Ca^{2+} response pattern was dramatically changed, when mitochondrial inhibitors were applied in combination with glutamate. Astrocyte-specific mechanisms are responsible for Ca^{2+} removal, which are largely not dependent on the mitochondrial polarization. Continuous detection of the MgGreen fluorescence allows an analysis of the kinetics of ATP changes. in neurons the application of glutamate induced a strong increase in MgGreen fluorescence, indicating a significant ATP decline. In neurons, removal of Ca^{2+} is linked to an increase of cytosolic Mg^{2+}, released from Mg-ATP complex and mitochondrial activation, characterized by enhanced mitochondrial polarization and ROS generation. ROS increase was not due to inhibition of the respiratory chain, as NADH did not accumulate. Co-application of mitochondrial inhibitors of complex I or III, rotenone or antimycin A, with glutamate completely depolarized mitochondria, but did not further decrease the cellular ATP level. In these cases, the neuronal Ca^{2+} recovery was completely abrogated.

Conclusions: Hippocampal neurons are more susceptible than surrounding glial cells to ischemic insult with pathologic levels of the excitatory neurotransmitter glutamate. We conclude that inherent differences in energy supplementation of Ca^{2+} handling determine the sensitivity of neurons to oxygen limitation with mitochondrial impairment.

References:

(1) Kahlert, S., Zündorf, G., Reiser, G. Detection of de- and hyperpolarization of mitochondria of cultured astrocytes and neurons by the cationic fluorescent dye Rh123. J. Neurosci. Meth. 171 (2008) 87-92.

(2) Reiser, G., Schild, L. and Kahlert, S. Effect of excitotoxicity and experimental ischemia on mitochondria in neurons and astrocytes: targets for neuroprotection. Int. J. Neuroprotection Neuroregeneration 2 (2006) 103-109.

Brain Poster Session: Stem Cells & Gene Therapy

MRI-GUIDED TRANSPLANTATION AND MONITORING OF A MICROPARTICLE SCAFFOLD SYSTEM FOR TISSUE REPAIR AND REGENERATION IN STROKE

E. Bible[1], D. Chau[2], M. Alexander[2], J. Price[3], K. Shakesheff[2], **M. Modo**[1]

[1]King's College London, London, [2]University of Nottingham, [3]King's College London, Nottingham, UK

Introduction: An alternative to pharmacological intervention in stroke therapy is cell replacement via NSC (neural stem cell) transplantation. As yet, however, neither pharmacological intervention, nor stem cell transplantation has tackled the problem of the large cystic cavity that remains post-lesion. In the present study, MRI-derived stereotactic co-ordinates were used to transplant neural stem cells attached to a microparticle scaffold into the lesion core to facilitate tissue regeneration. T2-weighted images obtained before and after transplantation allowed confirmation of the correct targeting of microparticles and progressive monitoring of scaffold integration with surrounding parenchyma, indicating successful engraftment.

Methods: Cells from the MHP36 mouse hippocampal cell line were attached to PGLA (polyglycolic lactic acid) microparticles that had previously undergone surface chemistry modification by allylamine plasma polymerisation coating (ppAam) and surface adsorption with fibronectin. Animals were lesioned by 60' MCAo (middle cerebral artery occlusion) and subjected to MRI 2 weeks after stroke to select animals with striatal lesions and transplantation co-ordinates were derived from these images. A 30 ml volume of microparticles with attached cells suspended in N-acetyl-cysteine was injected directly into the lesion cavity. Animals were scanned on a 7.0 T horizontal bore magnet (Varian, Palo Alto, CA, USA) using a custom built head coil with a 40 mm field of view and 128 X 128 data matrix. T_2-weighted images were acquired at 4 days pre-transplantation, 1 day post-transplantation and 7 days post-transplantation. A multi-echo, multi-slice, spin-echo pulse sequence (MEMSP: TR = 4200 ms, TE=10, 20, 30, 40, 50, 60, 70, 80 ms) was used to acquire images. T_2 maps and T_2-weighted images were generated using VnmrJ software (v2.3, Varian, Palo Alto, CA, USA).

Results & discussion: Conventionally NSCs have been transplanted in suspension into the contralateral non-lesioned side or into intact parenchyma adjacent to the stroke lesion. Transplantation of NSCs on PGLA microparticles using MRI-derived stereotactic co-ordinates allowed for direct transplantation of cells into the lesion. Microparticles could be visualized on MRI and were observed to fill the lesion cavity and to induce a change in signal intensity over time. Changes in the relaxivity of T2-weighted images, provides a means to monitor microparticle engraftment with surrounding tissue non-invasively over time. Immunofluoresent staining of brain sections confirmed MRI findings of scaffold engraftment within the lesion cavity. MHP36 cells could be found still attached to microparticles, but also migrating into the surrounding tissue matrix. Transplanted cells successfully differentiated into neuronal and glial cell populations.

Conclusions: PGLA microparticles can be used to inject NSCs directly into stroke lesions using MRI-derived co-ordinates. MRI is essential for the correct targeting of scaffolds to the lesion and can be used to monitor the extent of engraftment over time.

CEREBRAL BLOOD FLOW IMPROVEMENT BY FENOFIBRATE IN ISCHEMIC BRAIN REQUIRES PPARALPHA EXPRESSION IN MICE

S. Namura, Q. Guo, G. Wang

Department of Anatomy and Neurobiology, Morehouse School of Medicine, Atlanta, GA, USA

Objectives: We previously demonstrated that fenofibrate and Wy-14643 attenuated infarct size after permanent focal cerebral ischemia in mice [1]. We are investigating the mode of in vivo brain protection by these fibrates. In this study, we examined the impact of fenofibrate on cerebral blood flow (CBF) dynamics in the ischemic brain during focal cerebral ischemia and after reperfusion.

Methods: Male SV129Ev wild type and PPARalpha knockout mice were used. Animals were treated for 7 days with fenofibrate (through feeding needle; 0, 30, or 100 mg/kg/bw in 0.1 mL of 0.5% carboxymethylcellulose). Mice were subjected to 2 hr of filamentous middle cerebral artery occlusion (MCAO) and 30 min of reperfusion under general anesthesia with isoflurane. Cortical surface CBF (cCBF) was continuously measured by laser speckle flowmetry throughout the ischemic period and up to 30 min after reperfusion. The impact of fenofibrate on regional CBF (rCBF) in non-ischemic animals were measured by ^{14}C-iodoantipyrine autoradiography.

Results: Fenofibrate did not affect rCBF and mean arterial blood pressure in non-ischemic animals (n = 5 in each group). In ischemic animals, mean hemispheric cCBF was higher in the fenofibrate-treated animals ($p < 0.05$ by two-way repeated measures ANOVA; n = 6 in each group). The mean value of hemispheric cCBF in the 30 mg/kg/bw group was 1.5 fold of that in the vehicle-treated group at 2 hr after MCAO. The cCBF improvement by fenofibrate was more marked in the distal area of the middle cerebral artery territory. However, such effects of fenofibrate were not observed in PPARalpha knockout mice (n = 5 in each group).

Conclusions: The observed temporal and regional pattern of CBF improvement suggests that fenofibrate facilitates collateral supply in the ischemic hemisphere. Moreover, fenofibrate requires PPARalpha expression to improve CBF in the ischemic brain. Fenofibrate pretreatment may be useful for the prophylaxy purpose against ischemic stroke.

Reference: [1] Inoue H, Jiang X-F, Katayama T, Osada S, Umesono K, Namura S. Resveratrol and fenofibrate require PPARalpha expression to limit brain infarct resulting from permanent focal ischemia in mice. Neurosci. Lett. 2003;352:203-206. Support Contributed By: National Institute of Neurological Disorders and Stroke Grant NS048532, NS034194.

Brain PET Oral 2: Novel Radiotracers and Modeling

MAXIMUM LIKELIHOOD ESTIMATION OF RECEPTOR OCCUPANCY IN PET STUDIES

G. Tomasi, R.E. Carson

Department of Diagnostic Radiology, Yale University, New Haven, CT, USA

Objectives: In Positron Emission Tomography (PET), receptor occupancy **r** ($0< \mathbf{r}< 1$) is the fraction of the receptors occupied by an administered drug or by the tracer itself. Theoretically **r** should be uniform across region-of-interest (ROI), but in measured data, there is always variability. We compare here different methods for **r** estimation based on simulated data.

Methods: Let N be the number of ROIs and let BP_i be any measure of the binding potential (BP_{ND},BP_P,BP_F) at the i^{th} ROI, either at baseline($BP_{BASEL,i}$) or in blocked condition ($BP_{BLOCK,i}$). Let $x_i = BP_{BASEL,i}$, $y_i = BP_{BLOCK,I}$, and $r_i = (x_i-y_i)/x_i$, To compute the **global r**, 5 equations were considered:

A. $[(\sum x_i)/N -(\sum y_i)/N] / [(\sum x_i)/N]$.
B. $\sum r_i/N$.
C. The weighted version of **A)** $[(\sum w_i x_i)/\sum w_i -(\sum w_j y_j)/\sum w_j] /[(\sum w_i x_i)/\sum w_i]$ with weights equal to the inverse of the variance (σ^2) of the corresponding BP_i.
D. The weighted version of **B)** $\sum w_i r_i / \sum w_i$ with weights equal to the inverse of the variance of r_i.
E. A Maximum Likelihood (ML) estimator of $\beta_{ML}= [\beta_1,\beta_2,... \beta_{N+1}]=[BP_{BASEL,1},.... BP_{BASEL,N}, \mathbf{r}]$ as the point of maximum of the likelihood function

$\Pi_i 1/[sqrt(2\pi)\sigma(x_i)] \exp[-(x_i-\beta_i)^2/ 2\sigma^2(x_i)] \Pi_i 1/[sqrt(2\pi)\sigma(y_i)] \exp[-(y_i-(1-r) \beta_i)^2/ 2\sigma^2(y_i)]$.
Simulations were performed with N=5 to 10 ROIs with a uniform distribution for their baseline BPs between 0.5 and 2.5. Occupancies of 25%,50% and 75% and 3 different models for σ^2 ([1] a=constant; [2] aBP+b; [3] aBP^2+b) were considered. For each value of N, occupancy, and variance model, 5 noise levels for σ^2were tested by increasing the value of a. M=1000 simulated datasets were created by adding Gaussian noise to the baseline and block BPs, to obtain, in the end, 1000 occupancy estimates for each combination of parameters. In the application of B) and D) the exact σ^2 were employed for w_i. In E) the correct model for σ^2 was used but with the parameters a and b randomly distributed between 75% and 125% of their true values as in real applications a and b are not known.

Performances were assessed using the indices $\%BIAS =100*[\sum_i (r_i - \mathbf{r}_{TRUE}) / \mathbf{r}_{TRUE}] / M$ and

$\%STD.=100*sqrt [(\sum_i (r_i - \mathbf{r}_{MEAN})^2/ M] /\mathbf{r}_{MEAN}$, with $\mathbf{r}_{MEAN}$ being the mean **r** of the method examined.

Results: Eq.**B)** and **D)** gave sometimes biased results (range ±[5%-10%]) whereas the other approaches yielded substantially unbiased estimates. The figure shows typical results for %STD. Except for the case of equal constant variance, where all methods gave very similar performances, the ML approach **E)** provided the lowest %STD.

Conclusion: The ML approach provided the lowest noise estimates in the case of non-uniform variance. Additional work is required to test this method on real datasets. In this case, the selection of the best variance model must be addressed carefully.

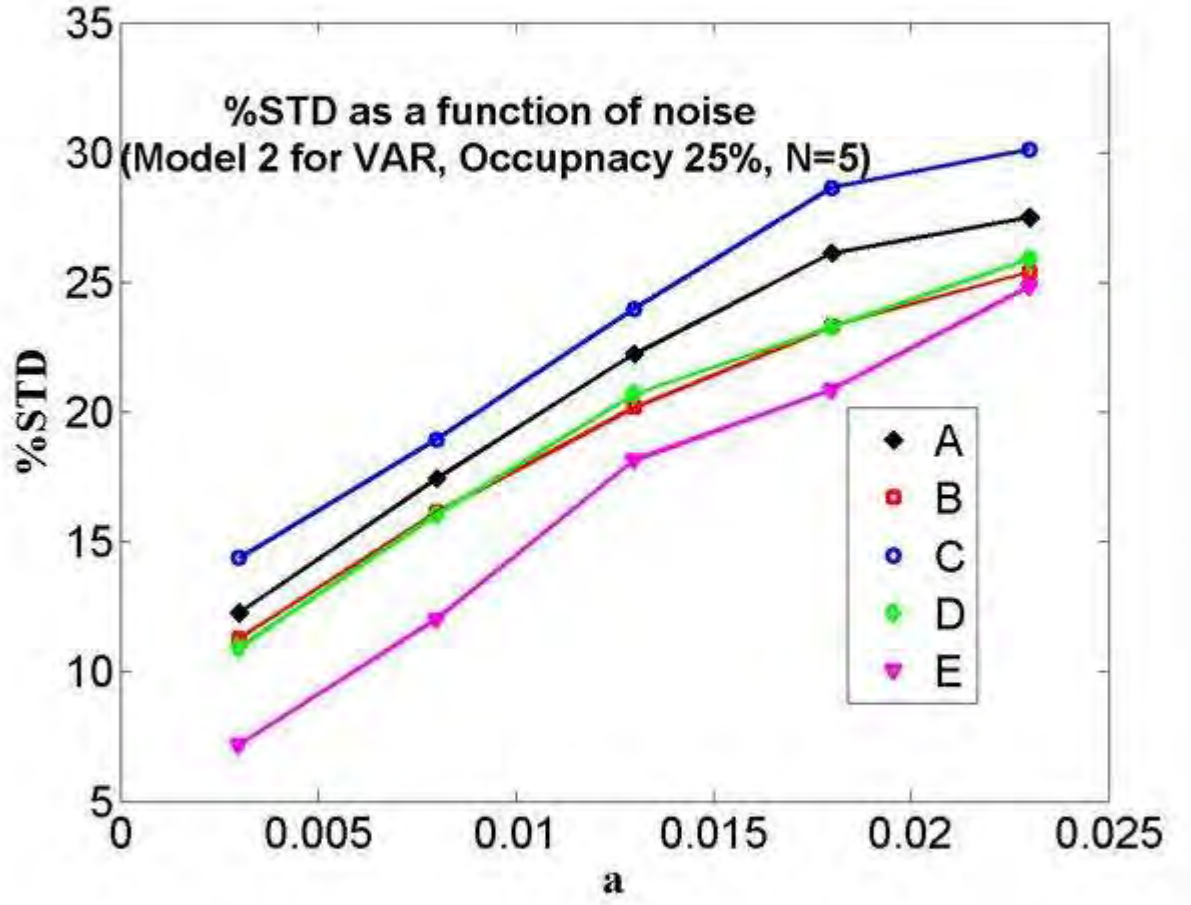
%STD as a function of noise
(Model 2 for VAR, Occupnacy 25%, N=5)
%STD
a
35
30
25
20
15
10
5
0
0.005
0.01
0.015
0.02
0.025
A
B
C
D
E

[Results]

736

Brain Poster Session: Brain Imaging: Neurologic Disease

NEED AND OPPORTUNITIES FOR IMAGING INVESTIGATION OF METABOLISM AND PERFUSION ABNORMALITIES IN AUTISM SPECTRUM DISORDERS AND THEIR RELATIONSHIP

N. Shetty[1,2], E. Ratai[2,3], M. Herbert[2,4]

[1]Neurology, [2]TRANSCEND Research Program, [3]Radiology, [4]Pediatric Neurology, Massachusetts General Hospital/Harvard Medical School, Boston, MA, USA

Objectives: Autism Spectrum Disorders (ASD) are a highly heritable set of conditions defined by deficits in three behavioral domains (communication, social interaction, repetitive/restricted range of behaviors) with onset before the age of 3 years and are commonly considered to be due to genetically caused perturbations of early brain development. High prevalence of immune dysfunction and metabolic disturbances (prominently oxidative stress) suggests that chronic pathophysiology is also present, which are known to impact cerebral perfusion and metabolism. There is much PET and SPECT documentation of reduced cerebral perfusion in ASD and much documentation of altered cerebral metabolism; there are no published studies yet to our knowledge utilizing ASL (arterial spin labeling). Overall atypically rapid brain growth in the first few years of life has been documented. This enlargement appears to occur most prominently in the outer (radiate) white matter, and neuropathological studies looking at the presence of activated glial cells has noted microgliosis in the cerebral cortex and astrogliosis in the radiate but not the deeper white matter. Overall, while there is developing an overall sense that perfusion and metabolism (as well as altered functional connectivity) may be altered for reasons that are related at an underlying level, investigations of these dimensions of altered brain function in ASD is poorly coordinated. Given the growing prevalence of ASD there is a great public health and medical need to gain clarity regarding its underlying mechanisms.

Given the difficulties involved in studying this population, the invasiveness constraining PET and SPECT studies; the low SNR of ASL and the impracticality of whole brain MRS acquisitions, as well as a paucity of practical non-invasive assessments of blood-brain barrier integrity, it is particularly important to formulate a well chosen set of measures and a strategically targeted research strategy. We therefore present a review of the evidence.

Methods: We will present the results of a PubMed literature search and the review of PET, SPECT and MRI papers related to perfusion, cerebral blood flow and metabolite quantification. We will show a tabulation of relevant papers based on regions of interest, metabolite/perfusion quantification, correlation with function (if done), modality, subject characteristics and objectives.

Results: The literature contains a large divergence of regions of interest, regions identified as abnormal, specific acquisition protocols, age ranges and subject characterization. Within this great heterogeneity a few common themes begin to emerge, such as the prominence of hypo- rather than hyper-perfusion, alterations in metabolites related to energetics, and reductions of N-acetylaspartate rather than the increases that might be expected if failure of pruning/high neuronal density were the reason for brain growth. The literature does not yet allow us to systematically evaluate perfusion-metabolism relationships.

Conclusions: Understanding the interplay between perfusion and metabolite quantification is crucial to explore the affected pathways in autism. Designing studies based on multi-modal imaging combining 31P MRS, ASL, Proton-MRS, BBB imaging could help contribute to clearer understanding of underlying pathophysiology which is vital for seeking treatment targets.

Brain Poster Session: Inflammation

ENDOGENOUS IMMUNOMODULATION AFTER EXPERIMENTAL FOCAL ISCHEMIA: MULTITARGETED CEREBROPROTECTION BY REGULATORY T CELLS IS THE KEY

R. Veltkamp[1], E. Suri-Payer[2], C. Veltkamp[3], C. Sommer[4], S. Rivest[5], **A. Liesz**[1]

[1]Neurology, University Heidelberg, [2]Immunogenetics, German Cancer Research Center, [3]Internal Medicine IV, University Heidelberg, Heidelberg, [4]Neuropathology, University Mainz, Mainz, Germany, [5]Molecular Endocrinology, Laval University, Quebec, QC, Canada

Background and objectives: Systemic and local inflammatory processes have come into the focus of translational cerebrovascular research because they play an important, mainly detrimental role in the pathophysiology of ischemic stroke[1,2]. To date, little is known about endogenous counterregulatory mechanisms preventing excessive inflammation after ischemia although they may represent powerful targets for therapy. $CD4^+CD25^+Foxp3^+$ regulatory T lymphocytes (T_{reg}) are key immunoregulators under physiological conditions and in various systemic and CNS inflammatory diseases[3]. However, their functional role in cerebral ischemia is largely unknown. Herein, we report the impact of Treg on outcome in various murine stroke models, and identify their protective pathways and targets.

Methods: In most experiments, focal ischemia was induced by permanent transtemporal MCAO; effect on outcome was also studied after 30min or 90min filament-MCAO. Infarct sizes and behavioural deficits were measured after 1, 3, and 7d. Mice were depleted of Treg either by CD25-specific antibodies or by selective transfer of $CD4^+CD25^-$ T cells into lymphocyte deficient $RAG^{-/-}$ mice. Cerebral cytokine expression was measured by RT-PCR, serum cytokine concentrations were quantified by ELISA. Leukocyte brain invasion and microglial activation was determined by immunohistochemistry. Lymphocyte subpopulations and quantitative intracellular cytokine production was analyzed by flow cytometry. Recombinant IL-10 was injected intraperitoneally (i.p.) or intracerebroventricularly (i.c.v.), in other experiments TNF-alpha or Interferon-gamma were neutralized by antibodies.

Results: Depletion of T_{reg} led to delayed infarct growth in models of MCA-coagulation and brief (30min) reversible MCAO. In contrast, anti-CD25 treatment did not exacerbate the already extensive lesions after 90min filament-MCAO. Corresponding to infarct volumes, behavioural outcome was significantly worse at day 3 and 7 in T_{reg} depleted mice. T_{reg} depletion resulted in highly increased expression of cerebral proinflammatory cytokines TNF-alpha, IL-1beta and Interferon-gamma, while i.c.v. neutralization of these cytokines in anti-CD25 treated mice reversed infarct volumes to values of control mice. Activated microglia and invading T lymphocytes were identified as the predominant cellular sources of TNF-alpha and Interferon-gamma, respectively. Anti-CD25 injection was associated with significantly increased number of invading granulocytes and activated (IBA-1+) microglia 24h after MCAO; quantitative analysis of intracellular Interferon-gamma production in brain invading T cells 5d after ischemia revealed multifold higher values in Treg depleted animals. Serum concentration of TNF-alpha and Interferon-gamma were significantly elevated at all measured time points from 6h to 7d after ischemia in anti-CD25 treated mice. Furthermore, i.c.v. (but not i.p.) administration of IL-10 prevented infarct enlargement in T_{reg} depleted mice and significantly lowered the postischemic overexpression of cerebral proinflammatory cytokines after T_{reg} depletion.

Conclusions: Treg are potent endogenous cerebroprotective modulators in models of cortical and subcortical stroke. IL-10 is their key mediator by suppressing proinflammatory cytokine expression and by targeting innate and adaptive immune cells.

References:

1. Dirnagl, U. Inflammation in stroke: the good, the bad, and the unknown. Ernst Schering Res Found Workshop (2004).

2. Wang et al. The inflammatory response in stroke. J Neuroimmunol (2007).

3. Tang & Bluestone The Foxp3 regulatory T cell: a jack of all trades, master of regulation. Nat Immunol (2008).

Supported by Else-Kröner-Fresenius Stiftung (R.V.).

KINASE ACTIVITIES OF JNK AND ERK DO NOT MATCH THEIR PHOSPHORYLATION LEVELS AFTER PRECONDITIONING IN FOCAL ISCHEMIA IN RATS

T. Takahashi, X. Gao, G. Steinberg, **H. Zhao**

Stanford University, Stanford, CA, USA

Objectives: Multiple cell signaling pathways, such as the Akt, JNK and ERK, are involved in neuronal injury induced by stroke [1]. These kinase activities have been thought to either protect (Akt), worsen (JNK), or protect or worsen (ERK) neuronal injury after stroke. Usually the activities of these kinases are represented by their phosphorylation levels[2]; however, we recently reported that changes in Akt phosphorylation levels do not match with the kinase activity assessed by in vitro kinase assay[3], suggesting that using the phosphorylation level as a sole marker as kinase activity is unreliable. In this study, we further investigate whether changes in phosphorylation levels of ERK (P-ERK) and JNK (P-JNK) coincide with their kinase activities in a focal ischemia model and have also studied the protective effects of rapid ischemic preconditioning on these changes.

Methods: Focal cerebral ischemia was generated as previously described in male Sprague-Dawley rats [3]. Bilateral common carotid arteries (CCAs) were occluded for 30 min after the distal portion of MCA was permanently cauterized. Ischemic preconditioning, which was induced by transient MCA occlusion for 15 minutes, was performed 1h prior to permanent MCA occlusion. Rats were sacrificed at 1, 5, 24 or 48h after MCAo, and tissue samples corresponding to the ischemic core and penumbra was dissected and prepared for Western blot. ERK and JNK kinase assay was processed using Kinase Assay Kits (Cell Signaling Technology, MA).

Results: Rapid ischemic preconditioning significantly reduced infarction size ($P< 0.01$). We first examined the effects of preconditioning without a test ischemia on P-ERK and P-JNK levelsand their kinase activities. Western blot results showed that both P-ERK and P-JNK levels were increased after preconditioning only, and in vitro kinase assay also showed that both of their activities were increased; suggesting that phosphorylation of ERK and JNK were consistent with their kinase activity. Next, we studied the effects of preconditioning after control ischemia on these pathways. As a result, both P-ERK and its activity were transiently increased at 1h and 5h after control ischemia; preconditioning increased P-ERK levels while it blocked its kinase activity. Thus, P-ERK levels did not match its kinase activity when preconditioning was introduced. At last, P-JNK and its activity were investigated. P-JNK levels were reduced in rats with control ischemia compared with sham; preconditioning attenuated such reductions. To the opposite, JNK activities estimated by the in vitro kinase assay were increased after control ischemia, and preconditioning showed a trend to inhibit JNK activites.

Conclusions: Phosphorylation levels of JNK and ERK do not always match with their kinase activites. Kinase assay should be performed along with Western blot to detect phosphorylation levels to understand the roles of JNK and ERK in stroke.

References:

1. Sawe et al. J Neurosci Res, 2008. 86(8): p. 1659-69.

2. Zhao et al, Mol Neurobiol, 2006. 34(3): p. 249-70. Zhao et al. J Neurosci, 2005. 25(42): p. 9794-806.

DETECTION AND CHARACTERIZATION OF MICROVASOSPASM FOLLOWING SUBARACHNOID HEMORRHAGE IN MICE

B. Friedrich[1], N. Plesnila[1,2]

[1]Institute for Surgical Research, [2]Department of Neurosurgery, University of Munich Medical Center - Großhadern, Munich, Germany

Objective: Subarachnoid hemorrhage (SAH) has a mortality of over 60% within the first 48 after the initial bleeding. Mortality and morbidity are highly associated with a decrease of cerebral blood flow (CBF). However, since cerebral perfusion pressure (CPP) is often normal and vasospasm of the large vessels has not developed yet, the mechanisms of SAH-induced cerebral ischemia is still unclear. The hypothesis of the current study was that early post-hemorrhagic ischemia is mostly caused by constriction of the microvasculature, i.e. microvasospasm. Therefore the aim of this study was to develop an experimental model for the visualization of the cerebral microvasculature and to characterize microvascular changes after SAH.

Methods: SAH was induced in intubated and ventilated male C57/Bl6 mice by the previously described filament perforation technique. 3 hours later the pial microcirculation was visualized through a cranial window using fluorescein isothiocyanate (FITC) dextran. A modified "Strahler-System" was used to classify cerebral arterioles according to their diameter. Thereby the diameters of resistance vessel in sham-operated mice could be compared to those of mice following SAH.

Results: Already three hours after induction of SAH cerebral arterioles were significantly constricted as compared to control animals. Vessels of "Strahler"-category 3 (~20 µm) showed a significant reduction of their diameter (21.86 ± 0.77 mm vs. 18.27 ± 1.13 mm; $p < 0.05$). A total of 115 microvasospasm were detected out of 355 investigated resistance vessels. Microvasospasms were segmental, showed pearl-string like pattern, and were associated with paravascular blood. The smallest vessels (10-20µm) showed the most significant microvasospasm (61.8 ± 2.4% vs. baseline; $p < 0.05$) while the largest investigated vessels showed the weakest constriction (76.8 ± 1.9% vs. baseline; $p < 0.05$).

Conclusion: We developed a model for the visualization of the cerebral microcirculation following SAH and detected already 3 hours after SAH severe and significant changes of the cerebral microcirculation, i.e. microvasospasm of cerebral resistance vessels as previously detected in man (Uhl et al., Neurosurgery, 2003, 52(6)). We suggest that these microvasospasms are responsible for post-hemorrhagic ischemia and the related early mortality and morbidity of SAH. Further investigations using our novel model will need to identify the mechanisms of this phenomenon and show if post-hemorrhagic microvasospasm progresses towards vasospasm of larger cerebral vessels.

Brain Poster Session: Traumatic Brain Injury

SEIZURE SUSCEPTIBILITY AFTER TRAUMATIC BRAIN INJURY IS ATTENUATED BY HYPOTHERMIA TREATMENT

D. Dietrich[1], C. Atkins[1], J. Truettner[1], G. Lotocki[1], J. Sanchez-Molano[1], O. Alonso[1], T. Sick[2], H. Bramlett[1]

[1]Neurological Surgery, [2]Neurology, University of Miami Miller School of Medicine, Miami, FL, USA

Objectives: A significant, debilitating consequence of traumatic brain injury (TBI) is the development of seizures. TBI patients have a 3-4 fold higher risk of developing epilepsy than the general population (1). The pathomechanisms underlying posttraumatic seizures include hippocampal interneuron loss, hyperexcitability of dentate granule cells and abnormal sprouting of the mossy fiber pathway in the dentate gyrus (2-5)). Hypothermia treatment is a highly promising therapy that targets multiple pathomechanisms caused by TBI. The objective of this study was to determine if hypothermia reduces posttraumatic seizure susceptibility by attenuating the histopathological mechanisms contributing to seizure development.

Methods: Adult male Sprague Dawley rats received moderate parasagittal fluid-percussion brain injury (FPI) or sham surgery. The animals were maintained at normothermia (37.0-37.5°C) or hypothermia (33.0-34.0°C) for 4 hr starting 30 min after TBI. Moderate FPI does not elicit behaviorally evident seizures. Thus, to ascertain seizure susceptibility, animals received a subconvulsant dose of pentylenetetrazole (PTZ, 30 mg/kg), a $GABA_A$ receptor antagonist at 1 or 12 weeks post-injury. Seizure class and frequency were scored with simultaneous EEG recordings to assess for seizure threshold changes. Mossy fiber sprouting was determined by TIMM staining. In another set of animals, hyperexcitability changes of dentate granule cells were assessed in acute hippocampal slices by measuring input/output curves of the perforant pathway onto dentate granule cells.

Results: We found that moderate FPI resulted in increases in input/output curves of dentate granule cells at 1 week post-injury. This paralleled a decrease in seizure threshold in TBI animals as compared to naïve animals and this was reduced with hypothermia treatment. Similarly, at 12 weeks post-injury, seizure threshold was decreased and the highest seizure class reached was increased in TBI animals; these traumatic outcomes were prevented by hypothermia. These behavioral findings correlated with epileptic seizure discharges recorded by EEG. Post-hoc analysis revealed that mossy fiber sprouting of the dentate gyrus after TBI was reduced with hypothermia therapy.

Conclusions: These results show for the first time that hypothermia therapy after TBI reduces posttraumatic seizure susceptibility and abnormal mossy fiber sprouting in the dentate gyrus. These preclinical studies demonstrate the promising potential of therapeutic hypothermia in improving outcome in TBI patients and open a new therapeutic avenue for the treatment of posttraumatic seizures.

References:

1. Garga N, Lowenstein DH (2006) Posttraumatic epilepsy: A major problem in desperate need of major advances. Epilepsy Curr 6:1-5.

2. D´Ambrosio R, Fairbanks JP, Fender JS, Born DE, Doyle DL, Miller JW (2004) Post-traumatic epilepsy following fluid percussion injury in the rat. Brain 127:304-14.

3. Golarai G, Greenwood AC, Feeney DM, Connor JA (2001) Physiological and structural evidence

for hippocampal involvement in persistent seizure susceptibility after traumatic brain injury. J Neurosci 21:8523-37.

4. Grady MS, Charleston JS, Maris D, Witgen BM, Lifshitz J (2003) Neuronal and glial cell number in the hippocampus after experimental traumatic brain injury: Analysis by stereological estimation. J Neurotrauma 20:929-41.

Santhakumar V, Ratzliff AD, Jeng J, Toth Z, Soltesz I (2001) Long-term hyperexcitability in the hippocampus after experimental head trauma. Ann Neurol 50:708-17.

743

Brain Oral Session: Experimental Cerebral Ischemia: Neuroprotection

THE PROTECTIVE EFFECTS OF ISHCEMIC POSTCONDITIONING ON POTENTIAL INFLAMMATORY FACTORS INVOVLED IN FOCAL ISCHEMIA IN RATS

D. Wei, X. Gao, X. Chen, **H. Zhao**

Stanford University, Stanford, CA, USA

Objectives: Ischemic postconditioning, which refers to a series of mechanical interruptions of reperfusion after ischemia, reduces infarction[1], but the protective mechanisms remain largely unknown. In this study we investigated its protective effects on some potential inflammatory molecules, including galectin-9, Tim-3, COX-2, iNOS and nitrotyrosine after stroke. Tim-3, which is a member of the T cell immunoglobulin and mucin domain (Tim) family, is activated by its ligand, galectin-9. It plays a double role, either promoting or inhibiting inflammatory response, depending on the cell types it activates [2]. COX-2, iNOS and nitrotyrosine are well-known inflammatory molecules.

Methods: Focal ischemia was induced by permanent distal MCA occlusion combined with 30 min of bilateral CCA occlusion in rats. For postconditioning[1], after 30 secs of CCA reperfusion, the CCAs were occluded again by tightening sutures around the CCA for 10 secs, followed with another 2 cycles of 30 secs reperfusion and 10 secs occlusion (total of 3 cycles). Western blot and immunofluorescence staining were used to examine protein expression. To detect the effects of immune suppression on protein expression, minocycline hydrochloride was intraperitoneally (i.p) injected at 60 min before and 8 hours after the MCA occlusion.

Results: Ischemic postconditioning significantly reduced infarct size after focal ischemia. The results of Western blot indicate that Tim-3 expression was increased after stroke, which was inhibited by postconditioning (n=6/group, $P< 0.001$). The results of confocal microscopy indicate that galecin-9 was expressed on blood vessels 1h after stroke, and on neurons from 5h to 24h. Such an expression was inhibited by postconditioning. Postconditioning also blocked iNOS and nitrotyrosine expression after stroke. However, postconditioning had no protective effects on COX-2 expression induced by stroke. At last, we found that minocycline injection attenuated increases in Tim-3 and iNOS, but promoted COX-2 expression.

Conclusions: the galectin -9/Tim-3 pathway is involved in brain injury after stroke. Ischemic postconditioning blocks increases in galectin-9, Tim-3, iNOS and nitrotyrosine, but promotes COX-2 expression. Minocycline, an inflammatory inhibitor, executed similar effects as postconditioning. Therefore, we conclude that ischemic postconditioning may prevent brain injury by regulating galectin-9/Tim-3 pathways, and inhibiting iNOS and nitrotyrosine activity.

References:

1. Zhao et al.,. J Cereb Blood Flow Metab, 2006. 26(9): p. 1114.

2. Anderson et al., Science, 2007. 318(5853): p. 1141-3.

744

Brain Poster Session: Traumatic Brain Injury

ACUTE AND CHRONIC METABOLIC ALTERATIONS IN THE BRAIN AFTER CERVICAL SPINAL CORD INJURY

H. Bramlett[1], L. Daniels[1], G. Lotocki[1], J. Truettner[1], W. Zhao[2], A. Marcillo[1], O. Alonso[1], D. Dietrich[1]

[1]Neurological Surgery, University of Miami Miller School of Medicine, [2]Biomedical Engineering, University of Miami, Miami, FL, USA

Objectives: Spinal cord injury (SCI) is a devastating clinical condition resulting in complex neurological consequences including sensory, motor and autonomic dysfunction. Recently, supraspinal changes have been documented after SCI including circuit plasticity as well as neuronal atrophy and cell death (1). Previous studies from our laboratory have utilized 2-deoxyglucose autoradiographic techniques combined with somatosensory circuit activation for measuring local cerebral metabolic rates of glucose utilization ($lCMR_{GLU}$) to understand the metabolic changes occurring in brain regions after injury (2). The purpose of this study was to assess baseline alterations in $lCMR_{GLU}$ occurring in spinal and supraspinal areas after acute and chronic cervical SCI and the metabolic responsiveness of the brain to vibrissae barrel-field circuit activation.

Methods: Adult male Wistar rats received moderate cervical SCI at C5 or sham laminectomy surgery. Forty-eight hours (n=4/group) or 6 weeks (n=6/group) after SCI, rats underwent 2-DG and vibrissae barrel-field circuit activation as previously described (2). Semi-serial coronal brain sections were cut while cervical spinal cord specimens were cut longitudinally. Autoradiographic images were analyzed as previously described (2) with region of interest analysis conducted on multiple brain regions including the three relay stations (ipsilateral trigeminal medullary nuclear complex (TMC), contralateral ventrobasal thalamic nucleus (VPM), contralateral barrel field cortex (S1 & S2)) of the vibrissae barrel-field circuit.

Results: In the non-stimulated condition, acute SCI animals showed widespread patterns of decreased $lCMR_{GLU}$ as compared to sham. Patterns of decreased $lCMR_{GLU}$ ranged from 10-40% reductions throughout multiple structures. In the 48 hr SCI animals, whisker stimulation resulted in normal increases in $lCMR_{GLU}$ within the barrel-field circuit relay stations as compared to uninjured animals. Interestingly, whisker stimulation also led to widespread increases in glucose metabolism outside of this circuit ranging from 20-100% compared to sham. At 6wks after SCI, normal levels of stimulation induced increases in $lCMR_{GLU}$ were seen in the relay stations compared to sham. However, in these animals, an expansion of the S1/S2 cortical field as well as aberrant metabolic activation of brain regions including cingulate cortex and striatum was observed. Finally, in addition to supraspinal structures, local alterations were seen within the injured spinal cord at both time points. At the site of injury, moderate hypometabolism was present while rostral and caudal spinal cord segments showed evidence for hypermetabolism compared to sham.

Conclusions: These data show that the brain and SC undergoes a complex pattern of metabolic changes following moderate cervical SCI. Such metabolic changes could indicate alterations in circuit activation after acute and chronic spinal cord injury. The findings suggest that it may be important to consider these consequences of SCI when designing strategies including rehabilitation and axonal regeneration to enhance recovery after SCI.

References:

1. Bramlett HM, Dietrich WD (2007) Progressive damage after brain and spinal cord injury: pathomechanisms and treatment strategies. Prog Brain Res 161:125-141.

2. Passineau MJ, Zhao W, Busto R, Dietrich WD, Alonso O, Loor JY, Bramlett HM, Ginsberg MD (2000) Chronic metabolic sequelae of traumatic brain injury: prolonged suppression of somatosensory activation. Am J Physiol Heart Circ Physiol 279:H924-H931.

745

Brain Poster Session: Experimental Stroke & Cerebral Ischemia

IS CYCLOOXYGENASE TYPE 2 A "GOOD" TARGET FOR STROKE TREATMENT?

D. Lerouet, M. Lechaftois, I. Popescu, B. Palmier, B. Coqueran, M. Plotkine, **I. Margaill**

Pharmacology of Cerebral Circulation, EA 2510, Paris Descartes University, Paris, France

Objectives: Cyclooxygenase type 2 (COX-2) has been demonstrated deleterious in various experimental models of cerebral ischemia, due to the production of prostaglandin E2 (PGE2) [1,2,3]. However, the recent reports of an increased risk of cardiovascular events, e.g. ischemic stroke, in patients receiving COX-2 selective anti-inflammatory drugs raised concern about the safety of these inhibitors[4]. In this context, the present study investigated the relevance of COX-2 as a therapeutic target in stroke.

Methods: Ischemia was induced by intravascular occlusion of the left middle cerebral artery for 1h in male Swiss mice (25-30g) anesthetized with ketamine/xylazine.

Experiment 1: Animals were euthanized 30 min, 2, 6, 24 or 48h after reperfusion. Their brains were removed and cut into 7 coronal sections to measure (1) COX-2 protein expression by western blot, and (2) lesion volume by the triphenyl-tetrazolium chloride (TTC) technique.

Experiment 2: The COX-2 inhibitor nimesulide (12 mg/kg, i.p) was administered just after the onset of ischemia and 4h later, and brain PGE2 production was measured 6h after reperfusion by Radio-Immuno Assay (RIA).

Experiment 3: Nimesulide was administered just after the onset of ischemia, then 4 and 8h later to study its effect on the lesion volume at 24h.

Results: Compared to sham-operated mice, COX-2 expression was significantly increased 6h (x1.7, $P< 0.01$) and 24h (x1.4, $P< 0.05$) after reperfusion. PGE2 was also increased at 6h (163 ± 22 pg/mg of proteins versus 83 ± 12 pg/mg of proteins in sham-operated animals, $P< 0.05$). Brain lesion was 17 ± 6 mm^3 after 2h of reperfusion and 61 ± 7 mm^3 at 24h ($P< 0.001$), and did not increase further at 48h (65 ± 2 mm^3).

Nimesulide totally suppressed post-ischemic PGE2 production at 6h ($P< 0.05$), but did not modify the brain lesion at 24h (66 ± 6 mm^3 versus 66 ± 4 mm^3).

Conclusions: Our results show that COX-2 induction associated with a PGE2 production occurred after cerebral ischemia. However, although the COX-2 inhibitor, nimesulide, suppresses post-ischemic PGE2 production, it has no neuroprotective effect. Thus COX-2 inhibition might not be a relevant strategy in every models of cerebral ischemia.

References:

1. Candelario-Jalil et al. 2004. Brain Res, 1007, 98-108.

2. Dore et al. 2003. Ann Neurol, 54, 155-62.

3. Iadecola et al. 2001. Proc Natl Acad Sci USA, 98, 1294-9.

4. Iadecola et al. 2005. Stroke, 36, 182-5.

EFFECT OF LEVODOPA AND DA AGONIST TREATMENT ON DA RELEASE PATTERNS AND DTBZ BINDING IN THE 6-OHDA PARKINSON´S RAT MODEL

V. Sossi[1], K. Dinelle[1], D. Doudet[2], R. de la Fuente Fernandez[2]

[1]Physics and Astronomy, University of British Columbia, [2]Medicine, University of British Columbia, Vancouver, BC, Canada

Background: There is still controversy on the effect of levodopa and dopamine (DA) agonist treatment on Parkinson´s disease (PD) progression as evaluated with imaging studies and on their impact on changes in synaptic DA levels. The latter point is of great clinical interest due to the established link between oscillations in synaptic DA levels and propensity to develop treatment-related motor complications. Here we investigated the effect of chronic levodopa and pramipexole treatment on the binding of the 11C-dihydrotetrabenazine (DTBZ) tracer to the vesicular transporter of type 2 (VMAT2), taken as a marker of dopaminergic integrity, and on changes in synaptic levodopa-derived synaptic DA levels (delta(DA) as measured by a double 11C-Racloprice (RAC) scan using the unilateral 6-OHDA rat model of PD.

Methods: 28 unilaterally 6-OHDA lesioned rats underwent a DTBZ, and two RAC scans (baseline and 45 min after I.P. administration of levodopa/benserazide (50 mg/kg, 15mg/kg prepared). After being assigned to three degree-of-denervation-matched treatment groups (saline (S, N= 7), pramipexole (PRA, N= 10) and levodopa (LD, N=11)) and undergoing treatment for approximately 4 weeks, they underwent an identical scanning protocol and imaging measures were compared. Dopaminergic denervation as estimated from the pre-treatment DTBZ scan ranged between 17% and 96%. ANOVA analysis was used to compare pre- and post-treatment results expressed in terms of BP_{ND} for the control and lesioned side respectively.

Results: On the control side, no treatment effect was found for DTBZ binding together with a significant overall reduction ($p=0.003$). On average the PRA group showed a slightly higher reduction (~7% vs ~3% for the other two groups). On the lesioned side a significant treatment effect was observed ($p=0.043$) with the PRA group only showing a slight decrease. After adjusting for baseline DTBZ and RAC binding values, a treatment effect ($p=0.018$) was observed for delta(DA) on the lesioned side with no change for the PRA and LD treated groups and a trend towards an increase in the S group. On the control side a significant treatment effect was observed ($p=0.032$) with a trend toward an increase of delta (DA) in the PRA treated group.

Conclusion: The most important finding of this study is that once denervation is present, neither pharmacological treatment changes delta (DA), thus neither treatment should influence the probability of developing motor complications. In addition, it shows that DTBZ might not be an objective marker to accurately monitor disease progression: the fact that a reduction in DTBZ binding on the control side was observed for all treatment groups, including saline, indicates that such reduction likely does not arise as a consequence of a possible treatment-induced terminal damage but rather from competition with DA arising either from increased synthesis (with the corollary that the control side might be susceptible to some of the regulatory changes occurring on the lesion side) or pharmacologically increased availability thus rendering this marker sensitive to either compensatory or pharmacological effects consistently with previous findings. Care must be thus taken when using PET markers to objectively determine either treatment effects or disease progression.

747

Brain Oral Session: Traumatic Brain Injury: Metabolism

EFFECT OF THE ANESTHETIC REGIMEN DURING EXPERIMENTAL BRAIN TRAUMA ON HISTOLOGICAL OUTCOME AND CEREBRAL INFLAMMATION

S. Thal, C. Ricken, K. Gierth, R. Timaru-Kast, C. Werner, K. Engelhard

Department of Anesthesiology, Johannes Gutenberg-University, Mainz, Germany

Objectives: Application of different anesthetics for 1 hour following traumatic brain injury (TBI) alters the extent of neuronal injury and influences functional outcome[1]. The question therefore arises, if already the use of anesthetics for a short period during induction of an experimental TBI influences secondary pathophysiological mechanisms. Knowledge about the effect of anesthetics on experimental data is essential for the selection of an appropriate anesthetic agent. The present study therefore compares the effect of two volatile and one intraperitoneal anesthesia on histological damage, functional outcome and expression of inflammatory marker genes after experimental brain trauma.

Methods: Male C57Bl/6 mice were randomly assigned to an anesthesia with 1.4 vol% isoflurane (iso), 3.5 vol% sevoflurane (sevo) or an i.p. injection (comb) of midazolam (5 mg/kg), fentanyl (0.05 mg/kg) and medetomidine (0.5 mg/kg). A pneumatic brain trauma was induced on the right parietal cortex (controlled cortical impact, CCI). 15 min and 24 hr after CCI brain contusion volume was determined in cresyl violet stained sections. mRNA expression of TNFα, IL1β, IL6, COX2 and iNOS was determined in contused brain tissue and normalized against Cyclophilin A as control gene. Neurological function was evaluated with a 10-point-neurological severity score. Statistics: ANOVA on ranks, $p < 0.05$.

Results: 15 min after CCI brain contusion volume was not different between the anesthesia regimens. Within 24 hours histological brain damage increased significantly in all groups (15 min: 19.4 $mm^3 \pm 4.5$; 24 hr: sevo=45.3 $mm^3 \pm 9.0$; iso=31.5 $mm^3 \pm 4.0$; comb=44.2 $mm^3 \pm 6.2$). Sevo and comb anesthesia resulted in a significantly larger contusion volume compared to iso. After 24 hours neurological function was significantly better in animals anesthetized with iso in comparison to comb (sevo: 4.6 pts.±1.3; iso: 3.9 pts.±0.8; comb: 5.1 pts.±1.6). The expression of inflammatory marker genes increased significantly from 15 min to 24 hours after CCI, but without differences between the anesthesia protocols.

Conclusion: The data demonstrate that a short anesthesia during the induction of a brain trauma has a profound impact on extent of secondary brain damage. Despite differences in histological brain damage, cerebral inflammation was similar between the anesthetic regimens. Differences in histological brain damage are therefore not mediated by variation in cerebral inflammation. Differences in post-traumatic cerebral perfusion or influence on apoptotic processes might account of the observed effects. In conclusion, in order to investigate the pathophysiological mechanisms of brain trauma selection of the anesthetic agent may influence results and interpretation of a study.

References: (1) K. D. Statler and H. Alexander and V. Vagni and C. E. Dixon and R. S. B. Clark and L. Jenkins and P. M. Kochanek. Comparison of seven anesthetic agents on outcome after experimental traumatic brain injury in adult, male rats. J Neurotrauma 23: 97-108, 2006.

748

Brain Oral Session: Neurological Diseases

CEREBRAL HAEMODYNAMICS CHANGES AFTER 20 ML LUMBAR DRAINAGE IN PATIENTS WITH GOOD GRADE SUBARACHNOID HAEMORRHAGE. A PET STUDY

E. Schmidt[1], J.F. Al Bucher[2], S. Silva Sifontes[3], P. Payoux[4], A. Luzi[3], I. Loubinoux[2], C. Cognard[5], F. Chollet[2]

[1]Service de Neurochirurgie, [2]Service de Neurologie, [3]Service d'Anesthésie, [4]Service de Médecine Nuclaire, [5]Service de Neuroradiologie, Toulouse, France

Background: After subarachnoid haemorrhage (SAH), vasospasm -i.e. delayed ischemia- and hydrocephalus greatly contribute in a context of cerebral energy crisis to unfavourable outcome. The link between hydrocephalus and vasospasm is rather unclear, but it has been shown that after SAH the ventricular size seems correlated with vasospasm [Black 1986] and a CSF lumbar drainage protocol reduces the risk of vasospasm [Klimo 2004]. In clinical practice, lumbar punctures to withdraw CSF are often performed to release headaches. However there are no clear evidences of the benefit of this procedure in terms of headache, but also no data on the cerebral haemodynamics consequences of a drop in intracranial pressure (ICP). We hypothesize that in patients with good grade SAH, a 20 ml CSF lumbar drainage significantly reduces the intensity of headache and improves cerebral blood flow measured with O^{15} PET scan.

Methods: 7 patients were included in our study (mean age 47, sex ratio 4/3) after signed consent. They were all good grade SAH (WFNS 1-2); 5 patients had an anterior communicating artery aneurysm and 2 a right middle cerebral artery aneurysm. All aneurysms have been successfully coiled. Every patient was complaining of severe headache. A 2O ml lumbar CSF withdrawal was performed in the PET scanner. ICP and arterial blood pressure (ABP) were continuously monitored throughout the procedure. Regional CBF changes was measured with O^{15} PET scan before and after CSF drainage. We applied masks (Pickatlas software) on the vascular territory related to the aneurysm. Global differences in CBF were covaried for all voxels and comparisons across conditions were made using t statistics with appropriate linear contrasts and then converted to Z scores. Only regions which exceeded a threshold of $P_{uncorrected} < 0.01$ (Z score > 3.2) were considered significant.

Results: A 20 ml CSF drainage yielded a significant:

i. drop in ICP from 23.5 ± 11.3 to 6.9 ± 3.8 mmHg,
ii. reduction in visual pain scale (-5), but
iii. no change in ABP (105.2 ± 22.6 vs 103.8 ± 10.6 mmHg).

O^{15} PET study demonstrated in all patients highly significant changes in cerebral haemodynamics before and after the CSF withdrawal (z > 3.2). The augmentation of CBF was prominent in the vascular territory of the aneurysm and the reduction of CBF took place in the rest of the vasculature.

Conclusions: In good grade SAH, a 20 ml CSF withdrawal significantly reduces headaches and lowers ICP. This drop in ICP seems to yield a redistribution of the whole CBF at the benefit of the vascular territory of the aneurysm, prone to vasopasm. Our study supports the use of lumbar drainage after SAH not only to reduce headaches but also to improve CBF in potentially jeopardized vascular regions.

References: Klimo P et al. J Neurosurg 100:215-224, 2004Black PM J Neurosurg 18(1):12-6, 1986.

749

Brain Poster Session: Experimental Stroke & Cerebral Ischemia

THE "SKIMMING LESION" MODEL OF CORTICAL PHOTOCHEMICAL STROKE MINIMIZES ARTIFACTUAL EDEMA

R. DeFazio, **B.D. Watson**

Neurology, University of Miami, Miami, FL, USA

Objectives: Small-vessel cortical models of Type II (rose Bengal, erythrosin B) photochemically induced stroke in rodents have been widely utilized owing to their relative noninvasiveness and high reproducibility. Although the lesion features acute occlusion of cortical vessels specifically by platelets (no fibrin), vasogenic edema due to blood-brain barrier damage can induce occlusion by vascular compression even in the absence of platelet aggregation [1-3]. We hypothesized that the contribution of blood-brain barrier breakdown to infarct volume can be minimized by inducing a "skimming" lesion, wherein a laser beam is focused into a line shape directed onto the skull parallel to the parietal convexity. The beam traverses the skull at a shallow grazing angle, effecting photothrombosis of only the pial vessels at the cortical surface.

Methods: We used adult mice of either sex. After anesthesia and femoral artery catheterization, the skull was exposed and coated with mineral oil. A 532nm Nd:YAG laser beam was applied perpendicular to (standard model), or focused as a line beam parallel to ("skimming" model), the skull surface. Both beams were 2mm in width with a total power of 4mW. The laser was applied for 1 minute upon injection of 20mg/kg erythrosin B. To investigate the volume of edema, Evans Blue was injected immediately after photo-excitation. Four hours after injury, the mice were cardiac perfused and the cortical surface area of Evans Blue labeling measured. With a separate set of mice, animals were perfusion-fixed at 3 days post-injury and infarct width was quantified using standard hematoxylin and eosin staining.

Results: In both models, Evans Blue revealed an intense staining in the center of the lesion, surrounded by a fainter ring of staining. The skimming lesion greatly reduced the surface area of Evans Blue staining. After the skimming lesion, intense Evans Blue labeling occurred only within the boundaries of the initial stimulation and was 75% less than the extravasation observed using the standard model (2.9 mm^2 vs. 12.4 mm^2, skimming vs. standard, n=2; initial photo-excitation region area = 3.1 mm^2). Faint Evans Blue extravasation infiltrated an area 63% less than the standard model (9.5 mm^2 vs. 25.7 mm^2, skimming vs. standard, n=2). We compared the histological impact of skimming photothrombosis with published reports using the standard model. Skimming photothrombosis resulted in a sharp-edged infarction delimited by boundaries perpendicular to the cortical surface. The width of infarction was 95% of the stimulation line beam width (n=2). Published results using the standard model have demonstrated bowl-shaped boundaries indicating edematous expansion of the infarction beyond the initial photo-excitation dimensions (>100% spot diameter).

Conclusions: Skimming photothrombosis minimizes the impact of edema yet maintains the powerful advantage of a reproducible infarct volume determined by the pattern of illumination. The skimming lesion results in a state of relatively pure ischemia in the absence of widespread blood-brain-barrier breakdown.

References:

1. Stoll G, et al. J Cereb Blood Flow Metab. In press.

2. Kleinschnitz C, et al. Stroke 39:1262, 2008.

3. Dietrich WD, et al. Stroke 19:857,1988.

Supported by the UM SJ Glaser Foundation.

750

BrainPET Poster Session: In Vivo Pharmacology and Clinical Applications

POSSIBLE EFFECTS OF FAMILY HISTORY OF ALCOHOLISM ON THE TEST-RETEST VARIABILITY OF STRIATAL D2 AVAILABILITY

K. Yoder[1,2], M. Normandin[1,3], C. Cox[4], C. Herring[1], K. Perry[1], D. Garzon[4], D. Kareken[4], E. Morris[1,5], D. Albrecht[1]

[1]Radiology, [2]Stark Neurosciences Research Institute, Indiana University School of Medicine, Indianapolis, [3]Weldon School of Biomedical Engineering, Purdue University, West Lafayette, [4]Neurology, Indiana University School of Medicine, [5]Biomedical Engineering, Indiana University-Purdue University Indianapolis, Indianapolis, IN, USA

A commonly used method for studying relative changes in endogenous dopamine concentration is the two-scan paradigm with [^{11}C]raclopride (RAC). In a 2-scan design, D2 receptor binding potential (BP) during a challenge state is compared to BP estimated from a resting or baseline state. Any detected changes in BP are attributed to changes in striatal dopamine levels. One of the inherent assumptions of this method is that basal dopamine tone is relatively stable in individuals. Indeed, the majority of available literature supports the notion that intra-individual RAC BP is consistent, with most reports citing between-scan differences in baseline BP in healthy subjects of approximately 10% [1-5]. However, the test-retest variability (TRV) has not been determined for individuals who have a family history of alcoholism (FHA).

Objective: The TRV of baseline RAC binding was determined as part of an ongoing study investigating the reproducibility of dopaminergic responses to alcohol.

Methods: Data are reported from 7 subjects who underwent 2 baseline RAC scans on separate days. Scan start times were between 1-3:30 p.m. Subjects were male, right-handed smokers who had > 1 blood relative with a history of alcoholism. Three subjects were social drinkers (SD), and 4 were nontreatment-seeking alcoholics (NTS). Subjects received a nicotine patch to prevent craving. Timing and dose of last alcohol exposure were controlled by administering a controlled IV infusion of alcohol 5 hours prior to scanning (target breath alcohol concentration (BrAC): 60 mg%; BrAC returned to zero prior to baseline RAC). RAC BP was estimated for right and left caudate, putamen, and ventral striatum using conventional reference region methods [6]. TRV was calculated as $|BP_1-BP_2| / [(BP_1+BP_2)/2]$.

Results: Across all subjects and all regions, the average TRV was very high (19.4 ± 0.04%). There was no consistency in directionality of change in BP between scan days, either across all subjects or between SD and NTS. Exploratory analyses were conducted to identify putative sources of the high TRV. SD subjects had a significantly higher TRV in the left putamen relative to NTS ($p < 0.02$). Light smokers (≤15 cigarettes/day) tended to have greater TRV in the left ventral striatum than heavy smokers (> 15/day; $p = 0.08$). The number of alcoholic relatives was significantly correlated with TRV in the left caudate and putamen ($n = 7$; $p < 0.05$). There were no interaction effects between smoking and FHA in any region. No variables were associated with TRV in the right striatum; small sample size may have precluded detection of any effects.

Conclusions: Striatal DA tone may be highly labile in smokers with a FHA. It is unclear what is contributing to the high TRV in this sample; a larger cohort is needed for more definitive conclusions. These preliminary data suggest that, without knowledge of the TRV in a population, "negative results" from DA challenge data should be interpreted with caution.

References:

(1) Cervenka 2006 Brain 129(pt8):2017-28.

(2) Hietala 1999 JCBFM 19(2):210-217.

(3) Mawlawi 2001 JCBFM 21(9):1034-1057.

(4) Schlosser 1998 Synapse 28(1):66-70.

(5) Volkow 1993 JNM 34(4):609-613.

(6) Ichise 2003 JCBFM 23(9):1096-1112.

751

Brain Poster Session: Angiogenesis

ROLE OF SOLUBLE EPOXIDE HYDROLASE IN POST-ISCHEMIC ANGIOGENESIS

W. Zhang, M. Grafe, J. Palmateer, P. Herson, N. Alkayed

Oregon Health & Sciences University, Portland, OR, USA

Objectives: Ischemia induces cerebral angiogenesis, which is part of a vascular remodeling response that necessary for regeneration and functional recovery. The mechanisms of post-ischemic angiogenesis remain unknown. Epoxyeicosatrienoic acids (EETs), P450 eicosanoids produced in brain by astrocytes, play an important role in blood flow regulation and protection after cerebral ischemia, and have been shown to exhibit angiogenic properties in multiple in vitro models of angiogenesis. EETs' actions are terminated by soluble epoxide hydrolase (sEH). We here tested the hypothesis that sEH gene deletion promotes post-ischemic angiogenesis and functional recovery after focal cerebral ischemia in mice.

Methods: Mice with targeted deletion of sEH (sEH knockout, sEHKO) and their wild type (WT) littermates were subjected to 45 min of middle cerebral artery occlusion (MCAO), followed by 8 days of recovery. A battery of somatosensory and cognitive neurobehavioral tests were performed during recovery. At the end of the experiment on day 8, mice were perfused, and brains were fixed, sections and stained for CD34, which identifies endothelial cells, as well as endothelial progenitor cells. Unbiased, stereology-based estimates of vascular density were obtained from the density of CD34-positive vascular profiles in these brain sections using computer-assisted optical dissector probe.

Results: Microvascular density was numerically higher in sEHKO compared to WT mice both within infarct zone (272 ± 50 vs 239 ± 31 profiles/mm^2, mean ± sem,) and contralateral cerebral cortex (262 ± 40 vs 181 ± 26, n=4 per group).

Conclusion: The preliminary results are consistent with higher post-ischemic angiogenic capacity in sEHKO vs WT mice, consistent with higher EETs-mediated angiogenesis. Ongoing studies will determine if increased vascular density is associated with improved functional recovery.

HYPOTHERMIA ALTERS PROTEIN SUMOYLATION DURING EARLY REPERFUSION AFTER FOCAL BRAIN ISHEMIA IN THE RAT

J. Sullivan[1], A. Lagina[2], R. Kumar[1], J. Wang[2]

[1]Emergency Medicine and Physiology, [2]Emergency Medicine, Wayne State University, Detroit, MI, USA

Objectives: Recent reports indicate that the Small Ubiquitin-Like Modifier (SUMO) protein participates in extensive protein conjugation (sumoylation) during early reperfusion after brain ischemia, with signal for extensive protein sumoylation present as early as 30 min of reperfusion. The relative salutary/detrimental effect of this massive sumoylation remains unclear. Moreover, there is evidence that both hypothermia and hibernation topor increase protein sumoylation. We hypothesized that hypothermia administered at the onset of reperfusion after focal brain ischemia would accelerate or accentuate overall protein sumoylation.

Methods: Male Sprague-Dawley rats (N=3) were subjected to 2h focal brain ischemia under isoflurane/N_2O using MCAO technique. At the onset of reperfusion, hypothermia was instituted utilizing a water-cooled extracorporeal system consisting of a modified veterinary heating blanket coupled to an Amersham gel cooling apparatus. Body core, brain and temporalis muscle temperatures were monitored throughout the hypothermic interval by thermocouples (Physitemp), and MAP, serum glucose and heart rate were monitored via arterial catheter. At the end of the reperfusion/hypothermic interval, animals were transcardially perfused with ice-cold isotonic saline and the brains rapidly removed. Cortex and striatium in the MCA distribution were taken from both ischemic and contralateral hemispheres and used for gel electrophoresis and Western blotting with antibody directed against SUMO 2/3.

Results: Sham-operated control animals demonstrated no protein sumoylation in any brain region. Animals subjected to 2h of brain ischemia and 2 hours of normothermic reperfusion demonstrated heavy protein sumoylation in both cortex and striatum, but no sumoylation in contralateral brain. Animals subjected to 2 h of brain ischemia and 2 hour of hypothermic reperfusion demonstrated markedly decreased protein sumoylation compared with ischemic animals.

Conclusions: These results suggests that hypothermia significantly alters the pattern and timing of protein sumoylation in ischemic brain when instituted at the onset of reperfusion after MCAO. Detailed time course studies are underway, as well as experiments to determine whether ischemia-induced sumoylation is a truly neuroprotective phenomenon and, if so, which sumoylated proteins mediate any effect on neuronal survival.

References: Yang W, Sheng H, Homi HM, Warner D, Paschen W. Cerebral Ischemia/Stroke and small ubiquitin-like modifier (SUMO) conjugation - a new target for therapeutic intervention? J. Neurochem. (2008) 106, 989-999.

753

Brain Oral Session: Cortical Spreading Depression

DECREASED CA^{2+} SPARK AND ASSOCIATED BK CHANNEL ACTIVITY IN PARENCHYMAL ARTERIOLAR MYOCYTES FOLLOWING SUBARACHNOID HEMORRHAGE

G. Wellman, M. Koide, K. O'Connor

Pharmacology, University of Vermont, Burlington, VT, USA

Objectives: Aneurysmal subarachnoid hemorrhage (SAH) is associated with high rates of morbidity and mortality. It has been a long-held notion that delayed blood-induced vasospasm of large diameter conduit arteries on the brain's surface is a major cause of this death and disability. However, compelling data are emerging to suggest additional phenomena, including enhanced constriction of the microcirculation, may also contribute to the development of neurological deficits in SAH patients. The objective of the present study was to determine whether impairment of a key vasodilator pathway, Ca^{2+} sparks and associated activity of large-conductance Ca^{2+} activated K^+ (BK) channels, contribute to enhanced constriction of parenchymal arterioles following SAH.

Methods: Using a rabbit SAH model, parenchymal arterioles were isolated from the temporal lobe of the cerebral cortex and cannulated for in vitro diameter measurements. Individual myocytes were also enzymatically isolated from parenchymal arterioles for Ca^{2+} spark, single channel and whole-cell BK current measurements. To evaluate Ca^{2+} sparks, fluorescence intensity changes were monitored using laser scanning confocal microscopy in freshly isolated parenchymal arteriolar myocytes loaded with the Ca^{2+} indicator, fluo-4. Expression of BK channel alpha and beta-1 subunits and ryanodine receptor-2 (RyR2) was examined by RT-PCR.

Results: Ca^{2+} spark frequency was decreased by greater than 50% in parenchymal arteriolar myocytes following SAH (0.31 ± 0.07 Hz, $n = 16$) compared to healthy controls (0.78 ± 0.09 Hz, $n = 11$). Although Ca^{2+} spark frequency was dramatically reduced, mean Ca^{2+} spark amplitude, expressed as a fractional change in fluorescence (F/F_0), was similar in myocytes isolated from control and SAH animals. Additional spatio-temporal characteristics such as rise-time, duration, size, and decay were similar for Ca^{2+} sparks recorded from myocytes of control and SAH animals. This decrease in Ca^{2+} spark frequency corresponded to decreased RyR2 expression in myocytes from SAH animals. Using perforated patch whole-cell electrophysiology, transient BK currents were observed in parenchymal myocytes isolated from both control and SAH rabbits. As with Ca^{2+} sparks, the frequency of transient BK currents was decreased by approximately 60% following SAH, with no change in current amplitude. Single channel recordings obtained from excised “inside-out” membrane patches demonstrated no change in the Ca^{2+} or voltage sensitivity of BK channels following SAH. Further, the density of functional BK channels detected in excised membrane patches was similar between groups, and BK channel alpha and beta-1 subunit expression was unaltered following SAH. Consistent with decreased Ca^{2+} spark/BK channel activity, parenchymal arterioles isolated from SAH rabbits exhibited enhanced constriction compared to arterioles isolated from healthy control animals.

Conclusions: In summary, we report the frequency of Ca^{2+} sparks and associated transient BK currents are significantly decreased in smooth muscle of parenchymal arterioles following SAH, contributing to enhanced vasoconstriction. This study may help to explain the impact of SAH leading to enhanced constriction of arterioles within the brain parenchyma following cerebral aneurysm rupture.

Brain PET Oral 6: Neurodegenerative Disorders

EVALUATION OF REFERENCE MODELS FOR [11C]ABP688 TARGETING THE METABOTROPIC GLUTAMATE RECEPTOR 5 IN RATS - APPLICATION TO AN EPILEPSY MODEL

D. Elmenhorst[1,2,3], G. Biagini[1,4], L. Minuzzi[3], A. Aliaga[1], G. Massarweh[1], M. Diksic[1], M. Avoli[1], A. Bauer[2], P. Rosa-Neto[3]

[1]Montreal Neurological Institute, McGill University, Montreal, QC, Canada, [2]Institute for Neurosciences and Biophysics INB-3, Research Center Juelich, Jülich, Germany, [3]Translational Neuroimaging Laboratory, Douglas Hospital, McGill University, Montreal, QC, Canada, [4]Department of Biomedical Sciences, University of Modena and Reggio Emilia, Modena, Italy

Objectives: An increase of metabotropic glutamate receptors type 5 (mGluR5) immunoreactivity was found in hippocampal specimens from patients suffering from pharmaco-resistant temporal lobe epilepsy. Further, pharmacologically induced myoclonic seizures could be suppressed by the systemic application of mGluR5 antagonists in mice. Based on this evidence, the primary objective of the present study was to determine the changes in receptor density of mGluR5 possibly occurring in the pilocarpine model of epilepsy in rats. Reference tissue methods for [11C]ABP688 were evaluated by in-vivo blocking experiments in control rats in order to avoid invasive blood collection procedures for quantifying receptor changes and to allow repeated scans in the same animal.

Methods: In order to evaluate if the rat cerebellum is a suitable reference region, 2 Sprague-Dawley (SD) rats were scanned twice in a microPET R4 scanner under isoflurane anesthesia for 60 min. Following a baseline scan, the selective antagonist M-MPEP (6mg/kg) was administered before the 2nd scan to block specific binding. Twelve arterial blood samples were drawn per each scan and corrected for metabolites. To compare changes in binding potential (BPnd) between control (n=9) and chronically epileptic (n=7) animals, SD rats were scanned for 60 min without blood sampling. The simplified reference tissue model (SRTM) and the 2 parameter version of the multi-linear reference tissue model (MRTM2) were used in a ROI based and voxel wise manner, respectively. The average time delay between pilocarpine induction of epilepsy and scanning was 88 days.

Results: Total distribution volumes (Vt) of cerebellum changed after M-MPEP blockade on average +1% and -7% using 2 tissue compartment modeling (2TCM) and Logan's non-invasive graphical analysis (NIGA), respectively. Binding in caudate-putamen was reduced by -66% and -67% to a Vt of 3.2-4.2 ml/ml (for comparison: cerebellum Vt: 2.9-3.4 ml/ml) for 2TCM and NIGA, respectively. BPnd based on 2TCM correlated well with BPnd derived from various reference models (SRTM, MRTM and its 2 parameter versions, NIGA). Time stability evaluation showed that BPnd and Vt determinations were stable after 50 min of scanning. Chronic epilepsy did not reveal significant changes in the ROI based analysis in the present sample. In the cingulate cortex - prelimbic cortex area, BPnd increased by 11% increase showing a trend towards significance (t-test, $p = 0.11$). Voxel wise statistical analysis showed significant clusters with decreased BPnd on the posterior ventral part of the hippocampus and with increased BPnd in mesial ventral frontal cortex.

Conclusions: The cerebellum is a suitable reference region for the quantification of mGluR5 availability with [11C]ABP688. Blood sample based quantification of BPnd correlates well with reference region based analyses. Scan duration of 50 min is required. The observed increase in receptor density in humans (hippocampal specimens) suffering from temporal lobe epilepsy was not observed in the pilocarpine model, but the stastical power has to be increased to confirm these results. The present results in the pilocarpine model contrast with the immunohistochemical studies in humans but are in agreement with receptor binding studies conducted by our group.

756

Brain Oral Session: Cerebrovascular Regulation

SEXUAL DIMORPHISM IN THE RESPONSE OF THE MIDDLE CEREBRAL ARTERY TO ACUTE HYPONATREMIA IN THE PRESENCE OF VASOPRESSIN

K. Klapczynska, **E. Kozniewska**

Neurosurgery, Mossakowski Medical Research Centre, Polish Academy of Sciences, Warsaw, Poland

Objectives: Hyponatremia contributes to impaired recovery of neurosurgical patients after subarachnoid hemorrhage (SAH), brain injury or stroke. The decrease in serum sodium concentration in these patients is usually caused either by natriuresis or retention of water. Both effects depend on vasoactive hormones. One of them - vasopressin is a strong vasoconstrictor, particularly under pathological conditions. In our previous study we have found that isolated, male middle cerebral artery (MCA) dilates in endothelium-dependent manner in response to hyponatremia. Our present study addresses the question of the effect of hyponatremia on female MCA and the influence of vasopressin on the response of male and female MCA to hyponatremia.

Methods: MCAs harvested from the brains of the adult male and female (in estrus phase of the menstrual cycle) Wistar rats were used for this study. The vessels were mounted in the small organ chamber filled with 3-(N- morpholino) propanesulfonic acid (MOPS) - buffered saline solution and pressurized. The chamber was placed on inverted microscope equipped with videocamera for the recording of changes in the diameter of MCA. Hyponatremia was induced by decreasing intra - and extraluminal concentration of Na^+ from 144 to 120 mM. In the experiments with vasopressin (AVP), the peptide was added to the extravascular bath before induction of hyponatremia in a concentration of 15 pg/ml which is comparable with that found in the cerebrospinal fluid of patients after SAH.

Results: Lowering of Na^+ concentration to 120 mM resulted in a comparable endothelium-dependent dilation of male and female MCA by about 20% ($p< 0.05$). Inhibition of NO/cGMP pathway abolished the effect of hyponatremia on male MCA and attenuated, but did not eliminate, hyponatremic response of female MCA. This suggests that hyponatremia stimulates production of another vasodilator, in addition to NO, in the endothelium of female MCA. Addition of AVP to the extraluminal bath before hyponatremia reversed hyponatremic response of male MCA to 14% constriction ($p< 0.005$). This effect of AVP was eliminated by pretreatment of MCA with a selective V1a receptor antagonist and attenuated by a nonselective endothelin receptor antagonist. In the case of female MCA, pretreatment with AVP attenuated only the hyponatremic dilation.

Conclusions: These results demonstrate that hyponatremic dilation of male and female MCA depends on different endothelium-dependent factors. They also indicate that modulation of hyponatremic response of MCA by vasopressin is sexually dimorphic and suggest that vasopressin-induced hyponatremia may increase the risk of vasospasm in male subjects.

Acknowledgements: This study was supported by the grant N401 19032/3924 from the Ministry of Science and Higher Education.

757

Brain Poster Session: Cerebral Vascular Regulation

THE RELATIVE ROLES OF CYCLOOXYGENASE-1 AND -2 AND EPOXYGENASE IN THE BLOOD FLOW RESPONSE TO WHISKER STIMULATION

X. Liu[1], C. Li[1], D.R. Harder[2], R.C. Koehler[1]

[1]Department of Anesthesiology/Critical Care Medicine, Johns Hopkins University, Baltimore, MD, [2]Cardiovascular Research Center, Medical College of Wisconsin, Milwaukee, WI, USA

Objectives: In mice, cortical superfusion of 100 μM of the cyclooxygenase-2 (COX-2) inhibitor NS-398 decreased the laser-Doppler flow (LDF) response to whisker stimulation, whereas superfusion of 25 μM of the COX-1 inhibitor SC-560, which was sufficient to inhibit other vascular responses, had no effect on the whisker response (1,2). In contrast, SC-560 at a higher concentration of 500 μM inhibited vasodilation evoked by photolysis of astrocytic caged calcium in mouse cerebral cortex (3) and to odorant stimulation in olfactory glomeruli (4). One explanation for the differences in SC-560 efficacy among studies is that a COX-1 metabolite plays a permissive role in the vasodilatory response and that the high concentration of SC-560 reduces basal metabolites to critically low levels. The first objective of the present study was to compare the whisker stimulation-evoked LDF response at both concentrations of SC-560 and to determine if adding exogenous PGE2 restores the evoked response. Furthermore, inhibition of epoxygenase activity reduced the LDF response to whisker stimulation with and without indomethacin in the rat (5). Because most studies with COX-specific inhibitors were performed in mice, the second objective was to compare the efficacy of COX-1 and -2 inhibitors in the whisker response in rats and to determine if the EETs antagonist, 14,15-EEZE, decreased the LDF response further after COX inhibition.

Methods: The LDF response to 60 s of whisker stimulation was measured before and after 1 h of cortical superfusion of inhibitors in anesthetized rats and mice.

Results: In agreement with work in mice, cortical superfusion of 25 μM of SC-560 in rats did not affect the percent increase in LDF during whisker stimulation (21.7±2.5% to 22.1±2.4%; ±SD; n=6). Combined superfusion of 25 μM SC-560 with 30 μM 14,15-EEZE decreased the response (14.7±1.9%). With the high concentration of 500 μM SC-560 in rats, the LDF response decreased from 20.3±1.4% to 16.0±2.1%. Co-superfusion with PGE2 (5 μM) significantly restored the response to 18.9±0.8% (n=6), whereas co-superfusion with 14,15-EEZE (30 μM) reduced the response further to 13.7±1.8% (n=6). Superfusion of NS-398 (100 μM) in rats also reduced the CBF response from 20.3±1.1% to 17.8±1.6%, and combined superfusion with 14,15-EEZE further reduced the response to 16.0±1.6%. In mice, superfusion of 500 μM SC-560 had no effect on the LDF response to whisker stimulation (25.5±4.3% to 25.6±9.2%; n=9), whereas 100 μM NS-398 decreased the response (27.3±7.2% to 19.2±6.6%).

Conclusion: A COX-2 metabolite appears to contribute to neurovascular coupling in both mice and rat whisker barrel cortex, whereas a COX-1 metabolite is less important. The decrease in the LDF response to whisker stimulation at the high dose of SC560 in rats may be related to an obligatory role of maintaining a minimal basal level of a COX-1 metabolite. The epoxygenase pathway still contributes to the neurovascular response after inhibition of either COX isoform.

References:

1. Niwa et al. J Neurosci. 2000;20:763-70.

2. Niwa et al. Circ Res. 2001;88:600-608.

3. Takano et al. Nat Neurosci. 2006;9:260-267.

4. Petzold et al. Neuron. 2008;58:897-910.

5. Peng et al. Am J Physiol 2002;283:H2029-37.

760

Brain Oral Session: Cortical Spreading Depression

COMBINED LASER SPECKLE AND MULTISPECTRAL REFLECTANCE IMAGING OF CORTICAL SPREADING DEPRESSION IN WILD TYPE AND FAMILIAL HEMIPLEGIC MIGRAINE 1 MICE

I. Yuzawa[1], K. Eikermann-Haerter[1], S. Sakadzic[2], D.A. Boas[2], M.A. Moskowitz[1], C. Ayata[1,3]

[1]Stroke and Neurovascular Regulation Laboratory, Neuroscience Center, Massachusetts General Hospital & Harvard Medical School, [2]MGH/MIT/HMS Athinuola A. Martinos Center for Biomedical Imaging, Department of Radiology, [3]Stroke Service and Neuroscience Intensive Care Unit, Department of Neurology, Massachusetts General Hospital, Harvard Medical School, Charlestown, MA, USA

Objectives: Unlike in most other species, cortical spreading depression (CSD) is associated with a triphasic cerebral blood flow (CBF) response in mice, with a profound initial hypoperfusion followed by transient normalization of flow and a long-lasting post-CSD oligemia. We aimed to investigate the hemodynamic and metabolic impact of CSD non-invasively with high spatiotemporal resolution in mice using multimodal optical imaging. Using the model, we tested whether familial hemiplegic migraine type 1 (FHM1) R192Q mutation in $Ca_v2.1$ (P/Q-type) voltage-gated calcium channels augment the hemodynamic and metabolic impact of CSD.

Methods: Changes in CBF, oxyhemoglobin (oxyHb), deoxyhemoglobin (deoxyHb), total hemoglobin (as a surrogate measure for cerebral blood volume, CBV), mixed arteriovenous O_2 saturation ($S_{AV}O_2$), and cerebral metabolic rate of oxygen ($CMRO_2$) were simultaneously measured through intact skull using combined laser speckle flowmetry and multispectral reflectance imaging during CSD in isoflurane-anesthetized ($70\%N_2O/30\%O_2$) male wild-type (C57/BL6) and female Cacna1a R192Q knockin mice (n=5 each). The region of interest was within middle cerebral artery territory away from large surface vessels. Two consecutive CSDs were induced in frontal cortex 15 min apart by topical KCl (1M).

Results: The first CSD in cortex was associated with a profound hypoperfusion reaching ~30% of baseline. CBV was also reduced by 30% confirming vasoconstriction as a mechanism. OxyHb and deoxyHb showed reciprocal changes simultaneously with and dominated by the CBF and CBV changes. Consequently, $S_{AV}O_2$ decreased by ~50%. Although $CMRO_2$ showed a small early rise at the onset of CSD (< 10%), it rapidly dropped to ~50% of baseline, presumably due to O_2 supply limitation. After a characteristic transient normalization 1-2 min after CSD onset, post-CSD oligemia ensued (CBF ~30%, CBV ~70%, $CMRO_2$ ~50%, $S_{AV}O_2$ ~60% of pre-CSD baseline). The hemodynamic and metabolic response to the second CSD was dramatically different: superimposed on the post-CSD oligemia, all measured parameters showed a monophasic increase lasting 3-4 min. No significant difference was observed between wild type and R192Q knockin mice in any measured parameter. [Figure: Data are average of all mice shown as % of baseline (except $S_{AV}O_2$ expressed as % Hb saturation, resting state empirically taken as 65%). Horizontal axis shows time in min.].

Conclusions: Our data demonstrate the unique vasoconstrictive vascular response to SD in mouse cortex, and show that O_2 metabolism becomes supply-limited. Post-CSD oligemia is associated with tissue hypoxia as evidenced by hemoglobin desaturation. Caution must be exercised to monitor for CSD occurrence during experimental preparation, and to distinguish the first CSD occurring in naïve mouse cortex and subsequent ones, as the vascular response to subsequent CSDs, and the baseline that they are superimposed upon, are very different.

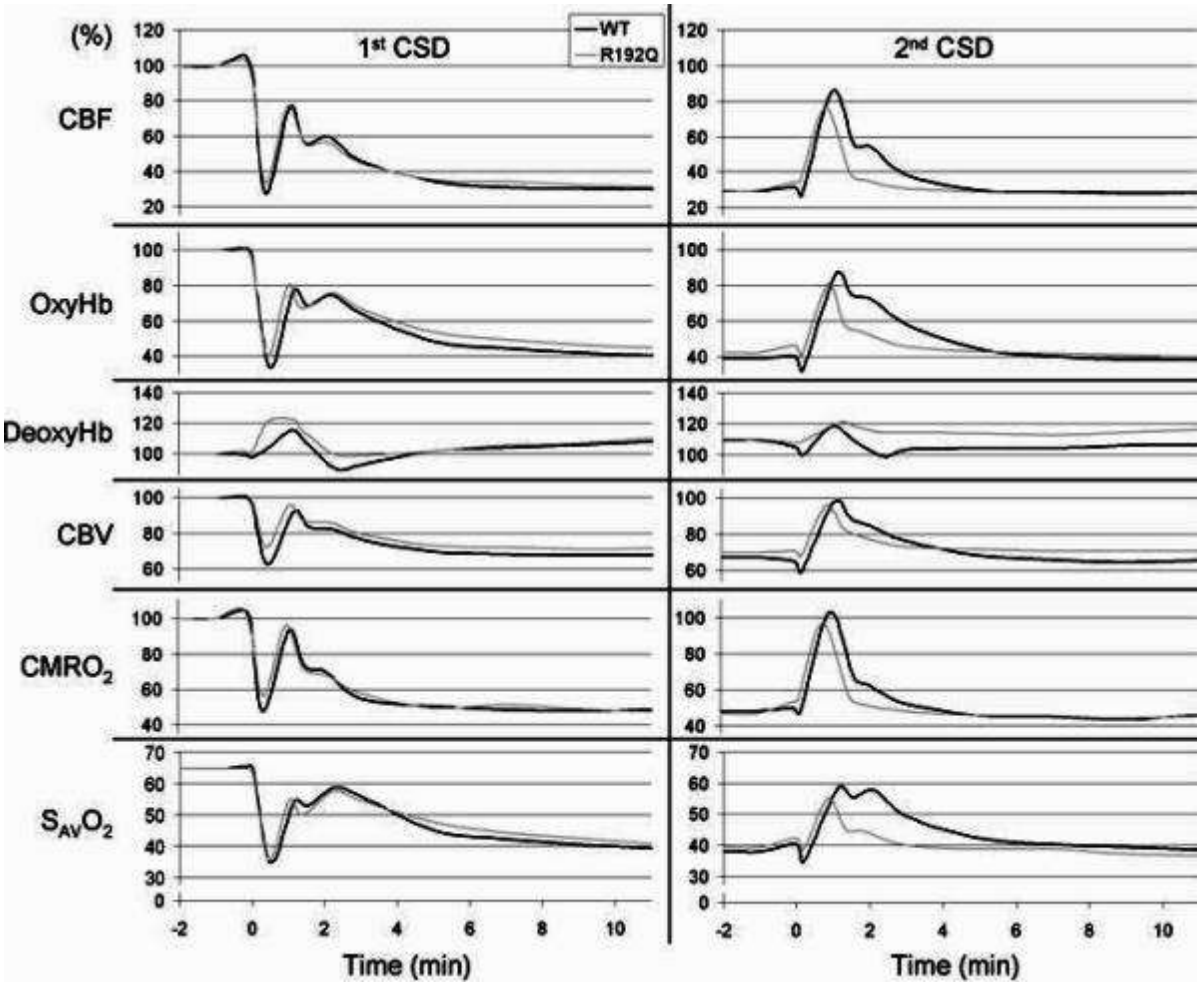
(%)
1st CSD
2nd CSD
WT
R192Q
CBF
OxyHb
DeoxyHb
CBV
CMRO2
SAVO2
Time (min)
Time (min)

[Figure]

761

Brain Poster Session: Neurologic Disease

MAPPING PROGRESSIVE LOSSES IN [^{18}F]FPCIT BINDING IN EARLY STAGE PARKINSON'S DISEASE: A LONGITUDINAL PET STUDY

Y. Ma, S. Peng, P. Spetsieris, V. Dhawan, D. Eidelberg

Center for Neurosciences, The Feinstein Institute for Medical Research, Manhasset, NY, USA

Objectives: PET imaging with radioligand [^{18}F]FPCIT provides a valuable means for quantifying regional abnormality and clinical correlate in dopamine transporter (DAT) binding associated with Parkinson's disease (PD). We have previously shown bilateral losses of DAT binding in the posterior putamen in hemi-PD subjects. In this study, we sought to delineate the topographic distribution of striatal DAT binding reductions in PD patients and its longitudinal change during early phases of the disease progression.

Methods: We performed dynamic [^{18}F]FPCIT PET studies over 100 minutes in eight parkinsonian patients (age= 59.2 ± 8.0 yr; Hoehn & Yahr stages 1-2.5; UPDRS= 8.5 ± 5.3) at baseline and at approximately four years. Ten age-matched normal subjects (age= 62 ± 10.4 yr) served as controls. Volumetric maps of [^{18}F]FPCIT binding were calculated on a voxel-by-voxel basis at 95 min post-injection and spatially normalized based on corresponding mean images generated over early frames. Statistical parametric mapping (SPM) was then used to localize binding reductions in PD relative to controls as well as to detect interval changes between the two time points in PD patients. The analysis was restricted within a striatal brain mask due to the existence of a prior hypothesis. Local changes in FPCIT binding was assessed post-hoc over spherical volumes (8 mm in diameter) centered at the peak coordinates of interest.

Results: Relative to the normal mean, [^{18}F]FPCIT binding decreased significantly in the bilateral putamen of the PD group at baseline (contralateral: -26 -8 4, Zmax= 6.36, cluster= 5.5 ml; ipsilateral: 34 -16 2, Zmax= 5.33, cluster= 5.1 ml; $p< 0.001$; Figure 1A). The decrease was larger in extent at the follow-up time point (contralateral: -28 -8 4, Zmax= 6.70, cluster= 7.1 ml; ipsilateral: 32 -10 4, Zmax= 5.67, cluster= 5.9 ml; $p< 0.001$). The cluster in the ipsilateral putamen was smaller in size than that in the contralateral side, but localized slightly more posterior. A significant reduction was also seen between the two time points only at a lower threshold of $p< 0.01$, with more DAT binding loss in the ipsilateral putamen. Progressive losses of [^{18}F]FPCIT binding were evident in the post-hoc analysis (e.g. Figure 1B). By contrast, there were no increases in DAT binding within the striatum of PD patients.

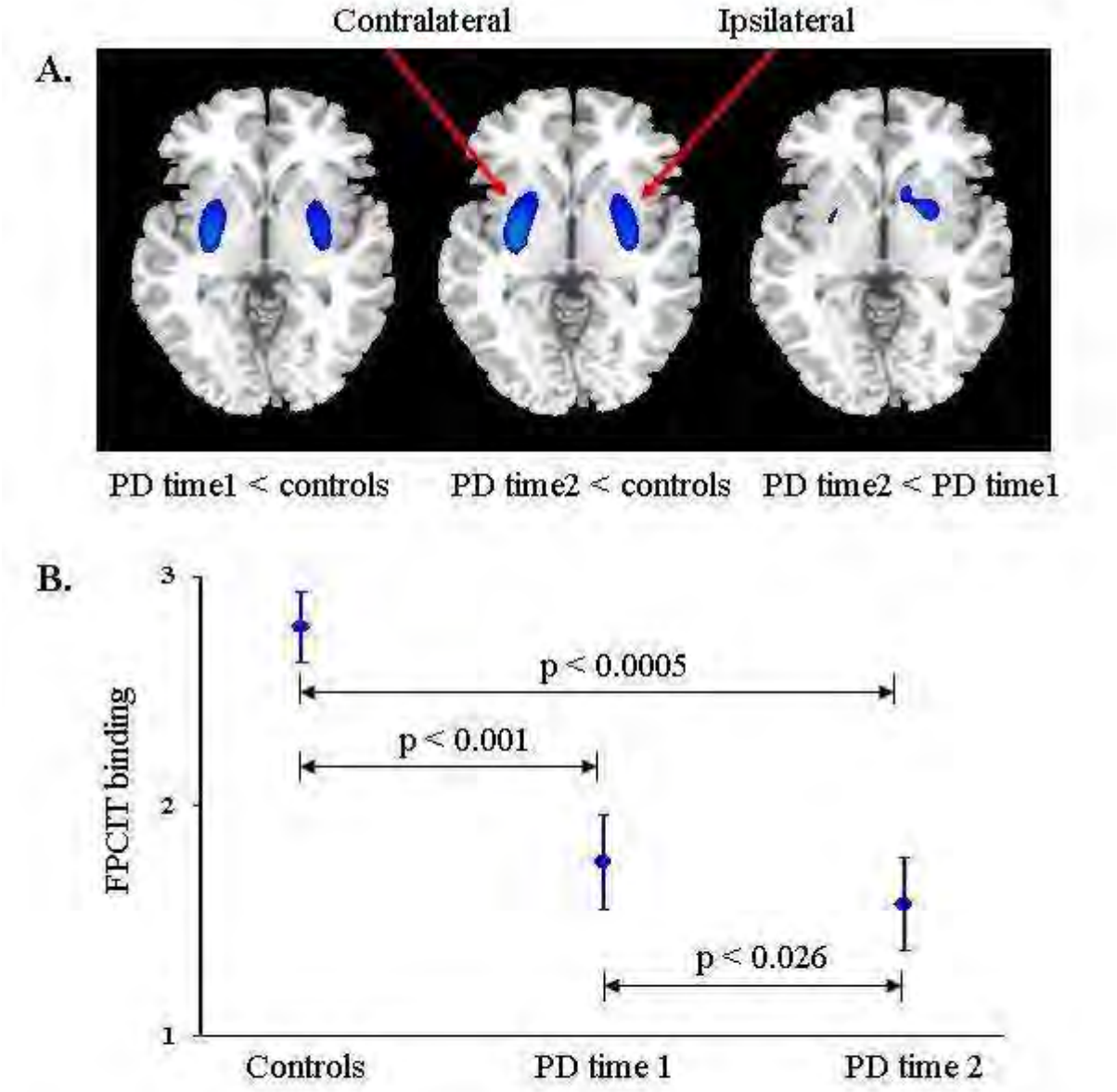

Decreased FPCIT binding in the putamen of PD patients relative to controls, with the mean values and standard errors plotted over the spheres at (24, 4, -2).

[Figure 1: SPM maps (A) and post-hoc VOI plot (B).]

Conclusions: Brain mapping analysis of [^{18}F]FPCIT PET data is capable of quantifying and mapping anatomically specific abnormalities in straital DAT activity in patients with PD. Our data seem to suggest different rates of decline in striatal DAT binding in the contralateral and ipsilateral putamen. This method offers a useful tool to track the onset and progression of PD at its early stages.

References: 1. Ma, Y et al (2002), 'Parametric Mapping of [^{18}F]FPCIT Binding in Early Stage Parkinson's Disease: a PET Study'. Synapse, 45:125-133.

762

Brain Oral Session: Traumatic Brain Injury: Metabolism

PROLONGED CEREBRAL HYPOMETABOLISM FOLLOWING MILD TRAUMATIC BRAIN INJURY DETECTED BY ^{1}H MAGNETIC RESONANCE SPECTROSCOPIC IMAGING AT 3T

B. Bartnik-Olson[1], K. Tong[1], S. Uffindell[2], V. Wong[3], S. Ashwal[4], B. Holshouser[1]

[1]Radiology, [2]Neurology, Loma Linda University, Loma Linda, [3]Redlands Pediatric and Adult Medicine, Redlands, [4]Pediatrics, Loma Linda University, Loma Linda, CA, USA

Objectives: Approximately 80% of traumatic brain injuries (TBI) are classified as mild (1). Neurocognitive deficits are estimated to occur in 50-80% of patients, which may persist for several years after injury (2) even though conventional imaging findings may be normal. ^{1}H magnetic resonance spectroscopic imaging (MRSI) offers an alternative approach to non-invasively measure cerebral metabolism; specifically, N-acetlyaspartate (NAA), representing neuronal metabolism; total creatine (Cr), indicative of energy metabolism and total choline (Cho), representing membrane metabolism. The study objective was to compare cerebral metabolism in mild TBI subjects (mTBI) with neurocognitive deficits to controls using 3D ^{1}H MRSI. We hypothesized that mTBI subjects would have areas of hypometabolism, as defined by decreased Cr levels, which may explain cognitive deficits.

Methods: Five adult mTBI (90 - 1050 days post-injury) and 3 control subjects were retrospectively identified for this study. Using a Siemens Tim Trio 3T scanner, 3D MRSI (PRESS TR/TE = 1700/144 msec, voxel size 1cm^3) of a 9 cm A-P x 8 cm R-L x 6 cm S-I volume of interest (VOI) covering the centrum semiovale through the midbrain was obtained. 3D fast spin echo T2-weighted MRI (SPACE, TR/TE = 3200/458 msec, pixel size = 1 mm^3) was used for VOI positioning. LCmodel was used to semi-quantitatively measure NAA, Cr, and Cho peak integrals with NAA/Cr, NAA/Cho, and Cho/Cr ratios calculated for each voxel. MRSI voxels were manually selected in normal appearing brain in the frontal grey (FG), frontal white (FW), parieto-occipital grey (POG) and parieto-occipital white (POW) matter. Voxels containing >10% CSF were excluded. Spectral findings were classified as hypometabolic if ratios were 2 standard deviations above the mean control ratio for that region due to decreased Cr but normal NAA . Pooled regional ratios were calculated for each subject. Statistical significance was measured using independent samples t-test with a significance = $p < 0.05$.

Results: Pooled regional ratios did not differ between mTBI and controls. In contrast, 58% of FW and 49% of FG voxels in mTBI subjects showed evidence of hypometabolism as seen by increased NAA/Cr ($p < 0.001$) and Cho/Cr (31% and 39%, respectively; voxel $p < 0.001$). In addition, 56% of FW and 37% of FG voxels showed increased NAA/Cho ($p < 0.001$) compared to controls. Less than 5% of voxels in the POG or POW showed an increase in any metabolite ratio.

Conclusions: To our knowledge this is the first study to report decreased Cr and Cho in mTBI adults. Decreased Cr indicates a prolonged reduction in energy metabolism and may be related to decreased perfusion reported in SPECT studies following mTBI (3). Decreased Cho may suggest altered membrane biosynthesis, resulting in decreased cholinergic function and memory impairment (4). These findings show metabolic abnormalities in normal appearing brain that may help explain cognitive deficits.

References:

1. Esselman PC, Umoto JM. 1995. Brain Inj 9:417-424.

2. Govindaraju V, et al. 2005. AJNR Am J Neuroradiol 25:730-737.

3. Gowda NK, et al. 2006. AJNR Am J Neuroradiol 27:447-451.

4. Arciniegas DB. 2003. Curr Psychiatry Rep 5:391-399.

763

Brain Poster Session: Neuroprotection

NOVEL MECHANISM OF NEUROPROTECTION OF GINSENG AGAINST OXIDATIVE STRESS

S. Dore, Y.-S. Kim

Anesthesiology and Critical Care Medicine, Johns Hopkins University School of Medicine, Baltimore, MD, USA

Objectives: Ginseng, the root of Panax ginseng (Araliaceae), which has been reported to have antioxidant properties and neuroprotective effects against transient and permanent ischemic damage, is used in complementary and alternative medicine. We have postulated that some of ginseng's associated neuroprotective action might be mediated by the induction of heme oxygenase 1 (HO1) enzyme. Heme oxygenase is the only enzyme that can degrade heme (iron protoporphyrin-IX) to release free iron, carbon monoxide, and biliverdin/bilirubin. In the present study, we examined the neuroprotective actions of ginseng in primary neuronal cells and the potential biological mechanisms.

Methods: Primary cortical neurons isolated from 17-day-old embryos of timed-pregnant mice were plated onto poly-d-lysine-coated 24-well plates at a high density in high-glucose neurobasal medium supplemented with B27. To investigate the neuroprotective effects of ginseng, we pretreated neuronal cells with ginseng for 7h. Pretreatment is required to increase intracellular antioxidant components and endogenous antioxidant proteins. Then we changed the medium to that without antioxidant and exposed the cells to 10 μM tert-butyl hydroperoxide (t-BuOOH) for 16h. t-BuOOH was freshly diluted in the culture medium immediately before use. The cell viability was measured by MTT assay. Experiments were performed in triplicate and reproduced three times with different primary culture batches.

Results: We found that pretreatment of primary neuronal cells with ginseng (0, 25, 75, 100, 200, and 400 μg/ml) for 7h significantly increased the expression of HO1 in a dose-dependent manner and attenuated cell death induced by t-BuOOH (10 μM) cytotoxicity ($p< 0.05$). The HO inhibitor SnPPIX (5 μM) inhibited the neuroprotective effects of ginseng, and the protein synthesis inhibitor cycloheximide (5 μg/ml) inhibited the neuronal protective effects of ginseng against t-BuOOH-induced oxidative stress. Moreover, we did not detect a significant cytoprotective effect of ginseng in neuronal cultures derived from HO1 knockout mice. Ongoing work is being performed in in vivo models of focal and global ischemia.

Conclusions: Together, our results suggest that the neuroprotective effects of ginseng could be mediated at least partially by HO1 activity and its by-products. This mechanism of action could potentially address the preventive properties associated with ginseng, which might not necessarily occur by its direct antioxidant properties, but rather by stimulation of an endogenous system capable of resisting various stress stimuli associated with age, acute, and/or chronic neurodegenerative conditions.

(This work was supported by a NIH-NCCAM grant.)

CARBON MONOXIDE IS PROTECTIVE AGAINST PERMANENT FOCAL BRAIN ISCHEMIA

B. Wang, S. Doré

Anesthesiology and Critical Care Medicine, Johns Hopkins University School of Medicine, Baltimore, MD, USA

Objectives: Historically, carbon monoxide (CO) gas has been considered to be toxic. We have recently shown that CO can be neuroprotective in transient focal cerebral ischemia [Zeynalov E, Doré S, Neurotox. Res. In Press]. Using in vivo and in vitro approaches, we demonstrated that the rate-limiting enzyme for the endogenous synthesis of CO, heme oxygenase, is highly neuroprotective against various types of insults. Our long term goals are to determine whether low levels of CO would also limit histological and functional outcomes in the permanent focal ischemia and determine the optimal therapeutic window.

Methods: Two-month-old male C57BL/6 mice (22-28g) were subjected to the permanent middle cerebral artery occlusion model (pMCAO). Mice were then immediately exposed to room air or 250ppm CO for 18h. Mice were maintained for 7d after surgery. Neurological deficits were assessed at 1 and 7d after pMCAO using the sticky tape task. To measure infarct volume, brains were harvested, sliced into 50-µm thick sections, collected at 500-µm intervals, and stained with luxol fast blue/cresyl violet. In a separate cohort, blood levels of carboxyhemoglobin (COHb) and methemoglobin (MetHb) were determined. In addition to these standard measures and to determine whether low levels of CO exposure are sufficient to increase the inducible heme oxygenase-1 within the brain, immunohistology and Western blots were performed. All animal protocols were in accordance to NIH guidelines and approved by the JHU Animal Care and Use Committee.

Results: Mice that received 18h exposure to 250ppm CO beginning immediately after pMCAO developed a significantly smaller infarct size than control mice exposed to air only ($p< 0.05$; $n=12$). Under this experimental protocol, mice developed no obvious signs of intoxication or histological changes. The animals exposed to CO had a trend toward shorter time to remove the sticky tape from the paws of the ischemic side compared to animals exposed to air. Moreover, in the other mouse cohort, levels of COHb were only transiently increased after CO exposure, from 4.3% to 17.1%, no detectable changes were observed in the MetHb levels (n=6/group), and no anatomical changes following H&E staining. Finally, for the CO-induced HO1 expression, a significant increase at 48h and 7d after 18h-CO exposure as compared to controls was observed.

Conclusions: A brief exposure to low levels of CO limits brain damage following permanent ischemia. Together, these results support the hypothesis that CO per se has neuroprotective actions and that its effects on stroke do not only result from a decrease in ischemic-reperfusion induced injury. Physiological amounts of CO play a key role in many cytoprotective mechanisms. Low concentrations of exogenous CO have anti-inflammatory/anti-apoptotic effects, which would protect tissues and organs against a variety of hypoxic/ischemic insults. CO can also mediate vascular signaling leading to vasodilatation, improved collateral blood flow, and improved brain perfusion. Development of a protocol to maintain CO within optimal and safe levels could be a novel therapeutic tool to fight brain damage and improve neurological outcome associated with stroke and other age/vascular-related neurodegenerative disorders.

(Supported by a GEMI award, and NIH grants)

SEX DIFFERENCES IN RESPONSE TO DIHYDROTESTOSTERONE AND FLUTAMIDE IN ASTROCYTE CELL DEATH

M. Liu, P.D. Hurn

Anesthesiology and Peri-Operative Medicine, Oregon Health & Sciences University, Portland, OR, USA

Introduction: Male sex is an acknowledged risk factor for stroke. Testosterone (T) can be converted to 17 β-estradiol via the aromatase, or metabolized to dihydrotestosterone (DHT) via the enzyme 5a-reductase, a step that then does not permit aromatization to estradiol. We previously demonstrated that astrocytic cell death induced by oxygen-glucose deprivation (OGD) is sex-specific (1, 2). However, it is not clear if sex differences in response to T and DHT in astrocyte cell death contributes to the observed sex difference in response to ischemia. In the current study, we tested the hypothesis that male (XY) and female (XX) astrocytes are respond differently to T and DHT.

Methods: Primary sex-specific cultured cortical astrocytes were prepared from 1-3-day old male and female rat pups separately and grown to confluency in steroid-free medium (1, 2). Confluent monolayers (10-14 days in vitro) were incubated in anoxia chamber in glucose-, serum-free medium for 6 hours (oxygen-glucose deprivation, OGD), and then returned to normoxia and glucose-containing medium for 24 hours. Cell death was induced by OGD alone, or in combination with T, DHT, or Flutamide. These reagents were added 24 hours before OGD, and maintained during OGD and re-oxygenation. Cell death was estimated by lactate dehydrogenase (LDH) assay.

Results: Female astrocytes are less sensitive to OGD alone, or in combination with T or DHT than male astrocyte. Androgen receptor antagonist, Flutamide, protect against T or DHT combined with OGD-induced cell death in male astrocytes but not in female astrocytes.

Conclusions: We conclude that there are sex differences in ischemic sensitivity in female and male astrocytes, and male astrocytes (but not female) metabolize testosterone to DHT via the enzyme 5 alpha reductase, resulting in androgen receptor activation and enhanced cell death after OGD.

References:

1. Liu M, Hurn PD, Roselli CE and Alakyed NJ. Role Of P450 aromatase in sex-specific astrocytic cell death. Journal of Cerebral Blood Flow & Metabolism. 2007;27:135-41.

2. Liu M, Oyarzabal EA, Yang R, Murphy MJ, Hurn PD. A novel method for assessing sex specific and genotype specific response to injury in astrocyte culture. Journal of Neuroscience Methods. 2008; 171:214-217.

768

Brain PET Oral 4: In Vivo Pharmacology I: Dopamine and Norepinephrine

DOSE OCCUPANCY RELATIONSHIP FOR A DOPAMINE D1 RECEPTOR AGONIST USING [11C] NNC 112 IN NON-HUMAN PRIMATES

M. Slifstein[1,2], R. Nardi[3], J. Javitch[1,4], T. Cooper[5], J. Lieberman[1,4], A. Abi-Dargham[1,2]

[1]Psychiatry, Columbia University, [2]Division of Translational Imaging, New York State Psychiatric Institute, New York, NY, [3]Sentia Therapeutics Inc., NA, [4]Psychiatry, New York State Psychiatric Institute, New York, [5]Analytical Psychopharmacology, Nathan Kline Institute, Orangeburg, NY, USA

Objectives: DAR100A is the active enantiomer of DAR100 and is a potent D1 agonist under development to treat cognitive impairment and negative symptoms in schizophrenia. Our aim here was to demonstrate a dose-occupancy relationship for DAR100A using PET imaging in baboons with [11C]NNC112. Knowledge of the dose occupancy relationship would inform the choice of doses to be investigated in humans.

Methods: 2 adult male baboons were scanned at baseline and following 5 doses of DAR100A (total scans: 10= 3*2 +2*2) on the HR+ scanner. Scans were 90 min. DAR100A was given as a constant infusion starting 10 min prior to scanning and lasting through the entire scan. Arterial blood samples were taken to measure concentration of DAR100A in plasma. PET data were analyzed by SRTM with cerebellum as reference region. Plasma data were analyzed by HPLC. Brain regions were cortical (frontal, parietal, temporal and occipital) and striatum. Occupancy was computed as the fractional decrease in BPND (ΔBP) following DAR100A.

Results: A clear relationship was observed between plasma concentration of DAR100A (both the integral and initial value at the start of the scan) and ΔBP. Average occupancy across cortical regions was lower than in striatum at each plasma level of DAR100A (Figure 1, left). Fits to a concentration-occupancy relationship showed maximal occupancy of 53% in striatum and 22% in cortex (Figure 1, right) when maximal occupancy and EC50 were treated as free parameters, or 51% and 26% when EC50 was constrained to the same value in both regions (constrained EC50 of DAR100A concentration at start of scan = 85 ng/mL), consistent with literature showing approximately 25% of the specific binding signal of [11C]NNC112 in baboon cortex is due to 5HT2A binding [1], whereas striatal binding is due entirely to D1-like receptors.

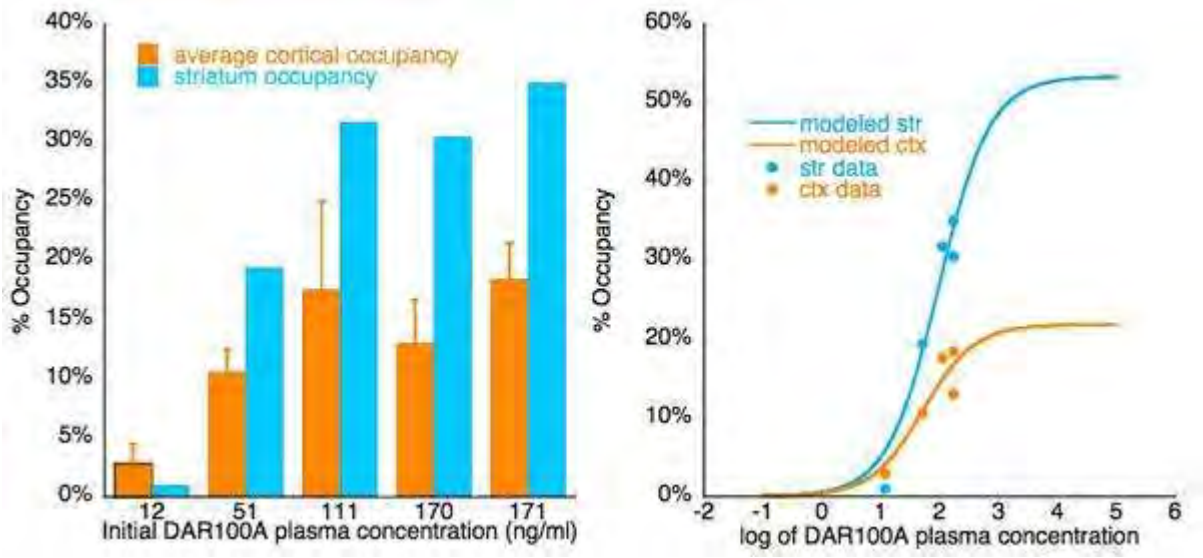

Conclusions: DAR100A reduces D1 binding of [11C]NNC112 in a dose dependent manner. Cortical ΔBP was lower than striatal ΔBP consistent with the known D1:5HT2A binding profile of [11C]NNC112. Estimated maximal occupancy was 53%, but this pharmacological ceiling effect will need confirmation with additional studies at higher doses than those described here. Previous failure to show vulnerability of dopamine D1 PET tracers to endogenous dopamine release has suggested that these tracers may not be sensitive to agonist competition. This is the first demonstration of significant occupancy by a full D1 agonist in vivo.

References: 1. Ekelund, J., et al., In vivo DA D-1 receptor selectivity of NNC 112 and SCH 23390. Molecular Imaging and Biology, 2007. 9(3): p. 117-125.

TRANSFORMING GROWTH FACTOR-β (TGF-β) SIGNALING IS INVOLVED IN THE REGULATION OF BLOOD-BRAIN BARRIER (BBB) FUNCTIONAL INTEGRITY DURING PERIPHERAL INFLAMMATORY PAIN

P.T. Ronaldson, K.M. DeMarco, L. Sanchez-Covarrubias, C.M. Solinsky, T.P. Davis

Department of Pharmacology, University of Arizona, Tucson, AZ, USA

Objectives: Our laboratory has shown altered BBB functional integrity during λ-carrageenan-induced peripheral inflammatory pain (CIP) characterized by changes in tight junction (TJ) protein expression and sucrose permeability (Huber et al. 2002; Brooks et al. 2005; Huber et al. 2006; Campos et al. 2008). However, the intracellular signaling mechanisms involved have not been elucidated. One pathway that may be involved is the transforming growth factor-β (TGF-β) system, which is known to regulate endothelial cell function. Of particular interest are processes mediated by activin receptor-like kinase 5 (ALK5), a TGF-β receptor that may decrease vascular permeability (Lebrin et al. 2005). The objectives of this study were to investigate, in vivo, the role of TGF-β/ALK5-mediated signaling on i) TJ protein expression in brain microvessels and ii) BBB permeability to ^{14}C-sucrose. Both objectives were evaluated in the context of CIP.

Methods: CIP was induced in female Sprague-Dawley rats (200-250 g) by subcutaneous injection of 3% λ-carrageenan into the plantar surface of the right hind paw. Control animals were injected with 0.9% saline instead of λ-carrageenan. SB431542 (1.5 mg/kg, i.p.), a selective ALK5 inhibitor, was administered 30 min prior to footpad injection. Similarly, human recombinant TGF-β1 (12.5 ng/kg, i.p.) was injected 30 min prior to CIP or control treatment. After 3 h, animals were sacrificed, blood samples collected, and brain microvessels isolated. ELISA was used to measure serum TGF-β1 concentrations. Protein expression of TGF-β receptors (i.e., ALK5), TJ proteins (i.e., claudin-3, claudin-5, occludin, ZO-1), and intracellular TGF-β signaling molecules (i.e., Smad2-4) were determined using immunoblot analysis. Brain permeability to ^{14}C-sucrose (10 μCi/ 20 ml perfusate) was assessed using the in situ brain perfusion technique.

Results: During CIP, serum TGF-β1 and ALK5 protein expression were reduced. Brain permeability to ^{14}C-sucrose was increased and expression of TJ proteins (i.e., claudin-5, occludin, ZO-1) were altered after 3 h CIP. Pharmacological inhibition of ALK5 with SB431542 further enhanced brain uptake of ^{14}C-sucrose, increased TJ protein expression (i.e., claudin-3, claudin-5, occludin, ZO-1), and decreased nuclear expression of TGF-β/ALK5 signaling molecules (i.e., Smad2, Smad3), suggesting a role for TGF-β/ALK5 signaling in the regulation of BBB functional integrity. Interestingly, administration of exogenous TGF-β1 prior to CIP activated the TGF-β/ALK5 pathway and reduced BBB permeability to ^{14}C-sucrose.

Conclusions: Our data show that TGF-β/ALK5 signaling is involved in the regulation of BBB functional integrity. Overall, these observations suggest that complex mechanisms are involved in controlling the dynamic nature of the BBB and may represent a novel target for pharmacological manipulation of brain microvascular permeability.

References:

1. Brooks T. A. et al. (2005). Am J Physiol Heart Circ Physiol 289, H738-H743.

2. Campos C. R. et al. (2008). Brain Res 1221, 6-13.

3. Huber J. D. et al. (2006). Am J Physiol Heart Circ Physiol 290, H732-H740.

4. Huber J. D. et al. (2002). Am J Physiol Heart Circ Physiol 283, H1531-H1537.

5. Lebrin F. et al. (2005). Cardiovasc Res 65, 599-608.

This work was supported by NIH grants R01-NS42652 and R01-DA12684 to TPD.

770

Brain Poster Session: Glial Functions

DIFFERENTIAL ACTIVATION OF MICROGLIA IN THE WHITE MATTER AFTER CLOSED SKULL TRAUMATIC BRAIN INJURY IN THE MOUSE

C. Venkatesan[1,2], M. Chrzaszcz[1,2], N. Choi[1,2], M. Wainwright[1,2]

[1]Department of Pediatrics, Division of Neurology, Northwestern University, Feinberg School of Medicine, [2]Center for Interdisciplinary Research in Pediatric Critical Illness and Injury, Children's Memorial Research Center, Chicago, IL, USA

Background and aims: The specific mechanisms by which microglia are activated and contribute to injury and repair following traumatic brain injury (TBI) have not been elucidated. In a mouse closed skull model, we have previously shown sustained long-term activation of glia as well as neurobehavioral deficits following TBI (Lloyd et al., J Neuroinflammation 2008, 5:28). The differential role of microglia in the mechanisms of injury and repair of the white matter following TBI is not known.

Methods: Adult CD1 mice were subject to midline closed skull injury or sham operation using a stereotactically guided pneumatic compression device. Animals were sacrificed 8 or 14 days after injury or sham procedure. Coronal frozen brain sections were cut at 40 micrometers on a freezing microtome and processed using standard immunohistochemical techniques. Antibody to the microglial marker IBA-1 was used to identify both resting and activated microglia. Antibody to Mac-2 was used to identify activated microglia alone. In order to evaluate the functional role of activated microglia, expression of the trophic factor Insulin-like growth factor (IGF) within microglia was also examined using an anti-IGF antibody. Patterns of labeling within the white matter underlying the impact site were analyzed qualitatively and quantitatively. Semi-quantitative analysis was performed in a blinded manner on digitized images.

Purpose: We tested the hypothesis that following TBI, there is a specific increase in the expression both of activated (Mac-2 immunoreactive) microglia, and a change in the functional properties of these activated microglia (increased IGF-expressing microglia) within the white matter.

Results: Qualitative and quantitative evaluation of IBA-1 immunureactive microglia showed no statistically significant differences between the sham and TBI groups. In contrast, there was a significant increase in the density of Mac-2 immunoreactive microglia within the white matter underlying the impact site 8 and 14 days post-injury ($p < 0.01$ vs sham). The increase was greatest 8 days after TBI. Comparison of Mac-2 staining in the two injury groups showed that there was a significant attenuation in the density of labeled cells 14 days following injury ($p < 0.01$ vs 8-days post injury). There was also an increase in IGF-immunoreactive microglia following TBI within the white matter.

Conclusions: These studies show that microglia have diverse phenotypes and a subset of microglia (identified by MAC-2 immunoreactivity) within the white matter are activated after TBI. This activation may involve a phenotypic switch of pre-existing microglia since there was no increase in the region examined in the density of IBA-1-immunoreactive cells following TBI. Further, the finding of an increase in the density of IGF-immunoreactive microglia supports a protective role for microglia for this microglial phenotype. Greater understanding of the mechanisms which distinguish the protective and pathologic phenotypes of activated microglia may advance the development of new therapeutic strategies to prevent the long term neurologic sequelae of TBI.

771

Brain Poster Session: Cerebral Vascular Regulation

INHIBITION OF TRPC3 BY PROTEIN KINASE G (PKG): A NOVEL COMPONENT OF NO-MEDIATED VASODILATION

J. Chen[1], M. Noorani[2], R. Crossland[3], **S. Marrelli**[1,3,4]

[1]Anesthesiology, [2]Pediatrics, [3]Graduate Program in Cardiovascular Sciences, [4]Molecular Physiology and Biophysics, Baylor College of Medicine, Houston, TX, USA

Objectives: A subset of the TRPC channels (TRPC3/6/7) are reported to be inhibited by NO/cGMP/PKG in expression systems. The purpose of the present study was to evaluate a possible role for TRPC3 channel regulation by NO in the vasculature. We sought to determine:

1. if the TRPC3 channel is inhibited by the NO-signaling pathway in freshly isolated smooth muscle cells and
2. if NO-mediated vasorelaxation involves TRPC3 channel inhibition.

Methods: We evaluated the role of the NO regulation of TRPC3 in freshly isolated smooth muscle cells (SMC) of the rat carotid artery using whole cell patch clamp. Extracellular UTP was used to activate TRPC3 channel currents. Contractions and relaxations of isolated carotid artery were measured in an isometric tension bath. L-NAME was present throughout to inhibit endogenous production of NO. Evaluation of TRPC channel expression was performed by standard RT-PCR, Western, and immunofluorescence techniques.

Results: TRPC3 and TRPC6 mRNA was expressed in carotid artery, whereas TRPC7 mRNA was not. TRPC3 protein was found in whole carotid artery by Western and further localized to the smooth muscle by immunofluorescence.

Whole cell patch clamp studies demonstrated that UTP (60 μM) produced a non-selective cation current (I_{UTP}) that was completely inhibited by La^{3+} (100 μM). We confirmed that the current was carried by TRPC3 by including selective TRPC channel antibodies in the patch clamp pipette solution. Intracellular delivery of TRPC3 antibody, but not TRPC6 antibody, significantly inhibited I_{UTP}. These studies demonstrated that I_{UTP} is dependent primarily on TRPC3 channel activation.

We next evaluated the ability of the NO signaling pathway to inhibit TRPC3 channels. Incubation with an NO donor (MAHMA-NONOate; 10 μM) or a cell-permeant cGMP analog (8Br-cGMP; 100 μM) led to a decrease in I_{UTP}. The inhibitory response of 8Br-cGMP on I_{UTP} was reversed in the presence of a PKG inhibitor (KT5823; 1 μM), demonstrating the requirement of PKG activation in the inhibition of TRPC3 by the NO-signaling pathway.

Lastly, we examined the role of TRPC3 channel inhibition in the mechanism of NO-mediated vasorelaxation in intact arteries. Carotid artery rings were contracted to UTP (100 μM) in the presence or absence of La^{3+} (100 μM). We then performed a concentration-response curve to an NO donor (SNP; 1 nM to 1 μM). The relaxations to SNP in the La^{3+}-treated group were significantly less compared with the untreated group. These results demonstrated that NO inhibits a La^{3+}-sensitive channel in the mechanism of vasorelaxation.

Conclusions: Carotid artery SMC expresses TRPC3 channels that are activated by extracellular UTP. These channels are significantly inhibited by NO or cGMP via a PKG-dependent mechanism. In the

intact artery, NO promotes relaxation in part by inhibition of a La^{3+}-sensitive channel. When the intact vessel and the patch clamp data are considered together, the data are highly suggestive of a role for TRPC3 channel inhibition in NO-mediated vasorelaxation. We propose that NO-inhibition of TRPC3 contributes to the overall mechanism of NO-mediated vasorelaxation.

(Supported by NIH R01-HL088435)

Brain Poster Session: Neurovascular Unit in Health & Disease

NEURONAL PGE_2 IS INVOLVED IN CEREBRAL BLOOD FLOW RESPONSE TO SOMATOSENSORY STIMULATION IN CHLORALOSE ANESTHETIZED RATS

A. Kocharyan[1], B. Stefanovic[2,3], A.C. Silva[1]

[1]Cerebral Microcirculation Unit, Laboratory of Functional and Molecular Imaging, National Institute of Neurological Disorders and Stroke, National Institutes of Health, Bethesda, MD, USA, [2]Imaging Research, Sunnybrook Health Sciences Centre, [3]Medical Biophysics, University of Toronto, Toronto, ON, Canada

Objectives: Cyclooxygenase (COX-1 and COX-2) products are important factors in the fine physiological processes of neurovascular coupling (Wang H. et al., 2005; Stefanovic B. et al., 2006). However, the specific roles of each COX isoform in eliciting the local vascular response to neural activity remains poorly understood and conflicting data exist (Niwa K et al., 2000; Takano et al., 2006).

In the present study we investigated the influence of the selective COX-1 and COX-2 inhibitors and prostaglandin E_2 (PGE_2) EP_1 subtype receptor antagonist on the cerebral blood flow (CBF) response and the microcirculatory volume in the superficial cortical layers in a rodent model of somatosensory stimulation.

Methods: Laser-Doppler flow and somatosensory-evoked potentials (SEPs) elicited in response to electrical stimulation of the contralateral forepaw (2mA, 333μs, 3Hz) were recorded in alpha-chloralose-anesthetized rats (n=5-8 per group) with implanted cranial windows during local superfusion (5μl/min) of SC-560 ($5x10^{-4}$M), NS-398 ($6x10^{-4}$M), SC-19220 (10^{-4}M) or respective vehicle. Arterial blood pressure, respiration patterns, oxygen saturation, arterial blood gases, arterial pH and rectal temperature were maintained during the experiments.

To estimate vessel volume we used two-photon imaging of intravenously administered rhodamine-labeled dextran (70,000 MW) with 805 nm excitation through a cranial window. High-resolution images at 5μm axial steps before and during forepaw stimulation from 3 different levels (pial vessels, layer I and layer II-III) were 3D reconstructed (Metamorph) and the areas covered by the microvasculature were compared in different conditions.

For immunohistochemistry 30μm thick cryosections were incubated first in either anti-COX-1 or anti-COX-2 antibodies (Cayman), stained with DAB or fluorescent secondary antibodies then in anti-c-Fos (Calbiochem) or anti-rat brain pyramidal cells or anti-s100β (SWANT) or Iba1 (Wako) antibodies and stained with DAB-Ni or respective fluorescent secondary antibodies.

Results: We found that cortical superfusion with the specific COX-2 inhibitor NS-398 and EP_1 antagonist SC-19220 caused a significant attenuation of the CBF response to somatosensory stimulation to 61.5 and 74.2%, respectively, ($p< 0.05$) of the response obtained during superfusion with vehicle. In contrast, the preferential COX-1 inhibitor SC-560 did not change the CBF response ($p>0.05$). Furthermore, local superfusion of the responsive area with PGE_2 (10^{-5}M), one of the vasoactive products of cyclooxygenase, resulted in recovery of the NS-398 attenuated CBF response back to 84.6% ($p< 0.05$) of the original response. Double-immunohistochemistry shows that numerous cortical COX-2-positive cells are expressing c-Fos after somatosensory stimulation. All the investigated COX-2 cells also are positive for pyramidal cell marker. In contrast, COX-1 cells are co-localized with microglial cell marker Iba1 and do not co-localize with the astrocytic marker s100β.

We also found an increase in the rhodamine covered area in 3D reconstructed two-photon images by 7.4, 52.2 and 24.6% respectively in the level of pial vessels, layer I and layer II-III in response to

forepaw stimulation. Superfusion with NS-398 significantly attenuated this vasodilatation response of pial vessels and in layer II-III.

Conclusion: Products of cyclooxygenase are modulators of the neurovascular coupling and production of the neuron-originated prostaglandins such as PGE_2 is necessary for the normal cerebrovascular reactivity to forepaw stimulation.

773

Brain Poster Session: Neurologic Disease

A PROGRESSIVE INCREASE IN BRAIN MICROHEMORRHAGES CORRELATES WITH SPORADIC LATE-ONSET DEMENTIA DEVELOPMENT

W.M. Kirsch[1], M. Schrag[1], G. McAuley[1], J.P. Larsen[2], S. Peterson[2], W. Britt III[3], F. Petersen[4], C. Dickson[1], D. Kido[5], M. Ayaz[6], E.M. Haacke[6], **W.J. Pearce**[7], L. Liotta[8], H.V. Vinters[9]

[1]Neurosurgery Center for Research, Training, and Education, [2]Department of Medicine, Geriatric Medicine, [3]Department of Psychiatry, [4]Health Research Consulting Group, [5]Department of Radiology, Loma Linda University, Loma Linda, CA, [6]MRI Institute for Biomedical Research, Detroit, MI, [7]Center for Perinatal Biology, Division of Physiology, Loma Linda University, Loma Linda, CA, [8]Department of Molecular and Microbiology, George Mason University, Manassas, VA, [9]Division of Neuropathology, UCLA Medical Center, Los Angeles, CA, USA

Objectives: Our goal is to define the pathogenesis of sporadic late-onset dementias studying brain microvasculature with new minimally invasive technologies.

Methods: For the past 5.5 years we have monitored the cognitive course of 76 mildly cognitively impaired (MCI) and 28 cognitively normal elderly individuals applying new MR contrast (Susceptibility Weighted Imaging, SWI) and proteomic tools ("carrier protein stripping"). The protein discovery tools are novel and are yielding previously unknown blood proteins and peptides considered to be of very low abundance. Low molecular weight fragments in the range of 40 kDa or less are being detected. Validation of these biomarkers has been conducted using antibodies raised against the candidates. The SWI sequence at 1.5T is at least fourfold more sensitive than conventional 1.5T GE-T2* for the detection of brain microbleeds (BMB). SWI is a 3-dimensional velocity compensated gradient echo sequence combining magnitude information with phase information that enhances contrast of magnetic field inhomogeneities combing phase and magnitude information permits shorter echo times, improves signal to noise ratio and detection of subvoxel susceptibility scores.

Results: SWI at 1.5T revealed an unanticipated association of cognitive loss with increasing BMB typical for "cerebral amyloid angiopathy (CAA)." SWI is superior to conventional gradient echo T2* (GE-T2*) for BMB detection. Nine of 26 MCI participants followed to dementia have significant MH and unique serum proteins, peptides from the heme degradation pathway. Our human experiment is the first prospective evidence for CAA microvasculopathy in the pathogenesis of late onset dementia.

Conclusions: As a result of the association between cerebral MH and progression to dementia, 3 key endpoints have been added to our study:

a. quantifying the location of MH by 3T SWI during the course of dementia,
b. proteomic studies of peripheral blood to complement SWI BMB detection to develop a clinical test for CAA and
c. determine the role of CAA hypoxic and apoptotic mechanisms responsible for neuronal and cognitive loss in an appropriate transgenic mouse model.

Defining the role of microvasculopathies in the pathogenesis of sporadic late-onset dementia may result in new therapeutic strategies.

This research was funded by NIH grant AG20948.

Kirsch WM, McAuley G, Petersen F, Chen LH, Kim I, Baqai W, Schrag M, Haacke EM, Ayaz M,

Khan A, Britt III W, Larsen J, Peterson S, Dickson C, Oyoyo U, Holshouser B, Mueller C, Vinters HA, Kido D. Serial Susceptibility Weighted MRI measures brain iron and microbleeds in dementia. Journal of Alzheimer's Disease, accepted Jan 2009.

Brain Oral Session: Neurological Diseases

[^{18}F]FETA PET - A NEW METHOD FOR HOT SPOT IMAGING OF THE ISCHEMIC PENUMBRA IN ACUTE STROKE

H. Barthel[1,2], U. Großmann[2], V. Zeisig[3], M. Patt[1], D. Wagner[3], J. Patt[1], M. Kluge[1], H. Franke[4], D. Sorger[1], J. Luthardt[1], B. Nitzsche[3], A. Dreyer[3], P. Brust[5], J. Steinbach[5,6], J. Boltze[2,3], F. Emmrich[2,3], O. Sabri[1]

[1]Department of Nuclear Medicine, University of Leipzig, [2]Translational Centre for Regenerative Medicine, University of Leipzig, [3]Fraunhofer Institute for Cell Therapy and Immunology, [4]Rudolph-Boehm-Institute of Pharmacology and Toxicology, [5]Institute of Interdisciplinary Isotope Research, University of Leipzig, Leipzig, [6]Institute of Radiopharmacy, Forschungszentrum Dresden-Rossendorf, Dresden-Rossendorf, Germany

Objectives: In acute ischemic stroke, an imaging method to directly visualize the ischemic penumbra - the salvageable part of the affected brain - in positive image contrast would potentially improve therapy stratification and monitoring. This study aimed to test [^{18}F]fluoroetanidazole ([^{18}F]FETA), a second-generation radiolabeled 2-nitroimidazole, for the first time with respect to its suitability to image brain hypoxia with positron emission tomography (PET).

Methods: Primary embryonal corticoencephalic cells (Wistar rats) and necortical brain slices (Sprague Dawley rats) were ex vivo exposed to nitrogen or air. The cells and brain slices were incubated with 5MBq [^{18}F]FETA up to 120min, respectively. The activities of three nitroreductases - enzymes which mediate the intracellular [^{18}F]FETA accumulation - were determined in the corticoencephalic cells. Further, organ distribution was determined in Sprague Dawley rats up to 2h after i.v. injection of 20MBq [^{18}F]FETA, and ex vivo brain autoradiography was performed up to 24h after permanent middle cerebral artery occlusion (pMCAO). Target-to-background image contrast of [^{18}F]FETA autoradiograms at 3h after pMCAO was compared with that of corresponding [^{18}F]fluoromisonidazole ([^{18}F]FMISO) autoradiograms. At 24h after pMCAO, animals were additionally i.v. injected with 1MBq [^{14}C]iodoantipyrine to determine the local cerebral blood flow (lCBF). Nissl staining of brain slices as well as stroke-specific MRI were carried out at 24h after pMCAO to confirm the existence and localization of ischemic brain tissue damage.

Results: In vitro, the oxygen concentration in the cell suspension was < 1 mm Hg and ~70 mm Hg under nitrogen and air, respectively. The normoxic [^{18}F]FETA uptake by the cells and the brain slices was low and constant over time (0.3±0.08 %ID.mio cells^{-1} and 0.04±0.01 %ID.g tissue^{-1}). In contrast, under hypoxia a time-dependent linear increase of the [^{18}F]FETA uptake was found which was 2.0- and 2.5-fold by the cells and 2.0- and 2.4-fold by the brain slices at 60min and 120min ($p < 0.05$), respectively. The analyses of nitroreductases activities showed that cell oxygenation does not affect the enzyme activities. The biodistribution studies revealed a fast blood clearance, a rapid urinary excretion and a constantly low uptake in unaffected brain tissue (0.1±0.02 %ID.g^{-1}). Ex vivo brain autoradiography in the pMCAO rats showed a relevant time-dependent [^{18}F]FETA uptake in ipsilateral brain regions which reached maximum target-to-background ratios of 3.3±0.2 at 3h. The corresponding [^{18}F]FMISO uptake ratios were only 1.5±0.3 ($p < 0.05$). Furthermore, at 24h after pMCAO the lCBF was reduced in the infarction core (as determined by Nissl staining and MRI) and surrounding brain areas by 25% and 10%, respectively.

Conclusions: These results demonstrate that [^{18}F]FETA has a better potential than [^{18}F]FMISO to serve as a brain hypoxia marker. Further testing of this promising new stroke PET marker is warranted. First results employing a new sheep stroke model developed recently by our group [1] are encouraging.

References: [1] Boltze et al., J Cereb Blood F Metab 2008.

First and second author contributed equally to this study.

This research was supported by the Translational Centre for Regenerative Medicine Leipzig / BMBF (PtJ-Bio 0313909).

776

Brain Poster Session: Brain Imaging: Neurologic Disease

CORRELATION OF HYPOINTENSITIES IN SUSCEPTIBILITY WEIGHTED MAGNETIC RESONANCE IMAGES TO TISSUE HISTOLOGY IN DEMENTIA PATIENTS WITH CEREBRAL AMYLOID ANGIOPATHY

M. Schrag[1], G. McAuley[1], J. Pomakian[2], H. Vinters[2], C. Mueller[1], W. Kirsch[1], **W.J. Pearce**[3]

[1]Loma Linda University School of Medicine, Loma Linda, [2]University of California Los Angeles, Los Angeles, [3]Center for Perinatal Biology, Division of Physiology, Loma Linda University, Loma Linda, CA, USA

Objectives: Recent neuroimaging studies of the Alzheimer's disease (AD) brain using susceptibility weighted (SWI) or conventional gradient echo T2* magnetic resonance have noted focal hypointensities distributed in a lobar pattern. The presence of these hypointensities has been shown to correlate with reduced global cognitive function and a significant risk for the progression of mild cognitive impairment to outright dementia. Because these imaging protocols are sensitive to iron, these findings were interpreted as small hemorrhages which have been termed “brain microbleeds." This study undertakes a systematic correlation of SWI hypointensities to tissue pathology in post mortem AD and cerebral amyloid angiopathic (CAA) brain to evaluate whether they are in fact related to hemorrhages.

Methods: Eight cases were imaged by susceptibility weighted imaging in a 3T MR scanner. Each was found to contain hypointensities and the corresponding foci in the tissue were carefully dissected.

Results: Post-hemorrhagic sites in various stages of resolution were detected in all but one specimen which was found to contain a thrombus enclosed within a vessel. The lesions measured between 1-7mm in diameter. When the ruptured vessel was still present, beta-amyloid immunohistochemistry confirmed the presence of amyloid in the vessel wall. Significant cellular apoptosis was noted in the perifocal region of recent bleeds along with heme oxygenase 1 activity and late complement activation.

Conclusions: Correlation of imaging findings to tissue pathology is time-consuming, but is a necessary validation of these techniques which will potentially offer AD patients and their families diagnostic and prognostic information which will guide therapy.

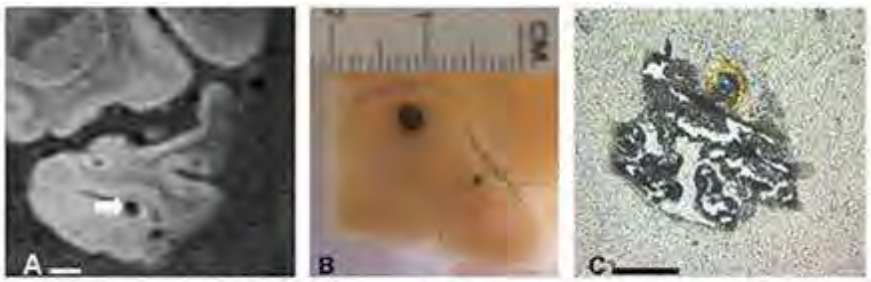

FIGURE: The hypointensities in SWI of the left temporal lobe shown in image A are localized in the tissue as shown in image B. Under microscopy it is clear that the lesion is closely associated with a vessel, which is stained a brilliant yellow by hemotoiden, an endogenous pigment produced by heme degradation.

[Schrag]

777

Brain Poster Session: Ischemic Preconditioning

THE ANTI-INFLAMMATORY CHEMOKINE CXCL12, AND ITS RECEPTOR CXCR4, IN HYPOXIC PRECONDITIONING: EXPRESSION CHANGES AND CELL-SPECIFIC ROLES IN ESTABLISHING ISCHEMIC TOLERANCE

A. Stowe[1], A. Freie[1], R. Hu[1], R. Klein[2], J. Gidday[1]

[1]Neurological Surgery, [2]Internal Medicine, Washington University, School of Medicine, St. Louis, MO, USA

Objectives: Preconditioning to mild systemic hypoxia two days prior to transient middle cerebral artery occlusion (tMCAo) significantly reduces injury[1]. We found that a series of repetitive hypoxic preconditioning (RHP) stimuli extends the duration of ischemic tolerance for many weeks, concomitant with reductions in post-stroke leukocyte-endothelial adherence[2]. As chemokines regulate inflammatory neutrophil chemotaxis, the present study investigated chemokine participation - specifically, the role of the anti-inflammatory chemokine CXCL12 (SDF-1)[3] - in establishing the ischemia-tolerant phenotype. We examined spatio-temporal responses of CXCL12α/β (two splice variants identified at the mRNA level only) and one of its receptors, CXCR4, to single hypoxic preconditioning (SHP) and RHP, and to tMCAo with and without prior RHP.

Methods: Adult, male SW/ND4 mice were sacrificed 6, 12, or 24h, 2d, or 2wks after SHP (4h, 8%O_2) or RHP (9 exposures over 2 wks; 8% or 11%O_2; 2 or 4h). Additional mice were sacrificed 24h after 60-min tMCAo 2d, or 2 or 4wks after RHP (n=6/group). Cortical whole brain homogenates and capillary-rich fractions (isolated by differential centrifugation) were analyzed for CXCL12/CXCR4 message and protein expression by rtPCR (n=8/group) and immunoblot (n=4/group), or brains were sectioned for cellular localization by immunohistochemistry (n=3/group). One-way ANOVA determined significance ($p< 0.05$).

Results: CXCL12α mRNA increased four-fold ($p< 0.05$), and CXCR4 mRNA doubled ($p< 0.01$), in whole brain 12h after SHP, returning to baseline at 2d, a time when capillary expression of both CXCL12α and CXCR4 mRNA transiently doubled ($p< 0.05$). Neither whole brain nor capillary expression of CXCL12α or CXCR4 mRNA was elevated following RHP. SHP doubled CXCL12β mRNA ($p< 0.01$) by 2d in brain, but not capillaries; following RHP, this elevated expression in whole brain was maintained through 2wks ($p< 0.05$). RHP elevated brain CXCL12 protein at 2d and 2wks. CXCL12 and CXCR4 co-localized to neurons and endothelial cells, with strong peri-endothelial CXCL12 immunoreactivity after RHP. From 2d to 4wks following tMCAo, capillary CXCL12β mRNA, but not CXCL12α or CXCR4 mRNA, declined by half ($p< 0.05$) in mice with RHP relative to untreated ischemic controls.

Conclusions: The tightly-coupled, transient upregulation of CXCL12α/CXCR4 mRNA expression[4] after SHP may initiate growth factor- and angiogenesis-related gene expression changes[3] that likely contribute to ischemic tolerance; lack of a similar upregulation following RHP could reflect tachyphylaxis. The sustained increases in CXCL12β mRNA and protein in whole brain, elevated through 2wks after RHP and localized to the peri-vascular space, may strengthen the blood-brain barrier prior to stroke[5]. Post-stroke reductions in capillary CXCL12β expression are consistent with an anti-inflammatory phenotype at the endothelial-blood interface, lowering leukocyte recruitment and endothelial adherence in preconditioned animals[4]. Thus, these changes support roles for this chemokine ligand/receptor pair in establishing and maintaining the anti-inflammatory, ischemia-tolerant phenotype. Causal studies with pharmacologic inhibitors and in conditional knockout mice are underway.

References:

1) Miller BA, NeuroReport 12(8), 1663-9, 2001.

2) Rangel YM, Soc Neurosci Abstr 457.6, 2004.

3) Shyu WC, JPET 324(2), 834-49, 2008.

4) Stumm RK, J Neurosci 22(14), 5865-78, 2002.

5) McCandless EE, Am J Path 172(3), 799-808, 2008.

Brain Poster Session: Translational Studies

A NOVEL MULTIMODAL APPROACH TO TRACK NEURAL PROGENITOR CELLS IN VIVO

A. Pendharkar[1], A. De[2], H. Wang[2], X. Gaeta[1], N. Wang[1], J.Y. Chua[1], R. Andres[1], X. Chen[2], S.S. Gambhir[2], R. Guzman[1]

[1]Department of Neurosurgery, [2]Molecular Imaging Program at Stanford, Stanford University School of Medicine, Stanford, CA, USA

Objectives: Stem cell transplantation represents a promising experimental therapeutic avenue for central nervous system disorders. Before these therapies can come to fruition, however, in depth studies must be conducted to assess stem cell survival and biodistribution, especially in developing minimally invasive intravascular delivery techniques.

In the present study, we have designed a multi-modality approach with which intravascular transplants can be studied for their biodistribution and survival. We have created a mouse neural progenitor cell line harboring a triple-fusion reporter gene encoding a luciferase, red fluorescent protein, and thymidine kinase PET reporter gene. To combine high sensitivity and spatial resolution, we have also included SPIO labeling for MR imaging to create a clinically applicable system to monitor neural stem cells after transplantation.

Methods: C17.2 mouse neural progenitor cells were transduced by a Lentivirus harboring a tri-fusion reporter gene containing a synthetic Renilla luciferase, monomeric RFP, and a truncated version of sr39 thymidine kinase (TK). Cells were also transfected with SPIO particles. Following transduction, RFP positive cells were selected using FACS.

Cells were analyzed for TK and Luciferase activity 48 h after FACS. Negative controls for both assays were performed using the parental C17.2 cells.

Adult nude mice were injected with either FACS isolated C17.2 cells positive for the triple-fusion reporter gene or parental C17.2 neural progenitor cells. $5x10^5$ FACS-sorted or wild-type cells were transplanted into the right or left striatum, respectively. Control injections of the respective cells were also performed subcutaneously into the shoulders.

In vivo bioluminescence imaging and T2*-weighted MRI was performed 3 days following transplantation. FHBG-PET imaging was also performed.

Results: FACS analysis confirmed the presence of RFP, and thus the triple-fusion reporter gene in the C17.2 mouse neural progenitor cell line. In vitro assays also demonstrated luciferase and thymidine kinase activity in the RFP sorted cell line. Wild type cells did not exhibit any thymidine kinase and luciferase activity.

The in vivo data validated the activity of the triple-fusion reporter gene after transplant, both in subcutaneous and intracerebral locations. Figure 1 demonstrates specific luciferase signal emission from the bolus of transduced cells from the shoulder, as well as the brain after intracerebral transplantation. Wild type cells transplanted on the contralateral shoulder and striatum did not emit any signal above background levels. PET confirmed the presence of the transduced cells and activity of the triple-fusion gene in vivo. SPIO transfection resulted in a typical susceptibility artifact on T2 and T2* weighted MRI.

Conclusions: We describe a novel method for tracking cells after transplant. With this approach we

obtain high spatial resolution from MRI and high sensitivity with PET. This method will enable studies of biodistribution and cell migration in both short and long term studies of CNS disorders.

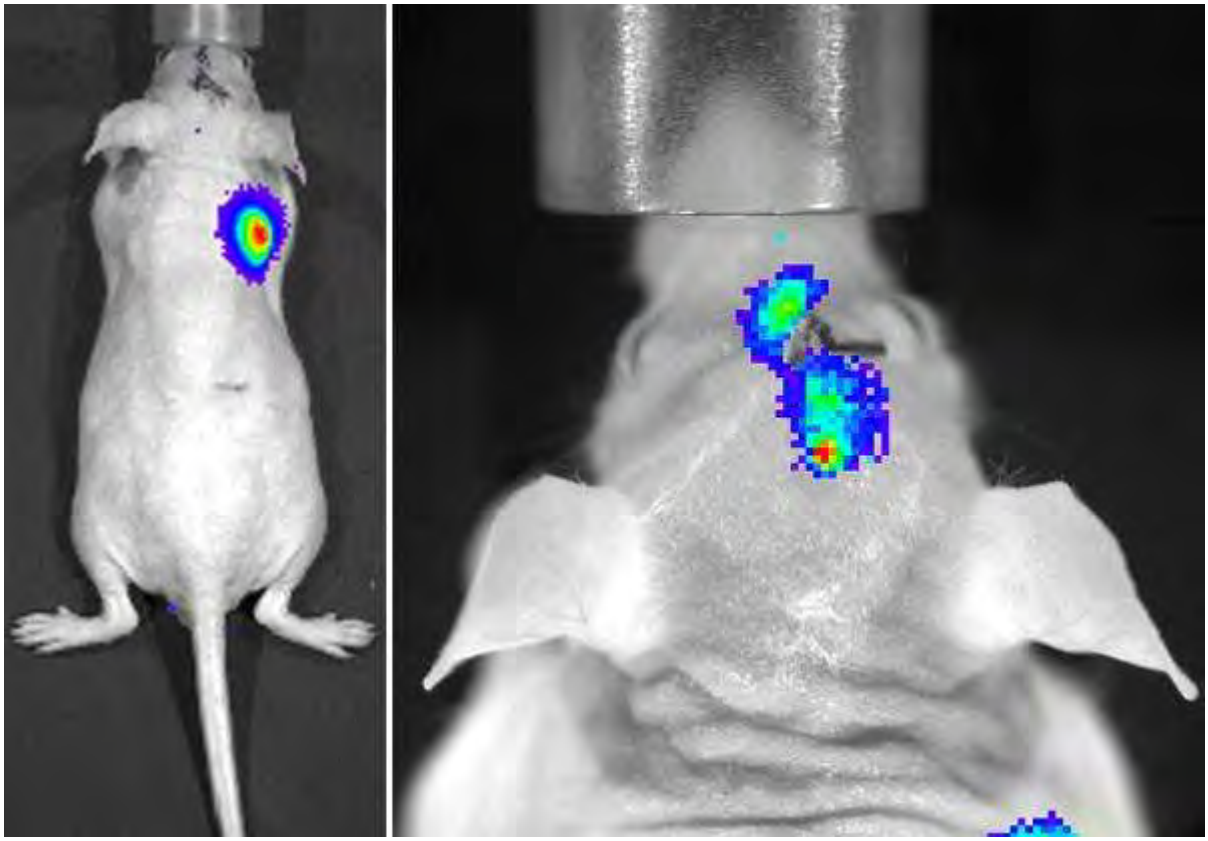

[Figure 1]

779

Brain Poster Session: Inflammation

BRAIN PERIHEMATOMA GENE PROFILE FOLLOWING SPONTANEOUS HUMAN INTRACEREBRAL HEMORRHAGE

A. Rosell[1], E. Cuadrado[1], I. Ferández-Cadenas[1], P. Delgado[1], T. García[1], M. Ribó[1], M. Hernández-Guillamon[1], A. Ortega-Aznar[2], J. Montaner[1]

[1]Neurovascular Research Laboratory, Vall d'Hebron Research Institut, [2]Neuropathology, Vall d'Hebron Hospital, Barcelona, Spain

Objectives: Spontaneous intracerebral hemorrhage (ICH) occurs from spontaneous rupture of an intracranial vessel. It represents about 15% of all strokes and is associated with high mortality rates and dreadful functional outcome. Neuroimaging studies have demonstrated a dynamic process where hematomas might expand over time and are associated with cerebral edema and perihematomal injury. Our aim was to identify the biological pathways activated in perihematomal areas by determining differences in the gene expression profile when compared to contraleteral healthy brain areas.

Methods: Twelve brain samples were obtained from four deceased patients who suffered a spontaneous ICH, including perihematomal tissue (PH) and the corresponding contralateral white (CW) and grey (CG) matter. Importantly, brain tissue was obtained within the first 6 hours after death to preserve RNA integrity and to avoid post-mortem autolysis. After isolation, total RNA was analyzed for quality (Agilent-BioAnalyzer). Finally, samples were processed using the Affymetrix GeneChip platform for analysis of over 47,000 transcripts (human U133 Plus 2.0). Paired samples from the same individual were used for comparisons between the 3 studied areas (PHvsCW, PHvsCG and CWvsCG). In order to deal with the multiple testing issues, p-values were adjusted using the Benjamini and Hochberg method. Microarray Analysis Suite 5.0 was used to process array iamges and the Ingenuity Pathway Analysis System was used to model and analyze the ontology pathways of the differentially expressed genes.

Results: Quality control parameters (standard Affymetrix parameters and a Probe-Level Model) and plots indicated that the quality of the arrays was good and with a relatively low background. Over 4,000 genes expressed and showing some variability were screened: of these 359 were differentially expressed in the PHvsCW group and over 2,000 in both PHvsCG and CWvsCG groups (adj.P.Val < 0.05 for all groups). All genes showing significant differences in their expression between CWvsCG groups were discarded since they most likely represent inherent differences due to different cellular populations and physiological functions. Finally, we identified 472 genes in the PH areas displaying a different expression pattern with a fold change between -3.74 and +5.15 when compared to the contralateral areas (309 were over-expressed and 163 were under-expressed). Of them, 6.5% of the genes represented differences between PHvsCW, 82.5% between PHvsCG and 11% between PH and both control areas. Bioinformatics analysis revealed important gene interactions in 8 key networks of cell death, cell signaling interactions, antigen presentation, cell-mediated immune response, immune cell trafficking, leukocyte-extravasation signaling pathways. Besides, gene overexpression related to cellular growth, development and proliferation was also found to be activated in the perihematomal areas. The top genes which appeared most significantly overexpressed in the PH areas codify for cytokines, chemokines, blood coagulation factors or cell growth and proliferation factors while the underexpressed codify for proteins involved in axonal guidance, cell cycle or neurotrophins.

Conclusions: The genetic-expression analysis of perihematomal areas after hemorrhagic stroke reveals changes in multiple pathological pathways but also in brain repair processes. This perihematomal area with putative secondary edema injury might also undergo endogenous repair mechanisms of therapeutical interest.

Brain Poster Session: Neuroprotection

PROTEINASE - ACTIVATED RECEPTOR TYPE I (PAR1) IS NECESSARY FOR NEUROPROTECTIVE ACTION OF ACTIVATED PROTEIN C AND THROMBIN

L. Gorbacheva[1], S. Strukova[1], V. Pinelis[2], G. Reiser[3]

[1]The Lomonosov Moscow State University, [2]The Scientific Centre for Children`s Health, Moscow, Russia, [3]Institute for Neurobiochemistry, Medical Faculty of Otto-von-Guericke University, Magdeburg, Germany

It is known, that serine proteinases participate in regulatory process in CNS. Glutamate (Glu)-induced citotoxicity is an important mechanism in ischemic brain injury and neuron death. Our early findings suggest that at low concentrations (up to 10 nM) thrombin has a protective effect on cortical and hippocampal neurons against Glu-induced toxicity (Gorbacheva et al., 2006). However, the role of PARs and activated protein C (APC) in regulation of neurons survival is not clearly.

Studies were performed using 8-10-day primary culture of neurons from cortex obtained from brain of 1-3 day-old Wistar rats. Neuron viability was determined by morphological method using fluorescent probes (Hoechst 33342, Ethidium bromide and Syto-13), and biochemical method with MTT-test. Statistical treatment of data was performed using one-way analysis of variance with GraphPrism software within multiple groups.

At 24 h after Glu exposure (100μM, 30 min) there was a increase in death of cortical neurons, reaching 30%. Preincubation of cell culture with APC at concentrations from 0,05 to 10 nM (0.05; 0.1; 1.0; 10.0 nM) reduced the Glu-induced neuronal death to 15,1; 10.1; 13.5 and 10.0%, accordingly. These findings suggest that at low concentrations (up to 10 nM) APC has a protective effect on cortical neurons against Glu-induced toxicity. 0,1 nM APC is the most effective neuroprotactive concentration in cortical neurons, but such concentration in hippocampal culture of neurons was 0,05 nM APC. Thus, the cortical neurons sensitivity to APC is some higher than in hippocampal cells.

The presence of proteolytic activity is absolutely necessary for displaying the neuroprotective effects of APC and thrombin, as 10 nM APC or thrombin, inactivated by PMSF did not protect cortical neurons from Glu-cytotoxicity.

To analyze the role of PAR-1 and PAR-3 in the neuroprotective effect of APC, cells were preincubated for 30 min with blocking and control antibodies to these receptors prior to addition of APC and glutamate. We showed that APC at low doses via PAR-1 protected rat hippocampal and cortical neurons against glutamate-induced cell death.

Thrombin was shown to protect hippocampal rat neurons against Glu-induced death via PAR1 activation. Because PAR1 antagonist Mrp(Cha) (100 μM) abolish the protective effect of thrombin and peptide-agonist PAR1 (PAR1AP) reduced the neuronal death induced by Glu.

Moreover, activation of PAR-1 by thrombin, the principal PAR-1 activator, triggers proinflammatory events, enhances endothelial permeability and initiates apoptosis (Feistritzer and Riewald 2005). We showed that pretreatment cells with APC before the high concentration of thrombin protected cells from death. These results point to PAR-1-desensitization by APC before the action of thrombin.

Taken together, our results demonstrate PAR-1-dependent neuroprotective effects of APC and thrombin at excitotoxicity. These findings can be of importance for developing novel therapeutic strategies to treat neurodegenerative disorders, where the modulation of PAR1-activity can used.

ALLOXAN INDUCED NEUROPROTECTION IN CULTURED CORTICAL NEURONS EXPOSED TO OXYGEN GLUCOSE DEPRIVATION IS MEDIATED THROUGH NMDA RECEPTOR ANTAGONISM

W.J. Costain, I. Rasquinha, A. Burgess, J. Slinn, J.S. Tauskela

Institute for Biological Sciences, National Research Council, Ottawa, ON, Canada

Objectives: Protein O-GlcNAcation is a stress-induced post-translational modification of intracellular proteins [1]. A variety of neuronal proteins have been shown to harbor O-GlcNAc modifications [2], which are dynamically regulated by two enzymes, OGT (O-GlcNAc transferase) and O-GlcNAcase. Protein O-GlcNAcation is proposed to be involved in mediating cellular responses to injurious conditions and is likely to play a protective role in mediating cellular stress responses [3]. The objective of this study was to assess the role of O-GlcNAcation in mediating neuronal cell death in response to oxygen glucose deprivation (OGD) and NMDA excitotoxicity.

Methods: E18 rat primary cortical neurons were cultured and studied on day 14. Neurotoxicity was performed by subjecting neurons to OGD (1 hour) or NMDA (10 - 300 μm) and viability was determined using propidium iodide (PI) staining. Intracellular Ca^{++} concentrations were determined in individual neurons using Fura-2, and in neuronal populations using Fluo-4 AM fluorescence. Neurotoxicity was compared in the absence and presence of PUGNAC (0 - 300 μM) and alloxan (0.3 - 3.0 mM). Western blots were performed in primary cortical neuronal homogenates using anti-O-GlcNAc (CTD110.6).

Results: We examined the effect of blocking OGT and O-GlcNAcase on OGD-induced cell death in primary cortical neurons. Western blot analysis revealed that OGD induced only moderate changes in O-GlcNAcation. However, O-GlcNAcase inhibition with PUGNAC induced a marked increase in protein O-GlcNAcation but did not impart a neuroprotective effect against OGD. OGT inhibition, with alloxan, had no overt effect on protein O-GlcNAcation, but produced a significant neuroprotective effect against OGD (68% reduction in cell death) and NMDA toxicity. Alloxan inhibited NMDA-mediated neuronal death and Ca^{++} currents in a dose dependent manner consistent with NMDA receptor blockade.

Conclusions: This study demonstrates that inhibition of O-GlcNAcase was not neuroprotective against OGD in cultured primary cortical neurons. Further, it was shown that alloxan-mediated neuroprotection was likely to be due to inhibition of NMDA receptor mediated excitotoxicity and not inhibition of OGT activity.

References:

1. Zachara, N.E. and G.W. Hart, O-GlcNAc a sensor of cellular state: the role of nucleocytoplasmic glycosylation in modulating cellular function in response to nutrition and stress. Biochim Biophys Acta, 2004. 1673(1-2): p. 13-28.

2. Cole, R.N. and G.W. Hart, Cytosolic O-glycosylation is abundant in nerve terminals. J Neurochem, 2001. 79(5): p. 1080-9.

3. Zachara, N.E., et al., Dynamic O-GlcNAc modification of nucleocytoplasmic proteins in response to stress. A survival response of mammalian cells. J Biol Chem, 2004. 279(29): p. 30133-42.

783

Brain Poster Session: Neuroprotection

DOCOSAHEXAENOIC ACID-MEDIATED NEUROPROTECTION IN FOCAL CEREBRAL ISCHEMIA IN RATS: CHARACTERIZATION BY SEQUENTIAL MAGNETIC RESONANCE IMAGING, BEHAVIOR, AND HISTOPATHOLOGY

N.G. Bazan[1], L. Khoutorova[1], T. Niemoller[1], K.D. Atkins[1], A. Obenaus[2], P. Hayes[2], E. Titova[2], **L. Belayev**[1]

[1]Neuroscience, Louisiana State University, New Orleans, LA, [2]Radiation Medicine, Loma Linda University School of Medicine, Loma Linda, CA, USA

Introduction: Docosahexaenoic (DHA 22:6n-3) acid is the precursor of NPD1, which inhibits oxidative stress-mediated proinflammatory gene induction and promotes cell survival (Bazan, 2005). DHA involved in memory formation, excitable membrane function, neuronal signaling and promotes neurogenesis both in vitro and in vivo, and has been implicated in neuroprotection (Bazan, 2003). We have recently showed DHA therapy to confer histological protection in the focal cerebral ischemia in rats (Belayev et al, 2005). We have now used diffusion-weighted magnetic resonance imaging (DWI) in conjunction with behavior and histological methods to expand our understanding of this therapeutic approach.

Methods: Sprague-Dawley rats were anesthetized with isoflurane/nitrous oxide and mechanically ventilated; rectal and cranial temperatures were regulated at 36-37.5°C. Rats received 2 h middle cerebral artery occlusion (MCAo) by retrograde insertion of an intraluminal suture (Belayev et al, 1996). Susceptibility-weighted (SWI) and T2-weighted (T2WI) MRI was carried out on a 4.7T magnet at 24 h, 72 h, and 7 days after MCAo. Animals were treated with either DHA (n=5), 5mg/kg, or saline vehicle (n=4) i.v. at 1 h after reperfusion. Neurological status was evaluated before MCAo and after treatment (at 24 h, 72 h, and 7 days), a grading scale of 0-12 was employed, as previously described. Brains were perfusion-fixed on day 7 and infarct volumes were determined.

Results: All animals showed similar values for rectal and cranial temperature, arterial blood gases, and plasma glucose during and after MCAo. DHA treatment significantly improved neurological scores compared to saline treatment at 72 h (3.3 ± 0.6 vs. 7.3 ± 1.0) and 7 days (2.7 ± 0.3 vs. 18.0 ± 1.0, respectively, $p < 0.05$). Lesion volumes computed from T2WI images and by histopathology agreed closely with one another, but histological infarct volume was underestimated by approximately 2.5-fold. DHA treatment significantly reduced subcortical infarct volumes computed from T2WI images compared to the Alb treatment on day 1 (62 ± 10 vs. 123 ±13 mm^3) and day 3 (26 ± 5 vs. 80 ±20 mm^3), but not on day 7 (12 ± 2 vs. 55 ±39 mm^3). Cortex was completely protected by DHA treatment and none of the rats had cortical infarction compared to the saline treated rats.

Conclusions: DHA experimental therapy improves neurological and histological outcome following focal cerebral ischemia and might provide the basis for future therapeutics in patients suffering ischemic stroke.

This study was supported by NS23002 and NS046741 (NGB).

Brain Poster Session: Neuroprotection: Hypothermia

AN EVALUATION OF THE SAFETY OF 3 WEEKS OF FOCAL CORTICAL HYPOTHERMIA IN RAT

A. Auriat[1], M. Penner[1], G. Silasi[2], D. Clark[2], F. Colbourne[1,2]

[1]Psychology, [2]Centre for Neuroscience, University of Alberta, Edmonton, AB, Canada

Objectives: Hypothermia is neuroprotective following global and focal cerebral ischemia. Cooling is frequently limited to a short period during the acute phase of injury (e.g., 48 hr treatment), but several types of brain injury produce cell death over a longer period and edema can persist for many days. Thus, extended cooling might provide additional benefit. However, before treatment efficacy can be addressed the safety of long-term cooling must be determined.

Methods: Rats were cooled with a metal cooling strip placed on the skull overlying the motor cortex in the right hemisphere. This strip was cooled by flushing it with cold water via a tethered system (Clark and Colbourne, 2007). Cooling was quickly initiated and maintained at a mildly hypothermic level for 3 weeks prior to gradual re-warming over 24 hours. Control rats were treated similarly, but not cooled. In part 1, several physiological parameters were measured including blood pressure, heart rate, body and cortex temperature (n=2). In part 2, brains were assessed for histological damage (hematoxylin and eosin (H&E) and fluoro jade B) 3 days after control (n=8) or hypothermia treatment (n=8) ended. In part 3, Golgi-Cox staining was used to assess neuronal complexity 3 days after re-warming (n=8) or at the same time in control rats (n=8). Finally, in part 4 electron microscopy was used to look for ultrastructural signs of tissue abnormalities in cooled and control brain. In several of these experiments we looked for behavioral abnormalities at 3 days after cooling or control treatment ceased. The corner turn, cylinder and horizontal ladder tests were used.

Results: Part 1: None of the physiological parameters were significantly affected by cooling. Brain temperature was lowered by 3-4°C for the duration of cooling. Part 2: No cell death was labeled with fluoro jade B in either cooled or control brains. H&E staining produced some dark neurons, however, these cells were present in both cooled and control hemispheres of cooled rats as well as in controls. No other indications of significant histological damage were present. The Golgi-Cox and electron microscopy data are yet to be completely analyzed. However, behavioral data indicate that no asymmetries or deficits occur with 3 weeks of focal brain cooling.

Conclusions: Studies have consistently shown great protection with longer bouts of systemic hypothermia (e.g., 48 vs. 12 hr; Clark et al., 2008). We have observed similar effects with focal cooling after ischemic stroke. The current findings suggest that local brain cooling may be administered for a prolonged period (3 weeks) without any significant physiological, anatomical or behavioral side effects.

References:

Clark, D. and Colbourne, F. A simple method to induce focal brain hypothermia in rats. Journal of Cerebral Blood Flow and Metabolism, 27: 115-122, 2007.

Clark, D., Penner, M., Orellana-Jordan, I. and Colbourne, F. Comparison of 12, 24 and 48 hours of systemic hypothermia on outcome after permanent focal ischemia in rat. Experimental Neurology, 212:386-92, 2008.

785

Brain Poster Session: Neurologic Disease

WHOLE-BRAIN PET STUDY OF PARKINSON'S PATIENTS REVEALS A COMPLEX PATTERN OF RCBF CHANGES ASSOCIATED WITH DEEP BRAIN STIMULATION

A. Tabesh[1], B. Ardekani[1,2], M. Tagliati[3], V. Dhawan[4], D. Eidelberg[4], J. Sidtis[1,2]

[1]The Nathan S. Kline Institute for Psychiatric Research, Orangeburg, [2]Department of Psychiatry, New York University School of Medicine, [3]Department of Neurology, Mount Sinai School of Medicine, New York, [4]Center for Neuroscience, Feinstein Institute for Medical Research, Manhasset, NY, USA

Objective: To investigate changes in the whole-brain multivariate pattern of regional cerebral blood flow (rCBF) quantified using positron emission tomography (PET) in Parkinson's patients with deep brain stimulation (DBS) on (ON) and off (OFF) during rest and speech motor tasks.

Methods: Six subjects with Parkinson's disease and bilateral DBS implants underwent PET scans in two sessions. In each session, PET images were acquired at rest (2 images) and while performing five speech motor tasks (10 images), with both the ON and OFF conditions. A total of 142 (72 ON and 70 OFF) images were obtained (two missing OFF images). All images were spatially normalized to a template using SPM [1] and their non-brain voxels were masked out. The remaining voxels ($2 \times 2 \times 2$ mm^3) were used for multivariate classification using the linear Gaussian classifier (LGC) [2]. Classification accuracy was estimated using the leave-one-out scheme [2].

Results: The classification accuracy of the LGC was 96.5% (sensitivity = 97.2%; specificity = 95.7%). Figure 1 shows the discriminant pattern of the LGC superimposed on the SPM PET template in neurological convention. Coefficients of the discriminant function with the largest 5% absolute values are shown. Blue and red scales indicate negative and positive coefficients, respectively. Slices are in the inferior to superior order and are 10 mm apart. Regions with increased rCBF due to DBS (in red) were thalamus, globus pallidus, caudate, and putamen. Regions with decreased rCBF were supplementary motor area and cerebellum. Increased and decreased rCBF were both observed in different regions of the frontal and temporal lobes.

Conclusions: Using a whole-brain multivariate classification approach, we showed that PET images corresponding to DBS OFF and ON conditions can be reliably differentiated. The high accuracy of classification confirms the reproducibility of the observed differences in the sense that they accurately predict the OFF or ON status of a previously unseen PET image. The whole-brain approach enables analysis without the need for specific a priori hypotheses regarding regions of interest. Previous PET studies had applied voxel-wise analysis techniques to investigate rCBF differences between the OFF and ON conditions [3, 4]. The multivariate classification approach offers the additional benefit of accounting for potential correlations between rCBF in different brain regions overlooked by voxel-wise techniques. The multivariate approach also allows for assigning a significance level to each brain region analogous to p-values in voxel-wise analysis [5].

Acknowledgment: Supported by R01 DC007658.

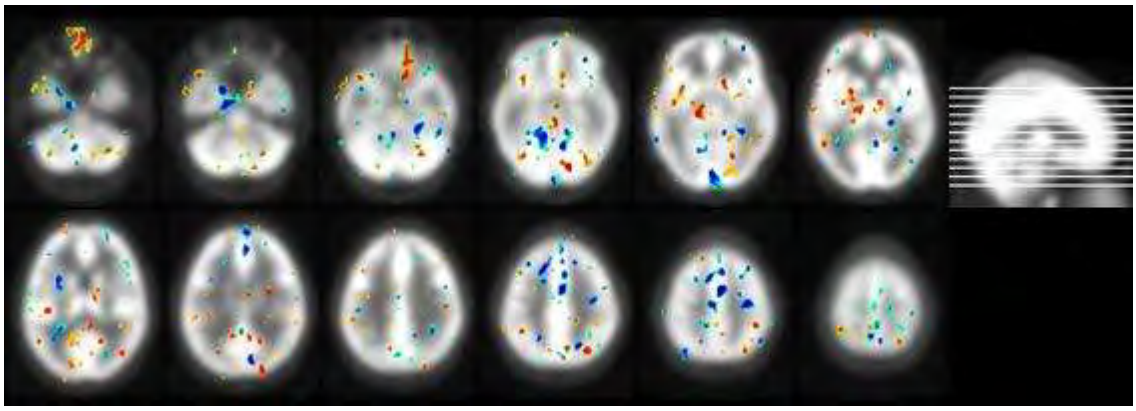

[Figure 1]

References:

1. http://www.fil.ion.ucl.ac.uk/spm/.

2. Duda et al. (2001), Pattern Classification. Wiley.

3. Schroeder et al. (2003), Ann Neurol 54, 445-450.

4. Trost et al. (2006), NeuroImage 31, 301-307.

5. Ardekani et al. (1998), in Carson et al. (eds.), Quantitative functional brain imaging with positron emission tomography. Academic, 253-257.

787

Brain Poster Session: Neuroprotection: Hypothermia

A COMPARISON OF 12 AND 48 HR OF SELECTIVE BRAIN HYPOTHERMIA AFTER PERMANENT FOCAL ISCHEMIA IN RAT

D. Clark[1], M. Penner[2], S. Wowk[2], F. Colbourne[1,2]

[1]Neuroscience, [2]Psychology, University of Alberta, Edmonton, AB, Canada

Objectives: Hypothermia provides significant neuroprotection in rodent models of ischemic brain damage. Indeed, we recently showed a duration-dependent treatment effect such that 48 hr of systemic hypothermia provided greater histological and behavioral protection at 7 days after onset of permanent focal ischemia[1]. However, the ideal treatment parameters and method of inducing hypothermia has not been determined. It is also important to evaluate whether treatments provide enduring protection. Thus, we examined the long-term impact of 12 and 48 hr of hypothermia treatment (33°C, 1 hr delay) on outcome after permanent middle cerebral artery occlusion (pMCAO). Importantly, we used a novel method of inducing focal brain hypothermia developed in our lab[2].

Methods: Rats were trained on a skilled reaching task and evaluated for baseline neurological status and walking ability. Stroke was induced by cauterization of the distal middle cerebral artery. Rats were randomly assigned to remain normothermic or receive focal hypothermia treatment one hour following occlusion for either 12 or 48 hours as described previously[2]. Rats were cooled at 2°C/h and rewarmed slowly at 1°C/h. Walking ability was measured on days 7 and 28 after stroke onset. Neurological deficits were measured on day 7 while skilled reaching ability was evaluated over 5 days starting one month following stroke onset. Animals were then euthanized to determine lesion volume.

Results: The 48 hr treatment (vs. control normothermic rats) significantly improved skilled reaching and walking ability while neurological impairment was reduced. No significant benefit was observed with the 12 hr cooling protocol. Histological analysis is ongoing and will be presented at the meeting.

Conclusions: Our results thus far indicate that delayed brain-selective hypothermia provides significant long-term behavioral protection in rats experiencing a pMCAO. Similar to our previous findings with systemic cooling[1], there is a clear duration-dependent effect. These findings suggest that either brain-selective or systemic cooling treatments, if prolonged, will improve outcome following ischemic stroke.

References:

[1]Clark, D., Penner, M., Orellana-Jordan, I. and Colbourne, F. Comparison of 12, 24 and 48 hours of systemic hypothermia on outcome after permanent focal ischemia in rat. Experimental Neurology, 212:386-92, 2008.

[2]Clark, D. and Colbourne, F. A simple method to induce focal brain hypothermia in rats. Journal of Cerebral Blood Flow and Metabolism, 27: 115-122, 2007.

789

Brain Poster Session: Neuroprotection: Hypothermia

TREATMENT OF INTRACEREBRAL HEMORRHAGE IN RATS WITH 12 H, 3 DAYS AND 6 DAYS OF SELECTIVE BRAIN HYPOTHERMIA

M. Penner[1], M. Fingas[2], G. Silasi[2], F. Colbourne[1,2]

[1]Psychology, [2]Centre for Neuroscience, University of Alberta, Edmonton, AB, Canada

Objectives: Intracerebral hemorrhage (ICH) is a devastating stroke, which accounts for 10 to 20% of all strokes. There is no proven treatment to reduce morbidity and mortality. In this study, we wanted to assess whether focally cooling the injured hemisphere following ICH would be beneficial. We also wanted to vary the duration of hypothermia to assess whether prolonged cooling is more beneficial than brief cooling.

Methods: We caused an ICH in rats by injecting 100 μL of autologous blood into the striatum. Systemic hypothermia has reduced blood-brain-barrier disruption, inflammation and edema, but has not consistently improved behavioral or histological outcome after ICH in animal studies. As this might relate to the choice of cooling method, we used a method that selectively cools the injured hemisphere to ~32ºC (striatum) while the body remained normothermic. Cooling was initiated 1 hour after ICH and lasted for 12 hours, 3 days, or 6 days, and was followed by slow rewarming (~1ºC / h). These groups were compared to a control group, which remained normothermic. We assessed functional outcome during weeks 2 and 3 post-ICH, and euthanized the rats on day 21 post-ICH. We used several behavioral tasks to assess general impairment (neurological deficit scale), walking ability (grid walk test), forelimb asymmetry (cylinder), and reaching ability (tray reaching task). We also assessed lesion volume at the end of the experiment (day 21 post-ICH).

Results: The ICH caused significant impairments in all of the behavioral tasks. The longest hypothermia treatment (6 days) significantly reduced forelimb asymmetry for both post-lesion assessments. However, none of the treatments significantly improved outcome on any of the other behavioral tasks. In addition, there was no significant reduction in lesion volume in any of the groups.

Conclusions: These results, as well as previous studies[1] indicate that hypothermia is not a substantial neuroprotectant following ICH. However, it may still improve functional recovery, as well as reduce life-threatening edema.

References: 1. Fingas, M., Clark, D. and Colbourne, F. The effects of selective brain hypothermia on intracerebral hemorrhage in rats. Experimental Neurology, 208:277-284, 2007.

790

Brain Poster Session: Spreading Depression

EVIDENCE THAT CORTICAL SPREADING DEPOLARIZATION (CSD) PROPAGATES PREFERENTIALLY ALONG GYRI IN THE HUMAN BRAIN

D. Milakara[1], G. Bohner[1], S. Major[2], J. Dreier[2]

[1]Radiology, [2]Neurology, Charité - Universitätsmedizin Berlin, Berlin, Germany

Objectives: Observations in gyrencephalic animals suggest that CSDs do not spread concentrically but propagate predominantly along gyri (Smith et al. 2001 J Anat 537-554). The relatively thin layer of grey matter lining the sulci may limit the spread of CSD between neighbouring gyri, thus preventing concentrical spread. Here, we developed a method to study whether CSD propagation in the human brain is consistent with a spread along gyri rather than a concentrical spread.

Methods: Eight CSDs were recorded in a patient with aneurysmal subarachnoid hemorrhage (aSAH) using subdural electrocorticography (ECoG). ECoG recordings were acquired continuously in 5 active channels from the 6-electrode (linear array) subdural strips. Electrode 1 served as ground while electrodes 2-6 (interelectrode distance 10 mm) were connected in sequential unipolar fashion to an amplifier, each referenced to an ipsilateral subgaleal platinum electrode. CSD was defined by the sequential onset in adjacent channels of a propagating slow potential change (SPC). A CT scan was performed during ECoG monitoring to visualize the platinum electrodes which are invisible in MRI scans. The electrode strip was then superimposed from the CT scan onto the 3D rendered brain surface of the MRI. If two electrodes were positioned on one gyrus, the shortest pathlength between the two electrodes was determined following the ridge of that gyrus. Then the CSD velocity was calculated from the latencies of the SPC onsets between electrode pairs divided by the measured pathlength. This MRI-corrected velocity was compared with the uncorrected velocity assuming an ideal linear spread between electrodes.

Results: The boxplots demonstrate that large differences of the propagation velocities were observed between different electrode pairs assuming a linear spread along the recording strip. Between subsequent CSDs propagation velocity was remarkably stable. If the velocities were corrected according to the anatomical brain surface assuming a preferential spread of CSD along a gyrus, the differences of the propagation velocities between different electrode pairs decreased significantly (difference between highest and lowest recorded speed: 1.0 (0.8, 1.1) versus 3.2 (3.1, 3.3) mm/min, paired t-test, n=8, $P < 0.0001$).

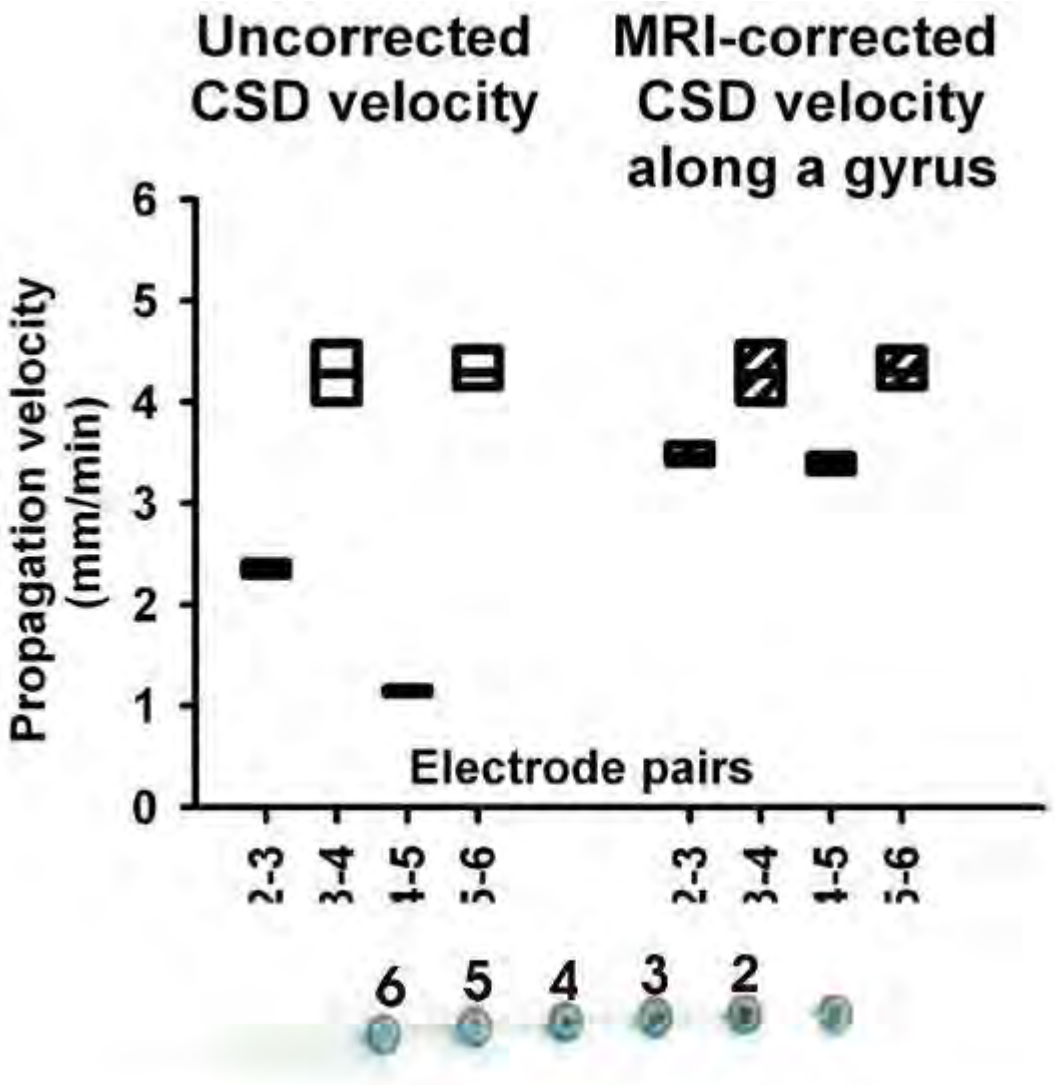

[CSD velocity]

Conclusions: The data suggest that CSD spread is hindered by sulci in the human brain in a fashion similar to that in other gyrencephalic species. This has to be confirmed in a larger study.

791

Brain Poster Session: Experimental Stroke & Cerebral Ischemia

SPATIAL MATCH OF MAXIMUM CHANGES OF SODIUM AND POTASSIUM IN ISCHEMIC RAT BRAIN

V.E. Yushmanov[1], A. Kharlamov[1], B. Yanovski[1], G. LaVerde[2], F.E. Boada[2], S.C. Jones[1,2,3]

[1]Anesthesiology, Allegheny-Singer Research Institute, [2]Radiology, MR Research Center, University of Pittsburgh School of Medicine, [3]Neurology, Allegheny-Singer Research Institute, Pittsburgh, PA, USA

Background: Regional inhomogeneities in sodium concentration ($[Na^+]_{br}$) increase (1,2) and potassium brain concentration ($[K^+]_{br}$) decrease (3) in ischemic brain have been observed. The peripheral edge of the infarct is characterized by more prominent edema formation (4) and transient BBB disruption (5) consistent with higher residual blood flow in these areas than in the infarct center. We hypothesize that the maximum rate of sodium increase occurs in the same peripheral ischemic regions where the decrease of potassium is maximal.

Methods: The rate of sodium increase by ^{23}Na MRI (2,6), $[Na^+]_{br}$ and $[K^+]_{br}$ by flame photometry (7), and $[K^+]_{br}$ spatial distribution by K^+ histostaining (3,8) were measured on the same rat brain after permanent MCA occlusion (9). The ischemic region was localized by ADC mapping with MRI (2), and by microtubule-associated protein-2 immunohistochemistry and changes in surface reflectivity (10). Flame photometry and K^+ histostaining were performed at 4.4 h after ischemia. The images were aligned and analyzed using AMIDE software.

Results: The maximum rate of Na^+ increase and maximum decrease of $[K^+]_{br}$ were observed in peripheral regions of ischemic core (Fig. 1, regions 1 and 3). $[Na^+]_{br}$ and $[K^+]_{br}$ from flame photometry confirmed normal values in non-ischemic cortex and the differences between the central and peripheral ischemic regions noted in Fig. 1: at the infarct edge (regions 1 and 3), $[Na^+]_{br}$ was increased to 125% in comparison to the central region, whereas $[K^+]_{br}$ was decreased to 56%.

Conclusion: Maximum changes in sodium and potassium in the peripheral regions of infarct indicate differences in pathophysiologic processes between the center and periphery of the infarct. The periphery of the infarct requires more attention for better understanding the mechanisms of ischemic pathology.

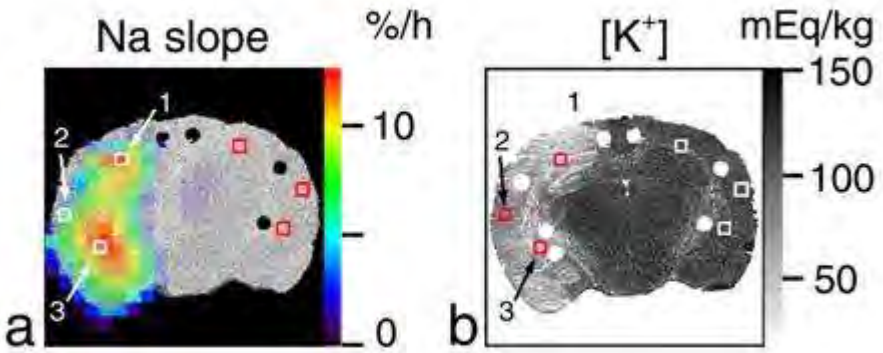

[Fig. 1]

Figure 1. (a) Pseudocolor image of the ^{23}Na slope superimposed over the grayscale 3D reconstruction of the brain from the slices. (b) K^+-stained slice. 1 - frontoparietal cortex at the dorsal edge of ischemic core; 2 - central ischemic core; 3 - ischemic region near the ventral edge. The maximum rate of Na^+ increase in the peripheral regions of ischemic core (a: regions 1 and 3) corresponds to the maximum decrease of $[K^+]_{br}$ in the same regions (b).

Support: NIH-NS030839.

References:

1. Jones et al. (2006) Stroke 37:883-888.

2. Yushmanov et al. (2009) JMRI, in press.

3. Kharlamov et al. (2007) JCBFM 27(S1):BP53-7W.

4. Kato et al. (1987) Exp Neurol 96:118-126.

5. Jones et al. (2007) JCBFM 27(S1):BO5-9.

6. Boada et al. (1997) Magn Reson Med 37:706-715.

7. Yushmanov et al. (2007) Magn Reson Med 57:494-500.

8. Mies et al. (1984) Ann Neurol 16:232-237.

9. Belayev et al. (1996) Stroke 27:1616-1622.

10. Kharlamov et al. (2001) J Neurosci Methods 111:67-73.

DYNAMIC CALIBRATED FMRI FOR EVENT RELATED OXIDATIVE ENERGETICS

B.G. Sanganahalli[1,2], P. Herman[1,2,3], H. Blumenfeld[4,5], F. Hyder[1,2,6]

[1]Diagnostic Radiology, [2]QNMR, Yale University School of Medicine, New Haven, CT, USA, [3]Semmelweis University, Budapest, Hungary, [4]Department of Neurology, [5]Neuroscience, [6]Biomedical Engineering, Yale University School of Medicine, New Haven, CT, USA

Objectives: Energetic basis of neural activity provides a solid foundation for non-invasive neuroimaging with calibrated fMRI. Calculating dynamic changes in cerebral oxidative energy utilization (CMR_{O2}) is limited by uncertainties about whether or not the conventional BOLD model can be applied transiently using multi-modal measurements of blood flow (CBF) and volume (CBV) that affect the blood oxygenation level dependent (BOLD) signal. A prerequisite for dynamic calibrated fMRI is testing the linearity of multi-modal signals within a temporal regime, as assessed by signal strength (i.e., both intensity and width). If each hyperemic component (BOLD, CBV, CBF) is demonstrated to be linear with neural activity under various experimental conditions, then the respective transfer functions generated by deconvolution with neural activity should be time invariant and thus could potentially be used for calculating CMR_{O2} transients.

Methods: Sprague-Dawley rats ($n_{(fMRI)}$ = 12, $n_{(neurophysiology)}$ = 8) were used under α-chloralose anesthesia (46±4 mg/kg/hr). The stimulation ranged from a single pulse to several pulses (1 to 4). Each pulse was 2 mA in amplitude and 0.3 ms in duration. The frequency ranged from 1.5 to 6 Hz. All fMRI data were obtained on a modified 11.7T Bruker horizontal-bore spectrometer (Billerica, MA) using a ^{1}H resonator/surface coil RF probe. LFP and MUA were recorded extracellularly in layer 4 of the rat somatosensory cortex. Electrical (e.g., LFP) non-electrical (e.g., BOLD, CBF, CBV) signals were measured during forepaw stimulation. Changes in CMR_{O2} were calculated using multi-modal measurements of changes in BOLD signal (ΔS/S), blood flow (ΔCBF/CBF), and blood volume (ΔCBV/CBV) from the relationship originally described by Ogawa et al, 1993.

Results: We found variable dependencies of each hyperemic component (BOLD, CBF, CBV) and neuronal activity (LFP, MUA) with the inter-pulse interval. Although relationships between neural activity and stimulus features ranged from linear to non-linear, associations between hyperemic components and neural activity were linear. Specific to each hyperemic component, a universal transfer function was calculated using iterative convolution method with LFP or MUA as input signal. In this process the residual signal (difference between the modeled and measured signal) was minimized. For stimulus frequencies of 1.5 and 3 Hz, the CMR_{O2} response (intensity, width) increased linearly with higher number of stimulus pulses, whereas for the same number of stimulus pulses the CMR_{O2} response decreased with higher stimulus frequency. For stimulus frequency of 6 Hz, the CMR_{O2} responses were nearly identical for different number of stimulus pulses. Existing methods cannot provide high temporal resolution CMR_{O2} data. Therefore, based on the thermodynamic principle of relating energy expended for the work done, we used the neural activity as a pseudo-validation for the predicted CMR_{O2} transients. Furthermore, given that the BOLD signal is dependent on oxygen transport from blood to tissue, we compared our CBF-CMR_{O2} coupling with theoretical predictions and experimental observations.

Conclusion: The results identified a component of the BOLD signal that can be attributed to significant changes in CMR_{O2}, even for temporal events separated by less than 200 ms.

Acknowledgements: Supported by grants from NIH (R01 MH-067528, R01 DC-003710, P30 NS-52519).

FMRI AND ELECTROPHYSIOLOGICAL STUDIES WITH α-CHLORALOSE AND DOMITOR ANESTHESIA

B.G. Sanganahalli[1,2], P. Herman[1,2,3], H. Blumenfeld[4,5], F. Hyder[1,2,6]

[1]Diagnostic Radiology, [2]QNMR, Yale University School of Medicine, New Haven, CT, USA, [3]Semmelweis University, Budapest, Hungary, [4]Department of Neurology, [5]Neuroscience, [6]Biomedical Engineering, Yale University School of Medicine, New Haven, CT, USA

Objectives: Anesthetized animal studies are valuable for many experimental situations and settings including high resolution fMRI, electrophysiology and optical imaging. Different anesthetics have diverse effects on systems responsible for arousal and conscious states, and the design of such studies may be affected by the profound metabolic and electrical effects of using different anesthetics. Recently, domitor (α_2-adrenergic agonist) has been studied as a potential anesthetic for longitudinal studies in rodents. α-chloralose and domitor have different powers in the γ band range of neural activity, which presumably reflect different arousal states. Therefore, we were interested in comparing the functional responses obtained under domitor and α-chloralose anesthesia during sensory stimulation in rodents.

Methods: Sprague-Dawley rats were tracheotomized and artificially ventilated (70% N_2O, 30% O_2). During the animal preparation isoflorane (2 to 3%) was used for induction. Intraperitoneal lines were inserted for administration of α-chloralose (46±4 mg/kg/hr) or domitor (0.1mg/kg/hr) and D-tubocurarine chloride (1 mg/kg/hr). Forepaw stimulation was achieved by insertion of thin needle copper electrodes under the skin of the forepaw. Electrical stimulation consisted of 0.3ms square wave pulses provided with a stimulus isolation unit (World Precession Instruments, FL, and USA). Variation of functional response was achieved by varying the frequency (1 - 24 Hz) of the stimulus. The stimulus was controlled with a computer by custom written scripts with a 30s off 30s on block design. All fMRI data were obtained on a modified 11.7T Bruker horizontal-bore spectrometer (Billerica, MA) using a ^{1}H resonator/surface coil RF probe. LFP and MUA were recorded extracellularly in layer 4 of the rat somatosensory cortex.

Results: We evaluated forepaw stimulation-induced activity patterns in the rat somatosensory area. Electrical stimulation (2 mA) of the forepaw with 0.3 ms duration pulses for 30 s evoked a strong positive BOLD signal change in the contralateral primary somatosensory area of the forelimb ($S1_{FL}$) under both anesthetics with stimulus frequency above 1Hz. We found frequency tuning response curves for a- chloralose and domitor where the BOLD and CBV responses peaked at 3 Hz for chloralose and 9 Hz for domitor. There were significant differences in the amplitude and shape of the BOLD and CBV response curves under domitor as compared to a-chloralose (3Hz) and (9Hz). The reproducibility of responses from inter and intra subjects was better with a- chloralose as compared to domitor. Baseline multiunit (MUA) and local field potential (LFP) recordings from $S1_{FL}$ regions under α-chloralose and domitor showed different power in the γ band range of neural activity, which presumably reflects different arousal states. There is a dramatic difference in the power of the γ band range of neural activity in the cortex, where activity/energy is significantly higher in the domitor state.

Conclusion: Differences in baseline spontaneous neuronal activity may be responsible for differential response magnitudes in BOLD and CBV under these two anesthetics. These results will benefit interpretation of fMRI experiments in anesthetized rodents as well as the understanding of brain function.

Achnowledgements: Supported by grants from National Institutes of Health (R01 MH-067528, R01 DC-003710, P30 NS-52519).

BOLD IMPULSE RESPONSES ACROSS CORTICAL LAYERS: IMPLICATIONS FOR CMR_{O2}

P. Herman[1,2,3], B.G. Sanganahalli[1,2], H. Blumenfeld[2,4,5,6], F. Hyder[1,2,7]

[1]Department of Diagnostic Radiology, [2]Quantitative Neuroscience with Magnetic Resonance, Yale University, New Haven, CT, USA, [3]Institute of Human Physiology and Clinical Experimental Research, Semmelweis University, Budapest, Hungary, [4]Department of Neurology, [5]Department of Neurosurgery, [6]Department of Neurobiology, [7]Department of Biomedical Engineering, Yale University, New Haven, CT, USA

Objectives: The calibrated fMRI technique can be used to extract oxygen consumption (CMR_{O2}) from BOLD signal using multi-modal measurements of blood flow (CBF) and volume (CBV) [1-2]. This model based approach describes tissue oxygen extraction at steady-state [3-4]. It is not clear how the cortical localization of the measurements can modify the calibration procedure since the neuronal and vascular microstructure is not homogenous across the cortex. How are the neural signals connected to the functional BOLD responses in different layers of the cortex? We described the BOLD transfer functions in the upper, middle and lower cortical layers with convolution analysis. The same experimental model was used in two groups of rats to measure the fMRI-BOLD signals and the conjunctive neural responses.

Methods: Sprague-Dawley rats were anesthetized with Halothane or Isoflurane which switched to i.p. α-chloralose after the surgery. **Forepaw stimulation:** Each stimulus train lasted 30s with 3Hz frequency, 2 mA in amplitude and 0.3 ms in duration. **BOLD** (n=7): All gradient echo EPI fMRI data were obtained on a modified 11.74T Bruker horizontal-bore spectrometer (Billerica, MA) using a ^{1}H resonator/surface coil RF probe. **Electrophysiology** (n=31) In the second group of animals microelectrodes were inserted step-by-step into three different depths of the cortex (upper, lower and middle part; 0.3mm, 1mm and 1.5mm, respectively) with stereotaxic manipulator. Local field potentials (LFP) were obtained applying low pass filter (< 150Hz) to the raw time series. **Transfer function**: The transfer function between the LFP and the BOLD signal was modeled by the gamma variate function [5]. The input function was defined as the average of the LFP series, where the individual events were normalized to the largest evoked potential (first evoked potential in the middle layer).

Results: The BOLD signal has the largest response in the upper layer and decreases toward the deeper cortical layers. The LFP signal is the most explicit in the middle layer and the smallest in the lower layer. The amplitude of transfer function follows the amplitude of the functional BOLD response. The normalized signals show very good correlation between the layers. The correlations between the electrical signals are very good because of the high number data point and similar pattern of the signals. BOLD signals show the best correlation between the upper and middle layers, while in the lower layer there is a small hysteresis in the correlation. Similarly the transfer functions of the upper and middle layers are well correlated.

Conclusion: Despite the differences in amplitudes, the normalized responses of the upper and middle layers are interchangeable for CMR_{O2} calculation. On the other hand, the lower layer of the cortex needs separate calibration.

References:

[1] Hyder et al (2001) NMR Biomed 14, 413-431.

[2] Kida et al (2000) J Cereb Blood Flow Metab 20, 847-860.

[3] Ogawa et al (1993) Magn Reson Med 29:205-210.

[4] Kennan et al. (1994) Magn Reson Med 31, 9-21.

[5] Boynton et al (1996) J Neurosci 16, 4207-4221.

This work was supported by grants from NIH (R01 MH-067528, R01 DC-003710, P30 NS-52519).

798

Brain Oral Session: Neurovascular Unit

CORTICAL AND SUB-CORTICAL ACTIVATIONS IN RAT BRAIN BY FMRI

B.G. Sanganahalli[1,2], P. Herman[1,2,3], D.L. Rothman[1,4], F. Hyder[1,2,4]

[1]Diagnostic Radiology, Yale University School of Medicine, New haven, [2]QNMR, Yale University School of Medicine, New Haven, CT, USA, [3]Semmelweis University, Budapest, Hungary, [4]Biomedical Engineering, Yale University School of Medicine, New Haven, CT, USA

Objectives: Current understanding about BOLD signal and the underlying neurophysiology is based predominantly on functions of the cerebral cortex. BOLD activations of subcortical regions, in contrast, are hard to detect because of low sensitivity and/or difficult access. The goal of the present work is to study subcortical mechanisms underlying dispersed cortical activations during sensory stimulation in rat brain by fMRI. Our results demonstrate reproducible thalamus and superior colliculus activity during forepaw, whisker, and visual stimuli in anesthetized rats. These experiments should provide insights into understudied interactions between cortical / subcortical areas and provide a mechanistic basis to understand multisensory integration.

Methods: Sprague-Dawley rats were tracheotomized and artificially ventilated (70% N_2O, 30% O_2). During the animal preparation isoflorane (2 to 3%) used for induction. Intraperitoneal lines were inserted for administration of α-chloralose (46±4 mg/kg/hr) and D-tubocurarine chloride (1 mg/kg/hr). **Forepaw stimulation** (2mA, 0.3 ms, 3Hz): Stimulation was achieved by insertion of thin needle copper electrodes under the skin of the forepaw. **Whiskers stimulation** (8Hz): Contralateral whiskers were trimmed to a length of ~14 mm. Air puffs were used to stimulate the whiskers. **Visual Stimulus delivery** (8Hz, blue light)**:** Fibre optic cables (Φ : 1mm) were used to guide the light of two strong LEDs, placed outside the scanner room, into the eyes of the animal as it lay positioned in the imaging bore. The details of the forepaw, whisker and visual stimulation procedure are available in our previous papers. All fMRI data were obtained on a modified 11.7T Bruker horizontal-bore spectrometer (Billerica, MA) using a ^1H resonator/surface coil RF probe.

Results: Independent stimulation of forepaw or whisker or visual activated the contralateral $S1_{FL}$ or $S1_{BF}$ or V1 regions. Our results demonstrate reproducible thalamus and superior colliculus activity during forepaw, whisker, and visual stimuli in rats. Forepaw stimulation activates the medial portions of the laterodorsal (LD) thalamic nucleus. Whisker stimulation activates broader regions within the thalamus: a small caudal part of the lateral thalamic nucleus, the dorsal and medial parts of the lateral geniculate nucleus, and small portions of the dentate gyrus. Visual stimulation activates superior colliculus and lateral geniculate nucleus quite robustly and even parts of the periaqueductal gray. The stimulation frequencies used for forepaw, whisker and visual stimuli were 3, 8 and 8 Hz respectively. Cortical BOLD responses were significantly larger as compared to the thalamic responses during forepaw and whisker stimulation. However, we found no differences in the BOLD response in cortical and superior colliculus during visual stimulation.

Conclusion: We can apply high field fMRI (high S/N ratio) to study thalamo-cortical, colliculo-cortical, thalamo-colliculor as well as their reciprocal interactions with crossmodal sensory mixing. The three regions in the cortex represent the primary areas activated during tactile (somatosensory; $S1_{FL}$, $S1_{BF}$) and non-tactile (visual; V1) stimuli, which are connected to the subcortex (thalamus and superior colliculus, respectively). These results have significance in understanding the role of both cortical and subcortical areas during multisensory integration.

Achnowledgements: Supported by grants from NIH (R01 MH-067528, R01 DC-003710, P30 NS-52519).

799

Brain Oral Session: Functional Brain Imaging

BOLD IMPULSE RESPONSES FOR EVENT RELATED AND STEADY-STATE PARADIGMS: IMPLICATIONS FOR CMR_{O2}

P. Herman[1,2,3], B.G. Sanganahalli[1,2], H. Blumenfeld[2,4,5,6], F. Hyder[1,2,7]

[1]Department of Diagnostic Radiology, [2]Quantitative Neuroscience with Magnetic Resonance, Yale University, New Haven, CT, USA, [3]Institute of Human Physiology and Clinical Experimental Research, Semmelweis University, Budapest, Hungary, [4]Department of Neurology, [5]Department of Neurosurgery, [6]Department of Neurobiology, [7]Department of Biomedical Engineering, Yale University, New Haven, CT, USA

Objectives: Quantitative mapping of changes in cerebral oxygen consumption with calibrated fMRI has become a popular modality for studying functional brain activity [1] because it is proportional to changes in energy consumption associated with alterations in neuronal activity induced by the stimulation [2]. This approach is based on a model which describes tissue oxygen extraction at steady-state [3-4], and this model is not proved to use for dynamic calculation. Experimental demonstration of linearity between neural and BOLD-related responses to short and long-lasting stimulations is needed to achieve an empirical proof of the feasibility of the steady-state BOLD model to dynamic events, then it may be possible to use calibrated fMRI in a dynamic manner.

Methods: Sprague-Dawley rats were anesthetized with Halothane or Isoflurane which switched to i.p. α-chloralose after the surgery. **Forepaw Stimulation:** Each stimulus train used 2mA in amplitude and 0.3ms in duration with 3Hz frequency. The stimulus number of the event related stimuli was varied from 1 to 4. 90 pulses train was used for steady-state stimulation. **BOLD** (n=12): All gradient echo EPI fMRI data were obtained on a modified 11.74T Bruker horizontal-bore spectrometer (Billerica, MA) using a ^{1}H resonator/surface coil RF probe. **Electrophysiology** (n=14): A separate group of animals were subject of the electrophysiological measurement with microelectrodes above the forepaw somatosensory region. Local field potentials (LFP) were obtained applying low pass filter (< 150Hz) to the raw time series. **Convolution analysis**: The transfer function between the LFP and the BOLD signal was modeled by the gamma variate function [5]. The parameters of the transfer function were calculated with iterative steps. The input function was defined as the average of the LFP series. The input signal covered not only one stimulus response, but consecutively all of the short stimulus conditions. The individual events were normalized to the largest evoked potential.

Results: The same transfer function was used not only for modeling event-related responses, but for long lasting stimulation events too. The precision of the simulated signal was checked by the comparison of the residual signal (i.e. difference between the modeled and measured signal) and the standard deviation of the measured signal. We considered the precision of the model adequate since the root mean square of the residual signal was smaller then the mean standard deviation of the measured signal. We got similar results from other modalities (CBV and CBF) (data not shown).

Conclusion: We showed that the transfer functions of fMRI responses generated by convolution analysis with neural activity are time invariant for events in the second to minute range, therefore the steady-state BOLD model [3] may be used for dynamic CMR_{O2} calculation.

References:

[1] Hoge and Pike (2001) J Chem Neuroanat 22:43-52.

[2] Smith et al (2002) Proc Natl Acad Sci USA 99: 10765-10770.

[3] Ogawa et al (1993) Magn Reson Med 29:205-210.

[4] Kennan et al. (1994) Magn Reson Med 31, 9-21.

[5] Boynton et al (1996) J Neurosci 16, 4207-4221.

This work was supported by grants from NIH (R01 MH-067528, R01 DC-003710, P30 NS-52519).

800

BrainPET Poster Session: Brain Imaging: MRI/fMRI

BOLD IMPULSE RESPONSES FOR DIFFERENT SOMATOSENSORY MODALITIES: IMPLICATIONS FOR CMR_{O2}

P. Herman[1,2,3], B.G. Sanganahalli[1,2], H. Blumenfeld[2,4,5,6], F. Hyder[1,2,7]

[1]Department of Diagnostic Radiology, [2]Quantitative Neuroscience with Magnetic Resonance, Yale University, New Haven, CT, USA, [3]Institute of Human Physiology and Clinical Experimental Research, Semmelweis University, Budapest, Hungary, [4]Department of Neurology, [5]Department of Neurosurgery, [6]Department of Neurobiology, [7]Department of Biomedical Engineering, Yale University, New Haven, CT, USA

Objectives: Quantitative mapping of changes in CMR_{O2} with calibrated fMRI [1] is proportional to changes in energy consumption of neuronal activities induced by different type of stimulations [2]. The calibrated fMRI is based on a tissue oxygen extraction model [3-4]. This model includes measured or modeled hemodynamic parameters (CBV, CBF), and their responses are different in different areas of the cortex. If these responses will differ only because of the different neural responses, than the same CMR_{O2} calibration can be used through different cortical areas. We measured BOLD and LFP signals in the forelimb and the whisker barrel cortex and calculated the impulse response functions with convolution analysis between these modalities. We assume the transfer function can linearly convert the electrical activity to the co-localized BOLD response, therefore similar transfer functions can establish the same CMR_{O2} calibration.

Methods: Sprague-Dawley rats were artificially ventilated. The anesthesia was switched to i.p. α-chloralose from Halothane or Isoflurane after the surgery. **Stimulation:** Electrical forepaw stimulus trains used 2 mA in amplitude, with 3 Hz frequency, and 0.3 ms in duration. For whisker stimulation we used air-puffs through a solenoid controlled plastic tube [5] with 8Hz of stimulus frequency. All stimulus presentation lasted 30s. **BOLD** (n=13): All gradient echo EPI fMRI data were obtained on a modified 11.74T Bruker horizontal-bore spectrometer (Billerica, MA) using a ^1H resonator/surface coil RF probe. **Electrophysiology** (n=33): Microelectrodes were inserted with stereotaxic manipulator either into the somatosensory forelimb or into the whisker barrel region. Local field potentials (LFP) were obtained applying low pass filter (< 150Hz) to the raw time series. **Convolution analysis**: The transfer function between the LFP and the BOLD signal was modeled by the gamma variate function [6]. The input function was defined as the average of the LFP series.

Results: We studied the responses only in the middle (III-IV) cortical layer, from where the electrical activity was measured. The BOLD response and LFP activity for whisker stimulation were weaker than that for the forepaw stimulation. However their normalized values were correlated very well (r^2 was 0.86 and 0.99, respectively). Transfer functions were calculated for both areas. The precision of the simulation was adequate if the root mean square of the residual signal (i.e. difference between the modeled and measured signal) was smaller then the standard deviation of the measured signal (Forepaw: 0.2 vs. 0.58, Whisker: 0.41 vs. 1.36).

Conclusion: Despite the similar characteristics of the transfer functions and the high correlation of the normalized signals, there is a marked hysteresis in the correlation of impulse response functions, which indicates caution in the CMR_{O2} calibration.

References:

[1] Hoge and Pike (2001) J Chem Neuroanat 22:43-52.

[2] Smith et al (2002) Proc Natl Acad Sci USA 99: 10765-10770.

[3] Ogawa et al (1993) Magn Reson Med 29:205-210.

[4] Kennan et al. (1994) Magn Reson Med 31, 9-21.

[5] Sanganahalli et al. (2008) NMR Biomed 21:410-416.

[6] Boynton et al (1996) J Neurosci 16, 4207-4221.

This work was supported by grants from NIH (R01 MH-067528, R01 DC-003710, P30 NS-52519).

801

BrainPET Poster Session: Brain Imaging: MRI/fMRI

MULTI-COMPARTMENT CBV CHANGES WITH LASER-DOPPLER AND FMRI

P. Herman[1,2,3], B.G. Sanganahalli[1,2], F. Hyder[1,2,4]

[1]Department of Diagnostic Radiology, [2]Quantitative Neuroscience with Magnetic Resonance, Yale University, New Haven, CT, USA, [3]Institute of Human Physiology and Clinical Experimental Research, Semmelweis University, Budapest, Hungary, [4]Department of Biomedical Engineering, Yale University, New Haven, CT, USA

Objectives: Quantitative mapping of changes in CMR_{O2} proportionally describes the energy consumption of neural activities [1-2], therefore it is popular for studying functional brain activity. Calibrated fMRI experiments require measurements of CBF, CBV, and BOLD signal to predict CMR_{O2} changes. Injection of long-lasting MRI contrast agent is necessary to obtain an MRI signal that was highly weighted by CBV. The aim of this study was to find an alternative method to estimate the CBV changes during stimulation [3].

Methods: Animal preparation: Sprague-Dawley rats were anesthetized with Halothane which switched to i.p. α-chloralose after the surgery. **Forepaw stimulation:** Each stimulus train lasted 30s with 3Hz frequency, 2 mA in amplitude and 0.3 ms in duration. **CBV fMRI measurement** (n=6): All gradient echo EPI fMRI data were obtained on a modified 11.74T Bruker horizontal-bore spectrometer (Billerica, MA) using a ^{1}H resonator/surface coil RF probe. The focal CBV response was measured by injection of iron oxide nanocolloid (Combidex 15 mg/ml) [2]. **LDF and backscatter measurement** (n=12): Fiber optodes (interoptode distance: 200 μm) were inserted into the three different depth of the forepaw somatosensory cortex with stereotaxic manipulators to measure the laser-Doppler flux and backscattered light intensity.

Results: We found a strong correlations between the MRI measured CBV and the optically measured back scattered light intensity in every three measured layers during onset (r^2=0.96±0.02), activation plateau (r^2=0.86±0.16), and offset (r^2=0.97±0.02) phases of the functional hyperemic response (overall r^2=0.95).

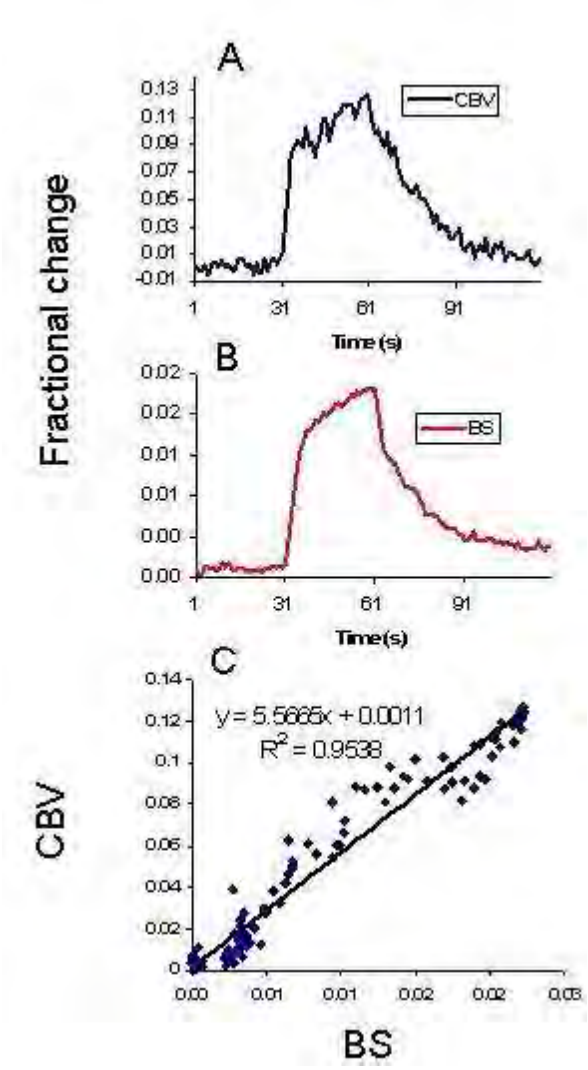

[Figure]

The contrast agent used in the fMRI CBV measurement is diluted in plasma volume which follows CBV changes after hematocrit correction. The BS signal intensity depends the scattering property of the brain tissue and the concentration of absorbers (i.e. oxy- and deoxyhemoglobins). Higher signal intensity means lower concentration of absorbers. If the wavelength of the applied laser light is an isosbestic point of the hemoglobin absorption curves, then only the number of the hemoglobin molecules can affect the BS intensity. Since oxygenation change doesn't influence the BS signal, it refers to the RBC volume which follows the change of the CBV. The instantaneous hematocrit (tube hematocrit) has to vary in the small vessels, because of the Fahraeus-effect, the discharge hematocrit seems to remain constant.

Conclusion: These results suggest that CBV measurements from both blood compartments may be used to reflect dynamic changes in total CBV. Furthermore, by assuming steady-state mass balance and negligible counter flow, these results indicate that discharge (volume) hematocrit is not appreciably affected during functional activation.

References:

[1] Hoge and Pike (2001) J Chem Neuroanat 22:43-52.

[2] Smith et al (2002) Proc Natl Acad Sci USA 99: 10765-10770.

[3] Herman et al (2009) JCBFM 29:19-24.

This work was supported by grants from National Institutes of Health (R01 MH-067528, R01 DC-003710, P30 NS-52519).

802

BrainPET Poster Session: Brain Imaging: MRI/fMRI

QUANTIFICATION OF PUNCTATE IRON SOURCES USING SUSCEPTIBILITY WEIGHTED PHASE IMAGES

G. McAuley[1], M. Schrag[1], P. Sipos[2], R. Sun[3,4], A. Obenaus[5], B. Holshouser[6], W. Kirsch[1], **W.J. Pearce**[7]

[1]Neurosurgery Center for Research, Loma Linda University, Loma Linda, CA, USA, [2]Department of Inorganic Biochemisty, University of Szeged, Szeged, Hungary, [3]Non-Invasive Imaging Laboratory, [4]School of Science and Technology, [5]Non-Invasive Imaging Laboratory, Radiobiology Program, [6]Radiology, [7]Center for Perinatal Biology, Division of Physiology, Loma Linda University, Loma Linda, CA, USA

Objectives: Iron deposition and dysregulation have clearly been implicated in neurodegenerative diseases including Alzheimer's disease (AD). Whether changes in iron content and metabolism are causal or epiphenomena, there is strong evidence that iron-mediated tissue damage occurs. We recently reported increasing BMB in a subset of subjects with progressing dementia in our prospective study. The BMB were located spatially in the brain in a pattern that is characteristic of cerebral amyolid angiopathy (CAA), a disease where beta amyloid is deposited in small cerebral arteries and microvessels, and typically present in AD cases.

Extravasated blood following BMB is a pathological source of brain iron that may contributes to the dementia associated with AD and CAA, and is potentially informative regarding the extent of cerebral vessel pathology. The potential role of paramagnetic iron as a biomarker or agent of disease makes its noninvasive quantification by MR very valuable for monitoring disease progression and treatment efficacy both clinically and experimentally. Past efforts to quantify brain iron have focused on estimation of content in distributed brain regions. However, BMB represent punctate iron sources where quantification is desirable.

Susceptibility weighted imaging (SWI) is a MR modality that uses magnetization phase to create or enhance contrast. It has been shown to be more sensitive to BMB detection than gradient echo T2* (GRE T2*) methods. Magnetization phase is directly related to tissue susceptibility differences, and therefore is sensitive to the presence of paramagnetic iron.

The present study investigates the possibility of using phase images to quantify iron content in punctate iron sources. We hypothesize a theoretical relationship between the iron content of samples modeled as magnetic dipoles and a measureed parameter in the phase images.

Methods: Magnetic resonance phantoms were constructed containing samples of a chitosan-ferric oxyhydroxide composite material which serves as a mimic for hemosiderin (the iron-containing blood breakdown product that marks the location of BMB in GRE T2* and SWI images). The phantoms were imaged using a SWI sequence at 11.7T. An easily recognized parameter from the resulting phase images theoretically related to the iron content of the sample was then measured from the resulting phase images. A plot relating the parameter with the known sample iron content was constructed.

Results: The hypothesized relationship between dipole pattern properties and sample iron content in phase images was corroborated by a plot of theoretically related variables that displayed the predicted mathematical form.

Conclusions: A simple and effective method is presented that relates parameters from phase images to iron content of punctat samples modeled as magnetic dipoles. Phantoms were constructed with a chitosan-ferric oxyhydroxide composite which serves as a mimic for hemosiderin. Results are in excellent agreement with theory, and serve as a 'proof of concept' of the quantification technique. The

research is potentially a first step toward experimental or clinical quantification of puntate iron sources such as BMB marked by hemosiderin deposits.

803

Brain Poster Session: Experimental Stroke & Cerebral Ischemia

PPAR-GAMMA AGONIST ROSIGLITAZONE IS NEUROPROTECTIVE AFTER STROKE IN TYPE II DIABETIC RODENTS

R. Vemuganti[1], K. Tureyen[1], I. Satriotomo[1], K. Bowen[1], R. Kapadia[1], D. Feinstein[2]

[1]Neurological Surgery, University of Wisconsin, Madison, WI, [2]Dept of Anesthesiology, University of Illinois-Chicago, Chicago, IL, USA

Type-2 diabetics show exacerbated brain damage, neurological dysfunction and mortality following stroke. Millions of type-2 diabetics use rosiglitazone (rosi; a potent agonist of the transcription factor PPAR-gamma) to control blood glucose and lipid balance. Rosi was also shown to induce neuroprotection against ischemic neuronal death in rodents. We currently tested the efficacy of rosi in adult db/db mice (a genetic model of type-2 diabetes) with 4 times higher blood sugar level than their normoglycemic littermates (db/+ mice). Following a 2h transient middle cerebral artery occlusion (MCAO), the mortality rate in the first day of reperfusion was observed to be 75% for the db/db compared to 13% for the db/+ mice (n=13/group). Following a 45 min transient MCAO and 3 days reperfusion, rosi treatment (2 mg/Kg at 2h reperfusion; i.p.) decreased the infarct volume by 54% in the db/+, but only by 21% in the db/db mice compared to vehicle control ($p< 0.05$; n = 7/group). Even pre-treatment (at -4h and 1 min reperfusion) with 4 mg/Kg rosi decreased the infarct volume by only 30% in the db/db compared to 68% in db/+ over vehicle control ($p< 0.05$; n = 7/group). The acute pre- or post-MCAO treatment with rosi had no significant effect on the blood glucose levels measured at 6h, 1 day and 3 days of reperfusion compared to pre-MCAO levels in either genotype. In human type-2 diabetics, there is a lag phase of ~3 weeks before the beneficial blood glucose lowering effect can be seen after starting rosi treatment. Hence, we fed a cohort of db/db and db/+ mice with rosi-fortified chow for 3 weeks. Rosi chow fed db/db mice showed a 32% decreased blood glucose level at 21 days compared to pretreatment levels. In the db/db (but not db/+) mice, the long-term oral pre-treatment with rosi induced a significantly better neuroprotection (47% decrease in infarct volume over normal chow fed controls; $p< 0.05$; n = 7/group) and decreased mortality than bolus injections. On the other hand db/db mice fed on metformin for 3 weeks show decreased blood sugar level, but not infarction volume following transient MCAO. Both the genotypes (db/db and db/+) fed on control chow showed significantly elevated mRNA expression of the pro-inflammatory transcripts IL6, MCP1, ICAM1 and E-selectin following transient MCAO. However, the post-ischemic fold increases for all the transcripts were significantly higher for the db/db group compared to db/+ group. Feeding mice on rosi chow significantly prevented the post-ischemic induction of all these transcripts by ~60 to 90% in both the db/db and db/+ mice indicating that prevention of inflammation is a mechanism of the neuroprotection induced by rosi. In addition, the rosi-fed db/db mice showed significantly less neutrophil infiltration and brain water accumulation following transient MCAO. Thus, rosi is a potentially beneficial therapeutic agent that not only decreases blood glucose but also prevents stroke-induced inflammation, edema, brain damage and mortality in type-2 diabetics.

ARTERIAL INPUT FUNCTION SAMPLING VIA AN INTRA-ARTERIAL POSITRON (β^+) PROBE: HUMAN $H_2{}^{15}O$ VALIDATION

K. Lee, P. Fox, J. Lancaster

Research Imaging Center, University of Texas Health Science Center at San Antonio, San Antonio, TX, USA

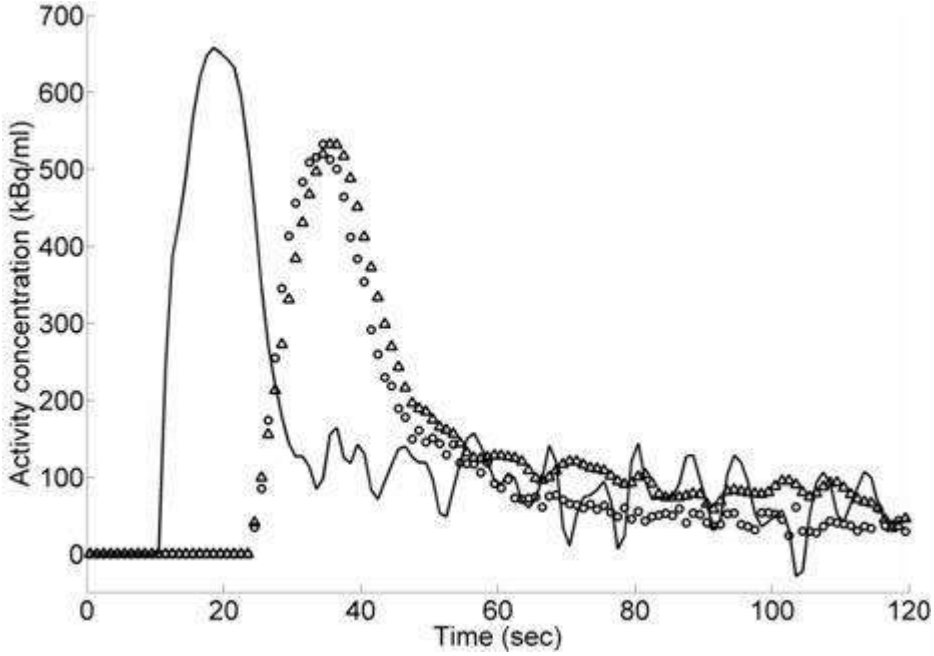

[An image-derived aortic and radial AIFs]

Objectives: An important advantage of positron emission tomography (PET) relative to other functional imaging methods is its capacity for quantification in physiological units. For physiological quantification, the arterial-radiotracer concentration must be measured throughout the tracer-uptake period. Typically, this is done by sampling the arterial blood during scanning, to obtain an arterial input function (AIF). The goal of this study was to validate use of an intra-arterial β^+ probe for measuring the AIF in humans. In a within-subject design, AIFs obtained via a β^+ probe placed in the radial artery were compared to AIFs obtained by dynamic imaging of the descending aorta.

Methods: Eight healthy, normal volunteers participated. Each subject underwent 12 PET scans (6-thorax; 6-brain) and 2 MRI scans (1-thorax; 1-brain). Thoracic images were used to obtain intra-aortic AIFs. For each PET scan, 555 MBq of $H_2{}^{15}O$ in 6-ml saline was injected as an intravenous bolus. Image acquisition consisted of 90 two-sec frames, beginning ~ 20 sec before injection. MRI was used to determine aortic diameter and location. Aortic ROIs created on MRI images were transferred to PET images for AIF. From the ROI, an aortic AIF was obtained. The aortic ROI values were corrected for partial volume effects using the recovery coefficient method. Radial AIFs were obtained using a β^+ probe fabricated in-house [1]. The probe consists of a 0.5-mm-diameter plastic scintillating fiber coupled to a photosensor module and was placed in the radial artery via a 22-gauge catheter. Intra-arterial β^+-probe counts were corrected for gamma interactions using an identical external probe attached to the wrist. Both β^+ probes were sampled at 1 Hz. The time-delay between the aortic and radials AIFs was measured and then corrected for prior to statistical comparison of the two AIFs. Full-width half maximum (FWHM), peak amplitude, area and correlation coefficient were used to characterize and compare the radial and aortic AIFs.

Results: Good-quality radial (circles) and disperse-corrected aortic (triangles) AIFs were successfully obtained for every injection in every subject (Figure). The time delay between the disperse-uncorrected aortic (solid-lines) and radial bolus arrival times was 19.6 sec (±1.8 sec, SD). AIF-curve shapes were appropriate for a rapid bolus injection and frame-to-frame variability (noise) was very low. Radial AIFs were more dispersed than aortic AIFs. After delay and dispersion correction, the shapes of the two AIFs curve did not differ. This was statistically confirmed (paired-t test) by comparing the FWHMs ($p=0.401$), peak amplitudes ($p=0.889$), and areas under the curves ($p=0.401$), none of which differed. The correlation between the aortic and radial AIFs was excellent ($r = 0.90 \pm 0.07$ (mean ± SD)).

Conclusion: An intra-arterial β^+ probe is reliable, low-noise, high-temporal-resolution, method for obtaining an AIF for PET quantitative.

Reference: [1] Lee et al., Rev. Sci. Instrum. 2008; 79: 064301-1-7.

807

Brain Poster Session: Spreading Depression

SHIFT OF FREQUENCY DISTRIBUTION FUNCTION OF RBC VELOCITY IN PARENCHYMAL CAPILLARIES DURING POTASSIUM-INDUCED CORTICAL SPREADING DEPRESSION IN ANESTHETIZED RATS

M. Unekawa[1], M. Tomita[1], Y. Tomita[1,2], H. Hattori[1], H. Toriumi[1], N. Suzuki[1]

[1]Neurology, [2]Preventive Medicine for Cerebrovascular Disease, School of Medicine, Keio University, Tokyo, Japan

Object: Cortical spreading depression (CSD) is a mass depolarization of neurons, and vascular changes occur concomitantly with CSD. We have already reported a repetitive wave-ring spread of decrease and increase of microvascular flow during potassium-induced CSD in rats (Tomita, M. et al. JCBFM 25:742, 2005). In this experiment, we focused on the velocity distribution of red blood cells (RBCs) in capillaries after application of potassium in cerebral cortex of anesthetized rat by employing an automated analyzing system developed by us (Tomita, M. et al. Microcirculation 15:163, 2008).

Methods: In urethane-anesthetized male Wistar rats (n=12), a cranial window was made in the left temporo-parietal region. FITC-labeled RBCs were injected through the femoral vein, and the labeled RBCs appearing in the region of interest (ROI) at 50 μm depth below the brain surface were tracked by means of high-speed camera (500 fps) laser-scanning confocal microscopy. Their velocities were calculated with Matlab-domain software, KEIO-IS2. Capillaries were defined as microvessels having a diameter of less than 10 μm. The frequency distribution function of RBC velocity was obtained in the control state and at 3 min after KCl application by counting RBCs with velocities in each successive 0.5 mm/s range (Unekawa, M. et al. Asian Biomed. 2:203, 2008). CSD was induced by application of approximately 10 μl of KCl solution of 0.3 M or more on the brain surface around the ROI.

Results: Nine pairs (control and 3 min after application) of microscopic images (3 - 10 s, or 1500 - 5000 frames each) were successfully obtained. From the data, 97 and 174 RBCs were defined as flowing in single capillaries among 3611 and 3894 detected RBCs, respectively. The average velocity decreased from 2.05±1.31 mm/s to 1.97±1.27 mm/s, but this decrease was not statistically significant. During CSD, there was transient flow cessation. However, it was too short to affect the average value. Analysis every 0.1 or 0.2 s revealed transient suppression of RBC appearance lasting 0.3 - 0.6 s in 4 rats. During the suppression period, the frequency distribution of RBC velocity in all vessels, including capillaries, arterioles, venules and veins, showed a notable decrease of RBCs with velocity in the range of 1.0 - 2.5 mm/s, but fast-flowing RBCs (more than 5 mm/s) persisted (Figure). During the same period, capillary RBCs disappeared or their velocity fell below the calculable limit of ca. 0.2 mm/s. Exceptionally, RBCs flow remained consistently fast in one capillary.

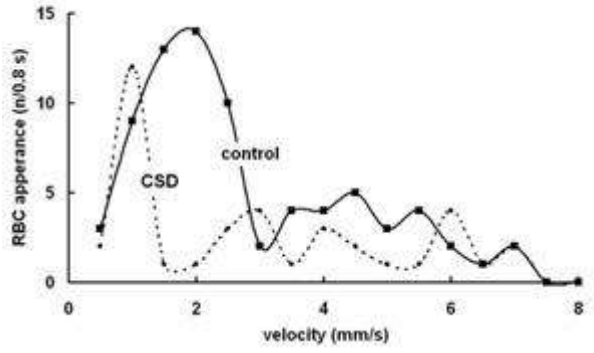

[Frequency distribution function of RBC velocity]

Conclusion: Potassium-induced CSD decreased the number of RBCs flowing in capillaries in the velocity range that was most frequently seen in the control, and a similar tendency was seen in non-capillary vessels.

ESTROGEN RECEPTOR-MEDIATED PROTECTION OF ASTROCYTES AND CEREBRAL ENDOTHELIAL CELLS DURING ISCHEMIC CONDITIONS IN VITRO

D.N. Krause[1], J. Guo[1,2], J.H. Weiss[3], S.P. Duckles[1]

[1]Pharmacology, University of California, Irvine, Irvine, CA, USA, [2]Pharmacology, Peking University, Beijing, China, [3]Neurology, University of California, Irvine, Irvine, CA, USA

We recently demonstrated that 17β-estradiol (E) improves mitochondrial efficiency and reduces mitochondrial free radical formation in brain blood vessels and endothelial cells. We hypothesized that during ischemic insult, E would protect mitochondrial function and enhance cell viability in two key supportive cells in the brain: endothelial cells and astrocytes. To test this, oxygen-glucose deprivation (OGD)/reperfusion was applied in culture to either primary neonatal mouse astrocytes or immortalized mouse cerebral endothelial cells (bEnd.3). In both cases, cell death induced by 6 hr OGD was prevented by long-term (24, 48 h), but not short-term (< 12 h) pretreatment with E (10 nM). E also suppressed OGD-induced translocation of apoptosis-inducing factor (AIF) from mitochondria to nuclei. E inhibited lactate dehydrogenase (LDH) leakage during OGD and reperfusion and abrogated OGD-induced ATP depletion. The latter effects were blocked by the estrogen receptor (ER) antagonist, ICI-182,780 and mimicked by an ERalpha-selective agonst but not an ERbeta agonist. E treatment also suppressed free radical formation that was evident after only 1 h OGD and preserved the integrity of the mitochondrial membrane potential. Interestingly, E stimulated mitochondrial protein expression in endothelial cells but not astrocytes, suggesting that suppression of free radical formation, not mitochondrial biogenesis, may be a common protective mechanism of E in both cell types.

[Supported by NIH Grant R01 HL-50775 and Chinese Government Scholarship 20073020].

809

Brain Poster Session: Neurogenesis

DOSE DEPENDENCE OF ISOFLURANE EFFECTS IN THE ADULT MOUSE BRAIN

R. Dallasen, A. Hirko, **Y. Xu**

Department of Anesthesiology, University of Pittsburgh School of Medicine, Pittsburgh, PA, USA

Objective: The general anesthetic isoflurane has been shown to confer neuroprotection against ischemic insults by a number of mechanisms including enhancing hyperpolarization by GABA, increasing levels of anti-apoptotic proteins, and reducing glutamate release. On the other hand, isoflurane has been implicated in the generation and accumulation of Aß plaques found in Alzheimer's disease (AD) and apoptosis in the developing brain. To investigate mechanisms of isoflurane-induced neurological change, levels of doublecortin (DCX), a marker of neurogenesis, c-Fos, a marker of gene activation, HSP70, a marker of cellular stress, and Bcl-xL, an anti-apoptotic marker, were compared in adult mice exposed to various concentrations of isoflurane and recovered for different lengths of time after exposure.

Method: Adult, male CD-1 mice were exposed to 2 hours of 0.6%, 1.3%, or 2% isoflurane anesthesia. After exposure, mice were given 2 hours, 1, 6, or 14 days to recover. Immunohistochemistry involved staining for DCX, c-Fos, HSP70, and Bcl-xL. Blue fluorescence 4,6′-diamidino-2-phenylindole (DAPI) staining was used to identify cell nuclei. Doublecortin positive cells were assessed in the dentate gyrus. Cells positive for c-fos were counted in the cortex, amygdala, dentate gyrus, and CA1 region of the hippocampus.

Results: No cells positive for HSP70 or Bcl-xL were detected in any brain region. There were DCX positive cells found in the dentate gyrus in all animals. Whether DCX immunoactivity is significantly increased in the anesthetized animals has yet to be determined. Three-way ANOVA showed that levels of c-Fos were significantly different with respect to brain region ($P< 0.001$), the number of days after isoflurane exposure ($P< 0.001$), and doses of isoflurane ($P< 0.001$) and that there was a statistically significant interaction between region, day, and dose. The overall level of c-Fos expression in the dentate gyrus was lower than that observed in any of the other assessed brain regions. In the hippocampal CA1 region, dentate gyrus, and amygdala, c-fos expression was elevated at the day 0 time point. In the cortex, c-fos expression on day 0 was lower in the anesthetized animals than in the control animals.

Conclusion: Isoflurane anesthesia at sub-clinical and clinical concentrations caused neither cellular stress, as measured by HSP70, nor upregulation of anti-apoptotic genes, as measured by Bcl-xL, in the adult mouse brain. Isoflurane did affect the expression of c-Fos, an immediate early gene. The effects of isoflurane on c-Fos expression are dose dependent, time dependent, and region dependent. DCX positive cells found in the dentate gyrus after isoflurane exposure may indicate induction of neurogenesis and is worthy of further investigation.

(Funded by NIH R37GM049202 and R01NS036124.)

ARTERIAL INPUT FUNCTION SAMPLING VIA AN INTRA-ARTERIAL POSITRON PROBE: HUMAN PROOF-OF-CONCEPT APPLICATION

K. Lee, P. Fox, J. Lancaster

Research Imaging Center, University of Texas Health Science Center at San Antonio, San Antonio, TX, USA

Objectives: An important advantage of positron emission tomography (PET) relative to other functional imaging methods is its capacity for quantification in physiological units. For physiological quantification, the arterial radiotracer concentration must be measured throughout the tracer uptake period. Typically, this is done by sampling the arterial blood during scanning, to obtain an arterial input function (AIF). As an alternative to blood extraction, we have developed an intra-arterial, positron-detecting probe (β^+ probe) system for measuring the AIF [1]. The goal of this study was to demonstrate the use of the β^+ probe system for $H_2{}^{15}O$ PET studies in humans. In a within-subject design, $H_2{}^{15}O$ PET measurements of cerebral blood flow (CBF) were obtained during normal ventilation and volitional hyperventilation, a maneuver know to lower whole-brain CBF.

Methods: Eight healthy, normal volunteers participated. Each subject underwent 12 PET scans (6 thorax; 6 brain) and 2 MRI scans (1 thorax; 1 brain). Thoracic images were used to validate the β^+ probe-derived AIFs relative to aortic, image-derived AIFs (reported in a separate abstract [2]). Brain images were used to compare brain blood flow in the two physiological states. For each $H_2{}^{15}O$ PET scan, 555 MBq of $H_2{}^{15}O$ in 6 ml of saline was injected as an intravenous bolus. For the six brain scans, physiological state was alternated between normoventilation and hyperventilation. Radial artery AIFs were obtained using the β^+ probe system, which consists of a 0.5 mm-diameter plastic scintillating fiber coupled to a photosensor module (Hamamatsu, H7826P) via a luer-lock hub. The probe fiber was placed in the radial artery via a 22-gauge catheter. Intra-arterial β^+ probe counts were corrected for gamma interactions using an identical external probe attached to the wrist. Both β^+ probes were sampled at 1 Hz. Global CBF (ml/100g/min) was calculated using the Ohta method [3]. CBF values were computed with and without dispersion correction using two-sample pair t-tests.

Results: Values for whole-brain CBF were in excellent agreement with literature values [3] for both physiological states, both with and without dispersion correction. In normal ventilation, whole-brain CBF values were 51.7 ± 7.7 (mean ± SD) uncorrected and 50.6 ± 6.8 corrected, which were not significantly different. In hyperventilation, whole brain CBF values were 35.6 ± 4.8 (mean ± SD) uncorrected and 34.0 ± 4.8 corrected, which also were not significantly different. As expected, hyperventilation dramatically lowered whole-brain CBF, this change being highly significant ($p< 0.0002$).

Conclusion: Physiologically quantitative PET studies can be obtained using an intra-arterial, positron-detecting probe system to obtain the arterial input function. This internal tracer quantification method is safer, simpler and more convenient than methods which rely on external counting of blood samples removed from the subject. Dispersion correction of AIFs obtained by this method is not necessary.

References:

[1] Lee et al., Rev. Sci. Instrum. 2008; 79: 064301-1-7.

[2] Lee et al., Abstract of the XXIV International Symposium on Cerebral Blood Flow, Metabolism and Function, 2009, A-164-0011-00804.

[3] Ohta et al., J Cereb Blood Flow Metab. 1996;16:765-780.

811

Brain Poster Session: Experimental Cerebral Ischemia: Vascular & Endothelial

THE DISTRIBUTION OF COLLATERAL CIRCULATIONS AFTER A MINI-ISCHEMIA IN RAT CORTEX EVALUATED BY OPTICAL IMAGING

W. Luo, P. Li, S. Chen, Q. Luo

Wuhan National Laboratory for Optoelectronics, Huazhong University of Science and Technology (HUST), Wuhan, China

Objectives: The cerebral collateral circulation is recruited as a subsidiary vascular network to stabilize the local cerebral blood flow (CBF) when the principal supplying arteries are constricted or occluded, and is crucial for the pathophysiology and outcome of acute cortical ischemia. Current understanding of collateral circulation still remains sparse, largely due to prior limitations of spatial or/and temporal resolution in methods to evaluate these diminutive redistributive routes of cerebral blood flow especially in leptomeningeal anastomoses that connected cortical arteries. The leptomeningeal anastomoses can be divided into 2 types according to their position and original source: inter-arterial and intra-arterial anastomoses, which connect the adjacent branches from same common artery and from different arteries, respectively. The aim of the present report was to evaluate the priority and kinetics of developing inter-arterial or intra-arterial anastomoses after mini-ischemia in rat cortex by optical imaging techniques with the utility of high spatiotemporal resolution, including laser speckle imaging and optical imaging of intrinsic signal.

Methods: Adult male Sprague-Dawley rats (n=10) were anesthetized with α-chloralose/urethane and the parietal-temporal cortex was exposed through craniectomy mini-ischemia (3-4 mm in diameter) was formed in rat cortex by ligating one or several small branches of middle cerebral artery (MCA) with short pieces of 11-0 suture passed through the dura and under the vessels. The animals were divided into two groups. One group (n=6) were subjected to cerebral blood flow measurement using laser speckle flowmetry. The animals in another group were adopted for tracing changes in cerebral blood volume after ischemia in rat cortex by optical imaging of intrinsic signal at a wavelength of 550 nm, which is an isoabsorptive point of oxy and deoxy-hemoglobin.

Results: The blood flow and diameter in the intra-arterial anastomoses were enhanced immediately after the ligation of one branch of middle cerebral artery and recovered to baseline level as arterial recirculation was performed. Whereas the communicative flow through the posterior cerebral artery-middle cerebral artery anastomoses was not significant enough to be determined. A step-size increase in local blood volume initially occurs in the cortical regions proximal to the adjacent unligated branches of MCA, and then forms a ring-shape zone surrounding the ischemic core. It is interesting that a gradual decrease in blood flow was indicated in the medial part of the parietal cortex, which supplied by anterior cerebral artery of posterior cerebral artery.

Conclusions: This is the evidence that in some case intra-arterial anastomoses were the primary routes to restore the blood flow into the ischemic territory during the acute phase of focal ischemia, whereas the inter-arterial anastomoses was not well established shortly after the ligation of the branches originating from MCA. This finding suggests the inter-anastomoses would be a potential therapeutic target when a sudden occlusion of the MCA was encountered, although the underlying mechanism is in need of further investigations.

Keywords: Collateral circulation, anastomoses, optical intrinsic signals, laser speckle imaging.

REGIONAL PATTERN AND TIME COURSE OF INJURY IN NEAR TERM RABBIT FETAL HYPOXIA-ISCHEMIA

A. Drobyshevsky, M. Derrick, X. Ji, L. Yu, S. Tan

Pediatrics, NorthShore University Healthcare System Research Institute, Evanston, IL, USA

Introduction: Premature infants with periventricular leucomalacia are at high risk to develop cerebral palsy. However, the type and site of lesions varies with gestational age. In late gestation, a basal ganglia type of injury often occurs with extrapyramidal clinical manifestations.

Objective: To reveal patterns of regional injury in near-term fetal brain and correlate it with the development of ensuing motor deficits in a rabbit model of fetal hypoxia-ischemia (Derrick et al., Stroke, 2007. 38(2 Suppl): p. 731-5).

Methods: New Zealand White rabbits at 29 days gestation (E29, 90% gestation) were subjected to 32 min uterine ischemia that results in global fetal-ischemia (H-I). Fetuses were imaged serially in utero on a 3T magnet, delivered by C-section and imaged on 4.7 Bruker magnet at 4, 24, 72 hours after H-I. A diffusion-weighted sequence with b=0,800 s/mm^2 was employed and apparent diffusion coefficient (ADC) calculated. At P1 the full diffusion tensor sequence (DTI) was acquired to estimate fractional anisotropy (FA). Muscle resistance to passive stretch in the rabbit kits after near term (E29) fetal H-I was measured using a recently developed torque-displacement apparatus.

Results: Out of 31 fetuses, 12 were found dead on c-section 4 hours after the H-I insult. Out of 19 survivors, 10 failed to maintain respiration 5-15 min after delivery. Out of the remaining 9 surviving kits, 4 developed hypertonia of hind limbs at 72 hours after H-I.

These kits had marked and persistent reduction of ADC in basal ganglia, thalamus and brainstem compared to non-hypertonic kits (fig.1). Massive cell death occurred by 72 hours after H-I in the areas of initially decreased ADC as indicated by formation of cystic lesions, tissue loss or hyperintensities on T2 and DWI- weighted images. Kits that developed hypertonia by 72 hour after H-I were initially hypotonic at 24 hour after H-I (fig. 2). At P1 (72 hours after H-I) FA values of hypertonic kits in corpus callosum and internal capsule showed a trend to be lower than in non-hypertonic kits.

Conclusions: The biphasic response is strikingly similar to the development of human hypertonia in infants, but in a much compressed time frame. Basal ganglia, thalamus and brain stem sustain larger injury than cortex and white matter after near term H-I in rabbits. ADC at 4 hours after H-I is informative to predict hypertonia in surviving kits. Development of hypertonia after near tem H-I in rabbits occurs within 72 hours making the model a convenient platform to study pathophysiology of hypertonia in cerebral palsy.

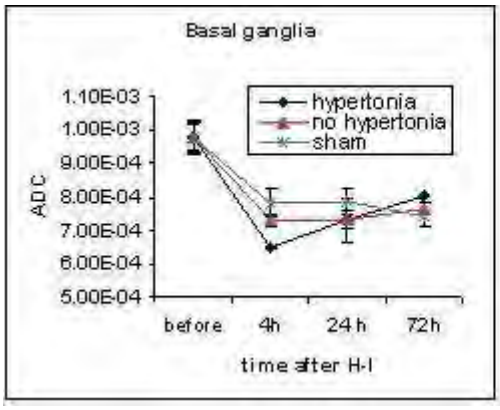
Basal ganglia
1.10E-03
1.00E-03
9.00E-04
8.00E-04
7.00E-04
6.00E-04
5.00E-04
ADC
hypertonia
no hypertonia
sham
before
4h
24 h
72h
time after H-I

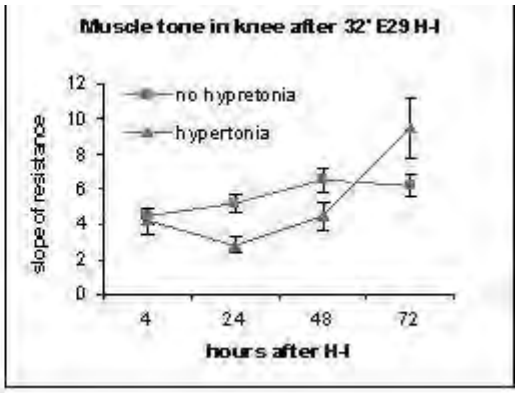
Muscle tone in knee after 32' E29 H-I
slope of resistance
12
10
8
6
4
2
0
no hypretonia
hypertonia
4
24
48
72
hours after H-I

[fig1-2]

813

Brain Poster Session: Glial Functions

LOSS OF ASTROCYTIC GLUTAMATE TRANSPORTERS IN WERNICKE´S ENCEPHALOPATHY; INVOLVEMENT OF OXIDATIVE STRESS

A. Hazell[1], D. Sheedy[2], C. Wang[1], D. Wang[1], R. Oanea[1], M. Aghourian[1], S. Sun[1], J. Yong[1]

[1]Department of Medicine, University of Montreal, Montreal, QC, Canada, [2]Department of Pathology, University of Sydney, Sydney, NSW, Australia

Objectives: Wernicke´s encephalopathy (WE), a neurological disorder caused by thiamine deficiency (TD), is characterized by structural damage in brain regions that include the thalamus and cerebral cortex (Victor et al., 1989). The basis for these lesions is unclear but evidence suggest it may involve a disturbance of glutamatergic neurotransmission (Hazell et al., 2001). We have therefore investigated levels of the astrocytic glutamate transporters EAAT1 and EAAT2 in these vulnerable areas in order to evaluate their role in the pathophysiology of this disorder.

Methods: Postmortem samples of frontal cortex were studied from patients with a neuropathological diagnosis of WE and a clinical history of consumption of greater than 80 g of absolute alcohol per day, and from control cases with a history that included consumption of less than 20 g of absolute alcohol per day. Tissue was provided by the New South Wales Tissue Resource Centre which is supported by the University of Sydney, Neuroscience Institute of Schizophrenia and Allied Disorders, National Institutes of Alcohol Abuse and Alcoholism and New South Wales Department of Health. In addition, TD rats and their pair-fed controls were prepared as previously described (Hazell and Wang, 2005), with and without co-treatment with N-acetylcysteine (NAC), and their brains studied at the loss of righting reflex stage. WE and TD samples were examined by immunoblotting and immunohistochemical methods.

Results: Histological assessment of the frontal cortex revealed a significant loss of neurons in WE cases compared to age-matched controls, concomitant with decreases in α-internexin and synaptophysin protein content of 67% and 52% by immunoblotting. EAAT2 levels were diminished by 71% in WE, with levels of EAAT1 also reduced by 62%. Development of TD in rats caused a profound loss of EAAT1 and EAAT2 in the thalamus accompanied by decreases in other astrocytic-specific proteins including GFAP, glutamine synthetase, and the GABA transporter GAT-3, which in the thalamus is localized in these cells, while β-actin levels were unchanged. Treatment of TD rats with NAC prevented the downregulation of both EAAT1 and EAAT2 in the medial thalamus, concomitant with increased neuronal survival.

Conclusions: Our results suggest that:

1. loss of astrocytic glutamate transporters is associated with structural damage to the frontal cortex in patients with WE,
2. oxidative stress plays an important role in this process, and
3. TD has a profound effect on the functional integrity of astrocytes.

Based on these findings, we recommend that early treatment using a combination of thiamine replenishment AND antioxidant approaches should be an important consideration in cases of WE, particularly those in which recurrent bouts of TD are part of the clinical history and where the underlying damaging processes may therefore be having a cumulative effect.

References:

Hazell, A.S., Wang, C. (2005) J. Neurosci. Res. 79, 200-207.

Hazell, A.S., Rama Rao, K.V., Danbolt, N.C., Pow, D.V., Butterworth, R.F. (2001) J. Neurochem. 78, 560-568.

Victor, M., Adams, R.D., Collins, G.H. (1989) The Wernicke-Korsakoff Syndrome and Related Neurologic Disorders due to Alcoholism and Malnutrition. F.A. Davies, Philadelphia.

FOCAL HYPOTHERMIA BY EPIDURAL COOLING PROVIDES BRAIN PROTECTION IN PORCINE MODEL OF MIDDLE CEREBRAL ARTERY OCCLUSION

H. Cheng

Department of Neurosurgery, Jinling Hospital, School of Medicine, Nanjing University, Nanjing, China

Objectives: Hypothermia has been shown to be neuroprotective in many animal models and several human trials of brain ischemia. However The protective effect against ischemic stroke by systemic hypothermia is limited by the cooling rate and it has severe complications. Our perior researchs show that the selective brian hypothermia (moderate and deep brian temperature) by epidural space cooling can be induced rapidly, and may be a useful strategy for reducing infarct volume after the onset fo ischemia. This study was designed to observe the histological morphology and differences of apoptosis on the brain tissue in a swine model of permanent middle cerebral artery occlusion (PMCAO) and eveluated the effect of protection by epidural cooling.

Methods: PMCAO was performed in 12 domestic swine assigned to groups A and B. In group A, the cranial and rectal temperatures were maintained at normal range for six hours after PMCAO. In group B, Cranial temperature was reduced to moderate (deep brain) and deep (brain surface) temperature and maintained at the level for 5 hours following one hour after PMCAO, by the method of epidural cooling. Epidural cooling was performed using cold-saline (4 degrees C) perfusion into the epidural space through a flexible double-lumen catheter. The dripping speed of cold saline was controlled to maintain the target temperature. All animals were euthanized 6 hours after MCAO; brain sections were perfusion-fixed and cryopreserved. Hematoxylin and eosin histology were used to characterize cell damage morphologically. Neuronal apoptosis were characterized by TUNEL histochemistry.

Results: Following the epidural cooling, the target temperatures were easily controlled (from mild to deep hypothermia on focal brain region). The body temperature was maintained at normal range within 6 perfusion hours. The structure of brain tissue in the infarcted regions maintained more intact, and TUNEL-positive cells were significantly fewer in the hypothermic group than in the normal temperature group.

Conclusions: The present study has demonstrated, with histological confirmation and apoptosis mechanisms, that epidural cooling may be a useful strategy for neuroprotection after the onset of ischemia.

References:

1. Cheng H, Shi J, Zhang L, Zhang Q, Yin H, and Wang L. Epidural cooling for selective brain hypothermia in porcine model. Acta Neurochir (Wien), 2006, 148: 559-564.

2. Ginsberg MD. Neuroprotection for ischemic stroke: past, present and future. Neuropharmacology. 2008;55(3):363-389.

3. Lihua Zhang, Huilin Cheng, Jixin Shi, Jun Chen.Focal epidural cooling reduces the infarction volume of permanent middle cerebral artery occlusion in swine. Surgical Neurology. 2007;67:117-121.

4. Miyazawa T, Tamura A, Fukui S, Hossmann KA. Effect of mild hypothermia on focal cerebral ischemia. Review of experimental studies. Neurol Res. 2003;25(5):457-464. 5. Wagner KR,

Zuccarello M. Local brain hypothermia for neuroprotection in stroke treatment and aneurysm repair. Neurol Res. 2005;27(3):238-245.

CEREBRO-VASCULAR RESPONSES TO BRIEF GLOBAL ASPHYXIA IN LATE GESTATION FETAL SHEEP: EVIDENCE FOR VASCULAR RE-MODELLING?

A. Baburamani, D. Walker, M. Castillo-Melendez

Physiology, Monash University, Melbourne, VIC, Australia

Background: The developing brain is vulnerable to hypoxia, resulting in damage due to cerebral edema, hemorrhage and vascular leakage. In the adult brain, angiogenic responses to hypoxia/ischemia include up-regulation of vascular endothelial growth factor (VEGF) and the formation of new, immature blood vessels that are leaky and prone to rupture [1]. During cerebral ischemia, the functional and structural integrity of the blood brain barrier (BBB) is rapidly destroyed [2]; this may extend beyond the endothelial component of the BBB to the basal lamina, which is also vulnerable to hypoxia-ischemia.

Aim: To investigate the early cerebrovascular responses (24-48h) that occur in the late gestation fetal brain following brief global asphyxia produced by umbilical cord occlusion (UCO).

Methods: At 124-127 days gestation (term = 147 days), singleton fetal sheep underwent surgery for catheterization and placing an inflatable cuff around the umbilical cord. At 132 days gestation, UCO was produced for 10 mins. Fetal brains were collected at 24 (n=5) and 48h (n=5) after UCO following transcardial perfusion with 4% paraformaldehyde. Control fetuses (n=5) underwent a sham UCO. Immunohistochemistry was carried out on 10mm sections using mouse monoclonal anti-VEGF, rabbit monoclonal anti-Ki67 (proliferative marker) and polyclonal rabbit anti-laminin (an important component of the basal lamina) primary antibody and visualized with metal-enhanced diaminobenzydine. VEGF and Ki67 immunoreactivity (IR) was visualized using Image J. Laminin was quantified with AdobePhotoshop7.

Results: Following UCO, a 10-20 fold increase in VEGF-IR was seen at 24 and 48h in the subventricular zone (SVZ), striatum terminalus (ST), caudo-putamen, cortex, white matter and corpus callosum (CC). Endothelial cell proliferation (Ki-67) showed a 8-18 fold increase at 24h in the ST, cortex and caudo-putamen and was maintained at 48h. The SVZ showed a 300 fold increase at 24h which was still elevated at 48 h. The amount of laminin present in blood vessels, quantified by densitometric analysis revealed no change in most brain regions at either time point. However, in the CC, SVZ and ST a marked decrease in the number of blood vessels/mm^2 was seen at 24 and maintained at 48h after UCO.

Conclusions: Brief, global asphyxia results in the up-regulation of VEGF and endothelial cell proliferation, adaptive responses known to result in the formation of new blood vessels. A wide-spread and sustained increase was observed at 24 and 48h following UCO, suggesting that the VEGF system is induced by brief asphyxia in the late gestation fetal sheep, leading to endothelial cell proliferation. The density of laminin-IR blood vessels/mm^2 was either unchanged or reduced in the brain regions examined suggesting that growth of new vessels had not taken place by 24 or 48h following UCO. However, as degradation of cerebral microvascular laminin reportedly occurs following brain hypoxia, further investigation into alternative vascular markers as well as assessment of the structural stability of the basal lamina (using collagen type IV and fibronectin) following fetal hypoxia needs to be carried out.

References:

[1] Kaur C et al (2006) Glia 54, 826-839.

[2] del Zoppo GJ and Hallenback JM (2000) Thromb Res 98, 73-81.

Brain Poster Session: Brain Edema & Water Transport

INVOLVEMENT OF MITOGEN-ACTIVATED PROTEIN KINASE PATHWAYS IN EXPRESSION OF AQUAPORIN-4 IN RAT CORTICAL ASTROCYTES AFTER OXYGEN GLUCOSE DEPRIVATION

C. Nito[1,2], M. Ueda[1], P.H. Chan[2], Y. Katayama[1]

[1]Department of Internal Medicine, Divisions of Neurology, Nephrology, and Rheumatology, Nippon Medical School, Tokyo, Japan, [2]Department of Neurosurgery, Department of Neurology and Neurological Sciences, and Program in Neurosciences, Stanford University Medical School, Stanford, CA, USA

Objectives: Brain edema is a key determinant of morbidity and mortality following ischemic brain injury. Aquaporin-4 (AQP4) plays an important role in water transport in the central nervous system and is highly expressed in astrocytes. However, the AQP4 regulatory mechanisms under pathological conditions like ischemia are unknown. In this study, we investigated whether the mitogen-activated protein kinases (MAPKs), which are involved in changes in osmolality (1,2), may mediate AQP4 expression in models of rat cortical astrocytes after oxygen-glucose deprivation (OGD), an in vitro ischemic-like condition. We hypothesized that AQP4 expression is regulated by a MAPK signaling pathway, which is affected by ischemic conditions.

Methods: Astrocyte cultures were prepared from the cerebral cortices of postnatal Sprague-Dawley rats. Cells were pretreated with selective inhibitors of ERK1/2 (PD98059), JNK (SP600125), p38 (SB203580), or DMSO (control) prior to OGD injury. AQP4 protein levels were measured by Western blot after 6h of OGD. To analyze the contribution of MAPKs after OGD, ERK1/2, JNK, and p38 were examined by measuring levels of phosphorylation and activation on immunoblotting. Cell death was determined after 24h of recovery in the normoxic incubator using a lactate dehydrogenase assay (3).

Results: p38 MAPK and JNK were activated in response to OGD. Increased AQP4 protein levels in astrocytes were observed after OGD and 2h of reperfusion, after which they decreased temporarily, as detected by immunoblotting. AQP4 was significantly upregulated at 16h compared with the control. Phosphorylation of all three MAPKs was significantly decreased by OGD and increased during reoxygenation. Treatment with SB203580 and SP600125 attenuated the increase in AQP4 to normal levels, and only SB203580 significantly decreased cell death ($p< 0.05$).

Conclusions: These results suggest that p38 MAPK positively regulates AQP4 expression in astrocytes after ischemic-like injury. We suggest that p38 MAPK signaling can be a molecular target for regulating brain edema formation under ischemic conditions.

References:

(1) Arima H, Yamamoto N, Sobue K, Umenishi F, Tada T, Katsuya H, Asai K. (2003) Hyperosmolar mannitol stimulates expression of aquaporins 4 and 9 through a p38 mitogen-activated protein kinase-dependent pathway in rat astrocytes. J Biol Chem 278:44525-44534.

(2) Han J, Lee J-D, Bibbs L, Ulevitch RJ. (1994) A MAP kinase targeted by endotoxin and hyperosmolarity in mammalian cells. Science 265:808-811.

(3) Koh JY, Choi DW. (1987) Quantitative determination of glutamate mediated cortical neuronal injury in cell culture by lactate dehydrogenase efflux assay. J Neurosci Methods 20:83-90.

KINETIC ANALYSIS OF A NOVEL RADIOLIGAND FOR α7 NICOTINIC ACETYLCHOLINE RECEPTOR, [^{11}C]CHIBA-1001 IN HUMAN BRAIN

M. Sakata[1], Y. Kimura[1,2], M. Ishikawa[1,3], J. Toyohara[1,4], J. Wu[1,4], K. Oda[1], K. Ishii[1], K. Hashimoto[4], K. Ishiwata[1]

[1]Positron Medical Center, Tokyo Metropolitan Institute of Gerontology, Tokyo, [2]Molecular Imaging Center, National Institute of Radiological Sciences, [3]Department of Psychiatry, [4]Center for Forensic Mental Health, Chiba University, Chiba, Japan

Objectives: α7 nicotinic acetylcholine receptor (nAChR) is one of the predominant nAChR subtypes in the brain and is suggested to play an important role in the pathologic states of psychiatric and neurological disorders, such as schizophrenia, Alzheimer's disease, and other dementia. 4-[^{11}C]methylphenyl 2,5-diazabicyclo[3.2.2]nonane-2-carboxylate ([^{11}C]CHIBA-1001) is recently developed as a novel PET tracer for α7nAChR in the brain [1]. Here we performed human PET studies with [^{11}C]CHIBA-1001, and analyzed the kinetics of the tracer in the brain.

Methods: Dynamic PET scans (90-min) were performed in four normal male volunteers (33 ±14 ages, non-smoker) on SET-2400W (Shimadzu Co., Kyoto, Japan). The doses of [^{11}C]CHIBA-1001 were 521 ± 107 MBq, and the specific activities were 28.7 ± 9.8 MBq/nmol. Arterial blood was sampled at various time intervals, and the fraction of parent compound in the plasma was determined by HPLC analysis. Eleven ROIs are placed on major cortices, cerebellum, and basal ganglia. ROI-averaged time-activity curves (TACs) were analyzed using one- and two-tissue (1T, 2T) compartment model and Logan graphical analysis (LGA, t* = 30 min). Total distribution volume (V_T) images of [^{11}C]CHIBA-1001 were also estimated by LGA.

Results: [^{11}C]CHIBA-1001 readily entered the brain. The radioactivity peaked about 15 min after administration. Metabolism of the [^{11}C]CHIBA-1001 was relatively slow with the percentage of unchanged form in the plasma remaining 73 ± 7 % at 60 min after administration. Figure 1 shows V_T images of [^{11}C]CHIBA-1001 estimated by LGA. The tracer was widely distributed in all gray matter regions and no candidate of reference region was found. Regional TACs were well described with 1T model and it caused unstable estimations in 2T model. K_1/k_2 using 1T model and V_T using LGA matched well ((K_1/k_2) = 1.03 (V_T) - 0.3 (r^2 = 0.92)). The region which has the highest V_T [mL/cm^3] was the thalamus (18.2±3.2), followed by the cerebellum (17.8±4.6), amygdala (16.6±3.0), hippocampus (16.5±3.0), posterior cingulate gyrus (16.5±2.1), putamen (16.4±2.8), temporal cortex (16.2±2.5), frontal cortex (15.6±2.4), parietal cortex (15.0±2.4), occipital cortex (14.5±2.2), and caudate (14.5±2.0). Although the distribution of α7nAChR in all regions of primate brains is still not completely known, the regional distribution pattern of [^{11}C]CHIBA-1001 is consistent with the in vitro results previously reported [2, 3].

Conclusion: [^{11}C]CHIBA-1001 was suggested to be applicable for further evaluations as a PET tracer for α7nAChR in human brain.

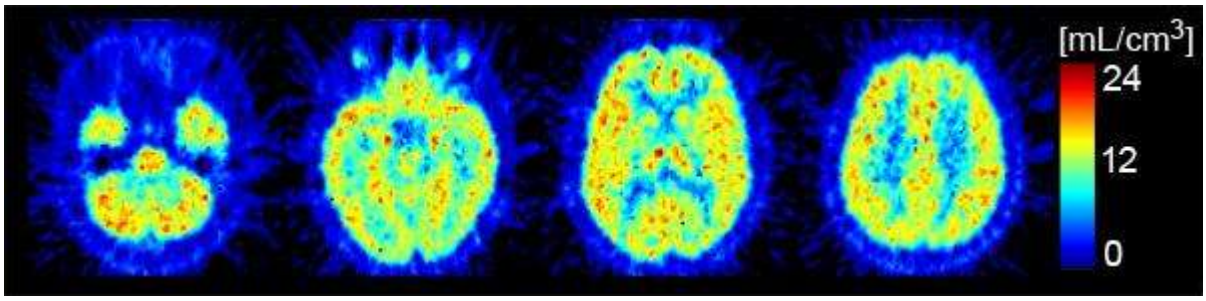

[VT images of [C-11]CHIBA-1001]

Fig. 1. Total distribution volume images of [^{11}C]CHIBA-1001.

References:

[1] Hashimoto K, et al., PLoS ONE 2008; 3:e3231.

[2] Court J, et al., Biol Psychiatry 2001; 49:175-184.

[3] Court J, et al., J Neurochem 1999; 73:1590-1597.

Acknowledgments: This research was supported by grant from the Program for Promotion of Fundamental Studies in Health Sciences of the National Institute of Biomedical Innovation of Japan.

820

Brain Oral Session: Experimental Stroke and Cerebral Ischemia 2

MITOCHONDRIAL DYSFUNCTION INDUCED BY FOCAL CEREBRAL ISCHEMIA IN THE TNFα-TRANSGENIC RAT

J. Pandya[1], P. Sullivan[1], L. Pettigrew[2,3]

[1]Spinal Cord & Brain Injury Research Center, [2]Stroke Program, Sanders-Brown Center on Aging, University of Kentucky, [3]Department of Veterans Affairs Medical Center, Lexington, KY, USA

Objectives: Tumor necrosis factor-alpha (TNFα) induces neurodegeneration in ischemic brain through cytokine-receptor mediated signalling pathways. Current evidence suggests that neuronal mitochondria stressed by ischemia may contribute synergistically to TNFα-mediated cell death. We tested the hypothesis that increased synthesis of TNFα in ischemic brain will promote oxidative stress through mitochondrial dysfunction.

Methods: TNFα-transgenic (TNFα-Tg) rats were constructed to overexpress the murine TNFα gene, resulting in elevated brain levels of active TNFα protein (Pettigrew et al., 2008). Both TNFα-Tg rats and non-Tg littermates of male sex underwent reversible middle cerebral artery occlusion (MCAO) for 1 hr. Mitochondria were isolated from ischemic cortex (IC) sampled after 3 hr of reperfusion. Production of reactive oxygen species (ROS) in mitochondria was measured with 2,7-dichlorodihydrofluorescein (Pandya et al., 2007).

Results: The mean ROS level in cortical mitochondria sampled from non-ischemic TNFα-Tg brain (n=7) was 349 ± 26.7 (SEM) relative fluorescence units, compared to 277.4 ± 20 in non-Tg brain (n=8; p=0.05; unpaired t-test). After MCAO, the ROS level peaked within IC in TNFα-Tg brain (518.3 ± 41.9) and was significantly greater than in unaffected cortex sampled from the same transgenic animals (385.3 ± 51.9; p=0.05) or from non-Tg littermates (293.8 ± 15.1; p=0.003; Fisher's test; n=6 per group for all comparisons). The mean ROS level measured within IC in TNFα-Tg brain also exceeded that in ischemic brain of non-Tg rats (393.3 ± 50) by a margin that approached statistical significance (p=0.06).

Conclusions: Our results show that ROS is produced at higher basal levels in neural mitochondria isolated from TNFα-Tg rats than in non-Tg littermates, suggesting that elevated TNFα protein induces free radical synthesis even without physiological stress. After MCAO, we found that ROS synthesis was further amplified in ischemic brain sampled from TNFα-Tg animals. We conclude that ischemic stress and synthesis of inflammatory cytokines, such as may occur during post-ischemic reperfusion in human brain, will synergistically augment ROS production to promote neuronal death.

References:

1) Pettigrew LC, et al. Focal cerebral ischemia in the TNFα-transgenic rat. J Neuroinflammation 5, 47 [e-pub] (2008).

2) Pandya JD, et al. Post-injury administration of mitochondrial uncouplers increases tissue sparing and improves behavioral outcome following traumatic brain injury in rodents. J Neurotrauma 24, 798-811 (2007).

Grant support: NIH/NINDS NS047395 and Merit Review Award from the Veterans Administration (LCP).

821

Brain Poster Session: Stem Cells & Gene Therapy

INTRAARTERIAL NEURAL STEM CELL DELIVERY DOES NOT REDUCE CEREBRAL BLOOD FLOW

J.Y. Chua, X. Gaeta, N. Wang, R.H. Andres, A.V. Pendharkar, R. Guzman

Neurosurgery, Stanford University School of Medicine, Stanford, CA, USA

Introduction: Stem cells have been recognized as a potential therapy for stroke and various methods have been developed to deliver these cells. One of these methods, the intraarterial (IA) delivery of cells, provides several benefits such as direct targeting of ischemic tissue, circumventing systemic cell trapping and feasibility in translating into clinical practice. However, it has been reported recently that the IA delivery potentially poses the risk of vascular occlusion. In this study, we compared the cerebral blood flow (CBF) effects of two IA delivery methods - a high volume catheter injection with permanent Common Carotid Artery (CCA) ligation and a low volume needle injection with CCA flow.

Methods: 24 hours after undergoing 2 hours of middle cerebral artery occlusion (MCAO) with intraluminal suture, adult female Wistar rats had a Laser Doppler probe placed on a thinned portion of the skull above the corpus striatum to monitor CBF. For transplantation, special care was taken to obtain single cell suspensions of Murine C17 cells in phosphate-buffered saline (PBS). In Group 1, the ipsilateral internal carotid artery (ICA) was cannulated with a catheter followed by the infusion of $1X10^6$ C17 cells in 1mL PBS. The Group 1 control animal underwent the same procedure but was infused with 1ml PBS. In Group 2 animals, $1X10^6$ C17 cells in 5μL and $0.5X10^6$ C17 cells in 5μL were injected into the CCA lumen via the External Carotid Artery. CBF measurements were recorded up to 15 minutes after IA delivery.

Results: IA delivery in Group 1 animals resulted in a sharp drop in CBF to about 10% of baseline within the first minute and a recovery to near baseline within 2 minutes. 1 animal in Group 1 did not show a recovery in CBF after 1 minute and was hemiplegic before dying. This is consistent with the variability in CBF and mortality reported for this method. The control animal experienced the same drop and recovery in CBF.

The IA delivery in Group 2 animals for both cell concentrations experienced a 20% spike in CBF after CCA reperfusion and maintained its CBF slightly above baseline for 15 minutes. The overall comparison between group 1 and 2 demonstrated a statistically significant difference ($p< 0.05$).

Conclusions: The lack of drop in CBF of Group 2 indicates that the reported risk of vascular occlusion and mortality may be confined to the high volume and the CCA occlusion catheter method of IA delivery. Furthermore, the drop in Laser Doppler values during the first minute of the control indicates that the initial drop is an artifact of PBS infusion and is most likely not an indicator of reduced CBF due to an occlusion. Depending on the method, IA delivery of therapeutic cells does not pose a clear risk of vascular occlusion.

823

Brain Poster Session: Subarachnoid Hemorrhage

CERVICAL SPINAL CORD STIMULATION FOR PREVENTION OF CEREBRAL VASOSPASM IN ANEURYSMAL SUBARACHNOID HAEMORRHAGE: PRELIMINARY RESULTS OF FIRST NORTH AMERICAN STUDY

K. Slavin, E. Goellner, P. Eboli, S. Aydin, E. Colpan, N. Mlinarevich, K. Watson, R. Deveshwar, S. Amin-Hanjani, F. Charbel

Neurosurgery, University of Illinois at Chicago, Chicago, IL, USA

Objective: The goal of this study was to establish feasibility and safety of prolonged cervical spinal cord stimulation (SCS) in the setting of acute aneurysmal subarachnoid hemorrhage (aSAH), as well as to evaluate clinical effects of cervical SCS in a small group of selected aSAH patients. The study was undertaken in preparation for a larger scale randomized trial of SCS for prevention of cerebral arterial vasospasm following aSAH.

Material and methods: A single arm non-randomized prospective study of cervical SCS in aSAH patients was performed in University of Illinois at Chicago. Standard percutaneous 8-contact SCS electrodes were implanted under an Investigational Device Exemption protocol in 12 consecutive patients that satisfied the following inclusion criteria: age 18-65, angiography-confirmed aSAH within 3 days prior to the electrode implantation, Hunt/Hess (H&H) grade 2-4, Fischer grade 2-4, no history of previous cervical spine surgery, ability to obtain informed consent from the patient or family. All electrodes were inserted using percutaneous approach under general anesthesia immediately upon completion of the definitive surgical or endovascular procedure to secure the ruptured aneurysm. SCS was then delivered for the soonest of either 14 consecutive days or until the patient's discharge. Daily vital signs, laboratory values, transcranial Doppler, computed tomography and angiography results were recorded along with the information on presence of clinical vasospasm and all interventions aimed at vasospasm prevention and treatment.

Results: Mean age of implanted patients was 49 years (range - 27-62), average H&H grade - 2.9, average Fisher grade - 3.3. Three had aneurysms coiled and 9 - clipped. One patient developed multisystem failure and expired on post-operative day 11. In two patients, electrode was inadvertently pulled out on days 7 and 13 after the implantation. There were no complications related to the electrode insertion or to SCS during the entire study period. The angiographic vasospasm was observed in 6 out of 12 patients, and clinical vasospasm - in 2 out of 12; no patient suffered any vasospasm-related neurological complication. Both incidences were smaller than predicted based on the patients' Fisher and H&H grades.

Conclusions: This is the first North American study of SCS for prevention of vasospasm after aSAH; it conclusively shows both safety and feasibility of this promising invasive treatment approach. Our data indicate that despite high level of acuity in patients after aSAH, general severity of medical condition, impaired level of consciousness, frequent patient re-positioning, need in multiple tests and variety of monitors, SCS electrodes may be safely implanted and maintained for the two-week period. Further data analysis and additional studies will be needed to evaluate its therapeutic benefit.

CREATINE MODULATES SURVIVAL, MIGRATION AND DIFFERENTIATION IN NEURAL STEM CELLS

R.H. Andres[1], A. Pendharkar[1], R. Guzman[1], A. De[2], T.M. Bliss[1], E. MacMillan[3], C. Svendsen[3], S.S. Gambhir[2], H. Widmer[4], T. Wallimann[5]

[1]Department of Neurosurgery, [2]Molecular Imaging Program at Stanford, Stanford University School of Medicine, Stanford, CA, [3]The Waisman Center, University of Wisconsin-Madison, Madison, WI, USA, [4]Department of Neurosurgery, University of Berne, Bern, [5]Department of Cell Biology, Swiss Federal Institute of Technology (ETH), Zurich, Switzerland

Objectives: Creatine kinase (CK) catalyzes the reversible transphosphorylation of creatine (Cr) by ATP. CK isoenzymes are specifically localized at strategic sites of ATP consumption to efficiently regenerate ATP in situ via phosphocreatine (PCr) or at sites of ATP generation to build-up a PCr pool. Accordingly, the CK/PCr system plays a key role in cellular energy buffering and energy transport, particularly in cells with high and fluctuating energy requirements like neurons, and exogenous Cr supplementation results in higher cellular ATP reserves and improved metabolic channeling. Given the high expression of CKs in the developing CNS, we hypothesize that Cr supplementation might be effective in improving the metabolic state of neural stem cells (NSCs). In the present study, we investigated the effects of Cr on survival, migration, and differentiation of mouse NSCs isolated from the subventricular zone (mNSCs) and NSCs derived from the human fetal cortex (hNSCs).

Methods and results: We found both the brain-specific cytosolic (BB-CK) and the ubiquitous mitochondrial (uMt-CK) isoform of CK expressed in mNSC and hNSC, as well as the key enzymes for endogenous Cr synthesis, AGAT and GAMT, and the specific transporter for cellular Cr uptake, CRT. Cr supplementation at 5 mM for 7 days resulted in higher ATP levels in mNSCs and hNSCs, as compared to untreated controls ($p< 0.01$).

Chronic Cr exposure of cultured mNSCs and hNSCs resulted in a dose-dependent increase in neurosphere size and total cell numbers with a maximal effect at 5 mM after 7 days in vitro ($p< 0.05$). Analysis of BrdU incorporation did not reveal a significant increase in proliferation activity, but Cr-treated cultures contained less cells with immunoreactivity for active Caspase-3 ($p< 0.05$), pointing towards an antiapoptotic effect of Cr.

In a modified Boyden chamber assay, both Cr-pretreated mNSCs and hNSCs demonstrated an improved migratory potential ($p< 0.01$) after 60 min, as compared to untreated controls. In line with this finding, we found that Cr-pretreated, GFP-labeled mNSCs showed improved migration to the ischemic brain area after intrastriatal transplantation in a distal MCA occlusion stroke model in C57/Bl6 mice ($p< 0.05$).

Next we examined the effects of Cr on differentiation of NSCs. Chronic Cr exposure at 5 mM resulted in significantly higher neuronal cell numbers (NeuN+, $p< 0.05$) at the expense of the glial fate (GFAP+, $p< 0.05$) after differentiation conditions in vitro for 5 days. In addition, we found disproportionally higher numbers of GABA-immunoreactive cells in the Cr-treated groups ($p< 0.05$), suggesting that Cr acts as a differentiation factor for specific neuronal subpopulations.

Conclusion: Our findings suggest that the CK/PCr system is critically involved in maintaining the energy metabolism of NSCs. Chronic Cr supplementation resulted in increased cellular ATP levels, inhibited apoptosis during in vitro expansion, and improved NSC migration in vitro and in vivo. Cr exposure also promoted the differentiation of NSCs towards the neuronal lineage, particularly supporting the GABAergic phenotype. Cr pretreatment of NSCs might therefore offer new ways for improving cell replacement approaches for stroke and other diseases of the nervous system.

825

Brain Poster Session: Glial Functions

ASTROCYTIC METABOLISM ASSESSED FROM ^{14}C-ACETATE AFTER OXYGEN GLUCOSE DEPRIVATION AND CHEMICAL ACTIVATION IN VITRO

T. Sasaki[1], K. Kitagawa[2], K. Kajimoto[3], Y. Terasaki[1], E. Omura-Matsuoka[1], N. Ohyama[1], Y. Sugiyama[2], S. Okazaki[2], Y. Yagita[2], J. Hatazawa[4]

[1]Division of Stroke Center, Department of Internal Medicine, [2]Department of Neurology, Osaka University Graduate School of Medicine, Osaka, [3]Stroke Divison, Department of Internal Medicine, National Cardiovascular Center, Suita, Osaka, [4]Department of Nuclear Medicine, Osaka University Graduate School of Medicine, Osaka, Japan

Background: Increasing evidence has suggested that stroke should be integrative, and thus a concept of dynamic interaction between cells belonging to the neurovascular unit, such as endothelial cells, astrocytes and neurons, is emerging. In the neurovascular unit, astrocyte supports their maintenance of the permeability barrier. Also, considering the coupling of neuronal activation to cerebral blood vessel responses, astrocytes play key roles between these cells. Thus, whereas astrocytes play crucial roles in both normal and injured brain, the astrocytic metabolism after ischemia are not yet fully known. Exogenous acetate is preferentially metabolized by astrocytes in the CNS. Acetate uptake by astrocytes appears to be mediated by a carrier of monocarboxylate transporter (MCT). We have assessed astrocytic metabolism based on the incorporation of radiolabel ^{14}C-acetate after in vitro ischemia and chemical stimulation by lipopolysaccharide (LPS).

Subjects and methods: Astrocytes for culture were obtained from 1-2 day neonatal Wister rats and grown in DMEM + 10% fetal bovine serum (FBS) + antibiotics. The purity of astrocytes has been shown to be > 95% glial fibrillary acidic protein positive cells. For oxygen-glucose deprivation (OGD), the culture medium was replaced with a glucose-free EBSS that had previously been saturated with 95% N_2/5% CO_2 and heated to 37°C. The cultures were then put into an anaerobic incubator (pO_2 < 2 mm Hg) with an atmosphere of 95% N_2 and 5% CO_2 (1% O_2) at 37°C for 6 hours. The cells were subjected to 6 hours of OGD followed by reoxygenation. Reoxygenation was achieved by returning cell cultures to normoxic conditions (37°C in a humidified 5% CO_2 atmosphere). To elucidate the mechanism of acetate uptake, we assessed the ability of selective inhibitor of TCA cycle, fluoroacetate, or MCT 1, 2 or 4 siRNAi. On the other hand, the cultures were exposed for 24 hours to 0.5-2.0 μg/ml LPS to study the incorporation of ^{14}C-acetate under chemical activated conditions of astrocyte.

Results: Following OGD, acetate uptake significantly increased at 3 to 24 hours after reoxygenation than basal control levels (Figure). Fluoroacetate produced significant inhibition at 10mM. In addition, MCT-1 siRNAi, but not MCT-2 or MCT-4 siRNAi, significantly decreased the acetate uptake. We also observed the increase of acetate uptake following LPS treatment.

Conclusion: These findings indicate that astrocytic function dynamically changes following ischemia and chemical activation. The images of ^{14}C-acetate may be particularly useful in the elucidation of mechanism of human stroke and neurodegenerative disease.

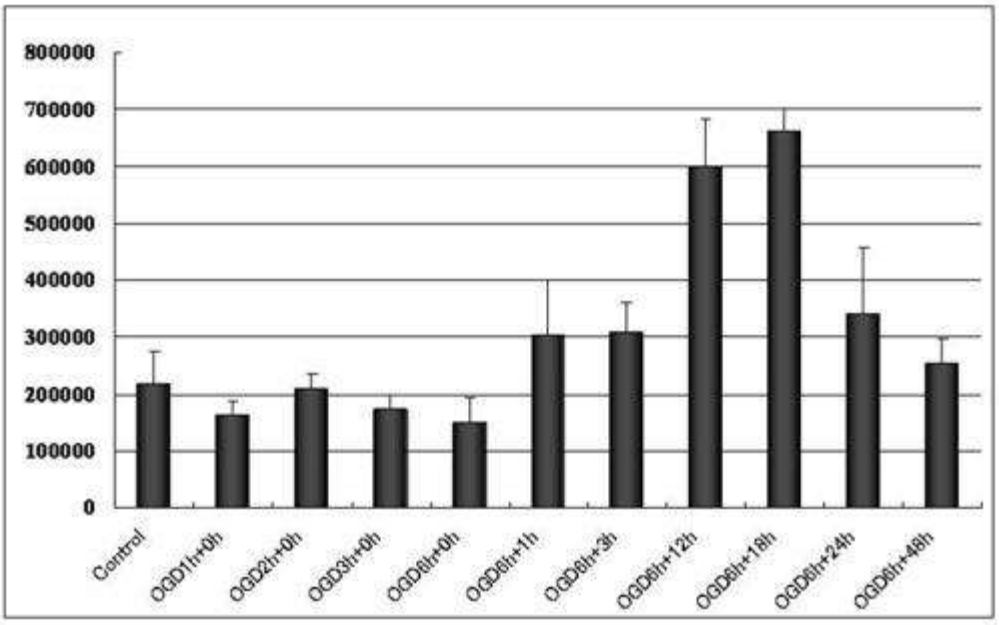
800000
700000
600000
500000
400000
300000
200000
100000
0
Control
OGD1h+0h
OGD2h+0h
OGD3h+0h
OGD6h+0h
OGD6h+1h
OGD6h+3h
OGD6h+12h
OGD6h+18h
OGD6h+24h
OGD6h+48h

[Figure]

827

Brain Poster Session: Traumatic Brain Injury

ROLE OF VASOPRESSIN V1 RECEPTORS FOR POST-TRAUMATIC BRAIN EDEMA FORMATION, CEREBRAL BLOOD FLOW, AND SECONDARY BRAIN DAMAGE

R. Trabold, S. Krieg, P. Nikolaus

Department of Neurosurgery, University of Munich Medical Center - Grosshadern, Ludwig Maximilians University, Munich, Germany

Objective: Reductions of cerebral blood flow (CBF) and the formation of brain edema are still among of the most deleterious sequels of traumatic brain injury (TBI) and their pathophysiology is still not well understood. The aim of the current study was to investigate the effect of arginine-vasopressin (AVP, antidiuretic hormone, ADH) receptors, important regulators of water homeostasis and blood flow, on post-traumatic brain edema, cerebral blood flow, neurological function, and secondary brain damage.

Methods: Male C57/Bl6 mice (n=8-10 per group) were randomized to six experimental groups and subjected to controlled cortical impact (CCI; 8 m/s, 1 mm). 5 min after trauma animals received the AVP V1-receptor antagonist SR-49059/g either systemically (10 µg/g) or intracerebroventricularly (icv, 40 ng/g). CBF was assessed immediately after trauma by laser Doppler fluxmetry while cerebral water content (wet-dry method), ICP, neurological function (beam walk), and contusion volume (histomorphometry) were assessed 24 h after the impact.

Results: The systemic inhibition of AVP V1 reduced post-traumatic (30 min) by 26% as compared to controls ($p < 0.05$) while the central application had no effect on CBF. Further experiments using the icv protocol reduced post-traumatic brain edema formation by 68% ($p < 0.05$), intracranial hypertension by 46% ($p < 0.05$), secondary contusion expansion by 46% ($p < 0.05$), and significantly improved the neurological function ($p < 0.05$).

Conclusion: The current results demonstrate that vasopressin V1 receptors are involved in the pathogenesis of post-traumatic brain damage. Although the underlying mechanisms of AVP-mediated brain edema formation and CBF remain to be elucidated, our study suggests that vasopressin V1 receptors may represent a novel pharmacological target for the treatment of secondary brain damage following traumatic brain injury.

DISPLACEMENT OF ^{18}F-FALLYPRIDE BINDING WITH HALOPERIDOL IN A WITHIN-SUBJECT DESIGN USING A BETA MICROPROBE

G. Warnock[1], D. Goblet[1], C. Lemaire[1], F. Giacomelli[1], M. Bahri[1], X. Langlois[2], A. Luxen[1], A. Plenevaux[1]

[1]Centre de Recherches du Cyclotron, Universite De Liege, Liège, [2]Johnson & Johnson Pharmaceutical Research & Development, Division of Janssen Pharmaceutica N.V., Beerse, Belgium

The dopamine D2 receptor is of interest for its role in the action of antipsychotic drugs, and therefore its implied role in the pathology of psychotic illness. A linear relationship exists between clinical potency and affinity for D2 receptors for many antipsychotic drugs.

^{18}F-Fallypride is a high affinity dopamine D2/D3 radioligand used for quantifying striatal but also extrastriatal dopamine D2/D3 receptors with positron emission tomography (PET) and related techniques. We have successfully accomplished the automation of ^{18}F-fallypride radiosynthesis, purification and formulation. The full synthesis has been accomplished in a total time of 80 min with a radiochemical yield of 40%. ^{18}F-fallypride can be obtained with excellent radiochemical purity (> 96%) and enantiomeric excess (94%), with specific activities of 1-3 Ci/μmol.

In the present studies we have used a beta microprobe system to measure ^{18}F-fallypride binding in the striatum of Sprague-Dawley rats, using the cerebellum as a reference region. For displacement of ^{18}F-fallypride, the antipsychotic haloperidol was chosen for its high affinity for D2 receptors.

Beta microprobe systems have recently become commercially available as an affordable alternative to PET. These systems utilise implantable probes consisting of a small (0.25-1mm) scintillation crystal bonded to a fibre optic cable, which can be stereotactically located in a specific region of the rodent brain. Scintillation in the crystal is carried by fibre optic to a photomultiplier tube from which a time-activity curve is generated.

^{18}F-fallypride was injected intravenously through a catheter in the femoral vein and activity in the striatum and cerebellum measured for 90 minutes. After 30 minutes a bolus of saline was injected as a control before the injection of haloperidol (0.025-0.25mg/kg) 30 minutes later. Specific striatal binding was calculated as [total binding striatum]-[binding cerebellum]. The effect of saline and haloperidol on specific binding was calculated as the percentage change in specific binding from the 30 or 60 minute maximum.

Haloperidol displaced ^{18}F-fallypride binding in the striatum in a clear dose- and time-dependent manner. Measurement of binding for a longer duration could be useful to confirm the maximum change in binding after haloperidol treatment. These results confirm the usefulness of the beta microprobe system for the measurement of D2 binding using ^{18}F-fallypride.

Brain Poster Session: Neuroprotection

NEUROPROTECTIVE EFFECT OF GENISTEIN AND DAIDZEIN IS DEPENDENT ON PPARγ ACTIVATION

O. Hurtado[1], G. Torregrosa[2,3], J.B. Salom[2,3], F.J. Miranda[3], E. Alborch[2,3], M. Sobrado[1], I. Lizasoain[1], **M.A. Moro**[1]

[1]Departamento de Farmacología, Facultad de Medicina, Universidad Complutense de Madrid (UCM), Madrid, [2]Centro de Investigación, Hospital Universitario La Fe, [3]Departamento de Fisiología, Universitat de València, Valencia, Spain

Objectives: Phytoestrogens are a group of plant-derived compounds which include mainly isoflavones (genistein, daidzein, glycitein, equol and biochanin A), lignans, coumestans, flavonoids, stilbenes and mycotoxins. Phytoestrogens prevent neuronal damage (1) and improve outcome in experimental stroke (2); however, mechanism of their neuroprotective action has not been fully elucidated. In this context, Peroxisome proliferator-activated receptor-γ (PPARγ) agonists have been shown to exert antiinflammatory effects in several settings, including the central nervous system (CNS) (3). The aim of this study is to determine whether phytoestrogen-induced neuroprotection is brought about by selective stimulation of PPARγ.

Methods: Primary cultures of rat mixed cortical cells and oxygen and glucose deprivation (OGD) were performed as described (4): Culture medium was replaced by OGD solution. OGD cells were transferred to an anaerobic chamber containing a gas mixture of 95%N_2/5%CO_2 at 37°C. The time of exposure to OGD was 150 min. In another set of experiments, cultures were exposed to the specific PPARγ antagonist (5) T0070907 (Tularik, San Francisco, CA, USA) for 24 h. As a marker of necrotic tissue damage, LDH (lactate dehydrogenase) activity released from damaged cells was determined 24 h after OGD.For preparation of nuclear extracts cells were collected 24 h after treatment with phytoestrogens in phosphate-buffered saline. The homogenate was centrifuged at 4°C, 12,000g. Supernatant was discarded and nuclear extracts were prepared as described (6). PPARγ activity was assessed in nuclei using PPARγ Transcription Factor Assay kit (Cayman Chemical Company, Ann Arbor, MI, USA).

Results: Administration of genistein or daidzein 24 hours before, during and after exposure to OGD decreased lethal OGD-induced LDH release measured 24 hr after the ischemia and caused neuroprotection in pure neuronal cultures (LDH: 92, 88 and 72% vs 100% OGD with 0.05, 0.5 and 5 μM genistein and 46, 45% vs 100% OGD with daidzein 0.5 and 5 μM respectively) but not in mixed cultures. The PPARγ antagonist T0070907 (1μM) inhibited the protective effect caused by the administration of 5 μM genistein or daidzein.To check the role of genistein and daidzein in PPARγ activation, we next quantified PPARγ transcriptional activity by the ability of nuclear proteins to bind a specific oligonucleotide containing the PPRE consensus sequence using an assay kit. Indeed, both phytoestrogens induced an increase in PPARγ activation in pure neuronal cultures: 129 and 125% vs control (100%) with 0.5 and 5 μM genistein and 122 and 117% vs control (100%) with 0.5 and 5 μM daidzein.

Conclusions: These results demonstrate that genistein and daidzein could be used as preventive agents in cerebral ischemia and suggest that these phytoestrogens act as agonists of PPARγ nuclear receptor.

Supported by RETICS-RENEVAS from ISCIII. RD06/0026/0005.

References:

1. Kajta et al. 2007. Neuroscience. 145:592-604.

2. Burguete et al. 2006. Eur J Neurosci. 23:703-10.

3. Jiang et al. 2008. CNS Drugs. 22:1-14.

4. Hurtado et al. 2002. J Cereb Blood Flow Metab. 22:576-85.

5. Lee et al. 2002. J Biol Chem. 277:19649-57.

6. Cárdenas et al. 2000. J. Neurochem. 74:2041-48.

Brain Poster Session: Experimental Cerebral Ischemia: In Vitro

ENDOPLASMIC RETICULUM STRESS WITH INCREASED XBP-1 ACTIVATION LEADING TO AGGRAVATED CEREBRAL INFARCTION IN SOD1 KNOCK-OUT MICE

S. Nakajima[1,2], M. Nibuya[1], K. Isoda[2]

[1]Neurology/Psychiatry, [2]1st Internal Medicine, NDMC, Tokorozawa, Japan

Objectives: Endoplasmic Reticulum (ER) plays important roles in maintaining intra-cellular Ca^{2+}, folding proteins, and responding to various cellular stresses. Ischemia might be the maximum ER stress when combined with reactive oxygen species (ROS). Hypo-functions of CuZn superoxide disumutase (SOD1) are known to worsen tissue damages by ROS, but the grade of ER stress in this condition is not well analyzed compared to that of mitochondrial damage. We aimed to examine the possible overt ER stress in the stroke model induced by the singlet oxygen and ROS exposure.

Methods: SOD1 knockout (hetero n=19, and homo n=18) and C57BL/6 (wild n=43) mice were anesthetized by the intra-peritoneal injection of 1% chloralose and 10% urethane mixture, keeping rectal temperatures at 37.5 degrees on the heating pad. Animals were fixed on the stereotactic apparatus and the non-invasive photothrombosis (PT) was created in the right distal-MCA by the transcranial irradiation of attenuated He-Ne laser beam (532 nm) guided through a single glass-fiber in the micromanipulator, after the injection of Rose-Bengal solution via a tail vein. Cerebral blood flow changes were recorded by a video-microscope and measured by a laser-Doppler flow (LDF) probe on the ischemic lesion. Ischemic changes were observed sequentially by the 9.4 T MRI (Bruker), and analyzed histologically up to the end-point of 1 month after loads. As the indicator of ER stress, spliced XBP-1 mRNA was measured by a RT-PCR method from samples of ischemic and contra-lateral hemispheres at 3, 12, and 24 hours after ischemic insults, and effects of cilostazol (60 mg/kg, po) and edaravone (6 mg/kg, iv) combination therapy were also evaluated in each group of mice.

Results: Microscopic observation of distal-MCA demonstrated recurrent occlusion/recanalization by micro-emboli flown from the laser-irradiated locus, showing cyclic hyperemias in LDF before the complete occlusion. Time to occlusions were shorter in SOD1 knockout mice, and elongated in the treated groups. MRI disclosed superficial spindle-shaped ischemic changes within 1 hour after distal-MCA occlusion, and enlarged gradually with surrounding edema. Ischemic T2WI area after 1 day in the wild group was 24.5±3.9 % (M±SEM) of the ipsi-lesional hemisphere in the untreated group, and reduced to 10.1±3.7 % in the therapy group ($p< 0.05$). SOD1 knockout groups demonstrated broader edematous lesions, which subsided after 1 week revealing larger infractions. Spliced XBP-1 transcription in the ischemic hemisphere showed the highest increase in SOD1 homo-knockout mice at each time spans, and significantly reduced by the combined therapy.

Conclusions: During the acute stroke stage, SOD1 hypo-function elicited the marked ER stress response with exaggerated XBP1 splicing, and induced the larger cerebral infarction. Excessive and sustained ER stress may trigger the apoptotic cell death around necrotic foci, and the early treatment with potent free radical scavenger and anti-thrombotic drugs will salvage this vicious process, as shown in the present study. Non-invasive PT stroke model in this experiment enabled the individual analysis of ischemic lesions using the MRI, and might be suitable for the long-term study of SOD1 hypo- or hyper-function in combination with free radical inducers and scavengers.

843

Brain Poster Session: Experimental Cerebral Ischemia: In Vitro

INDUCTION OF AUTOPHAGY IN THE RAT HIPPOCAMPUS AND CULTURED NEURONS BY IRON

Y. He, Y. Hua, S. Song, W. Liu, R.F. Keep, G. Xi

Department of Neurosurgery, University of Michigan, Ann Arbor, MI, USA

Objectives: Autophagy occurs in the brain after intracerebral hemorrhage (ICH)(He et al 2008). Iron is an important factor causing neuronal death and brain atrophy after ICH (Hua et al 2007; Xi et al 2006). In this study, we examined whether iron can induce autophagy in the hippocampus and in cultured neurons.

Methods: For in vivo studies, rats received an infusion of either saline or ferrous iron into the right hippocampus and were killed at 1, 3, or 7 days later for Western blot analysis of microtubule--associated protein light chain-3 (LC3). For in vitro studies, primary cultured cortex neurons from rat embryos were exposed to ferrous iron. Cells were used for Western blot analysis of LC3 and monodansylcadaverine (MDC) staining 24 hours later.

Results: Physiological variables including mean arterial blood pressure, blood pH, PaO_2, $PaCO_2$, hematocrit, and blood glucose level were controlled within normal ranges.

Using Western blot analysis, a time course study of LC3 showed that the ratio of LC3-II to LC3-I in the ipsilateral hippocampus was significantly increased at day 3 and remained at high levels at day 7 after intrahippocampal injection of ferrous iron. The ratio of LC3-II to LC3-I in the ipsilateral hippocampus at day 3 after ferrous iron injection was markedly higher than that in the ipsilateral hippocampus after saline injection (2.48 ± 0.57 versus 0.42 ± 0.08; $p< 0.01$).

To test whether autophagy also happens after ferrous iron treatment in cultured neurons, cells were exposed to ferrous iron or control medium. Western blotting showed that cells treated with ferrous iron had a higher ratio of LC3-II to LC3-I compared with vehicle control (0.40 ± 0.15 versus 0.13 ± 0.05; $p< 0.01$). MDC labeling showed an increase in the number of vacuoles and their size in cells treated with ferrous iron.

Conclusions: These results indicate that autophagy is induced by iron in neurons and that iron-induced autophagy may contribute to brain injury after ICH.

References:

He Y, Wan S, Hua Y, Keep RF, Xi G (2008) Autophagy after experimental intracerebral hemorrhage. J Cereb Blood Flow Metab 28:897-905.

Hua Y, Keep R, Hoff J, Xi G (2007) Brain injury after intracerebral hemorrhage: the role of thrombin and iron. Stroke 38:759-62.

Xi G, Keep RF, Hoff JT (2006) Mechanisms of brain injury after intracerebral hemorrhage. Lancet Neurol 5:53-63.

Brain PET Oral 1: PET Image Reconstruction and Processing

EFFECT OF IMAGE RECONSTRUCTION ALGORITHMS ON BINDING POTENTIAL CALCULATIONS IN [^{18}F]-FALLYPRIDE PET

J. Dunn[1], P. Marsden[1], M. O'Doherty[1], M. Cleij[1], L. Reed[2]

[1]PET Imaging Centre, Kings College London, [2]Section of Addiction Neurobiology, Institute of Psychiatry, Kings College London, London, UK

Objectives: The PET radioligand [^{18}F]-fallypride binds to D2/D3 receptors with high affinity in both striatal and extrastriatal regions (Slifstein et al 2004). We investigated the effect of PET reconstruction algorithms on the quantification of binding potential (BP) in selected regions.

Methods: Six healthy male volunteers were injected with 250MBq of [^{18}F]-fallypride and had a brain scan for 90 minutes on a GE Discovery STE PET camera with a 3D acquisition. CT attenuation corrected dynamic images were reconstructed after 2D Fourier rebinning (FORE) with filtered back projection (FBP) and iterative (FORE-ITER) reconstruction algorithms. Also, VUE Point, a fully 3D iterative algorithm (3D-ITER), was used to reconstruct both attenuation corrected (AC) and non-attenuation corrected (NAC) dynamic PET images. The frames in each NAC 3D-ITER image were realigned using the rigid-body realignment algorithm in SPM5 (www.fil.ion.ucl.ac.uk/spm) and these transforms were applied to the FBP, FORE-ITER and AC 3D-ITER images of each subject. Time activity curves from these images were extracted from regions defining the cerebellum, amygdala, caudate, putamen, thalamus, mid temporal lobes and inferior temporal lobes, all bilaterally, from the Automated Anatomical Atlas (Tzourio-Mazoyer et al 2002). The cerebellum was used a reference region to calculate the binding potential using the simplified reference tissue models of Lammertsma and Hume (1996).

Results: When corrected for multiple comparisons repeated measures ANOVA revealed a significant effect of reconstruction method on BP in bilateral amygdala, right putamen and all temporal regions (see table). Post-hoc analysis revealed significant differences in BP (denoted * in the table) between the FORE-ITER and 3D-ITER images in bilateral amygdala, right putamen, bilateral mid temporal lobes and right inferior temporal lobe.

	Mean (sd) BP across subjects			Mean fractional difference in BP (%)		
Region Name	FBP	FORE-ITER	3D-ITER	FBP v FORE-ITER	FORE-ITER v 3D ITER	FBP v 3D-ITER
Amygdala L	2.91 (0.43)	3.01 (0.44)	2.73 (0.43)	-3.3	9.9*	6.7
Amygdala R	3.10 (0.47)	3.18 (0.47)	2.93 (0.43)	-2.5	8.4*	5.8
Putamen R	14.10 (1.59)	13.94 (0.67)	14.86 (0.97)	1.0	-6.3*	-5.3
Mid Temp.	0.67 (0.24)	0.62 (0.23)	0.67 (0.22)	8.1	-9.3*	-1.3

Lobe L						
Mid Temp. Lobe R	0.63 (0.20)	0.59 (0.20)	0.64 (0.19)	6.8	-9.0*	-2.3
Inf. Temp. Lobe L	0.90 (0.28)	0.84 (0.26)	0.88 (0.26)	6.7	-4.81	1.9
Inf. Temp. Lobe R	0.84 (0.26)	0.79 (0.25)	0.83 (0.25)	6.1	-4.7*	1.4

[Descriptive statistics and comparisons of BP.]

Conclusions: The spatially variant convergence of iterative reconstruction algorithms is known to affect quantified PET especially in regions of low activity (Reilhac et al 2008). In most of the regions investigated BP was affected by reconstruction method, with the largest pairwise fractional differences between FORE-ITER and 3D-ITER, approaching 10% in the amygdala and mid temporal lobes. In conclusion choice of reconstruction algorithm is important especially between choices of iterative algorithms.

References:

Lammertsma AA, Hume SP (1996) Neuroimage 4(3):153-8.

Reilhac A et al. (2008) Neuroimage 39(1):359-68.

Slifstein M, et al. (2004) Synapse 54(1):46-63.

Tzourio-Mazoyer N et al. (2002) NeuroImage 15(1):273-89.

ENLARGED INFARCTS IN MICE EXPRESSING THE ARCHETYPAL NOTCH3 R90C CADASIL MUTATION

J.H. Lee[1], K. Eikermann-Haerter[1], A. Joutel[2], M.A. Moskowitz[1], C. Ayata[1,3]

[1]Stroke and Neurovascular Regulation Lab, Department of Radiology, Massachusetts General Hospital, Harvard Medical School, Charlestown, MA, USA, [2]Université Paris 7-Denis Diderot, Faculté de Médecine, Site Lariboisière, Paris, France, [3]Stroke Service and Neuroscience Intensive Care Unit, Department of Neurology, Massachusetts General Hospital, Harvard Medical School, Charlestown, MA, USA

Background and aims: Cerebral autosomal dominant arteriopathy with subcortical infarcts and leukoencephalopathy (CADASIL) is the most common inherited small vessel disease responsible for strokes, migraines, mental disorders, and dementia. The disease is caused by highly stereotyped mutations in NOTCH3, resulting in progressive degeneration of cerebrovascular smooth muscle cells. We recently reported increased sensitivity to cerebral ischemia in notch3 knockout mice. However, the impact of CADASIL mutations on focal ischemic outcome has not been tested [1].

Methods: All experiments were conducted by a blinded investigator. Transgenic mice overexpressing mutant human NOTCH3 R90C (TgR90C) were compared to those overexpressing wild-type human NOTCH3 (TgWT) and to non-transgenic wild-type (WT) mice (C57BL/6 background). Mice were anesthetized with isoflurane (2% induction, 1.5% maintenance, in 70% N_2O/30% O_2), and subjected to 1h transient middle cerebral artery occlusion (MCAO) using an intraluminal filament inserted via the external carotid artery. Regional CBF was monitored using a laser Doppler probed placed over the core MCA territory. Systemic physiological parameters were monitored before and during ischemia, and after reperfusion. Neurological deficits were assessed before sacrifice at 24h, using five-point grading. Circle of Willis was examined after intracardiac carbon black perfusion. Indirect infarct volumes were calculated using 1mm-thick TTC-stained coronal sections.

Purpose: To test whether NOTCH3 R90C CADASIL mutation worsens outcome after focal ischemia.

Results: Arterial blood pressure, pO_2, pCO_2 and pH were within normal range in all groups. Regional CBF did not differ among the groups after common carotid occlusion (CCAO), MCAO, and reperfusion. TgR90C mice developed significantly larger infarcts in both cortex and striatum compared to both TgWT and WT mice (*$p < 0.05$). Neurological deficits were significantly more severe in TgR90C mice compared to both TgWT and WT strains. Circle of Willis anatomy and presence of a posterior communicating artery did not differ among groups.

Strain	BW (g)	N	Mortality	CBF post-CCAO (%)	CBF post-MCAO (%)	Deficit	Indirect infarct (mm3)	Edema (mm3)
WT	31±4	12	3	73±16	11±4	2 [1-2]	68±15	14±7

TgWT	31±2	10	3	59±16	10±4	2 [2-3]	74±14	12±6
TgR90C	32±4	9	2	65±13	10±4	3 [2-3]*	93±24*	15±9

[Results]

Conclusions: To our knowledge, this is the first demonstration of worse ischemic tissue and neurological outcome associated with a CADASIL mutation. Although R90C NOTCH3 retains Notch3 function, in vivo [2], mutants develop impaired cerebrovascular autoregulation and an age-dependent arteriopathy similar to CADASIL [3, 4], suggesting a hemodynamic mechanism for the enlarged infarcts in NOTCH3 R90C mutants.

References:

1. Arboleda-Velasquez, J.F., et al., Linking Notch signaling to ischemic stroke. Proc Natl Acad Sci U S A, 2008. 105(12): p. 4856-61.

2. Monet, M., et al., The archetypal R90C CADASIL-NOTCH3 mutation retains NOTCH3 function in vivo. Hum Mol Genet, 2007.

3. Lacombe, P., et al., Impaired cerebral vasoreactivity in a transgenic mouse model of cerebral autosomal dominant arteriopathy with subcortical infarcts and leukoencephalopathy arteriopathy. Stroke, 2005. 36(5): p. 1053-8.

4. Ruchoux, M.M., et al., Transgenic mice expressing mutant Notch3 develop vascular alterations characteristic of cerebral autosomal dominant arteriopathy with subcortical infarcts and leukoencephalopathy. Am J Pathol, 2003. 162(1): p. 329-42.

Brain Poster Session: Experimental Stroke & Cerebral Ischemia

THE EFFECT OF PRE-MORBID INTRAVENOUS ADMINISTRATION OF DIPYRIDAMOLE IN A RABBIT MODEL OF EMBOLIC MIDDLE CEREBRAL ARTERY OCCLUSION

C.D. d'Esterre[1], W.G. Eisert[2], T.Y. Lee[1,3]

[1]Medical Biophysics, University of Western Ontario, London, ON, Canada, [2]Corp. Dept. Medical Affairs, Boehringer Ingelheim, Ingelheim, Germany, [3]Robarts Research Institute, London, ON, Canada

Objective: In twenty-nine trials examining the use of anti-platelet agents in patients with cerebrovascular disease, dipyridamole (DP) reduced the rate of vascular events but not vascular death. Thus, the role of DP to decrease stroke severity remains unclear. We investigated the potential of pre-morbid intravenous DP administration to minimize stroke severity in a rabbit embolic model.

Methods: Fourteen male New Zealand white rabbits (2.7-3.6 kg) were randomized to DP (n = 7) or Saline (sham) treatment (n = 7). Animals were infused via the right common jugular vein with DP or saline for 7 days prior to stroke induction. DP plasma concentrations were measured and maintained at > 1μg/ml plasma. The left middle cerebral artery was occluded by injection of an autologous blood clot into the corresponding internal carotid artery.

On day of stroke induction, three computed tomography perfusion (CTP) scans were performed: baseline (pre), 10 and 30 minutes (post embolus injection). A neurological assessment, with a 25 point scale, and a CTP scan were performed on days 1,4,7,14,21, and 28 post stroke. On completion of the study, the animals were sacrificed and 2,3,5-tetrazolium chloride (TTC) and H & E stained brain slices were analyzed for viability. For each animal, mean CBF and CBV in the ipsilateral cerebral hemisphere (CBF_{ih}, CBV_{ih}, respectively) were determined with CT Perfusion 4 software (GE Healthcare) at each time point. An omnibus repeated measures ANOVA and post-hoc Tukey test were used to identify significant differences in the collected data.

Results: The DP and Saline groups survived 15.3 ± 12.7 and 5.6 ± 3.1 days, respectively. 66% of the DP group survived past 28 days, while the Saline group were euthanized by day 7 due to severe neurological deficits. The DP group had more viable ipsilateral hemisphere tissue, shown with TTC staining, than the Saline group, 78.5 ± 36.4% vs. 46.7 ± % ($P< 0.05$) at sacrifice. On both day 4 and 7, the DP group had decreased deficit (lower neurological scores) than Saline group, 6.8 ± 5.3 vs. 17.9 ± 7.3 ($P < 0.05$).

Mean CBF_{ih} between DP and Saline groups were significantly different on day 1 (75.6 ± 24.7 vs. 55.1 ± 21.2) and 4 (77.2 ± 19.7 vs. 59.3 ± 16.8) post stroke induction; however, mean CBF_{ih} between groups were not different on the day of stroke induction. Within the DP group, mean CBF_{ih} at day 1 post stroke was 15% higher than that at 30 min post stroke ($P < 0.05$) but not different from subsequent days. Within the Saline group, day 1 and 4 mean CBF_{ih} was not different from that at 30 minutes post stroke. An inter-group comparison demonstrated a significant difference in mean CBF_{ih} on days 1 and 4. For CBV_{ih}, there were no differences between or within groups.

Two non-treated animals presented with small microbleeds within the infarcted tissue, observed on H&E staining.

Conclusion: Pre-morbid dipyridamole administration was shown to aid in the maintenance of cerebral perfusion, and long term recovery during an acute embolic stroke.

TOLL-LIKE RECEPTOR 2/1 SIGNALING IN CEREBRAL ISCHEMIA REQUIRES THE SCAVENGER RECEPTOR CD36

T. Abe, M. Shimamura, J. Anrather, P. Zhou, G. Racchumi, C. Iadecola

Neurobiology, Weill Cornell Medical Colledge, New York, NY, USA

Objectives: The scavenger receptor CD36 plays an important role in focal cerebral ischemic injury by triggering NF-κB activation and inducing post-ischemic inflammation (1). CD36 can be part of a receptor complex that includes toll-like receptors (TLRs), transmembrane receptors involved in innate immunity. TLR2 form heterodimers with TLR1 or 6, and CD36 may act as a co-receptor for TLR2/6 in macrophages (2). Furthermore, TLR2, like CD36, contributes to cerebral ischemic damage, raising the possibility of a co-receptor interaction between CD36 and TLR2 also in brain injury. Therefore, we investigated whether CD36 is required for TLR2-induced inflammatory signaling and for its deleterious effects on the ischemic brain.

Methods: The TLR2/6 activator FSL-1, the TLR2/1 activator Pam3 and the TLR4 activator LPS were administrated into the cerebral ventricles (ICV) in wild type, TLR2-/- and CD36-/- mice. Inflammatory genes expression in brain was examined by quantitative real-time PCR. The middle cerebral artery was transiently occluded in CD36-/-, or TLR2 -/- mice and,10 min after reperfusion, vehicle, FSL-1, Pam3, or LPS was injected ICV. Infarct volume was assessed 3 days later in Nissl stained sections and data corrected for swelling. The microglia-macrophage marker F4/80 and the neutrophil marker MPO were examined immunohistochemically 3 days after ischemia.

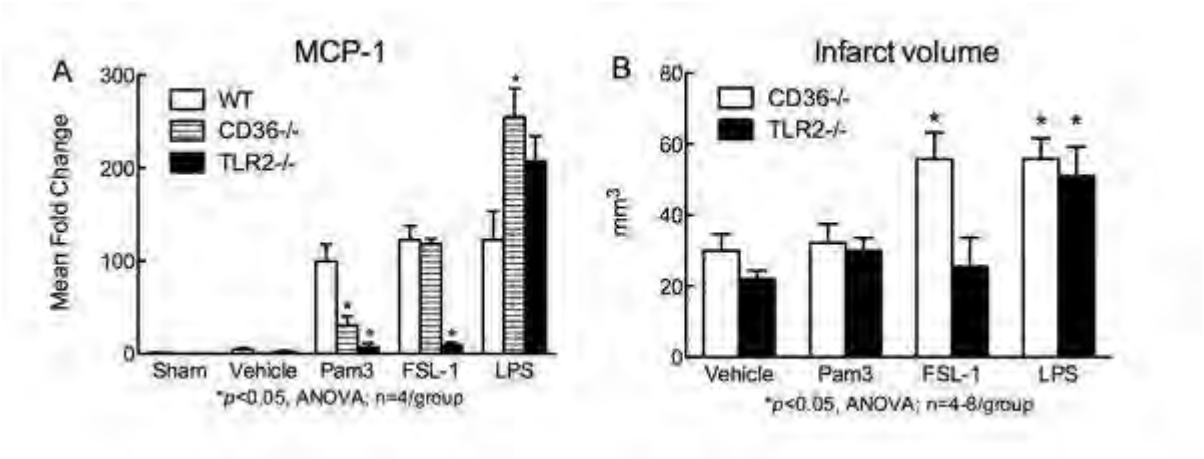

[figure 1]

Results: ICV injection of the FSL-1 in CD36+/+ mice upregulated inflammatory gene expression (MCP-1 figure 1A; ICAM-1 19±5 fold induction; ELAM-1 64±17; IL-6 22±4; $p< 0.05$; n=4/group). FSL-1 induced similar upregulation in CD36-/- mice, as did LPS ($p>0.05$ from CD36+/+; n=4/group). In contrast, the inflammatory response induced by Pam3 was markedly attenuated in CD36-/- and TLR2-/- mice. Therefore, TLR2/1 inflammatory signaling in brain requires CD36. ICV injection of FSL-1 or LPS after reperfusion increased stroke volume in CD36-/- mice (figure 1B). However, Pam3 did not increase stroke volume in either CD36-/- or in TLR2-/- mice (n=4-8/group; $p>0.05$).

Furthermore, microglial activation and neutrophil infiltration were markedly attenuated in CD36-/- mice compared to WT. Post-ischemic administration of FSL-1, but not Pam3, re-established the cellular inflammatory response in CD36-/- mice.

Conclusions: CD36 is required for TLR2/1-induced neuroinflammation and for the deleterious effects of TLR2/1 ligands in the post-ischemic brain. The findings suggest that in focal cerebral ischemia the endogenous ligands activating TLR2/1 require CD36 for triggering post-ischemic inflammation. Thus, CD36 is a critical sensor of "danger signals" in the post-ischemic brain and, as such, is a potential target for therapeutic interventions.

References:

1. Kunz, A., et al., Nuclear factor-kappaB activation and postischemic inflammation are suppressed in CD36-null mice after middle cerebral artery occlusion.J Neurosci 28:1649-1658.

2. Hoebe, K., P. et al., CD36 is a sensor of diacylglycerides. Nature 433:523-527.

850

Brain Poster Session: Inflammation

DOWNREGULATION OF INFLAMMATORY GENE EXPRESSION BY ROSIGLITAZONE THROUGH A 5-LIPOXIGENASE DEPENDENT MECHANISM IN EXPERIMENTAL STROKE

I. Ballesteros[1], M. Sobrado[1], J. Vivancos[2], F. Nombela[2], J.M. Pradillo[1], I. Lizasoain[1], M.A. Moro[1]

[1]Pharmacology, Universidad Complutense de Madrid, [2]Neurology, Hospital Universitario La Princesa, Madrid, Spain

Background: PPARg is a ligand-activated transcription factor belonging to the nuclear receptors superfamily. The PPARg agonist rosiglitazone (RSG) is neuroprotective in experimental acute stroke and reduces inflammation. We have recently shown that RSG induces 5-lipoxygenase (5-LO) expression in ischemic rat brain (1;2). Since 5-LO plays a key role in inflammatory responses and its inhibition abolishes RSG induced neuroprotection, we aimed to study the 5-LO dependent mechanisms which underlie RSG neuroprotective efects in experimental stroke.

Methods: Focal permanent ischemia was induced by middle cerebral artery occlusion (MCAO) in Fisher rats. RSG was administered 10 min after MCAO and BWA4C (selective 5-LO inhibitor) was administered 3h after MCAO. mRNA levels of inflammatory mediators (COX-2, TNFalpha, MMP9 and iNOS) were measured by real time PCR (5h after MCAO). Protein levels were also determined by western blot (18h after MCAO).

Results: RSG inhibited the expression of COX-2, iNOS, and mature forms of TNF-α and MMP9. More interesting, the 5-LO inhibitor BWA4C reversed RSG-induced inhibition of the gene expression of COX-2, iNOS and TNF-α. For MMP9, reversal of expression was observed only at the mRNA level.

Conclusions: inhibition of inflammatory gene expression is a mechanism involved in the neuroprotective actions of 5-LO induction by RSG, suggesting that 5-LO by-products mediates RSG-induced neuroprotection.

References:

1. Pereira MP, Hurtado O, Cárdenas A, Boscá L, Castillo J, Dávalos A, Vivancos J, Serena J, Lorenzo P, Lizasoain I, Moro MA (2006) Rosiglitazone and 15-Deoxy-Delta(12,14)-Prostaglandin J(2) Cause Potent Neuroprotection After Experimental Stroke Through Noncompletely Overlapping Mechanisms. J Cereb Blood Flow Metab 26:218-229.

2. Sobrado M, Pereira MP, Hurtado O, Nombela F, Escolar E, Romera VG, Lizasoain I, Vivancos J, Moro MA (2008) Rosiglitazone induces a switch to an anti-inflammatory status through 5-Lipoxigenase in experimental stroke. 17th European Stroke Conference. Cerebrovasc Dis. 2008 25:36.

851

BrainPET Poster Session: In Vivo Pharmacology and Clinical Applications

[F-18]MEFWAY AND [F-18]MPPF BINDING TO THE 5-HT$_{1A}$ RECEPTOR IN THE NONHUMAN PRIMATE

B. Christian[1], N. Vandehey[1], J. Moirano[1], D. Murali[1], D. Wootin[1], O. Dejesus[1], T. Barnhart[1], A. Converse[2], R. Nickles[1], T. Oakes[2], J. Mukherjee[3], R. Davidson[2], M. Schneider[4]

[1]Medical Physics, [2]Waisman Brain Imaging Lab, University of Wisconsin-Madison, Madison, WI, [3]University of California Irvine, Irvine, CA, [4]Kinesiology, University of Wisconsin-Madison, Madison, WI, USA

Introduction: Preliminary studies suggest [F-18]MEFWAY will offer significant improvements as a PET biomarker for the 5-HT$_{1A}$ system (1). The objective of this work was to compare the binding of 5-HT$_{1A}$ antagonists [F-18]MEFWAY and [F-18]MPPF in the rhesus monkey.

Methods: Dynamic microPET scans of MEFWAY and MPPF were acquired on 2 anesthetized rhesus monkeys. Arterial plasma samples were drawn throughout the 2 hour scan to assay parent compound. Time activity curves were obtained for the regions of the anterior cingulate (AC), hippocampus complex(HP), raphe nuclei (RN) and prefrontal cortex (PFC) the obtain a measure of binding potential (BP_{ND}) with the cerebellum (CBM) as a reference region using the Logan DVR and MRTM2 methods.

Results: In the arterial plasma, both radiotracers cleared from the plasma at a similar rate, with a slow component of 0.0088 and 0.0093 min^{-1} for MEFWAY and MPPF. The CBM to plasma ratios plateaued at 3:1 for MEFWAY and 1.5:1 for MPPF. Throughout the regions of the brain, MEFWAY revealed significantly higher binding.

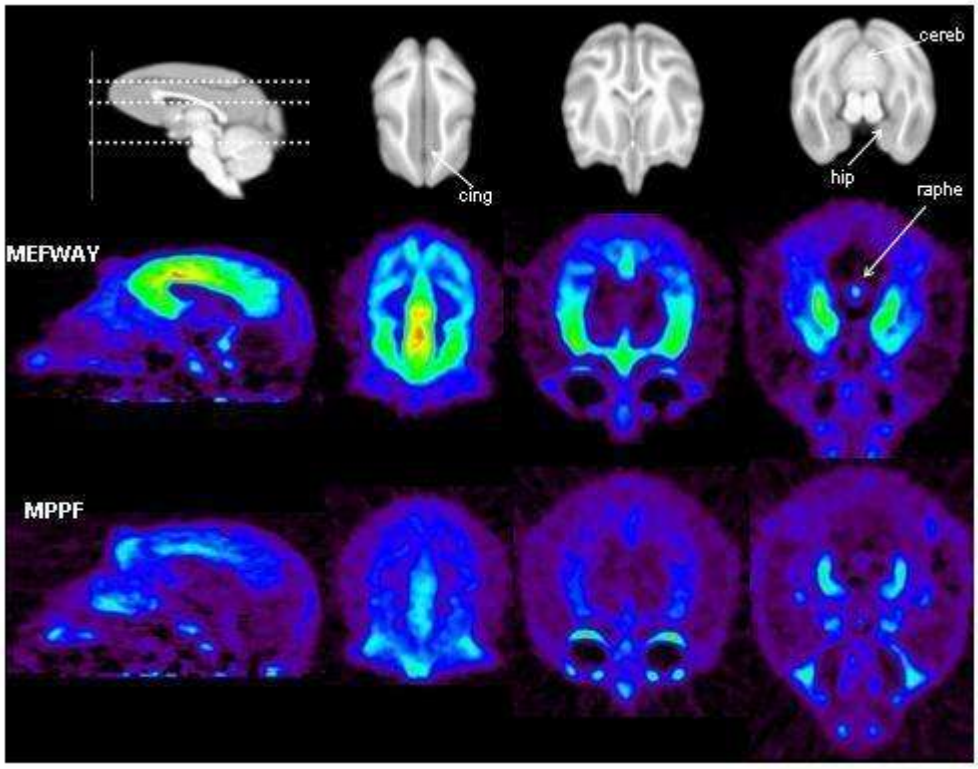

Using the ROI data, BP_{ND} was (MEFWAY and MPPF): AC - 12 and 3.6, HP - 11 and 3.1, RN - 3.8 and 1.3, PFC - 7.9 and 2.5 with less than 5% difference between the Logan and MRTM2 methods. Stable measurements of MEFWAY BP_{ND} were obtained using less than 90 minutes of dynamic data.

Conclusions: MEFWAY demonstrates a dramatic improvement as a PET biomarker for the 5-HT_{1A} site, yielding almost 3-fold increases in BP_{ND} over MPPF. Interestingly, MPPF demonstrated approximately double the BP_{ND} in rhesus monkeys over literature values in humans (2). Further investigation is required to see if this difference is species or methods specific.

Research support: AA017706,AG030524,AA012277.

[1] Saigal N, Pichika R, Easwaramoorthy B, Collins D, Christian BT, Shi B, Narayanan TK, Potkin SG, Mukherjee J.J Nucl Med. 2006;47(10):1697-706.

[2] Costes N, Merlet I, Zimmer L, Lavenne, Cinotti, Delforge J, Luxen A, Pujol JF, LeBars D. J Cereb Blood Flow Metab 2002;22(6):753-765.

QUANTITATIVE ASSESSMENT OF [^{18}F]-ANNEXIN V UPTAKE BY MICROPET IMAGING AS A BIOMARKER OF KETAMINE-INDUCED NEURONAL DEATH

X. Zhang, G. Newport, T. Patterson, M. Paule, W. Slikker, C. Wang

Neurotoxicology, NCTR/FDA, Jefferson, AR, USA

Ketamine is a dissociative anesthetic that is primarily used for the induction and maintenance of general anesthesia. Recent reports indicate that ketamine anesthesia for 6-12 h triggers neuronal apoptosis in postnatal day (PND) 7 rats. In all apoptotic neurons, phosphatidylserine (PS) is rapidly redistributed from the inner to outer surface of the plasma membrane and can be selectively recognized and bound by annexin V. Because the high-resolution positron emission tomography scanner (microPET) provides in vivo molecular imaging at sufficient resolution to resolve neuronal activities in the rat brain, it has been proposed as a minimally invasive method for detecting apoptosis in the brain using the tracer [^{18}F]-labeled annexin V. In this study, the effect of ketamine on the uptake and retention of [^{18}F]-annexin V in the rat brain was investigated using microPET imaging. On PND 7, rat pups in the experimental group were exposed to 6 injections of ketamine (20 mg/kg at 2 h intervals) and control rat pups received 6 injections of saline. On PND 35, [^{18}F]-annexin V (1 mci) was injected into the tail vein of treated and control rats and static microPET images were obtained over 2 h following the injection. Radiolabeled tracer accumulation in the region of interest (ROI) in the frontal cortex and hippocampus were converted into Standard Uptake Values (SUVs). After the injection, radiotracer was quickly distributed into the brains of both ketamine- and saline-treated rats. Compared with the control group, the uptake of [^{18}F]-annexin V was significantly increased in the ROI of ketamine-treated rats. Additionally, the duration for wash-out of the tracer was prolonged in the ketamine-treated animals. This preliminary study demonstrates that microPET imaging is capable of distinguishing differences in retention of [^{18}F]-annexin in different brain regions and suggests that this approach may provide a minimally invasive biomarker of neuronal apoptosis.

853

Brain Poster Session: Neonatal Ischemia

A BROADBAND MULTI-CHANNEL NIRS SYSTEM FOR MEASURING FOCAL ISCHEMIC BRAIN INJURY IN NEWBORNS

M. Diop[1,2], J. Elliott[1,2], K. Tichauer[1,2], T.-Y. Lee[1,2,3], K. St. Lawrence[1,2]

[1]Imaging Division, The Lawson Health Research Institute, St. Joseph's Health Care, [2]Department of Medical Biophysics, University of Western Ontario, [3]Imaging Research Laboratories, Robarts Research Institute, London, ON, Canada

Objectives: Near-infrared spectroscopy (NIRS) is a promising technique for assessing brain function in newborns. We have previously developed a method for measuring cerebral blood flow (CBF) using broadband NIRS [1]. However, broadband systems typically have one detector, which limits their clinical applicability. To address this limitation, we developed a multiplexing approach based on electronically controlled mechanical shutters to expand the detection capabilities to eight channels. This work was intended to demonstrate that broadband NIRS can detect focal ischemic brain injury caused by injecting Endothelin-1 (ET-1). For validation, CBF was measured by computed tomography (CT) perfusion [2].

Methods: Four newborn piglets were studied: 2 females, 2 males; median age 1.5 days. Animals were anaesthetized using isoflurane and physiological parameters were maintained within normal limits throughout the experiments. Piglets were placed in a CT scanner with the NIRS emission optode and four detection optodes positioned on the head. All detectors were placed 3 cm from the emitter, spanning an arc of 90°. Two sets of CBF measurements were obtained by CT [2] and NIRS [1] before and following the infusion of ET-1 (5 μmol in 50 ml of water) into the cerebral cortex [3].

All data are presented as means ± S.E.M. For both NIRS and CT, the two CBF measurements acquired prior to and following ET-1 infusion were averaged to generate single pre- and post-injection values. Comparison between the techniques was conducted for two regions: the site of ET-1 infusion (injury region) and a region remote from infusion (healthy region). Significant differences were determined by paired Student's t-test ($p < 0.05$) corrected for multiple comparisons.

Results: Baseline measurements showed no statistical differences between CBF measured by the four NIRS optodes and average CBF from the corresponding regions in the CT perfusion images. Infusion of ET-1 caused a general reduction in global CBF with the magnitude of the reduction diminishing with distance from the infusion site. With NIRS, a significant decrease was found only in the injured region (51 ± 9%) and not in the healthy region (14 ± 9%). Significant decreases in CBF for the corresponding regions (55 ± 5 and 23 ± 8%, respectively) were measured by CT.

Conclusion: Regional CBF measured by NIRS and CT were in good agreement with each other and both techniques measured approximately a 50% reduction in CBF in the injury region following ET-1 infusion. This study shows that the multi-channel broadband NIRS system can reliably measure regional CBF. It would be possible to also measure the cerebral metabolic rate of oxygen by combining measurements of CBF and cerebral deoxy-hemoglobin [4], making this mobile NIRS apparatus a valuable tool for bedside monitoring of critically-ill neonates.

References:

1. Brown et al., Pediatr Res 51:564 (2002).

2. Cenic et al., AJNR Am. J. Neuroradiol 20, 63 (1999).

3. Huges et al., J Neuropathol Exp Neurol 62,1276 (2003).

4. Tichauer et al., J Cereb Blood Flow Metab 26, 722 (2006).

855

BrainPET Poster Session: In Vivo Pharmacology and Clinical Applications

SENSITIVITY OF 11C-RACLOPRIDE SMALL ANIMAL PET TO STRIATAL DOPAMINE RELEASE INDUCED BY ALCOHOL OR COCAINE: EFFECTS OF ANESTHESIA/PROTOCOL

J.M. Sullivan[1,2], M.D. Normandin[1,2], S.L. Risacher[1], S.A. Berg[1], R.A. Chambers[1], J.C. Froehlich[1], E.D. Morris[1,2,3]

[1]IU School of Medicine, Indianapolis, [2]Purdue University, West Lafayette, [3]Purdue School of Eng & Tech, IUPUI, Indianapolis, IN, USA

Objectives: Microdialysis experiments have shown that drugs of abuse, such as alcohol and cocaine, produce an increase in extracellular dopamine (DA) in the striatum of rats [1,2]. This study examined if similar changes in striatal DA can be detected in Wistar or P rats using small animal PET. We also sought to establish optimal doses and times for imaging the dopaminergic response to drugs of abuse; we varied the time of IV cocaine administration, the type and mode of anesthesia delivery, and the dose of IP alcohol. We gauged DA release by calculating change in raclopride [RAC] binding potential (BP).

Methods: PET images were acquired in drug-naïve male Wistar and P rats. All scans were performed on IndyPETIII (~1mm FWHM in-plane resolution). Prior to each scan, all animals were anesthetized and secured on a stereotaxic holder. Time activity curves were extracted from the striatum and cerebellum and BPs were calculated as a measure of D_2 receptor availability [3,4].

Only Wistars were given cocaine and both Wistars and P rats were given alcohol. In cocaine studies, Wistars received up to three 11-C RAC scans (one rest and two cocaine) and were anesthetized with isoflurane or a ketamine/xylazine cocktail. Ket/Xyl boosters were given ~20mins after 11C-RAC injection. These animals received 2.0mg/kg cocaine intravenously 10mins ("early cocaine") or 25mins ("late cocaine") after tracer injection. In alcohol studies, Wistars and P rats received up to three 11C-RAC scans (rest, alcohol, saline) and were anesthetized with isoflurane only. These animals received 3.0 g/kg ethanol (20%v/v), 1.5 g/kg ethanol (15%v/v), or 2.25 g/kg ethanol (15%v/v) IP 5mins before tracer injection. Venous blood samples were collected from animals 10mins after tracer injection for determination of blood alcohol content (BAC).

Results: There was a significant decrease in BP in Wistars given 3g/kg ethanol IP, as well as in Wistars under ketamine/xylazine given 2mg/kg cocaine IV. There was no significant decrease in BP due to cocaine if Wistars were anesthetized with isoflurane. There was no detectable change in BP in P rats who received IP alcohol at either 1.5g/kg or 2.25g/kg ethanol. In P rats, decreased BP was positively correlated with BAC ($r=0.78$, $p< 0.04$). In fact, large decreases in BP were observed mainly in rats with BACs above 200mg%. No significant change in BP was found between rest and saline scans.

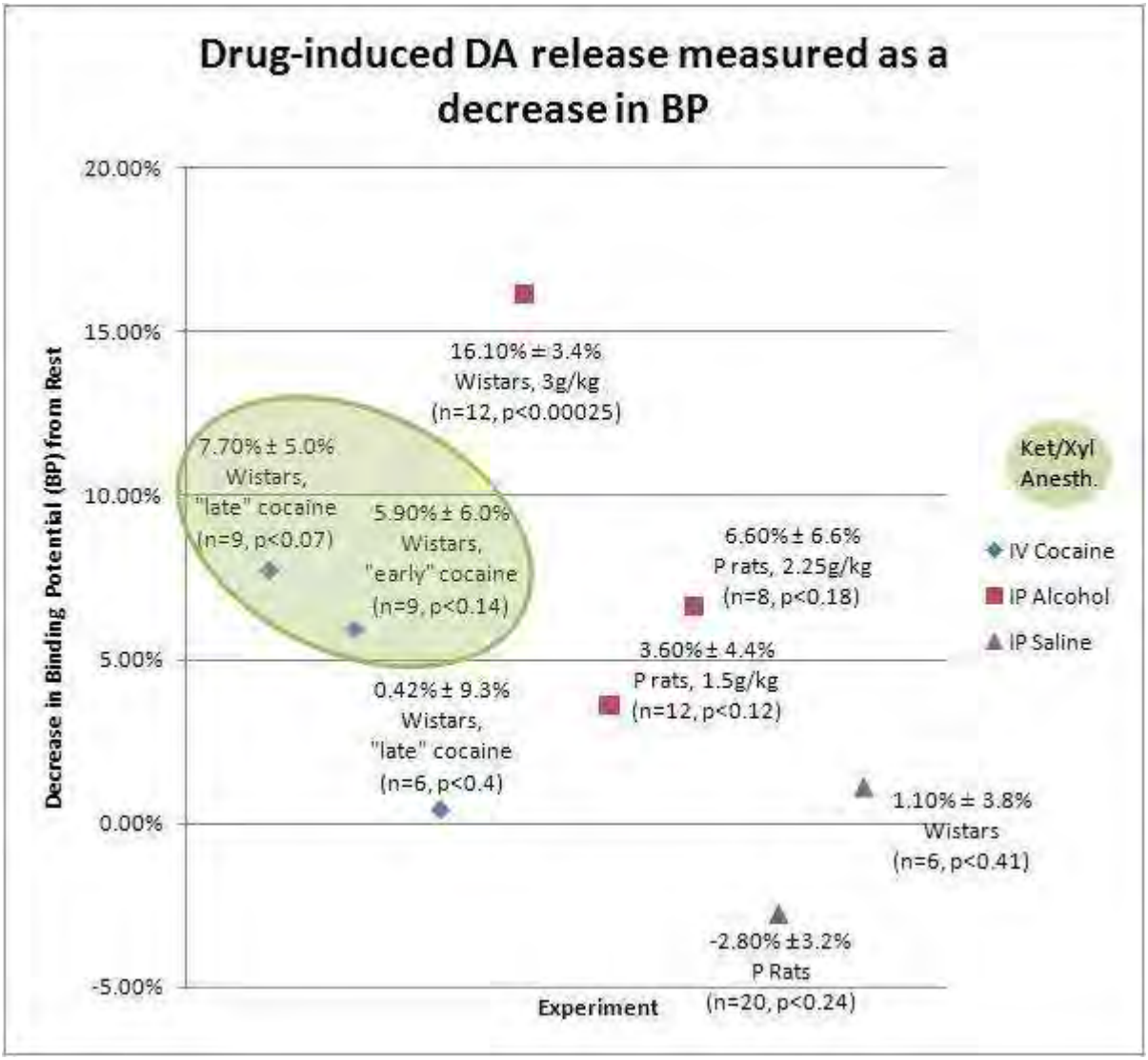

[Drug-induced DA release measured as BP decrease]

Conclusions: To maximize detectability of alcohol-induced DA release in the striatum, it may be necessary to achieve BAC levels of at least 200mg%. Cocaine-induced DA release may be quenched by isoflurane, which would be consistent with work of Votaw et al [5]. No effect of cocaine injection time was observed, but timing of ketamine boosters may have interacted with "late" cocaine [6].

References:

[1] Bradberry. NeuroSciLet:103(1).

[2] Heidbreder. PharmBiochemBehavior:46(2).

[3] Ichise. JCBF:22(10).

[4] Logan. JCBF:16(5).

[5] Votaw. Anesthesiology:98(2).

[6]Tsukada. Synapse:42(4).

TREHALOSE INDUCES NEUROPROTECTION VIA AUTOPHAGY ACTIVATION IN CEREBRAL ISCHEMIA

J.-S. Sunwoo, H.-K. Park, K. Chu, K.-H. Jung, S.-T. Lee, J.-J. Bahn, M. Kim, S.-K. Lee, J.-K. Roh

Neurology, Seoul National University Hospital, Seoul, South Korea

Objective: Trehalose is a non-reducing disaccharide found in many organisms including plants and yeast. By inducing autophagy and chemical chaperone, trehalose protects mammalian cells against neurodegenerative diseases, although it is not endogenously synthesized in mammalian cells. Recently, it is known that the autophagy induced by mild hypoxia is neuroprotective by modulating the biogenesis of mitochondria and the is related to the molecules like PGC-1 alpha, BNIP3, and Beclin-1. Here, we investigated whether the addition of trehalose could enhance the neuroprotection against the ischemia.

Methods: Using cell viability assay (WST-1) and flow cytometry (FACS), we measured the difference of cell viability of PC 12 cell line under oxygen-glucose deprivation (OGD), between trehalose treatment group (0.1, 1, 10 mM) and controls. The protein levels of molecules related to the autophagy and ischemia were evaluated before and after trehalose treatment. To find the neuroprotection of trehalose in vivo models, we measured the infarcted volume, modified limb placing tests (MLPT) and hemispheric atrophy after 90 minutes - transient MCA occlusion (MCAO) by thread insertion.

Results: The cell viability assay and FACS showed the trehalose addition enhanced the cell viability after OGD significantly and this neuroprotective effect was dose-dependent. The trehalose treatment (2% of drinking water, 7 days) reduced the infarcted volume one day after MCAO. Trehalose also improved hemispheric atrophy and the MLPT over 30 days after MCAO. We found that the increased protein expression of PGC-1alpha, BNIP-3, Beclin-1 and LC3-II after trehalose treatment, suggesting that enhanced hypoxia-induced mitochondrial autophagy. The amount of Hsp70 increased after addition of trehalose and this fact indicated that trehalose also enhanced the survival-related molecules. FACS and TTC staining showed that the inhibitors of BNIP3 (Ibuprofen) and autophagy (Bafilomycin, Wortmannin) reduced the cell viability and increased the infarcted volume of trehalose treatment group.

Conclusions: Trehalose exerted the neuroprotection against ischemic injury. The beneficial effect is associated with the pathway of hypoxia-induced mitochondrial autophagy. The modulation of mitochondrial autophagy can be one of the new therapeutic strategies for stroke treatment.

858

Brain Poster Session: Neuroprotection

TOLERANCE TO OXYGEN NUTRIENT DEPRIVATION IN THE HIPPOCAMPAL SLIDES OF THE NAKED MOLE RAT

T. Nathaniel[1], F. Umesiric[2], A. Saras[3], F. Olajuyigbe[4]

[1]Center for Health and Natural Sciences, Marywood University, Scranton, PA, [2]Chemistry, University of AlbertaToledo, Toledo, OH, [3]Department of Molecular and Cell Biology, University of California, Irvine,111 Life Sciences Addition, Berkeley, CA, USA, [4]Science, College of Education, Ondo, Nigeria

Hypoxia tolerance in the naked mole rats (Heterocephalus glaber), represents a unique physiological phenomenon characterized by the capability to regulate oxygen demand to attenuate energetically costly response to hypoxia. Several aspects of tolerance to hypoxia in the naked mole rat is consistent with a state of neuroprotection, however, it remains to be established if such protective capability is expressed in the brain cells of mole rats subjected to hypoxia insults. The objective of this study was determine whether evidence of tolerance to oxygen nutrient deprivation exists in the chronic cultures of the naked mole rats hippocampal slices. We used oxygen nutrient deprivation (OND) an in vitro model of hypoxia tolerance to determine neuronal survival in the hippocampal slices from mole rats and Rattus sp. At 4hours OND, followed by 20hours recovery, slices of neurons in CA1 of mole rats resist cell death, while slices of Rattus sp were susceptible to OND with a significant decrease in CA1 neurons after 4 to 24hrs in culture. These results demonstrate that hippocampal slices of mole rats kept in hypoxia condition, consistently tolerate OND right from the onset time point in cultured slices, and maintained for 24hrs.

859

Brain Poster Session: Stem Cells & Gene Therapy

DUAL SENSITIVITY OF EARLY AND LATE EMBRYONIC STEM CELL-DERIVED NEURAL PROGENITORS TO THE ISCHEMIC ENVIRONMENT

C. Seminatore[1], J. Polentes[1], D. Ellman[2], N. Kozubenko[3], S. Tine[1], L. Tritschler[4], J. Blondeau[1], E. Guidou[4], M. Luillhier[4], A. Bugi[4], L. Aubry[4], A. Perrier[4], P. Jendelova[3], E. Sykova[3], B. Finsen[2], B. Onteniente[1]

[1]I-STEM, INSERM UMR894/861, Evry Cedex, France, [2]Medical Biotechnology Center, University of Southern Denmark, Odense, Denmark, [3]Institute of Experimental Medicine, Prague, Czech Republic, [4]I-STEM, INSERM UMR861, Evry Cedex, France

Objectives: Teratoma/tumor formation is a major obstacle to embryonic stem cell (ESC) therapy. However, while it has been described in models of neurodegenerative diseases, teratoma/tumor formation has not been reported for stroke after transplantation of neural progenitors and/or neuronal precursors. This study aimed at understanding the reasons of this discrepancy.

Methods: Neural induction of the SA01 hESC (Cellartis AB, Sweden) line was performed using the rosette protocol with a minimal culture medium. qPCR expression of differentiation and proliferation markers identified 4 maturation stages, named early-, mid-, late-hES-NP, and neuronal precursors (NP). hES-NP and NP were transplanted into rats with no, small or large ischemic lesions. The fate of transplanted hES-NP and NP and their functional effects were investigated 1 to 4 months after transplantation.

Results: The lesion size significantly impacted graft survival of early-hES-NP. This influence was lost with mid- and late hES-NP and with NP. Similar relationships to the lesion were observed with the derivation of non-neuroectodermal cell types. Although teratoma with derivatives of the 3 germ layers were rarely observed (1 out of 12), early-hES-NP generated non-neural cell types of the ectodermal (epidermal cells) and endodermal (cartilage) lineages. The expression of frizzled-3, an inducer of the neural crest, suggested that non-neural formations from early-hES-NP were derived from neural crest-like structures. The sensitivity to the ischemic lesion was lost after the appearance of neuronal markers. Late progenitors and NP nicely integrated into the host brain, underwent a correct neurogenesis sequence by producing neurons then astrocytes, and contained patches of DARPP-32 neurons innervated by host TH afferents. The integration of transplanted cells and the benefit to the host were confirmed by reversal of ischemia-induced rotation behaviour after apomorphin administration.

Conclusions: The influence of the ischemic environment on hESC-NP is limited to the early stages of differentiation and is lost after neural commitment, confirming that intracerebral transplantation of hESC-NP is a safe and reliable approach for stroke.

860

Brain Poster Session: Neurologic Disease

BRAIN ARACHIDONIC ACID METABOLIC PATHWAY IS ALTERED DURING CUPRIZONE-INDUCED DEMYELINATION

S. Palumbo[1], C.D. Toscano[2], A. Silva[3], F. Bosetti[1]

[1]BPMS, NIA/NIH, Bethesda, [2]Center for Drug Evaluation and Research, Office of New Drugs, Office of Drug Evaluation I, Division of Neurology Products, Food and Drug Administration, Silver Sprig, [3]NINDS, NIH, Bethesda, MD, USA

Objectives: Multiple sclerosis (MS) is characterized by recurrent and progressive demyelination/ remyelination cycles which result in development of scleroses (scars) in white and gray matter of CNS, axonal damage and neuronal loss. There is no cure for MS, and only symptomatic treatments are available [1]. Chronic cuprizone exposure produces progressive demyelination in mice brain which reverses upon its removal from the diet [2]. Since there is limited evidence of altered arachidonic acid (AA) metabolism in MS, we hypothesized that cuprizone exposure would alter the expression of genes involved in AA metabolism, and that these genes represent potential therapeutic targets.

Methods: Adult C57B16 mice were exposed to cuprizone for 6 weeks and then returned to a normal diet. Demyelination was assessed by histochemistry and magnetic resonance imaging. Real-Time PCR and western blotting were used to determine gene and protein expression, respectively, of critical enzymes involved in AA metabolism.

Results: We demonstrated that the Magnetization Prepared Rapid Gradient Echo (MPRAGE) is a useful MRI technique to assess quantitatively structural changes in myelin rate in the corpus callosum during cuprizone exposure. Histochemistry with the myelin stains Black Gold and Fluoromyelin demonstrated that frank demyelination and influx of glial cells into the corpus callosum begins at week 3 and peaks at week 5. However, a decrease in myelin and oligodendrocyte markers, myelin basic protein (MBP) and 2, 3-cyclic nucleotide 3-phosphodiesterase (CNPase), was evident at week 1. Increased expression of CD11b and glial acidic fibrillary protein (GFAP), evidence of activated microglia and astrocytes, was also observed at week 1. Coincident with these early changes, we found an increase in cyclooxygenase (COX)-2 that persisted throughout the demyelination process as well as lipoxygenase 15-LO which was increased at week 1 and peaked in the height of frank demyelination suggesting that these AA metabolism genes are either involved in or respond to the earliest sign of demyelination. Moreover, western blotting analysis showed that 15-LO protein levels, peaked in the height of frank demyelination. Both gene and protein expression of 5-LO was not significantly changed during the early stages of demyelination but it peaked during week 5, when glial markers and frank demyelination also reached their peak of expression. While expression of 12-LO was not consistently increased during demyelination, increased 12-LO expression was observed during the remyelination, suggesting a role for this isoform in the recovery process. The expression $cPLA_2$ and $sPLA_2$ also increased at the peak of frank demyelination, while Ca^{2+}-independent $iPLA_2$ expression was not changed.

Conclusions: Multiple enzymes involved in AA metabolism are altered in the cuprizone model of MS suggesting that COX- and LO- derived AA metabolites are involved in demyelination and remyelination. Moreover, MPRAGE is a sensitive and non invasive method that allows to arrange longitudinal studies and to create a bridge between animal and human studies. These data may help to develop new biomarkers and therapeutic targets to treat demyelinating diseases.

References:

1. Franklin RJ, Ffrench-Constant C. Nat Rev Neurosci. 2008 Nov; 9(11):839-55.

2. Ludwin SK. Ann Neurol. 1994; 36 Suppl: S143-5. Review.

861

Brain Poster Session: Experimental Cerebral Ischemia: Vascular & Endothelial

ENVIRONMENTAL ENRICHMENT PROMOTES THE RESOLUTION OF POST STROKE MILD COGNITIVE IMPAIRMENT IN RATS

Y. Wang[1,2], B. Bontempi[3], X. Leinekugel[3], P. Weinstein[1], **J. Liu**[1]

[1]Neurosurgery, UCSF, San Francisco, CA, USA, [2]Neurosurgery, Beijing Tiantan Hospital, Capital University of Medical Science, Beijing, China, [3]Centre de Neurosciences Intégratives et Cognitives, CNRS UMR 5228 and Université Bordeaux 1, Bordeaux, France

Objective: While motor impairment due to ischemic damage of motor pathways is a hallmark of clinical and experimental stroke, post-stroke cognitive dysfunction can be observed without direct injury to brain regions supporting cognitive functions. The hippocampus plays a crucial role in learning and memory processes, however this structure is typically spared in both human stroke syndromes, and animal models of stroke. Here we examine whether hippocampal hypoactivity and memory impairments could result from damage to remotely connected cortical regions and whether post-ischemic hippocampal dysfunction can be reversed by environmental enrichment (EE).

Methods: Spatial memory in the Barnes maze and multi-channel in vivo electrophysiological recordings of cortical and intrahippocampal transmission were assessed in adult rats following distal middle cerebral artery occlusion (dMCAO). Imaging of the activity-dependent gene c-fos, a sensible proxy for neuronal activity, was used to map the brain regions exhibiting neuronal dysfunction immediately following spatial exploration or performing memory task. The effects of EE on hippocampal neuronal activity, neurogenesis and spatial memory were examined. The anterograde tracer biotinylated dextranamine (BDA) was injected iontophoretically into the parietal cortex of intact rats to reveal topographical projections between the cortex and hippocampus.

Results: Ischemic rats exhibited cortical damage and impaired hippocampal-dependent spatial learning at 5 weeks post-ischemia while hippocampal structural integrity was preserved. Contrasting with the expected reduction of ipsilateral cortical activity, functional spontaneous and evoked local field potentials recorded from hippocampal CA1 pyramidal layer and stratum radiatum were not disrupted following reperfusion in the ischemic rats. Fos imaging in dMCAO rats exploring a novel environment or submitted to memory testing revealed widespread, but region-specific, hypoactivations in hippocampus and connected brain regions of the hippocampal formation remote from the ischemic damage, including the entorhinal and perirhinal cortices. This hippocampal hypofunction and spatial memory deficits were reversed by rearing in the EE for 4 weeks, which also stimulated neurogenesis. Anatomical tracing with BDA demonstrated that parietal cortex project extensively to the parahippocampal regions, which include the perirhinal cortex.

Conclusions: Our results indicate that the experimental stroke-induced mild cognitive impairment is attributed to hippocampal hypofunction. Considering the absence of hippocampal damage in dMCAO rats, the, post-stroke cognitive deficit could be the consequence of a reduced source of cortical information (i.e. deactivation) or increased inhibition through the parahippocampal region that acts as a key gateway for information exchange between cortical areas and the hippocampus. EE reversed this diaschisis-like hippocampal hypofunction and associated spatial memory deficits. Thus, EE serves as a rehabilitative therapy to restore memory function by promoting the resolution of hippocampal diaschisis via an array of plasticity mechanisms that may include hippocampal neurogenesis.

862

Brain Poster Session: Neurologic Disease

PERFUSION ANGIOGRAPHY: A NOVEL TECHNIQUE FOR CHARACTERIZATION OF PERFUSION IN CEREBRAL ISCHEMIA

D. Liebeskind[1], G. Szilagyi[2], S. Black[2], B. Buck[3]

[1]University California Los Angeles, Los Angeles, CA, USA, [2]Neurology, University of Toronto, Toronto, ON, [3]Neurology, University of Alberta, Edmonton, AB, Canada

Objectives: Most perfusion imaging modalities for acute stroke or cerebral ischemia depend on contrast bolus tracking, yet the anatomy of specific flow routes remains obscure. Conversely, conventional angiography is increasingly used for endovascular procedures in acute stroke; however, standard perfusion parameters may be difficult to ascertain. We developed a novel post-processing technique that allows for rapid determination of various perfusion parameters from digital subtraction angiography (DSA).

Methods: Angiodensitometry of DSA data acquired in acute stroke was utilized to estimate perfusion. A standalone computer software algorithm was developed to iteratively process temporal changes in contrast intensity, yielding concentration-time curves based on the known arterial inflow within each pixel. Cerebral blood volume (CBV) is calculated at each pixel by numerical integration over the entire corresponding concentrationtime curve. Cerebral blood flow (CBF) is determined by deconvolving the tissue concentration-time curve with the arterial input function (AIF) using singular-value decomposition with a block-circulant deconvolution matrix.

Subsequent generation of multiparametric perfusion maps allowed for region of interest analyses.

Results: Perfusion angiography images were processed in 20 cases of acute ischemic stroke, exhibiting various types of occlusive lesions and degrees of collateral circulation. Perfusion maps were generated to display cerebral blood flow (CBF), cerebral blood volume (CBV), mean transit time (MTT) and cerebral perfusion pressure (CPP).

Simultaneous visualization of anatomic structures allowed the user to identify specific flow routes. Perfusion images were generated in frontal, lateral, and oblique planes. Software capability included use of DSA data with variable frame rates and spatial resolution. Validation was performed on multicenter datasets and correlation assessed with noninvasive perfusion imaging modalities.

Conclusions: Perfusion angiography provides a novel means to rapidly assess numerous perfusion parameters at the time of endovascular procedures. Serial changes in perfusion associated with treatment may be evaluated with this software in a multicenter setting.

863

BrainPET Poster Session: Brain Imaging: Stroke

FLOW HETEROGENEITY MRI REVEALS COMPENSATORY CHANGES IN THE MICROCIRCULATION DURING ACUTE ISCHEMIC STROKE

D. Liebeskind, J. Alger, B. Buck, T. Schaewe, O.Y. Bang, S. Starkman, D. Kim, L. Ali, B. Ovbiagele, J. Saver

University California Los Angeles, Los Angeles, CA, USA

Objectives: Perfusion MRI may demonstrate changes in the flow distributions of the microcirculation as derangements of the normal flow heterogeneity (FH) within a voxel of the ischemic brain. Such FH abnormalities have been used to predict final infarct evolution. We used FH MRI to explore the specific microcirculatory derangements associated with collateral perfusion in acute MCA ischemia.

Methods: FH MRI measures were derived in 75 consecutive cases of acute ischemic stroke with complete occlusion of the MCA on conventional angiography. Separate maps were generated reflecting the width or standard deviation (FHD), skewness (FHS), and kurtosis (FHK) of flow distributions in the microcirculation. In addition standard perfusion MR images were obtained of CBF, CBV, MTT and CPP. Region of interest analyses were performed to compare values of FHD, FHS, and FHK in the ischemic territory with homologous regions of the contralateral hemisphere.

Collateral circulation evident on catheter angiography was graded with the ASITN/SIR scale.

Results: Pretreatment FH MRI revealed microcirculatory flow abnormalities in all 75 cases. FHD or the width of the flow distribution was increased in all cases ($p < 0.001$). FHS images revealed redistribution of flow within slower routes of the microcirculation ($p < 0.001$). FHK images demonstrated the predominance of particular flow routes in all cases ($p < 0.001$). Topographic features of the FH abnormalities correlated with the degree of collateral flow noted at angiography.

Conclusions: Multiparametric FH MRI reveals consistent changes in the microcirculation associated with collateral perfusion in acute ischemic stroke due to MCA occlusion. Flow redistribution may involve recruitment of specific preferential routes with slower flow to enhance oxygen extraction. FH images can be rapidly generated and provide unique insights into tissue state that may help guide management.

864

Brain Oral Session: Experimental Stroke and Cerebral Ischemia 2

CALPAIN-DEPENDENT CLEAVAGE OF EUKARYOTIC TRANSLATION INITIATION FACTOR 4G MEDIATES TRANSLATION ARREST AND CELL DEATH AFTER ISCHEMIC INJURY

P. Vosler, C. Brennan, J. Chen

Neurology, University of Pittsburgh School of Medicine, Pittsburgh, PA, USA

Objectives: Focal ischemia results in uniform translation arrest in all ischemia-affected neurons. Importantly, the area of translation arrest is consistent throughout reperfusion and nearly completely coincides with total infarct area. Thus, translation arrest is a robust predictor of brain infarct. Our overarching hypothesis is that alleviation of translation arrest will confer neuroprotection. Previous in vivo studies have shown there is a decrease in the protein levels of the scaffolding protein responsible for transporting mRNA to the ribosome, eukaryotic initiation factor (eIF) 4G. It has been suggested that eIF4G is cleaved by the protease calpain. Our experiments attempt to determine if prevention of eIF4G cleavage is sufficient to restore translation and increase neuronal viability following ischemia.

Methods: The in vitro ischemia model oxygen glucose deprivation (OGD) was used on rat primary cortical neurons. Alamar blue and Hoechst staining measured cell viability and translation was measured with TCA precipitation. Calpain activity was confirmed using calpain activity assay and a-spectrin cleavage. In vitro cleavage assays were performed with recombinant proteins. Lentiviral vectors were used to overexpress eIF4G constructs.

Results: Sublethal OGD resulted in a significant decrease in translation immediately after OGD with complete recovery by 12-24 hours of reperfusion. In contrast, lethal OGD resulted in a similar initial inhibition of translation but with recovery to only 50% of control values. Translation recovery was correlated with cell viability, as sublethal OGD did not result in decreased viability and lethal OGD resulted in approximately 50% viability. The levels of translation initiation factors were unchanged except for eIF4G, which progressively decreased from 2h to 24h reperfusion. Further examination demonstrated that eIF4G was cleaved in a caspase-independent manner by calpain, as overexpression of the endogenous calpain inhibitor, calpastatin, inhibited eIF4G cleavage, restored translation, and increased neuronal viability above vector-treated control following OGD. To definitively establish eIF4GI as a calpain substrate, an in vitro assay was performed. Activation of recombinant calpain with Ca^{2+} progressively cleaved recombinant eIF4GI over 30min-an effect that was blocked by calpain-specific inhibitors. We next determined if neuronal death following ischemia was directly related to maintenance of critical levels of eIF4G. Overexpression of HA-eIF4G, but not a mutant eIF4G lacking the cap-binding protein binding site, increased translation and viability above eGFP-vector controls. This suggests that increased neuronal viability due to eIF4G overexpression is due to the restoration of cap-dependent translation.

Conclusions: This work describes the novel mechanism of calpain-mediated cleavage of eIF4G in ischemia-induced translation arrest and neuronal death following in vitro ischemia. Our findings suggest that the level and integrity of eIF4G are crucial to the maintenance of translation and neuronal viability after ischemia. Future work is aimed at determining the biological significance of eIF4G in terms of the types of mRNA translated following ischemia. Using luciferase constructs we are attempting to determine if the 5'UTRs of various viral and cellular internal ribosomal entry sequences (IRES) are preferentially translated following ischemia. Understanding the pathophysiological consequences of eIF4G cleavage and translation arrest may lead to novel therapeutic strategies to ameliorate neuronal death following stroke.

865

Brain Poster Session: Neurogenesis

CANONICAL WNT SIGNALING PROMOTES NEUROGENESIS IN THE ADULT MURINE BRAIN AND REDUCES APOPTOTIC CELL DEATH FOLLOWING FOCAL CEREBRAL ISCHEMIA

I. Iordanova[1], R. Guzman[1], C. Fuerer[2], R. Nusse[2], G. Steinberg[1]

[1]Department of Neurosurgery, Stanford Stroke Center, [2]Department of Developmental Biology, Stanford University, Stanford, CA, USA

Objectives: Canonical Wnt signaling is a conserved pathway during neural development (1-3). It is essential for the expansion of the pool of neural progenitors (4) and in conferring neuronal identity (5). Wnt signaling is also indispensable for hippocampal neurogenesis (6). However, the role of Wnt signaling in promoting neurogenesis within the adult cortex has not been examined to date. With this work we aimed to determine the role of Canonical Wnt signaling in the context of:

1. adult neurogenesis and
2. neuroprotection following focal cerebral ischemia in mice.

Methods: 100 ng of purified Wnt-3a murine protein was injected intra-parenchymally into the cortex and striatum of 12-week old C57/Bl6 male mice. This was followed by daily administration of 5-bromo-2-deoxyuridine, BrdU, for one week followed by immunohistochemical analyses of the cell types present. Wnt-3a was injected in a similar manner 1 day after middle cerebral artery occlusion (MCAO), a model of focal cerebral ischemia, followed by BrdU administration for one week and immunohistochemical analyses, using activated Caspase-3 as a marker of apoptosis.

Results: When injected into the naïve adult cerebral cortex and striatum, Wnt-3a promoted de novo neurogenesis as indicated by the expression of GFAP, Nestin and Doublecortin. Cells positive for these markers were situated along the needle track and were also positive for the mature astroglial cell marker s-100β. In addition, there was a large pool of BrdU-positive IBA-1 (microglial) cells situated close to the neural progenitor cells.

Injecting Wnt-3a after MCAO resulted in a significant (6-fold, $p< 0.0001$) reduction in apoptosis of the BrdU positive cells within the cortex and the striatum. This effect was also seen when Wnt-3a was injected prior to the insult, as well as up to 3 days after it and persisted at 6 months post-Wnt-3a and BrdU injection ($p< 0.0001$).

Conclusions: Canonical Wnt signaling is able to induce de novo neurogenesis within the adult murine cortex and striatum, possibly by causing de-differentiation of mature astrocytes. The role of the pool of proliferating microglial cells is yet to be established. Both pre- and post- MCAO injection of Wnt-3a has a protective effect on the proliferating cells within the murine cortex and striatum.

References:

1. F. Ille, L. Sommer, Cell Mol Life Sci 62, 1100 (May, 2005).

2. F. Kubo, M. Takeichi, S. Nakagawa, Development 130, 587 (Feb, 2003).

3. A. Patapoutian, L. F. Reichardt, Curr Opin Neurobiol 10, 392 (Jun, 2000).

4. S. G. Megason, A. P. McMahon, Development 129, 2087 (May, 2002).

5. T. J. Van Raay et al., Neuron 46, 23 (Apr 7, 2005).

6. D. C. Lie et al., Nature 437, 1370 (Oct 27, 2005).

Brain Poster Session: Brain Imaging: Neurologic Disease

CEREBELLAR VOLUME RATIO TO TOTAL INTRACRANIAL IN CENTRAL CAUSES OF VERTIGO: A STEREOLOGICAL STUDY

N. Gocmen-Mas[1], S. Karabekir[2], O. Kusbeci Yilmaz[3], B. Sahin[4], T. Ertekin[5], O. Bas[6], A.C. Yazici[7], S. Senan[8]

[1]Anatomy, [2]Neurosurgery, [3]Neurology, Kocatepe University School of Medicine, Afyon, [4]Anatomy, Ondokuz Mayis Universityt, Samsun, [5]Anatomy, Kocatepe University Ataturk Vocational School of Health Services, Afyon, [6]Anatomy, Rize University, Rize, [7]Biostatistics, Baskent University School of Medicine, Ankara, [8]Anatomy, Istanbul, Turkey

Objectives: The volume of organs or structures can be obtained using the Cavalieri principle of stereological approaches. Several investigations focused on defination of brain structures and tried to find out MR imaging detectable discriminators of healthy aging and pathological cases in neurological diseases. The normal relation between cerebellar volume and total intracranial volume is fixed .This proportion is significant in determining maybe a result of a cerebellar developmental malformation or atrophy. Proportional relations of the volume of neural structures may have a constant value of the size of the subject. The volume and volume fraction approach of stereological methods provides information about volumetric relations of the components of structures.The central cause of vertigo is often prolonged, permanent and chronic duration. Signs and symptoms of dysfunction of neighboring structures include the central brainstem and cerebellar structures. In literature, we have not able to find adequate data about volume relation between cerebella and total intracranial in central causes of vertigo. So, in this study, we aimed to evaluate the relevant methods of magnetic resonance and stereology to define cerebellar volume ratio to total intracranial volume according to gender in central causes of vertigo cases.

Material and methods: The study included 14 (7 men, 7 women) healthy adult subjects aged between 25-54; and 15 (7men, 8 women) cases with vertigo aged between 26 -55. The volumes of cerebellum and total intracranial were determined on MR images using the point-counting approach of stereological methods.

Results: The TIV volumes in control group were 1082.49±71.01 in males; 1067.76±80.41 in females on sagittal plane. The TIV volumes in vertigo group were 1043.13±27.43 in males; 1011.14±60.76 in females on sagittal plane. The cerebella volumes in control group were 106.64±5.23 in males; 100.81±12.25 in females on sagittal plane. The cerebella volumes in vertigo group were 98.06±7.46 in males; 100.49±5.83 in females on sagittal plane. There was not a difference the volumes of TIV between control group and the cases with vertigo both males and females ($p > 0.05$). The cerebellar volume in the cases with vertigo were significantly smaller than the control subjects in male subject ($p=0.028$). While, cerebellar volumes were small in females with vertigo ($P < 0.05$), but volume difference between two groups were not statistically significant. The volume fraction of the cerebella to TIV in control group were 0.099±0.008, in vertigo were 0.094±0.007 in male subjects. The volume fraction of the cerebella to TIV in control group were 0.095±0.012, in vertigo were 0.099±0.009 in female subjects. The cases of vertigo showed lower cerebella to TIV fraction than the control subjects in both male subjects ($p=0.018$) and female subjects ($P>0.05$). The proportion of cerebellum to TIV the cases with vertigo showed significantly lower cerebellar volume proportion to TIV than the control subjects ($P < 0.05$). No significant statistically difference was found in both groups with regard to the gender ($P>0.05$).

Conclusion: As a result, estimating the cerebella and TIV volumes proportion using the stereological method may be significant tool in defining brain anatomy and pathological changes in central causes of vertigo.

870

Brain Poster Session: Experimental Cerebral Ischemia: Blood Flow & Metabolism

EFFECT OF GINKGO BILOBA (EGB 761) AND ITS BIOACTIVE COMPONENTS ON CEREBRAL BLOOD FLOW

Z. Shah, S. Dore

Anesthesiology and Critical Care Medicine, Johns Hopkins University, Baltimore, MD, USA

Objectives: Ginkgo biloba standardized extract (EGb 761) has been consumed for its potential in treating neurological disorders. Substantial available evidence supports its benefits to cognitive function and in neurodegenerative diseases. We showed that EGb selectively increases heme oxygenase-1 (HO1) proteins in primary neuronal cultures (Zhuang et al. Cell Mol Biol 2002), and recently, we demonstrated its protective effect in an in vivo ischemic reperfusion model (Saleem et al. Stroke 2008). The mechanism involved in the protective effect of EGb has been attributed mostly to its antioxidant properties. However, we believe that part of its neuroprotective effect is dependent on HO1 activity. HO1 degrades the prooxidant heme into iron, biliverdin/bilirubin, and carbon monoxide (a vasodilator). Here we evaluated the effect of EGb on cerebral blood flow (CBF).

Methods: We treated mice orally with different Ginkgo components or vehicle control (n=5/group), immediately anesthetized the mice with halothane, and began monitoring CBF by laser Doppler flowmetry over the middle cerebral artery (MCA) territory for 180min.

Results: Within 30min, we observed a trend toward increased CBF in EGb-treated mice (126% of baseline) as compared with that of the vehicle-treated group (81% of baseline). Therefore, EGb and its bioactive components bilobalide (BB), Ginkgolide A (GA), Ginkgolide B (GB) and Terpene Free Material (TFM) might enhance CBF in mice subjected to transient MCA occlusion (tMCAO). Mice pretreated orally for 7d with vehicle, 6mg/kg BB, GA, or GB, 10mg/kg TFM, or 100mg/kg EGb were anesthetized to monitor CBF by laser Doppler flowmetry over the MCA territory for 3h before, during, and after occlusion. Physiologic parameters were measured by drawing blood through a femoral artery catheter at baseline, 1h after MCAO, and 1h after reperfusion. Compared with vehicle-treated mice, those pretreated with EGb for 7d had higher CBF levels 15min after reperfusion, CBF remained elevated for 90min (94% restoration of CBF vs 53% vehicle). Mice pretreated with BB for 7d had higher CBF levels immediately after reperfusion, but they stayed elevated for only 30min (106% restoration vs 53% vehicle). Similarly the CBF of TFM-pretreated mice were higher after 15min of reperfusion and stayed high for 45min (97% restoration vs 53% vehicle). However, GA and GB pre-treated mice did not show any differences in CBF levels after reperfusion. In the vehicle-treated group, CBF remained steady throughout the process at 54% of baseline. Additionally, no differences in physiologic parameters were observed in mice treated with different constituents of EGb as compared to vehicle group.

Conclusions: These findings suggest that EGb and its bioactive components enhance CBF and may prove beneficial in conditions in which blood flow is impaired, such as in stroke.

INVESTIGATING AMPHETAMINE-STIMULATED DOPAMINE RELEASE IN METHAMPHETAMINE USERS USING THE PET $D_{2/3}$ AGONIST LIGAND [^{11}C]PHNO

I. Boileau[1], S. Houle[1], D. Wilkins[2], P. Selby[1], P. Rusjan[1], A. Wilson[1], S. Kish[1]

[1]CAMH, Toronto, ON, Canada, [2]University of Utah, Salt Lake City, UT, USA

Background: PET/[^{11}C]raclopride neuroimaging data suggests a hypo-dopaminergic state (decreased $D_{2/3}$-receptor density and dopamine release) in the striatum of withdrawn addicted subjects. The goal of the present study was to use PET and the recently developed D_3 receptor-preferring agonist, [^{11}C]PHNO to assess dopamine receptor density and dopaminergic response to an open challenge with amphetamine in recently withdrawn methamphetamine users (MA).

Methods: 14 MA and 14 matched-controls (HC) underwent [^{11}C]PHNO scans during a non-placebo-controlled baseline and after a low oral-dose of amphetamine (0.4 mg /kg).

Results: MA abuse was associated with a trend for increased baseline $D_{2/3}$-receptor density corresponding to 15%($p=0.1$) and 16%($p=0.06$) in the ventral striatum and globus pallidus respectively and 9% in the dorsal striatum ($p=0.2$). Relative to HC, MA had greater amphetamine-induced increases in heart-rate, and subjective effects ($p< 0.01$) together with decreases in [^{11}C]PHNO binding potential slightly above HC value in the ventral striatum (-21% MA vs -13% HC, $p=0.1$) and globus-pallidus (-30% MA vs -14% HC, $p=0.04$) but not in the dorsal striatum.

Conclusion: Contrasting with the current PET/[^{11}C]raclopride imaging literature, these preliminary [^{11}C]PHNO data suggest increased $D_{2/3}$ receptors density and greater apparent DA release in MA users relative to HC. This could be explained by pharmacological differences between the in-vivo binding of [^{11}C]PHNO and [^{11}C]raclopride (consistent with our recent finding in Parkinson's disease, Brain, 2008). Specifically, its in-vivo distribution as well as its higher vulnerability to endogenous DA relative to [^{11}C]raclopride could be related to some degree to its selectivity for D_3 compared to D_2 receptors.

873

Brain Poster Session: Ischemic Preconditioning

PRESERVATION OF BLOOD-BRAIN BARRIER INTEGRITY IN ISCHEMIC TOLERANCE BY MICROVASCULAR SPHINGOSINE KINASE 2

B. Wacker, T. Park, J. Gidday

Neurosurgery, Washington University School of Medicine, St. Louis, MO, USA

Background: Hypoxic preconditioning (HPC) provides protection against cerebral ischemia-induced neurovascular dysfunction and cell death in mice[1], allowing for the study of endogenous pathways of ischemic protection. Studies in isolated mouse hearts have shown that the ischemia-protective preconditioning mechanisms depend on sphingosine kinase (SphK)-1[2]. Recent work in the brain documented a heterogeneous distribution of SphK isoform activity in normal and ischemic brain suggesting bioactive lipid signaling may differ from other organs[3]. Our preliminary studies indicate that, in the cerebral microvasculature, HPC leads to increased SphK2 protein expression, peaking 2-4 h after preconditioning, without a concomitant change in the protein levels of the SphK1 isoform.

Objectives: The present study was undertaken to document that increased microvascular SphK2 activity in response to HPC is vital to the mechanism of HPC-induced tolerance to focal cerebral ischemia. We also sought to confirm SphK2-dependent protection of the blood-brain barrier in the HPC-induced ischemia-tolerant brain.

Methods: Temporal changes in microvascular SphK activity were measured following HPC using an established assay[4]. The nonselective SphK inhibitor dimethylsphingosine (DMS, 0.33 mg/kg, i.v.) was administered to adult male Swiss-Webster ND4 mice by retroorbital injection 30 min prior to HPC (4 h of 8% oxygen, systemic). Two days later, mice were subjected to a 60-min transient middle cerebral artery occlusion (tMCAO) under halothane anesthesia by the intraluminal suture method. After 24 h of reperfusion, neurological deficit was determined, and infarct volume was measured using TTC staining in conjunction with ipsilateral hemispheric swelling. In a separate set of mice, neurological deficit and vasogenic edema (brain water content) were assessed at 24 h of reperfusion.

Results: Microvascular SphK2 activity increased following HPC, while SphK1 was unchanged (which paralleled the microvascular protein expression levels of these respective isoforms we observed earlier). Reductions in infarct volume, neurological deficit, hemispheric swelling, and vasogenic edema in HPC-treated mice were abrogated when SphK was inhibited during HPC. Administering the SphK2 agonist FTY720 (0.24 mg/kg, i.p) as an HPC mimic did not promote ischemic tolerance alone, but when combined with HPC, provided even greater (DMS-reversible) protection of the neurovascular unit, suggesting that HPC-induced increases in SphK2 activity, not additional substrate, are needed as an induction signal for ischemic tolerance.

Conclusions: These findings indicate that sphingosine-1-phosphate, formed by hypoxia-sensitive increases in SphK2 activity, serves as a proximal signaling mediator that ultimately leads to alterations in gene expression and the promotion of an ischemia-tolerant vasculoprotective phenotype. Thus, components of this bioactive lipid signaling pathway may be suitable therapeutic targets for protecting the blood-brain barrier and neurovascular unit in stroke.

References:

1. Miller BA et al., NeuroReport 2001; 12(8):1663-9.

2. Jin ZQ et al., Circulation 2004; 110(14):1980-9.

3. Blondeau N et al., J Neurochem 2007; 103(2):509-17.

4. Don AS et al., J Biol Chem 2007; 282(21):15833-42.

874

Brain Poster Session: Transcriptional Regulation

EFFECTS OF GLUCOSE AVAILABILITY ON HIF1ALPHA FUNCTION IN SH-SY5Y CELLS SUBJECTED TO HYPOXIA-REOXYGENATION

T. Santalucia[1], A. Serra-Perez[1], E. Berra[2], A. Planas[1]

[1]Brain Ischemia and Neurodegeneration, IIBB-CSIC/IDIBAPS, Barcelona, [2]Cell Biology & Stem Cells Unit, CICbioGUNE, Derio, Spain

Objectives: Hypoxia-induced Factor (HIF) regulates the cellular response against decreasing oxygen concentrations by activating genes involved in ATP production by glycolysis, among other mechanisms. HIF is a transcription factor that consists of an oxygen-regulated subunit (HIFalpha) and a constitutively expressed one (HIFbeta). HIFalpha expression is low under normoxia owing to proteasomal degradation. This is due to oxygen-dependent hydroxylation of certain proline residues in HIFalpha catalysed by prolylhydroxylases (PHD). Hypoxia inhibits degradation causing accumulation of HIFalpha[1]. Despite the regulation of HIFalpha expression and its transcriptional activity under hypoxia have been the subject of intense study, the putative contribution of glucose has not been examined so thoroughly.

Methods: SH-SY5Y (SH) cells were incubated in anoxic conditions for 15 h and either in the presence or absence of glucose. Cells were then allowed to reoxygenate and incubated for variable periods prior to preparing cell extracts[2]. These were analysed for the expression of HIF-1alpha and some of its target genes by Western blotting or ELISA. HIF transcriptional activity was measured by transient transfection with a luciferase reporter vector. Functionality of the proteasome was monitored by using SH clones engineered to express a ubiquitin-EGFP fusion protein that is constitutively targeted for proteasomal degradation[3].

Results: The expression of HIF-1 target genes (GLUT-1, HKII and VEGF) and the transcriptional activity of HIF after a period of 15h of anoxia were higher in the presence of glucose in the culture medium. These results were paralleled by differences in the expression of HIF-1alpha. HIF-1alpha was immediately degraded at reoxygenation following incubation of the cells in anoxia and in the presence of glucose. Surprisingly, the HIF-1alpha expressed under conditions of oxygen and glucose deprivation (OGD) remained stable after reoxygenation of the cells. The analysis of the proteasome activity under both conditions revealed no overt differences. However, we observed a specific change in the apparent molecular weight of HIF-1alpha at the end of the 15h OGD incubation. Whether this is related to the stabilisation is currently under study, together with the possible contribution of metabolites intervening in the PHD reaction[4].

Conclusions: The presence of glucose during anoxia enhances the induction of HIF-1alpha as well as of HIF-1 responsive genes, while OGD conditions are less favourable for the activation of HIF-1 in SH cells. Moreover, our data suggest the existence of some mechanism under OGD conditions that either affects the degradation of HIF-1alpha or renders it resistant to degradation triggered by oxygen.

References:

1. Semenza GL. (2007). Science 318, 62-64.

2. Serra-Perez A, Verdaguer E, Planas AM, and Santalucia T (2008) J Neurochem 106, 1237-1247.

3. Dantuma NP, Lindsten K, Glas R, Jellne M, and Masucci MG (2000) Nature Biotech 18, 538-543.

4. Puchowicz MA, Zechel JL, Valerio J, Emancipator DS, Xu K, Pundik S, LaManna JC, Lust WD (2008) J Cereb Blood Flow Metab 28, 1907-1916.

Acknowledgements: ASP has a predoctoral fellowship from AGAUR (Generalitat de Catalunya). TS is a "Ramón y Cajal" scientist (Spanish Ministry of Science and Innovation, MICINN). Project funded by grants from MICINN (SAF2005-05793-C02-02 and SAF2008-04515-C02-02).

875

Brain Poster Session: Experimental Stroke & Cerebral Ischemia

ENDOVASCULAR CANINE TRANSIENT MIDDLE CEREBRAL ARTERY OCCLUSION MODEL WITH LEPTOMENINGEAL COLLATERAL ASSESSMENT

G. Christoforidis, C. Rink, R. Koch, M. Kontzialis, A. Abduljalil, Y. Mohammad, V. Bergdall, S. Roy, S. Khanna, A. Slivka, M. Knopp, C. Sen

The Ohio State University, Columbus, OH, USA

Objective: In an effort to bridge the translational gap between laboratory and clinical research the goal of this work was to develop a large animal minimally invasive reversible middle cerebral artery occlusion (MCAO) model which also takes into account leptomeningeal collateral formation.

Methods: Endovascular MCAO materials and methods were optimized in 15 mongrel canines. Subsequently, 11 mongrel dogs (20-30 kg) received 300mg clopidogrel and intravenous heparin. Using isofluorane anesthesia and bilateral common femoral artery punctures digital subtraction angiography (OEC 9800) was used to guide a microcatheter (SL10, Boston Scientific) through the third spinal ramus artery to access the middle cerebral artery (MCA) through the circle of Willis and deploy a 3mm by 20 centimeter coil (Matrix, Boston Scientific) to occlude the middle cerebral artery and carotid terminus for one hour. Repetitive 4 vessel cerebral arteriography confirmed occlusion and reperfusion and allowed assessment of pial collateral formation using an 11-point scale. Infarct volumes were calculated from MRI (3T Achieva, Philips) using a threshold method by two observers on 1 hour post reperfusion mean diffusivity (MD) maps and 24 hour FLAIR MRI. A ten point canine stroke scale modified from the National Institutes of Health stroke scale score was developed to quantify neurologic assessments following reperfusion.

Results: MCAO was successful in 7 of 11 dogs (63% efficiency). Angiography was able to confirm that external carotid and circle of Willis colaterals were not present. Following coil removal reperfusion occurred in all successful MCAOs. Between two observers, Bland-Altman statistic indicated that infarct volume calculations from MD maps (15.9%) and FLAIR MRI (5.6%) and scoring of pial collateral formation (22.6%) were reproducible. One hour post-reperfusion infarct volumes calculated on MD maps was predictive of 24 hour post-reperfusion infarct volumes calculated on FLAIR MRI (linear fit; r^2= 0.970; p=0.0022). Pial collateral formation was found to be predictive of infarct volumes calculated on 1 hour post reperfusion mean diffusivity maps (linear fit; r^2=0.950; p=0.0003) and 24 hour FLAIR MRI (linear fit; r2=0.961; p=0.0033). The canine stroke scale score correlated with both infarct volume calculated at one hour post-reperfusion and 24 hours post reperfusion as well as pial collateral score.

Conclusion: An endovascular approach to transient MCA occlusion which takes into account leptomeningeal collateral formation is feasible and can consistently produce defined infarct lesions in the canine neocortex.

Note: First two authors provided equal effort towards this work.

Acknowledgements: Supported by NIH NS42617 (CKS) and Boston Scientific (GAC).

876

Brain Poster Session: Neurologic Disease

DIAGNOSTIC ACCURACY OF VISUAL VERSUS STATISTICAL PET IMAGE ANALYSIS FOR DISTINGUISHING BETWEEN NORMAL CONTROLS AND ALZHEIMER´S DISEASE

J. Mountz[1], A. Muthukrishnan[1], J. Price[2], E. Deeb[1], M. Rudolph[2], C. Mathis[2], W. Klunk[2]

[1]University of Pittsburgh Medical Center, [2]University of Pittsburgh, Pittsburgh, PA, USA

Objectives: Visual assessment of F-18 FDG brain PET scans for diagnosis of Alzheimer's Disease (AD) is widely used. Software programs for image analysis compare FDG PET scans to normal controls (NC) and generate statistical maps of hypometabolic regions. We examined NC and dementia patients to compare the accuracy of visual assessment to 3D-SSP and PMOD.

Methods: Patients were screened through the University of Pittsburgh Alzheimer's Disease Research Center using the NINCDS-ADRDA criteria. Nineteen NC, 17 MCI, and 16 AD subjects underwent F-18 FDG brain PET scans on the Siemens HR+ PET scanner after i.v. injection of approximately 7 mCi F-18 FDG. Analysis was performed by two expert brain PET scan interpreters (JM and AM). Scans were randomly sampled for visual interpretation and rated using the 3D-SSP and PMOD algorithms. Raters scored each scan from 1-4 where 1=definitely normal, 2=questionably normal, 3=questionably abnormal, and 4=definitely abnormal. The same rating scale was used for assessment of AD where 1 was definitely not AD and 4 was definitely AD. Agreement by both readers was necessary to score as either normal or AD, and differences were resolved by consensus.

Results: Figure shows two representative F-18 FDG PET scans. Normal control (left) and Alzheimer's disease patient (right) are represented. Image shows the format by which each scan was interpreted: Visual Assessment (top), 3D-SSP (middle), and Pmod (bottom). Table shows sensitivity and specificity for diagnosis of Alzheimer's disease for each test: Visual Interpretation, 3D-SSP, and Pmod. Sensitivity (top left) and specificity (bottom right) are shown bolded as percentages. False positive percent (top right) and false negative percent (bottom left) are also shown. AD was correctly classified as 56% visual, 50% by 3D SSP and 75% by PMOD. Normal controls were correctly classified as 79% visual, 95% by 3D-SSP and 89% by PMOD. PMOD was more sensitive to identify AD, but with a mild loss in specificity compared to 3D-SSP.

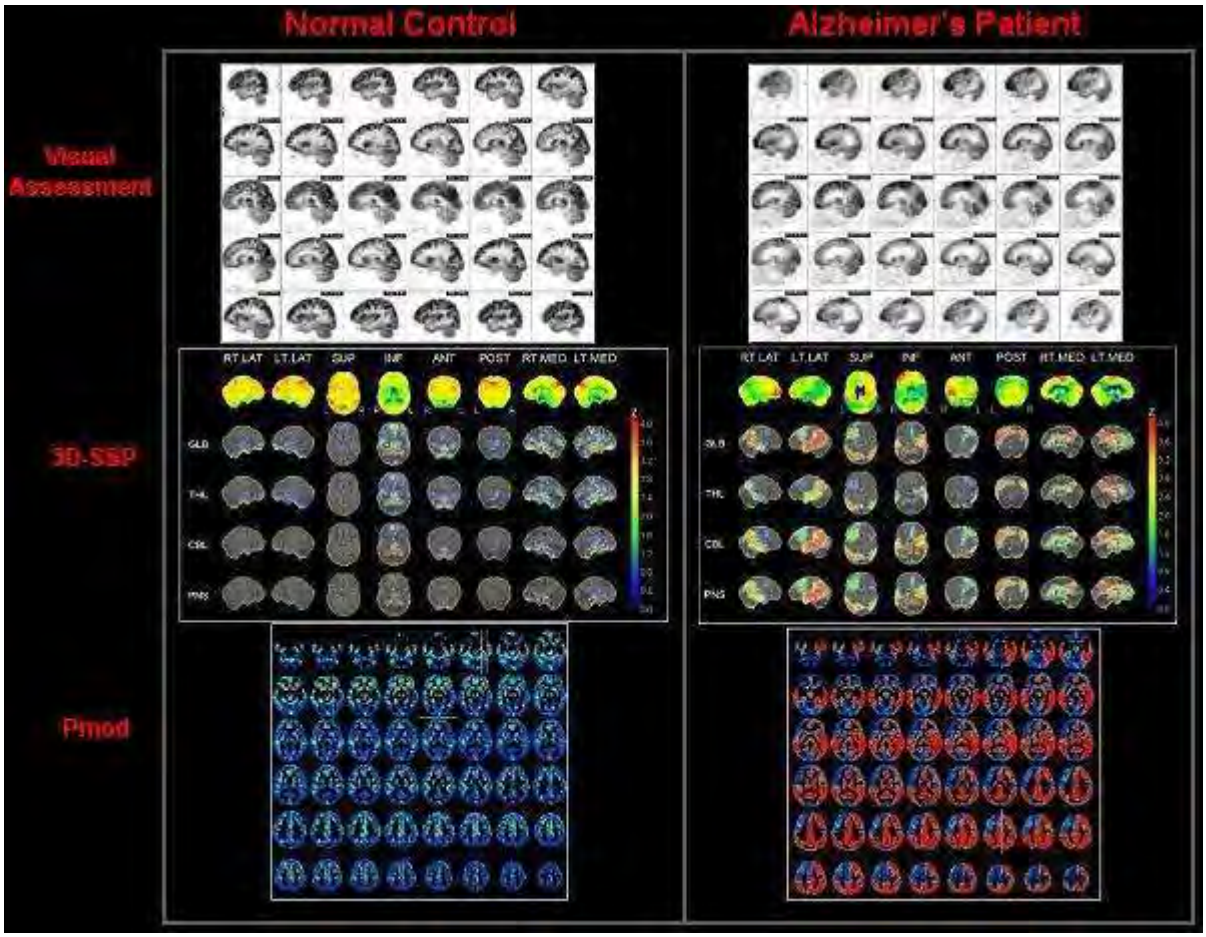

[Figure]

	Visual Interpretation of PET		3D-SSP		Pmod	
	AD patient	**Control patient**	**AD patient**	**Control patient**	**AD patient**	**Control patient**
Scan +	**56%**	21%	**50%**	5%	**75%**	11%
Scan -	44%	**79%**	50%	**95%**	25%	**89%**

[Table]

Conclusions: Visual assessment provides fair accuracy in discriminating NC from AD, but when

combined with a statistical method the accuracy significantly increases. Caution should be exercised when using visual or statistical methods alone to diagnosis AD.

877

Brain Poster Session: Stem Cells & Gene Therapy

TARGETED DELIVERY OF FERUMOXIDE LABELED HUMAN NEURAL STEM CELLS USING A NEODYMIUM MAGNET IN FOCAL CEREBRAL ISCHEMIC RATS

M. Song[1,2], Y.-J. Kim[1], Y.-H. Kim[1], J. Roh[1], B.-W. Yoon[1,2]

[1]Department of Neurology, Clinical Research Institute, Seoul National University Hospital, [2]Medical Research Center, Seoul National University, Seoul, South Korea

Objectives: It was reported that human neural stem cells (hNSCs) can be used to treat damaged tissues in various brain diseases. Injected hNSCs have limitations of delivery to target areas, so more effective methods are required. In our previous study, we established effective labeling of human neural stem cells with ferumoxide, FDA-approved iron oxide nanoparticle, complexed to transfection agent, poly-L-lysine (PLL). We hypothesized that ferumoxides labeled human neural stem cells can be delivered more effectively targeting to an area of interest by magnetic fields in vitro and in vivo.

Methods: hNSCs (HB1.F3 cells) were incubated for 24 hr in cell culture media with ferumoxides and PLL or without (control). Cellular iron uptake was identified by Prussian blue staining and iron contents of the cell were analyzed using iron reagents by a 560 nm UV/VIS spectrophotometer. hNSCs were incubated in a culture dish, under which a neodymium magnet was attached. Proliferation, viability and differentiation of the cells were evaluated using an increasing of cell number, trypan blue dye exclusion test, and immunofluorescence cytochemistry with cell-type specific makers, respectively. To investigate the targeted delivery, rats were allocated into three groups (i.e. ischemia only, cell injection with magnet and without magnet). After middle cerebral artery occlusion (MCAo), human NSCs were injected via tail vein 24 hours after. In histological sections, transplanted cells were identified by Prussian blue and anti-human nuclei fluorescence staining. Infarct size was analyzed by Nissl staining and the iron contents of rat brain were determined.

Results: Magnetic fields appeared not to affect cell proliferation, viability and differentiation. Cellular iron was detected in hNSCs by Prussian blue stain and mean iron contents was 261±9.8 pg/cell (n=3). An increased number of labeled hNSCs retained in the area of magnet field. Histological analysis of cell injection with magnet group at 7 days after transplantation revealed significantly reduced infarction volume and significantly increased hNSCs in rat brains comparing with other groups.

Conclusions: Our study suggests that this targeting system may be a useful tool for the cell therapy.

878

Brain Oral Session: Experimental Cerebral Ischemia: Neuroinflammation

CHARACTERIZATION OF THE IMMUNE RESPONSE IN PERIPHERAL ORGANS AFTER CEREBRAL ISCHEMIA IN MICE

A. Arac, T.M. Bliss, G.K. Steinberg

Neurosurgery, Stanford University School of Medicine, Stanford, CA, USA

Objectives: Inflammation plays an important role in central nervous system ischemia. Clinical and experimental data show acute and prolonged inflammatory response in the brain after stroke. In addition, there are changes in immune cells in peripheral organs following stroke. However, such immune cell changes in blood and secondary lymphoid organs such as lymph nodes and spleen after stroke have not been extensively studied. Here we investigate the response of the immune system in these organs after different stroke severities.

Methods: 12-week-old, male C57BL6J mice were subjected to 30 minutes (mild) or 90 minutes (severe) middle cerebral artery occlusion (MCAo) or sham surgery. 96 hours later, cells from cervical, axillary and abdominal (extra-peritoneal) lymph nodes, splenocytes and white blood cells from blood were isolated and analyzed by flow cytometry. The brains were processed and infarct sizes were determined from cresyl violet stained sections. Spleen size was also measured.

Results: Spleen size decreased after stroke. Consistent with this, the total number of splenocytes decreased after stroke compared to sham animals (42% and 73%, $p< 0.05$ in 30min and 90min MCAo groups, respectively, consistent with previous reports (1). This decrease in splenocyte number correlated with lesion size, with greater loss of splenocytes measured with increasing lesion size ($r=-0.918$, $p< 0.001$). Flow cytometric analysis of immune cells in the spleen confirmed a significant decrease after stroke in the total number of all immune cell types tested, except for the following which showed no significant change: NK1.1+ natural killer cells, CD4+ Th cells and CD8+ Tcyt cells in the 30min MCAo group and CD4+CD62L- effector T cells in both stroke groups. The number of all the cell types, except NK1.1+ natural killer cells, also correlated negatively with the infarct size. Although the total number of the different immune cells changed after stroke, the percentage of the different immune cells in the spleen was not different between sham and stroke animals except for: 1) regulatory T cells (Tregs, CD4+CD25+Foxp3+), that increased 42% ($p< 0.05$) after 90min MCAo, 2) B cells (B220+), which decreased 17.8% ($p< 0.05$) after 30min MCAo and 14% ($p< 0.05$) after 90min MCAo. In lymph nodes only Tregs changed and only after 90min MCAO, increasing 30% ($p< 0.05$). This increase correlated with infarct size ($r=0.867$, $p< 0.01$. In the blood, changes were only seen in granulocytes (Gr1+) and monocytes/macrophages (CD11b+), which significantly increased ($p< 0.05$) in both stroke groups (granulocytes: 213% in 30min and 276% in 90min MCAo groups; monocytes/macrophages: 185% in 30min and 210% in 90min MCAo groups).

Conclusions: There is a systemic response of the immune system to stroke. These data are the first to show that some components of this response correlate with infarct size. Modulation of the immune system may provide a new strategy for stroke treatment.

References: 1. Offner, H. et al., Splenic atrophy in experimental stroke is accompanied by increased regulatory T cells and circulating macrophages. J Immunol 176 (11), 6523 (2006).

879

Brain Poster Session: Blood-Brain Barrier

IDENTIFICATION OF NEUROINFLAMMATION-ASSOCIATED PROTEINS AND GLYCOPROTEINS IN HUMAN BRAIN ENDOTHELIAL CELLS USING MASS SPECTROMETRY-BASED QUANTITATIVE PROTEOMICS

A. Haqqani[1], J. Mullen[1], W. Zhang[1], P. Couraud[2], D. Stanimirovic[1]

[1]Institute for Biological Sciences, National Research Council, Ottawa, ON, Canada, [2]Université Paris Descartes, Paris, France

The luminal surface of brain vascular endothelium is decorated with proteins, glycoproteins and proteoglycans that form a thick coating called glycocalyx. The glycocalyx is involved in various vascular functions including endothelial permeability, leukocyte adhesion/emigration and vascular blood flow. Recent work has shown that the true interface between the endothelium and flowing blood is the endothelial glycocalyx rather than the endothelial plasma membrane. The glycocalyx is significantly altered in response to ischemia/reperfusion or various inflammatory stimuli; for example, most of the endothelial surface and adhesion molecules that are up-regulated as hallmarks of cerebrovascular inflammation are glycosylated proteins. However, the complex nature of the brain endothelial glycocalyx, has so far hindered deeper understanding of its molecular alterations in pathological conditions.

Objectives: To identify proteins and glycoproteins present in the membranes of human brain endothelial cells (HBEC) and their quantitative changes in response to inflammatory stimulus using advanced (glyco)proteomics and bioinformatics tools.

Methods: Total membrane extracts were isolated from Immortalized HBEC (HCMEC/D3 obtained from P. Couraud) exposed to 100 U/mL IL-1b for 16 h by ultracentrifugation and sucrose gradient. The membranes were then treated with N-linked deglycosylating enzyme (PNGase F) and fractionated using cation exchange chromatography. Each fraction was analyzed by label-free mass spectrometry-based quantitative proteomics using nanoLC-MS and MS/MS followed by a suite of bioinformatics tools. Three biological replicates and two technical replicates were carried out. The quantitative variability of the proteomic analyses was < 10% for technical replicates and < 20% for biological replicates.

Results: 10,608 high-quality unique peptide sequences have been identified in the total HBEC membranes, corresponding to 2,817 proteins (Table 1). More than 400 proteins were found to be glycoproteins as determined by PNGase F treatment (e.g., TMEM30A, various solute carrier family and ABC transporters). While most (68%) of the PNGase F-responsive proteins are known glycosylated proteins, many novel N-glycosylated proteins were identified. In addition, >750 proteins showed differential expression in response to IL-1b treatment (>2.5-fold up- or down-regulated, $p < 0.05$, 3 biological and 2 technical replicates). The majority of these proteins have not been previously reported as IL-1b-responsive, and >10% were of unknown function. Classification of the proteins using Panther Classification System showed their functions/processes consistent with pathophysiology of neuroinflammation.

Table 1: Number and examples of proteins up- or down-regulated in response to IL-1β in HCMEC/D3 total membranes

	Total	Upregulated	Downregulated	Examples
TOTAL	2817	390	378	
Signal Transduction	317	37	26	IL22RA1, erbB-2
Adhesion Molecules & Tight Junctions	192	21	20	ICAM1, integrins, ALCAM, PECAM1, ZO1, ZO2
ECM proteins	154	16	6	MMPs, ECM2
Transporters	140	21	19	SLC1A5, ABCs
Immunity and Defense	126	18	9	HSPs, GSH synthase
MMPs and other Proteases	67	11	8	MMP9
Protein Traffic	38	3	1	
MHC Antigens Associated Proteins	33	7	3	
Chemokines and Cytokines	26	6	2	
Angiogenesis	23	3	1	
Unclassified/Unknwon Category	298	35	32	

[Table1]

Conclusion: These analyses identified many proteins of yet unknown function as well as previously unknown glycoproteins that respond to inflammatory stimuli in brain endothelium. The data suggest an important role for glycocalyx in physiological and pathological responses of brain endothelium.

NITRIC OXIDE AS A MAJOR MEDIATOR OF NEUROVASCULAR COUPLING IN HYPOXIA: FREE RADICAL HYPOTHESIS

H. Takuwa[1], T. Matsuura[2], R. Bakalova[1], T. Obata[1], I. Kanno[1]

[1]Molecular Imaging Center, National Institute of Radiological Sciences, Chiba, [2]Iwate University, Morioka, Japan

Objectives: The tight spatial and temporal coupling of synaptic activity with local cerebral blood flow (known as neurovascular coupling) is a hallmark of brain function. Any obstruction of the neurovascular coupling mechanism disturbs brain homeostasis and provokes brain pathology and cell death. To clarify and find ways to control the key molecular targets underlying the regulation of neurovascular coupling could be an important way to increase the life of brain cells, to overcome neurodegenerative diseases, and to delay the processes of senescence.

The present study was designed to clarify whether nitric oxide participates in the regulation of neurovascular coupling during hypoxia. Hypoxia is a characteristic of many brain disorders (e.g., stroke, infraction, inflammation, necrosis, etc.) and its control is of outstanding importance for brain homeostasis.

Methods: Seventeen male Sprague-Dawley rats (385.4 ± 3.2 g) were used to investigate the effect of hypoxia and LNA [L-nitro-arginine - a selective inhibitor of nitric oxide synthase (NOS)] on the evoked regional cerebral blood flow response (rCBF) to hind-paw stimulation. The rats were anesthetized with isoflurane during the surgery and alpha-chloralose during the measurements. The animals were ventilated with a respirator using a mixture of air and oxygen to achieve physiological arterial blood levels of PaO_2 and $PaCO_2$ (PaO_2 was ~110-130 mmHg; $PaCO_2$ ~33-40 mmHg), as well as to induce hypoxia (PaO2 ~45-49 mmHg, PaCO2 ~33-40 mmHg). To avoid side-effects of systematic changes, the experimental protocol was designed to ensure hypoxia and normotension conditions. The rCBF response to hind-paw stimulation was measured by laser-Doppler flowmetry (LDF) with stimulus frequency of 5 Hz, current 1.5 mA, and duration 5 sec before and after induction of hypoxia, as well as before and after intravenous infusion of LNA. The field potentials were also recorded using an Ag-AgCl indifferent electrode.

Results: Hypoxia was accompanied by an enhancement of the baseline (~18%) and rCBF response to hind-paw stimulation. The peak-amplitude of the rCBF response curve increased significantly (~31%), while the rise-time and termination-time were constant. The infusion of LNA completely abolished the effect of hypoxia on the baseline and evoked rCBF response. During hypoxia, the peak-amplitude of the evoked rCBF decreased significantly after LNA infusion (~48%) to a value even lower than that obtained during normoxia without LNA administration. The infusion of LNA was accompanied by vasoconstriction and hypertension. The termination time of the rCBF response curve decreased slightly (~15%) after LNA infusion during hypoxia, while the rise-time was constant. The field potential was constant for all experimental protocols.

Conclusions: The data confirm the major role of nitric oxide in the regulation of neurovascular coupling during hypoxia. Since the hypoxia is accompanied by abnormal generation of reactive oxygen species,[1] e.g., superoxide radicals known to interact rapidly with nitric oxide, we hypothesize that the resulting peroxinitril radical is the most likely candidate for regulation of neurovascular coupling during hypoxia and hypoxia-induced vasodialtion.

References: [1]Packer L.,et al, (1992) Free Radicals in the Brain: Aging, Neurological and Mental Disorders, Springer-Verlag, Berlin.

881

Brain Poster Session: Ischemic Preconditioning

HYPOTHERMIC PRECONDITIONING INDUCES RAPID TOLERANCE TO HYPOXIA IN HIPPOCAMPAL SLICES: POTENTIAL MEDIATION BY ERYTHROPOIETIN

N. Kreisman[1], L. Wooliscroft[2], C. Campbell[3], A. Scanduro[4]

[1]Department of Physiology, [2]Neuroscience Program, [3]Department of Pharmacology, [4]Department of Microbiology and Immunology, Tulane University School of Medicine, New Orleans, LA, USA

Objectives: Preconditioning is a procedure where exposure to a mild insult renders tissue less vulnerable to injury following a subsequent, more severe insult. Hypothermia is a conditioning procedure that has minimal risk of injury to brain tissue. This investigation had two major objectives:

1. determine whether preconditioning hippocampal slices with hypothermia could induce rapid tolerance to a subsequent episode of severe hypoxia and
2. determine whether rapid tolerance to severe hypoxia is mediated by erythropoietin (EPO) and its downstream signaling cascade.

Methods: Sprague-Dawley rats were anesthetized with ether, decapitated, and the brain was placed in buffered saline at 0°C for 10 min. 400 μm slices of hippocampus were cut with a manual chopper and slices were either placed in an interface recording chamber at 35-36°C (normothermia) or in a preincubation chamber at 22-23°C (hypothermia). Orthodromic population spikes evoked in CA1 were used to verify slice viability. Thereafter, the recording electrode was moved to the inner blade of the dentate gyrus to monitor the extracellular potential. Light transmittance (LT) was measured as an index of tissue swelling/depolarization either in the whole slice, using a dissecting microscope with a digital video camera attached to one eyepiece (Kreisman et al 2000), or in the dentate gyrus with a photodiode. After two hours of incubation in 95% O_2+5% CO_2 (normoxia) normothermic slices were exposed to 10 min of hypoxia (95% N_2+5% CO_2). Normothermic slices were removed from the recording chamber and replaced with hypothermic slices, which were then incubated for 60 min at 35-36ºC before being exposed to 10 min of hypoxia. Comparisons were made of the LT index of hypoxic swelling in normothermic slices versus slices preconditioned with hypothermia.

Results: Slices preconditioned with hypothermia (n=11) had a 46.9% decrease in the LT index of swelling in response to 10 min of hypoxia, compared to normothermic slices (n=12). Swelling was prevented completely in the CA3 region and parts of the dentate gyrus. The tolerance mediated by hypothermia was mimicked by bathing normothermic slices (n=12) in recombinant rat EPO (10 ng/ml), which decreased the LT index of hypoxic swelling by 38.8% ($p< 0.01$ by Student's T test). Wortmannin (0.1 μM), which blocks activation of Akt by PI3 kinase (downstream of the EPO receptor) reduced the tolerance mediated by hypothermic conditioning, as indicated by a decrease in the LT index of hypoxic swelling from 44.7% to 17.1% (n=10).

Conclusions:

1. Hypothermic preconditioning produces rapid tolerance to subsequent hypoxic injury in hippocampal slices.
2. EPO may mediate hypothermic tolerance.
3. EPO's putative protective effect involves signaling via Akt.

References: Kreisman NR, Soliman S, and Gozal D (2000) Regional differences in hypoxic depolarization and swelling in hippocampal slices. J Neurophysiol 83: 1031-1038.

CHEMICAL PRECONDITIONING AMELIORATES POST-ISCHEMIC BRAIN EDEMA BY AQUAPORIN-4 DOWNREGULATION

A. Hoshi, T. Yamamoto, T. Kumagai, K. Shimizu, Y. Sugiura, Y. Ugawa

Neurology, Fukushima Medical University, Fukushima, Japan

Objectives: Aquaporin-4 (AQP4) is abundantly expressed in the astrocyte foot processes at the blood-brain barrier. In general, it has been believed that AQP4 plays an important role in the generation of cytotoxic edema under ischemic stroke (Manley et al., 2000). So far, we have shown that 3-nitropropionic acid (3-NP) of mitochondrial inhibitor was one of tolerance-inducers to ischemia, and astrocytic glutamine synthetase (GS) was induced by the chemical preconditioning (Hoshi et al., 2005; Hoshi et al., 2006). Using this model, we investigated whether the AQP4 or GS expression is affected by 3-NP preconditioning. The effectiveness of the chemical preconditioning on the post-ischemic edema was also studied.

Methods: Male Sprague-Dawley rats were used in all experiments. Three groups of animals were studied: control, preconditioned at two different stages. The animals were preconditioned by intraperitoneal injection with 10 mg/kg of 3-NPA at tolerance-inducible stage (TS: 24-48 hours) or non tolerance-inducible stage (NTS: 96 hours) before middle cerebral artery (MCA) occlusion (Hoshi et al., 2006). The control group was injected with physiological saline. All of the animals were sacrificed 4 days after MCA occlusion for the measurement of the cerebral hemisphere swelling. The cerebral hemisphere swelling was analyzed by measuring the percentage of hemispheric enlargement (HE) [(ipsilateral hemisphere volume - contralateral hemisphere volume)/contralateral hemisphere volume] ×100, which represents the amount of edema formation. In addition, single or double immunofluorescence analysis of AQP4 and GS was conducted after the each 3-NP treatment and vehicle applied. Fluorescence intensities of AQP4 were analyzed quantitatively by image analysis software (Lumina vision, Mitani Corp., Japan).

Results: The HE was significantly reduced in TS group compared with the control group ($P< 0.01$) or NTS group ($P< 0.05$). Temporal profiles of AQP4 immunoreactivity in the cortex and striatum revealed that the AQP4 expression was downregulated by 3-NP preconditioning at the tolerance-inducible period but not at another period. On the contrary, GS immunoreactivity was enhanced by the preconditioning at any periods (in particular tolerance-induced) as our previous report (Hoshi et al., 2006).

Conclusions: 3-NP preconditioning may attenuate post-ischemic brain edema by AQP4 downregulation. Inhibition of AQP4 by pharmacologic agents would offer a new therapeutic option for some forms of cerebral edema.

References:

Hoshi A, Nakahara T, Kayama H, Yamamoto T (2006) Ischemic tolerance in chemical preconditioning: Possible role of astrocytic glutamine synthetase buffering glutamate-mediated neurotoxicity. J Neurosci Res 84: 130-141.

Hoshi A, Nakahara T, Ogata M, Yamamoto T (2005) The critical threshold of 3-nitropropionic acid-induced ischemic tolerance in the rat. Brain Res 1050: 33-39.

Manley GT, Fujimura M, Ma T, Noshita N, Filiz F, Bollen AW, Chan P, Verkman AS (2000) Aquaporin-4 deletion in mice reduces brain edema after acute water intoxication and ischemic stroke. Nat Med 6: 159-163.

885

Brain PET Oral 5: In Vivo Pharmacology II: Serotonin

INVESTIGATION OF ATOMOXETINE OCCUPANCY OF SEROTONIN TRANSPORTERS

M. Naganawa[1,2], D. Weinzimmer[1], S.-F. Lin[1], C. Sandiego[1], J.-D. Gallezot[1], Y. Huang[1], R.E. Carson[1], E.A. Rabiner[3], M. Laruelle[3], Y.-S. Ding[1]

[1]Yale PET Center, Yale University School of Medicine, New Haven, CT, USA, [2]Molecular Imaging Center, National Institute of Radiological Sciences, Chiba, Japan, [3]GlaxoSmithKline, London, UK

Objectives: Atomoxetine (ATX) is a putative selective norepinephrine transporter (NET) reuptake inhibitor and is used for treatment of depression and attention-deficit/hyperactivity disorder. We have shown that ATX displayed a dose-dependent occupancy on NET using PET and [^{11}C]MRB, a selective NET radioligand [1]. Our previous study also indicated that ATX (1.5 mg/kg) blocked the binding of the SERT ligand [^{11}C]DASB in the baboon brain, an effect similar to that of fluoxetine (an SSRI) [2]. The purpose of this study was to determine if ATX, at clinically relevant doses, occupied SERT in a dose-dependent fashion in rhesus monkeys, using PET and [^{11}C]AFM, a highly selective radioligand for SERT [3].

Methods: Following a similar scanning paradigm as our previous study using [^{11}C]MRB [1], rhesus monkeys were scanned four times with [^{11}C]AFM (baseline & medium dose of ATX on day 1; low & high doses of ATX on day 2). ATX or saline infusion began 2 h before each scan, lasting until the end of the 2 h scan, to mimic the human oral dose PK profile. Infusion rates ranged 0.045-1.054 mg/kg/h. ATX plasma levels and arterial input functions were measured. Distribution volumes (V_T) were estimated by one-tissue compartment model and ATX IC_{50} values were calculated.

Results: In baseline scans, regional brain [^{11}C]AFM V_T [mL/cm^3] reflected the known distribution of SERT, with high binding in the brainstem (V_T = 127±52) and thalamus (V_T = 114±23), intermediate binding in temporal cortex (V_T = 73±13), and lowest binding in the cerebellum (V_T = 36±0.6). V_T in the cerebellum was reduced by up to 32% with increasing ATX dose, suggesting that there was some contribution of specific binding to the cerebellum signal. Receptor occupancy (r) and non-displaceable volume of distribution (V_{ND}) were calculated from the occupancy model in the absence of an ideal reference region [4]: V_T(baseline) - V_T(post-drug) = r × (V_T(baseline) - V_{ND}). After administration of ATX, a dose-dependent occupancy from 49 to 90% was observed. The IC_{50} was estimated to be 167±16 ng/mL of plasma ATX concentration (corresponding to an infusion rate of 0.126±0.013 mg/kg/h). At a therapeutic ATX dose (1.8 mg/kg, ~600 ng/mL plasma) ATX would have occupied ~80% of SERT.

Conclusions: This study demonstrated that ATX inhibited [^{11}C]AFM binding in rhesus monkey brain in a dose-dependent fashion. Compared with our reported ATX IC_{50} value for NET with [^{11}C]MRB [3], the ATX in vivo IC_{50} ratio of SERT to NET was ~6, consistent with the reported in vitro affinity (K_d) ratio of ~4.5 (8.9 and 2 nM for SERT and NET, respectively) [5]. Our comparative studies of ATX effects on NET and SERT suggest that ATX at clinical doses occupies both transporters. Thus, PET occupancy studies are important in clarifying the mechanism of ATX therapeutic action.

References:

[1] Gallezot J-D, et al., NeuroImage, 41:T49, 2008.

[2] Ding Y-S and Fowler, J, NMB, 32:707-718, 2005.

[3] Huang Y, et al., NMB, 31:543-556, 2004.

[4] Lassen NA, et al., JCBFM, 15: 152-165, 1995.

[5] Tatsumi M, et. al., EJP, 340: 249-258, 1997.

886

Brain Poster Session: Transcriptional Regulation

CALCIUM-DEPENDENT TRANSCRIPTION IN CEREBRAL ISCHEMIA: ROLE OF ASTROCYTES

M. Sobrado[1], B.G. Ramírez[2], M. Arbonés[3], D. Fernández-López[1], I. Lizasoaín[1], M.A. Moro[1], E. Cano[2]

[1]Complutense University of Madrid, [2]National Centre of Cardiovascular Research (CNIC), Madrid, [3]Center for Genomic Regulation (CRG-UPF), Barcelona, Spain

Background: Increase in intracellular calcium concentration $[Ca^{2+}]i$ is a common feature of many neurodegenerative, ischemic and ageing-related processes that likely involve astrocytes. Work from our laboratory, demonstrated the existence of an inducible calcium/calcineurin/Nuclear Activated Factor of T cells (NFAT) signalling pathway in primary cultured astrocytes. Moreover, the increase in $[Ca^{2+}]i$ activates NFAT-dependent mRNA and protein expression of targets such as cyclooxygenase 2 and Rcan 1.4 in this cell type [1]. Here, we have studied the induction of the calcineurin/NFAT signalling pathway in response to ischemia in astrocytes, using "in vivo" and "in vitro" experimental ischemia models in rodents. We show here that there is a specific up-regulation of total Rcan 1.4 protein in brain cortex after ischemia. We have focused in the induction of Rcan protein in astrocytes around the infarcted area.

Methods and results: Western blot and quantitative RT-PCR showed that oxygen and glucose deprivation (OGD) activates calcium/calcineurin/NFAT pathway in astrocytes cultures. Protein and mRNA time course shows that RCAN 1.4 increases at early times after OGD. We have found that Rcan 1.4 overexpression in astrocytes, using adenoviral vector, inhibits the expression of inflammatory markers such as Cyclooxigenase. The occlusion of middle cerebral artery for 1h produced an increased expression of RCAN 1.4 as soon as 1h after ischemia and it was maximal 24h after reperfusion. At the moment, we are carrying out a more thorough analysis of the inflammation process after brain ischemia, and the role of Rcan1.4 overexpression.

Conclusions: These results demonstrate the activation of calcium/calcineurin/NFAT pathway and the up-regulation of RCAN 1.4 after experimental cerebral ischemia. Moreover, our results suggest that the study of the calcium-dependent signalling pathway in general and the Ca/CN/NFAT pathway in particular in the ischemic context, together with its role in the regulation of genes-induced might be essential for a better understanding of neuroprotection and recovery of damaged tissue.

*These authors contributed equally to this work.

887

Brain Poster Session: Cerebral Vascular Regulation

PHOSPHORYLATION OF ENDOTHELIAL NITRIC OXIDE SYNTHASE IS INCREASED BY RHO-KINASE INHIBITION IN THE BRAIN

Y. Yagita[1], K. Kitagawa[1], N. Oyama[2], S. Okazaki[1], Y. Sugiyama[1], Y. Terasaki[2], E. Omura-Matsuoka[2], T. Sasaki[2], S. Sakoda[1]

[1]Stroke Division, Department of Neurology, [2]Stroke Division, Department of Cardiovascular Medicine, Osaka University Graduate School of Medicine, Suita, Japan

Objectives: Endothelial dysfunction and microcirculatory disturbance cause infarct expansion in the ischemic brain. Thus, vascular protection is a promising therapeutic strategy for brain protection against ischemic injury. Rho-kinase is small GTPase protein Rho dependent serine/threonine kinase. Abnormal activation of Rho-kinase perturbs endothelial function via impairment of endothelial nitric oxide synthase (eNOS) function. Chronic treatment of Rho-kinase inhibitor can increase eNOS protein expression and ameliorate ischemic brain injury [1]. Additionally, acute effect of Rho-kinase inhibitor against ischemic brain injury has been also reported [2, 3]. Post-ischemic treatment with Rho-kinase inhibitor can improve microcirculatory disturbance and ameliorate ischemic injury in the ischemic brain [3]. Phosphorylation of eNOS may be involved in this acute brain protective effect. However, there are few reports that directly show acute effect of Rho-kinase inhibitor on eNOS phosphorylation in the in vivo brain. In this study, we investigated the acute effect of Rho-kinase inhibitor, fasudil, on the phosphorylation of eNOS in the brain.

Methods: Male Wistar rats were subjected to focal cerebral ischemia with the use of a 4-0 nylon monofilament and reperfusion 80 min after induction of ischemia. Rho-kinase inhibitor, fasudil (10mg/kgBW), was injected intraperitoneally. Ischemic rats were injected fasudil at the period of reperfusion. Rho-kinase activation was histologically evaluated by analyzing the phosphorylation of direct substrates of Rho-kinase. Phosphorylation of eNOS (Ser1177) and neuronal NOS (Ser1412) were assessed by Western blot using phospho-specific antibody. Brain samples were obtained from the cortices of middle cerebral artery area for Western blot.

Results: Treatment of fasudil enhanced eNOS phosphorylation in the normal rat brain and lasted up to 8 hours after injection. In contrast, up-regulation of nNOS phosphorylation was not observed after fasudil injection. In the ischemic brain cortex of middle cerebral artery area, Rho-kinase was activated in the endothelial cells of microvessel and glial cells 6 hours after induction of ischemia. In this region, the level of eNOS phosphorylation was not altered significantly following ischemia/reperfusion injury. Fasudil treatment could enhance eNOS phosphorylation in the ischemic cerebral cortex, as well as in the normal brain.

Conclusions: Inhibition of Rho-kinase activity can acutely augment eNOS phosphorylation in the in vivo brain. Our findings suggest that Rho-kinase inhibitor can acutely enhance eNOS activity in the brain microvessels, as well as increase eNOS protein expression by chronic treatment. This effect may be one of the molecular mechanisms involved in the protective effect against brain ischemia.

References:

[1] Rikitake Y et al. Inhibition of Rho kinase (ROCK) leads to increased cerebral blood flow and stroke protection. Stroke 36:2251-2257, 2005.

[2] Shin HK et al. Rho-kinase inhibition acutely augments blood flow in focal cerebral ischemia via endothelial mechanisms. J Cereb Blood Flow Metab 27:998-1009, 2007.

[3] Yagita Y et al. Rho-kinase activation in endothelial cells contributes to expansion of infarction after focal cerebral ischemia. J Neurosci Res 85:2460-2469, 2007.

888

BrainPET Poster Session: Molecular Brain Imaging: Clinical Applications

[^{11}C]DASB PET AND SEROTONIN TRANSPORTER (SERT) AVAILABILITY IN PATIENTS WITH EARLY (EO) AND LATE - ONSET (LO) OF OBSESSIVE-COMPULSIVE DISORDER

K. Stengler[1], S. Hesse[2], D. Assmann[1], I. Jahn[1], R. Regenthal[3], G. Becker[2], M. Patt[2], H. Knuepfer[3], O. Sabri[2], U. Hegerl[1]

[1]Psychiatry, [2]Nuclear Medicine, [3]Clinical Pharmacology, University of Leipzig, Leipzig, Germany

Introduction: First in vivo imaging studies on SERT employing SPECT and PET in patients with OCD did not reveal consistent results. Previous research has investigated whether there are clinical, demographic and neurobiological differences between subgroups of OCD, e.g. individuals who have experienced onset of OCD at an early or later age. Results suggest that patients with an early onset (EO) of the disorder report greater severity and persistence of symptoms. Additional, few studies have investigated whether there are differences in treatment response between these subgroups of OCD. Therefore, the aim of the present study was to measure selectively SERT availability using [^{11}C]DASB and PET in patients with early and late onset of the disorder.

Methods: Seventeen unmedicated patients with OCD (ICD 10: F42.0-42.2; 8 females, age 37 ± 9 years; age of onset 26.3 ± 14.5 years [10-53]; 4 patients with early onset OCD [EOCD]) and 11 healthy age- and gender-matched controls underwent dynamic PET after the IV injection of 570 MBq [^{11}C]DASB. Distribution volume ratios (DVR) were generated using MRTM2 and VOI analysis after co-registration of the DVR maps with the individual 3D MRI data set. Severity of OCD was estimated using the Yale-Brown Obsessive Compulsive Scale (Y-BOCS). Patients must have Y-BOCS ³ 20 points for inclusion into the study. Depressive symptoms were rated using the Beck Depression Inventory (BDI).

Results: There was a negative relationship between DVR and age of onset (e.g. for the left thalamus R=-0.467, P=0.044, age-corrected) with significant lower values in the LO-OCD compared with EO-OCD. DVR of EO-OCD patients did not differ from controls. Lower than normal DVR in OCD were found in LO-OCD in any brain region (ranging from P=0.175 in the right dorsolateral prefrontal cortex, P=0.003 in the hippocampus-amygdala region to P< 0.001 in the corpora striatum and the thalamus). YBOCS and DVR were correlated in the right dorsolateral prefrontal cortex (R=0.504, P=0.028) and the left medial frontal cortex (0.473, 0.041) but there were no significant association between BDI and DVR. Age had a significant effect on DVR across the brain regions (except cerebellum) in patients (from R=-0.713, P=0.001 in the insula to R=-0.473, P=0.055 in the left dorsolateral frontal cortex) but not in healthy controls. Neither age nor age of onset did correlate with YBOCS.

Conclusion: The SERT availability differs depending on the age of onset in patients with OCD. Compared with either EO-OCD or healthy controls patients with LO-OCD have abnormal low SERT availability in frontal cortical areas as well as in the striatum and the thalamus.

890

Brain Poster Session: Epilepsy

ICTAL SPECT DURING SEIZURES PHARMACOLOGICALLY PROVOKED IN PRE-SURGICAL EVALUATION OF EXTRATEMPORAL LOBE EPILEPSY

D. Di Giuda[1], C. Caldarella[1], C. Barba[2], R. Mazza[1], F. Cocciolillo[1], D.P. Dambra[1], G. Colicchio[3], A. Giordano[1]

[1]Nuclear Medicine Institute, Catholic University of the Sacred Heart, Rome, [2]Pediatric Neurology Unit, Children's Hospital A. Meyer, Florence, [3]Neurosurgery Department, Catholic University of the Sacred Heart, Rome, Italy

Objectives: Ictal SPECT is a reliable indicator of the seizure onset zone in patients with intractable epilepsy. Contrarily to the contribution in temporal epilepsy, the localising ability of ictal SPECT in the pre-surgical work-up of extratemporal epilepsy (ETE) is lower due to several factors affecting results. Obtaining true ictal radiotracer injections remains a challenge at most Centres, mainly for logistical reasons. Aim of the study was to assess the diagnostic value of pharmacologically provoked ictal SPECT in surgical ETE.

Methods: 26 patients (15 m, 11 f, mean age: 27.7±8.8 yrs) underwent the following pre-surgical protocol: neurological examination, MRI, neuropsychological and psychodynamic assessments, scalp-video-EEG monitoring, interictal and ictal SPECT with ^{99m}Tc-Ethyl-Cysteinate-Dimer (ECD) and invasive neurophysiologic recordings if necessary. Interictal SPECT was carried out after a seizure-free period of > 24 hours. Ictal SPECT was performed during seizure provoked with pentylenetetrazol slow injection and recorded by scalp-video-EEG and/or intracranial-EEG monitoring. Visual interpretation of images was performed blind to clinical data. SPM analysis of individual ictal SPECT in comparison with a normal brain SPECT database was available in 16/26 cases.

Results: MRI was normal in 3/26 cases. In all patients radiotracer injections were performed during provoked seizures semiologically identical to the spontaneous ones. The average delay from clinical and EEG seizure onset to radiotracer injection was 6 sec and 16 sec, respectively. Visual analysis of interictal and provoked ictal SPECT was concordant with the epileptogenic zone (EZ) in 22/26 (84.6%) epileptic patients: 19/22 subjects showed the typical hypo-hyperperfusion pattern, while in the remaining three cases no interictal hypoperfusion areas were detected. Fifteen of these 22 patients with concordant results underwent ablative surgery: 13 patients were seizure-free after at least 2 years of follow-up while in 2 subjects surgical follow-up was too short to be considered. Discordant results between SPECT findings and the EZ were observed in 2 patients while in 2 cases with large anatomical lesions provoked ictal SPECT failed to demonstrate focal hyperperfusion. In these two cases ablative surgery was performed with poor outcome. SPM analysis of provoked ictal SPECT was concordant with visual interpretation and final definition of the EZ in 14/16 and 12/16 cases, respectively.

Conclusions: This study demonstrated the localising value of provoked ictal SPECT in refractory ETE. The diagnostic efficacy of our procedure was supported by the satisfying results at surgical outcome, also in patients with non-localising MRI. The optimisation of ^{99m}Tc-ECD injection timing is the main advantage of our procedure, indispensable for unambiguous localisation of extratemporal foci. SPM analysis may improve localisation of the seizure onset zone and aid in distinguishing it from seizure propagation areas.

References:

Correlation between provoked ictal SPECT and depth recordings in adult drug-resistant epilepsy patients. Barba C, Di Giuda D, Policicchio D, Bruno I, Papacci F, Colicchio G. Epilepsia 2007;48(2):278-85.

Ictal brain SPET during seizures pharmacologically provoked with pentylenetetrazol: a new diagnostic procedure in drug-resistant epileptic patients. Calcagni ML, Giordano A, Bruno I, Parbonetti G, Di Giuda D, De Rossi G, Troncone L, Colicchio G. Eur J Nucl Med Mol Imaging. 2002;29(10):1298-306.

MODELING BLOOD/TISSUE TRANSFERS AT THE VOXEL SCALE FOR BLOOD FLOW QUANTIFICATION WITH PET

I. Billanou[1], S. Lorthois[1], M. Quintard[1], P. Celsis[2]

[1]Institut de Mécanique des Fluides de Toulouse, UMR CNRS/INPT/UPS 5502, [2]Inserm U825 'Cerebral Imaging and Neurological Handicap', CHU Purpan, Toulouse, France

Objectives: The current practice for analyzing dynamic PET scans is based on compartmental models, which relate the kinetics of the measured activity and the function under study [1]. In particular, cerebral blood flow modifications during activation studies are determined by considering two well-mixed compartments: an arterial compartment (AC) and a tissue compartment (TC). The Renkin-Crone theoretical description of the exchange between these two compartments, which introduces kinetic rate constants related to the flow rate, considers one single capillary and its surrounding tissue, modeled as two coaxial cylinders (Krogh cylinder). The obtained rate constants, which implicitly describe exchanges at local scale, are nevertheless used in the compartmental model to describe exchanges between AC and TC at the voxel scale, i.e. macroscopic scale. Moreover, the compartmental approach is based on extremely simplifying assumptions. For example, axial diffusion (concentration gradients in the longitudinal direction) is neglected. The limits of the compartmental approach have been recognized and may explain some illogical results obtained by PET [2]. In this context, our goal is to propose an improved kinetic model for diffusible tracers (H_2O^{15} PET) valid at the voxel scale.

Methods: Based on the Krogh cylinder geometry, we use the volume averaging method [3] to obtain the coefficients describing the blood/tissue exchange at the voxel scale, accounting for axial diffusion. In other words, the purpose is to replace, in the usual compartmental model, the tissue compartment (which also includes microciculation) by a fictitious homogeneous compartment (Fig. 1.A). The validity of this approach is tested by comparisons with complete solutions of the transport equations at capillary scale using numerical simulations.

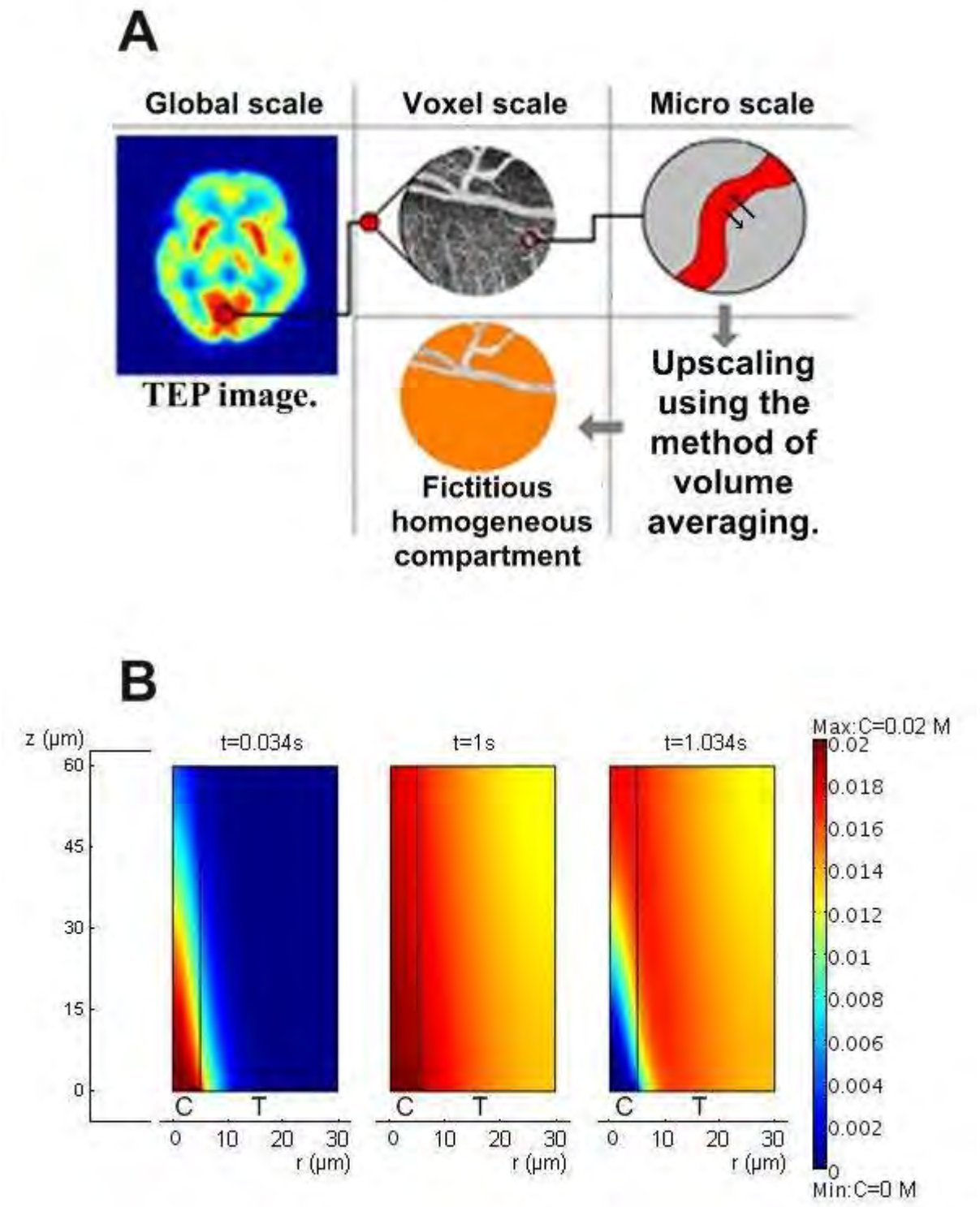

[Figure 1]

Results: Fig. 1.B displays the concentration field of H_2O^{15} in a 10µm diameter capillary and its

surrounding tissue at the beginning and end of injection, and 0.034s after the end of injection (clearance) for a Gaussian bolus of H_2O^{15} injected at the capillary inlet. The results highlight the presence of non-negligible longitudinal gradients. When averaged over a cross section, the longitudinal evolution of these concentration fields are correctly described by the volume averaged model.

Conclusions: The blood/tissue transfers at the voxel scale are properly described by this model. Its relevance for PET in comparison with the classical approach will be discussed.

Acknowledgments: This work is supported by the Skin Research Centre of Pierre Fabre Dermocosmetique and by a doctoral fellowship from "Region Midi Pyrénées".

References:

[1] Morris et al., in Emission Tomography: The Fundamentals of PET and SPECT. Ch. 23, Academic Press, 2004.

[2] Lawrence et al. J. Cereb. Blood Flow Metab. 18, 1378-1385, 1998; Munk et al. J. Nucl. Med., 44, 1862-1870, 2003.

[3] Quintard and Whitaker, in Handbook of Heat Transfer in Porous Media. Ch. 1, Marcel Decker Inc, 2000.

892

BrainPET Poster Session: Molecular Brain Imaging: Clinical Applications

COMPARISON OF 3T PROTON SPECTROSCOPY WITH F-18 FDG PET IN ASSOCIATION WITH GENETIC BIOMARKERS FOR ASSESSMENT OF BRAIN TUMOR RECURRENCE

F. Imani[1], F. Boada[1], F. Lieberman[2], D. Davis[1], E. Deeb[1], R. Hamilton[3], B. Bencherif[1], J. Mountz[1]

[1]Radiology, [2]Neuro-Oncology, [3]Pathology, University of Pittsburgh Medical Center, Pittsburgh, PA, USA

Objectives: With the advancements in discovery of genetic biomarkers, targeted chemotherapy and stereotactic radiation, it is critical that an accurate noninvasive assessment of tumor grade and viability be made. We evaluated 12 patients with new symptoms, suggestive of recurrence.

Methods: Magnetic Resonance Spectroscopy Imaging (MRSI) was performed on the GE MAGNETOM Trio to provide 3D maps of Choline (Ch) over Creatine (Cr) presented on a rainbow scale. Patients also underwent FDG PET scan. Intensity of FDG uptake was rated 0 (no uptake), 1 (< white matter), 2 (=white matter), 3 (>white matter, < gray matter), 4 (=gray matter), 5 (>gray matter). FDG uptake was compared with tumor grading based on histology and genetic biomarkers (N=7), including the loss of heterozygosity (LOH) of 1p, 19q, 9p, 10q, 17p, Ki-67 index, mutation in p53, amplification of EGFR and GFAP.

Results: Three patients with high grade viable tumor recurrence showed grade 3 to 5 FDG uptake but only 2 had high Ch/Cr. In 6 patients with low grade viable tumors, FDG uptake was grade 1 to 3 and Ch/Cr was elevated in all. Two of 3 patients in the low grade group with FDG uptake grade 3 showed LOH in 1p, 19q, 9p, or 10q; the third patient had high Ki-67 suggestive of high grade transformation. Three patients with necrosis showed no FDG uptake, but Ch/Cr was elevated in 1. Spearman's analysis demonstrated strong correlation between FDG uptake and tumor grading (r=0.91).

Conclusion: 3D co-registered MRSI maps provide complementary information to FDG PET for assessment of tumor recurrence particularly in low grade tumors. Genetic biomarkers suggestive of high grade transformation were associated with higher FDG uptake.

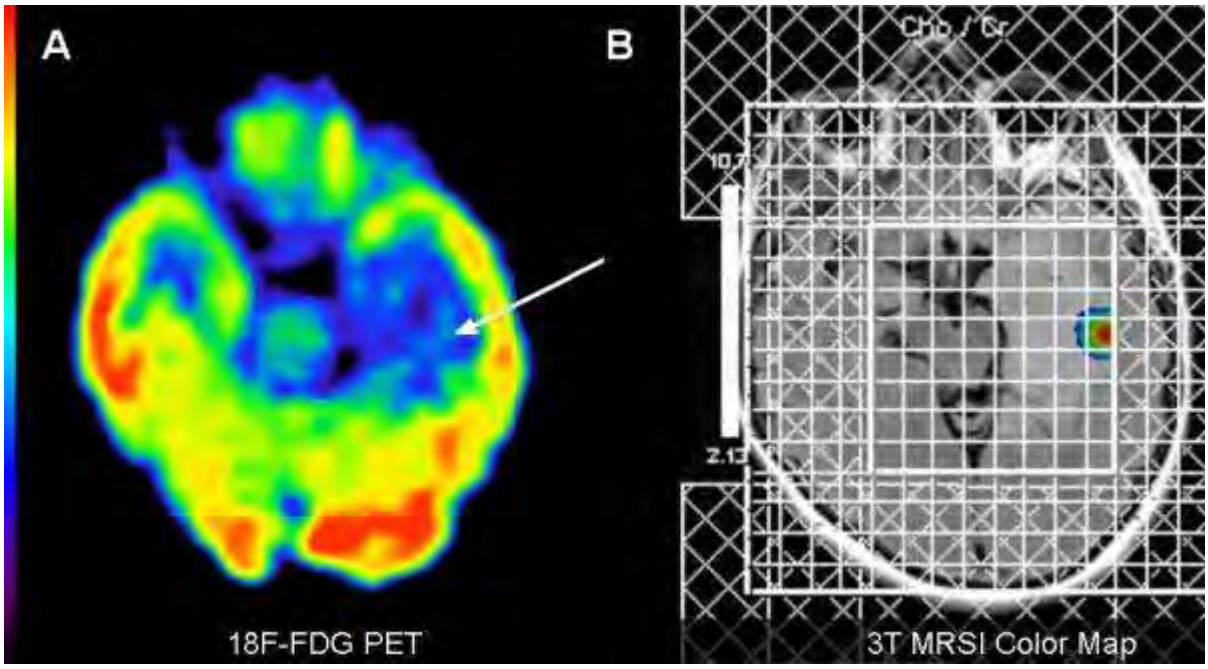

[Figure 1.]

Oligodendroglioma, WHO grade 2 (case 8). A. FDG PET scan shows a focus of increased tracer activity (grade 3) in the left temporal lobe. B. Map of Choline/Creatine demonstrates one focus of signal intensity in the left temporal lobe.

MRSI signal intensity is presented on a rainbow color scale where blue-green is normal background and bright red corresponds to greatly elevated signal intensity.

MRSI	PET Grade	Viability	Histology	LOH	Ki-67	p53	EGFR	GFAP	MGMT methylation
Positive	0	Necrosis	ANAPLASTIC OLIGODEN-DROGLIOMA	Nega-tive	10%	Posi-tive	Nega-tive	Nega-tive	
Negative	0	Necrosis	ANAPLASTIC ASTROCYTOMA, WHO GRADE 3	Nega-tive	12%	Nega-tive	Nega-tive	Posi-tive	

Negative	5	Tumor	ANAPLASTIC ASTROCYTOMA, WHO GRADE 3						
Positive	4	Tumor	INFILTRATING MALIGNANT ASTROCYTOMA	1p, 10q, 17p		Nega-tive	Posi-tive	Posi-tive	Nega-tive
Positive	3	Tumor	ANAPLASTIC ASTROCYTOMA, WHO GRADE 3						
Positive	3	Tumor	ASTROCYTOMA, WHO GRADE 2	1p, 10q		Nega-tive	Posi-tive	Posi-tive	
Positive	1	Tumor	OLIGODEN-DROGLIOMA, WHO GRADE 2	Nega-tive	< 5%	Posi-tive	Nega-tive	Posi-tive	
Positive	3	Tumor	OLIGODEN-DROGLIOMA, WHO GRADE 2	Nega-tive	14%	Nega-tive	Nega-tive	Posi-tive	Nega-tive
Positive	3	Tumor	OLIGODEN-DROGLIOMA, WHO GRADE 2	1p, 19q, 9p	6%	Nega-tive	Nega-tive	Posi-tive	Posi-tive

[Table 1]

Results of 3T MRSI, FDG PET, histology and genetic biomarkers for 9 cases.

893

Brain Poster Session: Neurologic Disease

BLOCKADE OF ADENOSINE A_{2A} RECEPTOR BY ANTAGONIST INCREASES $[CA^{2+}]_I$ IN HEK CELLS: POSSIBLE RELEVANCE TO NEUROPROTECTIVE INTERVENTIONS IN PARKINSON'S DISEASE

P.M. Luthra, S.K. Barodia

Dr. B.R. Ambedkar Center for Biomedical Research, University of Delhi, Delhi, India

Objective: A_{2a} receptor antagonists showed neuroprotective effects in models of diseases, such as brain ischemia (1), and MPTP-induced neuronal damage (2). Hence, adenosine A_{2a} receptor antagonists may possess neuroprotective effects in neurodegenerative diseases such as Parkinson's Disease, although the mechanisms responsible for such effects are primarily unknown (3). In the nervous system, Ca^{2+} acts as an important second messenger in regulating neurotransmitter release, synaptic activity, and even neuronal survival (4). It has been reported that large elevations in $[Ca^{2+}]_i$ do not always correlate with neurotoxicity but may instead have neuroprotective signaling effects (5). In the present work modulation of $[Ca^{2+}]_i$ concentration was studied in the presence of A_{2a} receptor antagonist SCH 58261 and agonist NECA using stably transfected HEK 293 cells with human A_{2a} receptor.

Methods: HEK 293 cells were stably transfected with pcDNA3.1 (+) containing human A_{2a} receptor cDNA using $CaPO_4$ method. Western blot analysis (using anti-HA mouse antibody) indicated the presence of moderate levels of A_{2a} receptor proteins in stably transfected HEK 293 cells. Modulation of free cytosolic Ca^{2+} concentration in human embryonic kidney (HEK 293) cell line was studied with A_{2a} receptor antagonist SCH 58261 and agonist NECA using the fluorescent Ca^{2+} indicator fura-2AM.

Results: Activation of adenosine A_{2a} receptor in transfected HEK 293 cell line with A_{2a} receptor antagonist SCH 58261 leads to 20% increase in intracellular Ca^{2+} i.e. $[Ca^{2+}]_i$ level. The present study on the human A_{2a} receptor transfected HEK 293 cells activation lead to inhibition of cAMP-dependent protein kinase A (PKA) activity.

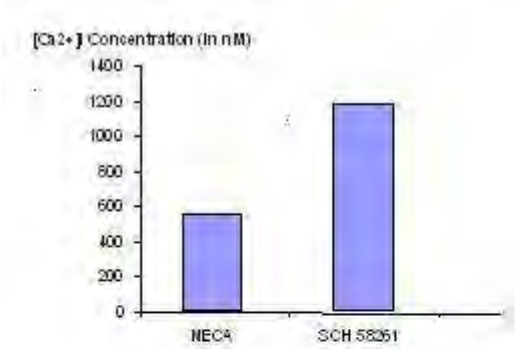

[Increase in [Ca2+]i by A2a receptor antagonist]

Conclusion: The studies illustrate that the elevation of intracellular Ca^{2+} i.e. $[Ca^{2+}]_i$ level by A_{2a} receptor antagonists inhibited the cAMP-dependent PKA activity. A_{2a} receptor antagonists induced enhancement of $[Ca^{2+}]_i$ may be related to striatal neuroprotection.

References:

1. Monopoli A, Lozza G, Forlani A, Mattavelli A, Ongini E (1998b) Blockade of adenosine A2A receptors results in neuroprotective effects in cerebral ischaemia in rats. NeuroReport 9:3955-3959.

2. Chen JF, Xu K, Petzer JP, Staal R, Xu YH, Belstein M, Sonsalla PK, Castagnoli K, Castagnoli Jr N, Schwarzschild MA (2001) Neuroprotection by caffeine and A2A adenosine receptor inactivation in a model of Parkinson's disease. J Neurosci 21:RC143(1-6).

3. Impagnatiello F, Bastia E, Ongini E, Monopoli A (2000) Adenosine receptors in neurological disorders. Emerg Ther Targets 4:635-664.

4. Fang Ba, Peter K.T. Pang, Christina G. Benishin (2004) The role of Ca2+ channel modulation in the neuroprotective actions of estrogen in _-amyloid protein and 1-methyl-4- phenyl-1,2,3,6-tetrahydropyridine (MPTP) cytotoxic models. Neurochemistry International 45, 31-38.

5. Friedman LK (2006) Calcium: A role for neuroprotection and sustained adaptation. Molecular Interventions 6, 315-329.

LOSARTAN ALLEVIATES GLOBAL CEREBRAL ISCHEMIA INDUCED MEMORY DYSFUNCTION ASSOCIATED WITH APOPTOSIS IN MOUSE

K.F. Ahamed[1], M. Reddy Chaparapu[1], R. Srinivas[1], V. Ravichandiran[1], P.T.-H. Wong[2]

[1]Department of Pharmacology, Vels University, Chennai, India, [2]Department of Pharmacology, Young Loo Lin School of Medicine, National University of Singapore, Singapore, Singapore

Objective: A mouse model Global cerebral ischemia (GCI) mimics the vascular dementia, through cholinergic dysfunction, neuronal apoptosis and memory impairment. Previous studies on losartan indicated that reduced GCI -induced delayed neuron death. However the effect of Losartan on GCI induced vascular dementia has not yet established. In this study, treatment of losartan (10 mg/kg) after ischemia for 45 days, we evaluated the long-term influence of losartan on behavior and biochemical changes.

Methods: Global cerebral ischemia (GCI) was induced by bilateral common carotid artery occlusion (BCCAo) for 30 min followed by reperfusion for 45 days. Learning and memory was assessed in step through passive avoidance task. Western blot analysis was carried out to express the apoptotic markers in brain.

Results: Step-through passive avoidance tests suggested that ischemic mice showed decreases in step-through latency throughout the entire learning trial and memory session, which suggested learning and memory impairment. Additionally, Acetyl cholinesterase (AChE) activity also increased in the frontal cortex and hippocampus of ischemic mice compared with sham control. However, losartan significantly alleviated GCI induced antrograde memory deficits and increased AChE activity in the frontal cortex and hippocampus of ischemic mice. Expression of apoptotic markers were present in the neurons of the ischemic mice, losartan reduced the expression apoptotic markers in ischemic mouse brain.

Conclusion: Our results indicate that neuroprotection by losartan is partly related to modulation of apoptosis and protection of the cholinergic neurons. Early rational losartan interventions may be one of the most promising therapeutic approach for cerebrovascular and neurodegenerative diseases.

TH1-TYPE MODULATION OF THE PERIPHERAL IMMUNE RESPONSE EXACERBATES ISCHEMIC BRAIN DAMAGE

A. Denes, N. Rothwell, R. Grencis, N. Humphreys

Faculty of Life Sciences, University of Manchester, Manchester, UK

Objectives: Peripheral infection and inflammation have been associated with pathological processes in the CNS including autoimmune, neurodegenerative disorders and cerebral ischemia. To date, the exact mechanisms by which the peripheral immune response can modify central inflammatory conditions and damage formation in stroke have not been revealed. Our aim was to investigate the effect of the Th1- and Th2-polarized peripheral immune responses on focal cerebral ischemia in mouse. To achieve this, we used a well-established model of parasitic infection of the gut. This model enables us to modulate the nature of the immune response, making it possible to evaluate the effects of Th1 and Th2 type immune responses on the ischemic brain damage in the same model system.

Methods: Male C57BL/6 mice were infected orally with a high or low dose of Trichuris muris eggs, to induce Th2- or Th1-polarized peripheral immune responses, respectively. Post-infection intervals were selected on the basis of previous experiments to obtain the peak of Th2- and Th1-type responses. Infected mice and age/weight matched controls were subjected to 45 minutes of middle cerebral artery occlusion (MCAo) or sham surgery. 24 and 48 hours after reperfusion, blood was taken and brains were perfusion-fixed or homogenized. Unfixed spleen, bone marrow, liver samples and mesenteric lymph nodes were collected. Ischemic and blood brain barrier damage as well as the number of apoptotic neurons in the brain were determined.

Results: Simultaneous measurement of 16 different cytokines by cytometric bead array in the periphery, analysis of bone marrow cells by flow cytometry and evaluation of anti-parasite IgG levels by ELISA confirmed appropriate Th1- and Th2-type response in infected mice. The Th1-type response significantly exacerbated ischemic- and BBB damage as well as neuronal death compared to control mice. Proinflammatory cytokine levels were elevated in the lymph nodes compared to control- and Th2-type mice. Anti-parasite IgG1 levels showed a negative correlation with the ischemic damage in mice with Th1-type response. IL-6, KC, MCP-1, G-CSF and RANTES in brain homogenates of Th1-shifted mice showed sustained elevation after MCAo compared to controls. RANTES levels were significantly higher in plasma, liver and blood cells of sham Th1-polarized mice compared to control sham animals. Ischemic brain damage was not augmented in mice with Th2-polarized response compared to controls, but showed positive correlation with the peripheral levels of proinflammatory cytokines and anti-parasite IgG2a antibodies.

Conclusions: Our results show that a peripheral Th1-type immune response can significantly exacerbate ischemic brain damage in mice. Analysis of multiple cytokines in plasma and several peripheral organs indicate augmented inflammation in these mice after MCAo and identifies RANTES as the most likely candidate to mediate peripheral Th1-type response induced changes to the brain.

899

Brain Oral Session: Experimental Cerebral Ischemia: Neuroinflammation

VASCULAR ADHESION PROTEIN-1 (VAP-1) INHIBITION PROVIDES NEUROPROTECTION IN RATS FOLLOWING REVERSIBLE MIDDLE CEREBRAL ARTERY OCCLUSION AND 14 DAYS REPERFUSION

L.Z. Mao, H.L. Xu, F. Vetri, D.A. Pelligrino

Neuroanesthesia Research Laboratory, University of Illinois at Chicago, Chicago, IL, USA

Introduction: VAP-1, also called semicarbazide-sensitive amine oxidase (SSAO), is reported to play an important role in adhesion and, especially, endothelial transmigration of multiple leukocyte subsets (i.e., neutrophils, monocytes, lymphocytes). Our laboratory previously reported that treatment with a novel and selective VAP-1/SSAO blocker, LJP-1207, at 6h reperfusion following transient forebrain ischemia (TFI), prevented neutrophil infiltration into the brain, and provided significant neuroprotection (1). A similar level of neuroprotection was seen in TFI rats rendered neutropenic (anti-PMNL antibody treatment). In preliminary experiments (2), we found little or no neuroprotection associated with neutropenia in rats exposed to 1h right middle cerebral artery occlusion (MCAo) and 72h reperfusion; yet LJP-1207 treatment was neuroprotective, even when introduced 6-12h post-MCAo. This suggested that the long therapeutic window associated with pharmacologic blockade of VAP-1/SSAO arises from actions toward non-PMNL leukocytes, at least over short (several days) post-ischemic recovery periods. In the present study, we evaluated whether neuroprotection could be extended over longer (2 weeks) post-MCAo recovery.

Methods: We compared control rats and rats treated with the highly-selective, non-hydrazine VAP-1/SSAO blocker, LJP-1586. Neurobehavioral function and histopathology were evaluated in male Sprague-Dawley rats, subjected to 1h of MCAo (suture model) followed by 14d of reperfusion. Administration of LJP-1586 (10 mg/kg, iv) was initiated at 6h of reperfusion, followed by repeated doses every 24h, until sacrifice. Neurobehavioral tests included beam walking speed, which assesses deficits in coordination and integration of motor movement, especially in the hindlimb; and adhesive-removal, which evaluates forelimb somatosensory asymmetries. For histopathology, 30 μm frozen coronal sections were stained with hematoxylin & eosin (H&E), and the infarct area was calculated (with corrections for ischemic vs non-ischemic hemisphere areas).

Results: Treatment with the VAP-1/SSAO inhibitor was associated with smaller infarcts, at 14 days, compared to controls. Representative brain sections (bregma ~-1.0 mm) are shown in the figure (infarct areas were 19.9 and 8.2 mm^2 in controls and LJP-treated rats, respectively). Both neurobehavioral function tests indicated a better outcome, at 14 days, in the VAP-1/SSAO-inhibited animals (see figure).

Conclusions: In conclusion, VAP-1/SSAO inhibitors are promising neuroprotective compounds with a wide therapeutic window and substantial translational potential.

References:

(1) J Pharmacol Exp Ther. 317:19-29, 2006.

(2) Program No. 512.5, Society for Neuroscience, 2008.

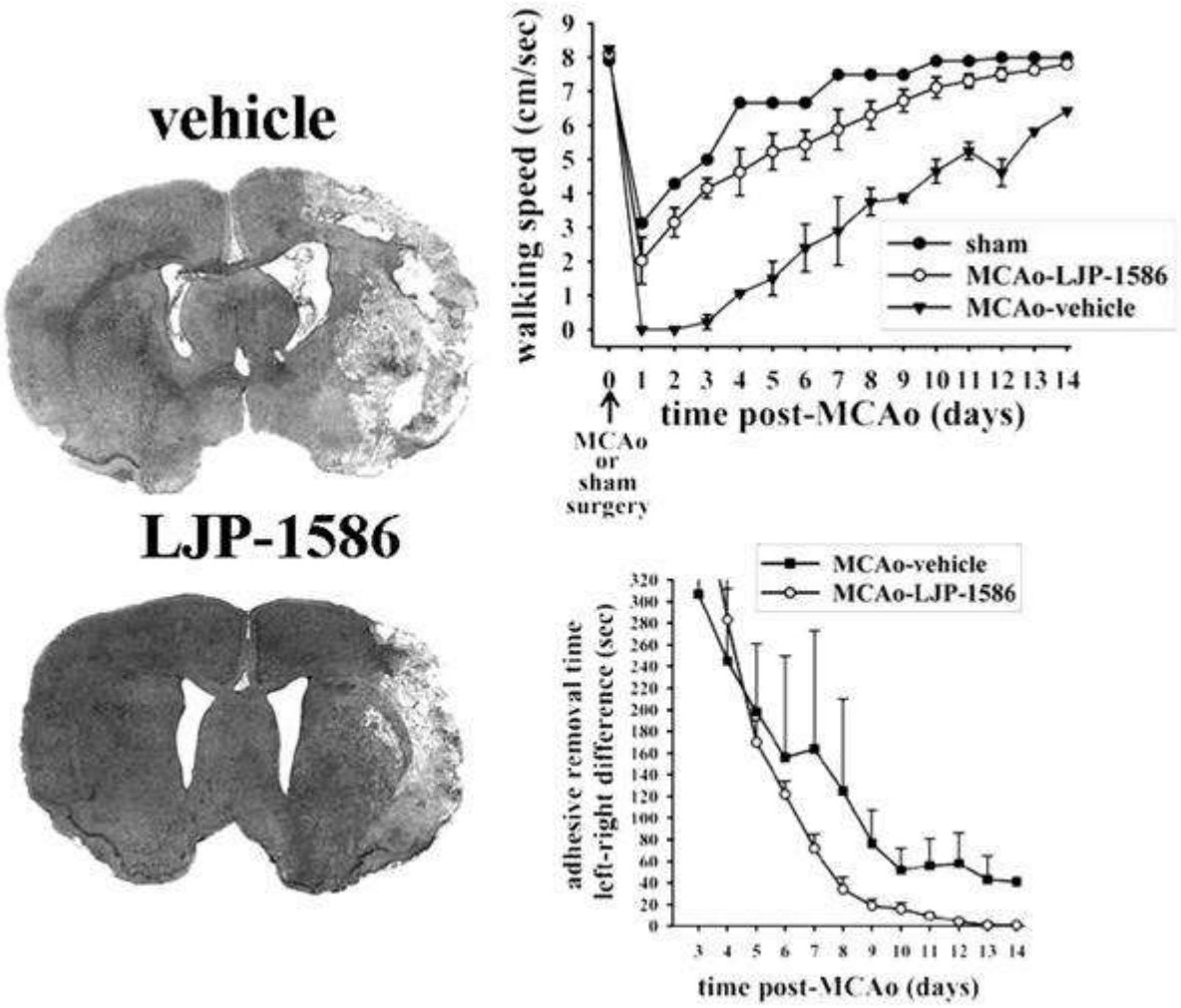
vehicle
LJP-1586
walking speed (cm/sec)
0 1 2 3 4 5 6 7 8 9
sham
MCAo-LJP-1586
MCAo-vehicle
0 1 2 3 4 5 6 7 8 9 10 11 12 13 14
time post-MCAo (days)
MCAo or sham surgery
MCAo-vehicle
MCAo-LJP-1586
adhesive removal time left-right difference (sec)
0 20 40 60 80 100 120 140 160 180 200 220 240 260 280 300 320
3 4 5 6 7 8 9 10 11 12 13 14
time post-MCAo (days)

[Figure]

900

Brain Poster Session: Blood-Brain Barrier

MR CHARACTERIZATION OF SMART CONTRAST AGENTS: TOXICITY, STABILITY, AND PERMEABILITY

D. Coman[1,2], M. Gattas-Sethi[3,4], H.K.F. Trubel[5,6], P. Herman[1,2,7], **F. Hyder**[1,2,3], G. Kiefer[8], F. d'Errico[3,4]

[1]Diagnostic Radiology, [2]Quantitative Neuroscience with Magnetic Resonance (QNMR), [3]Biomedical Engineering, [4]Therapeutic Radiology, Yale University, New Haven, CT, USA, [5]Department of Pediatrics, University Witten/Herdecke, HELIOS-Klinikum Wuppertal, [6]Bayer HealthCare Research Center, Wuppertal, Germany, [7]Semmelweis University, Budapest, Hungary, [8]Macrocyclics, Dallas, TX, USA

Introduction: The measurement of ex vivo kinetic inertness, in vivo blood-brain barrier permeability and in vivo cytotoxicity are three important steps in assessing the feasibility of using any smart contrast agent (SCA) for any ulterior biological studies. Over the past decade, a new non-invasive method for simultaneous measurements of temperature and pH was developed, based on the strong dependence on temperature and pH of the proton chemical shifts from the complex between the thulium ion and the macrocyclic chelate 1,4,7,10-tetraazacyclododecane-N,N',N'',N'''-tetra (methylene phosphonate) or $TmDOTP^{5-}$ [1,2,4]. More recently, another temperature probe was introduced, for which the macrocyclic chelate is 1,4,7,10-tetraazacyclododecane-1,4,7,10-tetramethyl-1,4,7,10-tetraacetate or $TmDOTMA^{-}$ [3]. In the present work, we measured ex vivo kinetic inertness, in vivo blood-brain barrier permeability and in vivo cytotoxicity of $TmDOTP^{5-}$ and $TmDOTMA^{-}$ agents.

Methods: Animal studies: Sprague-Dawley rats were tracheotomized and artificially ventilated (70% N_2O, 30% O_2). During the animal preparation, isoflurane (1 to 2 %) was used for induction. The anesthetized rats were prepared with renal ligation as previously described [4]. CBF was measured by a laser Doppler flowmetry probe and pO_2 was measured by an oxygen fluorescence probe. **Cytotoxicity:** The colony-forming ability of the CCL16 Chinese hamster lung cells in the cultures exposed to the SCAs was compared with that of cells from untreated cultures to calculate the relative surviving fraction.

Results: Kinetic stabilities of the SCAs in blood extracts from the sagittal sinus were estimated by the intensity of their ^1H NMR resonances over time. For both $TmDOTP^{5-}$ and $TmDOTMA^{-}$, the results indicate that there is no change in the intensity of the methyl group resonance from day 1 to day 59. Our observations suggest that $TmDOTP^{5-}$ does cross the blood-brain barrier quite efficiently, which allows quantifying brain temperature and pH [4]. Concomitant ^1H signals of $TmDOTP^{5-}$ in blood plasma and cerebral spinal fluid (CSF) confirm that the majority of the in vivo MR signals emanate from tissue [4]. A plausible delivery path into the extracellular space may be through the fenestrated vessels of the circumventricular organs. The in vivo cytotoxicity tests consistently showed survival rates between 90 and 95%. Our electrophysiological measurements suggest that an infusion dose of 1-2 mmol/kg results in stable systemic physiology without affecting normal brain function. Localized changes in CBF and pO_2 during forepaw stimulation in α-chloralose anesthetized rats are nearly identical before and after SCAs infusion.

Conclusion: Our results indicate that these two SCAs are kinetically stable, they cross the blood-brain barrier, they clearly exclude acute toxicity on Chinese hamster lung cells and they demonstrate that the brain's activity is unaffected by their presence in the extracellular space.

References:

[1] Zuo CS et al., Magn Reson Med 36: 955-999, 1996.

[2] Trubel HK et al., J Appl Physiol 94: 1641-1649, 2003.

[3] Pakin SK et al., NMR Biomed. 19(1): 116-124, 2006.

[4] Coman D et al., NMR in Biomed., in press.

Acknowledgements: Supported in part by a pilot grant from P30 NS052519 of the QNMR Program.

901

Brain Poster Session: Traumatic Brain Injury

LOCALIZED TEMPERATURE DYNAMICS DURING PHARYNGEAL SELECTIVE BRAIN COOLING

D. Coman[1,2], H.K.F. Trubel[3,4], P. Herman[1,2,5], **F. Hyder**[1,2,6]

[1]Diagnostic Radiology, [2]Quantitative Neuroscience with Magnetic Resonance (QNMR), Yale University, New Haven, CT, USA, [3]Department of Pediatrics, University Witten/Herdecke, HELIOS-Klinikum Wuppertal, [4]Bayer HealthCare Research Center, Wuppertal, Germany, [5]Semmelweis University, Budapest, Hungary, [6]Biomedical Engineering, Yale University, New Haven, CT, USA

Introduction: Recently, we described a new approach to obtain pharyngeal selective brain cooling (pSBC) [1, 2]. In this method a cooling coil is inserted into the pharynx in order to cool the brain selectively. Temperature distributions in rat brain can be obtained within minutes by using a new temperature-sensitive probe which is based on the complex between thulium ion (Tm^{3+}) and the macrocyclic chelate 1,4,7,10-tetraazacyclododecane-1,4,7,10- tetramethyl-1,4,7,10-tetraacetate or $DOTMA^{4-}$ [3]. In the present study we use $TmDOTMA^{-}$ agent to measure time-dependent temperature distributions and we calculate the corresponding cooling rate constants in rat brain.

Materials and methods: Animal preparation: Sprague-Dawley rats (220-315 g) were tracheotomized and artificially ventilated (70% N_2O, 30% O_2). During the animal preparation, isoflurane (1 to 2%) was used for induction. The anesthetized rats were prepared with renal ligation as previously described [4]. pSBC was achieved by running ice-cold water for 2 hours through the cooling coil inserted into the pharynx. **In vivo (n=4):** A gaussian pulse of 200 ms was used for excitation of a 6 mm slice with FOV of 2.56 cm x 2.56 cm. The following parameters were used: 16x16 encode steps, TR=11 ms, 100 averages and 4 min 40s acquisition time. The temperature maps were calculated from the chemical shifts of $TmDOTMA^{-}$ methyl group according to the equation: $\mathbf{T=346+4.6\cdot\delta_{CH3}+0.0152\cdot\delta_{CH3}^2}$. For each animal, the cooling and the recovering rate constants were calculated by fitting the temperature variation over time to a single exponential.

Results: The results for all the animals investigated indicate that there is a negative correlation (R=0.88) between the average cooling rate constants (k_c) and the average recovering rate constants (k_r) in each animal. This correlation is probably mediated by the local net heat contribution, which includes metabolic heat production, heat due to changes in cerebral blood flow or conductive heat exchange with the neighboring regions [5]. The temperature maps show a relatively homogeneous temperature distribution across the entire cortical region, with standard deviations of less than 0.4°C. The distribution of the cooling rate constants is also relatively homogeneous within the same animal, although somewhat larger variations are observed between different animals**.** In each animal, the recovering rate constants show a distribution which is slightly more dispersed than that of the cooling rate constants. However, the range of the recovering rate constants for different animals investigated is relatively small (1 to 1.5 h^{-1}), compared with a relatively larger range for the cooling rate constants (0.3 to 1.43 h^{-1}).

Conclusion: Our results indicate that the pSBC rate constants are tightly dependent on the local net heat contribution, measured indirectly by the recovering rate constants.

References:

[1] Trübel H et al., Biomed Tech 48: 298-300, 2003.

[2] Trübel H et al., Intensive Care Med 30: 1829-1833, 2004.

[3] Pakin SK et al., NMR Biomed. 19(1): 116-124, 2006.

[4] Coman D et al., NMR in Biomed., in press.

[5] Trübel H et al., J. Cereb. Blood Flow Metab. 26: 68-78, 2006.

Acknowledgements: Supported in part by P30 NS052519 of the QNMR Program.

902

Brain Poster Session: Traumatic Brain Injury

MDMA-INDUCED TEMPERATURE CHANGES AND DYNAMICS IN RAT BRAIN

D. Coman[1,2], L. Jiang[1], **F. Hyder**[1,2,3], K. Behar[4]

[1]Diagnostic Radiology, [2]Quantitative Neuroscience with Magnetic Resonance (QNMR), [3]Biomedical Engineering, [4]Department of Psychiatry, Yale University, New Haven, CT, USA

Objectives: 3,4-Methylenedioxymethamphetamine (MDMA, ecstasy) is a heavily abused psychostimulant which has seen explosive growth in its use during the last decade [1]. The most severe and potentially fatal acute effects of MDMA involve extreme hyperthermia and its consequences on multiple organ systems, e.g., rhabdomyolysis, coagulopathy, kidney, heart, and liver failure [2, 3]. The magnitude, distribution, and dynamics of MDMA induced temperature changes are thus of critical importance in neurotoxicity, where core body temperature is most frequently reported. Recently, we showed that temperature distributions in rat brain can be obtained within minutes by using a new temperature-sensitive probe which is based on the complex between the thulium ion (Tm^{3+}) and the macrocyclic chelate 1,4,7,10-tetraazacyclododecane-1,4,7,10-tetramethyl-1,4,7,10-tetraacetate or $DOTMA^{4-}$ [4]. In the present study we use the $TmDOTMA^{-}$ agent to measure time-dependent temperature distributions and from these we calculate the maps of temperature changes and those of MDMA-induced warming rate constants in rat brain.

Methods: Animal preparation: Sprague-Dawley rats (250-300 g) were tracheotomized and artificially ventilated (30% O_2). The animals were anesthetized with an intraperitonial injection of urethane (1.3 g/Kg). The anesthetized rats were prepared with renal ligation as previously described [4]. $TmDOTMA^{-}$ was continuously infused for ~2 hours, followed by the MDMA injection. **In vivo (n=3):** A gaussian pulse of 200 ms was used for excitation of a 6 mm slice with FOV of 2.56 cm x 2.56 cm. The following parameters were used: 16x16 encode steps, TR=11 ms, 100 averages and 4 min 40s acquisition time. The temperature maps were calculated from the chemical shifts of $TmDOTMA^{-}$ methyl group according to the equation: $\mathbf{T=346+4.6\cdot\delta_{CH3}+0.0152\cdot\delta_{CH3}^{2}}$**.** For each animal, the MDMA-induced warming rate constants were calculated by fitting the temperature variation over time to a single exponential function**.**

Results: The results indicate a relatively homogenous distribution of warming rate constants, with subcortical regions showing slightly faster temperature increase than the cortical regions. The average rate constant of MDMA-induced temperature change was 1.05 ± 0.13 h^{-1}, while the average temperature change was 2.1 ± 0.3°C. Although the distributions of both warming rate constants and temperature changes are relatively homogenous within the same animal, somewhat larger variations are observed when comparing different animals**.** The average warming rate constant was 1.4 ± 0.4 h^{-1}, while the average temperature change was +1.7 ± 0.4°C. On average, the brain temperature increased from 35.5 ± 0.2°C to 37.2 ± 0.5°C, while the core temperature increased from 37.4 ± 0.4°C to 39.8 ± 0.4°C.

Conclusion: The current results indicate that the temperature increase in the rat brain after a dose of 20 mg/kg MDMA is relatively homogenous, with subcortical regions showing slightly faster temperature increase than the cortical regions.

References:

[1] http://www.drugabuse.gov/PDF/RRmdma.pdf, (2006).

[2] Hall AP and Henry JA. Br J Anaesth., 96(6):678-685, (2006).

[3] Green AR et al., Pharmacol Rev., 55(3):463-508, (2003).

[4] Coman D and Hyder F, Proc. Intl. Soc. Mag. Reson. Med. 16: 273, (2008).

Acknowledgenments: Supported in part by a pilot grant from P30 NS052519 of the QNMR Program.

903

Brain Poster Session: Cerebral Vascular Regulation

ROLE OF SYMPATHETIC NERVOUS SYSTEM IN CEREBRAL AUTOREGULATION AND ACTIVATION-INDUCED PERFUSION

J. Gierthmühlen, A. Allardt, M. Sawade, G. Wasner, R. Baron

Department of Neurology, University of Kiel, Kiel, Germany

Objective: The role of the sympathetic nervous system (SNS) in regulation of cerebral perfusion is still discussed controversely. The aims of this study were to investigate the functional role of the sympathetic innervation (1) on cerebral autoregulation (CA) under induced decrease of perfusion pressure and (2) on activity-induced changes of cerebral perfusion and (3) to investigate possible differences in functional cerebral blood flow regulation between the anterior and posterior circulation.

Methods: Cerebral blood flow velocity (CBFV) in the medial (MCA) and posterior cerebral artery (PCA) using transcranial dopplersonography (TCD) during induced decrease of perfusion pressure and cortical activation of MCA or PCA territories was investigated in 27 healthy controls and 17 patients with Wallenberg´s syndrome.

Results: Cardio- and cerebrovascular regulation was similar in patients and controls under induced decrease of perfusion pressure. However, patients with a central sympathetic deficit had a prolonged decrease of resistance in the MCA and showed a slower and less pronounced decrease of resistance in the PCA upon cortical activation. No difference was observed between the side with and without sympathetic deficit.

Conclusions: We suggest that (1) the SNS does not have an influence on CA after decrease of perfusion pressure under normotonous conditions, but (2) sympathetic efferents seem to be involved in economisation of activity-induced changes of cerebral perfusion and (3) activation-induced sympathetic regulation of blood flow differs in the anterior and posterior circulation in humans.

904

Brain Oral Session: Cerebrovascular Regulation

REGULATION OF VASCULAR TONE IN THE CEREBRAL CIRCULATION IS MARKEDLY IMPAIRED FOLLOWING CELL-SPECIFIC INTERFERENCE WITH PPARγ FUNCTION

M. Modrick, S. Chrissobolis, C. Halabi, C. Sigmund, **F. Faraci**

University of Iowa, Iowa City, IA, USA

Objective: in vascular muscle would alter regulation of vasomotor tone in the cerebral circulation.Peroxisome proliferator-activated receptor-gamma (PPARγ) is a nuclear receptor that may play an important protective role in the vasculature. We examined the hypothesis that selective interference with PPARγ

Methods: We studied basilar arteries from mice expressing a dominant negative mutation in human PPARγ (P467L) under the control of the smooth muscle myosin heavy chain promoter (S-P467L). We examined responses in vitro to stimuli that produce vasodilation via nitric oxide and cGMP (acetylcholine, nitroprusside), cAMP (forskolin), and potassium channels [cromakalim and potassium ion (K+)]. Because products of arachidonic acid metabolism may be endogenous activators of PPARγ, we also examined effects of arachidonic acid on vascular tone.

Results: In non-transgenic controls, all agonists produced dilation of the basilar artery. In S-P467L mice, responses to acetylcholine, nitroprusside, forskolin, and activators of K+ channels were reduced by 40-70% compared to controls ($P< 0.01$). For example, vasodilation to K+ (10 mM) was 67±6 and 22±4% in control (n=9) and S-P467L (n=6) mice, respectively ($P< 0.01$). Arachidonic acid (1 μM) dilated arteries from non-transgenic and S-P467L mice by 63±3 and 20±3%, respectively ($P< 0.01$). Arteries from both groups responded similarly to the calcium channel agonist Bay K8644 and the calcium channel antagonist nifedipine and dilated fully to papaverine.

Conclusions: These data provide the first evidence that cell-specific interference with the function of PPARγ in vascular muscle produces marked, but selective, impairment of diverse vasodilator pathways. Thus, normal PPARγ function in vascular muscle plays an essential role in regulation of cerebral vascular tone.

905

Brain Poster Session: Cerebral Vascular Regulation

CHARACTERIZATION OF CORTICAL BLOOD FLOW (COBF) RESPONSES WITH LASER DOPPLER FLOWMETRY IN ZUCKER OBESE AND ZUCKER LEAN RATS

A. Institoris[1,2], L. Lenti[2], T. Gaspar[1], F. Domoki[2], F. Bari[2], D.W. Busija[1]

[1]Department of Physiology and Pharmacology, Wake Forest University Health Sciences, Winston-Salem, NC, USA, [2]Department of Physiology, University of Szeged, Szeged, Hungary

Introduction: Insulin resistance, a condition that often precedes development of type II diabetes, has been shown to cause dysfunction of isolated cerebral arteries or of exposed arterial segments on the brain surface of rats (Busija et al., 2004; Erdos et al., 2004). However, cortical blood flow (CoBF) responses, which would characterize the dynamics of the entire cerebral vasculature, have not been examined previously. The objective of the present study was to examine the effects of insulin resistance on CoBF to:

1. sensory nerve stimulation,
2. arterial hypercapnia,
3. localized bicuculline-induced cortical seizure, and
4. systemic hypotension.

Methods: 11-week-old Zucker Lean (ZL) (N=12) and Zucker Obese (ZO) (N=10-12) rats were anesthetized with pentobarbital (80 mg/kg intraperitoneally then 20 mg/kg/h intravenously), mechanically ventilated (end-tidal CO_2 pressure was kept at 40 mmHg), and blood pressure and temperature controlled (37°C). A closed cranial window filled with artificial cerebrospinal fluid was prepared above the parietal cortex. CoBF was measured with laser Doppler (LD) flowmetry within the closed cranial window and a silver-silver chloride electrode was used for electroencephalograph monitoring. Sensory nerve stimulation was achieved by the intranasal irrigation with 10^{-5}M, 10^{-6}M, and 10^{-7}M capsaicin for 10 min. Hypercapnia was induced by ventilating with 5% and 10% CO_2 for 5-5 min. Cortical seizure was evoked with the topical application of bicuculline (10^{-4}, 5x 10^{-4},and 10^{-3}M) for 10 min. Systemic hypotension was created with the withdrawal of venous blood to reach 40 mmHg mean arterial blood pressure for 10 min. The average change in LD signal was calculated for each minute.

Results: Capsaicin stimulation at a concentration of 10^{-5}M caused an increased CoBF for ZL of 7±2% (mean±S.E.M.) vs 3.1±2% for ZO animals (N= 12-12; P=0.31). CoBF responses to 5 and 10% CO_2 were 21±5% and 38±7% in ZO vs 20±6% and 53±9% in ZL rats, respectively (N= 10-10; $P_{5\%}$=0.74 and $P_{10\%}$=0.5). Bicuculline induced a dose-dependent elevation in CoBF for both ZL (30±10%, 66±11% and 95±12%) and ZO (36±15%, 68±18% and 88±19%) groups (N= 12-12; P=0.7). CoBF changes in response to arterial hypotension were -14±4% in ZL and 8±10% in ZO rats (N= 9-7; P=0.28).

Conclusions: While insulin resistance affects responses of isolated cerebral arterial segments to a number of vasoactive stimuli, the overall CoBF responses are largely intact. We speculate that in this early stage of insulin resistance, when arterial blood pressure and fasting blood glucose levels are not elevated beyond normal values, compensatory mechanisms are able to maintain CoBF responses. However, the nature and location along the cerebral vasculature of these beneficial adjustments during insulin resistance are not known.

References:

Busija DW, Miller AW, Katakam P, Simandle S, Erdös B. (2004) Mechanisms of vascular dysfunctionin insulin resistance. Curr Opin Investig Drugs. 5(9):929-35.

Erdös B, Snipes JA, Miller AW, Busija DW. (2004) Cerebrovascular dysfunction in Zucker obese rats is mediated by oxidative stress and protein kinase C. Diabetes. 53(5):1352-9.

906

Brain Poster Session: Neurovascular Unit in Health & Disease

BK_{CA} AND K_{IR} CHANNEL PHOSPHORYLATION CONTRIBUTES TO THE IMPAIRMENT OF NEUROVASCULAR COUPLING IN DIABETES MELLITUS

H.-L. Xu, F. Vetri, L.-Z. Mao, D.A. Pelligrino

Neuroanesthesia Research Laboratory, Department of Anesthesiology, University of Illinois-Chicago, Chicago, IL, USA

Introduction: Protein kinase (PKC) activation has been linked to diabetes mellitus-associated cerebral vasodilatory dysfunctions. However, its effect on cerebral neurovascular coupling in diabetes is virtually unexplored. The in vivo properties of large conductance Ca^{2+}-operated K^+ (BK_{Ca}) and inward rectifier K^+ (K_{ir}) channels that participate in the process of neurovascular coupling have been reported to be impaired in the diabetic cerebrovasculature (1). Since those channels have been reported to play a role in neurovascular coupling (2), the possibility exists of an aberrant neurovascular coupling in diabetes. In this study, we tested the hypothesis that diabetes mellitus leads to the impairment of neurovascular coupling, due to PKC activation.

Methods: The in vivo reactivity of pial arterioles was evaluated in age-matched rats (streptozotocin-induced diabetics [8 weeks] and non-diabetic controls) using a closed cranial window and intravital microscopy. Neurovascular coupling was assessed via the measurement of diameter changes in pial arterioles, localized to the hindlimb region of the somatosensory cortex, during sciatic nerve stimulation (SNS).

Results: Compared to non-diabetic controls, diabetic rats showed a significant attenuation in the pial arteriolar relaxation response to SNS, which was consistently accompanied by a substantially decreased responses to suffusion of the BK_{Ca} channel opener, NS1619, and the K_{ir} agonist, KCl. Topical applications of the PKC inhibitor, Calphostin C, which did not alter pial arteriolar reactivity in non-diabetic rats, largely restored these diabetes-impaired pial arteriolar responses, suggesting the involvement of PKC activation in BK_{Ca} and K_{ir} channel dysfunction and the disruption of neurovascular coupling during diabetes. These findings were further supported by the inhibitory effect of the acute PKC activation on all the aforementioned pial arteriolar responses in non-diabetic rats. That is, pial arteriolar responses to SNS, NS1619 and KCl were revealed to be markedly decreased by topical application of PKC agonist phorbol 12,13-dibutyrate (PdBu). The fact that PdBu suffusion did not affect the pial arteriolar responses to adenosine, SNAP, and hypercapnia ruled out the possibility of non-specific effects of PdBu application.

Conclusions: Collectively, these results suggest that PKC-mediated phosphorylation may be linked to diminished BK_{Ca} and K_{ir} channel function. One manifestation of this may be an impairment of neurovascular coupling during diabetes mellitus.

References:

(1) Microcirculation. 11:605-613, 2004.

(2) Nature Neurosci.9:1397-1403, 2006.

This work was supported by Juvenile Diabetes Research Foundation (JDRF 3-2008-462) to F.Vetri., NIH grant (HL 088259) to Dale.A.Pelligrino, and American Heart Association grant (AHA 0635337N) to H.L. Xu.

907

Brain Oral Session: Neonatal Ischemia

ALTERNATIVE SPLICING OF BCL-X REGULATES NEURAL CELL DEATH AFTER NEONATAL HYPOXIA-ISCHEMIA

J.-M. Lee, A. Ford, P. Yan, E. Gonzales, R. Perez, Q. Xiao

Neurology, Washington University School of Medicine, St. Louis, MO, USA

Objectives: Perinatal hypoxia-ischemia (H-I) is increasingly recognized as a common neurological disorder. What distinguishes perinatal H-I from adult stroke is the prominence of apoptosis as a form of cell death. Preliminary evidence suggests that pre-mRNA alternative splicing may play a role in the regulation of apoptosis. For example, the apoptotic regulatory gene, bcl-x, generates two mRNA isoforms with opposing actions: Bcl-xL (the longer form) is anti-apoptotic, while Bcl-xS (the short form) is pro-apoptotic. This study aimed to investigate the role of alternative splicing of Bcl-x in neural injury following neonatal H-I.

Methods: P7 Sprague Dawley rat pups were subjected to unilateral carotid ligation and hypoxia (8% O2 for 2.5 h). Bcl-x splicing was determined by RT-PCR from the ischemic and contralateral hippocampus and cortex. Because oligodendrocyte progenitors (OPs) are particularly vulnerable to H-I at this age, Bcl-x splicing was evaluated in OP cells induced to undergo apoptosis with C2-ceramide. Cell death was assessed by LDH assay and DNA fragmentation. Western blotting was used to detect Bcl-x, activated caspase-3 and CUG-BP1. Minigene mutagenesis experiments and RNA EMSA were performed to examine RNA binding proteins that might regulate Bcl-x splicing. RNA interference was employed to knockdown Bcl-xS and CUG-BP1 in vitro.

Results: Neonatal H-I resulted in a significant decrease of the Bcl-xL and a concurrent increase of Bcl-xS in the ischemic hippocampus and cortex (well before procaspase-3 cleavage), while the contralateral side remained unchanged compared to controls. Within 1 hour of exposing OP cells to C2-ceramide, the Bcl-xL/Bcl-xS ratio was decreased prior to capase-3 activation and cell death. Specific knockdown of Bcl-xS (without significantly altering Bcl-xL) attenuated ceramide-induced cell death. Using a transfected bcl-x minigene, we identified a UG rich motif immediately downstream of Bcl-xL 5' spicing site that altered Bcl-x splicing patterns. Supershift analysis indicated that splicing factor CUG-BP1 bound to this UG motif, and dephosphorylation of the CUG-BP1 abolished this RNA-binding activity. Overexpression of CUG-BP1 in OP cells altered splicing of the Bcl-x, favoring Bcl-xL, and protected cells from ceramide-induced cell death. In contrast, knockdown of CUG-BP1 aggravated cell vulnerability to ceramide. While CUG-BP1 is found predominantly in the nucleus, ceramide induced its translocation to the cytosol and consequently decreased the Bcl-xL/Bcl-xS ratio in OP cultures. In the brains of neonatal rats, CUG-BP1 decreased in nuclei within 3 hours after H-I (concurrent or prior to Bcl-x splicing changes).

Conclusions: Bcl-x alternative splicing may be an important regulatory mechanism for apoptosis following hypoxia-ischemia in neonates. The splicing factor CUG-BP1 appears to be a critical regulator of Bcl-x pre-mRNA splicing, and is altered following H-I. These results raise the possibility that regulators of alternative splicing may provide a novel target for neuroprotective intervention, increasing pro-survival factors (Bcl-xL) while decreasing anti-survival factors (Bcl-xS).

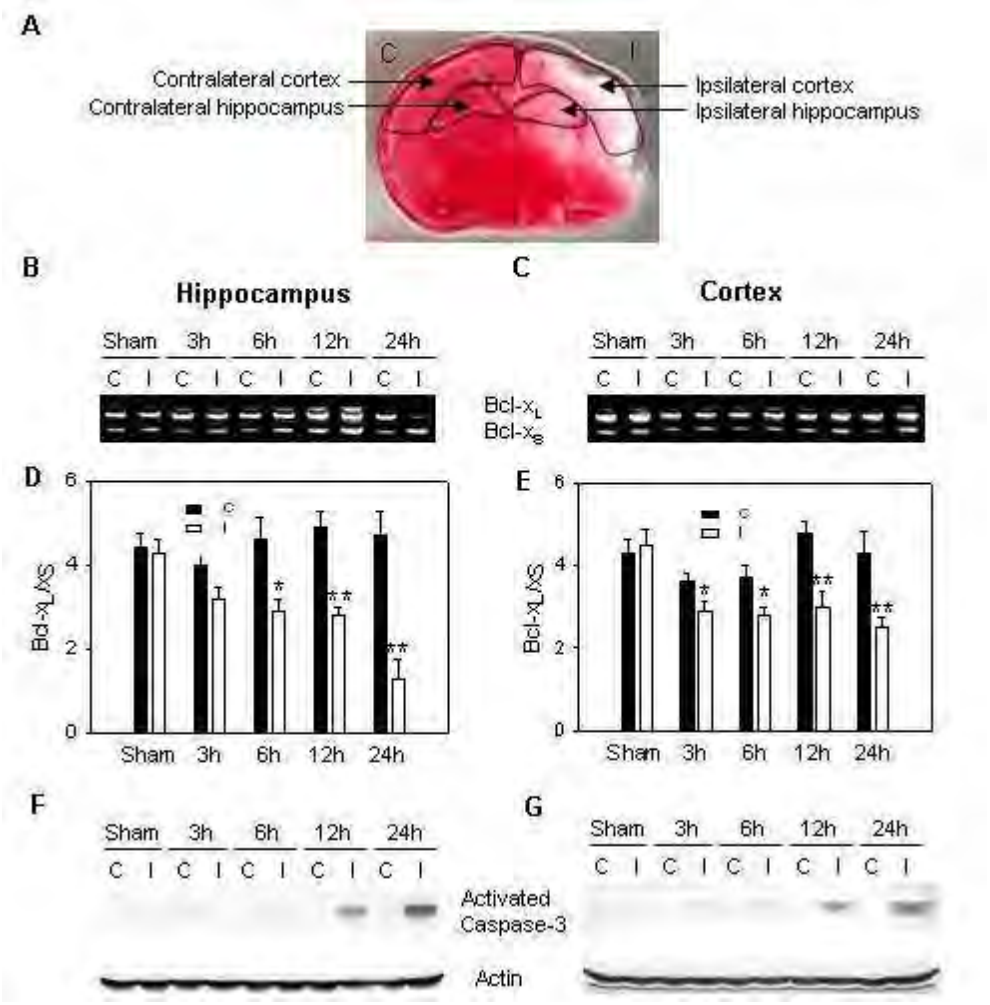

[Neonatal H-I alters Bcl-x alternative splicing]

908

Brain Poster Session: Subarachnoid Hemorrhage

HIGH FAT DIET HAS LITTLE DETRIMENTAL EFFECT ON STRESS GENE EXPRESSION POST INTRACEREBRAL HEMORRHAGE

J. Clark[1], S. Benoit[2], A. Harm[1], D. Caudell[1], A. Lu[1], G. Pyne-Geithman[1]

[1]Neurology, [2]Psychiatry, University of Cincinnati, Cincinnati, OH, USA

We hypothesized that high fat diet would increase stress gene expression in the brains of rats post intracerebral hemorrhage (ICH). Obesity and diet are risk factors for having stroke and we wanted to determine whether high fat diet alone would have an impact on the recovery and/or complications seen post hemorrhage.

Using male rats 12-13 weeks of age we injected 50 ml of autologous arterial blood or an equal volume of normal saline for control. Normal chow consisted of 4.5% fat and high fat chow consisted of 20% fat. After the surgery the animals were allowed to recover. One group of animals on normal diet were sacrificed at 1 week post ICH and analyzed for hemoxygenase-1 (HO-1) and heatshock protein 25 (HSP-25). All other groups were aged for 6 weeks on either normal diet or high fat diet.

For all groups and all time points ICH induced significantly greater levels of HO-1 and HSP-25 compared to saline controls. When we compared high fat versus ICH there was no significant change in HO-1 expression and a slight not significant decrease in HSP-25 expression. In a post hoc analysis we found that the return towards saline control levels post ICH between 1 week and 6 weeks was similar for all groups.

In conclusion, we found that diet did not affect stress gene expression of HO-1 or HSP-25 following ICH.

909

Brain Oral Session: Neurovascular Unit

IN VIVO PIAL ARTERIOLAR REGULATION ASSOCIATED WITH ATP HYDROLYSIS IN THE RAT

F. Vetri, H.L. Xu, L. Mao, D.A. Pelligrino

Neuroanesthesia Research Laboratory, University of Illinois at Chicago, Chicago, IL, USA

Objectives: ATP and adenosine (ADO) have been shown to have important roles in intercellular communication both in physiological and pathophysiological conditions. Furthermore, ATP has been linked to neural activity-induced vasodilation. Whether that vascular response relates to ATP itself, via interactions with purinergic P2 receptors, or is more closely linked to products of ATP hydrolysis, like ADO (and interactions with purinergic P1 receptors), is not precisely known. In the present study, we tested the hypothesis that extracellular ATP elicits vasodilation primarily via its rapid conversion to ADO.

Methods: We assessed vascular effects of exogenous ATP or ADO, topically applied through a closed cranial window, by measuring pial arterial dilation in the absence and presence of the ecto-5'-nucleotidase (e-N) inhibitor α,β-methylene ADP (AOPCP) or the selective ADO A_{2A} receptor blocker, ZM241385. ATP induced a dose-dependent dilation of pial arterioles (14 and 27% at 1 and 10 μM, respectively). Those dilations could be reduced to 2 and 10% in the presence of ZM241385 (10 μM). When co-applied with AOPCP (300 μM), ATP (1 and 10 μM) elicited only 3 and 13% dilations, respectively. On the other hand, ADO elicited 15 and 32% pial arteriolar dilation at 10 and 100 μM, but, when suffused with ZM241385, the dilation was completely blocked. Conversely, as expected, AOPCP did not interfere with ADO-induced pial arteriolar dilation.

Discussion: In the present study, we showed that ATP acts to dilate pial arterioles mainly in the form of ADO. Upon the conversion of ATP to AMP, via ecto-nucleotide pyrophosphatase phosphodiesterase (e-NPP), e-N removes a P_i to produce ADO, which, in turn, dilates vessels through ADO A_{2A} receptors. This cascade can be effectively blocked either by inhibiting e-N with AOPCP or the ADO A_{2A} receptor with ZM241385. The specificity of ZM241385 was proven by its ability to completely block ADO dilatory responses. Similarly, the specificity of AOPCP was demonstrated by the lack of any effect on ADO-induced dilation. As a further indication of the primacy of the ecto-pyrophosphatase (i.e., ecto-diphosphohydrolase; apyrase) pathway, over ecto-monophosphohydrolase activity (i.e., ATP→ADP→AMP), we previously reported that ADP-induced pial arteriolar dilation was unaffected by ADO receptor blockade with 8-sulfophenyltheophylline (1). This indicates that comparatively little ADP is formed from ATP extracellularly.

Conclusions: These data suggest that ADO is the major mediator of ATP-induced pial arteriolar dilation in vivo in rats.

References: (1) Am J Physiol Heart Circ Physiol. 281: H2105-H2112, 2001.

MEASUREMENT OF CEREBRAL BLOOD FLOW IN THE ADULT PIG BY DEPTH-RESOLVED BROADBAND NEAR-INFRARED SPECTROSCOPY

J.T. Elliott[1,2], M. Diop[1,2], K.M. Tichauer[1,2], T.-Y. Lee[1,2,3], K. St. Lawrence[1,2]

[1]Imaging Division, Lawson Health Research Institute, [2]Department of Medical Biophysics, The Universty of Western Ontario, [3]Imaging Research Laboratories, Robarts Research Institute, London, ON, Canada

Objectives: Near-infrared spectroscopy (NIRS) has the potential to improve management of life-threatening neurological emergencies by providing bedside measurements of cerebral blood flow (CBF). We have developed a method for measuring CBF using the NIRS contrast agent, indocyanine green (ICG)[1]. The challenge to adapting our technique to adult studies is to remove signal contamination caused by the extra-cerebral layer (ECL). To achieve this, we developed a multi-channel, broadband NIRS system. Multi-distance measurements provide some depth sensitivity to assist in separating cerebral and extra-cerebral signals and broadband spectroscopy is used to quantify ICG concentration. The objective of this study was to compare depth-resolved NIRS measurements of CBF to those obtained by CT perfusion[2].

Methods: Experiments were conducted on four pigs (3-4 weeks old) anesthetized with isoflurane; a cannula was inserted into an ear vein of each pig for administrating ICG and a CT contrast agent (Omnipaque). Animals were placed in the CT scanner with three NIRS optodes positioned on the head: one emission optode and two detection optodes placed 1 and 4-cm from the emitter. Brain and ECL ICG concentration curves were extracted from multi-distance NIRS data using a two-layer modified Beer-Lambert Law. Partial pathlengths (PPL) for each layer were selected from a library generated by Monte Carlo simulations[3] based on the geometry of the ECL and with the constraint that water concentration in the brain is 80%[4]. CBF was determined from brain ICG concentration curves as described previously[1]. For comparison, CBF was also calculated using 4-cm emitter-detector distance raw ICG curves. All NIRS results were evaluated against concomitant CT perfusion measurements of CBF.

Results: Figure 1 shows ICG curves obtained at source-detector distances of 1 and 4-cm and the corresponding ICG curves for brain and ECL from the PPL approach. CBF from CT perfusion ranged from 37 to 83 mL/min/100g and the mean thickness of the ECL was 9.2±1.7mm. Analysis of the 4-cm ICG data resulted in underestimations in CBF (by 33±23%), and was more erroneous for pigs with thicker ECLs. In contrast, there was a significant correlation between CBF measurements from CT perfusion and the PPL approach (mean difference of -2±20% between the techniques).

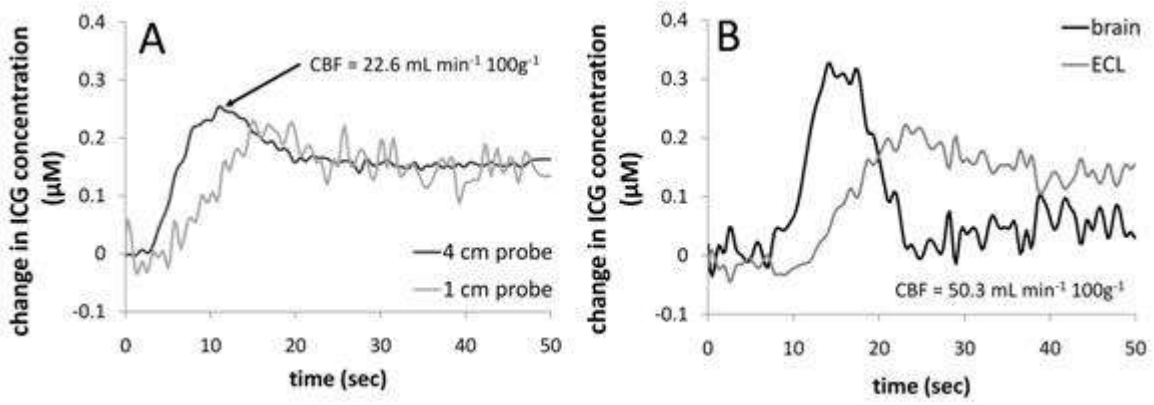

[Figure 1 - ICG curves]

Figure 1 - ICG curves from one pig: (A) From the 1cm and 4-cm detectors and (B) brain and ECL ICG curves determined from PPL approach. The CBF determined by CT perfusion was 51.2 ml/min/100g.

Conclusion: These preliminary results suggest that CBF in adults could be measured by depth-resolved broadband NIRS using our PPL approach. Further work is required to assess the precision of the CBF measurements and the sensitivity to the thickness of the ECL.

References:

1. Brown Pediatr Res 2;51:564.

2. Cenic AJNR 99;20:63.

3. Wang Comput Methods Prog Biomed 47;131:146.

4. Matcher Phys Med Biol 94;39:177.

VISUALIZATION OF DOPAMINE DYNAMICS FROM PET IMAGES

E. Morris[1,2,3], C. Constantinescu[4], J. Sullivan[2,3], M. Normandin[2,3], K. Yoder[2], S. Risacher[2], L. Christopher[5]

[1]Biomedical Engineering, Indiana University-Purdue University at Indianapolis, [2]Radiology, Indiana University School of Medicine, Indianapolis, [3]Biomedical Engineering, Purdue University, West Lafayette, IN, [4]Psychiatry & Human Behavior, University of California Irvine, Irvine, CA, [5]Electrical Engineering, Indiana University-Purdue University at Indianapolis, Indianapolis, IN, USA

Introduction: We recently introduced multiple strategies ("ntPET") for extracting temporal patterns of brain dopamine (DA) fluctuations from dynamic PET using 11C-raclopride [1-5]. Each of these modeling and parameter estimation methods yields a collection of time-concentration curves for endogenous DA. When the collection of DA curves is dense (i.e., one curve for every voxel), we can produce images of DA concentration at each time-frame; the 4D data set can be thought of as a volumetric DA "movie". Viewing a single slice of the movie or viewing parametric maps that we derive from it can reveal clusters of brain regions whose DA activity is synched to a task performance or other DA-ergic stimulus.

Methods: A male subject underwent 3 bolus PET studies. One study was a "rest" condition, the remaining two were "task" conditions. The latter two sessions involved an identical right-handed finger-tapping task lasting 10 minutes. Once, the task was initiated near the midpoint (25 min.) of the scan session. Another time, the task was initiated near the end (40 min.). Data were processed according to non-parametric ntPET [4] to produce DA movies. We generated mages of the DA peak time at each voxel for each of the two tasks [5]. Finally, we created an image of the time-difference between peak times for "early" and "late" tasks, respectively. This image was segmented with a Guassian mixture model [6] to identify clusters of temporally like-responding voxels.

Results: The segmented image of time-difference between peaks of DA activity for the two tasks is shown in the Figure for 12 contiguous (axial) striatal slices The units in the image are minutes and the largest cluster of striatal voxels (red) involved in the right-handed task are on the left. The time-difference for the dominant cluster is 14.6 +/- 0.08 (SEM) min. Analysis of a control study yielded no clusters of comparable size or contiguity.

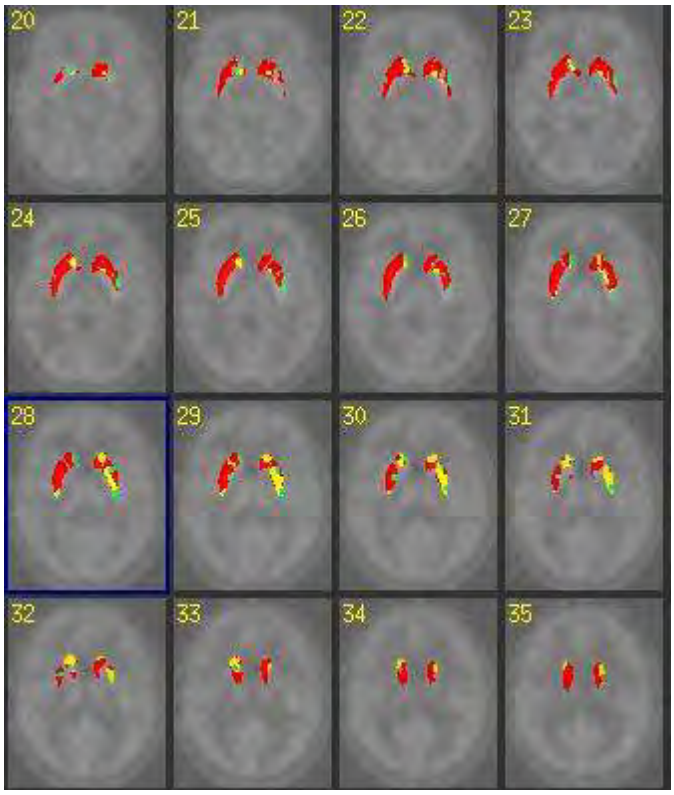

[Figure 1.]

Conclusion: Given that "early" and "late" tasks were identical except for timing, we would expect the DA-ergic response of voxels involved in execution of the task to be delayed by 15 min. in the late task relative to the early one. This appears to be true of the largest cluster of (primarily contralateral) voxels whose peak activity shifts in time by 15 min. from early to late task performance. We believe our images of DA timing are the first of their kind and may enhance our ability to identify clusters and sequencing responsible for responses to motor and other DA-ergic stimuli such as drugs of abuse.

References:

1. Morris, Mol Imag, 2005.

2. Morris, Mol Imag Biol, 2008.

3. Normandin, NeuroImage, 2008.

4. Constantinescu, IEEE Trans Med Imag, 2007.

5. Constantinescu, Phys Med Biol, 2008.

6. Christopher, submitted.

Acknowledgements: R21 AA015077.

913

Brain Poster Session: Experimental Cerebral Ischemia: In Vitro

PROTECTION OF ASTROCYTES FROM ISCHEMIA-LIKE INJURY BY ENDOPLASMIC RETICULUM CHAPERONE PROTEIN GRP78

R.G. Giffard[1], J.F. Emery[1], L.-J. Xu[1], A.S. Lee[2], Y.-B. Ouyang[1]

[1]Anesthesia, Stanford University, Stanford, [2]Department of Biochemistry and Molecular Biology, University of Southern California, Los Angeles, CA, USA

Objectives: Grp78 (BiP, Hsp78) is an endoplasmic reticulum (ER)-localized member of the 70kD heat shock protein (HSP70) family. Many studies of animal and cell-culture models of stroke have shown the neuroprotective properties of other members of the HSP70 family,[1,2] but little has been done with Grp78. In this study, we investigate the ability of Grp78 over-expression to protect primary astrocyte cultures under ischemic conditions.

Methods: Primary astrocyte cultures were prepared from postnatal (days 1-3) Swiss Webster mice (Charles River, Hollister, CA) as previously described.[3] After three days, cultures were co-transfected with equimolar amounts of pcDNA-Grp78[4] and pAcGFP1-Mito (BD Biosciences) using FuGene6 (Roche).

Cultures were subjected to ischemic conditions by either glucose deprivation (GD), or oxygen-glucose deprivation (OGD) as previously described.[2]

Cell viability was quantified after GD or OGD by microscopic evaluation of Hoechst 33342 (5 μM) and propidium iodide (PI, 5 μM) labeled cells.

Fluorescence immunocytochemistry and immunoblotting were performed as previously described[2] with anti-Grp78 (Stressgen, Ann Arbor, MI) or anti-activating transcription factor (ATF)-4 primary antibody.

Mitochondria were isolated by percoll gradient centrifugation. Reactive oxygen species (ROS) and mitochondrial membrane potential were measured over a three hour time course as described previously.[2] Mitochondrial complex I activity was measured using coenzyme Q0 as acceptor and NADH as donor, complex IV activity was measured using a CYTOX-OX1 kit (Sigma).

Results: The percentage of GFP-expressing cells after co-transfection was as high as 78% and the GFP signal was detectable through 25 days. The great majority of GFP positive cells also over-expressed Grp78 by immunostaining.

Over-expression of Grp78 protected primary cultured astrocytes against ischemic injury. Cultures over-expressing Grp78 demonstrated significantly reduced cell damage after both GD and OGD. ATF-4, a marker of ER stress, showed a smaller increase in Grp78 transfected cultures after GD, compared to controls. Grp78 immunostaining in unstressed cells demonstrated perinuclear distribution, consistent with ER localization. After GD, immunoblots from isolated mitochondria clearly showed that Grp78 was present in the mitochondria of Grp78-transfected cells. ROS production was reduced, and mitochondrial membrane potential and complex I and IV activities were better preserved in Grp78 transfected cells.

Conclusions: The ER-resident chaperone Grp78 can protect astrocytes from ischemic injury, and this is associated with reduced ER stress response and reduced ROS production. Under ischemic stress Grp78 retargets to mitochondria in over-expressing astrocytes. Mitochondrial functions are better preserved in these cells, indicating that part of the protection observed may be mediated by direct effects on mitochondria by Grp78.

References:

1. Giffard R. G. and M. A. Yenari (2004). Many mechanisms for hsp70 protection from cerebral ischemia. J Neurosurg Anesthesiol 16(1): 53-61.

2. Volobouéva L. A., et al. (2008). Overexpression of mitochondrial Hsp70/Hsp75 protects astrocytes against ischemic injury in vitro. J Cereb Blood Flow Metab 28(5):1009-16.

3. Dugan, L. L., et al. (1995). Glia modulate the response of murine cortical neurons to excitotoxicity: glia exacerbate AMPA neurotoxicity. J Neurosci 15(6): 4545-55.

4. Fu Y., et al. (2007). GRP78/BiP inhibits endoplasmic reticulum BIK and protects human breast cancer cells against estrogen starvation-induced apoptosis. Cancer Res 67:3734-40.

Brain Poster Session: Cerebral Vascular Regulation

DECREASED AUTOREGULATORY PATTERN DURING HYPOTENSION IN ENOS KNOCK-OUT MICE

T.E. Karwoski[1], R.K. Czambel[1], **S.C. Jones**[2,3]

[1]Anesthesiology, [2]Anesthesiology and Neurology, Allegheny-Singer Research Institute, [3]Radiology, Univ of Pittsburgh, Pittsburgh, PA, USA

Although CBF-blood pressure autoregulation is primarily attributed to the myogenic mechanism, CBF at arterial pressures near the hypotensive end of the autoregulatory plateau is also influenced by nitric oxide (1,2,3). Variations in the shape of the autoregulatory curve, characterized as the autoregulatory pattern (1,4,5) are distributed evenly within a large range, but can be divided into three distinct groups:

1. pressure-passive (none),
2. classical, and
3. hyper-autoregulation (peak).

The peak pattern is the most striking variation, as CBF paradoxically increases above the autoregulatory plateau during hypotension in what appears to be an exaggerated attempt to maintain CBF as the myogenic response becomes exhausted (4). Although the mean autoregulatory curve has been shown to be lower in eNOS knockout mice (6), here we investigate individual variations in autoregulatory pattern. Our hypothesis is that the peak autoregulatory pattern will be less frequent or non-existent if nitric oxide released from eNOS is not available in eNOS knockout mice.

Methods: Nine male mice (28±3 g), 7 wild type (WT, C57BL/6) and 2 eNOS knockouts (KO, genetic background: 129P2/OlaHsd*C57BL/6), were induced with 4.5% isoflurane, intubated, and femoral arteries cannulated under mechanical ventilation. Arterial blood gases and femoral artery blood pressure were recorded. Mice were further anesthetized with chloralose/urethane (50 mg/kg, 750 mg/kg, IP) and maintenance isoflurane was discontinued. CBF reactivities to CO_2 and to the blood-brain barrier permeant muscarinic receptor agonist, oxotremorine (1 μg/kg, IP) with systemic responses blocked with atropine methyl bromide, were determined.

CBF was determined using laser Doppler flowmetry at MABP steps of 10 mmHg during sequential hemorrhagic hypotension. Autoregulatory curves were categorized into peak, classical, and none patterns of autoregulation as previously described (4).

Results: The CO_2 vascular reactivity was greater for KO mice ($p=0.01$), whereas oxotremorine reactivities were present and not different for both WT and KO mice. Wild-type mice exhibited 2 none, 3 classical, and 2 peak patterns, whereas the eNOS KO mice exhibited 2 none patterns ($p=0.36$, chi-square), suggesting that the autoregulatory pattern is decreased by eNOS gene deletion.

Conclusions: The vascular reactivities were consistent were others' results (7,8). The absence of the peak autoregulatory pattern in the eNOS KO mice represents the loss of an important mechanism for increasing CBF during hypotension and suggests that the peak pattern is associated with eNOS. eNOS's role in the hypotension response represents a positive factor in maintaining CBF. The

exploitation of this potentially positive factor could well involve the upregulation of eNOS by the statins (9).

Support: Pennsylvania Tobacco Settlement Funds.

References:

1. Jones et al. (2003) JCBFM 23:1085-1095.

2. Toyoda et al. (1997) JCBFM 17:1089-1096.

3. Jones et al. (1999) Am J Physiol Heart Circ Physiol 276:H1253-H1262.

4. Jones et al. (2002) Anesthesiology 97:488-496.

5. Kharlamov et al. (2004) Neurosci Lett 368:151-156.

6. Huang et al. (1996) JCBFM 16:981-987.

7. Ma et al. (1996) Am J Physiol Heart Circ Physiol 271:H1717-H1719.

8. Meng et al. (1996) Am J Physiol Heart Circ Physiol 271:H1145-H1150.

9. Endres et al. (2004) TINS 27:283-289.

Brain Poster Session: Experimental Cerebral Ischemia: Global Ischemia

EFFECT OF DONEPEZIL ON NITRIC OXIDE PRODUCTION IN THE BRAIN DURING GLOBAL ISCHEMIA AND REPERFUSION IN MICE

Y. Asano[1], T. Ohkubo[2], K. Hattori[2], T. Shimazu[1], H. Nagoya[2], M. Yamazato[2], Y. Ito[2], Y. Kato[2], **N. Araki**[2]

[1]Neurology, Saitama Neuropsychiatric Institute, Saitama-shi, [2]Neurology, Saitama Medical University, Moroyama-machi, Japan

Objectives: Donepezil(DON), a selective acetylcholinesterase (AChE) inhibitor, may induce neuroprotective factors by stimulating nicotinic acetylcholine receptors (nAChRs) and protect cortical neurons by against glutamate neurotoxicity (1, 2). In addition, it was reported that donepezil protects the brain ischemia induced by MCA occlusion and that this effect may be due to, at least in part, to donepezil stimulation of α7-nAChRs (3).Nitric oxide (NO) plays an important role in the pathogenesis of neuronal cell injury which is closely related to glutamate neurotoxicity. However, effect of donepezil on NO production in the brain during ischemia have not been previously determined. Therefore, we examined the effect of donepezil on generation of NO metabolites during global ischemia and reperfusion in mice and striatum using an in vivo microdialysis technique.

Methods: Male C57BL/6 mice were anesthetized with halothane. Polyethylene catheter (PE-10) was inserted into the right femoral artery for measuring blood pressure. A Microdialysis probe was inserted into left striatum. After 2 hour equilibrium period, fractions were collected every 10 minutes. A Laser Doppler probe was placed on the right skull surface. In doenepzil group and control group, global ischemia was produced by clipping both common carotid arteries using Zen clips for 10 minutes. Donepezil (1mg/kg or 5mg/kg) was administered subcutaneously at 30 minutes before ischemia. The levels of nitrite (NO_2^-) and nitrate (NO_3^-) in the dialysate samples were measured by the Griess reaction. After euthanasia, the brains were immunostained using a primary antibody directed against nNOS in an immunoperoxidase method and visualized by diaminobenzidine in striatum.

Results: In steady state, blood pressure was transiently increased at 10 minutes and cerebral blood flow was increased at 10 (107.5±6.9 %, mean±SD), 20 (109.4±10.8) and 30 minutes (109.4±10.6) after administration of 5mg/kg doenepzil. Total NO (amount of nitrite and nitrate) levels in the dialysate from striatum were decreased significantly at 10 (3.27±0.97 μmol/L) and 20 minutes (3.24±0.91) after administration of 1mg/kg donepezil and 20 minutes (4.08±1.07) after administration of 5mg/kg donepezil as compared with each baseline (3.69±0.86, 4.64±1.03) (fig.). In addition, total NO levels in 1mg/kg donepezil group were significantly higher (99.30±22.76 %) during ischemia and significantly lower at 60 minutes after reperfusion (113.57±32.74) than those of control (82.65±19.50, 144.92±40.92). nNOS-positive area were decreased in 1mg/kg (1.14±0.39 %) and 5mg/kg donepezil group (1.24±0.54) as compared with control (1.51±0.70), but there was no significant differences between three groups.

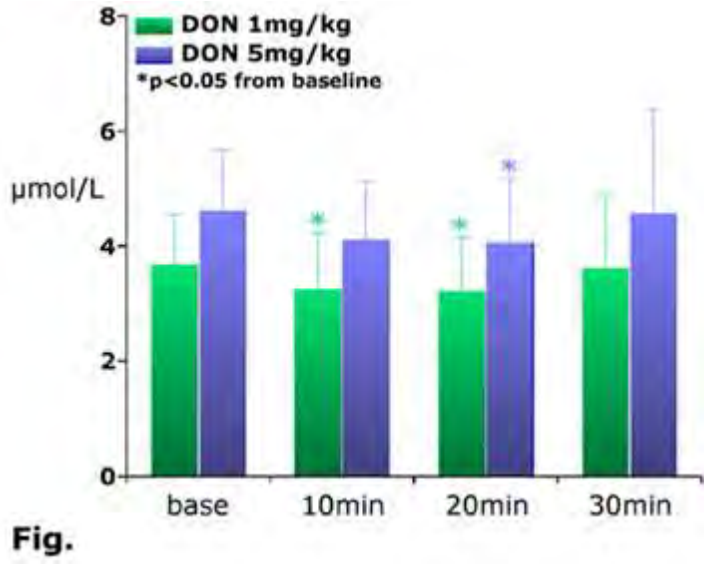

Fig.

[Changes in total NO levels]

Conclusions: These data indicate that donepezil attenuates NO production in the brain and may afford neuroprotective effects against ischemia and reperfusion injury.

References:

[1] Takada Y: J Pharmacol Exp Ther 306, 772-7 (2003).

[2] Kume T et al: Eur J Pharmacol 527, 77-85 (2005).

[3] Fujiki M et al: Brain Res 1043, 236-41 (2005).

IMAGING SEROTONIN RECEPTORS USING 18F-MEFWAY IN AGING

T. Dinh, S. Faheem, N. Rana, N. Saigal, S. Pandey, M.L. Pan, E. Head, J. Mukherjee

University of California Irvine, Irvine, CA, USA

Objectives: Serotonin $5HT_{1A}$ receptors have been implicated in aging. Effects of aging on the $5HT_{1A}$ receptor have been studied using post-mortem tissue as well as by PET imaging (eg., Costes et al., 2005). Results have varied from no effect to reductions and observed gender effects. Using the selective $5HT_{1A}$ radiotracer ^{18}F-trans-Mefway (Saigal et al., 2006) we have evaluated postmortem in the aging canine model. Ages of the dogs varied from 1 to 15.4 years (equivalent to ~15 to 90 human years).

Methods: Radiosynthesis of ^{18}F-Mefway was carried out with a specific activity of >2 Ci/mmol. Brain tissue was obtained from the cerebellum (CB) and temporal cortex (COR) of beagle dogs of various ages. Sections (10 µm thick) of the tissue were obtained including the cortex (COR) and cerebellum (CB). Sections were preincubated at room temperature for 15 min in 50 mM Tris-HCl buffer (pH 7.4). Incubation with 1 to 2 µCi/cc of ^{18}F-Mefway at 37 ^{o}C took place for 1 hour. Nonspecific binding was with 10 µm serotonin. Post incubation, sections were washed twice for 3 min in cold buffer, submerged quickly in cold distilled water and laid out to dry and exposed to phosphor films. Optiquant imaging software was used to quantify binding to the various cortical layers.

Results: Binding of ^{18}F-Mefway in the various cortical layers were observed and were in agreement with reported $5HT_{1A}$ distribution (Eickhoff et al., 2007). Serotonin displaced >90% of binding. Binding in CB was very low; each animal was used as reference in ratio measurements. In the youngest dog (1 Yr) ratio COR/CB= 19. Highest binding was in layers I, II (100%) and least in III, IV (31%), similar to that found in humans. Over the age range evaluated, no significant reduction in ^{18}F-Mefway was observed.

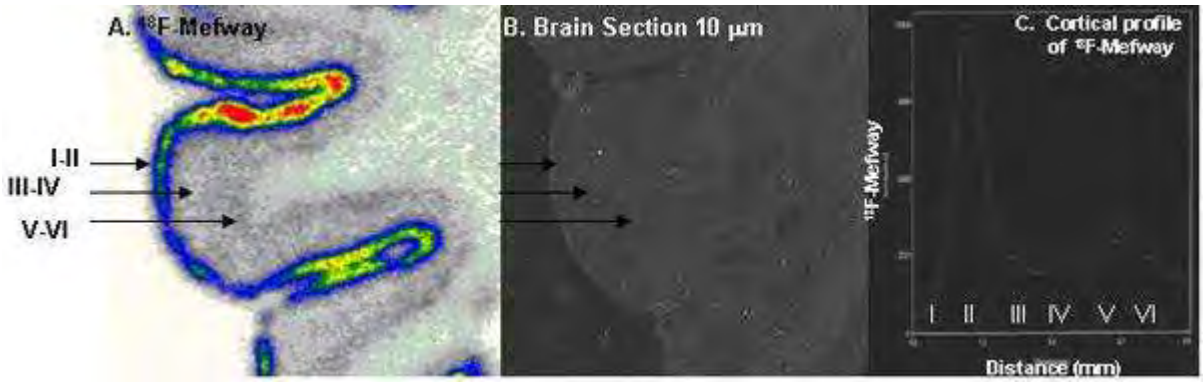

[18F-Mefway binding in canine]

Figure-1: (A). 18F-Mefway binding to cortical layers in canine model (14.8 yr old); (B). Scan of brain slice in image (A) showing cortical layers; (C). Binding profile in cortical layers showing maximal binding layers I-II followed by V-VI.

Conclusions: The canine model offers the ability to study aging effects. It has also been studied as a potential animal model for human AD (Head et al., 2008). Further studies are underway in additional old animals. Evaluation of D2/D3 receptors using ^{18}F-fallypride in the canine model is also underway in order to correlate our findings of aging in humans (Mukherjee et al., 2002).

References:

Costes, N. et al., J. Nucl. Med., 46:1980-1989 (2005); Eickhoff et al., Neuroimage, 34:1317-1330 (2007); Head et al., J. Neurosci., 28:3555-3566 (2008); Mukherjee J. et al., Synapse, 46:170-188 (2002); Saigal et al., J. Nucl. Med., 47: 1697-1706 (2006).

Research Supported by NIH R21AG030524.

STANDERDIZATION OF CBF QUANTIFICATION USING 123I-IMP SPECT AND DUAL TABLE ARG METHO

N. Jyoji[1], K. Kamiyama[1], T. Osato[1], H. Nakamura[1], H. Iida[2]

[1]Neurosurgery, Stroke Center, Nakamura Memorial Hospital, Sapporo, [2]Investigative Radiology, National Cardiovascular Center Research Institute, Osaka, Japan

Objectives: In assessment of hemodynamic cerebral ischemia using CBF-SPECT, resting and acetazolamide-activated CBF quantifications has been performed on different day using 123-I-IMP SPECT and ARG method (1). However, 2-days CBF quantification could not overcome the errors from different arterial input functions calculated using well-counter. Also, arbitrary assessment could be occurred using non-stereotactic ROI analysis on axial plane. In this study, the accuracy of dual table ARG (DTARG) (2) which was developed as 1-day CBF quantification was investigated to establish the standardization of CBF quantification.

Methods: Sixteen normal volunteers were involved in this study, and DTARG was performed using a split equivalent dose of 123-I-IMP and common arterial input function. In resting CBF quantification, a relationship between the pixel value of 1st SPECT and resting CBF was tabled using two-compartment model, and then the 1st SPECT was transformed to resting CBF map. In acetazolamide-activated CBF quantification, a relationship between the pixel values of the 2nd SPECT and acetazolamide-activated CBF was tabled using dual two-compartment model for both resting and acetazolamide- activated CBF. Vascular reserve (VR) was defined as [(acetazolamide-activated CBF - resting CBF) / resting CBF×100%]. For estimating diagnostic accuracy, CBF in vascular territories were measured by standardized ROI template (Flexer algorism) and segmental extraction estimation (SEE) (3). SEE could demonstrate resting and acetazolamide-activated CBF, VR, stage of hemodynamic ischemia on the standardized brain surface image developed in 3D-SSP (4).

Results: Using standardized ROI analysis for axial plane of mid-basal ganglia, mean resting CBF +/- S.D. was measured as 38.7+/-9.1(Rt), 38.0+/-8.3(Lt) ml/100g/min in ACA, 40.4+/-8.5, 39.2+/-8.7 ml/100g/min in MCA, 39.7+/-7.8, 39.2+/-7.1 ml/100g/min in PCA territories. Mean VR was measured as 42+/-20, 44+/-15 % in ACA, 46+/-15, 47+/-17 % in MCA, 44+/-19, 42+/-18 % in PCA territories. Using SEE analysis, mean resting CBF was measured as 38.2+/-7.9, 38.1+/-8.2 ml/100g/min in ACA, 38.1+/-7.3, 38.6+/-7.5 ml/100g/min in MCA, 38.7+/-6.7, 38.1+/-6.4 ml/100g/min in PCA territories. Mean VR was measured as 45+/-13, 45+/-16% in ACA, 48+/-15, 47+/-14% in MCA, 45+/-16, 47+/-15% in PCA territories. Territorial CBF in standardized ROI analysis was compatible to surface CBF using SEE analysis. Stage2 hemodynamic ischemia has been defined as both CBF less than 80% of normal mean CBF and VR less than 10% in MCA territory, significant reduction of renting CBF was comparable to mean CBF - 1S.D. and significant reduction of VR was comparable to mean VR - 2S.D.

Conclusions: Introduction of DTARG could make 1-day quantification of both resting and acetazolamide-activated CBF which overcomes measurement errors associated with 2-days CBF quantification. Also, introduction of SEE could make stereotactic assessment of severity of hemodynamic cerebral ischemia and its serial changes. These newly developed assessments for CBF-SPECT could improve the accuracy of SPECT quantification and diagnostic decision, and could promote the standardization of CBF quantification using SPECT.

References:

(1) Iida H, et al. J Nucl Med 35: 2019-2030, 1994.

(2) Kim KM, et al: Neuroimage 33: 1126-1135, 2006.

(3) Mizumura S, et al: Ann Nucl Med 18: 13-21, 2004.

(4) Minoshima S, et al. J Nucl Med 36: 1238-1248, 1995.

BIODISTRIBUTION STUDY OF [^{61}CU]PYRUVALDEHYDE-BIS(N_4-METHYLTHIOSEMICARBAZONE) IN NORMAL RATS AS A BRAIN PET TRACER

A.R. Jalilian[1], P. Rowshanfarzad[2], F. Bolourinovin[1], M. Kamalidehghan[1], A. Majdabadi[3], S. Moradkhani[1]

[1]Nuclear Medicine Research Group, [2]Nuclear Medicine Group, [3]Agricultural, Medical and Industrial Research School (AMIRS), Karaj, Iran

Background: [^{61}Cu]-labeled pyruvaldehyde-bis(N4-methylthiosemicarbazone) (^{61}Cu-PTSM) is a promising agent for imaging of blood perfusion that can be prepared in large amounts in the country.

Materials and methods: Copper-61 ($T_{1/2}$=3.33h) was produced via the ^{nat}Zn(p,x)^{61}Cu nuclear reaction in a 30 MeV cyclotron. ^{61}Cu was separated from the irradiated target by a two-step column chromatography method developed in our laboratory using a cation and an anion exchange resin. The radionuclide was then added to the in-house synthesized PTSM ligand for radiolabeling following the quality control procedures using RTLC and HPLC. The tracer was finaly injected to normal rats and percentages of injected dose per gram was calculated.

Results: After 150 μA irradiation of the target for 76 min, about 6.006 Ci of $^{61}Cu^{2+}$ was obtained with a radiochemical separation yield of more than 95% and a radionuclidic purity of more than 99% (^{60}Cu as impurity). Final ^{61}Cu-PTSM was prepared using the optimized method with a purity more than 98% following administration to normal rats. The tracer is mostly incorporated in heart, kidneys and brain compared to free copper cation as a control which is in agreement with former reports.

Conclusion: [^{61}Cu]-PTSM was prepared at the radiopharmaceutical scales with high quality and is a potential PET tracer in the perfusion study of the heart, kidey, brain and tumors.

Brain Poster Session: Oxidative Mechanisms

BIODISTRIBUTION OF [^{61}CU]-OXINATE IN FIBROSARCOMA TUMORS FOR PET IMAGING

A.R. Jalilian[1], S. Zolghadri[2], R. Faghihi[2], J. Garousi[1], H. Yousefnia[2], A. Majdabadi[1], F. Bolourinovin[1]

[1]Nuclear Medicine Research Group, Agricultural, Medical and Industrial Research School, Karaj, [2]Department of Nuclear Engineering, School of Engineering, Shiraz University, Shiraz, Iran

Objectives: This work was conducted for production of an radiolabeled anticancer copper complex, i.e. ^{61}Cu-oxinate as a potential PET in oncology.

Methods: Cu-61 was prepared from natural zinc target irradiation by 22 MeV protons (150 uA) via nuclear reaction with a yield of 3.33 mCi/μAh. In order to obtain the best labeling method optimization reactions were performed for pH, temperature and concentration and finally best solid phase extraction method. Biodistribution of the tracer was studied in normal and fibrosarcoma bearing mice.

Results: At the optimized conditions, ITLC showed radiochemical purity more than 97% with a specific activity of 0.06 Ci/mM. This was kept unchanged even with presence of human serum as well as room temperature for 5h.

conclusion: Biodistribution of the tracer in fibrosarcoma bearing mice demonstrated significant tumor uptake after 2h. This tracer can be used in the detection of some brain tumors using PET scan.

PLASMA CONCENTRATION OF PENTRAXIN3 (PTX3) IN ACUTE CEREBRAL INFARCTION

T. Tajima, M. Yamazato, W. Hara, A. Saitou, J. Akiyama, A. Kubota, S. Narukawa, M. Kojima, S. Izaki, N. Yoshida, S. Ohji, T. Iguchi, T. Mitui, M. Tkahama, M. Ohnuki, K. Nomura

Neuroogy, Saitama Medical Center, Saitama Medical University, Kawagoe, Saitama, Japan

Objectives: The utility of high sensitivity CRP (hs-CRP) is reported as a blood vessel inflammation marker of arteriosclerosis. However, the uniqueness to the blood vessel inflammation is low. Pentraxin3(PTX3) is an acute inflammation protein that belongs to Petraxin family as well as CRP, and it has exhibted on endothelial cell, smooth muscle cell, and macrophage. It has the possibility to become a specific biomarker for the blood vessel inflammation. There are some reports that plasma PTX3 concentration increased in the acute coronary syndrome [1] .However, there is no report in acute cerebral infarction (ACI).

Methods: We measured the concentration of plasma PTX3 and serum hs-CRP, 45 patients with ACI containing five patients treated with t-PA, admitted acute stroke within 48 hours (36 men and 9 women; mean age, 69.1±7.8 years; 15 cardiac embolism (CE), 16 atherothrombotic infarction (ATI), 10 lacnar infarction (LI), 4 TIA and 56 age-matched healthy control (HC)).

Results:

1. Plasma PTX3 concentration within 24 hours was no significant difference in four types of ACI (CE 4.31±1.89, ATI 3.57±3.86, LI 2.02±0.24, and TIA 2.29±0.47ng/ml).
2. Plasma PTX3 concentration of CE in 48 hours was significantly higher than that of ATI, LI, TIA, and HC ($P< 0.01$, respectively) (CE 12.52±8.68, ATI 4.62±3.38, LI 2.58±1.59, TIA 2.07±0.76, and HC 1.98±1.14ng/ml, Fig.1).
3. Serum hs-CRP concentration within 48 hours was no significant difference in four types of ACI (n=48, P=0.13).
4. There is no correlation between PTX3 and hs-CRP within 48 hours (n=24, P=0.45).
5. There is a significant correlation between PTX3 in 48hours and modified Rankin scale (mRS) in the discharge (n=40, $P< 0.01$, Fig.2).

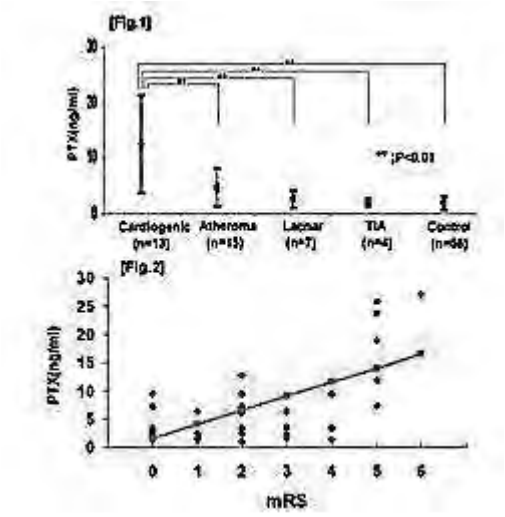

[tajima]

Conclusions:

1. Plasma PTX3 concentration increased after cardiac embolism, and it was suggested to be a useful indicator of ACI.
2. Plasma PTX3 within 48 hours after stroke was suggested to be a prognostic indicator to estimate of functional grade in the discharge.

References: [1] Inoue K et al.;Arterioscler Thromb Vasc Biol.2007;27:161-167.

Brain Oral Session: Traumatic Brain Injury

EVIDENCE FOR BRAIN TRAUMA FOLLOWING FIVE TWO MINUTE ROUNDS IN BOXING

M. Graham[1], C. Graham[1], P. Ryan[1], P. Evans[2], D. Renn[2], B. Davies[3], N.-E. Thomas[4], S.-M. Cooper[4], J. Baker[5]

[1]The Newman Centre for Sport and Exercise Research, Newman University, Birmingham, [2]Department of Endocrinology, Royal Gwent Hospital, Newport, [3]Health and Exercise Science Research Unit, University of Glamorgan, [4]Cardiff School of Sport, University of Wales Institute Cardiff, Cardiff, [5]Division of Sport, University of the West of Scotland, Glasgow, UK

Objectives: Severe cerebral acute injuries, resulting in morbidity or fatality, are rare in boxing compared with other sports (Zazryn et al., 2009). The British Medical Association has campaigned for a complete ban on boxing because of alleged chronic traumatic brain injury (White, 2007). A recent epidemiological study has concluded that such evidence is weak (Loosemore et al., 2008). The aim of this unique study was to analyse whether punches to the head (PTH), sustained during a boxing event, resulted in cerebral damage as quantified by elevated levels of neurochemical markers of brain tissue damage compared with punches to the body (PTB). Systemic stress was quantified by measuring serum cortisol.

Methods: Sixteen amateur boxers were divided into two groups: PTH, (n=8, mean ± SD, age: 17.6 ± 5.3 years; height: 168.4 ± 13; weight: 65.4 ± 20.3; punches to the head: 35.5 ± 18.4), PTB (n=8, mean ± SD, age: 19.1 ± 3.2 years; height: 169.6 ± 7.5; weight: 68.5 ± 15). The PTH group received punches to the head and body, while group PTB received only punches to the body. Blood samples were taken pre- and immediately post combat for analysis of S-100B, neurone specific enolase (NSE) and cortisol.

Results: Significant increases ($P < 0.05$) in serum concentrations of S-100B (0.35 ± 0.61 vs 0.54 ± 0.73, $\mu g.L^{-1}$) and NSE (19.7 ± 14 vs 31.1 ± 26.6, $ng.ml^{-1}$) and cortisol (372.9 ± 201.5 vs 755.8 ± 93, $nmol.L^{-1}$) were encountered pre- and immediately post combat in the PTH group but not in the PTB group.

Conclusions: PTH in boxing are sufficient enough to cause biochemically discernible damage of brain tissue. The risk of having an intra-cerebral haemorrhage from a mild brain injury (MBI) is 38%, with 7% requiring neurosurgical intervention (Thiruppathy and Muthukumar, 2004). The consequences of a MBI may be a transitory post-concussive syndrome (Kosakevitch-Ricbourg, 2006). Traumatic stress states are a well known pathology and consist of a psychological reaction against the trauma.

References:

Zazryn TR, McCrory PR, Cameron PA. Neurologic injuries in boxing and other combat sports. Phys Med Rehabil Clin N Am. 2009; 20: 227-239.

White C. Mixed martial arts and boxing should be banned, says BMA.BMJ. 2007; 335: 469.

Loosemore M, Knowles CH, Whyte GP. Amateur boxing and risk of chronic traumatic brain injury: systematic review of observational studies. Br J Sports Med. 2008; 42: 564-567.

Thiruppathy SP, Muthukumar N. Mild head injury: revisited. Acta Neurochirurgica (Wien) 2004; 146: 1075-1082.

Kosakevitch-Ricbourg, L. Clinical scoring scales for brain injury. Rev Stomatol Chir Maxillofac. 2006; 107: 211-217.

Disclosures: The authors have nothing to declare. All research complied with the Declaration of Helsinki. Ethical approval was provided by the University Ethics Committee.

EFFECT OF EXTERNAL COUNTERPULSATION ON CEREBRAL VASOREACTIVITY IN PATIENTS WITH ACUTE ISCHEMIC STROKE

L. Xiong, J.H. Han, X.Y. Chen, T. Leung, H. Leung, Y. Soo, K.S. Wong

Department of Medicine & Therapeutics, The Chinese University of Hong Kong, Hong Kong, Hong Kong S.A.R.

Objectives: Cerebral blood flow augmentation may play a key role in acute stroke management . External counterpulsation (ECP) is an established noninvasive method to improve the perfusion of vital organs. This study investigated whether cerebral blood flow velocities (CBFV) and cerebral vascular reactivity (CVR) in acute ischemic stroke patients with large artery disease are altered by ECP and whether the change of CBFV from baseline correlates with the change of CVR under ECP treatment.

Methods: Nineteen patients with unilateral acute ischemic stroke patients and fourteen healthy controls were enrolled. All stroke patients received 35 daily one-hour sessions of ECP therapy and controls received one session. During ECP treatment, bilateral middle cerebral arteries (MCAs) were monitored by transcranial Doppler ultrasonography (TCD) on day 1, 3, 5, 7, 10, 14, 18, 21, 24, 28, 35 and 60 after stroke onset in stroke patients and on the first ECP session in controls. Beat to beat heart rate, continuous finger blood pressure and CBFVs of MCAs were obtained before, during and after ECP. Pulsatility index (PI) and cerebral vascular resistance index (CVRi) were used to reflect cerebral vascular reactivity under ECP treatment.

Results: There were significant differences to the responses of ECP between stroke patients and controls. In both stoke patients and controls, mean blood pressure and CVRi increased and PI decreased immediately after ECP began. An increase in mean CBFV in relevant side on day 1, 5, 7, 14 and in irrelevant side on day 1, 7, 14, 18 was recorded in stroke patients during ECP, while a slight increase was shown in the controls. The increase in stroke patients was significant when compared with controls ($p< 0.05$). Significant differences were also seen in changes of mean CBFV, PI and mean blood pressure from baseline between different TCD monitoring days ($p< 0.01$). No significant difference was seen in the change of CVRi from baseline between different TCD monitoring days. Change of mean CBFV from baseline in right and left sides in controls significantly negatively correlated with CVRi ($r =-0.458$ and -0.528 respectively, $P< 0.01$), as well as in relevant and irrelevant sides in patients correlated with PI ($r = -0.183$ and -0.225 respectively, $P< 0.05$) and CVRi ($r =-0.572$ and -0.468 respectively, $P< 0.01$).

Conclusions: This study suggests that ECP exerts clear arterial effects on large vessels of the cerebral circulation. The different response in CBFV to ECP between stroke patients and controls may be attributed to the different status of cerebral autoregulation. These effects are of particular interest in ischemic cerebrovascular disease, in which techniques that increase regional blood flow may be beneficial.

References:

1. Enhanced external counterpulsation does not compromise cerebral autoregulation. Marthol H, Werner D, et al. Acta Neurol Scand 2005; 111(1):34-41.

2. Effects of enhanced external counterpulsation on carotid circulation in patients with coronary artery disease. Levenson J, Simon A, et al. Cardiology 2007; 108(2):104-110.

3. Cerebral blood flow responses to severe orthostatic stress in fit and unfit young and older adults. Franke WD, Allbee KA. Gerontology 2006; 52(5): 282-289.

A BRAIN PHANTOM STUDY OF ITERATIVE DECONVOLUTION VERSUS ANATOMICAL-BASED PARTIAL-VOLUME CORRECTION TECHNIQUES

B. Thomas[1], K. Erlandsson[1], S. Ourselin[2], L. Thurfjell[3], B. Hutton[1]

[1]Institute of Nuclear Medicine, [2]Centre for Medical Image Computing, University College London, London, [3]Medical Diagnostics R&D, GE Healthcare, Amersham, UK

Objectives: Partial-volume (PV) correction techniques require a measure of the scanner point-spread function (PSF) to operate. Two anatomical-based partial-volume correction (PVC) methods were evaluated: Müller-Gärtner (MG) and Multi-target correction (MTC). An iterative deconvolution method, Van-Cittert (VC), that requires no anatomical data, was also applied. The objective is to evaluate whether the performance of Van-Cittert deconvolution is comparable to anatomical PVC techniques when faced with measurement errors and noise.

Methods: Synthetic phantom images were generated using the Zubal phantom in Matlab with a 4:1 grey matter (GM) to white matter ratio. 10% variability in regional GM concentrations was applied. The image was forward projected with attenuation, adding approximations for scatter and randoms. Poisson distributed noise was added to the sinograms. Reconstruction was performed using filtered back-projection (FBP) with a Ramp filter. Ten realisations were generated at each noise level. Images were analysed in terms of recovery coefficient (RC) and standard deviation (SD) across noise realisations. A position-invariant PSF of 7.75mm was found by measurement.

MG and MTC were executed in Matlab. The VC method was implemented in C++ and uses a Deriche-style recursive approximation Gaussian filter. MTC is a “hybrid” anatomical PVC method, performing a Geometric Transfer Matrix (GTM) PV correction and using the estimated regional values as a basis for voxel-based PV correction. PVC was executed with PSF errors of +/- 2mm (5.75-9.75mm). MG and MTC PV correction was performed with perfect VOIs. Five count levels were tested (1.20e+07 to 3.84e+08).

Results: The results indicate that VC performance degrades at higher noise levels. Both MTC and MG were more reliant on an accurate measure of the PSF than VC. Errors in the PSF alter the number of iterations performed during VC PV correction, changing recovery and noise. The table below shows performance of the PVC techniques for one noise level.

	Van-Cittert (VC)	Müller-Gärtner (MG)	Multi-target correction (MTC)	Uncorrected
Frontal	0.925 (0.179)	0.989 (0.128)	1.007 (0.153)	0.663 (0.113)
Temporal	0.936 (0.208)	1.010 (0.135)	1.012 (0.167)	0.693 (0.130)
Occipital	0.887 (0.172)	1.025 (0.116)	0.994 (0.133)	0.631 (0.096)
Parietal	0.948 (0.165)	1.026 (0.116)	1.001 (0.134)	0.733 (0.117)

[RC (SD/mean). FWHM 7.75mm, 1.8e8 counts.]

Conclusions: Where a perfectly registered and segmented anatomical image is available, MTC outperforms both MG and VC in terms of recovery. However, MTC requires anatomical parcellation. MG is unable to account for variability in grey matter. VC does not achieve the same level of recovery as the other two methods, but has the advantage of requiring no anatomical information. VC is a viable alternative to anatomical PV correction.

References:

Kjell Erlandsson, Andrew Wong, Ramin Parsey, Ronald van Heertum, and J Mann (2006), ´A new voxel-based partial volume correction method for PET and SPECT´, J Nucl Med Meeting Abstracts, 47:191P.

Boon-Keng Teo, Youngho Seo, Stephen L. Bacharach, Jorge A. Carrasquillo, Steven K. Libutti, Himanshu Shukla, Bruce H. Hasegawa, Randall A. Hawkins, and Benjamin L. Franc (2007), ´Partial-Volume Correction in PET: Validation of an Iterative Postreconstruction Method with Phantom and Patient Data´, J Nucl Med 48(5), 802--810.

926

Brain Oral Session: Traumatic Brain Injury

CONTINUOUS MONITORING OF CEREBROVASCULAR REACTIVITY AFTER TRAUMATIC BRAIN INJURY IN CHILDREN

K. Brady[1], D. Shaffner[1], J. Lee[1], R.B. Easley[1], P. Smielewski[2], M. Czosnyka[2], G. Jallo[3], A.-M. Guerguerian[4]

[1]Pediatric Anesthesiology and Critical Care Medicine, Johns Hopkins University School of Medicine, Baltimore, MD, USA, [2]Academic Neurosurgery, Addenbrooke's Hospital, Cambirdge University, Cambridge, UK, [3]Neurosurgery, Johns Hopkins University School of Medicine, Baltimore, MD, USA, [4]Critical Care and Pediatrics, Hospital for Sick Children, Toronto, ON, Canada

Objective: Traumatic brain injury (TBI) is the foremost cause of death and disability in infants and children. In adults with TBI, monitoring of autoregulation has been utilized to define optimal cerebral perfusion pressure[1], but the methods have not been applied to children. Our objective was to test the hypothesis that the pressure-reactivity index, or PRx values, indicating preserved autoregulation would be associated with survival in children with TBI.

Methods: Twenty-one patients under 18 years of age admitted between May 2006 and September 2008 with severe traumatic brain injury requiring invasive intracranial pressure monitoring were enrolled in this prospective observational cohort study. The PRx was continuously monitored as a moving, linear correlation coefficient between low frequency waves of intracranial and arterial blood pressures. Positive values of PRx approaching 1 indicate impaired cerebrovascular reactivity, whereas negative PRx values or those close to zero indicate preserved cerebrovascular reactivity.[2] The average PRx over the entire monitoring period was compared between survivors and non-survivors. Values of PRx were sorted according to the cerebral perfusion pressure at which they were obtained to construct autoregulation curves for each patient.

Results: Positive values of PRx were associated with death in this cohort. Survivors (N=15) had a mean PRx (±S.D.) of 0.08 ± 0.19, and non-survivors (N = 6) had a mean PRx of 0.69 ± 0.21 (P=0.0009). In this sample, PRx monitoring suggested impaired cerebrovascular reactivity at low levels of cerebral perfusion pressure and intact cerebrovascular reactivity at higher levels of perfusion pressure (see figure).

Conclusions: Intact cerebrovascular reactivity quantified by the PRx is associated with survival after severe head trauma in children. The PRx is cerebral perfusion pressure dependent in children. In this cohort, the range of cerebral perfusion pressure in which cerebrovascular reactivity was found to be preserved was higher than the current pediatric guidelines set by the Brain Trauma Foundation.

References:

1) Steiner LA et al. Crit Care Med 2002;30:733-8.

2) Czosnyka M et al. Neurosurgery 1997;41:11,7.

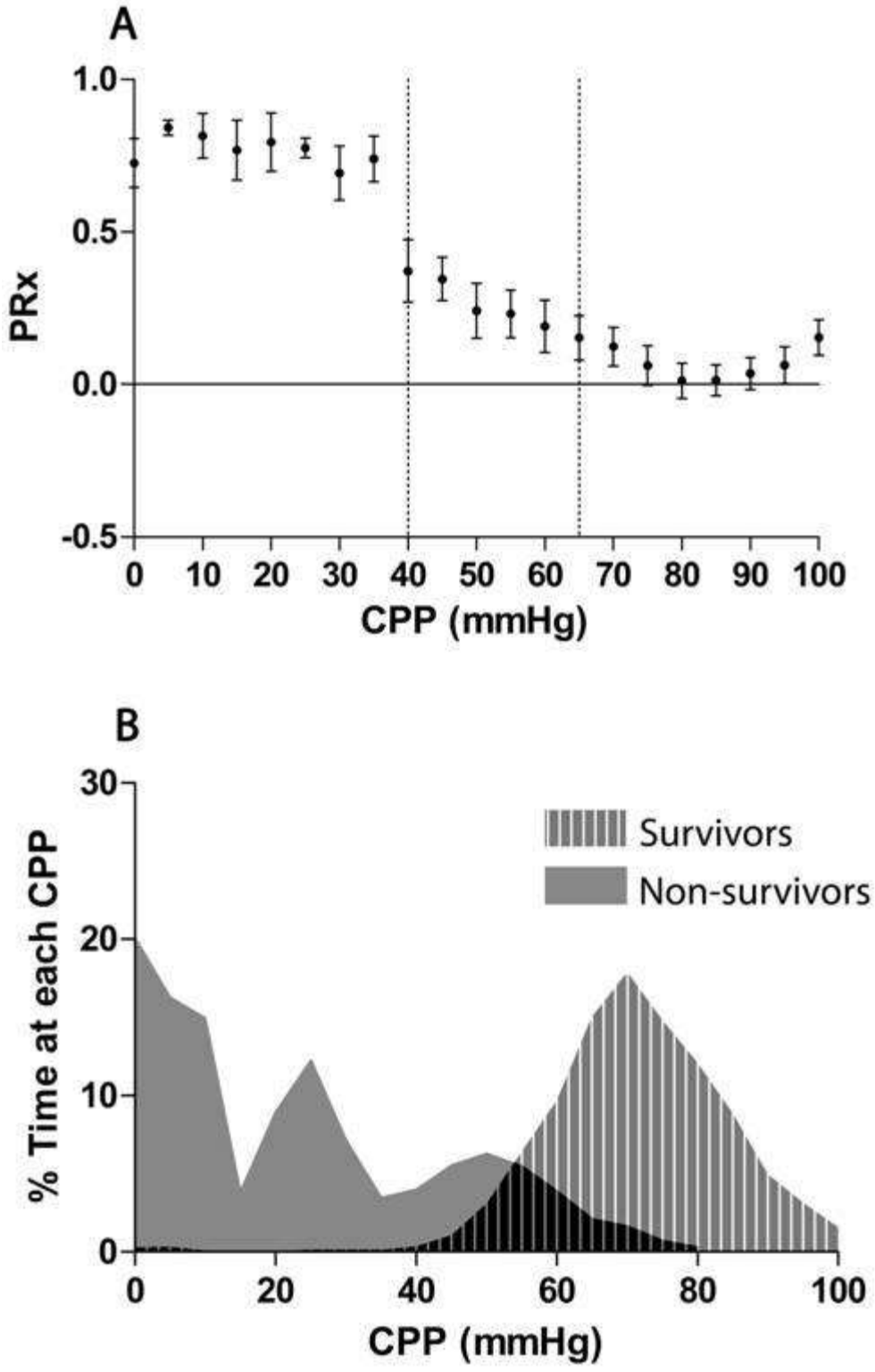

[Pediatric Autoregulation Curves]

Vascular reactivity is cerebral perfusion pressure dependent.

Autoregulation curves were estimated for each of 21 patients by sorting discrete values of PRx

according to cerebral perfusion pressure (CPP). In Panel A, the histogram was created by combining individual curves to create a mean of means (mean PRx ± SE). Vertical lines at 40 mmHg and 65 mmHg indicate the current Brain Trauma Foundation CPP guidelines. High PRx scores, seen below the guideline range, indicate vasomotor paralysis. Mean PRx values within the guideline range show a trend toward improvement with increasing CPP. The trend of PRx worsening with lower CPP is significant ($P < 0.0001$). Panel B shows the percentage of time spent by survivors and non-survivors at each CPP. Non-survivors experienced more time at low cerebral perfusion pressure than did survivors.

DIVERSITY OF NEURAL-HEMODYNAMIC RELATIONSHIPS DEPENDING ON PATTERNS OF CORTICAL PROCESSING DURING BILATERAL SOMATOSENSORY ACTIVATION IN RATS

M. Nemoto, Y. Hoshi, Y. Iguchi

Integrated Neuroscience, Tokyo Institute of Psychiatry, Tokyo, Japan

Objectives: Neural-hemodynamic relationships may vary depending on patterns of cortical processing. The purpose of this study is to investigate how cortical hemodynamics represents neural activity in functional paradigms that drive different patterns of cortical processing, and which facets of neural activity are reflected in hemodynamic changes.

Methods: Ten adult male Sprague-Dawley rats were studied. We introduced functional paradigms consisting of unilateral and bilateral electrical stimulation to rat hindpaws under alpha-chloralose anesthesia, and simultaneously measured broad-band extracellular field potentials and optical intrinsic signals at 586 nm wavelengths, which are associated with changes in CBV, in the somatosensory cortices. We analyzed the field potential signals through frequency-band filtering (local field potential, LFP< 100 Hz; multi-unit activity, MUA>300 Hz, using finite impulse response filters) to estimate synaptic and population spiking activities, and examined LFP-MUA-hemodynamic relationships. In the bilateral stimulation paradigms, we modulated neural interactions by varying time-lag between contra- and ipsilateral stimuli. Furthermore, to assess dependence of their relationships on the temporal structure within the LFPs, we extracted low-frequency (< 25 Hz) and high-frequency (>30 Hz) components from the LFPs. We evaluated differences between the low- and high-frequency components of LFPs in correlations with MUA and hemodynamic responses.

Results: While applying unilateral stimulation, we observed both neural and optical signals in the bilateral somatosensory cortices. Ipsilateral optical responses indicating CBV-increase had peak magnitudes of ~30% and mediocaudal shifts relative to contralateral responses. Correlation analyses revealed different scale factors between the contra- and ipsilateral responses in LFP-MUA and LFP-CBV relationships. While applying bilateral stimulation with varying time-lags, hemodynamic responses were strongly suppressed at 40 and 60 ms time-lags. This hemodynamic suppression quantitatively reflected suppressed LFP responses to contralateral testing stimulation rather than linear summation, with slowly-fluctuating LFP responses to ipsilateral conditioning stimulation. Consequently, CBV-related responses more linearly correlated with MUA than with LFPs in overall responses to bilateral stimulation. However, when extracting high-frequency components (>30 Hz) from LFPs, we found a similar scale factor between the contra- and ipsilateral responses in the LFP-MUA and LFP-CBV relationships, resulting in a significant linear relationship among high-frequency LFPs, MUA and cortical hemodynamics even in overall responses to bilateral stimulation.

Conclusions: There existed diversity of LFP-MUA-hemodynamic relationships depending on patterns of cortical processing during bilateral somatosensory activation. Cortical hemodynamics was not equally susceptible to overall LFP signals but particularly to a certain components of LFP signals. Furthermore, application of broad-band gamma LFPs may restore linear relationships between LFPs and cortical hemodynamics in such complex functional paradigms that drive different cortical processing.

References:

(1) Logothetis, N.K. et al. Nature 412, 150-157 (2001).

(2) Kayser, C. et al. Cereb. Cortex 14, 881-891 (2004).

(3) Niessing, J. et al. Science 309, 948-951 (2005).

(4) Mukamel, R. et al. Science 309, 951-954 (2005).

(5) Nir, Y. et al. Curr. Biol. 17, 1275-1285 (2007).

(6) Privman, E. et al. J. Neurosci. 27, 6234-6242 (2007).

THREE-DIMENSIONAL REALISTIC BRAIN PHANTOM CONTAINING BONE AND GREY MATTER STRUCTURES FOR EVALUATING PET/SPECT IMAGING TECHNIQUES

H. Iida[1,2,3], E. Imabayashi[2], K. Ishida[1], H. Matsuda[2], A. Yamamoto[1], C. Svarer[3]

[1]Dept Investigative Radiology, National Cardiovascular Center Research Institute, Osaka, [2]Dept Nucl Med, Saitama International Medical Center, Saitama Medical University, Saitama, Japan, [3]Neurobiology Research Unit, Rigshospitalet, Copenhagen, Denmark

Introduction: A sophisticated 3-dimensional brain phantom simulating a realistic head model that contains bone and detailed grey matter structures has been developed. Adequacy of the laser-modeling technique for constructing a detailed structure and its usefulness for evaluating a partial-volume effect (PVE) has been tested for PET/SPECT imaging.

Materials and methods: The phantom was made of transparent photo-curable polymer of density 1.09 g/mL, and constructed with the laser-modeling technique. The grey matter structure was designed slice-by-slice by tracing a high-resolution MRI on a healthy volunteer, consisting of cortical grey matter regions, striatum, thalamus, and the cerebellum. Additional component was made for skull structure, to which bone-equivalent solution of K_2HPO_4 was inserted. These multiple slice images were combined to establish two volume compartments, in which axial interpolation was made carefully so that each component does not lose connection. This volume data was then deformed 3-dimensionally to fit to a mannequin head model. Careful attention was made so that the liquid can be diluted to each component without air-bubble contamination. X-ray CT images were acquired to confirm the design structure, and also the bubbles not being contaminated. PET images were then acquired using Siemens ACCEL tomograph with F-18. A sophisticated program for correcting for the partial-volume effect, PVElab [1] has been applied, and the accuracy of the correction was tested.

Results and discussion: The volume of the grey-matter component was 550mL, and the bone 250 mL. The apparent attenuation coefficient for the whole brain was 0.173 cm-1 for Tc-99m, slightly higher than typical values for normal volunteers (0.168 cm^{-1}). Air bubbles have been removed relatively easily from each of compartments, as confirmed with the X-ray CT. X-ray CT also demonstrated a good agreement with the original design of the phantom, suggesting adequacy of the laser-modeling technique. PET images also showed a good agreement with the design after smoothing. The pixel counts in the grey matter area, which varied from region to region, became closer after the PVE correction, as shown in Figure. Counts in frontal and temporal regions relative to striatum was 0.92 and 0.89, which became 0.96 and 0.92, respectively. However, counts in the occipital, parietal, cerebellum regions did not show improvement after PVE correction, which might partly be attributed to misalignment between PET and the anatomical image.

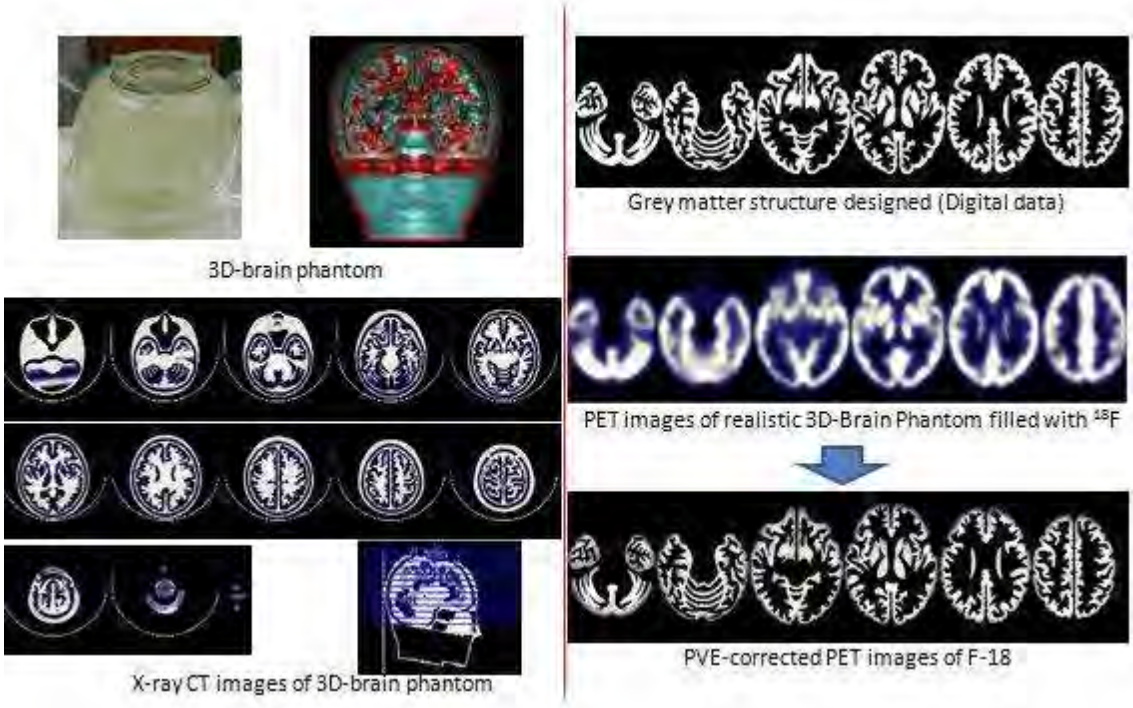

[Phantom design and results for PVE correction]

Conclusion: Use of the realistic 3D-brain phantom may be an adequate approach for evaluating accuracy of various PVE correction techniques in brain PET.

Reference: [1] Svarer C, et al., Neuroimage 24 (4):969-79, 2005.

SIMPLIFIED QUANTIFICATION OF ADENOSINE A_1 RECEPTOR WITH [^{11}C]MPDX AND GRAPHICAL ANALYSIS

Y. Kimura[1,2], M. Naganawa[1,2], M. Mishina[2,3], M. Sakata[1,2], K. Oda[2], K. Ishii[2], K. Ishiwata[2]

[1]Molecular Imaging Center, National Institute of Radiological Sciences, Chiba, [2]Positron Medical Center, Tokyo Metropolitan Institute of GerontologyMetropolitan Institute of Gerontology, Tokyo, [3]Neurological Institute, Nippon Medical School Chiba-Hokusoh Hospital, Chiba, Japan

Objectives: [^{11}C]MPDX is a clinically available radioligand for quantification of the adenosine A_1 receptor (A1R) [1], and its kinetic analysis was reported in [2]. The purpose of this study was to investigate an applicability of simplified graphical algorithms for human studies based on ROI analysis.

Methods: Six normal subjects were included in this study. The dose was 610±126 MBq, and the specific activity was 53±37 MBq/nmol. Dynamic PET scans were performed for 1 hour using SET-2400W (Shimadzu, Kyoto, Japan) in two-dimensional mode with arterial blood sampling. A total of 24 ROIs was placed manually on the summed images: cerebellum (reference), pons, midbrain, caudate, putamen, thalamus, posterior cingulate, and frontal, temporal, occipital, and parietal lobes. The ROI-averaged tissue time activity curves (tTACs) were analyzed using five algorithms: one- and two-tissue compartment models (1T and 2T), Logan graphical analysis (LGA), and a reference LGA with or without a clearance rate of a reference region (k_2) (LGAR-k2 and LGAR-Nok2) [3]. For LGAR-k2, the k_2 in a reference region was derived from the cerebellum using 1T. All graphical analyses were applied after 20-minute post-injection.

Results: The metabolism of [^{11}C]MPDX was slow; the parent fraction was 0.74±0.07 at 60 min after injection. The tTACs were well described using 2T with a constraint of V_{ND} that was estimated from the reference region using 1T. The values of V_T and K_1 ranged from 0.52±0.11 (cerebellum) to 0.72±0.13 mL/cm^3 (posterior putamen) and from 0.10±0.03 (cerebellum) to 0.13±0.04 mL/min/cm^3 (posterior putamen), respectively. The k_2 in reference regions were (0.45±0.11 min^{-1}). The kinetics in reference regions was described using 1T model, and 2T fitting could not give us reasonable V_{ND}, $V_{ND}(1T)=0.98\times V_{ND}(LGA)-0.06$ ($r^2=0.96$). In the graphical analyses, BP_{ND} using the simplified algorithms of LGAR-k2 and LGAR-Nok2 matched well with those using LGA: $BP_{ND}(LGAR\text{-}k2)= 0.99\times BP_{ND}(LGA)+0.01$ ($r^2=0.95$) and $BP_{ND}(LGAR\text{-}Nok2)= 0.96\times BP_{ND}(LGA)-0.01$ ($r^2=0.94$).

Conclusions: Both the simplified algorithms based on Logan graphical analysis without an arterial input function provided corresponding BP_{ND} with those of LGA using an input function in ROI-based analysis. These results implied that LGAR-Nok2 was applicable for the quantification of A1Rs using [^{11}C]MPDX.

References:

[1] Ishiwata, et al., Ann Nucl Med, 16, 377−382, 2002.

[2] Y Kimura, et al., Nucl Med Biol, 31, 975-981, 2004.

[3] J Logan, et al., J Cereb Blood Flow Metabo, 16, 834-840, 1996.

Acknowledgement: This work was supported by Grants-in-Aid for Scientific Research (B) No. 20390333, (B) 20390334 and (B) No. 16390348.

CEREBRAL PERFUSION IN PATIENTS AFTER ACUTE ANEURYSMAL SAH WITH OR WITHOUT INTRAVENOUS MAGNESIUM SULFATE INFUSION

G. Wong, R. Kwok, D. Yeung, A. King, A. Ahuja, K. Tang, W. Poon

The Chinese University of Hong Kong, Hong Kong, Hong Kong S.A.R.

Objective: A meta-analysis of current data suggests that magnesium sulfate infusion improves the outcome after aneurysmal subarachnoid hemorrhage through a reduction in delayed ischemic neurological deficit. Two multi-center randomized controlled trials are currently underway to investigate this hypothesis. The possible pharmacological basis of this hypothesis includes neuroprotection and vasodilatation. We aim to investigate the cerebral hemodynamic effects of magnesium sulfate infusion in aneurysmal subarachnoid hemorrhage patients.

Method: A total of 12 patients who had experienced aneurysmal subarachnoid hemorrhage were randomized to magnesium sulfate infusion (n=6) or placebo infusion (n=6) for 14 days. Each patient had two perfusion MRIs performed, one in the first week after subarachnoid hemorrhage and one in the second week after subarachnoid hemorrhage.

Results: Age, sex, and Fisher CT grade were not different between the two groups. All but one patient were of WFNS Grade I to II on presentation. No patient developed delayed ischemic neurological deficit. There was no increase in rCBV, rCBF and MTT between the two perfusion scans within the same group or between the two groups.

Conclusion: Magnesium sulfate infusion, in the dosage of current clinical trials, did not increase cerebral blood volume and cerebral blood flow, as postulated by dilation of small vessels and/or collateral pathways.

933

Brain Poster Session: Hemorrhagic Transformation

HEMORRHAGIC STROKE ASSOCIATED WITH POOR OUTCOME AFTER INFECTIVE ENDOCARDITIS

T. Ohtsuki, E. Nomura, S. Aoki, Y. Sueda, T. Kono, K. Kawase, K. Ochi, T. Ohshita, T. Nakamura, T. Kohriyama, M. Matsumoto

Department of Neurology, Hiroshima University Hospital, Hiroshima, Japan

Objectives: Infective endocarditis causes not only ischemic stroke by bacterial emboli, but also hemorrhagic stroke by inflamed arteries or aneurysms prone to rupture that often makes our decision for the requisite surgery hard. We examined if hemorrhagic stroke detected by CT was associated with poor outcome after stroke caused by infective endocarditis, as compared with pure ischemic stroke.

Patients and methods: We conducted the observational study on 22 consecutive patients (12 men, aged 23-82, median 57) with acute symptomatic stroke after definite or possible infective endocarditis according to the Duke University criteria from October 2005 to September 2008. Brain hemorrhage and infarction responsible for neurological signs were verified by CT and diffusion-weighed image of MRI, respectively. We evaluated modified Rankin Scale (mRS) at 3 months after stroke and divided each patient into either favorable outcome with mRS score of 0 to 1 or poor outcome of from disability to death, mRS score of 2 to 6. Best medical treatment and surgical repair of the damaged heart valves that cardiovascular doctors decided for if necessary were provided to each patient according to the Japanese Circulation Society guideline for treatment of infective endocarditis.

Results: While 2 hemorrhage and 13 infarction were noted in 15 patients of the favorable outcome group, 7 patients of the poor outcome group consisted of subarachnoid hemorrhage in 3, parenchymal hematoma on infarcts in 3 and multiple infarction in 1. Out of the poor outcome group, 4 died of recurrent intracranial bleeding. The poor consequence group had brain hemorrhage detected by CT more frequently than the favorable outcome group ($p < 0.01$: Mann-Whitney U-test). Statistically observed between the poor outcome and favorable outcome groups were no significant differences of age, gender, presence of disturbed consciousness or hemiplegia on admission, involvement of mitral valve, attachment of 1-cm or larger vegetations to valves, isolation of staphylococcus aureus from blood, recurrence of stroke, embolization to other organs than the brain and complication of meningitis/brain and intraocular abscess.The 8 of 13 ischemic patients had cardiac valves repaired 2 to 4 weeks after stroke to lead to favorable outcome. In contrast, out of 9 hemorrhagic stroke patients 4 cancelled the expected operations, while 5 underwent open-heart surgery, one of which led to parenchymal hematoma in vain during surgery. As a result, 6 of 8 hemorrhagic stroke led to poor prognosis, while 13 out of 14 ischemic stroke got advantageous outcome. Poor outcomes were more frequent in hemorrhagic stroke than in infarction (Hazards ratio 39.0: 95% CI, 2.9-518).

Conclusions: Hemorrhagic stroke on CT was independently associated with poor neurological outcome after infective endocarditis, as well as the formidable complication of intracranial hemorrhage during extracorporeal circulation as described previously (1), that could make us deferring open-heart surgery after infective endocarditis.

Reference: 1. Ruttmann E et al. Neurological outcomes of septic cardioembolic stroke after infective endocarditis. Stroke 37:2094-2099, 2006.

Brain Poster Session: rt-PA

CHANGES IN ARRIVAL TIME TO HOSPITAL FROM ONSET OF CEREBRAL INFARCTION IN THE T-PA ERA

S. Takagi, S. Takizawa, F. Yoshii, H. Takahashi, W. Takahashi, E. Nagata, Y. Ohnuki, T. Ishikawa, Y. Ohnuki, R. Kumazawa, S. Kontani, Y. Tsukamoto, Y. Moriya, E. Sakabe, A. Mizuma

Neurology, Tokai University School of Medicine, Isehara-shi, Kanagawa-ken, Japan

Background: Tissue plasminogen activator (t-PA) has been used to treat acute cerebral infarction for more than 10 years. In order to increase the number of patients who benefit from t-PA, early arrival of patients to the hospital is essential. Efforts to facilitate early arrival include:

1. giving appropriate information to public, physician, and ambulance, and
2. medical control over an ambulance department.

Purpose: The purpose of this presentation is to find out whether the arrival of stroke patients to the hospital after onset is getting earlier or not in the t-PA era.

Subjects and method: The subjects included 71 and 62 patients with acute cerebral embolism admitted to the Neurological and Cerebrovascular Center of Tokai University Hospital in the first year (from November 2005 to October 2006) and the second year (from November 2006 to October 2007), respectively. The age was 72 ± 11, and 73 ± 14, respectively. We evaluated medical records and calculated arrival time of these patients.

Results: In the first year, 36 of 71 (50.7%) patients came to hospital within 2 hours after onset. t-PA was used in 13 of these 36 (37.1%) patients. In the second year, 35 of 62 (56.5%) patients came to hospital within 2 hours after onset. t-PA was used in 15 of these 35 (42.9%) patients. In total, 13 of 71 (18.3%) patients with cerebral embolism were treated using t-PA in the first year, and this rate was increased to 15 of 62 (24.2%) in the second year.

Discussion and conclusion: Our data showed that patients come to hospital earlier in the second year, and that the frequency of using t-PA in the early-arrived patients is also getting higher in the second year. In order to increase the number of patients who benefit from t-PA, firstly, continuous effort is necessary to facilitate further the early arrival of patients. Secondly, enough human power and inter- and intra-department collaboration is necessary. Thirdly, the indication of t-PA should be re-evaluated, from the aspect of time window, age, severity, and so on.

GENETICALLY MODIFIED MESENCHYMAL STEM CELLS ARE MORE EFFECTIVE THAN UNMODIFIED IN REDUCING INFARCT VOLUME IN RODENT MCAO MODELS: A META-ANALYSIS

N. Karlupia[1], M. Prasad[2], K. Prasad[1]

[1]Neurology, All India Institute of Medical Sciences, Delhi, [2]Pt. B. D. Sharma PG Institute of Medical Sciences, Rohtak, India

Objective: To determine through meta-analysis the magnitude and consistency of effects on infarct volume with the use of genetically modified Mesenchymal stem cell (MSC) transplantation as compared to primary MSCs (control group), in rodent models of stroke.

Methods: Stem cell intervention studies were identified through a high sensitivity search of Pubmed. We used multiple search strategies to identify the studies. Hits obtained with different key terms (written in parenthesis) were 117{[human stem cells] AND [stroke in rats]}, 24{[human mesenchymal stem cells] AND [stroke in rats]}, 11{[hMSCs] AND [stroke in rats], upto 2008; 44{[MCAo] AND [stem cells]} from 2003 to 2008. The quality assessment of the studies was done independently by two reviewers with an overall agreement of 98.4%. As there was significant heterogeneity, relevant data were synthesized using random effect model of DerSimonian and Laird in Revman 4.2.7 software, to obtain standardized mean difference and 95% confidence interval (CI) for volume of infarction.

Results: We scanned the titles of 117 studies and abstracts of 79 studies to select eight studies for the meta-analysis in rodent MCAo models (five permanent and three transient). Studies were excluded if the primary outcome was not infarct volume or if the treatment group was not of genetically modified mesenchymal stem cells. One study (Kurozumi et al.2005) was excluded because the effect of primary stem cell group on infarct volume was not measured. The number of rats per group varied from 5 to 46. The cell dose ranged from 0.5 to 10 million cells. The time between occlusion and cell administration was three hours (two studies), six hours (two studies), 12 hours (one study) and 24 hours (two studies). Treatment with genetically modified mesenchymal stem cells resulted in statistically significant reduction in infarct volume (standardized mean difference -3.06 [-4.70 -1.42]) as compared to primary mesenchymal stem cells, but there was substantial heterogeneity ($P< 0.00001$, $I^2=82.1\%$).

Conclusion: Pre-clinical studies in rodent stroke models lead to reduction in infarct volume with the use of modified stem cells as compared to primary MSCs, but the results are heterogenous. More studies are required to investigate the factors responsible for the heterogeneity.

References:

Macleod M R etal.2004 ; Kurozumi K etal. 2004; Ikeda et al 2005.

Nomura T et al.2005; Honma T, etal. 2006; Horita Y etal. 2006; Liu H, et al. 2006.

Brain Poster Session: Cerebral Vascular Regulation

EFFECTS OF ACUTE VS. CHRONIC ERYTHROPOIETIN TREATMENT AND O_2 AVAILABILITY ON THE CARDIO- AND CEREBROVASCULAR RESPONSES TO EXERCISE IN HUMANS

P. Rasmussen[1], J.J. van Lieshout[2], R. Krogh-Madsen[1], J.J. Thomsen[1], C. Lundby[1], Y.-S. Kim[2], N.V. Olsen[1], N.H. Secher[1], S. Ogoh[3], P.B. Raven[3]

[1]University of Copenhagen, Copenhagen, Denmark, [2]AMC Center for Heart Failure Research, Academic Medical Center, University of Amsterdam, Amsterdam, The Netherlands, [3]University of North Texas, Health Science Center, Fort Worth, TX, USA

Erythropoietin (EPO) is a glycoprotein, regulating red cell production in humans with additional cell protective effects. EPO increases blood pressure following prolonged administration, but it is unknown whether this influences the cerebral vasculature. We hypothesized that EPO treatment enhances the effects of exercise on systemic and cerebrovascular vascular resistance, with potential consequences for blood pressure, cardiac output, and cerebral blood flow. We further addressed whether EPO affects cerebrovascular vs. systemic vascular control differently, considering that cerebral blood flow control has been reported as being tightly regulated. We measured the acute cardio- and cerebrovascular effects of a 3 day high dose vs. 3 month low dose EPO treatment on blood pressure, cardiac output, systemic vascular resistance, global cerebral arterio-venous differences for oxygen, glucose and lactate, as well as the regional transcranial Doppler-determined cerebral blood flow velocity at rest and during exercise. Dynamic cerebral autoregulation was assessed by transfer function analysis. EPO, regardless of dosage, increased blood pressure and cerebral blood flow velocity, but reduced cardiac output and increased cerebral arterio-venous differences for oxygen without an effect on dynamic cerebral autoregulation. In conclusion, EPO is a potent vasoconstrictor also encompassing the cerebral arteries without affecting cerebral autoregulatory capacity.

Brain Poster Session: Cerebral Vascular Regulation

QUANTITATIVE MEASUREMENT OF BLOOD FLOW IN THE RETINA AND BRAIN OF DIABETIC RATS BY AUTORADIOGRAPHY USING [^{14}C]-IMP

M. Pouliot[1,2], S. Hétu[1,2], R. Couture[2], E. Vaucher[1]

[1]School of Optometry, [2]Department of Physiology, Université de Montréal, Montreal, QC, Canada

Objectives: Quantitative and regional measurement of retinal blood flow in rodents is of prime interest for the investigation of regulatory mechanisms of ocular circulation in physiological and pathological conditions. In this study, a quantitative autoradiographic method using N-isopropyl-p-^{14}C-iodoamphetamine ([^{14}C]-IMP), a diffusible radioactive tracer, was evaluated for its ability to detect changes in retinal blood perfusion during hypercapnic challenges. Findings were compared to cerebral blood flow values measured simultaneously. Moreover, this technique was used to measure early blood flow changes in the retina and brain of diabetic rats, since microvascular damage is an early event in diabetes and could lead to retinopathy and blindness.

Methods: Hypercapnia was induced in awake Wistar rats by inhalation of 5% or 8% CO_2 in medical air 5 minutes prior to [^{14}C]-IMP injection (100 µCi/kg, 30s) in the femoral vein. Two minutes later, the rat was sacrificed, the brain and eyes were harvested, then frontal cortex and retinas were dissected out. The cortex and one retina were digested overnight in soluene and the amount of radioactivity was determined with a scintillation counter. The other retina was whole-mounted on a glass slide and processed for autoradiography. Type 1 diabetes was induced in male Wistar rats by a single i.p. injection of Streptozotocin (STZ, 65 mg/kg) while age-matched controls received sodium citrate buffer vehicle. Retinal and cerebral blood flows were measured 6 weeks after diabetes induction.

Results:

	Control (n=9)	5% CO_2 (n=4)	8% CO_2 (n=5)		Vehicle (n=7)	Diabetes (n=7)
Retinal blood flow(ml/100g/min)	**92 ± 21**	**110 ± 13**	**121 ± 7***		**74 ± 9**	**66 ± 16**
Cerebral blood flow (ml/100g/min)	**97 ± 4**	**197 ± 18***	**218 ± 3***		**104 ± 19**	**74 ± 22**
Mean blood pressure (mmHg)	113 ± 13	116 ± 5	116 ± 2		119 ± 15	122 ± 9
pCO_2 (mmHg)	38 ± 2	58 ± 4*	104 ± 16*		39 ± 1	33 ± 5 †

pO_2 (mmHg)	86 ± 4	107 ± 9*	103 ± 7*		86 ± 4	87 ± 6

*p≤0.05, Mann-Whitney test CO_2 compared to controls; † p≤0.01 Student t-test STZ compared to vehicle

[Blood flow and physiological parameters]
Physiological parameters changed as expected related to the treatment. Retinal and cerebral blood flows were significantly increased under hypercapnic conditions. The blood flow changes were uniform amongst all retinal regions examined. Retinal and cerebral blood flows were not significantly affected in STZ-diabetic rats.

Conclusions: Retinal blood flow changes could be quantified by this autoradiographic method using [^{14}C]-IMP. The results further showed that retinal blood flow is not affected in early diabetes and is not a primary event leading to retina damage in diabetic retinopathy.

942

Brain Poster Session: Experimental Cerebral Ischemia: In Vitro

ACTIVATION OF PROTEIN KINASE C DELTA FOLLOWING OXYGEN GLUCOSE DEPRIVATION LEADS TO RELEASE OF CYTOCHROME C FROM MITOCHONDRIA

M. Perez-Pinzon, K. Dave, A. Raval, R.A. DeFazio, I. Saul

Neurology, University of Miami, Miami, FL, USA

Objectives: Mitochondrial damage including release of pro-apoptotic factors such as cytochrome c from mitochondria following cerebral ischemia is a key event leading to cell death. In a previous study we observed release of cytochrome c and activation of δPKC following cerebral ischemia occurred closed to each other[1,2]. However, the mechanism by which early activation of δPKC leads to cytochrome c release is not understood. In the present study we tested hypothesis that early activation of δPKC following cerebral ischemia phosphorylates protein phosphatase 2A (PP2A) leading to release of cytochrome c from mitochondria via activation of pro-apoptotic factor BAD.

Methods: To test this hypotheses, we used an asphyxial cardiac arrest (CA) model of cerebral ischemia in rats where we studied translocation of δPKC from cytosol to mitochondria, release of cytochrome c from mitochondria, and the extent of BAD (ser 136) phosphorylation by Western blotting at 1 h of reperfusion following 8 min of CA. Mechanistic studies were performed using synaptosomes as a model system. Synaptosomes were subjected to 60 min of oxygen glucose deprivation (OGD) in presence of δPKC inhibitor peptide (Tat- δV1-1) or carrier peptide (Tat) alone.

Results: Levels of δPKC increased in the mitochondrial fraction by 99±19% ($p< 0.02$, n=4) and cytochrome c increased in cytosolic fraction by 76±14% ($p< 0.05$, n = 4) in CA group when compared to sham CA group. BAD phosphorylation decreased by 46±6% ($p< 0.005$, n=4) in CA animals vs. Sham treatment. These results suggest that early activation of δPKC initiates the release of cytochrome c from mitochondria by decreasing phosphorylation of BAD via activation of PP2A. To confirm the role of δPKC following cerebral ischemia, we used synaptosomes as a model system. OGD increased levels of δPKC in mitochondria by 72% ($p< 0.05$, n = 4). OGD in presence of δPKC inhibitor peptide (Tat- δV1-1) decreased cytochrome c release by 71% (n = 4, $p< 0.004$) and increased BAD phosphorylation by 312% (n = 4, $p< 0.01$) as compared to the Tat control group. Similarly, OGD in presence of PP2A inhibitor okadaic acid, prevented OGD induced cytochrome c release by 52% (n = 4, $p< 0.05$) and BAD dephosphorylation by 144% (n=4), respectively. The protein phosphatase 1 inhibitor calyculin had no effect.

Conclusion: These results suggest that early activation of δPKC following OGD initiates the release of cytochrome c from mitochondria by decreasing phosphorylation of BAD via activation of PP2A.

References:

1) Bright et al. J Neurosci. 2004, 24:6880.

2) Raval et al. J Cereb Blood Flow Metab. 2005, 25:730.

Support: PHS grants NS34773, NS05820, NS045676 and NS054147.

943

BrainPET Poster Session: Kinetic Modeling

A CONSISTENT GRAPHICAL ANALYSIS METHOD TO QUANTIFY NON-EQUILIBRIUM TRACER KINETICS IN LIGAND-RECEPTOR DYNAMIC PET STUDIES

Y. Zhou, W. Ye, J.R. Brasic, M. Guevara, D.F. Wong

Department of Radiology, Johns Hopkins University, Baltimore, MD, USA

A new graphical plot (nGP) was recently proposed to quantify tracer kinetics that attain equilibrium relative to plasma input as $t \geq t^*$ in radioligand receptor dynamic PET studies [1].

Objectives: The objectives of the study are:

1. to extend the nGP for quantification of non-equilibrium tracer kinetics relative to plasma input and
2. to evaluate the extended nGP method by human dynamic PET studies.

Methods: A bi-graphical plot (BiGP), consisting of the Patlak plot and the nGP, was first derived to estimate distribution volume (DV). [11C]CFT (19), [11C]diprenorphine ([11C]DNP) (26), and [11C]MDL100,907 ([11C]MDL) (10) human dynamic PET studies with metabolite-corrected plasma input were studied for dopamine transporter, opiate receptor, and serotonin receptor 5HT2A imaging, respectively. Eleven regions of interest (ROIs) were defined on coregistered MRIs and applied to dynamic PET for ROI time activity curves (TACs). The ratio of ROI TAC to plasma input was calculated to evaluate whether the ROI TAC would attain relative equilibrium states. For comparison, the BiGP, the Logan plot (LP), and a two-tissue compartment model (2TCM) with nonlinear regression were applied to ROI TACs for DV estimation. The BiGP with a spatial constraint algorithm was developed to generate DV images, and the ROI estimates from DV images were compared to the estimates from ROI TACs. The DV images generated by the BiGP and the LP were compared.

Results: The ratio of ROI TAC to plasma input increased linearly as $t \geq 40$ min in all ROIs except cerebellum in [11C]CFT and occiptal cortex in [11C]DNP. The plots from BiGP and the LP attained straight lines for $t \geq 40$ min. The DVs obtained by the BiGP were linearly correlated ($R^2 = 0.99$) to those estimated by the 2TCM, and the LP from ROI TACs with very comparable magnitudes (Fig. 1). For the ROI estimates from DV images using the BiGP, DV(images) = 1.00DV(ROI TACs) - 0.22, $R^2 = 0.97$, for all ROIs of the 3 tracer studies. In contrast to the DVs from ROI TACs, the ROI estimates from the DV images generated by the LP were underestimated ((13±2)%, (51±8)%) in (cerebellum, striatum), ((22±5)%, (68±8)%) in (occipital, thalamus), and ((39±12)%, (68±9)%) in (cerebellum, lateral temporal cortex) for the [11C]CFT, the [11C]DNP, and the [11C]MDL, respectively. The computational time for generating DV images was reduced by 71% on average by the BiGP in contrast to the LP.

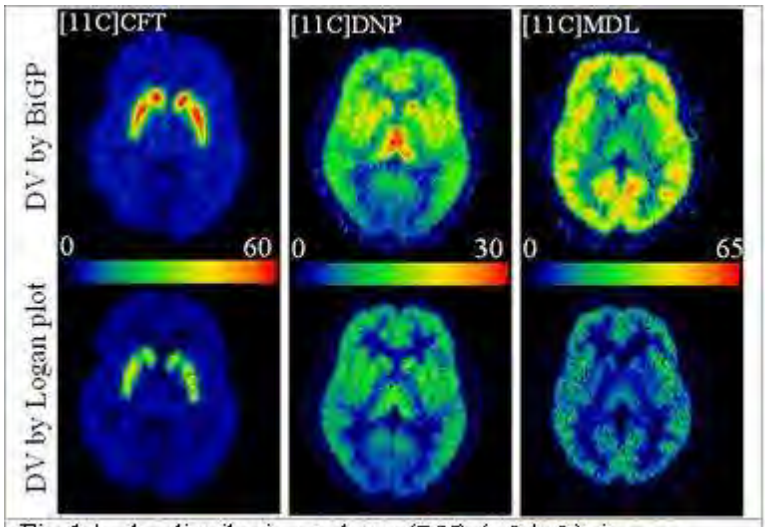

Fig.1A. the distribution volume (DV) (mL/mL) images generated by the BiGP and the LP from three typical human dynamic PET studies.

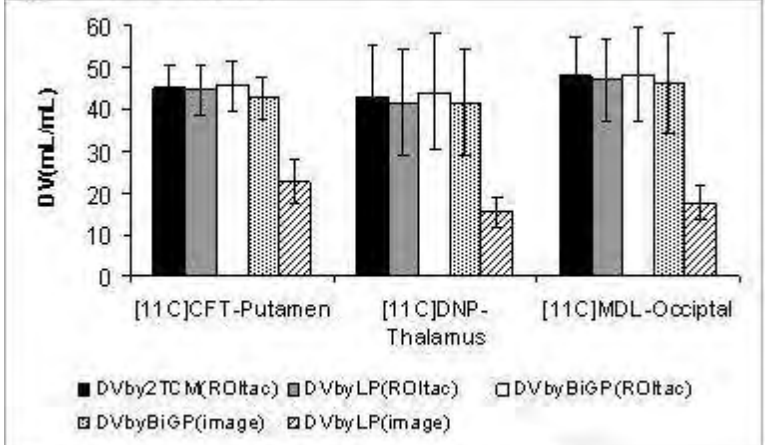

Fig.1B. The means ± SDs of ROI DV estimates.

[DV images and Mean (SD) of ROI DVs]

Conclusions: The BiGP is a consistent and computationally efficient graphical method for estimating DV from non-equilibrium tracer kinetics in both ROI and pixel levels.

Reference: [1] Zhou et al., 2009. Neuroiamge 44(3): 661-670.

This work was supported in part by NIH grants MH078175, DA000412, and AA012839.

VENTRICULAR FIBRILLATION INDUCED CARDIAC ARREST IN THE RAT AS A MODEL OF GLOBAL CEREBRAL ISCHEMIA

K. Dave, D. Della-Morte, I. Saul, M. Perez-Pinzon

Neurology, University of Miami, Miami, FL, USA

Objectives: Cardiopulmonary arrest (CA) remains one of the leading causes of death and disability in the USA. Although ventricular fibrillation (VF) models in rodents mimic the "square wave" type of insult (rapid loss of pulse and pressure) commonly observed in adult humans at the onset of CA, those approaches are not popular because of complicated animal procedure, poor animal survival and thermal injury[1,2,3]. Here we present modified, improvised, simple, reliable, ventricular fibrillation-induced rat model of CA that could be useful in studying the mechanisms of cerebral ischemia induced delayed cell death as well as efficacy of neuroprotective drugs.

Methods: CA was induced in male Sprague-Dawley rats weighing 300 - 370 g using modified method from von Planta[3]. In brief, VF was induced in anesthetized, paralyzed, mechanically ventilated rats by an alternating current delivered to the entrance of the superior vena cava. The electrode was placed at the correct location using a fluoroscope. The fluoroscope enabled us to lower the VF-inducing current, and identify the exact location to place the electrode and overcome minor rat-to-rat anatomical differences. The head and body temperatures were maintained at 37°C using heating lamp and heating pad, respectively. After 5 min 30 seconds, resuscitation was initiated by administering a bolus injection of epinephrine and sodium bicarbonate followed by mechanical ventilation and manual chest compressions and counter shocked with a 10-J DC current. Neurologic deficit score (NDS) was quantified up to three days of reperfusion. Seven days after ischemia, rat brains were fixed for histopathological assessment. Hippocampal sections at the level of 3.8 mm posterior to bregma were examined for normal neurons.

Results: During the induction of CA, an immediate VF was observed followed by a sudden drop in blood pressure to close to 0 mmHg. When the fibrillating current was stopped, asystole was observed and blood pressure remained zero mmHg until resuscitation. Ten minutes after resuscitation, ECG appeared normal. After 10 minutes of VF all rats returned to normal sinus rhythm with a heart rate of 367±22 beats per min and exhibited normal electrical heart conduction. In CA rats at 3, 24, 48 and 72h following CA, NDS score was 63±5, 26±2, 14±2 and 6±1, respectively. The NDS remained zero at all time points studied in sham rats. The number of normal neurons in the CA1 hippocampal region in sham CA rats was 1263±43 (n=6). The number of normal neurons was decreased by 79% (261±58, n=5, $p < 0.001$) in CA group as compared to the sham CA group. No signs of thermal injury were observed at the site of electrode placement.

Conclusion: The presently described ventricular fibrillation-induced model of cardiac arrest in rat as a model of whole body ischemia provides a tool to study the mechanism of cardiac arrest-induced neuronal death without compromising heart functions.

References:

1) Chen et al. Am J Emerg Med, 25, 2007, 623.

2) Chen et al. Resuscitation, 74, 2007, 546.

3) von Planta et al. J Appl Physiol 65, 1988, 2641.

Support: PHS grants NS34773, NS05820, NS045676 and NS054147.

945

BrainPET Poster Session: Molecular Brain Imaging: Clinical Applications

REDUCTION OF MGLUR5 BINDING SITES IN HIPPOCAMPI FROM PATIENTS WITH PHARMACO-RESISTANT TEMPORAL LOBE EPILEPSY: AN AUTORADIOGRAPHIC STUDY

L. Minuzzi[1], E. Kobayashi[2], J. Hall[2], M.-C. Guiot[3], F. Andermann[2], F. Dubeau[2], M. Diksic[2], G. Massarweh[4], J.-P. Soucy[4], P. Rosa-Neto[1]

[1]Translational Neuroimaging Laboratory - MCSA, Douglas Hospital, McGill University, [2]Department of Neurology and Neurosurgery, [3]Department of Pathology, [4]Brain Imaging Center, Montreal Neurological Institute, McGill University, Montreal, QC, Canada

Objectives: Metabotropic glutamate receptors (mGluR) have an important role in the regulation of neuronal excitability. Immunohistochemistry studies have found abnormalities in the mGluR type 5 (mGluR5) in the hippocampus of patients with temporal lobe epilepsy (TLE). The objective of this study is to determine the maximum concentration and affinity of mGluR5 in cryosections of human hippocampus from healthy controls and TLE patients who underwent surgical treatment for refractory seizures. In vitro quantitative autoradiography was performed using the mGluR5 radioligand [^{3}H]ABP688.

Methods: Human hippocampi were obtained from five healthy controls (Brain Bank, Douglas Hospital) and five patients operated for refractory TLE (Montreal Neurological Institute). The tissue was cryosectioned at 20 μm and a saturation binding study was carried out according to Hintermann et al. (2007) with some modifications. The slides were pre-incubated for 20 min in buffer containing 30 mM Na-HEPES, 110 nM NaCl, 5 mM KCl, 2.5 mM $CaCl_2$ and 1.2 mM $MgCl_2$ (pH 7.4) and then incubated for 60 min in the presence of [^{3}H]ABP688 (74 Ci/mmol) at a range of concentrations from 0.125 to 8 nM. Non-specific binding was determined with addition of 10 μM MPEP. The slides were washed (3x5 min) in cold buffer, dipped in ice-cold water and dried. The sections along with autoradiographic standards were exposed for five days to phosphor imaging plates. The Bmax and KD of [^{3}H]ABP688 from both groups were calculated by saturation binding analysis and compared using F-test ($p< 0.05$).

Results: Saturation binding of [^{3}H]ABP688 revealed higher Bmax in the control group in comparison to patients (1.31±0.06 and 0.89±0.16 pmol/mg of tissue, respectively). The 30% reduction of Bmax in the epileptic hippocampi was statistically significant ($p=0.01$). Control group showed slightly higher KD (1.43±0.2 nM) in comparison to the epileptic group (1.0±0.5 nM) with no statistical difference.

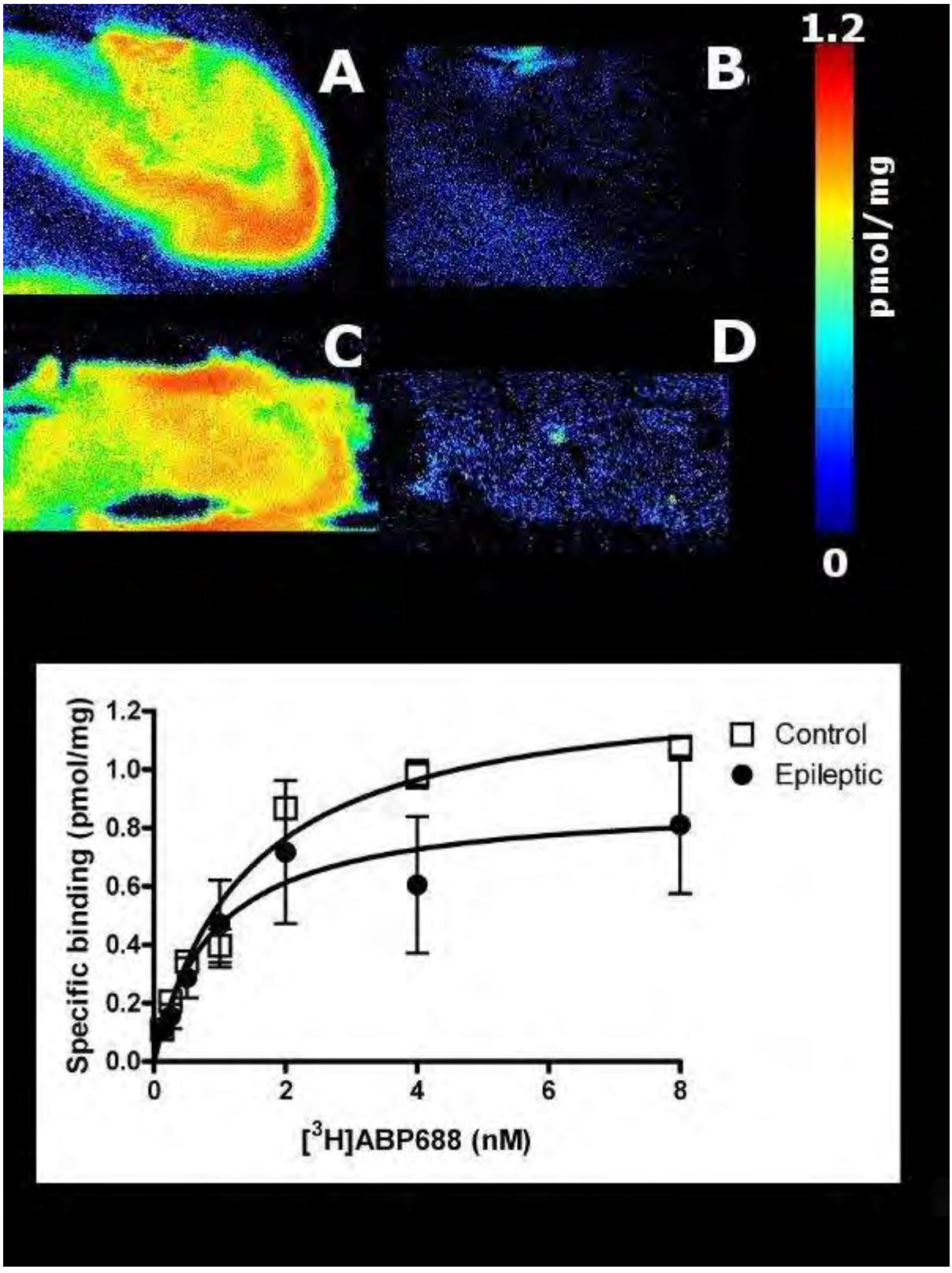

[Binding of [3H]ABP688 in controls and epillepsy]

Conclusions: The present study showed a reduction of the total amount of mGluR5 in epileptic

hippocampi in comparison to controls. Autoradiography provides gold standard quantification of receptors in human tissue, establishing the mGluR5 reduction in hippocampus as a possible phenomenon involved in the hyperexcitable circuitry in the seizure focus. This reduction is in agreement with in vivo mGluR5 binding studies with positron emission tomography performed in these same patients before the surgical treatment.

References:

1. Hintermann, S., I. Vranesic, et al.(2007). ABP688, a novel selective and high affinity ligand for the labeling of mGlu5 receptors: identification, in vitro pharmacology, pharmacokinetic and biodistribution studies. Bioorg Med Chem 15(2):903-14.

2. Notenboom, R. G., D. R. Hampson, et al.(2006). Up-regulation of hippocampal metabotropic glutamate receptor 5 in temporal lobe epilepsy patients. Brain 129:96-107.

3. Tang F-R, Lee W-L.(2001). Expression of the group II and III metabotropic glutamate receptors in the hippocampus of patients with mesial temporal lobe epilepsy. J Neurocytol 30:137-43.

946

Brain Poster Session: Angiogenesis

SYMPATHETIC DENERVATION DIFFERENTIALLY MODULATES DIRECT TROPHIC EFFECTS OF VEGF ON CONTRACTILE DIFFERENTIATION IN OVINE FETAL MIDDLE CEREBRAL ARTERIES

S. Butler, J. Abrassart, J. Williams, W. Pearce

Center for Perinatal Biology, Loma Linda University School of Medicine, Loma Linda, CA, USA

Objectives: Perivascular nerves dramatically influence the growth and functional maturation of cerebral arteries (1), but the mechanisms involved remain uncertain. Norepinephrine (NE) released from perivascular nerves may directly stimulate the gene transcription and protein synthesis governing vascular maturation (3). Alternatively, patterns of vascular activation may predominantly influence cerebrovascular development, as predicted by the "excitation-transcription" hypothesis (2); NE release could indirectly "prime" arterial reactivity to growth factors, such as VEGF, which in turn could regulate transcription. The present study tested this hypothesis.

Methods: In fetal lambs at 124d gestation (term≈143d) the left superior cervical ganglion was preganglionically denervated. After denervation the fetuses were returned to the womb and maintained for 14 days, at which time their middle cerebral arteries were harvested.

Contractile characteristics of intact and denervated fetal middle cerebral arteries were determined immediately after sacrifice, and after 48 hours of organ culture. In organ culture, arteries were serum starved in DMEM with: 30 ng/ml VEGF; 10 μM NE; 30 ng/ml VEGF plus 10 μM NE; or no additions (control). The contractility protocol measured myogenic stresses (dynes/mm^2), active stresses (120 mM potassium), and passive stresses (5 mM EGTA) at graded stretch. Young's Modulus was calculated to quantitate artery stiffness. After contractility measurements, segments were sectioned and imaged following fluorescent immunohistochemical staining for smooth muscle α-actin and Myosin Light Chain Kinase to identify smooth muscle phenotypic changes.

Results: Sympathectomy generally had opposite effects on VEGF- and NE-induced changes in culture. It enhanced VEGF-induced loss of stiffness, but enhanced NE-induced increases in stiffness. Sympathectomy enhanced loss of myogenic tone during serum starvation, eliminated VEGF-induced increases in myogenic tone but enhanced NE-induced increases. Sympathectomy enhanced active tone after serum starvation, enhanced VEGF-induced depression of active tone, and attenuated NE-induced increases in active tone. The effects of VEGF and NE on stiffness, myogenic tone, and active tone were additive in control arteries, but competitive following denervation. Imaging revealed that serum starvation enhanced smooth muscle proliferation and contractile dedifferentiation, and that these effects were amplified by VEGF but attenuated by NE in control arteries. Sympathectomy further enhanced these competitive effects of VEGF and NE on smooth muscle phenotype.

Conclusion: These results demonstrate that perivascular NE release stimulates contractile maturation and increased stiffness in cerebral arteries though both direct effects on contractile protein expression, and through indirect inhibition of VEGF-induced proliferative influences. Because NE-mediated influences were interrupted by preganglionic denervation, physiological patterns of perivascular NE release appear critical for normal vessel development; this helps explain why attempts to restore trophic effects of NE by readdition have been unsuccessful. These results also suggest that both the direct effect (3) and "excitation-transcription" (2) hypotheses apply to cerebrovascular maturation. These findings have important consequences for neonates with cerebrovascular injury sufficient to compromise the perivascular adrenergic innervation, and thus the normal development of cerebral artery structure and function.

References:

1. Bevan RD, Tsuru H, Bevan JA. (1983) Stroke 14:393-396.

2. Wamhoff BR, Bowles DK, Owens GK. (2006) Circ Res 98:868-878.

3. Zhang H, Faber JE. (2001) Circ Res 89:815-822.

947

Brain Oral Session: Experimental Cerebral Ischemia: Neuroinflammation

A CELL TYPE SPECIFIC ROLE FOR MYD88 FOLLOWING ISCHEMIC INSULT

P.J. Crack, C.E. Downes, C.H.C. Wong, P. Guio

Pharmacology, The University of Melbourne, Melbourne, VIC, Australia

Objectives: Myeloid differentiation factor 88 (MyD88) is an adaptor protein that is integral to many immune linked pathways including certain Toll Like Receptors (TLR). This study is designed to understand the role of MyD88 in coordinating inflammatory pathways in the brain that are activated after ischemia/reperfusion injury. Data generated through this study suggests a complex role for MyD88 during ischemic insult, involving both pro-survival and pro-death signalling.

Methods: Primary fibroblast, neuronal and glial cultures were isolated from wild type (WT) and MyD88 knockout mice (MyD88-/-). A novel membrane-based method of culture was used to study neurones and glia separately, whilst still being able to communicate with one another. WT and MyD88-/- neurons were cultured in the presence of both WT and MyD88-/- glia, these combinations of cells were then exposed to 4 hours of oxygen glucose deprivation (OGD). Cellular survival was assessed with a mitochondrial viability assay. Activation by phosphorylation of the TLR system downstream signalling components ERK, JNK, TPL2 and NFκB was measured by Western blot.

Results: Cellular viability following OGD shows that fibroblasts and neurons lacking MyD88 are more susceptible to ischemic injury, suggesting a pro-survival role for MyD88 in these cell types. This correlates with in vivo data showing MyD88-/- mice exposed to mid-cerebral artery occlusion exhibit a two fold increase in infarct volume when compare to WT mice (n=12). The presence of glia increases the survival of neurons after OGD by 30%, and MyD88-/- glia potentate this increase in survival of neurons by a further 15%, suggesting a pro-death signalling role for MyD88 in glia. MyD88 -/- neurons show delayed phosphorylation of mediators (ERK, JNK, TPL2 & NFκB) known to play a role in the determination of cellular fate as evidenced by Western blots.

Conclusions: Together these data suggest that there is a dual role for MyD88 dependant signalling. These results highlight the role of MyD88 as cell type specific and that responses controlled by MyD88 are more complex than originally thought.

MILD HYPOTHERMIA ATTENUATES OXIDATIVE/NITROSATIVE STRESS AND CYTOTOXIC BRAIN EDEMA IN EXPERIMENTAL ACUTE LIVER FAILURE

C. Bemeur, W. Jiang, P. Desjardins, R.F. Butterworth

Neuroscience Research Unit, CHUM, St-Luc Hospital, University of Montreal, Montreal, QC, Canada

Objectives: Encephalopathy and brain edema are serious neurological complications of acute liver failure (ALF). The precise pathophysiologic mechanisms responsible have not been fully elucidated but it has been suggested that oxidative/nitrosative stress is involved (Kosenko and al., 2003). In the present study, we evaluated the role of oxidative/nitrosative stress in the pathogenesis of hepatic encephalopathy and brain edema in rats with ALF resulting from hepatic devascularization and mice with ALF resulting from azoxymethane hepatotoxicity (Bélanger and Butterworth, 2005). We also studied the effect of hypothermia, a treatment previously shown to delay the progression of encephalopathy and the onset of brain edema, on ALF-induced oxidative stress (Rose et al., 2000).

Methods: ALF animals were sacrificed at precoma and coma stages of encephalopathy along with their appropriate controls. Hypothermic ALF animals were sacrificed in parallel with normothermic comatose ALF animals. Cerebral GSH/GSSG ratio were assessed spectrophotometrically. Nitrite/nitrate levels in plasma and brain were measured using the Griess reaction and expression of nitric oxide synthase (NOS) isoforms and heme oxygenase-1 (HO-1) were measured using real-time quantitative PCR and western blot analysis.

Results: Cerebral GSH/GSSG ratio was significantly decreased in ALF comatose animals compared to the controls. Increased nitrite/nitrate levels were observed in the plasma and frontal cortex in ALF animals at coma stage of encephalopathy compared to controls. Increased expression of HO-1 protein and mRNA was observed in the frontal cortex of ALF animals at both precoma and coma stages of encephalopathy. Significant increases in expression of endothelial and inducible nitric oxide synthase (NOS) mRNA isoforms also occured at precoma and coma stages of encephalopathy. Expression of the neuronal nitric oxide synthase isoform (nNOS) was not altered by ALF. Hypothermia normalized GSH/GSSG ratio and nitrite/nitrate levels in brain and significantly attenuated HO-1, eNOS and iNOS expression.

Conclusions: These results suggest that, oxidative/nitrosative stress participates in the pathogenesis of brain edema and its complications in ALF and that the beneficial effect of hypothermia depends on its ability to inhibit oxidative/nitrosative stress-related mechanisms.

References: Bélanger, M., Butterworth, R.F., 2005. Acute liver failure: a critical appraisal of available animal models. Metab. Brain Dis. 20, 409-423.Kosenko, E., Venediktova, N., Kaminsky, Y., Montoliu, C., Felipo, V., 2003. Sources of oxygen radicals in brain in acute ammonia intoxication in vivo. Brain Res. 981, 193-200.Rose, C., Michalak, A., Pannunzio, M., Chatauret, N., Rambaldi, A., Butterworth, R.F., 2000. Mild hypothermia delays the onset of coma and prevents brain edema and extracellular brain glutamate accumulation in rats with acute liver failure. Hepatology 31, 872-877.

949

Brain Poster Session: Experimental Cerebral Ischemia: Global Ischemia

CEREBRAL REPERFUSION UPREGULATES GENES DISTINCT FROM ISCHEMIA ALONE IN THE RAT

B. Ander, X. Zhan, D. Liu, F. Sharp

Neurology, UC Davis MIND Institute, Sacramento, CA, USA

Objectives: Ischemia and reperfusion are distinct phases of cerebral injury contributing to stroke. Previously, we have examined gene expression in the rat following permanent focal ischemia. We hypothesize that reperfusion will elicit its own change in gene expression and that this change can be measured in the blood.

Methods: Adult male Sprague Dawley rats were anaesthetized and subjected to middle cerebral artery occlusion using the intraluminal suture technique. The suture was left in place for either two hours (reperfusion group) or permanently for 24 hours (ischemia group). At 24 hours following the surgery, rats were anaesthetized and whole blood was collected into PAXgene blood collection tubes to stabilize RNA. Total RNA was isolated with the PAXgene system and processed using reagents from NuGEN Technologies to generate labelled cDNA for hybridization onto Affymetrix Rat Genome 230 2.0 arrays. Partek software was used to create gene lists. A false discovery rate ≤ 0.05 and two-fold change cutoff were applied for each stroke group compared to normal and sham controls.

Results: A total of 344 and 31 gene transcripts were upregulated in the reperfusion and ischemia groups, respectively. Of these, a unique set of 97 gene transcripts were significantly upregulated only in the reperfusion group and common in comparisons to both normal and sham groups. These 97 transcripts represented genes with significant representation in many biogroups including enzyme regulation, binding of calcium ions, inflammation and responses to stress and wounding.

Conclusions: Cerebral reperfusion injury results in upregulation of many genes that are not induced by ischemic injury alone. These specific gene profiles are measureable in the blood.

950

Brain Poster Session: Neurogenesis

REGULATION OF POST ISCHEMIC NEUROGENESIS BY IGFBP-3

R. Dempsey[1], H. Kalluri[2]

[1]Neurological Surgery, University of Wisconsin-Madison, [2]University of Wisconsin - Madison, Madison, WI, USA

Objectives: Cerebral ischemia enchances the proliferation of neural progenitor cells in the neurogenic regions, while upregulating the expression of several growth factors including, IGF-1 and IGFBP-3 in the ischemic cortex. Although, IGF-1 increases the proliferation, differentiation and survival of neural progenitor cells, the role of Insulin like growth factor binding protein-3 (IGFBP-3) in the ischemic brain is not clear.

Methods: To understand the role of IGFBP-3 in the post ischemic brain, we analyzed the effect of IGFBP-3 on the IGF-1 mediated proliferation of neural progenitor cells (NPC) in vitro. We used cultured neural progenitor cells stimulated by the tested agents and measured cell proliferation, release of LDH, incorporation of BrdU and analysis of phospho-Akt and cyclin D1.

Results: The stimulation of neural progenitor cells with IGF-1 (50ng/ml) and FGF2 (20ng/ml) enhanched the proliferation of cells. Incubation of NPC´s with IGFBP-3 (5, 50, 500ng/ml) reduced the neurosphere formation only at 500 ng/ml. The decrease in the neurosphere formation was consistent with the decline in the metabolic activity of the cells, however IGFBP-3 did not cause cell death as measured by the release of LDH. Consistent with these observations, BrdU incorporation studies established a role for IGFBP-3 in the inhibition of cell proliferation. Furthermore, immunoblot analysis demonstrated a decrease in the content of phospho-Akt and cyclin D1 following incubation with IGFBP-3, suggesting an inhibitory role for IGFBP-3 in the IGF-1 mediated proliferation of cells.

Conclusions: These results together suggest that IGFBP-3 may play an important role in regulating post ischemic neurogenesis. These results may have wider implications for the modulation of brain repair processes after a variety of insults.

951

Brain Oral Session: Cerebrovascular Regulation

VEGF RESCUES LOSS OF MYOGENIC TONE INDUCED BY HYPOXIC-ISCHEMIA IN NEONATAL RAT MIDDLE CEREBRAL ARTERIES

S. Charles[1], S. Butler[1], J. Abrassart[1], J. Williams[1], B. Tone[2], S. Ashwal[2], **W. Pearce**[1]

[1]Center for Perinatal Biology, [2]Department of Pediatrics, Loma Linda University School of Medicine, Loma Linda, CA, USA

Objectives: Whereas vascular injury undoubtedly contributes to cerebral infarct development following neonatal hypoxic-ischemic insults, the direct effects of such insults on cerebrovascular contractility remain poorly understood due largely to the technical challenges involved in such measurements. Nonetheless, better understanding of how hypoxic-ischemic insults compromise neonatal cerebrovascular contractility could greatly facilitate management of many NICU infants. In particular, it is important to know if neonatal ischemic vascular injury is irreversible, or if vascular function can be restored, and if so, how. The present study examines the hypothesis that neonatal ischemia compromises contractility by stimulating dedifferentiation of contractile smooth muscle, and that this process can be mitigated or reversed by treatment with the angiogenic growth factor, VEGF.

Methods: Sprague-Dawley rat pups at postnatal day 10 were anesthetized and the left common carotid was permanently ligated, as previously described (1). After a 90-min post-surgical recovery the pups were exposed to 8% oxygen for 90 minutes, then allowed to recover for 90 min at which time the cerebral arteries were harvested. The brains were stained with TTC to determine infarct volume, as previously described (1).

Contractile characteristics of control and ischemic middle cerebral arteries were determined immediately after sacrifice, and after 48 hours of organ culture. In organ culture, arteries were serum starved in DMEM in the presence or absence of 30 ng/ml VEGF. The contractility protocol measured in cannulated arteries the pressure-induced (myogenic) and potassium-induced changes in diameter at 20, 40, 60, and 80 mm Hg of transmural pressure. After contractility measurements, segments were sectioned and imaged following fluorescent immunohistochemical staining for smooth muscle α-actin and Myosin Light Chain Kinase (MLCK) to identify smooth muscle phenotypic changes.

Results: Before organ culture, ischemic injury completely ablated both stretch-induced and depolarization-induced contractility; at 20, 40, 60, and 80 mm Hg pressure-induced diameter differences averaged 39, 51, 58, and 75 μm in control arteries but only 5, 4, 2, and 0 μm in ischemic arteries. Organ culture with VEGF significantly improved contractility in the ischemic arteries; at 20, 40, 60, and 80 mm Hg diameter differences averaged 83, 79, 72, and 18 μm in control arteries and 45, 23, 4, and 1 μm in ischemic arteries. Fluorescent immunohistochemistry revealed that ischemia potently stimulated smooth muscle proliferation, as indicated by increased volume and density of staining for smooth muscle α-actin. VEGF treatment amplified this effect. Ischemia alone had little effect on MLCK expression, but ischemia plus VEGF dramatically enhanced MLCK expression, and by inference, the relative fraction of contractile smooth muscle cells.

Conclusion: The present results support the hypothesis that neonatal hypoxic-ischemia induces loss of vascular contractility via stimulation of contractile dedifferentiation in arterial smooth muscle. The data further suggest that this effect can be ameliorated by VEGF, which stimulates smooth muscle proliferation but also promotes expression of MLCK, a predominant regulatory contractile protein and marker for contractile, as opposed to proliferative, smooth muscle.

References: 1. Ashwal S, Tone B, Tian HR, Chong S, Obenaus A. (2007) Pediatr Res 61:9-14.

DECREASED NUMBER AND FUNCTION OF ENDOTHELIAL PROGENITOR CELLS IN ALZHEIMER´S DISEASE

K. Chu, S.-T. Lee, K.-H. Jung, J. Sunwoo, J.-J. Bahn, S. Lee, M. Kim, J.-K. Roh

Department of Neurology, Seoul National University Hospital, Seoul, South Korea

Objects: Neurovascular senescence contributes to the progression of Alzheimer´s disease (AD). Because circulating endothelial progenitor cells (EPCs) provide a cellular reservoir for the endothelial replacement, we investigated whether AD patients have dysfunctional EPCs to study the involvement of EPCs in AD pathogenesis.

Methods: We enrolled consecutive newly-diagnosed AD (n=55), non-AD neurodegenerative diseases (n=37), and non-demented risk factor control subjects (RF control, n=55 and 37) after matching for age, sex, and Framingham risk score. EPC colony forming units (CFU-EPC) were cultured in peripheral blood samples and used for various ex vivo assays.

Results: CFU-EPC was significantly lower in the AD patients than in ithe RF controls. In the AD patients, a lower CFU-EPC was independently associated with either a lower mini mental state examination or a higher clinical dementia rating scale score, indicating a greater reduction in CFU-EPC in advanced AD. Patients with non-AD neurodegenerative diseases showed similar CFU-EPC levels compared to their RF controls. EPCs from AD patients showed reduced chemotaxis, increased senescence, reduced paracrine angiogenic activity, and altered gene expression pattern compared to EPCs from RF controls. Ex vivo addition of Aβ1-42 to the EPC culture reduced EPC counts and endothelial nitric oxide synthase/Akt phosphorylations.

Conclusion: Our results showed that AD patients have dysfunctional, suggesting that an abnormal capacity to regenerate endothelium is associated with AD.

ARTIFICIAL RBCS TRANSIENTLY IMPROVED MICROCIRCULATORY DERANGEMENT PRODUCED BY MCA OCCLUSION OR HEMORRHAGIC HYPOTENSION IN MICE

Y. Tomita[1,2], H. Toriumi[1], H. Hattori[1], M. Unekawa[1], M. Tomita[1], Y. Itoh[1], H. Hoshino[1,2], H. Sakai[3], E. Tsuchida[3], H. Horinouchi[4], K. Kobayashi[4], N. Suzuki[1]

[1]Department of Neurology, [2]Department of Preventive Medicine for Cerebrovascular Disease, Keio University, School of Medicine, [3]Research Institute for Science and Engineering, Waseda University, [4]Division of General Thoracic Surgery, Department of Surgery, Keio University, Tokyo, Japan

Background: In acute brain ischemia, RBCs disappear from the capillary network, due probably to an RBC sieving effect. Since RBCs carry twenty times more oxygen than plasma does, neurons might suffer from anoxia. Even under such microcirculatory derangement, plasma flow in capillaries seems to persist, due probably to a plasma skimming effect. The effectiveness of artificial RBCs (aRBCs: 0.25μm in diameter) in these circumstances remains uncertain. Therefore, we examined the effect of rhodamine-labeled aRBCs (Artif Cells, Blood Substitutes, Biotechnol. 35: 81, 2007) on cerebral ischemia and hemorrhagic hypotension in mice.

Methods: Under isoflurane anesthesia, a cranial window was opened above the left parieto-temporal cortex of C57BL/6J mice (n=16). A femoral artery and tail vein were catheterized. An oxygen electrode (Eikoh Kagaku) was placed near the branch of the left MCA with a reference Ag-AgCl electrode inserted into the space between scalp and skull bone. The changes in brain microvasculature, blood pressure (Muromachi) and tissue oxygen tension (PO_2) were continuously recorded. FITC-labeled RBCs were injected into the circulating blood in all cases, and their movement through single capillaries in the ROI of brain parenchyma (50μm depth) was monitored and recorded continuously (Microcirculation. 15: 163, 2008) with a video camera (30 frames/s) or a high-speed laser scanning confocal fluorescence microscope (500 frames/s) under illumination at 488 or 533 nm. In the ischemia group (n=5), the root of the left MCA was thermo-coagulated surgically and cut (MCAO); 3 sham-operated mice were used as controls. Then 0.02ml of aRBCs were injected to both group. While in a hemorrhagic hypotension group (n=8), after withdrawal of 0.3-0.5 ml blood, the same amount of saline (n=3) or aRBCs (n=5) was systemically injected.

Results: Both MCAO and hemorrhagic hypotension to 31.8±3.6% of the baseline blood pressure produced severe microvascular derangement with sluggish flow, disappearance of most FITC-labeled RBCs from capillaries, and development of RBC sludge and aggregates in arterioles and venules. Tissue PO_2 decreased to 55.2±22.8% of the control value after MCAO ($P< 0.05$) and to 70.0±5.2% ($P< 0.05$) after hypotension. However, when aRBCs were given intravenously, we observed penetration of red 0.25μm aRBCs through capillaries and PO_2 recovered to 80.9±45.5% of the baseline value ($P< 0.05$) in the ischemia group and to the almost baseline level in a hemorrhagic hypotension group. Surprisingly, we noted transient resumption of capillary flow. Improvement of microcirculation persisted at least for 10 min. However, after the improvement, there were a few cases which showed slight reperfusion injury, due probably to free radical production, in the ischemia group. In the sham-operated group, tissue PO_2 was transiently elevated to 172.2±62.9% ($P< 0.05$) after aRBCs injection. In a hemorrhagic hypotension group, after injection of the saline, tissue PO_2 was slightly elevated then decreased again.

Discussion: Administration of aRBCs to emergent ischemic tissue improved the microcirculation transiently. Supply of oxygen via improved capillary flow might temporarily rescue anoxic neurons.

Conclusion: Use of aRBCs may be transiently helpful in acute ischemia and hemorrhagic hypotension.

FUNDAMENTAL CONSIDERATION OF ^{31}P-NMR STUDY ON BRAIN ENERGY METABOLISM

O. Tokumaru[1], C. Kuroki[1], K. Ogata[1], T. Kitano[2], I. Yokoi[1]

[1]Neurophysiology, [2]Medical Education Center, Oita University Faculty of Medicine, Yufu, Japan

Objectives: We have studied brain energy metabolism by measuring high energy phosphates, phosphocreatine (PCr) and ATP, using ^{31}P-NMR spectroscopy. PCr serves as a reserve of high-energy phosphate for ATP (Lohmann, 1934), and reflects the status of the energy metabolism. In order to conduct experiments under various conditions such as "body temperature", "hypothermia", "hyperglycemia" or "hypoglycemia", we reviewed our experimental protocols and investigated effects of temperature, [K^+] and [glucose] of the superfusate on energy metabolism of rat brain.

Methods: The original protocol: Brain slices (400 μm-thick) prepared from a male Wistar rat (6 week-old) were superfused with standard artificial cerebrospinal fluid (ACSF) at a flow rate of 1 ml/min in an NMR sample tube at 25°C. Ex-vivo ^{31}P-NMR spectra were obtained using an NMR spectrometer (DRX-300wb, Bruker Biospin) operating at 121 MHz. Free induction decays (FIDs) were acquired by 45° radio-frequency pulses repeated at intervals of 4 seconds. An accumulation of 64 FIDs were taken as a unit of observation. Relative quantities of PCr and ATP were obtained from areas under curves fit to resonance peaks.

Responses of PCr and ATP levels to the following insults were evaluated.

Ischemia-reperfusion model: Brain slices were exposed to ischemia by halting the perfusion for 1 hr at 25°C, followed by the recovery period for 2 hrs.

Depolarization model: Slices were superfused with ACSF with higher [K^+] to depolarize the cell membrane, increasing the energy expenditure of the slices.

Re-evaluation of the experimental conditions: The effects of temperature (25°C ~ 37°C), [glucose] (hypoglycemia: 5 mM; normoglycemia: 10 mM; hyperglycemia: 20 mM) and [K^+] (5 mM ~ 60 mM) of superfusate on brain energy metabolism were evaluated.

Results: When the temperature was raised from 25°C to 37°C without an increase in the flow rate, PCr and ATP signals disappeared. After ischemia longer than 10 min, recovery of PCr was too poor in ischemia-reperfusion model conducted at 37°C. Intracellular pH during ischemia was 6.6, 6.3 and 5.8 when [glucose] = 5, 10 and 20 mM, respectively. Recovery levels of PCr and ATP were poor when [glucose] = 5mM. Energy expenditure during the depolarization model was linearly correlated with extracellular [K^+] ($p < 0.0001$). Such increase in energy expenditure was suppressed by tetrodotoxin.

Conclusions: When temperature is raised from 25°C to 37°C, it is speculated that the energy consumption is increased by about 2.5 times and that the flow rate used at room temperature (1 ml/min) was insufficient to meet higher oxygen demand at body temperature. We have adopted a flow rate of 10 ml/min at 37°C with a safety factor of 4. In addition, the duration of ischemia should be shorter than 10 min in the ischemia-reperfusion model at 37°C. During ischemia under hyperglycemic condition, intracellular pH is more acidic probably due to increased production of lactate by glycolysis. By increasing extracellular [K^+], it is possible to control energy consumption in the depolarization model, which is dependent on voltage-gated Na^+ channel.

References:

Tokumaru et al., J Neurosurg 105(Suppl):202-207, 2006.

Tokumaru et al., Neurochem Res (in press).

955

Brain Poster Session: Cerebral Vascular Regulation

DYNAMIC RECORDING OF ONGOING NEUROVASCULAR ACTIVITY IN AWAKE-BEHAVING MICE

H. Takuwa[1], K. Masamoto[2], T. Obata[1], I. Kanno[1]

[1]Molecular Imaging Center, National Institute of Radiological Sciences, Chiba, [2]University of Electro-Communications, Tokyo, Japan

Background: There have been a number of studies concerning the mechanism regulating CBF induced by neuronal activity (neurovascular coupling) in animals. However, most studies were performed under the anesthetized condition. Since anesthesia greatly affects neurovascular coupling[1] and systemic physiology (e.g., blood pressure, heart rate, etc.), the implications from the anesthetized animal studies may not be directly applicable to human fMRI studies that are usually performed on awake subjects in clinical and neuroscience research. In the present study, we therefore aimed to develop a novel model for neurovascular physiologic studies in awake-behaving mice.

Material and methods: This study was conducted in C57BL/6J mice (5-7 weeks). The regional CBF (rCBF) in the somatosensory cortex was continuously measured with laser-Doppler flowmetry (LDF), while the mice were fully awake. A metal head plate was attached to the skull and the mice were tethered by screwing the head plate onto a metal rod. Below the animals, a styrofoam ball supported by a jet of air was set in the apparatus. The styrofoam ball freely rotated while the mice walked on it. In order to record the walking velocity of the mice, an optical computer mouse was set so that movement of the ball could be detected. The behavior of the mice was video-recorded using a digital camera. The animal behavior, while being tethered (e.g. running, resting and grooming, etc) was later analyzed by displaying it on a CRT and comparison was made with LDF data recorded simultaneously. The dynamic LDF data were compared across the conditions of resting, running, grooming and whisker stimulation (stimulus frequency 10 Hz and duration 10 sec).

Results and discussion: During the resting state, the spontaneous fluctuation (standard deviation) of the rCBF was ±2.7% relative to the mean LDF. The baseline level of the LDF signal did not change significantly over 1.5 hours recording. The rCBF change was also stable (SD = ±3.5%) when the animals were running. These results show that a motion artifact caused by running did not significantly affect the LDF measurements. The rCBF increased by about 20% during a period of spontaneous grooming. The rCBF change induced by whisker stimulation was observed to be about 30% of the baseline level at the peak intensity.

In conclusion, the present awake-behaving mice model allows for the study of ongoing rCBF activity, and leads to better comparison with awake-behaving humans studied with fMRI noninvasively.

References: [1] Kazuto Masamoto, Tae Kim, Mitsuhiro Fukuda, Ping Wang and Seong-Gi Kim, (2007) Relationship between Neural, Vascular, and BOLD Signals in Isoflurane-Anesthetized Rat Somatosensory Cortex: Cereb Cortex, 17(4), 942-950.

Brain Poster Session: Cerebral Vascular Regulation

DYNAMICS OF VASCULAR REARRANGEMENTS AND VASOGENIC EDEMA AFTER TRANSIENT BRAIN ISCHEMIA REVEALED BY TWO-PHOTON MICROSCOPY

S. Fumagalli[1], F. Ortolano[1,2], F. Pischiutta[1], P. Maffia[3], H.V. Carswell[3], P. Garside[3,4], **M.G. De Simoni**[1]

[1]Laboratory of Inflammation and Nervous System Diseases, Department of Neuroscience, Mario Negri Institute, [2]Anaesthesia and Critical Care Medicine, University of Milan, Milan, Italy, [3]Strathclyde Institute of Pharmacy & Biomedical Sciences, [4]Centre for Biophotonics, University of Strathclyde, Glasgow, UK

Objectives: Ischemia causes a number of vascular modifications including vessel diameter change and blood brain barrier (BBB) leakage. The mechanisms and effects of ischemia/reperfusion on vascular dynamics and on BBB damage are still largely unknown. The aim of our study was to assess the dynamics of vascular rearrangements and extravasation during and after transient ischemia using in vivo real time two-photon microscopy [1,2].

Methods: Anesthetized 11-week C57BL6 male mice underwent surgical preparation for two-photon microscopy observation. A cranial window was opened at AP -1mm and L -3.5mm from bregma to expose vessels lying in a region fed by the middle cerebral artery (MCA). After an intravenous injection of 70 kDa Texas-Red Dextran (150 µl solution 0.5%), mice were observed at baseline conditions. Imaging was performed on 250µm thick cortical area. Blood flow speed (expressed as erythrocyte speed, mm/s) and dextran extravasation (expressed as ratio between intra-vascular and extra-vascular pixel intensities) were evaluated before, during and after (at 10 minutes and 24 hours of reperfusion) 30 minute MCA occlusion in the same mouse. A group of mice receiving anesthesia and surgical preparation but not ischemia served as sham group.

Results: A total of 22 vessels visualized in 4 ischemic mice were analyzed and showed a mean blood flow speed of 3.326 mm/s. During MCA occlusion blood flow was completely prevented in 8/22 vessels, while in 10/22 the speed decreased to a mean value of 0.184 mm/s. Notably, in 4/22 vessels the blood flow was inverted, with a mean speed of -0.414 mm/s. Ten minutes after reperfusion blood flow appeared to be only weakly restored in 18/22 vessels, with a mean speed of 0.184 mm/s, while 4 vessels did not reperfuse, in spite of the confirmation of blood flow restoration assessed by Doppler probe at the same stereotactic coordinates of the cranial window. Similar data were obtained 24 hours after reperfusion.

Extravasation was significantly increased as early as 20 minutes after occlusion onset. It was preceeded by morphological changes in the vessel profile which became markedly irregular possibly due to the incipient BBB damage. No blood flow changes nor extravasation were detected in sham-operated animals (12 vessels from 3 animals).

Conclusions: In this study we report a feasible protocol to perform in vivo real time imaging of the microvasculature and surrounding brain parenchyma before, during and after ischemia. We could show the interruption/reduction of blood flow during ischemia and the presence of small percentage of vessels in which blood flow is inverted, perhaps as a result of redundancy in the cortical vascular architecture. Moreover we report that up to 24 hours after reperfusion, cerebral blood flow is not adequately restored in the microcirculation belonging to an area fed by the MCA. BBB damage, evaluated as extravasated fluorescent dextran, occurs as early as 20 minutes after MCA occlusion, quickly contributing to edema formation during ischemia.

References:

1. Nimmagadda, A., et al.. Stroke, 2008. 39(1): p. 198-204.

2. Schaffer, C.B., et al.. PLoS Biol, 2006. 4(2): p. e22.

957

Brain Poster Session: Epilepsy

^{1}H HRMAS NMR METABOLIC PROFILE OF MOUSE BRAIN INTOXICATED BY AN ORGANOPHOSPHORUS COMPOUND

F. Fauvelle, G. Testylier, F. Dorandeu, P. Arvers, A. Foquin, P. Carpentier

CRSSA, La Tronche, France

Soman is an organophosphorus neurotoxic. It induces epileptic seizures that can last for several hours leading to brain oedema and neuronal lesions, mainly in the piriform cortex and the hippocampus. Limited amount of data is available on the associated brain metabolic disturbances. The purpose of this study was to analyse by HRMAS ^{1}H-NMR spectroscopy the brain metabolic profile in piriform cortex (Pir) and cerebellum (Cvl) from the initial phase (1h) to 7 days after soman intoxication.

Methods: Mice were intoxicated with soman (172 µg/kg SC) and sacrificed 1h, 4h, 24h, 48h, 72h and 7 days after. Pir and Cvl biopsies were immediately stored in liquid nitrogen after dissection.

The HRMAS ^{1}H-NMR experiments were performed on a Bruker DRX Avance spectrometer at 9.4Tesla, at 4°C and 4KHz spinning. A spin-echo sequence with a 30 ms total echo time was used.

In a first analyse, 17 metabolites have been quantitated using jMRUI-sofware [1]. Then the Projection to Latent Structure by means of partial least squares Discriminant Analysis (PLS-DA) was applied to rough NMR data. All spectral region between 4.65 and 0.5ppm were segmented in 0.02 ppm rectangular buckets and loaded in the SIMCA-P software version 10 (Umetrics, Umea, Sweden) for PLS-DA analysis.

Results: Metabolite variations:

- In the initial phase of intoxication (1h and 4h), epileptic seizures have evolved into a severe status epilepticus. Alanine and GABA in Pir reached their maximum level at 1h while Choline and Acetate were maximum at 4h.
- 24h after soman injection, seizures are not totally arrested but are now discontinuous. Pir biopsies were characterized by a strong increase of Lactate and a strong decrease of NAA . Myo-inositol exhibited a significant decrease at 24h and 48h in Pir. Glutamine strongly increased not only in Pir but also in Cvl.
- Seven days after intoxication only lactate and NAA in Pir remained at an abnormal level.

Multivariate analysis: PLS-DA score plot showed the very good separation between samples based upon brain structure, even for samples of intoxicated animals (figure 1). However, a clear difference appear between the two strutures: cortex samples are much more dispersed than cerebellum samples. The second effect that is superimposed on structural effect for the class separation is the kinetic effect; samples appear separated according to their metabolic profile at different phases after intoxication.

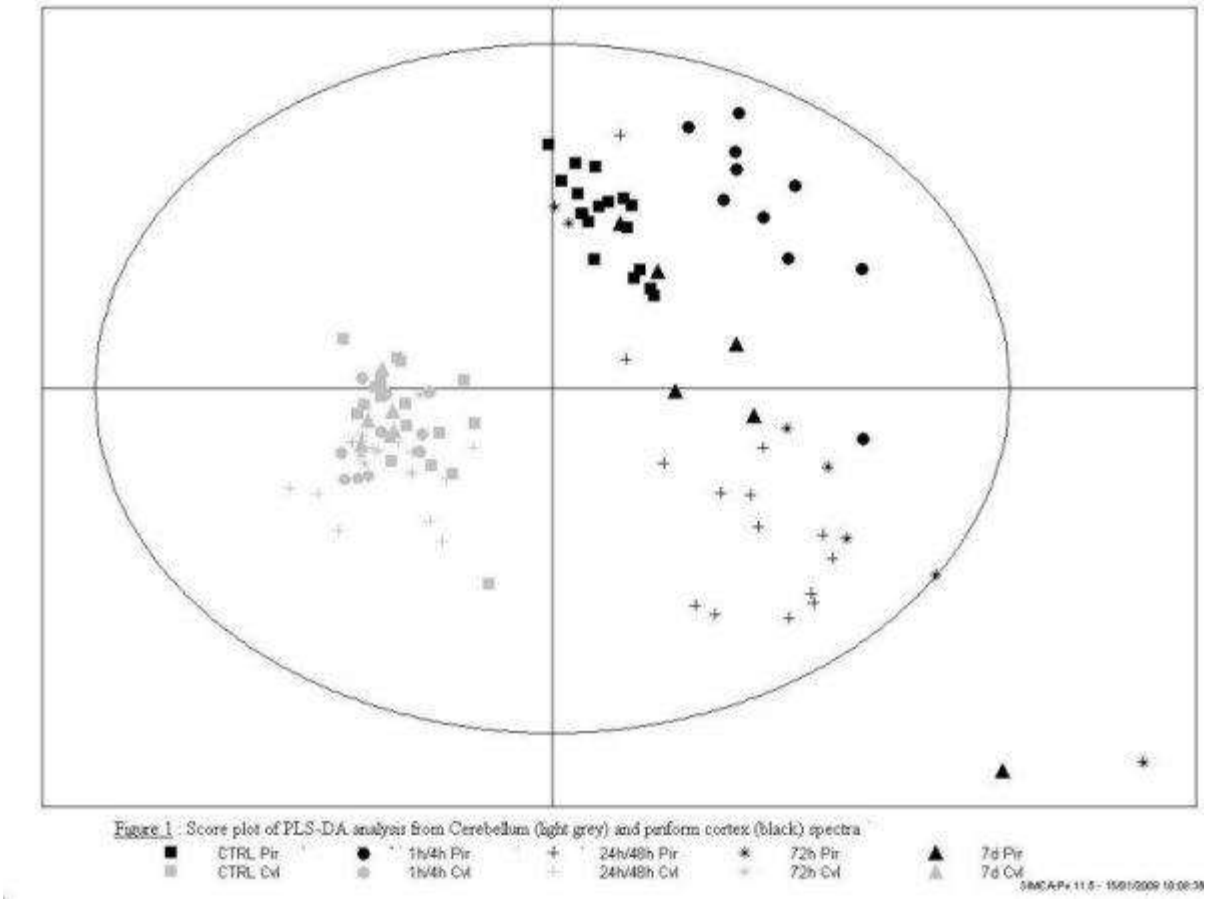

[figure 1]

Conclusion: This study enabled the acute observation of metabolic disturbances at different time points after soman intoxication. The metabolites identified reflected the different diseases occurring during soman intoxication from epileptic activity, brain oedema, neuro inflammation to neuronal death and brain adaptation.

[1] H. Rabeson et al., Magn. Reson. Med. 59(6) (2008) : 1266-1273.

Brain Poster Session: Neurogenesis

ROLE OF IL10 IN THE NEUROGENESIS OF THE POSTNATAL SVZ OF RODENTS

E. Pozas, R. Medina, A.M. Planas

Cerebral Ischemia and Neurodegeneration, Institute of Biomedical Research of Barcelona-CSIC-IDIBAPS, Barcelona, Spain

Objectives: The subventricular zone (SVZ) is the main neurogenic area in adult brain and after experimental models of stroke. In normal conditions the neuroblasts generated in the SVZ migrate and differentiate into mature interneurons in the olfactory bulb. After ischemia these neuroblasts migrate to the lesion areas indicating that adult neurogenesis can be modulated by pathological situations (Ardvisson et al., 2002, Doetsch et al., 1999). The specific relevance of the inflammation associated to CNS pathologies in adult neurogenesis is unclear. The first studies showed that inflammation was detrimental for hippocampal neurogenesis but the most recent studies indicated that this context is much more complex (Monje et al., 2003; Ekdahl et al., 2003; 2008). The aim of this study is to explore the effects of IL10 in the differentiation of the neural stem cell (NSC) from the postnatal SVZ in normal and pathological situations.

Methods: Several primary cultures (dissociated, explants, neurospheres) from the postnatal SVZ were performed from postnatal rats. Cell viability, proliferation and differentiation were explored after interleukins treatment. In living cultures cell viability was measured by IdPr incorporation and cell proliferation was evaluated by a pulse of Brdu. Cellular markers (nestin, BIII tubulin, DCX, and others) were detected by immunofluorescence on fix cultures. By western blotting the intracellular pathways activated after interleukin stimulation were quantified. The studies were mainly focused in detect the intracellular activation of the Jak/Stat and MAPK pathways. By RT-PCR the levels of interleukins and its receptors were analyzed in cell culture and in in vivo samples. Histological analyses by immunofluorescence and western blotting of different cellular markers were evaluated in neurogenic and non neurogenic areas of the adult mice.

Results: The postnatal SVZ express high levels of IL10 receptor. On primary cultures of the SVZ the exposure to IL10 stimulates the phosphorylation of STAT 3 as well as ERK1/2 p42-p44 (pErk). The inhibition of the MAPK pathway abolished the phosphorylation of Stat3. This observation indicates that pERK is upstream of STAT3 activation after IL10 stimulation. Double immunofluorescences techniques show that pERK is specifically activated on NSC (Nestin+). The presence of IL10 on primary culture of SVZ for several days induces cell death but have not effects on cell proliferation. In these cultures Il10 induces changes in the number of NSC. Preliminary in vivo studies in IL10 KO mice indicate that the neurogenesis in the SVZ is altered.

Conclusions: The present results show that NSC respond to IL10 by activation of ERK 1/2 that induces the phosphorylation of STAT3, and suggest that this anti-inflammatory cytokine plays a role in the NSC differentiation.

References:

Arvidsson et al. Nat Med. 8: 963-70, 2002; Doetsch et al. Cell. 97:703-16, 1999. Ekdahl et al. Proc Natl Acad Sci U S A 100:13632-7, 2003.

Ekdahl et al. doi: 10.1016/j.neuroscience.2008.06.052.

Monje et al. Science 302: 1760-5, 2003.

Acknowledgment: The project was funded by grant PI070917 from FIS (Spain) and CIDEM

(Catalonian Government). EP was supported by I3P and Ramón y Cajal programs from CSIC and MICINN respectively.

Brain Poster Session: Neuroprotection

NEUROPROTECTIVE EFFECTS OF HYDROGEN GAS ON BRAIN IN THREE TYPES OF STRESS MODELS: A ^{31}P-NMR STUDY

C. Kuroki, O. Tokumaru, H. Koga, I. Yokoi

Department of Neurophysiology, Oita University Faculty of Medicine, Oita, Japan

It has recently been reported that hydrogen gas (H_2) acts as a radical scavenger by reducing the hydroxyl radical and reduces acute oxidative stress on brain in ischemia-reperfusion stress (Ohsawa et al., Nat. Med. 2007). We measured high-energy phosphates in rat brain slices by phosphorus nuclear magnetic resonance (^{31}P-NMR) and evaluated neuroprotective effects of H_2 using a hypoxic stress model, an ischemia-reperfusion model and a high-K^+ stress model. Brain slices were superfused with well-oxygenated ($PO_2 \approx 500$torr) artificial cerebrospinal fluid (ACSF) equilibrated with (H_2+ group) or without 4% H_2 gas (H_2- group) at 27.5°C. In the hypoxic stress model, slices were superfused with hypoxic ACSF ($PO_2 \approx 120$torr) for 2 hours. In the ischemia-reperfusion model, perfusion was stopped for 1 hour. In the high-K^+ stress model, slices were superfused with ACSF containing 60mM K^+ for 1 hour. In the hypoxic stress model, phosphocreatine (PCr) level of H_2+ group recovered to 81% relative to the pre-stress level, whereas that of H_2- group was 85% (n.s.). There was no significant difference in γ-ATP levels. In the ischemia-reperfusion model, PCr levels after stress were not significantly different between the two groups (H_2+: 45%, H_2-: 47%; $p > 0.05$). But γ-ATP level of H_2+ group 1-2 hours after stress was significantly higher than that of H_2- group (H_2+: 60%, H_2-: 39%; $p < 0.05$). In the high-K^+ stress model, PCr level of H_2+ group at the early stage of the stress was significantly higher than that of H_2- group (H_2+: 71%, H_2-: 54%; $p < 0.05$). Our result in the ischemia-reperfusion model is consistent with the previous report that H_2 may exert neuroprotective effects on brain slices against strong oxidative stress by scavenging hydroxyl radical. But we observed the significant difference of PCr level in the high-K^+ stress model, because the high-K^+ stress has distinct mechanisms from oxidative stress, this difference is in conflict with the previous report.

Conclusion: Our result showed that H_2 may have neuroprotective effects on brain slices from a viewpoint of energy metabolism. In addition, our results indicated that careful consideration must be given to neuroprotective mechanisms other than that H_2 acts as a radical scavenger by reducing the hydroxyl radical.

ANALYSIS OF REGIONAL HYPOPERFUSION IN TRAUMATIC BRAIN INJURY USING 123I-IMP SPECT WITH 3D-SSP

T. Hayakawa, Y. Takasato, H. Masaoka, N. Otani, Y. Yoshino, H. Yatsushige, T. Sugawara, T. Momose, C. Aoyagi, G. Suzuki

Neurosurgery, National Disaster Medical Center, Tokyo, Japan

Objective: Cognitive function after head injury is important for the patients to be reintegrated in the society, but the lesion on conventional CT/MRI does not exactly correlate the neuropshychological impairment. In the previous studies, experience with SPECT in the assessment of head injury has shown that SPECT may reveal abnormalities that are not detected by CT or MRI. Three-dimensional stereotactic surface projection (3D-SSP) is one of the methods of statistical analysis, that allows more objective and clearer detection of decreased regional CBF than conventional SPECT analysis. This study investigated regional cerebral blood flow (CBF) in head injured patients using 3D-SSP to detect hypoperfusion on 123I-IMP SPECT scans.

Methods: 39 patients with traumatic brain injury (TBI) who underwent 123I-IMP SPECT at discharge (mean Day 36.7) were included in this study. Patients were divided into three groups according to the main lesion on CT scans; DAI group(diffuse axonal injury): 12cases, mean age 28.0, mean GCS score on admission 8.8, ASEDH group(acute subdural or epidural hematoma): 13 cases, mean age 37.1, mean GCS 11.2, Contusion group(cerebral contusion or contusional intracerebral hematoma): 14 cases, mean age 44.4, mean GCS 10.1. The SPECT images were analyzed statistically using 3D-SSP with Stereotactic extraction estimation (SEE) program.

Results: DAI group displayed low blood flow extensively in the basal frontal lobes (rectal gyrus, orbital gyrus) and the medial frontal lobes (i.e. anterior cingulate). This group also showed CBF decrease in the basal temporal lobes (parahippocampal gyrus, uncus) and the lateral frontal lobes (middle and inferior frontal gyrus). Examination of ASEDH group indicated the involvement of the contralateral frontal lobe in addition to the ipsilateral temporal and parietal lobe. In Contusion group, many patients showed CBF decrease in the basal frontal lobes and the basal temporal lobes in addition to the contusional region on CT. The hypoperfusion was common in the basal frontal lobes, medial frontal lobes and basal temporal lobes. In any type of the lesion on CT.

Conclusion: The SPECT analysis with 3D-SSP demonstrated hypoperfusion in many area where CT/MRI showed no abnormalities in TBI patients. The CBF reduction in the basal frontal lobes, medial frontal lobes and basal temporal lobes was found in any type of head injury, so this may be the characteristic pattern in TBI. 3D-SSP is useful in detecting functional abnormalities in TBI.

DIETARY VIRGIN OLIVE OIL REDUCE ISCHEMIA- REPERFUSION INJURY IN RAT BRAIN IN VIVO

F. Mohagheghi[1], M. Bigdeli[1], B. Rasoulian[2], A.A. Zeinallou[3]

[1]Biological Science, Shahid Beheshti, Tehran, [2]Lorestan University (Medical Sciences), Razi Herbal Medicines Research Center, Lorestan, [3]Agricultural Science, Seed and Plant Instrument Institut, Karaj, Iran

Background: Recent studies suggest that dietary virgin olive oil results in ischemic tolerance to reduce brain ischemia injury in rat brain slices. In this research, we attempted to investigate effects of virgin olive oil pretreatment against ischemia- reperfusion injury to the rat brain tissue.

Methods: Experimental rats were treated orally with virgin olive oil for 30 days at 0.25, 0.5 and 0.75 ml/kg/day (doses A, B and C, respectively). Control group treated with saline for 30 days. At the end of day 30, each group was exposed to middle cerebral artery occlusion for 60 minutes. After 24 hours reperfusion, neurologic deficit scores and infarct volume were measured in all groups.

Results: Median neurologic deficit scores (NDS) were reduced by virgin olive oil, being 2, 1, 1 and 2 in doses 0.25, 0.5, 0.75 and control group, respectively. Virgin olive oil reduced infarct volume (dose A 13%, dose B 41% and dose C 45% vs. control group). Neurologic deficit scores and infarct volume were reduced in doses B and C in comparison to control group significantly.

Conclusion: virgin olive oil induces ischemic preconditioning via effects against ischemic injury in the brain tissue partly by monounsaturated fatty acids and antioxidant agent found in virgin olive oil.

References:

1. González-Correa JA. Muñoz-Marín J. Arrebola MM. Guerrero A. Narbona F.López-Villodres JA and De La Cruz JP. (2007). Dietary Virgin Olive Oil Reduces Oxidative Stress and Cellular Damage in Rat Brain Slices Subjected to Hypoxia-Reoxygenation. Lipids. 42,921-929.

2. Longa E.Z. Weinstein P.R. Carlson S and Cummins R.(1989). Reversible middle cerebral artery occlusion without craniectomy in rats. Stroke 20,84-91.

Brain Poster Session: Neurologic Disease

EXTRADURAL MOTOR CORTEX STIMULATION AND DOPAMINE TRANSPORTER IMAGING IN ADVANCED PARKINSON´S DISEASE: A PILOT STUDY

D. Di Giuda[1], I. Bruno[1], B. Cioni[2], A.R. Bentivoglio[3], D.P. Dambra[1], R. Mazza[1], F. Cocciolillo[1], A. Giordano[1]

[1]Nuclear Medicine Institute, [2]Neurosurgery Institute, [3]Neurology Institute, Catholic University of the Sacred Heart, Rome, Italy

Objectives: Extradural motor cortex stimulation (EMCS) has recently been proposed as a possible alternative to deep brain stimulation in the treatment of advanced Parkinson's Disease (PD). Aim of this pilot study was to investigate long-term effects of EMCS on striatal Dopamine Transporter (DAT) availability in PD patients using ^{123}I-Ioflupane SPECT.

Methods: Six advanced PD patients (5 f, 1 m; mean age: 63.2±5.6 yrs) were enrolled in the study. A quadripolar electrode strip was placed epidurally over the motor cortex, unilaterally in 2 and bilaterally in 4 patients. Therapeutic stimulation during one year of follow-up was applied through the electrode contralateral to the worst clinical side. Neurological assessment (UPDRS) and ^{123}I-Ioflupane SPECT were performed before implant and after 6 and 12 months of continuous EMCS. Caudate-to-occipital cortex and putamen-to-occipital cortex radiotracer uptake ratios were calculated using a region of interest method.

Results: Five patients showed clinical improvement during EMCS, while 1 was unresponsive. Mean total UPDRS score was reduced by 22% at 6 months and 16% at 12 months; UPDRS III in "off-med" showed a mean decrease of 20% at 6 months and 10% at 12 months. No side effects because of surgery or stimulation were reported at follow-up. At baseline SPECT, all patients showed severe nigrostriatal impairment. Changes in specific to non-specific ^{123}I-Ioflupane uptake ratios were observed between pre-operative and follow-up investigations but did not reach statistical significance. However, a progressive decrease in radiotracer uptake was observed in the striatum contralateral to the implant side, reflecting a loss of DATs from baseline to the one-year follow-up scan. On the contrary, a tendency towards stability of uptake ratios was detected in the striatum ipsilateral to the implant. Semi-quantitative analysis results for striatal subregions showed a trend towards reduction of DAT availability in the caudate contralateral to the implant side. On the other hand, ^{123}I-Ioflupane uptake ratios remained stable in bilateral putamen during the observation period. In particular, a trend towards increase was detected in the putamen, more evident after 6 months and ipsilaterally to the implant.

Conclusions: This preliminary study showed that clinical improvement in patients with advanced PD undergoing continuous unilateral EMCS was paralleled by stable DAT availability in the putamen, especially on the side ipsilateral to the implant. On the contrary, the loss of DATs measured with ^{123}I-Ioflupane SPECT continued to progress in the caudate, particularly on the side contralateral to the implant. Given the absence of progressive DAT decline in bilateral putamen, it might be hypothesised that chronic EMCS could act as a "protective" mechanism against further putaminal neuronal degeneration. However, a possible pharmacological effect of long-term treatments and changes in medication dosage on DAT expression or affinity cannot be excluded.

References:

Chronic epidural motor cortical stimulation for movement disorders. Priori A, Lefaucheur JP. Lancet Neurol. 2007;6(3):279-86.

Motor cortex stimulation for Parkinson´s disease. Cioni B. Acta Neurochir Suppl. 2007;97(Pt 2):233-8.

963

Brain Poster Session: Migraine

FAMILIAL HEMIPLEGIC MIGRAINE IS ASSOCIATED WITH INCREASED HABITUATION OF EVOKED RESPONSES: A CONTRAST WITH THE COMMON FORMS OF MIGRAINE

J.M. Hansen[1], M. Bolla[2,3], D. Magis[2], L.L. Thomsen[4], V. de Pasqua[2], M. Ashina[1], J. Olesen[1], J. Schoenen[2]

[1]Danish Headache Center, Department of Neurology, Glostrup Hospital, University of Copenhagen, Glostrup, Copenhagen, Denmark, [2]Headache Research Unit, Department of Neurology and Neurobiology Research Center CNCM, Liège University, Liège, Belgium, [3]IRRCS C. Mondino, University of Pavia, Pavia, Italy, [4]Danish Headache Center, Department of Pediatrics, Glostrup Hospital, University of Copenhagen, Glostrup, Copenhagen, Denmark

Objectives: Familial hemiplegic migraine (FHM) is a dominantly inherited subtype of migraine with aura and transient hemiplegia associated with several mutations in genes coding for neuronal ion channels. These mutations lead to neuronal hyperexcitability and decreased threshold for cortical spreading depression in transgenic animal models. FHM and the common forms of migraine are thought to belong to a spectrum of migraine phenotypes with similar pathophysiology. The common forms of migraine are characterised interictally by a habituation deficit of cortical and subcortical evoked responses, which has been attributed to neuronal dysexcitability.

The FHM genotype has been linked to neuronal hyper excitability, and we therefore tested the hypothesis that a similar abnormal habituation pattern would be found in FHM patients.

Methods: We included 9 FHM patients with known gene mutations and 7 healthy controls. To optimize recruitment, we used portable devices to record most subjects with their agreement at their own homes.

We recorded: Habituation of visual evoked potentials (VEP), auditory evoked potentials including intensity dependence (IDAP) and the nociception-specific blink reflex (nsBR).

Results: FHM patients had a more pronounced habituation during VEP ($p=0.025$) and nsBR recordings ($p= 0.023$) than HV. There was no significant difference for IDAP, but the slope tended to be steeper in FHM.

Conclusion: Contrary to the common forms of migraine, FHM patients are not characterized by a deficient, but rather by an increased habituation in cortical/brain stem evoked activities. These results suggest that there may be some striking pathophysiological differences between FHM and the common forms of migraine, as far as central neuronal processing is concerned.

SPATIO-TEMPORAL CHANGES OF APOLIPOPROTEIN E (APOE) IN THE RAT BRAIN AFTER EXPERIMENTAL STROKE. ENRICHED HOUSING CONDITION ATTENUATES APOE EXPRESSION

K. Ruscher, E. Johannesson, M. Rickhag, T. Wieloch

Laboratory for Experimental Brain Research, Lund University, Lund, Sweden

Objectives: Apolipoprotein E (ApoE), a cholesterol transporter and an immunomodulator, is brain protective after stroke and implicated in brain repair. The present study was designed to assess the involvement of ApoE in the restoration of brain function after experimental stroke, by employing animal housing conditions that differentially improve recovery after brain injury (1).

Methods: The temporal and cellular pattern of ApoE expression was analyzed from different brain regions from rats subjected to 2 hours of transient occlusion middle cerebral artery (tMCAO). Permanent MCAO was induced in spontaneous hypertensive rats, housed in either standard or enriched housing conditions (starting 2 days after pMCAO), and the tissue levels and cellular cellular distribution of ApoE determined.

Results: ApoE levels increased in the injured hemisphere over a 30 days recovery period, with the exception of a proximal narrow peri-infarct rim, conspicuously devoid of ApoE at 4-7 days after tMCAO. In contrast to the ischemic core, this region showed no accumulation of $CD11b^+$ microglial cells but presented a normal distribution of $NeuN^+$ neurons indicative of a proximal non-injured peri-infarct zone. In this region, we further observed only a limited amount of $GFAP^+$ astrocytes suggesting an inhibition of astrocyte proliferation in this zone. Still, in the peri-infarct rim, ramified $S100\beta^+$ reactive astrocytes with high expression of ApoE are present. Further, enriched housing following pMCAO caused an approximately 50% decrease in ApoE levels compared to standard housing conditions, particularly in the peri-infarct region and in ApoE/$S100\beta^+$ reactive astrocytes.

Conclusions: The reduced levels of ApoE and reduced number of ApoE/$S100\beta^+$ reactive astrocytes in animals housed in an ee implies that enriched housing conditions might attenuate the inflammatory response after stroke. Our study also support the notion of a proximal regenerative zone in the peri-infarct zone after stroke, with low levels of ApoE.

Reference: Rickhag M, Deierborg T, Patel S, Ruscher K, Wieloch T. J Cereb Blood Flow Metab. 2008 28(3):551-62.

Grant support: The EU 7^{th} workprogram through the European Stroke Network, Swedish Research Council, Pia Ståhls Foundation, The Swedish Brain Fund, the Kungliga Fysiografiska Sällskapet i Lund, and the Greta and Johan Kocks stiftelser.

965

Brain Poster Session: Subarachnoid Hemorrhage

MRI OF CEREBRAL ISCHEMIA AND CHRONIC HYPERPERFUSION AFTER SUBARACHNOID HEMORRHAGE IN RATS

I.A.C.W. Tiebosch[1], W.M. van den Bergh[2], R. Zwartbol[1], K. van der Marel[1], R.M. Dijkhuizen[1]

[1]Image Sciences Institute, [2]Dpt. of Intensive Care, University Medical Center Utrecht, Utrecht, The Netherlands

Objectives: Subarachnoid hemorrhage (SAH) carries poor prognosis, which has been attributed to vasospasm-related delayed cerebral ischemia. With MRI we have demonstrated that vasoconstriction, loss of cerebral blood flow (CBF) and ischemic tissue damage develop within 48 h after SAH in rats.[1] Goal of the current study was to characterize the progression of tissue and perfusion changes in relation to outcome at chronic time-points after experimental SAH.

Methods: SAH was induced in isoflurane-anesthetized adult male Wistar rats (n=17) by puncturing the right middle cerebral artery or the internal carotid artery at the level of their bifurcation, with a sharpened 4-0 polypropylene suture.[2] MRI was conducted after 48 h and 7 days, and included multislice T_2- and diffusion-weighted MRI, dynamic susceptibility contrast-enhanced MRI in combination with an intravenous injection of gadobutrol, and pre- and post-contrast T_1-weighted MRI. Maps of the T_2, apparent diffusion coefficient (ADC), cerebral blood volume (CBV), CBF index (CBF_i) and contrast-induced T_1-weighted signal change were calculated[3] and co-registered to a stereotaxic rat brain atlas[4]. MR parameters were measured in ipsi- and contralateral primary somatosensory fore- and hindlimb regions (S1) and caudate putamen (CPu) and statistically analyzed with a paired Student's t-test.

Results: Ten rats died before the first MRI scan at 48 h, and four animals died between the first and second MRI scan at 7 days. At 48 h SAH-induced brain lesions were characterized by areas of reduced ADC and, more particularly, prolonged T_2, in large part of the ipsilateral somatosensory cortex and CPu (n=7). Relative T_2 in ipsilateral S1 and CPu were 142±26% and 132±31%, respectively (% of contralateral; $P< 0.05$). CBV and CBF_i were increased in these regions; on average by more than 40% ($P< 0.05$). Also, there was significant contrast leakage in ipsilateral S1 and CPu. Three animals with significantly smaller ADC and T_2 alterations in the lesioned area as compared to the other four animals, survived between 2 and 7 days. In these animals, lesion T_2 and ADC values had largely normalized, but CBV and CBF_i remained elevated after 7 days.

Conclusions: Experimental SAH was accompanied by a relatively high mortality rate. In animals that survived until at least 48 h post-SAH, ADC reduction and T_2 prolongation in the MCA territory point toward cerebral ischemia. However, elevated CBV and CBF_i suggest that perfusion loss occurs before this time-point. Animals with least signs of ischemia survived beyond 48 h. Our study corroborates the significant role of cerebral ischemia in outcome after SAH. Hyperperfusion at later time-points, which has also been observed in aneurysmal SAH patients[5], may be related to impaired autoregulation, but its effect on brain tissue status needs to be further investigated.

References:

1. Van den Bergh et al. (2005) Acta Neurochirurgica 147:977-983.

2. Veelken et al. (1995) Stroke 26:1279-1283.

3. Dijkhuizen et al. (2001) JCBFM 21:964-961.

4. Paxinos and Watson (1998) Academic Press (New York).

5. Egge et al. (2005) Neurosurgery 57:237-242.

Funding:

Netherlands Heart Foundation (2005B156).

Netherlands Brain Foundation (15F07(2).08).

Brain Poster Session: Cerebral Vascular Regulation

BETWEEN AND WITHIN ANIMAL VARIATIONS IN MICRO-PUNCH RAT BRAIN CORTEX ENOS CONCENTRATIONS

R.K. Czambel[1], A. Kharlamov[1], J.L. Timpona[1], **S.C. Jones**[2,3]

[1]Anesthesiology, [2]Anesthesiology and Neurology, Allegheny-Singer Research Institute, [3]Radiology, Univ of Pittsburgh, Pittsburgh, PA, USA

Endothelial nitric oxide synthase (eNOS) is an important component of the multiple cerebro-vasoregulatory mechanisms in hypotension and ischemia. Measurements of NOS enzyme activity are usually done in vitro under optimal cofactor conditions, which can obscure in vivo behavior, and are rarely if ever isoform specific. Phosphorylation state measurements, primarily focused on ser1179, can ignore the complex regulatory mechanisms that involve many other phosphorylation sites, both stimulatory and inhibitory. We thus propose that eNOS brain concentration, $[eNOS]_{br}$, itself, measured in micro-punch cortical brain samples with a modified ELISA assay, can provide crucial insights. We hypothesize that significant variations in $[eNOS]_{br}$ exist both within and between animals.

Methods: To investigate $[eNOS]_{br}$ variability, micro-punch (1,2) cortical brain samples (718±97 µg, n=76, mean±sd) from both the right and the left hemispheres of four adult male Sprague-Dawley rats were obtained after the brain was cooled in situ postmortem to -14°C. To each tissue punch was added 140 uL of ice-cold lysis buffer. All samples were frozen at -80°C until assayed using a modified eNOS ELISA procedure (R&D Systems, Minneapolis, MN). Modifications included the adjustment of the sample volume and the preparation of the calibration standards in an "eNOS free" matrix obtained from the brain cortex tissue of a mutant eNOS knock-out mouse and prepared in the same fashion as the micro-punch samples. Spike-and-recovery analysis was performed on all samples. After correcting for recovery, the resulting $[eNOS]_{br}$ were compared for within and between animal variability with repeated measure analysis of variance.

Results: Mean $[eNOS]_{br}$ for all samples (n=76) was 6.66±1.90 fmol/mg-wet weight. Significant differences were detected ($p< 0.001$) between animals but there were no differences between right and left samples. The between- and within-animal variances were 41% and 59%, respectively. Thus even though there was significant differences between animals, there was also significant variability within the brain cortex for each animal.

Conclusion: Our results demonstrating $[eNOS]_{br}$ variability, both between and within animals, validate the concept that concentration alone is important in this protein's function in cerebrovascular regulation. The concentration of eNOS, as a constitutively expressed protein, is commonly considered static. Our result, that concentration alone is important, could well complement the established concept that the cerebrovascular regulation via eNOS is tightly controlled by many modulators. Ours and others' previous measurements of heterogeneity in the cerebral circulation's response to hypotension (3,4,5), presumably based on nitric oxide from eNOS (6), correspond to the between and within animal variations in $[eNOS]_{br}$ documented in this work. These issues could potentially be further investigated by combining this quantitative micro-punch method with CBF laser Doppler flowmetry.

Support: Pennsylvania Tobacco Settlement Funds.

References:

1. Yushmanov et al. (2007) Magn Reson Med 57:494-500.

2. Hu et al. (2000) Brain Res 868:370-375.

3. Kharlamov et al. (2004) Neurosci Lett 368:151-156.

4. Heimann et al. (1994) J Cereb Blood Flow Metab 14:1100-1105.

5. Todd et al. (1998) Neuroanesthesia: a critical review. In: Principles and practice of anesthesiology (Longnecker et al.):1607-1658.

6. Toyoda et al. (1997) J Cereb Blood Flow Metab 17:1089-1096.

DUAL-ASSESSMENT OF FUNCTIONAL AND PATHOLOGICAL CHANGES IN ALZHEIMER'S DISEASE USING SINGLE ^{11}C-PIB PET

S.J. Kim, Y.K. Kim, J.S. Lee, E.J. Yoon, S.E. Kim, D.S. Lee

Department of Nuclear Medicine, Seoul National University College of Medicine, Seoul, South Korea

Objectives: In most studies, the association between functional (regional cerebral glucose metabolism) and pathological information (brain amyloid plaque load) have been separately investigated using two different traceres, ^{11}C-PIB and ^{18}F-FDG PET in assessment of of Alzheimer's disease (AD). In this study, we investigated the possibility of functional R_1 map (relative flow delivery, K_1 region of interest/K_1 reference region) from PIB PET as alternative functional map in stead of FDG PET.

Methods: Thirty eight subjects (8 AD and 12 MCI patients, 18 normal volunteers) underwent dynamic ^{11}C-PIB PET scans with 90 min scan duration and ^{18}F-FDG scans with 30min after injection. Parametric images of R_1 for ^{11}C-PIB PET were generated using multilinear reference tissue models (MRTM2) [1]. To compare the brain regions with perfusion and metabolic abnormalities on ^{11}C-PIB and FDG PET quantitatively, R_1 map and FDG images underwent z-transformation with respect to each normal average and SD. The association of the number of abnormal voxels and mean z-value between R_1 map obtained from PIB PET and glucose metabolism obtained from FDG PET was evaluated in the entire brain excluding cerebellum.

Results: Z-values of each group were well reflected the severity of AD. At a z threshold of -2.97 for both R_1 PIB and FDG, the number of abnormal voxels across the entire brain showed a correlation, and the mean z-values of abnormal voxels between them were highly correlated ($r = 0.86$, $p < 0.0001$).

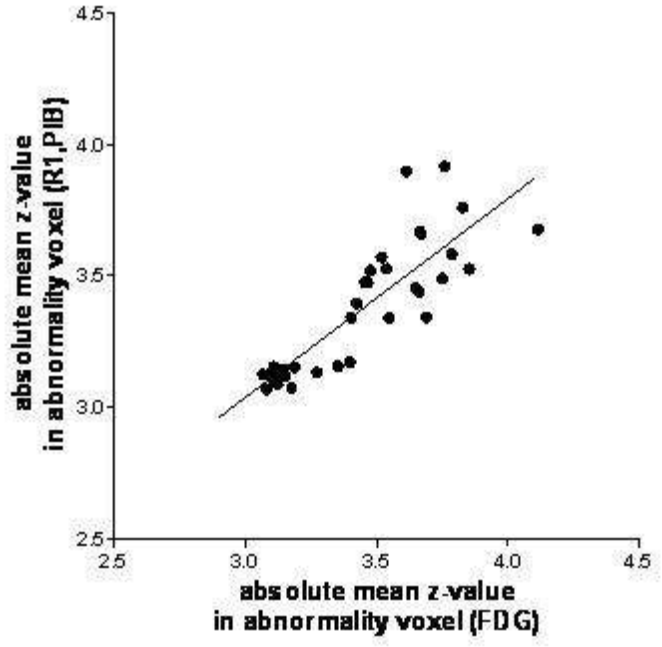

[Correlation mean z-value between FDG and PIB PET]

Conclusions: The relative perfusion obtained from PIB PET was well correlated with those of metabolic abnormality in the entire brain. This study may suggest that a single PIB PET study with R_1 map could provide the sufficient information in the distribution of pathologic and metabolic abnormalities in disease progression.

Reference: [1] Masanori Ichise, Jeih-San Liow, Jian-Qiang Lu, et al., "Linearized Reference Tissue Parametric Imaging Methods : Application to [^{11}C]DASB Positron Emission Tomography Studies of the Serotonin Transporter in Human Brain " JCBFM, 23:p1096-1112.

971

Brain Poster Session: Neuroprotection

CYCLIC PATTERN OF 17β-ESTRADIOL PRETREATMENT PROTECTS THE HIPPOCAMPAL CA1 REGION AGAINST CEREBRAL ISCHEMIA

N. Hirsch[1], I. Saul[1], K. Dave[1], R.A. DeFazio[1], H. Bramlett[2], M. Perez-Pinzon[1], **A. Raval**[1]

[1]Department of Neurology, University of Miami, [2]Department of Neurological Surgery, Miami Project to Cure Paralysis, University of Miami, Miami, FL, USA

Objectives: Chronic 17β-estradiol treatment improves pathophysiological outcome after brain ischemia in experimental animal models (1-3). In contrast to chronic 17β-estradiol treatment strategy, our recent study demonstrated that a single 17β-estradiol bolus 48 h prior to ischemia induces neuroprotection in the hippocampal CA1 region in slice culture and rat models of global cerebral ischemia (4, 5). Based on these results, we hypothesized that cyclic 17β-estradiol treatment provides neuroprotection against cerebral ischemia in the rat model.

Method: Normal cycling female rats were ovariectomized (OvX) and 7 days later an injection schedule of 17ß-estradiol (5 µg/Kg; i.p) or vehicle (oil) was started. Rats were injected with 17ß-estradiol/oil at an interval of every 48 or 72h for 4 cycles over the period of one month. Forty eight or seventy two hours following the last hormone treatment rats were exposed to cerebral ischemia produced by 10 min of bilateral carotid occlusion and systemic hypotension (50mmHg). Seven days after ischemia, rat brains were fixed for histopathological assessment. Hippocampal sections at the level of 3.8 mm posterior to bregma were examined for normal neurons. Results are expressed as mean ± SEM. Statistical significance was determined with an ANOVA test followed by a Bonferroni's post-hoc test.

Results: The number of normal neurons per slice in the CA1 hippocampal region in naïve rats was 1100 ± 45 (n = 4). The ischemic insult in OvX rats decreased the number of normal neurons to 18% of naïve (192 ± 10, n = 6, $p < 0.05$). Intermittent estradiol-17β treatment to ovariectomized rats prior to cerebral ischemia increased the number of normal neurons to 51% (559 ± 13, n = 7, dose 5 µg/Kg/every 48h for 21 days) and 41% (446 ± 14, n = 7, dose 5 µg/Kg/every 72h for 21 days) as compared to OvX group ($p < 0.05$). Vehicle treatment did not show any significant difference in the number of normal neurons versus OvX groups. Female rats receiving sham-OvX showed no difference from OVX in neuron loss after ischemia.

Conclusion: A cyclic pattern of 17β-estradiol bolus treatment conferred protection against ischemia in ovariectomized rats. This study emphasizes the need to investigate a cyclical estrogen hormone replacement regimen to promote improved cardio- and cerebro-vascular health and reduce stroke/cerebral ischemia incidents in post-menopausal women while avoiding the known side effects of chronic estradiol treatment.

References:

1. Alkayed et al, Stroke 31, 161 (2000).

2. McCullough and Hurn, Trends Endocrinol Metab 14, 228 (2003).

3. Jover et al., J Neurosci 22, 2115 (2002).

4. Raval et al Neuroscience (2006).

5. Raval et al Journal Cerebral Blood Flow and Metabolism 27, BP10 (2007).

Grant support: AHA-SDG-National Center #0730089N and James and Esther King Biomedical Research Program, Florida Department of Health 07KN-10.

ISCHEMIC PRECONDITIONING MEDIATED CYCLOOXYGENASE-2 EXPRESSION VIA NUCLEAR FACTOR KAPPA-B ACTIVATION: AN IN VITRO STUDY

E.J. Kim, A. Raval, N. Hirsch, M. Perez-Pinzon

Department of Neurology, University of Miami, Miami, FL, USA

Objectives: Ischemic preconditioning (IPC) is an endogenous protective mechanism invoked by a brief, sublethal ischemic insult prior to a subsequent lethal ischemic insult. Nuclear Factor-kappaB (NF-kappaB) activation occurs following IPC in brain [1]. However, the upstream signaling messengers and down-stream targets of NF-kappaB required for induction of IPC remain undefined. Previously, we demonstrated that epsilon protein kinase c (ePKC) is the key mediator of IPC- and ePKC-induced cyclooygenase-2 (COX-2) expression in the in vitro models [2]. Here, we hypothesized that IPC-mediated COX-2 expression was regulated by NF-kappaB.

Method: Mixed cortical neuron/astrocyte cell cultures were prepared from rat embryo/neonatal rat (18-19/1-2 days old), respectively. To simulate preconditioning or ischemia, cell cultures were exposed to 1h or 4h of oxygen-glucose deprivation (OGD), respectively. Epsilon PKC agonist peptide (100 nM) was applied to cell culture for 1 h. Cell lysates were isolated at different time points after IPC or ePKC agonist treatment for immunoblotting with antibody against p65 and p50 subunits of NF-kappaB. To determine assessment of cell death, cytotoxicity was measured by lactate dehydrogenase (LDH) released for 48 h into culture medium. Maximal neuronal LDH release was measured in neuronal cultures exposed to NMDA (500 μM; 48 h; maximal neuronal death). LDH release was measured by absorbance at 340 nm using a microplate reader (Molecular Devices, CA). Values were expressed relative to LDH measurement from maximal neuronal LDH. Results are expressed as mean ± SEM. Statistical significance was determined with an ANOVA test followed by a Bonferroni's post-hoc test.

Results: Translocation of p65 and p50 subunit of NF-kappaB to the nucleus occurred at 15 min after IPC and lasted for 2 hours. To verify whether NF-kappaB activation was required for IPC-induced neuroprotection, NF-kappaB inhibitor (pyrrolidine dithiocarbamate, PDTC, 10 μM), was applied during IPC. Forty-eight hours later, cells were exposed to OGD (4h) and neuronal cell death was measured. Results showed that IPC reduced the neuronal death by 30% as compared to ischemic injury (45 ± 2% vs. 75 ± 1.8% of maximal cell death; IPC vs. OGD, $P< 0.05$, $n = 20$) and PDTC treatment during IPC significantly abolished IPC-induced neuroprotection (45 ± 2% vs. 65.7 ± 2.5% of maximal cell death: IPC vs. IPC+PDTC+OGD, $P< 0.05$, $n = 20$). In parallel, inhibition of either ePKC or the ERK 1/2 pathway reduced IPC-induced NF-kappaB activation. To determine whether NF-kappaB activation was involved in IPC-induced COX-2 expression in neurons, cells were treated with NF-kappaB inhibitor during IPC. Results demonstrated that NF-kappaB inhibition significantly reduced IPC-induced COX-2 expression (0.6 ± 0.2 vs. 0.15 ± 0.02 optical density: IPC vs. IPC+PDTC, $p< 0.05$ compared with IPC, $n = 5$).

Conclusion: We demonstrated that IPC-signaling activates NF-kappaB via ePKC and ERK1/2 pathway and translocation of NF-kappaB to nucleus mediates COX-2 expression, resulting in neuroprotection in an in vitro model.

Reference:

1. Blondeau et at., 2001. J Neurosci 21 (2001) 4668-4677.

2. Kim et al., 2007. Neuroscience. 145, 931-941.

Grant support: PHS grants NS34773, NS054147, NS045676, NS05820.

IMAGING OF REGIONAL RED BLOOD CELL MASS IN THE RAT BRAIN BY HIGH-RESOLUTION, QUANTITATIVE NANOSPECT/CT TECHNOLOGY

D. Máthé[1], I. Portörő[2], G. Németh[1], **A. Eke**[2]

[1]Mediso Ltd., [2]Institute of Human Physiology and Clinical Experimental Research, Semmelweis University, Budapest, Hungary

Objectives: Regional oxygen supply by red blood cells (RBCs) within the regional cerebral blood volume (rCBV) has a major impact on brain functions. Hence, our motivation - by using a NanoSPECT/CT small animal imaging system with its proprietary Multiplexed-Multipinhole Collimation for in vivo quantitative SPECT [1] - was to develop a method for imaging RBC mass in the brain. As a test, rCBV was decreased by increasing the vascular tone via the NO/cGMP pathway by L-NAME.

Methods: Male Wistar rats (n=4) were anesthetized by a 1:1 mixture of Ketamine-Xylasine solutions (100 mg/mL and 5 mg/mL, respectively) given i.p. in a dose of 2.5 mL/kg bdw for induction, followed by an hourly maintaining dose of 1.5 mL/kg bdw. Catheters were inserted into the femoral artery and vein.

RBCs were labeled with ^{99m}Tc using stannous pyrophosphate as reducing agent (20 μg Sn (II)/kg bdw, i.v.). Thirty minutes later, 1 mL of pre-treated arterial blood was withdrawn and gently mixed with 1 mL of ^{99m}Tc-pertechnetate solution of ~ 200 MBq activity, and allowed to stand for 10 minutes prior to re-injection. Labeled RBCs were re-injected (in 0.7 mL with approximate activity of 70 MBq) for mapping RBCs 5 minutes post-injection.

Two animals were treated by L-NAME (100 mg/kg bdw, i.v.). Scans were acquired for control and at 44 minutes following the L-NAME injection. Animals were sacrificed by saline infusion (a total of 100 mL) given via the arterial line with concomitant drainage via the venous line in order to remove blood from the brain's parenchyma.

Cerebral RBC mass (CRBCM) was characterized by activities normalized by the brain's volume (as shown in an exemplary experiment in the Figure).

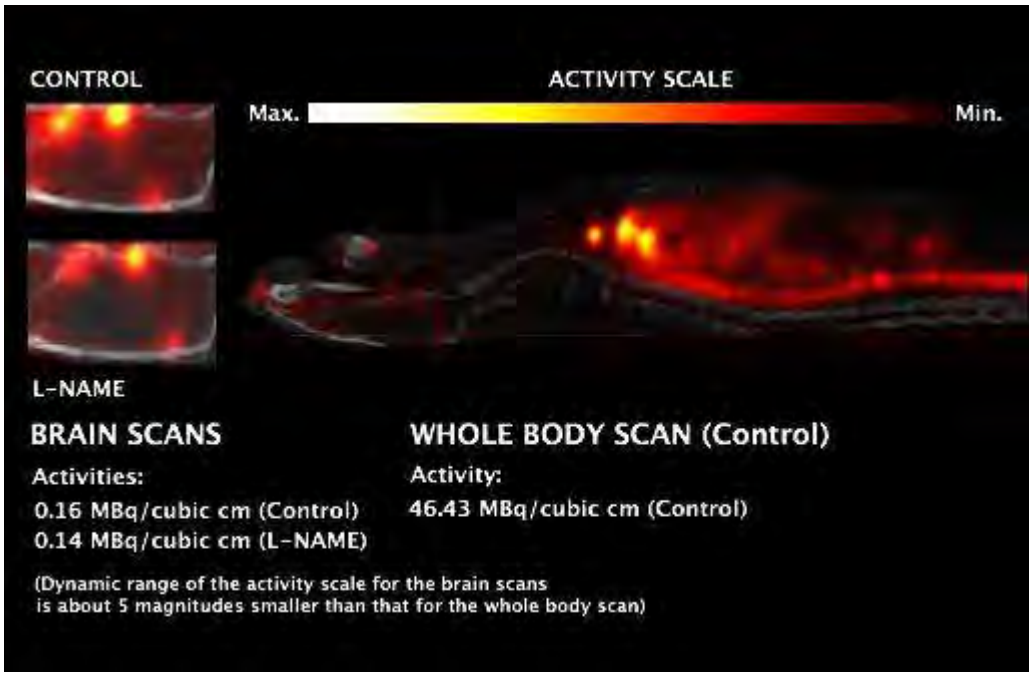

[Biodistribution of 99mTc-labeled red blood cells]

Results: No activities were found in the thyroids and in the stomach, the sites where free ^{99m}Tc-pertechnetate in blood accumulates if present; an evidence of a larger then 99% purity of radiolabeling. Hot spots in the brain were detected at sites of venous sinuses and the circus of Willis. CRBCM decreased in the L-NAME treated animals, as anticipated, while ^{99m}Tc-activity became about a magnitude smaller (0.03 mBq/cm^3) after saline infusion demonstrating the specificity of the ^{99m}Tc-radiolabeling for RBCs.

Conclusions: Quantitative NanoSPECT technology is efficient to assess regional RBC mass in the rodent brain.

References: 1. S. Nikolaus et al (2005) European Journal of Nuclear Medicine and Molecular Imaging, 32:308-313.

Acknowledgement: Supported by the National Office for Research and Technology Grant 2008ALAP1-01569/2008 given to A. Eke.

975

Brain Poster Session: Neurovascular Unit in Health & Disease

NICOTINE EXPOSURE INHIBITS 17β-ESTRADIOL-MEDIATED PROTECTION OF THE HIPPOCAMPAL CA1 REGION AGAINST CEREBRAL ISCHEMIA IN FEMALE RATS

A. Raval, A. Bhatt, I. Saul, M. Perez-Pinzon

Department of Neurology, University of Miami, Miami, FL, USA

Objective: Women are naturally protected against cerebral ischemia owing to the effects of circulating estrogens [1, 2]. Nicotine addiction in women modulates estrogen metabolism, reduces circulating estrogen levels and increases the risk/damage of ischemic stroke. The exact mechanism by which nicotine abrogates the protective effects of endogenous estrogen leading to increased incidence of ischemia in females is not known. Here, using a rat model of global cerebral ischemia, our goals are:

1. to determine whether chronic nicotine treatment abrogates beneficial effects of estrogen on hippocampal neurons subjected to ischemia, and
2. to determine whether nicotine exposure antagonizes estrogen signaling by reducing the number of estrogen receptor(s).

Method: Normally cycling or 7 days post-ovariectomized rats were injected with nicotine/saline daily (1mg/kg BW in saline; i.p.) for 15 days. To investigate the efficacy of estrogen in nicotine-exposed rats, ovariectomized and nicotine-treated rats were injected with a bolus of 17β-estradiol (5 μg/Kg in oil; i.p.). Following last treatment rats were divided in to two groups. Rats of the first group were exposed to cerebral ischemia produced by 10 min of bilateral carotid occlusion and systemic hypotension (50mmHg). Seven days after ischemia rat brains were fixed for histopathological assessment. Hippocampal sections at the level of 3.8 mm posterior to bregma were examined for normal neurons. For Western blot analysis, hippocampi were collected from second group of treated rats. The Western blots were quantified by densitometric analysis. Results are expressed as mean ± SEM. Statistical significance was determined with an ANOVA test followed by a Bonferroni's post-hoc test.

Results: The number of normal neurons per slice in the CA1 hippocampal region in naïve rats was 1268±31 (n=5) and the ischemic insult to saline-treated females rats decreased the normal neuronal count to 29% (496±57; n=4; $p< 0.001$). Nicotine exposure followed by ischemic insult to normal cycling rats decreased the number of live neurons to only 13% (177±21; n=6; $p < 0.05$ as against ischemia). The ischemic insult to ovariectomized rats resulted in 18% of normal neurons in the CA1 region (250±58; n=6; $p< 0.001$ as compared to naïve). A bolus of 17β-estradiol to ovariectomized rats significantly protected CA1 region against ischemia (47% of naïve; 601±89; n=5). In contrast, 17β-estradiol treatment to nicotine-exposed ovariectomized rats could not confer a similar degree of protection (27% of naïve; 373±52; n=6). In parallel, nicotine exposure reduced hippocampal ERβ protein levels by 47% and 40% in normally cycling or ovariectomized plus 17β-estradiol treated rats, respectively, as compared to the non-treated control groups ($p< 0.05$). In contrast to ERβ, the ERα protein level remained unchanged following nicotine exposure.

Conclusion: Chronic nicotine exposure reduced protein levels of estrogen receptor-β in the hippocampus and abrogated estrogen-conferred protection against cerebral ischemia in the female rat.

References:

1. McCullough LD and Hurn PD, Trends Endocrinol Metab 14, 228 (2003).

2. Bramlett H, Pathophysiology 12, 17 (2005).

Grant support: AHA-SDG-National Center #0730089N and James and Esther King Biomedical Research Program, Florida Department of Health 07KN-10.

COLLATERAL PERFUSION AND CEREBRAL BLOOD VOLUME DIMINISH INFARCT CORE AND PENUMBRA IN ACUTE ISCHEMIC STROKE DUE TO INTRACRANIAL ATHEROSCLEROSIS

D. Liebeskind[1], J. Alger[1], G. Kim[2], N. Sanossian[3], C. Chung[2], K. Lee[2], O.Y. Bang[2]

[1]University California Los Angeles, Los Angeles, CA, USA, [2]Samsung Medical Center, Seoul, South Korea, [3]University of Southern California, Los Angeles, CA, USA

Objectives: Etiology is rarely considered when evaluating perfusion abnormalities in acute ischemic stroke. Arterial occlusion due to progressive luminal stenosis with intracranial atherosclerosis (IA) may allow collateral perfusion to develop compared with abrupt cardioembolic (CE) occlusion. Diversion of cerebral blood volume (CBV) from core to periphery, leading to CBV collapse may also be offset by enhance collateral perfusion in the setting of IA. We analyzed diffusion and perfusion MRI in acute ischemic stroke based on etiology.

Methods: A consecutive series of acute stroke cases with MCA ischemia and NIHSS score>4 had MRI< 6 hours from symptom onset. Post-processing generated Tmax>2 sec (Tmax2), Tmax>8 sec (Tmax8), and CBV maps. Volumetric measures of lesions were extracted for Tmax and CBV (ischemic core (IC)< .50 ml/100 g; penumbra to infarct (PI)=.51-.75; penumbra to reverse (PR)=.76-1.00; normal (N)=1.01-6.99; hyperemia (H)=7.00-15.00). Lesion volumes were compared based on SSS TOAST classification (IA versus CE) and the subset with isolated M1 occlusion.

Results: Age and time to MRI did not differ between groups (20 IA and 46 CE). NIHSS scores were much lower with IA (mean 8.6 vs. 13.8, p=.002) and diffusion volumes were 10-fold smaller with IA (p=.004). Tmax2 volumes were equivalent, yet Tmax8 volumes were far smaller in IA (p=.016) suggesting greater sensitivity to Tmax thresholds. CBV IC lesions were much smaller than CE cases (p=.02) and far more variability in IC lesions was noted amongst CE cases likely reflecting a broad range of collateral perfusion. PI and PR lesions trended smaller in IA with no difference in H volumes. The extent of abnormal tissue (IC, PI, PR, H) was far greater in CE reflecting larger gradients of CBV (p=.015). Similar patterns with significant discrepancies of CBV based on etiology were noted in the isolated M1 occlusions (12 IA, 12 CE). Isolated occlusion of M1 resulted in dramatically lower NIHSS scores (mean 10.4 vs. 16.0, p=.005) and revealed strikingly smaller areas of ischemic core and penumbra. Gradients of CBV from core to penumbra and hyperemia downstream from isolated M1 occlusion were considerably smaller in IA (p=.039) likely reflecting well-developed arterial collateral inflow to balance cerebral venous diversion from core to periphery.

Conclusions: Ischemic stroke due to IA results in dramatically less sever neurological deficits and diminished lesion volumes. Time-domain perfusion parameters (e.g. Tmax) may not accurately reflect ischemic severity unless stroke etiology is considered. Collateral perfusion, reflected by preserved CBV, is more robust in IA with less variability across cases likely due to arteriogenesis. Smaller CBV gradients across the territory may make IA cases less vulnerable to collateral failure. Future predictive imaging models and treatment strategies must account for stroke etiologies such as IA.

Brain Poster Session: Oxidative Mechanisms

HYPERBARIC OXYGEN STIMULATES THE TRANSCRIPTION RATE OF THE ANTIOXIDANT ENZYME CUPPER/ZINC-SUPEROXIDE DISMUTASE IN RAT BRAIN CORTEX TISSUE

S. Oter[1], S. Sadir[1], B. Uysal[1], M. Ozler[1], K. Simsek[2], H. Ay[2], H. Yaman[3], R. Ogur[4], R.J. Reiter[5], T. Topal[1], A. Korkmaz[1]

[1]Physiology, [2]Undersea and Hyperbaric Medicine, [3]Biochemistry, [4]Public Health, Gulhane Military Medical Academy, Ankara, Turkey, [5]Cellular and Structural Biology, University of Texas Health Science Center at San Antonio, San Antonio, TX, USA

Objectives: HBO therapy is a treatment method known to cause oxidative stress [1] while having beneficial effects in several pathophysiological processes where free radical damage is contributory [2]. Moreover, antioxidant enzyme activities are usually increased with HBO exposure [3, 4], which may be a compensatory response to enhanced production of reactive oxygen species. Another hypothesis suggests that HBO has the ability to stimulate antioxidant enzyme synthesis directly [5]. Evidence for both these potential explanations is not completely understood. Therefore, taken the brain as one of the main target organs affected by HBO exposure, we aimed to elucidate this matter via detecting the transcription rate of cupper/zinc-superoxide dismutase (Cu/Zn-SOD) in rats.

Methods: eventy-two male Sprague-Dawley rats were divided into 6 (n=12 for each) groups: control, HBO, HBO+Glutathione (GSH) and HBO+SOD, HBO+melatonin, and melatonin. HBO was administered once for 2 hours at 3 atmospheres pressure. GSH, SOD, and melatonin were administred intraperitoneally one hour before HBO exposure. Right after exposure, their brain cortexes were harvested immediately and following biochemical assay was performed: malondialdehyde (MDA) and protein carbonyl (PCO) levels, catalase, glutathione peroxidase and SOD activities, and reduced/oxidized glutathione (GSH/GSSG) ratio. Additionally, the transcription rate of Cu/Zn-SOD mRNA was determined via RT-PCR.

The reason for establishing study groups with antioxidants (GSH, SOD, melatonin) was to distinguish a potential effect of HBO on the transcription rate of SOD with an indirectly stimulated effect via enhanced radical production. Melatonin itself is known to induce antioxidant enzymes expression [6]; therefore, the melatonin only group will give the ability to compare the strongivity of the results.

Results: O clearly increased oxidative stress indices MDA and PCO. SOD activity as well as its mRNA transcription rate was also increased with HBO exposure. Melatonin and GSH were able to reduce the oxidative action of HBO. Nevertheless, neither SOD nor GSH could block the mRNA enhancing effect of HBO for Cu/Zn-SOD. Interestingly, melatonin increased the SOD mRNA transcription itself, but limited (not blocked) the increasing effect of HBO. The Cu/Zn-SOD mRNA expression rates of all study groups are demonstrated in figure.

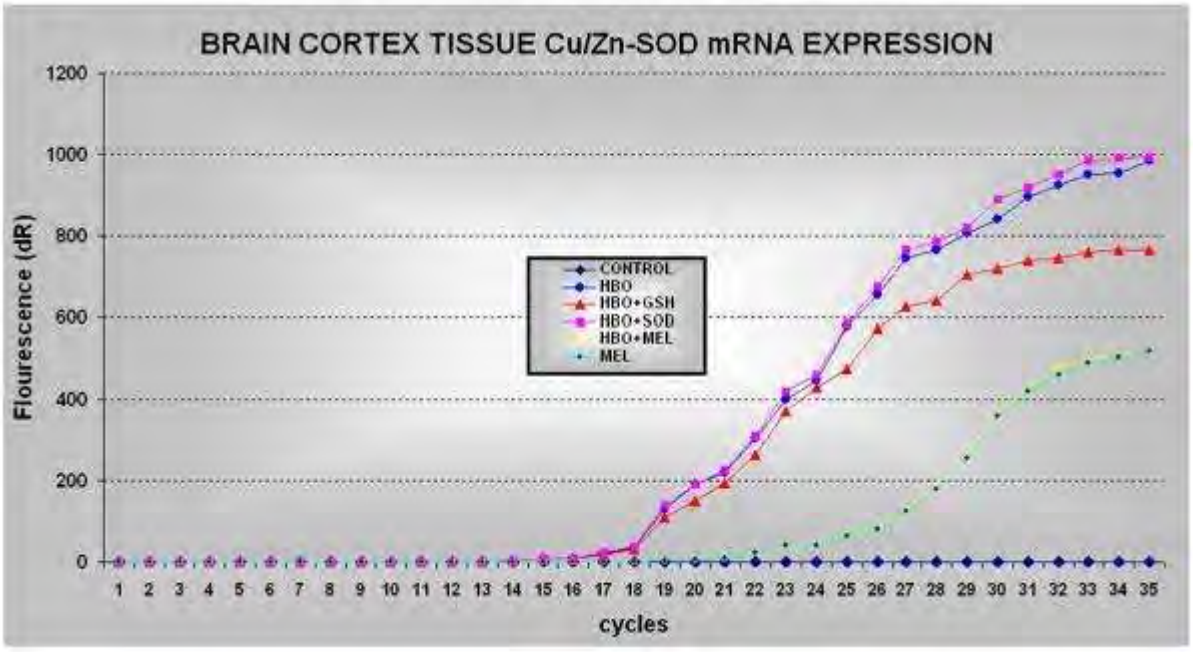

[Cortical SOD mRNA Expression]

Conclusion: The present findings support the suggestion that HBO have the ability to stimulate directly the mRNA transcription of SOD in rat's brain cortex. The limiting effect of melatonin indicates a molecular interaction and has to be further elucidated.

References:

[1] Narkowicz et al. Free Radic Res Commun 1993;19:71.

[2] Buras J. Int Anesthesiol Clin 2000;38:91.

[3] Li et al. Brain Res 2008;1210:223.

[4] Nie et al. J Cereb Blood Flow Metab 2006;26:666.

[5] Freiberger et al. Undersea Hyperb Med 2004;31:227.

[6] Rodriguez et al. J Pineal Res 2004;36:1.

Grant: This study was supported by the “Scientific & Technological Research Council of Turkey” with the grant Nr.105S060.

978

Brain Poster Session: Cerebral Vascular Regulation

NO REFLOW: OPEN ARTERIES WITHOUT TISSUE PERFUSION IN ACUTE ISCHEMIC STROKE

D. Liebeskind, G. Duckwiler, S. Starkman, D. Kim, L. Ali, B. Ovbiagele, A. Ohanian, J. Panagotacos, J. Gadhia, S. Tateshima, N. Gonzalez, R. Jahan, F. Vinuela, J. Saver

University California Los Angeles, Los Angeles, CA, USA

Objectives: Prior studies have reported that visualized distal emboli that limit reflow can cause dissociation of target artery recanalization and territorial reperfusion after endovascular recanalization. No reflow due to ischemic microvascular compromise has been described in preclinical work, yet never chronicled in humans. We investigated the frequency and mechanisms of constrained reperfusion following successful mechanical thrombectomy for acute ischemic stroke.

Methods: Retrospective analysis of angiographic findings was conducted in consecutive patients treated with the MERCI Retriever device for acute ischemic stroke at a single center from May 2001 through June 2007. Thrombolysis in Cerebral Infarction (TICI) grades and ASITN/SIR collateral flow scores were measured on posttreatment angiograms. The standard TICI 3 category was subdivided into TICI 3a - generally complete reperfusion but with subtle defects, and TICI 3b - complete, defect-free reperfusion. Demographic, clinical, and radiographic variables were examined to identify potential predictors of no reflow. Evidence of thrombi associated with distal emboli occlusion was also examined on post-treatment GRE MRI when available.

Results: One-hundred fourteen acute stroke patients were treated with mechanical thrombectomy using the MERCI device. Mean age was 65±19 years, median baseline National Institutes of Health Stroke Scale (NIHSS) score was 19±7. All (48/48) cases of TICI 2 reperfusion demonstrated residual distal vessel occlusions, yet tapering without abrupt arterial occlusion was often noted in other regions. Complete TICI 3b reperfusion without defects at angiography was noted in only 4/27 (15%) of TICI 3 cases, 4/114 (3.5%) of all cases. In the remaining 23 TICI 3a cases, overt evidence of distal embolic occlusions was noted in 11/23 (48%) and gradual arterial tapering without abrupt occlusion in 12/23 (52%). Cases with visualized distal emboli demonstrated retrograde collateral flow; in contrast, only marginal retrograde collateral flow was noted downstream from tapered arteries. GRE evidence of distal thrombotic occlusion was associated only with cases of distal emboli at angiography. No pretreatment clinical variables predicted development of no reflow with arterial tapering.

Conclusions: The microcirculatory no reflow phenomenon may limit reperfusion in half of all patients in whom all angiographically visualizable arteries are successful cleared by endovascular recanalization therapy. Regions with no reflow may be delineated by distal arterial tapering without overt embolic occlusion and lack of collateral inflow, consistent with increased downstream resistance. Further observational studies of no reflow and potential therapeutic approaches to improve tissue reperfusion beyond the clot are warranted.

For Endovascular Therapy Investigators, University California Los Angeles, USA.

980

Brain Poster Session: Cerebral Vascular Regulation

DYNAMIC CEREBRAL AUTOREGULATION- FROM MATHEMATICAL MODELLING TO CLINICAL PRACTICE AND BACK AGAIN

E. Carrera[1], M. Czosnyka[1], L.A. Steiner[2], E. Schmidt[3], S. Piechnik[4], P. Smielewski[1], K. Brady[5], J.D. Pickard[1]

[1]Clinical Neurosciences/ Neurosurgery Unit, Cambridge, Cambridge, UK, [2]Anaesthesiology, University Hospital, Basel, Switzerland, [3]Hopital Pourpan, Toulouse, France, [4]University of Oxford, Oxford, UK, [5]Anaesthesiology and Critical Care, Johns Hopkins University, Baltimore, MD, USA

Objectives: The role of dynamic cerebral autoregulation monitoring in the injured brain (TBI and SAH) has been highlighted in recent years. However, not all methods can be tested directly in clinical practice, because of ethical concerns regarding more invasive technologies. Apart from experimental laboratory, mathematical simulation is a strategy that can help in identifying the properties of potential indices suitable for the clinical testing of cerebrovascular reactivity and autoregulatory reserve.

Methods: Time-dependent interactions between pressure, flow and volume of cerebral blood and cerebrospinal fluid were modelled using a set of non-linear differential equations. The model simulates arterial blood inflow and storage, arteriolar and capillary blood flow controlled by cerebral autoregulation, venous blood storage and venous outflow modulated by intracranial pressure, cerebrospinal fluid production, storage, and reabsorption. The model was used to simulate three methods for assessment/monitoring of dynamic cerebral autoregulation:

- transient hyperaemia response (THR) after short lasting compression of common carotid artery,
- correlation between slow waves in mean blood flow velocity and cerebral perfusion pressure (CPP), generating the so-called Mx index (mean flow velocity index),
- correlation between slow waves in ICP and arterial pressure generating the pressure-reactivity index (PRx).

Material: Modelling data were compared to clinical findings. Tests were used to guide clinical management of 147 patients after subarachnoid haemorrhage (THR) and 602 patients after head injury (PRx- in 352 cases and Mx- in 298 cases).

Results: THR was demonstrated by modelling to depend on autoregulation strength (expressed as the static rate of autoregulation). This agrees with an absent hyperaemic response in patients after SAH suffering from vasospasm ($p< 0.001$). Delayed ischemic deficit could be predicted ($p< 0.03$) by coincidence of worsening autoregulation preceding vasospasm (1).

The Mx index proved to correlate with outcome after head injury showing worse autoregulation associated with higher mortality rate ($p< 0.001$), independent of intracranial hypertension.

In patients with asymmetrical CT scans (midline shift), cerebral autoregulation was worse on the side of brain expansion ($p< 0.02$)(2).

Pressure-reactivity (PRx) occurred to be a robust index in continuous bedside monitoring. Based on the results predicted by modelling, (3) U-shape relationships between PRx and CPP, PRx occurred to

be useful to optimize CPP by indicating preventable hypo- and hyperperfusion. Patients with current CPP closer to optimal CPP had more favourable outcome ($p < 0.002$) (4).

Conclusions: Modelling studies provide additional insight into the interpretation of clinical appearances of the varying states of cerebral autoregulation. Feedback from the clinical studies, in turn, provides data for verification of novel modelling structures: example is expansion from unilateral to bilateral model (5).

References:

1. Lam JM et al. Neurosurgery. 2000;47(4):819-25.

2. Schmidt EA et al. J Neurosurg. 2003;99(6):991-8.

3. Piechnik SK et al. Acta Neurochir (Suppl) 1998; 71:269-271.

4. Steiner LA et al. Crit Care Med. 2002;30(4):733-8.

5. Piechnik SK et al J Cereb Blood Flow Metab. 2001;21(2):182-92.

BrainPET Poster Session: Brain Imaging: MRI/fMRI

CONTRIBUTION OF PERIPHERAL IL-1BETA EXPRESSION IN THE SYSTEMIC REACTIVATION OF FOCAL MOG-EAE LESIONS IN RAT BRAIN

S. Serres[1,2], D.C. Anthony[3], Y. Jiang[3], S.J. Campbell[3], D. Merkler[4], W. Bruck[4], J. Recton[5], **N.R. Sibson**[2]

[1]Physiology, Anatomy & Genetics, [2]Gray Institute for Radiation Oncology and Biology, [3]Pharmacology, University of Oxford, Oxford, UK, [4]Neuropathology, Georg-August University, Gottingen, Germany, [5]Biogen IDEC, Boston, MA, USA

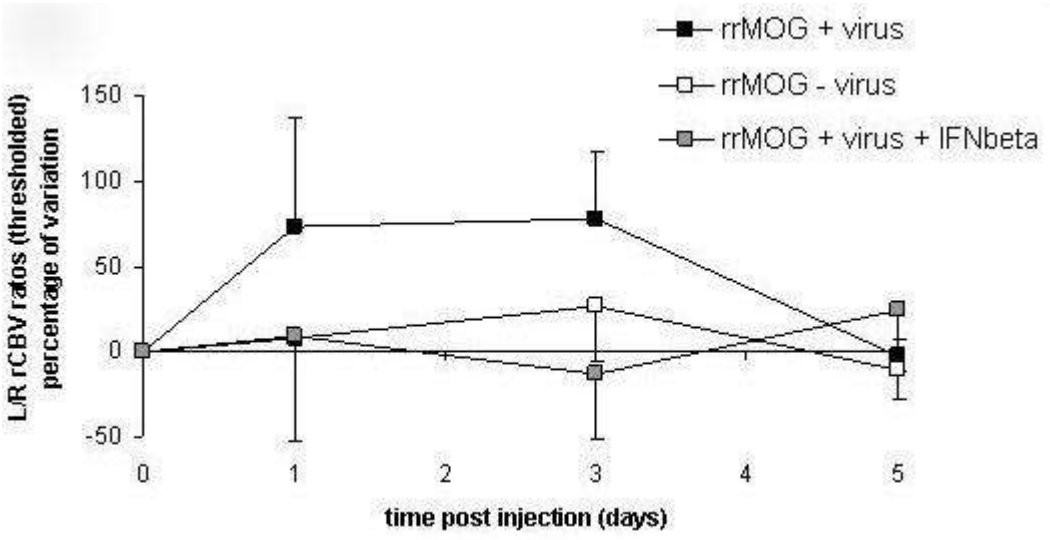

[Figure]

Objectives: Multiple sclerosis (MS) is a chronic inflammatory disorder associated with demyelination and axonal injury. Most MS patients display a relapsing-remitting form of disease in which bacterial and viral infections may play a key role. We have previously demonstrated that systemic endotoxin injection induced reactivation of inflammatory processes in focal MOG-EAE lesions. It has also been shown that systemic infection increases peripheral IL-1beta expression.

Methods: Therefore, in this study, we have investigated the contribution of systemic IL-1beta in the reactivation of focal MOG-EAE lesions. Two groups of rats with dormant CNS lesions were challenged with an i.v. injection of adenovirus expressing IL-1beta cDNA ($4x10^{10}$ plaque forming units). In addition, one of the groups was treated with a therapeutic dose of rrIFNbeta ($5x10^{6}$ U/kg, intraperitonally).

Results: We found a significant increase in the left/right regional cerebral blood volume (rCBV) ratio (~ 2 fold) from 1 to 3 days after administration of adenovirus expressing IL-1beta cDNA, an effect that we have previously shown to be associated with new macrophages recruitment and increased myelin loss following systemic endotoxin challenge. Post-gadolinium-DTPA T1-weighted images revealed contrast enhancement in the ipsilateral meninges indicating breakdown of the blood-CSF barrier, probably caused by extravasations of leukocytes into the brain. To determine whether a commonly used therapeutic agent IFNbeta could combat this IL-1beta induced reactivation of an MS-like lesion, rats were treated with therapeutic doses of rrIFNbeta and showed marked amelioration of the increased rCBV ratio together with a reduction in the gadolinium enhancement in the ipsilateral meninges.

Conclusion: These findings demonstrate the key role of peripheral IL-1beta expression in the mechanism of systemic reactivation of MS lesions and as the potential for therapy using IFNbeta.

982

Brain Poster Session: Cerebral Metabolic Regulation

ALTERATION OF BRAIN GLYCOGEN TURNOVER IN THE AWAKE RAT

F.D. Morgenthaler[1], **B. Lanz**[1], J.-M. Petit[2], H. Frenkel[1], P.J. Magistretti[2], R. Gruetter[1,3]

[1]Center for Biomedical Imaging, [2]Laboratory of Neuroenergetics and Cellular Dynamics, EPFL, Lausanne, [3]Department of Radiology, University of Geneva, Geneva, Switzerland

Objectives: Sleep deprivation elicit complex responses in brain glycogen (Glyc) synthesis and breakdown [1, 2]. Moreover, brief sensory stimulation alters Glyc turnover [3]. The increased Glyc turnover during activation complicates interpretation of standard approaches that assess concentration ([ ]) and metabolism to evaluate roles or utilization of Glyc under various conditions [3].

The aim of this study was to determine brain Glyc concentration ([ ]) and turnover time (tau) in euglycemic conscious rats maintained awake during 5 h using stable isotopes.

Methods: The metabolism of [1-^{13}C]-labeled glucose (Glc) into Glyc was measured in rats that had previously received a 10% w/v [1-^{13}C]-labeled Glc solution ad libitum as their sole source of exogenous carbon for either 5 (n=6+7), 24 (n=5) or 48 h (n=5). Six animals were continuously aroused by acoustic, tactile and olfactory stimuli for 5 h, and otherwise treated identically, resulting in elevated plasma corticosterone levels (97±21 ng/mL, n=6) compared to the control - undisturbed - rats (66±52 ng/mL, n=7, [mean] ± SD). To minimize postmortem degradation, rats were sacrificed using a focused microwave fixation device, brains dissected and assayed for tissue glycogen and Glc concentrations using biochemical measurements [4]. ^{13}C enrichment of N-acetyl-aspartate (NAA) and Glc (as well as digested glycogen) was evaluated in vitro by high field ^{1}H Nuclear Magnetic Resonance (NMR) spectroscopy (600 MHz)[5].

Results: Brain [Glyc] of the aroused rats (3.9±0.6 μmol/g, n=6) was not significantly different from that of the control group (4.0±0.4 μmol/g, n=7; t-test, P>0.5). To account for potential variations in plasma Glc Isotopic Enrichment (IE), Glyc IE was normalized by NAA IE, which has a turnover time on the same order of magnitude. A simple mathematical model was developed to derive brain Glyc and NAA turnover times as 5.3±3.2 h and 15.6±6.5 h (fitted value±SD) respectively, in the control rats. Finally, assuming that tau_{NAA} was not altered by 5 h of awakening, a faster tau_{Glyc} (2.9±1.2 h) was estimated in the aroused rats. Moreover, the model established in the present study shows that a calculated value of tau_{Glyc} in case of a shorter tau_{NAA} would anyway be smaller than the value found with an assumption of unchanged tau_{NAA}. Subsequently, the difference in tau_{Glyc} in case of a shorter tau_{NAA} between control and aroused rats would be even bigger than reported.

Conclusion: In conclusion, 5 h of prolonged wakefulness mainly activates glycogen metabolism, but has minimal effect on brain [Glyc].

References:

1. P. Gip, et al. (2002) Am J Physiol Regul Integr Comp Physiol 283 : R1057-1062.

2. J. Kong, et al. (2002) J Neurosci 22 : 5581-5587.

3. G. A. Dienel et al. (2007) J Neurochem 102(2) : 466-478.

4. F. D. Morgenthaler, et al. (2006) Neurochem. Int. 48(6-7) : 612-622.

5. F. D. Morgenthaler, et al. (2008) J. Neurochem. 107(5) : 1414-1423.

983

Brain Poster Session: Spreading Depression

CYCLOSPORIN A AMELIORATES PROLONGED OLIGEMIA IN THE WAKE OF CORTICAL SPREADING DEPRESSION

H. Piilgaard[1], P. Rasmussen[1], B. Witgen[1], M. Lauritzen[1,2]

[1]Department of Neuroscience and Pharmacology, University of Copenhagen, Copenhagen N,
[2]Department of Clinical Neurophysiology, Glostrup Hospital, University of Copenhagen, Glostrup, Denmark

Introduction: Cortical spreading depression (CSD) is a slowly propagating depolarization wave of cerebral gray matter, which occurs in the cerebral cortex during migraine aura or traumatic brain injury. Associated to CSD are changes in Cerebral blood Flow (CBF): Initial vasoconstriction (not always seen) followed by vasodilation (during DC shift) followed by prolonged oligemia for up to 2 hours. During an episode of CSD, neurons accumulate Ca^{2+} while free fatty acids and NO are released. This combination of events favors opening of the mitochondrial permeability transition pore (mPTP). Cyclosporin A (CsA) is a potent blocker of the mPTP and was used here to test the hypothesis that the mPTP was activated during CSD.

Methods: CBF changes were monitored through an open cranial window over the right somatosensory cortex by laser-Doppler flowmetry. Also tissue oxygenation (tpO_2), local field potentials (LFP) and electrocorticogram (ECoG) were measured in the same area. Bipolar stimulation of transcallosal fibers projecting was performed in the homologous left somatosensory cortex by inserting a stimulation electrode directly into the cortex. Stimulations were given in 1 s lasting trains at 1, 6 and 20 Hz.(1.5 mA, 0.1 ms lasting square pulses) Cerebral metabolic rate of oxygen ($CMRO_2$) was calculated from the simultaneously recorded values of tpO_2 and CBF as described by Gjedde[1]. Episodes of CSD were elicited by a brief needle stab to the right frontal cortex. After initial recordings of evoked responses, 0.1 mM CsA was topically applied to the somatosensory cortex of the right hemisphere as desribed by Sullivan[2] for 40 min before repeating evoked responses and eliciting CSD. The impact of CsA on baseline CBF and $CMRO_2$, and evoked synaptic, vascular, and metabolic responses after CSD (n=8) was compared to the effect of CSD in untreated animals (n=7).

Results: CsA augmented the maximal CBF response during CSD by 43.9% for the first few minutes (p=0.04). CsA also reduced the maximum undershoot in CBF after CSD from 25.3±4.1% to 11. 9±2.1% (p=0.02), an improvement of 53.1% without changing the time taken for CBF to return to normal. In comparison, baseline tpO_2 and $CMRO_2$ remained unchanged following CsA treatment. CsA itself had no influence on the evoked LFP, CBF, or $CMRO_2$ response amplitudes following TC stimulation.

Conclusion: We conclude that CsA augments the acute CBF response during CSD and ameliorates the prolonged oligemia after CSD.

Perspectives: CSD causes CBF reduction by direct interaction with the blood vessels. We here hypothesise that this change of function relates mechanistically to activation of mPTP in the vessel walls. If so, this opens the possibility that blockers of mPTP may be useful for treating vascular dysfunction in neurological disorders in which CSD or CSD-like phenomena are implicated.

References:

1. Gjedde A et al (2005) J Cereb Blood Flow Metab 25:1183-1196.

2. Sullivan PG et al (2005) J Neurosci Res 79:231-239.

Grant support: Lundbeck Foundation via the Lundbeck Foundation Centre for Neurovascular Signalling (LUCENS), the NOVO Nordisk Foundation, and the Danish Medical Research Council.

.

Brain Poster Session: Oxidative Mechanisms

CHANGES IN NITRIC OXIDE SYNTHASE (NOS), CYCLOOXYGENASE-2 (COX-2) AND SUPEROXIDE DISMUTASE (SOD) PROTEIN LEVELS IN CHRONIC CEREBRAL HYPOPERFUSION IN RATS

A. Institoris[1,2], E. Mracsko[2], M. Hugyecz[2], A. Matyas[3], Z. Sule[3], E. Farkas[2], F. Bari[2]

[1]Department of Physiology and Pharmacology, Wake Forest University Health Sciences, Winston-Salem, NC, USA, [2]Department of Physiology, University of Szeged, [3]Department of Anatomy, University of Szeged, Szeged, Hungary

Chronic cerebral hypoperfusion (CCH) is a condititon which contributes to cognitive decline during senescence and in several types of dementia. Its experimental model is the permanent bilateral common carotid artery occlusion (2VO) in rats. Following 2VO, the slow but progressive restoration of cerebral blood flow is accompanied with ischemic neuronal damage, neuroinflammation and cognitive dysfunction. The nitric oxide synthase (NOS) and cyclooxygenase (COX) enzyme systems participate in the maintenance of cerebral perfusion, meanwhile under acute ischemia these prooxidant enzymes aggrevate oxidative damage via producing neurotoxic free radicals. However, the temporal characteristics of oxidative stress and the involvement of these enzyme systems in CCH have not yet been described.

Our objective was to detect the expression of endothelial (e)NOS, inducible (i)NOS, neuronal (n)NOS (nNOS), COX-2 enzyme and manganase (Mn)SOD with Western blot analysis and immunocytochemistry (ICC) in the cerebral cortex and in the hippocampus in a temporal manner following 2VO.

Male Wistar rats were exposed to the 2VO (n=41) or SHAM operation (n=42). Alternatively, some rats were not operated on (naive) (n=20). Western blot analysis was carried out from tissue samples of the hippocampus and frontal cortex taken 1 day, 3 days, 1 week, 3 - 6 - and 12 months following surgery. ICC detection of eNOS, nNOS and MnSOD was performed on paraformaldehyde-fixed brain samples taken 3 - 6 - and 12 months after 2VO.

In the hippocampus, the expression of eNOS enzymes significantly increased ($P< 0.01$), COX-2 expression only mildly increased, while iNOS and nNOS levels decreased at the early phase of CCH. Three months after 2VO, lower eNOS production could be detected ($P< 0.05$). In the cortex, the early upregulation of eNOS and nNOS was followed by a reduction of COX-2 and eNOS production at 3 months of CCH. Finally, eNOS level increased again at 12 months after 2VO. There was no change in the MnSOD enzyme level in any of the observed regions. ICC failed to show significant changes.

The significant elevation of eNOS in the early stage of CCH is probably an important compensatory mechanism against the reduced perfusion in both areas, while the lower eNOS expression at the later phase of CCH might be a consequence of capillary degeneration. The early suppression of iNOS production indicates that the enzyme is probably not the origin of reactive oxygen species. The early activation of nNOS following 2VO in the cortex may reflect the effort of ischemic neurons to obtain more oxygen and glucose by releasing the vasodilator NO. The elevation of nNOS one year after 2VO might indicate synaptic remodeling in the hippocampus. Decreased levels of COX-2 in the cortex 3 months after 2VO are probably due to the loss of COX-2-positive neurons. The constant level of MnSOD suggests that the degree of oxidative stress is not remarkable in this model or other antioxidant mechanisms are induced against oxidative agents. In summary, the NOS system is substantially affected by CCH, however, the exact role of these prooxidant enzymes in the 2VO model remains to be elucidated.

985

BrainPET Poster Session: Radiotracers and Quantification

MICROGLIAL ACTIVATION IN LEUKOARAIOSIS: A [^{11}C]-PK11195 PET STUDY

A. Bertoldo[1], I. Florea[2,3,4], V. Di Piero[5], A. Panzacchi[3,4], M.C. Gilardi[2,3,4], G.L. Lenzi[5], F. Fazio[2,3], C. Cobelli[1], R.M. Moresco[2,3,4,6]

[1]Department of Information Engineering, University of Padova, Padova, [2]University of Milan 'Bicocca', [3]San Raffaele Scientific Institute, [4]IBFM CNR, Milan, [5]University of Rome 'La Sapienza', Rome, [6]Vita-Salute San Raffaele University, Milan, Italy

Objective: Leukoaraiosis describes diffuse white matter abnormalities on CT or MR brain scans, often seen in the normal elderly and in association with vascular risk factors or stroke [1]. The aim of this study was to evaluate by PET [^{11}C] PK11195 the microglia activation taking into account for both its tissue and vascular expression in patient diagnosed with leukoaraiosis.

Methods: Four healthy controls HC (age 44 ± 11) and two patients with leukoaraiosis (LK), one female (age 64) and one male (age 82) were enrolled in this pilot study. The non invasive simplified reference tissue model [2] modified by accounting for cerebral blood volume and vascular binding presence both in reference and target tissues [3,4] (SRTMV) was applied to the PET images on a voxel basis to estimate RI (ratio of tissue compared to that in the reference region delivery), k_2 (efflux rate constant from tissue), binding potential (BP) and blood volume (V_b). Receptor free regions (C_{ref}) were identify by cluster analysis. The whole blood tracer activity (C_b) was extracted from the dynamic images by averaging the tracer activities in 6 pixels selected by cluster analysis. C_{ref} and C_b were used as input functions to SRTMV, V_b in the reference region was fixed to 5%. Regional BP and V_b values were obtained by drawing regions of interest (ROIs) on BP and V_b parametric images.

Results: The results reveal significant group level effect for both BP and V_b, in cortical and subcortical ROIs. In particular, LK BPs show an increase respect to HC BPs in cortical areas as cuneus, precuneus of about 3 and 3.7 fold, respectively, with a mean fold of 2 ± 0.4 overall the neocortex and in subcortical areas a mean fold increase of about 1.7 ± 0.2. V_b estimates in HC group are >30% lower in cortical area as cuneus, posterior cingulate, insula and parietal cortex. Noteworthy, a variation between groups of more than 20% in V_b values was also identified for occipital cortex, posterior cingulate and thalamus. Average Vb values for HC was 5.7 ± 1 % while for LK 7.2 ± 2%.

Conclusion: As observed in patients with AD, Vb correction promotes an increase in BP values in different brain regions. However, differently to what observed for AD patients, in the two subjects with LK, we found Vb values higher than these present in HC group This might be cause by inflammation or modification in peripheral benzodiazepine receptor availability in micro-vessel wall. A blood-brain barrier dysfunction, due to toxic effects of serum protein, and/or the occurrence of "incomplete infarction" have been hypothesized as LK mechanisms, which might be both part of a broader failure of endothelial function. This preliminary study provides new information on the inflammatory process that accompany the LK disease.

References:

1. McCombe PA, Read SJ: Int J Stroke, 3 :254-265, 2008.

2. Lammertsma AA, Hume SP: Neuroimage, 3:153-158, 1996.

3. Gunn et al: Neuroimage, 8:426-440, 1998.

4. Tomasi G et al: J Nucl Med, 49:1249-1256, 2008.

988

Brain Poster Session: Inflammation

BETA 1 ADRENERGIC ACTIVATION OFFERS NEUROPROTECTION AFTER ISCHEMIA IN ORGANOTYPIC HIPPOCAMPAL SLICES BY INDUCING ANTI-INFLAMMATION, ANTI-APOPTOSIS AND ACTIVATING OXIDATIVE DEFENSE

T. Markus[1], T. Wieloch[2], T. Cronberg[3], S. Hansson[4], C. Cilio[5], D. Ley[1]

[1]Pediatrics, [2]Experimental Brain Research, [3]Neurology, [4]Obstetrics & Gynecology, Lund University, Lund, [5]Cellular Autoimmunity, Malmo University Hospital, Malmo, Sweden

Objectives: Adrenergic agonists have potent anti-inflammatory (Szelenyi and Vizi 2007) and anti-epileptic effects (Chauvel and Trottier 1986). We evaluated the neuroprotective and anti-inflammatory effects of beta adrenergic agonists in a previously developed model of perinatal brain inflammation and ischemia using immature organotypic hippocampal slices (Markus et al 2008). To assess the level of inflammation we measure the levels of pro- and anti-inflammatory cytokines released by the hippocampal slice culture and to evaluate the neuronal cell death we measure levels of incorporation of propidium iodide (PI) in cells of the neuronal regions of the hippocampus. We further characterize the mechanisms of induced anti-inflammation and neuroprotection by beta adrenergic stimulation in hippocampal slice cultures by analyzing profiles of gene expression using microarray technology.

Methods: Hippocampal slices from balb/c mice were obtained at postnatal day 6 and grown in vitro up until in vitro day 9. To induce inflammation hippocampal slices were exposed to lipopolysaccharide (LPS) during 24 hours followed by 15 minutes of in vitro ischemia, induced by exposure to oxygen and glucose deprivation (OGD). To study the modifying effects of beta adrenergic agonists on inflammation and ischemia, hippocampal slices were exposed to the beta1 adrenergic agonist dobutamine during the 24 hours of LPS exposure. Neuronal cell death was determined with PI which was measured by fluorescent light microscopy. Inflammation was assessed by measuring cytokine release using cytometric bead array (Becton Dickinson). Microglial activation and neuronal depletion was studied by immunohistochemistry. Gene expression profiles were studied by microarray technology, using slides which were printed with 33k oligos. A commercial mouse RNA (Stratagene) was used for quantification of specific gene transcripts in culture samples.

Results: Exposure to LPS + OGD resulted in extensive cell death in neuronal sub-regions CA1, -2, -3 and the dentate gyrus. Co-incubation with beta1 adrenergic agonist (50uM) during LPS exposure conferred complete protection from cell death in all neuronal subregions ($p < 0.001$). The neuroprotective effect of beta1 agonist was associated with decreased levels of inflammatory cytokines in medium and an inhibition of morphological microglial activation. Gene expression analysis revealed a suppressed inflammatory activation, increased defense against oxidative damage, and increased expression of anti-apoptotic mediators in association with beta1 adrenergic neuroprotection after induced inflammation and ischemia.

Conclusions: Enhanced signaling through the beta1 adrenoceptor may enable neuroprotection in the context of perinatal inflammation and ischemia. Differences in endogenous adrenergic input could explain varied individual vulnerability to inflammatory and ischemic insults. Expression profiling of endogenous neuroprotective strategies might aid in the development of neuroprotective drug discovery.

References:

Chauvel P, Trottier S (1986) Role of noradrenergic ascending system in extinction of epileptic phenomena. Advances in neurology 44:475-87.

Markus T, Cronberg T, Cilio C, Pronk C, Wieloch T, Ley D (2008) Tumor necrosis factor receptor-1 is essential for LPS-induced sensitization and tolerance to oxygen-glucose deprivation in murine neonatal organotypic hippocampal slices. J Cereb Blood Flow Metab.

Szelenyi J, Vizi ES (2007) The catecholamine cytokine balance: interaction between the brain and the immune system. Annals of the New York Academy of Sciences 1113:311-24.

Brain Poster Session: Cerebral Metabolic Regulation

THE BRAIN RELEASES IL-6 IN RECOVERY FROM EXERCISE CONCOMITANT WITH INCREASED IL-6 MRNA EXPRESSION

P. Rasmussen[1], J.-C. Vedel[1], M.V. Pedersen[1], E. Hart[2], N.H. Secher[1], H. Adser[1], H. Pilegaard[1], B.K. Pedersen[1]

[1]University of Copenhagen, Copenhagen, Denmark, [2]Brunel University, Uxbridge, UK

Interleukin-6 influences metabolism including inducing lipolysis and fat oxidation. Plasma IL-6 increases during exercise as well as in the recovery maybe mediating some of the health benefits of exercise. Both active muscles and the brain contribute to plasma IL-6, but whether the brain also increases IL-6 release in the recovery from exercise is unknown. To address this question, nine healthy male subjects completed a 4 h bout of ergometer rowing, while arterio-jugular venous difference (a-v diff) of IL-6 was measured. The IL-6 a-v diff was -2.2 ± 1.9 pg ml^{-1} ($P < 0.05$) after 4 h of exercise and importantly, the IL-6 a-v diff over the brain was still -2.1 ± 2.1 pg ml^{-1} ($P < 0.05$) after 1 h of recovery. To examine whether the exercise-induced IL-6 release may be associated with increased cerebral IL-6 expression, the IL-6 mRNA content was determined in mice hippocampus, cerebellum and cortex immediately after a single treadmill exercise and at 2h, 6h and 24h hours of recovery and compared with mice not run acutely. IL-6 mRNA was expressed in all three brain parts examined with higher ($P < 0.05$) content in cortex than in hippocampus and cerebellum. Exercise induced 2-3 fold increase ($P< 0.05$) in the IL-6 mRNA content in hippocampus only. In conclusion, the results indicate that hippocampus is a likely source of exercise-induced brain-derived IL-6. As IL-6 release in the human brain correlated to cerebral lactate release, we speculate that increased cerebral IL-6 expression and release may be elicited by changes in cerebral metabolism.

990

Brain Oral Session: Blood Brain Barrier

BLOOD BRAIN BARRIER ENDOTHELIAL CELLS ARE DIRECTLY INVOLVED IN ISCHEMIC PRECONDITIONING

R. Gesuete[1], E.R. Zanier[1], F. Orsini[1], L. Garzetti[1], M. Deli[2], M.G. De Simoni[1]

[1]Mario Negri Institute, Milan, Italy, [2]Biological Research Centre, Szeged, Hungary

Objective: Ischemic PreConditioning (IPC) is a phenomenon whereby a sub-threshold ischemic insult activates neuroprotective pathways (1). Although the concept of preconditioning has been widely studied, little attention has focused on the effects of preconditioning on cerebrovascular unit. Endothelial cell dysfunction may play an important role in the pathophysiology of cerebral ischemia. Disruption of the endothelial cells that form the blood-brain barrier (BBB) may lead to edema formation that can exacerbate brain injury. In this study we addressed the involvement of the cerebrovascular unit in IPC using an in vitro model of BBB.

Methods: Primary mouse Brain Microvessel Endothelial Cells (BMECs) co-cultured with primary mouse mixed glial cells were used to model BBB. In this condition the endothelial cells form a differentiated monolayer that retains the endothelial markers and the same properties of in vivo cerebral endothelium (2). Short Oxygen-Glucose Deprivation (1h-OGD) was used as preconditioning stimulus (PC) and administered 24h before severe 5h-OGD. Twenty-four and 48 hours after the severe OGD we evaluated the effect of IPC on the trans-endothelium electrical resistance (TEER), endothelial permeability coefficient (Pe) for paracellular (NaFluorescein) and transcellular (Albumin) transport and the presence of tight junction proteins.

Results: In basal conditions the endothelial cells showed the typical features of functional cerebral endothelium, i.e. high TEER values ($\geq$100Ωcm^2), low Pe for NaFluorescein ($0.53\pm0.02x10^{-3}$cm/min) and Albumin ($0.02\pm0.005x10^{-3}$cm/min) values and expression of the tight junction protein ZO-1.

Twenty-four hours after severe OGD the endothelial cells showed a dramatic reduction in TEER values (73.1±2.2 Ωcm^2), a significant increase in Pe values for both NaFluorescein ($1.8\pm0.35x10^{-3}$cm/min) and Albumin ($0.29\pm0.07x10^{-3}$cm/min) and a loss of the ZO-1 continuous staining pattern. The administration of 1h-OGD 24 hours before a severe OGD significantly ameliorated all the parameters observed. In particular 24 hours after severe OGD the preconditioned cells did not show significant changes in TEER values (111.2±5.8 Ωcm^2) and Pe values for both NaFluorescein ($0.98\pm0.11x10^{-3}$cm/min) and Albumin ($0.12\pm0.01x10^{-3}$cm/min) compared to control condition. Similarly, the immunostaining for ZO-1 showed that the pattern of the staining for this tight junction protein was not affected in preconditioned cells compared to control cells.

Conclusions: The present study shows for the first time that IPC significantly attenuates OGD-induced brain endothelial dysfunction. We observed that a short exposure to OGD acts as an IPC stimulus preventing the reduction of TEER values, the loss of paracelluar and transcelluar Pe selectivity and the disruption of the ZO-1 organization induced by OGD. These data indicate that the BBB endothelial cells can be directly preconditioned and that the cerebrovascular unit may have an important role in IPC neuroprotection.

References:

(1) Dirnagl U, Meisel A. Endogenous neuroprotection: mitochondria as gateways to cerebral preconditioning? Neuropharmacology. 2008 Sep;55(3):334-44.

(2) Deli MA, Abrahám CS, Kataoka Y, Niwa M. Permeability studies on in vitro blood-brain barrier models: physiology, pathology, and pharmacology. Cell Mol Neurobiol. 2005 Feb;25(1):59-127.

993

Brain Poster Session: Blood-Brain Barrier

INHIBITION OF MYOSIN LIGHT CHAIN KINASE AMELIORATES BRAIN EDEMA FORMATION AFTER TRAUMATIC BRAIN INJURY

C. Ricken[1], C. Kuhlmann[2], H. Luhmann[2], K. Engelhard[1], C. Werner[1], S. Thal[1]

[1]Department of Anesthesiology, [2]Department of Physiology, Johannes Gutenberg-University, Mainz, Germany

Introduction: The role of the endothelial contractile apparatus in the process of brain edema formation after brain trauma is not clarified. Myosin light chain kinase (MLCK) regulates the contraction of endothelial cells through phosphorylation of regulatory myosin light chains (MLC). The integrity of the blood brain barrier (BBB) may therefore be influenced by the phosphorylation state of the MLC. In endothelial cells hypoxia results in an up-regulation of MLCK and leads to increased phosphorylation of MLCs. This mediates a cytoskeletal rearrangement, which may result in blood-brain-barrier (BBB) dysfunction[1]. The present study investigates the effect of selective MLCK inhibition on brain edema formation and histological outcome after experimental brain trauma.

Methods: Male C57Bl/6 mice were anesthetized with midazolam, fentanyl and medetomidine and were subjected to controlled cortical impact brain injury (CCI). Mice were treated with intraperitoneal injection of the selective MLCK inhibitor ML-7 (1 mg/kg) or vehicle solution (0.9% NaCl) 1 hr prior to and 6 hr after trauma. Brain water content was determined 24 hr after CCI in animals randomized to:

1. vehicle + sham surgery;
2. vehicle + CCI;
3. ML-7 + sham surgery;
4. ML-7 + CCI (n=7 per group).

Brain contusion volume was determined 15 min and 24 hr post CCI in two separate set (small trauma: depth 1 mm; large trauma: depth 1.5 mm) of animals randomized to:

1. vehicle + CCI and
2. ML-7 + CCI (n=8 per group).

Statistics: ANOVA on RANKS, $p< 0.05$.

Results: 24 hr after CCI brain water content increased significantly in vehicle treated animals (CCI: 79.95%±0.69) in comparison to sham animals (78.64%±0.46). ML-7 significantly reduced edema formation (CCI: 78.97%±0.53). Brain damage expanded significantly between 15 min and 24 hr after CCI in vehicle and ML-7 treated animals. Independent of trauma size, brain contusion volume was not influence by ML-7 application (1.0 mm: vehicle=22.3mm³±3.7; ML-7=22.4mm³±3.4; 1.5 mm: vehicle=44.6mm³±10.9; ML-7=41.1mm³±6.8).

Conclusion: The present study demonstrates that inhibition of MLCK prevents brain edema formation 24 hr following trauma. The data are in accordance to a previous study, where ML-7 significantly reduced brain water content in focal cerebral ischemia[1]. Despite experimental evidence for the detrimental effects of brain edema formation after brain trauma, prevention of brain edema

formation did not result in reduction of contusion volume or improved neurological outcome. In this model increase of intracranial pressure and impairment of cerebral perfusion might have been not severe enough to demonstrate a histological or neurological effect of brain edema reduction by MLCK inhibition. The results suggest that brain edema formation depends on the phosphorylation state of MLC. This might present an important mechanism of BBB leakage after head trauma.

Literature: (1) C.R.W. Kuhlmann, R. Tamaki, M. Gamerdinger, V. Lessmann, C. Behl, O. S. Kempski, and H. J. Luhmann. Inhibition of the myosin light chain kinase prevents hypoxia-induced blood-brain barrier disruption. J Neurochem, 102(2):501-507, 2007.

DECREASED HYPOXIC VENTILATORY RESPONSE IN AGED RAT FOLLOWING TRANSIT GLOBAL ISCHEMIA

K. Xu[1], M.A. Puchowicz[2], X. Sun[1], J.C. LaManna[1]

[1]Physiology and Biophysics, [2]Nutrition, Case Western Reserve University, Cleveland, OH, USA

Introduction: Transient global brain ischemia induced by cardiac arrest and resuscitation results in reperfusion injury. There is increased incidence of cardiac arrest with aging. The age-related changes in the brain could alter the outcome of diseases as well as the potential therapeutic strategies. In this study we investigated the effects of an antioxidant, alpha-phenyl-tert-butyl-nitrone (PBN) in the aged rats following cardiac arrest and resuscitation.

Methods: Male Fischer 344 rats (Young: 6-month old; Aged: 24-month old) underwent cardiac arrest and resuscitation, and 4-day overall survival rats were determined. Brainstem function was assessed by measuring hypoxic ventilatory response (HVR; ratio of minute volume, hypoxia vs. normoxia). For the PBN-treated rats, PBN (100 mg/kg) was infused intravenously immediately after resuscitation for 60 min. The untreated rats were given normal saline instead.

Results: With aging the 4-day overall survival rates were decreased; with greater mortality during the first 2 days of recovery. The overall survival rate in the aged untreated rats was significantly less than that of the young rats (38.5%, 5/13 total vs. 69.2%, 9/13 total); however, PBN treatment significantly improved the overall survival rate by 28%.Compared to the young rats (3.0 ± 0.3, n = 5), the aged group had significantly lower pre-arrest HVR values (2.2 ± 0.4, n = 15), with similar normoxic ventilation (minute volume, ml, 206 ± 33 vs. 205 ± 35) but lower hypoxic ventilation (minute volume, ml, 455 ± 74 vs. 600 ± 117). During the first 4 days of recovery, the untreated aged rats have significantly lower HVR compared to their pre-arrest values; but the PBN-treated rats had similar ventilation performance in response to hypoxia (see figure, * indicates significance compared to the untreated group).

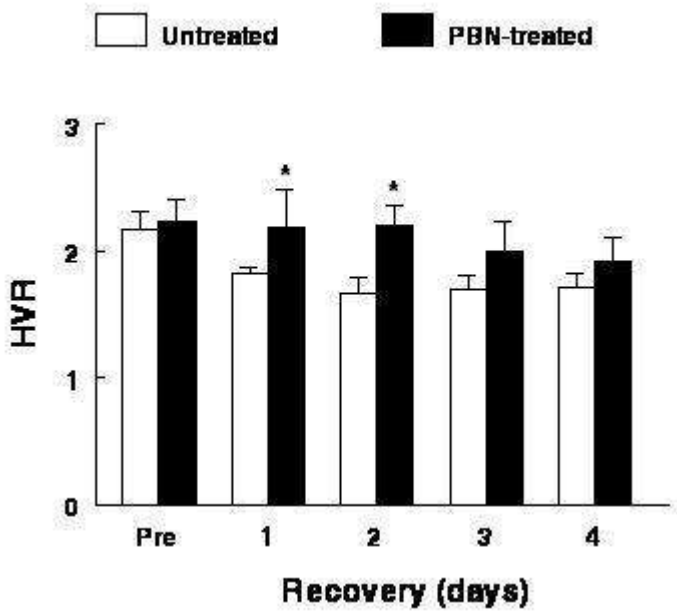

[Hypoxic Ventilatory Response in the Aged Rats]

Conclusion: These data suggest increased mortality in the aged may be associated with brainstem dysfunction. The antioxidant treatment with PBN improved recovery following cardiac arrest and resuscitation in the aged.

INTRAVENOUS ADMINISTRATION OF HUMAN UMBILICAL CORD BLOOD CELLS DID NOT REDUCE INFARCT VOLUME AND CASPASE-3-DEPENDENT APOPTOSIS

A. Kranz[1,2], U.-M. Riegelsberger[1,2], C. Poesel[1], J. Boltze[1,2,3], F. Emmrich[1,2,3], D.-C. Wagner[1]

[1]Neurorepair Research Group, Fraunhofer Institute for Cell Therapy and Immunology, [2]Institute for Clinical Immunology and Transfusion Medicine, University of Leipzig, [3]Translational Centre for Regenerative Medicine, University of Leipzig, Leipzig, Germany

Objectives: Beneficial effects of human umbilical cord blood (HUCBC) administration in animal models of ischemic stroke have been repeatedly described over the past decade. This cell population was predominantly used in intravenous approaches. Originally, the accepted opinion about the mechanism was a homing of transplanted cells into the lesioned brain areas and a subsequent integration and differentiation. Nevertheless, later studies substantiated alternative mechanisms of action, focusing on neuroprotective factors released by transplanted cells. Even the CNS entry of administered cells seemed unnecessary for providing substantial improvements within the readout parameters. A modulation of the inflammatory response, the release of neurotrophic factors and an enhancement of endogenous neurogenesis are imaginable mechanisms for a beneficial HUCBC treatment. In the present experiment, we aimed to investigate the potential neuroprotective and antiapoptotic effects of intravenously transplanted HUCBC within a 96 hour time window.

Methods: Forty male spontaneously hypertensive rats were subjected to a permanent occlusion of the right middle cerebral artery. Subsequently, the animals were randomly assigned into control and cell treatment group (n=20 each). The infusion of 8x10E6 HUCBC per kilogram bodyweight or the administration of vehicle solution was performed 24 hours upon stroke onset by an investigator blinded to the group allocation. Five subjects of each group were sacrificed 25h, 48h, 72h and 96h following the release of brain ischemia. Formalin fixed brain specimen were cut into 20 µm thick coronal slides. Every fifteenth slide was selected for the evaluation of the infarct volume, determined by the absence of MAP-2 immunoreactivity. The slides at bregma +1.6, +0.7, -0.2 and -1.1 were selected for the quantification of caspase-3 positive cells adjacent to the ischemic lesion. An investigation for RNA expression of caspase-3 and the antiapoptotic protein survivin within the cortical infarct border was performed for both experimental groups before MCAO, respectively 6h, 24h, 36h and 48h thereafter (n=3 each). All post mortem analyses were conducted by investigators blinded to the experimental groups.

Results: The infarct volume of both experimental groups did not show a significant variation during the experiment. No significant difference between cell treated and control animals was evident at any investigation time point. The amount of caspase+ cells increased from 25h to 72h and remained stable between 72h and 96h. Again, there was no significant difference between the treatment and the control group. Quantification of caspase-3 mRNA expression increased significantly between 6h and 24h and levelled off until 48h following stroke onset. We measured a cumulation of antiapoptotic protein survivin from 6h to 48h following stroke. Once more, we found no significant difference between the experimental groups for both investigated markers.

Conclusions: Regarding those surrogate parameters, we found no evidence for a significant neuroprotective or antiapoptotic effect of the used transplantation setup. The investigation of lesion development showed a constant infarct volume during the experiment despite ascending amounts of apoptotic cells. Possibly, the used therapeutic time point was too late to produce a neuroprotective effect in a permanent occlusion model.

996

Brain Poster Session: Glial Functions

IMPACT OF CELL THERAPIES ON POST-ISCHEMIC ASTROGLIOSIS

D.-C. Wagner[1], A. Kranz[1,2], U.-M. Riegelsberger[1,2], C. Poesel[1], F. Emmrich[1,2,3], J. Boltze[1,2,3]

[1]Neurorepair Research Group, Fraunhofer Institute for Cell Therapy and Immunology, [2]Institute for Clinical Immunology and Transfusion Medicine, [3]Translational Centre for Regenerative Medicine, University of Leipzig, Leipzig, Germany

Objectives: Astrogliosis is a common phenomenon following brain injury. However, the actual role of astrocytes within the complex spatio-temporal events after ischemic stroke is still not elucidated satisfactorily. On the one hand, multitude of evidence displayed a negative influence of activated astrocytes such as the release of proinflammatory cytokines, an increase of ischemic damage by the astrocytic gap-junction system and the formation of an anti-regenerative glial scar. Nevertheless, several aspects also support the hypothesis of a beneficial role of astrocytes after brain damage. The ablation of reactive astrocytes after traumatic brain injury resulted in the augmentation of CNS damage and inflammatory response. Hence, astrocytes may be an interesting target for modulating therapeutic approaches such as cell therapies. A recent study showed increased astrocytic survival by BMSC after hypoxic conditions. The aim of this study is the investigation of a potential interrelation between cell therapies and a modulation of astrocytic characteristics.

Methods: We examined the astrocytic reaction to permanent middle cerebral artery occlusion (pMCAO) dependent on cell therapy in two different experiments. Firstly, we investigated brain specimen of an effective long-term cell transplantation experiment. Sixteen male spontaneously hypertensive rats (SHR) were subjected to pMCAO and randomly assigned to therapy (intravenous administration of 2x10E6 human placenta cells; n=8) and control group (intravenous application of vehicle solution; n=8). Efficacy of cell treatment was examined weekly by behavioral tests and MR investigations until Day 60. Secondly, we performed a short-term investigation of astrocyte-associated markers within a 48h time window following stroke. Twenty-seven SHRs were subjected to pMCAO and received either 8x10E6 human umbilical cord blood cells (HUCBC) per kilogram bodyweight (n=9) or vehicle solution (n=9) intravenously. The animals were sacrificed 30h, 36h and 48h after stroke onset. Additional control subjects were sacrificed without pMCAO (n=3) and 6h and 24h after pMCAO (n=6), respectively. Messenger RNA expression of IL-1β, nestin, GFAP, and glutamate transporter-1 (GLT-1) was quantified by real time PCR within two areas in the cortical lesion border or corresponding contralateral domains.

Results: The long-term investigation of astrocytic reactions to brain ischemia and cell therapy showed a significant increase of GFAP+ cells in the infarct border of cell treated subjects at Day 60 after stroke onset. This observation was associated with a reduced infarct volume and a decline of functional deficits. The short-term investigation showed a fast increase of IL-1β followed by increased values of GFAP and nestin and a decline of GLT-1 mRNA expression. The development of IL-1β, GLT-1 and nestin appeared homogenously while there was a strong trend towards less GFAP expression in control animals compared to cell treated subjects at 36h and 48h.

Conclusions: Efficacy of cell therapies after stroke is, at least partly, mediated by a modulation of astrocytic survival or activation. The mentioned developments proceed within a comparatively short time upon stroke onset and might therefore determine a limited window for experimental therapies aiming to modulate these processes. However, an increase of the group size and further immunohistological examinations are under evaluation to confirm these preliminary results.

Brain Poster Session: Blood-Brain Barrier

ENDOTHELIAL NITRIC OXIDE SYNTHASE MEDIATES BLOOD-BRAIN BARRIER INJURY IN THE THIAMINE-DEFICIENT MOUSE BRAIN

É. Beauchesne, P. Desjardins, A.S. Hazell, R.F. Butterworth

Neurosciences Research Unit, CHUM, St-Luc Hospital, University of Montreal, Montreal, QC, Canada

Objectives: Wernicke's Encephalopathy (WE) in humans is a chronic metabolic disorder caused by thiamine deficiency (TD) characterized clinically by ophthalmoplegia, ataxia and confusion. TD leads to cerebral impaired oxidative metabolism, due to the inhibition of α-ketoglutarate dehydrogenase (α-KGDH), a rate-limiting enzyme of the TCA cycle. Neuropathologic consequences of TD include selective neuronal cell death and petechial hemorrhagic lesions in medial thalamus. Blood-brain barrier (BBB) breakdown plays an important role in TD pathogenesis (Harata and Iwasaki, 1995). Among early changes in TD, increased expression of the endothelial isoform of nitric oxide synthase (eNOS) occurs selectively in vulnerable regions of the brain (Kruse et al., 2004). We hypothesized that eNOS induction in TD leads to oxidative/nitrosative stress, tight junction protein (TJP) alterations and BBB breakdown.

Methods: TD was induced in C57BL6 and $eNOS^{-/-}$ mice by feeding with a thiamine-deficient diet and by treatment with the thiamine antagonist pyrithiamine. Pair-fed control (PFC) mice (from both strains) were fed the same diet and treated with thiamine. Experiments were conducted in medial thalamus versus frontal cortex (spared area) from the brains of PFC and TD (WT and $eNOS^{-/-}$) mice. Cresyl violet was used for histological evaluation, and oxidative/nitrosative stress was assessed by measuring levels of NO_x (nitrites/nitrates) and by heme oxygenase-1 (HO-1) immunohistochemistry. BBB integrity was assessed by measuring immunoglobulin-G (IgG) extravasation, expression of TJPs occludin, zonula occludens-1 and -2 (ZO-1, ZO-2), as well as activity of the related matrix-metalloproteinases (MMPs).

Results: In the medial thalamus of TD-WT mice, we observed increased levels of NO_x and that HO-1 immunostaining was co-localized with eNOS in vessel walls, showing the presence of oxidative/nitrosative stress in thalamic vessels. BBB breakdown was demonstrated by the presence of hemorrhagic lesions, an increase in BBB permeability to IgG, a loss in expression of occludin, ZO-1 and ZO-2, and a concomitant increase in MMP-9 activity. No such changes were observed in frontal cortex. eNOS gene deletion prevented NO_x increase and led to attenuation of neuronal cell death, confirming the neurotoxic role of eNOS-derived nitric oxide (NO) in TD (Calingasan et al., 2000). Moreover, HO-1 immunostaining was eliminated in vessels, and BBB breakdown was prevented as shown by absence of haemorrhages, prevention of IgG extravasation, normalization of TJP expression and prevention of the increase in MMP-9 activity in the medial thalamus of TD-$eNOS^{-/-}$ mice, compared to TD-WT mice.

Conclusions: These data demonstrate that eNOS-derived NO is a major factor leading to oxidative/nitrosative stress, alterations of the cerebrovascular endothelial cells and BBB breakdown in TD.

References:

Calingasan, N.Y., Huang, P.L., Chun, H.S., Fabian, A., Gibson, G.E., 2000. Vascular factors are critical in selective neuronal loss in an animal model of impaired oxidative metabolism. J. Neuropathol. Exp. Neurol. 59, 207-217.

Harata, N., Iwasaki, Y., 1995. Evidence for early blood-brain barrier breakdown in experimental thiamine deficiency in the mouse. Metab. Brain Dis. 10, 159-174.

Kruse, M., Navarro, D., Desjardins, P., Butterworth, R.F., 2004. Increased brain endothelial nitric oxide synthase expression in thiamine deficiency: relationship to selective vulnerability. Neurochem. Int. 45, 49-56.

FUNCTIONAL MRI DURING DIRECT STIMULATION OF THE SENSORIMOTOR CORTEX IN RATS AFTER UNILATERAL STROKE

M.P.A. van Meer[1,2], K. van der Marel[1], W.M. Otte[1,2], J.W. Berkelbach van der Sprenkel[2], R.M. Dijkhuizen[1]

[1]Image Sciences Institute, [2]Rudolf Magnus Institute of Neuroscience, University Medical Center Utrecht, Utrecht, The Netherlands

Objectives: Functional MRI studies with peripheral somatosensory stimulation or, in patients, execution of a task have provided important insights in rearrangement of ipsi- and contralesional functional brain fields during recovery from stroke[1,2]. In this study we applied blood oxygenation level-dependent (BOLD) fMRI during direct intracortical stimulation (DICS) of the primary motor cortex (M1) in rats recovering from stroke. Our goal was to assess possible changes in excitability of ipsi- and contralateral sensorimotor network regions following DICS of contralesional M1 at different time points after experimental unilateral stroke.

Methods: Stroke was induced by 90-min transient intraluminal occlusion of the right middle cerebral artery (tMCAO) in adult male rats. MRI was conducted on a 4.7 T MR system at 3 days (n=2) and 4 weeks (n=2) after stroke. Nine rats served as controls. Animals were anesthetized with 1-2% isoflurane in air/O_2 (2:1) and paralyzed with pancuronium bromide during MRI to prevent head motion. MRI-compatible custom-made bipolar insulated gold electrodes were positioned in contralesional (=left) M1. BOLD echo planar imaging was done in combination with a DICS paradigm[3] that involved 5 blocks of 3-s periods of stimulation, followed by 60-s rest. The BOLD signal intensity time series were coregistered to a T_2-weighted rat brain template. Statistical activation maps were calculated using FEAT (www.fmrib.ox.ac.uk). Z-statistic images were thresholded at a Z-value of 2.3 (uncorrected, equal to a corrected P=0.05).

Results: The figure displays average fMRI activation maps of the different groups (Z=2.3-25.5). Various cortical and subcortical sensorimotor areas ipsilateral to the stimulation site (=left) showed significant BOLD activation after stimulation of M1 in healthy control animals. Contralateral to the stimulation site (=right) M1, clear activation responses were evident in secondary motor cortex (M2), primary somatosensory cortex of the forelimb (S1fl) and caudate putamen. DICS-induced activation responses were decreased at 3 days after stroke in ipsilesional intact motor regions and contralesional subcortical areas. At 4 weeks after stroke activation was recovered in various ipsi- and contralesional sensorimotor regions.

Conclusions: This study demonstrates that fMRI during DICS allows assessment of central functional connectivity in rat brain. Our preliminary data in stroke rats point toward loss of ipsi- and contralesional activation at a subacute stage. At 4 weeks after tMCAO, when animals had recovered considerably, the activation pattern more clearly resembled the control situation, which is in agreement with previous fMRI data based on peripheral forelimb stimulation.[2]

References:

[1] Cramer SC. Stroke 2004;35:2695-2698.

[2] Dijkhuizen RM et al. J Neurosci 2003;23:510-517.

[3] Austin VC et al. MRM 2003;49:838-847.

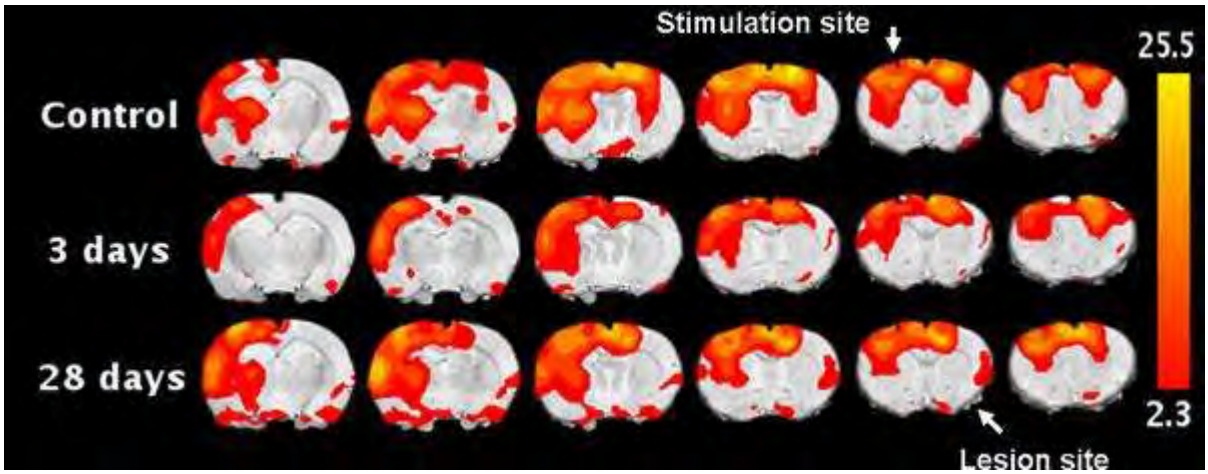

[Fig_DICSfMRI]

1001

Brain Oral Session: Brain Imaging

ULTRA-FAST HIGH RESOLUTION COMPUTERIZED TOMOGRAPHY ANGIOGRAPHY OF THE MURINE CEREBROVASCULAR SYSTEM IN VIVO

S.J. Schambach[1], S. Bag[1], C. Isaza[1], C. Groden[1], M.A. Brockmann[1], L. Schilling[2]

[1]Division of Neuroradiology, [2]Division of Neurosurgical Research, Medical Faculty Manheim, University of Heidelberg, Mannheim, Germany

Background: Animal models developed in rats and mice are of major importance in preclinical cerebrovascular research. Points of interest include the investigation of the morphology and function of the arterial, capillary and venous vessels. However, due to their extremely small caliber, in vivo examination of these vessels is extremely difficult. In the present study we present a new method to provide fast 3D in vivo analysis of cerebral murine vessels using volume computed tomography-angiography (vCTA).

Methods: An industrial X-ray inspection system equipped with a multifocus cone beam X-ray source and a 12-bit direct digital flatbed detector was used. The distance between the object, i.e. the animal's head and the detector is variable allowing for a zoom-like alteration of the geometric magnification. Mice were anesthetized with a ketamine / xylazin mixture (10 mg / 0.5 mg per 100g body weight) injected intraperitoneally. A 23G catheter was inserted into a tail vein and used for infusion of iodinated contrast medium (Imeron300®, 350µl) during each scan period.

A quick scan algorithm was developed consisting of 180° rotation within 40 sec and continuous recording of pictures at 30 Hz frequency (fps). During the scan procedure the animal rotates while the X-ray tube and the detector do not move. Images were reconstructed using a filtered back projection algorithm. Image analysis was performed by maximum intensity projection (MIP) and 3D volume reconstruction.

Results: All mice tolerated the infusion of the iodinated contrast agent well. The smallest voxel size of raw data to be achieved with the entire neurocranium depicted was 16µm. The anatomy of the arteries at the base of the brain making up the circle of Willis was nicely detectable in all animals. The posterior communicating artery connecting the anterior and the posterior part of the circulation was well developed in all C57/black6-mice while it was only small or completely absent in all balb/c mice studied. In these animals the posterior cerebral artery (PCA) was more prominently expressed than in C57/black6-mice. In accord, the mean diameter of the basilar artery (BA) was suspiciously larger in C57/black-6 mice (221±27 µm; mean±SD) than in balb/c animals (154±4 µm). In contrast, the diameter of the internal cerebral artery (ICA) did not differ (197.3±27.4 in C57/black6 vs 181.8±38.7µm in balb/c). Mean vessel diameters could be measured all animals. Dilatation ranging from 57% in the BA to 9.2% in the middle cerebral artery (MCA) was observed during ventilation with a hypoxic/hypercapnic gas mixture (5% CO_2, 12% O_2).

Conclusions: Ultra-fast in vivo vCTA of the murine cerebral vasculature is feasible at a resolution down to 16 µm. The technique allows the assessment of the vascular pattern and of vessel calibre changes in living mice even repeatedly, thus providing a worthwhile new tool to monitor in small laboratory animals different features of the cerebrovasculature in a non-invasive manner.

1002

Brain Oral Session: Brain Imaging

BOLUS-TRACKING ARTERIAL SPIN LABELING; A NEW MARKER FOR AGING AND AGE RELATED NEUROLOGICAL DISEASES

M. Kelly, C. Blau, R. Bechara, M. Lynch, C. Kerskens

Trinity College Institute of Neuroscience, Trinity College Dublin, Dublin, Ireland

Objectives: Arterial spin labeling (ASL) can be used to provide a quantitative assessment of cerebral perfusion. The purpose of this study is to develop a quantitative ASL technique, bolus-tracking arterial spin labeling, which quantifies both the mean and capillary transit times (MTT and CTT). It is expected that these parameters will vary under varying physiological and pathophysiological conditions. In order to test this hypothesis, a study was carried out in groups of rats of different ages.

Methods: A Fokker-Planck equation of motion that describes the distribution of labeled water in the brain was derived (Kelly et al, 2009). A bolus-tracking ASL sequence was designed to provide concentration-time curves that represent the passage of a bolus of labeled arterial water through the ROI. ROIs were selected in the cerebral cortex, hippocampus and whole brain. The solution to Fokker-Planck equation was fitted to the ASL concentration-time curves. The MTT and CTT were calculated from the first and second moments of the resultant curve respectively (Meier & Zierler, 1954; Kim & Kim, 2006). Male Wistar rats of varying age (young: 3 to 5 months, middle aged: 12 to 14 months, aged: 22 to 24 months) were used in the study.

Results: The theoretical model was found to be in excellent agreement with the experimental data for all datasets (chi-square ≈ 0.0001 for 20 iterations). The mean MTT value for the young, middle-aged and aged groups were 1.79s ± 0.14s, 1.75 ± 0.12s and 2.2s ± 0.26s respectively (error = 2 std. dev.). The mean CTT value for these groups was 1.39s ± 0.2s, 1.32 ± 0.21s and 1.93s ± 0.27s respectively. A significant difference in both the MTT and CTT between the young and middle aged groups and the aged group was identified (one-way ANOVA, $p < 0.01$), as shown in the graph below.

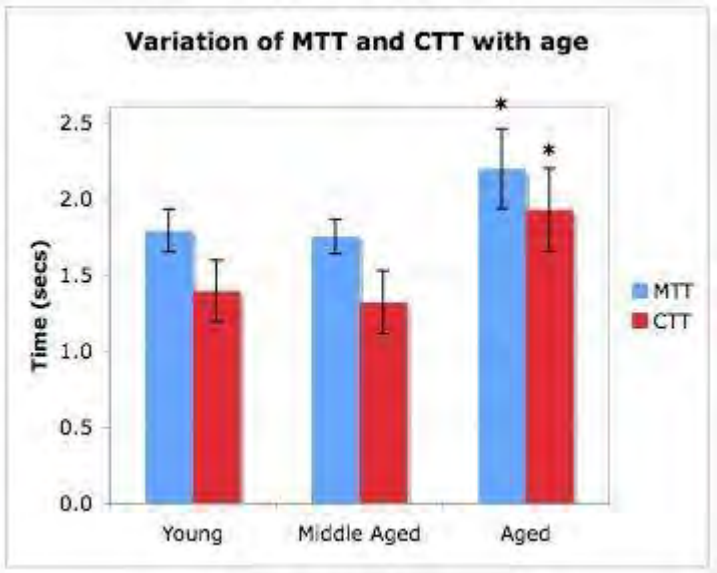

[Significant difference (*one-way ANOVA)]

Conclusions: We have developed a new ASL protocol that is capable of consistently and non-invasively measuring both the MTT and CTT. The technique is applied here to an aging study and a marked difference in both transit times for varying age has been demonstrated. Alterations in vascular dynamics due to aging, such as increased vessel tortuosity, atherosclerosis and reduced vascular reactivity are known to affect cerebral perfusion (D'Esposito et al, 2003). Consequently, a comparison between healthy aged subjects and subjects with various neurological diseases that affect resting CBF using this technique would be of particular interest.

References:

D'Esposito et al, Nature Neuroscience, 2003, vol.4, pp. 863-872.

Kelly et al, Physics in Medicine and Biology, 2009, article in press.

Kim & Kim, Magnetic Resonance in Medicine, 2006, vol.55, no.5, pp1047-1057.

Meier & Zierler, Journal of Applied Physiology, 1954, vol.6, pp731-744.

1003

Brain Poster Session: Neonatal Ischemia

A NEW SWIM TEST QUANTIFIES MOVEMENT DEFICITS IN PERINATAL RABBITS AFTER FETAL HYPOXIA-ISCHEMIA

M. Derrick[1,2], A. Drobyshevsky[1], X. Ji[1], Y. Yang[1], R. Silverman[3], H. Ji[3], S. Tan[1,2]

[1]Pediatrics, Northshore University Healthsystems, [2]Pediatrics, [3]Chemistry, Northwestern University, Evanston, IL, USA

The relationship of movement of different muscle groups has not been quantified before in the newborn period. Cerebral palsy (CP) which often occurs as a result of perinatal hypoxia-ischemia (H-I) is categorized to different types depending on clinical presentation, involvement of brain region and extent of involvement. In order to test involvement of different brain regions, this study investigates individual and multi-joint involvement in a rabbit model of CP. Pregnant rabbits at 70% gestation were subjected to 40-min uterine ischemia. Newborn rabbit kits were subjected to a swim test at 5 time points over the first 1-11 days of life. H-I kits were divided into hypertonic and non-hypertonic groups based on muscle tone at birth. The ranges and velocity of angular movement of the upper and hind-limb joints (wrist, elbow, shoulder, ankle, knee and hip) during supported swimming were determined. Severely impaired (hypertonic) animals have significantly reduced range and angular velocity of joint motion which do not improve over time. The non-hypertonic group showed deficits in wrist and hind-limb movements that were not evident on prolonged observation. Preventive treatment with an inhibitor of neuronal nitric oxide synthase decreased the incidence of severely impaired kits; the non-hypertonic kits showed a different pattern of swimming. Supported swimming allows easy quantification of limb and joint motion in the principal plane of movement in the absence of weight bearing and decreases the need for control of balance. Identification and quantification of milder deficits allows mechanistic studies in the causation of H-I injury as well as estimation of recovery from therapeutic agents.

1006

Brain Poster Session: Angiogenesis

PLATELET DEPLETION DOES NOT AFFECT GLIOBLASTOMA GROWTH AND ANGIOGENESIS IN VIVO DESPITE PROLIFERATIVE AND MIGRATORY EFFECTS OF PLATELET CYTOKINES

L. Schilling[1], B. Bender[2], E. Plaxina[2], I. Noelte[2], R. Erber[1], S. Schambach[2], C. Groden[2], M.A. Brockmann[2]

[1]Division of Neurosurgical Research, [2]Division of Neuroradiology, Medical Faculty Manheim, University of Heidelberg, Mannheim, Germany

Background: The main function of circulating platelets appears to be in the control of vessel wall integrity and regulation of hemostasis. Upon activation by exposure to subendothelial components of the vessel wall or alterations of endothelial cell function including tumor microcirculation, platelets undergo a shift of their phenotype along with the release of vasoactive and angiogenesis-relevant factors and cytokines. An elevated platelet count is considered an independent predictor of short survival in glioblastoma, one of the most densely vascularized tumor types and various peripheral tumors as well.

Methods: IWe investigated the effects of platelet releasate resulting form activation of human platelets with thrombin receptor agonist peptide (TRAP)-6 upon:

i. proliferation of glioma cell lines (U87, U373) and human umbilical venous endothelial cells (HUVECs),
ii. migratory behavior of HUVECs using the Boyden chamber assay, and
iii. of angiogenic activity in HUVECs using the tube formation assay.

We also studied the effect of platelet depletion in nude mice by an anti-GPIb alpha antibody in xenograft models of subcutaneously and intracerebrally grown glioma using volumetric analysis, immunohistochemistry, and magnetic resonance imaging (MRI). Furthermore, the relationship between platelet count on the one hand and tumor proliferation (proliferative index) and vascularization (determined as vessel density) on the other hand was studied in patients undergoing surgical removal of a glioblastoma.

Results: Upon incubation with platelet releasate proliferation of tumor cells and HUVECs was increased in a dilution-related manner. In HUVECs, platelet releasate also stimulated migration activity and tube formation. In contrast, platelet depletion starting on day 1 after tumor implantation did not affect tumor volume grown either subcutaneously (volumetric analysis ex vivo of tumor grown two weeks) or intracerebrally (measured by MRI after three weeks of tumor growth). In the subcutaneously grown tumors volumes were 1251±334 cm^3 (n=5) in saline-treated controls and 1147±178 cm^3 (n=5) in platelet-depleted animals. The respective values in the intracerebrally grown tumors are 163.9±24.0 cm^3 (n=8, saline-treated controls) and 153.6±30.2 cm^3 (n=7, platelet-depleted animals). The vessel density was not affected by platelet depletion in the subcutaneous tumor model determined in randomly chosen areas and in so-called “hot spots” with highly increased angiogenic activity. In patients we did not observe any relationship between the pre-operative platelet count and the proliferative index or vessel density determined in the surgically removed tumor tissue.

Conclusions: Despite distinct proliferation-, chemotaxis-, and angiogenesis-stimulating effects of a platelet-derived cytokine cocktail in vitro, platelet count does not exert a major influence on tumor

growth and angiogenesis in experimental and clinical conditions in vivo. Thus, the frequently observed relationship between an increased platelet count and reduced survival time in patients with malignant tumors is most likely to result from a tumor-induced increase of platelet counts, but not vice versa.

1008

Brain Poster Session: Brain Imaging: Neurologic Disease

PROSPECTIVE TARGETING AND CONTROL OF END - TIDAL PCO_2 AND PO_2 DURING FMRI SCANNING IN HEALTHY SUBJECTS AND PATIENTS

J. Han[1,2], S. Dorner[3], M. Slessarev[1], A. Mardimae[1], D. Mikulis[4], J. Fisher[1,2]

[1]Anesthesia, University Health Network, University of Toronto, [2]Physiology, University of Toronto, [3]Respiratory Therapy, [4]Medical Imaging, University Health Network, University of Toronto, Toronto, ON, Canada

Objectives: Cerebrovascular reactivity (CVR) is defined as change in cerebral blood flow (CBF) for a given vasoactive stimulus. Blood oxygen dependent (BOLD) MRI signal can be used as the surrogate for CBF, and changes in end-tidal PCO_2 ($PetCO_2$) as the stimulus-if end-tidal PO_2 ($PetO_2$) can be kept constant. We set out to develop and test a system that, for the first time, will provide a repeatable $PetCO_2$ stimulus to both healthy subjects and patients in an MR environment.

Methods: We used a custom gas blender (RespirAct™, TRI, Toronto Canada) and a sequential rebreathing circuit to study CVR in a 3T MRI unit (GE Healthcare, Milwalkee, Wisconsin) in 10 healthy subjects (ages 20-50) and 24 patients (ages 20-70) being investigated for neurological symptoms. The target end-tidal values consisted of normoxic (100mmHg) quasi-square wave changes in target $PetCO_2$'s between 40 and 50 mmHg of 45 - 130 s durations. We analyzed the $PetCO_2$'s of the last 30 seconds of each stage and the $PetO_2$ for the entire test.

Results: In healthy subjects the $PetCO_2$'s in mmHg (m ± SD) at each stage were: stage 1-(40.3 ± 0.8), 2-(49.6 ± 1.0), 3-(40.3 ± 1.0), 4-(50.0 ± 0.67), 5-(40.6 ± 1.2). In patients: stage 1- (40.2 ± 0.7), 2-(48.9 ± 2.2), 3-(40.8 ± 1.2), 4-(49.5 ± 1.1), 5-(41.2 ± 1.6). $PetO_2$ was 103.0 ± 2.7 in subjects and 103.5 ± 2.0 in patients. There were no differences at any stage in $PetCO_2$ or $PetO_2$ between healthy subjects and patients.

Conclusions: We conclude that the prospective targeting of $PetCO_2$ and $PetO_2$ provides a highly repeatable stimulus to both healthy subjects and patients during MRI scanning.

1009

Brain Poster Session: Neonatal Ischemia

NEURONAL NITRIC OXIDE SYNTHASE LEVEL IS A CRITICAL DETERMINANT OF NEURONAL DEATH FOLLOWING FETAL HYPOXIA-ISCHEMIA

L. Yu[1], A. Drobyshevsky[1], X. Ji[1], M. Derrick[2], S. Tan[2]

[1]NorthShore University Healthcare System Research Institute, [2]Northshore University Healthsystems, Evanston, IL, USA

Background: We have previously published that apparent diffusion coefficient (ADC) by MRI in fetal hypoxia-ischemia (HI) differentiates fetuses that are destined to be hypertonic postnatally from those that do not have motor deficits (A. Drobyshevsky et al 2007). We have also shown that neuronal nitric oxide synthase (nNOS) inhibitors prevent the motor deficits and perinatal deaths if given prior to HI (H. Ji et al 2009).

Objectives: We hypothesized that nNOS is a critical determinant of neuronal death that results in hypertonia. We tested a novel methodology combining ADC prediction with high speed flow cytometric sorting of cells and quantitative RTPCR.

Methods: Rabbit dams at E25 were subjected to 40 min uterine ischemia in the 3T magnet and serial ADC measurements obtained. ADC threshold was used to categorize fetuses destined to be hypertonic. After 30 min of reperfusion, fetal brains were removed and dissociated into single cell suspensions. Cells were stained by Rhodamine 123 and propidium iodide (PI) and sorted. Sorted cells were then assessed for nNOS gene expression by quantitative RTPCR.

Results: Cells were categorized into dead, injured and healthy cells based on Rhodamine and PI staining. Dead cells (PI+ and rhodamine-) showed higher nNOS expression than injured (PI+ and rhodamine+) or healthy cells (PI- and rhodamine+). In fetuses destined to be hypertonic, nNOS expression was even higher.

Conclusions: We conclude that nNOS is a critical determinant of cell death. We speculate that a certain threshold level of nNOS tips the fetus from a low risk to a high risk fetus for subsequent hypertonia.

References:

1. Drobyshevsky A, et al. Annals of Neurology, 2007, 61(4):307-314.

2. Ji H, et al. Annals Neurol in press.

1010

Brain Poster Session: Cerebral Vascular Regulation

REDUCED CEREBROVASCULAR REACTIVITY IN AREAS SUSCEPTIBLE TO HYPOXIA AND ISCHEMIA

J. Han[1,2], D. Mandell[3], J. Poublanc[3], A. Crawley[3], A. Mardimae[1], J. Fisher[1,2], D. Mikulis[3]

[1]Anesthesia, University Health Network, University of Toronto, [2]Physiology, University of Toronto, [3]Medical Imaging, University Health Network, University of Toronto, Toronto, ON, Canada

Objectives: Paradoxical reductions in blood flow in response to cerebral vasodilatory stimuli have been demonstrated in the peri-ventricular white matter (PVWM) (where elderly patients with dementia and stroke develop leukoariosis) but not in sub-cortical white matter (SCWM)[1]. We set out to administer a standard, repeatable stimulus and document values for normal cerebrovascular reactivity (CVR; change in cerebral blood flow (CBF) (for a given vasoactive stimulus) in white matter in 6 healthy subjects (age 20 - 50).

Methods: We assessed CVR using a 3T MR to generate blood oxygen dependent (BOLD) signal as the surrogate for CBF. We used a custom gas blender (RespirAct™, TRI, Toronto Canada) and a sequential rebreathing circuit to apply two ventilatory sequences consisting of normoxic (100 mmHg) near-square wave changes in target end-tidal PCO_2 ($PetCO_2$), first stepping between 30 and 40, and then 40 and 50 mmHg. Steps were of 45 - 130 s duration. In post hoc brain segmentation analysis, PVWM (Figure 1A) and SCWM (Figure 1B) regions of interest where identified from two axial sections above the head of the caudate nucleus. CVR was quantified as %Δ BOLD signal/Δ $PetCO_2$ and mapped voxel by voxel.

[Figure1]

Results: Hypercapnic stimuli (Figure1C) showed reduced CVR in PVWM compared to the SCWM (0.105 ± 0.034 vs. 0.145 ± 0.03 respectively, P = < 0.05; mean ± SD). Hypocapnic stimuli (Figure1D) did not affect CVR (0.120 ± 0.042 vs 0.116 ± 0.027, P = > 0.05, in PVWM and SCWM, respectively).

Conclusions: PVWM is supplied by the long penetrating arteries which lack distal collateralizaton. This may account for its reduced vascular reserve compared to that of the SCWM. The data supports the concept[1] that the PVWM is more susceptible to developing ischemic demyelination than the SCWM.

References: (1) Mandell DM. et al. Stroke 2008 July;39(7):1993-8.

1011

Brain Poster Session: Experimental Cerebral Ischemia: Vascular & Endothelial

AGMATINE REDUCES BRAIN EDEMA BY REGULATING THE EXPRESSION OF AQUAPORINS AND MATRIX METALLOPROTEINASES AFTER COLLAGENASE INDUCED INTRACEREBRAL HEMORRHAGE IN RATS

J.Y. Kim[1], S.H. Kim[2], J.H. Kim[3], W.T. Lee[3], K.A. Park[3], J.E. Lee[1]

[1]Anatomy, BK21 Project for Medical Science, Yonsei University, College of Medicine, Seoul, [2]Neurosurgery, Ajou University, School of Medicine, Suwon, [3]Anatomy, Yonsei University, College of Medicine, Seoul, South Korea

Objectives: we investigate the effect of agmatine on the expression of matrix metalloproteinases (MMPs) and aquaporines after collagenase induced intracerebral hemorrhage in rat.

Methods: ICH was induced on adult male Sprague-Dawley rats (280~300g) by stereotactic injection of collagenase type Ⅶ 0.5$\mu\ell$ using 32-Guage needle on right caudate putamen (0.2mm Anterior and 3mm Lateral to bregma, 6mm ventral for dura) [1]. Agmatine (100mg/kg, intraperitoneally) was administrated at 6hr, it has delayed initial treatment at 6hr to a more clinically relevant time [2], and 1 to 7days after ICH onset. Brains were cut into 2mm thick coronal sections in a cutting block, the sections were used for evaluated western blot, immunohistochemistry and swelling volume analysis.

Results: Agmatine treatment significantly increased the immunoreactivity of AQP4 and MMP9 in the peri-hematoma region. Swelling volume was clearly stabilized at 3day to 7day in agmatine treatment group. Western blot analysis showed that agmatine treatment decreased the expression of MMP2 and AQP9, correlated with brain edema as water channels. The expression of MMP2 and AQP9 were reduced in agmatine treatment group. Agmatine could attenuate brain edema through lessening water content by suppression of the expression of aquaporins and also play a critical role in maintaining the integrity of the BBB.

Conclusions: These results may suggest agmatine as a novel therapeutic material for vasogenic and cytosolic edema including traumatic brain injury and intracerebral hemorrhage.

References:

[1] Gary A. R et al., Stroke 21 (1990) 801-807.

[2] Jason K. Wet al., Exp Neurol. 207 (2007) 227-237.

1012

Brain Poster Session: Oxidative Mechanisms

HYPERBARIC OXYGEN INDUCED OXIDATIVE STRESS IN RATS' BRAIN CORTEX TISSUE WITH RELATION TO THE PRESSURE/DURATION RANGE OF THE TREATMENT

S. Oter[1], K. Simsek[2], S. Sadir[1], M. Ozler[1], B. Uysal[1], T. Topal[1], H. Ay[2], A. Korkmaz[1]

[1]Physiology, [2]Undersea and Hyperbaric Medicine, Gulhane Military Medical Academy, Ankara, Turkey

Objective: The toxicity risk of hyperbaric oxygen (HBO) has long been of interest [1, 2]. Since having a high rate of blood flow and oxygen consumption, the brain is one of the most sensible organs to hyperoxic injury [3]. During the last decade, our laboratory has been focused on pressure-related and exposure time-related correlation of HBO exposure in a series of experimental studies performed with rats; another study set elucidated the persistence of oxidative stress markers following HBO procedure. The results of have been published previously [4-6]. This presentation will summarize the outcome of our lab's recent work.

Methods: A total of 162 male Sprague-Dawley rats were used for the abovementioned experimental sets. The approved and clinically used maximal pressure/duration range, 3 ATA/2 hours [7], was chosen as HBO exposure limit. After HBO treatment procedures, brain tissues of the rats were harvested immediately and their cortexes were reserved to be used for biochemical assay. Thiobarbituric acid reactive substances (TBARS), indicator of lipid peroxidation, were measured in all tissue samples. Antioxidant enzymes superoxide dismutase (SOD) and glutathione peroxidase (GSH-Px) were also determined. In some of the experiments nitrite-nitrate values (NO_x) were measured in order to evaluate nitric oxide production.

Results: TBARS levels as well as SOD activities of brain cortex samples represented significant pressure-related increasing courses, estimated to be positively correlated with each other. A relation of HBO-induced oxidative action with exposure time was also found for TBARS and SOD, whereas GSH-Px activity increased independently. NO_x increased only at the maximal exposure level of 3 ATA for 2 hours. Anyway, all of the aforesaid oxidative stress and antioxidant defense indices returned to their baseline levels within 90 min at the most. The collective outcome was summarized in the table.

	HBO exposure pressure (at 2 h duration for each) [4]			HBO exposure time (at 3 atm pressure for each) [6]			Time after HBO treatment (with 3 atm for 2 h) [5]		
	1 atm	**2 atm**	**3 atm**	**30 min**	**60 min**	**120 min**	**30 min**	**60 min**	**90 min**
TBARS	**	**	**	**	**	**	**	---	---
SOD	---	**	**	---	**	**	**	**	---
GSH-Px	n.d.	n.d.	n.d.	**	**	**	**	**	---

NO_X	n.d.	n.d.	n.d.	---	---	**	**	---	---

[HBO & Oxidative Stress: **Significantly different]

Conclusion: The combined conclusion of these studies proves the oxidative effect of HBO, but also supports its safety as a treatment modality within its approved therapeutic limits. Especially, the increased activities of antioxidant enzymes and the relative short persistence time of oxidant molecules support this debate. However, to avoid unwanted oxidative side-effects as low pressure/duration ranges as possible should be used in clinical applications.

References:

[1] Narkowicz et al. Free Radic Res Commun 1993;19:71.

[2] Chavko & Harabin. Free Radic Biol Med 1996;20:973.

[3] Harabin et al. J Appl Physiol 1990;69:328.

[4] Oter et al. Clin Biochem 2005;38:706.

[5] Ay et al. Clin Exp Pharmacol Physiol 2007;34:787.

[6] Korkmaz et al. Neurochem Res 2008;33:160.

[7] Feldmeier J. The hyperbaric oxygen therapy committee report. UHMS 2003.

Grant: These studies were supported by the Gulhane Military Medical Academy Research and Progress Center with grants Nr.AR-2003/37 and AR-2005/25.

1013

Brain Poster Session: Cerebral Vascular Regulation

FREQUENCY-DEPENDENT CEREBRAL BLOOD FLOW-VOLUME COUPLING IN ACTIVATED HUMAN VISUAL CORTEX

A.-L. Lin, P. Fox

Research Imaging Center, University of Texas, San Antonio, TX, USA

Objectives: The understanding for coupling between relative changes in cerebral blood flow (rCBF (%)) and cerebral blood volume (rCBV (%)) is important due for investigating BOLD signals mechanisms and oxygen metabolism determination (1, 2). Nonetheless, it remains unclear that whether the coupling persists unchanged, i.e., with a fixed power law constant $\alpha = 0.38$ (Eq. [1]), or varies with brain activities. The purpose of this study was to verify the flow-volume coupling during graded visual stimulation with fMRI methods. $(1+ rCBV) = (1+ rCBF)^{\alpha}$ [1].

Methods: Five males (aged 20-34) participated the study. The studies were performed on a 3T Siemens Trio MRI Scanner with the experimental paradigm of 3-min 4Hz/3-min off/3-min 8Hz visual stimulation using a black-white checkerboard. Four slices with thickness of 5 mm. Field-of-view (FOV) = 24 cm; image matrix size = 64 x 64. rCBF(%) was determined using arterial spin labeling (ASL) techniques, with $TR/TE/TI_1/TI_2$ = 2000 ms/19 ms/700 ms/1000 ms (3). rCBV(%) was determined using 0.1 mmol/kg Gd-DTPA contrast agent per condition with the gradient echo EPI: TR/TE = 2000 ms/30 ms. The voxels of the ASL images that passed through the threshold (Student t test, $P < 0.005$) were used to determine rCBF. Changes in brain signal intensity occurring during cerebral transit of the high magnetic susceptibility Gd-DTPA were converted to contrast agent concentration--time curves. The area under the concentration-time curve is proportional to the local rCBV. These calculations were performed on a voxel-by-voxel basis to generate images of rCBV (4). Those passed through the threshold ($P < 0.005$) and had common area with rCBF were used to calculate the α values.

Results: The magnitudes of rCBF(%) and rCBV(%) averaged over the five subjects are shown in Table 1. Both rCBF and rCBV were higher at 8 Hz than at 4 Hz. The α values were then calculated with Eq. [1]. As shown in Table 1, α varies with stimulus frequency with $\alpha = 0.28$ and 0.50 at 4 and 8 Hz, respectively. The result is in good agreement with a previous PET study with a similar visual stimulus design (α =0.37-0.64), though $\alpha = 0.3$ was demonstrated in the paper with the mixture of all three conditions, i.e., resting, 2 and 8 Hz with quantitative values (5).

Conclusions: The results suggest that the flow-volume coupling is not constant, but varies with stimuli and brain activity, andthe calculation of cerebral metabolic rate of oxygen ($CMRO_2$) cannot depend on the assumption of α=0.38 for all stimuli. The frequency-dependent flow-volume coupling would facilitate our future understanding of BOLD and $CMRO_2$ mechanisms.

References:

(1) Grubb, Stroke 1974, 5:630-639.

(2) Davis, PNAS 1998, 95:1834-1839.

(3) Wang,MRM 2003, 49:796-802.

(4) Belliveau, Science 1991, 254:716-719.

(5) Ito, JCBFM 2001, 21:608-612.

Stimulus Rate	Imaging Method	rCBV(%)	rCBF(%)	α
4Hz	fMRI	12±3	49±10	0.28
8Hz	fMRI	27±5	62±12	0.50
2Hz	PET(5)	10±13	16±16	0.64
8Hz	PET(5)	21±5	68±20	0.37

[Table 1]

1014

Brain Oral Session: Cortical Spreading Depression

ACCELERATION OF ISCHEMIC TISSUE DAMAGE BY MODERATELY DECREASED BLOOD PRESSURE: ROLE OF TISSUE HYPOXIA BUT NOT OF CORTICAL SPREADING DEPRESSION

K. Waehner, N. Weinzierl, L. Schilling

Division of Neurosurgical Research, Medical Faculty Manheim, University of Heidelberg, Mannheim, Germany

Background: The pathophysiology of focal brain ischemia is complex and still poorly understood. The size of brain damage may be influenced by local and systemic changes of a variety of parameters such as arterial blood pressure (BP), occurrence of cortical spreading depression (CSD) or CSD-like episodes, and changes of blood sugar content occurring early, i.e. within hours after vessel occlusion. We addressed the question whether BP at a level around the lower range of autoregulation, i.e. around 80 mm Hg will affect development of ischemic damage by increasing the rate of CSD episodes.

Methods: Male Sprague-Dawley rats were intubated in isoflurane anesthesia the and artificially ventilated to maintain blood gases within physiological ranges. The femoral artery and vein were catheterized for BP monitoring and injection of pimonidazole (6 ml/100 g body weight), respectively. The right common carotid artery was exposed and a 4-0 nylon filament with the tip covered with a layer of silicone introduced. A burr hole was created in the right dorsal skull bone in the middle cerebral artery (MCA) territory to position:

i. a calomel electrode for monitoring DC potential changes in the epidural space and
ii. a laser Doppler flowmeter (LDF) probe to measure changes of regional cerebral blood flow (rCBF).

Additional burr holes to measure rCBF changes were created in the right anterior cerebral artery and left MCA territory. Two experimental groups were studied: a moderate BP level group in which the animals were kept at a blood pressure above 95 mmHg and a the second one in which BP was maintained around 80 mmHg for at least two hours by applying negative pressure to the abdomen and the hindlimbs (low level BP group). At the end of the 4 h observation period the brain was removed and serial coronal sections were cut. Adjacent sections were taken every 500 µm and used for either silver nitrate staining to detect brain damage or pimonidazole adducts staining to detect tissue hypoxia. The sections were scanned, areas where measured and processed to yield the volumes of structural damage and of hypoxia.

Results: Decreasing BP after establishing focal ischemia did not result in fall of LDF signal in the left MCA territory. The numbers of negative DC potential shifts occurring during 4 h after MCAO ranged from 1- 10 in the moderate and 1-8 in the low level BP group. Volume of ischemic damage was 92.3±25.8 cm^3 (mean±SEM; n=11) in the moderate level PB group and 157.1±24.6 cm^3 (n=5) in the low level BP group (p=0.1). Tissue hypoxia amounted to 168.8+20.6 cm^3 (moderate level BP group) and 195+31.6 cm^3 (low level BP group).

Conclusion: The results indicate that BP levels in the lower range of autoregulation occurring early after induction of focal cerebral ischemia accelerates the development of ischemic damage, probably by increasing the hypoxic burden to the tissue. Facilitation of CSD episodes, however, does not appear to play a major role.

1016

Brain Poster Session: Neonatal Ischemia

PROSTAGLANDIN E_2-EP4 RECEPTOR AGONIST PROTECTS NEONATAL BRAIN FROM HYPOXIA-ISCHEMIA

H. Taniguchi, C. Anacker, X. Liang, Q. Wang, F. Sabar, K. Andreasson

Neurology and Neurological Sciences, Stanford University School of Medicine, Stanford, CA, USA

Objectives: The pathogenesis of neonatal hypoxic-ischemic encephalopathy (HIE) involves increased production of prostaglandins (Taniguchi et al. 2007). It is known that two Gαs-coupled receptors, prostaglandin D_2-DP1 receptor and prostaglandin E_2-EP2 receptor, mediate neuroprotection in vivo in models of brain ischemia (McCullough et al. 2004; Liu et al. 2005; Saleem et al. 2007; Taniguchi et al. 2007; Li et al. 2008). In this study, we sought to clarify the role of the prostaglandin E_2-EP4 receptor, another Gαs-coupled receptor, in a model of neonatal brain ischemia.

Methods: The neonatal HIE model was performed as previously described (Rice et al. 1981; Taniguchi and Andreasson 2008). Briefly, the left common carotid artery of postnatal day 7 Sprague-Dawley rat pups was ligated and pups were placed in hypoxic chamber for 100min. Either ONO-AE1-329 (selective EP4 agonist; Ono Pharmaceuticals, Osaka, Japan) or vehicle were injected subcutaneously before and/or after hypoxia. At 24 hours after the end of hypoxia, the pups were sacrificed and brains were sliced and stained with 2,3,5-Triphenyltetrazolium chloride. Infarct area and infarct volume were measured using Image J (NIH, Bethesda, MD).

Results: Immunostaining of the EP4 receptor shows that the EP4 receptor is expressed in neurons and endothelium of cerebral cortex, striatum, and hippocampus. Stimulation of EP4 receptor with ONO-AE1-329 protected organotypic slice CA1 hippocampal neurons from N-methyl-d-aspartate (NMDA) toxicity or oxygen-glucose deprivation.

The infarct size was in HIE model significantly reduced in the EP4 agonist treated group compared with the vehicle treatment group. The EP4 agonist was most effective when administered before hypoxia.

Conclusions: We found that the EP4 agonist, ONO-AE1-329 reduced the infarct size in our neonatal HIE model. Taken together, these findings indicate that in vitro and in vivo, stimulation of the EP4 receptor leads to neuronal protection. Early administration of this EP4 agonist may provide a novel approach to protect the neonatal brain from hypoxic-ischemic insult.

References:

Li J, Liang X, Wang Q, Breyer RM, McCullough L, Andreasson K. (2008) Misoprostol, an anti-ulcer agent and PGE2 receptor agonist, protects against cerebral ischemia. Neurosci Lett 438:210-215.

Liu D, Wu L, Breyer R, Mattson MP, Andreasson K. (2005) Neuroprotection by the PGE2 EP2 receptor in permanent focal cerebral ischemia. Ann Neurol 57:758-761. McCullough L, Wu L, Haughey N, Liang X, Hand T, Wang Q, Breyer RM, Andreasson K. (2004) Neuroprotective function of the PGE2 EP2 receptor in cerebral ischemia. J Neurosci 24:257-268.

Rice JE, 3rd, Vannucci RC, Brierley JB. (1981) The influence of immaturity on hypoxic-ischemic brain damage in the rat. Ann Neurol 9:131-141.

Saleem S, Zhuang H, de Brum-Fernandes AJ, Maruyama T, Narumiya S, Dore S. (2007) PGD(2) DP1 receptor protects brain from ischemia-reperfusion injury. Eur J Neurosci 26:73-78.

Taniguchi H, Andreasson K. (2008) The hypoxic-ischemic encephalopathy model of perinatal ischemia. J Vis Exp.

Taniguchi H, Mohri I, Okabe-Arahori H, Aritake K, Wada K, Kanekiyo T, Narumiya S, Nakayama M, Ozono K, Urade Y, Taniike M. (2007) Prostaglandin D2 protects neonatal mouse brain from hypoxic ischemic injury. J Neurosci 27:4303-4312.

1017

Brain Poster Session: Neonatal Ischemia

CEREBRAL PALSY PHENOTYPE IN RABBITS MODELING PROGRESSION FROM PARTIAL TO COMPLETE PLACENTAL INSUFFICIENCY

X. Ji[1], M. Derrick[2], L. Yu[1], A. Drobyshevsky[1], A. Liu[1], S. Tan[3]

[1]NorthShore University Healthcare System Research Institute, [2]Pediatrics, [3]Peditrics, NorthShore University Healthcare System Research Institute, Evanston, IL, USA

Objective: Fetal hypoxia-ischemia is one of the important causes of cerebral palsy in children. The clinical scenario of abruptio placenta is a significant cause of fetal hypoxia-ischemia. Abruptio placenta progresses from partial to total abruptio in a variable period of time. To model the progression of partial to complete placental insufficiency, we modified our previously published animal model mimicking cerebral palsy (Derrick et al 2004). The objective was to make the animal model a more clinically relevant model.

Methods: Pregnant New Zealand White rabbits at 70% gestation (E22) were subjected to partial uterine ischemia for 30 min by inflation of a balloon catheter in the distal aorta using 75 µl. Fetal bradycardia was noted within 5 min of the balloon inflation. Then complete uterine ischemia was implemented for 40 min by further inflation of balloon to 250µl. The balloon was then deflated, the aortic catheter removed, wound sites sutured, and the pregnant dams were allowed to survive. The dams spontaneously gave birth at term gestation (E31.5 days). The newborn kits were subjected to a battery of neurobehavior tests on the first postnatal day.

Results: Of the 52 kits born to 8 dams, there were 25 stillbirths or fetal deaths (48%). 85% of the survivors manifested hypertonia based on a modified Ashworth scale. Based on the total neurobehavioral score of the survivors, there were 15% normal, 33% mild and 52% severely affected kits. Weights of survivors were 56±2 and dead kits were 35±3 G.

Conclusions: This outcome is slightly more severe than our previous model. We conclude that this modified model more closely mimics the clinical situation of the human mother who undergoes first partial then complete abruptio placenta. The rabbit kits show a spectrum of injury suggesting that some rabbits are intrinsically more vulnerable than others. The incidence of hypertonic survivors may be an underestimate because most of the stillbirths/fetal deaths may be hypertonic if we were able to resuscitate them. Furthermore, this model is suitable for testing neuroprotectants administered in the antenatal period.

References: Derrick M, et al. J. Neurosci. 24:24-34, 2004.

1018

Brain Poster Session: Cerebral Metabolic Regulation

OXYGEN EXTRACTION FRACTION IS UNCHANGED IN HEALTHY AGING

J. Aanerud[1], P. Borghammer[1], A. Gjedde[2]

[1]PET Centre, Aarhus University Hospitals, [2]CFIN, Aarhus University, Aarhus, Denmark

Introduction: We tested the hypothesis that the oxygen extraction fraction increases with age. Kety (1956) reported an increased arteriovenous oxygen difference with age in a meta-analysis of 16 studies, in which mean age ranged from 5 to 93 years. In our case PET measurements of cerebral blood flow (CBF) and oxygen consumption (CMRO2) were used to estimate oxygen extraction fraction (OEF), which corresponds to arteriovenous oxygen difference.

Materials and methods: Fifty-nine healthy subjects (39 men) aged 21-73 years were included. Parametric maps of CBF, OEF and CMRO2 were calculated from the PET image volumes, and non-linearly co-registered to common space, via individual anatomical MR images. Linear voxelwise regression of CBF, CMRO2, and OEF on age were performed using fMRIstat. OEF-maps were created by dividing CMRO2- maps with CBF-maps and hemoglobin concentration.

Results: The regression showed no significant changes in OEF with increasing age. Throughout the brain t-values remained close to zero, i.e. 95.7% of the intra-cerebral voxels exhibited t-values ranging from -2 (decreased OEF) to 2 (increased OEF).

Discussion: Based on this dataset the hypothesis of increased OEF with aging cannot be upheld. On the contrary, the result indicates that blood flow is tightly regulated across the age span investigated.

1019

Brain Poster Session: Cerebral Vascular Regulation

BLOOD FLOW AUTOREGULATION IN THE RAT BRAIN CORTEX IS A HETEROGENEOUS PHENOMENON

P. Herman[1,2], L. Kocsis[1], I. Portörő[1], A. Eke[1]

[1]Institute of Human Physiology and Clinical Experimental Research, Semmelweis University, Budapest, Hungary, [2]Department of Diagnostic Radiology, Yale University, New Haven, CT, USA

Objectives: Blood flow autoregulation in the brain is a spatio-temporal phenomenon. The cerebrovascular system distributes flow among great number of microregions in the brain cortex. In this study the effectiveness of autoregulation was investigated in the intravascular and parenchymal compartments of the brain cortex, and was characterized by the autoregulatory threshold.

Methods: Animal preparation: Artificially ventilated Wistar rats (n=8) were anesthetized by Urethane (1.3 g/kg, i.p.). An arterial line was used for monitoring blood pressure and taking samples for blood pH, pO2, pCO2 throughout the experiment. The bone was thickened to translucency over the parietal cortex 2 days prior the experiment. A metal platform was fixed to the skull to secure the head's position during the measurement. Laser Speckle measurements: The speckle contrast images (4096 images/150s) were collected with a Coolsnap CF camera with 256x256 resolution (voxelsize: 16 μm2) at 655nm. A 5x5 kernel was used to calculate flow velocity. The hypotensive steps (of 90, 80, 70, 60, 50 and 40 mmHg) were maintained by a computer controlled hypobaric method which has been described previously [1]. The duration of each hypotensive step was ~2.5 min. During the transient between steps, pressure slowly ramped to target level at a rate of ~0.07mmHg/s, for the purpose of maintaining autoregulation [2]. The 4096 velocity images were averaged for each hypotensive period. The autoregulatory threshold for CBF was determined for each microregion within the mapped area at 80% of the respective control level.

Results: The group mean perfusion in the intravascular space changed from 110 to 85 A.U. (i.e. 77%) from control to 40 mmHg, respectively, while in the parenchymal space from 85 to 73 A.U. (i.e. 88%). The intravascular compartments showed higher autoregulation threshold than the parenchymal regions. The threshold level, hence the effectiveness of autoregulation, in the parenchymal compartment was found to depend on regionally averaged baseline flow: lower and higher flow is associated with a higher threshold (see Figure).

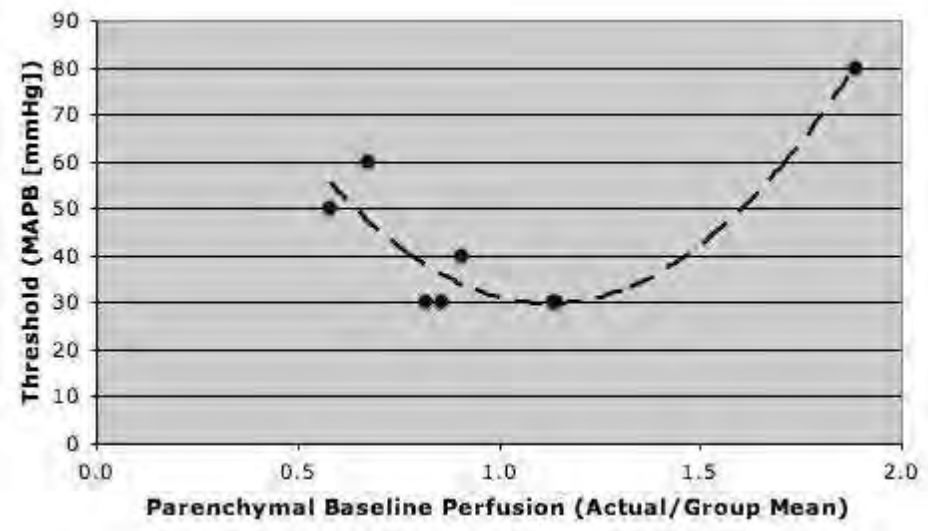

[Autoregulatory thresholds]

Conclusion: The autoregulatory threshold is spatially heterogeneous within the parenchymal and intravascular compartment, alike. In the parenchyma, autoregulation is most effective when the regionally averaged baseline flow is normal, while it is weakened when baseline flow is low or high.

References:

1. Herman et al (2006) J Cereb Blood Flow Metab 26:1189-97.

2. Barzo et al (1993) Neurosurgery 32:611-8.

Acknowledgements: Supported by OTKA (T34122) and EuroBloodSubstitues Consortium (LSHB-CT-2004-503023) grants given to A. Eke.

1020

Brain Poster Session: Cerebral Vascular Regulation

BOLD FMRI MEASURED CEREBROVASCULAR REACTIVITY IN WHITE MATTER: IS IT DIFFERENT WITH HYPERCAPNIC AND HYPOCAPNIC STIMULI?

J. Han[1,2], D. Mandell[3], J. Poublanc[3], A. Crawley[3], A. Mardimae[1], J. Fisher[1,2], D. Mikulis[3]

[1]Anesthesia, University Health Network, University of Toronto, [2]Physiology, University of Toronto, [3]Medical Imaging, University Health Network, University of Toronto, Toronto, ON, Canada

Objectives: Cerebrovascular reactivity (CVR) is defined as change in cerebral blood flow (CBF) per unit of vasoactive stimulus. Blood oxygen dependent (BOLD) MRI signal can be used as the surrogate for CBF, and changes in end-tidal PCO_2 ($PetCO_2$) as the stimulus if end-tidal PO_2 ($PetO_2$) can be kept constant. The reported consistency of CVR calculations from changes of $PetCO_2$ in the hypercapnic and hypocapnic ranges are conflicting. Having previously quantified the CVR in grey matter we now set out to study white matter CVR to standardized CO_2 stimuli in the hypercapnic and hypocapnic range.

Methods: We studied CVR in 10 healthy subjects aged 20-50 yrs, in a 3T MRI using a gradient echo EPI sequence with TE = 30 msec. We used a custom gas blender (RespirAct™, TRI, Toronto Canada) and a sequential rebreathing circuit to target end-tidal values. We applied two sequences consisting of normoxic (100mmHg) near-square wave changes in target $PetCO_2$'s stepping between 30 and 40, and then again from 40 to 50 mmHg. Steps were of 45 - 120 s durations. Post hoc brain segmentation was used to isolate the white matter (Figure1A). CVR was quantified % Δ BOLD signal/Δ $PetCO_2$ and mapped voxel by voxel.

Results: White matter CVR isolated from whole brain CVR with hypercapnic (Figure1B) and hypocapnic (Figure1C) stimuli were 0.155 ± 0.03 and 0.130 ± 0.03 respectively, P = > 0.05. These values are reduced compared to grey matter CVR, 0.295 ± 0.07 for hypercapnia and 0.207 ± 0.05 for hypocapnia, demonstrated from a previous study[1].

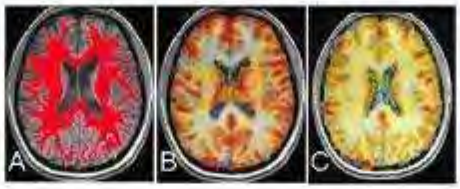

[Figure1]

Conclusions: In summary, there is no statistically significant difference in CVR between hypercapnea and hypocapnea in the cerebral white matter. This is in contradistinction to that seen in the gray matter. However, a trend is present in the white matter that might become significant if a larger sample of subjects is studied. In addition, the magnitude of the response to CO2 in both the hypercapnic ($P = < 0.05$) and hypocpanic ($P = < 0.05$) ranges are significantly smaller than that seen in gray matter. Therefore, CVR in the grey matter can not be extrapolated to the white matter and both therefore need to be studied separately. This indicates the need for accurate gray - white segmentation when quantitating results to avoid volume averaging effects (white matter CVR contaminates gray matter CVR measurement and vice versa) on the accuracy of the result.

References: 1. Han et al. BOLD FMRI measured cerebrovascular reactivity in grey matter: is it different with hypercapnic and hypocapnic stimuli?

Submitted abstract: Brain Chicago 2009.

1021

Brain Poster Session: Cerebral Vascular Regulation

BOLD FMRI MEASURED CEREBROVASCULAR REACTIVITY IN GREY MATTER: IS IT DIFFERENT WITH HYPERCAPNIC AND HYPOCAPNIC STIMULI?

J. Han[1,2], D. Mandell[3], J. Poublanc[3], A. Crawley[3], A. Mardimae[1], J. Fisher[1,2], D. Mikulis[3]

[1]Anesthesia, University Health Network, University of Toronto, [2]Physiology, University of Toronto, [3]Medical Imaging, University Health Network, University of Toronto, Toronto, ON, Canada

Objectives: Cerebrovascular reactivity (CVR) is defined as change in cerebral blood flow (CBF) for a given vasoactive stimulus. Blood oxygen dependent (BOLD) MRI signal can be used as the surrogate for CBF, and changes in end-tidal PCO_2 ($PetCO_2$) as the stimulus-if end-tidal PO_2 ($PetO_2$) can be kept constant. The reported consistency of CVR calculations from changes of $PetCO_2$ in the hypercapnic and hypocapnic are conflicting. We used fMRI to compare the grey matter CVR to standardized stimuli in the hypercapnic and hypocapnic range.

Methods: We studied CVR in 10 healthy subjects aged 20-50 y, in a 3T MRI (GE Healthcare, Milwalkee, Wisconsin) using a gradient echo EPI sequence with TE = 30 msec. We used a custom gas blender (RespirAct™, TRI, Toronto Canada) and a sequential rebreathing circuit to target end-tidal values. We applied two sequences consisting of normoxic (100mmHg) near-square wave changes in target $PetCO_2$'s stepping between 30 and 40, and 40 and 50 mmHg. Steps were of 45 - 130 s durations. Post hoc brain segmentation was used to isolate grey matter (Figure 1A) in each vascular territory. CVR was quantified % Δ BOLD signal/Δ $PetCO_2$ and mapped voxel by voxel.

Results: Grey matter CVR isolated from whole brain CVR with hypercapnic (Figure 1B) and hypocapnic (Figure 1C) stimuli were 0.295 ± 0.07 and 0.207 ± 0.05 respectively $P = < 0.05$. There was no difference in CVR between vascular territories at either hypercapnic or hypocapnic ranges.

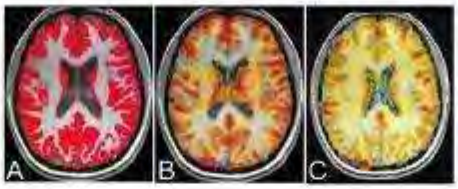

[Figure1]

Conclusions: We conclude that CVR in grey matter is greater with hypercapnic compared to hypocapnic stimuli. Further work is necessary to test the linearity of the response within the range of CO2 applied. For purposes of establishing normal ranges and performing population or sequential comparisons, “CVR” data need to be qualified by the stimulus range in which the data were collected, as well as the MR field strength and pulse sequence applied.

1023

Brain Poster Session: Neurogenesis

AGMATINE ENHANCES NEUROGENESIS OF TRANSPLANTED STRIATUM-DERIVED NEURAL STEM CELLS IN RAT BRAIN AFTER EXPERIMENTAL STROKE

J.Y. Kim[1], J.H. Kim[2], K.K. Bokara[2], Y.M. Nho[1], Y.M. Park[1], K.A. Park[2], W.T. Lee[2], J.E. Lee[1]

[1]Anatomy, BK21 Project for Medical Science, Yonsei University, College of Medicine, [2]Anatomy, Yonsei University, College of Medicine, Seoul, South Korea

Objectives: Transient ischemic attack (TIA) has long been identified as a risk factor for stroke. Ischemic injury can cause massive damage from extensive tissue loss, following the neuronal cells and the connections that reside there. Agmatine has been shown to have neuroprotective effect and ability to modulate differentiation of neural stem cells in various neuronal disease models [1, 2]. To better repair following stroke injury, stroke damaged animal models were transplanted with striatum-derived neural progenitor cells and treated agmatine in this study.

Methods: Using a well established models of focal cerebral ischemia, male Sprague-Dawley rats (300±30g) were subjected to 60min middle cerebral artery occlusion (MCAO)[2]. Before transplantation, striatum-derived neural progenitor stem cells isolated from E14 fetal ICR mice brain were formed undifferentiated neurospheres in vitro stained by BrdU. Animals were transplanted with striatum-derived neural stem cells at 1week after MACO injury and agmatine was co-treated for 7days to 21days at the end of occlusion (100mg/kg, I.P.). Animals were pretreated by agmatine after the injury was also transplanted with the neural stem cells at 1week. To analyze behavior performances, rotarod test, limb placing test were executed after MCAO. To investigate whether agmatine involved the differentiation and proliferation of striatum-derived neural progenitor cells, double immunohistochemical staining was performed with anti-BrdU antibody for donor-derived cells, neuronal marker NeuN and MAP2, migrating neuroblast marker DCX, and astrogial marker GFAP antibodies.

Results: Pretreatment of agmatine helped the neural progenitor cells differentiate to become mature neural cells at 7days to 14days after transplantation. Histological analysis supported that implantation of the striatum-derived neural progenitor cells with agmatine promoted functional recovery, and decreased infarction cavity and scar tissue formation compared to lesion-control group. The striatum-derived neuronal progenitor cells transplanted groups with agmatine regained approximately normal reflex in response to the stimuli within 3weeks. In contrast, lesion-control group regained only about 50% of reflex response for 4weeks.

Conclusions: Here, we show that agmatine which has been known as a neuromodulator in the brain enhances neurogenesis of striatum-derived neural stem cells. These results displayed that cell derived from neural progenitor cells exhibited the differentiation of functional neurons and synapse formation by agmatine treatment.

1024

Brain Poster Session: Cerebral Vascular Regulation

DYNAMIC PRESSURE-FLOW RELATIONSHIP OF THE CEREBRAL CIRCULATION DURING ACUTE INCREASE IN ARTERIAL PRESSURE

R. Zhang[1], K. Behbehani[2], B. Levine[1]

[1]Institute for Exercise and Environmental Medicine, UT Southwestern Medical Center at Dallas, Dallas, [2]Biomedical Engineering, The University of Texas at Arlington, Arlington, TX, USA

The physiological mechanism(s) for the regulation of the dynamic pressure-flow relationship of the cerebral circulation are not well understood. We studied the effects of acute cerebral vasoconstriction on the transfer function between spontaneous changes in blood pressure (BP) and cerebral blood flow velocity (CBFV) in 13 healthy subjects (30 ± 7 yrs). CBFV was measured in the middle cerebral artery using transcranial Doppler. BP was increased stepwise with phenylephrine infusion at 0.5, 1.0 and 2.0 ug/kg/min. During phenylephrine, BP was increased by 11, 23 and 37% from baseline, while CBFV increased only by 11% with the highest increases in BP. Cerebrovascular resistance index (BP / CBFV) increased progressively by 6, 17 and 23%, demonstrating effective steady-state autoregulation. Transfer function gain at the low frequencies (0.07 - 0.20 Hz) was reduced by 15, 14 and 14%, while the phase was reduced by 10, 17 and 31%. A similar trend of changes was observed at the high frequencies (0.20 - 0.35 Hz), but gain and phase were unchanged at the very low frequencies (0.02 - 0.07 Hz). Windkessel model simulation suggested that increases in steady-state cerebrovascular resistance and/or decreases in vascular compliance during cerebral vasoconstriction may contribute to the changes in transfer function gain and phase. These findings suggest that cerebral vasoconstriction attenuates CBFV responses to changes in BP at the low frequencies, whereas dynamic autoregulation may counteract these effects at the very low frequencies. Thus, oscillations in CBFV are likely to be modulated not only by dynamic autoregulation, but also by changes in steady-state cerebrovascular resistance and/or vascular compliance during cerebral vasoconstriction.

1026

BrainPET Poster Session: Kinetic Modeling

MEASUREMENT OF [18F]MPPF BINDING IN RAT HIPPOCAMPUS AND CORTEX BY PET

K. Tennessen, E. Ahlers, J. Moirano, D. Murali, A. Converse

Waisman Brain Imaging Lab, University of Wisconsin - Madison, Madison, WI, USA

Objectives: [18F]MPPF is a radiotracer used in positron emission tomography (PET) to image the location of serotonin-1A (5- HT1A) receptors. As part of an attempt to develop a noninvasive assay to measure in vivo changes in synaptic serotonin levels we imaged [18F]MPPF binding in rats.

Methods: Rats were anesthetized with isofluorane, catherterized for venous injection, and positioned four at a time in a microPET P4 small animal scanner. Following a transmission scan, [18F]MPPF was administered and emission scans were performed. Dynamic images were reconstructed with attenuation and scatter correction and aligned to template regions of interest (ROI) and time activity curves (TAC) were determined. Hipppocampus and cortex to cerebellum distribution volume ratios (DVR) were calculated using the Logan graphical reference tissue method.

Results: At the regions of highest binding, the observed DVRs for the period 20-40 minutes post injection of [18F]MPPF were hippocampus: 2.04 +/- 0.159 and anterior cortex: 1.95 +/- 0.124 (mean +/- SD, n=8).

Conclusions: Binding of the 5-HT1A receptor ligand [18F]MPPF has been measured by PET in rat hippocampus. Future work will focus on attempts to measure pharmacologically induced serotonin release.

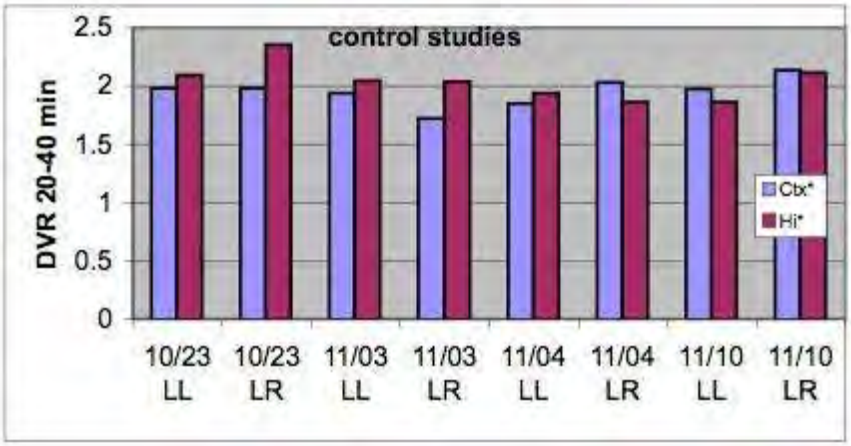

[Measurement of [18F]MPPF binding]

1027

Brain Poster Session: Neurovascular Unit in Health & Disease

EXHAUSTED CEREBRAL AUTOREGULATION IS SPATIALLY ASSOCIATED WITH CORTICAL ATROPHY

J. Fierstra[1], J. Poublanc[1], H. Wang[1], J. Han[2], J. Fisher[2], A. Crawley[1], **D. Mikulis**[1]

[1]Medical Imaging, [2]Anesthesia, University Health Network, University of Toronto, Toronto, ON, Canada

Objectives: The physiological impact of severely impaired cerebral autoregulatory vascular reactivity on gray matter integrity is unknown. We hypothesized that cortical gray matter supplied by a defective vascular system with exhausted dilatory autoregulation reserve will show evidence of cortical atrophy.

Methods: 250 BOLD-MRI cerebrovascular reactivity (CVR) studies were reviewed to identify subjects with severe unilateral impairment in CVR (impaired blood flow response to a vasoactive stimulus such as a change in PetCO2.), vasodilatory reserve (negative CVR) but with normal appearing gray matter on FLAIR. Patients with lacunar infarcts in the white matter were excluded. 17 patients were identified each having a high grade stenosis or occlusion of the ICA or MCA on one side regardless of etiology, secondary to Moyamoya, atherosclerosis, or unknown. CVR studies were performed by applying precision control of imposing acute transient vasodilatory stimulus end-tidal pCO2 CO2 between baseline (40mmHg) and to 50mmHg, (Respiract, TRI, Toronto, Canada) during BOLD MRI acquisition on a GE T HDX MRI system. [1] A D T1-weighted volume (voxel 0.78 x 0.78 x 2.2 mm) was acquired and analyzed for cortical thickness using freesurfer (http://surfer.nmr.mgh.harvard.edu/). CVR and cortical thickness maps were overlapped to determine a ROI encompassing the region of negative impaired CVR. This ROI was mirrored to the normal hemisphere providing a normal versus abnormal hemisphere ROI comparison in each subject. Mean cortical thickness between right and left hemisphere ROIs for each subject was measured and a paired t-test was applied.

Results: The ROI with negative impaired CVR showed thinner cortex (2.23 mm +/- 0.077) than the corresponding contra lateral side (2.42 mm +/- 0.052) ($p = 0.0005$) in 16 of the 17 cases. Mean cortical thickness was 2.23 mm +/- 0.077 on the abnormal side, and 2.42 mm +/- 0.052 on the normal side ($p = 0.0005$). The figure shows the relationship between the spatial extent of abnormal impaired CVR (blue) and the spatial extent of cortical thinning (light blue) in one subject, (decreased extent of light blue in right hemisphere = thinner cortex and increased extent of blue in right hemisphere = negative CVR).

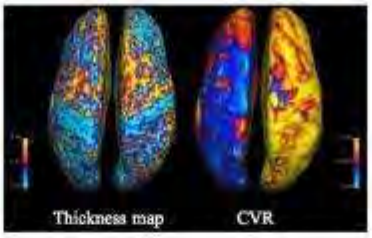

[Figure]

Conclusions: The data indicates that a spatial correspondence exists between exhaustion of autoregulatory capacitiy, vasodilatory capacity and cortical thinning. The findings imply that relate the inability to augment flow in response to metabolic stimuli, (as is also normally seen with neuronal activation), may be deleterious to the health of the preservation of gray matter.

References: 1. Vesely et al. MRM 2001;45:1011-1013.

1028

Brain Oral Session: Blood Brain Barrier

ASSESSMENT OF CEREBRAL BLOOD FLOW AND BLOOD-TO-BRAIN TRANSFER CONSTANT FOR GD-DTPA IN ISCHEMIC BRAIN TISSUE IN DIABETIC AND NORMAL RATS

R. Knight[1], T. Nagaraja[2], K. Keenan[2], J. Xu[2], K. Karki[3], P. Whitton[3], A. Ergul[4]

[1]Neurology NMR Research, Henry Ford Health System Hospital, [2]Anesthesiology, [3]Neurology NMR Research, Henry Ford Hospital, Detroit, MI, [4]Physiology, Medical College of Georgia, Augusta, GA, USA

Introduction: Diabetes increases the risk of cerebrovascular disease four- to six-fold and produces marked remodeling of cerebral vessels.[1] To evaluate the effects of diabetes in stroke, transient focal cerebral ischemia was induced in Wistar and Goto Kakizake (GK) rats by middle cerebral artery occlusion (MCAO). The GK strain is analogous to Wistars, but the animals develop type 2 diabetes spontaneously at 4-6 weeks of age. This study uses magnetic resonance imaging (MRI) measures of cerebral blood flow (CBF) and blood-brain barrier permeability to assess the effects of diabetes on stroke outcome.

Methods: Transient ischemia was induced in male Wistar (n=6) and GK rats (n=7) by intraluminal suture MCAO and reperfusion by withdrawal of the occluding filament after 3 hrs. Blood glucose and glycosylated hemoglobin (A1c) levels were measured in all GK animals, whereas blood glucose was measured in 3 Wistar rats. MRI data included T2-weighted imaging, CBF and BBB permeability assessments and were performed at 7 Tesla. Quantitative assessment of ischemia induced CBF changes was performed at baseline, during ischemia and acute reperfusion and at 24 hrs. BBB permeability changes were assessed at approximately 2 and 24 hrs after reperfusion using Look-Locker based T_1-weighted imaging to generate estimates of the blood-to-brain transfer constant (K_i) for Gd-DTPA via Patlak plot methodology[2]. Ischemia damaged regions of interest (ROIs) were identified by thresholding T2 values, whereas ROIs with BBB opening were indentied based on an F-test statistic. After MRI, the rats were sacrificed and brain tissues stained with 2,3,5-Triphenyltetrazolium chloride (TTC).

Results: Average blood glucose levels for the Wistar and GK groups were 145±12 and 255±12, respectively. A1c values were 5.5±0.4 for the GK group. Average baseline CBF values (Fig 1) in the GK group were significantly lower than in the Wistar group. Ischemic region CBF values for the GK animals decreased significantly during ischemia and then rebounded slightly toward baseline levels during acute reperfusion and at 24 hours. CBF values fell to roughly the same level during ischemia in the Wistar group. Contralateral ROI CBF became significantly elevated compared to baseline levels in the GK group during ischemia and early reperfusion, but not in Wistars. Acute BBB disruption was detected in the preoptic area and/or striatum in all rats by Gd-DTPA enhanced MRI. Measured K_i values were significantly elevated relative to corresponding contralateral brain regions with intact BBB function, but did not differ significantly between Wistar and GK groups. The average size of the BBB damaged ROI, however, was marginally larger in the Wistar group (154±72) than in the GK group (89±84) during acute reperfusion ($p=0.08$) and significantly larger (236±134 vs. 122±96, respectively) at 24 hrs ($p=0.05$). Likewise, the size of the ischemia-damaged region was larger in Wistars than in GK rats as assessed from the TTC stained sections.

Conclusions: The differences noted in CBF and BBB permeability between control and diabetic rats suggest that diabetes may play an important role in influencing outcome in stroke.

References:

1. Harris et al. Diabetes (2005);54:2638-44.

2. Ewing et al. Magn Reson Med (2003);50:283-292.

1029

Brain Poster Session: Cerebral Vascular Regulation

INTERNAL CAROTID ARTERY BLOOD FLOW DURING THE COURSE OF PREGNANCY MEASURED BY ANGLE INDEPENDENT DOPPLER ULTRASOUND

I. Thaler[1,2], O. Nevo[3], J. Soustiel.[4]

[1]Obstetrics & Gynecology, Rambam Medical Center, [2]Faculty of Medicine, Technion Israel Institute of Technology, Haifa, Israel, [3]Obstetrics & Gynecolgy, University of Toronto, Toronto, ON, Canada, [4]Neurosurgery, Technion Israel Institute of TechnologyIsrael Institute of Technoloigy, Haifa, Israel

Objective: Maternal cerebral perfusion pressure increases during the course of pregnancy. However, measurement of cerebral blood flow (CBF) was reported only in a small group of patients in the first trimester, probably due to technical difficulties in measurement of CBF. We aimed to investigate the effect of pregnancy on maternal cerebral blood flow by direct measurement of internal carotid artery blood flow with a new angle independent Doppler ultrasound.

Study design: Seventy women having a low-risk pregnancy at different gestational ages and 10 non-pregnant women participated in the study. Blood flow in the internal carotid artery was measured by a new angle independent Doppler ultrasound (Flowguard, Biosonix, Israel). The device is based on a dual Doppler beam that automatically measure vessel diameter and flow velocity profile. A novel algorithm calculates blood flow. Results were validated using a phantom model and in compared to SPECT measurement of cerebral blood flow.

Results: Internal carotid artery blood flow (mean±SE) increased during pregnancy from 330 ± before pregnancy to 350 ± in the first trimester and 380 ± in the third trimester (p<).

Conclusion: Our results demonstrate that maternal cerebral blood flow is increasing during the course of pregnancy as measured by internal carotid artery blood flow. The cause of maternal CBF increase is probably a result of elevated levels of estrogens and progesterone accompanied by elevated cardiac output.

1032

Brain Poster Session: Neonatal Ischemia

ARTICULATION CHARACTERISTICS OF DEVELOPMENTAL VERBAL APRAXIA

V. Djordjevic[1], **S. Golubovic**[2]

[1]Institute for Experimental Phonetic and Speech Pathology, Belgrade, [2]Speech and Language Pathology, Faculty of Special Education and Rehabilitation, University of Belgrade, Belgrade, Serbia

Introduction: Verbal apraxia or apraxia of speech is impaired ability to execute voluntarily the appropriate movements for articulation of speech in absence of parallysis, weakness, or incoordination of the speech musculature. Errors are inconsistent, involuntary speech is better than voluntary speech, errors include substitution, repetition, simplification, distortion, and addition. The errors increase with complexity and word length.

Method: We researched articulation ability in 15 children with verbal apraxia, 15 with developmental dysphasia and 15 with developmental phonological disorders (age 4 to 5) with Test of Articulatin sounds in Serbian Language.

Results: Analys of results showed us that substitution of sounds have 25,5% of children with dysphasia, 12,8% with verbal apraxia and 10,4% with phonological disorders. Distortion of sounds have 20,4% of children with verbal apraxia, 13, 7% with phonological disorders and 6% with dysphasia. Omision of sounds have 7,7% of children with verbal apraxia 7,3%, with dysphasia and 3,3% with phonological disorders. Children with developmental dysphasia and verbal apraxia must recent have substitution and distortion of affricates, fricatives, laterals, nasals, plosives, and vowels, while children with phonological disorders have more recent substitution of nasals than plosives. The largest frequency articulation of disorders consonant (substitution and distortion) is in children with dysphasia and than with verbal apraxia and phonological disorders. Between children with phonological disorders and dysphasia and verbal apraxia there is no difference in number of omision consonant clusters, distortions CVCV, and CVC.

Conclusion: Affricates and fricatives tend, as classes, to be more often in error than plosives, laterals, nasals, and vowels, although order varies with the position in utterance. Consonant errors are more likely than vowel errors, some children may make no more consonant errors than vowel errors.

1034

BrainPET Poster Session: In Vivo Pharmacology and Clinical Applications

ABNORMAL [11C]ABP688 BINDING IN PATIENTS WITH TEMPORAL LOBE EPILEPSY

E. Kobayashi[1], J. Hall[1], M.-C. Guiot[2], F. Andermann[1], F. Dubeau[1], M. Diksic[3], G. Massarweh[3], J.-P. Soucy[3], **P. Rosa-Neto**[4]

[1]Department of Neurology and Neurosurgery, [2]Department of Pathology, [3]Brain Imaging Center, Montreal Neurological Institute, McGill University, [4]Translational Neuroimaging Laboratory - MCSA, Douglas Hospital, McGill University, Montreal, QC, Canada

Objective: Immunohistochemistry studies suggested overexpression of metabotropic glutamate receptor type 5 (mGLUR5) in the epileptogenic hippocampus of patients with mesial temporal lobe epilepsy (MTLE). We performed in vivo mGUR5 binding studies using [11C]ABP688, a recently developed Positron Emission Tomography (PET) radioligand which binds specifically to mGUR5 as a potential clinical tool for identification of the seizure focus in a group of patients with unilateral MTLE.

Design/methods: We studied 9 patients (3 M, 6 F, mean age =39yo, range, 22 to 67) with unilateral MTLE (5 left, 4 right). Six patients had MRI evidence of hippocampal atrophy. PET images were obtained in a Siemens HR+ scanner following a venous injection of 10 mCi of [11C]ABP688 with high specific activity. Parametric images representing binding potentials (BPND) were generated using the cerebellum as reference tissue. BPND parametric images were co-registered using the MRI and subsequently non-linearly resampled to a standard stereotaxic space. We used voxel-by-voxel statistical parametric analysis: BPND differences between patients (right and left MTLE) and controls (7 healthy volunteers, 4 F, mean age=37, range 19-71) were computed. R1 maps were evaluated.

Results: Figure 1 shows a typical [11C]ABP688 binding study in MTLE patient.

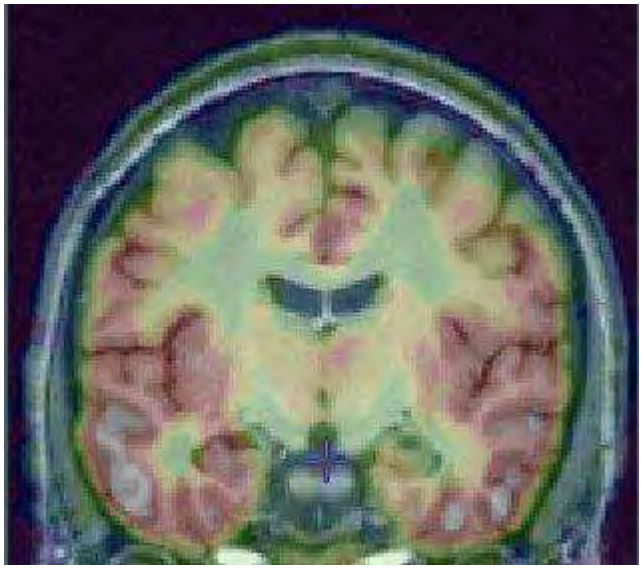

[Figure 1]

[11C]ABP688 BPND was reduced in the epileptogenic hippocampus for left and right MTLE patients (maximum t=4.74 for left and t=8.37 for right) as compared to controls. No differences in the contralateral hippocampus were seen. Finally, there was no significant differences on R1 maps.

Conclusions/relevance: Our finding of reduced mGLUR5 binding in the epileptogenic hippocampus

contrast with previous demonstration of hippocampal mGLUR5 upregulation. The discrepancy between our in vivo receptor binding study and the post mortem immunohistochemistry might be explained by abnormalities on mGLUR5 structure and function. It remains to be elucidated whether this is a cause or consequence of the seizures, but we were able to demonstrate that mGLUR5 binding studies can have clinical application in the identification of the abnormal hippocampus in MTLE patients.

Study supported by: Savoy Foundation for Epilepsy and the American Epilepsy Society Early Career Physician Scientist Award.

1035

BrainPET Poster Session: Radiotracers and Quantification

METABOLIC CHARACTERIZATION OF ^{18}F-FEOBV, AN ACETYLCHOLINE VESICULAR TRANSPORTER LIGAND, IN THE RODENT

J.-P. Soucy[1], É. Landry St-Pierre[1], M.-A. Bédard[2], P. Rosa[1], A. Aliaga[1], G. Massarweh[1]

[1]McConnell Brain Imaging Centre, Montreal Neurological Institute, McGill University,
[2]Neuropsychology, Université du Québec à Montréal, Montreal, QC, Canada

^{18}F]-Fluoroethoxy-benzovesamicol (^{18}F-FEOBV) is a high speicificity positron emitting ligand of the acetylcholine (ACh) vesicular transporter, which shows reversible binding kinetics. It holds promise as a potential ACh system pre-synaptic marker which could be useful for early detection of neurodegenerative diseases where ACh neurotransmission is altered such as Alzheimer's, Parkinson´s disease or Progressive Supranuclear Paralysis. In order to prepare for its use it in humans, characterizarion of its kinetics and metabolic fate in animals is necessary.

We therefore set up 2 experiments to perform this initial evaluation. In the first one, seven male Sprague-Dawley rats (anaesthetized with isofluorane 2%) were placed in a CTI Concorde R4 microPET scanner. Physiological parameters (respiration rate, EKG and temperature) were recorded throughout the imaging sessions. They received an i.v. dose of 4.3 to 16.7 MBq of high specific activity ^{18}F-FEOBV. Emission scans were obtained for 60 min. Images were co-registered to a rat brain anatomical (MRI) template. In the second study, five male Sprague-Dawley rats received an average i.v. dose of 37 MBq of high specific activity ^{18}F-FEOBV and were then sacrificed at 5, 7, 10, 24 and 70 minutes. Blood was drained and centrifuged and plasma was analyzed for metabolites using reverse-phase HPLC.

Physiological parameters remained constant during the imaging experiment. Rats manifested no overt acute nor subacute (days) signs of toxicity . Distribution of the tracer was found to be as expected from the literature on ACh systems anatomy. There was a fast washout of radioactivity from the cerebellum. On parametric images, the highest binding potentials were detected in the caudate, amygdala, hippocampus and basal forebrain. In the second study, blood analysis showed the presence of a single,hydrophilic, metabolite. The parent compound had a mean retention time of 120 seconds with the HPLC set-up we used, whih required extensive fine-tuning do define optimal conditions. Importantly, no lipophilic metabolite was found. Although no physiologic monitoring was done, rats showed no overt sign of physiological distress until sacrifice (up to 70 minutes), except for one animal who received a significantly higher mass of the compound.

These results show that ^{18}F-FEOBV is a promising ligand for imaging the innervations density of the cholinergic system, a potentially important parameter in neurodegenerative diseases assessment, which could lead to earlier detection of disease. In the current (and other) experiments, ^{18}F-FEOBV induced no overt toxicity, an encouraging result in terms of its potential clinical and research application in humans. Its metabolism is fairly rapid but as only a hydrophilic metabolite was found, modeling tracer uptake should be straightforward; moreover, the absence of significant uptake in the cerebellum should allow for a non-invasive, Simplified Reference Tissue Analysis type of approach to be used. We are now going through more advanced toxicology testing and are working on optimisation of the tracer imaging and quantification protocol. We will also assess its defluorination in primates before proceeding to human imaging.

1036

BrainPET Poster Session: Brain Imaging: Stroke

BRAIN TISSUE SURVIVAL PROBABILITY IS A FUNCTION OF EARLY MTT AND SUBSEQUENT EVOLUTION

H. An[1], A.L. Ford[2], K.D. Vo[2], A.M. Nassief[2], C.P. Derdeyn[2], W.J. Powers[1], J.-M. Lee[2], W. Lin[1]

[1]University of North Carolina at Chapel Hill, Chapel Hill, NC, [2]Washington University in St. Louis, St. Louis, MO, USA

Objectives: Dynamic susceptibility contrast (DSC) perfusion method is widely used to study acute stroke patients, because it provides assessments of cerebral blood volume (CBV), mean transit time (MTT), and cerebral blood flow (CBF). Quantitative measures of CBV and CBF are difficult to obtain and their values differ between gray and white matter. On the other hand, MTT values in normal brain are quite uniform across the entire brain. Thus, MTT is commonly used to discern regions of ischemia. It has been suggested that MTT overestimates the size of the ischemic lesions, but it is unclear if this overestimation is caused by an inappropriate MTT threshold value. In this study, we aimed to examine brain tissue survival probability using the temporal evolution of MTT at 3hrs and 6hrs after symptom onset.

Methods: Eight acute ischemic stroke patients were studied at three sequential time points: 2.7 ± 0.8 hours (tp1) and 6.2 ± 0.2 hours (tp2) and 1mo (tp3). MTT values were obtained at both tp1 and tp2. In addition, FLAIR images were acquired one month (tp3) to delineate the final infarct. Six patients received intravenous tPA, while the remaining two patients did not due to contraindications. Changes in MTT (ΔMTT = MTT(tp2)-MTT(tp1)) were calculated, and negative values of ΔMTT were considered reperfusion from tp1 and tp2. Conditional probability density function of tissue survival (1-infarction) was computed at given MTT and ΔMTT values. To minimize the effects of variation induced by noise, small isolated volumes (< 2cc) were excluded from this analysis.

Results: Mean MTT in the unaffected hemisphere was 6.2±0.1 seconds. The survival probability for tp1 MTT and tp2 MTT were very similar for MTT shorter than 15 seconds. However, the survival probability was higher at tp1 than at tp2 for MTT values longer than 15 second, and this deviation reached its maximum for values of 20 to 25 seconds (Figure, a). These data suggest that the survival rate is only time dependent for MTT values greater than a certain threshold (15 seconds). Furthermore, very long MTT delays (as long as 25-30 seconds) still had substantial survival probabilities especially at tp1, suggesting these regions may still include both tissue at risk and core. Moreover, brain tissue survival probability was a function of both MTT change as well as initial MTT delay at tp1; shorter initial MTT delays and greater ΔMTT's improvement resulted in higher survival probability (Figure, b). Conversely, worsening MTT at tp2 (positive ΔMTT) decreased the chance of tissue survival.

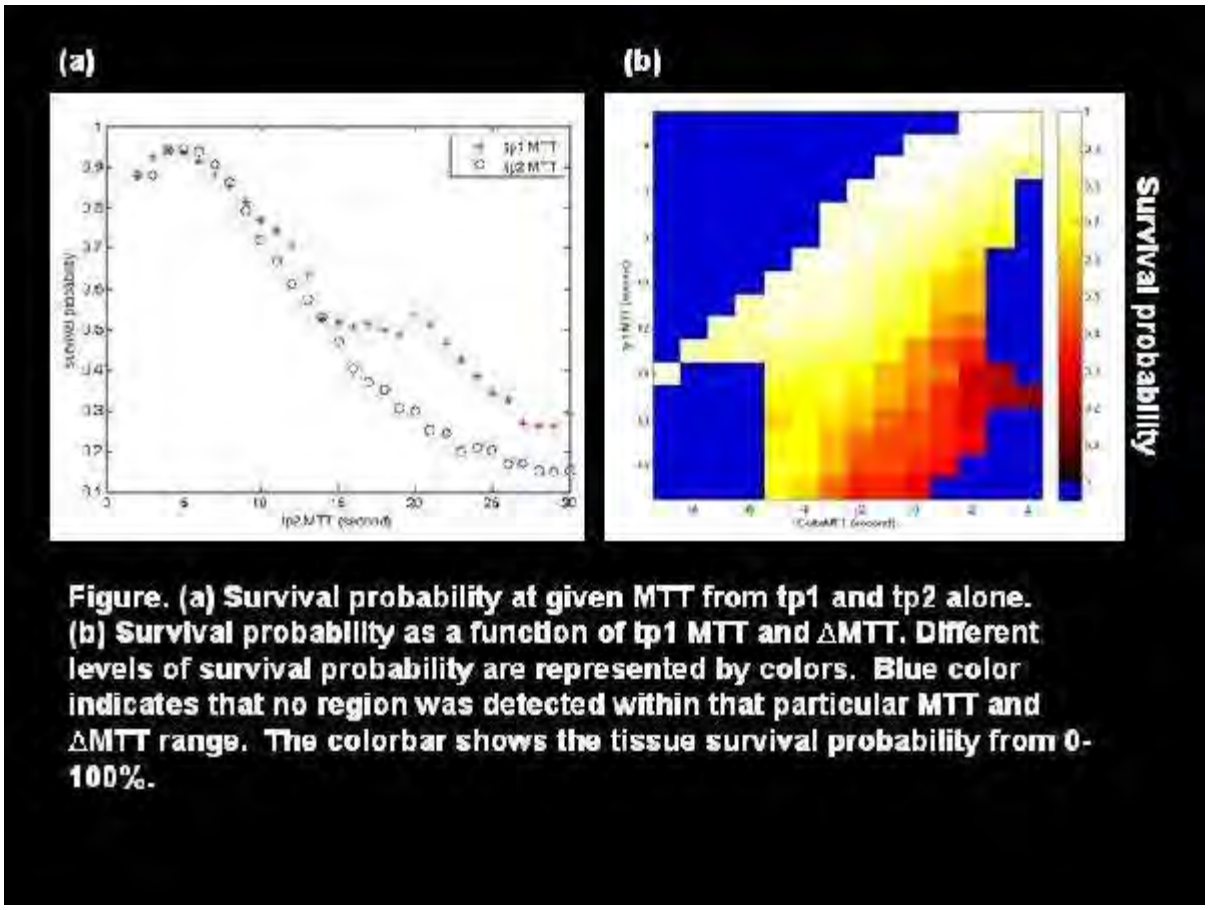

Figure. (a) Survival probability at given MTT from tp1 and tp2 alone. (b) Survival probability as a function of tp1 MTT and ΔMTT. Different levels of survival probability are represented by colors. Blue color indicates that no region was detected within that particular MTT and ΔMTT range. The colorbar shows the tissue survival probability from 0-100%.

[MTTFigure]

Conclusion: Our results suggest that survival of ischemic tissue depends on both initial MTT values and subsequent evolution during the hyperacute phase of stroke. The survival rate was only time dependent for MTT values greater than 15 seconds.

1037

BrainPET Poster Session: PET Acquisition and Processing

HAMNET: A TOOLBOX FOR CONNECTIVITY ANALYSIS FROM NEUROIMAGING DATA

S. Bose[1], R. Wise[2,3], S. Brownsett[2,3], G. Torresan[1], F. Turkheimer[1,3]

[1]PET Methodology, MRC Clinical Sciences Centre, [2]MRC Clinical Sciences Centre, Imperial College, [3]Division of Neuroscience and Mental Health, Imperial College, Hammersmith Hospital, London, UK

Objectives: To present a methodological platform for effective connectivity analysis for positron emission tomography (PET) or functional MRI (fMRI). It works with an input dataset composed from the activation time course of specific brain regions for several subjects under study and gives as outputs the estimation of the connectivity coefficient between the regions, the corresponding p-values, the regression coefficients and the acceptance value of the FDR and the Hochberg tests for the significance level of the connectivity detected.

Methods: Partial correlation has been considered as an effective measure of functional connectivity between a given pair of brain regions by removing the effects caused by other regions (Marrelec, 2008). We combined data from two studies of focal activation in response to the different conditions, which had two identical conditions, the implicit processing of passages of narrative speech and their spectrally-rotated (unintelligible) transformations. The partial correlation values were calculated using a fixed effect model whereas one regional data-point was extracted from each PET [O^{15}]water PET and all scans for all subjects were pooled together in the same data matrix. Individual regional values were normalized to the global brain radioactivity; this was achieved by using the average of brain counts as additional variable in the partial correlation analysis. Partial correlation coefficients were then transformed in normal z-scores using the Fisher z-transform. The ensuing set of p-values was thresholded using the false positive rate correction (0.05 false positive rate) calculated using the adaptive methodology detailed in (Benjamini and Hochberg, 2000) that used an estimator of the number of true null hypothesis presented in (Turkheimer et al., 2001).

Results: The pattern of connectivity indicated that the angular gyrus exerts top-down influence over activity within the part of the language network distributed across left posterior temporal cortex, contrary to other influential models of speech comprehension. In addition, there were also anterior temporal lobe functional connections, incorporating top-down influence from the anterior part of Broca's area in the inferior frontal gyrus; and between a number of mirror regions in the left and right cerebral hemispheres.

Conclusions: This work demonstrates that the partial correlations between pairs of brain regions can be a useful tool for effective connectivity analysis. This allows the effect of other nodes in the network to be subtracted (as well as removing the effect of nuisance factors such as global radioactivity counts), leaving a more accurate approximation of the interaction between pairs of regions.

Availability: The software is available free for academic use upon request.

References:

Benjamini and Hochberg, (2000) J. Educ. Behav. Stat. 25 60-83.

Turkheimer et al., (2001) Neuroimage. 13:920-930.

Fransson P, Marrelec G. (2008) Neuroimage 42(3):1178-84.

1038

Brain Poster Session: Neonatal Ischemia

ABILITY OF SPEECH PRODUCTION AND COMPREHENSION IN CHILDREN WITH DEVELOPMENTAL LANGUAGE DISORDER

L. Zecevic-Filipovic[1], S. Golubovic[2]

[1]Kindergarten Tivat, Tivat, Montenegro, [2]Faculty of Special Education and Rehabilitation, University of Belgrade Education and Rehabilitation, University of Belgrade, Belgrade, Serbia

Objectives: Developmental language disorder (DLD) is defined as a failure of normal language development in a child with normal nonverbal intelligence, no other neurologic or psychiatric disease, and no hearing loss. Children with this form of DLD exibit predominant receptive and expressive impairments of phonology and grammar. Dysphasic children are also characterized by speech production errors including misproduction and omission. As was found for speech perception, dysphasic children are preferentially impaired for producing speech sounds characterized by rapid changes.

Method: Sample of examinees includes 30 children, age of 5,6 years, 15 girls and 15 boys. All of there are tested with Reynell scale of language development, which is standardizes by Croatia and Serbian language of examinees. Test examinees level of ability of understanding speech reception and speeech production. Scale of speech understanding is composite part of test which examine structure, vocabulary and content, and on the basis of summarized points and equivalent age it is calculated deviation related to arithmetic mean. It is expressed in standard deviation and with that method is obtained standard evaluation which is equivalent to language development for certain calendar age.

Result: Result of examined sample of children shows small difference between boys and girls (of same calendar age =5,6) on tasks of Scale of speech understanding. But, it is noticed significantly better understanding in 6 boys and 4 girls, than acquirement on scale of speaking expression, and especially on part related to structure and content of speech, and which examine semantic and syntatic level.

Conclusion: Developmental expressive language disorder with impaired ability to express oneself and difficulty with vocabulary, complex sentences and recall of words. In severe cases DLD may persist until school-age, and the majority of affected children will develop additional learning disabilities or reading deficits.

1040

Brain Poster Session: Ischemic Preconditioning

PRECONDITIONING WITH OZONE/OXYGEN MIXTURE PRESENTED IMPROVED HISTOPATHOLOGICAL PROTECTION COMPARED TO HYPERBARIC OXYGEN TREATMENT IN A RAT GLOBAL CEREBRAL ISCHEMIA MODEL

S. Oter[1], E. Oztas[2], M. Seyrek[3], B. Uysal[1], B. Duz[4], M. Kaplan[4,5], A. Korkmaz[1], R. Ogur[6], S. Kahraman[4]

[1]Physiology, [2]Histology & Embryology, [3]Pharmacology, [4]Neurosurgery, Gulhane Military Medical Academy, Ankara, [5]Neurosurgery, Firat University, Medical School, Elazig, [6]Public Health, Gulhane Military Medical Academy, Ankara, Turkey

Objective: Hyperbaric oxygen (HBO) therapy is an accepted treatment alternative for preconditioning in both focal [1] and global [2] cerebral ischemia. Medical ozone therapy, a new therapeutic approach, has been reported similar molecular mechanisms to HBO in ischemic conditions [3]. One mechanism of the protective effects of HBO against central nervous system ischemia was explained with heme oxygenase-1 (HO-1) induction [4]. Interestingly, HO-1 is also known to play role in ozone/oxygen applications [3] and seems to be an intersection point among these two treatment modalities [5]. In the present study we compared HBO and ozone/oxygen pretreatments in the 2-VO rat model [6].

Methods: Sprague-Dawley rats were divided into 4 groups: control, global ischemia, HBO and ozone/oxygen. HBO was administered one time a day at 2,5 atmosphere / 1,5 hour sessions. Daily intraperitoneally ozone/oxygen (5%/95%) injections at a dose estimated to supply 0.7 mg/kg-BW of ozone. Twentyfour hours after the third applications of HBO or ozone/oxygen, global cerebral ischemia (GI) was induced via bilateral carotid artery occlusion for 10 min. Prior to sacrificing, the neurological deficit was evaluated by a blinded expert usind the Garcia score [7]. The rats were then sacrificed 24 h following GI induction and their brains were taken for for histopathological evaluation, namely Nissl and Tunel staining, and determination of HO-1 mRNA expression.

Results: Functional evaluation according to Garcia's method resulted with comparable scores; only a slight but insignificant improvement was observed. HO-1 was found to be depressed in GI group, whereas both HBO and ozone/oxygen treatments induced increased transcripton of HO-1 mRNA with nearly the same rates.

In the Nissl-stained slices, neuronal tissue loss was apparent in the hippocampal and cortical regions of GI animals. Pretreatment with HBO was able to reduce this injury, whereas in ozone/oxygen treated animals more protection was observed. Strong TUNEL-positive staining appeared in the hippocampus and cortex after GI. Both HBO and ozone/oxygen pretreatment reduced TUNEL-positive staining in neuronal tissue, of which ozone/oxygen mixture was significantly more effective.

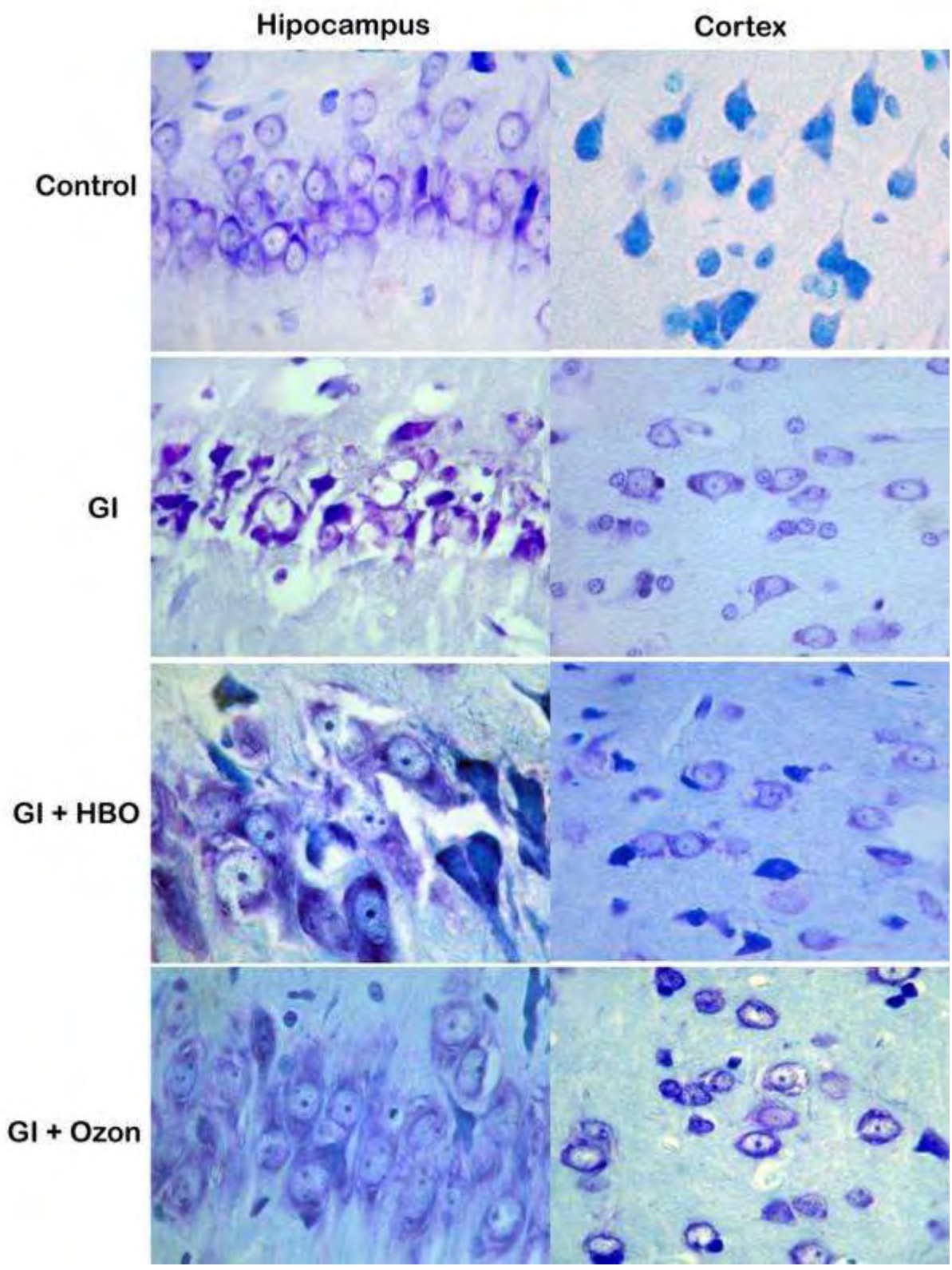

[Representative photos of Nissl-stained slices]

Conclusion: The present findings suggest that pretreatment with ozone/oxygen mixture, at least from the histopathological viewpoint, may exert more satisfying outcome than HBO. Therefore, this new

treatment modality have to be taken into consideration and further detailed studies have to be performed on this area.

References:

[1] Gu et al. J Appl Physiol 2008;104:1185.

[2] Ostrowski et al. Neurobiol Dis 2008;29:1.

[3] Bocci VA. Arch Med Res 2006;37:425.

[4] Li al. Life Sci 2007;80:1087.

[5] Oter & Korkmaz. Arch Med Res 2006;37:917.

[6] Clark et al. Can J Physiol Pharmacol 2007;85:1263.

[7] Beynon et al. Neurosci Lett 2007;425:141.

Grant: This study was supported by the Gulhane Military Medical Academy Research and Progress Center with the grant Nr.AR-2003/56.

1041

Brain Poster Session: Subarachnoid Hemorrhage

CORRELATION BETWEEN RCBF REDUCTION OBTAINED BY 3D-SSP AND NEUROPSYCHOLOGICAL IMPAIRMENT ON THE PATIENTS OF SUBARACHNOID HEMORRHAGE TREATED BY COIL EMBOLIZATION

H. Yatsushige, Y. Takasato, H. Masaoka, T. Hayakawa, N. Otani, Y. Yoshino, T. Momose, C. Aoyagi, G. Suzuki

Neurosurgery, National Hospital Organization Disaster Medical Center, Tokyo, Japan

Objectives: Patients treated ruptured intracranial aneurysms often suffer from neuropsychological deficits in spite of a good neurological outcome. This study focuses on relates the neuropsychological test results to regional cerebral blood flow (rCBF) on 3D stereotactic surface projections (3D-SSP).

Methods: N-isopropyl-p-(123) I iodoamphetamine single photon emission computed tomography (IMP-SPECT) and neuropsychological examinations was performed in 16 patients with subarachnoid hemorrhage (SAH) treated by coil embolization (average age: 50 years old and average post-SAH days: 51). Z-score maps of IMP-SPECT images of a patient were obtained by comparison with data obtained from control subjects. The neuropsychological tests included the Wechsler Adult Intelligence Scale-Revised (WAIS-R) and Wisconsin Card Sorting Test (Keio version: KWCST).

Results: The mean of full scale Intelligence Quotient (IQ), performance IQ (PIQ), and verbal IQ (VIQ) of WAIS-R were 97.8, 90.7, and 96.9, respectively. Number of Categories Achieved (CA) of KWCST was poor in the 66% of patients. On statistical Z-score maps, the half of patients was significantly lower rCBF in cingulate gyrus, orbital gyrus, rectal gyrus, and uncus. A correlation was observed between the VIQ score and rCBF in left superior frontal gyrus and left medial frontal gyrus. The PIQ score was correlated with rCBF in right middle frontal gyrus. No correlation was showed between CA of KWCST and rCBF.

Conclusions: Previous study showed that surgical intervention significantly decreased mean rCBF in the operated frontal lobe compared with the unoperated side. However, even if all patients were treated with coil intervention in this study, rCBF in particular area was significant lower than control subjects. Therefore, these findings indicated that primary damage of SAH may result in the decrease of rCBF. Moreover, rCBF on 3D-SSP might be useful for prognosis of the neuropsychological impairment.

1042

Brain Poster Session: Blood-Brain Barrier

EVALUATION OF BLOOD-BRAIN BARRIER PERMEABILITIES OF CLINICAL PET TRACERS USING IN VITRO MODEL OF HUMAN ADULT BLOOD-BRAIN BARRIER

A. Mabondzo[1], M. Bottlaender[2], J.R. Deverre[2]

[1]Insitut de Biologie et de Technologie de Scalay, CEA/Service de Pharmacologie et d'Immunoanalyse, Gif sur Yvette, [2]I2BM, CEA, Orsay, France

Background and objectives: The development of drugs targeting the central nervous system (CNS) requires precise knowledge of their brain penetration and, ideally, this information should be obtained as early as possible. The physical transport and metabolic blood-brain barrier (BBB) is highly complex and numerous in vitro models have been designed to study kinetic parameters in the CNS. In vitro BBB models must be carefully assessed for their capacity to reflect accurately the passage of drugs into the CNS in vivo. In this study, we report for the first time the evaluation of BBB permeabilities of compounds studied in human subjects by PET and using the in vitro human BBB model, in order to reassess the predictive power of the in vitro system.

Materials and methods: Six clinical PET tracer with different molecular size ranges and degree BBB passage were used (2 of them [^{18}F]-FDOPA and [^{18}F]-FDG are ligand of amino acid and glucose transporters, respectively). The k1 and k2 in human brain of those 6 tracers were available. The human BBB model was a coculture of primary human BECs and astrocytes as previously described (Mégard, 2002; Josserand et al., 2006). Before drug permeation screening, the integrity of the in vitro system was evaluated.

Results: Our findings indicate that the in vitro co-culture model of human BBB has important features of the BBB in vivo (low paracellular permeation, well developed tight junctions, functional expression of efflux transporters) and is suitable for discriminating between CNS and non-CNS compounds. We evaluated drug permeation into the human brain using PET imaging in parallel to the assessment of drug permeability across the in vitro model of the human BBB. 2-[^{18}F]fluoro-A-85380 and [^{11}C]-raclopride show absent or low cerebral uptake with the distribution volume under 0.6, while [^{11}C]-flumazenil, [^{11}C]-befloxatone, [^{18}F]-FDOPA and [^{18}F]-FDG show a cerebral uptake with the distribution volume above 0.6. The in vitro human BBB model discriminates the compounds in the same way as in vivo human brain PET imaging analysis. We cast new light on the close relationship between in vitro and in vivo pharmacokinetic data (r^2: 0.90, $P < 0.001$).

Discussion and conclusion: Past in vivo-in vitro studies often did not have good correlations for substances with transporters. This is probably because experiments have been performed with too much material in vitro, saturing transporters and so obscurancing that contribution. Using the radioactive labeled probes and the small amounts of compounds, this problem could be avoid. This first double study in human subjects demonstrates a close relationship between the assessment of in vitro human BBB passage and in vivo human brain penetration. These findings which can be extended to peptides, proteins, viruses and with substances with high degrees of protein binding in vivo or other non BBB factors dictating their penetration need to be specifically studies. The in vitro human BBB model offers the possibility of subtle discrimination between different BBB permeabilities and transport mechanisms. This in vitro human BBB model may help to test compounds of pharmaceutical importance for CNS diseases.

1046

BrainPET Poster Session: PET Acquisition and Processing

A COMPARISON OF LINEAR AND NONLINEAR METHODS FOR REGISTRATION OF PET IMAGES

J. Rowley[1], E. Kobayashi[2], J. Hall[2], F. Andermann[2], F. Dubeau[2], M. Diksic[3], G. Massarweh[3], P. Rosa-Neto[4]

[1]Translational Neuroimaging Laboratory, Douglas Hospital-McGill University, [2]Department of Neurology and Neurosurgery, [3]Brain Imaging Center, Montreal Neurological Institute, McGill University, [4]Translational Neuroimaging Laboratory - MCSA, Douglas Hospital, McGill University, Montreal, QC, Canada

Objective: Anatomical differences between healthy and neurologically affected populations may constitute a significant confounding factor when PET images are analyzed using voxel based statistics. Non-linear registration of PET images based on MRI information can potentially minimize the impact of anatomical variability on group analysis of PET data. Here we compare the effect of MRI-based non-linear registration in voxel-based t-statistics maps contrasting [^{11}C]ABP688 binding potential (BP_{ND}) between normal controls (Ctrls) and patients harboring unilateral temporal lobe epilepsy (TLE). MRI examination of TLE patients commonly reveals atrophy of the temporal structures, especially in the hippocampus.

Methods: 10 TLE patients (5 right, 5 left; mean age 34 +-14 std) and 9 Ctrls (mean age 40+-20 std) had a dynamic scan conducted in a ECAT HR+ after injection of 370 MBq of [^{11}C]ABP688 IV followed by a 15 min. transmission scan. Images were reconstructed using filter back projection and subsequently analyzed using the Logan´s reference tissue method with the cerebellum as a reference region. All participants had a T1 weighted 1mm isotropic MRI for coregistration purposes. Individual PET-MRI images were linearly registered using rigid body transformation. The MRIs were then linearly registered to the MNI157 space using 9 parameters. The PET images subsequently underwent a nonlinear registration using a deformation field to warp the image to the best possible fit. Patients with right TLE had their PET flipped in the x-direction prior to registration in order to keep the epilepsy hippocampus in the left side. T-statistics were calculated by comparing the left hemisphere of TLE patients vs. Ctrls with linear and nonlinear registration.

Results: Unilateral abnormalities in the epileptogenic hippocampus of TLE patients could be clearly identified with both linear and nonlinearly-treated images, with significant declines of [^{11}C]ABP688 BP_{ND} (t (linear)=6.6 as compared to t(nonlinear)=5.6). However, nonlinearly registered maps could identify the maximum peak within subiculum-CA1 regions, whereas linearly registered images showed a more homogeneous cluster involving the whole hippocampal head. Hippocampal cluster peaks were 5mm apart and maximum t-value was higher for linearly coregistered maps (6.6 as compared to 5.6). No difference in cluster extent was observed (voxels of $t>3.0$ within the hippocampal clusters: 2906 vs 2896).

Conclusions: In TLE, we were able to show that in a group of patients with structural abnormalities involving small and complex structures such as the hippocampal formation, linear registration might bias the anatomical location of PET information. In the particular case of TLE, receptor binding studies such as [^{11}C]ABP688-PET can provide detailed information that can be later correlated with pathological findings of cell loss and gliosis within specific hippocampal subfields.

References:

Ashburner, J., & Friston, K. J. (1999). Nonlinear Spatial Normalization Using Basis Functions. Human Brain Mapping, 7, 254-266.

Myers, R. (2002). The application of PET-MR image registration in the brain. The British Journal of Radiology, 75, S31-S35.

1048

Brain Oral Session: Experimental Cerebral Ischemia: Neuroinflammation

GENETICALLY-DEFINED MANNOSE-BINDING LECTIN DEFICIENCY IS ASSOCIATED WITH BETTER STROKE OUTCOME IN MICE AND HUMANS

A. Cervera[1], C. Justicia[2], X. Urra[1], S. Amaro[1], M. Gomez-Choco[1], B. Suarez[3], V. Obach[1], I. Perez-de-Puig[2], J. Jensenius[4], A.M. Planas[2], F. Lozano[3], A. Chamorro[1]

[1]Stroke Unit, Hospital Clinic, [2]Department of Brain Ischemia and Neurodegeneration, IIBB-CSIC, IDIBAPS, [3]Immunology Department, Hospital Clinic, Barcelona, Spain, [4]Department of Medical Microbiology and Immunology, University of Aarhus, Aarhus, Denmark

Objectives: Stroke activates humoral and cellular innate immune responses whose contribution to brain injury and/or repair remains incompletely understood. Various innate immune responses, including activation of the complement system,[1,2] are increasingly recognized as players in stroke-induced brain damage. Several lines of evidence support that complement activation in stroke occurred through the non-classical pathways.[3,4] In this translational study, the association of acute stroke outcome with genetically-defined deficiencies of mannose-binding lectin (MBL), a key component of the lectin pathway of complement activation,[5] was investigated in humans and mice.

Methods: Functionally relevant MBL and MASP2 polymorphisms were studied in 135 stroke patients admitted into a clinical trial of antibiotic prophylaxis in non-septic stroke (ESPIAS).[6] Major clinical endpoints were compared with systemic levels of MBL and MASP-2, and with genetic MBL and MASP2 deficiencies. The time-course of white-cell counts, C-reactive protein (CRP), cytokines, C3 and C4 complement proteins, was studied from baseline to day 90. MBL and MASP-2 circulating protein levels were evaluated with ELISA assays. In experimental studies, brain ischemia was induced in mice by intraluminal occlusion of the middle cerebral artery for 2-hours. Adult male MBL-null mice (KO) and corresponding wild type (WT) mice of the same background (C57/Bl6) were used in this study. Infarct volume and the neurological deficit were evaluated at 48h. In a subset of animals the expression of myeloperoxidase in brain tissue was evaluated to assess neutrophil recruitment.

Results: Twenty-four (17.8%) patients had MBL2 genotypes associated with MBL-low levels and presented lower CRP, C3 and C4 concentrations than patients with MBL-sufficient genotypes. Genetic deficiencies correlated very well with low levels of circulating proteins. In logistic regression analyses adjusted for age, gender, stroke severity and clinical subtype, MBL-low genotypes and low levels of circulating protein were associated with good functional outcome. In mice, transient cerebral ischemia was induced in WT and KO mice. Ischemia reduced cerebral blood flow to a similar extent in both types of mice. However, infarct volume was significantly smaller (50%) in MBL-deficient mice (n=10) compared to WT (n=11), and the neurological deficit was minor in KO mice. Also, MBL-deficiency attenuated neutrophil recruitment to the ischemic tissue.

Conclusions: These results underscore the key role of the MBL pathway in post-stroke injury in both human and mouse, and have not only predictive but also therapeutic value, thus supporting interventions aimed to specifically inhibit this ancient pathway of complement activation.

References:

1. Huang et al. (1999) Science 285:595−9.

2. Ducruet et al (2008). J Cereb Blood Flow Metab 28:1048-58.

3. Mocco et al. (2006) Circ Res 99:209-17.

4. De Simoni et al (2004) Am J Pathol 164:1857-63.

5. Walsh et al., (2004) J Immunol 175:541-6.

6. Chamorro et al (2005) Stroke 36:1495-500.

Acknowledgement: Supported by the Spanish Ministry of Education and Science (CICYT) and by the European Community´s Seventh Framework Programme (FP7/2007-201, grant n° 201024, European Stroke Network).

1049

BrainPET Poster Session: Brain Imaging: MRI/fMRI

MRI ESTIMATES OF THE TRANSVASCULAR TRANSFER CONSTANT OF ALBUMIN AGREE WITH THOSE OF QUANTITATIVE AUTORADIOGRAPHY

J. Ewing[1], T. Nagaraja[2], R. Paudyal[1], H. Bagher-Ebadian[1], **R. Knight**[1], S. Panda[1], J. Fenstermacher[2]

[1]Neurology, [2]Anesthesiology, Henry Ford Hospital, Detroit, MI, USA

The apparent forward transfer constant, K_{1a}, for albumin was measured in implanted 9L cerebral tumors in 15 rats, 8 of which had been previously administered dexamethasone to broaden the range of vascular transfer constants present in the tumors[1]. An MRI study using Gd-labeled albumin (Gd-BSA) was followed by terminal quantitative autoradiography (QAR) using radioiodinated serum albumin (RISA). MRI procedures used Look-Locker estimates of T_1 to follow Gd-BSA tissue concentration. QAR and MRI maps of K_{1a} were co-registered, a region of interest (ROI) that included the tumor and its bordering tissue was selected, and the estimates of K_{1a} by two techniques were compared by calculating the correlation coefficient based on either summary data (i.e., mean per animal ROI) or on pixel-by-pixel data using a generalized estimating equation (GEE).

For 15 animals, the two estimates of K_{1a} did not differ ($p = 0.2$), and were significantly correlated ($r = 0.55$, $p=0.04$). A pixel-by-pixel GEE analysis, adjusting for clusters, showed a significant correlation between the two measures ($r=0.56$, $p < 0.0001$), consistent with the summary data.

We conclude that the MRI K_{1a} measure shows utility as a surrogate measure of QAR K_{1a}.

1. Ewing JR, Brown SL, Nagaraja TN, et al. MRI measurement of change in vascular parameters in the 9L rat cerebral tumor after dexamethasone administration. Journal of Magnetic Resonance Imaging 2008;27(6):1430-1438.

1050

Brain Poster Session: Neurovascular Unit in Health & Disease

EFFECTS OF GINKGO BILOBA ON CBF ASSESSED BY QUANTITATIVE MR PERFUSION

D. Lin, M. Dizon, D. Yousem, P. Barker

Radiology, Johns Hopkins University School of Medicine, Baltimore, MD, USA

Objectives: Ginkgo biloba, a frequently used dietary supplement for dementia, peripheral vascular and cerebrovascular insufficiency, is thought to mediate an increased blood flow. The purpose of this study was to determine the effects on regional cerebral blood flow (CBF), using dynamic susceptibility contrast perfusion MRI, in elderly healthy humans before and after 4 weeks of oral intake of Ginkgo supplements.

Methods: 11 healthy men (mean age 61± 10 years) participated in this study. Each subject underwent MRI studies at baseline and at 4 weeks after taking 60 mg Ginkgo biloba capsules twice daily. In one of the 11 subjects, six MRI studies were conducted on different days at baseline prior to Ginkgo administration to evaluate the reproducibility of perfusion measurements. Whole brain perfusion MRI was performed at 1.5T using a gradient echo EPI sequence (TR/TE 2000/60 ms, 30 dynamics) during bolus injection of 0.1 mmol/kg GdDTPA at 5 cc/sec. CBF maps were generated using an arterial input function and singular value decomposition. Regions of interest were drawn from each cerebral hemisphere at the level of the centrum semiovale, as well as the right and left frontal-parietal gray matter and white matter. CBF computed from each region was normalized to that in the cerebellar hemispheres. The effects of Ginkgo were analyzed by comparison of the normalized CBF before and after treatment using a paired t-test.

Results: Perfusion MRI provides reproducible measurements of CBF within the same individual, with a normalized CBF in the right cerebral hemisphere of 1.35 ± 0.14 (10.37% s.d.) and in the left cerebral hemisphere of 1.42 ± 0.14 (9.85% s.d.) For assessment of the effects of Ginkgo on CBF before and after treatment, 9 out of 11 studies were analyzable and shown in Figure. There was no significant difference between the normalized CBF measurements (N=9) before and after treatment in the right hemisphere (P=0.66), left hemisphere (P=0.9), right white matter (P=0.54), left white matter (P=0.14), right gray matter (P=0.57) and left gray matter (P=0.73).

Conclusions: Quantitative determination of CBF can be made by MR perfusion techniques with a good reproducibility within the same individual, therefore may provide a useful means to assess physiological changes in normal subjects and individuals with dementia. Based on this method, no significant difference could be detected in CBF after Ginkgo administration in normal elderly individuals using the study design described here.

References:

1. Ahlemeyer B, Krieglstein J. Neuroprotective effects of ginkgo biloba extract. Cell Mol Life Sci. 2003;60:1779-1792.

2. Santos RF, Galduroz JC, Barbieri A, Castiglioni ML, Ytaya LY, Bueno OF. Cognitive performance, spect, and blood viscosity in elderly non-demented people using ginkgo biloba. Pharmacopsychiatry. 2003;36:127-133.

1051

Brain Poster Session: Neuroprotection

GENOME-WIDE EXPRESSION ANALYSIS OF ISCHEMIC PRECONDITIONING IN ADULT HIPPOCAMPAL ORGANOTYPIC SLICE CULTURES

E. Benardete

Neurosurgery, SUNY Downstate Medical Center, Brooklyn, NY, USA

Objectives: Adult rat hippocampal slice cultures become resistant to ischemic injury by prior exposure to a sublethal ischemic insult. This process, called ischemic preconditioning (IPC), which also occurs in vivo, triggers protective cellular pathways. We sought to characterize the changes in gene expression that occur with IPC. We also sought to determine whether NMDA-receptor blockade with (RS)-3-(2-Carboxypiperazin-4-yl)-propyl-1-phosphonic acid (CPP) would inhibit IPC and change the pattern of gene expression associated with IPC.

Methods: Adult hippocampal slice cultures were obtained as previously described (Hassen et al., 2002). Briefly, hippocampal slices were prepared from P20 - P30 Sprague-Dawley rats. Slices were then cultured on filter inserts for two weeks at 32 C. Slices were then shifted to 37 C for 2-3 days. Slices were exposed to 5 mins. of oxygen-glucose deprivation (OGD) in a specially designed chamber. Total RNA was then isolated from slices at 3, 6, and 12 hours following OGD. Total RNA was also isolated from slices undergoing mock OGD and OGD in the presence of 100 uM CPP. Total RNA was then reverse-transcribed into cRNA and used to probe genome-wide expression arrays, Rat 230 2.0 (Affymetrix, Santa Clara, CA). Raw hybridization data was the processed using robust microarray analysis (RMA) and analyzed using GeneSifter (Geospiza, Inc., Seattle, WA), GeneSpring 7.0 (Agilent, Inc., Santa Clara, CA), and Ingenuity Pathway Analysis (Ingenuity Systems, Inc., Redwood City, CA) software. Changes in individual genes were confirmed using real-time PCR (RT-PCR) with primers from Applied Biosystems Inc. (Foster City, CA).

Results: Genes were identified based on statistically significant changes in gene expression levels relative to controls at 3, 6, and 12 hours post-IPC. Heat maps and hierarchical clustering were used to identify and sort individually regulated genes. These genes were then placed into Gene Ontology (GO) categories and Kyoto Encyclopedia of Genes and Genomes (KEGG) pathways. The mitogen-activated protein kinase (MAPK) pathway, the Toll-like receptor pathway, and apoptosis pathway were statistically significantly regulated across all time points. In addition, at 3 hours post-IPC, the Wnt signaling and at 6 hours post-IPC, the ErbB signaling pathways were identified as significantly regulated. Changes in individual transcripts at 3, 6, and 12 hours were confirmed using RT-PCR. CPP failed to block IPC and did not significantly alter the levels of most transcripts. However, certain genes were markedly down-regulated by NMDA-receptor blockade by CPP, such as prostaglandin-endoperoxide synthase 2 (COX-2).

Conclusions: Endogenous mechanisms of neuroprotection are important targets for therapeutic approaches to stroke and brain injury. Genome-wide expression analysis is a useful technique to identify candidate molecules involved in IPC. These data expand results from other studies that suggest a role for the MAPK, Toll-like receptor, and apoptosis pathways. Further experiments will focus on blocking these pathways in vitro to confirm their roles in IPC and looking at these molecular markers in clinical subjects.

References: Hassen, G.W., Tian, D., Ding, D., Bergold, P.J., 2004. A new model of ischemic preconditioning using young adult hippocampal slice cultures. Brain Res Brain Res Protoc. 13, 135-43.

1053

Brain Poster Session: Cerebral Metabolic Regulation

TRAUMATIC BRAIN INJURY-INDUCED EXPRESSION AND PHOSPHORYLATION OF PYRUVATE DEHYDROGENASE: A MECHANISM OF DYSREGULATED GLUCOSE METABOLISM

G. Xing, M. Ren, W. Watson, J.T. O'Neill, A. Verma

Departments of Psychiatry, Pediatrics and Neurology, Uniformed Services University, Bethesda, MD, USA

Background: Dysregulated brain glucose metabolism and lactate acidosis are metabolic characteristics in people with traumatic brain injury (TBI). The molecular mechanism is poorly understood. Pyruvate dehydrogenase (PDH), the rate-limiting enzyme coupling cytosolic glycolysis to mitochondrial citric acid cycle, plays a critical role in maintaining homeostasis of brain glucose metabolism. PDH activity is maintained by the expression of its E1α1 subunit (PDHE1α1) and inhibited by the phosphorylation of PDHE1α1 (p-PDHE1α1). We hypothesized that PDHE1α1 expression and phosphorylation was altered in rat brain following controlled cortical impact (CCI)-induced TBI.

Objectives: To determine PDHE1α1 mRNA and protein expression and phosphorylated PDHE1α1 (p-PDHE1α1) protein in rat brain homogenates at various time post- traumatic brain injuries induced by controlled cortical impact (CCI).

Methods: CCI was induced in young adult male Sprague-Daley rats (170-200g) with a penetration width of 6 mm, depth of 2.5 mm, and velocity of 4 m/s. Brains were analyzed at 4 hr, 1 d, 3 d and 7 d post TBI with immunohistochemistry, RT-PCR and western blot.

Results: Compared to naïve controls (=100%), PDHE1α1 protein decreased significantly in ipsilateral CCI (62%, $P< 0.05$; 75%, $P< 0.05$; 57%, $P< 0.05$; and 39%, $P< 0.01$) and contralateral CCI (77%, 78%, 78% and 36% $P< 0.01$) at 4h, 24h, 3- and 7-day post-CCI, respectively. p-PDHE1α1 protein level decreased significantly in ipsilateral CCI (31%, $P< 0.01$; 102%, $P>0.05$; 64%, $P< 0.05$; and 14%, $P< 0.01$) and contralateral CCI (35%, 74%, $P< 0.05$; 60%, $P< 0.05$; 20% $P< 0.01$) at 4h, 24h, 3- and 7-day post-CCI, respectively. Similar reduction in PDHE1α1 and p-PDHE1α1 protein was found in craniotomy (Sham CCI) group.

Conclusions: Our data showed that TBI-induced reduction in PDHE1α1 expression and phosphorylation could alter PDH activity and thus affect brain glucose metabolism.

1054

Brain Poster Session: Experimental Cerebral Ischemia: Global Ischemia

EFFECTIVENESS OF HYPERBARIC OXYGEN AND MEDICAL OZONE PRETREATMENT AGAINST OXIDATIVE STRESS AFTER GLOBAL CEREBRAL ISCHEMIA IN RATS

S. Oter[1], M. Seyrek[2], S. Sadir[1], B. Duz[3], T. Topal[1], M. Kaplan[3,4], A. Korkmaz[1], S. Kahraman[3], S. Obut[1]

[1]Physiology, [2]Pharmacology, [3]Neurosurgery, Gulhane Military Medical Academy, Ankara, [4]Neurosurgery, Firat University, Medical School, Elazig, Turkey

Objective: Albeit a considerable number of experimental work reporting beneficial effects of hyperbaric oxygen (HBO) therapy in ischemic brain incidents exist, the overall outcome is insufficient to prove its effectiveness in such conditions [1]. More and more studies focus on the preventive side of this therapy modality; therefore, preconditioning experiments are of particular interest. Preconditioning with HBO was shown to exert beneficial effects against ischemic brain injury by upregulation of antioxidant enzymes [2]. A new therapeutic approach, medical ozone therapy, is reported to present similar actions with HBO and upregulation of antioxidant enzymes is one of their common points [3]. The present study tests the efficacy of HBO and medical ozone treatments against oxidative brain injury in a rat global cerebral ischemia model.

Methods: Twenty-eight Sprague-Dawley rats were seperated into sham operated, ischemia-reperfusion, HBO- and ozone-pretreated groups. HBO was exposed as 2.5 atm for 1.5 hours, once daily for a total of 3 sessions. Ozone was administered daily intraperitoneal injections for 3 days; the ozone dosis was set as 0.7 mg/kg-BW/day. Twenty-four hours after the last HBO or ozone treatments, cerebral ischemia was induced for 10 minutes using the 2-VO model [4]. Then the animals were placed in metabolic cages to collect 24 h urine specimens and right after this period they were sacrificed. Their brain cortex and hippocampus tissues were reserved for biochemical assay. Protein carbonyl content, malondialdehyde, superoxide dismutase, glutathione peroxidase and nitrites+nitrates (NO_x) were determined.

Results: Oxidative stress as well as antioxidant function indices resulted with comparable levels; only slight changes occur in the ischemia-reperfusion group, and ozone and HBO treatments presented similar levels. Data collected from NO_x measurements, however, reflected interesting outcome. Cerebral ischemia-reperfusion tended to depress NO_x production; in cortex and urine samples. Both HBO and ozone therapy were able to reverse this effect, of which in ozone-treated animals the values returned near to control levels.

	Sham	Ischemia	HBO	Ozone
Cortex (mg/ml)	93.4 (90.9-102.1)	76.7* (55.5-93.4)	86.4 (72.1-103.1)	102.6** (88.9-136.3)
Hippocampus (mg/ml)	87.7 (73.7-99.4)	96.5 (86.7-102.1)	97.8 (83.3-109.7)	97.1 (94.1-106.1)

Urine (mg/ml)	471 (237-747)	273* (241-323)	351** (335-388)	475** (160-1252)
Urine (mg/24h)	3592 (2373-4484)	1613* (1203-2182)	2077 (1673-2297)	4079** (1440-6447)

[Nitrite-nitrate values (median and range)]

Conclusion: The NO_x results in the present study seem to be valuable for further discussion. It was reported that there are different stages of NO production, therefore decreased and increased levels at diferent time points, during global cerebral ischemia [5]. Another work reported protecting effects of a NO donor against ischemic brain damage [6]. Both HBO [7] and ozone [8] have stimulating effect on NO production. Therefore, this point seems to have particular importance and warrants further research on this matter.

References:

[1] Cerebrovasc Dis 2005;20:417.

[2] Brain Res 2008;1210:223.

[3] Free Radic Res 2003;37:1163.

[4] Can J Physiol Pharmacol 2007;85:1263.

[5] Neurochem Res 2008;33:73.

[6] Neurosci Lett 2007;415:149.

[7] J Neurophysiol 2000;83:2022.

[8] Mediators Inflamm 2000;9:271.

Grant: This study was supported by the Gulhane Military Medical Academy Research and Progress Center with the grant Nr.AR-2003/56.

1055

Brain Poster Session: Migraine

NOVEL OPTICAL IMAGING REVEALS CHANGES IN CEREBRAL BLOOD FLOW AND DEOXY-HEMOGLOBIN IN RESPONSE TO ABNORMAL TRIGEMINAL ACTIVATION

N. Li, K. Murari, A. Rege, P. Miao, X. Jia, N. Thakor

Biomedical Engineering, Johns Hopkins University School of Medicine, Baltimore, MD, USA

Objectives: A strong association between migraine headache and vascular malfunction has been shown in literature. Active cerebral vasodilation is believed to be a major factor in inducing migraine headaches. However the relation is unclear and a thorough study is required to understand the disturbance of cerebrovascular activity. Blood vessel size reflects the local response in vessels, blood flow reflects both local and global responses and oxy- and deoxy-hemoglobin concentration reflects the metabolism response. Using a revised laser speckle imaging system, we obtained the information on both deoxy-hemoglobin concentration and blood flow changes simultaneously using a single laser source. The responses in arterioles and venules were distinguished and analyzed separately.

Methods: In the experiment, peripheral trigeminal nerve fibers of adult female Wistar rats were electrically stimulated. A laser source at 632 nm was used to illuminate the region of interest through a thinned skull preparation. Without using any contrast agents, laser light reflectance images were acquired from the brain of a rat fixed in a stereotactic frame. Responses in deoxy-hemoglobin concentration were obtained by analyzing the reflectance images. Laser speckle contrast images of the same area were obtained by analyzing a stack of raw speckle images. Blood flow responses were also analyzed through the speckle contrast images Arterioles and venules were distinguished using a combination of speckle contrast and white light reflectance images.

Results: Eight animals were studied with similar ROIs in corresponding pairs of arterioles and venules being selected for comparison. The results showed that for each pair, hemodynamic changes were greater in the venules than in the arterioles. The venules showed a 71±6% mean peak increase in the blood velocity, versus a 62±3% mean peak increase in case of arterioles. The two main cortical venules close to the stimulation site showed a remarkable increase in deoxy-hemoglobin concentration, and the pattern of the increase is propagating from distal to proximal point of the venule branch. On the other hand arterioles did not show any such obvious deoxy-hemoglobin concentration increase as venules.

Conclusions: In this study we exploit the high temporal-spatial resolution revised laser speckle imaging. This is the first study to optically characterize responses of both deoxy-hemoglobin concentration and blood flow simultaneously. The instrumentation is very simple, no contrast agents are needed, and no post registration is needed for the two imaging modalities: reflectance image and contrast image. The study of both deoxy-hemoglobin concentration and blood flow simultaneously should provide a deeper understanding of migraine and other neurovascular studies.

References: Li, N., Jia, X., Murari, K., Parlapalli, R., Rege, A., Thakor, N.V., 2008. High spatiotemporal resolution imaging of the neurovascular response to electrical stimulation of rat peripheral trigeminal nerve as revealed by in vivo temporal laser speckle contrast. J Neurosci Methods.

Murari, K., Li, N., Rege, A., Jia, X., All, A., Thakor, N., 2007. Contrast-enhanced imaging of cerebral vasculature with laser speckle. Appl Opt 46, 5340-5346.

1056

Brain Oral Session: Experimental Cerebral Ischemia: Neuroinflammation

BRAIN TRYPTOPHAN METABOLISM USING SMALL ANIMAL PET IN A NEONATAL RABBIT MODEL OF MATERNAL INFLAMMATION INDUCED CEREBRAL PALSY

S. Kannan[1], F. Saadani-Makki[1], H. Dai[1], P. Chakraborthy[2], O. Muzik[1,2], R. Romero[3], D. Chugani[1]

[1]Pediatrics, [2]Radiology, Wayne State University, Detroit, MI, [3]Perinatology Research Branch, NICHD, NIH, DHHS, Bethesda, MD, USA

Objective: Maternal intrauterine infection has been implicated in the activation of microglia and astrocytes in the neonatal brain, that may lead to neuronal and oligodendrocyte death by production of excitotoxic metabolites, resulting in periventricular leukomalacia (PVL) and cerebral palsy. Indoleamine 2,3-dioxygenase, the rate-limiting enzyme in tryptophan metabolism by the kynurenine pathway, is known to be upregulated in activated microglia and astrocytes. Increased tryptophan metabolism by the kynurenine pathway results in the production of excitotoxic metabolites such as quinolinic acid causing seizures and white matter injury. We hypothesized that there is increased tryptophan metabolism in the periventricular regions in our previously established rabbit model of maternal inflammation induced cerebral palsy, as assessed in vivo by the uptake of [^{11}C]methyl-L-tryptophan (AMT) using microPET.

Material and methods: Pregnant New Zealand White rabbits were injected with saline or 20μg/Kg of E. Coli lipopolysaccharide (LPS, endotoxin) along the length of the uterus on day 28/31 of gestation. The kits exposed to endotoxin in utero were born with a phenotype of cerebral palsy. The endotoxin (n=6) and saline exposed kits (n=5) were compared with term newborn kits born to rabbits that had no surgical intervention (n=4). Term newborn kits were injected with ^{11}C-AMT intravenously and scanned for 60 minutes using microPET, followed by MRI scan (4.7T) for anatomical co-registration. 3D regions of interest were drawn for the periventricular region and the whole brain and ratio of tracer uptake at 20-40 mins of the scan was determined. After scanning, the kits were euthanized and brains fixed, sectioned and stained for microglial cells (tomato lectin) and astrocytes (glial fibrillary acidic protein).

Results: There was increased uptake of ^{11}C-AMT in the periventricular regions

Fig. 1 : [^{11}C] AMT uptake in the neonatal rabbit brain

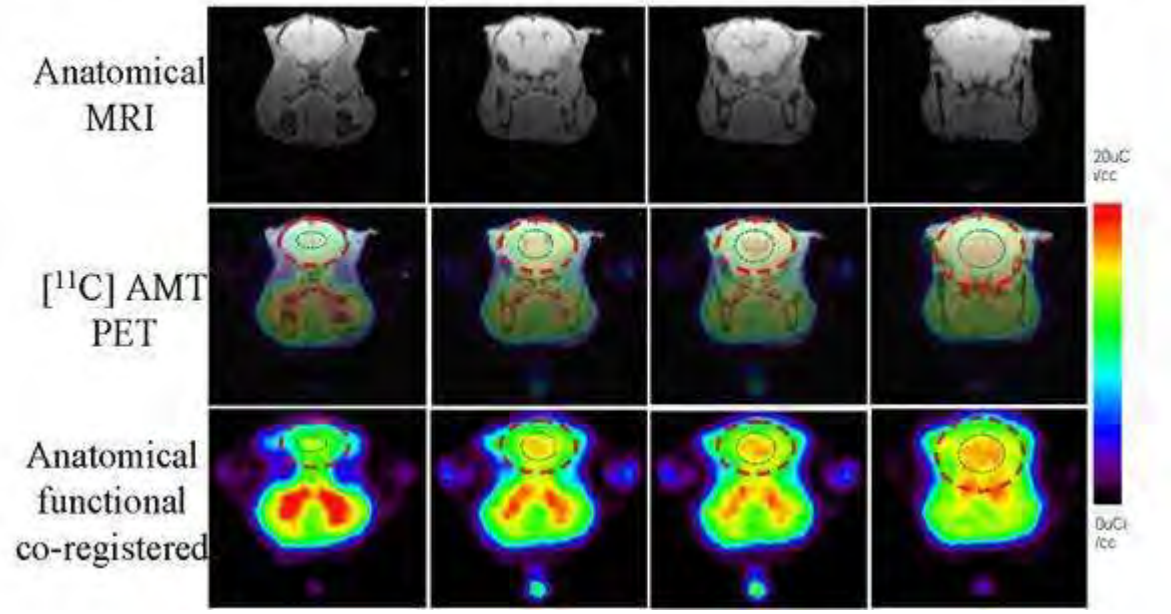

[11C AMT uptake in rabbit brain]

as determined by a significant increase in the ratio of tracer uptake in the periventricular region compared to the whole brain, in the endotoxin kits (mean ratio±SD was 1.46± 0.23) when compared to the saline controls (1.11±0.04) ($p< 0.001$) and the no-intervention control kits (1.02±0.10) ($p< 0.001$). Activated microglia and astrocytes as indicated by an increase in density and change in morphology of these cells were noted in periventricular regions and hippocampus of the brain kits exposed to intrauterine inflammation.

Conclusion: Increased tryptophan metabolism is noted in the periventricular regions of newborn kits exposed to maternal inflammation in utero when compared to age matched controls. This increase in tryptophan that is confined to the periventricular regions may be due to the increased presence of activated microglia and astrocytes in these regions. Tryptophan metabolism by the kynurenine pathway may be responsible for production of excitotoxic injury leading to seizures and motor deficits in neonates born to mothers with intrauterine infections.

References: IDO expression in the brain: a double-edged sword. Kwidzinski E, Bechmann I.J Mol Med. 2007;85(12):1351-9.

1057

Brain Poster Session: Mitochondria

IMPAIRED MITOCHONDRIAL ENERGY METABOLISM AND NEURONAL APOPTOTIC CELL DEATH AFTER CHRONIC ALUMINUM EXPOSURE IN RAT BRAIN

P. Khanna, **B. Nehru**

Biophysics Dept, Panjab University, Chandigarh, India

The present study elucidates a possible mechanism by which chronic aluminum exposure (100mg/kg b.wt. p.o. for 8 weeks daily) causes neuronal degeneration. Mitochondria, the primary site of cellular energy generation and oxygen consumption might **represent a** likely target for aluminum toxicity. Therefore, the objective of the current study was **to investigate the** effect of chronic aluminum exposure on mitochondrial energy metabolism, oxidative stress generation and its implication in the induction of neuronal apoptosis in rat model. Mitochondrial fractions were isolated from cerebral cortex, mid brain and cerebellar region of rat brain and the complexes were estimated biochemicaly in the same fractions. Our results indicated significant decrease in the activity of complex I, II and IV in all the three regions, though the changes were more pronounced in mid brain region. The MTT assay which indirectly shows the activity of complex III did not register any significant change except for mid brain. Mitochondria generate ROS that are thought to augment intracellular oxidative stress. The alterations in the mitochondrial electron transfer enzyme activities in **turn might have caused an increase in** malondialdehyde which is observed in all the three regions. Further the decreased levels of GSH and also decreased MnSOD activity in the mitochondrial fraction of rat brain enhanced oxidative stress. Thus, chronic aluminum exposure increases the oxidative stress both by mitochondrial damage as well as due to the failure in the ROS removal system which in turn causes oligonucleosomal DNA fragmentation and formation of comet, a hallmark of apoptosis. The present study provides an evidence of impaired mitochondrial bioenergetics and apoptotic neuronal degeneration after chronic exposure of aluminum.

1059

BrainPET Poster Session: Brain Imaging: Stroke

EVALUATION OF AUTOMATED-PARTIAL-VOLUME-CORRECTION SOFTWARE (PVEOUT) BY MEANS OF UN-BIASED RANDOM SAMPLING-BASED VOLUMETRIC ASSESSMENT FOR TWO SETS OF CLINICAL MRI DATA

A. Yamamoto[1,2], C. Svarer[3], K. Ishida[1], C. Yokota[4], Y. Tomii[4], M. Yamauchi[1], K. Iihara[5], S. Miyamoto[5], K. Minematsu[4], H. Iida[1,2,3]

[1]Dept Investigative Radiology, National Cardiovascular Center Research Institute, [2]Dept Medical Physics and Engineering, Graduate School of Medicine, Osaka University, Osaka, Japan, [3]Neurobiology Research Unit, Copenhagen University Hospital, Copenhagen, Denmark, [4]Cerebrovascular Division, Department of Medicine, [5]Neurosurgery Division, Department of Medicine, National Cardiovascular Center, Osaka, Japan

Introduction: Partial-volume-effect (PVE) is an essential source of errors, which degrades the accuracy in quantitative assessment of bio-physiologic functional parameters in PET and SPECT. A novel software, PVElab (running with SPM5), has been developed to automatically correct for PVE using clinical MRI images [1, 2]. The program is based on automatic registration of MRI to PET/SPECT, followed by automatic segmentation (SPM5) [3] and correction of PET/SPECT counts for fractional volume as determined from the segmentation. This study was intended to evaluate the accuracy and inter-subject consistency of this automatic segmentation procedure in two typical sets of clinical MRI.

Materials and methods: One data set was obtained from a 1.5-T MRI scanner (Siemens) performed on 13 clinical patients with lacunar infarction in white matter areas. The acquisition sequence was a spin-echo, with TR 630 msec, and TE 14 msec. Another was from a 3-T MRI scanner (GE) with 3D T_1 sequence on 8 healthy volunteers (1 male, and 7 female) whose age ranging from 20 to 35 year old. The acquisition sequence was a fast-spoiled-gradient-echo prepared with inversion-recovery (IR-FSPGR, TR/TE = 8.6/1.8 msec, FA 8°, TI 600 msec). Eight regions-of-interest (ROI) were delineated using the individual MR images for each subject, and grey-matter (GM) volume was obtained using PVElab. The un-biased random-sampling (RS) [4, 5] was also applied to obtain the GM volume as a reference. A sophisticated software program was developed for this purpose, with which the operator define points that hits the structure of interest within the ROI defined for PVElab. GM volume values were compared for each ROIs, and intra-subject and inter-subject consistency of GM volumes were evaluated by PVElab and RS.

Results and discussion: PVElab (SPM5) and RS provided GM volumes which were significantly correlated to each other in each subject for both 1.5-T and 3-T data sets. The averaged difference for all subjects was 0.93 ± 3.18% for 1.5-T and 1.17 ± 6.35% for 3-T, in which the subject-dependent variation was attributed to the fact that the MRI intensity varies, dependent on subject. The reason for greater variation with 3-T MRI is probably due to the fact that 3-T MRI is more sensitive to error sources. The variation of differences for ROIs within each subject was in most of cases 1-2%. However, large variations were observed in two cases for 1.5-T and in one case for 3-T MRI. The Exact reason for this is unknown, but probably both MRI acquisition and segmentation algorithm are responsible to this.

Conclusion: The automatic segmentation tool in PVElab for PVE correction is feasible for clinical use. The inter-subject consistency and intra-subject variations are reasonably small, but further studies and careful evaluation are still needed.

References:

1. Svarer C., et al. NeuroImage.2005;24:969-79.

2. Quarantelli M., et al. J.Nucl.Med.2004;45:192-201.

3. Ashburner J, Friston KJ. NeuroImage.2005;26:839-51.

4. Pakkenberg B., et al. Neuroradiology.1989;31:413-7.

5. Iida H., et al. JCBFM.2000;20:1237-51.

1063

BrainPET Poster Session: Brain Imaging: MRI/fMRI

VOLUMETRIC ASSESSMENT FOR MORPHOLOGICAL STRUCTURES OF MOUSE BRAIN LATERAL VENTRICLE USING ANATOMICAL MRI IMAGES BASED ON A RANDOM-SAMPLING THEOREM

A. Yamamoto[1,2], K. Koshino[1], Y. Hirano[1], C. Shen[3], Y. Niwa[3], N. Iwai[3], H. Sato[1], H. Fujiwara[2], H. Iida[1,2,4]

[1]Dept Investigative Radiology, National Cardiovascular Center Research Institute, [2]Dept Medical Physics and Engineering, Graduate School of Medicine, Osaka University, [3]Dept Epidemiology, National Cardiovascular Center Research Institute, Osaka, Japan, [4]Neurobiology Research Unit, Copenhagen University Hospital, Copenhagen, Denmark

Introduction: "Random Sampling" (RS)-based grid-point counting is an un-biased statistical procedure for assessing volumes for given structures [1]. A sophisticated program has been developed to assess volumes from tomographic images of MRI/PET with careful counting of randomly-generated grids those hit the volume-of-interest. Particle grids are generated randomly with arbitrary shift and/or rotation parameters, and observers are asked to highlight those grids on computer-screen, with careful judge for each point, based on anatomical/pathophysiological knowledge. This study was intended to evaluate the adequacy and usefulness of this program by applying to both numerical and physical phantoms. Applicability of this technique to anatomical/pathophysiological assessment on small animals has also been tested.

Materials and methods: The program is written in JAVA and can be applied to mutiple tomographic images which have been registered prior to the analysis. Grids are generated and overlaid to tomographic images, and the number of points hitting the structure-of-interest is counted. Volume assessment for multiple slice data is made by multiplying the area estimated from the number of grids at each slice by thickness of slice.

To test the statistical characteristics of RS approach, a simulation study was carried out, by assuming simple numerical phantoms of known volumes. Accuracy of the estimated volume was evaluated as a function of the number of grids hitting the structure.

The same evaluation was made for a small physical phantom of 436 microL obtained using a clinical MRI (GE, Signa HD) scanner with a small-animal dedicated coil. [2]. T_1W images (156×156×300μm) were obtained with 3D fast-spoiled-gradient-echo (FSPGR) sequence (TR/TE=16/3.4msec, FA30°)[3]. Agreement of estimated volume and the statistical uncertainty of RS approach were evaluated.

Study was also carried out on 9 normal mice (weight; 18-32g, age; 3.7±1.2 months) and a transgenic (TG) mouse (2-months old male) of ventricular distension.

MRI images were obtained using the same scanner, with visualizing images at constant signal intensity.

Results and discussion: Both numerical and physical phantom studies resulted in the volume estimates which agreed with the true value within errors < 5%, when the number of grids hitting the structure was >20 points in a slice. The normal animal study demonstrated the CSF volume 3.6+/-1.2 $\mu\ell$ in lateral ventricle (LV). This variation was attributed to the individual differences rather than the statistical errors. The TG mouse showed CSF volume of 24.6+/-1.2 $\mu\ell$ in LV, in which the variation was beyond the range of statistical variation of RS.

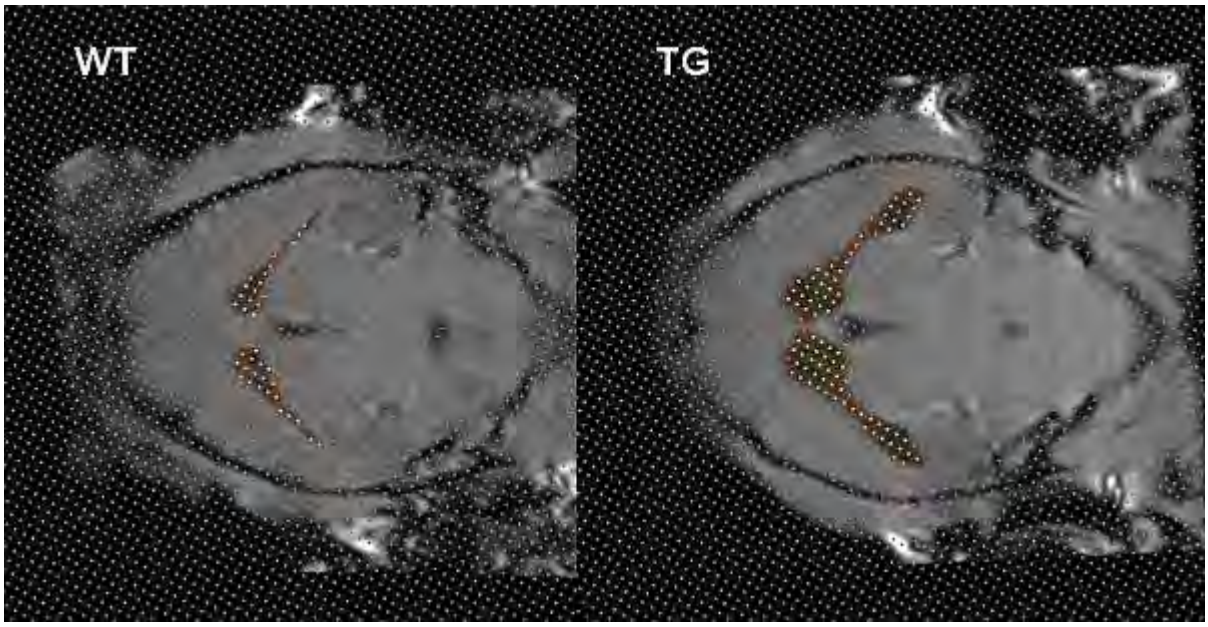

[RSinMiceBrainLV]

Conclusions: RS provides un-biased, expert knowledge-based assessment of volumetry in PET/MRI images. The practical procedures are minimal, and thus can be applied to a number of pathophysiological studies.

References:

1. Iida H., et al. JCBFM.2000;20:1237-51.

2. Yamamoto A., et al. Radiol Phys Technol. 2009;2:13-21.

3. Natt O., et al. J Neurosci Methods. 2002;120:203-09.

1065

Brain Poster Session: Brain Imaging: Neurologic Disease

CORRELATION OF COGNITIVE DEFICITS, ICP, AND CBF IN HYDROCEPHALUS USING NONINVASIVE MRI BASED MEASUREMENT (MR-ICP)

N. Alperin[1], R. Glick[2], S. Lee[1], T. Lichtor[3]

[1]Radiology, UIC, [2]Neurosurgery, Mount Sinai Hospital Hospital, Rush University, UIC, [3]Neurosurgery, Rush University Medical Center, Chicago, IL, USA

Objective: We previously reported the clinical utility of a noninvasive MRI-based measurement of intracranial pressure (MR-ICP) in hydrocephalic patients. We found that MR-ICP has a strong negative predictive i.e. patients with normal MR-ICP did not require surgical intervention. We now investigated this large group of hydrocephalic patients to determine if MR-ICP and tCBF, measured non-invasively, correlates with cognitive dysfunction.

Methods: 36 hydrocephalic patients underwent brain MRI study with measurements of CSF and CBF to and from the cranial vault, from which measurements of ICP and tCBF were derived, using a previously described algorithm. In addition, tCBF was normalized for brain volume. Neurologic exam with assessment of cognitive function and/or formal neuropsychological testing, was performed. Patients were divided into 2 groups: mild delay/cognitive deficits, or normal MS, and were compared to normal controls.

Results: MR-ICP values spanned a much wider range than normal controls, although the majority of MR-ICP values were within the normal range. Similarly, tCBF in these patients did not follow the "normal" distribution but spanned a much wider range. 12/36 patients had mental status (MS) changes on neurologic evaluation or neuropsych testing. Overall, tCBF in the hydrocephalic patients, whether they had normal MS or mild deficits, was lower than normal controls. However, when corrected for volume, only the patients with MS changes or cognitive deficits had a significant difference in tCBF versus normal controls. There was no difference in tCBF between the "normal MS" hydrocephalic patients versus normal controls.

Conclusion: MR-ICP and tCBF values in hydrocephalic patients did not follow the "normal" distribution but spanned a much wider range, suggesting possible dysautoregulation. Despite normal ICP and tCBF, many patients exhibited MS changes/ cognitive deficits, which correlated with changes in tCBF, measured noninvasively. We are now attempting to correlate ICP, tCBF, gray versus white matter volumetric changes and cognitive function in these cases.

1066

Brain Poster Session: Neurologic Disease

F-18 FDG PET IN PARKINSON'S SYNDROME PATIENTS WITH URINARY DYSFUNCTION

K.H. Hwang, W. Choe, M.K. Lee

Nucl Med, Gachon Univ. Gil Hosp, Incheon, South Korea

Introduction: Recently, it was reported that a relationship between dopaminergic degeneration and symptoms of urinary dysfunction. We investigated the difference in cerebral metabolism between Parkinson's syndrome (PS) patients with and without urinary dysfunction.

Methods: This study included 7 PS male patients without urinary dysfunction (mean age: 71 yr) and 3 PS patients with urinary dysfunction (mean age: 75 yr) who performed F-18 FDG Brain PET. Using SPM2 (Statistical parametric Mapping 2, Wellcome Department of Cognitive Neurology, London, UK) software, all the images were spatially normalized into the standard template, smoothed with 10 mm FWHM isotropic Gaussian kernel. The count of each voxel was normalized versus the total count for the brain (proportional scaling in SPM) to remove global cerebral metabolic differences between the individuals. Images of PS patients with urinary disturbance were compared with those of PS patients without in a voxel wise manner using SPM2 in group-to-group analysis (uncorrected $p < 0.01$).

Results: Decreased regional cerebral metabolism was demonstrated in bilateral superior cerebellar cortices and Rt parietal cortex in Parkinson's disease patients with urinary dysfunction, compared to those without. These findings are consistent with some study reports (1, 2), suggestive of connection of those areas to pontine micturition center.

Conclusions: Although the number of patients studied is small, these results suggest that urinary dysfunction in patients with Parkinson's disease may be associated with bilateral Cerebellum and Rt Parietal cortex.

References:

1. Zhang H, Reitz A, Kollias S, Summers P, Curt A and Schurch B. An fMRI study of the role of suprapontine brain structures in the voluntary voiding control induced by pelvic floor contraction. NeuroImage 2005;24:174-80.

2. Sakakibara R, Uchida Y, Uchiyama T,Yamanishi T and Hattori T. Reduced cerebellar vermis activation during urinary storage and micturition in multiple system atrophy: Tc-99m-labelled ECD SPECT study. Eur J Neurol 2004;11:705-8.

1068

Brain Poster Session: Oxidative Mechanisms

STRESS INDUCED ANXIOGENESIS AND BRAIN OXIDATIVE INJURY IN RATS: INFLUENCE OF AGE, SEX AND EMOTIONALITY

A. Ray, A. Chakraborty, K. Gulati

Department of Pharmacology, Vallabhbhai Patel Chest Institute, University of Delhi, Delhi, India

In biology and medicine, stress is defined as any external or internal stimulus capable of disrupting the physiological homeostasis and the ability to cope with such aversive inputs are crucial determinants of health and disease. A variety of stressful situations are known to induce complex neurobehavioral changes, the mechanisms of some of which are poorly understood. Anxiety is one such syndrome in which is regulated by the brain and has an impact on various body systems like neuroendocrine, cardiovascular and immune systems. The CNS, in addition to being the seat for interactive neural networking, is also highly susceptible to oxidative injury, and in view of this the present study evaluated the possible role of prooxidant/antioxidant balance in stress induced neurobehavioral and anxiogenic responses in rats. Further, interactions between both ROS and RNS were also evaluated during such stress induced anxiogenic responses. In addition, the role of physiological variables like age, sex and emotionality status was also assessed on stress susceptibility and their relationship with oxidative injury in the brain was studied. Restraint stress (RS), a universally model of behavioral stress, was used as the experimental stressor, and anxiety was measured by the elevated plus maze (EPM) test. Pharmacological modulation of stress induced behavioral responses were assessed and brain homogenates were assayed for oxidative and nitrosative stress markers, for corroborative purposes. Exposure to RS resulted in neurobehavioral suppression in the EPM test which was evidenced by a reduction in the number of open arm entries (OAE) and open arm time (OAT) during a 5 min period, and was indicative of an anxiogenic response. Pretreatment with the conventional anxiolytic, diazepam, attenuated this behavioral suppression, suggesting an anxiolytic response of the drug, which was, however, also accompanied by sedation. On the other hand, pretreatment with antioxidants (ascorbic acid, alpha tocopherol and melatonin) and NO mimetics (L-arginine and isosorbide dinitrate), showed clear-cut antagonizing effects on RS-induced EPM activity suppression. RS induced anxiogenic effects were accompanied by elevations in brain MDA levels and reductions in GSH and NOx activity, all of which were differentially reversed by the antioxidants and NO mimetics. Interestingly, in a parallel set of experiments, it was observed that RS induced anxiogenic responses were greater in:

a. male as compared to female rats, and
b. old as compared to young rats.

Further, “high emotional” rats were more susceptible to RS induced anxiogenic effects, as compared to “low emotional” rats. Concurrent assay of brain homogenates showed that brain oxidative injury was greater in:

a. males than in females,
b. old than in young, and
c. `high emotional` than `low emotional` rats, which were susceptible to reversal by antioxidants and NO mimetics.

These results are suggestive of the involvement of brain oxidative injury and ROS-RNS interactions during stress induced anxiogenic behavior. In addition, it is inferred that age, sex and emotionality status may play a crucial role in deciding the extent of stress induced anxiogenesis and oxidative injury.

1069

Brain Poster Session: Epilepsy

ROLE OF OXIDATIVE AND NITROSATIVE STRESS DURING THEOPHYLLINE INDUCED SEIZURES IN EXPERIMENTAL ANIMALS

K. Gulati, A. Ray, V. Vijayan

Department of Pharmacology, University of Delhi, Vallabhbhai Patel Chest Institute, Delhi, India

Theophylline, a methylxanthine, is a very effective bronchodilator in the treatment of obstructive airway disease. However, its narrow therapeutic index and propensity to induce neuroexcitatory effects are a major concern for this pharmaco-economically viable drug. Seizures can be problem during its use particularly in extremes of age and in epileptics, and identification of therapeutic strategies to counteract such iatrogenic seizures could lead to the development of an effective antidote for theophylline toxicity. Current therapeutic tools utilizing conventional anti-seizure approaches are ineffective in antagonizing such seizures, and thus the present study evaluated some novel mechanisms involved in theophylline induced convulsions in mice. Theophylline is metabolized by the xanthine-xanthine oxidase pathway, which is an important source of free radical generation, and thus the possible involvement of oxidative stress was studied in this phenomenon. Aminophylline (theophylline et ethylene diamine) induced seizures and mortality in mice in a dose related manner, which could not be replicated by phosphodiesterase inhibitors or the cerebral blood flow enhancer, pentoxyfylline. Further, such seizures were not consistently antagonized by conventional anticonvulsants or adenosine agonists. Interestingly, pretreatment with antioxidants (alpha tocopherol, ascorbic acid and melatonin) and the NO synthase inhibitor, L-NAME induced differential degrees of attenuations in aminophylline-induced seizures and mortality. The most potent effects were seen with the combination treatment of melatonin and L-NAME. Such seizures were paralleled by elevations in brain malondialdehyde (MDA), NO metabolites (NOx), and lowered reduced glutathione (GSH) levels, which were reversed by the antioxidant pretreatments. On the other hand, a combination of sub threshold doses of the methylxanthine and the NO precursor, L-arginine, had synergistic seizurogenic effects. Further, sub effective doses of aminophylline when combined with sub threshold intensities of electroshock also induced tonic clonic seizures which were also prevented by pretreatments with antioxidants, NO synthase inhibitors and their combination therapy. Biochemical assay of brain homogenates in these mice also showed elevations in MDA and NOx and reductions in GSH activity, which were normalized by antioxidant treatments. These results indicate that oxidative stress and ROS-RNS interactions may be involved in theophylline induced seizures and mortality, and antioxidants, alone or in combination with NO synthase inhibitors could form useful treatment strategies in such situations. Further, this hypothesis could provide a good nidus for translational research in co morbid situation involving asthma and epilepsy, and also other iatrogenic convulsive states.

1072

Brain Oral Session: Experimental Stroke and Cerebral Ischemia 1

PERLECAN DOMAIN V IMPROVES STROKE OUTCOME

D. Clarke, B. Lee, **G.J. Bix**

Texas A&M College of Medicine, College Station, TX, USA

Stroke is a significant world-wide cause of death and serious long-term disability. However, while advances have been made in acute stroke treatment, our understanding of the mechanisms underlying brain self-repair after stroke remains poor. Therefore, the problem of brain repair and stroke rehabilitation is an emerging research priority, with the underlying goal of identifying and improving brain reparative processes. Brain repair occurs in a close temporal-spatial neurovascular niche of revascularization (angiogenesis) and neuronal repopulation (neurogenesis), processes that both involve extracellular matrix (ECM) remodeling and subsequent generation of ECM fragments.

Objectives: We sought to demonstrate whether one of these ECM fragments, perlecan domain V (DV), could improve functional stroke outcome by stimulating angiogenesis, neurogenesis and neurovascular niche formation. Our objectives were based on previous observations that stroke rapidly generates bioactive fragments of perlecan (1), and perlecan is required for both angiogenesis and neurogenesis (2).

Methods: Rats underwent left middle cerebral artery occlusive stroke, or sham surgery control, via stereotactic injections of endothelin-1 (or PBS vehicle control) (3) followed by intraperitoneal injections of human recombinant DV (0.5 mg/kg) or PBS vehicle control on post-stroke days 1, 3, 5 and 7 (n=5 for each group, experiment repeated 3 times). Functional use of the affected contralateral limb was assessed via the cylinder test (4) and groups were statistically analyzed via ANOVA. Additionally, rat brain tissue was immunohistochemically processed to detect administered DV, as well as to measure post-stroke angiogenesis and neurogenesis. In parallel experiments, the effects of DV on angiogenesis and neurogenesis were studied in vitro with isolated rat brain microvascular endothelial cells, cortical neurons and neurospheres, respectively.

Results: From post-stroke day 3 onward, stroked rats treated with a total of 2 doses or more of DV were indistinguishable ($p=0.3$) from sham surgery controls in the spontaneous use of the contralaterally affected limb, while untreated stroked rats remained significantly impaired throughout testing ($p< 0.005$). Brain immunohistochemistry demonstrated that administered DV specifically homed to the ischemic core and peri-infarct cortex, depositing in a perivascular distribution, and increased both peri-infarct angiogenesis and neurogenesis. Additionally, a significant majority of these newborn neurons ($p< 0.001$) were closely associated with new blood vessels where administered DV deposited. In vitro studies further demonstrated that DV enhanced several aspects of angiogenesis including endothelial cell proliferation, migration and tube formation. Likewise, DV enhanced both neuronal migration and neurosphere formation.

Conclusions: In a stroke animal model, perlecan DV homes to stroked brain tissue and improves functional stroke outcome by enhancing post-stroke angiogenesis and neurogenesis. Our results suggest that DV could be a promising new stroke therapy.

References:

(1) Fukuda S, Fini CA, Mabuchi T, Koziol JA, Eggleston LL, Jr., del Zoppo GJ. Stroke. 35:998-1004, 2004.

(2) Bix G, and Iozzo R. Microsc. Res.Tech. 71:339-48, 2008.

(3) Sharkey J, Richie I, Kelley P. J Cereb Blood Flow Metab. 13:865-71, 1993.

(4) Hicks A, Hewlett K, Windle V, Chernenko G, Ploughman M, Jolkkonen J, Weiss S, Corbett D. Neuroscience. 146:31-40, 2007.

1073

Brain Poster Session: Cerebral Metabolic Regulation

CHARACTERIZATION OF LACTATE DEHYDROGENASE ISOZYMES IN JAPANESE QUAIL BRAIN (COTURNIX COTURNIX JAPONICA)

R.P. Singh[1], K.V.H. Sastry[1], N.K. Pandey[1], N. Shit[1], A. Ahuja[1], D. Radha[1], J. Mohan[1], K.B. Singh[2], R.P. Moudgal[1]

[1]Division of Physiology and Reproduction, Central Avian Research Institute, Izatnagar, Bareilly, [2]Depertment of Animal Science, M .J. P. Rohilkhand University Bareilly, Bareilly, India

Lactate dehydrogenase (LDH, EC 1.1.1.27) is a tetramer with two different types of polypeptide chains (subunits) viz. H and M. It exists in different molecular forms with different electrophoretic mobility. The distribution of different LDH isozymes is mostly tissue specific making them ideal molecular markers for the study of tissue energy metabolism. The LDH present in heart muscle consists of H-Type isozyme whereas in skeletal muscle it is of M-type isozyme. Presence of more than one LDH isozyme has been reported in brain. This distribution has been correlated with local oxygen tensions, pyruvate inhibition and lactate accumulation. Lactate dehydrogenase converts Pyruvate into lactate may use as a substrate in brain. The old hypothesis of brain energy metabolism was that oxidation of glucose is responsible for providing energy to the brain. However, recent research has suggested that lactate may be a major source in cerebral energy metabolism. In the functioning brain, lactate is the major end product of anaerobic glycolysis formed by one of the LDH isozyme and that lactate subsequently serves as a substrate for generation of significant amount of ATP to properly serve the metabolic functions of brain. Lactate dehydrogenase isozyme pattern of adult Japanese quail brain was investigated to examine brain energy metabolism by polyacrylamide-gel electrophoresis (PAGE) followed by densitometry. Twenty adult quails were sacrificed and separate brain tissue homogenate (10%) were prepared in 0.02 M Tris-Cl buffer (pH 7.4). The tissue homogenate was subjected to centrifuge. Supernatant was collected and used for enzyme activity and non-denaturing PAGE. The chicken brain tissue subjected to the same treatment was used as a reference for electrophoresis. The enzyme activity in the supernatant was 28.62±0.8400 μmol min-1 mg-1protein. The zymogram of quail brain isozymes revealed four different bands of LDH-1, LDH-2, LDH-3 and LDH-4 with a marked difference in their enzyme activity respectively as compare to chicken. The zymogram of chicken brain isozymes also showed four bands of equal enzyme activity at identical electrophoretic mobility to the quail brain. Among all four isozymes present in the quail brain the highest band intensity was observed in LDH-4. Densitometry again confirmed that LDH-4 was in highest (75.6%) proportion in quail brain. These results indicated that specifically higher amount of LDH-4 isozyme was only observed in quails was unique. The results are in support of the hypothesis that adult quail brain favors anaerobic tissue metabolism though it may function in both aerobic and anaerobic conditions.

1074

Brain Poster Session: Neurologic Disease

CEREBROSPINAL FLUID AND BLOOD FLOWS IN MILD COGNITIVE IMPAIRMENT, ALZHEIMER DISEASE AND NORMAL PRESSURE HYDROCEPHALUS

S. Stoquart-El Sankari[1,2], C. Gondry-Jouet[3], D. Mbayo[3], A. Fichten[4], O. Godefroy[2], M.-E. Meyer[1], **O. Balédent**[1]

[1]Department of Imaging and Biophysics, [2]Department of Neurology, [3]Department of Radiology, [4]Department of Neurosurgery, Amiens University Hospital, Amiens Cedex, France

Objectives: Phase-Contrast MRI (MRI) is a non invasive reliable technique which enables rapid quantification of cerebrospinal fluid (CSF) and cerebral blood (CBF) flows, and is helpful for aetiological diagnosis of Normal Pressure Hydrocephalus (NPH). In some patients, differential diagnosis with neurodegenerative pathologies (such as Alzheimer Disease: AD) may be difficult. Our purpose was to study the effects of AD or Mild Cognitive Impairment (MCI) on intracranial flows.

Methods: Nine MCI and 6 mild AD patients were identified after neuropsychological assessment and neurological examination. They underwent cerebral MRI using 3T scanner. PC-MRI pulse sequence was performed, and dynamic flow images were analyzed with home-made processing software. Results were compared to normal values recently published in age matched elderly healthy (EH) population (n=12), and to NPH patients, using multivariate analysis.

Results: Arterial flows didn't show statistical difference between AD patients (569 ± 69 ml/min) and EH (509 ± 103). Although not statistical, we found increased CBF in MCI patients (647 ± 124). Cervical CSF stroke volumes analysis showed similar values in the 3 populations (EH: 457 ± 147 µl; AD: 600 ± 194; MCI: 560 ± 146). Similarly, aqueductal CSF stroke volumes were comparable in EH (34 ± 16 µl) and AD (35 ± 17). Interestingly, aqueductal CSF was hyperdynamic in MCI patients (71 ± 24), but less than in NPH patients (196 ± 100).

Conclusion: These preliminary data suggest increased cerebral perfusion and ventricular CSF pulsations in predemential MCI patients. Surprisingly, we didn't find a significant difference between AD patients and healthy elderly. This may be due to small studied populations. PC-MRI enables reliable, safe and rapid measurements of CSF and blood flows. It provides complementary data helpful for the differential diagnosis between NPH and AD patients.

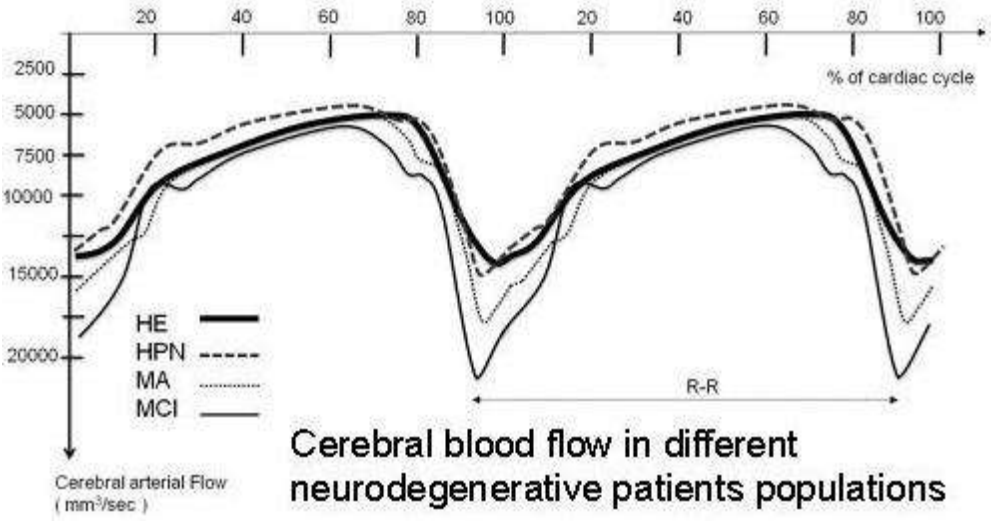

Cerebral blood flow in different neurodegenerative patients populations

[Figure 1]

References:

Baledent O, Henry-Feugeas MC, Idy-Peretti I (2001) Cerebrospinal fluid dynamics and relation with blood flow: a magnetic resonance study with semiautomated cerebrospinal fluid segmentation. Invest Radiol 36:368-77.

Stoquart-Elsankari S, Baledent O, Gondry-Jouet C, Makki M, Godefroy O, Meyer ME (2007) Aging effects on cerebral blood and cerebrospinal fluid flows. J Cereb Blood Flow Metab.

1075

Brain Poster Session: Neurologic Disease

CHOROIDS PLEXUS AND CSF ALTERATION IN MILD COGNITIVE IMPAIRMENT?

O. Balédent[1,2], M. Haddad-Rmeilly[1,2], S. Stoquart-El Sankari[1,3], J.-M. Serot[4], O. Godefroy[3], P. Bailly[2], M.-E. Meyer[1,2]

[1]Department of Imaging and Biophysics, [2]Department of Nuclear Medicine, [3]Department of Neurology, [4]Department of Geriatrics, Amiens University Hospital, Amiens Cedex, France

Objectives: Cerebrospinal fluid (CSF) plays a fundamental role in brain pathophysiology. Recent research has underlined the CSF´s involvement in neurodegenerative processes, such as Alzheimer´s disease (AD). The CSF is produced by the choroid plexus (CP) but the latter´s functional activity has only been studied in vitro. We present a new approach for studying these targets with [18F]fluorodeoxy-D-glucose (18F-FDG) positron emission tomography (PET) in Mild cognitive impairment popualtion.

Methods: The first population is constituted of 10 subjects (7 males and 3 females) aged of more than 65 years (73 ± 6 years) with a malignant pathology not affecting the brain. A neurological exam has been done to every patient to exclude all neurological pathology. The second population is constituted of 8 subjects (5 males and 3 females) identified as MCIa in the neurological department. a 45 min dyn-PET acquisition was scheduled in 34 time frames for each patient. CSF and CP regions of interest were manually selected on new reconstructed parametric map presented in other abstract of this congress. Mean raw uptake curves were reconstructed and FDG fixation was measured.

Results: The results show for the first time that it is possible to monitor the kinetics of FDG uptake by the CP and the CSF during a PET scan. The FDG kinetics in the CP differ from those seen in the CSF and all other brain tissues. CSF and CP FDG fixations were significantly decrease in MCI population.

Conclusion: This work is an initial step towards using PET to evaluate CSF production alteration in MCI population.

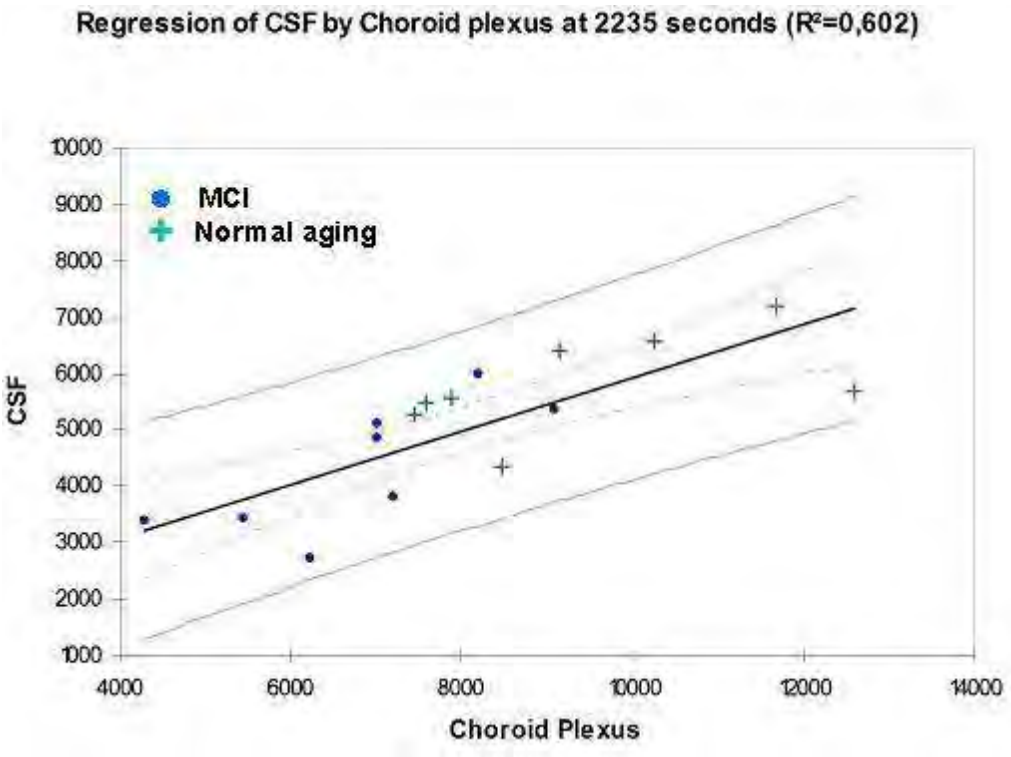

[Figure 1]

Figure: FDG fixation in choroid plexi presents a linear relationship with FDG fixation found in the CSF (R^2=0,602). This preliminary result shows the ability of PET for observation of CSF secretion.

References: Serot JM, Bene MC, Foliguet B, Faure GC (2000) Morphological alterations of the choroid plexus in late-onset Alzheimer´s disease. Acta Neuropathol 99:105-8.

1076

BrainPET Poster Session: Radiotracers and Quantification

THE KINETICS OF FDG UPTAKE IN THE CHOROID PLEXUS AND THE CSF

M. Haddad-Rmeilly[1,2], **O. Balédent**[1,2], S. Stoquart-El Sankari[1,3], J.-M. Serot[4], P. Bailly[2], M.-E. Meyer[1,2]

[1]Department of Imaging and Biophysics, [2]Department of Nuclear Medicine, [3]Department of Neurology, [4]Department of Geriatrics, Amiens University Hospital, Amiens Cedex, France

Objectives: Cerebrospinal fluid (CSF) plays a fundamental role in brain pathophysiology. Recent research has underlined the CSF´s involvement in neurodegenerative processes, such as Alzheimer´s disease (AD). The CSF is produced by the choroid plexus (CP) but the latter´s functional activity has only been studied in vitro. we present a new approach for studying these targets with [18F]fluorodeoxy-D-glucose (18F-FDG) positron emission tomography (PET).

Methods: The 45 min dyn-PET acquisition was scheduled in 34 time frames. Detection was performed in 3D mode. Our novel method provided successive images, representing the FDG uptake dynamics. Firstly, the analysis consisted in calculating 3 parameters (red + green + blue, RGB) for the fitting function (exponential fitting) for the 34 frames. This calculation was performed for every voxel in the brain volume. Secondly, the FDG uptake dynamic of each voxel was visualized as a new colour image generated from the 3 fundamental RGB colour maps. CSF and CP regions of interest were manually selected on the reconstructed map. Mean raw uptake curves were reconstructed.

Results: The Figure shows that inside the right ventricle, one can see a region of interest which appears only in our new parametric images and is absent on the conventional CT and static PET images. In our opinion, this region of interest corresponds to the choroid plexi**.** The results show for the first time that it is possible to monitor the kinetics of FDG uptake by the PC and the CSF during a PET scan.The FDG kinetics in the PC differ completely from those seen in the CSF and all other brain tissues.

Conclusion: This work is an initial step towards using PET to evaluate CSF production and PC function in vivo.

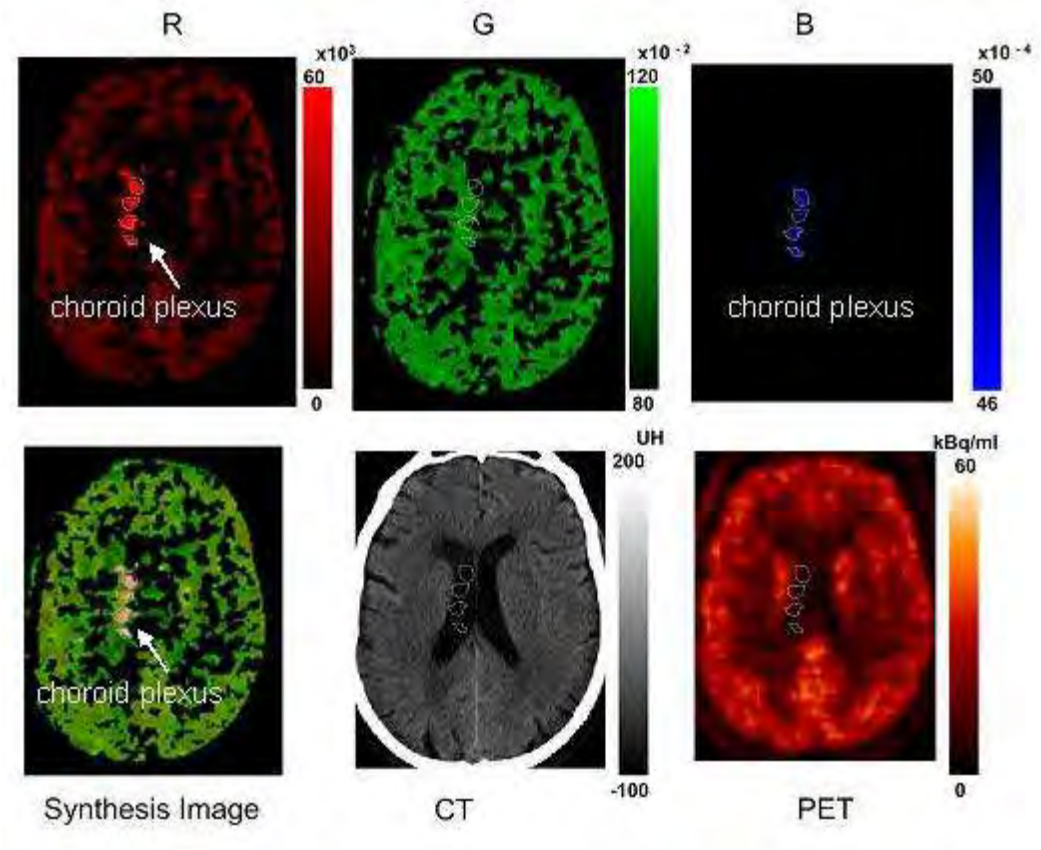

[Figure 1]

Figure: A sample patient image for the same brain slice presented in several difference image modes: the 3 parametric PET maps, the reconstructed PET map, the CT image and a static PET image.

References: Serot JM, Bene MC, Foliguet B, Faure GC (2000) Morphological alterations of the choroid plexus in late-onset Alzheimer´s disease. Acta Neuropathol 99:105-8.

1077

BrainPET Poster Session: Brain Imaging: Stroke

CEREBRAL VENOUS FLOW PHYSIOLOGY AND IMPACT OF CEREBRAL VENOUS THROMBOSIS: A PHASE-CONTRAST MRI STUDY

S. Stoquart-El Sankari[1,2], P. Lehmann[3], A. Villette[3], H. Deramond[3], M.-E. Meyer[1,4], **O. Balédent**[1,4]

[1]Department of Imaging and Biophysics, [2]Department of Neurology, [3]Department of Radiology, [4]Department of Nuclear Medicine, Amiens University Hospital, Amiens Cedex, France

Objectives: Although it is supposed to play a crucial role in regulating intracranial hydrodynamics, a few studies have been devoted to the cerebral venous system physiology and pathology. Phase-Contrast MRI (PC-MRI) enables non invasive and rapid measurements of cerebrospinal fluid (CSF) and blood flows, and has been used for venous evaluation in jugular veins, and intracerebral pathways, but physiological quantitative flow parameters are still lacking.

Material: PC-MRI sequences were added to brain MRI conventional protocol in 19 patients with suspected Cerebral Venous Thrombosis (CVT), among whom 6 patients had a positive diagnosis on MR venography. Results were compared to those of 18 age-matched healthy volunteers (HV). In each HV, we calculated the venous pulsatility index (VPI) at both cervical and cerebral levels. The VPI was calculated as follows: VPI= ((Fmax-Fmin/Fmax)) x100 where Fmax and Fmin represent respectively maximum and minimum venous flow amplitude.

Results: In HV, we found heterogeneous individual venous flows, as well as variable side dominance in paired veins and sinuses. PC-MRI enabled reproducible measurements of venous flows in Superior sagittal, straight and transverse sinuses. Arterial and CSF flows were normal. The VPI comparison showed a significant difference ($p < 0.05$) between the internal jugular veins (VPI= 38 ± 15), and the SSS (VPI= 21± 10). In CVT patients, PCMRI did not detect any venous flow in the veins and/or sinuses with thrombosis whereas arterial flows were preserved. Interestingly, aqueductal and cervical CSF flows were hyperdynamic in one patient with signs of increased intracranial pressure, and decreased in 3 patients with extended thrombosis in the Superior Sagittal and Transverse sinuses (figure).

Conclusion: We found heterogeneous types of venous pathways in HV, suggesting a variable role of accessory (epidural and vertebromedullar) drainage in physiological conditions. Besides, our study is the first to enable venous flow quantification in the major intracranial sinuses with excellent detection rates. VPI study showed higher pulsatility in the extracranial venous compartment. Heterogeneous results in patients with CVT show the complex role of veins in the regulation of intracranial hydrodynamics. PC-MRI enables reliable, safe and rapid measurements of CSF and blood flows. It helps understanding the complexity of the venous system and its role in regulating the intracranial pressure in physiological conditions and in pathologies like CVT.

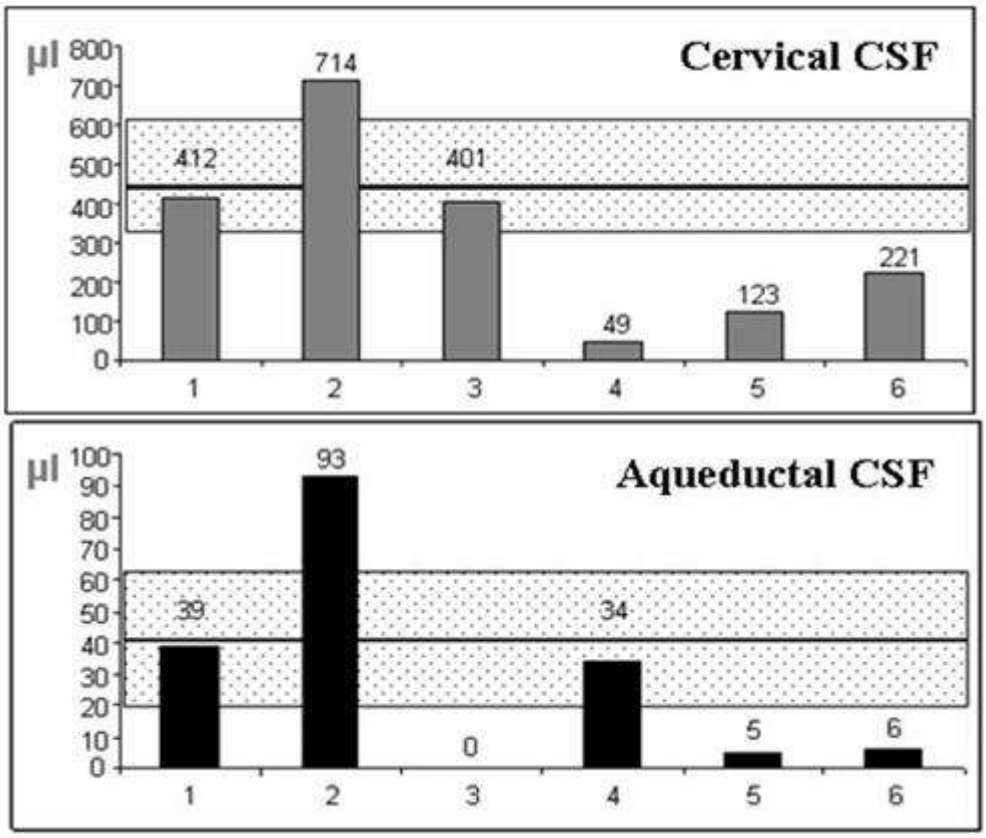

[Figure 1]

Figure: CSF stroke volumes in patients with cerebral venous Thrombosis. Stroke volumes are represented in µl per cardiac cycle. The dashed rectangle corresponds to the average ± 1 standard deviation observed in the HV population.

References:

Baledent O, Henry-Feugeas MC, Idy-Peretti I (2001) Cerebrospinal fluid dynamics and relation with blood flow: a magnetic resonance study with semiautomated cerebrospinal fluid segmentation. Invest Radiol 36:368-77.

Stoquart-Elsankari S, Baledent O, Gondry-Jouet C, Makki M, Godefroy O, Meyer ME (2007) Aging effects on cerebral blood and cerebrospinal fluid flows. J Cereb Blood Flow Metab.

1078

Brain Poster Session: Cerebral Vascular Regulation

DIFFERENTIAL REMODELING RESPONSES OF CEREBRAL AND SYSTEMIC ARTERIOLES IN A NOVEL EX VIVO CULTURE SYSTEM

S. Steelman[1], L.E. Niklason[2], J.D. Humphrey[3]

[1]Systems Biology and Translational Medicine, Texas A&M Health Science Center, College Station, TX, [2]Department of Anesthesiology, Yale University, New Haven, CT, [3]Department of Biomedical Engineering, Texas A&M University, College Station, TX, USA

Objective: Delayed cerebral vasospasm is a major cause of morbidity and mortality following subarachnoid hemorrhage. Recent evidence has suggested the involvement of the microcirculation in the development of cerebral ischemia associated with vasospasm. The difficulty of in vivo imaging of cerebral arterioles, however, makes investigation of this hypothesis difficult. We sought, therefore, to develop an ex vivo organ culture system with which to study the changes in cerebral arteriolar structure and function that might take place after subarachnoid hemorrhage.

Methods: Cerebral or skeletal muscle arterioles (~150 μm) were cannulated in a pressure myograph system and perfused and superfused with cell culture media (DMEM supplemented with L-glutamine, penicillin/streptomycin, and 10% plasma). Arterioles were cultured at physiological levels of pressure, temperature, axial stretch, and CO_2. The active and passive pressure-diameter relationships, as well as responsiveness to endothelin-1 and acetylcholine, were determined after 0, 24, 72, and 120 hours of culture.

Results: Culture using 10% plasma maintained cerebral arteriolar contractility for 3 days, with a moderate (44%) loss of the contractile response on day 5 (n = 6). Endothelial function, as assessed by dilation to acetylcholine, was diminished after 3 days and abolished at 5 days of culture. The passive pressure-diameter relationship, the circumferential stretch-stress relationship, and arteriolar wall thickness were not altered with culture. In contrast, skeletal muscle arterioles (n = 5) demonstrated enhanced production of extracellular matrix, total loss of smooth muscle cell contractility, and a dramatic reduction in passive diameter.

Conclusions: The pressure myograph-based culture system maintains arteriolar structure and smooth muscle function for up to 5 days, making it an appropriate technique with which to study the vascular remodeling that might contribute to cerebral ischemia following subarachnoid hemorrhage. Furthermore, these same culture conditions induced dramatic changes in skeletal muscle arterioles, suggesting that there are fundamental differences in the regulation of vascular structure and function between cerebral and systemic arterioles. Future studies using this novel culture system will focus on the responses of cerebral arterioles to vasospastic factors that may be produced by a subarachnoid clot.

1079

Brain Oral Session: Blood Brain Barrier

UPREGULATION OF BLOOD-BRAIN BARRIER DRUG EFFLUX PUMPS BY THE CONSTITUTIVE-ANDROSTANE RECEPTOR (CAR, NR1I3), A XENOBIOTIC-ACTIVATED NUCLEAR RECEPTOR

D.S. Miller, X. Wang

Laboratory of Pharmacology, NIH/NIEHS, Research Triangle Park, NC, USA

Objectives: p-Glycoprotein and breast cancer-related polypeptide (BCRP), are ATP-driven drug efflux pumps expressed at the blood-brain barrier. They are major obstacles to CNS pharmacotherapy, limiting delivery of drugs used to treat brain cancer, neuroAIDS and epilepsy (Miller et al 2008). In peripheral barrier and excretory tissues, several ligand-activated nuclear receptors, e.g., pregnane-X receptor (PXR) and CAR, are master regulators of drug metabolizing enzymes and drug efflux transporters. We previously found that PXR was expressed in rat and mouse brain capillaries and that receptor activation in vitro and in vivo substantially increased p-glycoprotein transport activity and protein expression (Bauer et al 2004; Bauer et al 2006). Here we demonstrate CAR-mediated upregulation of p-glycoprotein and BCRP in brain capillaries.

Methods: p-Glycoprotein and BCRP transport activity was measured in isolated brain capillaries from rats and mice using fluorescent substrates (cyclosporine A and prazosin derivatives, respectively), confocal microscopy and quantitative image analysis; transporter protein expression was measured in western blots of brain capillary plasma membranes (Bauer et al 2004; Bauer et al 2006).

Results: CAR protein was immunolocalized to the rat brain capillary endothelium; RT-PCR detected CAR mRNA in capillary extracts. Exposure of isolated rat capillaries to the CAR ligand, phenobarbital, roughly doubled protein expression and transport activity of both transporters. These increases were abolished by nanomolar concentrations of the protein phosphatase 2A (PP2A) inhibitor, okadaic acid, a finding consistent with the role of that phosphatase in CAR activation. In mouse brain capillaries, the specific murine CAR ligand, TCPOBOP, increased transport mediated by p-glycoprotein and BCRP, again by a PP2A-dependent mechanism. These increases were not seen in capillaries from CAR-null mice. Thus, CAR upregulated p-glycoprotein and BCRP expression and activity. Finally, dosing mice with TCPOBOP increased transport mediated by p-glycoprotein and BCRP, as well as p-glycoprotein and BCRP protein expression, all measured in isolated brain capillaries ex vivo.

Conclusions: CAR is a xenobiotic responsive transcription factor that is activated by a number of ligands, including, bilirubin, and a variety of foreign compounds, steroid hormones, and prescription drugs. The present in vitro and in vivo experiments with rats and mice show that CAR ligands upregulate expression of two key drug efflux pumps at the blood-brain barrier. Increases in transporter expression were comparable to that seen previously with PXR upregulation of p-glycoprotein. That level of transporter induction was previously associated with 70% reduction in the efficacy of the p-glycoprotein substrate, methadone, in an antinociception assay (Bauer et al 2006).

References:

Bauer B, Hartz AM, Fricker G, Miller DS (2004) Pregnane X receptor up-regulation of P-glycoprotein expression and transport function at the blood-brain barrier. Mol Pharmacol 66:413-9.

Bauer B, Yang X, Hartz AM, Olson ER, Zhao R, Kalvass JC, Pollack GM, Miller DS (2006) In vivo

activation of human pregnane X receptor tightens the blood-brain barrier to methadone through P-glycoprotein up-regulation. Mol Pharmacol 70:1212-9.

Miller DS, Bauer B, Hartz AM (2008) Modulation of P-glycoprotein at the blood-brain barrier: opportunities to improve central nervous system pharmacotherapy. Pharmacol Rev 60:196-209.

1080

Brain Poster Session: Blood-Brain Barrier

BLOOD-BRAIN BARRIER NA-K-CL COTRANSPORTER AND NA/H EXCHANGER: THERAPEUTIC TARGETS FOR ISCHEMIA-INDUCED BRAIN NA UPTAKE AND EDEMA FORMATION

Y.-J. Chen, T.I. Lam, S.E. Anderson, J.H. Walton, **M.E. O'Donnell**

Physiology and Membrane Biology, University of California, Davis, CA, USA

Objectives: Ischemia-induced brain edema is a major cause of morbidity and mortality in stroke although much is unknown about the processes involved. Previous studies have shown that during the early hours of cerebral ischemia, edema forms in the presence of an intact blood-brain barrier (BBB) by mechanisms involving increased secretion of Na, Cl and water across the barrier from blood into brain. The BBB ion transporters responsible for this have been largely unknown although luminal Na transporters appear to be rate limiting in the process. Our previous studies have provided evidence that a luminal BBB Na-K-Cl cotransporter participates in ischemia-induced cerebral edema formation. Among our findings are the observations that Na-K-Cl cotransporter activity of cerebral microvascular endothelial cells (CMEC) is stimulated by hypoxia, aglycemia and arginine vasopressin (AVP), three prominent factors present in ischemia, with a time course and sensitivity consistent with ischemia-induced edema formation. In addition, inhibition of the BBB Na-K-Cl cotransporter by intravenous administration of bumetanide significantly attenuates edema formation and infarct in the rat permanent middle cerebral artery occlusion (MCAO) model of ischemic stroke. In recent studies we have found evidence that a BBB Na/H exchanger is also stimulated by hypoxia, aglycemia and AVP and, further, that intravenous administration of the Na/H exchange inhibitor HOE642 also reduces edema formation and infarct in permanent MCAO. We also found that both NHE1 and NHE2 isoforms of the Na/H exchanger are present in cultured cerebral microvascular endothelial cells (CMEC). The present study had two goals: 1) to investigate NHE isoforms present in BBB in situ; and 2) to determine whether bumetanide and HOE642 reduce the brain Na uptake that underlies edema in ischemic stroke.

Methods: Perfusion-fixed brains of rats subjected to 90 min of permanent left MCAO were evaluated for the presence of NHE1 and NHE2 Na/H exchanger isoforms in BBB in situ using immunoelectron microscopy (immunoEM) and antibodies that specifically recognize NHE1 and NHE2 isoform proteins. For brain Na uptake studies, rats were given bumetanide (30 mg/kg), HOE642 (30 mg/kg) or vehicle i.v. 20 min before, or 1 or 2 hr after initiation of left MCAO. Localized 23Na magnetic resonance spectroscopy (MRS) with the shift reagent DyTTHA was then used to assess total and extravascular brain [Na] in selected regions of interest during up to 5 hr of MCAO.

Results: ImmunoEM revealed that both NHE1 and NHE2 isoforms are present predominantly in the luminal BBB membrane in situ, whether normoxic or ischemic cortex. For 23Na MRS studies, the ipsilateral/contralateral brain ratios of both total [Na] and extravascular [Na] increased linearly following induction of ischemia. Both bumetanide and HOE642 significantly reduced brain Na uptake and infarct whether given before or after the start of MCAO.

Conclusions: These findings support the hypothesis that the BBB Na/H exchanger, possibly both NHE1 and NHE2 isoforms, participates in ischemia-induced edema formation and that intravenous bumetanide and HOE642 are both effective in reducing brain Na uptake, edema and infarct even when given after the onset of ischemia.

Brain Poster Session: Cerebral Metabolic Regulation

CHROMIUM HISTIDINATE INCREASES BRAIN GLUT-1 AND GLUT-3 LEVELS IMPAIRED BY INSULIN RESISTANCE

J. Komorowski[1], M. Tuzcu[2], N. Sahin[2], K. Sahin[2]

[1]Technical Services & Scientific Affairs, Nutrition 21, Purchase, NY, USA, [2]Firat University, Elazig, Turkey

Objectives: Chromium is an essential trace mineral and a cofactor for insulin function. Chromium, in the form of chromium picolinate, has been shown to lower elevated blood glucose levels in people with type 2 diabetes (Broadhurst and Domenico, 2006). Chromium's beneficial effects on blood glucose levels may be due to its ability to increase insulin dependent membrane-associated GLUT-4 levels (Cefalu et al, 2002). Hou et al (2007) found that chronic hyperglycemia downregulated GLUT-1 and GLUT-3 expression in the brain. The current study was conducted to evaluate the effect of chromium, in the form of chromium histidinate (CrHis), on brain GLUT-1 and GLUT-3 levels in overweight, insulin resistant rats.

Methods: Insulin resistance and hyperglycemia were induced in male Wistar rats by feeding a high fat diet (HFD, 40% of calories as fat). A healthy control group received a standard diet (12% of calories as fat). Rats (10/group) were then divided into groups: healthy control (Control), HFD, and HFD + CrHis. Chromium (Cr) treated rats were fed CrHis (110 mcg/kg body wt/d). After 12 weeks, Cr levels and GLUT-1 and GLUT-3 expression (Western blot analysis) were measured from brain tissue homogenates. Body weight, serum Cr, and blood glucose levels were also measured.

Results: The study results are shown in Table 1. HFD significantly decreased brain Cr (-26%), GLUT-1 (-38%) and GLUT-3 (-11.2%) levels compared to Control. HFD also significantly increased body weight (+14%), increased blood glucose levels (+30%), and decreased serum Cr levels (-20%). Addition of CrHis to the HFD significantly increased brain and serum Cr levels, increased brain GLUT-1 and GLUT-3 levels, and decreased body weight and blood glucose levels, compared to HFD alone.

Table 1. Comparison of efficacy variables after treatment (mean ± s.e.m.)

	Control	HFD	HFD + CrHis
Body Weight (g)	288.7 ± 3.0^a	329.2 ± 1.3^b	315.1 ± 1.9^c
Blood Glucose (mg/dL)	101.5 ± 1.6^a	132.3 ± 2.3^b	116.4 ± 2.1^c
Serum Chromium (ng/g)	16.9 ± 0.4^a	13.6 ± 0.3^b	22.0 ± 0.6^c
Brain Chromium (ng/g)	15.6 ± 0.3^a	11.2 ± 0.2^b	17.7 ± 0.2^c
GLUT-1 (% of Control)	100.0 ± 1.2^a	62 ± 1.5^b	89.5 ± 0.3^c

GLUT-3 (% of Control)	100.0 ± 0.6[a]	88.8 ± 3.8[b]	106.3 ± 1.5[a]

[Table 1]

Different letters represent statistical significance ($p < 0.01$) between groups.

Conclusions: This is the first study to demonstrate that chromium administration can enhance brain GLUT-1 and GLUT-3 expression. This study also shows that a HFD decreases brain chromium levels, and brain GLUT-1 and GLUT-3 levels. The ability of chromium histidinate to enhance brain GLUT-1 and GLUT-3 levels may be directly related to: (1) actions of the chromium in the brain, (2) the indirect effects of chromium on systemic blood glucose levels, or (3) both. Additional research is warranted to further evaluate additional cerebral metabolic effects of chromium histidinate.

References:

1. Broadhurst CL, Domenico P (2006) Clinical studies on chromium picolinate supplementation in diabetes mellitus - A review. Diabetes Technol Ther **6**:677-687

2. Cefalu WT, Wang ZQ, Zhang XH, Baldor LC, Russell JC (2002) Oral chromium picolinate improves carbohydrate and lipid metabolism and enhances skeletal muscle Glut-4 translocation in obese, hyperinsulinemic (JCR-LA corpulent) rats. J Nutr **132**:1107-1114

3. Hou WK, Xian YX, Zhang L, Lai H, Hou XG, Xu YX, Yu T, Xu FY, Song J, Fu CL, Zhang WW and Chen L (2007) Influence of blood glucose on the expression of glucose transporter proteins 1 and 3 in the brain of diabetic rats. Chin Med J **19**:1704-1709

1083

Brain Poster Session: Experimental Stroke & Cerebral Ischemia

ENDURING DEFICITS IN NEUROPHYSIOLOGICAL AND BEHAVIORAL FUNCTIONS OF INTACT SOMATOSENSORY CORTEX FOLLOWING FOCAL INJURIES TO THE CONTRALATERAL SOMATOSENSORY CORTEX IN ADULT RATS

R. Chaudhary, Z. Darokhan, **V. Rema**

National Brain Research Centre, Manesar, India

Deleterious influences of brain injury could cause neurological deficits in people of all ages and can lead to significant, long-lasting behavioral and cognitive deficits. The degree of recovery of neurological functions, in most instances would depend on the type, severity, location and extent of injury. Functional impairments attributed to the site of injury are likely to be severe due to tissue loss and therefore limiting the possibilities for interventions. However ongoing secondary reactions in areas anatomically connected to the injured site could aggravate neurophysiological as well as behavioural deficits over time. Interventions using combination of pharmacological and rehabilitative therapy given at the right time could help in reducing deficits arising from secondary reactions. Designing optimal interventions requires in-depth knowledge of response of the brain to injuries. In this regard we addressed two major issues: (i) How do neurons in an intact region respond to focal lesions in a reciprocally connected area? (ii) What are the changes in behavioral functions controlled by an intact cortical region following lesion in a reciprocally connected site? For these studies we removed a part of the primary somatosensory (whisker barrel) cortex unilaterally and examined changes in neuronal activity and behavioral functions of the intact somatosensory cortex in adult rats. Surgical lesions were made by sub-pial aspiration of the whisker barrel cortex under anesthesia. Earlier studies have shown that such lesions caused deficits in activity of neurons in the intact contralesional barrel cortex after long survival times (Rema and Ebner 2003). We monitored ongoing changes at regular intervals for the first 12 hours post-lesion. Our results show early onset of laminar changes in spontaneous and stimulus evoked activities of neurons in the homotopic contralesional hemisphere. Neurons in cortical output layers 2/3 increased their activity whereas neurons in the thalamocortical input layer 4 do not change significantly. Alterations in neuronal functions could affect sensory behavior. To examine deficits in somatosensory behavior we used the whisker-sensitive gap-crossing task (Hutson and Masterton 1986). The rat uses its sensitive facial whisker to gather tactile information from its environment. The gap-crossing task tests the ability of rats to use sensory information from whiskers to judge and cross a gap between two raised platforms for food reward. The effect of lesion on behavioral functions of the intact barrel cortex in the opposite hemisphere was monitored at regular intervals upto 70 days post-lesion. The rats had all whiskers contralateral to lesion trimmed and all whiskers on the side ipsilateral to lesion were intact. This forced the use of whiskers that project to the intact cortex in the performing the gap-crossing task. Our results show that unilateral barrel cortex lesion produces long-term deficits in somatosensory behavioral functions controlled by intact somatosensory cortex in adult rats. Our preliminary experiments suggest that one of the mechanisms for these long-term impairments in neuronal activities and behavioral functions, of distant anatomically connected intact brain regions following focal cortical injuries is synaptic dysfunction at these regions.

Funding: Wellcome Trust International Senior Research Fellowship: WT066676 to V. Rema